VOLUME 28 / NUMBER 23
DECEMBER 8, 1990
ACC. NOS. N90-28489 TO N90-29298

STAR
AN ABSTRACT JOURNAL

Scientific and Technical Aerospace Reports

PRODUCED BY THE
SCIENTIFIC AND TECHNICAL
INFORMATION
DIVISION

NASA

NATIONAL AERONAUTICS AND SPACE ADMINISTRATION

WHAT YOU CAN DO FOR *STAR*

All users of this abstract service are urged to forward reports to be considered for announcement in *STAR*. This will aid NASA in its efforts to provide the fullest possible coverage of all scientific and technical publications that might support aeronautics and space research and development. If you have prepared relevant reports (other than those that you will transmit to NASA, DOD, or DOE through the usual contract- or grant-reporting channels), please send them for consideration to the NASA Scientific and Technical Information Facility, P.O. Box 8757, BWI Airport, MD 21240.

Reprints of journal articles, book chapters, and conference papers are also welcome. These will be considered for announcement in *STAR's* companion journal, *International Aerospace Abstracts*.

You may specify a particular source to be included in a report announcement if you wish; otherwise the report will be placed on public sale at the National Technical Information Service. Copyrighted publications will be announced but not distributed or sold.

PURCHASE OF *STAR*

The semimonthly issues are available to registered users on annual subscription from the NASA Scientific and Technical Information Facility, ATTN: Registration Services, P.O. Box 8757, BWI Airport, MD 21240. *STAR* is publicly available on annual subscription from the Superintendent of Documents, U.S. Government Printing Office, Washington, DC 20402.

PUBLISHED BY:

UNITED STATES GOVERNMENT
NATIONAL AERONAUTICS AND SPACE ADMINISTRATION
SCIENTIFIC AND TECHNICAL INFORMATION DIVISION
Scientific and Technical Aerospace Reports, Volume 28, is prepared by the NASA Scientific and Technical Information Facility operated for the National Aeronautics and Space Administration by RMS Associates.

The Administrator of the National Aeronautics and Space Administration has determined that the publication of this periodical is necessary in the transaction of the public business required by law of this agency. Use of funds for printing this periodical has been approved by the Director of the Office of Management and Budget through March 22, 1991.

US ISSN 0036-8741

Scientific and Technical Aerospace Reports (STAR) is issued twice a month and contains abstracts and indexes of meeting papers, conference proceedings, and unlimited distribution reports that have been added to the NASA Scientific and Technical Information Database during the preceding period. These citations may also be accessed online via NASA/RECON or via AIAA's Aerospace Database (File 108) through Dialog Information Services, Inc.

STAR subject coverage includes all aerospace-related areas that will help NASA achieve its mission. Material is gathered from all over the world and includes significant input from many countries under exchange and access agreements.

Consult the indexes at the back of this volume to help zero in on what you are looking for. These include:

Subject Index
Personal Author Index
Corporate Source Index
Contract Number Index
Report/Accession Number Index

STAR's companion abstract journal *International Aerospace Abstracts* should be used if you are looking for references to periodicals, books, and published meeting papers or conference proceedings.

Questions and comments should be addressed to:

NASA Scientific and Technical Information Facility
User Services
P.O. Box 8757
BWI Airport, MD 21240
301-621-0150

VOLUME 28 NUMBER 23 / DECEMBER 8, 1990

TABLE OF CONTENTS

AERONAUTICS

Includes aeronautics (general); aerodynamics; air transportation and safety; aircraft communications and navigation; aircraft design, testing and performance; aircraft instrumentation; aircraft propulsion and power; aircraft stability and control; and research and support facilities (air).

For related information see also *Astronautics.*

01 AERONAUTICS (GENERAL) 3267

02 AERODYNAMICS 3267

Includes aerodynamics of bodies, combinations, wings, rotors, and control surfaces; and internal flow in ducts and turbomachinery.

For related information see also *34 Fluid Mechanics and Heat Transfer.*

03 AIR TRANSPORTATION AND SAFETY 3270

Includes passenger and cargo air transport operations; and aircraft accidents.

For related information see also *16 Space Transportation* and *85 Urban Technology and Transportation.*

04 AIRCRAFT COMMUNICATIONS AND NAVIGATION 3270

Includes digital and voice communication with aircraft; air navigation systems (satellite and ground based); and air traffic control.

For related information see also *17 Space Communications, Spacecraft Communications, Command and Tracking* and *32 Communications and Radar.*

05 AIRCRAFT DESIGN, TESTING AND PERFORMANCE 3271

Includes aircraft simulation technology.

For related information see also *18 Spacecraft Design, Testing and Performance* and *39 Structural Mechanics.* For land transportation vehicles see *85 Urban Technology and Transportation.*

06 AIRCRAFT INSTRUMENTATION 3277

Includes cockpit and cabin display devices; and flight instruments.

For related information see also *19 Spacecraft Instrumentation* and *35 Instrumentation and Photography.*

07 AIRCRAFT PROPULSION AND POWER 3277

Includes prime propulsion systems and systems components, e.g., gas turbine engines and compressors; and onboard auxiliary power plants for aircraft.

For related information see also *20 Spacecraft Propulsion and Power, 28 Propellants and Fuels,* and *44 Energy Production and Conversion.*

08 AIRCRAFT STABILITY AND CONTROL 3282

Includes aircraft handling qualities; piloting; flight controls; and autopilots.

For related information see also *05 Aircraft Design, Testing and Performance.*

09 RESEARCH AND SUPPORT FACILITIES (AIR) 3284

Includes airports, hangars and runways; aircraft repair and overhaul facilities; wind tunnels; shock tubes; and aircraft engine test stands.

For related information see also *14 Ground Support Systems and Facilities (Space).*

ASTRONAUTICS

Includes astronautics (general); astrodynamics; ground support systems and facilities (space); launch vehicles and space vehicles; space transportation; space communications, spacecraft communications, command and tracking; spacecraft design, testing and performance; spacecraft instrumentation; and spacecraft propulsion and power.

For related information see also *Aeronautics.*

12 ASTRONAUTICS (GENERAL) N.A.

For extraterrestrial exploration see *91 Lunar and Planetary Exploration.*

13 ASTRODYNAMICS 3285

Includes powered and free-flight trajectories; and orbital and launching dynamics.

14 GROUND SUPPORT SYSTEMS AND FACILITIES (SPACE) 3285

Includes launch complexes, research and production facilities; ground support equipment, e.g., mobile transporters; and simulators.

For related information see also *09 Research and Support Facilities (Air).*

15 LAUNCH VEHICLES AND SPACE VEHICLES N.A.

Includes boosters; operating problems of launch/space vehicle systems; and reusable vehicles.

For related information see also *20 Spacecraft Propulsion and Power.*

16 SPACE TRANSPORTATION 3286

Includes passenger and cargo space transportation, e.g., shuttle operations; and space rescue techniques.

For related information see also *03 Air Transportation and Safety* and *18 Spacecraft Design, Testing and Performance.* For space suits see *54 Man/System Technology and Life Support.*

17 SPACE COMMUNICATIONS, SPACECRAFT COMMUNICATIONS, COMMAND AND TRACKING N.A.

Includes telemetry; space communications networks; astronavigation and guidance; and radio blackout.

For related information see also *04 Aircraft Communications and Navigation* and *32 Communications and Radar.*

18 SPACECRAFT DESIGN, TESTING AND PERFORMANCE **3286**

Includes satellites; space platforms; space stations; spacecraft systems and components such as thermal and environmental controls; and attitude controls.

For life support systems see *54 Man/System Technology and Life Support.* For related information see also *05 Aircraft Design, Testing and Performance, 39 Structural Mechanics,* and *16 Space Transportation.*

19 SPACECRAFT INSTRUMENTATION **N.A.**

For related information see also *06 Aircraft Instrumentation* and *35 Instrumentation and Photography.*

20 SPACECRAFT PROPULSION AND POWER **3288**

Includes main propulsion systems and components, e.g. rocket engines; and spacecraft auxiliary power sources.

For related information see also *07 Aircraft Propulsion and Power, 28 Propellants and Fuels, 44 Energy Production and Conversion,* and *15 Launch Vehicles and Space Vehicles.*

CHEMISTRY AND MATERIALS

Includes chemistry and materials (general); composite materials; inorganic and physical chemistry; metallic materials; nonmetallic materials; propellants and fuels; and materials processing.

23 CHEMISTRY AND MATERIALS (GENERAL) **N.A.**

24 COMPOSITE MATERIALS **3299**

Includes physical, chemical, and mechanical properties of laminates and other composite materials.

For ceramic materials see *27 Nonmetallic Materials.*

25 INORGANIC AND PHYSICAL CHEMISTRY **3303**

Includes chemical analysis, e.g., chromatography; combustion theory; electrochemistry; and photochemistry.

For related information see also *77 Thermodynamics and Statistical Physics.*

26 METALLIC MATERIALS **3306**

Includes physical, chemical, and mechanical properties of metals, e.g., corrosion; and metallurgy.

27 NONMETALLIC MATERIALS **3312**

Includes physical, chemical, and mechanical properties of plastics, elastomers, lubricants, polymers, textiles, adhesives, and ceramic materials.

For composite materials see *24 Composite Materials.*

28 PROPELLANTS AND FUELS **3315**

Includes rocket propellants, igniters and oxidizers; their storage and handling procedures; and aircraft fuels.

For related information see also *07 Aircraft Propulsion and Power, 20 Spacecraft Propulsion and Power,* and *44 Energy Production and Conversion.*

29 MATERIALS PROCESSING **3316**

Includes space-based development of products and processes for commercial application.

For biological materials see *55 Space Biology.*

ENGINEERING

Includes engineering (general); communications and radar; electronics and electrical engineering; fluid mechanics and heat transfer; instrumentation and photography; lasers and masers; mechanical engineering; quality assurance and reliability; and structural mechanics.

For related information see also *Physics.*

31 ENGINEERING (GENERAL) **3316**

Includes vacuum technology; control engineering; display engineering; cryogenics; and fire prevention.

32 COMMUNICATIONS AND RADAR **3317**

Includes radar; land and global communications; communications theory; and optical communications.

For related information see also *04 Aircraft Communications and Navigation* and *17 Space Communications, Spacecraft Communications, Command and Tracking.* For search and rescue see *03 Air Transportation and Safety,* and *16 Space Transportation.*

33 ELECTRONICS AND ELECTRICAL ENGINEERING **3320**

Includes test equipment and maintainability; components, e.g., tunnel diodes and transistors; microminiaturization; and integrated circuitry.

For related information see also *60 Computer Operations and Hardware* and *76 Solid-State Physics.*

34 FLUID MECHANICS AND HEAT TRANSFER **3323**

Includes boundary layers; hydrodynamics; fluidics; mass transfer and ablation cooling.

For related information see also *02 Aerodynamics* and *77 Thermodynamics and Statistical Physics.*

35 INSTRUMENTATION AND PHOTOGRAPHY **3329**

Includes remote sensors; measuring instruments and gauges; detectors; cameras and photographic supplies; and holography.

For aerial photography see *43 Earth Resources and Remote Sensing.* For related information see also *06 Aircraft Instrumentation* and *19 Spacecraft Instrumentation.*

36 LASERS AND MASERS **3330**

Includes parametric amplifiers.

For related information see also *76 Solid-State Physics.*

37 MECHANICAL ENGINEERING **3331**

Includes auxiliary systems (nonpower); machine elements and processes; and mechanical equipment.

38 QUALITY ASSURANCE AND RELIABILITY **3336**

Includes product sampling procedures and techniques; and quality control.

39 STRUCTURAL MECHANICS **3337**

Includes structural element design and weight analysis; fatigue; and thermal stress.

For applications see *05 Aircraft Design, Testing and Performance* and *18 Spacecraft Design, Testing and Performance.*

GEOSCIENCES

Includes geosciences (general); earth resources and remote sensing; energy production and conversion; environment pollution; geophysics; meteorology and climatology; and oceanography.

For related information see also *Space Sciences.*

42 GEOSCIENCES (GENERAL) **N.A.**

43 EARTH RESOURCES AND REMOTE SENSING **3341**

Includes remote sensing of earth resources by aircraft and spacecraft; photogrammetry; and aerial photography.

For instrumentation see *35 Instrumentation and Photography.*

44 ENERGY PRODUCTION AND CONVERSION **3344**

Includes specific energy conversion systems, e.g., fuel cells; global sources of energy; geophysical conversion; and windpower.

For related information see also *07 Aircraft Propulsion and Power, 20 Spacecraft Propulsion and Power,* and *28 Propellants and Fuels.*

45 ENVIRONMENT POLLUTION **3346**

Includes atmospheric, noise, thermal, and water pollution.

46 GEOPHYSICS **3349**

Includes aeronomy; upper and lower atmosphere studies; ionospheric and magnetospheric physics; and geomagnetism.

For space radiation see *93 Space Radiation.*

47 METEOROLOGY AND CLIMATOLOGY **3351**

Includes weather forecasting and modification.

48 OCEANOGRAPHY **3353**

Includes biological, dynamic, and physical oceanography; and marine resources.

For related information see also *43 Earth Resources and Remote Sensing.*

LIFE SCIENCES

Includes life sciences (general); aerospace medicine; behavioral sciences; man/system technology and life support; and space biology.

51 LIFE SCIENCES (GENERAL) **3354**

52 AEROSPACE MEDICINE **3355**

Includes physiological factors; biological effects of radiation; and effects of weightlessness on man and animals.

53 BEHAVIORAL SCIENCES **3357**

Includes psychological factors; individual and group behavior; crew training and evaluation; and psychiatric research.

54 MAN/SYSTEM TECHNOLOGY AND LIFE SUPPORT **3362**

Includes human engineering; biotechnology; and space suits and protective clothing.

For related information see also *16 Space Transportation.*

55 SPACE BIOLOGY **3378**

Includes exobiology; planetary biology; and extraterrestrial life.

MATHEMATICAL AND COMPUTER SCIENCES

Includes mathematical and computer sciences (general); computer operations and hardware; computer programming and software; computer systems; cybernetics; numerical analysis; statistics and probability; systems analysis; and theoretical mathematics.

59 MATHEMATICAL AND COMPUTER SCIENCES (GENERAL) **N.A.**

60 COMPUTER OPERATIONS AND HARDWARE **3379**

Includes hardware for computer graphics, firmware, and data processing.

For components see *33 Electronics and Electrical Engineering.*

61 COMPUTER PROGRAMMING AND SOFTWARE **3379**

Includes computer programs, routines, algorithms, and specific applications, e.g., CAD/CAM.

62 COMPUTER SYSTEMS **3384**

Includes computer networks and special application computer systems.

63 CYBERNETICS **3384**

Includes feedback and control theory, artificial intelligence, robotics and expert systems.

For related information see also *54 Man/System Technology and Life Support.*

64 NUMERICAL ANALYSIS **3386**

Includes iteration, difference equations, and numerical approximation.

65 STATISTICS AND PROBABILITY **3389**

Includes data sampling and smoothing; Monte Carlo method; and stochastic processes.

66 SYSTEMS ANALYSIS **3389**

Includes mathematical modeling; network analysis; and operations research.

67 THEORETICAL MATHEMATICS **3389**

Includes topology and number theory.

PHYSICS

Includes physics (general); acoustics; atomic and molecular physics; nuclear and high-energy physics; optics; plasma physics; solid-state physics; and thermodynamics and statistical physics.

For related information see also *Engineering.*

70 PHYSICS (GENERAL) **3391**

For precision time and time interval (PTTI) see *35 Instrumentation and Photography;* for geophysics, astrophysics or solar physics see *46 Geophysics, 90 Astrophysics,* or *92 Solar Physics.*

71 ACOUSTICS 3392
Includes sound generation, transmission, and attenuation.
For noise pollution see *45 Environment Pollution.*

72 ATOMIC AND MOLECULAR PHYSICS 3393
Includes atomic structure, electron properties, and molecular spectra.

73 NUCLEAR AND HIGH-ENERGY PHYSICS 3393
Includes elementary and nuclear particles; and reactor theory.
For space radiation see *93 Space Radiation.*

74 OPTICS 3395
Includes light phenomena and optical devices.
For lasers see *36 Lasers and Masers.*

75 PLASMA PHYSICS 3396
Includes magnetohydrodynamics and plasma fusion.
For ionospheric plasmas see *46 Geophysics.* For space plasmas see *90 Astrophysics.*

76 SOLID-STATE PHYSICS 3398
Includes superconductivity.
For related information see also *33 Electronics and Electrical Engineering* and *36 Lasers and Masers.*

77 THERMODYNAMICS AND STATISTICAL PHYSICS 3402
Includes quantum mechanics; theoretical physics; and Bose and Fermi statistics.
For related information see also *25 Inorganic and Physical Chemistry* and *34 Fluid Mechanics and Heat Transfer.*

SOCIAL SCIENCES

Includes social sciences (general); administration and management; documentation and information science; economics and cost analysis; law, political science, and space policy; and urban technology and transportation.

80 SOCIAL SCIENCES (GENERAL) N.A.
Includes educational matters.

81 ADMINISTRATION AND MANAGEMENT 3404
Includes management planning and research.

82 DOCUMENTATION AND INFORMATION SCIENCE 3405
Includes information management; information storage and retrieval technology; technical writing; graphic arts; and micrography.
For computer documentation see *61 Computer Programming and Software.*

83 ECONOMICS AND COST ANALYSIS 3407
Includes cost effectiveness studies.

84 LAW, POLITICAL SCIENCE AND SPACE POLICY N.A.
Includes NASA appropriation hearings; aviation law; space law and policy; international law; international cooperation; and patent policy.

85 URBAN TECHNOLOGY AND TRANSPORTATION 3407
Includes applications of space technology to urban problems; technology transfer; technology assessment; and surface and mass transportation.
For related information see *03 Air Transportation and Safety, 16 Space Transportation,* and *44 Energy Production and Conversion.*

SPACE SCIENCES

Includes space sciences (general); astronomy; astrophysics; lunar and planetary exploration; solar physics; and space radiation.
For related information see also *Geosciences.*

88 SPACE SCIENCES (GENERAL) N.A.

89 ASTRONOMY 3408
Includes radio, gamma-ray, and infrared astronomy; and astrometry.

90 ASTROPHYSICS 3410
Includes cosmology; celestial mechanics; space plasmas; and interstellar and interplanetary gases and dust.
For related information see also *75 Plasma Physics.*

91 LUNAR AND PLANETARY EXPLORATION 3412
Includes planetology; and manned and unmanned flights.
For spacecraft design or space stations see *18 Spacecraft Design, Testing and Performance.*

92 SOLAR PHYSICS 3413
Includes solar activity, solar flares, solar radiation and sunspots.
For related information see *93 Space Radiation.*

93 SPACE RADIATION 3414
Includes cosmic radiation; and inner and outer earth's radiation belts.
For biological effects of radiation see *52 Aerospace Medicine.* For theory see *73 Nuclear and High-Energy Physics.*

GENERAL

Includes aeronautical, astronautical, and space science related histories, biographies, and pertinent reports too broad for categorization; histories or broad overviews of NASA programs.

99 GENERAL 3415

Note: N.A. means that no abstracts were assigned to this category for this issue.

SUBJECT INDEX I-1
PERSONAL AUTHOR INDEX I-57
CORPORATE SOURCE INDEX I-65
CONTRACT NUMBER INDEX I-77
REPORT/ACCESSION NUMBER INDEX .. I-79
APPENDIX—ABOUT STAR A-1

TYPICAL CITATION AND ABSTRACT

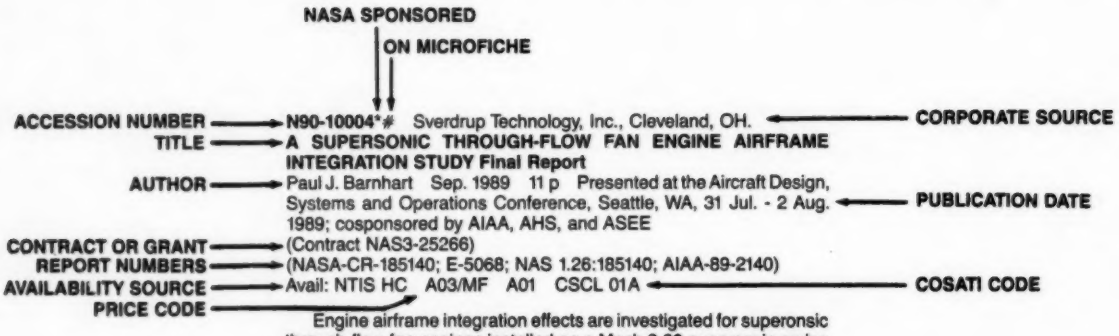
NASA SPONSORED
ON MICROFICHE
ACCESSION NUMBER
N90-10004*# Sverdrup Technology, Inc., Cleveland, OH.
CORPORATE SOURCE
TITLE
A SUPERSONIC THROUGH-FLOW FAN ENGINE AIRFRAME INTEGRATION STUDY Final Report
AUTHOR
Paul J. Barnhart Sep. 1989 11 p Presented at the Aircraft Design, Systems and Operations Conference, Seattle, WA, 31 Jul. - 2 Aug. 1989; cosponsored by AIAA, AHS, and ASEE
PUBLICATION DATE
CONTRACT OR GRANT
(Contract NAS3-25266)
REPORT NUMBERS
(NASA-CR-185140; E-5068; NAS 1.26:185140; AIAA-89-2140)
AVAILABILITY SOURCE
Avail: NTIS HC A03/MF A01 CSCL 01A
COSATI CODE
PRICE CODE

Engine airframe integration effects are investigated for superonsic through-flow fan engines installed on a Mach 3.20 supersonic cruise vehicle. Six different supersonic through-flow fan engine installations covering the effects of engine size, nacelle contour, nacelle placement, and approximate bypass plume effects are presented. The different supersonic through-flow fan installations are compared with a conventional turbine bypass engine configuration on the same basic airframe. The supersonic through-flow fan engine integrations are shown to be comparable to the turbine bypass engine configuration on the basis of installed nacelle wave drag. The supersonic through-flow fan engine airframe integrated vehicles have superior aerodynamic performance on the basis of maximum lift-to-drag ratio than the turbine bypass engine installation over the entire operating Mach number range from 1.10 to 3.20. When approximate bypass plume modeling is included, the supersonic through-flow fan engine configuration shows even larger improvements over the turbine bypass engine configuration. Author

VOLUME 28 NUMBER 23 / DECEMBER 8, 1990

Scientific and Technical Aerospace Reports

A Semimonthly Publication of the National Aeronautics and Space Administration

01 AERONAUTICS (GENERAL)

N90-28489# Boeing Commercial Airplane Co., Seattle, WA.
WORLD JET AIRPLANE INVENTORY AT YEAR-END 1989
Mar. 1990 101 p
(PB90-207218) Avail: NTIS HC A06/MF A01 CSCL 01B

Presented is the latest edition of World Jet Airplane Inventory, which contains data on the world commercial jet airplane fleet (including some military derivatives) and reflects the status of the fleet as accurately as possible as of December 31, 1989. Any fleet changes that have occurred since year-end 1989 will not be reflected in these data. GRA

N90-29160# European Space Agency, Paris (France).
FLIGHT TEST ENGINEERING WITH THE ATTAS
Peter Hamel and Heinz Winter (Deutsche Forschungsanstalt fuer Luft- und Raumfahrt, Cologne, Germany, F.R.) *In its* Scientific Colloquium in Honor of Prof. Dr. Rer. Nat. Hermann L. Jordan May 1990 p 10-44 Transl. into ENGLISH from Wissenschaftliches Kolloquim Gewidmet Herrn Professor Dr. Rer. Nat. Hermann L. Jordan zum 65 Geburtstag (Cologne, Fed. Republic of Germany, DFVLR), Jun. 1987 p 9-36 Original language document was announced as N88-17433 (For primary document see N90-29159 23-70)
Avail: NTIS HC A06/MF A01

02 AERODYNAMICS

Includes aerodynamics of bodies, combinations, wings, rotors, and control surfaces; and internal flow in ducts and turbomachinery.

For related information see also *34 Fluid Mechanics and Heat Transfer.*

N90-28490*# Texas A&M Univ., College Station. Dept. of Aerospace Engineering.
NONEQUILIBRIUM RADIATION AND CHEMISTRY MODELS FOR AEROCAPTURE VEHICLE FLOWFIELDS Semiannual Progress Report, Jun. - Dec. 1989
Leland A. Carlson Jan. 1990 50 p
(Grant NAG1-1003)
(NASA-CR-186379; NAS 1.26:186379; TAMRF-6382-90-01)
Avail: NTIS HC A03/MF A01 CSCL 01A

The continued development and improvement of the viscous shock layer (VSL) nonequilibrium chemistry blunt body engineering code, the incorporation in a coupled manner of radiation models into the VSL code, and the initial development of appropriate precursor models are presented. Author

N90-28491# National Aeronautical Lab., Bangalore (India). Computational and Theoretical Fluid Dynamics Div.
DO INVISCID VORTEX SHEETS ROLL-UP
Rajendra K. Bera May 1990 17 p
(PD-CF-9010) Avail: NTIS HC A03/MF A01

The Betz conjecture, its extensions and applications, regarding the final rolled-up structure of a vortex sheet in the absence of viscous effects is reexamined. It is argued that the conjecture, and consequently, its extensions and applications are theoretically incorrect. A plausible explanation is provided as to why, inspite of its incorrectness, the results correlate reasonably well with flight experiments on wakes behind aircraft wings. Author

N90-28492# National Aeronautical Lab., Bangalore (India). Experimental Aerodynamics Div.
STING-SUPPORT INTERFERENCE ON AFTERBODY DRAG AT TRANSONIC SPEEDS
P. R. Viswanath and G. Rajendra Nov. 1989 42 p
(NAL-TM-EA-8902) Avail: NTIS HC A03/MF A01

Experiments have been performed on several boat-tailed afterbodies and sting combinations with a view to assessing sting corrections on afterbody drag at transonic speeds. Measurements made included afterbody total drag and base pressure in the Mach number range of 0.6 to 1.0 and at relatively high Reynolds number. Correlations of base pressure and boat-tail pressure drag for the sting diameter and flare effects have been proposed using dimensional arguments. The correlations provide quick and reliable estimates of corrections to the zero lift drag of axisymmetric bodies with either contoured or conical boat-tailing. Author

N90-28493*# National Aeronautics and Space Administration. Langley Research Center, Hampton, VA.
CONTROL OF SUBMERSIBLE VORTEX FLOWS
D. M. Bushnell and C. D. Donaldson (Donaldson, C. D., Gloucester, VA) Jun. 1990 48 p Presented at the Submarine Technology Symposium, Baltimore, MD, 8-10 May 1990
(NASA-TM-102693; NAS 1.15:102693) Avail: NTIS HC A03/MF A01 CSCL 01A

Vortex flows produced by submersibles typically unfavorably influence key figures of merit such as acoustic and nonacoustic stealth, control effectiveness/maneuverability, and propulsor efficiency/body drag. Sources of such organized, primarily longitudinal, vorticity include the basic body (nose and sides) and appendages (both base/intersection and tip regions) such as the fairwater, dive planes, rear control surfaces, and propulsor stators/tips. Two fundamentally different vortex control approaches are available: (1) deintensification of the amplitude and/or organization of the vortex during its initiation process; and (2) downstream vortex disablement. Vortex control techniques applicable to the initiation region (deintensification approach) include transverse pressure gradient minimization via altered body cross section, appendage dillets, fillets, and sweep, and various appendage tip and spanload treatment along with the use of active controls to minimize control surface size and motions. Vortex disablement can be accomplished either via use of control vortices (which can also be used to steer the vortices off-board), direct unwinding, inducement of vortex bursting, or segmentation/tailoring for enhanced dissipation. Submersible-applicable vortex control technology is also included derived from various aeronautical applications such as mitigation of the wing wake vortex hazard and flight aircraft maneuverability at high angle of attack as well as the status of vortex effects upon, and mitigation of, nonlinear control forces on submersibles. Specific suggestions for submersible-applicable vortex control techniques are presented. Author

N90-28494*# Nielsen Engineering and Research, Inc., Mountain View, CA.
PREDICTION OF SUBSONIC VORTEX SHEDDING FROM FOREBODIES WITH CHINES Final Report
Michael R. Mendenhall and Daniel J. Lesieutre Washington NASA Sep. 1990 174 p
(Contract NAS1-17077)
(NASA-CR-4323; NAS 1.26:4323; TR-391) Avail: NTIS HC A08/MF A01 CSCL 01A

An engineering prediction method and associated computer code VTXCHN to predict nose vortex shedding from circular and noncircular forebodies with sharp chine edges in subsonic flow at angles of attack and roll are presented. Axisymmetric bodies are represented by point sources and doublets, and noncircular cross sections are transformed to a circle by either analytical or numerical conformal transformations. The lee side vortex wake is modeled by discrete vortices in crossflow planes along the body; thus the three-dimensional steady flow problem is reduced to a two-dimensional, unsteady, separated flow problem for solution. Comparison of measured and predicted surface pressure distributions, flow field surveys, and aerodynamic characteristics are presented for noncircular bodies alone and forebodies with sharp chines. Author

N90-28495# Sandia National Labs., Albuquerque, NM. Dept. of Advanced Systems Development.
HYPERSONIC ARBITRARY-BODY AERODYNAMICS (HABA) FOR CONCEPTUAL DESIGN
David E. Salguero 15 Mar. 1990 103 p
(Contract DE-AC04-76DP-00789)
(DE90-014750; SAND-90-0078) Avail: NTIS HC A06/MF A01

The Hypersonic Arbitrary-Body Aerodynamics (HABA) computer program predicts static and dynamic aerodynamic derivatives at hypersonic speeds for any vehicle geometry. It is intended to be used during conceptual design studies where fast computational speed is required. It uses the same geometry and hypersonic aerodynamic methods as the Mark IV Supersonic/Hypersonic Arbitrary-Body Program (SHABP) developed under sponsorship of the Air Force Flight Dynamics Laboratory; however, the input and output formats have been improved to make it easier to use. This program is available as part of the Department 9140 computer aided engineering (CAE) software. DOE

N90-28496 Arizona Univ., Tucson.
AERODYNAMICS OF BODIES IN SHEAR FLOW Ph.D. Thesis
Haldun Guvenen 1989 175 p
Avail: Univ. Microfilms Order No. DA9013174

Spanwise periodic shear flow past two-dimensional bodies is investigated. The flow is assumed to be inviscid and incompressible. Using singular perturbation techniques, the solution is developed for epsilon = L/l is much less than 1, where L represents body cross-sectional size, and l the period of the oncoming flow (U/z). The singular perturbation analysis involves three regions: the inner, wake and outer regions. The leading order solutions are developed in all regions, and in the inner region higher order terms are obtained. In the inner region near the body, the primary flow (U sub 0, V sub 0, P sub 0) corresponds to potential flow past the body with a local free stream value of U(z). The spanwise variation in U(z) produces a weak O(epsilon) secondary flow W(sub 1) in the spanwise direction. As the vortex lines of the upstream flow are convected dowstream, they wrap around the body, producing significant streamwise vorticity in a wake region of thickness O(L) directly behind the body. This streamwise vorticity induces a net volume flux into the wake. In the outer region far from the body, a nonlifting body appears as a distribution of three-dimensional dipoles, and the wake appears as a sheet of mass sinks. Both singularity structures must be included in describing the leading outer flow. For lifting bodies, the body appears as a lifting line, and the wake appears as a sheet of shed vorticity. The trailing vorticity is found to be equal to the spanwise derivative of the product of the circulation and the oncoming flow. For lifting bodies the first higher order correction to the inner flow is the response of the body to the downwash produced by the trailing vorticity. At large distances from the body, the flow takes on remarkably simple form. Dissert. Abstr.

N90-28497 California Inst. of Tech., Pasadena.
REGULAR AND CHAOTIC MOTION OF UNIFORM ELLIPTICAL VORTICES IN EXTERNAL LINEAR TIME DEPENDENT VELOCITY FIELDS Ph.D. Thesis
Kayo Ide 1990 169 p
Avail: Univ. Microfilms Order No. DA9014379

The motion of a uniform vorticity of an elliptical shape (UEV) induced by an external linear flow field and a self-induced effect in a two-dimensional incompressible inviscid flow is investigated. The fluid particle motion around the UEV is also investigated. The techniques from dynamical systems are intensively used. Researchers develop some modified versions of the Melnikov techniques which show how the perturbations influence the dynamics and allow us to predict the perturbed dynamics by knowing the unperturbed dynamics. The UEV motions in steady external linear flow fields are regular. However there are quite a few possibilities for types of motion depending on the UEV initial configuration and the external linear flow field parameters. When time periodic perturbation is imposed, the UEV motion drastically changes and various new types of motion become possible. This includes transition dynamics (i.e., the UEV changes its type of motion), chaotic motion, irregular oscillation and rotation, and quasiperiodic motion. The Melnikov techniques tell that the excess kinetic energy plays significant roles in determining the UEV dynamics. A periodic motion of the UEV in a steady external linear flow field results in the generation of chaotic fluid particle mixing regions around the UEV where the fluid particles from distinct flow regions are chaotically transported. The study emphasizes on the finite core size effect of the UEV in comparison to flow fields induced by a point vortex in unsteady external linear flow fields. Researchers show that the size of the UEV core and the UEV initial configuration are important factors in determining the size of the mixing region. Dissert. Abstr.

N90-28498# European Space Agency, Paris (France).
EXPERIMENTAL INVESTIGATIONS ON THE STABILITY AND VORTICITY OF THE VORTEX BREAKDOWN PHENOMENON ABOVE DELTA WINGS, MEASURED BY THE ULTRASONIC LASER METHOD
Rolf H. Engler (Deutsche Forschungs- und Versuchsanstalt fuer Luft- und Raumfahrt, Goettingen, Germany, F.R.) Feb. 1990 91 p Transl. into ENGLISH of Experimentelle Untersuchungen der Struktur und des Aufplatzens der Wirbel an Einem Schlanken Deltafluegel Ausgefuehrt im Windkanal Mittels Ultraschall (Goettingen, Fed. Republic of Germany, DFVLR), Feb. 1987 88 p Original language document was announced as N88-10017
(ESA-TT-1079; DFVLR-FB-87-06; ETN-90-97552) Avail: NTIS HC A05/MF A01

The breakdown of vortices above a delta wing is investigated by using a new, acoustical/optical measurement technique which does not interfere with the flow. The results from seven rows of measurements provide detailed information on the velocity and circulation distribution within the vortex. It is shown that four turns of the spirally wound shear layer can be clearly recognized in the vortex radius range between the viscous vortex core and a charateristic radius defined (in the stability theory by Ludwieg and Hall) as being relevant to this vortex. The circulation steps appearing on the individual turns were measured. Potential flow conditions can be used for calculations between the sheer layer turns. On the basis of this information and under these conditions, the validity of the Ludwieg stability theory can be confirmed; this theory requires that the shape parameter K at the breakdown position must be less than a critical value of 1.16. ESA

N90-28499# European Space Agency, Paris (France).
WIND TUNNEL INVESTIGATION OF PERIODIC VORTEX SEPARATION FROM ROUGH SURFACE CIRCULAR CYLINDERS BY MEANS OF ACOUSTIC MEASUREMENTS
Friedrich R. Grosche, Horst Stiewitt, and Hans Hoefer (Deutsche

Forschungs- und Versuchsanstalt fuer Luft- und Raumfahrt, Goettingen, Germany, F.R.) Feb. 1990 109 p Transl. into ENGLISH of Windkanaluntersuchungen mit Akustischen Messmethoden zur Periodischen Stroemungsabloesung an Kreiszylindern mit Rauher Oberflaeche (Goettingen, Fed. Republic of Germany, DFVLR), Jun. 1987 100 p Original language document was announced as N88-16665
(ESA-TT-1092; DFVLR-FB-87-24; ETN-90-97553) Avail: NTIS HC A06/MF A01

The sound generation due to periodic vortex separation from a circular cylinder in a cross flow (Aeolian tones) was measured at Reynolds numbers of between 10 to the 4th power and 4.10 to the 4th power in the large low speed wind tunnel of DFVLR, Goettingen, Germany. At low Reynolds numbers, below 2.10 to the 4th power, the results agree well with predictions based on flow measurements on smooth cylinders. Deviations occurring at higher Reynolds numbers are explained by effects due to the surface roughness of the model, which reduces the critical Reynolds number to about 2.10 to the 4th power. A helical trip wire wrapped around the cylinder decreases the sound emitted by up to 20 dB. Equations are derived for predicting the sound intensity at any given position in the acoustic far field from the experimental results. ESA

N90-28500# Office National d'Etudes et de Recherches Aerospatiales, Paris (France). Direction de l'Aerodynamique.
SOLUTION OF EULER EQUATIONS APPLIED TO A ROTOR OF A HELICOPTER IN STEADY FLIGHT Final Report [RESOLUTION DES EQUATIONS D'EULER APPLIQUEE A UN ROTOR D'HELICOPTERE EN VOL D'AVANCEMENT, RAPPORT DE SYNTHESE FINAL]
J. Sides Jan. 1990 37 p In FRENCH
(Contract DRET-89-34-001)
(ONERA-RSF-1/3731-AY-002A; ETN-90-97502) Avail: NTIS HC A03/MF A01

The three dimensional compressible flow, around a helicopter rotor during steady flight, is simulated by solving the Euler equation. An implicit multifield prospective approach, covering C and H meshes, for two dimensional analysis is proposed. The three dimensional modulus, initially defined for an arrow wing configuration, is extended to other configurations. A centered implicit method is used for solving a pseudo-unsteady Euler equation system. The simulation method is applied to the analysis of a single rotor blade in steady flight. ESA

N90-28501# Aeronautical Research Inst. of Sweden, Stockholm. Dept. of Aerodynamics.
TWO-DIMENSIONAL WIND TUNNEL TEST AND COMPARISON WITH CALCULATIONS FOR A 15.2 PERCENT THICK AIRFOIL SECTION FOR WIND TURBINES
Anders Bjoerck Apr. 1990 148 p
(Contract STEV-506266-489-06-22)
(FFA-TN-1990-16; ETN-90-97512) Avail: NTIS HC A06/MF A01

A low speed wind tunnel test of a 15.2 percent thick airfoil for horizontal axis wind turbines was carried out. Tests of the airfoil with a 700 mm chord were carried out at Re (Reynolds numbers) of 1, 2 and 3 million with smooth surfaces as well as with roughness strips applied at x/c = 2.5 and 5 percent. Tests were carried out with an adhesive film covering the airfoil leading edge. At the rearward end of the film at x/c = 7.5 percent there was a backwards facing step of 0.3 mm. Tests showed that this step causes premature boundary layer transition at Re above 1 to 2 million. The airfoil is designed for operation at Re above 2 to 3 million, and to attain high lift drag ratios with smooth surfaces, but with the constraint that performance with a rough leading edge should be as good as possible. Forces were obtained by an external balance during the wind tunnel test and drag measurements are somewhat uncertain. However, it is felt that results from calculations with the two dimensional analysis code ISES in general are verified. ESA

N90-28502*# National Aeronautics and Space Administration. Langley Research Center, Hampton, VA.
SECONDARY INSTABILITIES IN COMPRESSIBLE BOUNDARY LAYERS Final Report
Lian Ng and Gordon Erlebacher (Institute for Computer Applications in Science and Engineering, Hampton, VA.) Sep. 1990 52 p Submitted for publication
(Contracts NAS1-18605; NAS1-18599)
(NASA-CR-182091; NAS 1.26:182091; ICASE-90-58) Avail: NTIS HC A04/MF A01 CSCL 01A

Secondary instabilities are examined in compressible boundary layers at Mach numbers M(sub infinity) = 0, 0.8, 1.6, and 4.5. It is found that there is a broad-band of highly unstable 3-d secondary disturbances whose growth rates increase with increasing primary wave amplitude. At M(sub infinity) is less than or equal to 1.6, fundamental resonance dominates at relatively high (2-d) primary disturbance amplitude, while subharmonic resonance is characterized by a low (2-d) primary amplitude. At M(sub infinity) = 4.5, the subharmonic instability which arises from the second mode disturbance is the strongest type of secondary instability. The influence of the inclination, theta, of the primary wave with respect to the mean flow direction on secondary instability is investigated at M(sub infinity) = 1.6 for small to moderate values of theta. It is found that the strongest fundamental instability occurs when the primary wave is inclined at 10 deg to the mean flow direction, although a 2-d primary mode yields the most amplified subharmonic. The subharmonic instability at a high value of theta (namely, theta = 45 deg) is also discussed. Finally, a subset of the secondary instability results are compared against direct numerical simulations. Author

N90-28503*# National Aeronautics and Space Administration. Ames Research Center, Moffett Field, CA.
THE EFFECTS OF STRUCTURAL FLAP-LAG AND PITCH-LAG COUPLING ON SOFT INPLANE HINGELESS ROTOR STABILITY IN HOVER
William G. Bousman Washington May 1990 65 p Sponsored by Army Aviation Systems Command, Saint Louis, MO Prepared in cooperation with Army Aviation Systems Command, Moffett Field, CA
(NASA-TP-3002; A-89093; NAS 1.60:3002;
AVSCOM-TR-89-A-002) Avail: NTIS HC A04/MF A01 CSCL 01A

A 1.62-m-diameter rotor model was tested in hover to examine the effects of structural flap-lag and pitch-lag coupling on isolated rotor blade lead-lag stability. Flap-lag coupling was introduced by inclining the principal axes of the blade structure up to 60 degrees. Pitch-lag coupling was obtained either alone or in combination with flap-lag coupling through the use of skewed flexural hinges. The principal results confirm the predictions of theory, and show that both structural flap-lag and pitch-lag coupling when used separately are beneficial to blade stability. Moreover, when the couplings are combined, the lead-lag damping is significantly greater than it would be if the individual contributions were superimposed. Pitch-flap coupling is shown to have only a minor effect on blade lead-lag damping. Differences between theory and experiment observed at zero blade pitch and flexure angles during the initial testing were determined in a second test to be caused by stand flexibility. Other differences between theory and experiment warrant further investigation. Author

N90-28504*# Case Western Reserve Univ., Cleveland, OH. Dept. of Mechanical and Aerospace Engineering.
THE ENTRAINMENT RATE FOR A ROW OF TURBULENT JETS M.S. Thesis Final Report
Eliott B. Gordon and Isaac Greber Sep. 1990 135 p
(Grant NAG3-251)
(NASA-CR-185278; NAS 1.26:185278) Avail: NTIS HC A07/MF A01 CSCL 01A

Entrainment rates for a row of isothermal circular air jets issuing into a quiescent environment are found by integrating velocity distributions measured by a linearized hot-wire anemometer. Jet spacing to jet diameter ratios of 2.5, 5, 10, and 20 are studied at

jet Reynold's numbers ranging from 5110 to 12070. Velocity distributions are determined at regular downstream intervals at axial distances equal to 16.4 to 164 jet diameters from the jet source. The entrainment rates for the four spacing configurations vary monotonically with increasing spacing/diameter between the limiting case of the slot jet entrainment rate (where the jet spacing to diameter ratio is zero) and the circular jet entrainment rate (in which the spacing to diameter ratio is infinity). Author

N90-28505*# National Aeronautics and Space Administration. Hugh L. Dryden Flight Research Facility, Edwards, CA.
IN-FLIGHT FLOW VISUALIZATION WITH PRESSURE MEASUREMENTS AT LOW SPEEDS ON THE NASA F-18 HIGH ALPHA RESEARCH VEHICLE
John H. DelFrate, David F. Fisher, and Fanny A. Zuniga Oct. 1990 45 p Presented at the AGARD Vortex Flow Aerodynamics Conference, Scheveningen, Netherlands, 1-4 Oct. 1990
(NASA-TM-101726; H-1651; NAS 1.15:101726) Avail: NTIS HC A03/MF A01 CSCL 01A

In-flight results from surface and off-surface flow visualizations and from extensive pressure distributions document the vortical flow on the leading edge extensions (LEX) and forebody of the NASA F-18 high alpha research vehicle for low speeds and angles of attack up to 50 degs. Surface flow visualization data, obtained using the emitted fluid technique, were used to define separation lines and laminar separation bubbles. Off-surface flow visualization data, obtained by smoke injection, were used to document both the path of the vortex cores and the location of vortex core breakdown. The location of vortex core breakdown correlated well with the loss of suction pressure on the LEX and with the flow visualization results from ground facilities. Surface flow separation lines on the LEX and forebody corresponded well with the end of pressure recovery under the vortical flows. Correlation of the pressures with wind tunnel results show fair to good correlation. Author

N90-28506# Ballistic Research Labs., Aberdeen Proving Ground, MD.
PROJECTILE SUPERSONIC DRAG CHARACTERISTICS Final Report, Jan. - Jun. 1990
Ilmars Celmins Jul. 1990 29 p
(DA Proj. 1L1-62618-AH-80)
(AD-A224217; BRL-MR-3843) Avail: NTIS HC A03/MF A01 CSCL 19/10

An observation of projectile free flight behavior - that above Mach 2.5, velocity is linear with distance - leads to a proposed simple functional form for the drag coefficient. Equations are derived that allow the determination of both the zero-yaw drag coefficient (as a function of Mach number) and the yaw-drag coefficient from as few as two test firings. Good agreement with free-flight range data has been obtained. GRA

03 AIR TRANSPORTATION AND SAFETY

Includes passenger and cargo air transport operations; and aircraft accidents.

For related information see also *16 Space Transportation* and *85 Urban Technology and Transportation.*

N90-28507# Transportation Systems Center, Cambridge, MA.
AIRPORT CAPACITY ENHANCEMENT PLAN 1989 Final Report, May 1988 - Apr. 1989
May 1989 357 p
(PB90-197997; DOT-TSC-FAA-89-1; DOT/FAA/CP-89-4) Avail: NTIS HC A16/MF A02 CSCL 01E

The Airport Capacity Enhancement Plan plays a major role in the Federal Aviation Administration's (FAA) effort to increase airport capacity and efficiency without compromising the safety of passengers or the environment. The Plan identifies the cause and extent of capacity and delay problems currently associated with the U.S. air system, projects the effects of increased air traffic on airport capacity over the next decade, and outlines various planned and ongoing FAA projects intended to reduce capacity-related problems. The projects are directed toward one or more of four airport capacity enhancement areas: airport development; airspace control procedures; additional equipment and systems; and capacity planning studies. A description of each project is provided, along with significant milestones and expected capacity-related benefits. GRA

N90-28508 Physics and Electronics Lab. TNO, The Hague (Netherlands).
USER'S MANUAL ROBIN: A RESEARCH AND NOTIFICATION SYSTEM FOR BIRD MIGRATION Final Report
J. G. tenWolde May 1989 42 p In DUTCH; ENGLISH summary
(Contract A85/KLu/103)
(FEL-1989-103; TD-89-3097; ETN-90-97403) Copyright Avail: Physics and Electronics Lab. TNO, P.O. Box 96864, 2509 JG The Hague, Netherlands

The ROBIN (Radar Observation of Bird Intensity) system for the observation of bird migration is presented, with a view to the reduction of bird-aircraft collisions. The ROBIN system processes the radar signals in such a way that a distinction arises between the echoes of birds and the remaining echoes. If required the user obtains the unprocessed radar image or an image processed in a specified way. Besides a graphical display of the image all essential image parameters are shown. A general view of all system parts and a description of the user commands are given. With these commands the ROBIN system can be used to notify bird migration as well as to make further research into the improvements of these notifications. ESA

04 AIRCRAFT COMMUNICATIONS AND NAVIGATION

Includes digital and voice communication with aircraft; air navigation systems (satellite and ground based); and air traffic control.

For related information see also *17 Space Communications, Spacecraft Communications, Command and Tracking* and *Communications and Radar.*

N90-28509# Federal Aviation Administration, Atlantic City, NJ.
DALLAS/FORTH WORTH SIMULATION. PHASE 2: TRIPLE SIMULTANEOUS PARALLEL INSTRUMENT LANDING SYSTEM (ILS) APPROACHES (TURBOJETS) Final Report, Oct. - Jan. 1990
Mar. 1990 183 p Prepared in cooperation with Computer Technology Associates, Inc., McKee City, NJ
(Contract DTFA03-89-C-00023)
(DOT/FAA/CT-90/2) Avail: NTIS HC A09/MF A01

A dynamic, real-time simulation was conducted to evaluate triple simultaneous independent parallel approach operations for the Dallas/Fort Worth (D/FW) Airport. The simulation was part of an ongoing effort to evaluate plans for increasing air traffic capacity in the D/FW area and to evaluate multiple parallel approaches in general. An additional parallel runway (16L), with centerline 5,000 ft east of the existing 17L runway, was simulated in a triple simultaneous parallel operation conducted under Instrument Meteorological Conditions (IMC). The results of the study indicated that controllers were able to maintain miss distances, between blundering aircraft and nonblundering aircraft, in the proposed D/FW triple simultaneous parallel Instrument Landing System (ILS) approach operation, that were statistically equivalent to the miss distances maintained in the approved dual approach condition. None of the blunders in the triple or dual approach conditions resulted in a slant range miss distance of less than 1,000 ft. Finally, controllers, controller observers, and ATC management observers concluded that the triple simultaneous ILS approach operation at D/FW is acceptable, achievable, and safe. Author

N90-28510*# Army Aviation Systems Command, Moffett Field, CA.
COMPARISON OF SPEECH INTELLIGIBILITY IN COCKPIT NOISE USING SPH-4 FLIGHT HELMET WITH AND WITHOUT ACTIVE NOISE REDUCTION
Jeffrey W. Chan and Carol A. Simpson (Psycho-Linguistic Research Associates, Woodside, CA.) Jul. 1990 38 p
(Contracts NAS2-12425; NAS2-13188)
(NASA-CR-177564; A-90264; NAS 1.26:177564; USAAVSCOM-TR-90-G-1) Avail: NTIS HC A03/MF A01 CSCL 17B

Active Noise Reduction (ANR) is a new technology which can reduce the level of aircraft cockpit noise that reaches the pilot's ear while simultaneously improving the signal to noise ratio for voice communications and other information bearing sound signals in the cockpit. A miniature, ear-cup mounted ANR system was tested to determine whether speech intelligibility is better for helicopter pilots using ANR compared to a control condition of ANR turned off. Two signal to noise ratios (S/N), representative of actual cockpit conditions, were used for the ratio of the speech to cockpit noise sound pressure levels. Speech intelligibility was significantly better with ANR compared to no ANR for both S/N conditions. Variability of speech intelligibility among pilots was also significantly less with ANR. When the stock helmet was used with ANR turned off, the average PB Word speech intelligibility score was below the Normally Acceptable level. In comparison, it was above that level with ANR on in both S/N levels. Author

N90-28511# Transportation Research Board, Washington, DC.
MODELING AND ANALYSIS OF AIRPORT AND AIRCRAFT OPERATIONS
C. F. Wheeler, A. I. Oxoka, N. Ashford, D. Barol, and J. R. G. Brander 1989 64 p
(PB90-222167; TRB/TRR-1214; ISBN-0-309-04817-6; LC-90-31527) Avail: NTIS HC A04/MF A01 CSCL 01C

Strategies for maximizing the profitability of airline hub-and-spoke networks; application of disaggregate modeling in aviation systems planning in Nigeria; the measuring secondary economic impacts using regional input-output modeling system; entry, exclusion, and explusion in a single hub airport system; congestion, concentration, and contestability: the case of the airline industry; analysis of airline and aircraft safety posture using service difficulty reports; estimating practical maximum flight hours for general aviation turboprop and jet aircraft are discussed. GRA

N90-28512*# National Aeronautics and Space Administration. Ames Research Center, Moffett Field, CA.
VELOCITY FILTERING APPLIED TO OPTICAL FLOW CALCULATIONS
Yair Barniv Aug. 1990 58 p
(NASA-TM-102802; A-90108; NAS 1.15:102802) Avail: NTIS HC A04/MF A01 CSCL 20D

Optical flow is a method by which a stream of two-dimensional images obtained from a forward-looking passive sensor is used to map the three-dimensional volume in front of a moving vehicle. Passive ranging via optical flow is applied here to the helicopter obstacle-avoidance problem. Velocity filtering is used as a field-based method to determine range to all pixels in the initial image. The theoretical understanding and performance analysis of velocity filtering as applied to optical flow is expanded and experimental results are presented. Author

05 AIRCRAFT DESIGN, TESTING AND PERFORMANCE

Includes aircraft simulation technology.

For related information see also *18 Spacecraft Design, Testing and Performance* and *39 Structural Mechanics*.For land transportation vehicles see *85 Urban Technology and Transportation.*

N90-28513# Advisory Group for Aerospace Research and Development, Neuilly-Sur-Seine (France). Fluid Dynamics Panel.
AERODYNAMICS OF COMBAT AIRCRAFT CONTROLS AND OF GROUND EFFECTS
Apr. 1990 337 p In ENGLISH and FRENCH Symposium held in Madrid, Spain, 2-5 Oct. 1989
(AGARD-CP-465; ISBN-92-835-0555-7) Copyright Avail: NTIS HC A15/MF A02; Non-NATO Nationals requests available only from AGARD/Scientific Publications Executive

An updated review is provided for the aerodynamic design of controls for combat aircraft. The scope included the aerodynamic design of controls for take-off and landing conditions; for maneuvering at subsonic, transonic, and supersonic speeds; for high angles of attack and yaw; and for departure prevention and post-stall maneuvering. Ground effects; computational experimental methods; and jet effects on flow-field forces and intake flows were also reviewed. For individual titles, see N90-28514 through N90-28534.

N90-28514# Wright Research Development Center, Wright-Patterson AFB, OH.
AERODYNAMIC AND PROPULSIVE CONTROL DEVELOPMENT OF THE STOL AND MANEUVER TECHNOLOGY DEMONSTRATOR
David J. Moorhouse, James A. Laughrey, and Richard W. Thomas (McDonnell Aircraft Co., Saint Louis, MO.) *In* AGARD, Aerodynamics of Combat Aircraft Controls and of Ground Effects Apr. 1990 23 p (For primary document see N90-28513 23-05)
Copyright Avail: NTIS HC A15/MF A02; Non-NATO Nationals requests available only from AGARD/Scientific Publications Executive

The STOL and Maneuver Technology Demonstrator (S/MTD) program was structured to investigate, develop, and validate through analysis, experiment, and test flight, four specific technologies related to providing current and future high performance fighters with both STOL capability and enhanced combat mission performance. The four technologies are: two-dimensional thrust vectoring and reversing exhaust nozzle; integrated flight propulsion control (IFPC) system; advanced pilot vehicle interface (PVI) and rough/soft field landing gear. In addition to the required technologies, all-moving canard surfaces were also incorporated into the baseline F-15B. Starting with an existing aircraft, wind tunnel tests were performed to define the incremental effects of the specific technology items. A single data base was defined that was used by all the different functional design groups. The components of most interest are the canard and jet effects, both in and out of ground effects, and their use as control effectors. The intent is to present the progress of the S/MTD configuration towards meeting its goals. First, the design requirements and their rationale are discussed. Second, the aerodynamics of the canard and jet effects of vectoring and reversing are discussed followed by their implementation and impact on the control system. Ground effects with and without reversing are discussed, including a comparison of static and moving model test approaches. The results of a test to define inlet ingestion are presented. Then the control laws to counter the ground effects are discussed. Lastly, some preliminary flight test correlations are presented. Author

N90-28515# British Aerospace Public Ltd. Co., Lancashire (England). Military Aircraft Div.
COMBAT AIRCRAFT CONTROL REQUIREMENTS c08
T. B. Saunders and J. H. Tucker *In* AGARD, Aerodynamics of Combat Aircraft Controls and of Ground Effects Apr. 1990

20 p (For primary document see N90-28513 23-05)
Copyright Avail: NTIS HC A15/MF A02; Non-NATO Nationals requests available only from AGARD/Scientific Publications Executive

The various functions and requirements for combat aircraft controls which arise from consideration of the flight envelope, agility, handling qualities specifications, and control system design criteria are reviewed. Examples are drawn from supersonic and subsonic combat aircraft designed by British Aerospace including those employing powered lift (Harrier) and those which use a basically unstable airframe to enhance performance (EAP/EFA). The subject is discussed in terms of the basic functions of aircraft controls which are to trim, maneuver, and stabilize. These functions require certain forces and moments to be generated over the full design envelope of speed, Mach number, and angle of attack. A certain minimum level of linearity is desirable although, with some redundancy of controls, trim schedules can be chosen to avoid limited areas of ineffectiveness provided other constraints allow it. The achievable rate of application of control is an important variable which can have a serious impact on the sizing of actuators and power systems. Author

N90-28516*# National Aeronautics and Space Administration. Langley Research Center, Hampton, VA.
CONTROL RESEARCH IN THE NASA HIGH-ALPHA TECHNOLOGY PROGRAM **c08**
William P. Gilbert, Luat T. Nguyen, and Joseph Gera (National Aeronautics and Space Administration. Hugh L. Dryden Flight Research Facility, Edwards, CA.) *In* AGARD, Aerodynamics of Combat Aircraft Controls and of Ground Effects Apr. 1990 18 p (For primary document see N90-28513 23-05)
Copyright Avail: NTIS HC A15/MF A02; Non-NATO Nationals requests available only from AGARD/Scientific Publications Executive CSCL 01C

NASA is conducting a focused technology program, known as the High-Angle-of-Attack Technology Program, to accelerate the development of flight-validated technology applicable to the design of fighters with superior stall and post-stall characteristics and agility. A carefully integrated effort is underway combining wind tunnel testing, analytical predictions, piloted simulation, and full-scale flight research. A modified F-18 aircraft has been extensively instrumented for use as the NASA High-Angle-of-Attack Research Vehicle used for flight verification of new methods and concepts. This program stresses the importance of providing improved aircraft control capabilities both by powered control (such as thrust-vectoring) and by innovative aerodynamic control concepts. The program is accomplishing extensive coordinated ground and flight testing to assess and improve available experimental and analytical methods and to develop new concepts for enhanced aerodynamics and for effective control, guidance, and cockpit displays essential for effective pilot utilization of the increased agility provided. Author

N90-28517# Eidetics International, Inc., Torrance, CA.
COMBAT AIRCRAFT CONTROL REQUIREMENTS FOR AGILITY **c08**
Joseph R. Chody, John Hodgkinson, and Andrew M. Skow *In* AGARD, Aerodynamics of Combat Aircraft Controls and of Ground Effects Apr. 1990 21 p (For primary document see N90-28513 23-05)
Copyright Avail: NTIS HC A15/MF A02; Non-NATO Nationals requests available only from AGARD/Scientific Publications Executive

The positive effect of increased aircraft agility on air-to-air combat effectiveness has created a need to quantify the impact of preliminary design on the agility potential of candidate aerodynamic configurations. Recently developed measures of agility can provide an important supplement to traditional energy maneuverability measures like specific excess power and turn rate. The very nature of agility, characterized by the combination of traditional energy maneuverability plus controllability, places additional controllability and departure resistance requirements on the aircraft design. Specific issues of aircraft controllability that require close attention during the preliminary design process are highlighted. This will help ensure that the agility potential of the final configuration is not compromised at some point in the design process due to inadvertent oversight. Methods for estimating agility potential early in the design process are given as well as extensions of currently used departure susceptibility prediction techniques. A brief synopsis of agility is given from a historical standpoint and several agility measures of merit currently being used, are discussed. The benefits of improved lateral agility are illustrated by mapping potential lateral agility improvements as a function of angle of attack onto a typical energy-maneuverability envelope showing regions of enhanced combat capability. Author

N90-28518# Aeronautica Macchi S.p.A., Varese (Italy).
AERODYNAMIC CONTROL DESIGN: EXPERIENCE AND RESULTS AT AERMACCHI **c08**
B. Bufacchi, M. Lucchesini, L. Manfriani, and E. Valtorta *In* AGARD, Aerodynamics of Combat Aircraft Controls and of Ground Effects Apr. 1990 13 p (For primary document see N90-28513 23-05)
Copyright Avail: NTIS HC A15/MF A02; Non-NATO Nationals requests available only from AGARD/Scientific Publications Executive

A review of Aermacchi activities in the field of aerodynamic control design is presented. The aerodynamic balancing of the MB-326/339 elevator and of the AM-X control surfaces for the manual backup mode are described. The use of rotary balance wind tunnel testing and of simulation in assessing controllability at high angle of attack is discussed. Preliminary design studies of unconventional layouts are described and some features of control techniques on an unstable canard design are illustrated using wing tunnel results and flow visualization. Author

N90-28519# Technische Univ., Brunswick (Germany, F.R.). Institut fuer Stroemungsmechanik.
EFFECTS OF CANARD POSITION ON THE AERODYNAMIC CHARACTERISTICS OF A CLOSE-COUPLED CANARD CONFIGURATION AT LOW SPEED
D. Hummel and Hans-Christoph Oelker *In* AGARD, Aerodynamics of Combat Aircraft Controls and of Ground Effects Apr. 1990 18 p (For primary document see N90-28513 23-05)
(Contract DFG-HU-254/8)
Copyright Avail: NTIS HC A15/MF A02; Non-NATO Nationals requests available only from AGARD/Scientific Publications Executive

Comprehensive wing-tunnel investigations were carried out on a close-coupled A = 2.31 delta-canard configuration at low speed. Based on three-component, surface pressure, and flowfield measurements as well as on oilflow patterns, the flow about the coplanar normal configuration may be regarded as well understood. Three parameters describing the position of the canard relative to the wing were varied systematically within certain limits: vertical distance (3 locations: high, coplanar, low), longitudinal distance (3 locations: front, mid, rear), and canard setting angle (-12 deg is less than or equal to epsilon is less than or equal to 12 deg). The results of three-component measurements are presented and the corresponding flow structure is analyzed by means of pressure distribution measurements and oilflow patterns. For a large variety of parameter combinations in the vicinity of the normal configuration the same state of the flow with two separate vortex systems for canard and wing was found, and the effects of different canard positions relative to the wing on the aerodynamic coefficients could be explained by this mechanism. For low canard positions and large setting angles, however, the formation of vortices on the lower surface of the wing as well as the merging of the canard vortices with the wing vortex system on the upper surface was observed. This flow structure leads to abrupt changes in the aerodynamic coefficients which are unacceptable for practical flight conditions. Author

N90-28520# Royal Aerospace Establishment, Bedford (England). Dept. of Aerodynamics.
THE EFFECTS OF FOREPLANES ON THE STATIC AND DYNAMIC CHARACTERISTICS OF A COMBAT AIRCRAFT MODEL
C. O. OLeary and B. Weir *In* AGARD, Aerodynamics of Combat Aircraft Controls and of Ground Effects Apr. 1990 13 p (For primary document see N90-28513 23-05)
Copyright Avail: NTIS HC A15/MF A02; Non-NATO Nationals requests available only from AGARD/Scientific Publications Executive

On a close coupled canard configuration there are strong aerodynamic interactions between the forebody, foreplanes, and wings which are likely to affect both the longitudinal characteristics and the lateral/directional stability of the aircraft, especially at high angle-of-attack. The nature and strength of these interactions is likely to depend on the planform and deflection of the foreplanes. Tests were made to investigate these effects on the RAE HIRM2 model in the 4 x 2.7 m Low Speed Wind Tunnel. The model was tested with trapezoidal and gothic foreplanes on a static force balance and on a lateral oscillatory rig. Effects on lift and pitching moment were similar for the different types of foreplane. There were significant effects on lateral and directional stability due to foreplane and foreplane deflection. Author

N90-28521*# National Aeronautics and Space Administration. Langley Research Center, Hampton, VA.
INNOVATIVE CONTROL CONCEPTS AND COMPONENT INTEGRATION FOR A GENERIC SUPERCRUISE FIGHTER c08
Bret A. Marks (McDonnell Aircraft Co., Saint Louis, MO.) and David E. Hahne *In* AGARD, Aerodynamics of Combat Aircraft Controls and of Ground Effects Apr. 1990 14 p (For primary document see N90-28513 23-05)
Copyright Avail: NTIS HC A15/MF A02; Non-NATO Nationals requests available only from AGARD/Scientific Publications Executive CSCL 01C

The results of a series of low speed wind tunnel tests conducted in the NASA Langley Research Center (LaRC) 12 ft Low Speed Wind Tunnel (LSWT) are highlighted. The main objectives of the tests were to provide generalized component integration guidelines and to investigate a variety of innovative control concepts designed to improve the high angle of attack (AOA) controllability of a generic class of supercruise fighters. Author

N90-28522*# National Aeronautics and Space Administration. Langley Research Center, Hampton, VA.
DEVELOPMENT OF NON-CONVENTIONAL CONTROL METHODS FOR HIGH ANGLE OF ATTACK FLIGHT USING VORTEX MANIPULATION c08
Gerald N. Malcolm, T. Terry Ng, Liane C. Lewis (Eidetics International, Inc., Torrance, CA.), and Daniel G. Murri *In* AGARD, Aerodynamics of Combat Aircraft Controls and of Ground Effects Apr. 1990 17 p Previously announced in IAA as A89-47653 (For primary document see N90-28513 23-05)
(Contract F33615-86-C-3623)
Copyright Avail: NTIS HC A15/MF A02; Non-NATO Nationals requests available only from AGARD/Scientific Publications Executive CSCL 01C

Methods of manipulating the forebody vortices on a generic fighter model to produce controlled yawing moments at high angles of attack were investigated. Forces and moments were measured on the complete configuration and on the isolated forebody. Two schemes for vortex control on the forebody were evaluated: individually-controlled tip strakes and individually-controlled blowing ports. The effectiveness of the forebody strakes in controlling forebody side forces was strongly dependent on the size and location of the strakes. A yawing moment can be produced by deploying the forebody strakes asymmetrically, or can be eliminated by deploying the strakes symmetrically. The most effective strake position was found to be near the primary separation point, between 105 and 120 deg from windward. Blowing on the surface of the model was also shown to have a strong effect on the yawing moment. Blowing either forward or aft tangential to the surface appears to be more effective than blowing normal to the surface. The most effective method to control the yawing moment on the forebody was to minimize the natural asymmetry with a pair of small symmetrically mounted tip strakes and to perturb the vortex system away from the symmetric condition with asymmetric blowing. Author

N90-28523# Stanford Univ., CA. Dept. of Aeronautics and Astronautics.
CONTROL OF VORTEX AERODYNAMICS AT HIGH ANGLES OF ATTACK
L. Roberts and N. J. Wood (Bath Univ., England) *In* AGARD, Aerodynamics of Combat Aircraft Controls and of Ground Effects Apr. 1990 9 p (For primary document see N90-28513 23-05)
(Contract F49620-86-10-0020)
Copyright Avail: NTIS HC A15/MF A02; Non-NATO Nationals requests available only from AGARD/Scientific Publications Executive

The concept of tangential leading edge blowing was investigated as a means of controlling the vortical flow over delta wings at high angles of attack. At pre-stall angles of attack, tangential leading edge blowing exerts rapid control of the vertical flow and can control or impose asymmetries with either leading edge influence uncoupled from the other. At post-stall angles of attack, the response of the vortical flow to transient blowing is slower due to the presence of vortex burst. However, a burst vortex may be unburst by tangential leading edge blowing and significant rolling moments produced at conditions where conventional controls are ineffective. At these very high angles of attack, the left and right side vortical flows appear to be strongly coupled. Author

N90-28524# Wright Research Development Center, Wright-Patterson AFB, OH.
A LOOK AT TOMORROW TODAY
Lawrence A. Walchli *In* AGARD, Aerodynamics of Combat Aircraft Controls and of Ground Effects Apr. 1990 10 p (For primary document see N90-28513 23-05)
Copyright Avail: NTIS HC A15/MF A02; Non-NATO Nationals requests available only from AGARD/Scientific Publications Executive

A broad overview of the X-29 forward swept wing technology demonstrator traces its development and test path during the past five years. Brief descriptions of the aircraft and its flight control system provide insight for evaluating this vehicle. Results are presented in several key technical areas and some general comparisons are made with current frontline fighters. The baseline flight control system provided a starting point for safe concept evaluation and envelope expansion for the aircraft. Subsequent up-dates resulted in performance levels favorably comparable to current fighter aircraft. Plans are cited for expanding the X-29's capabilities into the high angle-of-attack regime of flight. Aircraft and flight control system modifications are described which will permit the X-29 to fully exploit its technologies. Author

N90-28525# London Univ. (England).
UNSTEADY AERODYNAMICS OF CONTROLS c08
G. J. Hancock and D. G. Mabey (Royal Aerospace Establishment, Bedford, England) *In* AGARD, Aerodynamics of Combat Aircraft Controls and of Ground Effects Apr. 1990 17 p (For primary document see N90-28513 23-05)
Copyright Avail: NTIS HC A15/MF A02; Non-NATO Nationals requests available only from AGARD/Scientific Publications Executive

The physics of quasi-steady aerodynamics are discussed. The concept of an aerodynamic rise time is defined, which indicates how quickly steady states are realized. Long rise times occur at low transonic speeds, but short rise times occur at high transonic speeds. Predictions of control surface characteristics compare poorly with experimental results. Experimental errors are possibly due to small gaps and wind tunnel wall interference while in the theoretical methods boundary layer approximations may be suspect. The interface of unsteady aerodynamics with control

system design and validation is described. It is pointed out that the unsteady aerodynamic input is limited to approximate and tailored forms of linearized aerodynamics. It is not clear how more accurate, nonlinear transonic aerodynamics can be incorporated in control design procedures. Author

N90-28526# Royal Aerospace Establishment, Bedford (England). Dept. of Aerodynamics.
THE STEADY AND TIME-DEPENDENT AERODYNAMIC CHARACTERISTICS OF A COMBAT AIRCRAFT WITH A DELTA OR SWEPT CANARD
D. G. Mabey, B. L. Welsh, and C. R. Pyne *In* AGARD, Aerodynamics of Combat Aircraft Controls and of Ground Effects Apr. 1990 13 p (For primary document see N90-28513 23-05)
Copyright Avail: NTIS HC A15/MF A02; Non-NATO Nationals requests available only from AGARD/Scientific Publications Executive

The steady and time-dependent aerodynamic characteristics for a low speed half model of a typical combat aircraft configuration fitted with a 65 deg delta canard are compared with those for the same model fitted with a 44.3 deg swept canard. The tests were made in the RAE 13 x 9 ft wind tunnel on a large model of the RAE High Incidence Research Model (HIRM 1), modified to represent the Experimental Aircraft (EAP) configuration. For the same platform area, the delta canard gives higher lift and comparable pitching moments for trimming. For canard and wing buffeting the differences are small. The pressures induced on the wing by oscillation of either the delta or the swept canard are very small and comparable. Overall, these low speed measurements suggest that delta canards might have advantages for future combat aircraft. Author

N90-28527# Imperial Coll. of Science and Technology, London (England). Dept. of Aeronautics.
THE EFFECT OF RAPID SPOILER DEPLOYMENT ON THE TRANSIENT FORCES ON AN AEROFOIL
P. W. Bearman, J. M. R. Graham, and P. Kalkanis *In* AGARD, Aerodynamics of Combat Aircraft Controls and of Ground Effects Apr. 1990 11 p (For primary document see N90-28513 23-05)
Copyright Avail: NTIS HC A15/MF A02; Non-NATO Nationals requests available only from AGARD/Scientific Publications Executive

The Discrete Vortex Method (DVM) is used to simulate the two-dimensional separated flow generated by a spoiler over the upper surface of an airfoil. Cases of fixed and moving spoilers are presented and particular attention is paid to the phenomenon of short duration adverse lift which can be induced by rapid spoiler deployment. Forces and pressure distributions on the airfoil and spoiler are calculated and compared, where possible, with experimental results. The model that was developed predicts the delay times to maximum adverse lift at very high spoiler deployment rates, as well as allowing the forces on the airfoil and the spoiler to be computed separately. Numerical results are in good agreement with the experiment. Author

N90-28528# Dornier-Werke G.m.b.H., Friedrichshafen (Germany, F.R.).
INFLIGHT THRUST VECTORING: A FURTHER DEGREE OF FREEDOM IN THE AERODYNAMIC/FLIGHT MECHANICAL DESIGN OF MODERN FIGHTER AIRCRAFT
P. Mangold and G. Wedekind *In* AGARD, Aerodynamics of Combat Aircraft Controls and of Ground Effects Apr. 1990 17 p (For primary document see N90-28513 23-05)
Copyright Avail: NTIS HC A15/MF A02; Non-NATO Nationals requests available only from AGARD/Scientific Publications Executive

Two different aspects of inflight thrust vectoring are discussed. In the first, more general part a rationale for the future use of thrust deflection including reverser modes is given by highlighting the overall possibilities and the potential of thrust vector devices within the aerodynamic/flight mechanical design of modern fighters. In the second part the most interesting results from 3 low speed wind tunnel test periods is presented showing beneficial and detrimental effects of in-flight thrust reverse on aerodynamic stability and control characteristics. Author

N90-28529# Dornier-Werke G.m.b.H., Friedrichshafen (Germany, F.R.).
AERODYNAMIC INTERFERENCES OF IN-FLIGHT THRUST REVERSERS IN GROUND EFFECT
G. Wedekind and P. Mangold *In* AGARD, Aerodynamics of Combat Aircraft Controls and of Ground Effects Apr. 1990 9 p (For primary document see N90-28513 23-05)
Copyright Avail: NTIS HC A15/MF A02; Non-NATO Nationals requests available only from AGARD/Scientific Publications Executive

Overall design studies for future fighter aircraft have shown that it may be desirable or even necessary to install an in-flight thrust reversing mode during approach and landing in order to fulfill the growing requirements for optimum mission, maneuver, and point performance. With this device an additional optimization task is introduced into the aerodynamic design process, because adverse aerodynamic interference effects have to be avoided. The problems related to approach and landing may roughly be divided into two main subjects. Reingestion of the hot exhaust gases into the inlet of the engines has to be retarded. Detrimental aerodynamic interferences in terms of abrupt changes of the aerodynamic forces and moments are not tolerable, because the controllability of the aircraft has to be guaranteed within the whole approach and landing phase. In a close cooperation between Dornier and Northrop a design study for a twin engine fighter equipped with an in-flight thrust-reverser (N/D-102) was performed. During this period several low speed wind tunnel test phases were run in order to study the principal effects of such a device. Test results including force measurements are summarized, flow visualization is presented, and some design rules for a reverser system are derived. To illustrate a possible optimization procedure the most interesting results of the two test periods are presented and discussed. Author

N90-28530# Centre d'Essais Aeronautique Toulouse (France).
STUDY OF THE GROUND EFFECTS IN THE CEAT AEROHYDRODYNAMIC TUNNEL: USING THE RESULTS [ETUDE DE L'EFFET DE SOL AU CEAT EXPLOITATION DES RESULTATS]
Georges Vidal and Jacques Deschamps (Avions Marcel Dassault-Breguet Aviation, Merignac, France) *In* AGARD, Aerodynamics of Combat Aircraft Control and of Ground Effects Apr. 1990 33 p In FRENCH; ENGLISH summary (For primary document see N90-28513 23-05)
Copyright Avail: NTIS HC A15/MF A02; Non-NATO Nationals requests available only from AGARD/Scientific Publications Executive

Since 1979, the Aero-Hydrodynamic Tunnel (AHT) of CEAT Toulouse is equipped with a faired platform powered by an electrical linear induction motor enabling a maximum speed of 40 m/s. This method is chiefly used in aerodynamic tests to analyze the aircraft behavior in ground effect. The purpose is to show the equipment and facilities used for the ground effect tests, and to provide measurement data. For aircraft manufacturers it is essential to know the effects of ground proximity on the aerodynamics of the wing. The ground effect was studied on a Falcon 900 model (scale 1/10) at the AHT of Toulouse. Results show that ground effect increases the lift coefficient and the pitching moment (nose down) for usual angle-of-attack. In the same way the drag decreases and the lift-to-drag ratio increases as the wing approaches the ground. On the contrary, stall C1 and stall angle-of-attack decrease in the ground effect. Numerical computation of pressure distribution by a panel method shows that on a wing profile the ground effect increases the pressure on the lower surface and decreases the pressure on the forward part ot the upper surface. The overall result of ground effect is an increase in normal force. The computational results are in good

agreement with the test results obtained at the Aero-Hydrodynamic Tunnel. Author

N90-28531*# National Aeronautics and Space Administration. Langley Research Center, Hampton, VA.
DYNAMIC GROUND EFFECTS
John W. Paulson, Jr., Guy T. Kemmerly, and William P. Gilbert *In* AGARD, Aerodynamics of Combat Aircraft Controls and of Ground Effects Apr. 1990 12 p (For primary document see N90-28513 23-05)
Copyright Avail: NTIS HC A15/MF A02; Non-NATO Nationals requests available only from AGARD/Scientific Publications Executive CSCL 01C

A research program is underway at the NASA Langley Research Center to study the effect of rate of descent on ground effects. A series of powered models were tested in the Vortex Research Facility under conditions with rate of descent and in the 14 x 22 Foot Subsonic Tunnel under identical conditions but without rate of descent. These results indicate that the rate of descent can have a significant impact on ground effects particularly if vectored or reversed thrust is used. Author

N90-28532# Institut de Mecanique des Fluides de Lille (France).
STUDY OF GROUND EFFECTS ON FLYING SCALED MODELS [ETUDE DE L'EFFET DE SOL SUR MAQUETTE EN VOL]
J. L. Cocquerez, P. Coton, and R. Verbrugge *In* AGARD, Aerodynamics of Combat Aircraft Controls and of Ground Effects Apr. 1990 11 p In FRENCH; ENGLISH summary Sponsored by Direction des Recherches, Etudes et Techniques (For primary document see N90-28513 23-05)
Copyright Avail: NTIS HC A15/MF A02; Non-NATO Nationals requests available only from AGARD/Scientific Publications Executive

The Institute of Fluid Mechanics of Lille (IFML), an establishment of ONERA, has developed for many years specific experimental methods based on the exploitation of flying scaled models in the laboratory. These methods are especially used to characterize and model the aircraft flight qualities in a disturbed or undisturbed environment. The methods were applied to ground effect studies in order to get a better control on approach and landing phases. The experimental technique and facilities are especially well adapted to this kind of study: realistic representation of the aircraft behavior and the involved aerodynamic phenomena (ground representation, no support interference, incompressible flow, and well-known environment); high accuracy on weight, inertia, and structural characteristics of the model; flight test data obtained through redundant measurements which allow an optimal evaluation of the state variables and the dynamic coefficients; application of parameters identification techniques widely complementary with low speed wind tunnel and other moving model techniques; and abilities to illustrate static and dynamic ground effect. The experimental techniques are emphasized. Some experimental results on ground effects, especially dynamic ones, are presented. The future developments of the mathematical modeling of the aircraft longitudinal behavior are also mentioned. Some ideas are suggested concerning aircraft on carrier or landing with atmospheric disturbances. Author

N90-28533*# National Aeronautics and Space Administration. Hugh L. Dryden Flight Research Facility, Edwards, CA.
AN IN-FLIGHT INVESTIGATION OF GROUND EFFECT ON A FORWARD-SWEPT WING AIRPLANE
Robert E. Curry, Bryan J. Moulton, and John Kresse *In* AGARD, Aerodynamics of Combat Aircraft Controls and of Ground Effects Apr. 1990 11 p Previously announced as N90-14202 (For primary document see N90-28513 23-05)
Copyright Avail: NTIS HC A15/MF A02; Non-NATO Nationals requests available only from AGARD/Scientific Publications Executive CSCL 01C

A limited flight experiment was conducted to document the ground effect characteristics of the X-29A research aircraft. This vehicle has an aerodynamic platform which includes a forward-swept wing and close-coupled, variable incidence canard. The flight-test program obtained results for errors in the air data measurement and for incremental normal force and pitching moment caused by ground effect. Correlations with wind-tunnel and computational analyses were made. The results are discussed with respect to the dynamic nature of the flight measurements, similar data from other configurations, and pilot comments. The ground effect results are necessary to obtain an accurate interpretation of the vehicle's landing characteristics. The flight data can also be used in the development of many modern aircraft systems such as autoland and piloted simulation. Author

N90-28534# Aerospatiale, Toulouse (France).
DETERMINATION OF THE GROUND EFFECT ON THE CHARACTERISTICS OF THE A320 AIRCRAFT [DETERMINATION DE L'EFFET DE SOL SUR LES CARACTERISTIQUES DE L'AVION A320]
A. Condaminas and J. P. Becle (Office National d'Etudes et de Recherches Aerospatiales, Modane, France) *In* AGARD, Aerodynamics of Combat Aircraft Controls and of Ground Effects Apr. 1990 12 p In FRENCH; ENGLISH summary Previously announced in IAA as A90-21048 (For primary document see N90-28513 23-05)
Copyright Avail: NTIS HC A15/MF A02; Non-NATO Nationals requests available only from AGARD/Scientific Publications Executive

The ground effect on the aerodynamic response of the A320 is investigated experimentally using a 1:7.6-scale model equipped with two motorized nacelles in the S1 wind tunnel at ONERA Modane-Avrieux. The design and instrumentation of the model are described; the measurement apparatus and procedures are explained; and the results are presented in extensive graphs and characterized in detail. Particular attention is given to the treatment of the floor boundary layer and the corrections for the side walls and model support in the data analysis. Good general agreement with flight-test data is demonstrated with respect to life and mean deflection; the airspeed errors are found to be comparable to the precision of the pressure sensors. Author

N90-28535 Kansas Univ., Lawrence.
LIFE CYCLE COST IN THE CONCEPTUAL DESIGN OF SUBSONIC COMMERCIAL AIRCRAFT, VOLUMES 1 AND 2 Ph.D. Thesis
Vicki S. Johnson 1989 391 p
Avail: Univ. Microfilms Order No. DA9009907

A methodology was developed which makes it possible to identify an aircraft concept that will meet the mission requirements and have the lowest life cycle cost (LCC). Provision is made in the methodology for sensitivities to advanced technologies to also be investigated. The methodology consists of: (1) a LCC module composed of elements to calculate RDT&E (research, development, testing, and evaluation) cost, production cost, DOC (direct operating cost), and IOC (indirect operating cost); and (2) an existing conceptual design and analysis code, the Flight Optimization System (FLOPS). Using this methodology, a configuration can be optimized for minimum life cycle cost, direct operating cost, or acquisition cost, in addition to minimum takeoff gross weight (TOGW), fuel burned, or maximum range. Use of the methodology on short-, medium-, and medium-to-long range subsonic commercial aircraft has demonstrated that optimization parameter has a definite effect on the aircraft; optimizing for minimum LCC results in a different airplane than when optimizing for minimum TOGW, fuel burned, DOC, or acquisition cost. Additionally, the economic assumptions can have a strong impact on the configurations optimized for minimum LCC or DOC. Also, results show that advanced technology can be worthwhile, even if it results in higher manufacturing and operating costs.
Dissert. Abstr.

N90-28536 Virginia Polytechnic Inst. and State Univ., Blacksburg.
SYSTEM RELIABILITY OPTIMIZATION OF AIRCRAFT WINGS

Ph.D Thesis
Ju-Sung Yang 1989 96 p
Avail: Univ. Microfilms Order No. DA9013527

System reliability based design of aircraft wings is studied. A wing of a light commuter aircraft designed according to the FAA regulations is compared with one designed by system reliability optimization. Both the level 3, and the advanced first order, second moment (AFOSM) method are employed to evaluate the probability of failure of each failure element of the system representing the wing. In the level 3 method the statistical correlation between failure modes is neglected. The AFOSM method allows evaluation of the sensitivity derivatives of the system safety index analytically. Furthermore, it accounts for the statistical correlation between failure modes. The results demonstrate the potential of stochastic optimization, and the importance of accounting for the statistical correlation between failure modes. Finally, it is shown that the problem associated with discontinuity of sensitivity derivatives encountered when using second order Ditlevsen upper bounds to estimate the system failure probability, is circumvented if a penalty function method is used for optimization. Dissert. Abstr.

N90-28537*# Boeing Commercial Airplane Co., Seattle, WA.
HIGH-SPEED CIVIL TRANSPORT STUDY: SPECIAL FACTORS Final Report, Sep. 1986 - Nov. 1988
Sep. 1990 126 p
(Contract NAS1-18377)
(NASA-CR-181881; NAS 1.26:181881) Avail: NTIS HC A07/MF A01 CSCL 01C

Studies relating to environmental factors associated with high speed civil transports were conducted. Projected total engine emissions for year 2015 fleets of several subsonic/supersonic transport fleet scenarios, discussion of sonic boom reduction methods, discussion of community noise level requirements, fuels considerations, and air traffic control impact are presented. Author

N90-28538# Aeronautical Research Inst. of Sweden, Stockholm. Dept. of Structures.
DAMAGE TOLERANCE OF THE FIGHTER AIRCRAFT 37 VIGGEN. PART 1: ANALYTICAL ASSESSMENT
Bjorn Palmberg, Per-Olof Boman, Mats-Olof Olsson, and Anders F. Blom 25 Feb. 1990 12 p Presented at FATIGUE 1990, Honolulu, HI, 15-20 Jul. 1990 Sponsored by Defence Materiel Administration, Stockholm, Sweden
(FFA-TN-1990-12-Pt-1; ETN-90-97510) Avail: NTIS HC A03/MF A01

The analytical part of an extensive damage tolerance evaluation of the fighter aircraft 37 Viggen is presented. The complementing experimental investigation is discussed in the companion paper. Topics addressed include load spectra, stress analysis, fracture mechanics and fatigue crack propagation. The following conclusions are made: the methodology used is verified and is state of the art; damage tolerance is analytically proven and experimentally demonstrated; extension of the original design life is currently being considered. ESA

N90-28539# Aeronautical Research Inst. of Sweden, Stockholm. Dept. of Structures.
DAMAGE TOLERANCE OF THE FIGHTER AIRCRAFT 37 VIGGEN. PART 2: EXPERIMENTAL VERIFICATION
Mats-Olof Olsson, Per-Olof Boman, Bjorn Palmberg, and Anders F. Blom 20 Mar. 1990 19 p Presented at FATIGUE 1990, Honolulu, HI, 15-20 Jul. 1990 Sponsored by Defence Materiel Administration, Stockholm, Sweden
(FFA-TN-1990-13-Pt-2; ETN-90-97511) Avail: NTIS HC A03/MF A01

An experimental test program carried out within a larger damage tolerance evaluation of the fighter aircraft 37 Viggen is presented. The analytical part of the work is described in the companion paper. Emphasis is put on full scale spectrum testing of both a fighter version main wing attachment frame as well as the fin of the same aircraft version. The following conclusions are made: the tested components are damage tolerant during their original fail safe design lives; analytical methodology is verified both in terms of global and local stress levels and spectrum fatigue crack growth prediction capability; extended usage of this aircraft may be possible following further considerations. ESA

N90-28540*# Stanford Univ., CA.
THE AERODYNAMIC DESIGN OF THE OBLIQUE FLYING WING SUPERSONIC TRANSPORT
Alexander J. M. VanDerVelden and Ilan Kroo Jun. 1990 69 p
(Contract NCA2-343)
(NASA-CR-177552; A-90168; NAS 1.26:177552) Avail: NTIS HC A04/MF A01 CSCL 01C

The aerodynamic design of a supersonic oblique flying wing is strongly influenced by the requirement that passengers must be accommodated inside the wing. It was revealed that thick oblique wings of very high sweep angle can be efficient at supersonic speeds when transonic normal Mach numbers are allowed on the upper surface of the wing. The goals were motivated by the ability to design a maximum thickness, minimum size oblique flying wing. A 2-D Navier-Stokes solver was used to design airfoils up to 16 percent thickness with specified lift, drag and pitching moment. A new method was developed to calculate the required pressure distribution on the wing based on the airfoil loading, normal Mach number distribution and theoretical knowledge of the minimum drag of oblique configurations at supersonic speeds. The wing mean surface for this pressure distribution was calculated using an inverse potential flow solver. The lift to drag ratio of this wing was significantly higher than that of a comparable delta wing for cruise speeds up to Mach 2. Author

N90-28541*# National Aeronautics and Space Administration. Langley Research Center, Hampton, VA.
NASA LANGLEY RESEARCH CENTER NATIONAL AERO-SPACE PLANE MISSION SIMULATION PROFILE SETS
Craig W. Ohlhorst, Wallace L. Vaughn, and John J. Bresina (National Aeronautics and Space Administration. Hugh L. Dryden Flight Research Facility, Edwards, CA.) Oct. 1990 18 p
(NASA-TM-102670; NAS 1.15:102670) Avail: NTIS HC A03/MF A01 CSCL 01C

To provide information on the potential for long life service of oxidation resistant carbon-carbon (ORCC) materials in the National Aero-Space Plane (NASP) airframe environment, NASP ascent, entry, and cruise trajectories were analytically flown. Temperature and pressure profiles were generated for 20 vehicle locations. Orbital (ascent and entry) and cruise profile sets from four locations are presented along with the humidity exposure and testing sequences that are being used to evaluate ORCC materials. The four profiles show peak temperatures during the ascent leg of an orbital mission of 2800, 2500, 2000, and 1700 F. These profiles bracket conditions where carbon-carbon might be used on the NASP vehicle. Author

N90-28542*# National Aeronautics and Space Administration. Hugh L. Dryden Flight Research Facility, Edwards, CA.
VALIDATION OF THE F-18 HIGH ALPHA RESEARCH VEHICLE FLIGHT CONTROL AND AVIONICS SYSTEMS MODIFICATIONS
Vince Chacon, Joseph W. Pahle, and Victoria A. Regenie Oct. 1990 13 p Presented at the IEEE 9th Digital Avionics Systems Conference, Virginia Beach, VA, 15-18 Oct. 1990
(NASA-TM-101723; H-1632; NAS 1.15:101723) Avail: NTIS HC A03/MF A01 CSCL 01C

The verification and validation process is a critical portion of the development of a flight system. Verification, the steps taken to assure the system meets the design specification, has become a reasonably understood and straightforward process. Validation is the method used to ensure that the system design meets the needs of the project. As systems become more integrated and more critical in their functions, the validation process becomes more complex and important. The tests, tools, and techniques which are being used for the validation of the high alpha research vehicle (HARV) turning vane control system (TVCS) are discussed

and the problems and their solutions are documented. The emphasis of this paper is on the validation of integrated system. Author

N90-28543# Naval Aerospace Medical Research Lab., Pensacola, FL.
PREDICTING F/A-18 FLEET REPLACEMENT SQUADRON PERFORMANCE USING AN AUTOMATED BATTERY OF PERFORMANCE-BASED TESTS Interim Report, Jun. 1986 - Jun. 1989
G. R. Griffin and R. N. Shull Mar. 1990 15 p
(AD-A223899; NAMRL-1354) Avail: NTIS HC A03/MF A01 CSCL 05/9

Several studies have suggested the possibility of predicting operational performance in fleet aviation environments. This report concerns the use of an automated performance-based test battery, involving cognitive and psychomotor functioning, to predict the operational performance of fighter pilots. Two groups of pilots who were completing fleet replacement squadron (FRS) training for the F/A-18 were tested on this battery. The older and more experienced pilot group got higher FRS grades than did the other group; test performance between these two groups was not significantly different. Those few significant correlations found between the test measures and the FRS grades were illogically patterned and of insufficient quantity or strength to demonstrate any reliable predictive ability. This could have been due to the homogeneous nature of each of these subject groups in terms of piloting skills and abilities. GRA

06 AIRCRAFT INSTRUMENTATION

Includes cockpit and cabin display devices; and flight instruments.

For related information see also *19 Spacecraft Instrumentation* and *35 Instrumentation and Photography.*

N90-28544# Air Force Wright Aeronautical Labs., Wright-Patterson AFB, OH.
THE INTERACTION OF CHROMOSTEREOPSIS AND STEREOPSIS IN STEREOSCOPIC CRT (CATHODE RAY TUBES) DISPLAYS M.S. Thesis
James Ennis McClain 1989 79 p
(AD-A217906; AFIT/CI/CIA-89-027) Avail: NTIS HC A05/MF A01 CSCL 01/3

With the increased complexity in aircraft and space system information display capabilities, conventional two-dimensional (2-D) displays will eventually be replaced by more capable 3-D stereoscopic displays. Three-dimensional stereoscopic displays allow the vehicle operator to more effectively interact with an increasingly dynamic environment by presenting information consistent with the operator's perceptual experience and stereotypes. Important to the development of stereoscopic 3-D displays is the interaction of perceived depth created by hues (chromostereopsis) and perceived depth created by presenting different images of a single object to the left and right eye of the observer (stereopsis). GRA

N90-28545# Aquanautics Corp., Alameda, CA.
A RELIABLE, MAINTENANCE-FREE OXYGEN SENSOR FOR AIRCRAFT USING AN OXYGEN-SENSITIVE COATING ON POTENTIOMETRIC ELECTRODES Final Report, Nov. 1988 - May 1989
Emory S. DeCastro and Mark E. Meyerhoff (Michigan Univ., Ann Arbor.) Mar. 1990 28 p
(Contract F33615-88-C-0638; AF Proj. 7930)
(AD-A222696; USAFSAM-TP-89-20) Avail: NTIS HC A03/MF A01 CSCL 17/8

This report is on the preliminary development of a new kind of oxygen sensor. Based on sensing a potentiometric signal from oxygen-specific compounds, this approach offers a potentially stable, reliable, and vastly simplified sensor. The report represents two configurations for the oxygen-specific compound (oxygen reagent). One makes use of the reagent in a thin solution film confined by a membrane. The other uses the reagent immobilized in a polymer film, without any additional solvents. This last embodiment is essentially a solid-state probe of oxygen. This report demonstrates the feasibility of such an approach by reviewing relevant work dealing with: (1) proof of principle, (2) calibration curves over a range of oxygen pressure, (3) temperature effects, and (4) pressure effects. GRA

N90-28546*# National Aeronautics and Space Administration. Langley Research Center, Hampton, VA.
DESCRIPTION OF THE PRIMARY FLIGHT DISPLAY AND FLIGHT GUIDANCE SYSTEM LOGIC IN THE NASA B-737 TRANSPORT SYSTEMS RESEARCH VEHICLE
Charles E. Knox Aug. 1990 25 p Original contains color illustrations
(NASA-TM-102710; NAS 1.15:102710) Avail: NTIS HC A03/MF A01; 1 functional color page CSCL 01D

A primary flight display format was integrated with the flight guidance and control system logic in support of various flight tests conducted with the NASA Transport Systems Research Vehicle B-737-100 airplane. The functional operation of the flight guidance mode control panel and the corresponding primary flight display formats are presented. Author

07 AIRCRAFT PROPULSION AND POWER

Includes prime propulsion systems and systems components, e.g., gas turbine engines and compressors; and onboard auxilliary power plants for aircraft.

For related information see also *20 Spacecraft Propulsion and Power, 28 Propellants and Fuels,* and *44 Energy Production and Conversion.*

N90-28547# Aeronautical Research Labs., Melbourne (Australia).
THE REDUCTION OF SMOKE EMISSIONS FROM ALLISON T56 ENGINES
F. W. Skidmore, D. R. Hunt, and P. N. Doogood Mar. 1990 43 p Original contains color illustrations
(ARL-PROP-R-182; AR-006-055) Avail: NTIS HC A03/MF A01; 2 functional color pages

Aeronautical Research Laboratory (ARL) has been working to reduce smoke emissions from the Allison T56 engines used in the Lockheed P-3C Orion aircraft operated by the Royal Australian Air Force (RAAF). The work consisted of a literature survey, design and manufacture of a water tunnel model, water tunnel testing of various modifications to improve the fluid dynamics of the combustion system, testing the modifications in a single liner combustion test rig, smoke emission comparative tests in ground run engine trials, performance tests in a calibrated test cell and flight trials of a modified engine. The modification that was developed in this program was found to significantly reduce smoke emissions and give substantial improvements in the specific fuel consumption of the engine. In addition, there were indications, in line with theoretical predictions, that the modification would extend the life of the hot end components of the engine. Author

N90-28548 University of Technology, Loughborough (England).
EFFECTIVE OPTIMAL CONTROL OF A FIGHTER AIRCRAFT ENGINE Ph.D. Thesis
Saad Mustafa Mahmoud 1988 330 p
Avail: Univ. Microfilms Order No. BRDX88310

Typical modern fighter aircraft use two-spool, low by-pass ratio, turbojet engines to provide the thrust needed to carry out the combat maneuvers required by present-day air warfare tactics. The dynamic characteristics of such aircraft engines are complex and non-linear. The need for fast, accurate control of the engine throughout the flight envelope is of paramount importance and this research was concerned with the study of such problems and subsequent design of an optimal linear control which would

improve the engine's dynamic response and provide the required correspondence between the output from the engine and the values commanded by a pilot. A detailed mathematical model was derived which, in accuracy and complexity of representation, was a large improvement upon existing analytical models, which assume linear operation over a very small region of the state space, and which was simpler than the large non-analytic representations, which are based on matching operational data. The non-linear model used in this work was based upon information obtained from DYNGEN, a computer program which is used to calculate the steady-state and transient responses of turbojet and turbofan engines. Dissert. Abstr.

N90-28549# Army Aviation Systems Command, Corpus Christi, TX. Depot Engineering and RCM Support Office.
ANALYSIS OF THE T63-A-700 ENGINE USED IN ALCOHOL TURBINE FUEL EXTENDER TEST
John S. Glaeser Aug. 1990 17 p Sponsored by FAA, Atlantic City, NJ
(DOT/FAA/CT-TN90/18) Avail: NTIS HC A03/MF A01

The teardown analysis of the T63-A-700 engine used in fuel extender research was conducted in order to evaluate the use of alcohols as extenders for the existing turbine fuels. The turbine section of the engine displayed burned vanes on the first stage gas producer. The blade tips of the second stage gas producer turbine rotor had rubbed the interior of the second stage gas producer nozzle. It was concluded that the vanes on the first stage gas producer burned during a series of hot or hung starts using extender fuels. The inefficiency of both the fuel nozzle and the fuel control unit using alcohol blends during starting operations caused the overtemperatures. The second stage gas producer nozzle was warped as a result of thermal cycling from ambient temperature to a hot or hung start condition that caused the turbine rotor tips to rub the nozzle. The remainder of the engine, including the seals, fuel control unit, fuel nozzle, bearings, and internal components, showed no discrepancies. Much of the change appears to have resulted from hung starts. Author

N90-28550 State Univ. of New York, Stony Brook.
CALCULATION OF TEMPERATURE DISTRIBUTION IN VARIOUS TURBINE BLADES USING A BOUNDARY-FITTED COORDINATE TRANSFORMATION METHOD Ph.D. Thesis
Byeong Soo Oh 1989 234 p
Avail: Univ. Microfilms Order No. DA9015633

Gas turbine engines operating at high temperature and high pressure ratio have been developed to increase power output and efficiency. However, due to the limitations of material properties, internal convective cooling is needed in many turbine blades. Knowledge of the temperature distribution in the cooled blade is necessary for its thermal stress analysis. Improvements in prediction capability in this area can benefit turbine life, reduce development and maintenance costs, and improve engine performance. Numerical solutions of partial differential equations in regions with arbitrarily shaped boundaries are relatively difficult. Finite-difference solutions in irregular domains have been hindered in the past by the problem of fitting curved boundaries into the computational grid. Here, the physical region where the heat transport occurs is mapped onto a rectangular computational domain by means of a boundary-fitted coordinate transformation method. The finite-difference approach is then used to give solutions that do not lack continuity of derivatives. A general convection-diffusion equation is derived for the transformed computational domain and a computer program is developed to solve the heat transfer in any blade shape. Only one outer blade shape, the Allison/NASA C3X vane, is studied with various inner hole geometries and boundary conditions. The study shows that by developing a multi-part technique the problem of complicated geometry can be solved. Regardless of the temperature distribution on the outer boundary, the best cooling effect is obtained when the inner cooling holes have a similar shape to the outer blade surface. It is shown that the cooling of the tail region is important especially at the tail end. Dissert. Abstr.

N90-28551*# National Aeronautics and Space Administration. Hugh L. Dryden Flight Research Facility, Edwards, CA.
PROPULSION SYSTEM-FLIGHT CONTROL INTEGRATION AND OPTIMIZATION: FLIGHT EVALUATION AND TECHNOLOGY TRANSITION
Frank W. Burcham, Jr., Glenn B. Gilyard, and Lawrence P. Myers Washington Jul. 1990 26 p Presented at the AIAA 26th Joint Propulsion Conference, Orlando, FL, 16-18 Jul. 1990
(NASA-TM-4207; H-1603; NAS 1.15:4207) Avail: NTIS HC A03/MF A01 CSCL 21E

Integration of propulsion and flight control systems and their optimization offers significant performance improvements. Research programs were conducted which have developed new propulsion and flight control integration concepts, implemented designs on high-performance airplanes, demonstrated these designs in flight, and measured the performance improvements. These programs, first on the YF-12 airplane, and later on the F-15, demonstrated increased thrust, reduced fuel consumption, increased engine life, and improved airplane performance; with improvements in the 5 to 10 percent range achieved with integration and with no changes to hardware. The design, software and hardware developments, and testing requirements were shown to be practical. Author

N90-28552*# Hamilton Standard, Windsor Locks, CT.
MEASUREMENT OF THE STEADY SURFACE PRESSURE DISTRIBUTION ON A SINGLE ROTATION LARGE SCALE ADVANCED PROP-FAN BLADE AT MACH NUMBERS FROM 0.03 TO 0.78 Final Report
Peter Bushnell Jul. 1988 540 p
(Contract NAS3-23051)
(NASA-CR-182124; E-4137; NAS 1.26:182124) Avail: NTIS HC A23/MF A03 CSCL 21E

The aerodynamic pressure distribution was determined on a rotating Prop-Fan blade at the S1-MA wind tunnel facility operated by the Office National D'Etudes et de Recherches Aerospatiale (ONERA) in Modane, France. The pressure distributions were measured at thirteen radial stations on a single rotation Large Scale Advanced Prop-Fan (LAP/SR7) blade, for a sequence of operating conditions including inflow Mach numbers ranging from 0.03 to 0.78. Pressure distributions for more than one power coefficient and/or advanced ratio setting were measured for most of the inflow Mach numbers investigated. Due to facility power limitations the Prop-Fan test installation was a two bladed version of the eight design configuration. The power coefficient range investigated was therefore selected to cover typical power loading per blade conditions which occur within the Prop-Fan operating envelope. The experimental results provide an extensive source of information on the aerodynamic behavior of the swept Prop-Fan blade, including details which were elusive to current computational models and do not appear in the two-dimensional airfoil data. Author

N90-28553*# General Electric Co., Cincinnati, OH. Aircraft Engine Group.
ENERGY EFFICIENT ENGINE HIGH PRESSURE TURBINE COMPONENT TEST PERFORMANCE REPORT
L. P. Timko 1984 173 p
(Contract NAS3-20643)
(NASA-CR-168289; NAS 1.26:168289; R82AEB406) Avail: NTIS HC A08/MF A01 CSCL 21E

The high pressure turbine for the General Electric Energy Efficient Engine is a two stage design of moderate loading. Results of detailed system studies led to selection of this configuration as the most appropriate in meeting the efficiency goals of the component development program. To verify the design features of the high pressure turbine, a full scale warm air turbine test rig with cooling flows simulated was run. Prior to this testing, an annular cascade test was run to select vane unguided turn for the first stage nozzle. Results of this test showed that the base configuration exceeded the lower unguided turning configuration by 0.48 percent in vane kinetic energy efficiency. The air turbine test program, consisting of extensive mapping and cooling flow

variation as well as design point evaluation, demonstrated a design point efficiency level of 90.0 percent based on the thermodynamic definition. In terms of General Electric cycle definition, this efficiency was 92.5 percent. Based on this test, it is concluded that efficiency goals for the Flight Propulsion System were met. Author

N90-28554*# General Electric Co., Cincinnati, OH. Aircraft Engine Business Group.
ENERGY EFFICIENT ENGINE COMBUSTOR TEST HARDWARE DETAILED DESIGN REPORT
D. L. Burrus, C. A. Chahrour, H. L. Foltz, P. E. Sabla, S. P. Seto, and J. R. Taylor Mar. 1984 474 p
(Contract NAS3-20643)
(NASA-CR-168301; NAS 1.26:168301; R82AEB472) Avail: NTIS HC A20/MF A03 CSCL 21E

The Energy Efficient Engine (E3) Combustor Development effort was conducted as part of the overall NASA/GE E3 Program. This effort included the selection of an advanced double-annular combustion system design. The primary intent was to evolve a design which meets the stringent emissions and life goals of the E3 as well as all of the usual performance requirements of combustion systems for modern turbofan engines. Numerous detailed design studies were conducted to define the features of the combustion system design. Development test hardware was fabricated, and an extensive testing effort was undertaken to evaluate the combustion system subcomponents in order to verify and refine the design. Technology derived from this development effort will be incorporated into the engine combustion system hardware design. This advanced engine combustion system will then be evaluated in component testing to verify the design intent. What is evolving from this development effort is an advanced combustion system capable of satisfying all of the combustion system design objectives and requirements of the E3. Fuel nozzle, diffuser, starting, and emissions design studies are discussed. R.J.F.

N90-28555*# General Electric Co., Cincinnati, OH. Aircraft Engine Business Group.
ENERGY EFFICIENT ENGINE (E3) COMBUSTION SYSTEM COMPONENT TECHNOLOGY PERFORMANCE REPORT Draft Report
D. L. Burrus, C. A. Chahrour, H. L. Foltz, P. E. Sabla, S. P. Seto, and J. R. Taylor Jul. 1984 494 p
(Contract NAS3-20643)
(NASA-CR-168274; NAS 1.26:168274; R82AEB401) Avail: NTIS HC A21/MF A03 CSCL 21E

The Energy Efficient Engine (E3) combustor effort was conducted as part of the overall NASA/GE E3 Program. This effort included the selection of an advanced double-annular combustion system design. The primary intent of this effort was to evolve a design that meets the stringent emissions and life goals of the E3, as well as all of the usual performance requirements of combustion systems for modern turbofan engines. Numerous detailed design studies were conducted to define the features of the combustion system design. Development test hardware was fabricated, and an extensive testing effort was undertaken to evaluate the combustion system subcomponents in order to verify and refine the design. Technology derived from this effort was incorporated into the engine combustion hardware design. The advanced engine combustion system was then evaluated in component testing to verify the design intent. What evolved from this effort was an advanced combustion system capable of satisfying all of the combustion system design objectives and requirements of the E3. R.J.F.

N90-28556*# Pratt and Whitney Aircraft, East Hartford, CT. Engineering Div.
ENERGY EFFICIENT ENGINE EXHAUST MIXER MODEL TECHNOLOGY REPORT ADDENDUM; PHASE 3 TEST PROGRAM
M. J. Larkin and J. R. Blatt Apr. 1984 197 p
(Contract NAS3-20646)
(NASA-CR-174799; NAS 1.26:174799; PWA-5594-271-Add)
Avail: NTIS HC A09/MF A02 CSCL 21E

The Phase 3 exhaust mixer test program was conducted to explore the trends established during previous Phases 1 and 2. Combinations of mixer design parameters were tested. Phase 3 testing showed that the best performance achievable within tailpipe length and diameter constraints is 2.55 percent better than an optimized separate flow base line. A reduced penetration design achieved about the same overall performance level at a substantially lower level of excess pressure loss but with a small reduction in mixing. To improve reliability of the data, the hot and cold flow thrust coefficient analysis used in Phases 1 and 2 was augmented by calculating percent mixing from traverse data. Relative change in percent mixing between configurations was determined from thrust and flow coefficient increments. The calculation procedure developed was found to be a useful tool in assessing mixer performance. Detailed flow field data were obtained to facilitate calibration of computer codes. Author

N90-28557*# General Electric Co., Cincinnati, OH. Aircraft Engine Business Group.
ENERGY EFFICIENT ENGINE ACOUSTIC SUPPORTING TECHNOLOGY REPORT
S. P. Lavin and P. Y. Ho Jun. 1985 371 p
(Contract NAS3-20643)
(NASA-CR-174834; NAS 1.26:174834; R84AEB246) Avail: NTIS HC A16/MF A02 CSCL 21E

The acoustic development of the Energy Efficient Engine combined testing and analysis using scale model rigs and an integrated Core/Low Spool demonstration engine. The scale model tests show that a cut-on blade/vane ratio fan with a large spacing (S/C = 2.3) is as quiet as a cut-off blade/vane ratio with a tighter spacing (S/C = 1.27). Scale model mixer tests show that separate flow nozzles are the noisiest, conic nozzles the quietest, with forced mixers in between. Based on projections of ICLS data the Energy Efficient Engine (E3) has FAR 36 margins of 3.7 EPNdB at approach, 4.5 EPNdB at full power takeoff, and 7.2 EPNdB at sideline conditions. Author

N90-28558*# General Electric Co., Evendale, OH. Aircraft Engine Business Group.
ENERGY EFFICIENT ENGINE: FLIGHT PROPULSION SYSTEM FINAL DESIGN AND ANALYSIS Report, Nov. 1978 - Aug. 1983
Donald Y. Davis and E. Marshall Stearns Aug. 1985 170 p
(Contract NAS3-20643)
(NASA-CR-168219; NAS 1.26:168219; R83AEB488) Avail: NTIS HC A08/MF A01 CSCL 21E

The Energy Efficient Engine (E3) is a NASA program to create fuel saving technology for future transport engines. The Flight Propulsion System (FPS) is the engine designed to achieve E3 goals. Achieving these goals required aerodynamic, mechanical and system technologies advanced beyond that of current production engines. These technologies were successfully demonstrated in component rigs, a core engine and a turbofan ground test engine. The design and benefits of the FPS are presented. All goals for efficiency, environmental considerations, and economic payoff were met. The FPS has, at maximum cruise, 10.67 km (35,000 ft), M0.8, standard day, a 16.9 percent lower installed specific fuel consumption than a CF6-50C. It provides an 8.6 percent reduction in direct operating cost for a short haul domestic transport and a 16.2 percent reduction for an international long distance transport. Author

N90-28559*# General Electric Co., Cincinnati, OH. Aircraft Engine Business Group.
ENERGY EFFICIENT ENGINE CORE DESIGN AND PERFORMANCE REPORT Report, Jan. 1978 - Dec. 1982
E. Marshall Stearns et al Dec. 1982 530 p
(Contract NAS3-20643)
(NASA-CR-168069; NAS 1.26:168069; R82AEB470) Avail: NTIS HC A23/MF A03 CSCL 21E

The Energy Efficient Engine (E3) is a NASA program to develop fuel saving technology for future large transport aircraft engines.

Testing of the General Electric E3 core showed that the core component performance and core system performance necessary to meet the program goals can be achieved. The E3 core design and test results are described. Author

N90-28560*# Pratt and Whitney Aircraft, East Hartford, CT. Engineering Div.
ENERGY EFFICIENT ENGINE PROGRAM ADVANCED TURBOFAN NACELLE DEFINITION STUDY
David C. Howe and T. A. Wynosky May 1985 165 p
(Contract NAS3-20646)
(NASA-CR-174942; NAS 1.26:174942; PWA-5394-315) Avail: NTIS HC A08/MF A01 CSCL 21E

Advanced, low drag, nacelle configurations were defined for some of the more promising propulsion systems identified in the earlier Benefit/Cost Study, to assess the benefits associated with these advanced technology nacelles and formulate programs for developing these nacelles and low volume thrust reversers/spoilers to a state of technology readiness in the early 1990's. The study results established the design feasibility of advanced technology, slim line nacelles applicable to advanced technology, high bypass ratio turbofan engines. Design feasibility was also established for two low volume thrust reverse/spoiler concepts that meet or exceed the required effectiveness for these engines. These nacelle and thrust reverse/spoiler designs were shown to be applicable in engines with takeoff thrust sizes ranging from 24,000 to 60,000 pounds. The reduced weight, drag, and cost of the advanced technology nacelle installations relative to current technology nacelles offer a mission fuel burn savings ranging from 3.0 to 4.5 percent and direct operating cost plus interest improvements from 1.6 to 2.2 percent. Author

N90-28561*# General Electric Co., Evendale, OH. Aircraft Engine Business Group.
ENERGY EFFICIENT ENGINE INTEGRATED CORE/LOW SPOOL DESIGN AND PERFORMANCE REPORT Topical Report, Jan. 1978 - Aug. 1983
E. Marshall Stearns et al Feb. 1985 649 p
(Contract NAS3-20643)
(NASA-CR-168211; NAS 1.26:168211; R83AEB503) Avail: NTIS HC A99/MF A04 CSCL 21E

The Energy Efficient Engine (E3) is a NASA program to create fuel saving technology for future transport aircraft engines. The E3 technology advancements were demonstrated to operate reliably and achieve goal performance in tests of the Integrated Core/Low Spool vehicle. The first build of this undeveloped technology research engine set a record for low fuel consumption. Its design and detailed test results are herein presented. Author

N90-28562*# General Electric Co., Evendale, OH. Aircraft Engine Business Group.
ENERGY EFFICIENT ENGINE: CONTROL SYSTEM COMPONENT PERFORMANCE REPORT
R. S. Beitler and G. W. Bennett Oct. 1984 205 p
(Contract NAS3-20643)
(NASA-CR-174651; NAS 1.26:174651; R83AEB623) Avail: NTIS HC A10/MF A02 CSCL 21E

An Energy Efficient Engine (E3) program was established to develop technology for improving the energy efficiency of future commercial transport aircraft engines. As part of this program, General Electric designed and tested a new engine. The design, fabrication, bench and engine testing of the Full Authority Digital Electronic Control (FADEC) system used for controlling the E3 Demonstrator Engine is described. The system design was based on many of the proven concepts and component designs used on the General Electric family of engines. One significant difference is the use of the FADEC in place of hydromechanical computation currently used. Author

N90-28563*# General Electric Co., Cincinnati, OH. Aircraft Engine Business Group.
NASA/GE ENERGY EFFICIENT ENGINE LOW PRESSURE TURBINE SCALED TEST VEHICLE PERFORMANCE REPORT Topical Report, 1979-1982
M. J. Bridgeman, D. G. Cherry, and J. Pedersen Jul. 1983 259 p
(Contract NAS3-20643)
(NASA-CR-168290; NAS 1.26:168290; R83AEB143) Avail: NTIS HC A12/MF A02 CSCL 21E

The low pressure turbine for the NASA/General Electric Energy Efficient Engine is a highly loaded five-stage design featuring high outer wall slope, controlled vortex aerodynamics, low stage flow coefficient, and reduced clearances. An assessment of the performance of the LPT has been made based on a series of scaled air-turbine tests divided into two phases: Block 1 and Block 2. The transition duct and the first two stages of the turbine were evaluated during the Block 1 phase from March through August 1979. The full five-stage scale model, representing the final integrated core/low spool (ICLS) design and incorporating redesigns of stages 1 and 2 based on Block 1 data analysis, was tested as Block 2 in June through September 1981. Results from the scaled air-turbine tests, reviewed herein, indicate that the five-stage turbine designed for the ICLS application will attain an efficiency level of 91.5 percent at the Mach 0.8/10.67-km (35,000-ft), max-climb design point. This is relative to program goals of 91.1 percent for the ICLS and 91.7 percent for the flight propulsion system (FPS). Author

N90-28564*# Pratt and Whitney Aircraft, East Hartford, CT. Engineering Div.
ENERGY EFFICIENT ENGINE PROGRAM TECHNOLOGY BENEFIT/COST STUDY. VOLUME 1: EXECUTIVE SUMMARY
D. E. Gray and William B. Gardner Oct. 1983 19 p
(Contract NAS3-20646)
(NASA-CR-174766-Vol-1; NAS 1.26:174766-Vol-1; PWA-5594-258-Vol-1) Avail: NTIS HC A03/MF A01 CSCL 21E

Under the NASA sponsored Energy Efficient Engine Program, Pratt and Whitney completed the Benefit/Cost Study to identify turbofan engine technologies required for the years 2000 to 2010, to assess the benefits of those technologies, and to formulate programs for developing the technologies required for that time period. The results verified that there are still many potential benefits to be realized from the advancement of gas turbine technology. The initial effort was to screen and rank preliminary technology concepts that might be amenable to future development. Cycle studies, flowpath definition studies, and mechanical configuration studies were then used to identify and establish the feasibility of the technologies that would be required in the 2000 to 2010 time frame. These efforts showed that a turbofan engine with advancements in aerodynamics, mechanical arrangements, and materials offered significant performance improvements over 1988 technology. The benefits of the technologies were assessed using fuel burn and direct operating cost plus interest (DOC+I). These concepts could yield thrust specific fuel consumption benefits of almost 16 percent, fuel burn benefits of up to 24 percent and DOC+I benefits of up to 14 percent in a long-range airplane relative to Energy Efficient Engine technology levels. Technology development programs were formulated and recommended to realize those benefits. Author

N90-28565*# Pratt and Whitney Aircraft, East Hartford, CT. Engineering Div.
ENERGY EFFICIENT ENGINE PROGRAM TECHNOLOGY BENEFIT/COST STUDY, VOLUME 2
D. E. Gray and William B. Gardner Oct. 1983 109 p
(Contract NAS3-20646)
(NASA-CR-174766-Vol-2; NAS 1.26:174766-Vol-2; PWA-5594-251-Vol-2) Avail: NTIS HC A06/MF A01 CSCL 21E

The Benefit/Cost Study portion of the NASA-sponsored Energy Efficient Engine Component Development and Integration program

was successful in achieving its objectives: identification of air transport propulsion system technology requirements for the years 2000 and 2010, and formulation of programs for developing these technologies. It is projected that the advanced technologies identified, when developed to a state of readiness, will provide future commercial and military turbofan engines with significant savings in fuel consumption and related operating costs. These benefits are significant and far from exhausted. The potential savings translate into billions of dollars in annual savings for the airlines. Analyses indicate that a significant portion of the overall savings is attributed to aerodynamic and structure advancements. Another important consideration in acquiring these benefits is developing a viable reference technology base that will permit engines to operate at substantially higher overall pressure ratios and bypass ratios. Results have pointed the direction for future research and a comprehensive program plan for achieving this was formulated. The next major step is initiating the program effort that will convert the advanced technologies into the expected benefits. Author

N90-28566*# Pratt and Whitney Aircraft, East Hartford, CT. Engineering Div.
ENERGY EFFICIENT ENGINE INTEGRATED CORE/LOW SPOOL TEST HARDWARE DESIGN REPORT
John W. Bisset and David C. Howe Mar. 1983 223 p
(Contract NAS3-20646)
(NASA-CR-168137; NAS 1.26:168137; PWA-5594-231) Avail: NTIS HC A10/MF A02 CSCL 21E

The Energy Efficient Engine Program is designed to identify and verify the technology required to significantly lower fuel consumption and operating cost for future commercial gas turbine engines. A major task that was completed under this program is the design and analysis of test hardware for the integrated core/low spool, which is a test simulation of the conceptual study engine defined to meet performance, economic and environmental goals. An evaluation and verification of critical technologies is intended in a full engine operating environment. The design and results of design-related analyses for the integrated core/low spool and its subsystems are described. The design effort included a definition of the engine, major components, internal and external subsystems, test ducting, and test instrumentation. Various analytical representations, in addition to results acquired from supporting component rig and subscale model tests, were used to verify aerodynamic and structural design concepts as well as to predict performance. Author

N90-28567*# Pratt and Whitney Aircraft, East Hartford, CT. Engineering Div.
ENERGY EFFICIENT ENGINE PIN FIN AND CERAMIC COMPOSITE SEGMENTED LINER COMBUSTOR SECTOR RIG TEST REPORT
D. J. Dubiel, R. P. Lohmann, S. Tanrikut, and P. M. Morris Sep. 1986 218 p
(Contract NAS3-20646)
(NASA-CR-179534; NAS 1.26:179534; PWA-5594-333; LC-86-23) Avail: NTIS HC A10/MF A02 CSCL 21E

Under the NASA-sponsored Energy Efficient Engine program, Pratt and Whitney has successfully completed a comprehensive test program using a 90-degree sector combustor rig that featured an advanced two-stage combustor with a succession of advanced segmented liners. Building on the successful characteristics of the first generation counter-parallel Finwall cooled segmented liner, design features of an improved performance metallic segmented liner were substantiated through representative high pressure and temperature testing in a combustor atmosphere. This second generation liner was substantially lighter and lower in cost than the predecessor configuration. The final test in this series provided an evaluation of ceramic composite liner segments in a representative combustor environment. It was demonstrated that the unique properties of ceramic composites, low density, high fracture toughness, and thermal fatigue resistance can be advantageously exploited in high temperature components. Overall, this Combustor Section Rig Test program has provided a firm basis for the design of advanced combustor liners. Author

N90-28568*# Pratt and Whitney Aircraft, East Hartford, CT. Engineering Div.
ENERGY EFFICIENT ENGINE: COMBUSTOR COMPONENT PERFORMANCE PROGRAM
D. J. Dubiel Sep. 1986 53 p
(Contract NAS3-20646)
(NASA-CR-179533; NAS 1.26:179533; PWA-5594-329) Avail: NTIS HC A04/MF A01 CSCL 21E

The results of the Combustor Component Performance analysis as developed under the Energy Efficient Engine (EEE) program are presented. This study was conducted to demonstrate the aerothermal and environmental goals established for the EEE program and to identify areas where refinements might be made to meet future combustor requirements. In this study, a full annular combustor test rig was used to establish emission levels and combustor performance for comparison with those indicated by the supporting technology program. In addition, a combustor sector test rig was employed to examine differences in emissions and liner temperatures obtained during the full annular performance and supporting technology tests. Author

N90-28569*# Pratt and Whitney Aircraft, East Hartford, CT. Engineering Div.
ENERGY EFFICIENT ENGINE: CONTROL SYSTEM PRELIMINARY DEFINITION REPORT
David C. Howe Sep. 1986 126 p
(Contract NAS3-20646)
(NASA-CR-179578; NAS 1.26:179578; PWA-5594-331) Avail: NTIS HC A07/MF A01 CSCL 21E

The object of the Control Preliminary Definition Program was to define a preliminary control system concept as a part of the Energy Efficient Engine program. The program was limited to a conceptual definition of a full authority digital electronic control system. System requirements were determined and a control system was conceptually defined to these requirements. Areas requiring technological development were identified and a plan was established for implementing the identified technological features, including a control technology demonstration. A significant element of this program was a study of the potential benefits of closed-loop active clearance control, along with laboratory tests of candidate clearance sensor elements for a closed loop system. Author

N90-28570*# Pratt and Whitney Aircraft, East Hartford, CT.
ENERGY EFFICIENT ENGINE: HIGH-PRESSURE COMPRESSOR TEST HARDWARE DETAILED DESIGN REPORT
David C. Howe and R. D. Marchant Mar. 1988 261 p
(Contract NAS3-20646)
(NASA-CR-180850; NAS 1.26:180850; PWA-5594-287) Avail: NTIS HC A12/MF A02 CSCL 21E

The objective of the NASA Energy Efficient Engine program is to identify and verify the technology required to achieve significant reductions in fuel consumption and operating cost for future commercial gas turbine engines. The design and analysis is documented of the high pressure compressor which was tested as part of the Pratt and Whitney effort under the Energy Efficient Engine program. This compressor was designed to produce a 14:1 pressure ratio in ten stages with an adiabatic efficiency of 88.2 percent in the flight propulsion system. The corresponding expected efficiency for the compressor component test rig is 86.5 percent. Other performance goals are a surge margin of 20 percent, a corrected flow rate of 35.2 kg/sec (77.5 lb/sec), and a life of 20,000 missions and 30,000 hours. Low loss, highly loaded airfoils are used to increase efficiency while reducing the parts count. Active clearance control and case trenches in abradable strips over the blade tips are included in the compressor component design to further increase the efficiency potential. The test rig incorporates variable geometry stator vanes in all stages to permit maximum flexibility in developing stage-to-stage matching. This

provision precluded active clearance control on the rear case of the test rig. Both the component and rig designs meet or exceed design requirements with the exception of life goals, which will be achievable with planned advances in materials technology.
Author

N90-28571# Air Force Human Resources Lab., Brooks AFB, TX.
SOURCE EMISSION TEST OF GAS TURBINE ENGINE TEST FACILITY, KELLY AFB, TX Final Report
Ronald W. Vaughn and Paul T. Scott Apr. 1990 44 p
(AD-A223869; AFOEHL-90-064EQ00094DEF) Avail: NTIS HC A03/MF A01 CSCL 24/1

Source emission testing was conducted on the F-15 JFS and GT CP 85-180 gas turbine engines for particulates, carbon monoxide, total hydrocarbons, sulfur dioxide and nitrogen oxide. The present Gas Turbine Engine Test Facility is grandfathered per Texas Air Control Board and Federal (40CFR60) Regulations. The data will be used to initiate a permit application for a new Gas Turbine Engine Test Facility. GRA

N90-28572# Naval Ship Research and Development Center, Bethesda, MD. Propulsion and Auxiliary Systems Dept.
FLOW COUPLING BETWEEN A ROTOR AND A STATOR IN TURBOMACHINERY
Yu-Tai Lee, Ivan Chen Wen Jiang, and Thomas W. Bein Apr. 1990 33 p
(AD-A223882; DTRC/PAS-90/15) Avail: NTIS HC A03/MF A01 CSCL 20/4

Successful turbomachine design requires detailed information about flow characteristics in order to predict the performance of a candidate geometry. The design needs information about the complex interaction between the blade rows when multistage blade rows are considered. A three-dimensional steady potential-flow code for a single blade row has been developed, where integral equations were derived to model the solid surfaces and the inlet condition for both external and internal flows with rotating or nonrotating lifting blades. Global iterations for the surface-panel source densities and the vortex strengths were used in conjunction with a Neumann iteration for solving the integral equations. In this paper, two numerical coupling procedures between the rotor and the stator are described. The phenomena of flow interaction between the rotor and the stator are studied and two test cases are presented. The performance of a vaneaxial fan is predicted using this procedure and the results indicate that the present numerical coupling procedure can be used by designers to select optimal blade shapes. GRA

N90-28573# Naval Research Lab., Washington, DC. Lab. for Computational Physics and Fluid Dynamics.
NUMERICAL SIMULATIONS OF FLOWFIELDS IN A CENTRAL-DUMP RAMJET COMBUSTOR. 3: EFFECTS OF CHEMISTRY Interim Report
Kazhikathra Kailasanath, John H. Gardner, Jay P. Boris, and Elaine S. Oran 23 Jul. 1990 52 p Sponsored by ONR, Arlington, VA and Naval Air Systems Command
(AD-A224145; NRL-MR-6682) Avail: NTIS HC A04/MF A01 CSCL 21/5

This report is the third in a series which presents the results of numerical simulations performed to isolate and study acoustic-vortex-chemical interactions in an idealized ramjet consisting of an axisymmetric inlet and combustor and a choked nozzle. Both reactive and nonreactive flows have been simulated. The nonreactive flow calculations show complex interactions among the natural instability frequency of the shear layer at the inlet-combustor junction and the acoustics of both the inlet and the combustor. The entire flow oscillates at a low frequency which corresponds to that of a quarter-mode in the inlet. For the reactive flow cases studied, energy release alters the flow field substantially. Energy release in a large vortex is in phase with the pressure oscillation over a substantial region of the combustor and results in the observed amplification of the low-frequency oscillations and leads to combustion instability. The large pressure oscillation also modifies the vortex shedding process. GRA

N90-28574# Universal Technology Corp., Dayton, OH.
STOVL FIGHTER PROPULSION RELIABILITY, MAINTAINABILITY, AND SUPPORTABILITY CHARACTERIZATION Final Report, Oct. 1988 - Sep. 1989
Randolph W. Spratt Mar. 1990 120 p
(Contract F33615-88-C-2823; AF Proj. 3066)
(AD-A224221; WRDC-TR-89-2150) Avail: NTIS HC A06/MF A01 CSCL 21/5

This report contains information on the Reliability, Maintainability and Supportability (RM and S) of STOVL fighter propulsion systems. Five STOVL propulsion concepts were investigated and evaluated. A RM and S evaluation method was developed for this project. This method could not be used to rate the propulsion concepts since the components of the propulsion systems had not been fully defined. An alternative method was to rank order the propulsion system for RM and S. Subjective ratings were given to the major components of each propulsion concept. These ratings were then weighted and summed to determine rank order of the propulsion concepts. Propulsion components critical to the RM and S ratings were identified. Recommendations for future RM and S study efforts are included in the report. GRA

N90-28615*# Rockwell International Corp., Canoga Park, CA. Rocketdyne Div.
BLADE TIP RUBBING STRESS PREDICTION
Gerald A. Brusher, Gary A. Davis, and Daniel M. Shea *In* NASA, Marshall Space Flight Center, Advanced Earth-to-Orbit Propulsion Technology 1988, Volume 1 Sep. 1988 p 43-53 (For primary document see N90-28611 23-20)
(Contract NAS8-36361)
Avail: NTIS HC A99/MF E06 CSCL 21E

08 AIRCRAFT STABILITY AND CONTROL

Includes aircraft handling qualities; piloting; flight controls; and autopilots.

For related information see also *05 Aircraft Design, Testing and Performance.*

N90-28575 Texas A&M Univ., College Station.
ACTIVE CONTROL OF FLEXIBLE STRUCTURES Ph.D. Thesis
Slim Choura 1989 223 p
Avail: Univ. Microfilms Order No. DA9015472

The active control of vibratory motion in distributed parameter systems (DPS) caused by an initial disturbance is considered. Control strategies that eliminate such vibrations in a finite time using a single fixed actuator are proposed. Also explored is possible elimination of vibratory motions by moving actuators. An open loop control strategy based on minimum energy control elminates totally in finite time a predetermined set of vibratory modes using a single force actuator. The proposed minimum energy strategy compares well with the true minimum time achieved by a bang-bang control and does not have any intermediate discontinuities that are present in a bang-bang control. It can only have two discontinuities at most. A combination of feedforward and feedback provides robustness. The feedforward is based on the minimum energy solution. The novel control strategies developed yield results that are comparable if not better than those achievable by conventional control strategies. A simple experiment supports the viability of the proposed strategies. Also explored is a novel concept for actively controlling DPS by moving force actuators. The elimination of a predetermined set of vibratory modes, by one or more moving force actuators is possible. Two such control strategies are proposed. The first strategy uses a finite number of distinct actuators to control an equal number of critical modes. The second uses only a single actuator to control a finite number of critical modes and is based on energy functions.
Dissert. Abstr.

N90-28576# Aeronautical Research Labs., Melbourne (Australia).
A FLIGHT DYNAMIC MODEL OF AIRCRAFT SPINNING
S. D. Hill and C. A. Martin Jun. 1990 45 p
(AR-005-600; ARL-Flight-Mech-R-180) Avail: NTIS HC A03/MF A01

A flight dynamic model of aircraft spinning was developed. It is capable of simulating aircraft behavior from conventional flight through stall, spin entry, steady spin, and spin recovery. A data base storage technique has been used to provide the six force and moment coefficients required. The data base embodies rotary balance data measured for a basic training aircraft plus computed small disturbance data calculated from a line vortex model.
Author

N90-28577# National Aeronautical Lab., Bangalore (India). Computational and Theoretical Fluids Dynamics Div.
A CONCEPTUAL FRAMEWORK FOR FIGHTER FLIGHT CONTROL SYSTEMS
Rajendra K. Bera Apr. 1990 28 p
(PD-CF-9009) Avail: NTIS HC A03/MF A01

A conceptual framework for the design of a combatworthy flight control system for air-superiority fighters is set down. An attempt is made to foresee possible pitfalls in attempting to implement a full-authority digital flight control system in the present Indian context and to suggest a viable means of circumventing them.
Author

N90-28578*# National Aeronautics and Space Administration. Langley Research Center, Hampton, VA.
AERODYNAMIC PARAMETERS OF HIGH-ANGLE-OF ATTACK RESEARCH VEHICLE (HARV) ESTIMATED FROM FLIGHT DATA
Vladislav Klein, Thomas R. Ratvasky, and Brent R. Cobleigh (George Washington Univ., Hampton, VA.) Aug. 1990 68 p
(NASA-TM-102692; NAS 1.15:102692) Avail: NTIS HC A04/MF A01 CSCL 01C

Aerodynamic parameters of the High-Angle-of-Attack Research Aircraft (HARV) were estimated from flight data at different values of the angle of attack between 10 degrees and 50 degrees. The main part of the data was obtained from small amplitude longitudinal and lateral maneuvers. A small number of large amplitude maneuvers was also used in the estimation. The measured data were first checked for their compatibility. It was found that the accuracy of air data was degraded by unexplained bias errors. Then, the data were analyzed by a stepwise regression method for obtaining a structure of aerodynamic model equations and least squares parameter estimates. Because of high data collinearity in several maneuvers, some of the longitudinal and all lateral maneuvers were reanalyzed by using two biased estimation techniques, the principal components regression and mixed estimation. The estimated parameters in the form of stability and control derivatives, and aerodynamic coefficients were plotted against the angle of attack and compared with the wind tunnel measurements. The influential parameters are, in general, estimated with acceptable accuracy and most of them are in agreement with wind tunnel results. The simulated responses of the aircraft showed good prediction capabilities of the resulting model.
Author

N90-28579# Defence Research Establishment Suffield, Ralston (Alberta).
A SENSOR STABILIZATION/TRACKING SYSTEM FOR UNMANNED AIR VEHICLES
Jean-Paul DeCruyenaere May 1990 45 p
(AD-A224008; DRES-SM-1321) Avail: NTIS HC A03/MF A01 CSCL 01/3

A control algorithm for the automatic steering of an imaging sensor has been developed at DRES. Both the tracking of a fixed ground point and the stabilization of the sensor are addressed. This system has been implemented in large part with pre-existing hardware and software in our unmanned air vehicles (UAV) system. This report describes the theoretical basis of the system as well as detailing the issues concerning the development of a working prototype.
GRA

N90-28515# British Aerospace Public Ltd. Co., Lancashire (England). Military Aircraft Div.
COMBAT AIRCRAFT CONTROL REQUIREMENTS
T. B. Saunders and J. H. Tucker *In* AGARD, Aerodynamics of Combat Aircraft Controls and of Ground Effects Apr. 1990 20 p (For primary document see N90-28513 23-05)
Copyright Avail: NTIS HC A15/MF A02; Non-NATO Nationals requests available only from AGARD/Scientific Publications Executive

N90-28516*# National Aeronautics and Space Administration. Langley Research Center, Hampton, VA.
CONTROL RESEARCH IN THE NASA HIGH-ALPHA TECHNOLOGY PROGRAM
William P. Gilbert, Luat T. Nguyen, and Joseph Gera (National Aeronautics and Space Administration. Hugh L. Dryden Flight Research Facility, Edwards, CA.) *In* AGARD, Aerodynamics of Combat Aircraft Controls and of Ground Effects Apr. 1990 18 p (For primary document see N90-28513 23-05)
Copyright Avail: NTIS HC A15/MF A02; Non-NATO Nationals requests available only from AGARD/Scientific Publications Executive CSCL 01C

N90-28517# Eidetics International, Inc., Torrance, CA.
COMBAT AIRCRAFT CONTROL REQUIREMENTS FOR AGILITY
Joseph R. Chody, John Hodgkinson, and Andrew M. Skow *In* AGARD, Aerodynamics of Combat Aircraft Controls and of Ground Effects Apr. 1990 21 p (For primary document see N90-28513 23-05)
Copyright Avail: NTIS HC A15/MF A02; Non-NATO Nationals requests available only from AGARD/Scientific Publications Executive

N90-28518# Aeronautica Macchi S.p.A., Varese (Italy).
AERODYNAMIC CONTROL DESIGN: EXPERIENCE AND RESULTS AT AERMACCHI
B. Bufacchi, M. Lucchesini, L. Manfriani, and E. Valtorta *In* AGARD, Aerodynamics of Combat Aircraft Controls and of Ground Effects Apr. 1990 13 p (For primary document see N90-28513 23-05)
Copyright Avail: NTIS HC A15/MF A02; Non-NATO Nationals requests available only from AGARD/Scientific Publications Executive

N90-28521*# National Aeronautics and Space Administration. Langley Research Center, Hampton, VA.
INNOVATIVE CONTROL CONCEPTS AND COMPONENT INTEGRATION FOR A GENERIC SUPERCRUISE FIGHTER
Bret A. Marks (McDonnell Aircraft Co., Saint Louis, MO.) and David E. Hahne *In* AGARD, Aerodynamics of Combat Aircraft Controls and of Ground Effects Apr. 1990 14 p (For primary document see N90-28513 23-05)
Copyright Avail: NTIS HC A15/MF A02; Non-NATO Nationals requests available only from AGARD/Scientific Publications Executive CSCL 01C

N90-28522*# National Aeronautics and Space Administration. Langley Research Center, Hampton, VA.
DEVELOPMENT OF NON-CONVENTIONAL CONTROL METHODS FOR HIGH ANGLE OF ATTACK FLIGHT USING VORTEX MANIPULATION
Gerald N. Malcolm, T. Terry Ng, Liane C. Lewis (Eidetics International, Inc., Torrance, CA.), and Daniel G. Murri *In* AGARD, Aerodynamics of Combat Aircraft Controls and of Ground Effects Apr. 1990 17 p Previously announced in IAA as A89-47653 (For primary document see N90-28513 23-05)
(Contract F33615-86-C-3623)
Copyright Avail: NTIS HC A15/MF A02; Non-NATO Nationals

requests available only from AGARD/Scientific Publications Executive CSCL 01C

N90-28525# London Univ. (England).
UNSTEADY AERODYNAMICS OF CONTROLS
G. J. Hancock and D. G. Mabey (Royal Aerospace Establishment, Bedford, England) *In* AGARD, Aerodynamics of Combat Aircraft Controls and of Ground Effects Apr. 1990 17 p (For primary document see N90-28513 23-05)
Copyright Avail: NTIS HC A15/MF A02; Non-NATO Nationals requests available only from AGARD/Scientific Publications Executive

09 RESEARCH AND SUPPORT FACILITIES (AIR)

Includes airports, hangars and runways; aircraft repair and overhaul facilities; wind tunnels; shock tubes; and aircraft engine test stands.

For related information see also *14 Ground Support Systems and Facilities (Space).*

N90-28580# National Academy of Sciences - National Research Council, Washington, DC. Building Research Board.
PROCEEDINGS OF A WORKSHOP ON FUTURE AIRPORT PASSENGER TERMINALS
A. C. Lemer 1989 45 p Workshop held in Washington, DC, 6-7 Jun. 1989; sponsored in part by Building Research Board and the Transportation Research Board
(PB90-213620) Avail: NTIS HC A03/MF A01 CSCL 01E

A report of a workshop on future airport passenger terminals, sponsored by the Building Research Board in cooperation with the Transportation Research held in the Washington Metropolitan Area Transit Authority (WMATA) is given. An introduction is given to the factors any jurisdiction has to look at when investing in transportation facilities. After reviewing the funding mechanisms and debt service already being borne by WMATA to set the context, the financial condition of each of the WMATA major funding contributors is examined in detail. Each jurisdiction's writeup includes its credit rating from Moody's and Standard and Poor's, its current mass transit service revenue commitment to the transit system, its economic situation, its current tax base and taxing rate restrictions, the composition of its general fund, its borrowing history (both in terms of amounts borrowed and from whom), and projected expenditures. Although oriented toward large projects, the document can introduce assessment of ability to pay to governments of any size. Author

N90-28581# Federal Aviation Administration, Washington, DC.
DEVELOPMENT OF ACCEPTANCE PLANS FOR AIRPORT PAVEMENT MATERIALS. VOLUME 1: DEVELOPMENT Final Report, 1 Oct. 1986 - 31 May 1990
John E. Foster and Kamran Majidzadeh (Resource International, Inc., Columbus, OH.) May 1990 197 p
(Contract DTFA01-86-Y-01046)
(DOT/FAA/RD-90/15) Avail: NTIS HC A09/MF A02

Statistically based acceptance/rejection plans and payment adjustment schedules were developed for five specifications: (1) excavation and embankment; (2) crushed aggregate base course; (3) cement treated base course; (4) econocrete subbase course; and (5) portland cement concrete pavement. The statistical analysis of data, development of payment adjustment plans (PAP), and development of PAP computer diskette system are presented. Test data used for this effort were collected from field sources. The developed PAP formulas, schedules, and computer diskette system were verified using new pavement construction projects. Author

N90-28582# Soil and Materials Engineers, Inc., Ann Arbor, MI.
DEVELOPMENT OF A THICKNESS DESIGN PROCEDURE FOR STABILIZED LAYERS UNDER RIGID AIRFIELD PAVEMENTS Final Report, May 1987 - May 1990
Starr D. Kohn and Chaouki A. Gemayel May 1990 150 p
(Contract DTFA01-81-Y-10555)
(DOT/FAA/RD-90/22) Avail: NTIS HC A07/MF A01

The results of an analysis of two rigid layer pavement systems are presented. The outcome of the study resulted in the development of a design procedure which can account for the materials properties of the stabilized materials layer. The study employed the use of elastic layer theory and regression analysis to predict the interior stress under aircraft loading. Equivalent interior stress is used as the design criteria such that a single layer rigid pavement on subgrade is equated to a two layer system with a cement-treated base course and a portland cement concrete surface. The comparison of the developed procedures to the existing procedures show both allowable decreases and increases in the thickness of the portland cement concrete layer. The design procedure is an iterative process and was computerized. Author

N90-28583 Southampton Univ. (England).
THREE-DIMENSIONAL MODEL TESTING IN THE TRANSONIC SELF-STREAMLINING WIND TUNNEL Ph.D. Thesis
Graeme Neal 1988 327 p
Avail: Univ. Microfilms Order No. BRDX88081

The wall interference effects present on three-dimensional models during wind tunnel testing are difficult to correct using post-test model data correction methods. Further, at transonic speeds, with the use of ventilated test sections these corrections become complex to apply and inaccurate. The high quality of wind tunnel testing that is required today means that such methods are no longer satisfactory. The flexible walled wind tunnel has in recent years shown its ability to obtain two-dimensional aerofoil data free from the effects of wall boundary restraint. The use of the two-dimensional Transonic Self-Streamlining Wind Tunnel was extended to the relief of wall interference effects on three-dimensional models. The compromise of using only two-wall single curvature movement avoids the problems that are inherent with the additional complexity of fully three-dimensional adaptive tunnels. A method of assessing the wall-induced interference velocity components from tunnel boundary pressure data, without reference to the model, was developed and validated against other wall interference assessment methods. The algorithm, suitable for use in adaptive tunnels, is used with a wall movement influence coefficient method of wall contour prediction resulting in the apparent removal of wall interference effects along a streamlining target line. A calibrated force-balance wing-body model was used to demonstrate the first successful streamlining around a three-dimensional model in the Transonic Self-Streamlining Wind Tunnel. Dissert. Abstr.

N90-28584# Federal Aviation Administration, Atlantic City, NJ.
ANALYSIS OF HELIPORT ENVIRONMENTAL DATA, INTRACOASTAL CITY
Rosanne M. Weiss Jul. 1990 81 p
(Contract FAA-T0701U)
(DOT/FAA/CT-TN89/43) Avail: NTIS HC A05/MF A01

During a 2 day period in May 1988, heliport environmental data were collected at Petroleum Helicopter Incorporated's Heliport in Intracoastal City, LA. The purpose of this data collection activity was to gather measurements of rotorwash at a heavy used heliport frequented by larger helicopters with higher gross weights then observed during previous data collection activities. During this operation, ten wind vector transmitters were situated at various locations around the facility in order to gather information to describe the rotorwash induced wind speed and wind direction changes. The results of this data collection activity are documented. The data collection and analysis methodology are explained. Graphical presentations of the heliport environment and or rotorwash induced wind speeds and wind speed and direction changes are included. The Concepts Analysis Division Report, ACD-330-89-10, Analysis of Heliport Environment Data, Intracoastal City, LA, contains the heliport wind speed and direction plots for each flight. The results of this study will be considered in future modifications of the Federal Aviation Administration (FAA) Heliport Design Advisory Circular (AC) 150/5390-2. Author

N90-28585# European Space Agency, Paris (France).
THE EQUIPMENT FOR MASS FLOW MEASUREMENTS IN THE LOW-SPEED WIND TUNNEL AT DFVLR IN BRUNSWICK (FEDERAL REPUBLIC OF GERMANY)
Reinhard Friedrichs (Deutsche Forschungs- und Versuchsanstalt fuer Luft- und Raumfahrt, Brunswick, Germany, F.R.) May 1990 103 p Transl. into ENGLISH of Die Durchsatzmesseinrichtung des Niedergeschwindigkeits- Windkanals der DFVLR in Braunschweig (Brunswick, Fed. Republic of Germany, DFVLR), Dec. 1987 54 p Original language document was announced as N88-27212
(ESA-TT-1125; DFVLR-Mitt-88-02; ETN-90-97555) Avail: NTIS HC A06/MF A01

The mass flow measurement equipment in the low speed wind tunnel is used for the accurate determination of the air mass flow in engine and intake models, for which the intake parameters can be determined simultaneously in static tests. The plant consists essentially of a vacuum tank for accommodating the models and a standard nozzle or orifice plate; the tank is connected to the existing induction pipe of the DEMAG vacuum pumps. The plant is located in the cellar underneath the test hall so that the normal wind tunnel test work is not affected. In order to ensure the accuracy of the mass flow measurements, the standard nozzle and orifice plate were calibrated, by means of choked nozzles, over their total measurement range of 0.5 to 2.5 kg/s. Test results on intake are given as an example. ESA

N90-28586# Naval Postgraduate School, Monterey, CA.
DEVELOPMENT AND TESTING OF RAPID REPAIR METHODS FOR WAR DAMAGED RUNWAYS M.S. Thesis - Florida Univ.
Paul A. Soares 1990 164 p
(AD-A223970) Avail: NTIS HC A08/MF A01 CSCL 01/5

A need exists to establish a main runway repair method that is rapid, effective, and easy to install. The primary objective of this research was to develop a rapid runway repair method that could be implemented by the armed forces within their current resources. A method of mixing fine aggregate, coarse aggregate, cement, and water was developed using soil stabilizing equipment. The required testslab thickness was selected from known slab thicknesses in existence today. The mix design was developed for a roller compacted mix. The mix design was tested in a laboratory for compressive, tensile and flexural strength. Simplified relationships were developed between the degree of compaction versus the strength of concrete. Moist Rodded Unit Weight tests were performed on the fine and coarse aggregates to determine a pre-mix unit weight of each material. The mix proportions by weight of fine aggregate, coarse aggregate, and cement were converted to pre-mix volumes. An angle of repose test was performed on the fine and coarse aggregates. The pre-mix volumes were converted to layer thicknesses. A field test procedure was developed to conduct a large scale test of the method. A large scale test was performed. GRA

N90-28613*# National Aeronautics and Space Administration. Marshall Space Flight Center, Huntsville, AL.
OXYGEN/HYDROGEN TECHNOLOGY TEST BED STATUS UPDATE
J. S. Richards *In its* Advanced Earth-to-Orbit Propulsion Technology 1988, Volume 1 Sep. 1988 p 21-28 (For primary document see N90-28611 23-20)
Avail: NTIS HC A99/MF E06 CSCL 14B

12 ASTRONAUTICS (GENERAL)

For extraterrestrial exploration see *91 Lunar and Planetary Exploration.*

No abstracts in this category.

13 ASTRODYNAMICS

Includes powered and free-flight trajectories; and orbital and launching dynamics.

N90-28587 Georgia Inst. of Tech., Atlanta.
REAL TIME GUIDANCE AND PROPULSION CONTROL FOR SINGLE-STAGE-TO-ORBIT AIRBREATHING VEHICLES Ph.D. Thesis
John Eric Corban 1989 312 p
Avail: Univ. Microfilms Order No. DA9014857

Problems associated with on-board trajectory optimization and with the synthesis of guidance laws are addressed for ascent to low-Earth-orbit of an air-breathing, single-stage-to-orbit vehicle. A multi-mode propulsion system is assumed which incorporates turbojet, ramjet, SCRAMJET, and rocket engines. An energy state approximation is applied to a four-state dynamic model for flight of a point mass over a spherical non-rotating Earth. An algorithm for generating fuel-optimal climb profiles is derived via singular perturbation theory. This algorithm results from application of the minimum principle to a low order dynamic model that includes general functional dependence on angle of attack and a component of thrust normal to the flight path. Maximum dynamic pressure and maximum aerodynamic heating rate constraints are considered in addition to acceleration limits. Switching conditions are derived which, under appropriate assumptions, govern optimal transition from one propulsion mode to another. The use of bank angle to modulate the magnitude of the vertical component of lift is shown to improve the index of performance slightly. A nonlinear transformation technique is employed to derive a feedback controller for tracking the computed trajectory. Numerical results illustrate the nature of the resulting fuel-optimal climb paths and the performance of the feedback control law. Dissert. Abstr.

14 GROUND SUPPORT SYSTEMS AND FACILITIES (SPACE)

Includes launch complexes, research and production facilities; ground support equipment, e.g., mobile transporters; and simulators.

For related information see also *09 Research and Support Facilities (Air).*

N90-28588*# National Aeronautics and Space Administration. Marshall Space Flight Center, Huntsville, AL.
MICROGRAVITY SCIENCE AND APPLICATIONS: APPARATUS AND FACILITIES
Jan. 1989 108 p
(NASA-TM-101892; NAS 1.15:101892) Avail: NTIS HC A06/MF A01 CSCL 14B

NASA support apparatus and facilities for microgravity research are summarized in fact sheets. The facilities are ground-based simulation environments for short-term experiments, and the shuttle orbiter environment for long duration experiments. The 17 items of the microgravitational experimental apparatus are described. Electronic materials, alloys, biotechnology, fluid dynamics and transport phenomena, glasses and ceramics, and combustion science are among the topics covered. Author

15 LAUNCH VEHICLES AND SPACE VEHICLES

Includes boosters; operating problems of launch/space vehicle systems; and reusable vehicles.

For related information see also *20 Spacecraft Propulsion and Power.*

No abstracts in this category.

16 SPACE TRANSPORTATION

Includes passenger and cargo space transportation, e.g., shuttle operations; and space rescue techniques.

For related information see also *03 Air Transportation and Safety* and *18 Spacecraft Design, Testing and Performance.* For space suits see *54 Man/System Technology and Life Support.*

N90-28589*# National Aeronautics and Space Administration. Langley Research Center, Hampton, VA.
SHUTTLE TO SHUTTLE 2: SUBSYSTEM WEIGHT REDUCTION POTENTIAL (ESTIMATED 1992 TECHNOLOGY READINESS DATE)
Ian O. MacConochie May 1988 54 p
(NASA-TM-89114; NAS 1.15:89114) Avail: NTIS HC A04/MF A01 CSCL 22B

The objective of this study was to make estimates of the weight savings that might be realized on all the subsystems on an advanced rocket-powered shuttle (designated Shuttle 2) by using advanced technologies having a projected maturity date of 1992. The current Shuttle with external tank was used as a baseline from which to make the estimates of weight savings on each subsystem. The subsystems with the greatest potential for weight reduction are the body shell and the thermal protection system. For the body shell, a reduction of 5.2 percent in the weight of the vehicle at main engine cutoff is projected through the application of new technologies, and an additional configuration-based reduction of 5 percent is projected through simplification of body shape. A reduction of 5 percent is projected for the thermal protection system through experience with the current Space Shuttle and the potential for reducing thermal protection system thicknesses in selected areas. Main propellant tanks are expected to increase slightly in weight. The main propulsion system is also projected to increase in weight because of the requirement to operate engines at derated power levels in order to accommodate one-engine-out capability. The projections for weight reductions through improvements in the remaining subsystems are relatively small. By summing all the technology factors, a projected reduction of 16 percent in the vehicle weight at main engine cutoff is obtained. By summarizing the configurational factors, a potential reduction of 12 percent in vehicle weight is obtained. Author

17 SPACE COMM., SPACECRAFT COMM., COMMAND & TRACKING

Includes telemetry; space communications networks; astronavigation and guidance; and radio blackout.

For related information see also *04 Aircraft Communications and Navigation* and *32 Communications and Radar.*

No abstracts in this category.

18 SPACECRAFT DESIGN, TESTING AND PERFORMANCE

Includes satellites; space platforms; space stations; spacecraft systems and components such as thermal and environmental controls; and attitude controls.

For life support systems see *54 Man/System Technology and Life Support.* For related information see also *05 Aircraft Design, Testing and Performance, 39 Structural Mechanics,* and *16 Space Transportation.*

N90-28590*# Science and Engineering Associates, Inc., Englewood, CO.
SPACE STATION CONTAMINATION MODELING Final Report
T. D. Gordon 15 Dec. 1989 17 p
(NASA Order H-80598-B)
(NASA-CR-183871; NAS 1.26:183871; SEA-D470-2) Avail: NTIS HC A03/MF A01 CSCL 22B

Current plans for the operation of Space Station Freedom allow the orbit to decay to approximately an altitude of 200 km before reboosting to approximately 450 km. The Space Station will encounter dramatically increasing ambient and induced environmental effects as the orbit decays. Unfortunately, Shuttle docking, which has been of concern as a high contamination period, will likely occur during the time when the station is in the lowest orbit. The combination of ambient and induced environments along with the presence of the docked Shuttle could cause very severe contamination conditions at the lower orbital altitudes prior to Space Station reboost. The purpose here is to determine the effects on the induced external environment of Space Station Freedom with regard to the proposed changes in altitude. The change in the induced environment will be manifest in several parameters. The ambient density buildup in front of ram facing surfaces will change. The source of such contaminants can be outgassing/offgassing surfaces, leakage from the pressurized modules or experiments, purposeful venting, and thruster firings. The third induced environment parameter with altitude dependence is the glow. In order to determine the altitude dependence of the induced environment parameters, researchers used the integrated Spacecraft Environment Model (ISEM) which was developed for Marshall Space Flight Center. The analysis required numerous ISEM runs. The assumptions and limitations for the ISEM runs are described. Author

N90-28591*# Howard Univ., Washington, DC. Dept. of Mechanical Engineering.
THE DYNAMICS AND CONTROL OF LARGE FLEXIBLE SPACE STRUCTURES - 13 Final Report
Peter M. Bainum, Feiyue Li, and Jianke Xu Sep. 1990 82 p
(Grant NsG-1414)
(NASA-CR-186930; NAS 1.26:186930) Avail: NTIS HC A05/MF A01 CSCL 22B

The optimal control of three-dimensional large angle maneuvers and vibrations of a Shuttle-mast-reflector system is considered. The nonlinear equations of motion are formulated by using Lagrange's formula, with the mast modeled as a continuous beam subject to three-dimensional deformations. Pontryagin's Maximum Principle is applied to the slewing problem, to derive the necessary conditions for the optimal controls, which are bounded by given saturation levels. The resulting two point boundary value problem is then solved by using the quasilinearization algorithm and the method of particular solutions. The study of the large angle maneuvering of the Shuttle-beam-reflector spacecraft in the plane of a circular earth orbit is extended to consider the effects of the structural offset connection, the axial shortening, and the gravitational torque on the slewing motion. Finally the effect of additional design parameters (such as related to additional payload requirement) on the linear quadratic regulator based design of an orbiting control/structural system is examined. Author

N90-28592*# Jet Propulsion Lab., California Inst. of Tech., Pasadena.
THE MAGELLAN VENUS EXPLORER'S GUIDE
Carolynn Young, ed. Aug. 1990 202 p
(Contract NAS7-918)
(NASA-CR-186968; NAS 1.26:186968; JPL-Publ-90-24) Avail: NTIS HC A10/MF A02 CSCL 22B

The Magellan radar-mapping mission to the planet Venus is described. Scientific highlights include the history of U.S. and Soviet missions, as well as ground-based radar observations, that have provided the current knowledge about the surface of Venus. Descriptions of the major Venusian surface features include controversial theories about the origin of some of the features. The organization of the Magellan science investigators into discipline-related task groups for data-analysis purposes is presented. The design of the Magellan spacecraft and the ability of its radar sensor to conduct radar imaging, altimetry, and radiometry measurements are discussed. Other topics report on

the May 1989 launch, the interplanetary cruise, the Venus orbit-insertion maneuver, and the in-orbit mapping strategy. The objectives of a possible extended mission emphasize the gravity experiment and explain why high-resolution gravity data cannot be acquired during the primary mission. A focus on the people of Magellan reveals how they fly the spacecraft and prepare for major mission events. Special items of interest associated with the Magellan mission are contained in windows interspersed throughout the text. Finally, short summaries describe the major objectives and schedules for several exciting space missions planned to take us into the 21st century. Author

N90-28593*# Jet Propulsion Lab., California Inst. of Tech., Pasadena.
AN AERONAUTICAL MOBILE SATELLITE EXPERIMENT External Report
T. C. Jedrey, K. I. Dessouky, and N. E. Lay 15 Aug. 1990 37 p
(Contract NAS7-918)
(NASA-CR-186971; NAS 1.26:186971; JPL-Publ-90-14; MSAT-X-163) Avail: NTIS HC A03/MF A01 CSCL 22B

The various activities and findings of a NASA/FAA/COMSAT/INMARSAT Collaborative aeronautical mobile satellite experiment are detailed. The primary objective of the experiment was to demonstrate and evaluate an advanced digital mobile satellite terminal developed at the Jet Propulsion Laboratory under the NASA Mobile Satellite Program. The experiment was a significant milestone for NASA/JPL, since it was the first test of the mobile terminal in a true mobile satellite environment. The results were also of interest to the general mobile satellite community because of the advanced nature of the technologies employed in the terminal. Author

N90-28594# Royal Aerospace Establishment, Farnborough (England).
SPACECRAFT CHARGING EFFECTS
G. L. Wrenn 6 Mar. 1990 15 p Presented at Solar Terrestrial Predictions Workshop, Sydney, Australia, 16-20 Oct. 1989
(RAE-TM-Space-375; BR113453; ETN-90-97529) Copyright Avail: NTIS HC A03/MF A01

The way in which spacecraft surfaces become electrostatically charged in their interactions with incident space radiations is described and consequential effects which can have dramatic impact on operations are discussed. An extensive chronicle of in-orbit anomalies gathered for geosynchronous satellites makes it possible to search for links between the timing and freqeuncy of these events, flux measurements of charging particles, and solar terrestrial sources. This is a difficult exercise, due to the scarcity of suitable data, but results from the ESA METEOSAT and MARECS satellites are presented to define the boundary conditions of the problem. Special consideration of differential charging and deep dielectric charging, with likely modes of breakdown, highlights the roles of energetic electrons, cold plasma concentration and secondary emission yields is given and recommended prevention techniques are outlined to stress the merit of improved solar-geomagnetic predictions. ESA

N90-28595# Sandia National Labs., Albuquerque, NM. Trident 2 Warhead Div.
PROCEDURES FOR DOE-NAVY EXCHANGE AND APPROVAL OF ENGINEERING INFORMATION AND MATERIAL MANAGEMENT REQUIRED FOR PRODUCTION OF W88-0/Mk5 RBA (REENTRY BODY ASSEMBLY)
Robert L. Alvis and Edward J. Barkocy Apr. 1990 41 p Revised
(Contract DE-AC04-76DP-00789)
(DE90-014763; SAND-85-2523-Rev-2) Avail: NTIS HC A03/MF A01

This report establishes the procedures whereby information pertaining to the W88-0/Mk5 RBA, Mk5 JTA, reentry body, and associated test equipment configurations and nonconformances will be exchanged and approved by the U.S. Navy and DOE agencies. Material management procedures common to the Navy and the DOE will be implemented according to the provisions agreed to and reported here. DOE

N90-28596*# National Aeronautics and Space Administration. Lewis Research Center, Cleveland, OH.
ATDRS PAYLOAD TECHNOLOGY RESEARCH AND DEVELOPMENT
G. Anzic, D. J. Connolly, G. Fujikawa, M. Andro, R. R. Kunath, and G. R. Sharp 1990 9 p Prepared for presentation at the IEEE Global Telecommunications Conference, San Diego, CA, 2-5 Dec. 1990; sponsored in part by IEEE
(NASA-TM-103256; E-5687; NAS 1.15:103256) Avail: NTIS HC A02/MF A01 CSCL 22B

Four technology development tasks were chosen to reduce (or at least better understand) the technology risks associated with proposed approaches to Advanced Tracking and Data Relay Satellite (ATDRS). The four tasks relate to a Tri-Band Antenna feed system, a Digital Beamforming System for the S Band Multiple Access System (SMA), an SMA Phased Array Antenna, and a Configuration Thermal/Mechanical Analysis task. The objective, approach, and status of each are discussed. Author

N90-28597*# National Aeronautics and Space Administration. Marshall Space Flight Center, Huntsville, AL.
SPACE STATION FREEDOM PRESSURIZED ELEMENT INTERIOR DESIGN PROCESS
George D. Hopson, John Aaron, and Richard L. Grant (Boeing Aerospace Co., Huntsville, AL.) 1990 29 p
(Contract NAS8-50000)
(NASA-CR-181297; NAS 1.26:181297) Avail: NTIS HC A03/MF A01 CSCL 22B

The process used to develop the on-orbit working and living environment of the Space Station Freedom has some very unique constraints and conditions to satisfy. The goal is to provide maximum efficiency and utilization of the available space, in on-orbit, zero G conditions that establishes a comfortable, productive, and safe working environment for the crew. The Space Station Freedom on-orbit living and working space can be divided into support for three major functions: (1) operations, maintenance, and management of the station; (2) conduct of experiments, both directly in the laboratories and remotely for experiments outside the pressurized environment; and (3) crew related functions for food preparation, housekeeping, storage, personal hygiene, health maintenance, zero G environment conditioning, and individual privacy, and rest. The process used to implement these functions, the major requirements driving the design, unique considerations and constraints that influence the design, and summaries of the analysis performed to establish the current configurations are described. Sketches and pictures showing the layout and internal arrangement of the Nodes, U.S. Laboratory and Habitation modules identify the current design relationships of the common and unique station housekeeping subsystems. The crew facilities, work stations, food preparation and eating areas (galley and wardroom), and exercise/health maintenance configurations, waste management and personal hygiene area configuration are shown. U.S. Laboratory experiment facilities and maintenance work areas planned to support the wide variety and mixtures of life science and materials processing payloads are described. Author

N90-28598*# National Aeronautics and Space Administration. Langley Research Center, Hampton, VA.
TRANSFORMATIONAL PART-COUNT IN LAYERED OCTAHEDRAL-TETRAHEDRAL TRUSS CONFIGURATIONS
Haresh Lalvani (Joint Inst. for Advancement of Flight Sciences, Hampton, VA.) Aug. 1990 20 p
(NASA-TM-102635; NAS 1.15:102635) Avail: NTIS HC A03/MF A01 CSCL 22B

The number of component part (nodes, struts and panels) termed part count, is an important factor in the design, manufacture, and assembly of modular space structures. Part count expressions are presented for a variety of profiles derived from the layered octahedral-tetrahedral truss configuration. Referred to as the

tetrahedral truss in the NASA projects, this specific geometry has been used in several missions. The general expressions presented here transforms to others as one profile changes to another. Such transformational part count relations provide a measure of flexibility and generality, and may be useful when dealing with a wider range of geometric configurations. Author

19 SPACECRAFT INSTRUMENTATION

For related information see also *06 Aircraft Instrumentation* and *35 Instrumentation and Photography.*

No abstracts in this category.

20 SPACECRAFT PROPULSION AND POWER

Includes main propulsion systems and components, e.g., rocket engines; and spacecraft auxilliary power sources.

For related information see also *07 Aircraft Propulsion and Power, 28 Propellants and Fuels, 44 Energy Production and Conversion,* and *15 Launch Vehicles and Space Vehicles.*

N90-28599*# Martin Marietta Corp., New Orleans, LA. Manned Space Systems.
LIQUID ROCKET BOOSTER (LRB) FOR THE SPACE TRANSPORTATION SYSTEM (STS) SYSTEMS STUDY. VOLUME 1: EXECUTIVE SUMMARY
Mar. 1989 55 p
(Contract NAS8-37136)
(NASA-CR-183822; NAS 1.26:183822) Avail: NTIS HC A04/MF A01 CSCL 21H

The feasibility of replacing the Space Transportation System (STS) Solid Rocket Boosters (SRBs) with Liquid Rocket Boosters (LRBs) was studied. Feasibility required acceptable technical risk, program costs, and a program plan which supports STS requirements. Three major goals were identified to direct booster design and operation: increased STS safety and reliability; STS/LRB integration with minimum impact; and increased STS performance. Two booster engine designs were studied. The first engine design was a turbopump-fed engine with state-of-the-art design, and the second was a pressure-fed engine which might provide a lower cost alternative to the pump-fed concept. Both booster concepts were carried through to completion of conceptual design and all system impacts and program costs were identified. Applications for LRB use in the Advanced Launch System (ALS) program were studied using the pump-fed LRB baseline concept and variations on the baseline concept. Support for the Pressure-Fed Booster Test Bed (PFBTB) included test program planning and costs and technical support. Author

N90-28600*# Martin Marietta Corp., New Orleans, LA. Manned Space Systems.
LIQUID ROCKET BOOSTER (LRB) FOR THE SPACE TRANSPORTATION SYSTEM (STS) SYSTEMS STUDY, VOLUME 2 Final Report
Mar. 1989 301 p
(Contract NAS8-37136)
(NASA-CR-183786; NAS 1.26:183786) Avail: NTIS HC A14/MF A02 CSCL 21H

The Liquid Rocket Booster (LRB) Systems Definition Handbook presents the analyses and design data developed during the study. The Systems Definition Handbook (SDH) contains three major parts: the LRB vehicles definition; the Pressure-Fed Booster Test Bed (PFBTB) study results; and the ALS/LRB study results. Included in this volume are the results of all trade studies; final configurations with supporting rationale and analyses; technology assessments; long lead requirements for facilities, materials, components, and subsystems; operational requirements and scenarios; and safety, reliability, and environmental analyses. B.G.

N90-28601*# Martin Marietta Corp., New Orleans, LA. Manned Space Systems.
LIQUID ROCKET BOOSTER (LRB) FOR THE SPACE TRANSPORTATION SYSTEM (STS) SYSTEMS STUDY. APPENDIX A: STRESS ANALYSIS REPORT FOR THE PUMP-FED AND PRESSURE-FED LIQUID ROCKET BOOSTER
Mar. 1989 56 p
(Contract NAS8-37136)
(NASA-CR-183787-App-A; NAS 1.26:183787-App-A) Avail: NTIS HC A04/MF A01 CSCL 21H

Pressure effects on the pump-fed Liquid Rocket Booster (LRB) of the Space Transportation System are examined. Results from the buckling tests; bending moments tests; barrel, propellant tanks, frame XB1513, nose cone, and intertank tests; and finite element examination of forward and aft skirts are presented. B.G.

N90-28602*# Martin Marietta Corp., New Orleans, LA. Manned Space Systems.
LIQUID ROCKET BOOSTER (LRB) FOR THE SPACE TRANSPORTATION SYSTEM (STS) SYSTEMS STUDY. APPENDIX B: LIQUID ROCKET BOOSTER ACOUSTIC AND THERMAL ENVIRONMENTS
Mar. 1989 50 p
(Contract NAS8-37136)
(NASA-CR-183788-App-B; NAS 1.26:183788-App-B; Remtech-RTN-186-02) Avail: NTIS HC A03/MF A01 CSCL 21H

The ascent thermal environment and propulsion acoustic sources for the Martin-Marietta Corporation designed Liquid Rocket Boosters (LRB) to be used with the Space Shuttle Orbiter and External Tank are described. Two designs were proposed: one using a pump-fed propulsion system and the other using a pressure-fed propulsion system. Both designs use LOX/RP-1 propellants, but differences in performance of the two propulsion systems produce significant differences in the proposed stage geometries, exhaust plumes, and resulting environments. The general characteristics of the two designs which are significant for environmental predictions are described. The methods of analysis and predictions for environments in acoustics, aerodynamic heating, and base heating (from exhaust plume effects) are also described. The acoustic section will compare the proposed exhaust plumes with the current SRB from the standpoint of acoustics and ignition overpressure. The sections on thermal environments will provide details of the LRB heating rates and indications of possible changes in the Orbiter and ET environments as a result of the change from SRBs to LRBs. Author

N90-28603*# Martin Marietta Corp., New Orleans, LA. Manned Space Systems.
LIQUID ROCKET BOOSTER (LRB) FOR THE SPACE TRANSPORTATION SYSTEM (STS) SYSTEMS STUDY. APPENDIX C: BATTERY REPORT FOR THE LIQUID ROCKET BOOSTER TVC ACTUATORS
Mar. 1989 7 p
(Contract NAS8-37136)
(NASA-CR-183789-App-C; NAS 1.26:183789-App-C) Avail: NTIS HC A02/MF A01 CSCL 21H

The actuators for control of engine valves and gimbals for a booster require 165 kW or more peak power at 270 volts direct current (VDC) during the 2 or 3 minutes of first stage ascent; other booster devices require much less power at 28 VDC. It is desired that a booster supply its own electrical power and satisfy redundancy requirements of the Solid Rocket Booster Shuttle, when applicable. The power of a Liquid Rocket Booster is therefore provided by two subsystems: Actuator Battery Power (270 VDC) Subsystem for the engine actuators, and Electrical Power and Distribution (28 VDC) Subsystem, to power everything else. Boosters will receive no electrical power from Orbiter, only

commands and data, according to current plans. It was concluded that nine 30 volt silver-zinc batteries-in-series be used to provide the 270 volt, 37 kW average (165 kW peak). Author

N90-28604*# Martin Marietta Corp., New Orleans, LA. Manned Space Systems.
LIQUID ROCKET BOOSTER (LRB) FOR THE SPACE TRANSPORTION SYSTEM (STS) SYSTEMS STUDY. APPENDIX D: TRADE STUDY SUMMARY FOR THE LIQUID ROCKET BOOSTER
Mar. 1989 60 p
(Contract NAS8-37136)
(NASA-CR-183790-App-D; NAS 1.26:183790-App-D) Avail: NTIS HC A04/MF A01 CSCL 21H

Trade studies plans for a number of elements in the Liquid Rocket Booster (LRB) component of the Space Transportation System (STS) are given in viewgraph form. Some of the elements covered include: avionics/flight control; avionics architecture; thrust vector control studies; engine control electronics; liquid rocket propellants; propellant pressurization systems; recoverable spacecraft; cryogenic tanks; and spacecraft construction materials. Author

N90-28605*# Martin Marietta Corp., New Orleans, LA. Manned Space Systems.
LIQUID ROCKET BOOSTER (LRB) FOR THE SPACE TRANSPORTATION SYSTEM (STS) SYSTEMS STUDY. APPENDIX E: PRESSURE-FED BOOSTER TEST BED FOR THE LIQUID ROCKET BOOSTER STUDY
Mar. 1989 225 p
(Contract NAS8-37136)
(NASA-CR-183791-App-E; NAS 1.26:183791-App-E) Avail: NTIS HC A10/MF A02 CSCL 21H

The stress analysis/structural design of the Pressure-Fed Booster Engine Test Bed using the existing F-1 Test Facility Test Stand at Huntsville, Alabama is described. The analysis has been coded and set up for solution on NASTRAN. A separate stress program was established to take the NASTRAN output and perform stress checks on the members. Joint checks and other necessary additional checks were performed by hand. The notes include a brief description of other programs which assist in reproducing and reviewing the NASTRAN results. The redesign of the test stand members and the stress analysis was performed per the A.I.S.C. Code. Loads on the stand consist of the loaded run tanks; wind loads; seismic loads; live loads consisting of snow and ice: live and dead loads of steel; and loaded pressurant bottle. In combining loads, wind loads and seismic loads were each combined with full live loads. Wind and seismic loads were not combined. No one third increase in allowables was taken for the environmental loads except at decks 147 and 214, where the increase was used when considering the stay rods, brackets and stay beams. Wind and seismic loads were considered from each of the four coordinate directions (i.e. N,S,E,W) to give eight basic conditions. The analysis was run with the pressurant tank mounted at level 125. One seismic condition was also run with the tank mounted at levels 169 and 214. No failures were noted with mounting at level 169, but extensive deck failure with mounting at level 214 (the loadsets used are included on the tape, but no detailed results are included in the package). Decking support beams at levels 147 and 214 are not included in the model. The stress program thus does not reduce strut lengths to the length between support beams (the struts are attached to the beams at intersection points) and gives stress ratios larger than one for some of the struts. The affected members were therefore checked by hand. Author

N90-28606*# Martin Marietta Corp., New Orleans, LA. Manned Space Systems.
LIQUID ROCKET BOOSTER (LRB) FOR THE SPACE TRANSPORTATION SYSTEM (STS) SYSTEMS STUDY. APPENDIX F: PERFORMANCE AND TRAJECTORY FOR ALS/LRB LAUNCH VEHICLES
Mar. 1989 6 p
(Contract NAS8-37136)
(NASA-CR-183792-App-F; NAS 1.26:183792-App-F) Avail: NTIS HC A02/MF A01 CSCL 21H

By simply combining two baseline pump-fed LOX/RP-1 Liquid Rocket Boosters (LRBs) with the Denver core, a launch vehicle (Option 1 Advanced Launch System (ALS)) is obtained that can perform both the 28.5 deg (ALS) mission and the polar orbit ALS mission. The Option 2 LRB was obtained by finding the optimum LOX/LH2 engine for the STS/LRB reference mission (70.5 K lb payload). Then this engine and booster were used to estimate ALS payload for the 28.5 deg inclination ALS mission. Previous studies indicated that the optimum number of STS/LRB engines is four. When the engine/booster sizing was performed, each engine had 478 K lb sea level thrust and the booster carried 625,000 lb of useable propellant. Two of these LRBs combined with the Denver core provided a launch vehicle that meets the payload requirements for both the ALS and STS reference missions. The Option 3 LRB uses common engines for the cores and boosters. The booster engines do not have the nozzle extension. These engines were sized as common ALS engines. An ALS launch vehicle that has six core engines and five engines per booster provides 109,100 lb payload for the 28.5 deg mission. Each of these LOX/LH2 LRBs carries 714,100 lb of useable propellant. It is estimated that the STS/LRB reference mission payload would be 75,900 lb. Author

N90-28607*# Martin Marietta Corp., New Orleans, LA. Manned Space Systems.
LIQUID ROCKET BOOSTER (LRB) FOR THE SPACE TRANSPORTATION SYSTEM (STS) SYSTEMS STUDY. APPENDIX G: LRB FOR THE STS SYSTEM STUDY LEVEL 2 REQUIREMENTS, REVISION 1
Mar. 1989 156 p
(Contract NAS8-37136)
(NASA-CR-183793-App-G; NAS 1.26:183793-App-G) Avail: NTIS HC A08/MF A01 CSCL 21H

Requirements are presented for shuttle system definition; performance and design characteristics; shuttle vehicle end item performance and design characteristics; ground operations complex performance and design characteristics; operability and system design and construction standards; and quality control. B.G.

N90-28608# Argonne National Lab., IL.
EFFECTS OF FRICTION AND END LOSSES ON MHD THRUSTER EFFICIENCY
E. D. Doss and H. K. Geyer 1990 8 p Presented at the 28th Symposium on Engineering Aspects of Magnetohydrodynamics, Chicago, IL, 26-28 Jun. 1990
(Contracts W-31-109-eng-38; N00014-89-F-0064)
(DE90-013673; CONF-9006105-9) Avail: NTIS HC A02/MF A01

A parametric study was performed to investigate the influence of friction and end losses on the performance of MHD thrusters. An MHD model that couples a one-dimensional flow model to a two-dimensional electrical model has been developed and used in the analysis. The parametric study includes the variation of the applied magnetic field (5 to 20 T), thruster diameter (0.5 to 2.0 m), wall roughness (0 to 3 mm), flow velocity (5 to 20 m/s), and the load factor (1 to 10). The results indicate that friction and end losses can have a deleterious effect on the thruster efficiency close to a load factor equal to unity. Furthermore, the parameter studies show that the thruster efficiency increases with the strength of the magnetic field and thruster diameter and decreases with the wall roughness and the flow velocity. Careful considerations should be given to the analysis and the design of MHD thrusters for load factors close to one. DOE

N90-28609*# Thiokol Corp., Brigham City, UT. Space Operations.
FLIGHT MOTOR SET 360L008 (STS-32R). VOLUME 1: SYSTEM OVERVIEW Final Report
D. M. Garecht Jul. 1990 164 p

(Contract NAS8-30490)
(NASA-CR-184010; NAS 1.26:184010; TWR-17547-1-Vol-1)
Avail: NTIS HC A08/MF A01 CSCL 21H

Flight motor set 360L008 was launched as part of NASA space shuttle mission STS-32R. As with all previous redesigned solid rocket motor launches, overall motor performance was excellent. All ballistic contract end item specification parameters were verified with the exception of ignition interval and rise rates, which could not be verified due to elimination of developmental flight instrumentation. But the available low sample rate data showed nominal propulsion performance. All ballistic and mass property parameters closely matched the predicted values and were well within the required contract end item specification levels that could be assessed. All field joint heaters and igniter joint heaters performed without anomalies. Redesigned field joint heaters and the redesigned left-hand igniter heater were used on this flight. The changes to the heaters were primarily to improve durability and reducing handling damage. Evaluation of the ground environment instrumentation measurements again verified thermal mode analysis data and showed agreement with predicted environmental effects. No launch commit criteria violation occurred. Postflight inspection again verified superior performance of the insulation, phenolics, metal parts, and seals. Postflight evaluation indicated both nozzles performed as expected during flight. All combustion gas was contained by insulation in the field and case-to-nozzle joints. Recommendations were made concerning improved thermal modeling and measurements. The rationale for these recommendations and complete result details are presented. Author

N90-28610*# Rockwell International Corp., Canoga Park, CA. Rocketdyne Div.
THE SPACE TRANSPORTATION MAIN ENGINE PHASE A' STUDY Interim Study Report, 1 Jun. - 31 Dec. 1987
31 Dec. 1987 203 p
(Contract NAS8-36869)
(NASA-CR-179399; NAS 1.26:179399; RI/RD87-207-2) Avail: NTIS HC A10/MF A02 CSCL 21H

The Space Transportation Main Engine Phase A prime study was conducted over a 7 month period as an extension to the Phase A study. The Phase A prime program was designed to expand the study effort completed in Phase A, focusing on the baseline engine configuration selected. Analysis and trade studies were conducted to further optimize some of the major engine subsystems. These changes resulted in improvements to the baseline engine. Several options were evaluated for consideration by vehicle contractors. Author

N90-28611*# National Aeronautics and Space Administration. Marshall Space Flight Center, Huntsville, AL.
ADVANCED EARTH-TO-ORBIT PROPULSION TECHNOLOGY 1988, VOLUME 1
Robert J. Richmond, ed. and S. T. Wu, ed. (Alabama Univ., Huntsville.) Washington Sep. 1988 775 p Conference held in Huntsville, AL, 10-12 May 1988
(NASA-CP-3012-Vol-1; M-593-Vol-1; NAS 1.55:3012-Vol-1) Avail: NTIS HC A99/MF E06 CSCL 21H

The purpose of this conference was to disseminate to the industry, government, and university propulsion community the results emerging from NASA's Advanced Earth-to-Orbit Propulsion Technology Program. There were 14 sessions, Volume 1 covers the sections on structure dynamics, bearings, ignition combustion processes, engine vehicle interaction, fatigue fracture and life prediction, turbomachinery, and manufacturing. For individual titles, see N90-28612 through N90-28656.

N90-28612*# National Aeronautics and Space Administration, Washington, DC.
ADVANCED EARTH-TO-ORBIT PROPULSION TECHNOLOGY PROGRAM OVERVIEW: IMPACT OF CIVIL SPACE TECHNOLOGY INITIATIVE
Frank W. Stephenson, Jr. *In* NASA, Marshall Space Flight Center, Advanced Earth-to-Orbit Propulsion Technology 1988, Volume 1 Sep. 1988 p 5-19 (For primary document see N90-28611 23-20)
Avail: NTIS HC A99/MF E06 CSCL 21H

The NASA Earth-to-Orbit (ETO) Propulsion Technology Program is dedicated to advancing rocket engine technologies for the development of fully reusable engine systems that will enable space transportation systems to achieve low cost, routine access to space. The program addresses technology advancements in the areas of engine life extension/prediction, performance enhancements, reduced ground operations costs, and in-flight fault tolerant engine operations. The primary objective is to acquire increased knowledge and understanding of rocket engine chemical and physical processes in order to evolve more realistic analytical simulations of engine internal environments, to derive more accurate predictions of steady and unsteady loads, and using improved structural analyses, to more accurately predict component life and performance, and finally to identify and verify more durable advanced design concepts. In addition, efforts were focused on engine diagnostic needs and advances that would allow integrated health monitoring systems to be developed for enhanced maintainability, automated servicing, inspection, and checkout, and ultimately, in-flight fault tolerant engine operations. Author

N90-28613*# National Aeronautics and Space Administration. Marshall Space Flight Center, Huntsville, AL.
OXYGEN/HYDROGEN TECHNOLOGY TEST BED STATUS UPDATE **c09**
J. S. Richards *In its* Advanced Earth-to-Orbit Propulsion Technology 1988, Volume 1 Sep. 1988 p 21-28 (For primary document see N90-28611 23-20)
Avail: NTIS HC A99/MF E06 CSCL 14B

An overview is provided of the Hydrogen/Oxygen Technology Test Bed program. The status of the program, the program direction, plans for testing, and plans for technology implementation within the program are delineated. Test Bed goals and objectives are defined and the current status of the Test Bed engine is provided. A test facility status and a summary of the test facility capabilities are given. Author

N90-28614*# Computational Mechanics Co., Austin, TX.
A HYBRID-STRESS FINITE ELEMENT FOR LINEAR ANISOTROPIC ELASTICITY **c39**
Gerald W. Fly, J. Tinsley Oden, and Mark L. Pearson (Softcom Systems, Inc., Huntsville, AL.) *In* NASA, Marshall Space Flight Center, Advanced Earth-to-Orbit Propulsion Technology 1988, Volume 1 Sep. 1988 p 30-42 (For primary document see N90-28611 23-20)
(Contract NAS8-37283)
Avail: NTIS HC A99/MF E06 CSCL 20K

Standard assumed displacement finite elements with anisotropic material properties perform poorly in complex stress fields such as combined bending and shear and combined bending and torsion. A set of three dimensional hybrid-stress brick elements were developed with fully anisotropic material properties. Both eight-node and twenty-node bricks were developed based on the symmetry group theory of Punch and Atluri. An eight-node brick was also developed using complete polynomials and stress basis functions and reducing the order of the resulting stress parameter matrix by applying equilibrium constraints and stress compatibility constraints. Here the stress compatibility constraints must be formulated assuming anisotropic material properties. The performance of these elements was examined in numerical examples covering a broad range of stress distributions. The stress predictions show significant improvement over the assumed displacement elements but the calculation time is increased. Author

N90-28615*# Rockwell International Corp., Canoga Park, CA. Rocketdyne Div.
BLADE TIP RUBBING STRESS PREDICTION **c07**
Gerald A. Brusher, Gary A. Davis, and Daniel M. Shea *In* NASA, Marshall Space Flight Center, Advanced Earth-to-Orbit Propulsion Technology 1988, Volume 1 Sep. 1988 p 43-53 (For primary

document see N90-28611 23-20)
(Contract NAS8-36361)
Avail: NTIS HC A99/MF E06 CSCL 21E

A linear analysis was performed to determine the dynamic response of a turbine blade to intermittent rubbing against a tip seal. The response analysis consisted of a parametric study where the rubbing friction force was assumed to vary as a half sine wave over a preselected contact arc. The length of the contact arc, as well as the pump speed, was varied to determine the effects of each. Results show that for a given contact arc there are distinct critical speeds at which the blade response becomes a maximum. Author

N90-28616*# National Aeronautics and Space Administration. Lewis Research Center, Cleveland, OH.

PROBABILISTIC STRUCTURAL ANALYSIS METHODS DEVELOPMENT FOR SSME

C. C. Chamis and D. A. Hopkins *In* NASA, Marshall Space Flight Center, Advanced Earth-to-Orbit Propulsion Technology 1988, Volume 1 Sep. 1988 p 54-68 (For primary document see N90-28611 23-20)
Avail: NTIS HC A99/MF E06 CSCL 21H

The development of probabilistic structural analysis methods is a major part of the SSME Structural Durability Program and consists of three program elements: composite load spectra, probabilistic finite element structural analysis, and probabilistic structural analysis applications. Recent progress includes: (1) the effects of the uncertainties of several factors on the HPFP blade temperature pressure and torque, (2) the evaluation of the cumulative distribution function of structural response variables based on assumed uncertainties on primitive structural variables, and (3) evaluation of the failure probability. Collectively, the results obtained demonstrate that the structural durability of critical SSME components can be probabilistically evaluated. Author

N90-28617*# State Univ. of New York, Buffalo. Dept. of Civil Engineering.

DEVELOPMENT OF AN INTEGRATED BEM FOR HOT FLUID-STRUCTURE INTERACTION **c39**

G. F. Dargush and P. K. Banerjee *In* NASA, Marshall Space Flight Center, Advanced Earth-to-Orbit Propulsion Technology 1988, Volume 1 Sep. 1988 p 69-86 (For primary document see N90-28611 23-20)
Avail: NTIS HC A99/MF E06 CSCL 20K

One of the most difficult problems in engine structural component durability analysis is the determination of the temperatures and fluxes in the structural components directly in contact with the hot gas flow path. Currently there exists no rational analytical or numerical technique which can effectively deal with this problem. Since the temperature distribution in the structural components are strongly influenced by both the fluid flow and the deformation as well as the cooling system in the structure, the only effective way to deal with this problem is to develop an integrated solid mechanics, fluid mechanics and heat transfer analysis for this problem. Herein, the Boundary Element Method (BEM) is chosen as the basic analysis tool principally because the definition of quantities like fluxes, temperatures, displacements, and velocities are very precise on a boundary based discretization scheme. One fundamental difficulty is that a BEM analysis requires a considerable amount of analytical work which is not present in other numerical methods. During the past year, all of this analytical work was completed and a two dimensional, general purpose code was written. A portion of the work is summarized. Author

N90-28618*# Spectra Research Systems, Inc., Huntsville, AL. Aerospace and Commercial Systems Directorate.

EVOLUTION AND USE OF COMBINED MECHANICAL AND THERMAL CODES FOR CRYOGENIC TURBOPUMP BEARINGS **c37**

Joe C. Cody, David E. Marty, and James D. Moore *In* NASA, Marshall Space Flight Center, Advanced Earth-to-Orbit Propulsion Technology 1988, Volume 1 Sep. 1988 p 88-101 (For primary document see N90-28611 23-20)
Avail: NTIS HC A99/MF E06 CSCL 13I

Shaft bearing system analysis codes were developed, improved, and used to investigate Space Shuttle Main Engine (SSME) Liquid Oxygen (LOX) turbopump bearing problems, and to support the Marshall Space Flight Center Bearing and Seal Materials Test (BSMT) program. Thermal network modeling uses the SINDA thermal code, and the modeling of bearing quasi-dynamic characteristics uses the SHABERTH bearing/shaft code. These codes are solved concurrently for a bearing/shaft system using software developed for this purpose. Simulation of the SSME LOX turbopump turbine and pump end bearings and the MSFC BSMT operating in liquid nitrogen (LN sub 2) and LOX was done. The thermal network models include the bearing components, bearing carriers, shaft, housing, frictional heat, and viscous fluid energy. A cage model was included to account for heat generation between the cage and rolling elements. Since most bearing surfaces operate at temperatures well above the coolant saturation temperature, and move at high speed relative to the coolant, forced convection boiling is the dominant mechanism for heat removal. Improved modeling of forced convection film boiling was incorporated to take into account the local vapor generation at the high temperature surfaces. Rearing preloads in the pump and tester are provided by preload springs. As bearing operating clearances and contact angles change due to thermal effects and loading, the bearing preload changes with these varying conditions. These characteristics were modeled and are included in the overall system models. Results from these models indicate an operational limit which, if exceeded, predicts a thermal excursion. Author

N90-28619*# Rockwell International Science Center, Thousand Oaks, CA.

DETERMINATION OF THE SSME HIGH PRESSURE OXIDIZER TURBOPUMP BEARING TEMPERATURE **c37**

Y. Naerheim, P. J. Stocker, and J. B. Lumsden *In* NASA, Marshall Space Flight Center, Advanced Earth-to-Orbit Propulsion Technology 1988, Volume 1 Sep. 1988 p 102-109 (For primary document see N90-28611 23-20)
(Contract NAS8-4000)
Avail: NTIS HC A99/MF E06 CSCL 13I

The SSME high pressure liquid oxygen turbopump (HPOTP) bearings sometimes wear and experience heating and oxidation of the ball and raceway surfaces. So far it has been impossible to measure the temperature of the bearings directly during operation of the turbopumps. However, a method was developed for determining the surface temperature of the bearings from the composition of the oxides using oxidation samples for calibration and Auger Electron Spectroscopy (AES) for chemical analysis. Author

N90-28620*# National Aeronautics and Space Administration. Marshall Space Flight Center, Huntsville, AL.

CRYOGENIC, HIGH SPEED, TURBOPUMP BEARING COOLING REQUIREMENTS **c37**

Fred J. Dolan, Howard G. Gibson, James L. Cannon, and Joe C. Cody (Spectra Research Systems, Inc., Huntsville, AL.) *In its* Advanced Earth-to-Orbit Propulsion Technology 1988, Volume 1 Sep. 1988 p 110-141 (For primary document see N90-28611 23-20)
Avail: NTIS HC A99/MF E06 CSCL 13I

Although the Space Shuttle Main Engine (SSME) has repeatedly demonstrated the capability to perform during launch, the High Pressure Oxidizer Turbopump (HPOTP) main shaft bearings have not met their 7.5 hour life requirement. A tester is being employed to provide the capability of subjecting full scale bearings and seals to speeds, loads, propellants, temperatures, and pressures which simulate engine operating conditions. The tester design permits much more elaborate instrumentation and diagnostics than could be accommodated in an SSME turbopump. Tests were made to demonstrate the facilities; and the devices' capabilities, to verify the instruments in its operating environment and to establish a performance baseline for the flight type SSME HPOTP Turbine Bearing design. Bearing performance data from tests are being

utilized to generate: (1) a high speed, cryogenic turbopump bearing computer mechanical model, and (2) a much improved, very detailed thermal model to better understand bearing internal operating conditions. Parametric tests were also made to determine the effects of speed, axial loads, coolant flow rate, and surface finish degradation on bearing performance. Author

N90-28621*# Rockwell International Corp., Canoga Park, CA. Rocketdyne Div.

POOL BOILING FROM ROTATING AND STATIONARY SPHERES IN LIQUID NITROGEN **c37**

Winston M. Cuan and Sidney H. Schwartz *In* NASA, Marshall Space Flight Center, Advanced Earth-to-Orbit Propulsion Technology 1988, Volume 1 Sep. 1988 p 142-157 Previously announced in IAA as A88-48028 (For primary document see N90-28611 23-20)

(Contract NAS8-40000)

Avail: NTIS HC A99/MF E06 CSCL 13I

Results are presented for a preliminary experiment involving saturated pool boiling at 1 atm from rotating 2 and 3 in. diameter spheres which were immersed in liquid nitrogen (LN2). Additional results are presented for a stationary, 2 inch diameter sphere, quenched in LN2, which were obtained utilizing a more versatile and complete experimental apparatus that will eventually be used for additional rotating sphere experiments. The speed for the rotational tests was varied from 0 to 10,000 rpm. The stationary experiments parametrically varied pressure and subcooling levels from 0 to 600 psig and from 0 to 50 F, respectively. During the rotational tests, a high speed photographic analysis was undertaken to measure the thickness of the vapor film surrounding the sphere. The average Nusselt number over the cooling period was plotted against the rotational Reynolds number. Stationary sphere results included local boiling heat transfer coefficients at different latitudinal locations, for various pressure and subcooling levels. Author

N90-28622*# National Aeronautics and Space Administration. Lewis Research Center, Cleveland, OH.

BEARING OPTIMIZATION FOR SSME HPOTP APPLICATION **c37**

Elizabeth S. Armstrong and Harold H. Coe *In* NASA, Marshall Space Flight Center, Advanced Earth-to-Orbit Propulsion Technology 1988, Volume 1 Sep. 1988 p 159-174 (For primary document see N90-28611 23-20)

Avail: NTIS HC A99/MF E06 CSCL 13I

The space shuttle main engine (SSME) high-pressure oxygen turbopumps (HPOTP) have not experienced the service life required of them. To improve the life of the existing turbopump bearings, modifications to the bearings that could be retrofitted into the present bearing cavity are being investigated. Several bearing parameters were optimized using the computer program SHABERTH, which performs a thermomechanical simulation of a load support system. The computer analysis showed that improved bearing performance is feasible if low friction coefficients can be attained. Bearing geometries were optimized considering heat generation, equilibrium temperatures, and relative life. Two sets of curvatures were selected from the optimization: an inner-raceway curvature of 0.54, an outer-raceway curvature of 0.52, and an inner-raceway curvature of 0.55, an outer-raceway curvature of 0.53. A contact angle of 16 deg was also selected. Thermal gradients through the bearings were found to be lower with liquid lubrication than with solid film lubrication. As the coolant flowrate through the bearing increased, the ball temperature decreased but at a continuously decreasing rate. The optimum flowrate was approximately 4 kg/s. The analytical modeling used to determine these feasible modifications to improve bearing performance is described. Author

N90-28623*# Battelle Columbus Labs., OH.

DEVELOPMENT OF IMPROVED SELF LUBRICATING CAGES FOR SSME HPOTP BEARINGS **c37**

J. W. Kannel, K. F. Dufrane, S. A. Barber, and J. Gleeson *In* NASA, Marshall Space Flight Center, Advanced Earth-to-Orbit Propulsion Technology 1988, Volume 1 Sep. 1988 p 175-189 (For primary document see N90-28611 23-20)

Avail: NTIS HC A99/MF E06 CSCL 13I

The reusability requirements of the Space Shuttle main engines (SSME) have put severe demands on the bearings for the high pressure oxygen turbopump (HPOTP) bearings. These bearings must operate at very high speeds with meager lubrication. The cages in the current bearings are fabricated from Armalon, which is a glass-fiber-reinforced polytetrafluoroethylene (PTFE) composite. Bearing lubrication occurs as a result of the PTFE transferring from cage to ball to race. One difficulty with the design is that the glass fibers impede the PTFE transfer to the balls. An alternative cage using a bronze filled PTFE material, Salox M was studied. Although experiments have shown that Salox M should provide much better PTFE transfer than Armalon does, Salox M does not have sufficient strength to be used as a bearing cage. Cage design concepts that can incorporate a bronze-PTFE interface at the ball pockets, but with a strength equivalent to Armalon were analyzed. An insert design appears to be an excellent candidate design. The housing for the insert can be fabricated from a high strength material to give sufficient cage strength. Further, the design can be configured so the Salox M contacts both the balls and the outer race surfaces. A sample cage was constructed to verify the feasibility of fabrication. Author

N90-28624*# Pratt and Whitney Aircraft, West Palm Beach, FL. Government Engine Business.

PRATT AND WHITNEY CRYOGENIC TURBOPUMP BEARING EXPERIENCE **c37**

W. E. Poole and R. W. Bursey, Jr. *In* NASA, Marshall Space Flight Center, Advanced Earth-to-Orbit Propulsion Technology 1988, Volume 1 Sep. 1988 p 190-199 (For primary document see N90-28611 23-20)

Avail: NTIS HC A99/MF E06 CSCL 13I

Successful, reusable bearings require lubrication, traditionally, a transfer film from sacrificial cage wear. Early testing included materials screening programs to identify suitable cryogenic cage materials. A specially developed element tester that simulated the function of a ball bearing cage was used. Suitable materials must provide lubrication with an acceptably low wear rate, without abrading contacting surfaces. The most promising materials were tested in full scale bearings at speeds up to 4 MDN. Teflon, filled with 40 percent bronze powder, was the best performing material. A variety of bearings were designed and successfully tested in LH2 and LOX. Bearings with bronze filled Teflon cages were successfully tested for 150 hrs. In overload tests, the same design was tested for 5 hrs at maximum Hertz stresses above 450 ksi and an additional 5 hrs with a maximum Hertz stress exceeding 500 ksi. Four bearings were tested in LOX for 25 hrs, with a maximum time per bearing of 10 hrs. Author

N90-28625*# Battelle Columbus Labs., OH.

CAGE STABILITY ANALYSIS FOR SSME HPOTP BEARINGS **c37**

T. L. Merriman and J. W. Kannel *In* NASA, Marshall Space Flight Center, Advanced Earth-to-Orbit Propulsion Technology 1988, Volume 1 Sep. 1988 p 200-212 (For primary document see N90-28611 23-20)

Avail: NTIS HC A99/MF E06 CSCL 13I

A numerical model of cage motion (CAGEDYN) was used to analyze the stability of bearing cages in the Space Shuttle main engine (SSME) high pressure oxygen turbopump (HPOTP). The stability of existing bearing geometries, as well as perturbations of these geometries, was analyzed for various operating conditions. Results of the analyses show that some combinations of operating parameters, exacerbated by the sparse lubrication that exist in the HPOTP bearings, can cause unstable cage oscillations. Frequencies of cage oscillations were predicted by the CAGEDYN numerical model by Fourier analysis of predicted cage motions. Under conditions that cause unstable cage motion, high frequency oscillations were predicted that could cause premature cage failures. Author

N90-28626*# Rockwell International Corp., Canoga Park, CA. Rocketdyne Div.
ROCKETDYNE LOX BEARING TESTER PROGRAM **c37**
J. E. Keba and R. F. Beatty *In* NASA, Marshall Space Flight Center, Advanced Earth-to-Orbit Propulsion Technology 1988, Volume 1 Sep. 1988 p 213-229 (For primary document see N90-28611 23-20)
(Contract NAS8-4000)
Avail: NTIS HC A99/MF E06 CSCL 13I

The cause, or causes, for the Space Shuttle Main Engine ball wear were unknown, however, several mechanisms were suspected. Two testers were designed and built for operation in liquid oxygen to empirically gain insight into the problems and iterate solutions in a timely and cost efficient manner independent of engine testing. Schedules and test plans were developed that defined a test matrix consisting of parametric variations of loading, cooling or vapor margin, cage lubrication, material, and geometry studies. Initial test results indicated that the low pressure pump thrust bearing surface distress is a function of high axial load. Initial high pressure turbopump bearing tests produced the wear phenomenon observed in the turbopump and identified an inadequate vapor margin problem and a coolant flowrate sensitivity issue. These tests provided calibration data of analytical model predictions to give high confidence in the positive impact of future turbopump design modification for flight. Various modifications will be evaluated in these testers, since similar turbopump conditions can be produced and the benefit of the modification will be quantified in measured wear life comparisons. Author

N90-28627*# National Aeronautics and Space Administration. Lewis Research Center, Cleveland, OH.
CATALYTIC IGNITION OF HYDROGEN/OXYGEN **c25**
James M. Green (Sverdrup Technology, Inc., Middleburg Heights, OH.) and Robert L. Zurawski *In* NASA, Marshall Space Flight Center, Advanced Earth-to-Orbit Propulsion Technology 1988, Volume 1 Sep. 1988 p 231-248 (For primary document see N90-28611 23-20)
Avail: NTIS HC A99/MF E06 CSCL 21B

An experimental program was conducted to evaluate the catalytic ignition of gaseous hydrogen and oxygen. Shell 405 granular catalyst and a unique monolithic sponge catalyst were tested. Mixture ratio, mass flow rate, propellant inlet temperature, and back pressure were varied parametrically in testing to determine the operational limits of a catalytic igniter. The test results showed that the gaseous hydrogen/oxygen propellant combination can be ignited catalytically using Shell 405 catalyst over a wide range of mixture ratios, mass flow rates, and propellant injection temperatures. These operating conditions must be optimized to ensure reliable ignition for an extended period of time. The results of the experimental program and the established operational limits for a catalytic igniter using both the granular and monolithic catalysts are presented. The capabilities of a facility constructed to conduct the igniter testing and the advantages of a catalytic igniter over other ignition systems for gaseous hydrogen and oxygen are also discussed. Author

N90-28628*# Rockwell International Corp., Canoga Park, CA. Rocketdyne Div.
OXYGEN/METHANE COMBUSTION STABILITY INVESTIGATION **c25**
R. J. Jensen, H. Dodson, and B. Trueblood *In* NASA, Marshall Space Flight Center, Advanced Earth-to-Orbit Propulsion Technology 1988, Volume 1 Sep. 1988 p 249-269 (For primary document see N90-28611 23-20)
(Contract NAS3-24612)
Avail: NTIS HC A99/MF E06 CSCL 21B

The LOX/Hydrocarbon Combustion Instability Investigation Program is structured to determine if the use of light hydrocarbon fuels (such as methane) with liquid oxygen (LOX) produces combustion performance and stability behavior similar to the LOX/hydrogen propellant combination. In particular, methane is being investigated to determine if that fuel can be rated for combustion instability using the same techniques as previously used for LOX/hydrogen. These techniques include fuel temperature ramping and stability bomb tests. The hot fire program probed the combustion behavior of methane from ambient to subambient (438 R) temperatures. The 5.66-in. diameter, 82-coaxial element hardware was operated over a mixture ratio range of 2.8 to 3.7 and mainstage durations from 0.1 to 8 sec in tests at a nominal chamber pressure of 2000 psig. Three tests were successfully driven unstable at low fuel temperature during fuel temperature ramping stability rating tests. Three other tests experienced self-induced instabilities at low mixture ratios and ambient fuel temperatures. Relationships between the data, stability analyses, and LOX/hydrogen stability trends are discussed. Author

N90-28629*# National Aeronautics and Space Administration. Lewis Research Center, Cleveland, OH.
COMBUSTION INSTABILITY COUPLING WITH FEED SYSTEM ACOUSTICS **c25**
Richard J. Priem (Priem Consultants, Inc., Cleveland, OH.) and Kevin J. Breisacher *In* NASA, Marshall Space Flight Center, Advanced Earth-to-Orbit Propulsion Technology 1988, Volume 1 Sep. 1988 p 270-301 (For primary document see N90-28611 23-20)
Avail: NTIS HC A99/MF E06 CSCL 21B

High frequency combustion instability has recently been observed by Rocketdyne in a 40K thrust methane/LOX combustion chamber. The oscillations had frequencies as high as 14,000 Hz with pressure amplitudes in the LOX dome of 500 psi at a chamber pressures of 2,000 psi. At this frequency the wave length associated with a period of oscillation is 2.3 inches in LOX and 1.4 inches in methane. These distances are comparable to the lengths of the injector elements which requires that acoustic waves be considered in the feed systems rather than using lumped parameters as is normally considered for feed system coupled oscillations. To expand the capability of existing models, the Feiler and Heidmann feed system coupled instability model was modified to include acoustic oscillations in the feed system. Similarly the vaporization controlled instability model of Heidmann and Wieber was modified to include flow oscillations that would be produced by feed system coupling. The major elements that control oscillations in a rocket combustion chamber are shown and discussed. Author

N90-28630*# Aerojet TechSystems Co., Sacramento, CA.
COMPUTER CODE FOR THE PREDICTION OF NOZZLE ADMITTANCE
Thong V. Nguyen *In* NASA, Marshall Space Flight Center, Advanced Earth-to-Orbit Propulsion Technology 1988, Volume 1 Sep. 1988 p 302-315 (For primary document see N90-28611 23-20)
(Contract F04611-85-C-0100)
Avail: NTIS HC A99/MF E06 CSCL 21H

A procedure which can accurately characterize injector designs for large thrust (0.5 to 1.5 million pounds), high pressure (500 to 3000 psia) LOX/hydrocarbon engines is currently under development. In this procedure, a rectangular cross-sectional combustion chamber is to be used to simulate the lower traverse frequency modes of the large scale chamber. The chamber will be sized so that the first width mode of the rectangular chamber corresponds to the first tangential mode of the full-scale chamber. Test data to be obtained from the rectangular chamber will be used to assess the full scale engine stability. This requires the development of combustion stability models for rectangular chambers. As part of the combustion stability model development, a computer code, NOAD based on existing theory was developed to calculate the nozzle admittances for both rectangular and axisymmetric nozzles. This code is detailed. Author

N90-28631*# Pratt and Whitney Aircraft, West Palm Beach, FL.
TRIPROPELLANT COMBUSTION PROCESS **c25**
T. D. Kmiec and R. G. Carroll *In* NASA, Marshall Space Flight Center, Advanced Earth-to-Orbit Propulsion Technology 1988, Volume 1 Sep. 1988 p 316-333 (For primary document see N90-28611 23-20)
Avail: NTIS HC A99/MF E06 CSCL 21B

The addition of small amounts of hydrogen to the combustion of LOX/hydrocarbon propellants in large rocket booster engines has the potential to enhance the system stability. Programs being conducted to evaluate the effects of hydrogen on the combustion of LOX/hydrocarbon propellants at supercritical pressures are described. Combustion instability has been a problem during the development of large hydrocarbon fueled rocket engines. At the higher combustion chamber pressures expected for the next generation of booster engines, the effect of unstable combustion could be even more destructive. The tripropellant engine cycle takes advantage of the superior cooling characteristics of hydrogen to cool the combustion chamber and a small amount of the hydrogen coolant can be used in the combustion process to enhance the system stability. Three aspects of work that will be accomplished to evaluate tripropellant combustion are described. The first is laboratory demonstration of the benefits through the evaluation of drop size, ignition delay and burning rate. The second is analytical modeling of the combustion process using the empirical relationship determined in the laboratory. The third is a subscale demonstration in which the system stability will be evaluated. The approach for each aspect is described and the analytical models that will be used are presented. Author

N90-28632*# Aerojet TechSystems Co., Sacramento, CA.
SWIRL COAXIAL INJECTOR ELEMENT CHARACTERIZATION FOR BOOSTER ENGINES
Gregory M. Meagher and Jeffrey A. Muss *In* NASA, Marshall Space Flight Center, Advanced Earth-to-Orbit Propulsion Technology 1988, Volume 1 Sep. 1988 p 334-347 (For primary document see N90-28611 23-20)
Avail: NTIS HC A99/MF E06 CSCL 21H

Recent hot fire testing at the Marshall Space Flight Center (MSFC) has indicated the swirl-coaxial element to be a viable candidate for the STBE injector. Plans are to test the current 40K lbf thrust injector at the higher chamber pressure and colder fuel temperature which are anticipated for STBE. A cold flow program to characterize the swirl coax element over a range of operating points was conducted. The results are presented and compared to the hot fire data. Predictions for compatibility, performance and stability are then presented for the uprated test conditions. Author

N90-28633*# Rockwell International Corp., Canoga Park, CA. Rocketdyne Div.
HEAVY HYDROCARBON MAIN INJECTOR TECHNOLOGY
S. C. Fisher and H. A. Arbit *In* NASA, Marshall Space Flight Center, Advanced Earth-to-Orbit Propulsion Technology 1988, Volume 1 Sep. 1988 p 348-374 (For primary document see N90-28611 23-20)
Avail: NTIS HC A99/MF E06 CSCL 21H

One of the key components of the Advanced Launch System (ALS) is a large liquid rocket, booster engine. To keep the overall vehicle size and cost down, this engine will probably use liquid oxygen (LOX) and a heavy hydrocarbon, such as RP-1, as propellants and operate at relatively high chamber pressures to increase overall performance. A technology program (Heavy Hydrocarbon Main Injector Technology) is being studied. The main objective of this effort is to develop a logic plan and supporting experimental data base to reduce the risk of developing a large scale (approximately 750,000 lb thrust), high performance main injector system. The overall approach and program plan, from initial analyses to large scale, two dimensional combustor design and test, and the current status of the program are discussed. Progress includes performance and stability analyses, cold flow tests of injector model, design and fabrication of subscale injectors and calorimeter combustors for performance, heat transfer, and dynamic stability tests, and preparation of hot fire test plans. Related, current, high pressure, LOX/RP-1 injector technology efforts are also briefly discussed. Author

N90-28634*# Pratt and Whitney Aircraft, West Palm Beach, FL. Government Engine Business.
INJECTOR ELEMENT CHARACTERIZATION METHODOLOGY
George B. Cox, Jr. *In* NASA, Marshall Space Flight Center, Advanced Earth-to-Orbit Propulsion Technology 1988, Volume 1 Sep. 1988 p 375-387 (For primary document see N90-28611 23-20)
Avail: NTIS HC A99/MF E06 CSCL 21H

Characterization of liquid rocket engine injector elements is an important part of the development process for rocket engine combustion devices. Modern nonintrusive instrumentation for flow velocity and spray droplet size measurement, and automated, computer-controlled test facilities allow rapid, low-cost evaluation of injector element performance and behavior. Application of these methods in rocket engine development, paralleling their use in gas turbine engine development, will reduce rocket engine development cost and risk. The Alternate Turbopump (ATP) Hot Gas Systems (HGS) preburner injector elements were characterized using such methods, and the methodology and some of the results obtained will be shown. Author

N90-28635*# Boeing Aerospace Co., Seattle, WA. Space Systems Preliminary Design.
SUMMARY OF BOOSTER PROPULSION/VEHICLE IMPACT STUDY RESULTS
Vincent A. Weldon, Lawrence E. Fink, and Dwight U. Phillips *In* NASA, Marshall Space Flight Center, Advanced Earth-to-Orbit Propulsion Technology 1988, Volume 1 Sep. 1988 p 389-413 (For primary document see N90-28611 23-20)
(Contract NAS8-36944)
Avail: NTIS HC A99/MF E06 CSCL 21H

Hydrogen, RP-1, propane, and methane were identified by propulsion technology studies as the most probable fuel candidates for the boost phase of future launch vehicles. The objective of this study was to determine the effects of booster engines using these fuels and coolant variations on representative future launch vehicles. An automated procedure for integrated launch vehicle, engine sizing, and design optimization was used to optimize two stage and single stage concepts for minimum dry weight. The two stage vehicles were unmanned and used a flyback booster and partially reusable orbiter. The single stage designs were fully reusable, manned flyback vehicles. Comparisons of these vehicle designs, showing the effects of using different fuels, as well as sensitivity and trending data, are presented. In addition, the automated design technique is described. Author

N90-28636*# National Aeronautics and Space Administration. John F. Kennedy Space Center, Cocoa Beach, FL.
OPERATIONAL COST DRIVERS **c66**
Arthur L. Scholz (Boeing Aerospace Co., Kennedy Space Center, FL.) and William J. Dickinson *In* NASA, Marshall Space Flight Center, Advanced Earth-to-Orbit Propulsion Technology 1988, Volume 1 Sep. 1988 p 414-421 (For primary document see N90-28611 23-20)
Avail: NTIS HC A99/MF E06 CSCL 12B

To be economically viable, the operations cost of launch vehicles must be reduced by an order of magnitude as compared to the Space Transportation System (STS). A summary of propulsion-related operations cost drivers derived from a two-year study of Shuttle ground operations is presented. Examples are given of the inordinate time and cost of launch operations caused by propulsion systems designs that did not adequately consider impacts on prelaunching processing. Typical of these cost drivers are those caused by central hydraulic systems, storable propellants, gimballed engines, multiple propellants, He and N2 systems and purges, hard starts, high maintenance turbopumps, accessibility problems, and most significantly, the use of multiple, nonintegrated RCS, OMS, and main propulsion systems. Recovery and refurbishment of SRBs have resulted in expensive crash and salvage operations. Vehicle system designers are encouraged to be acutely aware of these cost drivers and to incorporate solutions (beginning with the design concepts) to avoid business as usual and costs as usual. Author

N90-28637*# Acurex Corp., Huntsville, AL. Aerotherm Div.
HIGH/VARIABLE MIXTURE RATIO OXYGEN/HYDROGEN ENGINES
William H. Knuth and John H. Beveridge *In* NASA, Marshall Space Flight Center, Advanced Earth-to-Orbit Propulsion Technology 1988, Volume 1 Sep. 1988 p 422-440 (For primary document see N90-28611 23-20)
Avail: NTIS HC A99/MF E06 CSCL 21H

A LOX/LH2 high/variable mixture ratio booster upper stage is described. The engine has high thrust-weight ratio as a booster and high specific impulse as an upper stage engine. Operation at high mixture ratio utilizes the propellants at high bulk density. The engine may use multiple turbopump-preburners for higher thrust ratings. The engine uses the full flow cycle to obtain minimum turbine inlet temperatures for a given chamber pressure and to avoid interpropellant shaft seals and other single point failure modes. A portion of the liquid hydrogen is used to regeneratively cool the thrust chamber assembly. The warmed hydrogen coolant is then used to drive the fuel boost turbopump. All propellants arrive at the gas-gas injector ready to burn. Shear mixing of the parallel flowing high velocity, low density fuel-rich gases with the high density, low velocity oxidizer-rich gases provides complete combustion with a modest chamber volume. Combustion stability is assured by the injection of the heated fuel-rich gases and the comparatively low volume ratio of the propellants before and after combustion. The high area ratio nozzle skirt is fitted with a low area ratio nozzle skirt insert for optimum low altitude performance. The overall engine characteristics make it a candidate for ALS, Shuttle-C, LRB, and SSTO applications. Author

N90-28638*# Pratt and Whitney Aircraft, West Palm Beach, FL. Government Engine Business.
HIGH/VARIABLE MIXTURE RATIO O2/H2 ENGINE
A. Adams and R. C. Parsley *In* NASA, Marshall Space Flight Center, Advanced Earth-to-Orbit Propulsion Technology 1988, Volume 1 Sep. 1988 p 441-449 (For primary document see N90-28611 23-20)
Avail: NTIS HC A99/MF E06 CSCL 21H

Vehicle/engine analysis studies have identified the High/Dual Mixture Ratio O2/H2 Engine cycle as a leading candidate for an advanced Single Stage to Orbit (SSTO) propulsion system. This cycle is designed to allow operation at a higher than normal O/F ratio of 12 during liftoff and then transition to a more optimum O/F ratio of 6 at altitude. While operation at high mixture ratios lowers specific impulse, the resultant high propellant bulk density and high power density combine to minimize the influence of atmospheric drag and low altitude gravitational forces. Transition to a lower mixture ratio at altitude then provides improved specific impulse relative to a single mixture ratio engine that must select a mixture ratio that is balanced for both low and high altitude operation. This combination of increased altitude specific impulse and high propellant bulk density more than offsets the compromised low altitude performance and results in an overall mission benefit. Two areas of technical concern relative to the execution of this dual mixture ratio cycle concept are addressed. First, actions required to transition from high to low mixture ratio are examined, including an assessment of the main chamber environment as the main chamber mixture ratio passes through stoichiometric. Secondly, two approaches to meet a requirement for high turbine power at high mixture ratio condition are examined. One approach uses high turbine temperature to produce the power and requires cooled turbines. The other approach incorporates an oxidizer-rich preburner to increase turbine work capability via increased turbine mass flow. Author

N90-28639*# Aerojet TechSystems Co., Sacramento, CA.
VARIABLE MIXTURE RATIO PERFORMANCE THROUGH NITROGEN AUGMENTATION
R. Beichel, C. J. OBrien, and E. K. Bair *In* NASA, Marshall Space Flight Center, Advanced Earth-to-Orbit Propulsion Technology 1988, Volume 1 Sep. 1988 p 450-470 (For primary document see N90-28611 23-20)
(Contract NAS8-36867)
Avail: NTIS HC A99/MF E06 CSCL 21H

High/variable mixture ratio O2/H2 candidate engine cycles are examined for earth-to-orbit vehicle application. Engine performance and power balance information are presented for the candidate cycles relative to chamber pressure, bulk density, and mixture ratio. Included in the cycle screening are concepts where a third fluid (liquid nitrogen) is used to achieve a variable mixture ratio over the trajectory from liftoff to earth orbit. The third fluid cycles offer a very low risk, fully reusable, low operation cost alternative to high/variable mixture ratio bipropellant cycles. Variable mixture ratio engines with extendible nozzle are slightly lower performing than a single mixture ratio engine (MR = 7:1) with extendible nozzle. Dual expander engines (MR = 7:1) have slightly better performance than the single mixture ratio engine. Dual fuel dual expander engines offer a 16 percent improvement over the single mixture ratio engine. Author

N90-28640*# Rockwell International Corp., Canoga Park, CA. Rocketdyne Div.
HIGH VARIABLE MIXTURE RATIO OXYGEN/HYDROGEN ENGINE
C. M. Erickson, W. H. Tu, and A. H. Weiss *In* NASA, Marshall Space Flight Center, Advanced Earth-to-Orbit Propulsion Technology 1988, Volume 1 Sep. 1988 p 471-485 (For primary document see N90-28611 23-20)
(Contract NAS8-36869)
Avail: NTIS HC A99/MF E06 CSCL 21H

The ability of an O2/H2 engine to operate over a range of high-propellant mixture ratios was previously shown to be advantageous in single stage to orbit (SSTO) vehicles. The results are presented for the analysis of high-performance engine power cycles operating over propellant mixture ratio ranges of 12 to 6 and 9 to 6. A requirement to throttle up to 60 percent of nominal thrust was superimposed as a typical throttle range to limit vehicle acceleration as propellant is expended. The object of the analysis was to determine areas of concern relative to component and engine operability or potential hazards resulting from the operating requirements and ranges of conditions that derive from the overall engine requirements. The SSTO mission necessitates a high-performance, lightweight engine. Therefore, staged combustion power cycles employing either dual fuel-rich preburners or dual mixed (fuel-rich and oxygen-rich) preburners were examined. Engine mass flow and power balances were made and major component operating ranges were defined. Component size and arrangement were determined through engine layouts for one of the configurations evaluated. Each component is being examined to determine if there are areas of concern with respect to component efficiency, operability, reliability, or hazard. The effects of reducing the maximum chamber pressure were investigated for one of the cycles. Author

N90-28641*# Georgia Inst. of Tech., Atlanta. School of Materials Engineering.
MICROMECHANICS OF CYCLIC DEFORMATION IN SSME TURBOPUMP BLADE MATERIALS **c39**
Walter W. Milligan and Stephen D. Antolovich *In* NASA, Marshall Space Flight Center, Advanced Earth-to-Orbit Propulsion Technology 1988, Volume 1 Sep. 1988 p 487-496 (For primary document see N90-28611 23-20)
(Grant NAG3-503)
Avail: NTIS HC A99/MF E06 CSCL 20K

Current and candidate Space Shuttle Main Engine (SSME) turbopump blade materials are anisotropic, both in their elastic and plastic response. The major objective is to characterize the plastic deformation behavior of a typical single crystal nickel-base superalloy, PWA 1480, and to use this information to help guide the development of anisotropic constitutive models. Author

N90-28642*# National Aeronautics and Space Administration. Lewis Research Center, Cleveland, OH.
HIGH TEMPERATURE FATIGUE BEHAVIOR OF HAYNES 188 **c26**

Gary R. Halford, James F. Saltsman, and Sreeramesh Kalluri (Sverdrup Technology, Inc., Cleveland, OH.) *In* NASA, Marshall Space Flight Center, Advanced Earth-to-Orbit Propulsion Technology 1988, Volume 1 Sep. 1988 p 497-509 (For primary document see N90-28611 23-20)
Avail: NTIS HC A99/MF E06 CSCL 11F

The high temperature, creep-fatigue behavior of Haynes 188 was investigated as an element in a broader thermomechanical fatigue life prediction model development program at the NASA-Lewis. The models are still in the development stage, but the data that were generated possess intrinsic value on their own. Results generated to date is reported. Data were generated to characterize isothermal low cycle fatigue resistance at temperatures of 316, 704, and 927 C with cyclic failure lives ranging from 10 to more than 20,000. These results follow trends that would be predicted from a knowledge of tensile properties, i.e., as the tensile ductility varies with temperature, so varies the cyclic inelastic straining capacity. Likewise, as the tensile strength decreases, so does the high cyclic fatigue resistance. A few two-minute hold-time cycles at peak compressive strain were included in tests at 760 C. These results were obtained in support of a redesign effort for the Orbital Maneuverable System engine. No detrimental effects on cyclic life were noted despite the added exposure time for creep and oxidation. Finally, a series of simulated thermal fatigue tests, referred to as bithermal fatigue tests, were conducted using 316 C as the minimum and 760 C as the maximum temperature. Only out-of-phase bithermal tests were conducted to date. These test results are intended for use as input to a more general thermomechanical fatigue life prediction model based on the concepts of the total strain version of Strainrange Partitioning.
Author

N90-28643*# Pratt and Whitney Aircraft, East Hartford, CT.
CONSTITUTIVE AND LIFE MODELING OF SINGLE CRYSTAL BLADE ALLOYS FOR ROOT ATTACHMENT ANALYSIS **c26**
T. G. Meyer, G. J. McCarthy, L. H. Favrow, D. L. Anton, and Joe Bak (United Technologies Research Center, East Hartford, CT.) *In* NASA, Marshall Space Flight Center, Advanced Earth-to-Orbit Propulsion Technology 1988, Volume 1 Sep. 1988 p 510-518 (For primary document see N90-28611 23-20)
(Contract NAS3-23939)
Avail: NTIS HC A99/MF E06 CSCL 11F

Work to develop fatigue life prediction and constitutive models for uncoated attachment regions of single crystal gas turbine blades is described. At temperatures relevant to attachment regions, deformation is dominated by slip on crystallographic planes. However, fatigue crack initiation and early crack growth are not always observed to be crystallographic. The influence of natural occurring microporosity will be investigated by testing both hot isostatically pressed and conventionally cast PWA 1480 single crystal specimens. Several differnt specimen configurations and orientations relative to the natural crystal axes are being tested to investigate the influence of notch acuity and the material's anisotropy. Global and slip system stresses in the notched regions were determined from three dimensional stress analyses and will be used to develop fatigue life prediction models consistent with the observed lives and crack characteristics.
Author

N90-28644*# National Aeronautics and Space Administration. Lewis Research Center, Cleveland, OH.
THE FATIGUE DAMAGE BEHAVIOR OF A SINGLE CRYSTAL SUPERALLOY **c26**
Michael A. McGaw *In* NASA, Marshall Space Flight Center, Advanced Earth-to-Orbit Propulsion Technology 1988, Volume 1 Sep. 1988 p 519-562 (For primary document see N90-28611 23-20)
Avail: NTIS HC A99/MF E06 CSCL 11F

The uniaxial fatigue behavior of a single crystal superalloy, PWA 1480, is described. Both monotonic tensile and constant amplitude fatigue tests were conducted at room temperature, in an effort to assess the applicability of polycrystalline-based fatigue life prediction methods to a single crystal superalloy. The observed constant amplitude behavior correlated best using a stress-based life criterion. Nearly all specimens failed at surface or slightly subsurface microporosity; this is thought to be responsible for the unusually large amount of scatter in the test results. An additional term is developed in the stress-life equation for the purpose of accounting for the effect of microporosity on fatigue life. The form chosen is a function of the effective area of the failure-producing microporosity projected on a plane perpendicular to the loading axis, as well as the applied stress. This additional term correlated the data to within factors of two on life. Although speculative, extrapolation of the microporosity relation to zero micropore area indicates that approximately an order of magnitude improvement in fatigue life should result.
Author

N90-28645*# Failure Analysis Associates, Inc., Palo Alto, CA.
NASCRAC (TRADEMARK): A FRACTURE MECHANICS ANALYSIS CODE **c39**
D. O. Harris, D. D. Dedhia, R. A. Sire, P. J. Woytowitz, and E. E. Nelson *In* NASA, Marshall Space Flight Center, Advanced Earth-to-Orbit Propulsion Technology 1988, Volume 1 Sep. 1988 p 563-579 (For primary document see N90-28611 23-20)
Avail: NTIS HC A99/MF E06 CSCL 20K

The NASCRAC code, a computer program for fracture mechanics analysis, is described. The NASCRAC code is a comprehensive program applicable to a wide variety of fracture mechanics analyses. Although specifically tailored for analysis of fatigue crack growth by the use of linear elastic fracture mechanics, the code has many other capabilities. A brief overview of the code is provided and some of the particular code features are discussed. Emphasis is given to the many stress intensity and J-integral solutions contained in the code, along with provisions for generation of influence factors (for K) and values of fully-plastic J-integrals. The features in the NASCRAC code for automatically transitioning crack geometries as a crack grows due to fatigue are discussed, and provisions for analysis of creep crack growth are covered.
Author

N90-28646*# Southwest Research Inst., San Antonio, TX. Dept. of Materials Sciences.
A COMPARISON OF SINGLE-CYCLE VERSUS MULTI-CYCLE PROOF TESTING STRATEGIES **c39**
Stephen J. Hudak, Jr. and Dale A. Russell (Rockwell International Corp., Canoga Park, CA.) *In* NASA, Marshall Space Flight Center, Advanced Earth-to-Orbit Propulsion Technology 1988, Volume 1 Sep. 1988 p 580-595 (For primary document see N90-28611 23-20)
(Contract NAS8-37451)
Avail: NTIS HC A99/MF E06 CSCL 20K

Proof testing was a useful supplement to conventional nondestructive evaluation (NDE) of space shuttle main engine (SSME) components. Since many of these components involve thin sections and high toughness materials, such as Inconel 718, conventional single-cycle proof test logic is not applicable due to the propensity for stable crack growth during the proof tests. Experience with five-cycle proof testing of SSME components is summarized and a framework is outlined for understanding multi-cycle proof testing using the fracture mechanics concept of a resistance curve. Extreme value statistics are also used to propose an empirical approach to compare the advantages and disadvantages of single- versus multi-cycle proof testing. The importance of the initial flaw size distribution and specimen thickness in such a comparison is also discussed.
Author

N90-28647*# National Aeronautics and Space Administration. Lyndon B. Johnson Space Center, Houston, TX.
DATA BASE FOR CRACK GROWTH PROPERTIES OF MATERIALS **c39**
Royce G. Forman, Victor B. Lawrence, and Henry L. Nguy (Lockheed Engineering and Management Services Co., Inc., Houston, TX.) *In* NASA, Marshall Space Flight Center, Advanced Earth-to-Orbit Propulsion Technology 1988, Volume 1 Sep. 1988 p 596-608 (For primary document see N90-28611 23-20)
Avail: NTIS HC A99/MF E06 CSCL 20K

A computerized data base of crack growth properties of

materials was developed for use in fracture control analysis of rocket engine components and other NASA space hardware. The software system has files of basic crack growth rate data, other fracture mechanics material properties such as fracture toughness and environmental crack growth threshold values, and plotting and fitting routines for deriving material properties for use in fracture control analysis. An extensive amount of data was collected and entered, and work is continuing on compiling additional data. The data base and software codes are useful both for fracture control analysis and for evaluation or development of improved crack growth theories. Author

N90-28648*# National Aeronautics and Space Administration. Marshall Space Flight Center, Huntsville, AL.
COMPARISON OF TWO COMPUTER CODES FOR CRACK GROWTH ANALYSIS: NASCRAC VERSUS NASA/FLAGRO **c39**
Roderick Stallworth, Charles A. Meyers, and Helen C. Stinson *In its* Advanced Earth-to-Orbit Propulsion Technology 1988, Volume 1 Sep. 1988 p 609-633 (For primary document see N90-28611 23-20)
Avail: NTIS HC A99/MF E06 CSCL 20K

The service life calculations of two computer codes, NASCRAC and NASA/FLAGRO, are compared. The analysis technique is based on linear elastic fracture mechanics (LEFM), in which stresses remain below the yield strength of an elastic/plastic material. To perform service life calculations, a relationship expressing incremental crack growth, DA/DN, as a function of loading, geometry, and material properties is necessary. Load and geometry are expressed in terms of the cyclic stress intensity factor, delta K. The crack growth rate as a function of delta K is then determined by material tests, plotting DA/DN versus delta K for the given material, loading condition, and environment. Crack growth rate equations such as the Paris, Walker, and modified Forman equations are used to obtain a best fit curve to the laboratory DA/DN versus delta K data. Author

N90-28649*# National Aeronautics and Space Administration. Lewis Research Center, Cleveland, OH.
STRUCTURAL RESPONSE OF SSME TURBINE BLADE AIRFOILS **c39**
V. K. Arya, A. Abdul-Aziz (Sverdrup Technology, Inc., Cleveland, OH.), and R. L. Thompson *In* NASA, Marshall Space Flight Center, Advanced Earth-to-Orbit Propulsion Technology 1988, Volume 1 Sep. 1988 p 634-652 (For primary document see N90-28611 23-20)
Avail: NTIS HC A99/MF E06 CSCL 20K

Reusable space propulsion hot gas-path components are required to operate under severe thermal and mechanical loading conditions. These operating conditions produce elevated temperature and thermal transients which results in significant thermally induced inelastic strains, particularly, in the turbopump turbine blades. An inelastic analysis for this component may therefore be necessary. Anisotropic alloys such as MAR M-247 or PWA-1480 are being considered to meet the safety and durability requirements of this component. An anisotropic inelastic structural analysis for an SSME fuel turbopump turbine blade was performed. The thermal loads used resulted from a transient heat transfer analysis of a turbine blade. A comparison of preliminary results from the elastic and inelastic analyses is presented. Author

N90-28650*# Pratt and Whitney Aircraft, West Palm Beach, FL.
PROBABILISTIC MODEL FOR FRACTURE MECHANICS SERVICE LIFE ANALYSIS **c39**
Charles Annis and Tommie Watkins *In* NASA, Marshall Space Flight Center, Advanced Earth-to-Orbit Propulsion Technology 1988, Volume 1 Sep. 1988 p 653-659 (For primary document see N90-28611 23-20)
(Contract NAS8-36901)
Avail: NTIS HC A99/MF E06 CSCL 20K

The service longevity of complex propulsion systems, such as the Space Shuttle Main Engine (SSME), can be at risk from several competing failure modes. Conventional life assessment practice focuses upon the most severely life-limited feature of a given component, even though there may be other, less severe, potential failure locations. Primary, secondary, tertiary failure modes, as well as their associated probabilities, must also be considered. Futhermore, these probabilities are functions of accumulated service time. Thus a component may not always succumb to the most severe, or even the most probable failure mode. Propulsion system longevity must be assessed by considering simultaneously the actions of, and interactions among, life-limiting influences. These include, but are not limited to, high frequency fatigue (HFF), low cycle fatigue (LCF), and subsequent crack propagation, thermal and acoustic loadings, and the influence of less-than-ideal nondestructive evaluation (NDE). An outline is provided for a probabilistic model for service life analysis, and the progress towards its implementation is reported. Author

N90-28651*# National Aeronautics and Space Administration. Lewis Research Center, Cleveland, OH.
DURABILITY OF THERMAL BARRIER COATINGS IN A HIGH HEAT FLUX ENVIRONMENT **c27**
William J. Brindley and James A. Nesbitt *In* NASA, Marshall Space Flight Center, Advanced Earth-to-Orbit Propulsion Technology 1988, Volume 1 Sep. 1988 p 661-674 (For primary document see N90-28611 23-20)
Avail: NTIS HC A99/MF E06 CSCL 11C

Thermal shock is a significant factor in the limited service life of Space Shuttle Main Engine (SSME) high pressure, fuel turbopump (HPFTP) turbine blades. Addition of advanced thermal barrier coatings (TBCs) to the blades could serve to dampen the thermal shock, thereby increasing the life of the blades. However, testing and use of TBCs to date is performed primarily under moderate heat flux conditions which are typical of aircraft turbines. Only limited testing was conducted that addresses high heat flux and severe thermal shock conditions. Therefore, it is not clear if TBCs can survive severe thermal shocks or provide adequate thermal shock protection to the HPFTP turbine blades. The purpose is to experimentally evaluate the potential durability and protective capability of a variety of advanced TBCs in a cyclic thermal shock environment. A secondary goal is to identify significant parameters affecting TBC life during high heat flux testing. Parameters investigated include top coat thickness, bond coat thickness, substrate type, and substrate geometry. Author

N90-28652*# National Aeronautics and Space Administration. Lewis Research Center, Cleveland, OH.
THERMAL ANALYSIS OF THERMAL BARRIER COATINGS IN A HIGH HEAT FLUX ENVIRONMENT **c27**
James A. Nesbitt and William J. Brindley *In* NASA, Marshall Space Flight Center, Advanced Earth-to-Orbit Propulsion Technology 1988, Volume 1 Sep. 1988 p 675-691 (For primary document see N90-28611 23-20)
Avail: NTIS HC A99/MF E06 CSCL 11C

Gas temperatures and pressures were measured around the second test position in the H2/O2 rocket engine at NASA-Lewis. Measured gas temperatures generally varied from 1210 to 1390 C. Measured pressures were in good agreement with other studies for throat tubes in a square chamber rocket engine. Heat transfer coefficients were measured at 90 and 180 degrees from the stagnation point and resulted in values of 27.5 and 8.5 kW/sq m C, respectively. A thermal model was developed to predict temperatures in bare and coated tubes and rods. Agreement between measured and predicted temperatures below the surface of a bare Mar-M 246 tube was very good for most of the heat up and cool down period. Predicted temperatures were significantly below measured temperatures for the coated tubes. A thermal model to simulate heat transfer to the leading edge of an HPFTP blade was developed and showed that TBCs can significantly dampen the thermal transient which occurs in the HPFTP during the startup of the SSME. Author

N90-28653*# National Aeronautics and Space Administration. Marshall Space Flight Center, Huntsville, AL.
VACUUM APPLICATION OF THERMAL BARRIER PLASMA COATINGS **c27**
R. R. Holmes and T. N. McKechnie (Rockwell International Corp., Canoga Park, CA.) *In its* Advanced Earth-to-Orbit Propulsion Technology 1988, Volume 1 Sep. 1988 p 692-702 (For primary document see N90-28611 23-20)
Avail: NTIS HC A99/MF E06 CSCL 11C

Coatings are presently applied to Space Shuttle Main Engine (SSME) turbine blades for protection against the harsh environment realized in the engine during lift off-to-orbit. High performance nickel, chromium, aluminum, and yttrium (NiCrAlY) alloy coatings, which are applied by atmospheric plasma spraying, crack and spall off because of the severe thermal shock experienced during start-up and shut-down of the engine. Ceramic coatings of yttria stabilized zirconia (ZrO2-Y2O3) were applied initially as a thermal barrier over coating to the NiCrAlY but were removed because of even greater spalling. Utilizing a vacuum plasma spraying process, bond coatings of NiCrAlY were applied in a low pressure atmosphere of argon/helium, producing significantly improved coating-to-blade bonding. The improved coatings showed no spalling after 40 MSFC burner rig thermal shock cycles, cycling between 1700 and -423 F. The current atmospheric plasma NiCrAlY coatings spalled during 25 test cycles. Subsequently, a process was developed for applying a durable thermal barrier coating of ZrO2-Y2O3 to the turbine blades of first stage high-pressure fuel turbopumps utilizing the vacuum plasma process. The improved thermal barrier coating has successfully passed 40 burner rig thermal shock cycles without spalling. Hot firing in an SSME turbine engine is scheduled for the blades. Tooling was installed in preparation for vacuum plasma spray coating other SSME hardware, e.g., the titanium main fuel valve housing (MFVH) and the fuel turbopump nozzle/stator. Author

N90-28654*# IIT Research Inst., Chicago, IL. Surface Engineering Center.
APPLICATION OF ADVANCED COATING TECHNIQUES TO ROCKET ENGINE COMPONENTS **c27**
S. K. Verma *In* NASA, Marshall Space Flight Center, Advanced Earth-to-Orbit Propulsion Technology 1988, Volume 1 Sep. 1988 p 703-729 (For primary document see N90-28611 23-20)
Avail: NTIS HC A99/MF E06 CSCL 11C

The materials problem in the space shuttle main engine (SSME) is reviewed. Potential coatings and the method of their application for improved life of SSME components are discussed. A number of advanced coatings for turbine blade components and disks are being developed and tested in a multispecimen thermal fatigue fluidized bed facility at IIT Research Institute. This facility is capable of producing severe strains of the degree present in blades and disk components of the SSME. The potential coating systems and current efforts at IITRI being taken for life extension of the SSME components are summarized. Author

N90-28655*# National Aeronautics and Space Administration. Lewis Research Center, Cleveland, OH.
CERAMIC MATRIX COMPOSITES IN SIMULATED SSME ENVIRONMENTS **c24**
Thomas P. Herbell and Andrew J. Eckel (Sverdrup Technology, Inc., Middleburg Heights, OH.) *In* NASA, Marshall Space Flight Center, Advanced Earth-to-Orbit Propulsion Technology 1988, Volume 1 Sep. 1988 p 730-741 (For primary document see N90-28611 23-20)
Avail: NTIS HC A99/MF E06 CSCL 11D

Future Space Shuttle Main Engine (SSME)-type rocket engines can benefit from the use of fiber-reinforced ceramix matrix composites (FRCMC). Ceramics reinforced with long continuous fibers exhibit improved tolerance to severe thermomechanical and environmental exposures. An in-house NASA-Lewis program to evaluate the durability of FRCMC in simulated SSME environments is described. Primary tests involve multiple (one second) exposures of FRCMC specimens in a hydrogen/oxygen rocket test rig. This rig generates surface heating rates of 1000 to 2500 C/second. The FRCMC durability evaluation involves measurement of retained strength as a function of thermal shock severity and number of upshock cycles. Preliminary test results for monolithic silicon nitride (Si3N4) and silicon carbide (SiC), and one type of silicon based FRCMC, are presented. The test data are examined in terms of simple thermal shock theory. Author

N90-28656*# National Aeronautics and Space Administration. Marshall Space Flight Center, Huntsville, AL.
ROBOTIC AND AUTOMATIC WELDING DEVELOPMENT AT THE MARSHALL SPACE FLIGHT CENTER **c37**
C. S. Jones, M. E. Jackson, and L. A. Flanigan (Rockwell International Corp., Canoga Park, CA.) *In its* Advanced Earth-to-Orbit Propulsion Technology 1988, Volume 1 Sep. 1988 p 742-750 (For primary document see N90-28611 23-20)
Avail: NTIS HC A99/MF E06 CSCL 13H

Welding automation is the key to two major development programs to improve quality and reduce the cost of manufacturing space hardware currently undertaken by the Materials and Processes Laboratory of the NASA Marshall Space Flight Center. Variable polarity plasma arc welding has demonstrated its effectiveness on class 1 aluminum welding in external tank production. More than three miles of welds were completed without an internal defect. Much of this success can be credited to automation developments which stabilize the process. Robotic manipulation technology is under development for automation of welds on the Space Shuttle's main engines utilizing pathfinder systems in development of tooling and sensors for the production applications. The overall approach to welding automation development undertaken is outlined. Advanced sensors and control systems methodologies are described that combine to make aerospace quality welds with a minimum of dependence on operator skill. Author

N90-28657*# National Aeronautics and Space Administration. Lewis Research Center, Cleveland, OH.
LOW POWER ARCJET PERFORMANCE
Francis M. Curran and Charles J. Sarmiento Jul. 1990 15 p Presented at the 21st International Electric Propulsion Conference, Orlando, FL, 18-20 July 1990; cosponsored in part by AIAA, DGLR, and JSASS
(NASA-TM-103280; E-5734; NAS 1.15:103280; AIAA-90-2578)
Avail: NTIS HC A03/MF A01 CSCL 21H

An experimental investigation was performed to evaluate arc jet operation at low power. A standard, 1 kW, constricted arc jet was run using nozzles with three different constrictor diameters. Each nozzle was run over a range of current and mass flow rates to explore stability and performance in the low power engine. A standard pulse-width modulated power processor was modified to accommodate the high operating voltages required under certain conditions. Stable, reliable operation at power levels below 0.5 kW was obtained at efficiencies between 30 and 40 percent. The operating range was found to be somewhat dependent on constrictor geometry at low mass flow rates. Quasi-periodic voltage fluctuations were observed at the low power end of the operating envelope, The nozzle insert geometry was found to have little effect on the performance of the device. The observed performance levels show that specific impulse levels above 350 seconds can be obtained at the 0.5 kW power level. Author

N90-28658*# Stuttgart Univ. (Germany, F.R.). Inst. fuer Raumfahrtsysteme.
HIGH POWER ARCJET Progress Report No. 2
M. Auweter-Kurtz, B. Glocker, T. M. Goelz, H. Habiger, H. L. Kurtz, H. O. Schrade, and T. Wegmann Aug. 1990 26 p Original contains color illustrations
(Grant NAGw-1736)
(NASA-CR-183086; NAS 1.26:183086; IRS-90-P7) Avail: NTIS HC A03/MF A01; 7 functional color pages CSCL 21H

The activities on the development of the high power arc jet HIPARC, the thrust balance, and plasma diagnostic probes are discussed. Modifications of the HIPARC design and a synopsis of the materials used are given. Further experimental results with

the TT30 thruster in the 50 kW range are presented. Some first calibration measurements of the thrust balance are also included. Progress concerning the development of plasma diagnostic devices is documented. Author

N90-28659*# National Aeronautics and Space Administration. Lewis Research Center, Cleveland, OH.
A FAILURE DIAGNOSIS SYSTEM BASED ON A NEURAL NETWORK CLASSIFIER FOR THE SPACE SHUTTLE MAIN ENGINE
Ahmet Duyar (Florida Atlantic Univ., Boca Raton.) and Walter Merrill 1990 13 p Proposed for presentation at the 29th Conference on Decision and Control, Honolulu, HI, 5-7 Dec. 1990; sponsored by IEEE
(NASA-TM-103607; E-5756; NAS 1.15:103607) Avail: NTIS HC A03/MF A01 CSCL 21H

A conceptual design of a model based failure detection and diagnosis system is developed for the space shuttle main engine. This design relies on the accurate and reliable identification of the parameters of the highly nonlinear and very complex engine. The design approach is presented in some detail and results for a failed valve are presented. These preliminary results verify that the developed parameter identification technique together with a neural network classifier can be used for this purpose. Author

N90-28660*# Boeing Aerospace Co., Seattle, WA.
DESIGN OPTIMIZATION OF GAS GENERATOR HYBRID PROPULSION BOOSTERS
Vincent Weldon, Dwight U. Phillips, and Lawrence E. Fink 1990 24 p
(Contract NAS8-37776)
(NASA-CR-181096; NAS 1.26:181096) Avail: NTIS HC A03/MF A01 CSCL 21H

A methodology used in support of a contract study for NASA/MSFC to optimize the design of gas generator hybrid propulsion booster for uprating the National Space Transportation System (NSTS) is presented. The objective was to compare alternative configurations for this booster approach, optimizing each candidate concept on different bases, in order to develop data for a trade table on which a final decision was based. The methodology is capable of processing a large number of independent and dependent variables, adjusting the overall subsystems characteristics to arrive at a best compromise integrated design to meet various specified optimization criteria subject to selected constraints. For each system considered, a detailed weight statement was generated along with preliminary cost and reliability estimates. Author

N90-28661# Army Strategic Defense Command, Huntsville, AL.
USE OF NI63 OVERVOLTAGE GAP SWITCHES IN THE FLIGHT TERMINATION SYSTEMS ON BOOSTERS LAUNCHED FROM US ARMY KWAJALEIN ATOLL (USAKA)
Randy Gallien May 1990 84 p
(AD-A223866) Avail: NTIS HC A05/MF A01 CSCL 21/8

This Environmental Assessment documents the results of an analysis of the potential for and the magnitude of impacts resulting from using Overvoltage Gap Switches containing Ni63 radioisotopes in the Flight Termination System of the Ground-Based Interceptor Boosters launched from the U.S. Army Kwajalein Atoll. GRA

23 CHEMISTRY AND MATERIALS (GENERAL)

No abstracts in this category.

24 COMPOSITE MATERIALS

Includes physical, chemical, and mechanical properties of laminates and other composite materials.
For ceramic materials see *27 Nonmetallic Materials*.

N90-28662# Oak Ridge National Lab., TN. Metals and Ceramics Div.
FRICTION MICROPROBE STUDIES OF COMPOSITE SURFACES
Peter J. Blau 1990 10 p Presented at the Conference on the Tribology of Composite Materials, Oak Ridge, TN, 1-3 May 1990
(Contract DE-AC05-84OR-21400)
(DE90-014224; CONF-900513-2) Avail: NTIS HC A02/MF A01

A newly constructed friction microprobe was used to study the variations in friction force associated with unlubricated sliding of small 1.0 mm diameter, 440C stainless steel spheres over the surfaces of alumina, silicon nitride, silicon carbide, and silicon carbide whisker-reinforced composites with matrices of alumina and silicon nitride. The purpose of the work was to attempt to detect frictional transients associated with the sliding interaction of individual asperities and to relate these transients to the microstructures of the ceramics and their composites. Friction data could be obtained without detectable wear of either the spheres or the flat specimens. The presence of whiskers increased in the friction of alumina by about 28 percent and decreased the friction of silicon nitride by about 15 percent. Less than a 1 percent instantaneous variation in friction coefficient could be directly ascribed to contacts with whiskers. DOE

N90-28663# Oak Ridge National Lab., TN. Metals and Ceramics Div.
MICROMECHANICS ANALYSIS OF POWER CONSOLIDATION IN MANUFACTURING PARTICULATE-REINFORCED MMCS (METAL MATRIX COMPOSITES)
T. C. Tszeng 1990 9 p Presented at the International Conference on Fabrication of Particulates Reinforced Metal Composites, Montreal, Quebec, 16-19 Sep. 1990
(Contract DE-AC05-84OR-21400)
(DE90-014448; CONF-9009147-1) Avail: NTIS HC A02/MF A01

A micromechanics study of the interaction between a reinforcing particulate and matrix powder particles subjected to isostatic pressing has been carried out. The model enables us to examine the deformation, number of contacting particles, total contact area, and average contact pressure on an individual particulate or powder particle. Three different powder systems were analyzed. Particularly, the composite powder systems are typified by a dual-sized powder system consisting of 20 wt percent reinforcing particulate and 80 wt percent matrix particles of 1/2.6 size ratio. The analysis shows that the smaller reinforcing particulates experience larger specific contact area and higher average contact pressure in comparison with the larger matrix powder particles. DOE

N90-28664 Stanford Univ., CA.
MECHANICAL BEHAVIOR OF THICK, CURVED, LAMINATED COMPOSITES Ph.D. Thesis
Ehoud Graff 1989 159 p
Avail: Univ. Microfilms Order No. DA9011502

A finite element code was developed for calculating the stresses and strains in thick, curved, composite laminates subjected to an arbitrary, but consistent, combination of forces and displacements. The laminate may be arbitrarily curved in one plane but must have no curvature in the other two perpendicular planes. The accuracy of the stress analysis was evaluated by generating numerical results for three problems for which analytical solutions exist, and by comparing the numerical and the analytical results. In every case the agreement between the numerical and analytical results was excellent. The analysis and the computer code were specialized to racetrack shaped composite straps loaded by pins in tension. A procedure was also established for estimating the failure loads of such straps, by utilizing the strains provided by the finite element method and the Tsai-Wu failure criteria. Tests

were performed to validate the strap stress analysis and failure model. Forty-three straps were made of either T300/976, IM6/081, T1000/081 graphite-epoxy, K92/081 kevlar-epoxy, or S-2/081 glass-epoxy. The strains and failure loads of these straps were measured, and the data were compared to the calculated strains and failure loads. The calculated values agreed well with the data. Lastly, the use of the computer code in the design of composite straps is discussed, and charts for estimating the failure loads of different types of straps are presented. Dissert. Abstr.

N90-28665 Surrey Univ., London (England).
PROBABILITY MODELS FOR THE FAILURE OF FIBRES AND FIBROUS COMPOSITE MATERIALS Ph.D. Thesis
Linda C. Wolstenholme 1989 201 p
Avail: Univ. Microfilms Order No. BRDX88358

Probability models are developed for the failure of parallel brittle fibers embedded in a relatively soft plastic matrix. A loss of load-bearing occurs in the region surrounding a fiber break, resulting in a concentration of stress in neighboring fibers. These stress concentrations cannot be measured directly, but by assuming them to be a chosen function of unknown parameters, the failure of the composite may be modeled. It is then shown how the stress concentration parameters may be estimated using the method of maximum likelihood. The technique is illustrated using experimental data for different materials, and in particular, it is shown how the stress concentration parameters vary with fiber spacing. The appearance of breaks along a fiber is, in nature, a point process. Load-sharing between two fiber processes will lead to a degree of nearly coincidental breaks. The degree to which coincidences or matchings occur in two independent point processes is examined. An unusually high degree of matching can be defined, and used to infer that processes are not independent. The exact analysis for a fiber-break process is intractable, but several approximate alternatives are studied, and compared with real and simulated data. The probability models for composite failure rely on assumptions about the underlying strength of the fibers. Principally, the weakest-link property is assumed, frequently characterized by use of the Weibull distribution. A non-parametric test of this property is devised, and specially designed experiments show that weakest-link is apparently open to considerable doubt. It is shown that the existence of different causes of failure, all of which may not be present all of the time, give rise to some new types of failure model. It is demonstrated that these do not have the weakest-link property, even when based on the Weibull distribution, and that they are consistent with some experimental results. Dissert. Abstr.

N90-28666 Rutgers - The State Univ., New Brunswick, NJ.
STRENGTHENING AND TOUGHENING MECHANISMS IN CERAMIC FIBER-REINFORCED GLASS MATRIX COMPOSITES Ph.D. Thesis
Cheryl Ann Zern 1989 178 p
Avail: Univ. Microfilms Order No. DA9013470

A composite system containing FP-alumina fibers and a borosilicate glass matrix was studied. CVD carbon coatings were applied to the fibers to control the degree of bonding at the interface. Processing techniques of slurry infiltration and hot pressing were used to fabricate composites with fiber fractions ranging from 20 to 50 percent. The most significant result is the determination of the role of the fiber/matrix interface in dictating the mechanical properties. The carbon coatings enhanced the mechanical properties of the composites by reducing the shear strength of the fiber matrix interface. The interfacial shear stress for fiber movement was measured using an indentation method. Composites with uncoated fibers did not show fiber sliding due to the strong bonding. Fibers in the composites with 22 and 47 percent C-coated fibers slid in their matrix cavities during measurement and exhibited shear strength for fiber movement values of 100 and 43 MPa respectively. These values are greater than interfacial shear strength values from the literature for debonded fiber composites. Interfacial shear stress required for fiber movement after debonding the fiber from the matrix was measured on thin samples. Values of 37 and 10 MPa were found for the 22 and 47 percent fiber samples respectively. Contributions to the interfacial shear stress for fiber movement include: friction between two surfaces, surface roughness of the fibers, radial interfacial pressure due to thermal expansion differences, a chemical bonding effect, and a residual shear stress for fiber movement include: friction between two surfaces, surface roughness of the fibers, radial interfacial pressure due to thermal expansion differences, a chemical bonding effect, and a residual shear stress for fiber movement. These components may be combined to produce a model for the total interfacial shear stress for fiber movement. The work of fracture was measured on the composites and found to behave according to expected results. Work of fracture values for C-coated fiber composites were 3800 and 4969 J/sq m for 22 and 47 percent fiber levels. Uncoated fiber composites exhibited very low work of fracture. Dissert. Abstr.

N90-28667 Georgia Inst. of Tech., Atlanta.
CRASH-IMPACT BEHAVIOR OF GRAPHITE/EPOXY COMPOSITE SINE WAVE WEBS Ph.D. Thesis
Weiyu Zhou 1989 171 p
Avail: Univ. Microfilms Order No. DA9014874

This research focuses on the study of static and dynamic energy absorption behavior of graphite epoxy composite sine wave webs (corrugated webs). The principal objectives are: (1) comparison of the dynamic versus static properties in order to establish the reliability of using static energy absorption information to predict dynamic behavior; and (2) comparison of theory versus experiment in order to create a suitable theoretical model for understanding and explaining the energy absorption mechanisms based on the experimental work. The static energy absorption behavior of sine wave webs loaded in axial compression was investigated both in experimental and theoretical territories. Tests were conducted to study the effects of various geometric parameters of the web specimen including width and effective thickness. The importance of the failure initiator and its effect on energy absorption are described along with other observed energy absorption trends. A theoretical model for the static energy absorption mechanism in a sine wave web was developed. Good agreement was obtained between experiment data and the analytical model. The existence of a stability boundary within which efficient crushing occurs was shown in the case of effective thickness variation of the web, and verified by theoretical study. Boundary effects, more specifically specimen finite width effects, in the web were also studied experimentally and theoretically, and were predicated for this sine wave web based on the study. The dynamic energy absorption behavior of sine wave webs was also investigated experimentally. Dissert. Abstr.

N90-28668 Michigan Univ., Ann Arbor.
FACTORS INFLUENCING THE MODE I INTERLAMINAR FRACTURE RESISTANCE OF TOUGHENED MATRIX COMPOSITES Ph.D. Thesis
Douglas Scott Parker 1989 225 p
Avail: Univ. Microfilms Order No. DA9013986

Fiber reinforced polymeric composites which provide high stiffness and strength to weight ratios have become important for the production of weight sensitive structures. A major problem with polymer composites based on brittle matrices is that they have a low interlaminar fracture toughness and are sensitive to out of plane impact. Simply introducing a toughened resin as a matrix material does not necessarily bring about a substantial improvement in the fracture toughness of a composite. In this study, composites were produced utilizing epoxy and thermoplastic matrix materials both in the neat and rubber modified conditions. These composites allow evaluation over the extremes of matrix fracture toughness and the identification of factors which influence the mode I interlaminar fracture toughness of toughened matrix composites. The results of this work have identified several factors which limit the interlaminar fracture toughness of a composite. These include rubber particle agglomeration, solvent and molding induced crystallization of the matrix, and poor fiber matrix adhesion. It is observed that the plastic zone which develops in the composite is smaller than that of the bulk resin and extends beyond a single

interfibrillar spacing. Improvements made in the fracture toughness of the matrix resins do not lead to proportional increases in the interlaminar fracture toughness of a composite due to poor fiber matrix adhesion. In order to produce tough composites utilizing toughened matrices, any improvements in the matrix toughness must be coupled with improvements in the fiber/matrix adhesion. Dissert. Abstr.

N90-28669 Rensselaer Polytechnic Inst., Troy, NY.
INELASTIC ANALYSIS OF LAMINATED COMPOSITES Ph.D. Thesis
Bor Zen Hong 1989 251 p
Avail: Univ. Microfilms Order No. DA9018429

In an extension of classical laminate theory for in-plane loading and bending two new theories of rate-dependent behavior are introduced. It is assumed that the ply behavior can be represented by orthotropic continuum theories representative of metal matrix or polymer matrix behavior. The simplified orthotropic viscoplasticity theory based on overstress which does not use a yield surface and loading/unloading conditions is the basis of the formulations. It can represent rate sensitivity, creep and relaxation in a unified way. The inelastic strain rate is solely a function of overstress, the difference between stress and the equilibrium stress which is the state variable of the theory. The growth law for the equilibrium stress is incremental for the modeling of metal matrix laminates and is the repository for modeling hysteresis and permanent set after inelastic deformation. For polymer matrix composites the equilibrium stress depends solely on strain and therefore no permanent set can be modeled. Ease of use and formulations with a minimum number of material constants are the goal of both material models. The governing equations for in-plane loading and bending for arbitrary lay-ups are established. They consist of a set of coupled, non-linear, stiff ordinary differential equations which must be integrated numerically for either strain or stress boundary conditions. This is accomplished by a FORTRAN program. A semi-empirical method is established which assumes the rate dependence and allows the determination of the material constants of the theory from limited test data. Dissert. Abstr.

N90-28670*# National Aeronautics and Space Administration. Lewis Research Center, Cleveland, OH.
THE EFFECTS OF ATOMIC OXYGEN ON THE THERMAL EMITTANCE OF HIGH TEMPERATURE RADIATOR SURFACES
Sharon K. Rutledge, Deborah L. Hotes, and Phillip E. Paulsen (Cleveland State Univ., OH.) 1989 25 p Presented at the Spring Meeting of the Materials Research Society, San Diego, CA, 24-29 Apr. 1989
(NASA-TM-103224; E-5640; NAS 1.15:103224) Avail: NTIS HC A03/MF A01 CSCL 11D

Radiator surfaces on high temperature space power systems such as SP-100 space nuclear power system must maintain a high emittance level in order to reject waste heat effectively. One of the primary materials under consideration for the radiators is carbon-carbon composite. Since carbon is susceptible to attack by atomic oxygen in the low earth orbital environment, it is important to determine the durability of carbon composites in this environment as well as the effect atomic oxygen has on the thermal emittance of the surface if it is to be considered for use as a radiator. Results indicate that the thermal emittance of carbon-carbon composite (as low as 0.42) can be enhanced by exposure to a directed beam of atomic oxygen to levels above 0.85 at 800 K. This emittance enhancement is due to a change in the surface morphology as a result of oxidation. High aspect ratio cones are formed on the surface which allow more efficient trapping of incident radiation. Erosion of the surface due to oxidation is similar to that for carbon, so that at altitudes less than approximately 600 km, thickness loss of the radiator could be significant (as much as 0.1 cm/year). A protective coating or oxidation barrier forming additive may be needed to prevent atomic oxygen attack after the initial high emittance surface is formed. Textured surfaces can be formed in ground based facilities or possibly in space if emittance is not sensitive to the orientation of the atomic oxygen arrival that forms the texture. Author

N90-28671# National Defence Research Establishment, Stockholm (Sweden). Dept. of Weapon Systems, Effects, and Protection.
ARALL (ARAMID ALUMINUM LAMINATE), A LITERATURE SURVEY
Sven Bogegard Feb. 1990 20 p In SWEDISH, ENGLISH summary
(FOA-C-20782-2.5; ISSN-0347-3694; ETN-90-97101) Avail: NTIS HC A03/MF A01

ARALL is a high strength Kevlar composite bonded between thin sheets of a high strength aluminum alloy. It combines the good fatigue and crack growth properties of Kevlar-Epoxy composites with the environmental durability of aluminum. The material is 15 percent less dense than monolithic aluminum and the tensile properties are claimed to be 15 to 30 percent better. The material can be processed like ordinary aluminum alloys. ARALL protects well from lightning and has attractive dumping properties. ESA

N90-28672# Office National d'Etudes et de Recherches Aerospatiales, Paris (France). Direction Scientifique des Materiaux.
ELECTROCHEMICAL SURFACE FINISHING USING AMINO-SUBSTRATES ON CARBON FIBERS IN ORGANIC MEDIA. EFFECTS OF THE FINISHING ON THE MECHANICAL PROPERTIES OF CARBON-EPOXY COMPOSITES [TRAITEMENTS ELECTROCHIMIQUES A SUBSTRAT AMINE SUR DES FIBRES DE CARBONE, EN MILIEU ORGANIQUE. EFFETS DE CES TRAITEMENTS SUR DES PROPRIETES MECANIQUES DE COMPOSITES CARBONE-EPOXY]
B. Barbier and G. Desarmot Feb. 1989 222 p In FRENCH
(Contract DRET-88-34-001)
(ONERA-RT-9/3549-M; ETN-90-97489) Avail: NTIS HC A10/MF A02

The toughness of carbon-epoxy fibers submitted to electrochemical surface finishing using amino substrates is investigated. Such a finishing in organic media induces the grafting of an amino molecule by a cationic radical. The grafting kinetics depends on temperature and voltage of the process. The results of toughness from composite materials made of surface finished fibers, fibers without finishing and oxided fibers are compared. High values of toughness were obtained from triethylenetetramine substrates. ESA

N90-28673# Los Alamos National Lab., NM. Ceramic Science and Technology Group.
IS THERE ANYTHING OF PRACTICAL VALUE HIDDEN AMONGST THE COMPOSITE TOUGHENING THEORIES. A JIM MUELLER PROSPECTIVE
Frank D. Gac 1990 36 p Presented at the 14th Annual Conference on Composites and Advanced Ceramics, Cocoa Beach, FL, 14-17 Jan. 1990 Submitted for publication
(Contract W-7405-eng-36)
(DE90-014905; LA-UR-90-2431; CONF-900160-4) Avail: NTIS HC A03/MF A01

Numerous theories have been developed over the last three decades for explaining the toughening behavior of discontinuous fiber reinforced brittle matrix composites. The issue is the practical engineering utility of these theories. Upon compiling a table of fiber parameters that are identified in the predominant toughening mechanisms, a number of important features become evident for achieving high toughnesses. First, all of the mechanisms indicate that a high fiber volume fraction is desirable. Second, residual stresses appear to influence all of the composite toughening mechanisms. Third, the highest fiber tensile strength is preferred. Finally, fiber diameter and fiber-matrix interfacial shear strength are also important, but both are composite system and toughening mechanism specific. DOE

N90-28674# Atomic Energy of Canada Ltd., Pinawa (Manitoba). Nuclear Research Establishment.
RADIATION-CURABLE PREPREG COMPOSITES
Chris B. Saunders, Lawrence W. Dickson, Ajit Singh, Alistair A.

Carmichael, and Vince J. Lopata 1988 23 p
(DE90-629740; AECL-9560; ISSN-0067-0367) Avail: NTIS (US Sales Only) HC A03/MF A01

A potential application of electron-beam processing in composite manufacturing is curing carbon-fiber prepregs. These thermally curable prepregs, carbon fibers or fabrics preimpregnated with liquid polymer resin, are commonly used in the aircraft industry. A radiation-curable prepreg was designed to meet the mechanical and physical property specifications of a leading aircraft manufacturing company. Characterization studies showed that the maximum gel fraction in the cured polymer occurred at a dose of about 50 kGy and varied from 91 to 97 percent, depending on the type of atmosphere (air or nitrogen) and the pressure (100 to 1000 kPa) during irradiation. Only the acrylate groups of the resin took a significant part in the curing reactions. Some carbon dioxide was produced during radiation curing. The polymer was amorphous with a softening point of about 235 C and a linear thermal expansion coefficient of 1.3 x 10(exp -4) m/(m x C) between 25 and 150 C (30 to 50 kGy). Preliminary mechanical and physical testing of the prepreg composites was also started. DOE

N90-28675# Instituto de Pesquisas Espaciais, Sao Jose dos Campos (Brazil).
FABRICATION OF SPHERICAL PRESSURE VESSELS FROM COMPOSITE MATERIALS [FABRICACAO DE VASO DE PRESSAO ESFERICO EM MATERIAL COMPOSTO]
Thomas Leomil Shaw Jun. 1988 18 p In PORTUGESE
(INPE-4598-RPE/570) Avail: NTIS HC A03/MF A01

The high performance presented by spherical pressure vessels of composite materials, compared with conventional metallic pressure vessels, causes them to be very attractive for aerospace applications. The present work has as its objective fabrication of a spherical vessel with carbon fibers, which is identified as a critical stage in the process. Transl. by B. G.

N90-28676# Southwest Research Inst., San Antonio, TX.
MICROMECHANISMS OF FATIGUE CRACK GROWTH AND FRACTURE TOUGHNESS IN METAL MATRIX COMPOSITES Final Technical Report, 1 Aug. 1988 - 28 Apr. 1990
David L. Davidson 28 Jun. 1990 9 p
(Contract N00014-85-C-0206; NR Proj. 039283)
(AD-A223863) Avail: NTIS HC A02/MF A01 CSCL 11/4

Research objectives under which this work was initiated were as follows: To understand the mechanisms of subcritical crack extension and fracture toughness in particulate-reinforced metal matrix composites projected for Naval applications in which one or more of these parameters control service. The factors thought to be important in 1985 were the processing variables by which these materials were fabricated and the role of SiC particles in altering fatigue crack growth and fracture toughness of the matrix alloys. The methods used in reaching for these objectives include the techniques of experimental micromechanics. Experiments in fatigue crack growth and fast fracture were conducted for a variety of composites obtained from different manufacturers, and these materials were thoroughly characterized. Materials characterized were picked in order to: (1) determine the effects of differences in matrix composition and heat treatment, (2) determine the effect of SiC volume fraction, and (3) account for differences in particle size. Materials were obtained from two different manufacturers. IN-9051+15v/o SiC (essentially Al-4Mg) and IN-9021+15v/o SiC, both made by mechanically alloying and powder metallurgy were obtained from Novamet. The remainder of the composites made by ingot metallurgy by Dural Aluminum Composites Co., were: Al-4Mg+15v/o SiC, 2014+15v/o SiC, 2014+25v/o SiC, 2024+15v/o, 2014+15v/o SiC, and 7475+15v/o SiC. GRA

N90-28677# Georgia Inst. of Tech., Atlanta.
A THEORETICAL INVESTIGATION INTO THE INELASTIC BEHAVIOR OF METAL-MATRIX COMPOSITES Final Report, Jun. 1988 - Jun. 1990 M.S. Thesis
William F. Ward Jun. 1990 132 p
(AD-A223973) Avail: NTIS HC A07/MF A01 CSCL 11/4

Various self-consistent analyses have been proposed and used to approximately evaluate the elastic stiffness and elastic-plastic behavior of metal-matrix composites. Such analyses have generally relied on very simple theoretical models for the matrix inelastic stress-strain response. This was perhaps substantiated on the basis of a lack of combined stress state experiments. Weng (1988) successfully approximated the inelastic behavior of spherical particle-reinforced composites utilizing a modified self-consistent model called the equivalent inclusion-average stress (EIAS) method. Noting the overly stiff response of the basic EIAS model, he developed the secant modulus method to correct for the overconstraining power of the matrix. The purpose of this thesis is to reexamine the problem in the context of more sophisticated nonlinear kinematic hardening rules for the matrix. An EIAS method which incorporates a tangent stiffness formulation based on incremental plasticity is proposed. GRA

N90-28678*# Purdue Univ., West Lafayette, IN. Composite Materials Lab.
DISSIPATION OF MECHANICAL WORK AND TEMPERATURE RISE IN AS4/PEEK THERMOPLASTIC COMPOSITE
I. Georgiou and C. T. Sun Oct. 1990 82 p
(Grant NAG1-825)
(NASA-CR-186893; NAS 1.26:186893; CML-90-2) Avail: NTIS HC A05/MF A01 CSCL 11D

The dissipated mechanical work per cycle of sinusoidal stress in the thermoplastic composite material AS4/PEEK was measured as a function of stress amplitude for fixed frequency and fiber orientation. The experimental result shows that the dissipated work per cycle is proportional to the square of the stress amplitude. Using the concept of the equivalent isotropic material, it is shown that the relaxation modulus satisfies a proportionality condition. Also, the rate of temperature rise due to sinusoidal stresses has been measured as a function of stress amplitude. The result shows that the rate of temperature rise is not proportional to the square of the stress amplitude. Author

N90-28679*# Purdue Univ., West Lafayette, IN. Composite Materials Lab.
A CONSTITUTIVE MODEL FOR AS4/PEEK THERMOPLASTIC COMPOSITES UNDER CYCLIC LOADING Final Technical Report
Yuting Rui and C. T. Sun Oct. 1990 39 p
(Grant NAG1-825)
(NASA-CR-180393; NAS 1.26:180393; CML-90-3) Avail: NTIS HC A03/MF A01 CSCL 11D

Based on the basic and essential features of the elastic-plastic response of the AS4/PEEK thermoplastic composite subjected to off-axis cyclic loadings, a simple rate-independent constitutive model is proposed to describe the orthotropic material behavior for cyclic loadings. A one-parameter memory surface is introduced to distinguish the virgin deformation and the subsequent deformation process and to characterize the loading range effect. Cyclic softening is characterized by the change of generalized plastic modulus. By the vanishing yield surface assumption, a yield criterion is not needed and it is not necessary to consider loading and unloading separately. The model is compared with experimental results and good agreement is obtained. Author

N90-28655*# National Aeronautics and Space Administration. Lewis Research Center, Cleveland, OH.
CERAMIC MATRIX COMPOSITES IN SIMULATED SSME ENVIRONMENTS
Thomas P. Herbell and Andrew J. Eckel (Sverdrup Technology, Inc., Middleburg Heights, OH.) *In* NASA, Marshall Space Flight Center, Advanced Earth-to-Orbit Propulsion Technology 1988, Volume 1 Sep. 1988 p 730-741 (For primary document see N90-28611 23-20)
Avail: NTIS HC A99/MF E06 CSCL 11D

25 INORGANIC AND PHYSICAL CHEMISTRY

Includes chemical analysis, e.g., chromatography; combustion theory; electrochemistry; and photochemistry.

For related information see also *77 Thermodynamics and Statistical Physics.*.

N90-28680*# National Aeronautics and Space Administration. Ames Research Center, Moffett Field, CA.

ACCURATE QUANTUM CHEMICAL CALCULATIONS

Charles W. Bauschlicher, Jr., Stephen R. Langhoff, and Peter R. Taylor (Eloret Corp., Sunnyvale, CA.) 1989 77 p

(Contract NCC2-371)

(NASA-TM-101932; NAS 1.15:101932) Avail: NTIS HC A05/MF A01 CSCL 07D

An important goal of quantum chemical calculations is to provide an understanding of chemical bonding and molecular electronic structure. A second goal, the prediction of energy differences to chemical accuracy, has been much harder to attain. First, the computational resources required to achieve such accuracy are very large, and second, it is not straightforward to demonstrate that an apparently accurate result, in terms of agreement with experiment, does not result from a cancellation of errors. Recent advances in electronic structure methodology, coupled with the power of vector supercomputers, have made it possible to solve a number of electronic structure problems exactly using the full configuration interaction (FCI) method within a subspace of the complete Hilbert space. These exact results can be used to benchmark approximate techniques that are applicable to a wider range of chemical and physical problems. The methodology of many-electron quantum chemistry is reviewed. Methods are considered in detail for performing FCI calculations. The application of FCI methods to several three-electron problems in molecular physics are discussed. A number of benchmark applications of FCI wave functions are described. Atomic basis sets and the development of improved methods for handling very large basis sets are discussed: these are then applied to a number of chemical and spectroscopic problems; to transition metals; and to problems involving potential energy surfaces. Although the experiences described give considerable grounds for optimism about the general ability to perform accurate calculations, there are several problems that have proved less tractable, at least with current computer resources, and these and possible solutions are discussed. Author

N90-28681*# National Inst. of Standards and Technology, Boulder, CO. Chemical Engineering Science Div.

THERMOPHYSICAL PROPERTIES OF HELIUM-4 FROM 0.8 TO 1500 K WITH PRESSURES TO 2000 MPa

Vincent D. Arp and Robert D. McCarty Nov. 1989 143 p Sponsored in part by NASA, Ames Research Center; DOD, and AF

(NASA-CR-186992; NAS 1.26:186992; PB90-183351; NIST-TN/1334) Avail: NTIS HC A07/MF A01; also avail. from SOD as SN003-003-02991-2 CSCL 07D

Tabular summary data of the thermophysical properties of fluid helium are given for temperatures from 0.8 to 1500 K, with pressures to 2000 MPa between 75 and 300 K, or to 100 MPa outside of this temperature band. Properties include density, specific heats, enthalpy, entropy, internal energy, sound velocity, expansivity, compressibility, thermal conductivity, and viscosity. The data are calculated from a computer program which is available from the National Institute of Standards and Technology. The computer program is based on carefully fitted state equations for both normal and superfluid helium. GRA

N90-28682# Massachusetts Inst. of Tech., Cambridge. Research Lab. of Electronics.

SURFACE AND DEFECT EXCITATIONS IN COVALENTLY BONDED SOLIDS Final Report, 1 Feb. 1986 - 31 Jan. 1990

John D. Joannopoulos 31 Jan. 1990 19 p

(Contract N00014-86-K-0158)

(AD-A221995; AD-E501218) Avail: NTIS HC A03/MF A01 CSCL 07/4

Topics addressed include: direct current conductivity and the Meyer-Neldel rule in amorphous silicon; ab-initio pseudopotentials for highly electronegative first row elements; Monte Carlo study of the quantum Heisenberg antiferromagnet; magnetic properties of the Bose gas; symmetry breaking and quantum molecular dynamics; antisites, bond-switching reactions and negative U defects in chalcogenides. GRA

N90-28683# Massachusetts Inst. of Tech., Cambridge. Dept. of Chemistry.

QUENCHING OF N(2D) BY O(3P)

C. Fell, J. I. Steinfeld, and S. Miller (Air Force Geophysics Lab., Hanscom AFB, MA.) 15 Apr. 1990 10 p Previously announced in IAA as A90-30595

(Contract F19628-86-C-0139)

(AD-A221690; GL-TR-90-0122) Avail: NTIS HC A02/MF A01 CSCL 11/6

A definitive measurement of the rate coefficient for the quenching of N(2D) by O(3P) is reported. The O(3P) atoms were generated by titrating nitric oxide directly into the active nitrogen flow. Analysis of the results required that the rate coefficient for the reaction N(2D) + NO yields N2 + O be known accurately, and this was also determined. A finite mixing time correction is also necessary. GRA

N90-28684# EG and G Mound Applied Technologies, Miamisburg, OH.

THERMOGRAVIMETRY-MASS SPECTROMETRY ANALYSIS OF GAS BUBBLES IN MOLTEN GLASS

C. Chang, J. R. Tackett, and K. C. Coleman 1990 3 p Presented at the 38th ASMS Conference on Mass Spectrometry and Allied Topics, Tucson, AZ, 4-8 Jun. 1990

(Contract DE-AC04-88DP-43495)

(DE90-014116; MLM-3641(OP); CONF-9006241-3) Avail: NTIS HC A01/MF A01

A series of thermogravimetry mass spectrometry (TG-MS) experiments was carried out for the analysis and identification of gas bubbles formed inside P-glass. It was hoped that the analysis would shed light on the source of bubble formation and ultimately suggest ways to eliminate these bubbles. It was determined that possible ways to eliminate bubbles may include: (1) high purity glass with minimum carbonate impurities; (2) vacuum furnace heating; (3) higher furnace heating temperatures; and (4) longer furnace heating. E.R.

N90-28685# EG and G Mound Applied Technologies, Miamisburg, OH.

MASS SPECTROMETRIC ANALYSIS OF HYDROGEN ISOTOPES IN METALS AND METAL HYDRIDES

R. E. Ellefson 1990 3 p Presented at the 38th ASMS Conference on Mass Spectrometry and Allied Topics, Tucson, AZ, 4-8 Jun. 1990

(Contract DE-AC04-88DP-43495)

(DE90-014118; MLM-3642(OP); CONF-9006241-1) Avail: NTIS HC A01/MF A01

Methods are discussed of measuring the quantity of hydrogen present in metals or metal hydrides using mass spectrometers. DOE

N90-28686# California Univ., Berkeley. Lawrence Berkeley Lab. Combustion Group.

THE SPATIAL SCALAR STRUCTURE OF PREMIXED TURBULENT STAGNATION POINT FLAMES

I. G. Shepherd, R. K. Cheng, and P. J. Goix Apr. 1990 17 p Presented at the 23rd Combustion Institute Symposium on Combustion, Orleans, France, 22-27 Jul. 1990

(Contracts DE-AC03-76SF-00098; F44620-76-C-0083)

(DE90-014189; LBL-28884; CONF-900704-11) Avail: NTIS HC A03/MF A01

A high speed tomographic technique is used to quantify the

spatial scalar structure of stagnation flow stabilized premixed flames. Studies are performed on CH4/Air and C2H4/Air turbulent flames with equivalence ratios ranging from 0.75 to 1.0. The gas velocity at the nozzle exit is 5 m/s, the turbulence intensity is 7 percent, the integral length scale 3 mm and hence the turbulence Reynolds number is 70. The light source is a copper vapor laser which produces 20 ns, 5 mJ pulses at a 4 KHz repetition rate. Cylindrical lenses transform the 38 mm circular laser beam to a sheet 50 mm high and 0.6 mm thick. A high speed Fastax camera is used to record the tomographic images formed by the scattering of light from oil droplets seeded in the reactant flow which disappear at the flame front. The films are digitized and the wrinkled flame front extracted from the images by a thresholding technique. The integral scalar length scales proposed in the model of Bray-Champion-Libby are deduced from the tomographic movies by numerically constructing flame crossing sequences from the burned and unburned probability density functions of flame crossing length and performing a spectral analysis of these sequences. The integral scalar length scales are found to be similar to the integral length scales of the incident turbulence. A fractal analysis was performed on the flame boundaries to characterize the flame geometry and provide from an estimate of the flame surface area a measure of the turbulent burning rate. The flame area increase is found to underestimate the turbulent burning velocity when compared with direct measurements of the flow velocity at the cold boundary. DOE

N90-28687# Ames Lab., IA.
PEAK ANALYSIS IN GAS CHROMATOGRAPHY AND THE DEVELOPMENT OF NEW STATIONARY PHASES FOR ANION CHROMATOGRAPHY Ph.D. Thesis
Roy Francis Strasburg Jul. 1990 143 p
(Contract W-7405-eng-82)
(DE90-014428; IS-T-1467) Avail: NTIS HC A07/MF A01

Causes of band broadening in capillary, gas chromatography are investigated. Using the Golay equation, it is shown that the presence of a diluent significantly increases the extra-column variance, in early eluting peaks, when a liquid injection is used. The cause of this phenomenon is also discussed. A mathematical method based on an iterative method is developed to obtain the correct hold-up time of a capillary column using a flame ionization detector. This method takes advantage of the programmable ability of a common, hand-held calculator. Also discussed is the application of this method for calculating Kovats indices and the calculation of capacity factors. The injection peak in single-column, anion exchange chromatography is used to quantitatively determine simple mixtures of cations in solution. A new, low capacity, anion-exchange resin is developed which possesses a unique selectivity for sulfate and oxalate over bromide and nitrate. DOE

N90-28688 Illinois Univ., Chicago.
ANALYSES OF SPRAY AND DROPLET IGNITION FOR PURE AND MULTICOMPONENT FUELS Ph.D. Thesis
Mohammd Ahmed Mawid 1989 235 p
Avail: Univ. Microfilms Order No. DA9015760

Droplet and spray ignition phenomena are important from scientific as well as practical points of view. Here, these phenomena were examined for pure and multicomponent fuels. Many of the important physical and chemical aspects of the ignition process are studied. First the ignition behavior of an isolated droplet is analyzed. The influence of the chemical kinetics is examined using large activation energy asymptotics. Critical and system Damkohler numbers criteria for ignition, based on the quasi-steady assumption of the gas-phase processes, are derived and employed to predict the ignition behavior of pure and multicomponent fuel drops. Comparisons between predictions and measurements of the ignition delay times show good quantitative agreements for pure fuel droplets. Detailed transient analysis is performed for multicomponent fuel droplets. Comparisons between the predictions of the ignition Damkohler numbers criteria and the detailed transient analyses exhibit reasonable qualitative agreements. The transient analyses also reveal an extinction phenomenon characterized by the suppression of the mass vaporization rate after ignition occurs. The Damkohler number criterion obtained above is then utilized to determine the ignitability of individual droplets in a spray. A full numerical investigation in a one-dimensional combustion chamber is conducted to obtain the ignition conditions for droplets as well as for external sprays for both pure and multicomponent fuels. The mathematical formulation is based on Eulerian conservation equations for the gas-phase and Lagrangian equations for the dispersed phase. A hybrid Eulerian-Lagrangian numerical scheme has been employed to solve the two-phase systems of equations. The spray ignition behavior has been further investigated through the consideration of axisymmetric spray computations. The detailed numerical study shows good qualitative agreements of the one-dimensional and two-dimensional predictions for the effects of initial drop size, equivalence ratio, and ignition source temperature.

Dissert. Abstr.

N90-28689# Lawrence Livermore National Lab., CA.
SHOCK DYNAMICS IN THE SUB-NANOMETER FEMTOSECOND DOMAIN
A. M. Karo, T. M. DeBoni, J. R. Hardy, and G. A. Weiss (California Univ., Berkeley.) Apr. 1990 20 p Presented at the 1990 SANIBEL Symposia, St. Augustine, FL, Apr. 1990
(Contracts W-7405-eng-48; N00014-89-F-0082)
(DE90-014390; UCRL-JC-103246; CONF-9004234-1) Avail: NTIS HC A03/MF A01

New experimental techniques combined with computer molecular dynamics simulations of increasing complexity are beginning to permit a detailed examination of the initial steps in the complex chemistry describing the high-temperature, high-pressure regime associated with combustion and detonation as well as processes that may be involved in shock-induced chemistry. We present the results of several simulations that describe the generation of moderately strong shocks and their interaction with molecules embedded in weakly-bound clusters, with material defects such as microscopic voids, and with molecular species placed in the neighborhood of such defects. DOE

N90-28690# Sandia National Labs., Albuquerque, NM.
REFLECTION MASS SPECTROMETRY (REMS) DURING 3/5 MBE
J. Y. Tsao, T. M. Brennan, L. R. Dawson, B. E. Hammons, and R. E. Hibray 1990 3 p Presented at the BES Material Science Program Information and Review Meeting, Albuquerque, NM, 20-21 Jun. 1990
(Contract DE-AC04-76DP-00789)
(DE90-014568; SAND-90-1582C; CONF-9006246-1) Avail: NTIS HC A01/MF A01

Reflection Mass Spectrometry (REMS) consists of a cryo-shrouded mass spectrometer which measures mass-analyzed, line-of-sight chemical fluxes from a growing wafer. It is especially useful during III/V molecular beam epitaxy (MBE) for which there are always substantial group V fluxes and often some group III fluxes leaving the wafer during growth. These fluxes depend sensitively on the instantaneous chemical reactivity of the surface. That chemical reactivity in turn depends on instantaneous alloy composition (III/III ratio), surface stoichiometry (As coverage) and temperature. Two examples of the engineering usefulness of REMS are briefly described involving MBE of InAlAs and InGaAs and one example of measurements of basic scientific interest. DOE

N90-28691# Texas A&M Univ., College Station. Dept. of Chemistry.
A STUDY OF CATALYSTS AND MECHANISMS IN SYNTHESIS REACTIONS
1990 31 p
(Contract DE-FG05-88ER-13829)
(DE90-015064; DOE/ER-13829/3) Avail: NTIS HC A03/MF A01

Recent interest in the partial oxidation of alkanes has focused attention on the role of surface generated gas phase radicals in catalysis. During the oxidative coupling of methane the importance of gas phase CH3- radicals was demonstrated using a

matrix-isolation electron spin resonance (MIESR) system. This technique was employed to study several important problems associated with the formation and reactions of hydrocarbon radicals. The production of gas phase propyl radicals over a V-MgO-O catalyst was investigated to determine the intermediate that is responsible for the observed heterogeneous-homogeneous reaction. The nonoxidative formation of hydrocarbon radicals over supported CrO was explored to establish whether radical reactions over this catalyst involve gas phase intermediates. In the proposed experiments the cross coupling of methyl radicals with benzyl, allyl, 1-methylallyl and 2-methylallyl radicals was investigated, again to determine the role of surface generated gas phase radicals in these reactions. Secondary reactions of radicals with metal oxide surfaces often dictate product selectivity, therefore reactive sticking coefficients for methyl and allyl radicals colliding with metal oxides will be determined. Such quantitative information is essential for modeling complex heterogeneous-homogeneous reactions. A newly constructed laser induced fluorescence (LIF) spectrometer will be used to complement the data obtained using the MIESR technique. An initial LIF investigation will focus on the OH- radical, which is a key intermediate in hydrocarbon oxidation reactions. The research will be extended to include CH and possibly CH2 radicals. The proposed projects will provide conceptual information and quantitative data on an important class of catalytic reactions.
DOE

N90-28692# Office National d'Etudes et de Recherches Aerospatiales, Paris (France). Direction de la Physique Generale.
STUDY OF THE RADICAL OH IN A HIGH PRESSURE FLAME BY RESONANT DRASC Final Report [ETUDE DU RADICAL OH DANS UNE FLAMME A HAUTE PRESSION PAR DRASC RESONNANTE, RAPPORT FINAL]
B. Tretout Jan. 1990 66 p In FRENCH
(Contract DRET-89-001-40)
(ONERA-RF-57/7131-PY; ETN-90-97500) Avail: NTIS HC A04/MF A01

The concentration profiles of OH from high pressure CH4/air flame and from laser fluorescence are compared. The diffusion Raman Anti-Stokes Coherent (DRASC) is applied. The concentration absolute value is obtained by means of the measurement of the UV differential absorption on OH. The DRASC measurements under 10 and 20 bars allowed the evolution of the signal-to-noise ratio to be controlled. Different concentration profiles were compared with the calculations using both adiabatic flame concept and chemical reaction kinetics.
ESA

N90-28693*# Alabama Univ., Huntsville. Dept. of Mechanical Engineering.
DEVELOPMENT OF COMPREHENSIVE NUMERICAL SCHEMES FOR PREDICTING EVAPORATING GAS-DROPLETS FLOW PROCESSES OF A LIQUID-FUELED COMBUSTOR Semiannual Report, 15 Jun. 1988 - 30 Nov. 1988
C. P. Chen 1990 104 p
(Grant NAG8-092)
(NASA-CR-187018; NAS 1.26:187018) Avail: NTIS HC A06/MF A01 CSCL 21B

An existing Computational Fluid Dynamics code for simulating complex turbulent flows inside a liquid rocket combustion chamber was validated and further developed. The Advanced Rocket Injector/Combustor Code (ARICC) is simplified and validated against benchmark flow situations for laminar and turbulent flows. The numerical method used in ARICC Code is re-examined for incompressible flow calculations. For turbulent flows, both the subgrid and the two equation k-epsilon turbulence models are studied. Cases tested include idealized Burger's equation in complex geometries and boundaries, a laminar pipe flow, a high Reynolds number turbulent flow, and a confined coaxial jet with recirculations. The accuracy of the algorithm is examined by comparing the numerical results with the analytical solutions as well as experimented data with different grid sizes.
Author

N90-28694*# Alabama Univ., Huntsville.
SPECTROSCOPIC STUDY OF COMBUSTION DIAGNOSTICS ON HYDROXYL RADICALS Final Report
R. J. Hung 1990 35 p
(Grant NAG8-102)
(NASA-CR-186998; NAS 1.26:186998) Avail: NTIS HC A03/MF A01 CSCL 21B

Experimental observations of propane-air flames were performed. Measurements of hydroxyl (OH) radical concentration were made using resonance line absorption techniques. A microwave-pumped low pressure discharge in argon and water vapor is employed to produce strong OH radical band radiation in the 308 nm region. This radiation is transmitted through the plume and absorption data are taken at various radical positions using an optical multichannel analyzer. This absorption data is used to compute OH number density using a model for the absorption band characteristics as a function of temperature based on an atlas of line strengths. A numerical computation of flow fields, temperature profile and OH number density is carried out by using a technique of computational fluid dynamics (CFD). The results of CFD computation are good compared with experimental observation with a good agreement.
Author

N90-28695# IIT Research Inst., Bartlesville, OK.
FUELS RESEARCH, VOLUME 1 Quarterly Technical Report, 1 Apr. - 30 Jun. 1990
John Green 27 Jul. 1990 33 p
(Contract DE-FC22-83FE-60149)
(DE90-015393; NIPER-479-Vol-1) Avail: NTIS HC A03/MF A01

Fuels research from the National Institute for Petroleum and Energy Research (NIPER) is described. The following two topics are briefly discussed: Department of Analytical Methodology for Analysis of heavy Crudes, and Thermochemistry and Thermophysical Properties of Organic Nitrogen-, and Diheteroatom-Containing Compounds.
DOE

N90-28696*# National Aeronautics and Space Administration. Lewis Research Center, Cleveland, OH.
SYNTHESIS AND STRUCTURAL CHEMISTRY OF Au(III)-SUBSTITUTED Ba2YCu3O(7-DELTA)
A. F. Hepp, J. R. Gaier, J. J. Pouch, A. Banerjea, and P. D. Hambourger (Cleveland State Univ., OH.) Apr. 1988 9 p Presented at the 2nd Annual Conference on Superconductivity and Applications, Buffalo, NY, 18-20 Apr. 1988; sponsored in part by The New York State Institute on Superconductivity and The New York State Energy Research and Development Authority
(NASA-TM-103292; E-5752; NAS 1.15:103292) Avail: NTIS HC A02/MF A01 CSCL 07D

Gold-substituted superconductors, Ba2Y(Au(x)Cu(1-x))3O-(7-delta) (x = 0-0.1) were synthesized. For x = 0.1, there was no change in the a and b lattice parameters (a = 3.826 A and b = 3.889 A) but a 0.06 A c axis expansion to 11.75 A was observed. Substituted gold is found to be trivalent by XPS. Replacing Cu(1) in the copper oxide chain with a slight reordering of oxygen is consistent with c axis expansion. The formal charge of the site remains trivalent; remaining Cu in the chains may be reduced resulting in an oxygen stoichiometry is less than or equal to 7. A small effect on T(sub c)(89 K for x = 0.10) is observed upon gold substitution.
Author

N90-28697# California Inst. of Tech., Pasadena. Dept. of Chemistry.
ELECTROCHEMISTRY USING NANOMETER-SIZED ELECTRODES Technical Report No. 9, Jun. 1989 - May 1990
Reginald M. Penner, Michael J. Heben, Teresa L. Longin, and Nathan S. Lewis 29 May 1990 15 p Submitted for publication
(Contract N00014-88-K-0482)
(AD-A223890) Avail: NTIS HC A03/MF A01 CSCL 07/1

Electrodes with dimensions as small as 10 A have been fabricated and used for electrochemical studies. Remarkably large current densities are generated by these ultra small electrodes,

as predicted by conventional radial diffusion theory. These large current densities have enabled the measurement of electron transfer rate constants, k sub het, which are two orders of magnitude faster than k sub het values accessible using any other electrochemical method. GRA

N90-28627*# National Aeronautics and Space Administration. Lewis Research Center, Cleveland, OH.
CATALYTIC IGNITION OF HYDROGEN/OXYGEN
James M. Green (Sverdrup Technology, Inc., Middleburg Heights, OH.) and Robert L. Zurawski *In* NASA, Marshall Space Flight Center, Advanced Earth-to-Orbit Propulsion Technology 1988, Volume 1 Sep. 1988 p 231-248 (For primary document see N90-28611 23-20)
Avail: NTIS HC A99/MF E06 CSCL 21B

N90-28628*# Rockwell International Corp., Canoga Park, CA. Rocketdyne Div.
OXYGEN/METHANE COMBUSTION STABILITY INVESTIGATION
R. J. Jensen, H. Dodson, and B. Trueblood *In* NASA, Marshall Space Flight Center, Advanced Earth-to-Orbit Propulsion Technology 1988, Volume 1 Sep. 1988 p 249-269 (For primary document see N90-28611 23-20)
(Contract NAS3-24612)
Avail: NTIS HC A99/MF E06 CSCL 21B

N90-28629*# National Aeronautics and Space Administration. Lewis Research Center, Cleveland, OH.
COMBUSTION INSTABILITY COUPLING WITH FEED SYSTEM ACOUSTICS
Richard J. Priem (Priem Consultants, Inc., Cleveland, OH.) and Kevin J. Breisacher *In* NASA, Marshall Space Flight Center, Advanced Earth-to-Orbit Propulsion Technology 1988, Volume 1 Sep. 1988 p 270-301 (For primary document see N90-28611 23-20)
Avail: NTIS HC A99/MF E06 CSCL 21B

N90-28631*# Pratt and Whitney Aircraft, West Palm Beach, FL.
TRIPROPELLANT COMBUSTION PROCESS
T. D. Kmiec and R. G. Carroll *In* NASA, Marshall Space Flight Center, Advanced Earth-to-Orbit Propulsion Technology 1988, Volume 1 Sep. 1988 p 316-333 (For primary document see N90-28611 23-20)
Avail: NTIS HC A99/MF E06 CSCL 21B

26 METALLIC MATERIALS

Includes physical, chemical, and mechanical properties of metals, e.g., corrosion; and metallurgy.

N90-28698# Advisory Group for Aerospace Research and Development, Neuilly-Sur-Seine (France). Structures and Materials Panel.
HIGH TEMPERATURE SURFACE INTERACTIONS
Nov. 1989 239 p The 68th meeting was held in Ottawa, Ontario, 23-28 Apr. 1989
(AGARD-CP-461; ISBN-92-835-0533-6) Copyright Avail: NTIS HC A11/MF A02; Non-NATO Nationals requests available only from AGARD/Scientific Publications Executive

In today's climate of life extension for military aircraft, the topic of corrosion control assumes a role of greater importance. Controlling the degradative effects of flight environments on aircraft engine materials was emphasized. The chemical and mechanical mechanisms involved in degradative processes were reviewed and some state-of-the-art solutions considered. Emphasis in discussions centered on hot-salt corrosion topics but wear and erosion problems were also considered. For individual titles, see N90-28699 through N90-28714.

N90-28699# Ohio State Univ., Columbus. Dept. of Materials Science and Engineering.
HIGH TEMPERATURE SURFACE INTERACTIONS: OVERVIEW
Robert A. Rapp *In* AGARD, High Temperature Surface Interactions Nov. 1989 13 p (For primary document see N90-28698 23-26)
(Contract N00014-87-K-0030; NSF DMR-86-20311; ORNL Order 19X-SB154C)
Copyright Avail: NTIS HC A11/MF A02; Non-NATO Nationals requests available only from AGARD/Scientific Publications Executive

A mechanistic model is presented to explain and interrelate the means for vacancy annihilation, stress generation, and scale adherence for cation/vacancy diffusion-limited scale growth on a pure metal. Specifically, the climb into the metal of a fraction of the intrinsic interfacial misfit edge dislocations accounts for vacancy annihilation, ultimately leading to cooperative dislocation glide in both the metal and the scale. The hot corrosion of metals by thin fused salt films is treated in terms of oxide solubilities, electrochemical experimentation, and corrosion mechanisms. The chemistry of mixed sodium sulfate/vanadate melts, and the influence of vanadate on the solubilities of oxides, are presented. Temperature limitations to the protection of carbon/carbon substrates by SiC conversion coatings are discussed. Specifically, the rate of vitreous silica film growth on SiC, the partial pressures of SiO and CO at the SiC/SiO2 interface, and the conditions for active/passive volatilization of SiC are considered. The vapor pressures for volatile iridium oxides as a function of temperature and oxygen pressure are calculated. Analyses and experimental verification of simultaneous chromizing/aluminizing coating of Ni-base alloys in a chloride-activated cementation pack are explained. These inwardly grown diffusion coatings promise improved resistance to thermal fatigue and to hot corrosion. Author

N90-28700# National Physical Lab., Teddington (England). Div. of Materials Applications.
DEVELOPMENTS IN TEST PROCEDURES FOR HOT-SALT CORROSION OF SUPERALLOYS
S. R. J. Saunders and T. B. Gibbons *In* AGARD, High Temperature Surface Interactions Nov. 1989 8 p (For primary document see N90-28698 23-26)
Copyright Avail: NTIS HC A11/MF A02; Non-NATO Nationals requests available only from AGARD/Scientific Publications Executive

It is important that the test procedures used to assess the resistance of superalloys to hot salt corrosion should reliably simulate conditions expected in service and the results should be capable of interpretation to provide a prediction of likely long-term behavior. Past experience has shown that the many test methods available have frequently given conflicting measures of alloy performance and intercomparability between test procedures was frequently poor. As a result of extensive research in Europe, much of which was carried out within the COST Project, there is now a better understanding of the critical factors that must be controlled to provide a reliable and reproducible procedure and which gives corrosive attack similar to that encountered in service. In particular, contaminant flux rate was identified as a key parameter. These activities are briefly reviewed and progress towards the definition of a unified test procedure is outlined. Plans for a new international intercomparison, organized under the auspices of VAMAS, to probe the validity of the procedure are described. Author

N90-28701# National Research Council of Canada, Ottawa (Ontario).
THE EFFECTS OF A COMPRESSOR REBUILD ON GAS TURBINE ENGINE PERFORMANCE: FINAL RESULTS c27
J. D. MacLeod and J. C. G. Laflamme (Canadian Forces Base, Baden-Soellingen, Germany, F.R.) *In* AGARD, High Temperature Surface Interactions Nov. 1989 13 p (For primary document see N90-28698 23-26)
Copyright Avail: NTIS HC A11/MF A02; Non-NATO Nationals requests available only from AGARD/Scientific Publications Executive

The Canadian Department of National Defence, in conjunction with the Engine Laboratory of the National Research Council

Canada (NRCC), initiated a project for the evaluation of gas path coatings on the Allison T56 engine. The objective was to evaluate blade coatings in terms of engine performance effects and material durability. The project included a study of the influence of rebuilding the compressor on performance, since dismantling and rebuilding was required for the coating process. The compressor rebuild study, including the overall objectives, the test set-up, the performance effects, and the uncertainty of the measured results are described. The impact of this work on the coatings project is also documented. Author

N90-28702# Naval Air Development Center, Warminster, PA. Aerospace Materials Div.

OXIDATION, SULFIDATION, AND HOT CORROSION: MECHANISMS AND INTERRELATIONSHIPS

T. A. Kircher *In* AGARD, High Temperature Surface Interactions Nov. 1989 8 p (For primary document see N90-28698 23-26)

Copyright Avail: NTIS HC A11/MF A02; Non-NATO Nationals requests available only from AGARD/Scientific Publications Executive

A discussion of the various types of oxide growth laws which describe oxidation of metals and alloys was given. The formation and maintenance of a dense, adherent oxide scale will result in diffusion-limited scale growth and a parabolic-type rate equation. These protective scales are formed by selectively oxidizing their respective metallic components from a complex base alloy or coating. Exposure of alloys to a sulfidizing or hot-corrosive type environment reduces the ability for protective scales to adhere or recover from scale damage and shortens the time for which an alloy can form a protective scale via selective oxidation. Author

N90-28703# United Technologies Research Center, East Hartford, CT.

SCALE ADHERENCE EFFECTS IN OXIDATION AND SULFIDATION **c27**

M. A. DeCrescente and N. S. Bornstein *In* AGARD, High Temperature Surface Interactions Nov. 1989 10 p (For primary document see N90-28698 23-26)

Copyright Avail: NTIS HC A11/MF A02; Non-NATO Nationals requests available only from AGARD/Scientific Publications Executive

The most oxidation-resistant gas turbine alloys and coatings form adherent Al_2O_3 oxide scales which slowly thicken and resist spallation when thermally stressed. Work performed in the period 1966 to 1972 demonstrated that the onset of sulfidation was also affected by the adhesion of the Al_2O_3 scale. The relationship between sulfidation corrosion, and oxide scale adherence as it relates to oxidation resistance is reviewed. The sulfidation mechanism research is summarized to illustrate the role of Al_2O_3 scale in the sulfidation process; whereas more recent oxidation results of in-house and ONR and NADC-sponsored programs is presented which demonstrates that sulfur present in gas turbine materials, even at very low concentrations, degrades Al_2O_3 scale adhesion. Finally, results are disclosed which indicate that the very low sulfur-containing materials are extremely oxidation resistant and delay the onset of sulfidation. Author

N90-28704# Office National d'Etudes et de Recherches Aerospatiales, Paris (France). Dept. of Materials Science.

MOLTEN SALT INDUCED HIGH TEMPERATURE DEGRADATION OF THERMAL BARRIER COATINGS **c27**

Serge Alperine *In* AGARD, High Temperature Surface Interactions Nov. 1989 18 p Previously announced in IAA as A89-48745 (For primary document see N90-28698 23-26)

Copyright Avail: NTIS HC A11/MF A02; Non-NATO Nationals requests available only from AGARD/Scientific Publications Executive

Thermal barriers are now fairly well known as a new generation of protective coatings for components of the hot sections of conventional, diesel and turbine engines. The more performing system is a duplex coating consisting of a stabilized zirconia top coat generally air plasma sprayed on a approximately 100 micron thick MCrAlY bond coat. The service degradation modes of such coatings have been extensively studied during the past ten years. Their failure mechanisms are generally thought of in terms of thermomechanical stress, thermal expansion coefficient mismatch and bond coat high temperature oxidation. Efforts are thus made to design ceramic and bond coat composition, microstructure and processing parameters, according to these requirements. However, degradation of thermal barrier coatings by hot corrosion processes and, more generally, by fused salt thin films related phenomena, should also be taken into account. A review is given of the degradation modes that can be encountered when partially stabilized zirconia coatings are exposed to intermediate temperature range and sulphur and/or vanadium containing atmosphere. The interaction of the salt film with the coating is threefold: a chemical acidic or alkaline dissolution of the zirconia stabilizing oxide may occur, provoking zirconia tetragonal to monoclinic phase transformation and subsequent coating spallation on cooling. Fused salt may diffuse inside the ceramic microcracks network and solidify on cooling with a generation of extra stress inside the coating. Fused salt diffused throughout the microcracks network down to the ceramic/bond coat interface may also affect the MCrAlY bond coat. Careful distinction should be made between the working conditions encountered in diesel engines and marine turbines and those involved in aircraft turboengines. An illustration of the hot corrosion resistance of a ZrO_2-8wt percent Y_2O_3/NiCrAlY thermal barrier coating, plasma sprayed on a single crystal superalloy substrate, in a typical aircraft turbine environment is given. Author

N90-28705# Royal Aerospace Establishment, Farnborough (England). Dept. of Materials and Structures.

HIGH TEMPERATURE OXIDATION OF Al-Li ALLOYS

P. G. Partridge *In* AGARD, High Temperature Surface Interactions Nov. 1989 22 p (For primary document see N90-28698 23-26)

Copyright Avail: NTIS HC A11/MF A02; Non-NATO Nationals requests available only from AGARD/Scientific Publications Executive

Lithium additions increase the oxidation rate of Al-alloys in the solid and liquid states. At elevated temperatures in the solid state lithium diffuses rapidly through the aluminum alloy and through oxidized surfaces to become oxidized preferentially at the oxide/air interface where it forms non-protective oxidation products. The consequent lithium depletion causes changes in the near surface microstructure and hardness to depths of up to 800 microns depending on the temperature and exposure times. Depleted surface layers can lead to substantial reductions in the strength of thin sections. Procedures for minimizing lithium depletion during processing of Al-Li alloys are discussed. Oxidation in the liquid state is important in casting, in fusion welding and in rapid solidification processing and the behavior of Al-Li alloys under these conditions is described. Author

N90-28706# Nottingham Univ. (England). Dept. of Metallurgy and Materials Science.

FRETTING WEAR AND FRETTING FATIGUE AT TEMPERATURES UP TO 600 C

R. B. Waterhouse *In* AGARD, High Temperature Surface Interactions Nov. 1989 12 p (For primary document see N90-28698 23-26)

Copyright Avail: NTIS HC A11/MF A02; Non-NATO Nationals requests available only from AGARD/Scientific Publications Executive

Raising the temperature increases the oxidation rate of most alloys. The thicker oxide film prevents metal-to-metal contact and reduces the coefficient of friction. On ferrous materials a type of oxide layer develops which was first observed in high temperature unindirectional sliding and, because of its smoothness, was given the name glaze oxide. Both high temperature and sliding are necessary for its formation. The result is that the wear is much reduced and also fatigue strengths are increased. It is only stable at the high temperature. If the temperature falls to room temperature it is soon completely disrupted. The evidence is that the alloys which are capable of forming the glaze oxide are those

on which an oxide with a spinel structure can develop. The appearance of the oxide is a smooth, grooved outer surface, with a granular structure underneath. If the oxide is damaged it is soon repaired. Titanium alloys do not develop this type of oxide. Surface modification by implantation of Ba and Bi ions has produced significant improvements in the tribological behavior of these alloys in high temperature fretting. Author

N90-28707# Office National d'Etudes et de Recherches Aerospatiales, Paris (France). Dept. of Materials Science.
EFFECT OF PROTECTIVE COATINGS ON MECHANICAL PROPERTIES OF SUPERALLOYS
Remy Mevrel and Jean-Marie Veys (Service Technique des Programmes Aeronautiques, Paris, France) *In* AGARD, High Temperature Surface Interactions Nov. 1989 13 p Previously announced in IAA as A90-11126 (For primary document see N90-28698 23-26)
Copyright Avail: NTIS HC A11/MF A02; Non-NATO Nationals requests available only from AGARD/Scientific Publications Executive

The influence of protective coatings on the mechanical properties of superalloys employed in hot sections of gas turbine engines is investigated. The most used coatings are aluminide-based such as MCrAlY overlays and zirconia-based thermal barrier coatings, which may affect the mechanical properties of the superalloy substrates in several ways. Interdiffusion phenomena taking place between coating and substrate at high temperature during service may decrease the load bearing section of the superalloy and, as a consequence, may degrade its creep lifetime. Examples of possible effects of coating/substrate interdiffusion on the creep life of single crystal CMSX2 (no effect) and in the case of a directionally solidified eutectics superalloy (significant degradation) are considered. In the long run, the presence of a coating can enhance the creep life of a substrate due to its protective effect against high temperature corrosion. After considering different factors which can affect the mechanical behavior of the coated systems, a review of recent experimental results is presented. Author

N90-28708# Naval Air Development Center, Warminster, PA.
MICRODAMAGE TO CERAMIC SURFACES UNDER SLIDING CONDITIONS **c27**
P. J. Kennedy and A. Conte *In* AGARD, High Temperature Surface Interactions Nov. 1989 7 p (For primary document see N90-28698 23-26)
Copyright Avail: NTIS HC A11/MF A02; Non-NATO Nationals requests available only from AGARD/Scientific Publications Executive

Fretting studies were performed on silicon nitride in order to ascertain the effect of small amplitude slip (0.1 to 10 micrometers) on ceramic wear. The results indicate that the small amplitude fretting of silicon nitride on silicon nitride is primarily controlled by tribochemical reaction forming a soft silicon oxide layer. This reaction was not observed to any measurable extent at slip amplitudes of less than 3 micrometers. The tribochemical reaction was initially observed at the edge of the contact region and then progressed toward the center of the contact zone. The reacted material in the contact zone tended to flow out of the high pressure region to form a debris pile-up outside of the contact area. The wear ratio was found to be 4 x 10(exp -16) sq m/Nm. Author

N90-28709# Industrieanlagen-Betriebsgesellschaft m.b.H., Ottobrunn (Germany, F.R.).
FRETTING FATIGUE STRENGTH OF TI-6AL-4V AT ROOM AND ELEVATED TEMPERATURES AND WAYS OF IMPROVING IT
Rainer Schaefer and Walter Schuetz *In* AGARD, High Temperature Surface Interactions Nov. 1989 15 p Sponsored by BMFT, Fed. Republic of Germany (For primary document see N90-28698 23-26)
Copyright Avail: NTIS HC A11/MF A02; Non-NATO Nationals requests available only from AGARD/Scientific Publications Executive

The high sensitivity of titanium alloys to fretting fatigue has to be taken into account when oscillatory relative motion occurs in joints of fatigue loaded components, e.g., in the connection of the disc with the blades in compressors of aircraft engines. Against this background fretting fatigue behavior of Ti-6Al-4V was investigated at room temperature and service temperature (350 C) as well by testing flat specimens under fatigue loading and simultaneous fretting applied by a special fretting apparatus. The results show a complex system of parameters affecting fretting fatigue resistance: Fretting fatigue resistance decreases with increasing contact pressure and increasing amplitude of slip, down to a certain limit value for each. Other parameters investigated here are surface finish and stress ratios. The lowest value of fretting fatigue limit found was about 20 percent of the original fatigue limit of the unfretted material. Elevated temperature (350 C), however, had little additional detrimental effect. Among several methods to improve fretting fatigue resistance, shot peening and coating are also employed in compressor components. By shot peening the fretting fatigue limit could be increased by more than a factor of two, by coating with PVD systems by nearly a factor of two. Author

N90-28710# Office National d'Etudes et de Recherches Aerospatiales, Paris (France). Dept. of Materials Science.
HIGH TEMPERATURE PROTECTIVE COATINGS: RECENT TRENDS **c27**
Remy Mevrel *In* AGARD, High Temperature Surface Interactions Nov. 1989 10 p Previously announced in IAA as A90-21039 (For primary document see N90-28698 23-26)
Copyright Avail: NTIS HC A11/MF A02; Non-NATO Nationals requests available only from AGARD/Scientific Publications Executive

Major types of currently used high-temperature protective coatings, including modified aluminides, MCrAlY overlays, and ceramic thermal barrier coatings are described, and recent trends in the coating field research reviewed. These research trends include studies of high-temperature corrosion degradation mechanisms, the mechanical properties of coated components, and the diffusional stability of coating/substrate systems. Particular attention is given to the development of high-performance ceramic coatings and to alternative coating processes, such as the deposition of MCrAlY alloys by electrophoresis and coelectrodeposition, cladding, or replacing Pt by Pd in modified aluminide coatings. Author

N90-28711# National Aerospace Lab., Emmeloord (Netherlands).
THERMAL SHOCK AND OXIDATION RESISTANCE OF CERAMIC COATINGS **c27**
J. A. M. Boogers, R. J. H. Wanhill, and H. J. C. Hersbach *In* AGARD, High Temperature Surface Interactions Nov. 1989 16 p Sponsored by Royal Netherlands Air Force (For primary document see N90-28698 23-26)
Copyright Avail: NTIS HC A11/MF A02; Non-NATO Nationals requests available only from AGARD/Scientific Publications Executive

Thermal shock and long term oxidation tests on ceramic thermal barrier coatings were done under flight simulation conditions in a burner rig. Three coating combinations were investigated: magnesium stabilized zirconia topcoat with Ni-5 percent Al bondcoat; magnesium stabilized zirconia topcoat with NiCoCrAlY bondcoat; and yttrium stabilized zirconia topcoat with NiCoCrAlY bondcoat. The ZrO2/Y2O3 + NiCoCrAlY combination showed superior resistance to thermal shock and long term oxidation as compared to the ZrO2/MgO + Ni-5 percent Al coating. The long term oxidation resistance of the ZrO2/MgO + NiCoCrAlY combination was intermediate to that of the other two coatings. Degradation of the coatings was examined in detail, and the practical significance of the results is assessed. Author

N90-28712# National Aeronautical Establishment, Ottawa (Ontario).
EVALUATION OF HIGH TEMPERATURE PROTECTIVE COATINGS FOR GAS TURBINE ENGINES UNDER SIMULATED SERVICE CONDITIONS c27
A. K. Gupta, T. Terada, P. C. Patnaik (Hawker Siddeley Canada Ltd., Toronto, Ontario), and J.-P. Immarigeon *In* AGARD, High Temperature Surface Interactions Nov. 1989 31 p Sponsored by Department of National Defence, Ottawa, Ontario (For primary document see N90-28698 23-26)
Copyright Avail: NTIS HC A11/MF A02; Non-NATO Nationals requests available only from AGARD/Scientific Publications Executive

The surface degradation of turbine hot section components, due to oxidation, hot corrosion, erosion, and thermal fatigue, is discussed. The mechanisms of each mode of attack are summarized and the state-of-the-art in protective coatings for gas path components is reviewed. Durability evaluations of coatings under simulated service conditions are discussed, including evaluations conducted in high velocity burner rigs. Inconsistencies in the ranking of coatings in rigs is attributed to laboratory-to-laboratory variations in test procedures and/or test conditions. Finally, the important parameters for durability testing in rigs are discussed in terms of the environmental and operational factors that control hot gas chemistry and the extent of surface damage of hot parts. A description of commonly used burner rigs and test procedures employed is also provided to complete the paper. Author

N90-28713# Hawker Siddeley Canada Ltd., Toronto (Ontario). Research and Technology Development Group.
SURFACE PROPERTY IMPROVEMENT IN TITANIUM ALLOY GAS TURBINE COMPONENTS THROUGH ION IMPLANTATION
J. E. Elder, M. R. Pishva, N. C. Bellinger, P. C. Patnaik, and R. Thamburaj *In* AGARD, High Temperature Surface Interactions Nov. 1989 11 p Sponsored by Department of National Defence, Ottawa, Ontario (For primary document see N90-28698 23-26)
Copyright Avail: NTIS HC A11/MF A02; Non-NATO Nationals requests available only from AGARD/Scientific Publications Executive

The feasibility of applying ion implantation to produce substantial improvement in the wear/fretting fatigue resistance of titanium alloys used as gas turbine fan and compressor blade material was studied. Detailed/microscopy and mechanical test results were used to analyze the various mechanisms contributing to wear and fretting fatigue damage in titanium alloys at room and elevated temperatures. The manner in which ion implantation might modify the normal wear/fretting fatigue response of these alloys is discussed in detail, along with the factors to be considered in choosing optimum ion implantation parameters. Author

N90-28714# Deutsche Forschungsanstalt fuer Luft- und Raumfahrt, Cologne (Germany, F.R.). Inst. for Materials Research.
OVERVIEW ON HOT GAS TESTS AND MOLTEN SALT CORROSION EXPERIMENTS AT THE DLR
H.-J. Raetzer-Scheibe *In* AGARD, High Temperature Surface Interactions Nov. 1989 14 p (For primary document see N90-28698 23-26)
Copyright Avail: NTIS HC A11/MF A02; Non-NATO Nationals requests available only from AGARD/Scientific Publications Executive

The use of more corrosive low-grade fuels in combination with increasing combustion gas temperatures are major challenges in the present and future operation of heat engines. Improved thermal efficiency under practical operating conditions can only be accomplished by improved materials and/or coatings. This development motivated in 1982, the procurement of a high-velocity burner rig for simulation of the operation of gas turbines under service conditions. As an aircraft research and development establishment, corrosion and oxidation of aircraft gas turbines were the main interest. Working in this new field of research yielded a review on hot corrosion in aircraft engines. For an overview of the work, to date, in the field of hot corrosion and high temperature oxidation some topics are selected. Burner rig tests were started with investigations on the hot corrosion resistance of protective coating systems to evaluate coating alloys for use in highly contaminated combustion gases. Thermocyclic oxidation tests of coated aircraft turbine glade materials in hot gases of JP4 up to temperatures of 1100 C, followed later. Since hot corrosion is induced by molten salts or low-melting oxides deposited from the hot gas on the material surface the necessity is seen for fundamental investigations of molten salt corrosion. Therefore a device was developed for electrochemical experiments in molten salts. Another motivation for developing molten salt experimentation was to have an alternative test procedure to the high-cost burner rig tests. Author

N90-28715# Johns Hopkins Univ., Baltimore, MD.
PRELIMINARY EXPOSURE STUDY TO DETERMINE THE EFFECTS OF ACID DEPOSITION ON COATED STEEL SUBSTRATES Final Report
P. J. Moran, T. C. Simpson, H. Hampel, G. D. David, and B. A. Shaw Apr. 1990 38 p Prepared in cooperation with Martin Marietta Labs., Baltimore, MD, and Versar, Inc., Columbia, MD (Grant EPA-R-814347-01)
(PB90-201799; EPA/600/3-90/032) Avail: NTIS HC A03/MF A01 CSCL 11F

The project involves the evaluation of the effects of acidic pollutants on painted metal substrates. The project examined a commercially available alkyd paint/primer system applied to a low carbon steel substrate exposed under a variety of simulated acidic conditions to determine the micro/macro effects of such exposure. The techniques that were identified as those most sensitive and applicable during the study include tensile adhesion testing, electrochemical impedance spectroscopy, and x ray photoelectron spectroscopy. A novel electrochemical monitor was developed during this program that allowed the continual monitoring of coating degradation during chamber exposure. It was further found that a good correlation existed between tensile adhesion strength measurements and electrochemical impedance parameters. The program determined that the rate of degradation of the alkyd painted steel coupons was accelerated in the presence of SO2. This effect was most pronounced on samples that contained defects, that were allowed to form condensation during the exposure period, and that had a horizontal orientation during exposure. GRA

N90-28716# National Inst. of Standards and Technology, Gaithersburg, MD. Metallurgy Div.
DETERMINATION OF THE NDT TEMPERATURE AND CHARPY V-NOTCH IMPACT PROPERTIES OF AAR TC128 GRADES B STEEL AND A 8XX GRADE B STEEL
G. E. Hicho and J. H. Smith Apr. 1990 31 p Sponsored by Federal Railroad Admin., Washington, DC
(PB90-207804; NISTIR-4300; Rept-20) Avail: NTIS HC A03/MF A01 CSCL 11F

Charpy V-notch impact tests and the nil-ductility transition (NDT) temperature were redetermined for two steels. The two steels examined were normalized and inclusion shape controlled American Association of Railroads (AAR) TC128 grade B steel and control-rolled and inclusion shape controlled A 8XX grade B Steel. The notch toughness, as determined by Charpy V-notch impact test, and the NDT temperature of the AAR TC128 grade B steel was found again to be better than that of the A8XX grade B steel. Metallographic investigations showed that the ferrite/pearlite grain size of the AAR TC128 grade B steel was more uniform and finer than that of the A 8XX grade B steel. Charpy V-notch impact results and NDT temperatures, presented in an earlier report were confirmed. Plate chemistry and test specimen orientation were also confirmed. GRA

N90-28717# Sandia National Labs., Albuquerque, NM.
TENSILE BEHAVIOR OF BORATED STAINLESS STEELS, PHASE 1
J. J. Stephens and K. B. Sorenson 1990 16 p Presented at

the Pressure Vessels and Piping Conference: Be in Tune for the 1990's, Nashville, TN, 17-21 Jun. 1990
(Contract DE-AC04-76DP-00789)
(DE90-014368; SAND-90-1247C; CONF-900617-17) Avail: NTIS HC A03/MF A01

Borated stainless steel tensile testing is being conducted. The goal of the test program is to provide data to support a code case inquiry to the ASME Boiler and Pressure Vessel Code, Section 3. The adoption by ASME facilitates a materials qualification for structural use in transport cask applications. The borated stainless steel being tested conforms to ASTM specification A-887, which specifies 16 grades of material as a function of boron content (0.20 to 2.25 percent) and fabrication technique. For transport cask basket applications, the potential advantage to using borated stainless steel arises from the fact that the structural and criticality control functions can be combined into one material. The test program involves procuring material, machining test specimens, and conducting the tensile tests. From test measurements obtained so far, general trends indicate that tensile properties (yield strength and ultimate strength) increase with boron content and are in all cases superior to the minimum required properties established in SA-240, Type 304, a typical grade of austenitic stainless steel. Therefore, in a designed basket, web thickness using borated stainless steel would be comparable to or thinner than an equivalent basket manufactured from a typical stainless steel without boron additions. DOE

N90-28718# Oak Ridge National Lab., TN.
STRUCTURE OF METAL OVERLAYERS BY LOW ENERGY ALKALI ION SCATTERING: Cu/Ru(0001) AND Sn/Pt(111)
S. H. Overbury, D. R. Mullins, M. T. Paffett, and B. Koel (California Univ., Los Angeles.) 1990 7 p Presented at the 3rd International Conference on the Structure of Surfaces, Milwaukee, MN, 9-12 Jul. 1990
(Contract DE-AC05-84OR-21400)
(DE90-014453; CONF-9007131-1) Avail: NTIS HC A02/MF A01

Structural studies of metal adsorption on metals by incident angle dependent, low energy alkali ion scattering are presented for the systems of Cu on Ru(0001) and Sn on Pt(111). Cu forms well ordered islands which are pseudomorphic for two layers. Sub-monolayers of SN incorporate into the first Pt layer upon annealing, giving rise to a slightly buckled first layer. DOE

N90-28719# Lawrence Livermore National Lab., CA.
EXPERIMENTAL STUDY OF THE OPTICAL CONSTANTS OF METALS AT HIGH TEMPERATURES Thesis - Stanford Univ.
Mark A. Havstad May 1990 45 p Submitted for publication
(Contract W-7405-eng-48)
(DE90-014732; UCRL-ID-103911) Avail: NTIS HC A03/MF A01

This document summarizes the status of optical and radiative studies of selected metals at high temperature and serves as a dissertation proposal to the Thermosciences Division of the Department of Mechanical Engineering at Stanford University. This dissertation proposal summarizes work in progress. The final dissertation will be published in August 1990. Detailed descriptions of methods, results, and prior work will be fully reported in the dissertation and later in the open literature. DOE

N90-28720# Oak Ridge National Lab., TN.
EVALUATION OF ADVANCED AUSTENITIC ALLOYS RELATIVE TO ALLOY DESIGN CRITERIA FOR STEAM SERVICE. PART 1: LEAN STAINLESS STEEL
R. W. Swindeman, P. J. Maziasz, E. Bolling, J. F. King, and D. L. Balltrip May 1990 125 p
(Contract DE-AC05-84OR-21400)
(DE90-014765; ORNL-6629/P1) Avail: NTIS HC A06/MF A01

The results are summarized on advanced austenitic stainless steels for heat recovery systems. Commercial, near-commercial, and developmental alloys were evaluated relative to criteria for metallurgical stability, fabricability, weldability, and mechanical strength. Fireside and steamside corrosion were also considered, but no test data were collected. Lean stainless steel alloys that were given special attention were type 316 stainless steel, fine-grained type 347 stainless steel, 17-14CuMo stainless steel, Esshete 1250, Sumitomo ST3Cu stainless steel, and a group of alloys identified as HT-UPS (high temperature, ultrafine precipitation strengthened) steels that were basically 14Cr-16Ni-Mo steels modified by various additions of MC-forming elements. It was found that, by solution treating the MC-forming alloys to temperatures above 1150 C and subsequently cold or warm working, excellent metallurgical stability and creep strength could be achieved. Test data to beyond 35,000 h were collected. The ability to clad the steels for improved fireside corrosion resistance was demonstrated. Weldability of the alloys was of concern, and hot cracking was found to be a problem in the HT-UPS alloys. By reducing the phosphorous content and selecting either CRE 16-8-2 stainless steel or alloy 556 filler metal, weldments were produced that had excellent strength and ductility. The major issues related to the development of the advanced alloys were identified and ways to resolve the issues suggested. DOE

N90-28721# Brookhaven National Lab., Upton, NY.
MEASUREMENT OF LOCALIZED CORROSION USING CURRENT DENSITY MAPPING
H. S. Isaacs and A. J. Davenport 1989 7 p Presented at the American Institute of Chemical Engineers Annual Meeting, San Francisco, CA, 5-10 Nov. 1989
(Contract DE-AC02-76CH-00016)
(DE90-015086; BNL-44830; CONF-891113-12) Avail: NTIS HC A02/MF A01

The techniques for measuring distributions of currents over electrode surfaces have been reviewed. Simulation of current distributions in solutions, based on the substituting of elemental areas by point current sources is presented. Examples of the application of the technique using vibrating probe electrodes to study localized corrosion are discussed. The examples are stress corrosion cracking of sensitized stainless steels and inhibitor action during pitting of aluminum. DOE

N90-28722# Aerospatiale, Suresnes (France).
STATIC AND DYNAMIC CHARACTERIZATION OF THE ATR 72 RODS MADE OF Ti 10.2.3 TITANIUM ALLOY [CARACTERISATION STATIQUE ET DYNAMIQUE DE BIELLES ATR 72 EN ALLIAGE DU TITANE Ti 10.2.3]
R. Senger and M. H. Campagnac 10 Aug. 1989 40 p In FRENCH
(Contract STPA-86-91-021-00-471-75-86)
(Rept-49-238; ETN-90-97484) Copyright Avail: NTIS HC A03/MF A01

The mechanical properties of the airfoil-fuselage rods of the ATR 72 are investigated. The control rods are made of beta metastable Ti 10.2.3 titanium alloy. The static mechanical characteristics, for loads of about 1100 and 1200 MPa, concerning tensile tests and toughness are higher than those obtained for the annealed TA6V alloy. Optimal characteristics are obtained for R equal to 1100 MPa. The Ti 10.2.3 characteristics measured under fatigue notch tests are not satisfactory. ESA

N90-28723# Lawrence Livermore National Lab., CA.
BEHAVIOR OF Al-Mg ALLOYS IN HOT WORKING AND SUPERPLASTICITY
H. J. McQueen and M. E. Kassner (Oregon State Univ., Corvallis.) 27 Jun. 1990 19 p Presented at the 2nd Superplasticity in Aerospace Meeting, Anaheim, CA, 18-22 Feb. 1990
(Contract W-7405-eng-48)
(DE90-015193; UCRL-JC-103631; CONF-9002135-1) Avail: NTIS HC A03/MF A01

Al-Mg alloys offer a wide range of behaviors during deformation in the warm and high temperature domains. Below 250 C, the alloys exhibit high rates of strain hardening and serrated yielding. Through atmospheres pinning dislocations and reducing dynamic recovery in the same way as a drop in SFE, the Mg gives rise to non-uniform, non-cellular, high density substructures. This raises the rate of recrystallization despite the drag on grain boundaries

and also causes non-uniformity in grain size. Addition of Mn gives rise to large Al6Mn particles which induce high misorientation cells in the adjacent matrix and lead to nucleation on annealing. Fine Al6Mn particles stabilize the substructure and retard grain boundary migration. Alloys of 1 to 7 percent Mg exhibit creep domains of 3rd power stress dependence (strain rate sensitivity m=0.33) which results in tensile ductilities of 200 to 300 percent during which the large grains develop substructures. At 300 to 600 C (1--100/s), 1 to 3 percent Mg alloys develop a substructure almost as recovered as Al, which gives rise to slightly raised strain hardening, to steady state regimes and to ultra-ductility in torsion. At levels of 5 to 7 percent Mg, dynamic recrystallization is observed in limited domains. In alloys with 2 to 7 percent Mg having 0.5 to 0.8 Mn, dynamic recrystallization initiates at large constituent particles. Such alloys can be rendered superplastic though grain refinement by particle enhanced discontinuous static recrystallization. In contrast, Al-10Mg containing Al8Mg5 particles dynamically precipitated during T.M.P. also becomes capable through continuous recrystallization of superplasticity at higher rates than those above. DOE

N90-28724# Pacific Northwest Lab., Richland, WA.
DENSITY CHANGES OF GENERATION 1.5 AND 2.0 COPPER ALLOYS IRRADIATED AT 411 TO 414 C AND 529 C IN FFTF-MOTA
F. A. Garner, H. R. Brager, and K. R. Anderson (Illinois Univ., Urbana.) Jun. 1990 10 p Submitted for publication
(Contract DE-AC06-76RL-01830)
(DE90-015291; PNL-SA-17636) Avail: NTIS HC A02/MF A01

The intrinsic swelling rate of pure copper and Cu-5Ni appears to be approximately 5 percent/dpa at approximately 400 C. At 529 C the swelling rate of these alloys appears to be much lower. In more complex precipitation-strengthened alloys phase instabilities appear to play a role in determining the onset of void swelling and also the density of the unvoided matrix. Dispersion-hardened alloys were found to be very resistant to swelling. Large amounts of oxygen in an alloy, however, can overcome the swelling resistance imparted by very high densities of oxide dispersoids. Internally oxidized Gildcop alloys offer the most pronounced resistance to swelling, with the transient regime progressively extended as alumina content increases. Unfortunately, laser welding destroys the swelling resistance of dispersion-strengthened alloys. DOE

N90-28725# International Centre for Thecretical Physics, Trieste (Italy).
THERMODYNAMICS AND STRUCTURE OF LIQUID ALKALI METALS FROM THE CHARGED-HARD-SPHERE REFERENCE FLUID
S. K. Lai, O. Akinlade, and M. P. Tosi (Trieste Univ., Italy) Dec. 1989 26 p Submitted for publication
(Contract NSC79-0208-M008-23)
(DE90-627792; IC-89/418) Avail: NTIS (US Sales Only) HC A03/MF A01

The evaluation of thermodynamic properties of liquid alkali metals is re-examined in the approach based on the Gibbs-Bogoliubov inequality and using the fluid of charged hard spheres in the mean spherical approximation as the reference system, with a view to achieving consistency with the liquid structure factor. The perturbative variational calculation of the Helmholtz free energy is based on an ab initio and highly reliable nonlocal pseudopotential. Only limited improvement is found in the calculated thermodynamic functions, even when full advantage is taken of the two variational parameters inherent in this approach. The role of thermodynamic self-consistency between the equations of state of the reference fluid derived from the routes of the internal energy and of the virial theorem is then discussed, using previous results by Hoye and Stell. An approximate evaluation of the corresponding contribution to the free energy of liquid alkali metals yields appreciable improvements in both the thermodynamic functions and the liquid structure factor. It thus appears that an accurate treatment of thermodynamic self-consistency in the charged-hard-sphere system may help to resolve some of the difficulties that are commonly met in the evaluation of thermodynamic and structural properties of liquid metals. DOE

N90-28726# Centro Brasileiro de Pesquisas Fisicas, Rio de Janeiro.
EFFECTS OF Al SUBSTITUTION BY Fe IN CeAl2
A. Y. Takeuchi and S. F. daCunha 1989 18 p Submitted for publication
(DE90-627843; CBPF-NF-046/89) Avail: NTIS (US Sales Only) HC A03/MF A01

Magnetization and electrical resistivity measurements of the CeAl2 with Al substitution by Fe up to 10 percent at Fe show that the competition between the increasing Kondo effect and the antiferromagnetism persists. Change of the electronic density is followed by a decreasing Neel temperature and an increasing residual electrical resistivity. The probable appearance of ferromagnetism of the Ce moments, at intermediate temperature range, is discussed. The small decrease of the lattice parameter with Fe concentration or the magnetic behavior do not show evidence of valence changes in the Ce ion. DOE

N90-28727# Comision Nacional de Energia Atomica, San Carlos de Bariloche (Argentina).
THE STABILITY OF THE MARTENSITIC PHASES IN Cu-Zn-Al AT AN ELECTRON CONCENTRATION OF 1.534
J. L. Pelegrina and Manfred Ahlers 1989 11 p In SPANISH; ENGLISH summary Sponsored in part by Consejo Nacional de Investigaciones Cientificas y Tecnicas Prepared in cooperation with Universidad Nacional de Cuyo, Mendoza, Argentina
(DE90-628628; CNEA-CAB-89/22) Avail: NTIS (US Sales Only) HC A03/MF A01

The (beta) phase to martensite and the martensite to martensite transformations in Cu-Zn-Al single crystals of a high electron concentration have been studied as a function of the temperature. A stress temperature diagram, similar to that proposed in the Cu-Al-Ni system, is constructed and the stability of the different martensites is analyzed from thermodynamic considerations. The results for the 18R, the 6R and the 2H phase are compared with those obtained from other alloy compositions. DOE

N90-28728# Rensselaer Polytechnic Inst., Troy, NY. Dept. of Materials Engineering.
MICROSTRUCTURE AND IMPURITY EFFECTS ON TUNGSTEN HEAVY ALLOYS Final Report, May 1987 - Apr. 1990
Randall M. German 12 Jul. 1990 20 p
(Contract DAAL03-87-K-0072)
(AD-A224220; ARO-24667.16-MS) Avail: NTIS HC A03/MF A01 CSCL 11/6

The research performed in this study focused on improved tungsten heavy alloys through process optimization as measured by affects on microstructure and impurity concentrations. This largely was performed by alloying and adjusting the sintered microstructure through processing changes. Many past heavy alloy studies have failed to couple the two activities. As a consequence, potentially beneficial alloying effects have been masked by incomplete densification. Alternatively, novel processing approaches have been unsuccessful because they were applied to conventional alloys. This research has advanced both aspects, leading to novel heavy alloys with tantalum, rhenium, or molybdenum alloying. GRA

N90-28729# Army Missile Command, Redstone Arsenal, AL.
FARADAY ROTATION MAPPING OF MERCURY CADMIUM TELLURIDE Final Technical Report, Aug. - Dec. 1989
G. A. Tanton, C. R. Christensen, J. A. Grisham, and J. A. Stensby (Alabama Univ., Huntsville.) Mar. 1990 27 p
(AD-A224278; AD-E951507; AMSMI/CR-RD-RE-90-1) Avail: NTIS HC A03/MF A01 CSCL 20/6

This report summarizes the application of Faraday Rotation (FR) to determine the uniformity of free-carrier concentrations in samples of Mercury Cadmium Telluride as a function of position. This report is the first application of FR measurement techniques

on tertiary compounds. The results presented, demonstrate first order agreement of the technique with Hall measurements performed at cryogenic temperatures. Further studies and development of calibration standards are recommended. GRA

N90-28642*# National Aeronautics and Space Administration. Lewis Research Center, Cleveland, OH.
HIGH TEMPERATURE FATIGUE BEHAVIOR OF HAYNES 188
Gary R. Halford, James F. Saltsman, and Sreeramesh Kalluri (Sverdrup Technology, Inc., Cleveland, OH.) *In* NASA, Marshall Space Flight Center, Advanced Earth-to-Orbit Propulsion Technology 1988, Volume 1 Sep. 1988 p 497-509 (For primary document see N90-28611 23-20)
Avail: NTIS HC A99/MF E06 CSCL 11F

N90-28643*# Pratt and Whitney Aircraft, East Hartford, CT.
CONSTITUTIVE AND LIFE MODELING OF SINGLE CRYSTAL BLADE ALLOYS FOR ROOT ATTACHMENT ANALYSIS
T. G. Meyer, G. J. McCarthy, L. H. Favrow, D. L. Anton, and Joe Bak (United Technologies Research Center, East Hartford, CT.) *In* NASA, Marshall Space Flight Center, Advanced Earth-to-Orbit Propulsion Technology 1988, Volume 1 Sep. 1988 p 510-518 (For primary document see N90-28611 23-20)
(Contract NAS3-23939)
Avail: NTIS HC A99/MF E06 CSCL 11F

N90-28644*# National Aeronautics and Space Administration. Lewis Research Center, Cleveland, OH.
THE FATIGUE DAMAGE BEHAVIOR OF A SINGLE CRYSTAL SUPERALLOY
Michael A. McGaw *In* NASA, Marshall Space Flight Center, Advanced Earth-to-Orbit Propulsion Technology 1988, Volume 1 Sep. 1988 p 519-562 (For primary document see N90-28611 23-20)
Avail: NTIS HC A99/MF E06 CSCL 11F

27 NONMETALLIC MATERIALS

Includes physical, chemical, and mechanical properties of plastics, elastomers, lubricants, polymers, textiles, adhesives, and ceramic materials.

For composite materials see *24 Composite Materials.*

N90-28730# Xerox Palo Alto Research Center, CA.
RESEARCH ON THE STRUCTURAL AND ELECTRONIC PROPERTIES OF DEFECTS IN AMORPHOUS SILICON Annual Subcontract Report, Jul. 1988 - Aug. 1989
R. A. Street, J. B. Boyce, W. B. Jackson, N. Johnson, S. E. Ready, R. Thompson, C. C. Tsai, J. Walker, and K. Winer Jun. 1990 54 p Prepared for Midwest Research Inst., Golden, CO
(Contracts DE-AC02-83CH-10093; HB-7-06056-1)
(DE90-000342; SERI/TP-211-3830) Avail: NTIS HC A04/MF A01

The objective of this research program is to obtain a comprehensive understanding of the structure and electronic properties of a-Si:H. The main emphasis is on the phenomena of metastability and thermal equilibrium, in which the density of electronic states depend on the electronic and thermal history of the material. Metastability effects are a problem with solar cells and with other electronic devices. The studies provide an understanding of the complex interaction between the electronic states and the atomic structure which cause these effects. One of the main materials problems of amorphous silicon technology is the phenomenon of metastability, in which the electronic properties depend on the thermal and electrical history of the sample. A key observation is that the defects are in thermal equilibrium with the disordered structure. The experiments confirm that defect equilibration occurs over a range of temperatures and sample deposition conditions. The relaxation time depends on the growth conditions, and the thermal defects are shown to anneal more slowly than optically induced defects. The temperature dependence of the thermodynamic equilibrium defect density is calculated, based on a hydrogen mediated weak-bond/dangling-bond conversion model. The distribution of defect formation energies is introduced by associating a different density of valence band tail states with each formation energy. A detailed analysis of the connection between hydrogen diffusion and the relaxation kinetics finds excellent agreement with the data. DOE

N90-28731# EG and G Mound Applied Technologies, Miamisburg, OH.
EVALUATIONS OF NEW POLYIMIDE FILMS FOR FLEXIBLE CIRCUIT APPLICATIONS AT EG AND G MOUND APPLIED TECHNOLOGIES
Melvin K. Williams, Margaret Huelskamp, Jeanne Brandon, Mark Fisher, Andra Smith, and Thomas Wittberg (Dayton Univ., OH.) 1990 7 p Presented at the 4th International SAMPE Electronic Materials and Processes Conference, Albuquerque, NM, 12-14 Jun. 1990
(Contract DE-AC04-88DP-43495)
(DE90-014117; MLM-3644(OP); CONF-9006121-7) Avail: NTIS HC A02/MF A01

Until recently, flexible cable development and production at Mound had to rely heavily on Kapton polyimide from Dupont. The availability of new polyimide films has provided the opportunity to evaluate alternatives to Kapton for flexible cable work. The initial evaluations of the Upilex polyimides, Upilex-S, R, and SGA, distributed by ICI and Apical polyimide distributed by Allied Signal are described. The new polyimide films were analyzed, along with Kapton, by scanning electron microscopy/energy dispersion spectroscopy, infrared spectroscopy, and x ray photoelectron spectroscopy. Relative insulating strengths of the films were determined by high voltage electrical breakdown (HiPot) test. All the films were given a thin metal coating by physical vapor deposition, and the metal to polyimide adhesion was tested. Actual test cables were made using Upilex-S as a bridge material. These cables were fired and flyer performance was compared to that of flyers made from Kapton. The new polyimide films not only compare well to Kapton in all areas but also show some advantages in certain applications. DOE

N90-28732# National Inst. of Standards and Technology, Gaithersburg, MD. Metallurgy Div.
ELECTRODEPOSITION OF WEAR RESISTANT COATINGS Final Report
C. E. Johnson, D. S. Lashmore, D. R. Kelley, and J. L. Mullen Apr. 1990 105 p Sponsored by Bureau of Engraving and Printing, Washington, DC
(PB90-221839; NISTIR-4301) Avail: NTIS HC A06/MF A01 CSCL 11C

Analysis of premature plate failure resulted in a number of recommendations to address a series of problems that were identified in the plating process of printing plates. An accelerated wear tester was developed and applied to rank electrodeposited coatings for wear. Composite coatings of nickel-phosphorus-silicon carbide exhibited a factor of 10 increase in wear performance over the current chromium technology. Various chromium coatings exhibited a factor of 1.2 to 2 increase in abrasive wear performance. A new pulse plated duplex chromium coating exhibited the factor of two increase over the presently used chromium coating. In situ wear testing of chromium plated wiper blades exhibited a factor of two increase over the presently used chromium coatings. In situ wear testing of chromium plated wiper blades exhibited a 10 to 15 fold increase in the blade life compared to the currently used unplated blades. GRA

N90-28733# European Space Agency, Paris (France).
ASCERTAINING THE FRACTURE TOUGHNESS OF CERAMIC MATERIALS BY MEANS OF BENDING TESTPIECES OF VARIOUS NOTCH TYPES AT AMBIENT AND HIGH TEMPERATURES
Guenther Himsolt (Deutsche Forschungs- und Versuchsanstalt fuer Luft- und Raumfahrt, Cologne, Germany, F.R.) Feb. 1990 281 p Transl. into ENGLISH of Bestimmung des Bruchwiderstands

Keramischer Werkstoffe mit Biegeproben Unterschiedlicher Kerbform bei Raumtemperatur und Hohen Temperaturen (Cologne, Fed. Republic of Germany, DFVLR), Dec. 1985 255 p Original language document was announced as N86-31744
(ESA-TT-992; DFVLR-FB-85-67; ETN-90-97548) Avail: NTIS HC A13/MF A02

A new method which makes it possible to use simple relations in order to ascertain the corresponding crack length of a bending testpiece from its compliance is described. Investigations on HPSN (hot-pressed silicon nitride), RBSN (reaction-bonded silicon nitride) and HPSiC (hot-pressed silicon carbide) show that their fracture toughness is decisively governed by structural parameters and their dependance on test temperature. In the case of a notch sawn straight through, this can mean that there is dependency on the notch radius, and in the case of the chevron-notch testpiece the result may extend to failure of the method due to deteriorated crack initiation. Furthermore, some materials exhibit fracture toughness which increases hand in hand with crack length. Fractographic investigations reveal that the test method must be adapted to problems which are specific to the material. Where difficulties arise with either of the two notch types, a modified chevron notch is suggested. ESA

N90-28734# Oak Ridge National Lab., TN.
MECHANICAL TESTING ACTIVITIES RELATED TO HIGH-PERFORMANCE STRUCTURAL CERAMICS Foreign Trip Report
M. K. Ferber 17 Jul. 1990 11 p
(Contract DE-AC05-84OR-21400)
(DE90-014299; ORNL/FTR-3675) Avail: NTIS HC A03/MF A01

Current mechanical testing activities related to high-performance structural ceramics are examined. These discussions focused on a gripping arrangement for high-temperature tensile testing of single-phase and composite ceramics, which is particularly relevant to the tensile testing efforts in the Metals and Ceramics Division at ORNL. The 7th CIMTEC World Ceramics Congress in Montecatini Terme, Italy, consisted of papers on both classical and advanced technical ceramics. Papers of particular significance to the materials effort at ORNL covered both processing and property evaluation of advanced single-phase and composite ceramics. The pertinent material systems discussed included silicon carbide whisker- and particulate-reinforced silicon nitride; silicon carbide whisker- and particulate-reinforced zirconia; and silicon carbide whisker-reinforced alumina. DOE

N90-28735*# Ford Motor Co., Dearborn, MI.
IMPROVED SILICON CARBIDE FOR ADVANCED HEAT ENGINES Annual Report No. 3
Thomas J. Whalen Aug. 1988 69 p
(Contract NAS3-24384)
(NASA-CR-182186; NAS 1.26:182186) Avail: NTIS HC A04/MF A01 CSCL 11C

This is the third annual technical report for the program entitled, Improved Silicon Carbide for Advanced Heat Engines, for the period February 16, 1987 to February 15, 1988. The objective of the original program was the development of high strength, high reliability silicon carbide parts with complex shapes suitable for use in advanced heat engines. Injection molding is the forming method selected for the program because it is capable of forming complex parts adaptable for mass production on an economically sound basis. The goals of the revised program are to reach a Weibull characteristic strength of 550 MPa (80 ksi) and a Weibull modulus of 16 for bars tested in 4-point loading. Two tasks are discussed: Task 1 which involves materials and process improvements, and Task 2 which is a MOR bar matrix to improve strength and reliability. Many statistically designed experiments were completed under task 1 which improved the composition of the batches, the mixing of the powders, the sinter and anneal cycles. The best results were obtained by an attritor mixing process which yielded strengths in excess of 550 MPa (80 ksi) and an individual Weibull modulus of 16.8 for a 9-sample group. Strengths measured at 1200 and 1400 C were equal to the room temperature strength. Annealing of machined test bars significantly improved the strength. Molding yields were measured and flaw distributions were observed to follow a Poisson process. The second iteration of the Task 2 matrix experiment is described. Author

N90-28736# Societe Nationale des Poudres et Explosifs, Vert-Le-Petit (France).
TECHNICAL BIBLIOGRAPHY OF HIGH PERFORMANCE POLYETHYLENE FIBERS [BIBLIOGRAPHIE TECHNIQUE DES FIBRES DE POLYETHYLENE HAUTES PERFORMANCES]
Michel Gossant 10 Jul. 1989 41 p In FRENCH
(Contract DRET-88-302-15)
(SNPE-NT-106/89/GTR/RP/NP; ETN-90-97456) Avail: NTIS HC A03/MF A01

Polyethylene fibers are applied in several industrial manufacturing fields. The fabrication techniques and the characteristics of the fibers are summarized. The different surface finishing and properties obtained are underlined. The mechanical, electrical, chemical and thermal properties are reported. The effects of light and the thermal coefficient of expansion of the fibers are considered. Present and potential uses of such composite materials are included. ESA

N90-28737# Massachusetts Inst. of Tech., Cambridge. Center for Materials Science and Engineering.
POLYMER RESEARCH Annual Report, 1990
Apr. 1990 134 p
(PB90-246638) Avail: NTIS HC A07/MF A01 CSCL 11C

Phase transitions and interfacial phenomena in complex fluids; structure-property relations for polymeric materials; biomedical polymers; controlled polymerization of olefins and acetylenes by transition metal catalysts; electronic structure of conducting and conjugated polymers; graphite fibers; polymers in microelectronics; structure-property relationships in high-performance polymers; polymers and fiber reinforced polymer composites; mechanics of polymeric materials; design, synthesis, and processing of electrically and optically responsive polymers; ultrastructural studies of polymers; fibers and polymers laboratory; mechanical behavior of polymers; MIT-industry composites and polymer processing program; MIT-industry microcellular consortium; phase transitions and self association in aqueous solutions of micelles, microemulsions, and proteins; and structure, properties, and processing of biopolymers are discussed. GRA

N90-28738# Lawrence Livermore National Lab., CA.
DAMAGE RESISTANT OPTICAL COATINGS PREPARED USING HIGH TEMPERATURE, PLASMA CHEMICAL-VAPOR-DEPOSITION
J. H. Campbell, J. L. Emmett, R. M. Brusasco, F. Rainer, R. Th. Kersten, V. Paquet, and H. W. Etzkorn (Schott Glaswerke, Mainz, Germany, F.R.) 2 May 1990 17 p Presented at the Boulder Damage Symposium, Boulder, CO, 1-3 Nov. 1989
(Contract W-7405-eng-48)
(DE90-015042; UCRL-101769; CONF-8911192-5) Avail: NTIS HC A03/MF A01

Multilayer dielectric optical coatings, nominally consisting of 1000 or more optical-quarterwave layers, were prepared by reacting SiCl4 and a halogenated dopant (e.g., GeCl4) with O2 in a microwave-driven plasma. The dopant concentration is such that the index difference (Delta n) between adjacent quarterwave layers is about 0.02 or less. The deposition is carried out at high substrate temperatures (850 to 1100 C) producing a fully dense, fused silica coating. Surface damage thresholds of high reflectivity (HR) coatings prepared by this plasma process are comparable to those for fused silica. For example, at 1.06 micron and 16-ns surface damage thresholds were measured at greater than 45 J/sq cm compared to about 45 to 60 G/sq cm for super-polished optical fused silica. DOE

N90-28739# Lawrence Livermore National Lab., CA. Chemistry and Materials Science Dept.
A NEW LOW DENSITY, HIGH POROSITY LITHIUM HYDRIDE-BERYLLIUM HYDRIDE FOAM

J. L. Maienschein, P. E. Barry, F. E. McMurphy, and J. S. Bowers Jun. 1990 9 p Presented at the SPIE's International Symposium on Optical and Optoelectronic Applied Science and Engineering and Exhibit, San Diego, CA, 8-13 Jul. 1990 Submitted for publication
(Contract W-7405-eng-48)
(DE90-015150; UCRL-JC-103743; CONF-900756-18) Avail: NTIS HC A02/MF A01

A low density (30 to 670 kg/cu m), high porosity (up to 96 percent) foam was developed containing lithium hydride and amorphous beryllium hydride. This foam may be attractive as the x ray scattering element in experiments such as the Thomson Scattering Polarimeter as proposed for inclusion in the High Throughput X Ray Spectroscopy Space Mission, (XMM). Ways are discussed to synthesize the foam, and physical properties such as bulk density and porosity, electron density, uniformity of foam density, concentration of impurities, pore size distribution, and sensitivity to moisture are discussed. The composition of the foam can be varied, but equimolar mixtures of LiH and BeH2 give the most vigorous foaming reaction. The force needed to expand the plastic reaction mass into a foam is provided by hydrogen and organic contaminants in the beryllium hydride that are released during the foaming reaction. Simultaneous differential thermal analysis and thermogravimetric analysis show that the reaction is endothermic with very little mass loss. The presence of LiBeH3 as either a reaction intermediate or final product is suggested by the fact that the most vigorous foaming occurs with equimolar mixtures of lithium hydride and beryllium hydride. DOE

N90-28740*# National Aeronautics and Space Administration. Lewis Research Center, Cleveland, OH.
HIGH-TEMPERATURE DEFORMATION AND MICROSTRUCTURAL ANALYSIS FOR Si3N4-Sc2O3
Deock-Soo Cheong and William A. Sanders Apr. 1990 25 p Presented at the 92nd Annual Meeting of the American Ceramic Society, Dallas, TX, 23-27 Apr. 1990
(NASA-TM-103239; E-5593; NAS 1.15:103239) Avail: NTIS HC A03/MF A01 CSCL 11C

It was indicated that Si3N4 doped with Sc2O3 may exhibit high temperature mechanical properties superior to Si3N4 systems with various other oxide sintered additives. High temperature deformation of samples was studied by characterizing the microstructures before and after deformation. It was found that elements of the additive, such as Sc and O, exist in small amounts at very thin grain boundary layers and most of them stay in secondary phases at triple and multiple grain boundary junctions. These secondary phases are devitrified as crystalline Sc2Si2O7. Deformation of the samples was dominated by cavitational processes rather than movements of dislocations. Thus the excellent deformation resistance of the samples at high temperature can be attributed to the very small thickness of the grain boundary layers and the crystalline secondary phase. Author

N90-28741# Army Research Office, Research Triangle Park, NC.
PROCEEDINGS OF US ARMY RESEARCH OFFICE WORKSHOP ON US ARMY APPLICATIONS FOR DIAMOND AND DIAMONDLIKE MATERIALS
John T. Prater and Robert R. Reeber Nov. 1989 46 p Workshop held in Chapel Hill, NC, 13-14 Jun. 1989
(AD-A224193; ARO-WRKSP-RP8901) Avail: NTIS HC A03/MF A01 CSCL 11/2

The Materials Science Division of the U.S. Army Research Office Sponsored a one and one-half day workshop in June 1989 to review the status of diamond-related research in the U.S., and to identify Army system requirements that potentially could be met by this technology. Fourteen invited speakers provided an overview of diamond-related research in the U.S., and identified the particular applications where this technology could make a significant contribution to future Army missions. Applications that deserve increased attention include: erosion-resistant broad-band missile domes and detector windows, corrosion-and tribological resistant coatings, thermal heat dissipating structures, and high-strength ceramics/composites. Working discussions were then convened to determine whether there were specific recommendations which would promote the Army's implementation of this technology. GRA

N90-28651*# National Aeronautics and Space Administration. Lewis Research Center, Cleveland, OH.
DURABILITY OF THERMAL BARRIER COATINGS IN A HIGH HEAT FLUX ENVIRONMENT
William J. Brindley and James A. Nesbitt *In* NASA, Marshall Space Flight Center, Advanced Earth-to-Orbit Propulsion Technology 1988, Volume 1 Sep. 1988 p 661-674 (For primary document see N90-28611 23-20)
Avail: NTIS HC A99/MF E06 CSCL 11C

N90-28652*# National Aeronautics and Space Administration. Lewis Research Center, Cleveland, OH.
THERMAL ANALYSIS OF THERMAL BARRIER COATINGS IN A HIGH HEAT FLUX ENVIRONMENT
James A. Nesbitt and William J. Brindley *In* NASA, Marshall Space Flight Center, Advanced Earth-to-Orbit Propulsion Technology 1988, Volume 1 Sep. 1988 p 675-691 (For primary document see N90-28611 23-20)
Avail: NTIS HC A99/MF E06 CSCL 11C

N90-28653*# National Aeronautics and Space Administration. Marshall Space Flight Center, Huntsville, AL.
VACUUM APPLICATION OF THERMAL BARRIER PLASMA COATINGS
R. R. Holmes and T. N. McKechnie (Rockwell International Corp., Canoga Park, CA.) *In its* Advanced Earth-to-Orbit Propulsion Technology 1988, Volume 1 Sep. 1988 p 692-702 (For primary document see N90-28611 23-20)
Avail: NTIS HC A99/MF E06 CSCL 11C

N90-28654*# IIT Research Inst., Chicago, IL. Surface Engineering Center.
APPLICATION OF ADVANCED COATING TECHNIQUES TO ROCKET ENGINE COMPONENTS
S. K. Verma *In* NASA, Marshall Space Flight Center, Advanced Earth-to-Orbit Propulsion Technology 1988, Volume 1 Sep. 1988 p 703-729 (For primary document see N90-28611 23-20)
Avail: NTIS HC A99/MF E06 CSCL 11C

N90-28701# National Research Council of Canada, Ottawa (Ontario).
THE EFFECTS OF A COMPRESSOR REBUILD ON GAS TURBINE ENGINE PERFORMANCE: FINAL RESULTS
J. D. MacLeod and J. C. G. Laflamme (Canadian Forces Base, Baden-Soellingen, Germany, F.R.) *In* AGARD, High Temperature Surface Interactions Nov. 1989 13 p (For primary document see N90-28698 23-26)
Copyright Avail: NTIS HC A11/MF A02; Non-NATO Nationals requests available only from AGARD/Scientific Publications Executive

N90-28703# United Technologies Research Center, East Hartford, CT.
SCALE ADHERENCE EFFECTS IN OXIDATION AND SULFIDATION
M. A. DeCrescente and N. S. Bornstein *In* AGARD, High Temperature Surface Interactions Nov. 1989 10 p (For primary document see N90-28698 23-26)
Copyright Avail: NTIS HC A11/MF A02; Non-NATO Nationals requests available only from AGARD/Scientific Publications Executive

N90-28704# Office National d'Etudes et de Recherches Aerospatiales, Paris (France). Dept. of Materials Science.
MOLTEN SALT INDUCED HIGH TEMPERATURE DEGRADATION OF THERMAL BARRIER COATINGS
Serge Alperine *In* AGARD, High Temperature Surface Interactions Nov. 1989 18 p Previously announced in IAA as A89-48745 (For primary document see N90-28698 23-26)

Copyright Avail: NTIS HC A11/MF A02; Non-NATO Nationals requests available only from AGARD/Scientific Publications Executive

N90-28708# Naval Air Development Center, Warminster, PA.
MICRODAMAGE TO CERAMIC SURFACES UNDER SLIDING CONDITIONS
P. J. Kennedy and A. Conte *In* AGARD, High Temperature Surface Interactions Nov. 1989 7 p (For primary document see N90-28698 23-26)
Copyright Avail: NTIS HC A11/MF A02; Non-NATO Nationals requests available only from AGARD/Scientific Publications Executive

N90-28710# Office National d'Etudes et de Recherches Aerospatiales, Paris (France). Dept. of Materials Science.
HIGH TEMPERATURE PROTECTIVE COATINGS: RECENT TRENDS
Remy Mevrel *In* AGARD, High Temperature Surface Interactions Nov. 1989 10 p Previously announced in IAA as A90-21039 (For primary document see N90-28698 23-26)
Copyright Avail: NTIS HC A11/MF A02; Non-NATO Nationals requests available only from AGARD/Scientific Publications Executive

N90-28711# National Aerospace Lab., Emmeloord (Netherlands).
THERMAL SHOCK AND OXIDATION RESISTANCE OF CERAMIC COATINGS
J. A. M. Boogers, R. J. H. Wanhill, and H. J. C. Hersbach *In* AGARD, High Temperature Surface Interactions Nov. 1989 16 p Sponsored by Royal Netherlands Air Force (For primary document see N90-28698 23-26)
Copyright Avail: NTIS HC A11/MF A02; Non-NATO Nationals requests available only from AGARD/Scientific Publications Executive

N90-28712# National Aeronautical Establishment, Ottawa (Ontario).
EVALUATION OF HIGH TEMPERATURE PROTECTIVE COATINGS FOR GAS TURBINE ENGINES UNDER SIMULATED SERVICE CONDITIONS
A. K. Gupta, T. Terada, P. C. Patnaik (Hawker Siddeley Canada Ltd., Toronto, Ontario), and J.-P. Immarigeon *In* AGARD, High Temperature Surface Interactions Nov. 1989 31 p Sponsored by Department of National Defence, Ottawa, Ontario (For primary document see N90-28698 23-26)
Copyright Avail: NTIS HC A11/MF A02; Non-NATO Nationals requests available only from AGARD/Scientific Publications Executive

28 PROPELLANTS AND FUELS

Includes rocket propellants, igniters, and oxidizers; their storage and handling procedures; and aircraft fuels.

For related information see also *07 Aircraft Propulsion and Power, 20 Spacecraft Propulsion and Power,* and *44 Energy Production and Conversion.*

N90-28742*# Sverdrup Technology, Inc., Brook Park, OH.
HIGH ENERGY-DENSITY LIQUID ROCKET FUEL PERFORMANCE Final Report
Douglas C. Rapp Jul. 1990 14 p Presented at the 26th Joint Propulsion Conference, Orlando, FL, 16-18 Jul. 1990; cosponsored by AIAA, SAE, ASME, and ASEE
(Contract NAS3-25266)
(NASA-CR-185279; E-5667; NAS 1.26:185279; AIAA-90-1968) Avail: NTIS HC A03/MF A01 CSCL 21I

A fuel performance database of liquid hydrocarbons and aluminum-hydrocarbon fuels was compiled using engine parametrics from the Space Transportation Engine Program as a baseline. Propellant performance parameters are introduced. General hydrocarbon fuel performance trends are discussed with respect to hydrogen-to-carbon ratio and heat of formation. Aluminum-hydrocarbon fuel performance is discussed with respect to aluminum metal loading. Hydrocarbon and aluminum-hydrocarbon fuel performance is presented with respect to fuel density, specific impulse, and propellant density specific impulse. Author

N90-28743# Oak Ridge National Lab., TN.
RESULTS FROM THE FOURTH YEAR OF OPERATION OF THE FEDERAL METHANOL FLEET AT LAWRENCE BERKELEY LABORATORY
B. H. West, R. N. McGill, and S. L. Hillis (Tennessee Univ., Knoxville.) Aug. 1990 32 p
(Contract DE-AC05-84OR-21400)
(DE90-014741; ORNL/TM-11590) Avail: NTIS HC A03/MF A01

Lawrence Berkeley Laboratory has completed a fourth year of operation of five methanol vehicles for the Federal Methanol Fleet Project. Five comparable gasoline vehicles were involved in the project for the first three years, but were retired at the end of the third year. Approximately 25,000 miles were accumulated on the five methanol vehicles during the fourth year bringing the ten car total for all four years to nearly 310,000 miles. Fuel economy of the methanol vehicles was about the same as in previous years, while drivers' ratings of ease of starting and driveability declined. The cars required more frequent maintenance than in previous years, and the accumulation rates of wear metals in the engine oil continued to decline. DOE

N90-28744# National Defence Research Establishment, Stockholm (Sweden). Dept. of Weapon Systems, Effects, and Protection.
COMPOSITE PROPELLANTS WITH HIGH BURNING RATES
Torsten Liljegen Feb. 1990 28 p In SWEDISH; ENGLISH summary
(FOA-C-20781-2.1; ISSN-0347-3694; ETN-90-97100) Avail: NTIS HC A03/MF A01

Propellants with a burning rate up to 75 mm/s at 10 mPa, were manufactured by using Ultra-Fine Ammonium Perchlorate (UFAP). The manufacture of UFAP is safe when using freon as the suspending product for the perchlorates. The processing with freon will not be allowed after 1995. It is not easy to find a substitute for freon. The grinding process and the manufacture of propellants are described and discussed. Results concerning burning rates, mechanical properties, and migration of a liquid burning catalyst, catocene, are reported. ESA

N90-28745# Los Alamos National Lab., NM.
STUDY OF THE INDUCTION TIME IN ISOTHERMAL DECOMPOSITION OF EXPLOSIVES
Mary Margaret Stinecipher, Frederick W. DuBois, and John F. Baytos 1990 7 p Presented at the 19th Annual North American Thermal Analysis Society Conference, Boston, MA, 23-26 Sep. 1990 Submitted for publication
(Contract W-7405-eng-36)
(DE90-014906; LA-UR-90-2427; CONF-9009223-1) Avail: NTIS HC A02/MF A01

The high explosives (HEs) HMX, RDX, and TATB, were studied in the isothermal-age mode in the accelerating rate calorimeter (ARC) in the solid state at temperatures well below their rapid decomposition temperatures. The ARC maintained the temperature chosen until it detected an exotherm greater than 0.01 C/min, at which time heaters in the walls of the calorimeter were programmed to keep the calorimeter at the same temperature as the sample cell. If during its induction time at elevated temperature HMX was cooled and reheated, the total induction time remained the same as that of an uncooled sample. However, if the cooled sample was ground to release any trapped gases after the first heating, then the induction time was extended. Mass spectrometry was used to identify the trapped gases. DOE

N90-28746# California Univ., Davis.
IGNITION AND COMBUSTION OF LIQUID PROPELLANTS Final Report
Chung K. Law 15 Jan. 1990 41 p Prepared in cooperation with Princeton Univ., NJ
(Contracts DAAL03-89-K-0012; DAAL03-86-K-0098)
(AD-A224150; ARO-23610.5-EG; ARO-26308.1-EG) Avail: NTIS HC A03/MF A01 CSCL 21/9

A comprehensive experimental program has been conducted to gain fundamental understanding on the gasification and microexplosion characteristics of droplets of water-based liquid gun propellants consisting of hydroxylammonium nitrate and triethanol ammonium nitrate, under atmospheric as well as elevated pressures. Results demonstrate that the propellant microexplosion temperature is around 200 C and is substantially in excess of previously reported values, that liquid-phase reaction plays a key role in the droplet gasification characteristics, and that increasing the environment pressure increases the droplet gasification rate and advances the onset of droplet microexplosion. GRA

29 MATERIALS PROCESSING

Includes space-based development of products and processes for commercial applications.
For biological materials see *55 Space Biology.*

N90-28747*# Alabama Univ., Birmingham. Dept. of Material Science and Engineering.
CONTAINERLESS LOW GRAVITY PROCESSING OF GLASS FORMING AND IMMISCIBLE ALLOYS Final Report
J. Barry Andrews, Craig Briggs, and M. B. Robinson (National Aeronautics and Space Administration. Marshall Space Flight Center, Huntsville, AL.) Sep. 1990 22 p
(Grant NAG8-072)
(NASA-CR-186999; NAS 1.26:186999) Avail: NTIS HC A03/MF A01 CSCL 22A

Under normal one-g conditions immiscible alloys segregate extensively during solidification due to sedimentation of the more dense of the immiscible liquid phases. Immiscible (hypermonotectic) gold-rhodium alloys were processed in the 100 meter drop tube under low gravity, containerless conditions to determine the feasibility of producing dispersed structures. Three alloy compositions were utilized. Alloys containing 10 percent by volume of the gold-rich hypermonotectic phase exhibited a tendency for the gold-rich liquid to wet the outer surface of the samples. This wetting tendency led to extensive segregation in several cases. Alloys containing 80 and 90 percent by volume of the gold-rich phase possessed completely different microstructures from the 10 percent samples when processed under low-g, containerless conditions. Several samples exhibited microstructures consisting of well dispersed 2 to 3 microns diameter rhodium-rich spheres in a gold-rich matrix. Author

N90-29162# European Space Agency, Paris (France).
MICROGRAVITATION EXPERIMENTS IN SPACE: COMPATIBILITY WITH INTERFERING DYNAMIC INFLUENCES
Berndt Feuerbacher and Hans Hamacher (Deutsche Forschungsanstalt fuer Luft- und Raumfahrt, Cologne, Germany, F.R.) *In its* Scientific Colloquium in Honor of Prof. Dr. Rer. Nat. Hermann L. Jordan May 1990 p 69-89 Transl. into ENGLISH from Wissenschaftliches Kolloquim Gewidmet Herrn Professor Dr. Rer. Nat. Hermann L. Jordan zum 65 Geburtstag (Cologne, Fed. Republic of Germany, DFVLR), Jun. 1987 p 57-71 Original language document was announced as N88-17435 (For primary document see N90-29159 23-70)
Avail: NTIS HC A06/MF A01

31 ENGINEERING (GENERAL)

Includes vacuum technology; control engineering; display engineering; cryogenics; and fire prevention.

N90-28748# National Inst. of Standards and Technology, Gaithersburg, MD.
SPECIFICATIONS, TOLERANCES, AND OTHER TECHNICAL REQUIREMENTS FOR WEIGHING AND MEASURING DEVICES AS ADOPTED BY THE 74TH NATIONAL CONFERENCE ON WEIGHTS AND MEASURES, 1989 (1990 EDITION)
H. V. Oppermann Oct. 1989 281 p
(PB90-184961; NIST/HB-44) Avail: NTIS HC A13/MF A02; also avail. from SOD as SN003-003-02964-5 CSCL 13I

Handbook 44 was first published in 1949. The 1990 edition was developed by the Committee on Specifications and Tolerances of the National Conference on Weights and Measures with the assistance of the Office of Weights and Measures of the National Institute of Standards and Technology. It includes amendments adopted by the 74th annual meeting of the National Conference on Weights and Measures in 1989. Handbook 44 is published in its entirety each year following the annual meeting of the National Conference on Weights and Measures. The current edition includes new standards for mass flow meters in the Vehicle-Tank Meters Code and the Milk Meters Code. Author

N90-28749# National Inst. of Standards and Technology, Boulder, CO.
GUIDELINES FOR PRESSURE VESSEL SAFETY ASSESSMENT Final Report
S. Yukawa Apr. 1990 77 p Sponsored by Occupational Safety and Health Administration, Washington, DC
(PB90-219619; NIST/SP-780) Avail: NTIS HC A05/MF A01 CSCL 13B

A technical overview and information on metallic pressure containment vessels and tanks is given. The intent is to provide Occupational Safety and Health Administration (OSHA) personnel and other persons with information to assist in the evaluation of the safety of operating pressure vessels and low pressure storage tanks. The scope is limited to general industrial application vessels and tanks constructed of carbon or low alloy steels and used at temperatures between -75 and 315 C (-100 and 600 F). Information on design codes, materials, fabrication processes, inspection and testing applicable to the vessels and tanks are presented. The majority of the vessels and tanks are made to the rules and requirements of ASME Code Section VIII or API Standard 620. The causes of deterioration and damage in operation are described and methods and capabilities of detecting serious damage and cracking are discussed. Guidelines and recommendations formulated by various groups to inspect for the damages being found and to mitigate the causes and effects of the problems are presented. GRA

N90-28750# Harmony Thermal Co., Wichita, KS.
EXTENDED RANGE TANKLESS WATER HEATER Quarterly Report No. 5, 20 Apr. - 19 Jul. 1990
James A. Harris 27 Jul. 1990 3 p
(Contract DE-FG01-89CE-15407)
(DE90-014474; DOE/CE-15407/T5) Avail: NTIS HC A01/MF A01

The objective of this project is to develop an innovative gas-fired tankless water heater certified by AGA and ready for commercial sale. Effort in the past three months has been directed primarily at development of a burner that will meet the design criteria. Progress in this area has been made, and there is confidence that the objectives can be met. In addition to burner work, the other components in the gas train and ignition system have been procured, installed, and successfully tested on prototype units. DOE

N90-28751*# National Aeronautics and Space Administration. Langley Research Center, Hampton, VA.
AN LQR CONTROLLER DESIGN APPROACH FOR A LARGE GAP MAGNETIC SUSPENSION SYSTEM (LGMSS)

Nelson J. Groom and Philip R. Schaffner Jul. 1990 65 p
(NASA-TM-101606; NAS 1.15:101606) Avail: NTIS HC
A04/MF A01 CSCL 13B

Two control approaches for a Large Gap Magnetic Suspension System (LGMSS) are investigated and numerical results are presented. The approaches are based on Linear Quadratic Regulator (LQR) control theory and include a nonzero set point regulator with constant disturbance input and an integral feedback regulator. The LGMSS provides five degree of freedom control of a cylindrical suspended element which is composed of permanent magnet material. The magnetic actuators are air core electromagnets mounted in a planar way. Author

N90-28752# Lawrence Livermore National Lab., CA. Nuclear Test Engineering Div.

USING THE X RAY REGION OF THE ELECTROMAGNETIC SPECTRUM FOR ALIGNMENT: OVERVIEW, GEOMETRIC OPTICS, AND DESIGN CONSIDERATIONS

Robert B. Addis 30 May 1990 40 p
(Contract W-7405-eng-48)
(DE90-014798; UCRL-ID-104341) Avail: NTIS HC A03/MF A01

Traditional alignment systems based on the use of visible light are not practical when opaque materials obstruct the alignment axis. X ray Alignment Systems (XRA) have been designed specifically to overcome this limitation. XRA systems are analogous to visible light alignment methods, in that they both consist of placing an object to be aligned between a source of radiation and a detector. This report summarizes the interaction of the components which comprise an XRA System. Using physical principles and the knowledge developed by the traditional x ray fields, general design guidelines are established. The specialized requirements for these systems are also provided, with analytical relationships for the basic alignment configurations being derived. These equations are used to predict the alignment error of a proposed system, in addition to interpreting the resulting alignment images. While this report establishes the limitations of this technique, it also reveals that XRA has some substantial advantages over optical methods. Besides the ability to penetrate materials opaque to visible light, it is possible to eliminate all optical aberrations when using a polychromatic x ray source. This results in true geometric optics, making the measurements highly repeatable and accurate. This technique can readily position a fiducial within 0.001 in. of the alignment axis using off-the-shelf components. Typical alignment geometries are defined with an accuracy of one microradian through a distance of 100 feet. The ability of these systems to monitor the alignment in near real-time when using an x ray camera is another advantage. This allows active alignment to be performed from a remote location prior to an experiment or through its duration. DOE

N90-28753*# Texas A&M Univ., College Station. Surface Electrochemistry Lab.

ELECTROCHEMICAL INCINERATION OF WASTES Final Report, Feb. - Aug. 1990

R. C. Bhardwaj, D. K. Sharma, and J. OM. Bockris Aug. 1990 95 p
(Grant NAGw-1779)
(NASA-CR-187033; NAS 1.26:187033) Avail: NTIS HC
A05/MF A01 CSCL 13B

The novel technology of waste removal in space vehicles by electrochemical methods is presented to convert wastes into chemicals that can be eventually recycled. The important consideration for waste oxidation is to select a right kind of electrode (anode) material that should be stable under anodic conditions and also a poor electrocatalyst for oxygen and chlorine evolution. On the basis of long term electrolysis experiments on seven different electrodes and on the basis of total organic carbon reduced, two best electrodes were identified. The effect of redox ions on the electrolyte was studied. Though most of the experiments were done in mixtures of urine and waste, the experiments with redox couples involved 2.5 M sulfuric acid in order to avoid the precipitation of redox ions by urea. Two methods for long term electrolysis of waste were investigated: (1) the oxidation on Pt and lead dioxide electrodes using the galvanostatic methods; and (2) potentiostatic method on other electrodes. The advantage of the first method is the faster rate of oxidation. The chlorine evolution in the second method is ten times less then in the first. The accomplished research has shown that urine/feces mixtures can be oxidized to carbon dioxide and water, but current densities are low and must be improved. The perovskite and Ti4O7 coated with RuO2 are the best electrode materials found. Recent experiment with the redox agent improves the current density, however, sulphuric acid is required to keep the redox agent in solution to enhance oxidation effectively. It is desirable to reduce the use of acid and/or find substitutes. Author

N90-28754*# National Aeronautics and Space Administration. Lewis Research Center, Cleveland, OH.

DEVELOPMENT AND APPROACH TO LOW-FREQUENCY MICROGRAVITY ISOLATION SYSTEMS

Carlos M. Grodsinsky Washington Aug. 1990 24 p
(NASA-TP-2984; E-5287; NAS 1.60:2984) Avail: NTIS HC
A03/MF A01 CSCL 22A

The low-gravity environment provided by space flight has afforded the science community a unique arena for the study of fundamental and technological sciences. However, the dynamic environment observed on space shuttle flights and predicted for Space Station Freedom has complicated the analysis of prior microgravity experiments and prompted concern for the viability of proposed space experiments requiring long-term, low-gravity environments. Thus, isolation systems capable of providing significant improvements to this random environment are being developed. The design constraints imposed by acceleration-sensitive, microgravity experiment payloads in the unique environment of space and a theoretical background for active isolation are discussed. A design is presented for a six-degree-of-freedom, active, inertial isolation system based on the baseline relative and inertial isolation techniques described. Author

32 COMMUNICATIONS AND RADAR

Includes radar; land and global communications; communications theory; and optical communications.

For related information see also *04 Aircraft Communications and Navigation* and *17 Space Communications, Spacecraft Communications, Command and Tracking.* For search and rescue see *03 Air Transportation and Safety,* and *16 Space Transportation.*

N90-28755# National Telecommunications and Information Administration, Boulder, CO. Inst. for Telecommunication Sciences.

NEW APPROACH TO HF CHANNEL MODELING AND SIMULATION. PART 2: STOCHASTIC MODEL

L. E. Vogler and J. A. Hoffmeyer Feb. 1990 37 p
(PB90-200338; NTIA-90-255) Avail: NTIS HC A03/MF A01
CSCL 17B

A new and unique approach for modeling either narrowband or wideband high frequency (HF) channels is described. Although narrowband models of the HF channel have existed for many years, they are applicable to only a limited set of actual narrowband propagation conditions. The need for an HF channel model that is valid for both narrow and wideband widths over a more extensive range of propagation conditions motivated the research documented here. The stochastic portion of the model which simulates the time-varying distortion of a transmitted signal due to dispersion, scattering due to irregularities in the ionosphere, Doppler spread and Doppler shift is described. The development of the stochastic model is described. The model output is compared with measured propagation data obtained on a variety of HF links. The mechanism for the comparison is the channel scattering function which has been found to be an excellent descriptor of the time-varying dispersive HF channel. Author

N90-28756# National Telecommunications and Information Administration, Annapolis, MD.
GROUND-BASED WEATHER RADAR COMPATIBILITY WITH DIGITAL RADIO-RELAY MICROWAVE SYSTEMS
P. E. Gawthrop and G. M. Patrick Mar. 1990 124 p
(PB90-206236; NTIA-90-260) Avail: NTIS HC A06/MF A01
CSCL 17I

The potential for ground-based weather radar (meteorological radar) interference to digital microwave systems in the common carrier bands of 3700 to 4200 MHz and 5925 to 6425 MHz is examined. Reported cases of interference to microwave common carrier systems from ground-based weather radar systems have increased due to the trend towards digital modulations. Because of this interference, the National Telecommunications and Information Administration, the Federal Communications Commission and the National Spectrum Managers Association formed an informal working group to investigate and document the potential problems. The existing and planned spectrum uses by ground-based weather radars and digital microwave systems are addressed as well as regulations and policy pertaining to their electromagnetic compatibility. Methods to mitigate the interference in both the radar transmitter and microwave receiver are also provided. GRA

N90-28757# National Inst. of Standards and Technology, Gaithersburg, MD.
SECURE DATA NETWORK SYSTEM (SDNS) NETWORK, TRANSPORT, AND MESSAGE SECURITY PROTOCOLS
C. Dinkel Mar. 1990 89 p Sponsored by National Security Agency/Central Security Service, Fort George G. Meade, MD
(PB90-198946; NISTIR-90/4250) Avail: NTIS HC A05/MF A01
CSCL 17B

The Secure Data Network System (SDNS) project, implements computer to computer communications security for distributed applications. The internationally accepted Open Systems Interconnection (OSI) computer networking architecture provides the framework for SDNS. SDNS uses the layering principles of OSI to implement secure data transfers between computer nodes of local area and wide area networks. Four security protocol documents developed by the National Security Agency (NSA) as output from the SDNS project are included. SDN.301 provides the framework for security at layer 3 of the OSI Model. Cryptographic techniques to provide data protection for transport connections or for connectionless-mode transmission are described in SDN.401. Specifications for message security service and protocol are contained in SDN.701. Directory System Specifications for Message Security Protocol are covered in SDN.702. GRA

N90-28758# Institute for Telecommunication Sciences, Boulder, CO.
DESIGN AND PERFORMANCE OF A LONG, OVER-WATER MICROWAVE RADIO LINK
Joseph E. Farrow Feb. 1990 50 p Sponsored by Naval Air Test Center, Patuxent River, MD
(PB90-207994; NTIA-90-256) Avail: NTIS HC A03/MF A01
CSCL 20N

The design and the measured performance of a 76.8-km (47.7-mi) over-water 2.3 GHz microwave radio link is discussed. Since one of the terminals was located on an ocean tower, the maximum antenna height at that location was restricted to 49 m (160 ft). A 367-m (1200 ft) tower was used at the shore end to provide ray path clearance for normal and extreme refractivity gradients. The tower at the shore end supported antennas at 361 m (1180 ft), 345 m (1128 ft), 229 m (750 ft), and 49 m (160 ft) to provide quadruple diversity protection. Received signal level measurements were made over the link for several months including some of the summer period. Propagation performance of the link during the period was satisfactory. GRA

N90-28759 Council for National Academic Awards (England).
STUDIES IN AUTOMATIC SPEECH RECOGNITION AND ITS APPLICATION IN AEROSPACE Ph.D. Thesis
Michael Robinson Taylor 1989 1989 p
Avail: Univ. Microfilms Order No. BRDX88064

Human communication is characterized in terms of the spectral and temporal dimensions of speech waveforms. Electronic speech recognition strategies based on Dynamic Time Warping and Markov Model algorithms are described and typical digit recognition error rates are tabulated. The application of Direct Voice Input (DVI) as an interface between man and machine is explored within the context of civil and military aerospace programmes. Sources of physical and emotional stress affecting speech production within military high performance aircraft are identified. Experimental results are reported which quantify fundamental frequency and coarse temporal dimensions of male speech as a function of the vibration, linear acceleration and noise levels typical of aerospace environments; preliminary indications of acoustic phonetic variability reported by other researchers are summarized. Connected whole-word pattern recognition error rates are presented for digits spoken under controlled Gz sinusoidal whole-body vibration. Correlations are made between significant increases in recognition error rate and resonance of the abdomen-thorax and head subsystems of the body. The phenomenon of vibrato style speech produced under low frequency whole-body Gz vibration is also examined. Interactive DVI system architectures and avionic data bus integration concepts are outlined together with design procedures for the efficient development of pilot-vehicle command and control protocols. Dissert. Abstr.

N90-28760 Institute for Perception RVO-TNO, Soesterberg (Netherlands). Afd. Cognitieve Psychologie.
RESEARCH IN COMMAND AND CONTROL FOR THE DUTCH ARMY CORPS (1NL) Final Report
P. J. M. D. Essens 10 Aug. 1989 41 p In DUTCH; ENGLISH summary
(Contract A87/KL/154)
(IZF-1989-28; TD-89-1053; ETN-90-97393) Copyright Avail: Inst. for Perception RVO-TNO, P.O. Box 23, 3769 ZG Soesterberg, Netherlands

Decision making processes in a command and control system in the army corps were analyzed, with a view to the introduction of automated information systems and development for future air fights. A model for the analysis of the relation between task situation and the nature of the decision making is presented. The time dimension model characterizes typical aspects of the decision making process, based on the time reserved for that model. This model can serve as a framework for the analysis of decision making in future command and control systems. It is concluded that in the development of support systems for human information processing and decision making the differences in the task situations of the various levels of command have to be taken into account. ESA

N90-28761# Centre National d'Etudes Spatiales, Toulouse (France).
APPROXIMATION, SYNTHESIS, AND DEVELOPMENT OF BI-MODE CAVITIES MICROWAVE FILTERS PRESENTING UNSYMMETRICAL QUASI-ELLIPTIC RESPONSES [APPROXIMATION, SYNTHESE ET REALISATION DE FILTRES MICROONDES A CAVITES BIMODES, A REPONSES PSEUDO-ELLIPTIQUES DISSYMETRIQUES]
C. Guichaoua, P. Jarry, and C. Boschet Mar. 1990 190 p In FRENCH; ENGLISH summary Original contains color illustrations
(CNES-NT-124; ETN-90-97505) Copyright Avail: NTIS HC A09/MF A01

Communications, broadcasting, and recently Earth observation satellites have several channels and use microwave filtering and multiplexing techniques. Because of weight and volume constraints and increasing payload complexity, filtering techniques must be improved. A method for calculating and building unsymmetrical microwave filters leading to filtering optimization and narrower spectral occupancy in the case of multiplexers is proposed. The synthesis method, named quasi-elliptic, uses a Chebychev transfer function and transmission zeros located at finite frequencies. The

zeros may be arbitrarily situated on each side of the bandwidth. Filters are built using bi-mode cavities. This technique needs a complete characterization of the microwave cavities and coupling irises. The method is explained and validated. ESA

N90-28762# Federal Aviation Administration, Atlantic City, NJ.
COMMUNICATIONS INTERFACE DRIVER (CID) TEST PLAN
Thomas Bratton, James Davis, Charles Dudas, Jeffrey G. Livings, and Mark Schoenthal Sep. 1990 124 p
(DOT/FAA/CT-TN89/35) Avail: NTIS HC A06/MF A01

This test plan for the Communications Interface Driver (CID) systems will be used to evaluate and accept the CID. The CID system is a test tool whose purpose is to supply or receive a capacity level of communication (comm) messages to and from the air traffic control (ATC) and non-ATC ports of the Mode Select (Mode S) sensor. The primary concern of the CID test plan is written to establish the detailed test requirements, criteria, and methods to achieve the evaluation of the CID against the requirements set forth in the report, Functional Requirements of the Communications Interface Driver (CID), DOT/FAA/CT-TN87/41. Author

N90-28763# Allied-Signal Aerospace Co., Kansas City, MO.
USING EMBEDDED MICROCONTROLLERS IN RADAR TEST EQUIPMENT
Richard S. Binney and Loren E. Riblett Jul. 1990 32 p Presented at the Automatic RF Technology Group (ARFTG) Conference, Dallas, TX, 10-11 May 1990
(Contract DE-AC04-76DP-00611)
(DE90-014997; KCP-613-4292; CONF-9005175-2) Avail: NTIS HC A03/MF A01

With the recent advancements in microcontroller technology, radar test equipment can be designed to improve the accuracy of measurements being made and simplify designs. An embedded integrator monitor design application (hardware and software) is presented and comparisons are made between the embedded design and the more traditional discrete design approach. DOE

N90-28764# International Centre for Theoretical Physics, Trieste (Italy).
PROPAGATION OF ELECTROMAGNETIC RADIATION IN A RANDOM FIELD OF GRAVITATIONAL WAVES AND SPACE RADIO INTERFEROMETRY
V. B. Braginsky, N. S. Kardashev, A. G. Polnarev, and I. D. Novikov (Academy of Sciences, USSR, Moscow) Dec. 1989 26 p Submitted for publication
(DE90-627196; IC-89/392) Avail: NTIS (US Sales Only) HC A03/MF A01

Propagation of an electromagnetic wave in the field of gravitational waves is considered. Attention is given to the principal difference between the electromagnetic wave propagation in the field of random gravitational waves and the electromagnetic wave propagation in a medium with a randomly-inhomogeneous refraction index. It is shown that in the case of the gravitation wave field the phase shift of an electromagnetic wave does not increase with distance. The capability of space radio interferometry to detect relic gravitational waves as well as gravitational wave bursts of non cosmological origin are analyzed. DOE

N90-28765# Federal Aviation Administration, Atlantic City, NJ.
A FAA TECHNICAL CENTER PROJECT TRANSITION PLAN: MODE S
Leonard H. Baker, Philip S. Barbagallo, and Jeffrey G. Livings Sep. 1990 23 p
(Contract FAA-T1006B)
(DOT/FAA/CT-TN90/17) Avail: NTIS HC A03/MF A01

The provision for two-way communications with aircraft, via a digital data link, has long been considered a means of providing significant enhancements for safe and efficient flight operations. The Mode Select Beacon System (Mode S) system currently under development will provide the mechanism to allow a digital data link function. The Mode S also offers improvements in surveillance processing, and range and azimuth accuracy. The Mode S Project Transition Plan presents those activities and the organizations that are responsible to effect the transition of the Mode S into the Federal Aviation Administration (FAA) Technical Center. Author

N90-28766*# Ohio State Univ., Columbus. ElectroScience Lab.
TARGET SIGNATURE MODELING AND BISTATIC SCATTERING MEASUREMENT STUDIES Annual Report, Sep. 1988 - Aug. 1989
W. D. Burnside, T. H. Lee, R. Rojas, R. J. Marhefka, and D. Bensman 1989 49 p
(Grant NAG2-542)
(NASA-CR-186611; NAS 1.26:186611; OSU-721432-2; OSU-721446-2; OSU-721447-2; OSU-721711-3) Avail: NTIS HC A03/MF A01 CSCL 20N

An annual report that summarizes the work done on Grant No. NAG2-542 is presented. There are four areas of study to be summarized: (1) bistatic scattering measurement studies for a compact range; (2) target signature modeling for test and evaluation hardware in the loop situations; (3) aircraft code modification study; and (4) SATCOM antenna studies on aircraft. Author

N90-28767*# Michigan Univ., Ann Arbor. Radiation Lab.
ELECTROMAGNETIC SCATTERING FROM TWO-DIMENSIONAL THICK MATERIAL JUNCTIONS Report, Feb. - Sep. 1990
M. A. Ricoy and John L. Volakis Sep. 1990 77 p
(Grant NAG2-541)
(NASA-CR-186468; NAS 1.26:186468; MU-025921-14-T) Avail: NTIS HC A05/MF A01 CSCL 20N

The problem of the plane wave diffraction is examined by an arbitrary symmetric two dimensional junction, where Generalized Impedance Boundary Conditions (GIBCs) and Generalized Sheet Transition Conditions (GSTCs) are employed to simulate the slabs. GIBCs and GSTCs are constructed for multilayer planar slabs of arbitrary thickness and the resulting GIBC/GSTC reflection coefficients are compared with exact counterparts to evaluate the GIBCs/GSTCs. The plane wave diffraction by a multilayer material slab recessed in a perfectly conducting ground plane is formulated and solved via the Generalized Scattering Matrix Formulation (GDMF) in conjunction with the dual integral equation approach. Various scattering patterns are computed and validated with exact results where possible. The diffraction by a material discontinuity in a thick dielectric/ferrite slab is considered by modelling the constituent slabs with GSTCs. A non-unique solution in terms of unknown constants is obtained, and these constants are evaluated for the recessed slab geometry by comparison with the solution obtained therein. Several other simplified cases are also presented and discussed. An eigenfunction expansion method is introduced to determine the unknown solution constants in the general case. This procedure is applied to the non-unique solution in terms of unknown constants; and scattering patterns are presented for various slab junctions and compared with alternative results where possible. Author

N90-28768*# National Aeronautics and Space Administration. Lewis Research Center, Cleveland, OH.
RAIN-FADE SIMULATION AND POWER AUGMENTATION FOR SATELLITE COMMUNICATION SYSTEMS
Kurt A. Shalkhauser, Lawrence A. Nagy, and James S. Svoboda (Sverdrup Technology, Inc., Brook Park, OH.) Sep. 1990 11 p
(Contract NAS3-25266)
(NASA-TM-103134; E-5476; NAS 1.15:103134) Avail: NTIS HC A03/MF A01 CSCL 17B

The design and implementation of an automated rain-fade simulation and power augmentation system is presented. The system experimentally simulates and measures the effects of radiofrequency power fade on a 20 GHz communication link using a multimode travelling wave tube amplifier for loss compensation. Precision, computer-controlled attenuators are used in the fade simulation. Test plans for analog and digital testing are discussed. Author

N90-28769# Army Construction Engineering Research Lab., Champaign, IL.
METHODS FOR DETECTING LOW-FREQUENCY SIGNALS IN THE PRESENCE OF STRONG WINDS Final Report
Paul D. Schomer, Richard Raspet, Mark Wagner, Douglas Walker, and Daniel Marshall May 1990 113 p
(AD-A223980; CERL-TR-N-90/09) Avail: NTIS HC A06/MF A01 CSCL 17/1

This report looks at two methods to better separate blast noise from wind induced noise in unattended monitoring situations. One method is to use a windscreen, a device which prevents wind and wind induced pressures from reaching the microphone diaphragm while allowing the unimpeded passage of true acoustical pressures to the microphone. The second method is to make the microphone-black box system smarter so that it can separate wind induced noise from true blast noise. The results show both methods can do a good job of reducing wind induced noise. For blast noise, where the C-weighted sound is relevant, a special, two-layer wind screen can reduce the C-weighted sound level by almost 30 dB as compared with a bare microphone. Taking the integrated cross product of two vertically spaced microphones (about 60 cm spacing) reduces the C-weighted noise as compared with a bare microphone by about 22 dB. The two methods can be combined, but only when the wind induced noise level is very high and the C-weighted background noise ambient is very low. Otherwise, the two methods together are too good; the maximum useful reduction is the difference between the wind noise level and the background acoustical ambient. GRA

N90-28770# Naval Surface Warfare Center, Dahlgren, VA. Strategic Systems Dept.
TARGET DETECTION IN GAUSSIAN NOISE USING ARTIFICIAL NEURAL SYSTEMS Final Report
Jeffrey L. Solka and George Rogers Jun. 1990 23 p
(AD-A223983; NSWC/TR-90-171) Avail: NTIS HC A03/MF A01 CSCL 17/9

Radar signal processing with multilayered perceptrons was investigated. Networks with no hidden layer and a single hidden layer were tested on field collected millimeter wave target returns that have been corrupted with artificial Gaussian noise at a signal to noise level of 3 dB. Performance as a function of network architecture was characterized. GRA

N90-28771# Naval Postgraduate School, Monterey, CA. Dept. of Electrical Engineering.
BANDWIDTH AND SIGNAL-TO-NOISE RATIO ENHANCEMENT OF THE NPS TRANSIENT ELECTROMAGNETIC SCATTERING LABORATORY M.S. Thesis
Norman J. Walsh Dec. 1989 76 p
(AD-A224144) Avail: NTIS HC A05/MF A01 CSCL 17/9

The development of a parallel GaAs FET amplifier configuration is described for the Transient Electromagnetic Scattering Range at the Naval Postgraduate School. The implementation of the parallel amplifier configuration improved the bandwidth and the signal-to-noise ratio of the range. Existing software was used to process signals scattered from canonical targets. When interpreted, this data was used to optimize the new amplifier configuration. The upgraded facility is shown to provide measurements having excellent agreement with theoretically predicted signatures of simple canonical shapes. A significant improvement of the signal-to-noise ratio and bandwidth of scattered signature vis-a-vis that of the previous laboratory configuration is observed. Results are documented for a target library created to facilitate research into a number of scattering problems. GRA

N90-28772# Oklahoma Univ., Norman.
PHOENIX DATA ANALYSIS AND NUMERICAL SIMULATION Final Report, 1 Aug. 1985 - 31 Jul. 1989
Douglas K. Lilly 27 Jun. 1990 16 p
(Contract DAAG29-85-K-0198)
(AD-A224226; ARO-22880.1-GS) Avail: NTIS HC A03/MF A01 CSCL 17/9

The Phoenix 2 data analysis project was aimed at developing techniques for applying Doppler radar to observations of the turbulent boundary layer and at defining the important statistical properties and the large eddy structure more completely than is generally possible with direct sensors. An array of direct sensors was applied for comparison and to observe some of the finer scales of turbulence not accessible to the radar. A large eddy simulation experiment was also carried out for the purposes of observational comparison and improved interpretation. The original emphasis was on technique development in an environment thought to be moderately well understood. In outcome the technological developments are mixed in quality and some remain incomplete, while the scientific results are much more interesting than originally expected. Important improvements were made in single and dual Doppler processing, and satisfactory comparisons made between them. The errors in vertical velocity from the dual Doppler remain unpleasantly large in the upper levels and the effective resolution for some fields disappointingly coarse. GRA

33 ELECTRONICS AND ELECTRICAL ENGINEERING

Includes test equipment and maintainability; components, e.g., tunnel diodes and transistors; microminiaturization; and integrated circuitry.

For related information see also *60 Computer Operations and Hardware* and *76 Solid-State Physics*.

N90-28773# National Inst. of Standards and Technology, Gaithersburg, MD. Center for Electronics and Electrical Engineering.
EMERGING TECHNOLOGIES IN ELECTRONICS AND THEIR MEASUREMENT NEEDS, SECOND EDITION
Feb. 1990 195 p
(PB90-188087; NISTIR-90/4260) Avail: NTIS HC A09/MF A02 CSCL 09C

The National Institute of Standards and Technology (NIST) is the nation's lead organization for the development of measurement capability and for the maintenance of national reference standards that assure the uniformity of that capability. Within NIST, the Center for Electronics and Electrical Engineering (CEEE) is responsible for measurements that support the U.S. electronics industry. As part of fulfilling this responsibility, CEEE assesses measurement needs that affect the competitiveness of the U.S. electronics industry in emerging technologies. A comprehensive assessment of those needs is given. Author

N90-28774# EG and G Energy Measurements, Inc., Woburn, MA.
COMPUTER SIMULATION OF MICRO-TRIODE PERFORMANCE
Richard M. Mobley and Jack E. Boers (Boers, Jack E., Gloucester, MA) 1990 17 p Presented at the IEEE International Vacuum Microelectronics Conference, Monterey, CA, 23-25 Jul. 1990
(Contract DE-AC08-88NV-10617)
(DE90-014191; EGG-10617-1088; CONF-9007125-1) Avail: NTIS HC A03/MF A01

An evaluation is presented of the use of field emitter arrays (FEAs) for use in fast cathode ray oscilloscopes (CRTs). Fast CRTs typically have bandpass of several GHz, corresponding to step function risetime response of 100 picoseconds or less. High beam brightness is desirable since the limiting apertures of the deflection structures are small, typically .030 inches diameter at a distance of 10 inches from the gun. The spot size on the screen and the current are limited by the well known universal beam spreading relationship. It is generally possible to reach these limits using conventional oxide cathodes. Since FEAs are inherently patchy and bumpy emitters, which are known deleterious effects for flat cathodes, it is questionable whether such arrays can be used effectively in fast CRTs. If the answer is yes, then there are at least two advantageous features of FEA guns as follows: (1) faster turn-on using an impedance matched mounting, and (2) no grid emission. The simulations presented show that under certain

assumptions arrays with 10 microamps of emission/tip can produce beam brightness reaching the universal beam spread limit. DOE

N90-28775# National Inst. of Standards and Technology, Gaithersburg, MD. Electricity Div.
RESEARCH FOR ELECTRIC ENERGY SYSTEMS Annual Report
Richard J. VanBrunt, ed. Jun. 1990 83 p
(Contract DE-AI01-87CE-34011)
(DE90-014221; NISTIR-4339) Avail: NTIS HC A05/MF A01

Electrical Energy Systems investigations include: (1) an evaluation and critique of techniques for measuring ambient magnetic fields in support of epidemiological and in vitro studies of biological field effects; (2) development of techniques for detecting the toxic gas S2F10 in SF6 and measuring its production rate from corona discharges in SF6; (3) optical and electrical measurements of prebreakdown partial discharge phenomena in dielectric liquids; and (4) development of improved electro-optical methods for measurement and characterization of fast, transient high voltage impulses. DOE

N90-28776# Sandia National Labs., Albuquerque, NM.
INVESTIGATIONS INTO THE USE OF DIELECTRIC COATINGS IN MAGNETIC SWITCHES
H. C. Harjes, D. J. Sharp, G. A. Mann, F. A. Morgan, and W. G. Yelton 1990 6 p Presented at the 19th Power Modulator Symposium, San Diego, CA, Jun. 1990
(Contract DE-AC04-76DP-00789)
(DE90-014331; SAND-90-0415C; CONF-9006176-10) Avail: NTIS HC A02/MF A01

High reliability, high efficiency, long lifetime magnetic switches (saturable reactors) will be required in the high power pulse compression systems which are now being considered for use in several applications. One of the most critical components in a magnetic switch is its interlamina insulation. In high speed (high magnetization rate) magnetic switches, the insulation requirements are severe and the thermal management of core losses is a serious design issue. In such a switch, the interlamina voltage can approach 1000 V and, at present, dielectric films (such as Mylar, Polycarbonate, Kapton, etc.) are the only insulation options. These insulations, however, make the thermal management problem more difficult because they have low thermal conductivities and because substantial margins are required on the sides of the core. In addition, it is difficult to realize the normal holdoff strengths of thin films when they are wound with Metglas (the magnetic material of choice in most high speed switches) because the films can be degraded during the winding process by the rough Metglas surface. The results are reported of investigations into the possibility of using conformal dielectric coatings as a viable insulation option in high speed magnetic switches. DOE

N90-28777# Sandia National Labs., Albuquerque, NM.
ION DIVERGENCE AND THE STABILITY OF MAGNETICALLY INSULATED DIODES
S. A. Slutz 1990 6 p Presented at the 8th International Conference on High-power Particle Beams, Novosibirsk, USSR, 2-5 Jul. 1990
(Contract DE-AC04-76DP-00789)
(DE90-014565; SAND-89-2907C; CONF-9007111-10) Avail: NTIS HC A02/MF A01

Cold fluid equilibria for magnetically insulated ion diodes are unstable. The interaction of these unstable waves with electrons leads to loss above a threshold wave amplitude. The waves also interact with ions producing both divergence and energy spread. The magnitude of these effects depends strongly on the diode equilibrium and the wave parameters. Since previous stability analyses ignored the virtual cathode and the charge-neutral region, both important features of Applied-B ion diode equilibria, we have investigated diode stability with these features included. The nature of ion diode instability is changed dramatically. Ultimately one would like to control ion divergence and energy spread, which depend on the wave amplitudes. We present test particle calculations of wave-electron interactions within the diode. Comparison of our results with 3-D PIC simulations, indicate that wave amplitudes late in the simulations are just large enough to produce electron loss. This suggests that a reduction in ion divergence might result from decreasing the wave amplitude required to induce electron loss. This and other possible approaches for reducing ion divergence are discussed. DOE

N90-28778# Sheladia Associates, Inc., Rockville, MD.
ASSESSMENT OF BATTERY TECHNOLOGIES FOR ELECTRIC VEHICLES. VOLUME 2, PART 2: APPENDICES
E. Z. Ratner, ed. and G. L. Henriksen, ed. (Edgerton, Germeshausen and Grier, Inc., Idaho Falls, ID.) Feb. 1990 506 p Prepared for Edgerton, Germeshausen and Grier, Inc., Idaho Falls, ID
(Contracts DE-AC07-76ID-01570; C87-101249)
(DE90-014610; DOE/ID-10243/2-Vol-2-App-Pt-2; MISC-90024-Vol-2-App-Pt-2) Avail: NTIS HC A22/MF A03

This document, Part 2 of Volume 2, provides appendices to this report and includes the following technologies: zinc/air battery; lithium/molybdenum disulfide battery; sodium/sulfur battery; nickel/cadmium battery; nickel/iron battery; iron/oxygen battery and iron/air battery. DOE

N90-28779# Central Research Inst. of Electric Power Industry, Tokyo (Japan). Energy and Environment Lab.
ANALYSIS OF THREE-DIMENSIONAL EDDY CURRENT FIELD. APPLICATION TO CALCULATION OF MAGNETIC SCREENING EFFECT OF THE DAMPER SYSTEM IN A MODEL SUPERCONDUCTING GENERATOR
T. Kawamoto, T. Takuma, and S. Akita Nov. 1989 28 p In JAPANESE; ENGLISH abstract
(DE90-507869; CRIE-T-89015) Avail: NTIS (US Sales Only) HC A03

Based on the formulation proposed by Emson and Simkin, a method of calculating eddy current is given which uses a modified magnetic vector potential inside conducting regions and a magnetic scalar potential in non-conducting regions. Only the stationary field of alternating current expressed by complex number is dealt with and the code of calculation is established based on the finite element method. Applying this code to the calculation of eddy current generated in a hollow cylinder and a square plate being placed in homogeneous magnetic field, the results are compared with those calculated by the other method or an exact solution to show the validity of the present code. When damper is near the center of a model superconducting generator, the relation between its slip frequency and its magnetic screening effect is dealt with by this code. The result is in fairly good agreement with that obtained by experiment or calculated by the other method. Finally the result of calculation is given of 3-D eddy current induced on the inside wall of innermost SUS layer situated at the inner damper of the generator. DOE

N90-28780# Ebasco Services, Inc., Bellevue, WA.
ADJUSTABLE SPEED DRIVE APPLICATIONS GUIDEBOOK
H. M. Szablya, ed. Jan. 1990 101 p Prepared in cooperation with EA-Mueller, Inc., Baltimore, MD Prepared for Bonneville Power Administration, Portland, OR
(Contract DE-AC79-87BP-34906)
(DE90-014151; DOE/BP-34906/1) Avail: NTIS HC A06/MF A01

Reducing motor speed to match process requirements saves energy and improves process control. This guidebook looks at a number of industrial applications and processes that can be improved and made more energy efficient by applying adjustable speed drives (ASDs). It assists in determining suitable ASD applications in terms of technical and economic screening factors. It is intended for plant engineers, plant managers, and others concerned with better product quality and energy management in industrial processes. DOE

N90-28781# Sandia National Labs., Albuquerque, NM.
ZINC-BROMINE BATTERY DEVELOPMENT Final Report
Lew Richards, Walter Vanschalwijk, George Albert, Mike Tarjanyi, Anthony Leo, and Stephen Lott May 1990 101 p Prepared in

cooperation with Energy Research Corp., Danbury, CT
(Contract DE-AC04-76DP-00789)
(DE90-014751; SAND-90-7016) Avail: NTIS HC A06/MF A01

This report describes development activities on the zinc-bromine battery system conducted by Energy Research Corporation (ERC). The project was a cost-shared program supported by the U.S. Department of Energy and managed through Sandia. The project began in September 1985 and ran through January 1990. The zinc-bromine battery has been identified as a promising alternative to conventional energy storage options for many applications. The low cost of the battery reactants and the potential for long life make the system an attractive candidate for bulk energy storage applications, such as utility load leveling. The battery stores energy by the electrolysis of an aqueous zinc bromide salt to zinc metal and dissolved bromine. Zinc is plated as a layer on the electrode surface while bromine is dissolved in the electrolyte and carried out of the stack. The bromine is then extracted from the electrolyte with an organic complexing agent in the positive electrolyte storage tank. On discharge the zinc and bromine are consumed, regenerating the zinc bromide salt. DOE

N90-28782# Lawrence Livermore National Lab., CA.
MODELING TAPE-WOUND MAGNETIC SWITCHES
Jan-Mark Zentler 1990 5 p Presented at the 19th Power Modulator Symposium, San Diego, CA, 26-28 Jun. 1990 Submitted for publication
(Contract W-7405-eng-48)
(DE90-015121; UCRL-102850; CONF-9006176-11) Avail: NTIS HC A01/MF A01

An empirical ferromagnetic model developed by M. L. Hodgdon has been incorporated into the NET-2 Circuit Analysis Program to allow detailed simulation of magnetic modulators. The model is capable of representing rate dependency of the material B-H characteristics and internal losses. This tool has been used successfully to simulate non-uniform magnetization within magnetic switch cores during the switching process. Comparison is made with published experimental results on amorphous tape-wound cores subjected to 0.1 T/msec and 1 T/msec magnetization rates. DOE

N90-28783 Physics and Electronics Lab. TNO, The Hague (Netherlands).
DESIGN AND REALIZATION OF A TWO STAGE C-BAND LOW NOISE AMPLIFIER Final Report
T. C. B. Tieman Oct. 1989 34 p In DUTCH; ENGLISH summary
(FEL-89-B265; TD-89-3576; ETN-90-97410) Copyright Avail: Physics and Electronics Lab. TNO, P.O. Box 96864, 2509 JG The Hague, Netherlands

The design and some measuring results of a two stage low noise amplifier for the fequency band between 5.0 and 5.6 GHz are presented. The amplifier circuit consists of microstrip elements etched on 0.787 mm thick 5870 Duroid (a polytetrafluorethylene substrate with a relative dielectric constant of 2.33) and uses low cost GaAs FET's. The dimensions of the amplifier are 40 by 50 mm. The amplification in the frequency band between 5.0 and 5.6 GHz is at least 19 dB with a noise figure below 1.4 dB. The computer aided design program TOUCHSTONE was used. ESA

N90-28784# Instituto de Pesquisas Espaciais, Sao Jose dos Campos (Brazil).
SIMULATION OF INPE'S PRINTED CIRCUIT LABORATORY PRODUCTION LINE M.S. Thesis
Arthur TorgoGomes May 1988 179 p In PORTUGUESE; ENGLISH summary
(INPE-4556-TDL/331) Avail: NTIS HC A09/MF A01

The development of a tool intended to improve, plan, monitor, and control INPE's Printed Circuit Laboratory Production Line is presented. A manipulatable computer model was developed. The model simulates the behavior of the production line elements, when established demand is given. A discrete simulation model of stochastic nature was created departing from study and comprehension of technical and operational characteristics. The system was modeled encompassing physical and chronological dimensions. The computer model utilizes the GASP 4 language simulation. The source program for this language was worked out to make possible such an application. The model was tested and proved operational in a 6800 Burroughs computer. The major significant results that the model provides information on necessary time between an order placed with the Laboratory and the final product ready for delivery to the client; also statistics of waiting time elapsed and starting time for production. Currently, this program is operational. It is being successfully utilized by INPE's Printed Laboratory Production Line. Author

N90-28785# Lawrence Livermore National Lab., CA.
NOISE PERFORMANCE OF MICROCHANNEL PLATE IMAGING SYSTEMS
K. McCammon, K. Hagans, and A. Hankla 26 Jun. 1990 6 p Presented at the SPIE's International Symposium on Optical and Optoelectronic Applied Science and Engineering Exhibit, San Diego, CA, 8-13 Jul. 1990
(Contract W-7405-eng-48)
(DE90-015037; UCRL-JC-104338; CONF-900756-17) Avail: NTIS HC A02/MF A01

A characterization is presented of the significant noise mechanisms is a microchannel image intensifier and CCD image recording system intended for applications in ultrafast imaging systems used for nuclear science. The system under study consists of a generation two image intensifier, a relay lens, and a cooled CCD imaging array of 640 by 1024 pixels. Fixed pattern noise is significantly reduced by flat fielding techniques. The remaining major noise mechanisms are the intensifier shot noise and a noise factor that characterizes the non-idealness of the system. Results are given for the intensifier noise factor's functional dependence on input irradiance levels, gain settings, and accelerating voltages. DOE

N90-28786*# National Aeronautics and Space Administration. Lewis Research Center, Cleveland, OH.
HIGH TEMPERATURE SUPERCONDUCTING THIN FILM MICROWAVE CIRCUITS: FABRICATION, CHARACTERIZATION, AND APPLICATIONS
K. B. Bhasin, J. D. Warner, R. R. Romanofsky, V. O. Heinen, and C. M. Chorey (Sverdrup Technology, Inc., Brook Park, OH.) 1990 14 p Presented at the Technical Symposium on Optical Engineering and Photonics in Aerospace Sensing, Orlando, FL, 16-20 Apr. 1990; sponsored by Society of Photo-Optical Instrumentation Engineers
(NASA-TM-103235; E-5515; NAS 1.15:103235) Avail: NTIS HC A03/MF A01 CSCL 09A

Epitaxial YBa2Cu3O7 films were grown on several microwave substrates. Surface resistance and penetration depth measurements were performed to determine the quality of these films. Here the properties of these films on key microwave substrates are described. The fabrication and characterization of a microwave ring resonator circuit to determine transmission line losses are presented. Lower losses than those observed in gold resonator circuits were observed at temperatures lower than critical transition temperature. Based on these results, potential applications of microwave superconducting circuits such as filters, resonators, oscillators, phase shifters, and antenna elements in space communication systems are identified. Author

N90-28787# Naval Postgraduate School, Monterey, CA. Dept. of Physics.
UNIPOLAR ARCING ON THE CATHODE SURFACE OF A HIGH VOLTAGE DIODE M.S. Thesis
Stephen A. Minnick Dec. 1989 37 p
(AD-A224122) Avail: NTIS HC A03/MF A01 CSCL 20/3

The idea of electron emission from an exploding cathode whisker has been reported on many times by various research groups. However, since the reported estimates of current density from the cathode spots vary widely over several orders of magnitude, it is clear that the actual mechanism of explosive emission is not well understood. Plasma surface interaction via

unipolar arcing can be shown to be able to supply the necessary current density to initiate explosive emission. Joule heating of the whisker by unipolar arcing is much greater than for either field emitted or space charge limited current flow. It has now been shown experimentally that unipolar arcing occurs not only in a laser induced plasma surface interaction, but also in a vacuum diode discharge at the cathode surface. The unipolar arcing process forms the initial breakdown plasma in each case. GRA

N90-28788# Air Force Astronautics Lab., Edwards AFB, CA.
DEVELOPMENT OF THE ELECTRIC VEHICLE ANALYZER Final Report, Aug. 1986 - Dec. 1988
Michael R. Dickey, Raymond S. Klucz, Kimberly A. Ennix, and Leo M. Matuszak Jun. 1990 42 p
(AF Proj. 2864)
(AD-A224201; AL-TR-90-006) Avail: NTIS HC A03/MF A01 CSCL 21/3

The increasing technological maturity of high power (greater than 20 kW) electric propulsion devices has led to renewed interest in their use as a means of efficiently transferring payloads between earth orbits. Several systems and architecture studies have identified the potential cost benefits of high performance Electric Orbital Transfer Vehicles (EOTVs). These studies led to the initiation of the Electric Insertion Transfer Experiment (ELITE) in 1988. Managed by the Astronautics Laboratory, ELITE is a flight experiment designed to sufficiently demonstrate key technologies and options to pave the way for the full-scale development of an operational EOTV. An important consideration in the development of the ELITE program is the capability of available analytical tools to simulate the orbital mechanics of a low thrust, electric propulsion transfer vehicle. These tools are necessary not only for ELITE mission planning exercises but also for continued, efficient, accurate evaluation of DoD space transportation architectures which include EOTVs. This paper presents such a tool: the Electric Vehicle Analyzer (EVA). GRA

34 FLUID MECHANICS AND HEAT TRANSFER

Includes boundary layers; hydrodynamics; fluidics; mass transfer; and ablation cooling.

For related information see also *02 Aerodynamics* and *77 Thermodynamics and Statistical Physics.*

N90-28789*# Institute for Computer Applications in Science and Engineering, Hampton, VA.
ON THE USE OF LAGRANGIAN VARIABLES IN DESCRIPTIONS OF UNSTEADY BOUNDARY-LAYER SEPARATION Final Report
Stephen J. Cowley, Leon L. VanDommelen, and Shui T. Lam (National Power Technology and Environmental Centre, Leatherhead, England) Jul. 1990 68 p Submitted for publication
(Contract NAS1-18605)
(NASA-CR-182071; ICASE-90-47; NAS 1.26:182071) Avail: NTIS HC A04/MF A01 CSCL 20D

The Lagrangian description of unsteady boundary layer separation is reviewed from both analytical and numerical perspectives. It is explained in simple terms how particle distortion gives rise to unsteady separation, and why a theory centered on Lagrangian coordinates provides the clearest description of this phenomenon. Some of the more recent results for unsteady three dimensional compressible separation are included. The different forms of separation that can arise from symmetries are emphasized. A possible description of separation is also included when the detaching vorticity layer exits the classical boundary layer region, but still remains much closer to the surface than a typical body-lengthscale. Author

N90-28790# National Inst. of Standards and Technology, Gaithersburg, MD. Center for Computing and Applied Mathematics.
STABILIZATION OF TAYLOR-COUETTE FLOW DUE TO TIME-PERIODIC OUTER CYLINDER OSCILLATION
B. T. Murray, G. B. McFadden, and S. R. Coriell Apr. 1990 31 p
(PB90-219130; NISTIR-90/4283) Avail: NTIS HC A03/MF A01 CSCL 20D

The linear stability of circular Couette flow between concentric infinite cylinders is considered for the case when the inner cylinder is rotated at a constant angular velocity and the outer cylinder is driven sinusoidally in time with zero mean rotation. This configuration was studied experimentally by Walsh and Donnelly. The critical Reynolds numbers calculated from linear stability theory agree well with the experimental values, except at large modulation amplitudes and small frequencies. The theoretical values are obtained using Floquet theory implemented in two distinct approaches: a truncated Fourier series representation in time, and a fundamental solution matrix based on a Chebyshev pseudospectral representation in space. For large amplitude, low frequency modulation, the linear eigenfunctions are temporally complex, consisting of a quiescent region followed by rapid change in the perturbed flow velocities. Author

N90-28791*# Army Propulsion Lab., Cleveland, OH.
CURRENT RESEARCH IN CAVITATING FLUID FILMS
D. E. Brewe, ed., J. H. Ball, ed., and M. M. Khonsari, ed. (Pittsburgh Univ., PA.) Jul. 1990 66 p
(NASA-TM-103184; E-4924; NAS 1.15:103184) Avail: NTIS HC A04/MF A01 CSCL 20D

A review of the current research of cavitation in fluid films is presented. Phenomena and experimental observations include gaseous cavitation, vapor cavitation, and gas entrainment. Cavitation in flooded, starved, and dynamically loaded journal bearings, as well as squeeze films are reviewed. Observations of cavitation damage in bearings and the possibility of cavitation between parallel plates with microasperities were discussed. The transcavity fluid transport process, meniscus motion and geometry or form of the film during rupture, and reformation were summarized. Performance effects were related to heat transfer models in the cavitated region and hysteresis influence on rotor dynamics coefficients. A number of cavitation algorithms was presented together with solution procedures using the finite difference and finite element methods. Although Newtonian fluids were assumed in most of the discussions, the effect of non-Newtonian fluids on cavitation was also discussed. Author

N90-28792*# National Aeronautics and Space Administration. Lewis Research Center, Cleveland, OH.
EVALUATION OF A HYBRID KINETICS/MIXING-CONTROLLED COMBUSTION MODEL FOR TURBULENT PREMIXED AND DIFFUSION COMBUSTION USING KIVA-2
H. Lee Nguyen and Ming-Jyh Wey (MBR Combustion Research, Inc., Princeton, NJ.) 1990 22 p Presented at the 26th Joint Propulsion Conference, Orlando, FL, 16-18 Jul. 1990; cosponsored by AIAA, SAE, ASME, and ASEE
(NASA-TM-103196; E-5590; NAS 1.15:103196; AIAA-90-2450)
Avail: NTIS HC A03/MF A01 CSCL 20D

Two dimensional calculations were made of spark ignited premixed-charge combustion and direct injection stratified-charge combustion in gasoline fueled piston engines. Results are obtained using kinetic-controlled combustion submodel governed by a four-step global chemical reaction or a hybrid laminar kinetics/mixing-controlled combustion submodel that accounts for laminar kinetics and turbulent mixing effects. The numerical solutions are obtained by using KIVA-2 computer code which uses a kinetic-controlled combustion submodel governed by a four-step global chemical reaction (i.e., it assumes that the mixing time is smaller than the chemistry). A hybrid laminar/mixing-controlled combustion submodel was implemented into KIVA-2. In this model, chemical species approach their thermodynamics equilibrium with a rate that is a combination of the turbulent-mixing time and the

chemical-kinetics time. The combination is formed in such a way that the longer of the two times has more influence on the conversion rate and the energy release. An additional element of the model is that the laminar-flame kinetics strongly influence the early flame development following ignition. Author

N90-28793# Oak Ridge National Lab., TN.
GAS-FILM FLOW IN TUBES
Eckhart Blass (Technische Univ., Munich, Germany, F.R.) 1990 28 p Presented at the Annual Meeting of Chemical Engineers, Duesseldorf, Fed. Republic of Germany, 29 Sep. - 1 Oct. 1976
(Contract DE-AC05-84OR-21400)
(DE90-011528; ORNL/tr-90/9) Avail: NTIS HC A03/MF A01

The countercurrent flow of gases or vapors and falling films is used in many apparatus for thermal treatment or separation. This is because the heat and mass transfer efficiency of such apparatus relative to the expenditure of energy for gas flow and for falling film generation is relatively high compared to that of other separative apparatus. An overview is given of the current possibilities for calculating the flow, heat transfer and mass transfer in falling film apparatus. Steady state falling film flow is discussed with and without the countercurrent flow of gases, the upper and lower operating limit, heat transfer between non-boiling and boiling falling films and the tube wall, and heat and mass transfer between falling film and the gas. DOE

N90-28794 Rensselaer Polytechnic Inst., Troy, NY.
AN INVESTIGATION OF THE STEADY AND UNSTEADY NEAR WAKE AND ITS EFFECT ON A LAMINAR BOUNDARY LAYER Ph.D. Thesis
Daniel Edwin Paxson 1989 216 p
Avail: Univ. Microfilms Order No. DA9018443

An investigation was conducted to study the near wake and its unsteady effects on an accelerating laminar boundary layer as it is convected over the surface on which the boundary layer is formed. The experiment was divided into two major parts. The first portion of the experiment concerned the wake itself, in the region 40 to 90 diameters downstream from the wake source. Very little information is presently available on this 'near wake' region and it was felt that an adequate characterization was needed before any unsteady phenomena could be examined. Hot-wire measurements were made using the technique of conditional sampling. This portion of the investigation proved to be of independent interest due to the uniqueness of the measurements; thus, a theoretical interpretation of the results was also pursued. It was found that when the equations of motion are rewritten using the intermittency function, several new terms arise which are of importance to a physical understanding of the flow. These were experimentally measured and are presented along with the new equations. Several of the new terms are reasonably well modelled using relatively simple relationships between various flow quantities. The second part of the experiment involved wake induced, unsteady boundary layer velocity measurements on the forward portion of a bluff body. It was found that in this region, the unsteadiness manifests itself upon the boundary layer as inviscid oscillations. As a result the boundary layer equations remain valid. Furthermore, since the periodic and random oscillations induced by the passing wake are relatively small, a method of solution to the equations of motion could be obtained using perturbation techniques. Arguments supporting this approach are presented along with experimental results which confirm the theoretical predictions. Dissert. Abstr.

N90-28795 Council for National Academic Awards (England).
A STUDY OF HEAT AND FLUID FLOW PHENOMENA ON THE GAS SIDE OF CIRCULAR-TUBE PLATE-FIN HEAT EXCHANGERS Ph.D. Thesis
Stephen Baldwin 1989 366 p
Avail: Univ. Microfilms Order No. BRDX88699

The heat transfer and pressure drop characteristics of a circular-tube, plate-fin heat exchanger geometry were investigated. These parameters, expressed as the Colburn J factor and a friction factor f, are presented for Reynolds numbers from 100 to 3200, for exchanger samples with 1, 2 and 4 tube rows and 8, 10 and 12 fins per inch. These results are presented graphically and as a mathematical predictor model. The Taylor first order expansion and a Monte-Carlo numerical simulation of data were used to estimate the uncertainty in the values of J and f due to instrument discretization and random error. Comparisons with earlier work by other authors using simplified equations were undertaken. Dye-streak flow visualization was undertaken to study the flow field in four times scale models of circular-tube exchanger geometries with louvred and un-louvred plate-fins. Local heat transfer coefficients were obtained for the plain exchanger using a phase change paint in a transient condition. Correlations between the flow field and local heat transfer coefficient distribution were identified on the plain geometry and used to estimate the trends in heat transfer coefficient distribution for a louvred geometry. Numerical prediction of the flow fields present in a three dimensional plain circular-tube, plate-fin exchanger geometry, and two designs of multi-fin louvre bank were undertaken using the PHOENICS 81 code. Comparisons of predicted flow fields and experimental flow visualization showed good qualitative agreement. The development and manufacture of the various rigs, tools, and techniques used in the investigation are described.
Dissert. Abstr.

N90-28796 Washington State Univ., Pullman.
AN EXPERIMENTAL INVESTIGATION OF A SINGLE AND MULTIPHASE CONFINED COAXIAL JET Ph.D. Thesis
Robert Allen Gore 1989 190 p
Avail: Univ. Microfilms Order No. DA9015992

The purpose of the present investigation was to determine the effect of the addition of particles on the mixing process in a highly loaded confined coaxial jet. This geometry has similarities to ones in many practical situations (e.g., jet pumps). In order to quantify the mixing process it is necessary to obtain the velocities at all locations in the flow field. This was done using a laser-Doppler anemometer system which, at a high concentration of particles (in this case up to 15 percent by volume), required that the indices of refraction of the solid phase and liquid phase be matched. In the present investigation this was done using a 52 percent solution of NaI in distilled water as the liquid phase and silica gel as the solid phase. The results of the investigation show that the mixing rate in a confined coaxial jet is a strong function of the jet Reynolds number, velocity ratio of the two streams, the initial entrance profiles and the concentration (above a concentration of 3 percent). Higher velocity ratios, flatter initial profiles, and high solids concentrations lead to enhanced mixing of the two streams. Higher values of Reynolds number, however, correspond to reduced mixing. These trends will be useful in the development of viable physical and numerical models for slurry flows. Dissert. Abstr.

N90-28797 Stanford Univ., CA.
THE EFFECTS OF GRID-GENERATED TURBULENCE ON FLAT AND CONCAVE TURBULENT BOUNDARY LAYERS Ph.D. Thesis
Paul Leslie Johnson 1990 266 p
Avail: Univ. Microfilms Order No. DA9017859

This experiment examines the effects of grid-generated turbulence on flat and concave turbulent boundary layers. The work is motivated by interest in the combined effects of free-stream turbulence and concave curvature, which, when considered separately, increase skin friction and heat transfer over values in flat plate boundary layers without free-stream turbulence. Three-component laser Doppler velocimetry measurements were made in a water channel facility whose low Reynolds numbers and thick boundary layers allowed accurate velocity measurements into the viscous sublayer. A square, biplanar, square bar grid was used to generate turbulence best characterized as axisymmetric, rather than isotropic. Measurements of decaying grid turbulence were made in the inviscid core region of the channel, outside of the boundary layers growing on each wall. Results show that the irrotational mean strain rate due to streamline curvature decreases the rate of decay of turbulent kinetic energy, relative to flows without streamline curvature. Dissert. Abstr.

N90-28798# Nevada Univ., Reno.
FREE SHEAR LAYER AND SWIRL FLOW HEAT TRANSFER ENHANCEMENT Final Report, 1 Sep. 1987 - 31 Dec. 1989
R. A. Wirtz, M. Greiner, and B. Snyder 1 May 1990 32 p
(Contract GRI-5087-260-1562)
(PB90-228123; GRI-90/0088) Avail: NTIS HC A03/MF A01 CSCL 20D

Two wall shape induced convective heat transfer enhancement mechanisms for channel flows are investigated. The first uses transverse grooves in a channel wall to produce unstable free shear layers which cause traveling waves to be superimposed on the mean flow, thus augmenting heat transfer. The second uses streamline curvature to produce a swirling secondary flow. In this case, a serpentine channel is investigated. Flow visualization and heat transfer/pressure drop measurements with both air and water show that the expected augmentation mechanisms are operable in both the grooved and serpentine channel configurations at flow rates normally encountered in compact heat exchanger applications. When compared to other enhanced surfaces (such as offset strip fins or corrugated plate fins) on an equal pumping power basis, both the grooved and serpentine configurations of the present study produce performance curves which are comparable to, and in some cases superior to other conventional techniques. GRA

N90-28799# Maryland Univ., College Park. Dept. of Mechanical Engineering.
TRANSIENT COOLING OF A HOT SURFACE BY DROPLETS EVAPORATION Final Report
M. Klassen and M. diMarzo May 1990 109 p
(Grant NANB8H0890)
(PB90-227968; NIST/GCR-90/575) Avail: NTIS HC A06/MF A01 CSCL 20D

An infrared thermographic technique is developed to obtain the transient solid surface temperatures surrounding the droplet during vaporization. The technique is appealing because it is non-intrusive, detailing the surface response to the droplet without affecting the evaporation process. Surface recovery can also be monitored using the thermographic method. The transient temperature distribution of a Macor solid is detailed. It is found that contact temperature is held in the vicinity of the droplet during the majority of the droplet's evaporation until the droplet thickness diminished greatly, whereupon the temperature of the solid surrounding the droplet begins to rise. The non-dimensional radius of influence of droplet cooling is also detailed. The data obtained on the cooling effect induced on aluminum and on Macor from previous studies is used in concert with new data obtained on a quartz surface to characterize the induced cooking of a hot surface by an evaporating droplet. The role of the droplet size and shape is investigated for various high and low thermal conductivity surfaces. Droplet evaporation time, surface heat transfer coefficient and droplet shape parameter are also examined. GRA

N90-28800# Royal Aerospace Establishment, Farnborough (England).
USE OF LIQUID CRYSTALS FOR QUALITATIVE AND QUANTITATIVE 2-D STUDIES OF TRANSITION AND SKIN FRICTION
L. Gaudet and T. G. Gell 15 Jun. 1989 35 p Presented at the ICIASF 1989, Goettingen, Fed. Republic of Germany, 18-21 Sep. 1989 Previously announced in IAA as A90-28259 Original contains color illustrations
(RAE-TM-Aero-2159; BR112416; ETN-90-97063) Copyright Avail: NTIS HC A03/MF A01

The exploitation of the properties of liquid crystals to visualize transition and to measure skin friction is described. The effectiveness of a transition band to trip the laminar boundary layer on a swept wing is demonstrated by the growth of turbulent wedges with Reynolds number. The ability of liquid crystals to reveal intricate surface flow structure is clearly shown by subtle changes of color on an unswept rectangular wing when subjected to the combined effects of transition, separation, reattachment, and a normal shock. The time response of the liquid crystals to changes in shear stress is illustrated by the shock pattern on the model surface which was seen to be oscillating. A method involving the digitization of the video image into its three components colors has the potential for measuring skin friction in great detail. This involves using relationships firstly correlating the components colors with wavelength and secondly correlating shear stress with wavelength. ESA

N90-28801# European Space Agency, Paris (France).
OSCILLATORY CONVECTION
Roland Kessler (Deutsche Forschungs- und Versuchsanstalt fuer Luft- und Raumfahrt, Goettingen, Germany, F.R.) Feb. 1989 100 p Transl. into ENGLISH of Oszillatorische Konvektion (Goettingen, Fed. Republic of Germany, DFVLR), Feb. 1984 95 p Original language document was announced as N84-33756
(ESA-TT-890; DFVLR-FB-84-14; ETN-90-97547) Avail: NTIS HC A05/MF A01

The steady and oscillatory convection in a rectangular box heated from below and cooled from above is studied theoretically. The spatial structure of the three dimensional flow, caused by the vertical boundaries of the box, is influenced by the Prandtl number and thermal boundary conditions of the side walls. These three dimensional effects of the convection flow are discussed with reference to the theoretical steady flow. The onset and the frequency of the oscillatory instability are determined by solving the nonlinear time dependent equations. The numerical solutions show that the cause of this stability depends very heavily on the Prandtl number. The physics of the theoretical oscillatory flow is discussed and compared with experimental results. A Galerkin method for solving the three dimensional, time dependent Navier-Stokes equation is presented. This method proves to be an efficient algorithm for calculating three dimensional flows, especially on a vector computer like the Cray 1S. ESA

N90-28802# European Space Agency, Paris (France).
NUMERICAL SIMULATION OF THE FORMATION OF TWO-DIMENSIONAL AND THREE-DIMENSIONAL STRUCTURES IN SHEAR LAYERS AND WAKES
Eckart Meiburg (Deutsche Forschungs- und Versuchsanstalt fuer Luft- und Raumfahrt, Goettingen, Germany, F.R.) Feb. 1990 148 p Transl. into ENGLISH of Numerische Simulation der Zwei- und Dreidimensionalen Strukturbildung in Scherschichten un Nachlaeufen (Goettingen, Fed. Republic of Germany, DFVLR), Dec. 1985 Original language document was announced as N87-11136
(ESA-TT-1008; DFVLR-FB-86-10; ETN-90-97549) Avail: NTIS HC A07/MF A01

The nonlinear formation of two dimensional and three dimensional structures in nominally two dimensional shear layers and wakes is investigated numerically assuming spatially periodic flow. The simulation of the vorticity dynamics is based on the Biot-Savart law. In the case of the simple shear layer, the instability of the braid region, the translational instability of the vortex cores and the helical pairing mechanism are analyzed. The wake flow is investigated with respect to possible changes in the topological structure of the vorticity field. Comparison with experimental observations indicates the importance of subharmonic perturbations in the wake. ESA

N90-28803# European Space Agency, Paris (France).
EXPERIMENTAL INVESTIGATIONS ON THE STABILITY AND TRANSITION OF THREE-DIMENSIONAL BOUNDARY LAYERS
Petra Nitschke-Kowsky (Deutsche Forschungs- und Versuchsanstalt fuer Luft- und Raumfahrt, Goettingen, Germany, F.R.) Feb. 1990 143 p Transl. into ENGLISH of Experimentelle Untersuchungen zu Stabilitaet und Umschlag Dreidimensionaler Grenzschichten (Goettingen, Fed. Republic of Germany, DFVLR), Jun. 1986 136 p Original language document was announced as N87-14664 Previously announced as N87-24673
(ESA-TT-1026; DFVLR-FB-86-24; ETN-90-97550) Avail: NTIS HC A07/MF A01

Various experimental methods are used to investigate three-dimensional unstable boundary layers with respect to those

characteristic perturbations which lead to transition. Flow visualization of stationary crossflow instabilities on a swept cylinder (and also traveling waves in the boundary layer over the wall before transition) was successfully achieved using the hydrogen bubble method. Further investigations were carried out in the 1 m wind tunnel (using the sublimation method and hot wire technology) on a representative model consisting of a swept plate and a displacement body used to impose pressures on it. These experiments again indicated the presence, over a wide frequency band, of both stationary crossflow instabilities and traveling waves. In the case of the model used, selected to demonstrate principles and whose boundary layer is therefore a close approximation to the theoretical assumptions, the observed perturbation waves agree well with theory. ESA

N90-28804# Lawrence Livermore National Lab., CA.
AN ASYMPTOTICALLY INDUCED DOMAIN DECOMPOSITION METHOD FOR PARABOLIC BOUNDARY LAYER PROBLEMS
Garry Rodrigue and Edna Reiter (California State Univ., Hayward.) 1990 18 p Presented at the Workshop on Asymptotic Analysis and Numerical Solution of Partial Differential Equations, Argonne, IL, 26-28 Feb. 1990
(Contract W-7405-eng-48)
(DE90-014620; UCRL-JC-104001; CONF-9002131-1) Avail: NTIS HC A03/MF A01

An iterative method for computing an approximation to the solution of the singularly perturbed elliptic partial differential equations is described. Smoothness of the boundary conditions are established that will enable the iterates to asymptotically approximate the parabolic boundary layers of the solution. A domain decomposition technique based around the results of the asymptotic analysis is developed to numerically solve the differential equation when the boundary functions are discontinuous. Convergence results of the numerical scheme are established and a computational example is given. Divergence is computationally examined. DOE

N90-28805# Lawrence Livermore National Lab., CA.
LECTURE NOTES ON INCOMPRESSIBLE FLOW AND THE FINITE ELEMENT METHOD
P. M. Gresho and S. T. Chan 1989 456 p
(Contract W-7405-eng-48)
(DE90-014665; UCRL-ID-103169) Avail: NTIS HC A20/MF A03

Some areas of discussion are: scalar transport equations; incompressible flow equations; flows with coupled transport equations; and the FEM3 model. DOE

N90-28806*# National Aeronautics and Space Administration. Langley Research Center, Hampton, VA.
GAS-JET AND TANGENT-SLOT FILM COOLING TESTS OF A 12.5 DEG CONE AT MACH NUMBER OF 6.7
Robert J. Nowak May 1988 85 p
(NASA-TP-2786; L-16148; NAS 1.60:2786) Avail: NTIS HC A05/MF A01 CSCL 20D

Tests were conducted in the Langley 8-Foot High Temperature Tunnel to determine the aerothermal effects of gaseous nitrogen-coolant ejection on a 3-ft base-diameter, 12.5 degree half-angle cone. Free-stream Mach number, total temperature, and unit Reynolds number per foot were 6.7, 3300 deg R, and 1.4 million, respectively. Two coolant ejection noses were tested, an ogive frustum with a forward-facing 0.8-in radius gas-jet tip, and a 3-in radius hemisphere with a 0.243-in high rearward-facing tangent slot. Data include surface pressures and heating rates, shock shapes, and shock-layer profiles; results are compared with no-cooling data obtained with 1-in and 3-in radius solid noses. Surface pressures were reduced with gas-jet ejection but were affected little by tangent-slot ejection. For both gas-jet and tangent-slot ejection, high coolant flow rates reduced heating even far downstream from the region of ejection; however, low coolant rates caused transition to turbulence and increased heating. Shock-layer profiles of pitot pressure, Mach number, and total temperature were reduced for both gas-jet and tangent-slot ejection. Insight into the gas-jet heat-flux mechanisms was obtained by using shock-layer rake data and established, no-cooling, heat-transfer equations. Author

N90-28807# Haute-Normandie Univ., Mont Saint Aignan (France).
NUMERICAL SIMULATION OF REACTIVE TURBULENT FLOWS Final Report [SIMULATION NUMERIQUE D'ECOULEMENTS TURBULENTS REACTIFS, RAPPORT DE SYNTHESE FINALE]
A. Picart, R. Borghi, and J. P. Chollet (Institut de Mecanique de Grenoble, France) 1986 18 p In FRENCH
(Contract DRET-86-199)
(ETN-90-97476) Avail: NTIS HC A03/MF A01

The results of the direct numerical simulation of reactive turbulent flows are summarized. The study allows quantification of the importance of turbulence on the reaction rates and on the decrease of the scalar mean values. A semi-spectral method with periodic boundary conditions in three dimensions is used. The importance of turbulence on the reaction depends on the configuration considered and on the linearity of the reaction term. The hypothesis concerning the distribution probability of the inert scalar and the reactive scalar is verified by the simulation. ESA

N90-28808# Societe Nationale d'Etude et de Construction de Moteurs d'Aviation, Moissy-Cramayel (France).
NUMERICAL RESOLUTION OF NAVIER-STOKES EQUATIONS USING SEVERAL TURBULENCE MODELS AND APPLICATIONS ON TURBOMACHINES Final Report [RESOLUTION NUMERIQUE DES EQUATIONS DE NAVIER-STOKES AVEC PLUSIEURS MODELES DE TURBULENCE ET APPLICATIONS AUX TURBOMACHINES, RAPPORT FINAL]
J. Massines Sep. 1989 84 p In FRENCH
(Contract DRET-88-1457)
(ETN-90-97478) Avail: NTIS HC A05/MF A01

A method for calculating the aerodynamic field at the convergence region of turbomachine exhaustion jets and their emission in the atmosphere is presented. The phenomenon is mainly turbulent and the flow is disturbed by compressibility effects. In the model, the influence of viscosity, thermal conductivity and flow compressibility are taken into account. A two dimensional pseudo-steady code is used. The numerical scheme, based on the Ni finite volume method and multigrid method, is described. ESA

N90-28809# Laboratoire d'Informatique pour la Mecanique et les Sciences de l'Ingenieur, Paris (France).
VORTICE-PROPELLER INTERACTION Final Report
Alain Hemon and Serge Huberson Aug. 1989 76 p In FRENCH; ENGLISH summary
(Contract DRET-86-176)
(LIMSI-89-9; ETN-90-97485) Avail: NTIS HC A05/MF A01

The interactions between a ship's propeller blades and the boundary layer created by the ship are investigated. A finite element calculation method based on Navier-Stokes equation is developed. The application of an k-epsilon turbulence model for improving the analysis is considered. The flow azimuthal homogenization hypothesis is applied and leads to an accurate evaluation of the propeller performances. The unsteady effects generated by the interaction between the propeller blades and the vortices are analyzed. ESA

N90-28810# Institut de Mecanique des Fluides de Toulouse (France). Equipe Transferts en Ecoulements Laminaires et Turbulents.
DEVELOPMENT OF TURBULENCE MODELS FOR THE ANALYSIS OF COMPRESSIBLE OR INCOMPRESSIBLE UNSTEADY FLOW Final Report [LE DEVELOPPEMENT DE MODELES DE TURBULENCE ADAPTES AUX ECOULEMENTS INSTATIONNAIRES INCOMPRESSIBLES OU COMPRESSIBLES, RAPPORT DE SYNTHESE]
H. C. Boisson, M. Braza, P. Chassaing, H. HaMinh, A. Kourta, J.

Meyer, and A. Sevrain Jun. 1989 161 p In FRENCH
(Contract DRET-87-131)
(ETN-90-97486) Avail: NTIS HC A08/MF A01

The results of the investigations performed on the project for the development of turbulence models are summarized. Classical models of turbulence were developed and adapted to complex flow configurations. Models based on one-point schemes, numerical simulation of the aerodynamics around airfoils and a three dimensional analysis of the interaction of the turbulent flow shock and boundary layers are established. The characteristics of the flow transitions around a cylinder and in the layer in the planar neighborhood of a planar jet are analyzed. ESA

N90-28811# Aeronautical Research Inst. of Sweden, Stockholm. Dept. of Aerodynamics.
EXTRAPOLATION PROCEDURES AT OUTFLOW BOUNDARIES FOR THE NAVIER-STOKES EQUATIONS
Bertil Gustafsson (Uppsala Univ., Sweden) and Jan Nordstroem May 1990 21 p
(Contracts ANE-2/87-Step2; FMV-88260-88-203-73-001; STU-89/90)
(FFA-TN-1990-23; ETN-90-97514) Avail: NTIS HC A03/MF A01

A very common procedure when constructing boundary conditions at artificial boundaries is to extrapolate the solution from gridpoints near the boundary to the boundary itself. In general one cannot expect accurate solutions by this procedure but in the special case where there are large gradients tangential to the boundary, it is shown that extrapolation methods can be used. For example, if the subsonic part of the flow at an outflow boundary is contained in the boundary layer, then extrapolation of all variables can be used for the Navier-Stokes equations. ESA

N90-28812# Deutsche Forschungsanstalt fuer Luft- und Raumfahrt, Goettingen (Germany, F.R.). Abt. fuer Numerische Stroemungsmechanik.
DESIGN OF AN AXISYMMETRIC, CONTOURED NOZZLE FOR THE HEG
Klaus Hannemann 1990 73 p
(DLR-FB-90-04; ISSN-0171-1342; ETN-90-97543) Avail: NTIS HC A04/MF A01; DLR, VB-PL-DO, Postfach 90 60 58, 5000 Cologne, Fed. Republic of Germany, HC 28 DM

An axisymmetric contoured nozzle is designed for the High Entalpy wind tunnel Gottingen (HEG), Germany, Fed. Republic of Germany. In the first, conical part of the expansion, the flow is calculated using a quasi one dimensional approximation, taking into account finite rate chemical kinetics. Assuming a source flow and species freezing at the end of the conical section, the contoured part of the nozzle contour is subsequently determined using the method of characteristics for a perfect gas. The physical nozzle contour is finally obtained by adding the boundary layer displacement thickness, calculated by using an empirical correlation, to the inviscid contour. In addition to the discussion of the performance at off-design conditions, different chemical models and rate constants are used in the quasi one dimensional calculations in order to investigate the influence on the flow properties. ESA

N90-28813# Purdue Univ., West Lafayette, IN. School of Mechanical Engineering.
RADIATIVE HEAT TRANSFER Final Report, Jan. 1987 - Mar. 1990
K. S. Chapman, S. Ramadhyani, H. Ramamurthy, and R. Viskanta Apr. 1990 169 p
(Contract GRI-5086-260-1293)
(PB90-247602; GRI-90/0133) Avail: NTIS HC A08/MF A01 CSCL 20D

One and two-dimensional mathematical models have been developed to predict the steady state thermal performance and combustion characteristics of a natural gas-fired straight-through radiant tube. The effects of burner geometry, equivalence ratio, and preheat temperature and fuel firing rate on fuel burn-up have been investigated. The one-dimensional models for straight-through and single-ended recuperative radiant tubes have been validated using available experimental data. Thermal system models have been developed for the continuous and batch indirectly fired (radiant tube) furnaces to identify opportunities for fuel savings and enhanced productivity. Extensive parametric investigations were performed to examine the effects of load and refractory emissivities, load throughput rate and thickness on the thermal performance of the furnaces. Batch and continuous direct-fired furnace thermal system models were developed to analyze the effect of various design and operation parameters on the furnace thermal performance. An attempt was made to validate the batch furnace model by using experimental data from a small experimental furnace. Due to the size of the furnace, the two-dimensional heat conduction effects near the corners and edges of the furnace walls were significant. Since the effects were neglected in the system model, which is intended to simulate a large industrial furnace, the validation was unsuccessful. The parametric study consisted of examining the effect of the load and refractory emissivities and other operating and load parameters on the thermal performance of the batch and continuous furnaces. GRA

N90-28814*# Institute for Computer Applications in Science and Engineering, Hampton, VA.
A HYBRID PERTURBATION-GALERKIN TECHNIQUE FOR PARTIAL DIFFERENTIAL EQUATIONS Final Report
James F. Geer and Carl M. Anderson (College of William and Mary, Williamsburg, VA.) Aug. 1990 30 p Submitted for publication
(Contract NAS1-18605)
(NASA-CR-182085; ICASE-90-57; NAS 1.26:182085) Avail: NTIS HC A03/MF A01 CSCL 20D

A two-step hybrid perturbation-Galerkin technique for improving the usefulness of perturbation solutions to partial differential equations which contain a parameter is presented and discussed. In the first step of the method, the leading terms in the asymptotic expansion(s) of the solution about one or more values of the perturbation parameter are obtained using standard perturbation methods. In the second step, the perturbation functions obtained in the first step are used as trial functions in a Bubnov-Galerkin approximation. This semi-analytical, semi-numerical hybrid technique appears to overcome some of the drawbacks of the perturbation and Galerkin methods when they aree applied by themselves, while combining some of the good features of each. The technique is illustrated first by a simple example. It is then applied to the problem of determining the flow of a slightly compressible fluid past a circular cylinder and to the problem of determining the shape of a free surface due to a sink above the surface. Solutions obtained by the hybrid method are compared with other approximate solutions, and its possible application to certain problems associated with domain decomposition is discussed. Author

N90-28815*# National Aeronautics and Space Administration. Hugh L. Dryden Flight Research Facility, Edwards, CA.
REAL-TIME AERODYNAMIC HEATING AND SURFACE TEMPERATURE CALCULATIONS FOR HYPERSONIC FLIGHT SIMULATION
Robert D. Quinn and Leslie Gong Washington Aug. 1990 44 p
(NASA-TM-4222; H-1602; NAS 1.15:4222) Avail: NTIS HC A03/MF A01 CSCL 20D

A real-time heating algorithm was derived and installed on the Ames Research Center Dryden Flight Research Facility real-time flight simulator. This program can calculate two- and three-dimensional stagnation point surface heating rates and surface temperatures. The two-dimensional calculations can be made with or without leading-edge sweep. In addition, upper and lower surface heating rates and surface temperatures for flat plates, wedges, and cones can be calculated. Laminar or turbulent heating can be calculated, with boundary-layer transition made a function of free-stream Reynolds number and free-stream Mach number. Real-time heating rates and surface temperatures calculated for a generic hypersonic vehicle are presented and compared with more

exact values computed by a batch aeroheating program. As these comparisons show, the heating algorithm used on the flight simulator calculates surface heating rates and temperatures well within the accuracy required to evaluate flight profiles for acceptable heating trajectories. Author

N90-28816*# Institute for Computer Applications in Science and Engineering, Hampton, VA.
AN INVESTIGATION OF CHAOTIC KOLMOGOROV FLOWS Final Report
N. Platt, L. Sirovich, and N. Fitzmaurice (Case Western Reserve Univ., Cleveland, OH.) Aug. 1990 77 p Submitted for publication
(Contract NAS1-18605)
(NASA-CR-182079; ICASE-90-50; NAS 1.26:182079) Avail: NTIS HC A05/MF A01 CSCL 20D

A two dimensional flow governed by the incompressible Navier-Stokes equations with a steady spatially periodic forcing (known as the Kolmogorov flow) is numerically simulated. The behavior of the flow and its transition states as the Reynolds number (Re) varies is investigated in detail, as well as a number of the flow features. A sequence of bifurcations is shown to take place in the flow as Re varied. Two main regimes of the flow were observed: small and large scale structure regimes corresponding to different ranges of Re. Each of the regimes includes a number of quasiperiodic, chaotic, and relaminarization windows. In addition, each range contains a chaotic window with non-ergodic chaotic attractors. Spatially disordered, but temporally steady states were discovered in large scale structure regime. Features of the diverse cases are displayed in terms of the temporal power spectrum, Poincare sections and, where possible, Lyapunov exponents and Kaplan-Yorke dimension. Author

N90-28817# California Inst. of Tech., Pasadena. Graduate Aeronautical Labs.
STUDIES OF VORTEX INTERACTIONS Final Report, 1 Aug. 1984 - 31 Dec. 1989
Anatol Roshko and Theodore vonKarman 26 Jun. 1990 3 p
(Contract N00014-84-C-0618)
(AD-A223864) Avail: NTIS HC A01/MF A01 CSCL 20/4

Work accomplished under this contract includes the following: (1) The X-Y Tow Tank Facility was designed and constructed, and (2) Experimental techniques developed for flow visualization in the Tow Tank included improvement in laser-induced fluorescence and particle-streakline techniques. It was found that, for an oscillating body, it is the acceleration phase of the body's motion in each half cycle that synchronizes the vortex formation, and thereby influences both the magnitude and phase of the forces on the body (which are of central importance to flow-induced vibration). It was demonstrated how flows with truly two-dimensional parallel shedding can be achieved, which can now be directly compared with the many 2-D numerical simulations presently being carried out. It was shown that the transition to three-dimensionality in the cylinder wake involves two stages, each of which is associated with a discontinuous change in the mode of vortex formation (corresponding with different scales of streamwise vorticity). GRA

N90-28818# Naval Postgraduate School, Monterey, CA.
EFFECT OF VORTEX CIRCULATION ON INJECTANT FROM A SINGLE FILM-COOLING HOLE AND A ROW OF FILM-COOLING HOLES IN A TURBULENT BOUNDARY LAYER. PART 2: INJECTION BENEATH THE VORTEX UPWASH M.S. Thesis
Pisut Kaisuwan Dec. 1989 182 p
(AD-A223894) Avail: NTIS HC A09/MF A01 CSCL 20/13

Results are presented which illustrate the effects of single embedded longitudinal vortices on heat transfer and injectant downstream of a row of film cooling holes and downstream of a single hole in a turbulent boundary layer. Changes resulting from circulation magnitudes of the vortices are varied from 0.0 to 0.144 sq m/s are examined. Mean temperature results are presented which show how the injectant is distorted and redistributed by vortices, along with heat transfer measurements and mean velocity surveys. Injection hole diameter is 0.952 cm to give a ratio of vortex core diameter to hole diameter of about 1.5 to 1.6. Freestream velocity is maintained at 10 m/s, and the blowing ratio is approx. 0.5. Film cooling holes are oriented 30 deg with respect to the test surface. Stanton numbers are measured on a constant heat flux surface with a nondimensional temperature parameter of about 1.5. The situation studied is one where the middle injection hole is beneath the vortex upwash. For all results, vortex centers pass well within 2.9 vortex core diameters of the middle injection hole. To quantify influences of the vortices on the injectant, the parameter S is introduced, defined as the ratio of vortex circulation to injection hole diameter times mean injection velocity. The perturbation to film injectant and local heat transfer is determined by the magnitude of S. When S is greater than 1.0 to 1.5, injectant is swept into the vortex upwash and above the vortex core by secondary flows, and Stanton number data show evidence of injectant beneath the vortex core and downwash near the wall. GRA

N90-28819# Naval Postgraduate School, Monterey, CA. Dept. of Aeronautics and Astronautics.
EFFECTS OF FLOWFIELD TURBULENCE ON ASYMMETRIC VORTICES OVER A SLENDER BODY M.S. Thesis
James A. Pinaire, Jr. Dec. 1989 103 p
(AD-A224139) Avail: NTIS HC A06/MF A01 CSCL 16/2

The flowfield about a vertically-launched surface-to-air missile model at an angle of attack of 50 degrees and a Reynolds number 110000 was investigated in a low-speed wind tunnel at the Naval Postgraduate School. The location and intensity of the asymmetric vortices in the wake of the missile model were determined and the vortices were displayed using planar velocity vector, total pressure coefficient, and vorticity plots. The model configuration tested was a body-only configuration (wings, strakes, and tails removed). Two flowfield conditions were treated: the nominal ambient wind tunnel condition and grid-generated turbulence condition. Flow visualization was conducted and video-taped for both the body-only and winged configurations. The following conclusions were reached: (1) the addition of turbulence decreased the vorticity but did not significantly change the patterns of the plots; (2) the addition of turbulence reduced the vorticity more at eleven body diameters than at six diameters; (3) compared to the body-only case, the vorticity is reduced for the x case but not for the plus case for the turbulence condition; and (4) flow visualization verified vortices movement away from the missiles as the tested point was moved aft along the missile body. GRA

N90-28820*# National Aeronautics and Space Administration. Hugh L. Dryden Flight Research Facility, Edwards, CA.
IN-FLIGHT INVESTIGATION OF SHUTTLE TILE PRESSURE ORIFICE INSTALLATIONS
Timothy R. Moes and Robert R. Meyer, Jr. Washington Sep. 1990 38 p
(NASA-TM-4219; H-1575; NAS 1.15:4219) Avail: NTIS HC A03/MF A01 CSCL 20D

To determine shuttle orbiter wing loads during ascent, wing load instrumentation was added to Columbia (OV-102). This instrumentation included strain gages and pressure orifices on the wing. The loads derived from wing pressure measurements taken during STS 61-C did not agree with those derived from strain gage measurements or with the loads predicted from the aerodynamic database. Anomalies in the surface immediately surrounding the pressure orifices in the thermal protection system (TPS) tiles were one possible cause of errors in the loads derived from wing pressure measurements. These surface anomalies were caused by a ceramic filler material which was installed around the pressure tubing. The filler material allowed slight movement of the TPS tile and pressure tube as the airframe flexed and bent under aerodynamic loads during ascent and descent. Postflight inspection revealed that this filler material had protruded from or receeded beneath the surface, causing the orifice to lose its flushness. Flight tests were conducted at NASA Ames Research Center Dryden Flight Research Facility to determine the effects of

any anomaly in surface flushness of the orifice installation on the measured pressures at Mach numbers between 0.6 and 1.4. An F-104 aircraft with a flight test fixture mounted beneath the fuselage was used for these flights. Surface flushness anomalies typical of those on the orbiter after flight (STA 61-C) were tested. Also, cases with excessive protrusion and recession of the filler material were tested. This report shows that the anomalies in STS 61-C orifice installations adversely affected the pressure measurements. But the magnitude of the affect was not great enough to account for the discrepancies with the strain gage measurements and the aerodynamic predictions. Author

N90-29161# European Space Agency, Paris (France).
NUMERIC FLUID MECHANICS
Herbert Oertel (Deutsche Forschungsanstalt fuer Luft- und Raumfahrt, Cologne, Germany, F.R.) *In its* Scientific Colloquium in Honor of Prof. Dr. Rer. Nat. Hermann L. Jordan May 1990 p 45-68 Transl. into ENGLISH from Wissenschaftliches Kolloquim Gewidmet Herrn Professor Dr. Rer. Nat. Hermann L. Jordan zum 65 Geburtstag (Cologne, Fed. Republic of Germany, DFVLR), Jun. 1987 p 37-55 Original language document was announced as N88-17434 (For primary document see N90-29159 23-70)
Avail: NTIS HC A06/MF A01

35 INSTRUMENTATION AND PHOTOGRAPHY

Includes remote sensors; measuring instruments and gages; detectors; cameras and photographic supplies; and holography.

For aerial photography see *43 Earth Resources and Remote Sensing*. For related information see also *06 Aircraft Instrumentation*, and *19 Spacecraft Instrumentation*.

N90-28821# Aeronautical Research Labs., Melbourne (Australia).
A MICROPROCESSOR CONTROLLED STRAIN GAUGE CALIBRATION MODULE
J. F. Harvey, C. W. Sutton, and F. J. Bird Feb. 1989 39 p
(AR-005-579; ARL-Flight-Mech-TM-2) Avail: NTIS HC A03/MF A01

The electronics module is described which interfaces the recently developed strain gauge balance calibrating machine with the low speed wind tunnel data acquisition and control computer system. Author

N90-28822# National Inst. of Standards and Technology, Gaithersburg, MD. Electrosystems Div.
SPECIAL TEST AND EVALUATION METHODS USED FOR A NINE-AXIS ACCELEROMETER
John D. Ramboz Oct. 1989 39 p
(Contract DOT-HS-9-02193IA)
(PB90-209578; NISTIR-89/4195) Avail: NTIS HC A03/MF A01 CSCL 14B

The test methods used to characterize and evaluate the performance of a miniature nine-axis accelerometer are discussed. A special transducer containing nine separate linear accelerometers was examined. The intended application for this type of device is to derive angular acceleration data for dynamic head motion measurements relating to automobile crash studies. The accelerometers, amplifiers, multiplexer, frequency modulation telemetry transmitter and power supply are all to be molded into an athletic orthodontic mouthpiece and data will be obtained from measurements taken from boxer's head motions. The transducer parameters tested include axial and transverse linear vibration sensitivities, equivalent acceleration noise, effects of power supply voltage variations, and mouthpiece vibration transmissibility. Special test apparatus described includes a dual centrifuge and a dual spinaxis rate-table. Test philosophy and some test results are used to illustrate how apparently conflicting test results can be used to explain transducer performance under test conditions of combined environments. GRA

N90-28823# Naval Research Lab., Washington, DC. Beam Physics Branch.
MODE COMPETITION IN THE QUASIOPTICAL GYROTRON
S. Riyopoulos (Science Applications International Corp., McLean, VA.) and A. W. Fliflet 30 May 1990 63 p Sponsored in part by ONR
(Contract DE-AL05-83ER-52092)
(AD-A222181; NRL-MR-6532) Avail: NTIS HC A04/MF A01 CSCL 20/10

A set of equations describing the nonlinear multimode dynamics in the Quasioptical Gyrotron is derived. These equations, involving the slow amplitude and phase variation for each mode, result from an expansion of the nonlinear induced current up to fifth order in the wave amplitude. The interaction among various modes is mediated by coupling coefficients, of known analytic dependence on the normalized current 1, the interaction length mu, and the frequency detunings delta(sub i) corresponding to the competing frequencies omega(sub 1). The particular case when the modes form triads with frequencies omega(sub 1) + omega(sub 3) - 2 omega(sub 2) approximately = 0 is examined in more detail. The equations are quite general and can be used to study mode competition, the existence of a final steady state, its stability, as well as its accessibility from given initial conditions. It is shown that when mu/beta perp. is much greater than 1, mu can be eliminated as an independent parameter. The control space is then reduced to a new normalized current 1 and the desynchronism parameters nu(i) = delta(sub i) mu for the interacting frequencies. Each coupling coefficient G(sub ij) is written as G(sub ij) = I S(sub ij) G(sub ij) (nu sub i, nu sub j), where the nonlineer filling factor S(sub ij), carrying the information of the beam current spatial profile, can be computed independently. Therefore, it suffices to compute table of G(sub ij) as functions of nu(sub 1), nu (sub 2), and nu (sub 3) once to cover the parameter space. Results for a cold beam are presented here. GRA

N90-28824# California Univ., Berkeley. Lawrence Berkeley Lab. Center for Advanced Materials.
RHEOMETER STRAIN AND STRAIN-RATE ERRORS
D. W. Giles and M. M. Denn May 1990 4 p Presented at the Golden Jubilee Meeting of the British Society of Rheology and 3rd European Rheology Conference, Edinburgh, Scotland, 3-7 Sep. 1990 Prepared in cooperation with California Univ., Berkeley
(Contract DE-AC03-76SF-00098)
(DE90-013845; LBL-29040; CONF-9009209-1) Avail: NTIS HC A01/MF A01

Systematic errors were found which can affect measured rheological properties in the instrumentation of two commercial rheometers. Users of commercial instrumentation should establish the extent to which these and similar errors may exist in their systems. DOE

N90-28825*# Virginia Polytechnic Inst. and State Univ., Blacksburg. Fiber and Electro-Optics Research Center.
NONCONTACT MEASUREMENT OF HIGH TEMPERATURE USING OPTICAL FIBER SENSORS Final Report
R. O. Claus [1990] 95 p
(Grant NAG1-831)
(NASA-CR-186975; NAS 1.26:186975) Avail: NTIS HC A05/MF A01 CSCL 14B

The primary goal of this research program was the investigation and application of noncontact temperature measurement techniques using optical techniques and optical fiber methods. In particular, a pyrometer utilizing an infrared optical light pipe and a multiwavelength filtering approach was designed, revised, and tested. This work was motivated by the need to measure the temperatures of small metallic pellets (approximately 3 mm diameter) in free fall at the Microgravity Materials Processing Drop Tube at NASA Marshall Space Flight Center. In addition, research under this program investigated the adaptation of holography technology to optical fiber sensors, and also examined the use of rare-earth dopants in optical fibers for use in measuring temperature. The pyrometer development effort involved both theoretical analysis and experimental tests. For the analysis, a

mathematical model based on radiative transfer principles was derived. Key parameter values representative of the drop tube system, such as particle size, tube diameter and length, and particle temperature, were used to determine an estimate of the radiant flux that will be incident on the face of an optical fiber or light pipe used to collect radiation from the incandescent falling particle. An extension of this work examined the advantage of inclining or tilting the collecting fiber to increase the time that the falling particle remains in the fiber field-of-view. Those results indicate that increases in total power collected of about 15 percent may be realized by tilting the fiber. In order to determine the suitability of alternative light pipes and optical fibers, and experimental set-up for measuring the transmittance and insertion loss of infrared fibers considered for use in the pyrometer was assembled. A zirconium fluoride optical fiber and several bundles of hollow core fiber of varying diameters were tested. A prototype two-color pyrometer was assembled and tested at Virginia Tech, and then tested on the Drop Tube at Marshall Space Flight Center. Radiation from 5 mm diameter niobium drops falling in the Drop Tube was successfully detected, and recorded for later analysis. Subsequent analysis indicated that the imaging of light output from the light pipe onto the detector active areas was not identical for both detectors. Author

N90-28826# Oak Ridge National Lab., TN. Health and Safety Research Div.
CONCEPT FOR A NEUTRON SPECTROMETER BASED ON OPTICAL DETECTION OF (3)He(n, p)-3H REACTIONS IN A GAS
J. E. Turner, R. N. Hamm, H. A. Wright, G. S. Hurst, T. E. Huston, and W. A. Gibson (Pellissippi International, Knoxville, TN.) Jun. 1990 29 p
(Contract DE-AC05-84OR-21400)
(DE90-014776; ORNL/TM-11531) Avail: NTIS HC A03/MF A01

The conceptual framework is described for a new type of neutron spectrometer, based on the recently demonstrated principle of optical detection of charged-particle tracks in a gas. Whereas the elastic scattering of a neutron gives rise to the single track of a charged recoil particle, the reaction He-3(n,p)H-3 produces an event in which two tracks (those of the proton and triton) diverge from a common vertex at the capture site. The optical detection method, which allows direct visualization of tracks, could be used to distinguish between one- or two-pronged events. The measured total light output from an absorption event would be proportional to T(sub p) + T(sub t), the sum of the initial kinetic energies of the proton and triton. Independently of its incident direction, the energy of the absorbed neutron would be given by T = T(sub p) + T(sub t) - Q, where Q = 765 keV is the energy released by the reaction. DOE

N90-28827*# National Aeronautics and Space Administration. Lewis Research Center, Cleveland, OH.
FREQUENCY RESPONSE OF A THERMOCOUPLE WIRE: EFFECTS OF AXIAL CONDUCTION Progress Report, Apr. - Sep. 1990
L. J. Forney (Georgia Inst. of Tech., Atlanta.) and G. C. Fralick Sep. 1990 40 p
(Contract NCC3-135)
(NASA-CR-180454; NAS 1.26:180454; E19-666-1) Avail: NTIS HC A03/MF A01 CSCL 14B

Theoretical expressions are derived for the steady-state frequency response of a thermocouple wire. In particular, the effects of axial heat conduction are demonstrated for both a uniform thermocouple wire and a nonuniform wire with unequal material properties and wire diameters across the junction. For the case of a uniform wire, the amplitude ratio and phase angle compare favorably with the series solution of Scadron and Warshawsky (1952) except near the ends of the wire. For the case of a non-uniform wire, the amplitude ratio at low frequency omega yields 0 agrees with the results of Scadron and Warshawsky for a steady-state temperature distribution. Moreover, the frequency response for a non-uniform wire in the limit of infinite length I yields infinity is shown to reduce to a simple expression that is analogous to the classic first order solution for a thermocouple wire with uniform properties. Author

N90-28828# Kopin Corp., Taunton, MA.
SMART MICROSENSORS FOR HIGH TEMPERATURE APPLICATIONS, PHASE 1 Final Report, Aug. 1989 - Feb. 1990
Paul M. Zavracky 28 Jun. 1990 30 p
(Contract DAAL03-89-C-0024)
(AD-A224151; ARO-27323.1-SBI) Avail: NTIS HC A03/MF A01 CSCL 09/1

Microsensors find applications in many important areas of U.S. military hardware. Advances in aircraft and internal combustion engines are placing increasing demands on the electronics which play an increasingly important role in engine control. Complexity of control circuits has demanded increases in the scale of integration and in reliability, and have suggested the placement of high levels of functionality near the point of use. Engine performance must be evaluated with sensors and used intelligently to maintain optimum efficiency. Recent advances in microsensor technology have provided smaller, more economical sensors for these applications. With smaller sensors the need for signal conditioning electronics in close proximity to the sensor has become an increasingly important issue. The proposed three-phase project addresses the development of smart sensors for applications under high temperature ambients (up to 350 C). The approach proposed here is the demonstration of the usefulness of the SOI material obtained by the Isolated Silicon Epitaxy (ISE) process for high temperature sensor applications. This would couple with process development of sensor elements. GRA

36 LASERS AND MASERS

Includes parametric amplifiers.
For related information see also *76 Solid-State Physics*.

N90-28829# Rochester Univ., NY. Lab. for Laser Energetics.
LABORATORY FOR LASER ENERGETICS REVIEW Quarterly Report, Jan. - Mar. 1990
D. K. Bradley, ed. 1990 72 p
(Contract DE-FC03-85DP-40200)
(DE90-014666; DOE/DP-40200/124) Avail: NTIS HC A04/MF A01

This volume of the LLE Review contains a study of electron heat transport using two-dimensional Fokker-Planck simulations and an article describing how plastic microshells are being manufactured at LLE for future implosion studies. The advanced technology section reports on an experiment that has measured exponential gain in a number of x ray lasing transitions and discusses the continuing development of a 2-D high speed electro-optic probing system. Finally, the activities of the National Laser Users Facility and the GDL and OMEGA laser facilities are summarized. DOE

N90-28830# Los Alamos National Lab., NM.
THREE-DIMENSIONAL SIMULATIONS OF THE GENERATION OF ONE ANGSTROM RADIATION BY A SELF-AMPLIFIED SPONTANEOUS EMISSION FREE-ELECTRON LASER
J. C. Goldstein, C. J. Elliott, and M. J. Schmitt 1990 11 p
Presented at the Workshop on Propects for a One Angstrom Free Electron Laser, Sag Harbor, NY, 23-27 Apr. 1990
(Contract W-7405-eng-36)
(DE90-015032; LA-UR-90-2294; CONF-9004232-2) Avail: NTIS HC A03/MF A01

Three-dimensional numerical simulations of the generation of one Angstrom x rays by a free-electron laser operating in the self-amplified spontaneous emission mode have been performed. Using model electron beam and wiggler parameters, we have investigated the length of wiggler needed to just avoid bandwidth broadening effects associated with gain saturation, and we have also obtained requirements for wiggler field errors to avoid significant loss of performance. DOE

N90-28831# Lawrence Livermore National Lab., CA.
NEW RESONANTLY PHOTO-PUMPED X RAY LASER SCHEME
Joseph Nilsen 14 Jun. 1990 18 p Presented at the International Symposium on Short Wavelength Lasers and Their Applications, Samarkand, USSR, 14-18 May 1990 Submitted for publication
(Contract W-7405-eng-48)
(DE90-015044; UCRL-JC-104125; CONF-9005253-1) Avail: NTIS HC A03/MF A01

Over the last several years there has been tremendous progress in the development of x ray lasers. However, only two pumping mechanisms have been used to create gain and produce laser output, these have been collisional excitation, in the case of the Ne-like and Ni-like lasers, and recombination, in the case of the H-like and Li-like lasers. Other mechanisms such as photoionization and resonant photo-pumping have been proposed as possible candidates to build the x ray laser. However, the resonant photo-pumping mechanism has not yet been demonstrated in the soft x ray region. The shortest wavelength at which significant gain has been measured using resonant photo-pumping is at 2163 (angstrom) in Be-like C. This paper presents several new laboratory x ray laser schemes which show great promise based on resonant photo-pumping of Ne-like and Ni-like ions. DOE

N90-28832*# Physical Sciences, Inc., Alexandria, VA.
A LASER SPECTROMETER AND WAVEMETER FOR PULSED LASERS Final Report
J. A. McKay, P. M. Laufer, and L. J. Cotnoir Sep. 1989 34 p
(Contract NAS1-18243)
(NASA-CR-181731; NAS 1.26:181731; PSI-1011/TR-800) Avail: NTIS HC A03/MF A01 CSCL 20E

The design, construction, calibration, and evaluation of a pulsed laser wavemeter and spectral analyzer are described. This instrument, called the Laserscope for its oscilloscope-like display of laser spectral structure, was delivered to NASA Langley Research Center as a prototype of a laboratory instrument. The key component is a multibeam Fizeau wedge interferometer, providing high (0.2 pm) spectral resolution and a linear dispersion of spectral information, ideally suited to linear array photodiode detectors. Even operating alone, with the classic order-number ambiguity of interferometers unresolved, this optical element will provide a fast, real-time display of the spectral structure of a laser output. If precise wavelength information is also desired then additional stages must be provided to obtain a wavelength measurement within the order-number uncertainty, i.e., within the free spectral range of the Fizeau wedge interferometer. A Snyder (single-beam Fizeau) wedge is included to provide this initial wavelength measurement. Difficulties in achieving the required wide-spectrum calibration limit the usefulness of this function. Author

N90-28833*# National Aeronautics and Space Administration. Lewis Research Center, Cleveland, OH.
DESIGN OF A CO2 LASER POWER CONTROL SYSTEM FOR A SPACELAB MICROGRAVITY EXPERIMENT
Carl J. Wenzler and Dennis J. Eichenberg Aug. 1990 42 p
(NASA-TM-103112; E-5436; NAS 1.15:103112) Avail: NTIS HC A03/MF A01 CSCL 20E

The surface tension driven convection experiment (STDCE) is a Space Transportation System flight experiment manifested to fly aboard the USML-1 Spacelab mission. A CO2 laser is used to heat a spot on the surface of silicone oil contained inside a test chamber. Several CO2 laser control systems were evaluated and the selected system will be interfaced with the balance of the experimental hardware to constitute a working engineering model. Descriptions and a discussion of these various design approaches are presented. Author

N90-28834# Stanford Univ., CA. Lab. of Physics.
TUNABLE CW SINGLE-FREQUENCY SOURCE FOR INJECTION SEEDING 2-MICROMETER LASERS Final Technical Report, 1 Jul. - 31 Dec. 1988
Robert L. Byer Jun. 1990 63 p
(Contract N00014-88-K-0576)
(AD-A223979; GL-4697) Avail: NTIS HC A04/MF A01 CSCL 09/3

This program developed stable, single-frequency, continous-wave (CW) optical parametric oscillators (OPOs) for the application of injection seeding pulsed lasers. Progress has been made in the demonstration and performance characterization of a doubly resonant optical parametric oscillator (DROs) operating near degeneracy pumped by 532-nm CW radiation obtained from second harmonic generation of diode-array-pumped Nd:YAG lasers. It was observed that the OPO reproduced the coherence of the pump radiation with little additional noise. A detailed analysis of the tuning and control properties of the DRO helpful for development of active stabilization techniques has been completed. Design considerations for a 2-micron DRO based on this analysis are presented. Stabilization of the DRO requires synchronized control of at least three parameters; temperature, pump frequency, and applied potential for electro-optic tuning are considered. Research on this topic is continuingly motivated by the exceptional coherence and tuning properties of the OPO and applications involving optical frequency synthesis that will extend far beyond injection seeding. GRA

N90-28835# Illinois Univ., Urbana. Dept. of Electrical and Computer Engineering.
THE III-V SEMICONDUCTOR QUANTUM WELL LASERS AND RELATED OPTOELECTRONIC DEVICES ON SILICON
N. Holonyak, Jr., K. C. Hsieh, and G. E. Stillman Jun. 1990 30 p
(Contract DAAL03-89-K-0008)
(AD-A224120; ARO-26434.3-EL) Avail: NTIS HC A03/MF A01 CSCL 09/3

For some time interests have been aroused by the III-V quantum well heterostructures (QWHs) and superlattices (SLs) and, in addition to fundamental effects, the special opportunities QWHs and SLs afford in making possible improved forms of lasers, not to mention other devices and optoelectronic systems. In this report, studies have been made of: (1) Al(x)Ga(1-x)As-GaAs lasers on Si, (2) impurity induced layer disordering (which is an especially advantageous phenomenon in QWHs and SLs). (3) phonon-assisted laser operation and its unambiguous identification by control of the cavity Q of QWH samples, (4) the use of cavity Q to fill the recombination spectrum of QWHs, and (5) hydrolization and reliability of Al(x)Ga(1-x)As-GaAs QWHs and SLs, and (6) various other laser problems associated with higher gap crystals such as In(y)(Al(x)Ga(1-x)(1-y)P. GRA

37 MECHANICAL ENGINEERING

Includes auxiliary systems (nonpower); machine elements and processes; and mechanical equipment.

N90-28836# Dresser Industries, Inc., Waukesha, WI. Engine Div.
DEVELOPMENT OF ADVANCED COMBUSTION TECHNOLOGY FOR MEDIUM AND HIGH SPEED NATURAL GAS ENGINES Final Report, Jan. 1985 - Feb. 1989
W. E. Snyder Jul. 1989 414 p Prepared in cooperation with Ricardo Consulting Engineers Ltd., Shoreham-by-Sea, England
(Contract GRI-5084-243-0094)
(PB90-198565; GRI-89/0196) Avail: NTIS HC A18/MF A03 CSCL 21B

The project investigated the several variables which influence the performance of pre-chamber equipped, lean-burn natural gas engines in general, and of the pre-chamber in particular. The effort was divided into four closely inter-related phases: theoretical analysis, constant volume combustion (CVC) rig tests, single cylinder engine tests and multi-cylinder engine tests. The theoretical analysis was directed toward development of a computer program, called COGEN, which was then used to predict output performance trends resulting from changes to input parameters. The CVC Rig Test program was directed towards an improved understanding of

the pre-chamber combustion process using high speed photography and simultaneous measurement of instantaneous pressures. Variations of pre-chamber size, throat design and air-fuel ratio were studied to guide the later engine test programs. The Single Cylinder Engine Tests were directed towards bridging the gap between the CVC Test Rig and the performance to be expected from a commercial multi-cylinder engine. Variations in pre-chamber design as well as engine compression ratio, Intake Manifold Temperature and load were investigated. GRA

N90-28837# Ohio State Univ., Columbus. Dept. of Electrical Engineering.
MOTION COORDINATION FOR MOBILE ROBOTS IN UNSTRUCTURED ENVIRONMENTS
C. A. Klein Feb. 1990 39 p
(Grant NSF DMC-84-21321)
(PB90-199498; NSF/ENG-90001) Avail: NTIS HC A03/MF A01 CSCL 13I

The three main areas that are being pursued in order to advance the scientific database of technology to promote more advanced mobile manipulator systems are: posture optimization of the mobility and manipulation systems as a whole, taking into account the kinematic redundancy of the composite system; force allocation among the multiple actuators of such a system treating the closed kinematic chains properly and exploiting the mathematical dualism with the first problem; and obstacle avoidance of such a system in its workplace. Summaries of the sub-projects into which these topics have been divided, as well as abstracts of students' theses are included. GRA

N90-28838# Ohio State Univ., Columbus. Dept. of Electrical Engineering.
INVESTIGATION OF MAXIMUM ACHIEVABLE BODY TORQUE FOR A WALKING MACHINE WITH FRICTION CONE CONSTRAINTS M.S. Thesis
H. Hudiono Nov. 1989 143 p
(Grants NSF DMC-84-21321; MDA972-88-K-0003)
(PB90-203175; NSF/ENG-89058) Avail: NTIS HC A07/MF A01 CSCL 13I

Linear programming and the pseudoinverse methods are used to calculate the maximum body torque of a walking machine. An algorithm was developed to identify the torque polyhedron in the three dimensional torque space, which represents the maximum achievable body torques of the vehicle. The algorithm can accept other methods of computing maximum body torque, such as the gradient projection method. The thesis used the torque polyhedrons to analyze the effect of the input parameters on the torque performance of the vehicle. In general, the linear programming method can achieve larger body torque than the pseudoinverse method does at cost of long computing time. GRA

N90-28839# Ohio State Univ., Columbus. Dept. of Electrical Engineering.
MOTION COORDINATION FOR A MOBILE MANIPULATOR SYSTEM M.S. Thesis
A. C. Zeik Jan. 1989 132 p
(Grant NSF DDM-84-21321)
(PB90-203076; NSF/ENG-89056) Avail: NTIS HC A07/MF A01 CSCL 13I

In order for robotic systems to advance beyond the bounds of the traditional factory setting, mobility needs to be added. The combination of mobility and manipulation forms a kinematically redundant system that can be used to achieve secondary goals. The control of such a system is examined and its redundancy is used to satisfy a joint-range-availability secondary criterion. A Jacobian scaling technique is introduced which enables fast joint responses while still maintaining normalization between the joints. Although the results presented pertain to a mobile robot, they can also be applied to conventional robot arms. GRA

N90-28840# National Inst. of Standards and Technology, Gaithersburg, MD. Robot Systems Div.
DOE/NIST WORKSHOP ON COMMON ARCHITECTURES FOR ROBOTIC SYSTEMS Final Report
Richard Quintero, ed. Apr. 1990 156 p Workshop held in Gaithersburg, MD, 30-31 Jan. 1990 Sponsored by DOE, Washington, DC
(PB90-216839; NIST/SP-784) Avail: NTIS HC A08/MF A01; SOD HC $9.00 as 003-003-03001-5 CSCL 13I

At the request of the Department of Energy's (DOE's) Office of Technology Development the National Institute of Standards and Technology (NIST), Robot Systems Division organized and hosted the first DOE/National Institute of Standards and Technology (NIST) Workshop on common architectures for robotic systems. The workshop had three goals: An initial review of the methodologies currently used by the DOE sites for development and maintenance of software related to robotic and remote systems; presentations by representatives of other government agencies on lessons learned in the development of common architectures for robotic and remote systems; and a preliminary assessment of the methodology necessary to arrive at a DOE common architecture. Author

N90-28841# National Inst. of Standards and Technology, Gaithersburg, MD. Center for Building Technology.
COMPUTERIZATION OF WELDING DATA: PROCEEDINGS OF THE CONFERENCE AND WORKSHOP
T. A. Siewert, J. E. Jones, and H. G. Ziegenfuss Apr. 1990 47 p Conference held in New Orleans, LA, 19-21 Oct. 1988 Prepared in cooperation with American Welding Inst., Louisville, TN, and American Welding Society, Miami, FL
(PB90-219551; NST/SP-781) Avail: NTIS HC A03/MF A01; also available SOD HC $5.00 as 003-003-03006-6 CSCL 13I

The proceedings of an October 1988 conference on computerization of welding data are given. A written summary of each speaker's presentation is included in its appropriate conference session. Topics include an overview of computers and databases: databases for technology; a review of the 1986 workshop on computerization of welding information; on-line access to world-wide sources of materials performance data; ASM International's materials properties data system; application of artificial intelligence to welding; welding applications software: computerized software for welding engineers; computer applications in welding; welding case studies: update on procedure qualification records and welding procedure specifications; computers in welding; weld improvement program: weld and welder tracking system; and expert systems for diagnosing problems in welding power sources. GRA

N90-28842 Leeds Univ. (England).
SOME STUDIES OF THE VIBRATION WELDING OF THERMOPLASTICS Ph.D. Thesis
Stephen Mark Moody 1989 280 p
Avail: Univ. Microfilms Order No. BRD-88006

A study was performed on the mechanical and microstructural properties produced in vibration welded thermoplastics. The work has concentrated mainly upon two types of thermoplastics, polycarbonate which is amorphous and polypropylene which is semi-crystalline. Initially 6 mm thick sheets were welded using a range of welding parameters in order to determine optimum welding conditions. Weld qualities were assessed by the use of short term tests, such as tensile and impact tests, together with long term creep tests. Microstructural examinations were performed on the semi-crystalline thermoplastic welds using both optical and electron microscopy so that their mechanical properties could be related to their microstructures. Fracture studies were also performed on all the welded materials. The short term tests revealed that weld strengths equal to or greater than the parent material strength could be achieved in polycarbonate welds made using a range of welding conditions. On the other hand, good quality welds were difficult to make using polypropylene. An explanation was put forward for the reason why good quality welds can be made using

polycarbonate but not polypropylene in terms of differences in the microstructures and in the relaxation behavior of the two materials. Dissert. Abstr.

N90-28843 Ohio State Univ., Columbus.
DYNAMIC MODELING AND PAYLOAD-ADAPTATION CONTROL OF A FLEXIBLE ONE-LINK MANIPULATOR Ph.D. Thesis
Jian-Shiang Chen 1989 141 p
Avail: Univ. Microfilms Order No. DA9011142

The dynamic modeling and payload-adaptation of a flexible manipulator are described. Contributions are made in three areas: (1) Dynamic modeling: a dynamic model, including both structural flexibility and joint compliance, together with a spectral index for model reduction, is presented to obtain a lower order model for real-time application. The extension of this modeling scheme to multilink manipulators is indicated. (2) Payload adaptation: an on-line parameter identification scheme, which is based on an averaged gradient method, is presented to identify physical parameter(s) subject to variation, e.g., the payload. It is anticipated that this scheme will be less sensitive to unmodeled dynamics. (3) Experimental verification: a direct-drive flexible one-link manipulator is built to study the modeling scheme and the on-line identification scheme whn applied to a noncolocated system. Least-squares based identification schemes are also implemented for comparison. Two controller designs are implemented to explore the capability for rejecting load disturbances. Finally, an indirect self-tuning controller is implemented to investigate the payload-adaptability of this scheme. Dissert. Abstr.

N90-28844 California Univ., Los Angeles.
DYNAMIC INTERACTION OF MULTIPLE AUTONOMOUS MOBILE ROBOTS Ph.D. Thesis
Suck Gyu Lee 1990 159 p
Avail: Univ. Microfilms Order No. DA9014739

The global dynamic behavior of multiple autonomous mobile robots with simple navigation strategies is studied. Assuming that each robot has complete detectability with finite range, various navigation strategies are derived by introducing interactive forces between robots analogous to those between electric charges. Collision avoidance is ensured by introducing appropriate repulsive forces inversely related to the distance between objects. An analysis of the dynamic behavior of the interacting robots in both bounded and unbounded spatial domains are made. In navigation strategies of robots with vision, analytical and simulation results are obtained for two cases: (1) communication between robots is not permissible; and (2) communication between robots is maintained at all times. The convergence of robot motions to their goal states under certain conditions is established by considering their global dynamic behavior even when some objects (including domain boundaries) are close to their goal points. When the motions of robots are confined to move inside a bounded spatial domain, supercharges representing the domain boundary within the detectable range are introduced to simplify the navigation strategy. In this case, the rate of convergence to the goal state is studied by using pseudo-domain. Navigation strategies of a robot with tactile sensors for two situations are proposed: a robot with finite memory and a robot with infinite memory. A robot with finite memory navigates by selectively prioritizing its information on the surrounding environment based on a certain given criterion. Here, a robot stores the acquired information on a fixed number of pseudo-obstacles closest to its current positions, and uses this information for collision avoidance. The results of computer simulation studies on the dynamic behavior of multiple interacting robots with the proposed navigation strategies are given.
Dissert. Abstr.

N90-28845 Stanford Univ., CA.
EXPERIMENTS IN THE DYNAMIC AND STRATEGIC CONTROL OF COOPERATING MANIPULATORS Ph.D. Thesis
Stanley Aaron Schneider 1990 276 p
Avail: Univ. Microfilms Order No. DA9017925

This thesis comprises an experimental study of a semi-autonomous robotic system with multiple manipulators. Four topics are studied in detail: Hierarchical real-time system design, conceptual operator command, dynamic control of cooperative manipulators, and integrated real-time vision. The goal is to study simultaneously the dynamic and strategic issues of cooperative robotic manipulation. This work focuses not only on the various subsystems, but also on their interfaces and interactions. The system is structured as a four-level hierarchy. At the highest level, an iconic 'object-only' user interface allows an operator to direct the conceptual activities of the system. The operator commands only object motions; the arm actions required to effect these motions need not be specified. An event-driven tabular finite state machine provides strategic command. This technique encourages modular design of multi-process programs, provides an intuitive task programming environment, and naturally manages the concurrent system interactions. The dynamic controller implements 'object impedance control' - an extension of the impedance control concept to cooperative-arm manipulation of a single object. This controller presents an intuitive object behavior specification interface, and provides good dynamic performance both for free-motion positioning and environmental contact tasks. A real-time point-tracking two-dimensional vision system locates and tracks passive targets. Groups of targets can be identified and tracked as individual objects. The system can track multiple objects at 60 Hz with sub-millimeter resolution. The design was verified by experimental implementation: a multi-processor real-time computer controls a dual-arm planar manipulator system. Experimental results are presented, showing the system locating and identifying a moving object, catching it, and performing a simple cooperative assembly. These operations are controlled by a remote user entering only high-level conceptual object relations. Results from dynamic control experiments show excellent dynamic trajectory tracking performance, while also permitting control of environmental contact forces. Dissert. Abstr.

N90-28846 Minnesota Univ., Minneapolis.
SOLUTIONS TO THE FRICTIONAL DYNAMICS PROBLEM AND THE RECIPROCAL VARIABLE FEEDBACK METHODOLOGY FOR DESIGN AND CONTROL OF ROBOT MECHANISMS Ph.D. Thesis
Aristides Gogoussis 1989 412 p
Avail: Univ. Microfilms Order No. DA9014088

A rationale for incorporating friction into the robot dynamic equations based on three propositions has been developed and, subsequently, a general method was proposed for generating the equations of motion. Based on this method, an efficient algorithm was derived for solving the inverse robot dynamics problem including joint compliance, gyroscopic, and gravitational effects, as well as friction in the bearings and transmission mechanisms. Furthermore, a hybrid method for solving the forward robot dynamics problem in real-time was developed. Algebraic loops are resolved in the analog domain by exploiting the positive definiteness property of the inertia matrix of the dynamic equations of motion. A method for a digital solution to the forward robot dynamics problem was developed as well. The method is computationally efficient because it preserves the recursiveness of the inverse dynamics algorithm, which is used in the solution of the forward problem as part of a masking procedure that always converges. With respect to control, in order to overcome extensive computational requirements of control strategies based on inverse dynamics algorithms, the Reciprocal Variable Feedback method for design and control of robot mechanisms was developed.
Dissert. Abstr.

N90-28847# Environmental Protection Agency, Washington, DC. Office of Cooperative Environmental Management.
STUDY AND ANALYSIS OF LEAKING UNDERGROUND STORAGE TANK REMEDIATION TECHNIQUES INCORPORATED IN STATES IN EPA REGION 6 Final Report
E. Kennedy 23 May 1990 33 p
(PB90-214834; EPA/DF/DK-90/038A) Avail: NTIS HC A03/MF A01; aso avail. on diskette as PB90-502337 CSCL 13B

The intent of the research project was initially to determine the effectiveness of groundwater remediation techniques utilized within EPA Region VI for the cleanup of leaking underground storage tanks (LUST). It was concluded that effectiveness of groundwater remediation is primarily dependent on the choice of remediation parameters rather than the type of technique used. Furthermore, the choice of remediation parameters depends on the value of hydrogeologic parameters that characterize the site and are determined during the initial site assessment. GRA

N90-28848# Sandia National Labs., Albuquerque, NM.
USE OF ELECTRON SPECTROSCOPIES IN THE TRIBOLOGICAL EVALUATION OF DIAMOND FILMS
D. E. Peebles and L. E. Pope 1990 54 p Presented at the International Symposium on Industrial Tribology, Evanston, IL, 29-31 Aug. 1990
(Contract DE-AC04-76DP-00789; MIPR-FY1457-89-5004)
(DE90-014421; SAND-90-0186C; CONF-9008127-1) Avail: NTIS HC A04/MF A01

Diamond films hold a lot of promise as tribological protective coatings, especially for applications in harsh environments. However, thorough examinations of the mechanisms of film failure and wear must be completed in order to optimize the tribological performance of diamond films. In situ electron spectroscopic analysis has been very successfully applied to such studies for metal-metal wear systems and for systems involving several types of dry film lubricants. This work describes our application of these types of studies to protective diamond films on silicon. We have characterized the diamond films by selected techniques, including: Raman spectroscopy, Auger electron spectroscopy, x ray photoelectron spectroscopy, electron energy loss spectroscopy, and a specially developed charging probe technique. We have characterized the relative ability of each technique to discern film damage, while evaluating the conditions under which each technique may be used, including normal operations such as elastic peak optimization and sample imaging. Results are discussed for each technique which are representative of undamaged and damaged diamond bonding configurations. In addition, the effects of ion bombardment for cleaning and damaging the surface have been evaluated. Finally, applications of these techniques to studies of the tribology of 440C stainless steel pins on diamond films are discussed. These results show that in laboratory air, the observed friction coefficient is strongly correlated with the concentration of oxygen and the surface roughness in the wear track, with only a weak (if any) dependence on the type of carbon structure present (diamond versus graphite). DOE

N90-28849# Oak Ridge National Lab., TN.
INFLUENCE OF DIESEL ENGINE EXPOSURE ON THE RUPTURE STRENGTH OF SILICON NITRIDE AND PARTIALLY STABILIZED ZIRCONIA
C. R. Brinkman, G. M. Begun, R. L. Graves, W. K. Kahl, K. C. Liu, and B. H. West Jun. 1990 26 p
(Contract DE-AC05-84OR-21400)
(DE90-014759; ORNL-6612) Avail: NTIS HC A03/MF A01

Results are reported from studies in which several monolithic ceramic materials in the form of modulus-of-rupture bars were exposed for 100 h to the combustion conditions found in either a small single- or two-cylinder diesel engine. Fuels included a standard Phillips D-2 diesel or a synthetic mixture of the Phillips D-2 and an aromatic blend. The ceramics included two commercial grades of partially stabilized zirconia: (1) PSZ-TS, and (2) PSZ-MS and silicon nitride (GTE WESGO SNW-1000). Significant reductions in postexposure fracture strength occurred in the PSZ-TS material irrespective of whether it was exposed in the single- or two-cylinder engine. Only a small decrease in fracture strength occurred in the PSZ-MS material, and essentially no decrease in fracture strength occurred in the silicon nitride. DOE

N90-28850# Oak Ridge National Lab., TN. Engineering Physics and Mathematical Div.
TREATMENT OF SYSTEMATIC ERRORS 2: FUSION OF ULTRASOUND AND VISUAL SENSOR DATA
M. Beckerman, L. A. Farkas, and S. E. Johnston Jun. 1990 25 p
(Contract DE-AC05-84OR-21400)
(DE90-014780; ORNL/TM-11349; CESAR-89/38) Avail: NTIS HC A03/MF A01

In this work we present a methodology for the fusion of ultrasound and visual sensor data as acquired by a mobile robot. The objective of the methodology was the reduction of systematic errors which arise in the processing of the data in the individual sensor domains. In the initial processing of the ultrasound scan, rectilinear (Cartesian map) and polar (strings) data structures were built. In the initial processing of the CCD camera image, vertical edge segments were identified and labeled according to their connectivity. The systematic errors treated included ultrasound distortions in size, and visual ambiguities in discriminating depth discontinuities from intensity gradients generated by other details in the image. These systematic errors were first flagged by comparing the ultrasound strings and visual vertical edges to one another. The ranges, spatial orientation of the camera, and geometric information extracted from least-squares fits were then used in the fusion stage processing of the visual image. Vertical edge information was used in the subsequent fusion stage processing of the ultrasound data. By the end of this feedback-like fusion process the data structures in each sensor domain carried some information from the other domain. We had identified the vertical edges of interest, tagged them with range information, and removed the distortions from the Cartesian navigation maps. DOE

N90-28851# Oak Ridge National Lab., TN. Engineering Physics and Mathematics Div.
ROSES, A ROBOT OPERATING SYSTEM EXPERT SCHEDULER: METHODOLOGICAL FRAMEWORK
E. C. Halbert, J. Barhen, and P. C. Chen Aug. 1990 87 p
(Contract DE-AC05-84OR-21400)
(DE90-014782; ORNL/TM-9987) Avail: NTIS HC A05/MF A01

The optimal scheduling of tasks among which complex interrelationships (such as precedence constraints) may exist is essential for driving the new generation of concurrent supercomputers to their utmost performance. To address this need, the project ROSES (Robot Operating System Expert Scheduler) was initiated. The project, its method for optimizing schedules, and its implementing computer code are each called ROSES. The problem of finding optimum schedules is explosive in complexity (i.e., NP-complete). By combining heuristic techniques, graph-theoretic algorithms, and sophisticated data structures, ROSES achieves near optimal solutions in a highly efficient manner both with respect to computer time and memory space. The description of the methodology is followed by an overview of the ROSES computer code, including detailed outlines of selected algorithms. In addition, an application is described of ROSES to schedule inverse dynamics computations for a robot manipulator. DOE

N90-28852*# California Inst. of Tech., Pasadena. Div. of Engineering and Applied Science.
TURBOMACHINERY ROTOR FORCES Final Report, 30 Oct. 1978 - 30 Aug. 1988
Norbert Arndt Aug. 1988 18 p
(Contract NAS8-33108)
(NASA-CR-183779; NAS 1.26:183779; Rept-249.9) Avail: NTIS HC A03/MF A01 CSCL 13I

The fluid-induced forces, both steady and unsteady, acting upon an impeller of a centrifugal pump, and impeller blade-diffuser vane interaction in centrifugal pumps with vaned radial diffusers were evaluated experimentally and theoretically. Knowledge of the steady and unsteady forces, and the associated rotordynamic coefficients are required to effectively model the rotor dynamics of the High Pressure Fuel Turbopump (HPFTP) of the Space Shuttle Main Engine (SSME). These forces and rotordynamic coefficients were investigated using different impellers in combination with volutes and vaned diffusers, and axial inducers. These rotor forces are global. Local forces and pressures are also important in

impeller-diffuser interaction, for they may cause cavitation damage and even vane failures. Thus, in a separate investigation, impeller wake, and impeller blade and diffuser vane pressure measurements were made. The nature of the rotordynamic forces is discussed, the experimental facility is described, and the measurements of unsteady forces and pressure are reported together with a brief and incomplete attempt to calculate these flows. Author

N90-28853# Deutsche Forschungsanstalt fuer Luft- und Raumfahrt, Oberpfaffenhofen (Germany, F.R.). Abt. Mehrkoerperdynamik.

ON THE APPLICATION OF SIMILARITY LAWS TO A SCALED RAILWAY BOGIE MODEL Ph.D. Thesis - Technische Univ. Delft

Alfred Jaschinski 1990 166 p

(DLR-FB-90-06; ISSN-0171-1342; ETN-90-97544) Avail: NTIS HC A08/MF A01; DLR, VB-PL-DO, Postfach 90 60 58, 5000 Cologne, Fed. Republic of Germany, HC 21.50 DM

For a dicone moving on a pair of cylindrical rails the equations of motion are established. The frictions forces due to Kalker's theory of rolling contact are approximated by nonlinear functions. For this nonlinear system conditions for the dynamical similarity of a scaled and a full scale model are derived. The equations of motion are extended to a railway bogie model with two conical wheelsets. Numerical simulation results for the dicone as well as for the bogie model are obtained with a particular software taking into account the specific structure of the equations of motion. The simulation results are compared with experiments on a 1:5 scaled roller rig where the bogie model was designed with the aid of scaling factors for length, mass, inertia and suspension stiffness due to dynamical similarity laws. The results indicate that the nonlinear behavior of designs of railway running gears or even complete vehicles can be investigated in a wide range on a scaled test rig. ESA

N90-28854*# Michigan Univ., Ann Arbor. Robotics Research Lab.

TELE-AUTONOMOUS CONTROL INVOLVING CONTACT Final Report Thesis

Lejun Shao, Richard A. Volz, Lynn Conway, and Michael W. Walker 1 Mar. 1990 219 p Prepared in cooperation with Texas A&M Univ., College Station

(Grant NAG5-1024)

(NASA-CR-187004; NAS 1.26:187004) Avail: NTIS HC A10/MF A02 CSCL 13I

Object localization and its application in tele-autonomous systems are studied. Two object localization algorithms are presented together with the methods of extracting several important types of object features. The first algorithm is based on line-segment to line-segment matching. Line range sensors are used to extract line-segment features from an object. The extracted features are matched to corresponding model features to compute the location of the object. The inputs of the second algorithm are not limited only to the line features. Featured points (point to point matching) and featured unit direction vectors (vector to vector matching) can also be used as the inputs of the algorithm, and there is no upper limit on the number of the features inputed. The algorithm will allow the use of redundant features to find a better solution. The algorithm uses dual number quaternions to represent the position and orientation of an object and uses the least squares optimization method to find an optimal solution for the object's location. The advantage of using this representation is that the method solves for the location estimation by minimizing a single cost function associated with the sum of the orientation and position errors and thus has a better performance on the estimation, both in accuracy and speed, than that of other similar algorithms. The difficulties when the operator is controlling a remote robot to perform manipulation tasks are also discussed. The main problems facing the operator are time delays on the signal transmission and the uncertainties of the remote environment. How object localization techniques can be used together with other techniques such as predictor display and time desynchronization to help to overcome these difficulties are then discussed. Author

N90-28855*# North Carolina Univ., Charlotte. Dept. of Mechanical Engineering and Engineering Science.

MAGNETOSTRICTIVE DIRECT DRIVE MOTORS Semiannual Report, 1 Jan. - 30 Jun. 1990

Dipak Naik and P. H. DeHoff 1990 71 p

(Grant NAG5-1169)

(NASA-CR-186895; NAS 1.26:186895) Avail: NTIS HC A04/MF A01 CSCL 13I

Developing magnetostrictive direct drive research motors to power robot joints is discussed. These type motors are expected to produce extraordinary torque density, to be able to perform microradian incremental steps and to be self-braking and safe with the power off. Several types of motor designs have been attempted using magnetostrictive materials. One of the candidate approaches (the magnetostrictive roller drive) is described. The method in which the design will function is described as is the reason why this approach is inherently superior to the other approaches. Following this, the design will be modelled and its expected performance predicted. This particular candidate design is currently undergoing detailed engineering with prototype construction and testing scheduled for mid 1991. Author

N90-28618*# Spectra Research Systems, Inc., Huntsville, AL. Aerospace and Commercial Systems Directorate.

EVOLUTION AND USE OF COMBINED MECHANICAL AND THERMAL CODES FOR CRYOGENIC TURBOPUMP BEARINGS

Joe C. Cody, David E. Marty, and James D. Moore *In* NASA, Marshall Space Flight Center, Advanced Earth-to-Orbit Propulsion Technology 1988, Volume 1 Sep. 1988 p 88-101 (For primary document see N90-28611 23-20)

Avail: NTIS HC A99/MF E06 CSCL 13I

N90-28619*# Rockwell International Science Center, Thousand Oaks, CA.

DETERMINATION OF THE SSME HIGH PRESSURE OXIDIZER TURBOPUMP BEARING TEMPERATURE

Y. Naerheim, P. J. Stocker, and J. B. Lumsden *In* NASA, Marshall Space Flight Center, Advanced Earth-to-Orbit Propulsion Technology 1988, Volume 1 Sep. 1988 p 102-109 (For primary document see N90-28611 23-20)

(Contract NAS8-4000)

Avail: NTIS HC A99/MF E06 CSCL 13I

N90-28620*# National Aeronautics and Space Administration. Marshall Space Flight Center, Huntsville, AL.

CRYOGENIC, HIGH SPEED, TURBOPUMP BEARING COOLING REQUIREMENTS

Fred J. Dolan, Howard G. Gibson, James L. Cannon, and Joe C. Cody (Spectra Research Systems, Inc., Huntsville, AL.) *In its* Advanced Earth-to-Orbit Propulsion Technology 1988, Volume 1 Sep. 1988 p 110-141 (For primary document see N90-28611 23-20)

Avail: NTIS HC A99/MF E06 CSCL 13I

N90-28621*# Rockwell International Corp., Canoga Park, CA. Rocketdyne Div.

POOL BOILING FROM ROTATING AND STATIONARY SPHERES IN LIQUID NITROGEN

Winston M. Cuan and Sidney H. Schwartz *In* NASA, Marshall Space Flight Center, Advanced Earth-to-Orbit Propulsion Technology 1988, Volume 1 Sep. 1988 p 142-157 Previously announced in IAA as A88-48028 (For primary document see N90-28611 23-20)

(Contract NAS8-40000)

Avail: NTIS HC A99/MF E06 CSCL 13I

N90-28622*# National Aeronautics and Space Administration. Lewis Research Center, Cleveland, OH.

BEARING OPTIMIZATION FOR SSME HPOTP APPLICATION

Elizabeth S. Armstrong and Harold H. Coe *In* NASA, Marshall Space Flight Center, Advanced Earth-to-Orbit Propulsion Technology 1988, Volume 1 Sep. 1988 p 159-174 (For

primary document see N90-28611 23-20)
Avail: NTIS HC A99/MF E06 CSCL 13I

N90-28623*# Battelle Columbus Labs., OH.
DEVELOPMENT OF IMPROVED SELF LUBRICATING CAGES FOR SSME HPOTP BEARINGS
J. W. Kannel, K. F. Dufrane, S. A. Barber, and J. Gleeson *In* NASA, Marshall Space Flight Center, Advanced Earth-to-Orbit Propulsion Technology 1988, Volume 1 Sep. 1988 p 175-189 (For primary document see N90-28611 23-20)
Avail: NTIS HC A99/MF E06 CSCL 13I

N90-28624*# Pratt and Whitney Aircraft, West Palm Beach, FL. Government Engine Business.
PRATT AND WHITNEY CRYOGENIC TURBOPUMP BEARING EXPERIENCE
W. E. Poole and R. W. Bursey, Jr. *In* NASA, Marshall Space Flight Center, Advanced Earth-to-Orbit Propulsion Technology 1988, Volume 1 Sep. 1988 p 190-199 (For primary document see N90-28611 23-20)
Avail: NTIS HC A99/MF E06 CSCL 13I

N90-28625*# Battelle Columbus Labs., OH.
CAGE STABILITY ANALYSIS FOR SSME HPOTP BEARINGS
T. L. Merriman and J. W. Kannel *In* NASA, Marshall Space Flight Center, Advanced Earth-to-Orbit Propulsion Technology 1988, Volume 1 Sep. 1988 p 200-212 (For primary document see N90-28611 23-20)
Avail: NTIS HC A99/MF E06 CSCL 13I

N90-28626*# Rockwell International Corp., Canoga Park, CA. Rocketdyne Div.
ROCKETDYNE LOX BEARING TESTER PROGRAM
J. E. Keba and R. F. Beatty *In* NASA, Marshall Space Flight Center, Advanced Earth-to-Orbit Propulsion Technology 1988, Volume 1 Sep. 1988 p 213-229 (For primary document see N90-28611 23-20)
(Contract NAS8-4000)
Avail: NTIS HC A99/MF E06 CSCL 13I

N90-28656*# National Aeronautics and Space Administration. Marshall Space Flight Center, Huntsville, AL.
ROBOTIC AND AUTOMATIC WELDING DEVELOPMENT AT THE MARSHALL SPACE FLIGHT CENTER
C. S. Jones, M. E. Jackson, and L. A. Flanigan (Rockwell International Corp., Canoga Park, CA.) *In its* Advanced Earth-to-Orbit Propulsion Technology 1988, Volume 1 Sep. 1988 p 742-750 (For primary document see N90-28611 23-20)
Avail: NTIS HC A99/MF E06 CSCL 13H

N90-29027*# Carnegie-Mellon Univ., Pittsburgh, PA. Dept. of Mechanical Engineering.
PERIODIC GAITS FOR THE CMU AMBLER
Swaminathan Mahalingam and Suren N. Dwivedi (West Virginia Univ., Morgantown.) *In* JPL, California Inst. of Tech., Proceedings of the NASA Conference on Space Telerobotics, Volume 1 31 Jan. 1989 p 301-310 (For primary document see N90-29000 23-54)
(Grant NSF ROA-86-15072)
Avail: NTIS HC A21/MF A03 CSCL 13I

N90-29066*# Carnegie-Mellon Univ., Pittsburgh, PA. Robotics Inst.
FIRST RESULTS IN TERRAIN MAPPING FOR A ROVING PLANETARY EXPLORER
E. Krotkov, C. Caillas, M. Hebert, I. S. Kweon, and Takeo Kanade *In* JPL, California Inst. of Tech., Proceedings of the NASA Conference on Space Telerobotics, Volume 2 31 Jan. 1989 p 247-256 (For primary document see N90-29044 23-54)
(Grant NAGw-1175)
Avail: NTIS HC A17/MF A03 CSCL 13I

N90-29067*# National Aeronautics and Space Administration, Washington, DC.
PLANETARY ROVER TECHNOLOGY DEVELOPMENT REQUIREMENTS
Roger J. Bedard, Jr., Brian K. Muirhead (Jet Propulsion Lab., California Inst. of Tech., Pasadena.), Melvin D. Montemerlo, and Murray S. Hirschbein *In* JPL, California Inst. of Tech., Proceedings of the NASA Conference on Space Telerobotics, Volume 2 31 Jan. 1989 p 257-264 (For primary document see N90-29044 23-54)
Avail: NTIS HC A17/MF A03 CSCL 13I

N90-29068*# Rice Univ., Houston, TX. Dept. of Electrical and Computer Engineering.
RICE-OBOT 1: AN INTELLIGENT AUTONOMOUS MOBILE ROBOT
R. deFigueiredo, L. Ciscon, and D. Berberian *In* JPL, Californai Inst. of Tech., Proceedings of the NASA Conference on Space Telerobotics, Volume 2 31 Jan. 1989 p 265-274 Sponsored in part by Texas Instruments, Inc. (For primary document see N90-29044 23-54)
(Grant NAG9-208)
Avail: NTIS HC A17/MF A03 CSCL 13I

N90-29069*# Texas Univ., Austin. Dept. of Computer Science.
SATELLITE-MAP POSITION ESTIMATION FOR THE MARS ROVER
Akira Hayashi and Thomas Dean (Brown Univ., Providence, RI.) *In* JPL, California Inst. of Tech., Proceedings of the NASA Conference on Space Telerobotics, Volume 2 31 Jan. 1989 p 275-282 Sponsored in part by ARPA (For primary document see N90-29044 23-54)
(Contract F49620-88-C-0132; NSF IRI-86-12644)
Avail: NTIS HC A17/MF A03 CSCL 13I

N90-29070*# Martin Marietta Corp., Denver, CO. Astronautics Group.
ROBOTIC SAMPLING SYSTEM FOR AN UNMANNED MARS MISSION
Wendell Chun *In* JPL, California Inst. of Tech., Proceedings of the NASA Conference on Space Telerobotics, Volume 2 31 Jan. 1989 p 283-291 (For primary document see N90-29044 23-54)
(IR/D Proj. D-46S)
Avail: NTIS HC A17/MF A03 CSCL 13I

38 QUALITY ASSURANCE AND RELIABILITY

Includes product sampling procedures and techniques; and quality control.

N90-28856# National Inst. of Standards and Technology, Gaithersburg, MD. Center for Building Technology.
STUDY OF METEOROLOGICAL PROCESSES IMPORTANT IN THE DEGRADATION OF MATERIALS THROUGH SURFACE TEMPERATURE Final Report
S. C. Saunders, M. A. Jensen, and J. W. Martin Apr. 1990 47 p Prepared in cooperation with Scientific Consulting Services, Pullman, WA
(PB90-222720; NIST/TN-1275) Avail: NTIS HC A03/MF A01; also avail. SOD as 003-003-03005-8 HC $2.50 CSCL 14D

One of the greatest impediments in forecasting the service life of a material exposed outdoors is the uncontrolled and non-predictable nature of the ambient factors comprising its environment. This contributes to the difficulty of establishing the cause-and-effect relationship between these factors and the rate of material degradation. To surmount these difficulties it is necessary to characterize quantitatively each of the factors comprising the exposure environment which are thought to be important in the material's degradation. The selection and quantification of these factors must accommodate not only the

periodicity of the diurnal cycle but its statistical fluctuation. The objective of the research is to develop a general mathematical model, through Fourier analysis, characterizing the diurnal variation in the primary factor, material temperature. This factor is felt to be important in the degradation of a wide range of materials and protective systems, including coated steel panels. The steps taken and problems encountered in developing such a model are outlined. It is concluded that the simulated data generated from the model display virtually the same stochastic behavior as does the real data and that, if appropriate meteorological records are available, it will be possible to characterize and reproduce the statistical behavior for any locality, season and panel orientation. GRA

N90-28857# Allied-Signal Aerospace Co., Kansas City, MO.
QUALITY FUNCTION DEPLOYMENT AS A MECHANISM FOR PROCESS CHARACTERIZATION AND CONTROL Final Report
L. K. Gillespie, M. Maurer, L. Gillespie, J. Sims, and D. Ramos Jul. 1990 86 p
(Contract DE-AC04-76DP-00613)
(DE90-014755; KCP-613-4276) Avail: NTIS HC A05/MF A01

This study was initiated to determine how well quality function deployment (QFD) was suited for process characterization. The process chosen on which to test QFD was the mechanical process of flat lapping (flat sanding) metal parts to a specified flatness or finish. This is the first use of QFD at this facility. It is the first example seen of its use for generic process characterization. It is normally used to define product needs. DOE

N90-28858*# Massachusetts Inst. of Tech., Cambridge. Dept. of Mechanical Engineering.
ULTRASONIC VERIFICATION OF FIVE WAVE FRONTS IN UNIDIRECTIONAL GRAPHITE EPOXY COMPOSITE Final Report
Han-Song Seng and James H. Williams, Jr. Sep. 1990 55 p
(Grant NAG3-1105)
(NASA-CR-185288; NAS 1.26:185288) Avail: NTIS HC A04/MF A01 CSCL 14D

The existence of five different waves fronts in a unidirectional graphite fiber reinforced epoxy composite with energy flux propagation at the angle of 60 deg with respect to the fiber direction is verified by measuring their corresponding group and phase velocities of longitudinal and shear waves using the through transmission technique. The experimental and theoretical values of phase velocities show excellent agreement for all three modes of wave propagation. It is also verified that the maximum output voltage amplitude is obtained when the line joining the centers of the transmitting and receiving transducers is parallel to the energy propagation direction defined by the deviation angle. Author

39 STRUCTURAL MECHANICS

Includes structural element design and weight analysis; fatigue; and thermal stress.

For applications see *05 Aircraft Design, Testing and Performance* and *18 Spacecraft Design, Testing and Performance*.

N90-28859*# National Aeronautics and Space Administration. Langley Research Center, Hampton, VA.
BUCKLING AND POSTBUCKLING BEHAVIOR OF COMPRESSION-LOADED ISOTROPIC PLATES WITH CUTOUTS
Michael P. Nemeth Washington Sep. 1990 22 p Presented at the 31st AIAA/ASME/ASCE/AHS Structures, Structural Dynamics, and Materials Conference, Long Beach, CA, 2-4 Apr. 1990 Previously announced in IAA as A90-29311
(NASA-TP-3024; L-16789; NAS 1.60:3024) Avail: NTIS HC A03/MF A01 CSCL 20K

An experimental study of the buckling and postbuckling behavior of square and rectangular compression loaded aluminum plates with centrally located circular, square, and elliptical cutouts is presented. Experimental results indicate that the plates exhibit overall trends of increasing buckling strain and decreasing initial postbuckling stiffness with increasing cutout width. Corresponding plates with circular and square cutouts of the same width buckle at approximately the same strain level, and exhibit approximately the same initial postbuckling stiffness. Results show that the reduction in initial postbuckling stiffness due to a cutout generally decreases as the plate aspect ratio increases. Other results presented indicate that square plates with elliptical cutouts having a large cutout-width-to-plate-width ratio generally lose prebuckling and initial postbuckling stiffness as the cutout height increases. However, the plates buckle at essentially the same strain level. Results also indicate that postbuckling stiffness is more sensitive to changes in elliptical cutout height than are prebuckling stiffness and buckling strain. Author

N90-28860# Sydney Univ. (Australia). School of Civil and Mining Engineering.
FINITE ELEMENT ANALYSIS OF COUPLED THERMOELASTICITY
J. P. Carter and J. R. Booker May 1989 33 p
(PB90-201211; R-599) Avail: NTIS HC A03/MF A01 CSCL 20K

The governing equations for the fully coupled theory of thermoelasticity are developed and a method for solving these equations, based on the finite element technique, is proposed. The numerical method is used to obtain approximate solutions which are then compared with analytical solutions to a number of test problems. An assessment is also made of the importance of the full coupling. The use of the solution technique is further illustrated with some example problems from geotechnical engineering. GRA

N90-28861# Oak Ridge National Lab., TN. Metals and Ceramics Div.
MECHANICAL PROPERTIES TESTING OF DIAMOND AND DIAMOND-LIKE FILMS BY ULTRA-LOW LOAD INDENTATION
Michael E. OHern (Tennessee Univ., Knoxville.) and Carl J. McHargue 1990 8 p Presented at the NATO Advisory Study Inst. on Diamond and Diamond-Like Films, Castelvecchio Pascoli, Italy, 22 Jul. - 2 Aug. 1990
(Contract DE-AC05-84OR-21400)
(DE90-014456; CONF-900731-1) Avail: NTIS HC A02/MF A01

The mechanical properties of diamond-like carbon and diamond films have been studied using an ultra-low load indentation technique. The elastic/plastic properties of the films can be evaluated from the continuous load and displacement data acquired with a mechanical properties microprobe. Values for hardness and elastic modulus are given for both types of films relative to natural diamond and single-crystal sapphire. Determination of hardness and modulus of elasticity in thin films (particularly those with high values such as diamond) requires more information than can be obtained from conventional (e.g., Knoop or Vicker's) microhardness testing. The use of the mechanical properties microprobe to characterize these properties is addressed. DOE

N90-28862*# Virginia Polytechnic Inst. and State Univ., Blacksburg. Center for Composite Materials and Structures.
STRUCTURAL ANALYSIS AND OPTIMUM DESIGN OF GEODESICALLY STIFFENED COMPOSITE PANELS
John L. Phillips and Zafer Guerdal Jul. 1990 263 p
(Grant NAG1-643)
(NASA-CR-186944; NAS 1.26:186944; CCMS-90-05; VPI-E-90-08)
Avail: NTIS HC A12/MF A02 CSCL 20K

A computationally efficient analyses approach is developed to predict the buckling of geodesically stiffened composite panels under in-plane loads. This procedure accounts for the discrete flexural contribution of each stiffener through the use of Lagrange multipliers in an energy method solution. An analysis is also implemented for the buckling of simply supported anisotropic rhombic plates. Analysis routines are coupled with the numerical optimizer ADS to create a package for the design of minimum-mass stiffened panels, subject to constraints on buckling of the panel assembly, local buckling of the stiffeners, and material strength

failure. The design code is used to conduct a preliminary design study of structurally efficient stiffened aircraft wing rib panels. Design variables include thickness of the skin laminates, stiffener thickness, and stiffener height. Applied loads are uniaxial compression, pure shear, and combined compression-shear. Two different geodesically stiffened wing rib configurations with increasing numbers of stiffeners are considered. Results are presented in the form of structural efficiency charts and are compared with those for minimum-weight longitudinally stiffened panels and unstiffened flat plates. Trends in design parameters, including skin thickness, stiffener height, stiffener thickness, stiffener aspect ratio, stiffener load fraction, and stiffener mass fraction, are also examined for the panels under compression and shear. The effect of skin laminate geometry and anisotropy on the local buckling behavior of cross-stiffened geodesic panels are examined using the rhombic plate analysis. Author

N90-28863# Materials Research Labs., Ascot Vale (Australia).
OPERATION AND CALIBRATION OF MRL PERMEAMETER FOR MEASUREMENT OF DC MAGNETIC PROPERTIES OF MATERIALS UNDER STRESS
I. M. Robertson and P. S. Vincent May 1990 30 p
(MRL-TN-574) Avail: NTIS HC A03/MF A01

The operation and calibration of experimental apparatus constructed at MRL for the measurement of the DC magnetic properties of steels are described. The instrument is capable of measuring normal induction curves and hysteresis loops at applied magnetic field strengths up to about 1 kA/m. A special feature is the ability to apply mechanical stress to the specimens before or during magnetic measurements. The stress and magnetic field are applied in the same direction in the specimen, and the magnetic induction is also measured in this direction. Author

N90-28864 Case Western Reserve Univ., Cleveland, OH.
CRACK LAYER ANALYSIS OF FATIGUE FRACTURE OF A BETA TITANIUM ALLOY Ph.D. Thesis
Ibrahim Mohammed Mostafa 1989 203 p
Avail: Univ. Microfilms Order No. DA9012400

Fatigue crack propagation (FCP) in TiV15Cr3Al3Sn3 alloy (where the composition is in approximate weight percent) was studied using single-edge-notch specimens. The crack tip was preceded by a zone of transformation, the size of which increased considerably with crack advance. Microscopic examinations revealed a mixture of surface traces due to shear by dislocation slip and microcracking. The extent of microcracking increased markedly with the crack depth. The crack layer theory is employed to relate the rate of FCP to the observed damage mechanisms. The analysis revealed two stages of FCP. Dislocation slip process dominated the first stage with an average specific enthalpy of damage of 7 MJ/cu m. The second stage, approaching critical crack length, is dominated by microcracking and is characterized by an average specific enthalpy of damage of about 20 MJ/cu m. The investigation of the behavior of FCP under different maximum applied stresses showed that the two stages indicated by the crack layer theory still exist at all stress levels. However, the crack length at which the behavior of the crack changes from one stage to another decreases with the increase in the maximum applied stress. The average value of the specific enthalpy of damage is practically constant within each stage. Calculations of the strain energy of dislocations were made using the results from transmission electron microscopy on the first stage of crack propagation. The value of the total strain energy of dislocations is about 6.8 MH/cu m. Dissert. Abstr.

N90-28865*# McDonnell-Douglas Helicopter Co., Mesa, AZ.
CORRELATION OF AH-1G AIRFRAME FLIGHT VIBRATION DATA WITH A COUPLED ROTOR-FUSELAGE ANALYSIS
K. Sangha and J. Shamie Aug. 1990 172 p
(Contract NAS1-17498)
(NASA-CR-181974; NAS 1.26:181974) Avail: NTIS HC A08/MF A01 CSCL 20L

The formulation and features of the Rotor-Airframe Comprehensive Analysis Program (RACAP) is described. The analysis employs a frequency domain, transfer matrix approach for the blade structural model, a time domain wake or momentum theory aerodynamic model, and impedance matching for rotor-fuselage coupling. The analysis is applied to the AH-1G helicopter, and a correlation study is conducted on fuselage vibration predictions. The purpose of the study is to evaluate the state-of-the-art in helicopter fuselage vibration prediction technology. The fuselage vibration predicted using RACAP are fairly good in the vertical direction and somewhat deficient in the lateral/longitudinal directions. Some of these deficiencies are traced to the fuselage finite element model. Author

N90-28866*# McDonnell-Douglas Helicopter Co., Mesa, AZ.
PLAN, EXECUTE, AND DISCUSS VIBRATION MEASUREMENTS AND CORRELATIONS TO EVALUATE A NASTRAN FINITE ELEMENT MODEL OF THE AH-64 HELICOPTER AIRFRAME
D. Ferg, L. Foote, G. Korkosz, F. Straub, M. Toossi, and R. Weisenburger Jan. 1990 215 p
(Contract NAS1-17498)
(NASA-CR-181973; NAS 1.26:181973) Avail: NTIS HC A10/MF A02 CSCL 20K

A ground vibration test was performed on the AH-64 (Apache) helicopter to determine the frequency response of the airframe. The structure was excited at both the main and tail rotor hubs, separately, and response measurements were taken at 102 locations throughout the fuselage structure. Frequency responses were compared and correlated with results from a NASTRAN finite element model of AH-64. In addition, natural frequencies and mode shapes were estimated from the frequency response data and were correlated with analytical results. Author

N90-28867 Illinois Univ., Chicago.
A NONLINEAR FINITE ELEMENT FORMULATION FOR THE LARGE DISPLACEMENT ANALYSIS OF PLATES Ph.D. Thesis
Bilin Chang 1989 120 p
Avail: Univ. Microfilms Order No. DA9015743

A method for the dynamic analysis of plates that undergo large translational and rotational displacements is presented. The simple case of two-parameter screw motion in which the rigid body translation and rotation of the plate are along and about an axis fixed in space is considered; the equations of motion are derived using classical approximation methods and Lagrange's equations. The quadratic velocity terms that contain the gyroscopic and Coriolis forces are presented in a closed form in terms of a set of invariants of motion that depend on the assumed displacement field. A total nonlinear Lagrangian finite element formulation is also developed for the rectangular plate elements that undergo large translational and rotational displacements. The configuration of each rectangular plate element on the deformable body is identified using four coordinate systems: global, body, element, and intermediate element coordinate. By using these coordinate systems, the configuration of the rectangular plate element can be identified in the global coordinate system in terms of a coupled set of body reference and elastic nodal coordinates. The nonlinear differential equations of motions of the plate element are developed using Lagrange's equation of motion. These nonlinear equations are expressed in terms of unique set of invariants of the plate elements. The invariants of the deformable body that undergoes finite rotations are obtained by assembling the invariants of its elements. The effect of the coupling between the stretching and bending of the plate as the result of considering the rotary inertia is also examined. The use of the nonlinear dynamic formulation developed here is demonstrated using multibody systems that consist of a set of interconnected rigid and deformable bodies each of which may undergo large rigid body motion.
Dissert. Abstr.

N90-28868 Arizona Univ., Tucson.
RELIABILITY ANALYSIS OF MAINTAINED STRUCTURAL SYSTEM VULNERABLE TO FATIGUE AND FRACTURE Ph.D. Thesis

Tony Yi Torng 1989 246 p
Avail: Univ. Microfilms Order No. DA9014683

Metallic structures dominated by tensile loads are vulnerable to fatigue and fracture. Fatigue is produced by oscillatory loads. Quasi-static brittle or ductile fracture can result from a large load in the random sequence. Moreover, a fatigue or fracture failure in a member of a redundant structure produces impulsive redistributed loads to the intact members. These transient loads could produce a sequence of failures resulting in progressive collapse of the system. Fatigue and fracture design factors are subject to considerable uncertainty. Therefore, a probabilistic approach, which includes a system reliability assessment, is appropriate for design purposes. But system reliability can be improved by a maintenance program of periodic inspection with repair and/or replacement of damaged members. However, a maintenance program can be expensive. The ultimate goal of the engineer is to specify a design, inspection, and repair strategy to minimize life cycle costs. The fatigue/fracture reliability and maintainability (FRM) process for redundant structure can be a complicated random process. The structural model considered series, parallel, and parallel/series systems of elements. Applied to the system are fatigue loads including mean stress, an extreme load, as well as impulsive loads in parallel member systems. The failure modes are fatigue, brittle and ductile fracture. A refined fatigue model is employed which includes both the crack initiation and propagation phases. The FRM process cannot be solved easily using recently developed advanced structural reliability techniques. A hybrid simulation method which combines modified importance sampling (MIS) with inflated stress extrapolation (ISE) is proposed. MIS and ISE methods are developed and demonstrated using numerous examples which include series, parallel and series/parallel systems. Dissert. Abstr.

N90-28869# Illinois Univ., Urbana-Champaign. Dept. of Civil Engineering.
TORSIONAL EFFECTS IN STRUCTURES SUBJECTED TO STRONG GROUND MOTION Ph.D. Thesis
Shi Lu and William J. Hall Apr. 1990 201 p
(Grants NSF DFR-84-19191; NSF CES-88-03920; NSF BCS-88-03920)
(PB90-226960; SRS-552; UILU-ENG-89-2006; ISSN-0069-4274)
Avail: NTIS HC A10/MF A02 CSCL 20K

The purpose was to increase the understanding of torsional behavior in low-rise frame buildings and to assess its importance in the gross response of such buildings. One aspect of this investigation centered on understanding the strong coupling between translational and torsional response with closely spaced frequencies (including the beating phenomenon arising from modal instability); the study is believed to be the first conclusive theoretical demonstration of the beating phenomenon arising in the manner noted. It was found that the dynamic amplification factor in torsion (as measured by static eccentricity) was about 2.5. With the use of a theoretical model encompassing nonlinear material behavior, it was possible to predict the torsional effects in two low-rise buildings and to compare such results with response data recorded in these buildings in the 1987 Whittier Narrows Earthquake. The low-rise moment-resisting frame-building studies indicated that the fundamental frequencies identified earlier herein are usually not well separated, and if possible, to prevent damage arising from torsion (usually late in the response process), the translational frequency should be kept smaller in relation to the torsional frequency, to ensure that the fundamental translational mode is dominant. GRA

N90-28870# Sydney Observatory (Australia). School of Civil and Mining Engineering.
APPLICATION OF DISCRETE FOURIER SERIES TO THE FINITE ELEMENT STRESS ANALYSIS OF AXI-SYMMETRIC SOLIDS
J. Y. Lai and J. R. Booker Oct. 1989 45 p
(PB90-231010; R-603) Avail: NTIS HC A03/MF A01 CSCL 20K

An efficient formulation, based on a discrete Fourier series expansion, for the analysis of axi-symmetric solids subjected to non-symmetric loading is described. In contrast to the commonly adopted continuous Fourier series approach, the discrete Fourier series representation has largely overcome problems such as the presence of Gibb's phenomenon and the lack of conformity of elements. The computational advantage over a fully three-dimensional formulation is illustrated. Finally, the method is demonstrated through a finite element study of rigid caissons founded in both elastic and elasto-plastic materials. GRA

N90-28871*# National Aeronautics and Space Administration. Langley Research Center, Hampton, VA.
DEVELOPMENT OF TESTING AND ANALYSIS METHODOLOGY TO ASSESS THE LONG TERM DURABILITY OF POLYMERIC COMPOSITES AT HIGH TEMPERATURES
W. Steven Johnson Aug. 1990 14 p
(NASA-TM-102714; NAS 1.15:102714) Avail: NTIS HC A03/MF A01 CSCL 20K

A workshop was held to help assess the state-of-the-art in evaluating the long term durability of polymeric matrix composites (PMCs) and to recommend future activities. Design and evaluation of PMCs at elevated temperatures were discussed. The workshop presentations, the findings of the workshop sessions are briefly summarized. Author

N90-28872*# National Aeronautics and Space Administration. Langley Research Center, Hampton, VA.
EVALUATION OF SEVERAL MICROMECHANICS MODELS FOR DISCONTINUOUSLY REINFORCED METAL MATRIX COMPOSITES
W. Steven Johnson and M. J. Birt Sep. 1990 32 p
(NASA-TM-102719; NAS 1.15:102719) Avail: NTIS HC A03/MF A01 CSCL 20K

A systematic experimental evaluation of whisker and particulate reinforced aluminum matrix composites was conducted to assess the variation in tensile properties with reinforcement type, volume fraction, and specimen thickness. Each material was evaluated in three thicknesses, 1.8, 3.18, and 6.35 mm, to determine the size, distribution, and orientation of the reinforcements. This information was used to evaluate several micromechanical models that predict composite moduli. The longitudinal and transverse moduli were predicted for reinforced aluminum. The Paul model, the Cox model and the Halpin-Tsai model were evaluated. The Paul model gave a good upper bound prediction for the particulate reinforced composites but under predicted whisker reinforced composite moduli. The Cox model gave good moduli predictions for the whisker reinforcement, but was too low for the particulate. The Halpin-Tsai model gave good results for both whisker and particulate reinforced composites. An approach using a trigonometric projection of whisker length to predict the fiber contribution to the modulus in the longitudinal and transverse directions was compared to the more conventional lamination theory approach. Author

N90-28873# Etablissement Technique Central de l'Armement, Arcueil (France). Dept. Comportement des Materiaux.
BEHAVIOR OF ARAMID/EPOXY WOUNDED TUBES UNDER UNIAXIAL AND BIAXIAL LOADING Final Report [COMPORTEMENT DE TUBES BOBINES KEVLAR/EPOXY SOUS SOLLICITATIONS UNIAXIALES ET BIAXIALES AL]
P. Joguet and C. Oytana (Paris Univ., Besancon, France) 30 Oct. 1989 10 p Sponsored by Direction des Recherches, Etudes et Techniques
(ETCA-89-R-150; ETN-90-97470) Avail: NTIS HC A02/MF A01

A model for the prevision of the mechanical behavior of Kevlar/epoxy wound tubes is proposed. The aim of the study is to impose the quality of the dimensioning of industrial composite structures. The model is based on plate laminate theory, modulus damage laws. The structure behavior up to the nonlinearity limits can be estimated. ESA

N90-28874# Office National d'Etudes et de Recherches Aerospatiales, Paris (France). Direction Scientifique de la Resistance des Structures.
PARAMETRIC SOLUTION OF NONLINEAR STRUCTURE PROBLEMS Final Report [RESOLUTION PARAMETRIQUE DE PROBLEMES STRUCTURAUX NON LINEAIRES]
R. Girard Feb. 1990 33 p In FRENCH
(Contract DRET-88-34-001)
(ONERA-RT-21/3542-RY-082-R; ETN-90-97501) Avail: NTIS HC A03/MF A01

The solution of nonlinear structural problems concerning large displacements is discussed on the basis of the finite element method. Algorithms allowing the calculation of the equilibrium points for the loads considered are developed. The proposed method consists of the parameterization of arc length type. This parameterization is applied to the singularities existing in buckling phenomena. Numerical calculations are performed by a regularization procedure in order to allow an easy crossover of the singularities. ESA

N90-28875# Southampton Univ. (England). Inst. of Sound and Vibration Research.
ANALYSIS OF VIBRATIONAL POWER TRANSMISSION THROUGH A BEAM SYSTEM INCLUDING A FLEXIBLE SECTION
Jane Louise Horner Apr. 1989 45 p Sponsored by the Ministry of Defence Procurement Executive, London, England
(ISVR-TR-176; ETN-90-97515) Avail: NTIS HC A03/MF A01

The effect that the introduction of a flexible section has on the wave motion in a beam system is considered. Power flow analysis is used to compare the effects of the stiffness of the flexible section on both flexural and longitudinal wave transmission. To ensure accurate modeling of the power flow in the system, a closed form solution was used to model the multiple reflections within the flexible section. Results show that flexible sections attenuate longitudinal waves more than flexural waves. A very flexible section gives the best attenuation over a wide frequency band. ESA

N90-28876*# Institute for Computer Applications in Science and Engineering, Hampton, VA.
LANZ: SOFTWARE SOLVING THE LARGE SPARSE SYMMETRIC GENERALIZED EIGENPROBLEM Interim Report
Mark T. Jones and Merrell L. Patrick (Duke Univ., Durham, NC.) Aug. 1990 13 p
(Contract NAS1-18605; NAG1-466; AF-AFOSR-0117-88)
(NASA-CR-182086; ICASE-IR-12; NAS 1.26:182086) Avail: NTIS HC A03/MF A01 CSCL 20K

A package, LANZ, for solving the large symmetric generalized eigenproblem is described. The package was tested on four different architectures: Convex 200, CRAY Y-MP, Sun-3, and Sun-4. The package uses a Lanczos' method and is based on recent research into solving the generalized eigenproblem. Author

N90-28877*# National Aeronautics and Space Administration. Langley Research Center, Hampton, VA.
ERROR DETECTION AND CONTROL FOR NONLINEAR SHELL ANALYSIS
Susan L. McCleary (Lockheed Engineering and Sciences Co., Hampton, VA.) and Norman F. Knight, Jr. Aug. 1990 12 p Prepared for presentation at the 6th World Congress on Finite Element Methods, Banff, Alberta, 1-5 Oct. 1990
(NASA-TM-102723; NAS 1.15:102723) Avail: NTIS HC A03/MF A01 CSCL 20K

A problem-adaptive solution procedure for improving the reliability of finite element solutions to geometrically nonlinear shell-type problem is presented. The strategy incorporates automatic error detection and control and includes an iterative procedure which utilizes the solution at the same load step on a more refined model. Representative nonlinear shell problem are solved. Author

N90-28878*# Case Western Reserve Univ., Cleveland, OH. Dept. of Civil Engineering.
GREEN'S FUNCTIONS FOR DISLOCATIONS IN BONDED STRIPS AND RELATED CRACK PROBLEMS Final Report
R. Ballarini and H. A. Luo Sep. 1990 47 p
(Grant NAG3-856)
(NASA-CR-185291; NAS 1.26:185291) Avail: NTIS HC A03/MF A01 CSCL 20K

Green's functions are derived for the plane elastostatics problem of a dislocation in a bimaterial strip. Using these fundamental solutions as kernels, various problems involving cracks in a bimaterial strip are analyzed using singular integral equations. For each problem considered, stress intensity factors are calculated for several combinations of the parameters which describe loading, geometry and material mismatch. Author

N90-28879*# National Aeronautics and Space Administration. Marshall Space Flight Center, Huntsville, AL.
MINIMUM WEIGHT DESIGN OF A LEAF SPRING TAPERED IN THICKNESS AND WIDTH FOR THE HUBBLE SPACE TELESCOPE-SPACE SUPPORT EQUIPMENT
P. I. Rodriguez Washington Sep. 1990 41 p
(NASA-TM-4233; NAS 1.15:4233) Avail: NTIS HC A03/MF A01 CSCL 20K

A linear elastic solution to the problem of minimum weight design of cantilever beams with variable width and depth is presented. The solution shown is for the specific application of the Hubble Space Telescope maintenance mission hardware. During these maintenance missions, delicate instruments must be isolated from the potentially damaging vibration environment of the space shuttle cargo bay during the ascent and descent phases. The leaf springs are designed to maintain the isolation system natural frequency at a level where load transmission to the instruments in a minimum. Nonlinear programming is used for the optimization process. The weight of the beams is the objective function with the deflection and allowable bending stress as the constraint equations. The design variables are the width and depth of the beams at both the free and the fixed ends. Author

N90-28880*# Cincinnati Univ., OH. Dept. of Materials Science and Engineering.
MICROSTRUCTURE: PROPERTY CORRELATION Final Technical Report
N. Jayaraman 1 Oct. 1990 54 p
(Grant NAG3-506)
(NASA-CR-180406; NAS 1.26:180406) Avail: NTIS HC A04/MF A01 CSCL 20K

Strain controlled torsional and biaxial (tension-torsion) low cycle fatigue behavior of Waspaloy was studied at room temperature as a function of heat treatment. Biaxial tests were conducted under proportional (when the axial and torsional strain cycles are in-phase) and non-proportional (when the axial and torsional strain cycles are 90 deg out-of-phase) cyclic conditions. The deformation behavior under these different cyclic conditions were evaluated by slip trace analysis. For this, a Schmidt-type factor was defined for multiaxial loading conditions and it was shown that when the slip deformation is predominant, non-proportional cycles are more damaging than proportional or pure axial or torsional cycles. This was attributed to the fact that under non-proportional cyclic conditions, deformation was through multiple slip as opposed single slip for other loading conditions, which gave rise to increased hardening. The total life for a given test condition was found to be independent of heat treatment. This was interpreted as being due to the differences in the cycles to initiation and propagation of cracks. Author

N90-28614*# Computational Mechanics Co., Austin, TX.
A HYBRID-STRESS FINITE ELEMENT FOR LINEAR ANISOTROPIC ELASTICITY
Gerald W. Fly, J. Tinsley Oden, and Mark L. Pearson (Softcom Systems, Inc., Huntsville, AL.) *In* NASA, Marshall Space Flight Center, Advanced Earth-to-Orbit Propulsion Technology 1988, Volume 1 Sep. 1988 p 30-42 (For primary document see

N90-28611 23-20)
(Contract NAS8-37283)
Avail: NTIS HC A99/MF E06 CSCL 20K

N90-28617*# State Univ. of New York, Buffalo. Dept. of Civil Engineering.
DEVELOPMENT OF AN INTEGRATED BEM FOR HOT FLUID-STRUCTURE INTERACTION
G. F. Dargush and P. K. Banerjee *In* NASA, Marshall Space Flight Center, Advanced Earth-to-Orbit Propulsion Technology 1988, Volume 1 Sep. 1988 p 69-86 (For primary document see N90-28611 23-20)
Avail: NTIS HC A99/MF E06 CSCL 20K

N90-28641*# Georgia Inst. of Tech., Atlanta. School of Materials Engineering.
MICROMECHANICS OF CYCLIC DEFORMATION IN SSME TURBOPUMP BLADE MATERIALS
Walter W. Milligan and Stephen D. Antolovich *In* NASA, Marshall Space Flight Center, Advanced Earth-to-Orbit Propulsion Technology 1988, Volume 1 Sep. 1988 p 487-496 (For primary document see N90-28611 23-20)
(Grant NAG3-503)
Avail: NTIS HC A99/MF E06 CSCL 20K

N90-28645*# Failure Analysis Associates, Inc., Palo Alto, CA.
NASCRAC (TRADEMARK): A FRACTURE MECHANICS ANALYSIS CODE
D. O. Harris, D. D. Dedhia, R. A. Sire, P. J. Woytowitz, and E. E. Nelson *In* NASA, Marshall Space Flight Center, Advanced Earth-to-Orbit Propulsion Technology 1988, Volume 1 Sep. 1988 p 563-579 (For primary document see N90-28611 23-20)
Avail: NTIS HC A99/MF E06 CSCL 20K

N90-28646*# Southwest Research Inst., San Antonio, TX. Dept. of Materials Sciences.
A COMPARISON OF SINGLE-CYCLE VERSUS MULTI-CYCLE PROOF TESTING STRATEGIES
Stephen J. Hudak, Jr. and Dale A. Russell (Rockwell International Corp., Canoga Park, CA.) *In* NASA, Marshall Space Flight Center, Advanced Earth-to-Orbit Propulsion Technology 1988, Volume 1 Sep. 1988 p 580-595 (For primary document see N90-28611 23-20)
(Contract NAS8-37451)
Avail: NTIS HC A99/MF E06 CSCL 20K

N90-28647*# National Aeronautics and Space Administration. Lyndon B. Johnson Space Center, Houston, TX.
DATA BASE FOR CRACK GROWTH PROPERTIES OF MATERIALS
Royce G. Forman, Victor B. Lawrence, and Henry L. Nguy (Lockheed Engineering and Management Services Co., Inc., Houston, TX.) *In* NASA, Marshall Space Flight Center, Advanced Earth-to-Orbit Propulsion Technology 1988, Volume 1 Sep. 1988 p 596-608 (For primary document see N90-28611 23-20)
Avail: NTIS HC A99/MF E06 CSCL 20K

N90-28648*# National Aeronautics and Space Administration. Marshall Space Flight Center, Huntsville, AL.
COMPARISON OF TWO COMPUTER CODES FOR CRACK GROWTH ANALYSIS: NASCRAC VERSUS NASA/FLAGRO
Roderick Stallworth, Charles A. Meyers, and Helen C. Stinson *In its* Advanced Earth-to-Orbit Propulsion Technology 1988, Volume 1 Sep. 1988 p 609-633 (For primary document see N90-28611 23-20)
Avail: NTIS HC A99/MF E06 CSCL 20K

N90-28649*# National Aeronautics and Space Administration. Lewis Research Center, Cleveland, OH.
STRUCTURAL RESPONSE OF SSME TURBINE BLADE AIRFOILS
V. K. Arya, A. Abdul-Aziz (Sverdrup Technology, Inc., Cleveland, OH.), and R. L. Thompson *In* NASA, Marshall Space Flight Center, Advanced Earth-to-Orbit Propulsion Technology 1988, Volume 1 Sep. 1988 p 634-652 (For primary document see N90-28611 23-20)
Avail: NTIS HC A99/MF E06 CSCL 20K

N90-28650*# Pratt and Whitney Aircraft, West Palm Beach, FL.
PROBABILISTIC MODEL FOR FRACTURE MECHANICS SERVICE LIFE ANALYSIS
Charles Annis and Tommie Watkins *In* NASA, Marshall Space Flight Center, Advanced Earth-to-Orbit Propulsion Technology 1988, Volume 1 Sep. 1988 p 653-659 (For primary document see N90-28611 23-20)
(Contract NAS8-36901)
Avail: NTIS HC A99/MF E06 CSCL 20K

42 GEOSCIENCES (GENERAL)

No abstracts in this category.

43 EARTH RESOURCES AND REMOTE SENSING

Includes remote sensing of earth resources by aircraft and spacecraft; photogrammetry; and aerial photography.

For instrumentation see *35 Instrumentation and Photography.*

N90-28881# Instituto de Pesquisas Espaciais, Sao Jose dos Campos (Brazil).
COMPARISON OF METHODS OF SPACE COLOR TRANSFORMATIONS FOR ENHANCEMENT OF COLORED IMAGES [COMPARACAO DE METODOS DE TRANSFORMACOES DO ESPACO DE CORES PARA REALCE DE IMAGENS COLORIDAS]
Virginia RagonideMoraesCorreia and Luciano VieiraDutra Oct. 1989 11 p In PORTUGESE Presented at the 4th Latin American Symposium on Remote Sensors, Bariloche, Argentina, 20-24 Nov. 1989
(INPE-4977-PRE/1542) Avail: NTIS HC A03/MF A01

Photointerpretation of remote sensing imagery requires a good quality in the representation of data. Enhancement techniques of colors based on IHS (intensity, hue, and saturation) transformations has many uses for improving image aspects. Many modes are possible for RGB (red, green, and blue) imagery transformation for space perceptual IHS. Work is presented for three IHS techniques existing in literature to study, evaluate, and compare these techniques for processing time, mean quadratic error, and visual quality. Transl. by B.G.

N90-28882# Oak Ridge National Lab., TN. Energy Div.
GEOPHYSICAL DIFFRACTION TOMOGRAPHY: A COMPLEMENTARY REMOTE SENSING TECHNIQUE FOR HAZARDOUS WASTE SITE CHARACTERIZATION
W. Chris King (Army Environmental Hygiene Activity, Aurora, CO.) and Alan J. Witten 1990 13 p Presented at the 4th National Outdoor Action Conference on Aquifer Restoration, Groundwater Monitoring, and Geophysical Methods, Las Vegas, NV, 14-17 May 1990
(Contract DE-AC05-84OR-21400)
(DE90-013025; CONF-9005149-6) Avail: NTIS HC A03/MF A01

Use of surface geophysical methods for characterization of hazardous waste sites has well documented technical, health, and cost benefits when compared to intrusive data gathering methods. This statement is obviously predicated on the assumption that the geophysical methods being employed are applicable to the waste and shallow geologic features in the area of interest. This paper

places a new surface geophysical technique, geophysical diffraction tomography, into a context of its utility within the existing remote sensing technology. A procedure based on analyses of the propagating wave which accounts for the naturally occurring diffractions has more information available than simple time of travel, and therefore can provide information concerning subsurface features not recoverable from many existing surface sensing methods. The paper presents field results showing the application of the geophysical diffraction tomography method within the existing suite of remote sensing methods to maximize the site characterization information obtained. DOE

N90-28883# Geological Survey, Tallahassee, FL. Water Resources Div.
COMPUTER PROGRAM FOR CONVERTING RECTANGULAR COORDINATES TO LATITUDE-LONGITUDE COORDINATES
A. T. Rutledge 1989 21 p Prepared in cooperation with Southwest Florida Water Management Dist., Tallahassee; South Florida Water Management Dist., West Palm Beach, Northwest Florida Water Management Dist., Tallahassee, and St. John's River Water Mangement Dist., Palatka, FL
(PB90-231796; USGS/WRI-89-4070) Avail: NTIS HC A03/MF A01 CSCL 08B

A FORTRAN-77 computer program was developed for converting the coordinates of any rectangular grid on a map to coordinates on a grid that is parallel to lines of equal latitude and longitude. Using the program in conjunction with ground-water flow models, the user can extract data and results from models with varying grid orientations and place these data into a grid structure that is oriented parallel to lines of equal latitude and longitude. All cells in the rectangular grid must have equal dimensions, and all cells in the latitude-longitude grid must measure 1 minute by 1 minute. The program is applicable if the map used shows lines of equal latitude as arcs and lines of equal longitude as straight lines and assumes that the Earth's surface can be approximated as a sphere. GRA

N90-28884# Nevada Univ., Reno. Div. of Earth Sciences.
GEOTHERMAL FLUID GENESIS IN THE GREAT BASIN Final Report, 1 Aug. 1988 - 1 May 1990
T. Flynn and P. K. Buchanan 1990 154 p
(Contract DE-FG07-88ID-12784)
(DE90-014438; DOE/ID-12784/1) Avail: NTIS HC A08/MF A01

Early theories concerning geothermal recharge in the Great Basin implied recharge was by recent precipitation. Physical, chemical, and isotopic differences between thermal and non-thermal fluids and global paleoclimatic indicators suggest that recharge occurred during the late Pleistocene. Polar region isotopic studies demonstrate that a depletion in stable light-isotopes of precipitation existed during the late Pleistocene due to the colder, wetter climate. Isotopic analysis of calcite veins and packrat midden megafossils confirm the depletion event occurred in the Great Basin. Isotopic analysis of non-thermal springs is utilized as a proxy for local recent precipitation. Contoured plots of deuterium concentrations from non-thermal and thermal water show a regional, systematic variation. Subtracting contoured plots of non-thermal water from plots of thermal water reveals that thermal waters on a regional scale are generally isotopically more depleted. Isolated areas where thermal water is more enriched than non-thermal water correspond to locations of pluvial Lakes Lahontan and Bonneville, suggesting isotopically enriched lake water contributed to fluid recharge. These anomalous waters also contain high concentrations of sodium chloride, boron, and other dissolved species suggestive of evaporative enrichment. Carbon-age data and isotopic data from Great Basin thermal waters correlate with the polar paleoclimate studies. Recharge occurred along range bounding faults. DOE

N90-28885# Los Alamos National Lab., NM.
A MANUAL FOR ANALYSIS OF HEMISPHERICAL CANOPY PHOTOGRAPHY
Paul M. Rich (Stanford Univ., CA.) Dec. 1989 80 p
(Contract W-7405-eng-36)
(DE90-014718; LA-11733-MS) Avail: NTIS HC A05/MF A01

Hemispherical canopy photography involves taking photographs through a hemispherical (fisheye) lens pointed upward from beneath a plant canopy. The resulting photographs can be analyzed to determine the geometry of canopy openings and to calculate potential light penetration. This manual serves as a comprehensive guide to the program CANOPY (copyright), a public domain microcomputer program for image analysis of hemispherical canopy photography. Included are discussions of theory, research applications, field methodology, hardware setup and operation, and software setup and operation. CANOPY enables video digitization of negatives, real-time display of positive images, interactive determination of a threshold to distinguish foliage from canopy openings, editing of photographs with poor exposure, rapid calculation of various measures of canopy geometry and indices of potential light penetration, and convenient output of results. A series of utility programs allow user specification of theoretical or empirical distributions of direct sunlight and diffuse skylight for a given site. DOE

N90-28886# Instituto de Pesquisas Espaciais, Sao Jose dos Campos (Brazil).
DIGITAL GEOMETRIC CORRECTION FOR MSS-LANDSAT IMAGERY [CORRECAO GEOMETRICA DIGITAL DE IMAGENS MSS-LANDSAT]
Antonio Jose FerreiraMeSilva, Fernando AugustoMli, Gilberto CamaraNeto, Paulo Roberto MartinsSerra, and Ricardo CartaxoModestodeSouza Jul. 1988 12 p In PORTUGUESE; ENGLISH summary Presented at the 3rd Brazilian Symposium on Remote Sensing, Rio de Janeiro, Brazil, 1984
(INPE-4627-PRE/1345) Avail: NTIS HC A03/MF A01

An integrated software system for geometric correction of LANDSAT imagery is described. This system includes all phases of processing, from receiving a raw CCT (computer compatible tape) to the generation of a corrected CCT (of UTM mosaic). Emphasis is placed on a model which needs few control points, and on the creation of a ground control point library for Brazil. Author

N90-28887 Physics and Electronics Lab. TNO, The Hague (Netherlands).
DESCRIPTION OF THE MARC MEASURING SYSTEM Final Report
A. N. deJong, J. Winkel, and R. A. W. Kemp Nov. 1989 69 p In DUTCH; ENGLISH summary
(FEL-89-B170; TD-89-3873; ETN-90-97408) Copyright Avail: Physics and Electronics Lab. TNO, P.O. Box 96864, 2509 JG The Hague, Netherlands

The MARC (Multispectral Airborne Reference-aided Calibrated scanner) measuring system is presented. The MARC system for gathering multispectral reflection data of terrain elements contains 16 spectral bands from the UV to the IR range. Special attention was paid to the data collection and gathering system with a view to different applications. The system can either measure in the field or from an airplane. In the latter case the required accuracy cannot be obtained in all spectral bands. Some measurement results are discussed. ESA

N90-28888*# Purdue Univ., West Lafayette, IN. School of Electrical Engineering.
ON-LINE OBJECT FEATURE EXTRACTION FOR MULTISPECTRAL SCENE REPRESENTATION
Hassan Ghassemian and David Landgrebe Aug. 1988 168 p
(Grant NAGw-925)
(NASA-CR-187006; NAS 1.26:187006; TR-EE-88-34) Avail: NTIS HC A08/MF A01 CSCL 08B

A new on-line unsupervised object-feature extraction method is presented that reduces the complexity and costs associated with the analysis of the multispectral image data and data transmission, storage, archival and distribution. The ambiguity in the object detection process can be reduced if the spatial

dependencies, which exist among the adjacent pixels, are intelligently incorporated into the decision making process. The unity relation was defined that must exist among the pixels of an object. Automatic Multispectral Image Compaction Algorithm (AMICA) uses the within object pixel-feature gradient vector as a valuable contextual information to construct the object's features, which preserve the class separability information within the data. For on-line object extraction the path-hypothesis and the basic mathematical tools for its realization are introduced in terms of a specific similarity measure and adjacency relation. AMICA is applied to several sets of real image data, and the performance and reliability of features is evaluated. Author

N90-28889*# Purdue Univ., West Lafayette, IN. Lab. for Applications of Remote Sensing.

A METHOD OF CLASSIFICATION FOR MULTISOURCE DATA IN REMOTE SENSING BASED ON INTERVAL-VALUED PROBABILITIES

Hakil Kim and Philip H. Swain Jul. 1990 131 p
(Grant NAGw-925)
(NASA-CR-187007; NAS 1.26:187007; TR-EE90-48) Avail: NTIS HC A07/MF A01 CSCL 08B

An axiomatic approach to intervalued (IV) probabilities is presented, where the IV probability is defined by a pair of set-theoretic functions which satisfy some pre-specified axioms. On the basis of this approach representation of statistical evidence and combination of multiple bodies of evidence are emphasized. Although IV probabilities provide an innovative means for the representation and combination of evidential information, they make the decision process rather complicated. It entails more intelligent strategies for making decisions. The development of decision rules over IV probabilities is discussed from the viewpoint of statistical pattern recognition. The proposed method, so called evidential reasoning method, is applied to the ground-cover classification of a multisource data set consisting of Multispectral Scanner (MSS) data, Synthetic Aperture Radar (SAR) data, and digital terrain data such as elevation, slope, and aspect. By treating the data sources separately, the method is able to capture both parametric and nonparametric information and to combine them. Then the method is applied to two separate cases of classifying multiband data obtained by a single sensor. In each case a set of multiple sources is obtained by dividing the dimensionally huge data into smaller and more manageable pieces based on the global statistical correlation information. By a divide-and-combine process, the method is able to utilize more features than the conventional maximum likelihood method. Author

N90-28890*# Purdue Univ., West Lafayette, IN. Lab. for Applications of Remote Sensing.

METHODS FOR MULTISOURCE DATA ANALYSIS IN REMOTE SENSING

Jon Atli Benediktsson and Philip H. Swain May 1987 75 p
(Grants NAGw-925; NSF ECS-80-0324)
(NASA-CR-187005; NAS 1.26:187005; TR-EE-87-26) Avail: NTIS HC A04/MF A01 CSCL 08B

Methods for classifying remotely sensed data from multiple data sources are considered. Special interest is in general methods for multisource classification and three such approaches are considered: Dempster-Shafer theory; fuzzy set theory; and statistical multisource analysis. To apply statistical multisource analysis successfully it is necessary to characterize the reliability of each data source. Separability measures and classification accuracy are used to measure the reliability. These reliability measures are then associated with reliability factors included in the statistical multisource analysis to multispectral scanner data where different segments of the electromagnetic spectrum are treated as different sources. A discussion is included concerning future directions for investigating reliability measures. Author

N90-28891# Instituto de Pesquisas Espaciais, Sao Jose dos Campos (Brazil).

STUDY OF ANOMALIES IN TRANSITION VEGETATION IN ALTO XINGO-NT, THROUGH REMOTE SENSING TECHNIQUES M.S. Thesis [ESTUDO DE ANOMALIAS NA VEGETACAO DE TRANSICAO DO ALTO XINGU-MT, ATRAVES DE TECNICAS DE SENSORIAMENTO REMOTO]

Maria deLourdesBuenoTrindade Jun. 1988 131 p In PORTUGESE
(INPE-4601-TDL/334) Avail: NTIS HC A07/MF A01

MSS and TM/LANDSAT multitemporal data obtained in the near infrared spectral bands disclosed anomalies in the transition vegetation between Amazonian rain forest and Cerrado, Brazilian tropical savannah (Mato Grosso State, Brazil). The visual interpretation of TM/LANDSAT images showed the spatial, spectral, and temporal characteristics of the anomalies. Through digital analysis was carried out in two test areas, it was not possible to improve the anomaly patterns definition. Spectral parameters were more consistent than vegetation indices in the differentiation between anomalies and the surrounding vegetation. The first observation of this occurrence was done in pancromatic aerial photographs (obtained in 1967), and lately, in the near infrared spectral bands of the satellite images. This fact infers that the existence of these anomalies is related to the regeneration of the vegetation in these specific areas and demonstrated the application of these spectral bands in similar work. Author

N90-28892# Army Cold Regions Research and Engineering Lab., Hanover, NH.

THREE FUNCTIONS THAT MODEL EMPIRICALLY MEASURED UNFROZEN WATER CONTENT DATA AND PREDICT RELATIVE HYDRAULIC CONDUCTIVITY

Patrick B. Black May 1990 12 p
(AD-A223875; CRREL-90-5) Avail: NTIS HC A03/MF A01 CSCL 08/12

Empirically determined data on changes in unfrozen water content occurring as the result of changes in the state of ice and water in soil are discussed with reference to the changes in soil-water retention data for ice-free soil. The similarity between the two types of data is developed. The Brooks and Corey, van Genuchten and Gardner equations are then shown to be applicable to describing unfrozen water content data. These three functions are then used in the model of Mualem and the relative hydraulic conductivity of frozen soil is predicted. GRA

N90-28893# Army Cold Regions Research and Engineering Lab., Hanover, NH.

MULTIBAND IMAGING SYSTEMS

Harlan L. McKim, Carolyn J. Merry, and Nancy T. LaPotin May 1990 13 p
(AD-A223969; CRREL-SR-90-15) Avail: NTIS HC A03/MF A01 CSCL 15/4

Intelligence from satellites or other airborne platforms can give units on the battlefield an insurmountable advantage over the enemy. When multiband data from these devices are placed into a geographic information system, these results can vividly convey tactical information to the commander by providing an image backdrop to other attribute data, such as soil type, vegetation cover and slope. Geographic information systems can display both terrain analysis data, such as high resolution photographs, and multispectral data, such as thermal, radar or IR imagery. GRA

N90-28894# Army War Coll., Carlisle Barracks, PA.

SPACE-BASE MULTISPECTRAL IMAGERY: CURRENT AND FUTURE APPLICATIONS AND IMPLICATIONS TO THE UNITED STATES ARMY

James M. Weilbrenner 2 Feb. 1990 50 p
(AD-A224046; AD-F000153) Avail: NTIS HC A03/MF A01 CSCL 17/5

The Army expends considerable effort in attempts to pierce the fog of battle. Multispectral imagery (MSI), an emerging technology, has the ability to reduce this fog. Although MSI has been used by civil agencies for more than 15 years, the Army is

just beginning to realize and exploit its capabilities. One of the major attractions of MSI is the unclassified nature of its reconnaissance data which is usually highly classified. Operational and tactical commanders at all levels can use MSI products. This study provides a thorough description of MSI including its space-based assets and civil uses. Current Army utilization is also reviewed. The study concludes with an examination of possible future applications and implications. Research for the project included a comprehensive review and analysis of a wide spectrum of literature and personal interviews with experts in the MSI field. In addition to showing how MSI can benefit the Army, the study offers several recommendations to facilitate the development and utilization of MSI technology in the Army. GRA

N90-29025*# Brown Univ., Providence, RI. Dept. of Computer Science.
MAP LEARNING WITH INDISTINGUISHABLE LOCATIONS
Kenneth Basye and Thomas Dean *In* JPL, California Inst. of Tech., Proceedings of the NASA Conference on Space Telerobotics, Volume 1 31 Jan. 1989 p 285-290 (For primary document see N90-29000 23-54)
(Contract F49620-88-C-0132; NSF IRI-86-12644)
Avail: NTIS HC A21/MF A03 CSCL 05H

44 ENERGY PRODUCTION AND CONVERSION

Includes specific energy conversion systems, e.g., fuel cells; global sources of energy; geophysical conversion; and windpower.

For related information see also *07 Aircraft Propulsion and Power, 20 Spacecraft Propulsion and Power,* and *28 Propellants and Fuels.*

N90-28895# Helsinki Univ. of Technology, Espoo (Finland).
FUEL CELLS: THEIR APPLICATIONS, TECHNOLOGICAL STATUS, MARKET AND OPPORTUNITY
M. Yao (Yao International, Inc., Clarendon Hills, Il.) Oct. 1988 109 p
(DE90-796158; NEMO-4) Avail: NTIS (US Sales Only) HC A06/MF A01

Fuel cell applications are reviewed along with the global status of fuel cell development and demonstration, and the potential market and opportunity. A recommendation is made of potential strategies for Finnish industries and the government's role in the application and development of fuel cell technology in Finland. DOE

N90-28896# Energy Conversion Devices, Inc., Troy, MI.
RESEARCH ON HIGH-EFFICIENCY, MULTIPLE-GAP, MULTI-JUNCTION AMORPHOUS SILICON-BASED ALLOY THIN-FILM SOLAR CELLS Semiannual Subcontract Report, 1 Mar. - 31 Aug. 1989
S. Guha Jul. 1990 49 p Prepared for Midwest Research Inst., Golden, CO
(Contracts DE-AC02-83CH-10093; ZB-7-06003-4)
(DE90-000338; SERI/TP-211-3804) Avail: NTIS HC A03/MF A01

This research program is directed toward the advancement of understanding of amorphous silicon-based alloys and their use in small area multi-junction solar cells. The program is divided into subtasks on materials research, single-junction solar cell research, and multi-junction solar cell research. In this report we discuss progress made during the period from March through August 1989. A major focus of the program was to achieve improvement in the performance of the back reflector and the antireflection coating to optimize cell performance. Computer simulation work was also carried out to analyze performance trade-offs between triple and tandem a-Si alloy solar cells. DOE

N90-28897# Sandia National Labs., Albuquerque, NM. Solar Thermal Test Facility.
EVALUATION OF THE STM4-120 KINEMATIC STIRLING ENGINE
Kevin L. Linker, K. Scott Rawlinson, and Greg Smith 1990 7 p Presented at the 25th Intersociety Energy Conversion Engineering Conference, Reno, NV, 12-17 Aug. 1990
(Contract DE-AC04-76DP-00789)
(DE90-013836; SAND-90-0009C; CONF-900801-23) Avail: NTIS HC A02/MF A01

The Department of Energy's (DOE) Solar Thermal Program has identified the Stirling cycle heat engine as the conversion device for dish-electric systems with the most potential for meeting the program's goals. To advance the technology toward commercialization in a dish-electric system, Sandia National Laboratories has acquired a Stirling Thermal Motors, Inc. kinematic Stirling engine, STM4-120, for evaluation. During the past year this engine has been operating at Sandia's Engine Test Facility. The engine's heat input was provided through fossil fuel combustion and sodium heat pipes, while the output power was absorbed with an eddy-current dynamometer. The evaluation of the engine performance during the past year is presented. DOE

N90-28898# Sandia National Labs., Albuquerque, NM.
UV-INDUCED DEGRADATION OF THE Si-SiO2 INTERFACE: APPLICATIONS TO THE POINT CONTACT SOLAR CELL
W. K. Schubert, J. D. McBrayer, M. E. Buck, and J. W. Tingley 1990 5 p Presented at the 1990 DOE/Sandia Crystalline Photovoltaic Technology Project Review Meeting, Albuquerque, NM, 7-9 Aug. 1990
(Contract DE-AC04-76DP-00789)
(DE90-013843; SAND-90-1767C; CONF-9008124-1) Avail: NTIS HC A01/MF A01

Prior research has concentrated on damage at the Si-SiO2 interface caused by photoinjection of electrons into the oxide by near UV light. The damage processes involved may be similar to those responsible for degradation in the Stanford type, point contact solar cell (PCSC). DOE

N90-28899# Sandia National Labs., Albuquerque, NM. Dept. of Power Sources.
DEVELOPMENT OF THE SODIUM/SULFUR TECHNOLOGY FOR ENERGY STORAGE
Albert Landgrebe (Department of Energy, Washington, DC.) and Nicholas J. Magnani 1990 6 p Presented at the 8th Beta Battery Workshop, Chester, England, 12-18 Jun. 1990
(Contract DE-AC04-76DP-00789)
(DE90-014329; SAND-90-1829C; CONF-9006243-1) Avail: NTIS HC A02/MF A01

The sodium-sulfur programs have focused on progressing core aspects of the technology and completing initial battery engineering for both mobile and stationary applications. An overview of the Office of Energy Management (OEM) activities is presented. Two major development programs were active: the first with Ford Aerospace and Communications Corporation (1975 to 1985), and the second with Chloride Silent Power Limited (1985 to 1990). With the completion this year of the qualification of a cell suitable for initial Solar Energy Systems (SES) applications, the emphasis of future DOE/OEM sodium/sulfur programs will shift to SES-battery engineering and development. The initial effort will resolve a number of issues related to the feasibility of utilizing the sodium/sulfur technology in these large scale applications. This multi-year activity represents an integrated program to produce a commercially viable battery system. DOE

N90-28900# Central Research Inst. of Electric Power Industry, Tokyo (Japan).
A 10kW CLASS MOLTEN CARBONATE FUEL CELL TEST: THE STACK WITH ELECTROLYTE PLATE PREPARED WITH PAPER-MAKING METHOD
Y. Izaki, T. Watanabe, Y. Mugikura, T. Hayasaka, K. Shimazu, T. Hamamatsu, T. Abe, H. Ishikawa, N. Kusunose, and Y. Shundo

Oct. 1989 31 p In JAPANESE; ENGLISH abstract
(DE90-507841; CRIE-W-89012) Avail: NTIS (US Sales Only)
HC A03

In Central Research Institute of Electric Power Industry (CRIEPI) , 10kW class Molten Carbonate Fuel Cell (MCFC) Test Facility has been installed at Yokosuka Laboratory, and operation experiments have been performed. The experimental results are described. An operation experiment of about 250 hours was carried out, using large MCFC stack with the Electrolyte Plate prepared with a Paper Making Method made by Fuji Electric Co. Ltd. The test stack was designed by adopting internal manifold and co-flow type as gas flow structure. It was clarified that high fuel utilization operation is very important, because the energy conversion efficiency depends on fuel utilization ratio. Output power of the stack depends on the partial pressure of oxygen in cathode oxidizing agent gas, but the amount of dependency is not clear. It was recognized that the temperature control for keeping operation without any outside heater is possible, as the amount of producing heat by power generation becomes more than heat loss and gas removal heat at the electric current over 200A (2/3 load). DOE

N90-28901# Central Research Inst. of Electric Power Industry, Tokyo (Japan).
STUDY OF POWER GENERATION SYSTEMS FOR CO2 COLLECTION: LNG COMBINED CYCLE
H. Moritsuka, T. Hamamatsu, and H. Ishikawa Oct. 1989 34 p In JAPANESE; ENGLISH abstract
(DE90-507881; CRIE-W-89016) Avail: NTIS (US Sales Only)
HC A03

Power generation system for CO2 collection was studied. When a pressure swing adsorption method is used to separate CO2 from exhaust gas of conventional power plant (LNG (liquefied natural gas) combined cycle power plant), three stage process is required and 5.1 percent power of total power generation is consumed. For CO2 closed reheat gas turbine combined cycle power generation system where oxygen is used to combust fuel and to avoid nitrogen mixture in exhaust gas by oxygen blow out, net generation efficiency is 36.8 percent owing to oxygen generation and power plant consumtion. For a LNG reformed CO removal combined cycle power generating system where hydrogen is separared from LNG reformed gas to supply to gas turbine and remained CO is combusted in the reformer to collect CO2, net generation efficiency is 38.5 percent after subtracting power to generate oxygen and power consumed in the power plant. For a LNG reformed MC type fuel cell power generation system where LNG is reformed to supply fuel to the MC type fuel cell and oxygen is supplied to oxygen pole, final net generation efficiency becomes 49.2 percent, indicating very high efficiency. DOE

N90-28902 Deutsche Forschungs- und Versuchsanstalt fuer Luft- und Raumfahrt, Cologne (Germany, F.R.).
SOLAR ENERGY FOR HIGH TEMPERATURE TECHNOLOGY AND APPLICATIONS
W. Grasse, M. Becker, and B. Finnstrom (Energy Research Commission, Sweden) 1990 89 p Sponsored by BMFT
(ETN-90-97429) Avail: Fachinformationszentrum Karlsruhe, 7514 Eggenstein-Leopoldschafen 2, Fed. Republic of Germany

Information on the status of solar thermal technology and on the possibilities of its thermal applications is presented. The interactions between solar irradiation and chemical processes, including steam reforming, coal gasification, and hydrogen production, are outlined. The status of solar thermal power generation is described as prerequisite to following considerations. Some characteristic applications of solar thermal energy in chemical processes are given. Technological developments of the receiving and storing elements are explained. Actual work, test facilities, and further planning and results to be obtained are reported. ESA

N90-28903# Deutsche Forschungsanstalt fuer Luft- und Raumfahrt, Stuttgart (Germany, F.R.). Gruppe Solarenergiewandlung.
PERFORMANCE MEASUREMENTS AND ENERGY BALANCE OF AN SPS V160 STIRLING MOTOR AT THE GERMAN AEROSPACE RESEARCH ESTABLISHMENT
Gerold Noyes Feb. 1990 28 p
(DLR-Mitt-90-03; ISSN-0176-7739; ETN-90-97538) Avail: NTIS HC A03/MF A01; DLR, VB-PL-DO, Postfach 90 60 58, 5000 Cologne, Fed. Republic of Germany, HC 13.50 DM

Before conversion to solar operation to serve as a solar receiver test bed, a Stirling Power Systems (SPS) V160F natural gas-fired co-generation stirling motor was tested. A test stand was built and instrumented, and the motor performance was measured under various loads. An energy balance of the motor/generator unit was done including electric output and input, thermal input, waste heat in the cooling water, cooling air, exhaust, radiation and free convection from the motor housing. The influence of the internal cooling water temperature on motor performance was measured. Measurements, including an exhaust gas analysis and surface temperature distribution, were made to determine the combustion chamber efficiency. A magnetic eddy current brake was used to measure the shaft output of the stirling motor and measure the efficiency of the generator. The total natural gas to electric energy conversion efficiency was measured to be 23 percent above 2/3 of full power; 20 percent efficiency was achieved down to 1/3 power. Maximum power was measured at 8.9 kWc. ESA

N90-28904# Tecogen, Inc., Waltham, MA.
OPEN CYCLE HEAT PUMP DEVELOPMENT FOR LOCAL RESOURCE USE. PHASE 2: DISTRICT HEATING CASE STUDY ANALYSIS Final Report, 13 Sep. 1988 - 10 Apr. 1990
K. D. Patch, F. A. DiBella, J. F. Glick, and F. E. Becker Apr. 1990 91 p
(Contract DE-FG01-88CE-26561)
(DE90-011123; DOE/CE-26561/1; TR-4455-038-90) Avail: NTIS HC A05/MF A01

District heating (DH) systems provide thermal energy to their customers in the form of hot water or steam. These systems can use one or more types of heat sources to meet the thermal load, including boilers, cogeneration systems, or low-grade heat sources in conjunction with a heat pump. Most large-scale heat pumps operate using the closed-cycle concept and usually use a chlorinated fluorocarbon (CFC) as the working fluid. An alternative to this approach is the quasi open-cycle heat pump, which was first studied in a Phase 1 report entitled, Open-Cycle Heat Pump Development for Local Resource Use, DOE/CE/26563-5. The quasi open-cycle (QOC) heat pump actually uses the district heating transport medium as its working fluid. This document is the Final Report prepared as a part of Task 6 of Open-Cycle Heat Pump Development for Local Resource Use, Phase 2 District Heating Case Study Analysis. The objective of this study contract was to assess the application of the QOC heat pump in an actual case study. DOE

N90-28905# Texas A&M Univ., College Station. Dept. of Chemistry.
LIGHTWEIGHT SOLID POLYMER ELECTROLYTE FUEL CELL WITH STACK POWER DENSITY OF 3 kW/lb (7 kW/kg) Interim Report, Jan. - Mar. 1990
D. H. Swan, A. Parthasarathy, O. Velev, S. Srinivasan, and C. R. Martin 6 Jul. 1990 22 p
(Contract N00014-88-K-0389)
(AD-A223964; RF-6035) Avail: NTIS HC A03/MF A01 CSCL 10/3

Data for the physiochemical properties of the Pt/Solid polymer electrolyte interface were obtained using cyclic voltammetry and potential pulse techniques. The oxygen diffusion coefficient in Nafion was determined to be 7.4 x 10(exp -7) sq cm/s. Several single cells were assembled and their performance at different current densities tested. The maximum power density achieved was 1.4W/sq cm with a 50 microns thick membrane and electrodes with high Pt loading at 90 C and pressure of 5 atm. A design for

a fuel cell stack is proposed meeting the requirements for 7W/kg specific power density. The current collectors are from gold plated titanium. High flow rate of oxygen will be used in order to achieve high heat transfer rate between the stack and the gas flow as well as removal of the product water. GRA

45 ENVIRONMENT POLLUTION

Includes atmospheric, noise, thermal, and water pollution.

N90-28906*# National Aeronautics and Space Administration. Langley Research Center, Hampton, VA.
THE DISTRIBUTION OF MIDDLE TROPOSPHERIC CARBON MONOXIDE DURING EARLY OCTOBER 1984
Henry G. Reichle, Jr., Vickie S. Connors, H. Andrew Wallio, J. Alvin Holland, Robert T. Sherrill, Joseph C. Casas, and Barbara B. Gormsen (ST Systems Corp., Hampton, VA.) [1989] 49 p
(NASA-TM-103485; NAS 1.15:103485) Avail: NTIS HC A03/MF A01 CSCL 13B

The distribution of middle tropospheric carbon monoxide measure by the Measurement of Air Pollution from Satellites (MAPS) instrument carried aboard the space shuttle is reported. The data represent average mixing ratios in the middle troposphere and are presented in the form of maps that show the carbon monoxide mixing ratios averaged for 6 days of the mission. Comparisons with concurrent, direct measurements taken aboard aircraft show that the inferred concentrations are systematically low by from 20 to 40 percent depending upon which direct measurement calibration standard is used. The data show that there are very large CO sources resulting from biomass burning over South America and southern Africa. Measured mixing ratios were high over northeast Asia and were highly variable over Europe. Author

N90-28907# Office of Science and Technology, Washington, DC.
OUR CHANGING PLANET: THE FY 1991 US GLOBAL CHANGE RESEARCH PROGRAM. A REPORT BY THE COMMITTEE ON EARTH SCIENCES TO ACCOMPANY THE FY 1991 BUDGET
Jan. 1990 71 p
(PB90-202623) Avail: NTIS HC A04/MF A01 CSCL 13B

Although the Earth has been changing for millions of years, dramatic recent changes such as antarctic ozone depletion demonstrate that human activities are affecting the Earth system. Because of the high priority attached to the U.S. Global Change Research Program, the President is proposing $1,034 million for the research effort in the FY 1991 budget, a $374.8 million or 57 percent increase over the FY 1990 level. Summarized here are the key features and budget of the proposed U.S. Global Change Research Program for FY 1991. A more detailed FY 1991 research plan will be released in the spring of 1990. GRA

N90-28908# Environmental Protection Agency, Research Triangle Park, NC. Office of Air Quality Planning and Standards.
NATIONAL AIR POLLUTANT EMISSION ESTIMATES, 1940-1988 Final Report
Mar. 1990 74 p
(PB90-199266; EPA/450/4-90/001) Avail: NTIS HC A04/MF A01 CSCL 13B

Estimates of trends in nationwide air pollutant emissions for six major pollutants: particulate (PM/TSP), sulfur oxides, nitrogen oxides, reactive volatile organic compounds, carbon monoxide, and lead are given. Estimates are provided for major categories of air pollution sources. A short analysis of emission trends is given, along with a discussion of methods used to develop the data. GRA

N90-28909# Environmental Protection Agency, Research Triangle Park, NC. Office of Air Quality Planning and Standards.
NATIONAL AIR QUALITY AND EMISSIONS TRENDS REPORT, 1988
T. C. Curran, R. Faoro, T. Fitz-Simons, N. Frank, and W. Freas Mar. 1990 153 p
(PB90-200114; EPA/450/4-90/002) Avail: NTIS HC A08/MF A01 CSCL 13B

National and regional trends in air quality from 1979 through 1988 for total suspended particulate, sulfur dioxide, carbon monoxide, nitrogen dioxide, ozone and lead are presented. Air pollution trends were also examined for the 5-year period (1984 to 1988). Both national and regional trends in each of these pollutants are examined. National air quality trends are also presented for both the National Air Monitoring Sites (NAMS) and other site categories. In addition to ambient air quality, trends are also presented for annual nationwide emissions. The emissions are estimated using the best available engineering calculations; the ambient levels presented are averages of direct measurements. Also included is a section on levels in Metropolitan Statistical Areas (MSAs). Its purpose is to provide interested members of the air pollution control community, the private sector and the general public with greatly simplified air pollution information. Air quality statistics are presented for each of the pollutants for all MSAs with data in 1988. GRA

N90-28910# National Inst. of Standards and Technology, Gaithersburg, MD. Center for Fire Research.
LONG-RANGE PLAN FOR A RESEARCH PROJECT ON CARBON MONOXIDE PRODUCTION AND PREDICTION
William M. Pitts Oct. 1989 45 p
(PB90-209602; NISTIR-89/4185) Avail: NTIS HC A03/MF A01 CSCL 13B

A five-year plan for the Center for Fire Research (CFR) Priority Research Project on Carbon Monoxide Prediction is given. Sections of the report provide a justification for the priority project, assess the current state of knowledge, summarize current relevant CFR research efforts, discuss specific research needs, list major assumptions utilized in formulating the research program, outline a research plan designed to meet the goals of the project and address the specific research needs, provide a rough timetable and budget, and present a discussion of the project philosophy and management. GRA

N90-28911# Colorado State Univ., Fort Collins. Dept. of Atmospheric Science.
THE ROLE OF CLOUDS IN CO2-INDUCED CLIMATE CHANGE Technical Progress Report, Sep. 1989 - Jul. 1990
David A. Randall 1990 15 p
(Contract DE-FG02-89ER-69027)
(DE90-014380; DOE/ER-69027/T1) Avail: NTIS HC A03/MF A01

This three year project includes the following tasks: continue participation in the Department of Energy's General Circulation Model (GCM) Intercomparison Project, study the response of a one-dimensional coupled ocean-atmosphere model to changes in CO2, analyze cloud forcing simulations with the CSU GCM by comparison with observations from ISCCP, FIRE, and ERBE, perform CO2 sensitivity studies with a X-flux version of the CSU model, and begin a long term project to couple the CSU model with a global ocean model, in preparation for more definitive CO2 sensitivity studies. DOE

N90-28912*# National Aeronautics and Space Administration. Marshall Space Flight Center, Huntsville, AL.
ATMOSPHERIC ENVIRONMENT FOR SPACE SHUTTLE (STS-32) LAUNCH
G. L. Jasper and G. W. Batts (Computer Sciences Corp., Huntsville, AL.) Mar. 1990 41 p
(NASA-TM-100400; NAS 1.15:100400) Avail: NTIS HC A03/MF A01 CSCL 13B

A summary of selected atmospheric conditions observed near space shuttle STS-32 launch time on January 9, 1990, at Kennedy

Space Center, Florida, are presented. Values of ambient pressure, temperature, moisture, ground winds, visual observations (clouds), and winds aloft are included. The sequence of pre-launch Jimsphere-measured vertical wind profiles is also presented. The final atmospheric tape, which consists of wind and thermodynamic parameters versus altitude, for STS-32 vehicle ascent was constructed. The STS-32 ascent atmospheric data tape was constructed to provide an internally consistent data set for use in postflight performance assessments and represents the best estimate of the launch environment that was traversed by the STS-32 vehicle. Author

N90-28913*# National Aeronautics and Space Administration. Marshall Space Flight Center, Huntsville, AL.
ATMOSPHERIC ENVIRONMENT FOR SPACE SHUTTLE (STS-31) LAUNCH
G. L. Jasper and G. W. Batts (New Technology, Inc., Huntsville, AL.) Jun. 1990 46 p
(NASA-TM-103508; NAS 1.15:103508) Avail: NTIS HC A03/MF A01 CSCL 13B

A summary of selected atmospheric conditions observed near space shuttle STS-31 launch time on April 24, 1990, at Kennedy Space Center, Florida, are presented. Values of ambient pressure, temperature, moisture, ground winds, visual observations (clouds), and winds aloft are included. The sequence of pre-launch Jimsphere-measured vertical wind profiles is also presented. The final atmospheric tape, which consists if wind and thermodynamic parameters versus altitude, for STS-31 vehicle ascent was constructed. The STS-31 ascent atmospheric data tape was constructed to provide an internally consistent data set for use in postflight performance assessments and represent the best estimated of the launch environment to the 400,000 feet altitude that was traversed by the STS-31 vehicle. Author

N90-28914*# National Aeronautics and Space Administration. Marshall Space Flight Center, Huntsville, AL.
ATMOSPHERIC ENVIRONMENT FOR SPACE SHUTTLE (STS-36) LAUNCH
G. L. Jasper and G. W. Batts (Computer Sciences Corp., Huntsville, AL.) May 1990 43 p
(NASA-TM-100403; NAS 1.15:100403) Avail: NTIS HC A03/MF A01 CSCL 13B

A summary of selected atmospheric conditions observed near space shuttle STS-36 launch time on February 28, 1990, at Kennedy Space Center, Florida was presented. STS-36 carried a Department of Defense payload and the flight azimuth is not known. Values of ambient pressure, temperature, moisture, ground winds, visual observations (cloud), and winds aloft are included. The sequence of pre-launch Jimsphere-measured vertical wind profiles is given. The final atmospheric tape, which consists of wind and thermodynamic parameters versus altitude, for STS-36 vehicle ascent was constructed. The STS-36 ascent atmospheric data tape was constructed to provide an internally consistent data set for use in postflight performance assessments and represent the best estimate of the launch environment to the 400,000 feet altitude that was traversed by the STS-36 vehicle. Author

N90-28915*# National Aeronautics and Space Administration. Marshall Space Flight Center, Huntsville, AL.
ATMOSPHERIC ENVIRONMENT FOR SPACE SHUTTLE (STS-34) LAUNCH
G. L. Jasper and G. W. Batts (Computer Sciences Corp., Huntsville, AL.) Dec. 1989 44 p
(NASA-TM-100396; NAS 1.15:100396) Avail: NTIS HC A03/MF A01 CSCL 13B

A summary of selected atmospheric conditions observed near space shuttle STS-34 launch time on October 18, 1989, at Kennedy Space Center, Florida is presented. Values of ambient pressure, temperature, moisture, ground winds, visual observations (clouds), and winds aloft are included. The sequence of pre-launch Jimsphere-measured vertical wind profiles is given. The final atmospheric tape, which consists of wind and thermodynamic parameters vs. altitude, for STS-34 vehicle ascent was constructed to provide an internally consistent data set for use in post-flight performance assessments. It represents the best estimates of the launch environment to the 400,000 feet altitude that was traversed by the STS-34 vehicle. Author

N90-28916# Environmental Protection Agency, Cincinnati, OH. Risk Reduction Engineering Lab.
OZONE FOR TRACE ORGANIC CONTAMINANT REMOVAL
B. W. Lykins and W. E. Koffskey (Jefferson Parrish Dept. of Public Utilities, LA.) 1990 16 p Presented at the IOA Conference, Shreveport, LA, 27-29 Mar. 1990
(PB90-221680; EPA/600/D-90/016) Copyright Avail: NTIS HC A03/MF A01 CSCL 13B

Many drinking water utilities have recently changed or are seriously considering changing from disinfection with chlorine to some alternative disinfectant as a result of regulations to control trihalomethanes. Many of the water utilities that have changed to alternative disinfectants have done so without evaluating possible chemical impacts or health effects associated with the alternative disinfectant. Therefore, a research project was initiated at Jefferson Parish, Louisiana to evaluate these effects. Ozone was one of the alternative disinfectants evaluated. During the one year research study at Jefferson Parish, raw river water from the Mississippi River was pumped to the full-scale plant where it was clarified with diallyldimethyl ammonium chloride or dimethylamine-type cationic polymers. After fluoridation, but before disinfection, a portion of the clarified water was filtered through pressure sand filters before going to a 10 gallon-per-minute pilot plant. GRA

N90-28917# East Anglia Univ., Norwich (England).
CHASING A SPECTER: RISK MANAGEMENT FOR GLOBAL ENVIRONMENTAL CHANGE
Timothy ORiordan and Steve Rayner (Oak Ridge National Lab., TN.) Oct. 1989 19 p Presented at the International Workshop on Understanding Global Environmental Change, Worcester, 11-13 Oct. 1989
(Contract DE-AC05-84OR-21400)
(DE90-014455; CONF-8910434-1) Avail: NTIS HC A03/MF A01

Global environmental change is both a concept and a process that changes in meaning with scientific discovery, public concern, and political responsiveness. It is the relationship between the problems as perceived and the various institutions that help shape and adapt to such problems that defines global environmental change. There is a kind of race between scientific detective work and political adjustment to lessen the likely impacts that predictive science is trying to verify. Risk analysis, because of its capacity to recognize this relationship in many spheres of problem identification, can contribute to the political debate, mostly by proposing institutional redesign of the relationship among scientific research, public entry, and experimental readjustments to consensus formation and international action. This paper discusses the factors involved in global environmental change, the risk management involved, the holistic interpretation, and the environmental impacts. DOE

N90-28918# Argonne National Lab., IL.
RESPONDING TO THE THREAT OF GLOBAL WARMING: OPTIONS FOR THE PACIFIC AND ASIA
David G. Streets, ed. and Toufic A. Siddiqi, ed. 1989 526 p Presented at the Responding To the Threat of Global Warming: Options for the Pacific and Asia, Honolulu, HI, 21-27 Jun. 1989
(Contract W-31-109-eng-38)
(DE90-014756; ANL/EAIS/TM-17; CONF-8906244) Avail: NTIS HC A23/MF A03

The primary goal of the workshop was to explore the options that the countries of the Pacific and Asia have for dealing with the threat of global warming. The countries of the Pacific and Asia must address a variety of issues related to global warming, ranging from determining the advisability of reducing greenhouse-gas emissions to assessing the vulnerability of various communities to the consequences of climate change only adds to

the many other important health and socioeconomic problems they must face. The goal of this workshop was to bring together policy makers, scientists, and analysts who are concerned about the issue of climate change in this region so they could begin to develop information that will help decision makers formulate rational policy alternatives. Four principal areas of discussion: the current state of knowledge about global climate change and its likely consequences; energy policy options for slowing the expected growth in emissions of greenhouse gases; mitigation measures to cope with the impacts (including impacts related to agriculture and sea-level rise), should they occur, and research needs to assist decision makers in the Pacific and Asia. This volume compiles the proceedings of the workshop. DOE

N90-28919# Lawrence Livermore National Lab., CA. Atmospheric and Geophysical Sciences Div.

THE GLOBAL CYCLE OF REACTIVE NITROGEN

J. E. Penner, C. S. Atherton, J. J. Walton, and S. Hameed (State Univ. of New York, Stony Brook.) Jun. 1990 17 p Presented at the International Conference on Global and Regional Environmental Atmospheric Chemistry, Beijing, China, 3-10 May 1990

(Contract W-7405-eng-48)

(DE90-015041; UCRL-JC-104052; CONF-9005252-1) Avail: NTIS HC A03/MF A01

We have simulated the global cycle of reactive nitrogen in a three-dimensional chemistry-transport-deposition model. Our model is a Lagrangian parcel model in which trace species react and are carried in constant-mass air parcels; the parcels are advected by winds calculated by an atmospheric general circulation model (GCM). The GCM calculated winds, clouds, precipitation and other variables at nine levels in the atmosphere with a horizontal resolution of approximately 4.5(degree) latitude and 7.5(degree) longitude. The model includes the basic chemical reactions of NO, NO2, and HNO3 calculated with prescribed distributions of OH and O3. The model predicts atmospheric concentrations of NO(sub x) (NO + NO2) and HNO3 throughout the globe at nine altitudes. In addition, deposition of nitrogen in precipitation and in dry processes is also calculated. We present global maps of calculated atmospheric concentration with emphasis on the surface atmospheric concentration of NO(sub x). Comparisons between calculated and observed atmospheric concentrations and deposition rates are made for several parts of the world. The long-range transport of NO(sub x) is documented from the model by comparing the ratio of surface NO(sub x) concentrations for all sources to those for natural sources only. DOE

N90-28920# Brookhaven National Lab., Upton, NY. Environmental Chemistry Div.

ACID DEPOSITION: NO SUCH THING AS A FREE LAUNCH

Stephen E. Schwartz Jul. 1990 27 p Presented at the The Environment: Global Problems -- Local Solutions, Hempstead, NY, 7-9 Jun. 1990

(Contract DE-AC02-76CH-00016)

(DE90-015085; BNL-44821; CONF-9006249-1) Avail: NTIS HC A03/MF A01

This paper reviews the acid deposition process and outlines the issues of atmospheric science that have made it such a difficult issue on which to achieve consensus. The geographical focus of this review is eastern North America, but the considerations presented here are applicable also to other regions. Acid deposition consists of the delivery of acidic substances from the atmosphere to the earth's surface, principally sulfur and nitrogen oxides, acids, and salts. These compounds (mainly the oxides) are introduced into the atmosphere principally as by-products of fossil fuel combustion. Research on atmospheric processes examines the relations between the rates and spatial distributions of emissions of acidifying substances, the atmospheric concentrations and spatial distributions of these substances and of their atmospheric transformation products, and the rates and spatial distributions of deposition of these materials. The goal of this research is to determine how atmospheric concentrations and deposition fluxes would change in response to specified changes in emissions. Effects research is the study of the consequences of atmospheric concentrations and deposition rates of acidic and related substances on human health, on artificial structural and ornamental materials, on cultivated crops, and on natural terrestrial and aquatic ecosystems. The goal of this research is to determine standards for concentrations and deposition that are suitable for protecting human health and the general welfare from adverse effects of acid deposition. DOE

N90-28921# State Dept., Washington, DC. Bureau of Oceans and International Environmental and Scientific Affairs.

PUERTO RICO WORKSHOP ON LAND-BASED SOURCES OF MARINE POLLUTION IN THE WIDER CARIBBEAN REGION

Apr. 1990 34 p Workshop held in San Juan, Puerto Rico, 7-9 Aug. 1989 Sponsored by National Park Service, Washington, DC; Agency for International Development, Washington, DC; EPA, Washington, DC; and NOAA, Rockville, MD

(PB90-184094) Avail: NTIS HC A03/MF A01 CSCL 13B

The participants in the conference met August 7 to 9, 1989, in San Juan, Puerto Rico. The participants divided the report into four major sections, each succeeding section relying for inputs from the preceding sections. They are: inventory of land-based sources of marine pollution. The inventory, divided into point sources and non-point sources of pollutants, establishes the baseline data for dealing with marine pollution, and the impact of land-based sources of marine pollution. The extent of the impact of pollutants on the ecological and economic life dependent on the marine environment calls for scientific analyses involving the nature of the polluting substances as well as that of the receiving marine areas, development of tropical water quality and effluent standards. Tropical water quality criteria and standards provide essential analytical links between the use of marine waters and the control of marine pollution, and marine pollution control strategy. The means for managing land-based sources of marine pollution can be divided into utilizing marine water quality standards, effluent standards, environmental planning, and best management practices. The authors dealt with only man-made pollution, which is distinct from natural pollution such as oil seepage through ancient fissures in the seabed. GRA

N90-28922# Lawrence Livermore National Lab., CA. Atmospheric and Geophysical Sciences Div.

TROPOSPHERIC NITROGEN: THE INFLUENCE OF ANTHROPOGENIC SOURCES ON DISTRIBUTIONS AND DEPOSITION, EXECUTIVE SUMMARY Final Report

J. E. Penner, C. S. Atherton, and J. J. Walton Jul. 1990 28 p

(Contracts W-7405-eng-48; EPA-DW-89932676-01-0)

(DE90-015401; UCRL-CR-104490-Exec-Summ) Avail: NTIS HC A03/MF A01

Nitrogen oxides are important for global photochemistry because they determine whether O(sub 3) is produced or destroyed. In this paper, we describe our simulations of the global cycle of reactive nitrogen. We use a three-dimensional chemistry-transport-deposition model. Our model is a lagrangian model in which trance species react and are carried in constant-mass air parcels; the parcels are advected by winds calculated by the NCAR Community Climate Model (CCM), a nine-layer general circulation model. In Section 2, we describe the model, together with our specification of the reactive nitrogen sources. A comparison of our predicted concentrations and deposition amounts with measurements appears in Section 3. Section 4 describes our model results for predicted distributions, while Section 5 describes our results for deposition. Section 6 summarizes a regional analysis of sources and deposition. Our conclusions appear in Section 7. DOE

N90-28923# Atmospheric and Environmental Research, Inc., Cambridge, MA.

NATURAL AND ANTHROPOGENIC CLIMATE CHANGE Annual Technical Progress Report, 1 Sep. 1989 - 15 May 1990

W. J. Gutowski, S. A. Clough, G. Molnar, M. Iacono, and W.-C. Wang (State Univ. of New York, Albany.) Jul. 1990 9 p

(Contract DE-FG02-86ER-60485)
(DE90-015528; DOE/ER-60485/3) Avail: NTIS HC A02/MF A01

This report covers work on grant FG02-86ER60485 and consists of two parts: progress for the period 9/1/89 to 5/15/90 and the plan for the remaining period 5/16/90 to 8/31/90. The project includes two tasks: atmospheric radiation and improvement of climate models to evaluate the climatic effects of radiation changes. DOE

N90-28924# Colorado Univ., Boulder. Cooperative Inst. for Research in Environmental Sciences.
DIFFUSION IN THE SURFACE LAYER OF THE CONVECTIVE BOUNDARY LAYER Final Report, 14 Mar. 1988 - 30 Apr. 1990
J. C. Weil 30 Jun. 1990 18 p
(Contract DAAL03-88-K-0036)
(AD-A224125; ARO-25882.3-GS) Avail: NTIS HC A03/MF A01 CSCL 07/2

Dispersion in the planetary boundary layer (PBL) is important in a variety problems including air pollution and obscurant cloud behavior in a battlefield environment. Dispersion is a stochastic phenomena caused by the random or stochastic nature of PBL turbulence, and the fluctuating concentration field often is as important as the mean field. Indeed, laboratory measurements show that the root-mean-square (rms) fluctuating concentration, sigma sub c, in plumes from continuous point sources can be 5 times greater than the ensemble-mean concentration C; a similar situation exists in smoke clouds. Thus, sigma sub c, as well as C must be estimated to assess the visibility limits of an obscurant cloud or the air quality effects of a pollution source. Under this program, stochastic dispersion models have been developed for the C and sigma sub c fields due to a passive tracer source in the convective boundary layer (CBL), with the main aim of improving the understanding and predictability of dispersion in that layer. Effects were focused on the CBL because: (1) the PBL is in a convective state a substantial fraction of the time (equivalent 30 to 40 percent), (2) the turbulence structure of the CBL is well documented, and (3) laboratory data and numerical results exist for testing models. Furthermore, dispersion in the CBL cannot be modeled by the standard statistical or eddy-diffusion theories because of the complications caused by the CBL turbulence. GRA

N90-28925*# Bionetics Corp., Cocoa Beach, FL.
FLORA AND THREATENED AND ENDANGERED PLANTS OF JOHN F. KENNEDY SPACE CENTER, FLORIDA
Paul A. Schmalzer and C. Ross Hinkle 20 Aug. 1990 75 p
(Contracts NAS10-10285; NAS10-11624)
(NASA-TM-102791; NAS 1.15:102791; BIO-2) Avail: NTIS HC A04/MF A01 CSCL 13B

The vascular flora of the Kennedy Space Center (KSC) area was first studied in the 1970's. Nomenclatural and taxonomic changes as well as additional collections required revision of this list. The revised list includes 1045 taxa of which 850 are native and 195 are introduced. This appears to be a substantial proportion of the regional flora. Forty six taxa are endemic or nearly endemic to Florida, a level of endemism that appears high for the east coast of central Florida. Seventy three taxa (69 native) are listed as threatened, endangered, or of special concern on Federal or state lists. Taxa of special concern occur in all major habitats, but many are restricted to hammocks and hardwood swamps that constitute a minor proportion of the terrestrial vegetation. For some of these taxa, populations on KSC appear to be important for their regional and global survival. The bryophyte flora of the KSC area include 23 mosses and 20 liverworts and hornworts. The lichen flora is currently unknown. Author

46 GEOPHYSICS

Includes aeronomy; upper and lower atmosphere studies; ionospheric and magnetospheric physics; and geomagnetism.

For space radiation see *93 Space Radiation.*

N90-28926# National Inst. of Standards and Technology, Gaithersburg, MD.
GENESIS OF BOW ECHOES: A REAR-INFLOW INDUCED MESO-CONVECTIVE STRUCTURE Ph.D. Thesis
M. L. Weisman 1990 167 p Prepared in cooperation with Pennsylvania State Univ., University Park
(Grant NSF ATM-87-09659)
(PB90-209776; NCAR/CT-125) Avail: NTIS HC A08/MF A01 CSCL 04A

The goal is to use idealized simulations of bow echoes, achieved through the use of a nonhydrostatic numerical cloud model, to discern the important physical mechanisms responsible for their behavior, and to identify the environmental conditions most conducive to their development. In the process, the author demonstrates that the bow echo represents a unique stage in the evolution of a convective system that occurs only for a limited set of environmental conditions: in particular, large amounts of thermodynamic instability and strong low-level vertical wind shear. The primary factors giving rise to the structure are a convectively-induced elevated rear inflow jet, which develops in response to strong buoyancy gradients at the back edge of the convective system, and cyclonic and anticyclonic vortices at the northern and southern ends of the convective line segment, which develop in response to the tilting of the horizontal vorticity inherent in the ambient vertical wind shear. The elevated rear inflow is focused between these vortices and interacts with the cold pool and ambient vertical wind shear to produce a quasi-steady, bow-shaped updraft along the system's leading edge. The author reviews the observations and numerical modeling results that have motivated the study of the bow echo as a distinct meso-convective entity. GRA

N90-28927# National Oceanic and Atmospheric Administration, Boulder, CO. Wave Propagation Lab.
REMOTE ATMOSPHERIC PROFILING SYSTEMS FOR TROPOSPHERIC MONITORING
J. C. Kaimal Jan. 1990 79 p
(Contract ASL-89-8025)
(PB90-216789; NOAA-TM-ERL-WPL-175) Avail: NTIS HC A05/MF A01 CSCL 04A

A growing need to replace in situ sounding systems currently used in many tropospheric applications with a mobile remote sensing system using a combination of ground and satellite-based technologies is addressed. The performance characteristics of both the proven technologies and the new systems are reviewed to determine how they can be combined effectively. An assessment of cost vs. risk is given and several options for combined systems are proposed. GRA

N90-28928# National Oceanic and Atmospheric Administration, Oak Ridge, TN. Atmospheric Turbulence and Diffusion Div.
ESTIMATING THE SPATIAL VARIABILITY OF TRACE GAS DEPOSITION VELOCITIES
R. T. McMillen Mar. 1990 44 p Prepared in cooperation with National Acid Precipitation Assessment Program, Washington, DC Sponsored by Environmental Protection Agency, Washington, DC
(PB90-208570; NOAA-TM-ERL-181) Avail: NTIS HC A03/MF A01 CSCL 04A

Dry deposition of gaseous and particulate materials constitutes a significant fraction of the total acidic deposition. Dry deposition measurements are difficult to obtain and are usually available only for a single location. An understanding of the spatial variability of dry deposition is fundamental to extending site-specific measurements to subregional and regional scales. The study estimates the spatial variability of the dry deposition velocity over three 84 km by 84 km study areas by use of a deposition velocity

model. Inputs to the model consist of meteorology, land use type, and terrain roughness. Meteorological data were available from an ongoing dry deposition research program; terrain and land use data were derived from U.S. Geological Survey (USGS) Digital Elevation Models and LANDSAT Thematic Mapper data, respectively. Model run results are presented for one month's data at one site and for 12 weekly averages at all three sites. Verification of the technique is presented, but only at a single point. GRA

N90-28929*# National Aeronautics and Space Administration, Washington, DC.
PRESENT STATE OF KNOWLEDGE OF THE UPPER ATMOSPHERE 1990: AN ASSESSMENT REPORT Report to the Congress
R. T. Watson, M. J. Kurylo, M. J. Prather, and F. M. Ormond Sep. 1990 145 p
(NASA-RP-1242; NAS 1.61:1242) Avail: NTIS HC A07/MF A01 CSCL 04A

NASA is charged with the responsibility to report on the state of the knowledge of the Earth's upper atmosphere, particularly the stratosphere. Part 1 of this report, issued earlier this year, summarized the objectives, status, and accomplishments of the research tasks supported under NASA's Upper Atmosphere Research Program during the last two years. New findings since the last report to Congress was issued in 1988 are presented. Several scientific assessments of the current understanding of the chemical composition and physical structure of the stratosphere are included, in particular how the abundance and distribution of ozone is predicted to change in the future. These reviews include: a summary of the most recent international assessment of stratospheric ozone; a study of future chlorine and bromine loading of the atmosphere; a review of the photochemical and chemical kinetics data that are used as input parameters for the atmospheric models; a new assessment of the impact of Space Shuttle launches on the stratosphere; a summary of the environmental issues and needed research to evaluate the impact of the newly re-proposed fleet of stratospheric supersonic civil aircraft; and a list of the contributors to this report and the science assessments which have formed our present state of knowledge of the upper atmosphere and ozone depletion. Author

N90-28930# Rensselaer Polytechnic Inst., Troy, NY. Dept. of Mathematical Sciences.
SOUND PROPAGATION THROUGH ATMOSPHERIC TURBULENCE: A LITERATURE SUMMARY
I. W. Schurman, W. L. Siegmann, M. J. Jacobson, and C. G. Orio 18 Jun. 1990 32 p
(Contract DAAG60-90-M-1463)
(RPI-Math-184) Avail: NTIS HC A03/MF A01 CSCL 04A

A summary of literature dealing with sound propagation through atmospheric turbulence is presented. Fundamental components of the general problem include turbulence modeling, sound propagation through turbulence, and methodologies for handling sound-turbulence interaction. Key words which provide particularly illuminating discussions of these components are referenced and primary results are briefly described. Whenever possible, implications for the frequency range 10 to 250 Hz are emphasized. Future goals are outlined. Author

N90-28931 Texas A&M Univ., College Station.
PLANETARY-SCALE FLOW ON A TWO-LAYER BETA-PLANE CHANNEL MODEL WITH TOPOGRAPHY Ph. D. Thesis
Won-Tae Kwon Shin 1989 136 p
Avail: Univ. Microfilms Order No. DA9015581

A two-layer low-order spectral model on a beta-plane channel with topographic, thermal, and frictional forcing is designed as a compromise to resolve the relative importance and interaction of several relevant processes. The model is truncated at three zonal modes and three meridional modes. Topography forces the largest scale; the intermediate scale may be destabilized by zonal thermal forcing; the smallest scale permits barotropic scale-interaction and a rudimentary energy cascade. Multiple steady states of the simple one zonal mode and one wave mode (the 1 x 1 model) were found. There are seven possible steady states: a zonally symmetric state, a topographically resonant state, and five baroclinic and equivalent barotropic wave states. New results emphasize relevance of the barotropic and baroclinic zonal flows; most significantly, multiple steady states exist only for a restricted range of zonal wind and vertical shear in the vicinity of the topographically resonant values. The time-dependent behavior for the 3 x 3 model is classified into six different types: zonally symmetric, steady wave state, steady propagating (Rossby wave), periodic, quasi-periodic and chaotic solutions. The regimes of the solutions for three parameters (thermal forcing, topography, and friction) are investigated. Dissert. Abstr.

N90-28932 Reading Univ. (England).
A NONHYDROSTATIC NUMERICAL MODEL IN SIGMA-COORDINATES AND SIMULATIONS OF MESOSCALE PHENOMENA Ph.D. Thesis
Ming Xue 1989 274 p
Avail: Univ. Microfilms Order No. BRDX88621

A nonhydrostatic mesoscale numerical model is developed and simulations of various mesoscale phenomena using this model are described. The model is based on a quasi-nonhydrostatic equation system in the normalized pressure-sigma coordinates. The system is free of vertical sound waves but contains Lamb wave modes which are significantly retarded in nonhydrostatic regime. An integration time step comparable to that of an anelastic model system can be used when grid length is around a few kilometers. The current model includes also parameterized micro-physical processes. The solution procedure of the model is analogous to that of an anelastic system in terrain-following height-coordinates. An elliptic equation has to be solved for the geo-potential height perturbation. Conventional finite differencing techniques are used except in the advection of thermodynamical variables, where the flux-corrected transport scheme (FCT) is employed. FCT eliminates the problem of negative water generation and significantly improves the model accuracy. Radiative conditions are applied at the lateral boundaries, and at the upper boundary radiative condition is simulated by an absorbing layer. Subgrid scale turbulence is parameterized using the deformation and Richardson number dependent formulation. Three water phases, i.e., water vapor, cloud water and rain water, are present in the model with Kessler's microphysics parameterizations being adopted. A number of two dimensional mesoscale problems are studied using the model. They include, dry and moist gravity waves and related phenomena in stratified air streams flowing over a 2-D ridge, long-lived squall line systems and deep orographic convection. Dissert. Abstr.

N90-28933*# Alabama Univ., Huntsville.
GRAVITY WAVE INITIATED CONVECTION
R. J. Hung 24 Sep. 1990 130 p
(Grant NAGw-1165)
(NASA-CR-186868; NAS 1.26:186868) Avail: NTIS HC A07/MF A01 CSCL 04A

The vertical velocity of convection initiated by gravity waves was investigated. In one particular case, the convective motion-initiated and supported by the gravity wave-induced activity (excluding contributions made by other mechanisms) reached its maximum value about one hour before the production of the funnel clouds. In another case, both rawinsonde and geosynchronous satellite imagery were used to study the life cycles of severe convective storms. Cloud modelling with input sounding data and rapid-scan imagery from GOES were used to investigate storm cloud formation, development and dissipation in terms of growth and collapse of cloud tops, as well as, the life cycles of the penetration of overshooting turrets above the tropopause. The results based on these two approaches are presented and discussed. Author

N90-28934# Royal Aerospace Establishment, Farnborough (England). Dept. of Space.
MEASUREMENTS OF THE SINGLE EVENT UPSET ENVIRONMENT IN THE UPPER ATMOSPHERE
C. S. Dyer, A. J. Sims, J. Farren, and J. Stephen (United Kingdom Atomic Energy Authority, Harwell, England) 23 Nov. 1989 13 p
(RAE-TM-Space-373; BR113427; ETN-90-97528) Copyright Avail: NTIS HC A03/MF A01

Regular flights of a cosmic radiation environment monitor on-board supersonic transport enable mapping of the atmospheric environment to 60,000 ft. The CREAM (Cosmic Radiation Effects and Activation Monitor) packages are described. Thirty Concorde flights between London (England) and New York (U.S.) were analyzed. The routes are shown. Results show the importance of secondary particles produced by nuclear reactions into the atmosphere. ESA

N90-28935# National Oceanic and Atmospheric Administration, Boulder, CO. Space Environment Lab.
A RADIO FREQUENCY USER'S GUIDE TO THE SPACE ENVIRONMENT SERVICES CENTER GEOPHYSICAL ALERT BROADCASTS
David A. Rosenthal and Joseph W. Hirman Jun. 1990 26 p
(PB90-240631; NOAA-TM-ERL-SEL-80) Avail: NTIS HC A03/MF A01 CSCL 04A

The National Oceanic and Atmospheric Administration's hourly short-wave radio bulletins provide continually updated information on solar-activity-induced effects on the near-Earth space environment. Bulletins are 45 seconds or less in duration and contain a large amount of useful data. The User's Guide explains the standardized format and terminology of the bulletins. Specific terms are highlighted in bold type the first time they occur, and are defined in an appendix. Author

N90-28936# Woods Hole Oceanographic Inst., MA.
DRILLING THE OCEANIC LOWER CRUST AND MANTLE: A GLOBAL STRATEGY FOR EXPLORING THE DEEP OCEANIC CRUST AND MANTLE IN THE 1990'S
Nov. 1989 123 p Presented at the JOI/USSAC Workshop, Woods Hole, MA, 7-10 Mar. 1989 Sponsored by President's Science Advisory Committee, Washington, DC
(PB90-240953; WHOI-89-39) Avail: NTIS HC A06/MF A01 CSCL 08G

The workshop was convened to follow up on the Second Conference on Scientific Ocean Drilling (COSOD II) to devise a specific plan for deep crustal and mantle drilling over the next decade. Since COSOD II, however, there have been several developments which have had major impact on planning for this drilling. These include new and evolving models for volcanic segmentation at ocean ridges, a growing appreciation that faulting and deformation are an integral feature of the ocean crust, and the recent successful drilling during Ocean Drilling Project Leg 118 into a tectonically exposed section of layer 3 at Site 735B at the Atlantis II Fracture Zone in the Indian Ocean. The community has come to realize that while obtaining complete penetration of the crust at a few sites remains a critical goal for ocean drilling, these will be inadequate to characterize a heterogeneous ocean crust. Thus, in order to evaluate fully crustal composition and structure, crustal drilling must include both an ongoing attempt to attain total crustal penetration, and a major program to drill offset partial sections of the deep layers of the crust and their critical contacts. Accordingly, this workshop has formulated a global strategy for using drilling to systematically study an ocean crust whose composition and structure is laterally variable and changes with spreading rate and tectonic setting. Author

N90-28937# Brookhaven National Lab., Upton, NY.
A PRELIMINARY ARM (ATMOSPHERIC RADIATION MEASUREMENTS) GUIDE FOR CLIMATIC EVALUATIONS
Robert M. Brown Mar. 1990 63 p
(Contract DE-AC02-76CH-00016)
(DE90-015135; BNL-44770) Avail: NTIS HC A04/MF A01

This guide was made to assist in the task of selecting sites for the Atmospheric Radiation Measurements (ARM) study. It is a preliminary attempt to provide mean annual and seasonal meteorological data that might be useful in initial climatic evaluations. It is not a finished product and will be added to in time to give other important information on parameters such as standard deviations, percent of means and times, and other variances. In order to cover the spectrum of climatic factors to be considered, this generalized climatic guide was established from various publications to provide a diversified set of basic meteorological data that exists. To comply with other site selection restrictions, this guide covers only the United States, except for the material at the end on Koppens World Climate Classification. It is anticipated that a similar guide will be made to cover the world's climate at a later date. DOE

47 METEOROLOGY AND CLIMATOLOGY

Includes weather forecasting and modification.

N90-28938# National Weather Service, Washington, DC. Climate Analysis Center.
PROCEEDINGS OF THE 14TH ANNUAL CLIMATE DIAGNOSTICS WORKSHOP
Mar. 1990 501 p Workshop held in La Jolla, CA, 16-20 Oct. 1989
(PB90-198573) Avail: NTIS HC A22/MF A03 CSCL 04B

The Fourteenth Annual Climate Diagnostics Workshop was hosted by the Experimental Forecast Center at the Scripps Institution of Oceanography, in La Jolla, CA. The Proceedings provide a published record of the presentations made at the Workshop. The Workshop had sessions on the following topics: observed atmospheric responses to the 1986 to 1988 Pacific warm/cold evolution, numerical modeling of the El Nino Southern Oscillation (ENSO) phenomenon, atmospheric oscillations, atmospheric variability, ocean-atmosphere interaction from an observational perspective, climate monitoring, climatic variability from a modeling perspective, prediction on climatic time scales, aspects of predictability on climatic time scales, long-range prediction activities at operational forecast centers, and regional climatic studies. GRA

N90-28939# National Oceanic and Atmospheric Administration, Boulder, CO. Wave Propagation Lab.
TROPOSPHERIC WIND PROFILING USING RADAR INTERFEROMETRY: A FEASIBILITY STUDY OF A COMPACT MOBILE SYSTEM
Richard J. Lataitis, Steven F. Clifford, and Peter T. May (Colorado Univ., Boulder.) Feb. 1990 37 p
(Contract ASL-89-8025)
(PB90-217068; NOAA-TM-ERL-WPL-177) Avail: NTIS HC A03/MF A01 CSCL 04B

The authors compare the feasibility of using three-beam Doppler, Spaced-Antenna (SA), and Imaging Doppler Interferometer (IDI) techniques for tropospheric wind profiling at 400 MHz. The SA and IDI methods appear to be the most suited for a compact mobile system because narrow beams and therefore large antennas are not required. The SA technique is a proven technology in the troposphere at 50 MHz. An extension to a 400 MHz system appears to be straight forward. They found the IDI technique for measuring tropospheric winds at 400 MHz to be a particularly promising through yet unproven technology. Advantages include a potential capability of high resolution imaging of the wind field in the radar volume not attainable by the SA method. Disadvantages include the necessity for having several highly localized and persistent scattering centers in the volume, and the inherently low effective signal-to-noise ratios associated with the shorter dwell times needed to locate to detect the scatterers, which result in higher power requirements. Under ideal conditions, they expect uncertainties in the IDI wind estimates to be comparable to those obtained with the SA technique. GRA

N90-28940# National Weather Service, Fort Worth, TX. Scientific Services Div.
AN INVESTIGATION OF FORCING MECHANISMS DURING A SURPRISE TORNADIC THUNDERSTORM
Joseph A. Rogash (National Weather Service, Memphis, TN.) Apr. 1990 37 p
(PB90-216805; NOAA-TM-NWS-SR-128) Avail: NTIS HC A03/MF A01 CSCL 04B

On June 2, 1989 a tornado formed in the Missouri bootheel near the Arkansas border at a time and place where no severe weather was expected. The occurrence of the event was a surprise due to the existence of environmental conditions typically considered unfavorable for thunderstorm rotation. These included a vertical wind profile lacking both the speed and directional changes with height found conducive to mesocyclone formation. Thunderstorms were triggered in a convectively unstable air mass by convergence along a weak surface front with further lifting provided by lower level differential heating with respect to surrounding areas. Remote sensing of the thunderstorm during its tornadic phase strongly suggest it was a nonsupercell type. Thus, the tornado may have formed when the storm updraft converged and stretched positive relative vorticity which pre-existed near the intersection of the front and a weak surface trough. GRA

N90-28941# Westinghouse Hanford Co., Richland, WA.
DAILY TEMPERATURE, SOLAR RADIATION, WIND SPEED, CLOUD COVER, AND PRECIPITATION DATA RECORDED AT THE METEOROLOGICAL STATION FOR CALENDAR YEARS 1957–1988
W. A. Skelly Jun. 1990 257 p
(Contract DE-AC06-87RL-10930)
(DE90-014399; WHC-MR-0165) Avail: NTIS HC A12/MF A02

Daily values of maximum, minimum, and dew point temperature; wind speed; cloud cover; solar radiation; and precipitation measured at the Hanford Meteorological Station from January 1, 1957 to December 31, 1988 are presented. DOE

N90-28942# Oregon State Univ., Corvallis.
ANNUAL COURSE OF PRECIPITATION OVER MUCH OF THE US: OBSERVED VERSUS GCM SIMULATION
R. P. Neilson, G. A. King, J. Lenihan, and R. L. DeVelice (Montana Natural Heritage Program, Helena.) 1990 11 p Proceedings of the PACLIM (Pacific Climate) Workshop, Pacific Grove, CA, Mar. 1989 Sponsored by Corvallis Environmental Research Lab., OR Prepared in cooperation with NSI Technology Services Corp., Corvallis, OR
(Contract EPA-68-C8-0006)
(PB90-221656; EPA/600/D-90/019) Copyright Avail: NTIS HC A03/MF A01 CSCL 04B

General Circulation Models (GCMs) are being increasingly used to estimate the ecological impacts of global climatic change. The authors analyzed seasonal weather patterns over the conterminous USA and determined that regional patterns of rainfall seasonality appear to control the distributions of the major biomes of the country. These regional patterns were compared to the output from three GCMs for validation. The models appear to simulate the appropriate seasonal climates in the northern tier of states. However, the spatial extent of these regions is distorted. None of the models accurately portrayed the necessary seasonal rainfall patterns in the southern tier of states, where biomes are primarily influenced by the Bermuda High. GRA

N90-28943# National Severe Storms Lab., Norman, OK.
[PROGRAM ON DEVELOPMENT OF BASIC UNDERSTANDING OF SEVERE WEATHER PHENOMENA] Annual Report, period ending Dec. 1989
Dec. 1989 76 p
(PB90-226564) Avail: NTIS HC A05/MF A01 CSCL 04B

The National Severe Storms Laboratory (NSSL) conducts a broad program of research to develop basic understanding of severe weather phenomena, including the large and mesoscale environments that evolve and interact to produce intense storms. The focus is upon observational and theoretical studies of hazardous, middle latitude weather phenomena such as tornadoes, hailstorms, lightning, windstorms, floods, and blizzards. Sophisticated numerical models are often employed as research tools. The Laboratory's research projects provide sound scientific foundations upon which improvements to NOAA's weather and climate forecasting services may be built. NSSL participates in field programs and special projects intended to demonstrate or improve capabilities to detect, forecast, and warn of hazardous weather events. GRA

N90-28944# Geological Survey, Trenton, NJ.
A CONCEPTUAL WEATHER-TYPE CLASSIFICATION PROCEDURE FOR THE PHILADELPHIA, PENNSYLVANIA AREA Water-Resources Investigations Report
Gregory J. McCabe, Jr. 1990 30 p
(PB90-231705; USGS/WRI-89-4183) Avail: NTIS HC A03/MF A01 CSCL 04B

A simple method of weather-type classification, based on a conceptual model of pressure systems that pass through the Philadelphia, Pennsylvania, area, was developed. The only inputs required for the procedure are daily mean wind direction and cloud cover, which are used to index the relative position of pressure systems and fronts to Philadelphia. Daily mean wind-direction and cloud-cover data recorded at Philadelphia, Pennsylvania, from January 1954 through August 1988 were used to categorize daily weather conditions. The conceptual weather types reflect changes in daily air and dew-point temperatures, and changes in monthly mean temperature and monthly and annual precipitation. The weather-type classification produced by using the conceptual model was similar to a classification produced by using a multivariate statistical classification procedure. GRA

N90-28945# Instituto de Pesquisas Espaciais, Sao Jose dos Campos (Brazil).
AUTOMATED SYSTEM FOR METEOROLOGICAL ANALYSIS M.S. Thesis [SISTEMA AUTOMATIZADO DE ANALISE METEOROLOGICA]
Carlos HoShihNing Jun. 1988 145 p In PORTUGUESE; ENGLISH summary
(INPE-4586-TDL/332) Avail: NTIS HC A07/MF A01

An integrated system is presented for automatic analyses of meteorologic fields, for the purpose of being used in an advanced center of short (24 up to 72 hours) and medium (3 up to 10 days) range weather forecasting. The system covers all phases of preprocessing of meteorologic information, with special emphasis on objective analysis, although it can also be of practical use in subjective forecasting. Message decoding (SHIP, SYNOP, TEMP, PILOT, and GRID), tests of quality control, and the application of objective analysis schemes to data irregularly distributed are discussed in detail. A set of graphics subroutines built in the system is used to display the analyzed field for ready interpretation of the results in the case of the subjective forecasting or for validation of meteorological fields used as input data in numerical models. The whole work is characterized by: modularity in terms of system structure, so to help an easy inclusion and/or modification of the routines separately; and portability concerning other computer systems, because all the coding is written in FORTRAN. It's expected that this system will replace the whole process of manual elaboration or weather maps, after adequately and systematically being tested on an experimental basis. Author

N90-28946# Institut National des Sciences de l'Univers, Paris (France). Lab. d'Aerologie.
STUDY OF THE RELATIONSHIPS BETWEEN RADAR STRUCTURE AND THE ELECTRICAL ACTIVITY OF CLOUDS [ETUDE DES RELATIONS ENTRE LA STRUCTURE RADAR ET L'ACTIVITE ELECTRIQUE DES NUAGES]
Henri Sauvageot Dec. 1989 13 p In FRENCH
(Contract DRET-87-1170)
(ETN-90-97488) Avail: NTIS HC A03/MF A01

The three dimensional localization of the electrical discharges during storms is studied. Acquisition and processing of data from a millimeter wave and polarimetric radar is presented. The main

purpose of the study campaign was to determine the physical conditions associated with lightning propagation in clouds. The study shows that the main difficulties for accurate measurements come from the synchronization between radar beam orientation and lightning phenomena. ESA

N90-28947# Centre National d'Etudes Spatiales, Toulouse (France).
WIND LIDAR FOR BEST [LIDAR VENT DE BEST]
G. Chalon and J.-P. Sage Apr. 1990 58 p In FRENCH; ENGLISH summary
(CNES-NT-125; ETN-90-97506) Copyright Avail: NTIS HC A04/MF A01

The design of a four fixed telescope wind lidar for the BEST (Bilan Energetique du Systeme Tropical) space mission is presented. The fixed viewing geometry is chosen to avoid a complex system for dynamically compensating the temporal variation of lag angle and to provide the possibility of averaging lidar shots. Atmospheric effects on laser propagation are briefly described and considerations about pulsed CO2 laser and heterodyne detection package are given. Error and power budgets were simulated and different signal processing methods analyzed. The wind measurement accuracy is 3 m/s with a 6 joule pulsed laser, a 4 P processing and for a 5 times 10 to the power of minus 11/m.sr backscatter coefficient. With increased backscatter, accuracy can reach 1.5 m/s in the tropospheric boundary layer. ESA

N90-28948# National Weather Service, Fort Worth, TX. Scientific Services Div.
SEVERE THUNDERSTORM FORECASTING: AN OPERATIONAL REVIEW
Larry H. Eblen, Judson W. Ladd, and Thomas M. Hicks (National Weather Service, San Antonio, TX.) Jul. 1990 51 p
(PB90-215484; NOAA-TM-NWS-SR-130) Avail: NTIS HC A04/MF A01 CSCL 04B

A brief survey of pertinent literature regarding severe thunderstorm structure, detection and forecasting is given. It is organized so as to simulate the methodology or approach an average forecaster might take in preparing for and actually working on a severe thunderstorm event. The main group targeted by the publication and the planned final version is the new forecaster or intern whose knowledge of severe thunderstorm structure and forecasting may be quite limited. However, it is recognized that recent advances in the science can take their toll on experienced forecasters as well. GRA

N90-28949# Instituto de Pesquisas Espaciais, Sao Jose dos Campos (Brazil).
VORTICITY BALANCE STUDY FOR A TROPICAL REGION, DURING THE SOUTHERN HEMISPHERE SUMMER M.S. Thesis [UM ESTUDO DO BALANCO DE VORTICIDADE, PARA A REGIAO TROPICAL, DURANTE O VERAO DO HEMISFERIO SUL]
Celso Valim GomesMarinho Aug. 1988 82 p In PORTUGUESE; ENGLISH summary
(INPE-4634-TDL/336) Avail: NTIS HC A05/MF A01

Vorticity balance over the tropical region is examined during the Southern Hemisphere summer. Data obtained with the integration of a two-layer baroclinic model and data from the tropical operational objective analyses of the National Meteorological Center (NMC), are used. Absolute vorticity advection, by the divergent wind plays an important role as a vorticity source for Rossby waves in the tropical region. Although, the model limitations do not allow the observation of energy propagation from lower to higher latitudes, the final results suggest that the divergent circulation plays a relevent role in the meridional energy transport. Author

N90-28950# International Centre for Theoretical Physics, Trieste (Italy).
ON THE DYNAMICS OF SEVERE THUNDERSTORMS
M. Abdel Wahab (Alfateh Univ., Tripoli, Libya) Sep. 1989 11 p Submitted for publication
(DE90-627922; IC-89/244) Avail: NTIS (US Sales Only) HC A03/MF A01

A detailed study of widespread thunderstorm activity occurring in winter over the central and coastal parts of Egypt (Cairo 30 N, Marsa Matruh 31 N) is presented. The storm activity is associated with strong positive vorticity in the 300/200 mb layer. The maximum kinetic energy was located at the storm center. The divergent wind component was found to be very important in energy transformation and it is a major cause for energy generation by cross contour flow. DOE

N90-28951*# National Aeronautics and Space Administration. Marshall Space Flight Center, Huntsville, AL.
MESOSCALE LIGHTNING EXPERIMENT (MLE): A VIEW OF LIGHTNING AS SEEN FROM SPACE DURING THE STS-26 MISSION
O. H. Vaughan, Jr. Jul. 1990 64 p
(NASA-TM-103513; NAS 1.15:103513) Avail: NTIS HC A04/MF A01 CSCL 04B

Information on the data obtained from the Mesoscale Lightning Experiment flown on STS-26 is provided. The experiment used onboard TV cameras and a 35 mm film camera to obtain data. Data from the 35 mm camera are presented. During the mission, the crew had difficulty locating the various targets of opportunity with the TV cameras. To obtain as much data as possible in the short observational timeline allowed due to other commitments, the crew opted to use the hand-held 35 mm camera. Author

48 OCEANOGRAPHY

Includes biological, dynamic, and physical oceanography; and marine resources.

For related information see also *43 Earth Resources and Remote Sensing.*

N90-28952# National Oceanic and Atmospheric Administration, Washington, DC. Oceanography.
OCEANOGRAPHIC DATA EXCHANGE, 1988
R. E. Moffatt, E. G. Trammell, C. L. Sazama, and C. L. Forgy Dec. 1989 48 p
(PB90-232596; WDCA-OC-89-2) Avail: NTIS HC A03/MF A01 CSCL 08C

The oceanographic data exchange activities of World Data Center A (WDC-A), Oceanography during 1988 are discussed. Included are tabulations of data received during 1988, as well as summarizations of oceanographic station data, bathythermograph data, biological observations, and surface and subsurface current measurements received prior to 1988. International data inventory forms received by the Center are also summarized. Data and inventory forms received are tabulated by nation, ship, cruises, and types of format and observation as appropriate. Quantities of data, publications, and information supplied to other nations and international organizations are also tabulated. Author

N90-28953# Universite de Toulon et du Var (France). Lab. de Sondages Electromagnetiques de l'Environnement Terrestre.
DETECTION OF OCEAN INNER WAVES BY SYNTHETIC APERTURE RADAR: OBSERVATIONS AT GIBRALTAR PASS Final Report [TELEDETECTION DES ONDES INTERNES OCEANIQUES PAR RADAR A OUVERTURE SYNTHETIQUE. OBSERVATIONS DANS LE DETROIT DE GIBRALTAR, RAPPORT FINAL]
Philippe Forget and Pascale Bouruet-Aubertot Oct. 1989 118 p In FRENCH
(Contract DRET-87-1171)
(ETN-90-97477) Avail: NTIS HC A06/MF A01

The results of the image analysis of ocean inner waves by Synthetic Aperture Radar (SAR) remote sensing are discussed. The SAR data allows the morphological description of the phenomenon and, together with other information sources, the physical properties. The hydrodynamic effects contained in SAR

imagery as part of the acquired data are discussed. The interaction mechanisms between radar and ocean waves is studied. The parameters limiting the use of SAR images are underlined. The obtaining of high quality imagery is examined. ESA

N90-28954# Chesapeake Research Consortium, Inc., Gloucester Point, VA.
PERSPECTIVES ON THE CHESAPEAKE BAY, 1990: ADVANCES IN ESTUARINE SCIENCES
Michael Haire, comp. and Elizabeth C. Krome, comp. Apr. 1990 104 p Sponsored by EPA, Annapolis, MD
(PB90-248600; CBP/TRS-41/90) Avail: NTIS HC A06/MF A01 CSCL 08C

Coastal ecosystem models and the Chesapeake Bay Program; the functional role of estuarine benthos; role of best management practices in restoring the health of the Chesapeake Bay and developing an ecological risk assessment strategy for the Chesapeake Bay are discussed. GRA

N90-28955# Lamont-Doherty Geological Inst., Palisades, NY.
ROSS SEA OCEANOGRAPHIC DATA, 1983-1987: USCGC GLACIER, JANUARY-FEBRUARY 1983; USCGC POLAR SEA, JANUARY-FEBRUARY 1984; USCGC POLAR STAR, FEBRUARY 1984; USCGC POLAR SEA, FEBRUARY 1987
S. S. Jacobs, W. E. Haines, J. L. Ardai, and P. A. Mele 1989 480 p Sponsored in part by NSF, and DOE
(PB90-243932; LDGO-89-5) Avail: NTIS HC A21/MF A03 CSCL 08C

Oceanographic data collected in the Ross Sea from the U.S. Coast Guard icebreakers GLACIER (GL 83), POLAR SEA (PS 84 and PS 87), and POLAR STAR (ST 85) from January 1983 through February 1987 is included. The observations included continuous vertical profiles of temperature and salinity vs. depth (CTD data), temperature vs. depth (XBT data), and serial measurements of salinity, dissolved oxygen, silicate, phosphate, nitrate, chlorofluorocarbons, carbon dioxide and alkalinity. Most data were taken as part of the Ross Sea Heat Flux Experiment. The scientific objective of the program has been to better understand the ocean circulation on the Ross Sea continental shelf in relation to the sea ice, glacial ice and deep ocean ventilation. GRA

N90-28956# Applied Research Lab., State College, PA.
FACTORIZATION OF THE CHARACTERISTIC EQUATION FOR THREE LAYER DUCTS
E. B. Brosius and D. F. McCammon Jul. 1990 91 p
(Contract N00039-88-C-0051)
(AD-A223867; APL/PSU-TR-90-008) Avail: NTIS HC A05/MF A01 CSCL 08/3

The characteristic equation for a lossy three-layer ocean model is complex and transcendental and thus requires numerous, lengthy iterations to determine its eigenvalues. Factoring the equation, made possible by the introduction of a small error term, provides new equations that are quickly and easily solved. The eigenvalues of the simplified equations are examined and compared with those of the original characteristic equation for two water/sediment/bedrock models. The first model treats all three layers as liquids which can propagate only compressional waves. The second model represents both the sediment and bedrock layers as elastic materials which support the propagation of shear waves in addition to compressional waves. For the all-liquid model, the factored solutions showed too much mode attenuation compared to the exact solutions. A different type of factor was developed that had eigenvalues closer to the exact eigenvalues. The liquid/elastic/elastic model factored solutions also predicted too much loss, but no correction was found. GRA

N90-28957# Naval Underwater Systems Center, West Palm Beach, FL.
MEASURING THE VERTICAL DIRECTIONAL SPECTRA CAUSED BY SEA SURFACE SOUND
R. M. Kennedy 24 May 1990 29 p Presented at the 119th Acoustical Society of America Meeting, State College, PA, 24 May 1990
(AD-A223883; NUSC-TD-8733) Avail: NTIS HC A03/MF A01 CSCL 20/1

The objective of these measurements is the development of a database of directional spectra obtained in an acoustically isolated area (Tongue of the Ocean, The Bahamas) where the acoustic ambient is principally controlled by the local (observable) sea surface conditions. The purpose of the database is the identification of a model of the space-time statistics of sea surface sound. A wideband (40 to 4000 Hz) vertical acoustic linear antenna system was used. Data logging took place in a remote, autonomously operating subsurface buoy system. Recording restrictions limited each of the seven octavely nested apertures of the sensor system to four wavelengths. However, quite adequate spatial resolutions of the directional spectral estimates were obtained using a physically based parametric model of the random process. Results of the initial two-month deployment (wind speed range of 2 to 16 m/s) are discussed. The measured directional spectra are displayed as a function of frequency, elevation angle, and surface friction velocity. The sea surface sound source structure is discussed. GRA

51 LIFE SCIENCES (GENERAL)

N90-28958# Commerce Dept., Washington, DC. Japanese Technical Literature Program.
JAPANESE MOLECULAR BIOLOGY 1990: AN UPDATE
R. B. Wickner 1990 49 p
(PB90-188707) Avail: NTIS HC A03/MF A01 CSCL 06B

A series of summaries of the recent and current work of a number of selected top labs in molecular biology in Japan is given. Most of the work covered is not only important as basic science, but has important implications for applications. Separate brief discussions are included of the Human Genome Project, of the Human Frontiers Science Program and of some general observations on factors likely to influence the future course of the relative scientific situations in Japan and the U.S. Also presented is a summary of some of the work presented at the 12th Annual Meeting of the Japanese Society for Molecular Biology (November 29 to December 2, 1989) which the author attended during the laboratory visits in Japan. GRA

N90-28959*# Miriam Hospital, Providence, RI. Dept. of Pathology.
COMPUTER AIDED MECHANOGENESIS OF SKELETAL MUSCLE ORGANS FROM SINGLE CELLS IN VITRO
Herman H. Vandenburgh, Somporn Swasdison (Alabama Univ., Birmingham.), and Patricia Karlisch 1990 21 p
(Grant NAG2-414)
(NASA-CR-187025; NAS 1.26:187025) Avail: NTIS HC A03/MF A01 CSCL 06C

Complex mechanical forces generated in the growing embryo play an important role in organogenesis. Computerized application of similar forces to differentiating skeletal muscle myoblasts in vitro generate three dimensional artificial muscle organs. These organs contain parallel networks of long unbranched myofibers organized into fascicle-like structures. Tendon development is initiated and the muscles are capable of performing directed, functional work. Kinetically engineered organs provide a new method for studying the growth and development of normal and diseased skeletal muscle. Author

N90-28960*# Miriam Hospital, Providence, RI. Dept. of Pathology.
INSULIN AND INSULIN-LIKE GROWTH FACTOR-1 INDUCE PRONOUNCED HYPERTROPHY OF SKELETAL MYOFIBERS IN TISSUE CULTURE
Herman H. Vandenburgh, Patricia Karlisch, and Janet Shansky 1990 40 p

(Grant NAG2-414)
(NASA-CR-187026; NAS 1.26:187026) Avail: NTIS HC A03/MF A01 CSCL 06C

Skeletal myofibers differentiated from primary avian myoblasts in tissue culture can be maintained in positive nitrogen balance in a serum-free medium for at least 6 to 7 days when embedded in a three dimensional collagen gel matrix. The myofibers are metabolically sensitive to physiological concentrations of insulin but these concentrations do not stimulate cell growth. Higher insulin concentrations stimulate both cell hyperplasia and myofiber hypertrophy. Cell growth results from a long term 42 percent increase in total protein synthesis and a 38 percent increase in protein degradation. Myofiber diameters increase by 71 to 98 percent after 6 to 7 days in insulin-containing medium. Insulin-like growth factor-1 but not insulin-like growth factor-2, at 250 ng/ml, is as effective as insulin in stimulating cell hyperplasia and myofiber hypertrophy. This model system provides a new method for studying the long-term anabolic effects of insulin and insulin-like growth factors on myofiber hypertrophy under defined tissue culture conditions. Author

N90-28961# Total Army Personnel Agency (Provisional), Alexandria, VA.
A DESIGN TOOL UTILIZING STOICHIOMETRIC STRUCTURE FOR THE ANALYSIS OF BIOCHEMICAL REACTION NETWORKS Final Report M.S. Thesis - Wisconsin Univ., Madison
Stephen Edward Kelly 20 May 1990 173 p
(AD-A223873) Avail: NTIS HC A08/MF A01 CSCL 06/1

A method is proposed for the analysis of possible distributions of products in biochemical reaction networks using linear optimization techniques. Software to assist in the conduct of this analysis was developed. Several biochemical systems were analyzed to examine the effects of different constraining situations. Software was developed to simplify and reduce the manual data manipulation needed to conduct this analysis. The software consists of two major components: a specially constructed database and a commercial linear optimization package. The database program was constructed to store and manipulate information on chemical species and on the reactions involving them. The database can assemble information about many reactions to form a stoichiometric model of a reaction network. The solution provides information on the overall reaction the network performs as well as the relative rates of the individual reactions within the network. Several biochemical reaction networks were examined. A proposed pathway for the biosynthetic production of astaxanthin, a natural red pigment was analyzed. Penicillin production was examined for the effects of various carbon and reduction/oxidation limits. The production of 1,3-propanediol (1,3-PD) was examined with the pathway for 1,3-PD overlaid onto the general metabolic pathways of Escherichia coli. GRA

52 AEROSPACE MEDICINE

Includes physiological factors; biological effects of radiation; and effects of weightlessness on man and animals.

N90-28962# Midwest Research Inst., Kansas City, MO.
FURTHER STUDIES OF 60 Hz EXPOSURE EFFECTS ON HUMAN FUNCTION Quarterly Report No. 4, 1 Apr. - 30 Jun. 1990
Charles Graham and Harvey D. Cohen 20 Jul. 1990 7 p
(Contract DE-FG01-89CE-34025; MRI Proj. RA-111-C)
(DE90-014377; DOE/CE-34025/T4) Avail: NTIS HC A02/MF A01

Public concern has been expressed about possible health risks arising from exposure to the electric and magnetic fields generated by power distribution systems. This project is addressing this concern through a laboratory research program designed to evaluate the effects of brief exposure to known field conditions on multiple measures of human function. In this continuation effort, a series of exploratory studies are being performed, which will be followed by a confirmatory experiment, to determine if the above physiological effects differ as a function of exposure to the electric and magnetic fields separately and combined, time of day, and rate of intermittent exposure. Project status to date is as follows. An initial series of exploratory studies, involving 24 healthy male volunteers exposed over multiple sessions, was completed. These studies assessed whether effects on human physiology differ over the day as a function of intermittent exposure to the electric vs. the magnetic fields. Exposure to the magnetic fields produced a pattern of cardiac changes similar to that observed in our previous research. This pattern was not found when subjects were exposed to the electric field. Goals were to: continue performance of the probe studies; and present project findings at the 1990 meeting of the Bioelectromagnetics Society (BEMS). DOE

N90-28963* National Aeronautics and Space Administration, Washington, DC.
AEROSPACE MEDICINE AND BIOLOGY: A CONTINUING BIBLIOGRAPHY WITH INDEXES (SUPPLEMENT 340)
Feb. 1989 64 p
(NASA-SP-7011(340); NAS 1.21:7011(340)) Avail: NTIS HC A03; NTIS standing order as PB90-912300, $11.50 domestic, $23.00 foreign CSCL 06E

This bibliography lists 157 reports, articles and other documents introduced into the NASA Scientific and Technical Information System during August 1990. Subject coverage includes: aerospace medicine and psychology, life support systems and controlled environments, safety equipment, exobiology and extraterrestrial life, and flight crew behavior and performance. Author

N90-28964# Bordeaux 2 Univ. (France). U.F.R. des Sciences Medicales.
CARDIOVASCULAR DECONDITIONING OF COSMONAUTS: ROLE, IMPORTANCE AND APPLICATIONS OF THE LOWER BODY NEGATIVE PRESSURE Ph.D. Thesis [LE DECONDITIONNEMENT CARDIO VASCULAIRE CHEZ LES COSMONAUTES: ROLES, INTERETS ET APPLICATIONS DU LOWER BODY NEGATIVE PRESSURE]
Laurent Labreze 1990 178 p In FRENCH Original contains color illustrations
(ETN-90-97507) Avail: NTIS HC A09/MF A01

Microgravity effects on the cardiovascular system of cosmonauts are investigated. Experiments using the lower body negative pressure system are performed. Modifications in the cardiovascular system when the body is placed under microgravity conditions are studied. The consequences of the cardiovascular deconditioning syndrome under normal gravity conditions are examined. Special attention is given to the orthostatic intolerance. The importance of the lower body negative pressure device in future space missions is underlined. ESA

N90-28965*# National Aeronautics and Space Administration. Ames Research Center, Moffett Field, CA.
JOINT US/USSR STUDY: COMPARISON OF EFFECTS OF HORIZONTAL AND HEAD-DOWN BED REST
Harold Sandler and Anatoli I. Grigoriev (Institute of Biomedical Problems, Moscow, USSR) Washington Aug. 1990 102 p
(NASA-TP-3037; A-85177; NAS 1.60:3037) Avail: NTIS HC A06/MF A01 CSCL 06S

An account is given of the results of the first joint U.S./U.S.S.R. bed rest study. The study was accomplished in two parts: A soviet part (May to June 1979) and an American part (July to August 1979). Both studies were conducted under identical conditions and provided a basis for comparison of physiologic reactions and standardizing procedures and methods. Each experiment consisted of three periods: 14 days of pre-bed rest control, 7 days of bed rest, and a 10 to 14 day recovery period. Ten males participated in each study, with five subjects experiencing horizontal bed rest and five subjects a -6 deg head-down body position. Biochemical and hormonal measurements were made of blood and urine, with particular attention to electrolyte metabolism and kidney function; cardio-pulmonary changes at rest and exercise; influence of Lower Body Negative Pressure (LBNP); and incremental exercise using

a bicyle ergometer while supine and sitting. Expected moderate changes were noted to occur for various physiologic parameters. Clinical evidence pointed to the fact that head-down bed rest when compared to horizontal conditions more closely matched the conditions seen after manned spaceflight. For the most part, statistically significant differences between the two body positions were not observed. Author

N90-28966# Brookhaven National Lab., Upton, NY.
DNA DAMAGE AND REPAIR IN HUMAN SKIN: PATHWAYS AND QUESTIONS
B. M. Sutherland, H. Hacham, J. C. Sutherland, R. W. Gange, and D. Maytum (Harvard Medical School, Boston, MA.) 1989 12 p Presented at the DNA Damage and Repair in Human Tissues Conference, Upton, NY, 1-4 Oct. 1989 Sponsored in part by Wellman Foundation
(Contract DE-AC02-76CH-00016)
(DE90-015126; BNL-44839; CONF-8910354-2; BIO-4595) Avail: NTIS HC A03

Skin is assaulted daily with physical and chemical carcinogens, promoters, and modifiers of biological responses to such agents. DNA is the principal target for most carcinogens, and DNA in skin is particularly at risk. It is subject to damage not only from ingested compounds and their metabolic products, but also from externally applied or encountered chemicals, as well as from physical carcinogens such as sunlight and cosmetic or medical sources of ultraviolet radiation. Three major factors determine the balance between damage to DNA of skin and the biological consequences of that damage: the frequencies and types of lesions, the ability of the individual to repair a lesion, and the strategy that skin employs to deal with the different spectra of lesions inflicted under varying environmental conditions. Thus, cellular responses to DNA damage, including repair of DNA lesions, are critical factors in determining the final level of damage and its consequences. This paper discusses DNA damage and repair in human skin. DOE

N90-28967# School of Aerospace Medicine, Brooks AFB, TX.
DECOMPRESSION SICKNESS PRESENTING AS A VIRAL SYNDROME Final Report
Frederick W. Rudge 1989 8 p
(AD-A223880; USAFSAM-JA-90-22) Avail: NTIS HC A02/MF A01 CSCL 06/5

Decompression sickness (DCS) is a well-known hazard of exposure to significant variations in ambient pressure. The diagnosis and management of DCS is frequently a source of confusion. Although the majority of cases are manifested by joint or limb pains (Type I DCS), patients may present with a wide array of symptoms, such as neurologic deficits, headache, fatigue, nausea, and respiratory difficulty. A thorough knowledge of the differential diagnosis and a strong index of suspicion are crucial to the proper management of DCS. Presented herein are two cases of altitude-related DCS which were confused initially with a viral syndrome. A discussion of the symptoms of DCS is included. GRA

N90-28968# Naval Health Research Center, San Diego, CA.
PREVALENCE OF HYPERTENSION AMONG ACTIVE DUTY PERSONNEL Interim Report
D. Stephen Nice and Linda Kelly Trent 13 Apr. 1990 20 p
(AD-A223892; NHRC-90-5) Avail: NTIS HC A03/MF A01 CSCL 06/5

The prevalence of uncontrolled hypertension in the Navy was studied. Systolic and diastolic blood pressure readings were collected for 10,866 active duty men and women in conjunction with the Navy's current blood pressure screening program. Mean systolic blood pressure was 118.3 (millimeters of mercury) mmHg; mean diastolic blood pressure was 71.6 mmHg. Blood pressure was elevated in 8.9 percent of the total sample, which is lower than the adjusted rate for the nation at large (about 14 percent). Hypertension was more prevalent among enlisted personnel, older individuals, men, and blacks. The relatively low prevalence of hypertension in the Navy may be related to screening policies at accession and/or the Navy's ongoing health and fitness programs, including exercise, weight control, and nutrition. However, with nearly 1 in 10 sailors exhibiting high blood pressure, it is recommended that the Navy continue its efforts toward a comprehensive program for detection and treatment of hypertension. GRA

N90-28969# Florida Univ., Gainesville. Dept. of Psychology.
COMPLEX AUDITORY SIGNALS Annual Report, 14 Apr. 1989 - 15 Apr. 1990
David M. Green and Bruce G. Berg 13 Jun. 1990 7 p
(Grant AF-AFOSR-0333-88; AF Proj. 2313)
(AD-A224127; AFOSR-90-0749TR) Avail: NTIS HC A02/MF A01 CSCL 25/4

Efforts to understand the perception of complex auditory stimuli produced four different research undertakings. Studies have been done both with computer simulations and human listeners, the most precise psychophysical procedure to estimate a discrimination threshold. A technique to determine the listener's sensitivity to synchrony was perfected in envelope modulation produced at two separate regions, and have measured such sensitivity using a variety of different stimulus parameters. Sensitivity to modulation synchrony is essentially independent of the locus of the two frequency bands. Studies have also been done on temporal factors that influence the ability to discriminate an increment in the level of a single component of a multi-tonal complex. Very slight differences in the temporal onset (greater than 20 msec.) of tone and complex strongly influence the ability to make such discrimination even when the entire stimulus lasts 500 msec. Finally, we continue to study the estimates of spectral weights used in such intensity discrimination tasks. GRA

N90-28970# Loyola Univ., Chicago, IL. Hearing Inst.
AUDITORY PROCESSING OF COMPLEX SOUNDS ACROSS FREQUENCY CHANNELS Annual Technical Report, 1 May 1989 - 30 Apr. 1990
William P. Shofner, Raymond H. Dye, William A. Yost, and Stanley Sheft 24 May 1990 7 p
(Grant AF-AFOSR-0335-89; AF Proj. 2313)
(AD-A224147; AFOSR-90-0754TR) Avail: NTIS HC A02/MF A01 CSCL 06/4

Neurophysiological experiments have been directed at gaining an understanding of how auditory neurons encode pitch related information in the temporal properties of discharge. In general, all physiological neuronal types recorded to date in the chinchilla cochlear nuclea can show periodicities in their discharges that are related to the pitch of harmonic tone complexes, but only those neurons that show phase-locking at best frequency can encode the pitch related information in cost + rippled noise. The results of binaural psychophysical experiments suggest: (1) that spectrally synthetic binaural processing is the rule when the number of components in the tone complex are relatively few (less than 10) and there are no dynamic binaural cues to aid segregation of the target from the background, and (2) that waveforms having large effective envelope depths are on the average more easily lateralized than those having small effective envelope depths. GRA

N90-28987# Hamburg Univ. (Germany, F.R.). Dept. of Eyes.
EXPERIMENTAL TESTS ON THE MINIMAL VISUAL ACUITY REQUIRED FOR SAFE AIR CREW AND AIR CONTROL PERSONNEL PERFORMANCE
J. Draeger and R. Schwartz *In* AGARD, Situational Awareness in Aerospace Operations Apr. 1990 3 p (For primary document see N90-28972 23-53)
Copyright Avail: NTIS HC A09/MF A02; Non-NATO Nationals requests available only from AGARD/Scientific Publications Executive

N90-28991# Institute of Aviation Medicine, Madrid (Spain).
EVALUATION OF THE PERFORMANCE CAPABILITY OF THE AVIATOR UNDER HYPOXIC CONDITIONS OPERATIONAL EXPERIENCE
Francisco Rios Tejada, Luis Marquez delaPlata, Cesar Alonso

Rodriguez, and Juan J. Canton Romero *In* AGARD, Situational Awareness in Aerospace Operations Apr. 1990 6 p (For primary document see N90-28972 23-53)
Copyright Avail: NTIS HC A09/MF A02; Non-NATO Nationals requests available only from AGARD/Scientific Publications Executive

N90-28992# McGill Univ., Montreal (Quebec).
EFFECTS OF SHORT-TERM WEIGHTLESSNESS ON ROLL CIRCULARVECTION
D. G. D. Watt and J. P. Landolt *In* AGARD, Situational Awareness in Aerospace Operations Apr. 1990 6 p Sponsored in part by Medical Research Council of Canada and National Research Council of Canada Prepared in cooperation with Defence and Civil Inst. of Environmental Medicine, Toronto, Ontario (For primary document see N90-28972 23-53)
Copyright Avail: NTIS HC A09/MF A02; Non-NATO Nationals requests available only from AGARD/Scientific Publications Executive

N90-28993# Naval Aerospace Medical Research Lab., Pensacola, FL.
MAINTAINING SPATIAL ORIENTATION AWARENESS
A. Rupert, A. Mateczun, and F. E. Guedry, Jr. *In* AGARD, Situational Awareness in Aerospace Operations Apr. 1990 5 p (For primary document see N90-28972 23-53)
Copyright Avail: NTIS HC A09/MF A02; Non-NATO Nationals requests available only from AGARD/Scientific Publications Executive

53 BEHAVIORAL SCIENCES

Includes psychological factors; individual and group behavior; crew training and evaluation; and psychiatric research.

N90-28971# Rochester Univ., NY. Dept. of Computer Science.
TIME, SPACE AND FORM IN VISION
Jerome A. Feldman Nov. 1988 72 p
(Contract N00014-84-K-0655; NSF DCR-83-20136)
(AD-A213889; TR-244) Avail: NTIS HC A04/MF A01; also avail. as TR-88-011, International Computer Science Inst., 1947 Center St., Suite 600, Berkeley, CA CSCL 23/3

The prodigious spatial capabilities of the primate visual system are even more remarkable when temporal considerations are taken into account. Recent advances in neurophysiology, psychophysics and computer vision provide significant constraints on how the system could work. This paper presents a fairly detailed connectionist computational model of how the perception and recognition of objects is carried out by primate brains. The model is claimed to be functionally adequate and to satisfy all the constraints established by the various disciplines. One key notion introduced is a multi-input, multi-output network for inverting spatio-temporal cues. The central construct in intermediate level vision is taken to be the trajectory and these are used in recognition of dynamic situations called scenarios. The entire development is an extension of the author's 1985 Four Frames model, which required relatively little modification to accommodate temporal change (eventually). GRA

N90-28972# Advisory Group for Aerospace Research and Development, Neuilly-Sur-Seine (France). Aerospace Medical Panel.
SITUATIONAL AWARENESS IN AEROSPACE OPERATIONS
Apr. 1990 200 p In ENGLISH and FRENCH Symposium held in Copenhagen, Denmark, 2-6 Oct. 1989
(AGARD-CP-478; ISBN-92-835-0554-9) Copyright Avail: NTIS HC A09/MF A02; Non-NATO Nationals requests available only from AGARD/Scientific Publications Executive

The Symposium examined aviator situational awareness with consideration of conditions where problems occur, methods to assess situational awareness and latest methods for information management and presentation in the cockpit. Indications for future research needs were discussed. These Proceedings will be of interest to those involved with human perception and cognition and those responsible for design of modern aircraft cockpits. For individual titles, see N90-28973 through N90-28993.

N90-28973# Netherlands Aerospace Medical Centre, Soesterberg.
SPATIAL DISORIENTATION INCIDENTS IN THE RNLAF F16 AND F5 AIRCRAFT AND SUGGESTIONS FOR PREVENTION
A. Kuipers, A. Kappers, C. R. vanHolten, J. H. W. vanBergen, and W. J. Oosterveld (Amsterdam Univ., Netherlands) *In* AGARD, Situational Awareness in Aerospace Operations Apr. 1990 16 p (For primary document see N90-28972 23-53)
Copyright Avail: NTIS HC A09/MF A02; Non-NATO Nationals requests available only from AGARD/Scientific Publications Executive

Controlled flight into terrain caused several accidents within the Royal Netherlands Airforce. Two hundred and nine RNLAF fighter pilots were interviewed to obtain information about the occurrence of spatial disorientation in flight. The incident, which left the greatest impression on each pilot, was analyzed. Thirty-four percent of those incidents is considered by the aviators as a very serious risk for flight safety. The incidents are caused by a combination of factors, of which weather conditions, psychological factors and visual reference are the most important. Visual and vestibular illusions are common, as well as certain psychological conditions which lead to a wrong perception of position or motion. The aspects of the sensation of disorientation are described in detail. All pilots have experienced disorientation in some way and 26 percent report that it has caused one or more narrow escapes. Seventy-three percent of the pilots report a greater susceptibility for disorientation in a F16, compared with other types of aircraft. Suggestions for prevention of disorientation accidents are given. Author

N90-28974# Northrop Corp., Hawthorne, CA. Aircraft Div.
A METHODOLOGY FOR THE OBJECTIVE MEASUREMENT OF PILOT SITUATION AWARENESS
Mica R. Endsley *In* AGARD, Situational Awareness in Aerospace Operations Apr. 1990 9 p (For primary document see N90-28972 23-53)
Copyright Avail: NTIS HC A09/MF A02; Non-NATO Nationals requests available only from AGARD/Scientific Publications Executive

The ability of the pilot to maintain situation awareness is recognized in the pilot community as crucial to mission success and survivability. The design of the pilot vehicle interface must therefore be guided by the goal of maintaining and enhancing pilot situation awareness. A formal definition of situation awareness is presented in addition to a detailed description of the Situation Awareness Global Assessment Technique (SAGAT). SAGAT was developed as an objective measure of a pilot's situation awareness, including pilot knowledge of ownship status, the tactical environment, his overall comprehension of the situation, and his ability to project the tactical situation into the near future. SAGAT allows for a variety of system design concepts to be evaluated on the basis of situation awareness, as well as workload and performance, thus providing the design community with a much needed tool. Author

N90-28975# Royal Air Force Inst. of Aviation Medicine, Farnborough (England).
SITUATIONAL AWARENESS RATING TECHNIQUE (SART): THE DEVELOPMENT OF A TOOL FOR AIRCREW SYSTEMS DESIGN
R. M. Taylor *In* AGARD, Situational Awareness in Aerospace Operations Apr. 1990 17 p (For primary document see N90-28972 23-53)
Copyright Avail: NTIS HC A09/MF A02; Non-NATO Nationals requests available only from AGARD/Scientific Publications Executive

Human engineering activities in aircrew system design

traditionally were concerned with the reduction and management of operator workload. Recent advances in automation technology have radically changed the role of the human operator and highlighted the essential human function for making adaptive decisions in situations involving uncertainty. Improving and enhancing operator situational awareness has become the major crew station design driver for achieving survivability and mission effectiveness criteria. How aircrew understand situational awareness (SA) is investigated and tools were developed for its subjective estimation. Author

N90-28976# Aerospace Medical Research Labs., Wright-Patterson AFB, OH. Human Engineering Div.
PERFORMANCE-BASED MEASURES OF MERIT FOR TACTICAL SITUATION AWARENESS
Michael Venturino, William L. Hamilton, and Stephen R. Dvorchak (Hamilton and Associates, Las Vegas, NV.) *In* AGARD, Situational Awareness in Aerospace Operations Apr. 1990 5 p (For primary document see N90-28972 23-53)
Copyright Avail: NTIS HC A09/MF A02; Non-NATO Nationals requests available only from AGARD/Scientific Publications Executive

Pilot situation awareness is not a well-understood concept. Most attempts at understanding situation awareness have relied almost exclusively on subjective reports, and have not led to a clear understanding of the concept. A performance based approach to assessing situation awareness, where the relationship between pilot-reported situation awareness and tactical task performance is investigated is represented. Aspects of a high realism air combat simulation were analyzed in terms of a priori hypotheses regarding performance of a tactical task (fire point selection), its relation to pilot-reported situation awareness, and its relation with mission outcome. Results showed that pilot-reported situation awareness by itself was not a reliable indicator of pilot performance (based on mission outcome). Further, pilot performance by itself was not systematically related to fire point selection. Only when the simultaneous operation of pilot performance, fire point selection, and pilot-reported situation awareness are considered does a systematic relationship emerge. The highest mission performance scores were associated with both a FPS within a preferred zone (80 to 100 percent RMAX2) and high pilot-reported SA ratings. Lower performance scores were observed as pilots' FPS diverged from the preferred FPS area and reported lower SA scores. The drop-off in mission performance is more severe when pilots launched their weapons inside the 80 to 100 percent RMAX2 area relative to launching outside this preferred area. These findings are interpreted in terms of fire point selection as one potential measure of merit for tactical situation awareness. Author

N90-28977# Royal Air Force Inst. of Aviation Medicine, Farnborough (England).
EVALUATION OF THE SITUATIONAL AWARENESS RATING TECHNIQUE (SART) AS A TOOL FOR AIRCREW SYSTEMS DESIGN
S. J. Selcon and R. M. Taylor *In* AGARD, Situational Awareness in Aerospace Operations Apr. 1990 8 p (For primary document see N90-28972 23-53)
Copyright Avail: NTIS HC A09/MF A02; Non-NATO Nationals requests available only from AGARD/Scientific Publications Executive

The Situational Awareness Rating Technique (SART) was developed as an evaluation tool for aircrew systems design. SART provides subjective estimates of attentional Demand and Supply, and ratings of Understanding, which are postulated to be the three primary components of situational awareness. While consistent with contemporary theories of cognition, the application of SART requires knowledge of performance. SART sensitivity seems likely to depend on the contribution of skill, rule, and knowledge based behavior, and on the role of explicit and implicit knowledge in the candidate task situation. An evaluation of SART in three aircrew systems design studies with different task requirements is reported: (1) Multiple Task Compatibility Study; (2) Attitude Recovery/Attention-Switching Study; and (3) Warnings Comprehension Study. SART Demand, Supply, and Understanding ratings showed significant effects of experimental manipulations in all three studies. The relevance of the specific SART components was related to the contribution of skill, rule, and knowledge based behavior to the tasks. The SART ratings also highlighted weaknesses in the performance measures and improved their interpretation. Thus, in combination with performance measures, SART provides a powerful tool for aircrew system design. Author

N90-28978# Aerospace Medical Research Labs., Wright-Patterson AFB, OH. Human Engineering Div.
ATTENTION GRADIENTS IN SITUATION AWARENESS
Martin L. Fracker *In* AGARD, Situational Awareness in Aerospace Operations Apr. 1990 10 p (For primary document see N90-28972 23-53)
Copyright Avail: NTIS HC A09/MF A02; Non-NATO Nationals requests available only from AGARD/Scientific Publications Executive

A model of how people develop and maintain awareness was explored in a series of four experiments. These experiments focused on the role of attention allocation in situation awareness. All four experiments supported the hypothesis that attention is limited in supply contrary to recently proposed unlimited supply theories. Unlimited supply theories do not predict attention gradients in which more attention is allocated to some things than to others. Spatial awareness data from all four experiments showed that more attention was paid to enemy aircraft that directly threatened the subject than was paid to other aircraft. Experiment 2 showed that the resulting attention gradient steepened as enemy number increased: when attentional demand was increased by increasing the total number of aircraft, subjects seemed to increase the amount of attention paid to direct threats by reallocating attention previously paid to other aircraft. Experiments 3 and 4 provided additional support for the reallocation hypothesis by showing that less attention was paid to individual neutral aircraft when the number of enemy aircraft increased (even though the total number of aircraft had not changed). These data suggest that attention is allocated to objects based on the degree to which they threaten or can assist the subject's task performance. Author

N90-28979# Royal Aerospace Establishment, Farnborough (England).
TOWARDS A FUTURE COCKPIT: THE PROTOTYPING AND PILOT INTEGRATION OF THE MISSION MANAGEMENT AID (MMA) **c54**
C. P. Gibson and A. J. Garrett (British Aerospace Public Ltd. Co., Kingston-upon-Thames, England) *In* AGARD, Situational Awareness in Aerospace Operations Apr. 1990 9 p (For primary document see N90-28972 23-53)
Copyright Avail: NTIS HC A09/MF A02; Non-NATO Nationals requests available only from AGARD/Scientific Publications Executive

The Mission Management Aid (MMA) Joint Venture (MMAJV) is a three phase program, the objectives of which are to: (1) establish the functional requirements and feasibility of a device(s) such as the MMA; (2) to prove the techniques for accomplishing this in a rapid prototyping environment and produce a set of functional specifications; and (3) to optimize the MMA functionality and develop the MMI on a real time Mission Capable Simulation (MCS). With the ever increasing trend towards complex integrated avionics systems and the increased level and capability of threat anticipated in future hostile scenarios, the requirement for the pilot of the single seat aircraft to maximize his situational awareness at all times must be one of the prime issues in driving the development of such systems. The requirement is outlined for the MMA and the major functional areas of sensor fusion, situation assessment, dynamic planning and the Man-Machine Interface are introduced. Some of the Human Factors issues associated with the introduction of an intelligent Mission Management Aid (MMA) and the increasing need to promote situational awareness are discussed. Issues relating to the design requirements and evaluation of such systems are also discussed. Author

N90-28980# School of Aerospace Medicine, Brooks AFB, TX. Crew Technology Div.
THE THREE-DIMENSIONAL STRUCTURE OF VISUAL ATTENTION AND ITS IMPLICATIONS FOR DISPLAY DESIGN **c54**

Fred H. Previc *In* AGARD, Situational Awareness in Aerospace Operations Apr. 1990 7 p (For primary document see N90-28972 23-53)
Copyright Avail: NTIS HC A09/MF A02; Non-NATO Nationals requests available only from AGARD/Scientific Publications Executive

The ability to direct attention toward far visual space while maintaining good spatial orientation is imperative for pilots of high performance fighter aircraft. In actuality, this task is quite similar to that performed during such everyday activities as reaching and locomotion. A theoretical analysis of the three-dimensional (3-D) structure of visual attention and its involvement in normal perceptual activities leads to the conclusion that far attention is: (1) biased toward the upper right visual field; (2) associated with saccadic scanning confined to the central 30 degs of the visual field; and (3) primarily utilized in performing local perceptual processes. In properly designed aircraft displays, then, far attention can be encouraged both by restricting local perceptual analyses to certain regions of the visual field, and by enabling attitude control to be performed using more global (ambient) mechanisms. Author

N90-28981# Central Electricity Generating Board, Gloucester (England).
A REAL TIME EVALUATION OF THE USE OF A PERSPECTIVE FORMAT TO PROMOTE SITUATIONAL AWARENESS IN USERS OF AIR TO AIR TACTICAL DISPLAYS Abstract Only **c54**

D. Ridley *In* AGARD, Situational Awareness in Aerospace Operations Apr. 1990 1 p (For primary document see N90-28972 23-53)
Copyright Avail: NTIS HC A09/MF A02; Non-NATO Nationals requests available only from AGARD/Scientific Publications Executive

Networked data systems such as JTIDS (Joint Tactical Information Distribution System) promise a substantial increase in the amount of information available to aircrew involved in air defense. This will include more detailed information regarding relative heights of hostile and friendly airborne units. Such information will be an important factor in BVR (Beyond Visual Range) air defense engagements using missiles such as AMRAAM (Advanced Medium Range Air to Air Missile). On the basis of psychological theory it was predicted that a perspective display format, would allow a greater volume of situational awareness data to be shown intuitively than would be the case with a conventional plan format. Specifically it should allow information regarding relative height to be more easily comprehended. A real time, cockpit based, air defense simulation was used to compare pilot performance using a perspective situational awareness display with performance with an equivalent plan view display. Twelve subjects were instructed to attack and destroy a constantly evading target aircraft that had to be distinguished from a number of hostile aircraft. Performance measures showed that subjects had more difficulty in learning to use the perspective display. However once they were familiar with this format their results were significantly better than those achieved using the plan display. These results are discussed with reference to requirements for air defense displays in general and networked data displays. Author

N90-28982# Human Engineering Labs., Aberdeen Proving Ground, MD.
COUNTERAIR SITUATION AWARENESS DISPLAY FOR ARMY AVIATION **c54**

Christopher C. Smyth, Frank J. Malkin, and William B. DeBellis *In* AGARD, Situational Awareness in Aerospace Operations Apr. 1990 10 p (For primary document see N90-28972 23-53)
Copyright Avail: NTIS HC A09/MF A02; Non-NATO Nationals requests available only from AGARD/Scientific Publications Executive

An air combat display concept is proposed for Army aviation helicopter cockpits. The effects of the choice of the display size, the display symbol size, and the area of coverage as a counterair situation awareness display are discussed. The display shows the tracks of aircraft about the host helicopter on a Planar Position Indicator (PPI) graph via the open broadcast radio net of the division-wide air defense radar coverage. The display is used to alert the aircrew to the presence of aircraft in the area and cue to the location of enemy threats for the counterair role. It is concluded that with the relatively small display sizes used in helicopters, an accurate determination of the position of enemy threats during air-to-air combat cannot be made by an aviator from the PPI alone. It must be interactive allowing access to detailed information about a track of interest to be useful. Author

N90-28983# Laboratoire de Medecine Aerospatiale, Bretigny-sur-Orge (France).
TARGET ACQUISITION UNDER LOAD FACTORS: ADVANTAGES AND DISADVANTAGES OF A HELMET MOUNTED SIGHT [DESIGNATION D'OBJECTIFS SOUS FACTEUR DE CHARGE: INTERET ET LIMITES DU VISEUR DE CASQUE] **c54**

A. Leger and Patrick Sandor *In* AGARD, Situational Awareness in Aerospace Operations Apr. 1990 10 p In FRENCH (For primary document see N90-28972 23-53)
Copyright Avail: NTIS HC A09/MF A02; Non-NATO Nationals requests available only from AGARD/Scientific Publications Executive

Helmet mounted viewfinders are actually considered as a possible means for improving the consciousness of the situation of combat pilots. The potential advantage of this type of device can depend on the opening up of cramped aircraft interiors, like the +Gz acceleration of air to air combat. An experimental study in a centrifuge was conducted in order to attempt an evaluation of the impact of +Gz acceleration on the designated function of the helmet mounted viewfinder. The results show that up to +5Gz, the reduction of tracking performance under delayed load factor is moderated. These are tied to biomechanical characteristics and functional method of eye-head coordination. Transl. by E.R.

N90-28984# Royal Aerospace Establishment, Farnborough (England). Human Factors Div.
THE SIMULATION OF LOCALIZED SOUNDS FOR IMPROVED SITUATIONAL AWARENESS

Peter L. N. Naish *In* AGARD, Situational Awareness in Aerospace Operations Apr. 1990 9 p (For primary document see N90-28972 23-53)
Copyright Avail: NTIS HC A09/MF A02; Non-NATO Nationals requests available only from AGARD/Scientific Publications Executive

It is argued that, in everday life, the directional information available in sounds is automatically incorporated into the listener's overall awareness of the situation. The absence of such cues in the air-borne environment must inevitably impoverish the data base from which the pilot builds his appreciation of the situation. Experiments are reported, which indicate that modifying cockpit sounds, to give them a synthetic directional quality, would indeed facilitate spatial appreciation. Author

N90-28985# School of Aerospace Medicine, Brooks AFB, TX.
THE EFFECTS OF ACOUSTIC ORIENTATION CUES ON INSTRUMENT FLIGHT PERFORMANCE IN A FLIGHT SIMULATOR

Terence J. Lyons, Kent K. Gillingham, Don C. Teas, William R. Ercoline, and Carolyn Oakley *In* AGARD, Situational Awareness in Aerospace Operations Apr. 1990 10 p Prepared in cooperation with Krug International, Houston, TX (For primary document see N90-28972 23-53)
Copyright Avail: NTIS HC A09/MF A02; Non-NATO Nationals requests available only from AGARD/Scientific Publications Executive

An initial version of an Acoustic Orientation Instrument (AOI)--in which airspeed was displayed as sound frequency, vertical velocity

as amplitude modulation rate, and bank angle as right-left lateralization– was evaluated in a T-40 (Link GAT-3) motion-based simulator. Fifteen pilots and three non-pilots were taught to use the AOI and flew simulated flight profiles under conditions of neither visual nor auditory instrumentation (NO INPUT), AOI signals only (AOI), T-40 simulator instrumentation only (VISUAL), and T-40 simulator instrumentation with AOI signals (BOTH). Bank control under AOI conditions was significantly better than under the NO INPUT condition for all flying tasks. Bank control under VISUAL conditions was significantly better than under the AOI condition only during turning and when performing certain complex secondary tasks. The pilots' ability to use the AOI to control vertical velocity and airspeed was less apparent. However, during straight-and-level flight, turns, and descents the AOI provided the pilots with sufficient information to maintain controlled flight. Factors of potential importance in using sound to convey aircraft attitude and motion information are discussed. Author

N90-28986# Los Alamos National Lab., NM.
WORKLOAD INDUCED SPATIO-TEMPORAL DISTORTIONS AND SAFETY OF FLIGHT: AN INVESTIGATION OF COGNITIVE INTRUSIONS IN PERCEPTUAL PROCESSES
Christopher L. Barrett and Scott A. Weisgerber (Naval Weapons Center, China Lake, CA.) *In* AGARD, Situational Awareness in Aerospace Operations Apr. 1990 9 p Previously announced as N90-14771 (For primary document see N90-28972 23-53)
Copyright Avail: NTIS HC A09/MF A02; Non-NATO Nationals requests available only from AGARD/Scientific Publications Executive

A theoretical analysis of the relationship between cognitive complexity and the perception of time and distance is presented and experimentally verified. Complex tasks produce high rates of mental representation which affect the subjective sense of duration and, through the subjective time scale, the percept of distance derived from dynamic visual cues (i.e., visual cues requiring rate integration). The analysis of the interrelationship of subjective time and subjective distance yields the prediction that, as a function of cognitive complexity, distance estimates derived from dynamic visual cues will be longer than the actual distance whereas estimates based on perceived temporal duration will be shorter than the actual distance. This prediction was confirmed in an experiment in which subjects (both pilots and non-pilots) estimated distances using either temporal cues or dynamic visual cues. The distance estimation task was also combined with secondary loading tasks in order to vary the overall task complexity. The results indicated that distance estimates based on temporal cues were underestimated while estimates based on visual cues were overestimated. This spatio-temporal distortion effect increased with increases in overall task complexity. Author

N90-28987# Hamburg Univ. (Germany, F.R.). Dept. of Eyes.
EXPERIMENTAL TESTS ON THE MINIMAL VISUAL ACUITY REQUIRED FOR SAFE AIR CREW AND AIR CONTROL PERSONNEL PERFORMANCE **c52**
J. Draeger and R. Schwartz *In* AGARD, Situational Awareness in Aerospace Operations Apr. 1990 3 p (For primary document see N90-28972 23-53)
Copyright Avail: NTIS HC A09/MF A02; Non-NATO Nationals requests available only from AGARD/Scientific Publications Executive

National and international directives specify minimal requirements for corrected and uncorrected visual acuity in military as well as civil aviation. There is a striking difference between the corrected visual acuity and the minimal visual acuity specified as a lower limit. The present experimental study concerning military pilots deals intensively with the minimal requirements on visual acuity which guarantee the safe operation of an aircraft. The investigation revealed that the specified visual acuity without correction as stated in all directives is not acceptable as a lower border limit for safe operation of an aircraft. It would therefore be possible to dispense completely with specified minimal uncorrected visual acuity values. However, a safe wearing of visual aids at all times, considering cockpit environment specific conditions must then be guaranteed. For air control personnel the uncorrected visual acuity should not have further significances. In additional studies we examined the minimal requirements for the radar controller. While reducing the visual acuity in defined steps the radar controller had to recognize critical situations during a simulated approach. For the special situation of the tower controller a visual acuity of 1.0 is required. The tests with radar controllers reveal that a reduced visual acuity between 0.5 and 1.0 had no significant influence on the failure rates. The visual acuity in that range is not as important as for pilots and tower personnel. Author

N90-28988# Laboratoire de Medecine Aerospatiale, Bretigny-sur-Orge (France).
TRACKING PERFORMANCE AND INFLUENCE OF FIELD OF VIEW [PERFORMANCE DE TRACKING ET INFLUENCE DU CHAMP DE VISION]
Patrick Sandor and Alain Leger *In* AGARD, Situational Awareness in Aerospace Operations Apr. 1990 7 p In FRENCH (For primary document see N90-28972 23-53)
Copyright Avail: NTIS HC A09/MF A02; Non-NATO Nationals requests available only from AGARD/Scientific Publications Executive

Eyesight with limited field of view becomes habitual with the use of optronic systems mounted on a helmet. In order to evaluate the influence of these devices on operator performance, the effect of several levels of visual restriction on the task of visual-manual tracking and on eye-head coordination, was tested. The performance is moderately reduced when the available field or view is small (20 deg), without improvement in the intermediate field (70 deg). The origin of this reduction must be researched bringing into play the adaptive neuro-sensory mechanisms needed for the limitation of the field rather than the restricted biomechanics imposed by the target motion range. This aspect obeys the analysis of the change of eye-head coordination tied to the string restriction of the field. Transl. by E.R.

N90-28989# Italian Air Force Aerospace Medical Center, Rome. Neuropsychophysiology Group.
NEUROPHYSIOLOGICAL CORRELATES OF INFORMATION PROCESSING ABILITIES DURING DIVIDED ATTENTION SITUATIONS IN AIR TRAFFIC CONTROLLERS
S. Porcu, G. DellErba, L. Riccio, M. Peronti, and P. Venturi (La Sapienza Univ., Rome, Italy) *In* AGARD, Situational Awareness in Aerospace Operations Apr. 1990 9 p (For primary document see N90-28972 23-53)
Copyright Avail: NTIS HC A09/MF A02; Non-NATO Nationals requests available only from AGARD/Scientific Publications Executive

The relationships that exist between arousal, cognitive functioning and generalized expectancy of control in a group of air traffic controllers (ATC), are studied in conditions of single and dual tasks. Furthermore, under the same conditions and based on performance outcome, evidence was sought of eventual differences in cognitive functioning which could be related to the diversity of professional ATC skills. Data show that arousal is increased in the dual-task: (1) N2 peak latency is positively correlated to arousal in both tasks; (2) correlates inversely with perceived control in the single task; (3) relates inversely with activation in the dual task; and (4) adjusted arousal correlates with perceived control. Finally, N2 peak latency appears to be sensitive to ATC skill. Author

N90-28990# Paris V Univ. (France). Lab. d'Anthropologie Appliquee.
LOSS OF ALERTNESS AND CONSCIOUSNESS FROM PILOT POSITION DURING LONG RANGE FLIGHT [BAISSE DE LA VIGILANCE ET CONSCIENCE DE LA SITUATION DES PILOTES AU COURS DE VOLS LONG-COURRIERS]
A. Coblentz, J.-P. Fouillot, R. Mollard, and Ph. Cabon *In* AGARD, Situational Awareness in Aerospace Operations Apr. 1990 9 p In FRENCH (For primary document see N90-28972 23-53)

Copyright Avail: NTIS HC A09/MF A02; Non-NATO Nationals requests available only from AGARD/Scientific Publications Executive

The variations in levels of alertness over the course of monotonous activities have been presented by many authors. In aeronautics, during long flight, these variations in alertness can reduce pilot performance and ability to an appreciable amount. After study of pilot behavior during this type of flight, ground based research was undertaken. The objective was to identify phases of hyperalertness and to evaluate their impact on pilot performance and its effect on consciousness. The method rests on the use of ambulatory techniques such as EEG, EOG, heart rate, and motor function of the pilot during flight, as well as the observation of the task. The first results in the preliminary phase, supported by eight long range flights, are presented. Transl. by E.R.

N90-28991# Institute of Aviation Medicine, Madrid (Spain).
EVALUATION OF THE PERFORMANCE CAPABILITY OF THE AVIATOR UNDER HYPOXIC CONDITIONS OPERATIONAL EXPERIENCE **c52**
Francisco Rios Tejada, Luis Marquez delaPlata, Cesar Alonso Rodriguez, and Juan J. Canton Romero *In* AGARD, Situational Awareness in Aerospace Operations Apr. 1990 6 p (For primary document see N90-28972 23-53)
Copyright Avail: NTIS HC A09/MF A02; Non-NATO Nationals requests available only from AGARD/Scientific Publications Executive

Performance capacity under hypoxia conditions was determined in 48 subjects exposed to a simulated altitude of 25,000 feet (7,620 mts.). The method was a modified Toulouse-Pieron Test (TTM) and a Digit Span Test (DST), completed at 3 altitudinal conditions: Ground Level (GL), FL 250 and Placebo (PL). Maximum hypoxia time was 4 minutes and it was measured every 30 sec. The Direct Partial Score (DPS) 8 times through the 4 min., and the Direct Total Score (DTS) was obtained by the Tolouse application formula. Significant decrements in test performance were found by comparing GL to FL 250 and FL 250 to PL in pairs at .001 confidence level after point 90 sec. time for DPS. Similar results were obtained for DTS. For DTS, the comparative analysis of the average values were also significant. The application of the TTM is considered as useful, simple and profitable in the evaluation of Attention Capacity of the aviator under hypoxia conditions. The Incapacitation Curve is a term which expresses, in a quantitative and chronological way, the psychomotor performance. Both, the TTM and DTS, are between each other complementary tools in the evaluation of the psychomotor pilot efficiency. Author

N90-28992# McGill Univ., Montreal (Quebec).
EFFECTS OF SHORT-TERM WEIGHTLESSNESS ON ROLL CIRCULARVECTION **c52**
D. G. D. Watt and J. P. Landolt *In* AGARD, Situational Awareness in Aerospace Operations Apr. 1990 6 p Sponsored in part by Medical Research Council of Canada and National Research Council of Canada Prepared in cooperation with Defence and Civil Inst. of Environmental Medicine, Toronto, Ontario (For primary document see N90-28972 23-53)
Copyright Avail: NTIS HC A09/MF A02; Non-NATO Nationals requests available only from AGARD/Scientific Publications Executive

Roll circularvection is an illusion of self-rotation about the fore-aft axis experienced when a stationary subject is exposed to a visual field rotating in the frontal plane. In these experiments, subjects were asked to estimate the strength of this phenomenon while undergoing visual stimulation in the upright and supine positions, and during parabolic aircraft flight. The results indicate that the steady roll component of vection is not affected by the magnitude or direction of the gravity vector. The unpredictable and sudden loss of this compelling illusion could contribute to serious episodes of pilot disorientation. Author

N90-28993# Naval Aerospace Medical Research Lab., Pensacola, FL.
MAINTAINING SPATIAL ORIENTATION AWARENESS **c52**
A. Rupert, A. Mateczun, and F. E. Guedry, Jr. *In* AGARD, Situational Awareness in Aerospace Operations Apr. 1990 5 p (For primary document see N90-28972 23-53)
Copyright Avail: NTIS HC A09/MF A02; Non-NATO Nationals requests available only from AGARD/Scientific Publications Executive

It is believed that training paradigms which vividly demonstrate to pilots the need and way to maintain spatial orientation awareness during formation flight will reduce the incidence of these very costly mishaps. Several training paradigms are under development using the Dynasim, a cockpit mounted on a short-arm centrifuge. The pilot controls both pitch and roll axes of the Dynasim cockpit to maintain the position on a wing aircraft projected onto a visual surround. Pilot's attention is intermittently distracted from the lead aircraft and from attitude display(s) by simultaneous performance of other cockpit tasks. The orientation experienced by pilots is controlled by varying information in the visual surround and in the onboard instruments (including a Malcolm Horizon) and by controlling the direction of the gravitoinertial field of the short-arm centrifuge. A second stage of the research will investigate new concepts in displays to improve pilot orientation awareness. The inevitable distraction of visual attention, which accompanies emergency situations, engenders consideration of peripheral vision and nonvisual channels to convey aircraft attitude and target information and maintain spatial orientation awareness. Author

N90-28994 Institute for Perception RVO-TNO, Soesterberg (Netherlands). Afd. Verrichtingspsychologie.
SITUATIONAL AWARENESS AND VESTIBULAR STIMULATION: THE INFLUENCE OF WHOLE-BODY ROTATION UPON TASK PERFORMANCE Final Report
C. J. E. Wientjes and W. Bles 14 Aug. 1989 21 p In DUTCH; ENGLISH summary
(Contract A86/KLu/048)
(IZF-1989-14; TD-89-1051; ETN-90-97386) Copyright Avail: Inst. for Perception RVO-TNO, P.O. Box 23, 3769 ZG Soesterberg, Netherlands

The effects of vestibular stimulation (whole-body rotation) on performance memory comparison task, subjective well-being and visual perception were investigated. It was found that rotation results in a deterioration of the task performance, in motion sickness and anxiety responses; the visibility of the characters on the display that was used for the presentation of the task was also affected. It is concluded that rotation may result in adverse effects on the information processing, mainly as a consequence of problems with visual perception that seem to be due to insufficient suppression of the vestibular reflex. These findings are important for the problem of situational awareness because similar reactions may occur with vestibular stimulation in high performance aircrafts. ESA

N90-28995 Institute for Perception RVO-TNO, Soesterberg (Netherlands). Afd. Verrichtingspsychologie.
COGNITION VERSUS SENSATION: A PARADIGM FOR REORIENTATION Final Report
L. C. Boer Jul. 1989 25 p In DUTCH; ENGLISH summary
(Contract A85/K/077)
(IZF-1989-20; TD-89-1050; ETN-90-97388) Copyright Avail: Inst. for Perception RVO-TNO, P.O. Box 23, 3769 ZG Soesterberg, Netherlands

The progress in the research project Orientation and Navigation which is, for example, important for (fighter) pilots, is reported. A task of mental orientation is described in which subjects are required to image themselves rotating in the horizontal plane; at the same time they undergo an actual rotation in the same plane but in a different direction. It is found that the imagined reorientation angle has a strong effect on the cognitive processing time; the actual rotation, however, has no effect. Conflicts between actual and imagined orientation are not found. Suggestions for continued investigations are presented. ESA

N90-28996*# National Aeronautics and Space Administration. Ames Research Center, Moffett Field, CA.
TECHNIQUES AND APPLICATIONS FOR BINAURAL SOUND MANIPULATION IN HUMAN-MACHINE INTERFACES
Durand R. Begault and Elizabeth M. Wenzel Aug. 1990 27 p Submitted for publication
(NASA-TM-102279; A-90066; NAS 1.15:102279) Avail: NTIS HC A03/MF A01 CSCL 05I

The implementation of binaural sound to speech and auditory sound cues (auditory icons) is addressed from both an applications and technical standpoint. Techniques overviewed include processing by means of filtering with head-related transfer functions. Application to advanced cockpit human interface systems is discussed, although the techniques are extendable to any human-machine interface. Research issues pertaining to three-dimensional sound dispalys under investigation at the Aerospace Human Factors Division at NASA Ames Research Center are described. Author

N90-28997# Air Force Human Resources Lab., Brooks AFB, TX.
AIR FORCE OFFICER QUALIFYING TEST (AFOQT): DEVELOPMENT OF QUICK SCORE COMPOSITES FOR FORMS P1 AND P2 Interim Technical Report, Nov. 1987 - Jan. 1990
Todd C. Sperl and Malcolm James Ree Jun. 1990 39 p
(AD-A223868; AFHRL-TR-90-3) Avail: NTIS HC A03/MF A01 CSCL 05/8

The purpose of this effort was to develop an instrument to predict success on the Air Force Officer Qualifying Test (AFOQT) Forms P. This device, referred to as Quick Score Composites (QSC), will aid in the identification of individuals likely to pass AFOQT requirement in applying for a commission in the Air Force. The subjects were 6,192 applicants administered AFPQT Forms P1 and P2. Two item selection methods (point-biserial and random) were compared for accuracy, reliability, and control of differential score prediction for gender and ethnic groups. Results showed that QSC scores based on random item selection within subtest are effective predictors of the AFOQT composites. This was indicated by their comparable reliability to that of the other method, high positive correlation with the composites they represent, and introduction of less gender and ethnic bias than that introduced by the point-biserial method. GRA

N90-28998# Naval Surface Warfare Center, Dahlgren, VA. Strategic Systems Dept.
SELECTIVE LEARNING ALGORITHM FOR CERTAIN TYPES OF LEARNING FAILURE IN MULTILAYER PERCEPTRONS Final Report
George Rogers and Jeffrey L. Solka Jun. 1990 14 p
(AD-A223982; NSWC/TR-90-167) Avail: NTIS HC A03/MF A01 CSCL 05/8

A simple selective learning algorithm for use with Multilayer Perceptrons (MLPs) is presented. This algorithm has proved useful in certain types of problems where learning failure occurs using standard back propagation. Examples of these problems are included. The algorithm is based on the rms output error, computed across all output nodes and all training patterns. The learning rate is decreased for all individual output nodes each time the error is less than a user chosen multiple of the rms error corresponding to the previous pass. This algorithm has produced convergence where the standard fixed gain back propagation failed. GRA

54 MAN/SYSTEM TECHNOLOGY AND LIFE SUPPORT

Includes human engineering; biotechnology; and space suits and protective clothing.

For related information see also *16 Space Transportation.*

N90-28999# Aerospace Medical Research Labs., Wright-Patterson AFB, OH.
MILITARY AIRCREW SEATING: A HUMAN FACTORS ENGINEERING APPROACH Summary Report, Dec. 1985 - Dec. 1988 Ph.D. Thesis
James David Whiteley Dec. 1989 199 p
(AF Proj. 7231)
(AD-A218049; AAMRL-TR-89-046) Avail: NTIS HC A09/MF A02 CSCL 23/2

The application of human factors engineering to the realm of aerospace design is not a new or unique concept; however, its direct application to aircrew seat design considerations, human response to whole body vibration, new seat design concepts, and several methods of evaluating and contrasting aircrew seats is a new development. During this effort, two aircrew seats were developed. These primarily consisted of new seat pan and backrest structures. Two distinct experiments were performed. Data was collected to determine pressure distribution on the various seat pans in a static environment. The new seat pans were statistically different (lower maximum pressure) than the current seat pan. The current seat pan averaged almost double new seat pressure readings. The second experiment in which 12 active duty Air Force males participated in a series of dynamic vibration exposure tests which simulated the measurements was accomplished. GRA

N90-29000*# Jet Propulsion Lab., California Inst. of Tech., Pasadena.
PROCEEDINGS OF THE NASA CONFERENCE ON SPACE TELEROBOTICS, VOLUME 1
Guillermo Rodriguez, ed. and Homayoun Seraji, ed. 31 Jan. 1989 481 p Conference held in Pasadena, CA, 31 Jan. - 2 Feb. 1989
(Contract NAS7-918)
(NASA-CR-186856; JPL-Publ-89-7-Vol-1; NAS 1.26:186856)
Avail: NTIS HC A21/MF A03 CSCL 05H

The theme of the Conference was man-machine collaboration in space. Topics addressed include: redundant manipulators; man-machine systems; telerobot architecture; remote sensing and planning; navigation; neural networks; fundamental AI research; and reasoning under uncertainty. For individual titles, see N90-29001 through N90-29043.

N90-29001*# Robotics Research Corp., Milford, OH.
A 17 DEGREE OF FREEDOM ANTHROPOMORPHIC MANIPULATOR
Havard I. Vold, James P. Karlen, Jack M. Thompson, Jr., James D. Farrell, and Paul H. Eismann *In* JPL, California Inst. of Tech., Proceedings of the NASA Conference on Space Telerobotics, Volume 1 31 Jan. 1989 p 19-28 (For primary document see N90-29000 23-54)
Avail: NTIS HC A21/MF A03 CSCL 05H

A 17 axis anthropomorphic manipulator, providing coordinated control of two seven degree of freedom arms mounted on a three degree of freedom torso-waist assembly, is presented. This massively redundant telerobot, designated the Robotics Research K/B-2017 Dexterous Manipulator, employs a modular mechanism design with joint-mounted actuators based on brushless motors and harmonic drive gear reducers. Direct joint torque control at the servo level causes these high-output joint drives to behave like direct-drive actuators, facilitating the implementation of an effective impedance control scheme. The redundant, but conservative motion control system models the manipulator as a spring-loaded linkage with viscous damping and rotary inertia at each joint. This approach allows for real time, sensor-driven control of manipulator pose using a hierarchy of competing rules, or

objective functions, to avoid unplanned collisions with objects in the workplace, to produce energy-efficient, graceful motion, to increase leverage, to control effective impedance at the tool or to favor overloaded joints. Author

N90-29002*# Jet Propulsion Lab., California Inst. of Tech., Pasadena.
A NEW APPROACH TO GLOBAL CONTROL OF REDUNDANT MANIPULATORS
Homayoun Seraji *In its* Proceedings of the NASA Conference on Space Telerobotics, Volume 1 31 Jan. 1989 p 29-38 (For primary document see N90-29000 23-54)
Avail: NTIS HC A21/MF A03 CSCL 05H

A new and simple approach to configuration control of redundant manipulators is presented. In this approach, the redundancy is utilized to control the manipulator configuration directly in task space, where the task will be performed. A number of kinematic functions are defined to reflect the desirable configuration that will be achieved for a given end-effector position. The user-defined kinematic functions and the end-effector Cartesian coordinates are combined to form a set of task-related configuration variables as generalized coordinates for the manipulator. An adaptive scheme is then utilized to globally control the configuration variables so as to achieve tracking of some desired reference trajectories. This accomplishes the basic task of desired end-effector motion, while utilizing the redundancy to achieve any additional task through the desired time variation of the kinematic functions. The control law is simple and computationally very fast, and does not require the complex manipulator dynamic model. Author

N90-29003*# Jet Propulsion Lab., California Inst. of Tech., Pasadena.
KINEMATIC FUNCTIONS FOR THE 7 DOF ROBOTICS RESEARCH ARM
K. Kreutz, M. Long, and Homayoun Seraji *In its* Proceedings of the NASA Conference on Space Telerobotics, Volume 1 31 Jan. 1989 p 39-48 (For primary document see N90-29000 23-54)
Avail: NTIS HC A21/MF A03 CSCL 05H

The Robotics Research Model K-1207 manipulator is a redundant 7R serial link arm with offsets at all joints. To uniquely determine joint angles for a given end-effector configuration, the redundancy is parameterized by a scalar variable which corresponds to the angle between the manipulator elbow plane and the vertical plane. The forward kinematic mappings from joint-space to end-effector configuration and elbow angle, and the augmented Jacobian matrix which gives end-effector and elbow angle rates as a function of joint rates, are also derived. Author

N90-29004*# New Mexico State Univ., Las Cruces.
CARTESIAN CONTROL OF REDUNDANT ROBOTS
R. Colbaugh and K. Glass *In* JPL, California Inst. of Tech., Proceedings of the NASA Conference on Space Telerobotics, Volume 1 31 Jan. 1989 p 49-58 Sponsored in part by Sandia Labs. (For primary document see N90-29000 23-54)
Avail: NTIS HC A21/MF A03 CSCL 05H

A Cartesian-space position/force controller is presented for redundant robots. The proposed control structure partitions the control problem into a nonredundant position/force trajectory tracking problem and a redundant mapping problem between Cartesian control input F is a set member of the set R(sup m) and robot actuator torque T is a set member of the set R(sup n) (for redundant robots, m is less than n). The underdetermined nature of the F yields T map is exploited so that the robot redundancy is utilized to improve the dynamic response of the robot. This dynamically optimal F yields T map is implemented locally (in time) so that it is computationally efficient for on-line control; however, it is shown that the map possesses globally optimal characteristics. Additionally, it is demonstrated that the dynamically optimal F yields T map can be modified so that the robot redundancy is used to simultaneously improve the dynamic response and realize any specified kinematic performance objective (e.g., manipulability maximization or obstacle avoidance). Computer simulation results are given for a four degree of freedom planar redundant robot under Cartesian control, and demonstrate that position/force trajectory tracking and effective redundancy utilization can be achieved simultaneously with the proposed controller. Author

N90-29005*# Ford Aerospace and Communications Corp., Palo Alto, CA. Space Systems Div.
KINEMATICS, CONTROLS, AND PATH PLANNING RESULTS FOR A REDUNDANT MANIPULATOR
Bruce Gretz and Scott W. Tilley *In* JPL, California Inst. of Tech., Proceedings of the NASA Conference on Space Telerobotics, Volume 1 31 Jan. 1989 p 59-68 (For primary document see N90-29000 23-54)
Avail: NTIS HC A21/MF A03 CSCL 05H

The inverse kinematics solution, a modal position control algorithm, and path planning results for a 7 degree of freedom manipulator are presented. The redundant arm consists of two links with shoulder and elbow joints and a spherical wrist. The inverse kinematics problem for tip position is solved and the redundant joint is identified. It is also shown that a locus of tip positions exists in which there are kinematic limitations on self-motion. A computationally simple modal position control algorithm has been developed which guarantees a nearly constant closed-loop dynamic response throughout the workspace. If all closed-loop poles are assigned to the same location, the algorithm can be implemented with very little computation. To further reduce the required computation, the modal gains are updated only at discrete time intervals. Criteria are developed for the frequency of these updates. For commanding manipulator movements, a 5th-order spline which minimizes jerk provides a smooth tip-space path. Schemes for deriving a corresponding joint-space trajectory are discussed. Modifying the trajectory to avoid joint torque saturation when a tip payload is added is also considered. Simulation results are presented. Author

N90-29006*# Toronto Univ. (Ontario). Robotics and Automation Lab.
A COMPLETE ANALYTICAL SOLUTION FOR THE INVERSE INSTANTANEOUS KINEMATICS OF A SPHERICAL-REVOLUTE-SPHERICAL (7R) REDUNDANT MANIPULATOR
R. P. Podhorodeski, R. G. Fenton, and A. A. Goldenberg *In* JPL, California Inst. of Tech., Proceedings of the NASA Conference on Space Telerobotics, Volume 1 31 Jan. 1989 p 69-78 (For primary document see N90-29000 23-54)
Avail: NTIS HC A21/MF A03 CSCL 05H

Using a method based upon resolving joint velocities using reciprocal screw quantities, compact analytical expressions are generated for the inverse solution of the joint rates of a seven revolute (spherical-revolute-spherical) manipulator. The method uses a sequential decomposition of screw coordinates to identify reciprocal screw quantities used in the resolution of a particular joint rate solution, and also to identify a Jacobian null-space basis used for the direct solution of optimal joint rates. The results of the screw decomposition are used to study special configurations of the manipulator, generating expressions for the inverse velocity solution for all non-singular configurations of the manipulator, and identifying singular configurations and their characteristics. Two functions are therefore served: a new general method for the solution of the inverse velocity problem is presented; and complete analytical expressions are derived for the resolution of the joint rates of a seven degree of freedom manipulator useful for telerobotic and industrial robotic application. Author

N90-29007*# Massachusetts Inst. of Tech., Cambridge. Man-Machine Systems Lab.
ADJUSTABLE IMPEDANCE, FORCE FEEDBACK AND COMMAND LANGUAGE AIDS FOR TELEROBOTICS (PARTS 1-4 OF AN 8-PART MIT PROGRESS REPORT)
Thomas B. Sheridan, G. Jagganath Raju, Forrest T. Buzan, Wael Yared, and Jong Park *In* JPL, California Inst. of Tech., Proceedings

of the NASA Conference on Space Telerobotics, Volume 1 31 Jan. 1989 p 81-88 Sponsored in part by NASA, Ames Research Center (For primary document see N90-29000 23-54)
Avail: NTIS HC A21/MF A03 CSCL 05H

Projects recently completed or in progress at MIT Man-Machine Systems Laboratory are summarized. (1) A 2-part impedance network model of a single degree of freedom remote manipulation system is presented in which a human operator at the master port interacts with a task object at the slave port in a remote location is presented. (2) The extension of the predictor concept to include force feedback and dynamic modeling of the manipulator and the environment is addressed. (3) A system was constructed to infer intent from the operator's commands and the teleoperation context, and generalize this information to interpret future commands. (4) A command language system is being designed that is robust, easy to learn, and has more natural man-machine communication. A general telerobot problem selected as an important command language context is finding a collision-free path for a robot. Author

N90-29008*# Massachusetts Inst. of Tech., Cambridge.
VARIABLE FORCE AND VISUAL FEEDBACK EFFECTS ON TELEOPERATOR MAN/MACHINE PERFORMANCE
Michael J. Massimino and Thomas B. Sheridan *In* JPL, California Inst. of Tech., Proceedings of the NASA Conference on Space Telerobotics, Volume 1 31 Jan. 1989 p 89-98 (For primary document see N90-29000 23-54)
Avail: NTIS HC A21/MF A03 CSCL 05H

An experimental study was conducted to determine the effects of various forms of visual and force feedback on human performance for several telemanipulation tasks. Experiments were conducted with varying frame rates and subtended visual angles, with and without force feedback. Author

N90-29009*# Wisconsin Univ., Madison. Dept. of Industrial Engineering.
TELEOPERATOR COMFORT AND PSYCHOMETRIC STABILITY: CRITERIA FOR LIMITING MASTER-CONTROLLER FORCES OF OPERATION AND FEEDBACK DURING TELEMANIPULATION
Steven F. Wiker, Elaine Hershkowitz, and John Zik *In* JPL, California Inst. of Tech., Proceedings of the NASA Conference on Space Telerobotics, Volume 1 31 Jan. 1989 p 99-107 (For primary document see N90-29000 23-54)
Avail: NTIS HC A21/MF A03 CSCL 05H

The following question is addressed: How much force should operators exert, or experience, when operating a telemanipulator master-controller for sustained periods without encountering significant fatigue and discomfort, and without loss of stability in psychometric perception of force. The need to minimize exertion demands to avoid fatigue is diametrically opposed by the need to present a wide range of force stimuli to enhance perception of applied or reflected forces. For 104 minutes subjects repetitiously performed a series of 15 s isometric pinch grasps; controlled at 5, 15, and 25 percent of their maximum voluntary strength. Cyclic pinch grasps were separated by rest intervals of 7.5 and 15 s. Upon completion of every 10 minute period, subjects interrupted grasping activities to gage the intensity of fatigue and discomfort in the hand and forearm using a cross-modal matching technique. A series of psychometric tests were then conducted to determine accuracy and stability in the subject's perception of force experienced. Results showed that onset of sensations of discomfort and fatigue were dependent upon the magnitude of grasp force, work/rest ratio, and progression of task. Declines in force magnitude estimation slopes, indicating a reduction in force perception sensitivity, occurred with increased grasp force when work/rest ratios were greater than 1.0. Specific recommendations for avoiding discomfort and shifts in force perception, by limiting pinch grasp force required for master-controller operation and range of force reflection or work/rest ratios, are provided. Author

N90-29010*# Center for Engineering Applications, Memphis, TN.
MEASUREMENT OF HAND DYNAMICS IN A MICROSURGERY ENVIRONMENT: PRELIMINARY DATA IN THE DESIGN OF A BIMANUAL TELEMICRO-OPERATION TEST BED
Steve Charles and Roy Williams *In* JPL, California Inst. of Tech., Proceedings of the NASA Conference on Space Telerobotics, Volume 1 31 Jan. 1989 p 109-118 (For primary document see N90-29000 23-54)
Avail: NTIS HC A21/MF A03 CSCL 05H

Data describing the microsurgeon's hand dynamics was recorded and analyzed in order to provide an accurate model for the telemicrosurgery application of the Bimanual Telemicro-operation Test Bed. The model, in turn, will guide the development of algorithms for the control of robotic systems in bimanual telemicro-operation tasks. Measurements were made at the hand-tool interface and include position, acceleration and force between the tool-finger interface. Position information was captured using an orthogonal pulsed magnetic field positioning system resulting in measurements in all six degrees-of-freedom (DOF). Acceleration data at the hands was obtained using accelerometers positioned in a triaxial arrangement on the back of the hand allowing measurements in all three cartesian-coordinate axes. Force data was obtained by using miniature load cells positioned between the tool and the finger and included those forces experienced perpendicular to the tool shaft and those transferred from the tool-tissue site. Position data will provide a minimum/maximum reference frame for the robotic system's work space or envelope. Acceleration data will define the response times needed by the robotic system in order to emulate and subsequently outperform the human operator's tool movements. The force measurements will aid in designing a force-reflective, force-scaling system as well as defining the range of forces the robotic system will encounter. All analog data was acquired by a 16-channel analog-to-digital conversion system residing in an IBM PC/AT-compatible computer at the Center's laboratory. The same system was also used to analyze and present the data. Author

N90-29011*# Bureau of Mines, Pittsburgh, PA.
HUMAN FACTORS MODEL CONCERNING THE MAN-MACHINE INTERFACE OF MINING CREWSTATIONS
James P. Rider and Richard L. Unger *In* JPL, California Inst. of Tech., Proceedings of the NASA Conference on Space Telerobotics, Volume 1 31 Jan. 1989 p 119-127 (For primary document see N90-29000 23-54)
Avail: NTIS HC A21/MF A03 CSCL 05H

The U.S. Bureau of Mines is developing a computer model to analyze the human factors aspect of mining machine operator compartments. The model will be used as a research tool and as a design aid. It will have the capability to perform the following: simulated anthropometric or reach assessment, visibility analysis, illumination analysis, structural analysis of the protective canopy, operator fatigue analysis, and computation of an ingress-egress rating. The model will make extensive use of graphics to simplify data input and output. Two dimensional orthographic projections of the machine and its operator compartment are digitized and the data rebuilt into a three dimensional representation of the mining machine. Anthropometric data from either an individual or any size population may be used. The model is intended for use by equipment manufacturers and mining companies during initial design work on new machines. In addition to its use in machine design, the model should prove helpful as an accident investigation tool and for determining the effects of machine modifications made in the field on the critical areas of visibility and control reach ability. Author

N90-29012*# British Aerospace Public Ltd. Co., Bristol (England). Sowerby Research Centre.
DEVELOPMENT OF A FLEXIBLE TEST-BED FOR ROBOTICS, TELEMANIPULATION AND SERVICING RESEARCH
Barry F. Davies *In* JPL, California Inst. of Tech., Proceedings of the NASA Conference on Space Telerobotics, Volume 1 31

Jan. 1989 p 129-138 (For primary document see N90-29000 23-54)
Avail: NTIS HC A21/MF A03 CSCL 05H

The development of a flexible operation test-bed, based around a commercially available ASEA industrial robot is described. The test-bed was designed to investigate fundamental human factors issues concerned with the unique problems of robotic manipulation in the hostile environment of Space. Author

N90-29013*# Dortmund Univ. (Germany, F.R.). Inst. of Robotics Research.

CONTROL OF INTELLIGENT ROBOTS IN SPACE

E. Freund and Ch. Buehler *In* JPL, California Inst. of Tech., Proceedings of the NASA Conference on Space Telerobotics, Volume 1 31 Jan. 1989 p 141-150 Sponsored in part by Bundeminister fuer Forschung und Technologie, Federal Republic of Germany (For primary document see N90-29000 23-54)
Avail: NTIS HC A21/MF A03 CSCL 05H

In view of space activities like International Space Station, Man-Tended-Free-Flyer (MTFF) and free flying platforms, the development of intelligent robotic systems is gaining increasing importance. The range of applications that have to be performed by robotic systems in space includes e.g., the execution of experiments in space laboratories, the service and maintenance of satellites and flying platforms, the support of automatic production processes or the assembly of large network structures. Some of these tasks will require the development of bi-armed or of multiple robotic systems including functional redundancy. For the development of robotic systems which are able to perform this variety of tasks a hierarchically structured modular concept of automation is required. This concept is characterized by high flexibility as well as by automatic specialization to the particular sequence of tasks that have to be performed. On the other hand it has to be designed such that the human operator can influence or guide the system on different levels of control supervision, and decision. This leads to requirements for the hardware and software concept which permit a range of application of the robotic systems from telemanipulation to autonomous operation. The realization of this goal requires strong efforts in the development of new methods, software and hardware concepts, and the integration into an automation concept. Author

N90-29014*# Texas Univ., Austin. Dept. of Mechanical Engineering.

MODULARITY IN ROBOTIC SYSTEMS

Delbert Tesar and Michael S. Butler *In* JPL, California Inst. of Tech., Proceedings of the NASA Conference on Space Telerobotics, Volume 1 31 Jan. 1989 p 151-162 (For primary document see N90-29000 23-54)
Avail: NTIS HC A21/MF A03 CSCL 05H

Most robotic systems today are designed one at a time, at a high cost of time and money. This wasteful approach has been necessary because the industry has not established a foundation for the continued evolution of intelligent machines. The next generation of robots will have to be generic, versatile machines capable of absorbing new technology rapidly and economically. This approach is demonstrated in the success of the personal computer, which can be upgraded or expanded with new software and hardware at virtually every level. Modularity is perceived as a major opportunity to reduce the 6 to 7 year design cycle time now required for new robotic manipulators, greatly increasing the breadth and speed of diffusion of robotic systems in manufacturing. Modularity and its crucial role in the next generation of intelligent machines are the focus of interest. The main advantages that modularity provides are examined; types of modules needed to create a generic robot are discussed. Structural modules designed by the robotics group at the University of Texas at Austin are examined to demonstrate the advantages of modular design. Author

N90-29015*# Jet Propulsion Lab., California Inst. of Tech., Pasadena.

A SYSTEM ARCHITECTURE FOR A PLANETARY ROVER

D. B. Smith and J. R. Matijevic *In its* Proceedings of the NASA Conference on Space Telerobotics, Volume 1 31 Jan. 1989 p 163-184 (For primary document see N90-29000 23-54)
Avail: NTIS HC A21/MF A03 CSCL 05H

Each planetary mission requires a complex space vehicle which integrates several functions to accomplish the mission and science objectives. A Mars Rover is one of these vehicles, and extends the normal spacecraft functionality with two additional functions: surface mobility and sample acquisition. All functions are assembled into a hierarchical and structured format to understand the complexities of interactions between functions during different mission times. It can graphically show data flow between functions, and most importantly, the necessary control flow to avoid unambiguous results. Diagrams are presented organizing the functions into a structured, block format where each block represents a major function at the system level. As such, there are six blocks representing telecomm, power, thermal, science, mobility and sampling under a supervisory block called Data Management/Executive. Each block is a simple collection of state machines arranged into a hierarchical order very close to the NASREM model for Telerobotics. Each layer within a block represents a level of control for a set of state machines that do the three primary interface functions: command, telemetry, and fault protection. This latter function is expanded to include automatic reactions to the environment as well as internal faults. Lastly, diagrams are presented that trace the system operations involved in moving from site to site after site selection. The diagrams clearly illustrate both the data and control flows. They also illustrate inter-block data transfers and a hierarchical approach to fault protection. This systems architecture can be used to determine functional requirements, interface specifications and be used as a mechanism for grouping subsystems (i.e., collecting groups of machines, or blocks consistent with good and testable implementations). Author

N90-29016*# Jet Propulsion Lab., California Inst. of Tech., Pasadena.

THE NASA/OAST TELEROBOT TESTBED ARCHITECTURE

J. R. Matijevic, W. F. Zimmerman, and S. Dolinsky *In its* Proceedings of the NASA Conference on Space Telerobotics, Volume 1 31 Jan. 1989 p 185-195 (For primary document see N90-29000 23-54)
Avail: NTIS HC A21/MF A03 CSCL 05H

Through a phased development such as a laboratory-based research testbed, the NASA/OAST Telerobot Testbed provides an environment for system test and demonstration of the technology which will usefully complement, significantly enhance, or even replace manned space activities. By integrating advanced sensing, robotic manipulation and intelligent control under human-interactive supervision, the Testbed will ultimately demonstrate execution of a variety of generic tasks suggestive of space assembly, maintenance, repair, and telescience. The Testbed system features a hierarchical layered control structure compatible with the incorporation of evolving technologies as they become available. The Testbed system is physically implemented in a computing architecture which allows for ease of integration of these technologies while preserving the flexibility for test of a variety of man-machine modes. The development currently in progress on the functional and implementation architectures of the NASA/OAST Testbed and capabilities planned for the coming years are presented. Author

N90-29017*# National Aeronautics and Space Administration. Goddard Space Flight Center, Greenbelt, MD.

FORMULATION OF DESIGN GUIDELINES FOR AUTOMATED ROBOTIC ASSEMBLY IN OUTERSPACE

Suren N. Dwivedi, Gary Jones, S. Banerjee, and S. Srivastava (Bowie State Univ., MD.) *In* JPL, California Inst. of Tech., Proceedings of the NASA Conference on Space Telerobotics, Volume 1 31 Jan. 1989 p 197-206 (For primary document see N90-29000 23-54)
Avail: NTIS HC A21/MF A03 CSCL 05H

The approach for arriving at design guidelines for assembly by

robots in outerspace is illustrated. The use of robots in a zero gravity environment necessitates that extra factors over and above normal design guidelines be taken into account. Besides, many of the guidelines for assembly by robots on earth do not apply in space. However, considering the axioms for normal design and assembly as one set, guidelines for design and robotic assembly as another, and guidelines for design and assembly in space as the third set, unions and intersections of these sets can generate guidelines for two or more of these conditions taken together - say design and manual assembly in space. Therein lies the potential to develop expert systems in the future, which would use an exhaustive database and similar guidelines to arrive at those required by a superposition of these conditions. Author

N90-29018*# Bureau of Mines, Pittsburgh, PA.
AUTOMATION AND ROBOTICS TECHNOLOGY FOR INTELLIGENT MINING SYSTEMS
Jeffrey H. Welsh *In* JPL, California Inst. of Tech., Proceedings of the NASA Conference on Space Telerobotics, Volume 1 31 Jan. 1989 p 207-216 (For primary document see N90-29000 23-54)
Avail: NTIS HC A21/MF A03 CSCL 05H

The U.S. Bureau of Mines is approaching the problems of accidents and efficiency in the mining industry through the application of automation and robotics to mining systems. This technology can increase safety by removing workers from hazardous areas of the mines or from performing hazardous tasks. The short-term goal of the Automation and Robotics program is to develop technology that can be implemented in the form of an autonomous mining machine using current continuous mining machine equipment. In the longer term, the goal is to conduct research that will lead to new intelligent mining systems that capitalize on the capabilities of robotics. The Bureau of Mines Automation and Robotics program has been structured to produce the technology required for the short- and long-term goals. The short-term goal of application of automation and robotics to an existing mining machine, resulting in autonomous operation, is expected to be accomplished within five years. Key technology elements required for an autonomous continuous mining machine are well underway and include machine navigation systems; coal-rock interface detectors, machine condition monitoring, and intelligent computer systems. The Bureau of Mines program is described, including status of key technology elements for an autonomous continuous mining machine, the program schedule, and future work. Although the program is directed toward underground mining, much of the technology being developed may have applications for space systems or mining on the Moon or other planets. Author

N90-29019*# Carnegie-Mellon Univ., Pittsburgh, PA. Dept. of Electrical and Computer Engineering.
A FAST LIGHTSTRIPE RANGEFINDING SYSTEM WITH SMART VLSI SENSOR
Andrew Gruss, L. Richard Carley, and Takeo Kanade *In* JPL, California Inst. of Tech., Proceedings of the NASA Conference on Space Telerobotics, Volume 1 31 Jan. 1989 p 219-228 (For primary document see N90-29000 23-54)
Avail: NTIS HC A21/MF A03 CSCL 05H

The focus of the research is to build a compact, high performance lightstripe rangefinder using a Very Large Scale Integration (VLSI) smart photosensor array. Rangefinding, the measurement of the three-dimensional profile of an object or scene, is a critical component for many robotic applications, and therefore many techniques were developed. Of these, lightstripe rangefinding is one of the most widely used and reliable techniques available. Though practical, the speed of sampling range data by the conventional light stripe technique is severely limited. A conventional light stripe rangefinder operates in a step-and-repeat manner. A stripe source is projected on an object, a video image is acquired, range data is extracted from the image, the stripe is stepped, and the process repeats. Range acquisition is limited by the time needed to grab the video images, increasing linearly with the desired horizontal resolution. During the acquisition of a range image, the objects in the scene being scanned must be stationary. Thus, the long scene sampling time of step-and-repeat rangefinders limits their application. The fast range sensor proposed is based on the modification of this basic lightstripe ranging technique in a manner described by Sato and Kida. This technique does not require a sampling of images at various stripe positions to build a range map. Rather, an entire range image is acquired in parallel while the stripe source is swept continuously across the scene. Total time to acquire the range image data is independent of the range map resolution. The target rangefinding system will acquire 1,000 100 x 100 point range images per second with 0.5 percent range accuracy. It will be compact and rugged enough to be mounted on the end effector of a robot arm to aid in object manipulation and assembly tasks. Author

N90-29020*# Michigan Univ., Ann Arbor. Robot Systems Div.
METHODS AND STRATEGIES OF OBJECT LOCALIZATION
Lejun Shao and Richard A. Volz (Texas A&M Univ., College Station.) *In* JPL, California Inst. of Tech., Proceedings of the NASA Conference on Space Telerobotics, Volume 1 31 Jan. 1989 p 229-239 (For primary document see N90-29000 23-54)
Avail: NTIS HC A21/MF A03 CSCL 05H

An important property of an intelligent robot is to be able to determine the location of an object in 3-D space. A general object localization system structure is proposed, some important issues on localization discussed, and an overview given for current available object localization algorithms and systems. The algorithms reviewed are characterized by their feature extracting and matching strategies; the range finding methods; the types of locatable objects; and the mathematical formulating methods. Author

N90-29021*# Surrey Univ., Guildford (England). Dept. of Mechanical Engineering.
A LASER TRACKING DYNAMIC ROBOT METROLOGY INSTRUMENT
G. A. Parker and J. R. R. Mayer *In* JPL, California Inst. of Tech., Proceedings of the NASA Conference on Space Telerobotics, Volume 1 31 Jan. 1989 p 241-250 Sponsored in part by Bureau of Community Reference, Commission of the European Community, Brussels; and Department of Trade and Industry, England (For primary document see N90-29000 23-54)
Avail: NTIS HC A21/MF A03 CSCL 05H

Research work over several years has resulted in the development of a laser tracking instrument capable of dynamic 3-D measurements of robot end-effector trajectories. The instrument characteristics and experiments to measure the static and dynamic performance of a robot in an industrial manufacturing environment are described. The use of this technology for space applications is examined. Author

N90-29022*# Maryland Univ., College Park. Computer Vision Lab.
ROBOT ACTING ON MOVING BODIES (RAMBO): INTERACTION WITH TUMBLING OBJECTS
Larry S. Davis, Daniel DeMenthon, Thor Bestul, Sotirios Ziavras, H. V. Srinivasan, Madhu Siddalingaiah, and David Harwood *In* JPL, California Inst. of Tech., Proceedings of the NASA Conference on Space Telerobotics, Volume 1 31 Jan. 1989 p 251-260 (For primary document see N90-29000 23-54)
(Contract DACA-76-88-C-0008)
Avail: NTIS HC A21/MF A03 CSCL 05H

Interaction with tumbling objects will become more common as human activities in space expand. Attempting to interact with a large complex object translating and rotating in space, a human operator using only his visual and mental capacities may not be able to estimate the object motion, plan actions or control those actions. A robot system (RAMBO) equipped with a camera, which, given a sequence of simple tasks, can perform these tasks on a tumbling object, is being developed. RAMBO is given a complete geometric model of the object. A low level vision module extracts and groups characteristic features in images of the object. The

positions of the object are determined in a sequence of images, and a motion estimate of the object is obtained. This motion estimate is used to plan trajectories of the robot tool to relative locations nearby the object sufficient for achieving the tasks. More specifically, low level vision uses parallel algorithms for image enhancement by symmetric nearest neighbor filtering, edge detection by local gradient operators, and corner extraction by sector filtering. The object pose estimation is a Hough transform method accumulating position hypotheses obtained by matching triples of image features (corners) to triples of model features. To maximize computing speed, the estimate of the position in space of a triple of features is obtained by decomposing its perspective view into a product of rotations and a scaled orthographic projection. This allows use of 2-D lookup tables at each stage of the decomposition. The position hypotheses for each possible match of model feature triples and image feature triples are calculated in parallel. Trajectory planning combines heuristic and dynamic programming techniques. Then trajectories are created using dynamic interpolations between initial and goal trajectories. All the parallel algorithms run on a Connection Machine CM-2 with 16K processors. Author

N90-29023*# Carnegie-Mellon Univ., Pittsburgh, PA. Dept. of Electrical and Computer Engineering.

REAL-TIME EDGE TRACKING USING A TACTILE SENSOR

Alan D. Berger, Richard Volpe, and Pradeep K. Khosla *In* JPL, California Inst. of Tech., Proceedings of the NASA Conference on Space Telerobotics, Volume 1 31 Jan. 1989 p 261-271 (For primary document see N90-29000 23-54)

Avail: NTIS HC A21/MF A03 CSCL 05H

Object recognition through the use of input from multiple sensors is an important aspect of an autonomous manipulation system. In tactile object recognition, it is necessary to determine the location and orientation of object edges and surfaces. A controller is proposed that utilizes a tactile sensor in the feedback loop of a manipulator to track along edges. In the control system, the data from the tactile sensor is first processed to find edges. The parameters of these edges are then used to generate a control signal to a hybrid controller. Theory is presented for tactile edge detection and an edge tracking controller. In addition, experimental verification of the edge tracking controller is presented. Author

N90-29024*# Rensselaer Polytechnic Inst., Troy, NY. Dept. of Electrical, Computer, and Systems Engineering.

PLANNING 3-D COLLISION-FREE PATHS USING SPHERES

Susan Bonner and Robert B. Kelley *In* JPL, California Inst. of Tech., Proceedings of the NASA Conference on Space Telerobotics, Volume 1 31 Jan. 1989 p 273-282 (For primary document see N90-29000 23-54)

Avail: NTIS HC A21/MF A03 CSCL 05H

A scheme for the representation of objects, the Successive Spherical Approximation (SSA), facilitates the rapid planning of collision-free paths in a 3-D, dynamic environment. The hierarchical nature of the SSA allows collision-free paths to be determined efficiently while still providing for the exact representation of dynamic objects. The concept of a freespace cell is introduced to allow human 3-D conceptual knowledge to be used in facilitating satisfying choices for paths. Collisions can be detected at a rate better than 1 second per environment object per path. This speed enables the path planning process to apply a hierarchy of rules to create a heuristically satisfying collision-free path. Author

N90-29025*# Brown Univ., Providence, RI. Dept. of Computer Science.

MAP LEARNING WITH INDISTINGUISHABLE LOCATIONS c43

Kenneth Basye and Thomas Dean *In* JPL, California Inst. of Tech., Proceedings of the NASA Conference on Space Telerobotics, Volume 1 31 Jan. 1989 p 285-290 (For primary document see N90-29000 23-54)

(Contract F49620-88-C-0132; NSF IRI-86-12644)

Avail: NTIS HC A21/MF A03 CSCL 05H

Nearly all spatial reasoning problems involve uncertainty of one sort or another. Uncertainty arises due to the inaccuracies of sensors used in measuring distances and angels. This is inferred as directional uncertainty. Uncertainty also arises in combining spatial information when one location is mistakenly identified with another. This is referred to as recognition uncertainty. Most problems in constructing spatial representations (maps) for the purpose of navigation involve both directional and recognition uncertainty. It is shown that a particular class of spatial reasoning problems involving the construction of representations of large-scale space can be solved efficiently even in the presence of directional and recognition uncertainty. Particular attention is paid to the problems that arise due to recognition uncertainty. The results described are applicable to the construction of global maps from satellite data as well as the construction of local navigation maps from measurements made by a rover in exploring a planetary surface. Author

N90-29026*# Georgia Inst. of Tech., Atlanta. School of Information and Computer Science.

THREE-DIMENSIONAL MOTOR SCHEMA BASED NAVIGATION c63

Ronald C. Arkin *In* JPL, California Inst. of Tech., Proceedings of the NASA Conference on Space Telerobotics, Volume 1 31 Jan. 1989 p 291-299 (For primary document see N90-29000 23-54)

Avail: NTIS HC A21/MF A03 CSCL 09B

Reactive schema-based navigation is possible in space domains by extending the methods developed for ground-based navigation found within the Autonomous Robot Architecture (AuRA). Reformulation of two dimensional motor schemas for three dimensional applications is a straightforward process. The manifold advantages of schema-based control persist, including modular development, amenability to distributed processing, and responsiveness to environmental sensing. Simulation results show the feasibility of this methodology for space docking operations in a cluttered work area. Author

N90-29027*# Carnegie-Mellon Univ., Pittsburgh, PA. Dept. of Mechanical Engineering.

PERIODIC GAITS FOR THE CMU AMBLER c37

Swaminathan Mahalingam and Suren N. Dwivedi (West Virginia Univ., Morgantown.) *In* JPL, California Inst. of Tech., Proceedings of the NASA Conference on Space Telerobotics, Volume 1 31 Jan. 1989 p 301-310 (For primary document see N90-29000 23-54)

(Grant NSF ROA-86-15072)

Avail: NTIS HC A21/MF A03 CSCL 13I

The configuration of the Carnegie Mellon University Ambler, a six legged autonomous walking vehicle for exploring Mars, enables the recovery of a trailing leg past the leading leg to reduce the energy expenditure in terrain interactions. Gaits developed for this unprecedented configuration are described. A stability criterion was developed which ensures stability of the vehicle in the event of failure of any one of the supporting legs. Periodic gaits developed for the Ambler utilize the Ambler's unique abilities, and continuously satisfy the stability criterion. Author

N90-29028*# Hughes Research Labs., Malibu, CA. Artificial Intelligence Center.

EXPLOITING MAP PLANS AS RESOURCES FOR ACTION c63

David Payton *In* JPL, California Inst. of Tech., Proceedings of the NASA Conference on Space Telerobotics, Volume 1 31 Jan. 1989 p 311-320 (For primary document see N90-29000 23-54)

Avail: NTIS HC A21/MF A03 CSCL 09B

When plans are used as programs for controlling the action of autonomous or teleoperated robots, their abstract representation can easily obscure a great deal of the critical knowledge that originally led to the planned course of action. An autonomous vehicle experiment is highlighted which illustrates how the information barriers created by abstraction can result in undesirable action. It is then shown how the same task can be performed correctly using plans as a resource for action. As a result of this

simple change in outlook, problems requiring opportunistic reaction to unexpected changes in the environment can be solved.
Author

N90-29029*# Old Dominion Univ., Norfolk, VA. Dept. of Computer Science.
LEARNED NAVIGATION IN UNKNOWN TERRAINS: A RETRACTION METHOD **c63**
Nageswara S. V. Rao, N. Stoltzfus, and S. Sitharama Iyengar (Louisiana State Univ., Baton Rouge.) *In* JPL, California Inst. of Tech., Proceedings of the NASA Conference on Space Telerobotics, Volume 1 31 Jan. 1989 p 321-330 (For primary document see N90-29000 23-54)
Avail: NTIS HC A21/MF A03 CSCL 09B

The problem of learned navigation of a circular robot R, of radius delta (is greater than or equal to 0), through a terrain whose model is not a-priori known is considered. Two-dimensional finite-sized terrains populated by an unknown (but, finite) number of simple polygonal obstacles are also considered. The number and locations of the vertices of each obstacle are unknown to R. R is equipped with a sensor system that detects all vertices and edges that are visible from its present location. In this context two problems are covered. In the visit problem, the robot is required to visit a sequence of destination points, and in the terrain model acquisition problem, the robot is required to acquire the complete model of the terrain. An algorithmic framework is presented for solving these two problems using a retraction of the freespace onto the Voronoi diagram of the terrain. Algorithms are then presented to solve the visit problem and the terrain model acquisition problem.
Author

N90-29030*# Jet Propulsion Lab., California Inst. of Tech., Pasadena.
COMPUTATIONAL NEURAL LEARNING FORMALISMS FOR MANIPULATOR INVERSE KINEMATICS **c63**
Sandeep Gulati, Jacob Barhen, and S. Sitharama Iyengar (Louisiana State Univ., Baton Rouge.) *In its* Proceedings of the NASA Conference on Space Telerobotics, Volume 1 31 Jan. 1989 p 333-342 (For primary document see N90-29000 23-54)
Avail: NTIS HC A21/MF A03 CSCL 09B

An efficient, adaptive neural learning paradigm for addressing the inverse kinematics of redundant manipulators is presented. The proposed methodology exploits the infinite local stability of terminal attractors - a new class of mathematical constructs which provide unique information processing capabilities to artificial neural systems. For robotic applications, synaptic elements of such networks can rapidly acquire the kinematic invariances embedded within the presented samples. Subsequently, joint-space configurations, required to follow arbitrary end-effector trajectories, can readily be computed. In a significant departure from prior neuromorphic learning algorithms, this methodology provides mechanisms for incorporating an in-training skew to handle kinematics and environmental constraints.
Author

N90-29031*# University of Southern Illinois, Carbondale. Dept. of Electrical Engineering.
MULTI-LAYER NEURAL NETWORKS FOR ROBOT CONTROL **c63**
Farzad Pourboghrat *In* JPL, California Inst. of Tech., Proceedings of the NASA Conference on Space Telerobotics, Volume 1 31 Jan. 1989 p 343-352 (For primary document see N90-29000 23-54)
Avail: NTIS HC A21/MF A03 CSCL 09B

Two neural learning controller designs for manipulators are considered. The first design is based on a neural inverse-dynamics system. The second is the combination of the first one with a neural adaptive state feedback system. Both types of controllers enable the manipulator to perform any given task very well after a period of training and to do other untrained tasks satisfactorily. The second design also enables the manipulator to compensate for unpredictable perturbations.
Author

N90-29032*# Tulane Univ., New Orleans, LA. Dept. of Computer Science.
A HYBRID ARCHITECTURE FOR THE IMPLEMENTATION OF THE ATHENA NEURAL NET MODEL **c63**
C. Koutsougeras and C. Papachristou (Case Western Reserve Univ., Cleveland, OH.) *In* JPL, California Inst. of Tech., Proceedings of the NASA Conference on Space Telerobotics, Volume 1 31 Jan. 1989 p 353-361 (For primary document see N90-29000 23-54)
Avail: NTIS HC A21/MF A03 CSCL 09B

The implementation of an earlier introduced neural net model for pattern classification is considered. Data flow principles are employed in the development of a machine that efficiently implements the model and can be useful for real time classification tasks. Further enhancement with optical computing structures is also considered.
Author

N90-29033*# New Mexico Univ., Albuquerque. Dept. of Electrical and Computer Engineering.
A DESIGN PHILOSOPHY FOR MULTI-LAYER NEURAL NETWORKS WITH APPLICATIONS TO ROBOT CONTROL **c63**
Nader Vadiee and Mo Jamshidi *In* JPL, California Inst. of Tech., Proceedings of the NASA Conference on Space Telerobotics, Volume 1 31 Jan. 1989 p 363-372 (For primary document see N90-29000 23-54)
Avail: NTIS HC A21/MF A03 CSCL 09B

A system is proposed which receives input information from many sensors that may have diverse scaling, dimension, and data represnetations. The proposed system tolerates sensory information with faults. The proposed self-adaptive processing technique has great promise in integrating the techniques of artificial intelligence and neural networks in an attempt to build a more intelligent computing environment. The proposed architecture can provide a detailed decision tree based on the input information, information stored in a long-term memory, and the adapted rule-based knowledge. A mathematical model for analysis will be obtained to validate the cited hypotheses. An extensive software program will be developed to simulate a typical example of pattern recognition problem. It is shown that the proposed model displays attention, expectation, spatio-temporal, and predictory behavior which are specific to the human brain. The anticipated results of this research project are: (1) creation of a new dynamic neural network structure, and (2) applications to and comparison with conventional multi-layer neural network structures. The anticipated benefits from this research are vast. The model can be used in a neuro-computer architecture as a building block which can perform complicated, nonlinear, time-varying mapping from a multitude of input excitory classes to an output or decision environment. It can be used for coordinating different sensory inputs and past experience of a dynamic system and actuating signals. The commercial applications of this project can be the creation of a special-purpose neuro-computer hardware which can be used in spatio-temporal pattern recognitions in such areas as air defense systems, e.g., target tracking, and recognition. Potential robotics-related applications are trajectory planning, inverse dynamics computations, hierarchical control, task-oriented control, and collision avoidance.
Author

N90-29034*# Kobe Univ. (Japan). Div. of System Science.
A NEURAL NETWORK FOR CONTROLLING THE CONFIGURATION OF FRAME STRUCTURE WITH ELASTIC MEMBERS **c63**
Kazuyoshi Tsutsumi *In* JPL, California Inst. of Tech., Proceedings of the NASA Conference on Space Telerobotics, Volume 1 31 Jan. 1989 p 373-382 (For primary document see N90-29000 23-54)
Avail: NTIS HC A21/MF A03 CSCL 09B

A neural network for controlling the configuration of frame structure with elastic members is proposed. In the present network, the structure is modeled not by using the relative angles of the members but by using the distances between the joint locations alone. The relationship between the environment and the joints is

also defined by their mutual distances. The analog neural network attains the reaching motion of the manipulator as a minimization problem of the energy constructed by the distances between the joints, the target, and the obstacles. The network can generate not only the final but also the transient configurations and the trajectory. This framework with flexibility and parallelism is very suitable for controlling the Space Telerobotic systems with many degrees of freedom. Author

N90-29035*# Edinburgh Univ. (Scotland). Inst. of Artificial Intelligence Applications.

COORDINATING THE ACTIVITIES OF A PLANNER AND AN EXECUTION AGENT **c63**

Austin Tate *In* JPL, California Inst. of Tech., Proceedings of the NASA Conference on Space Telerobotics, Volume 1 31 Jan. 1989 p 385-393 (For primary document see N90-29000 23-54)

(Grants GR/D/5898-7; GR/E/98058)

Avail: NTIS HC A21/MF A03 CSCL 09B

A research program was defined that will explore the link between planning and execution systems. A simple scenario was defined in which a very capable off-line planning system interacts with the user and a smaller, less capable, on-line real-time system executing plans and reacting to faults. However, the on-line execution system may have a more flexible representation of the plans it is executing. This imbalance in the capabilities of the two agents involved should clarify some of the research objectives and give an experimental framework for the work. The task is to investigate the knowledge representations and communication protocols needed to link a user stating some requirements for a task to be carried out through a planning system to the (remote) execution agent that can carry out the user's wishes. The notion that a single representation can encapsulate the expression of the user's requirements, the capabilities for action, the communication to the execution agent, the successful or faulty response from the execution agent and the means of keeping the user informed, is examined. Methods of creating plan patches to update the plans separately held by each of the parties involved to keep them in step as they each react to changing circumstances in real-time is investigated. This involves the specification of plan patch attachment points that can be understood by the recipient. Transaction based methods are also investigated for coordinating the activities of the planner with those of the execution agent and user. The trial application area for the research is in the command and control of an advanced Earth Observation Space Platform. Author

N90-29036*# Bolt, Beranek, and Newman, Inc., Cambridge, MA.

PLAN RECOGNITION FOR SPACE TELEROBOTICS

Bradley A. Goodman and Diane J. Litman (Bell Telephone Labs., Inc., Murray Hill, NJ.) *In* JPL, California Inst. of Tech., Proceedings of the NASA Conference on Space Telerobotics, Volume 1 31 Jan. 1989 p 395-404 (For primary document see N90-29000 23-54)

(Grant NSF IRI-87-01874)

Avail: NTIS HC A21/MF A03 CSCL 05H

Current research on space telerobots has largely focused on two problem areas: executing remotely controlled actions (the tele part of telerobotics) or planning to execute them (the robot part). This work has largely ignored one of the key aspects of telerobots: the interaction between the machine and its operator. For this interaction to be felicitous, the machine must successfully understand what the operator is trying to accomplish with particular remote-controlled actions. Only with the understanding of the operator's purpose for performing these actions can the robot intelligently assist the operator, perhaps by warning of possible errors or taking over part of the task. There is a need for such an understanding in the telerobotics domain and an intelligent interface being developed in the chemical process design domain addresses the same issues. Author

N90-29037*# Jet Propulsion Lab., California Inst. of Tech., Pasadena.

CAUSAL SIMULATION AND SENSOR PLANNING IN PREDICTIVE MONITORING

Richard J. Doyle *In its* Proceedings of the NASA Conference on Space Telerobotics, Volume 1 31 Jan. 1989 p 405-414 (For primary document see N90-29000 23-54)

Avail: NTIS HC A21/MF A03 CSCL 05H

Two issues are addressed which arise in the task of detecting anomalous behavior in complex systems with numerous sensor channels: how to adjust alarm thresholds dynamically, within the changing operating context of the system, and how to utilize sensors selectively, so that nominal operation can be verified reliably without processing a prohibitive amount of sensor data. The approach involves simulation of a causal model of the system, which provides information on expected sensor values, and on dependencies between predicted events, useful in assessing the relative importance of events so that sensor resources can be allocated effectively. The potential applicability of this work to the execution monitoring of robot task plans is briefly discussed. Author

N90-29038*# Carnegie-Mellon Univ., Pittsburgh, PA. The Robotics Inst.

STATE-BASED SCHEDULING: AN ARCHITECTURE FOR TELESCOPE OBSERVATION SCHEDULING **c61**

Nicola Muscettola and Stephen F. Smith *In* JPL, California Inst. of Tech., Proceedings of the NASA Conference on Space Telerobotics, Volume 1 31 Jan. 1989 p 415-424 (For primary document see N90-29000 23-54)

(Contract NCC2-531)

Avail: NTIS HC A21/MF A03 CSCL 09B

The applicability of constraint-based scheduling, a methodology previously developed and validated in the domain of factory scheduling, is extended to problem domains that require attendance to a wider range of state-dependent constraints. The problem of constructing and maintaining a short-term observation schedule for the Hubble Space Telescope (HST), which typifies this type of domain is the focus of interest. The nature of the constraints encountered in the HST domain is examined, system requirements are discussed with respect to utilization of a constraint-based scheduling methodology in such domains, and a general framework for state-based scheduling is presented. Author

N90-29039*# Carnegie-Mellon Univ., Pittsburgh, PA. Dept. of Computer Science.

FOCUS OF ATTENTION IN AN ACTIVITY-BASED SCHEDULER **c61**

Norman Sadeh and Mark S. Fox *In* JPL, California Inst. of Tech., Proceedings of the NASA Conference on Space Telerobotics, Volume 1 31 Jan. 1989 p 425-434 Sponsored in part by McDonnell Aircraft Co., and by Digital Equipment Corp. (For primary document see N90-29000 23-54)

(Contract F30602-88-C-0001)

Avail: NTIS HC A21/MF A03 CSCL 09B

Earlier research in job shop scheduling has demonstrated the advantages of opportunistically combining order-based and resource-based scheduling techniques. An even more flexible approach is investigated where each activity is considered a decision point by itself. Heuristics to opportunistically select the next decision point on which to focus attention (i.e., variable ordering heuristics) and the next decision to be tried at this point (i.e., value ordering heuristics) are described that probabilistically account for both activity precedence and resource requirement interactions. Preliminary experimental results indicate that the variable ordering heuristic greatly increases search efficiency. While least constraining value ordering heuristics have been advocated in the literature, the experimental results suggest that other value ordering heuristics combined with our variable-ordering heuristic can produce much better schedules without significantly increasing search. Author

N90-29040*# Rensselaer Polytechnic Inst., Troy, NY. Center for Intelligent Robotic Systems for Space Exploration.

A BOLTZMANN MACHINE FOR THE ORGANIZATION OF INTELLIGENT MACHINES **c63**

Michael C. Moed and George N. Saridis *In* JPL, California Inst. of Tech., Proceedings of the NASA Conference on Space Telerobotics, Volume 1 31 Jan. 1989 p 437-446 (For primary document see N90-29000 23-54)

(Grant NAGw-1333)

Avail: NTIS HC A21/MF A03 CSCL 09B

In the present technological society, there is a major need to build machines that would execute intelligent tasks operating in uncertain environments with minimum interaction with a human operator. Although some designers have built smart robots, utilizing heuristic ideas, there is no systematic approach to design such machines in an engineering manner. Recently, cross-disciplinary research from the fields of computers, systems AI and information theory has served to set the foundations of the emerging area of the design of intelligent machines. Since 1977 Saridis has been developing an approach, defined as Hierarchical Intelligent Control, designed to organize, coordinate and execute anthropomorphic tasks by a machine with minimum interaction with a human operator. This approach utilizes analytical (probabilistic) models to describe and control the various functions of the intelligent machine structured by the intuitively defined principle of Increasing Precision with Decreasing Intelligence (IPDI) (Saridis 1979). This principle, even though resembles the managerial structure of organizational systems (Levis 1988), has been derived on an analytic basis by Saridis (1988). The purpose is to derive analytically a Boltzmann machine suitable for optimal connection of nodes in a neural net (Fahlman, Hinton, Sejnowski, 1985). Then this machine will serve to search for the optimal design of the organization level of an intelligent machine. In order to accomplish this, some mathematical theory of the intelligent machines will be first outlined. Then some definitions of the variables associated with the principle, like machine intelligence, machine knowledge, and precision will be made (Saridis, Valavanis 1988). Then a procedure to establish the Boltzmann machine on an analytic basis will be presented and illustrated by an example in designing the organization level of an Intelligent Machine. A new search technique, the Modified Genetic Algorithm, is presented and proved to converge to the minimum of a cost function. Finally, simulations will show the effectiveness of a variety of search techniques for the intelligent machine. Author

N90-29041*# George Mason Univ., Fairfax, VA. School of Information Technology and Engineering.

GRASP PLANNING UNDER UNCERTAINTY **c63**

A. M. Erkmen and H. E. Stephanou *In* JPL, California Inst. of Tech., Proceedings of the NASA Conference on Space Telerobotics, Volume 1 31 Jan. 1989 p 447-456 (For primary document see N90-29000 23-54)

Avail: NTIS HC A21/MF A03 CSCL 09B

The planning of dexterous grasps for multifingered robot hands operating in uncertain environments is covered. A sensor-based approach to the planning of a reach path prior to grasping is first described. An on-line, joint space finger path planning algorithm for the enclose phase of grasping was then developed. The algorithm minimizes the impact momentum of the hand. It uses a Preshape Jacobian matrix to map task-level hand preshape requirements into kinematic constraints. A master slave scheme avoids inter-finger collisions and reduces the dimensionality of the planning problem. Author

N90-29042*# Brown Univ., Providence, RI. Dept. of Computer Science.

APPROXIMATION ALGORITHMS FOR PLANNING AND CONTROL **c63**

Mark Boddy and Thomas Dean *In* JPL, California Inst. of Tech., Proceedings of the NASA Conference on Space Telerobotics, Volume 1 31 Jan. 1989 p 457-462 (For primary document see N90-29000 23-54)

(Contract F49620-88-C-0132; NSF IRI-86-12644)

Avail: NTIS HC A21/MF A03 CSCL 09B

A control system operating in a complex environment will encounter a variety of different situations, with varying amounts of time available to respond to critical events. Ideally, such a control system will do the best possible with the time available. In other words, its responses should approximate those that would result from having unlimited time for computation, where the degree of the approximation depends on the amount of time it actually has. There exist approximation algorithms for a wide variety of problems. Unfortunately, the solution to any reasonably complex control problem will require solving several computationally intensive problems. Algorithms for successive approximation are a subclass of the class of anytime algorithms, algorithms that return answers for any amount of computation time, where the answers improve as more time is allotted. An architecture is described for allocating computation time to a set of anytime algorithms, based on expectations regarding the value of the answers they return. The architecture described is quite general, producing optimal schedules for a set of algorithms under widely varying conditions. Author

N90-29043*# Drexel Univ., Philadelphia, PA. Dept. of Electrical and Computer Engineering.

MULTIRESOLUTIONAL MODELS OF UNCERTAINTY GENERATION AND REDUCTION **c63**

A. Meystel *In* JPL, California Inst. of Tech., Proceedings of the NASA Conference on Space Telerobotics, Volume 1 31 Jan. 1989 p 463-476 (For primary document see N90-29000 23-54)

Avail: NTIS HC A21/MF A03 CSCL 09B

Kolmogorov's axiomatic principles of the probability theory, are reconsidered in the scope of their applicability to the processes of knowledge acquisition and interpretation. The model of uncertainty generation is modified in order to reflect the reality of engineering problems, particularly in the area of intelligent control. This model implies algorithms of learning which are organized in three groups which reflect the degree of conceptualization of the knowledge the system is dealing with. It is essential that these algorithms are motivated by and consistent with the multiresolutional model of knowledge representation which is reflected in the structure of models and the algorithms of learning. Author

N90-29044*# Jet Propulsion Lab., California Inst. of Tech., Pasadena.

PROCEEDINGS OF THE NASA CONFERENCE ON SPACE TELEROBOTICS, VOLUME 2

Guillermo Rodriguez, ed. and Homayoun Seraji, ed. 31 Jan. 1989 393 p Conference held in Pasadena, CA, 31 Jan. - 2 Feb. 1989

(Contract NAS7-918)

(NASA-CR-186857; JPL-Publ-89-7-Vol-2; NAS 1.26:186857)

Avail: NTIS HC A17/MF A03 CSCL 05H

These proceedings contain papers presented at the NASA Conference on Space Telerobotics held in Pasadena, January 31 to February 2, 1989. The theme of the Conference was man-machine collaboration in space. The Conference provided a forum for researchers and engineers to exchange ideas on the research and development required for application of telerobotics technology to the space systems planned for the 1990s and beyond. The Conference: (1) provided a view of current NASA telerobotic research and development; (2) stimulated technical exchange on man-machine systems, manipulator control, machine sensing, machine intelligence, concurrent computation, and system architectures; and (3) identified important unsolved problems of current interest which can be dealt with by future research. For individual titles, see N90-29045 through N90-29079.

N90-29045*# Jet Propulsion Lab., California Inst. of Tech., Pasadena.

CHARACTERIZATION AND CONTROL OF SELF-MOTIONS IN REDUNDANT MANIPULATORS

J. Burdick (California Inst. of Tech., Pasadena.) and Homayoun

Seraji *In its* Proceedings of the NASA Conference on Space Telerobotics, Volume 2 31 Jan. 1989 p 3-14 Sponsored in part by System Development Foundation (For primary document see N90-29044 23-54)
Avail: NTIS HC A17/MF A03 CSCL 05H

The presence of redundant degrees of freedom in a manipulator structure leads to a physical phenomenon known as a self-motion, which is a continuous motion of the manipulator joints that leaves the end-effector motionless. In the first part of the paper, a global manifold mapping reformulation of manipulator kinematics is reviewed, and the inverse kinematic solution for redundant manipulators is developed in terms of self-motion manifolds. Global characterizations of the self-motion manifolds in terms of their number, geometry, homotopy class, and null space are reviewed using examples. Much previous work in redundant manipulator control has been concerned with the redundancy resolution problem, in which methods are developed to determine, or resolve, the motion of the joints in order to achieve end-effector trajectory control while optimizing additional objective functions. Redundancy resolution problems can be equivalently posed as the control of self-motions. Alternatives for redundancy resolution are briefly discussed. Author

N90-29046*# Texas Univ., Austin. Dept. of Electrical and Computer Engineering.
MULTIPLE COOPERATING MANIPULATORS: THE CASE OF KINEMATICALLY REDUNDANT ARMS
Ian D. Walker, Robert A. Freeman, and Steven I. Marcus *In* JPL, California Inst. of Tech., Proceedings of the NASA Conference on Space Telerobotics, Volume 2 31 Jan. 1989 p 15-24 Sponsored in part by Bureau of Engineering Research (For primary document see N90-29044 23-54)
(Contract F49620-86-C-0045; AF-AFOSR-0029-86; NSF ECS-86-17860)
Avail: NTIS HC A17/MF A03 CSCL 05H

Existing work concerning two or more manipulators simultaneously grasping and transferring a common load is continued and extended. Specifically considered is the case of one or more arms being kinematically redundant. Some existing results in the modeling and control of single redundant arms and multiple manipulators are reviewed. The cooperating situation is modeled in terms of a set of coordinates representing object motion and internal object squeezing. Nominal trajectories in these coordinates are produced via actuator load distribution algorithms introduced previously. A controller is developed to track these desired object trajectories while making use of the kinematic redundancy to additionally aid the cooperation and coordination of the system. It is shown how the existence of kinematic redundancy within the system may be used to enhance the degree of cooperation achievable. Author

N90-29047*# Robotics Research Corp., Milford, OH.
REFLEXIVE OBSTACLE AVOIDANCE FOR KINEMATICALLY-REDUNDANT MANIPULATORS
James P. Karlen, Jack M. Thompson, Jr., James D. Farrell, and Havard I. Vold *In* JPL, California Inst. of Tech., Proceedings of the NASA Conference on Space Telerobotics, Volume 2 31 Jan. 1989 p 25-37 Sponsored by NASA, Langley Research Center (For primary document see N90-29044 23-54)
Avail: NTIS HC A17/MF A03 CSCL 05H

Dexterous telerobots incorporating 17 or more degrees of freedom operating under coordinated, sensor-driven computer control will play important roles in future space operations. They will also be used on Earth in assignments like fire fighting, construction and battlefield support. A real time, reflexive obstacle avoidance system, seen as a functional requirement for such massively redundant manipulators, was developed using arm-mounted proximity sensors to control manipulator pose. The project involved a review and analysis of alternative proximity sensor technologies for space applications, the development of a general-purpose algorithm for synthesizing sensor inputs, and the implementation of a prototypical system for demonstration and testing. A 7 degree of freedom Robotics Research K-2107HR manipulator was outfitted with ultrasonic proximity sensors as a testbed, and Robotics Research's standard redundant motion control algorithm was modified such that an object detected by sensor arrays located at the elbow effectively applies a force to the manipulator elbow, normal to the axis. The arm is repelled by objects detected by the sensors, causing the robot to steer around objects in the workspace automatically while continuing to move its tool along the commanded path without interruption. The mathematical approach formulated for synthesizing sensor inputs can be employed for redundant robots of any kinematic configuration. Author

N90-29048*# McGill Univ., Montreal (Quebec). Research Center for Intelligent Machines.
PRELIMINARY STUDY OF A SERIAL-PARALLEL REDUNDANT MANIPULATOR
Vincent Hayward and Ronald Kurtz *In* JPL, California Inst. of Tech., Proceedings of the NASA Conference on Space Telerobotics, Volume 2 31 Jan. 1989 p 39-48 Sponsored in part by Natural Sciences and Engineering Research Council, Canada and Fonds pour la Formation des Chercheurs et l'Aide a la Recherche, Quebec (For primary document see N90-29044 23-54)
Avail: NTIS HC A17/MF A03 CSCL 05H

The manipulator design discussed here results from the examination of some of the reasons why redundancy is necessary in general purpose manipulation systems. A spherical joint design actuated in-parallel, having the many advantages of parallel actuation, is described. In addition, the benefits of using redundant actuators are discussed and illustrated in the design by the elimination of loci of singularities from the usable workspace with the addition of only one actuator. Finally, what is known by the authors about space robotics requirements is summarized and the relevance of the proposed design matched against these requirements. The design problems outlined here are viewed as much from the mechanical engineering aspect as from concerns arising from the control and the programming of manipulators. Author

N90-29049*# Jet Propulsion Lab., California Inst. of Tech., Pasadena.
THE JPL TELEROBOT OPERATOR CONTROL STATION. PART 1: HARDWARE
Edwin P. Kan, John T. Tower, George W. Hunka, and Glenn J. VanSant (General Electric Co., Moorestown, NJ.) *In its* Proceedings of the NASA Conference on Space Telerobotics, Volume 2 31 Jan. 1989 p 51-62 (For primary document see N90-29044 23-54)
Avail: NTIS HC A17/MF A03 CSCL 05H

The Operator Control Station of the Jet Propulsion Laboratory (JPL)/NASA Telerobot Demonstrator System provides the man-machine interface between the operator and the system. It provides all the hardware and software for accepting human input for the direct and indirect (supervised) manipulation of the robot arms and tools for task execution. Hardware and software are also provided for the display and feedback of information and control data for the operator's consumption and interaction with the task being executed. The hardware design, system architecture, and its integration and interface with the rest of the Telerobot Demonstrator System are discussed. Author

N90-29050*# Jet Propulsion Lab., California Inst. of Tech., Pasadena.
THE JPL TELEROBOT OPERATOR CONTROL STATION. PART 2: SOFTWARE
Edwin P. Kan, B. Patrick Landell, Sheldon Oxenberg, and Carl Morimoto (General Electric Co., San Jose, CA.) *In its* Proceedings of the NASA Conference on Space Telerobotics, Volume 2 31 Jan. 1989 p 63-73 (For primary document see N90-29044 23-54)
Avail: NTIS HC A17/MF A03 CSCL 05H

The Operator Control Station of the Jet Propulsion Laboratory (JPL)/NASA Telerobot Demonstrator System provides the

man-machine interface between the operator and the system. It provides all the hardware and software for accepting human input for the direct and indirect (supervised) manipulation of the robot arms and tools for task execution. Hardware and software are also provided for the display and feedback of information and control data for the operator's consumption and interaction with the task being executed. The software design of the operator control system is discussed. Author

N90-29051*# Teledyne Brown Engineering, Huntsville, AL.
DESIGN OF A MONITOR AND SIMULATION TERMINAL (MASTER) FOR SPACE STATION TELEROBOTICS AND TELESCIENCE
L. Lopez, C. Konkel, P. Harmon (System Dynamics, Inc., Huntsville, AL.), and S. King *In* JPL, California Inst. of Tech., Proceedings of the NASA Conference on Space Telerobotics, Volume 2 31 Jan. 1989 p 75-86 (For primary document see N90-29044 23-54)
Avail: NTIS HC A17/MF A03 CSCL 05H

Based on Space Station and planetary spacecraft communication time delays and bandwidth limitations, it will be necessary to develop an intelligent, general purpose ground monitor terminal capable of sophisticated data display and control of on-orbit facilities and remote spacecraft. The basic elements that make up a Monitor and Simulation Terminal (MASTER) include computer overlay video, data compression, forward simulation, mission resource optimization and high level robotic control. Hardware and software elements of a MASTER are being assembled for testbed use. Applications of Neural Networks (NNs) to some key functions of a MASTER are also discussed. These functions are overlay graphics adjustment, object correlation and kinematic-dynamic characterization of the manipulator. Author

N90-29052*# Jet Propulsion Lab., California Inst. of Tech., Pasadena.
PERFORMANCE EVALUATION OF A 6 AXIS HIGH FIDELITY GENERALIZED FORCE REFLECTING TELEOPERATOR
Blake Hannaford and Laurie Wood *In its* Proceedings of the NASA Conference on Space Telerobotics, Volume 2 31 Jan. 1989 p 87-96 (For primary document see N90-29044 23-54)
Avail: NTIS HC A17/MF A03 CSCL 05H

A few of the results of a major study of over 100 hours of experimental teleoperation are presented. Force and torque data recorded from the robot wrist is a rich source of information on the performance of tasks. Performance measures can be computed for whole tasks, or for specific task segments. As a general principle, the performance increases as manipulation capability is increased although the effects may depend on task and performance measure. This study has laid the groundwork for much future work. Further reports will detail additional results which could not be presented here due to lack of space as well as follow-on experiments investigating manipulation under time delay and shared control conditions. Author

N90-29053*# Jet Propulsion Lab., California Inst. of Tech., Pasadena.
IMPLEMENTATION AND DESIGN OF A TELEOPERATION SYSTEM BASED ON A VMEBUS/68020 PIPELINED ARCHITECTURE
Thomas S. Lee *In its* Proceedings of the NASA Conference on Space Telerobotics, Volume 2 31 Jan. 1989 p 97-107 (For primary document see N90-29044 23-54)
Avail: NTIS HC A17/MF A03 CSCL 05H

A pipelined control design and architecture for a force-feedback teleoperation system that is being implemented at the Jet Propulsion Laboratory and which will be integrated with the autonomous portion of the testbed to achieve share control is described. At the local site, the operator sees real-time force/torque displays and moves two 6-degree of freedom (dof) force-reflecting hand-controllers as his hands feel the contact force/torques generated at the remote site where the robots interact with the environment. He also uses a graphical user menu to monitor robot states and specify system options. The teleoperation software is written in the C language and runs on MC68020-based processor boards in the VME chassis, which utilizes a real-time operating system; the hardware is configured to realize a four-stage pipeline configuration. The environment is very flexible, such that the system can easily be configured as a stand-alone facility for performing independent research in human factors, force control, and time-delayed systems. Author

N90-29054*# Minnesota Univ., Minneapolis. Dept. of Mechanical Engineering.
HUMAN MACHINE INTERACTION VIA THE TRANSFER OF POWER AND INFORMATION SIGNALS
H. Kazerooni, W. K. Foslien, B. J. Anderson, and T. M. Hessburg *In* JPL, California Inst. of Tech., Proceedings of the NASA Conference on Space Telerobotics, Volume 2 31 Jan. 1989 p 109-119 (For primary document see N90-29044 23-54)
Avail: NTIS HC A17/MF A03 CSCL 05H

Robot manipulators are designed to perform tasks which would otherwise be executed by a human operator. No manipulator can even approach the speed and accuracy with which humans execute these tasks. But manipulators have the capability to exceed human ability in one particular area: strength. Through any reasonable observation and experience, the human's ability to perform a variety of physical tasks is limited not by his intelligence, but by his physical strength. If, in the appropriate environment, we can more closely integrate the mechanical power of a machine with intellectually driven human hand under the supervisory control of the human's intellect, we will then have a system which is superior to a loosely-integrated combination of a human and his fully automated robot as in the present day robotic systems. We must therefore develop a fundamental approach to the problem of this extending human mechanical power in certain environments. Extenders will be a class of robots worn by humans to increase human mechanical ability, while the wearer's intellect remains the central intelligent control system for manipulating the extender. The human body, in physical contact with the extender, exchanges information signals and power with the extender. Commands are transferred to the extender via the contact forces between the wearer and the extender as opposed to use of joystick (master arm), push-button or key-board to execute such commands that were used in previous man amplifiers. Instead, the operator becomes an integral part of the extender while executing the task. In this unique configuration the mechanical power transfer between the human and extender occurs in addition to information signal transfer. When the wearer uses the extender to touch and manipulate an object, the extender transfers to the wearer's hand, in feedback fashion, a scaled-down value of the actual external load which the extender is manipulating. This natural feedback force on the wearer's hand allows him to feel the scaled-down value of the external forces in the manipulations. Extenders can be utilized to maneuver very heavy loads in factories, shipyards, airports, and construction sites. In some instances, for example, extenders can replace forklifts. The experimental results for a prototype extender are discussed. Author

N90-29055*# National Inst. of Standards and Technology, Gaithersburg, MD.
TRAJECTORY GENERATION OF SPACE TELEROBOTS
R. Lumia and A. J. Wavering *In* JPL, California Inst. of Tech., Proceedings of the NASA Conference on Space Telerobotics, Volume 2 31 Jan. 1989 p 123-131 (For primary document see N90-29044 23-54)
Avail: NTIS HC A17/MF A03 CSCL 05H

The purpose is to review a variety of trajectory generation techniques which may be applied to space telerobots and to identify problems which need to be addressed in future telerobot motion control systems. As a starting point for the development of motion generation systems for space telerobots, the operation and limitations of traditional path-oriented trajectory generation approaches are discussed. This discussion leads to a description of more advanced techniques which have been demonstrated in research laboratories, and their potential applicability to space telerobots. Examples of this work include systems that incorporate

sensory-interactive motion capability and optimal motion planning. Additional considerations which need to be addressed for motion control of a space telerobot are described, such as redundancy resolution and the description and generation of constrained and multi-armed cooperative motions. A task decomposition module for a hierarchical telerobot control system which will serve as a testbed for trajectory generation approaches which address these issues is also discussed briefly. Author

N90-29056*# Michigan Univ., Ann Arbor. Robotics Research Lab.

ON THE SIMULATION OF SPACE BASED MANIPULATORS WITH CONTACT

Michael W. Walker and Joseph Dionise *In* JPL, California Inst. of Tech., Proceedings of the NASA Conference on Space Telerobotics, Volume 2 31 Jan. 1989 p 133-142 Sponsored in part by ERIM (For primary document see N90-29044 23-54)
Avail: NTIS HC A17/MF A03 CSCL 05H

An efficient method of simulating the motion of space based manipulators is presented. Since the manipulators will come into contact with different objects in their environment while carrying out different tasks, an important part of the simulation is the modeling of those contacts. An inverse dynamics controller is used to control a two armed manipulator whose task is to grasp an object floating in space. Simulation results are presented and an evaluation is made of the performance of the controller. Author

N90-29057*# Ford Aerospace Corp., Palo Alto, CA. Space Systems Div.

PRELIMINARY RESULTS ON NONCOLLOCATED TORQUE CONTROL OF SPACE ROBOT ACTUATORS

Scott W. Tilley, Colin M. Francis, Ken Emerick, and Michael G. Hollars *In* JPL, California Inst. of Tech., Proceedings of the NASA Conference on Space Telerobotics, Volume 2 31 Jan. 1989 p 143-152 (For primary document see N90-29044 23-54)
Avail: NTIS HC A17/MF A03 CSCL 05H

In the Space Station era, more operations will be performed robotically in space in the areas of servicing, assembly, and experiment tending among others. These robots may have various sets of requirements for accuracy, speed, and force generation, but there will be design constraints such as size, mass, and power dissipation limits. For actuation, a leading motor candidate is a dc brushless type, and there are numerous potential drive trains each with its own advantages and disadvantages. This experiment uses a harmonic drive and addresses some inherent limitations, namely its backdriveability and low frequency structural resonances. These effects are controlled and diminished by instrumenting the actuator system with a torque transducer on the output shaft. This noncollocated loop is closed to ensure that the commanded torque is accurately delivered to the manipulator link. The actuator system is modelled and its essential parameters identified. The nonlinear model for simulations will include inertias, gearing, stiction, flexibility, and the effects of output load variations. A linear model is extracted and used for designing the noncollocated torque and position feedback loops. These loops are simulated with the structural frequency encountered in the testbed system. Simulation results are given for various commands in position. The use of torque feedback is demonstrated to yield superior performance in settling time and positioning accuracy. An experimental setup being finished consists of a bench mounted motor and harmonic drive actuator system. A torque transducer and two position encoders, each with sufficient resolution and bandwidth, will provide sensory information. Parameters of the physical system are being identified and matched to analytical predictions. Initial feedback control laws will be incorporated in the bench test equipment and various experiments run to validate the designs. The status of these experiments is given. Author

N90-29058*# Rutgers - The State Univ., Piscataway, NJ. Dept. of Electrical and Computer Engineering.

PORTABLE DEXTROUS FORCE FEEDBACK MASTER FOR ROBOT TELEMANIPULATION (PDMFF)

Grigore C. Burdea and Thomas H. Speeter (Bell Telephone Labs., Inc., Holmdel, NJ.) *In* JPL, California Inst. of Tech., Proceedings of the NASA Conference on Space Telerobotics, Volume 2 31 Jan. 1989 p 153-161 Sponsored in part by Bell Telephone Labs., Inc. (For primary document see N90-29044 23-54)
Avail: NTIS HC A17/MF A03 CSCL 05H

A major drawback of open loop masters is a lack of force feedback, limiting their ability to perform complex tasks such as assembly and repair. Researchers present a simple dextrous force feedback master for computer assisted telemanipulation. The device is compact, portable and can be held in the operator hand, without the need for a special joystick or console. The system is capable of both position feed forward and force feedback, using electronic position sensors and a pneumatic micro-actuator. The level of forces exercised by the pneumatic actuator is such that near rigidity may be attained. Experimental results showing good system linearity and small time lag are given. Author

N90-29059*# Jet Propulsion Lab., California Inst. of Tech., Pasadena. Tele-Autonomous Systems Group.

EXPERIENCES WITH THE JPL TELEROBOT TESTBED: ISSUES AND INSIGHTS

Henry W. Stone, Bob Balaram, and John Beahan *In its* Proceedings of the NASA Conference on Space Telerobotics, Volume 2 31 Jan. 1989 p 163-172 (For primary document see N90-29044 23-54)
Avail: NTIS HC A17/MF A03 CSCL 05H

The Jet Propulsion Laboratory's (JPL) Telerobot Testbed is an integrated robotic testbed used to develop, implement, and evaluate the performance of advanced concepts in autonomous, tele-autonomous, and tele-operated control of robotic manipulators. Using the Telerobot Testbed, researchers demonstrated several of the capabilities and technological advances in the control and integration of robotic systems which have been under development at JPL for several years. In particular, the Telerobot Testbed was recently employed to perform a near completely automated, end-to-end, satellite grapple and repair sequence. The task of integrating existing as well as new concepts in robot control into the Telerobot Testbed has been a very difficult and timely one. Now that researchers have completed the first major milestone (i.e., the end-to-end demonstration) it is important to reflect back upon experiences and to collect the knowledge that has been gained so that improvements can be made to the existing system. It is also believed that the experiences are of value to the others in the robotics community. Therefore, the primary objective here will be to use the Telerobot Testbed as a case study to identify real problems and technological gaps which exist in the areas of robotics and in particular systems integration. Such problems have surely hindered the development of what could be reasonably called an intelligent robot. In addition to identifying such problems, researchers briefly discuss what approaches have been taken to resolve them or, in several cases, to circumvent them until better approaches can be developed. Author

N90-29060*# Jet Propulsion Lab., California Inst. of Tech., Pasadena.

THE KALI MULTI-ARM ROBOT PROGRAMMING AND CONTROL ENVIRONMENT

Paul Backes, Samad Hayati, Vincent Hayward (McGill Univ., Montreal, Quebec), and Kam Tso *In its* Proceedings of the NASA Conference on Space Telerobotics, Volume 2 31 Jan. 1989 p 173-182 (For primary document see N90-29044 23-54)
Avail: NTIS HC A17/MF A03 CSCL 05H

The KALI distributed robot programming and control environment is described within the context of its use in the Jet Propulsion Laboratory (JPL) telerobot project. The purpose of KALI is to provide a flexible robot programming and control environment for coordinated multi-arm robots. Flexibility, both in hardware configuration and software, is desired so that it can be easily modified to test various concepts in robot programming and control, e.g., multi-arm control, force control, sensor integration, teleoperation, and shared control. In the programming environment,

user programs written in the C programming language describe trajectories for multiple coordinated manipulators with the aid of KALI function libraries. A system of multiple coordinated manipulators is considered within the programming environment as one motion system. The user plans the trajectory of one controlled Cartesian frame associated with a motion system and describes the positions of the manipulators with respect to that frame. Smooth Cartesian trajectories are achieved through a blending of successive path segments. The manipulator and load dynamics are considered during trajectory generation so that given interface force limits are not exceeded. Author

N90-29061*# Pennsylvania Univ., Philadelphia. Dept. of Computer and Information Science.
HOW DO ROBOTS TAKE TWO PARTS APART
Ruzena K. Bajcsy and Constantine J. Tsikos *In* JPL, California Inst. of Tech., Proceedings of the NASA Conference on Space Telerobotics, Volume 2 31 Jan. 1989 p 185-195 Sponsored in part by DEC Systems Research Center, Palo Alto, CA; IBM; Lord Corp., Erie, PA; and North Atlantic Treaty Organization (For primary document see N90-29044 23-54)
(Contracts NAG5-1045; F49620-85-K-0018; ONR-SB-35923-0; NCGS-1-RO-1-23636-01; N00014-88-K-0632; DAAG29-84-K-0061; NSF DCR-82-19196; NSF INT-85-14199; NSF DMC-85-17315; NS-10939-11)
Avail: NTIS HC A17/MF A03 CSCL 05H

This research is a natural progression of efforts which begun with the introduction of a new research paradigm in machine perception, called Active Perception. There it was stated that Active Perception is a problem of intelligent control strategies applied to data acquisition processes which will depend on the current state of the data interpretation, including recognition. The disassembly/assembly problem is treated as an Active Perception problem, and a method for autonomous disassembly based on this framework is presented. Author

N90-29062*# Drexel Univ., Philadelphia, PA. Dept. of Electrical and Computer Engineering.
TECHNIQUES AND POTENTIAL CAPABILITIES OF MULTI-RESOLUTIONAL INFORMATION (KNOWLEDGE) PROCESSING **c63**
A. Meystel *In* JPL, California Inst. of Tech., Proceedings of the NASA Conference on Space Telerobotics, Volume 2 31 Jan. 1989 p 197-209 (For primary document see N90-29044 23-54)
Avail: NTIS HC A17/MF A03 CSCL 09B

A concept of nested hierarchical (multi-resolutional, pyramidal) information (knowledge) processing is introduced for a variety of systems including data and/or knowledge bases, vision, control, and manufacturing systems, industrial automated robots, and (self-programmed) autonomous intelligent machines. A set of practical recommendations is presented using a case study of a multiresolutional object representation. It is demonstrated here that any intelligent module transforms (sometimes, irreversibly) the knowledge it deals with, and this tranformation affects the subsequent computation processes, e.g., those of decision and control. Several types of knowledge transformation are reviewed. Definite conditions are analyzed, satisfaction of which is required for organization and processing of redundant information (knowledge) in the multi-resolutional systems. Providing a definite degree of redundancy is one of these conditions. Author

N90-29063*# Maryland Univ., College Park. Cybernetics Research Lab.
PERCEPTUAL TELEROBOTICS
Panos A. Ligomenides *In* JPL, California Inst. of Tech., Proceedings of the NASA Conference on Space Telerobotics, Volume 2 31 Jan. 1989 p 211-220 Prepared in cooperation with Caelum Research Corp., Silver Spring, MD (For primary document see N90-29044 23-54)
Avail: NTIS HC A17/MF A03 CSCL 05H

A sensory world modeling system, congruent with a human expert's perception, is proposed. The Experiential Knowledge Base (EKB) system can provide a highly intelligible communication interface for telemonitoring and telecontrol of a real time robotic system operating in space. Paradigmatic acquisition of empirical perceptual knowledge, and real time experiential pattern recognition and knowledge integration are reviewed. The cellular architecture and operation of the EKB system are also examined. Author

N90-29064*# Michigan Univ., Ann Arbor. Artificial Intelligence Lab.
BUILDING AN ENVIRONMENT MODEL USING DEPTH INFORMATION **c63**
Y. Roth-Tabak and Ramesh Jain *In* JPL, California Inst. of Tech., Proceedings of the NASA Conference on Space Telerobotics, Volume 2 31 Jan. 1989 p 221-230 (For primary document see N90-29044 23-54)
(Contract JPL-958086)
Avail: NTIS HC A17/MF A03 CSCL 09B

Modeling the environment is one of the most crucial issues for the development and research of autonomous robot and tele-perception. Though the physical robot operates (navigates and performs various tasks) in the real world, any type of reasoning, such as situation assessment, planning or reasoning about action, is performed based on information in its internal world. Hence, the robot's intentional actions are inherently constrained by the models it has. These models may serve as interfaces between sensing modules and reasoning modules, or in the case of telerobots serve as interface between the human operator and the distant robot. A robot operating in a known restricted environment may have a priori knowledge of its whole possible work domain, which will be assimilated in its World Model. As the information in the World Model is relatively fixed, an Environment Model must be introduced to cope with the changes in the environment and to allow exploring entirely new domains. Introduced here is an algorithm that uses dense range data collected at various positions in the environment to refine and update or generate a 3-D volumetric model of an environment. The model, which is intended for autonomous robot navigation and tele-perception, consists of cubic voxels with the possible attributes: Void, Full, and Unknown. Experimental results from simulations of range data in synthetic environments are given. The quality of the results show great promise for dealing with noisy input data. The performance measures for the algorithm are defined, and quantitative results for noisy data and positional uncertainty are presented. Author

N90-29065*# Oak Ridge National Lab., TN. Robotics and Intelligent Systems Program.
HERMIES-3: A STEP TOWARD AUTONOMOUS MOBILITY, MANIPULATION, AND PERCEPTION
C. R. Weisbin, B. L. Burks, J. R. Einstein, R. R. Feezell, W. W. Manges, and D. H. Thompson *In* JPL, California Inst. of Tech., Proceedings of the NASA Conference on Space Telerobotics, Volume 2 31 Jan. 1989 p 233-245 Previously announced as N89-17249 (For primary document see N90-29044 23-54)
Avail: NTIS HC A17/MF A03 CSCL 05H

HERMIES-III is an autonomous robot comprised of a seven degree-of-freedom (DOF) manipulator designed for human scale tasks, a laser range finder, a sonar array, an omni-directional wheel-driven chassis, multiple cameras, and a dual computer system containing a 16-node hypercube expandable to 128 nodes. The current experimental program involves performance of human-scale tasks (e.g., valve manipulation, use of tools), integration of a dexterous manipulator and platform motion in geometrically complex environments, and effective use of multiple cooperating robots (HERMIES-IIB and HERMIES-III). The environment in which the robots operate has been designed to include multiple valves, pipes, meters, obstacles on the floor, valves occluded from view, and multiple paths of differing navigation complexity. The ongoing research program supports the development of autonomous capability for HERMIES-IIB and III to perform complex navigation and manipulation under time constraints, while dealing with imprecise sensory information. Author

N90-29066*# Carnegie-Mellon Univ., Pittsburgh, PA. Robotics Inst.

FIRST RESULTS IN TERRAIN MAPPING FOR A ROVING PLANETARY EXPLORER **c37**

E. Krotkov, C. Caillas, M. Hebert, I. S. Kweon, and Takeo Kanade *In* JPL, California Inst. of Tech., Proceedings of the NASA Conference on Space Telerobotics, Volume 2 31 Jan. 1989 p 247-256 (For primary document see N90-29044 23-54)

(Grant NAGw-1175)

Avail: NTIS HC A17/MF A03 CSCL 13I

To perform planetary exploration without human supervision, a complete autonomous rover must be able to model its environment while exploring its surroundings. Researchers present a new algorithm to construct a geometric terrain representation from a single range image. The form of the representation is an elevation map that includes uncertainty, unknown areas, and local features. By virtue of working in spherical-polar space, the algorithm is independent of the desired map resolution and the orientation of the sensor, unlike other algorithms that work in Cartesian space. They also describe new methods to evaluate regions of the constructed elevation maps to support legged locomotion over rough terrain. Author

N90-29067*# National Aeronautics and Space Administration, Washington, DC.

PLANETARY ROVER TECHNOLOGY DEVELOPMENT REQUIREMENTS **c37**

Roger J. Bedard, Jr., Brian K. Muirhead (Jet Propulsion Lab., California Inst. of Tech., Pasadena.), Melvin D. Montemerlo, and Murray S. Hirschbein *In* JPL, California Inst. of Tech., Proceedings of the NASA Conference on Space Telerobotics, Volume 2 31 Jan. 1989 p 257-264 (For primary document see N90-29044 23-54)

Avail: NTIS HC A17/MF A03 CSCL 13I

Planetary surface (including lunar) mobility and sampling capability is required to support proposed future National Aeronautics and Space Administration (NASA) solar system exploration missions. The NASA Office of Aeronautics and Space Technology (OAST) is addressing some of these technology needs in its base research and development program, the Civil Space Technology Initiative (CSTI) and a new technology initiative entitled Pathfinder. The Pathfinder Planetary Rover (PPR) and Sample Acquisition, Analysis and Preservation (SAAP) programs will develop and validate the technologies needed to enable both robotic and piloted rovers on various planetary surfaces. The technology requirements for a planetary roving vehicle and the development plans of the PPR and SAAP programs are discussed. Author

N90-29068*# Rice Univ., Houston, TX. Dept. of Electrical and Computer Engineering.

RICE-OBOT 1: AN INTELLIGENT AUTONOMOUS MOBILE ROBOT **c37**

R. deFigueiredo, L. Ciscon, and D. Berberian *In* JPL, Californai Inst. of Tech., Proceedings of the NASA Conference on Space Telerobotics, Volume 2 31 Jan. 1989 p 265-274 Sponsored in part by Texas Instruments, Inc. (For primary document see N90-29044 23-54)

(Grant NAG9-208)

Avail: NTIS HC A17/MF A03 CSCL 13I

The Rice-obot I is the first in a series of Intelligent Autonomous Mobile Robots (IAMRs) being developed at Rice University's Cooperative Intelligent Mobile Robots (CIMR) lab. The Rice-obot I is mainly designed to be a testbed for various robotic and AI techniques, and a platform for developing intelligent control systems for exploratory robots. Researchers present the need for a generalized environment capable of combining all of the control, sensory and knowledge systems of an IAMR. They introduce Lisp-Nodes as such a system, and develop the basic concepts of nodes, messages and classes. Furthermore, they show how the control system of the Rice-obot I is implemented as sub-systems in Lisp-Nodes. Author

N90-29069*# Texas Univ., Austin. Dept. of Computer Science.

SATELLITE-MAP POSITION ESTIMATION FOR THE MARS ROVER **c37**

Akira Hayashi and Thomas Dean (Brown Univ., Providence, RI.) *In* JPL, California Inst. of Tech., Proceedings of the NASA Conference on Space Telerobotics, Volume 2 31 Jan. 1989 p 275-282 Sponsored in part by ARPA (For primary document see N90-29044 23-54)

(Contract F49620-88-C-0132; NSF IRI-86-12644)

Avail: NTIS HC A17/MF A03 CSCL 13I

A method for locating the Mars rover using an elevation map generated from satellite data is described. In exploring its environment, the rover is assumed to generate a local rover-centered elevation map that can be used to extract information about the relative position and orientation of landmarks corresponding to local maxima. These landmarks are integrated into a stochastic map which is then matched with the satellite map to obtain an estimate of the robot's current location. The landmarks are not explicitly represented in the satellite map. The results of the matching algorithm correspond to a probabilistic assessment of whether or not the robot is located within a given region of the satellite map. By assigning a probabilistic interpretation to the information stored in the satellite map, researchers are able to provide a precise characterization of the results computed by the matching algorithm. Author

N90-29070*# Martin Marietta Corp., Denver, CO. Astronautics Group.

ROBOTIC SAMPLING SYSTEM FOR AN UNMANNED MARS MISSION **c37**

Wendell Chun *In* JPL, California Inst. of Tech., Proceedings of the NASA Conference on Space Telerobotics, Volume 2 31 Jan. 1989 p 283-291 (For primary document see N90-29044 23-54)

(IR/D Proj. D-46S)

Avail: NTIS HC A17/MF A03 CSCL 13I

A major robotics opportunity for NASA will be the Mars Rover/Sample Return Mission which could be launched as early as the 1990s. The exploratory portion of this mission will include two autonomous subsystems: the rover vehicle and a sample handling system. The sample handling system is the key to the process of collecting Martian soils. This system could include a core drill, a general-purpose manipulator, tools, containers, a return canister, certification hardware and a labeling system. Integrated into a functional package, the sample handling system is analogous to a complex robotic workcell. Discussed here are the different components of the system, their interfaces, forseeable problem areas and many options based on the scientific goals of the mission. The various interfaces in the sample handling process (component to component and handling system to rover) will be a major engineering effort. Two critical evaluation criteria that will be imposed on the system are flexibility and reliability. It needs to be flexible enough to adapt to different scenarios and environments and acquire the most desirable specimens for return to Earth. Scientists may decide to change the distribution and ratio of core samples to rock samples in the canister. The long distance and duration of this planetary mission places a reliability burden on the hardware. The communication time delay between Earth and Mars minimizes operator interaction (teleoperation, supervisory modes) with the sample handler. An intelligent system will be required to plan the actions, make sample choices, interpret sensor inputs, and query unknown surroundings. A combination of autonomous functions and supervised movements will be integrated into the sample handling system. Author

N90-29071*# Purdue Univ., West Lafayette, IN. School of Electrical Engineering.

EFFICIENT MAPPING ALGORITHMS FOR SCHEDULING ROBOT INVERSE DYNAMICS COMPUTATION ON A MULTIPROCESSOR SYSTEM **c61**

C. S. G. Lee and C. L. Chen (Purdue Univ., Indianapolis, IN.) *In* JPL, California Inst. of Tech., Proceedings of the NASA Conference on Space Telerobotics, Volume 2 31 Jan. 1989 p 295-306

(For primary document see N90-29044 23-54)
(Grant NSF CDR-88-03017)
Avail: NTIS HC A17/MF A03 CSCL 09B

Two efficient mapping algorithms for scheduling the robot inverse dynamics computation consisting of m computational modules with precedence relationship to be executed on a multiprocessor system consisting of p identical homogeneous processors with processor and communication costs to achieve minimum computation time are presented. An objective function is defined in terms of the sum of the processor finishing time and the interprocessor communication time. The minimax optimization is performed on the objective function to obtain the best mapping. This mapping problem can be formulated as a combination of the graph partitioning and the scheduling problems; both have been known to be NP-complete. Thus, to speed up the searching for a solution, two heuristic algorithms were proposed to obtain fast but suboptimal mapping solutions. The first algorithm utilizes the level and the communication intensity of the task modules to construct an ordered priority list of ready modules and the module assignment is performed by a weighted bipartite matching algorithm. For a near-optimal mapping solution, the problem can be solved by the heuristic algorithm with simulated annealing. These proposed optimization algorithms can solve various large-scale problems within a reasonable time. Computer simulations were performed to evaluate and verify the performance and the validity of the proposed mapping algorithms. Finally, experiments for computing the inverse dynamics of a six-jointed PUMA-like manipulator based on the Newton-Euler dynamic equations were implemented on an NCUBE/ten hypercube computer to verify the proposed mapping algorithms. Computer simulation and experimental results are compared and discussed. Author

N90-29072*# Ohio State Univ., Columbus. Dept. of Electrical Engineering.
PARALLEL ALGORITHMS FOR COMPUTATION OF THE MANIPULATOR INERTIA MATRIX **c61**
Masoud Amin-Javaheri and David E. Orin *In* JPL, California Inst. of Tech., Proceedings of the NASA Conference on Space Telerobotics, Volume 2 31 Jan. 1989 p 307-316 (For primary document see N90-29044 23-54)
(Grant NSF EET-87-18434)
Avail: NTIS HC A17/MF A03 CSCL 09B

The development of an O(log2N) parallel algorithm for the manipulator inertia matrix is presented. It is based on the most efficient serial algorithm which uses the composite rigid body method. Recursive doubling is used to reformulate the linear recurrence equations which are required to compute the diagonal elements of the matrix. It results in O(log2N) levels of computation. Computation of the off-diagonal elements involves N linear recurrences of varying-size and a new method, which avoids redundant computation of position and orientation transforms for the manipulator, is developed. The O(log2N) algorithm is presented in both equation and graphic forms which clearly show the parallelism inherent in the algorithm. Author

N90-29073*# Grenoble-1 Univ. (France).
PLANNING ROBOT ACTIONS UNDER POSITION AND SHAPE UNCERTAINTY **c61**
Christian Laugier *In* JPL, California Inst. of Tech., Proceedings of the NASA Conference on Space Telerobotics, Volume 2 31 Jan. 1989 p 319-330 Sponsored in part by CNRS; ADI Agency; ITMI Co.; and Institut National de Recherche en Informatique et d'Automatique (For primary document see N90-29044 23-54)
Avail: NTIS HC A17/MF A03 CSCL 09B

Geometric uncertainty may cause various failures during the execution of a robot control program. Avoiding such failures makes it necessary to reason about the effects of uncertainty in order to implement robust strategies. Researchers first point out that a manipulation program has to be faced with two types of uncertainty: those that might be locally processed using appropriate sensor based motions, and those that require a more global processing leading to insert new sensing operations. Then, they briefly describe how they solved the two related problems in the SHARP system: how to automatically synthesize a fine motion strategy allowing the robot to progressively achieve a given assembly relation despite position uncertainty, and how to represent uncertainty and to determine the points where a given manipulation program might fail. Author

N90-29074*# Oxford Univ. (England). Robotics Group.
ORGANISING GEOMETRIC COMPUTATIONS FOR SPACE TELEROBOTICS **c61**
Stephen Cameron *In* JPL, California Inst. of Tech., Proceedings of the NASA Conference on Space Telerobotics, Volume 2 31 Jan. 1989 p 331-340 Sponsored in part by Science Research Council (For primary document see N90-29044 23-54)
Avail: NTIS HC A17/MF A03 CSCL 09B

A truly intelligent system that interacts with the physical world must be endowed with the ability the compute with shapes: despite this, spatial reasoning is rarely regarded as part of mainstream artificial intelligence. Here, researchers argue that the study of intelligent spatial algorithms is a worthwhile activity, and give opinions and suggestions for the way forward. Author

N90-29075*# Carnegie-Mellon Univ., Pittsburgh, PA. Robotics Inst.
A TESSELATED PROBABILISTIC REPRESENTATION FOR SPATIAL ROBOT PERCEPTION AND NAVIGATION **c61**
Alberto Elfes *In* JPL, California Inst. of Tech., Proceedings of the NASA Conference on Space Telerobotics, Volume 2 31 Jan. 1989 p 341-350 (For primary document see N90-29044 23-54)
(Contract N00014-81-K-0503; CNPq-200.986-80)
Avail: NTIS HC A17/MF A03 CSCL 09B

The ability to recover robust spatial descriptions from sensory information and to efficiently utilize these descriptions in appropriate planning and problem-solving activities are crucial requirements for the development of more powerful robotic systems. Traditional approaches to sensor interpretation, with their emphasis on geometric models, are of limited use for autonomous mobile robots operating in and exploring unknown and unstructured environments. Here, researchers present a new approach to robot perception that addresses such scenarios using a probabilistic tesselated representation of spatial information called the Occupancy Grid. The Occupancy Grid is a multi-dimensional random field that maintains stochastic estimates of the occupancy state of each cell in the grid. The cell estimates are obtained by interpreting incoming range readings using probabilistic models that capture the uncertainty in the spatial information provided by the sensor. A Bayesian estimation procedure allows the incremental updating of the map using readings taken from several sensors over multiple points of view. An overview of the Occupancy Grid framework is given, and its application to a number of problems in mobile robot mapping and navigation are illustrated. It is argued that a number of robotic problem-solving activities can be performed directly on the Occupancy Grid representation. Some parallels are drawn between operations on Occupancy Grids and related image processing operations. Author

N90-29076*# National Aeronautics and Space Administration. Ames Research Center, Moffett Field, CA.
A SURVEY OF PLANNING AND SCHEDULING RESEARCH AT THE NASA AMES RESEARCH CENTER **c81**
Monte Zweben *In* JPL, California Inst. of Tech., Proceedings of the NASA Conference on Space Telerobotics, Volume 2 31 Jan. 1989 p 353-358 Previously announced as N89-19820 (For primary document see N90-29044 23-54)
Avail: NTIS HC A17/MF A03 CSCL 05A

NASA Ames Research Center has a diverse program in planning and scheduling. Some research projects as well as some applications are highlighted. Topics addressed include machine learning techniques, action representations and constraint-based scheduling systems. The applications discussed are planetary rovers, Hubble Space Telescope scheduling, and Pioneer Venus orbit scheduling. Author

N90-29077*# Teleos Research, Palo Alto, CA.
INTEGRATING PLANNING AND REACTIVE CONTROL c81
Stanley J. Rosenschein and Leslie Pack Kaelbling *In* JPL, California Inst. of Tech., Proceedings of the NASA Conference on Space Telerobotics, Volume 2 31 Jan. 1989 p 359-366 Sponsored in part by System Development Foundation (For primary document see N90-29044 23-54)
(Contract NCC2-494; SU Proj. 6359)
Avail: NTIS HC A17/MF A03 CSCL 05A

Artificial intelligence research on planning is concerned with designing control systems that choose actions by manipulating explicit descriptions of the world state, the goal to be achieved, and the effects of elementary operations available to the system. Because planning shifts much of the burden of reasoning to the machine, it holds great appeal as a high-level programming method. Experience shows, however, that it cannot be used indiscriminately because even moderately rich languages for describing goals, states, and the elementary operators lead to computational inefficiencies that render the approach unsuitable for realistic applications. This inadequacy has spawned a recent wave of research on reactive control or situated activity in which control systems are modeled as reacting directly to the current situation rather than as reasoning about the future effects of alternative action sequences. While this research has confronted the issue of run-time tractability head on, in many cases it has done so by sacrificing the advantages of declarative planning techniques. Ways in which the two approaches can be unified are discussed. The authors begin by modeling reactive control systems as state machines that map a stream of sensory inputs to a stream of control outputs. These machines can be decomposed into two continuously active subsystems: the planner and the execution module. The planner computes a plan, which can be seen as a set of bits that control the behavior of the execution module. An important element of this work is the formulation of a precise semantic interpretation for the inputs and outputs of the planning system. They show that the distinction between planned and reactive behavior is largely in the eye of the beholder: systems that seem to compute explicit plans can be redescribed in situation-action terms and vice versa. They also discuss practical programming techniques that allow the advantages of declarative programming and guaranteed reactive response to be achieved simultaneously. Author

N90-29078*# Space Telescope Science Inst., Baltimore, MD.
LEARNING IN STOCHASTIC NEURAL NETWORKS FOR CONSTRAINT SATISFACTION PROBLEMS c63
Mark D. Johnston and Hans-Martin Adorf (European Southern Observatory, Garching, Germany, F.R.) *In* JPL, California Inst. of Tech., Proceedings of the NASA Conference on Space Telerobotics, Volume 2 31 Jan. 1989 p 367-376 (For primary document see N90-29044 23-54)
Avail: NTIS HC A17/MF A03 CSCL 09B

Researchers describe a newly-developed artificial neural network algorithm for solving constraint satisfaction problems (CSPs) which includes a learning component that can significantly improve the performance of the network from run to run. The network, referred to as the Guarded Discrete Stochastic (GDS) network, is based on the discrete Hopfield network but differs from it primarily in that auxiliary networks (guards) are asymmetrically coupled to the main network to enforce certain types of constraints. Although the presence of asymmetric connections implies that the network may not converge, it was found that, for certain classes of problems, the network often quickly converges to find satisfactory solutions when they exist. The network can run efficiently on serial machines and can find solutions to very large problems (e.g., N-queens for N as large as 1024). One advantage of the network architecture is that network connection strengths need not be instantiated when the network is established: they are needed only when a participating neural element transitions from off to on. They have exploited this feature to devise a learning algorithm, based on consistency techniques for discrete CSPs, that updates the network biases and connection strengths and thus improves the network performance. Author

N90-29079*# Carnegie-Mellon Univ., Pittsburgh, PA. Dept. of Computer Science.
INTEGRATING PLANNING, EXECUTION, AND LEARNING c81
Daniel R. Kuokka *In* JPL, California Inst. of Tech., Proceedings of the NASA Conference on Space Telerobotics, Volume 2 31 Jan. 1989 p 377-386 Sponsored in part by Hughes Aircraft Co. (For primary document see N90-29044 23-54)
(Contracts NCC2-463; N00014-79-C-0661; N00014-82-C-50767; F33615-84-K-1520)
Avail: NTIS HC A17/MF A03 CSCL 05A

To achieve the goal of building an autonomous agent, the usually disjoint capabilities of planning, execution, and learning must be used together. An architecture, called MAX, within which cognitive capabilities can be purposefully and intelligently integrated is described. The architecture supports the codification of capabilities as explicit knowledge that can be reasoned about. In addition, specific problem solving, learning, and integration knowledge is developed. Author

N90-29080# Army Safety Center, Fort Rucker, AL.
HELICOPTER AIRCREW HELMETS AND HEAD INJURY: A PROTECTIVE EFFECT Final Report, Jan. - May 1990
John Stephen Crowley 1 Jun. 1990 9 p
(AD-A223024; USASC-TR-90-1) Avail: NTIS HC A02/MF A01 CSCL 01/2

The effectiveness of the Army's SPH-4 flight helmet in reducing the severity of head injuries sustained during helicopter accidents was evaluated, using the accident data base at the U.S. Army Safety Center (USASC), Fort Rucker, Alabama. Analysis was restricted to severe (Class A) 1972 to 1988 accidents that were at least partially survivable, using USASC criteria. Occupants who were not wearing a protective helmet were significantly more likely to sustain severe and fatal head injuries than occupants wearing the SPH-4 (RR=3.8 and 6.3, respectively). Unhelmeted non-cockpit occupants faced higher risks (RR=5.3 and 7.5). All personnel regularly participating in helicopter flight, civilian or military, should be equipped with protective headgear. GRA

N90-29081# Lawrence Livermore National Lab., CA. Systems and Human Performance.
HUMAN FACTORS EVALUATION AND VALIDATION CRITERIA FOR QUALITY TRAINING PROGRAMS: DEVELOPMENT, PRESENTATION, AND ASSESSMENT
William W. Banks 15 May 1990 96 p
(Contract W-7405-eng-48)
(DE90-014724; UCRL-ID-103792) Avail: NTIS HC A05/MF A01

This paper provides LLNL managers with a rigorous and quantitative human factors method for assessing the development and validity of any training program at the Lab. A secondary purpose is to provide a checklist for course developers and evaluators. The checklist is easy to use and comprehensive, and it helps ensure that critical components of a training program are adequately addressed. DOE

N90-29082 Institute for Perception RVO-TNO, Soesterberg (Netherlands).
PROPRIOCEPTION IN AIRCRAFT CONTROL Final Report
R. N. H. W. vanGent 12 Oct. 1989 35 p In DUTCH; ENGLISH summary Sponsored by National Defense Research, The Hague, Netherlands
(IZF-1989-43; TD-89-4143; ETN-90-97397) Copyright Avail: Inst. for Perception RVO-TNO, P.O. Box 23, 3769 ZG Soesterberg, Netherlands

It was investigated whether with an active stick to feed back a flight variable through proprioception, the visual attention of the pilot for secondary tasks diminishes in a steering task with a remotely piloted vehicle. An experiment was set up in which a remotely piloted vehicle was simulated on a computer and in which the independent factors stick type (active versus passive), task speed, replication and the presence of a visual secondary task were introduced. The results show that with the control of remotely

piloted vehicles in the vertical plane proprioceptive feedback of the vertical speed enhances the accuracy of the steering task and the score on the visual secondary task. ESA

N90-29083*# National Aeronautics and Space Administration. Ames Research Center, Moffett Field, CA.
AUTOMATED SIMULATION AS PART OF A DESIGN WORKSTATION
Elizabeth Cantwell, T. Shenk, P. Robinson, and R. Upadhye (Lawrence Livermore National Lab., CA.) Aug. 1990 15 p Presented at the 20th Intersociety Conference on Environmental Systems, Williamsburg, VA, 9-12 Jul. 1990
(NASA-TM-102852; A-90245; NAS 1.15:102852) Avail: NTIS HC A03/MF A01 CSCL 05H

A development project for a design workstation for advanced life-support systems (called the DAWN Project, for Design Assistant Workstation), incorporating qualitative simulation, required the implementation of a useful qualitative simulation capability and the integration of qualitative and quantitative simulation such that simulation capabilities are maximized without duplication. The reason is that to produce design solutions to a system goal, the behavior of the system in both a steady and perturbed state must be represented. The Qualitative Simulation Tool (QST), on an expert-system-like model building and simulation interface toll called ScratchPad (SP), and on the integration of QST and SP with more conventional, commercially available simulation packages now being applied in the evaluation of life-support system processes and components are discussed. Author

N90-29084*# Perkin-Elmer Corp., Pomona, CA. Applied Science Operation.
ATMOSPHERE AND WATER QUALITY MONITORING ON SPACE STATION FREEDOM
William Niu 1990 22 p Presented at the Space Conference, Long Beach, CA, 22 Sep. 1990
(Contract NAS8-50000)
(NASA-CR-186707; NAS 1.26:186707) Avail: NTIS HC A03/MF A01 CSCL 06K

In Space Station Freedom air and water will be supplied in closed loop systems. The monitoring of air and water qualities will ensure the crew health for the long mission duration. The Atmosphere Composition Monitor consists of the following major instruments: (1) a single focusing mass spectrometer to monitor major air constituents and control the oxygen/nitrogen addition for the Space Station; (2) a gas chromatograph/mass spectrometer to detect trace contaminants; (3) a non-dispersive infrared spectrometer to determine carbon monoxide concentration; and (4) a laser particle counter for measuring particulates in the air. An overview of the design and development concepts for the air and water quality monitors is presented. Author

N90-28979# Royal Aerospace Establishment, Farnborough (England).
TOWARDS A FUTURE COCKPIT: THE PROTOTYPING AND PILOT INTEGRATION OF THE MISSION MANAGEMENT AID (MMA)
C. P. Gibson and A. J. Garrett (British Aerospace Public Ltd. Co., Kingston-upon-Thames, England) *In* AGARD, Situational Awareness in Aerospace Operations Apr. 1990 9 p (For primary document see N90-28972 23-53)
Copyright Avail: NTIS HC A09/MF A02; Non-NATO Nationals requests available only from AGARD/Scientific Publications Executive

N90-28980# School of Aerospace Medicine, Brooks AFB, TX. Crew Technology Div.
THE THREE-DIMENSIONAL STRUCTURE OF VISUAL ATTENTION AND ITS IMPLICATIONS FOR DISPLAY DESIGN
Fred H. Previc *In* AGARD, Situational Awareness in Aerospace Operations Apr. 1990 7 p (For primary document see N90-28972 23-53)
Copyright Avail: NTIS HC A09/MF A02; Non-NATO Nationals requests available only from AGARD/Scientific Publications Executive

N90-28981# Central Electricity Generating Board, Gloucester (England).
A REAL TIME EVALUATION OF THE USE OF A PERSPECTIVE FORMAT TO PROMOTE SITUATIONAL AWARENESS IN USERS OF AIR TO AIR TACTICAL DISPLAYS Abstract Only
D. Ridley *In* AGARD, Situational Awareness in Aerospace Operations Apr. 1990 1 p (For primary document see N90-28972 23-53)
Copyright Avail: NTIS HC A09/MF A02; Non-NATO Nationals requests available only from AGARD/Scientific Publications Executive

N90-28982# Human Engineering Labs., Aberdeen Proving Ground, MD.
COUNTERAIR SITUATION AWARENESS DISPLAY FOR ARMY AVIATION
Christopher C. Smyth, Frank J. Malkin, and William B. DeBellis *In* AGARD, Situational Awareness in Aerospace Operations Apr. 1990 10 p (For primary document see N90-28972 23-53)
Copyright Avail: NTIS HC A09/MF A02; Non-NATO Nationals requests available only from AGARD/Scientific Publications Executive

N90-28983# Laboratoire de Medecine Aerospatiale, Bretigny-sur-Orge (France).
TARGET ACQUISITION UNDER LOAD FACTORS: ADVANTAGES AND DISADVANTAGES OF A HELMET MOUNTED SIGHT [DESIGNATION D'OBJECTIFS SOUS FACTEUR DE CHARGE: INTERET ET LIMITES DU VISEUR DE CASQUE]
A. Leger and Patrick Sandor *In* AGARD, Situational Awareness in Aerospace Operations Apr. 1990 10 p In FRENCH (For primary document see N90-28972 23-53)
Copyright Avail: NTIS HC A09/MF A02; Non-NATO Nationals requests available only from AGARD/Scientific Publications Executive

55 SPACE BIOLOGY

Includes exobiology; planetary biology; and extraterrestrial life.

N90-29085*# Institute for Circadian Physiology, Boston, MA.
FLUID AND ELECTROLYTE HOMEOSTASIS DURING SPACEFLIGHT: ELUCIDATION OF MECHANISMS IN A PRIMATE
Susanne Churchill Apr. 1990 93 p
(Contract NAS2-10547)
(NASA-CR-177548; A-90095; NAS 1.26:177548) Avail: NTIS HC A05/MF A01 CSCL 06C

Although it is now well accepted that exposure to the hypogravic environment of space induces a shift of fluid from the lower extremities toward the upper body, the actual physiological responses to this central volume expansion have not been well characterized. Because it is likely that the fluid and electrolyte response to hypogravity plays a critical role in the development of Cardiovascular Deconditioning, elucidation of these mechanisms is of critical importance. The goal of flight experiment 223, scheduled to fly on SLS-2, is the definition of the basic renal, fluid and electrolyte response to spaceflight in four instrumented squirrel monkeys. The studies were those required to support the development of flight hardware and optimal inflight procedures, and to evaluate a ground-based model for weightlessness, lower body positive pressure (LBPP). Author

N90-29086*# Tennessee Univ., Knoxville.
REGULATION OF ERYTHROPOIESIS IN RATS DURING SPACE FLIGHT
Robert D. Lange Oct. 1989 26 p

(Contract NAS2-11586)
(NASA-CR-177537; NAS 1.26:177537) Copyright Avail: NTIS HC A03/MF A01 CSCL 06C

Astronauts who have flown in microgravity have experienced a loss in red cell mass. The pathogenesis of the anemia of space flight has not been ascertained, but it is probably multifactorial. In 1978, the laboratory was selected to participate in life sciences studies to be carried out in the space shuttle in an attempt to study the pathogenesis of space anemia. In particular, the original studies were to be made in mice. This was later changed to study erythropoiesis in rats during space flight. Author

59 MATHEMATICAL AND COMPUTER SCIENCES (GENERAL)

No abstracts in this category.

60 COMPUTER OPERATIONS AND HARDWARE

Includes hardware for computer graphics, firmware, and data processing.

For components see *33 Electronics and Electrical Engineering.*

N90-29087# Army War Coll., Carlisle Barracks, PA.
THE PERSONAL COMPUTER: AN UNTAPPED SOURCE FOR THE UNITED STATES ARMY WAR COLLEGE
Charles E. Persyn 2 May 1990 42 p
(AD-A223976) Avail: NTIS HC A03/MF A01 CSCL 12/6

This essay examines the dramatic changes made in the use of personal computers in civilian universities, and explores the concept of educational computing. The author presents the idea of an educational computing model and its application in the United States Army War College (USAWC). Department of Defense Policy and Army Information Management Regulations are discussed where applicable. Finally, the author presents some recommendations based on known fiscal constraints, an analysis of the present computer system at the USAWC, and on lessons learned in business and civilian universities. GRA

N90-29088# Colorado Univ., Boulder. Dept. of Computer Science.
A USER MODELLING APPROACH FOR COMPUTER-BASED CRITIQUING Ph.D. Thesis
Thomas Walter Mastaglio 1990 242 p
(AD-A224042; AD-F000153) Avail: NTIS HC A11/MF A02 CSCL 23/2

Theoretical studies and implementations of computer-based critiquing systems indicate that it is desirable to enhance that approach to better support human-computer collaborative effort. A user model will enable these systems to individualize explanations of their advice to provide better support for cooperative problem solving and enhance user learning. User modelling research in advice-giving dialog and intelligent educational systems was studied together with theoretical analyses of the limitations of human-computer interaction, and empirical observations of human-to-human collaborative effort. A framework for a user modelling component fo a critiquing system was developed and implemented in a critic for LISP programs. The user models developed by the system were compared to self-assessment questionnaires completed by subjects learning the LISP language. The analyses indicated a favorable correlation and potential improvements to the framework. The user model is based on the conceptual domain model required for explanations; its semantic structure allows the system to implicitly enrich the user model contents. The significance of this thesis is a framework for a user modelling component that can be used for a more general class of cooperative knowledge-based systems. GRA

N90-29089# Naval Postgraduate School, Monterey, CA. Dept. of Administrative Sciences.
A COMPARISON OF PASSWORD TECHNIQUES FOR MULTILEVEL AUTHENTICATION MECHANISMS
Moshe Zviran and William J. Haga Jun. 1990 40 p
(AD-A224245; NPS54-90-014) Avail: NTIS HC A03/MF A01 CSCL 12/8

Various mechanisms for authenticating users of computer-based information systems have been proposed. These include traditional, user-selected passwords, system-generated passwords, passphrases, cognitive passwords and associative passwords. While the mechanisms employed in primary passwords are determined by the operating systems' manufacturers, system designers can select any password mechanism for secondary passwords, to further protect sensitive applications and data files. This paper reports on the results of an empirically based study of passwords characteristics. It provides a comparative evaluation on the memorability and users' subjective preferences of the various passwords mechanisms, and suggest that cognitive passwords and associative passwords seem the most appropriate for secondary passwords. GRA

61 COMPUTER PROGRAMMING AND SOFTWARE

Includes computer programs, routines, alogorithms, and specific applications, e.g., CAD/CAM.

N90-29090# Los Alamos National Lab., NM.
LINTERP: A NUMERICAL ALGORITHM FOR INTERPOLATING QUADRILATERAL AND HEXAHEDRAL MESHES
T. L. Wilson Sep. 1990 11 p
(Contract W-7405-eng-36)
(DE90-014417; LA-11902-MS) Avail: NTIS HC A03/MF A01

A linear interpolation method, suitable for use on quadrilateral and hexahedral grids with logical or irregular mesh connectivity, is presented. LINTERP, a FORTRAN code that implements this method, is also described. DOE

N90-29091# Lawrence Livermore National Lab., CA.
WHO'S WHO IN SCIENTIFIC VISUALIZATION AT LLNL
Peter Keller, Palmer T. VanDyke, and John R. Strack 4 May 1990 159 p
(Contract W-7405-eng-48)
(DE90-014720; UCRL-53941) Avail: NTIS HC A08/MF A01

Who's Who In Scientific Visualization at LLNL is addressed to those involved in computer graphics activities at the Laboratory. Its broader purpose is to promote awareness and application of the new cluster of disciplines known as Visualization in Scientific Computing (VISC). VISC focuses on delivering information, rather than numbers, to the scientist. It combines computer graphics, image processing, computer vision, computer-aided design, signal processing, and user interface studies to provide information in a form that is understandable, relevant to the problem at hand, and useable. A major emphasis of VISC is the output or display of meaningful computer-generated images. The information in Who's Who is based on a Laboratory-wide survey of scientists, engineers, and programmers. With the cooperation of our respondents, we have assembled a catalog of current computer-graphics expertise and interests at LLNL. Our survey revealed -- not surprisingly -- a widespread interest in VISC and significant activity in VISC-related disciplines. Our hope is that by helping to knit together this community of interests, Who's Who will stimulate further progress in VISC. To maintain its utility as a timely resource, we plan to update Who's Who periodically. DOE

N90-29092# Instituto de Pesquisas Espaciais, Sao Jose dos Campos (Brazil). Dept. de Processamento de Imagens.
AUTOREGRESSIVE-MOVING AVERAGE MODELS FOR TEXTURE CLASSIFICATION [MODELOS AUTO-REGRESSIVOS - MEDIA MOVEL PARA CLASSIFICACAO DE TEXTURAS]
Luciano Vieira Dutra and Nelson Delfino dAvilaMascarenhas Oct. 1989 11 p In POLISH Presented at the 4th Latin American Symposium on Remote Sensing, Bariloche, Argentina, 20-24 Nov. 1989
(INPE-4987-PRE/1549) Avail: NTIS HC A03/MF A01

The development of a method for statistical characterization of images is presented using the autoregressive-moving average (ARMA) models. These models are utilized for improving the results of pattern classification of digital image texture. The models adjust each class through a process of adequate identification. The original image is filtered by an inverse filter derived from the obtained models. The many channels which were obtained for all the class textures, were defined a-priori for the original images. With the existing correlation between apertures, the filters become advantageous considering the residual distribution for defining the statistics of the unknown pattern. The classifiers were associated with the class which minimizes the statistical distance between the distribution which governs the pattern (assumed Gaussian) and the existing class. Author

N90-29093 Rensselaer Polytechnic Inst., Troy, NY.
AN IMPROVED METHOD FOR CHOOSING SAMPLING POINTS FOR THE INSPECTION OF COMPLEX SURFACES IN A COMPUTER-AIDED MANUFACTURING ENVIRONMENT Ph.D. Thesis
Charles Bernard Malloch 1989 172 p
Avail: Univ. Microfilms Order No. DA9018440

An improved method for sparsely probing a complex surface, using a technique which provides closer inspection of surface regions which are known to be critical to the resulting part or likely to be out-of-tolerance is developed. The 'desired inspection density', developed from the design parameters and intended use of a surface, provides a relative measure of how carefully any surface region must be inspected to maximize the probability of detecting flaws as a function of inspection cost. The desired inspection density takes into account process variability, tolerance tightness, measurement uncertainty, and information from neighboring probes. A simplified one-dimensional model is analyzed and criteria are given for exact optimal solutions to this model. Numerical results are presented. This analysis is not directly extendable to surfaces. An alternate is given which is suboptimal but more generally useful for surface inspection. This algorithm improves a given set of probe locations using the physical model of free electrons in a specified potential field. Repulsion between the electrons limits probe redundancy. The potential field is specified by the desired inspection density. The electrons' equilibrium positions correspond to improved probe locations. The thesis analyzes the optimal selection of the probe points' number and locations for a reduced discrete problem, develops a method to improve the probing point set to a local optimum, discusses the functioning of the algorithm, compares its results with those analytically determined from the reduced problem, and provides justification for the algorithm's use in an expanded range of problems using Monte Carlo simulations. Dissert. Abstr.

N90-29094# Admiralty Research Establishment, Portland (England).
A COMPUTER GRAPHICS PACKAGE
C. Richardson Jun. 1989 52 p Original contains color illustrations
(ARE-TM(UDT)-89111; ACCN-79353; BR112976; ETN-90-97070)
Copyright Avail: NTIS HC A04/MF A01

A general purpose graphic package is described. The package is an updated version of a graphics library first developed in 1969 on an ICL-1900 series computer and in use continously since that time with various modifications and informal documentation improvements. It is currently implemented on a DEC-MicroVAX computer and various hardware devices including the HP series of plotters (using HPGL), Regis devices (VT125, VT340), DEC Workstation, LN03 laser printer, and certain Ramtek, Sigma and Tektronix devices. Although commercial graphics packages are available this one is simple to understand and use, and together with its familiarity to existing users continues to provide useful graphic support. Examples are given to clarify usage of the software and lists of subroutines are also provided. ESA

N90-29095# Oak Ridge National Lab., TN. Engineering Physics and Mathematical Div.
THE EFFECT OF MULTIPROCESSOR RADIUS ON SCALING
Patrick H. Worley Jun. 1990 32 p
(Contract DE-AC05-84OR-21400)
(DE90-014772; ORNL/TM-11579) Avail: NTIS HC A03/MF A01

It was previously established that, for a large class of linear partial differential equations (PDEs), increasing the problem size necessarily increases the execution time, independent of the algorithm and the number of processors used to solve the problem. Herein, the analysis is extended to take into account the effect of the radius of the multiprocessor interconnection network on the growth in the execution time. Define r(p) to be the minimum radius over all subsets of p processors in a multiprocessor. An information-theoretic analysis is used to show that r(p) determines a lower bound on the communication cost of a parallel algorithm, and that this in turn determines a lower bound on the parallel execution time. Assume that r(p) greater than or = beta x p sup gamma - mu for positive constants beta, gamma, and mu for a given multiprocessor. For example, this type of lower bound on r(p) holds for a multiprocessor whose interconnection topology is a k-dimensional array. It is then established that, for the given class of PDEs, the time spent on interprocessor communication will be the dominant constraint on the performance of optimal algorithms when the problem and the multiprocessor are large. Moreover, as the problem and the multiprocessor increase in size, it is shown that the asymptotic increase in the parallel execution time will be determined by the communication cost and not by the computational requirements. The restriction to linear PDEs is not necessary, and similar results can be obtained for many problems in scientific computation. DOE

N90-29096# Los Alamos National Lab., NM. Mechanical and Electronic Engineering Div.
RECURSIVE LEAST-SQUARES LEARNING ALGORITHMS FOR NEURAL NETWORKS
Paul S. Lewis and Jenq-Neng Hwang (Washington Univ., Seattle.) 1990 12 p Presented at the SPIE Conference on Mathematical Imaging, San Diego, CA, Jul. 1990
(Contract W-7405-eng-36)
(DE90-014926; LA-UR-90-2358; CONF-9007117-3) Avail: NTIS HC A03/MF A01

The development is presented of a pair of recursive least squares (RLS) algorithms for online training of multilayer perceptrons, which are a class of feedforward artificial neural networks. These algorithms incorporate second order information about the training error surface in order to achieve faster learning rates than are possible using first order gradient descent algorithms such as the generalized delta rule. A least squares formulation is derived from a linearization of the training error function. Individual training pattern errors are linearized about the network parameters that were in effect when the pattern was presented. This permits the recursive solution of the least squares approximation, either via conventional RLS recursions or by recursive QR decomposition-based techniques. The computational complexity of the update is in the order of N sup 2, where N is the number of network parameters. This is due to the estimation of the N x N inverse Hessian matrix. Less computationally intensive approximations of the RLS algorithms can be easily derived by using only block diagonal elements of this matrix, thereby partitioning the learning into independent sets. A simulation example is presented in which a neural network is trained to approximate a two dimensional Gaussian bump. In this example,

RLS training required an order of magnitude fewer iterations on average (527) than did training with the generalized delta rule (6331). DOE

N90-29097# Los Alamos National Lab., NM. Safeguards Systems Group.
GRAPH STRUCTURE MODEL
Jared S. Dreicer 1990 7 p Presented at the Institute of Nuclear Materials Management Conference, Los Angeles, CA, 15-18 Jul. 1990
(Contract W-7405-eng-36)
(DE90-014930; LA-UR-90-2342; CONF-9007106-43) Avail: NTIS HC A02/MF A01

The Graph Structure (GRPHSTRUC) model is a generic software-system tool that was developed to allow a system analyst to conduct studies and design analysis concerning control flow in graph structures. The GRPHSTRUC model is a knowledge-based expert system using icons and object-oriented methodologies. This software tool was implemented using the expert system shell called Knowledge Engineering Environment (KEE), Common Lisp methods, and KEE Pictures for graphical display. The GRPHSTRUC model provides a user interface that is designed to allow the user to rapidly and efficiently represent graph components, interconnections, and interrelationships. GRPHSTRUC was generically designed and developed to use classical graph theory and to allow the display of vertices and links of a graph structure. In particular, the model was developed to assist a computer security analyst in assessing the security of and to conduct security studies and design analysis concerning computer networks. The model is applicable to other disciplines that can be portrayed by graph structures, in particular safeguards. DOE

N90-29098# Lister Hill National Center for Biomedical Communications, Bethesda, MD.
THE SPECIALIST: NATURAL LANGUAGE PROCESSING SYSTEM Interim Report, May 1987 - May 1990
Alexa T. McCray, Allen C. Browne, Suresh Srinivasan, Alan R. Aronson, Theresa A. Waldspurger, and Ingrid Pufahl Jun. 1990 33 p
(PB90-240029; NLM/LHC-90-02) Avail: NTIS HC A03/MF A01 CSCL 09B

The SPECIALIST system is an experimental system for parsing, analyzing and accessing biomedical text. The system is being developed by Natural Language Systems (NLS) program staff at the Lister Hill National Center for Biomedical Communications. The research of the NLS group is based on the testable hypothesis that natural language processing systems which combine sophisticated linguistic analysis with structured domain knowledge will lead to improved representation and retrieval of information. The SPECIALIST system is designed to capture the regularities of general English as well as the specialized nature of biomedical text. The parsing system is based on principles of linguistic analysis and includes a large lexicon together with rules of morphology, syntax, and semantics. The report describes the current status of the SPECIALIST system and ends with a brief discussion of future work. Author

N90-29099# Office of Software Development, Falls Church, VA. Federal Software Management Support Center.
PREPARING SOFTWARE CONVERSION STUDIES
Dec. 1989 64 p
(PB90-235623) Avail: NTIS HC A04/MF A01 CSCL 09B

The purpose is to provide Government agencies with a guideline for preparing software conversion studies. Software conversion is the transformation, without functional change, of computer programs or data elements to permit their use on a replacement or changed ADP equipment system or teleprocessing service. The required contents of a comprehensive software conversion study are defined in FIRMR 201-30.012-1 and 2. A conversion study should present the procurement alternatives that an agency is considering, associated conversion costs, benefits, and risks. An outline for software conversion studies that the Federal Software Management Support Center has found to be most successful is given. Section 1 contains the introduction to the software conversion study; Section 2 describes the current environment; Section 3 describes the target environment; Section 4 documents conversion cost estimating; Section 5 contains a summary of findings; and Section 6 provides the procurement and implementation schedule. Appendix A contains a set of sample inventory forms that may be used when collecting the software inventory. GRA

N90-29100# Instituto de Pesquisas Espaciais, Sao Jose dos Campos (Brazil).
COMPUTER VISION AND ITS POTENTIAL APPLICATIONS IN BRAZIL [VISAO POR COMPUTADOR E O POTENCIAL DE SUAS APLICACOES NO BRASIL]
Otavio S. CupertinoDurao Aug. 1988 13 p In PORTUGUESE; ENGLISH summary Presented at the Computer Graphics and Image Processing Seminar, INPE, San Jose dos Campos, Brazil, Oct. 1987
(INPE-4666-NTE/283) Avail: NTIS HC A03/MF A01

The two most common types of artificial vision systems are explained. The identification of the potential applications for implementation in Brazil is presented. B.G.

N90-29101# Technische Hochschule, Darmstadt (Germany, F.R.). Fachbereich Informatik.
A STUCTURE DEPENDENT SOFTWARE DEVELOPMENT ON A RELATIONAL BASIS: AN INTEGRAL APPROACH Ph.D. Thesis [STRUKTURGEBUNDENER SOFTWARE-ENTWURF AUF RELATIONALER BASIS: EIN INTEGRIERENDER ANSATZ]
Juergen R. Bergmann 1989 226 p In GERMAN
(ETN-90-97289) Avail: NTIS HC A11/MF A02

An integral approach to a structure dependent software development, based on a relational data model, is presented. The starting point for this approach was an analysis of the present status of software engineering and of the requirements for future developments. The theoretical fundamentals of the relational representation of syntactical objects and their management in an object system are outlined. The core system of an object oriented relational software development environment is described. The procedure of this core system is illustrated by an example. Further possible developments based on this approach are given. ESA

N90-29102# Technische Hochschule, Darmstadt (Germany, F.R.). Fachbereich Informatik.
FAST INTERACTIVE IMAGE GENERATION OF LINE AND SURFACE ORIENTED OBJECTS IN RASTER SYSTEMS Ph.D. Thesis [SCHNELLE INTERAKTIVE BILDGENERIERUNG VON LINIEN- UND FLAECHENORIENTIERTEN OBJEKTEN IN RASTERSYSTEMEN]
Joachim Rix 1988 119 p In GERMAN
(ETN-90-97290) Avail: NTIS HC A06/MF A01

The possibilities of using graphic raster systems for faster image construction and better interaction were investigated. The status of research and development in the field of graphical systems and their environment is outlined. The advantages and disadvantages of vector and raster systems are discussed. The properties of raster technology are described. The systems architecture including a flexible and modular driver structure is treated. The integration of the functionality in the interface hierarchy is presented. Further steps toward the standardization and harmonization of graphical data processing are suggested. ESA

N90-29103# National Inst. of Standards and Technology, Gaithersburg, MD. Center for Fire Research.
SOFTWARE DEVELOPMENT TOOLS Final Report
G. P. Forney and W. W. Jones Jul. 1990 43 p
(PB90-250051; NISTIR-4363) Avail: NTIS HC A03/MF A01 CSCL 09B

The use of software tools to aid in the development of models produced by the Center for Fire Research (CFR) is discussed. There are two types of tools described. The first type consists of executable programs that characterize the subroutine and data structures of FORTRAN programs. A second class of software

tools are subroutines that support various utility functions required by CFR models. The authors will discuss how each of these tools are used and why their development was necessary. In addition, the authors will indicate how these tools might be improved.
GRA

N90-29104# Instituto de Pesquisas Espaciais, Sao Jose dos Campos (Brazil).
INFERENCE ENGINE FOR EXPERT SYSTEMS [MOTOR DE INFERENCIA PARA SISTEMAS ESPECIALISTAS]
Edson L. F. Senne May 1988 13 p In PORTUGUESE; ENGLISH summary Presented at the 8th SCCC International Conference on Computer Science, Santiago, Chile, Jul. 1988
(INPE-4565-PRE/1306) Avail: NTIS HC A03/MF A01

The MOTIN system, a tool for building expert systems is discussed. In essence, the representation scheme of the decision rules that will be stored in the knowledge base of a expert system and a meta-knowledge-controlled inference mechanism that can be adapted to the characteristics of specific domains are shown. The use of a semantic network to store structured, well-established knowledge of a domain is presented and information is provided in order to determine suitable contexts for decision rules application. An approach to inexact reasoning based on the Dempster-Shafer theory is also presented. Author

N90-29105# Lawrence Livermore National Lab., CA.
ANIMATED COMPUTER-GENERATED VIDEO-TAPE INSTRUCTION USING DIGLIB (DEVICE INDEPENDENT GRAPHICS LIBRARY) Final Report
Zia Begg, Anthony Thomas, and Wolsey A. Semple (Howard Univ., Washington, DC.) 19 Jun. 1990 213 p
(Contract W-7405-eng-48)
(DE90-015360; UCRL-CR-104308) Avail: NTIS HC A10/MF A02

The objective of the manual is to discuss the details a software developer may need to develop educational movies. The manual is organized in a manner that the user can browse through each chapter of the manual and later can work on the functions provided in the driver. In the end, the user would be capable of developing the educational movies. The manual is intended both for the end user, who wants to write programs to develop movies, and for the system programmer/debugger, who either wants to extend the capabilities of the system or wants to debug the system.
DOE

N90-29106# International Centre for Theoretical Physics, Trieste (Italy).
PRODUCT INTEGRATION RULES AT CLENSHAW-CURTIS AND RELATED POINTS: A ROBUST IMPLEMENTATION
Gh. Adam (Institute of Physics and Technology of Radiation Devices, Bucharest, Romania) and A. Nobile Dec. 1989 35 p Submitted for publication
(DE90-627158; IC-89/422) Avail: NTIS (US Sales Only) HC A03/MF A01

Product integration rules generalizing the Fejer, Clenshaw-Curtis and Filippi quadrature rules respectively are derived for integrals with trigonometric and hyperbolic weight factors. The study puts in evidence the existence of well-conditioned fully analytic solutions, in terms of hypergeometric functions (sub 0)F(sub 1). An a priori error estimator is discussed which is shown both to avoid wasteful invocation of the integration rule and to increase significantly the robustness of the automatic quadrature procedure. Then, specializing to extended Clenshaw-Curtis (ECC) rules, three types of a posteriori error estimates are considered and the existence of a great risk of their failure is put into evidence by large scale validation tests. An empirical error estimator, superseding them at slowly varying integrands, is found to result in a spectacular increase in the output reliability. Finally, enhancements in the control of the interval subdivision strategy aiming at increasing code robustness is discussed. Comparison with the code DQAWO of QUADPACK, extending over a statistics of about hundred thousand solved integrals, is illustrative for the increased robustness and error estimate reliability of our computer code implementation of the ECC rules.
DOE

N90-29107*# National Aeronautics and Space Administration. Wallops Flight Facility, Wallops Island, VA.
A PERSONAL COMPUTER-BASED, MULTITASKING DATA ACQUISITION SYSTEM
Steven A. Bailey Washington Sep. 1990 15 p
(NASA-TM-4232; NAS 1.15:4232; Rept-90B00133) Avail: NTIS HC A03/MF A01 CSCL 09B

A multitasking, data acquisition system was written to simultaneously collect meteorological radar and telemetry data from two sources. This system is based on the personal computer architecture. Data is collected via two asynchronous serial ports and is deposited to disk. The system is written in both the C programming language and assembler. It consists of three parts: a multitasking kernel for data collection, a shell with pull down windows as user interface, and a graphics processor for editing data and creating coded messages. An explanation of both system principles and program structure is presented. Author

N90-29108*# Old Dominion Univ., Norfolk, VA. Dept. of Computer Science.
DOCUMENTING THE DECISION STRUCTURE IN SOFTWARE DEVELOPMENT Final Report, period ending 15 Aug. 1990
J. Christian Wild, Kurt Maly, and Stewart N. Shen Sep. 1990 39 p Revised
(Contract NAS1-18584; NAG1-1026)
(NASA-CR-186865; NAS 1.26:186865) Avail: NTIS HC A03/MF A01 CSCL 09B

Current software development paradigms focus on the products of the development process. Much of the decision making process which produces these products is outside the scope of these paradigms. The Decision-Based Software Development (DBSD) paradigm views the design process as a series of interrelated decisions which involve the identification and articulation of problems, alternates, solutions and justifications. Decisions made by programmers and analysts are recorded in a project data base. Unresolved problems are also recorded and resources for their resolution are allocated by management according to the overall development strategy. This decision structure is linked to the products affected by the relevant decision and provides a process oriented view of the resulted system. Software maintenance uses this decision view of the system to understand the rationale behind the decisions affecting the part of the system to be modified. D-HyperCase, a prototype Decision-Based Hypermedia System is described and results of applying the DBSD approach during its development are presented. Author

N90-29109# Carnegie-Mellon Univ., Pittsburgh, PA. Software Engineering Inst.
TECHNICAL WRITING FOR SOFTWARE ENGINEERS Final Report
Linda Levine, Linda H. Pesante, and Susan B. Dunkle May 1990 69 p
(Contract F19628-90-C-0003)
(AD-A223872; SEI-CM-23) Avail: NTIS HC A04/MF A01 CSCL 12/5

This module, which is directed specifically to software engineers, discusses the writing process in the context of software engineering. Its focus is on the basic problem-solving activities that underlie effective writing, many of which are similar to those underlying software development. The module draws on related work in a number of disciplines, including rhetorical theory, discourse analysis, linguistics, and document design. It suggests techniques for becoming an effective writer and offers criteria for evaluating writing.
GRA

N90-29110# Carnegie-Mellon Univ., Pittsburgh, PA. Software Engineering Inst.
CONCEPTS OF CONCURRENT PROGRAMMING Final Report
David W. Bustard (Ulster Coll., Newtownabbey, North Ireland)

Apr. 1990 55 p
(Contract F19628-90-C-0003)
(AD-A223897; SEI-CM-24) Avail: NTIS HC A04/MF A01
CSCL 12/5

A concurrent program is one defining actions that may be performed simultaneously. The nature of such programs are discussed and an overview is provided of the means by which they may be constructed and executed. Emphasis is given to the terminology used in this field and the underlying concepts involved. Explicit concurrency is examined where concurrent behavior is specified by the program designer. Particular attention is paid to programs that can be considered inherently concurrent, that is, programs that are constructed to control or model physical systems that involve parallel activity. The module also includes a brief introduction to performance oriented concurrency, where concurrency is used to improve program performance by taking advantage of hardware support for parallel processing. The module is divided into three sections. The first deals with basic concepts in concurrent programming, covering characteristic attributes, formal properties, standard design problems, and execution details. The second section discusses the steps in constructing concurrent programs for specification to coding. The final section briefly examines concurrency from the point of view of some common application areas. The module gives a foundation for a deeper study of specific topics in concurrent programming. It also provides the preparatory material for a study of the concurrent aspects of application areas such as real time (embedded) systems, database systems, operating systems, and many simulation systems. GRA

N90-29111# Naval Postgraduate School, Monterey, CA.
BLOCK LANCZOS ALGORITHM M.S. Thesis
Joo Kim Yong Dec. 1989 67 p
(AD-A224011) Avail: NTIS HC A04/MF A01 CSCL 12/1

We use a Lanczos algorithm for computing a few of the smallest eigenvalues and the corresponding eigenvectors of a large symmetric matrix rather than computing all the eigenvalue-eigenvector pairs. The basic Lanczos algorithm generates a similar matrix which is block tridiagonal from a given large symmetric matrix. The size of the generated tridiagonal matrix depends upon the number of the small eigenvalues to be computed. The result is the savings in computations and storage. The block Lanczos algorithm is well suited for problems involving multiple eigenvalues. In this thesis, we develop the block Lanczos algorithm to estimate the direction-of-arrival (DOA) of a point source based on the observations measured at a linear array of sensors and compare the performance with that of a single vector Lanczos algorithm. The results of the computer simulation experiments conducted with this method is presented and discussed. GRA

N90-29112# Anacapa Sciences, Inc., Fort Rucker, AL.
STRATEGIES OF COMPUTER-BASED INSTRUCTIONAL DESIGN: A REVIEW OF GUIDELINES AND EMPIRICAL RESEARCH Interim Report, Jun. 1988 - Sep. 1989
Dudley J. Terrell May 1990 67 p
(Contract MDA903-87-C-0523; DA Proj. 2Q2-63007-A-795)
(AD-A224038; ASI690-324-89; ARI-TR-888) Avail: NTIS HC A04/MF A01 CSCL 05/8

A survey of literature was conducted to examine empirical research for the numerous guidelines and recommendations that have been published about design strategies for computer-based instruction. The guidelines and experiments were categorized as pertaining to: (1) strategies for presenting instructional material, (2) strategies for questioning and interactivity, or (3) strategies for programming response feedback and remediation procedures. Strategies for presenting instructional material were analyzed in literature on orienting instructions and objectives, stimulus display duration, sequencing instructional material, sequencing levels of difficulty, graphics, and review of material. Strategies for questioning and interactivity were analyzed in literature on prelesson questions, question types, question placement, number of questions, and answering questions. Strategies for programming response feedback and remediation procedures were analyzed in literature on feedback for correct and incorrect responses, latency of feedback, and placement of feedback. GRA

N90-29113# Naval Postgraduate School, Monterey, CA. Dept. of Computer Science.
DESIGNING INTELLIGENT COMPUTER AIDED INSTRUCTION SYSTEMS WITH INTEGRATED KNOWLEDGE REPRESENTATION SCHEMES M.S. Thesis
Daniel Joseph Ragsdale and John Patrick Tidd Jun. 1990 110 p
(AD-A224178) Avail: NTIS HC A06/MF A01 CSCL 12/5

Over the past twenty years, automated tutoring systems have gained an increasing recognition as a prominent area of Artificial Intelligence (AI). During this period, Intelligent Computer Aided Instruction (ICAI) systems have been developed using a variety of AI techniques to enhance the learning process. The core AI issue in designing these systems concerns knowledge representation. A review of current AI literature shows that there are numerous, distinctly different knowledge representation schemes, and most conventional programming environments do not readily support all of these representation schemes. This thesis proposes that tutoring systems are best designed in a programming environment that supports multiple, integrated knowledge representation schemes. Such an environment allows the designer to select and employ, with ease, the most natural knowledge representation scheme for each type of knowledge in the tutoring system. In this thesis we describe the components of a generalized ICAI system; discuss the various types of knowledge and knowledge representation schemes; and review the knowledge representation schemes used in several noted ICAI systems. In addition, we describe two prototype ICAI systems (Map Reading Tutor and Pilot Emergency Procedure Tutor) which we designed and developed in a specific programming environment that supports multiple, integrated knowledge representation schemes. GRA

N90-29038*# Carnegie-Mellon Univ., Pittsburgh, PA. The Robotics Inst.
STATE-BASED SCHEDULING: AN ARCHITECTURE FOR TELESCOPE OBSERVATION SCHEDULING
Nicola Muscettola and Stephen F. Smith *In* JPL, California Inst. of Tech., Proceedings of the NASA Conference on Space Telerobotics, Volume 1 31 Jan. 1989 p 415-424 (For primary document see N90-29000 23-54)
(Contract NCC2-531)
Avail: NTIS HC A21/MF A03 CSCL 09B

N90-29039*# Carnegie-Mellon Univ., Pittsburgh, PA. Dept. of Computer Science.
FOCUS OF ATTENTION IN AN ACTIVITY-BASED SCHEDULER
Norman Sadeh and Mark S. Fox *In* JPL, California Inst. of Tech., Proceedings of the NASA Conference on Space Telerobotics, Volume 1 31 Jan. 1989 p 425-434 Sponsored in part by McDonnell Aircraft Co., and by Digital Equipment Corp.
(For primary document see N90-29000 23-54)
(Contract F30602-88-C-0001)
Avail: NTIS HC A21/MF A03 CSCL 09B

N90-29071*# Purdue Univ., West Lafayette, IN. School of Electrical Engineering.
EFFICIENT MAPPING ALGORITHMS FOR SCHEDULING ROBOT INVERSE DYNAMICS COMPUTATION ON A MULTIPROCESSOR SYSTEM
C. S. G. Lee and C. L. Chen (Purdue Univ., Indianapolis, IN.) *In* JPL, California Inst. of Tech., Proceedings of the NASA Conference on Space Telerobotics, Volume 2 31 Jan. 1989 p 295-306
(For primary document see N90-29044 23-54)
(Grant NSF CDR-88-03017)
Avail: NTIS HC A17/MF A03 CSCL 09B

N90-29072*# Ohio State Univ., Columbus. Dept. of Electrical Engineering.
PARALLEL ALGORITHMS FOR COMPUTATION OF THE MANIPULATOR INERTIA MATRIX

Masoud Amin-Javaheri and David E. Orin *In* JPL, California Inst. of Tech., Proceedings of the NASA Conference on Space Telerobotics, Volume 2 31 Jan. 1989 p 307-316 (For primary document see N90-29044 23-54)
(Grant NSF EET-87-18434)
Avail: NTIS HC A17/MF A03 CSCL 09B

N90-29073*# Grenoble-1 Univ. (France).
PLANNING ROBOT ACTIONS UNDER POSITION AND SHAPE UNCERTAINTY
Christian Laugier *In* JPL, California Inst. of Tech., Proceedings of the NASA Conference on Space Telerobotics, Volume 2 31 Jan. 1989 p 319-330 Sponsored in part by CNRS; ADI Agency; ITMI Co.; and Institut National de Recherche en Informatique et d'Automatique (For primary document see N90-29044 23-54)
Avail: NTIS HC A17/MF A03 CSCL 09B

N90-29074*# Oxford Univ. (England). Robotics Group.
ORGANISING GEOMETRIC COMPUTATIONS FOR SPACE TELEROBOTICS
Stephen Cameron *In* JPL, California Inst. of Tech., Proceedings of the NASA Conference on Space Telerobotics, Volume 2 31 Jan. 1989 p 331-340 Sponsored in part by Science Research Council (For primary document see N90-29044 23-54)
Avail: NTIS HC A17/MF A03 CSCL 09B

N90-29075*# Carnegie-Mellon Univ., Pittsburgh, PA. Robotics Inst.
A TESSELATED PROBABILISTIC REPRESENTATION FOR SPATIAL ROBOT PERCEPTION AND NAVIGATION
Alberto Elfes *In* JPL, California Inst. of Tech., Proceedings of the NASA Conference on Space Telerobotics, Volume 2 31 Jan. 1989 p 341-350 (For primary document see N90-29044 23-54)
(Contract N00014-81-K-0503; CNPq-200.986-80)
Avail: NTIS HC A17/MF A03 CSCL 09B

62 COMPUTER SYSTEMS

Includes computer networks and special application computer systems.

N90-29114# Office National d'Etudes et de Recherches Aerospatiales, Paris (France). Direction des Moyens d'Informatique.
PARALLELIZATION OF A SOFTWARE RELATING TO AERODYNAMICS ON MIMD TYPE COMPUTERS Annual Report, 1988 [PARALLELISATION DE PROGRAMME D'AERODYNAMIQUE SUR DES INSTALLATIONS DE TYPE MIMD (ACTIVITES DE L'ANNE 1988)]
D. Guiraud and L. Mane Jan. 1989 47 p In FRENCH
(Contract DRET-88-34-001)
(ONERA-RT-31/3479-CY; ETN-90-97498) Avail: NTIS HC A03/MF A01

The activities performed in 1988 concerning the project for the parallelization of computer codes on aerodynamics are presented. The investigation is performed on two microprocessors, the CRAY2 and iPSC2. On CRAY2 microprocessors, the parallelization of a code for calculating three dimensional potential flow in a channel of variable rectangular cross section is carried out. A method for solving three dimensional Navier-Stokes equations on microprocessors with memory distribution is studied. ESA

N90-29115# Oak Ridge National Lab., TN. Engineering Physics and Mathematical Div.
PIECEWISE LINEAR MODELS OF PROCESSOR UTILIZATION
Michael D. Vose (Tennessee Univ., Knoxville.) Jun. 1990 20 p
(Contract DE-AC05-84OR-21400)
(DE90-014774; ORNL/TM-11566) Avail: NTIS HC A03/MF A01

This paper is part of a larger research effort to characterize the performance of parallel programs on distributed memory multiprocessors. We consider modeling processor utilization data by continuous piecewise linear approximations. We describe interactive tools for the identification of underlying trends and for the suppression of superfluous detail in processor utilization graphs. DOE

N90-29116# Los Alamos National Lab., NM.
AN EVEN-PARITY/ODD-PARITY FORMULATION FOR DETERMINISTIC TRANSPORT CALCULATIONS ON MASSIVELY PARALLEL COMPUTERS
J. E. Morel, Laura A. Olvey, G. W. Claborn, and J. A. Josef 1990 10 p Presented at the Free Lagrange Conference, Jackson Hole, WY, 3-7 Jun. 1990 Submitted for publication
(Contract W-7405-eng-36)
(DE90-015036; LA-UR-90-2268; CONF-9006195-4) Avail: NTIS HC A02/MF A01

A highly parallel deterministic method was developed for performing time-dependent particle (neutron, gamma-ray, or thermal radiation) transport calculations on arbitrarily connected 3-D tetrahedral meshes. The standard discrete-ordinates method, which is used to solve the first-order form of the transport equation, is extremely cumbersome to apply on such meshes and is based upon a mesh sweeping algorithm that is highly sequential in nature. A serial 1-D code for the CRAY-YMP and a parallel 1-D code for the CM-2 (Connection Machine) were written to test the basic method. Comparisons between these two codes have shown that the new even/odd parity method is highly parallelizable. DOE

63 CYBERNETICS

Includes feedback and control theory, artificial intelligence, robotics and expert systems.

For related information see also *54 Man/System Technology and Life Support.*

N90-29117*# New Mexico State Univ., Las Cruces. Computing Research Lab.
OVERCOMING RULE-BASED RIGIDITY AND CONNECTIONIST LIMITATIONS THROUGH MASSIVELY-PARALLEL CASE-BASED REASONING Memoranda in Computer and Cognitive Science
John Barnden and Kankanahalli Srinivas [1990] 33 p
(Grants NAGw-1592; AF-AFOSR-0215-88)
(NASA-CR-186963; NAS 1.26:186963; MCCS-90-187) Avail: NTIS HC A03/MF A01 CSCL 09B

Symbol manipulation as used in traditional Artificial Intelligence has been criticized by neural net researchers for being excessively inflexible and sequential. On the other hand, the application of neural net techniques to the types of high-level cognitive processing studied in traditional artificial intelligence presents major problems as well. A promising way out of this impasse is to build neural net models that accomplish massively parallel case-based reasoning. Case-based reasoning, which has received much attention recently, is essentially the same as analogy-based reasoning, and avoids many of the problems leveled at traditional artificial intelligence. Further problems are avoided by doing many strands of case-based reasoning in parallel, and by implementing the whole system as a neural net. In addition, such a system provides an approach to some aspects of the problems of noise, uncertainty and novelty in reasoning systems. The current neural net system (Conposit), which performs standard rule-based reasoning, is being modified into a massively parallel case-based reasoning version. Author

N90-29118# European Space Agency, Paris (France).
ROBUST CONTROLLER DESIGN BY CONTRACTION OF A POLE REGION
Dieter Kaesbauer (Deutsche Forschungs- und Versuchsanstalt fuer Luft- und Raumfahrt, Oberpfaffenhofen, Germany, F.R.) Feb. 1990 81 p Transl. into ENGLISH of Robuster Reglerentwurf durch Kontraktion eines Polgebiets (Oberpfaffenhofen, Fed. Republic of Germany, DFVLR), Jul. 1986 81 p Original language document was announced as N87-18360

(ESA-TT-1042; DFVLR-FB-86-34; ETN-90-97551) Avail: NTIS HC A05/MF A01

Stability is the prime requirement imposed upon a closed loop control circuit. By intensifying this requirement, assignment of a pole zone is achieved. A systematic, interactive method for specifically shifting a linear system's eigenvalues into an assigned zone on the complex plane is stated. The quality criteria used for the assessment of the eigenvalue clustering take account of all eigenvalues. Variations in sector parameters produce the multimodel problem. In this instance, too, extrapolation of the method is found to provide the approach to a solution. ESA

N90-29119# Oak Ridge National Lab., TN. Center for Engineering Systems Advanced Research.

A HARDWARE/SOFTWARE ENVIRONMENT TO SUPPORT R/D IN INTELLIGENT MACHINES AND MOBILE ROBOTIC SYSTEMS

Reinhold C. Mann 1990 7 p Presented at the DARPA Workshop on Distributed Intelligent Control Systems, Pacifica, CA, 17-19 Jul. 1990

(Contract DE-AC05-84OR-21400)

(DE90-014458; CONF-9007134-1; CESAR-90/30) Avail: NTIS HC A02/MF A01

The Center for Engineering Systems Advanced Research (CESAR) serves as a focal point at the Oak Ridge National Laboratory (ORNL) for basic and applied research in intelligent machines. Research and development at CESAR addresses issues related to autonomous systems, unstructured (i.e., incompletely known) operational environments, and multiple performing agents. Two mobile robot prototypes (HERMIES-2B and HERMIES-3) are being used to test new developments in several robot component technologies. This paper briefly introduces the computing environment at CESAR which includes three hypercube concurrent computers (two on-board the mobile robots), a graphics workstation, VAX, and multiple VME-based systems (several on-board the mobile robots). The current software environment at CESAR is intended to satisfy several goals, e.g.: code portability, re-usability in different experimental scenarios, modularity, concurrent computer hardware transparent to applications programmer, future support for multiple mobile robots, support human-machine interface modules, and support for integration of software from other, geographically disparate laboratories with different hardware set-ups. DOE

N90-29120# Oak Ridge National Lab., TN. Data Systems Research and Development Program.

WORKSHOP ON NEURAL NETWORKS

Robert E. Uhrig and M. L. Emrich Jan. 1990 373 p Workshop held in Oak Ridge, TN, 20-21 Nov. 1989; cosponsored by Tennessee Univ. and Tennessee Center for Neural Engineering and Applications

(Contract DE-AC05-84OR-21400)

(DE90-014794; ORNL/DSRD-25; CONF-8911136-Vugraphs)

Avail: NTIS HC A16/MF A02

The topics covered in this report are: Learning, Memory, and Artificial Neural Systems; Emerging Neural Network Technology; Neural Networks; Digital Signal Processing and Neural Networks; Application of Neural Networks to In-Core Fuel Management; Neural Networks in Process Control; Neural Network Applications in Image Processing; Neural Networks for Multi-Sensor Information Fusion; Neural Network Research in Instruments and Controls Division; Neural Networks Research in the ORNL Engineering Physics and Mathematics Division; Neural Network Applications for Linear Programming; Neural Network Applications to Signal Processing and Diagnostics; Neural Networks in Filtering and Control; Neural Network Research at Tennessee Technological University; and Global Minima within the Hopfield Hypercube. DOE

N90-29121*# National Aeronautics and Space Administration. Lewis Research Center, Cleveland, OH.

AN EXPERT SYSTEM TO PERFORM ON-LINE CONTROLLER RESTRUCTURING FOR ABRUPT MODEL CHANGES

Jonathan S. Litt 1990 12 p Prepared for presentation at the Rotary Wing Propulsion Specialists' Meeting, Williamsburg, VA, 13-15 Nov. 1990; sponsored in part by the Hampton Roads Chapter of the Southeast Region of the American Helicopter Society Prepared in cooperation with Army Aviation Systems Command, Cleveland, OH

(DA Proj. 1L1-61102-AH-45)

(NASA-TM-103609; E-5761; NAS 1.15:103609; AVSCOM-TR-90-C-018) Avail: NTIS HC A03/MF A01 CSCL 09B

Work in progress on an expert system used to reconfigure and tune airframe/engine control systems on-line in real time in response to battle damage or structural failures is presented. The closed loop system is monitored constantly for changes in structure and performance, the detection of which prompts the expert system to choose and apply a particular control restructuring algorithm based on the type and severity of the damage. Each algorithm is designed to handle specific types of failures and each is applicable only in certain situations. The expert system uses information about the system model to identify the failure and to select the technique best suited to compensate for it. A depth-first search is used to find a solution. Once a new controller is designed and implemented it must be tuned to recover the original closed-loop handling qualities and responsiveness from the degraded system. Ideally, the pilot should not be able to tell the difference between the original and redesigned systems. The key is that the system must have inherent redundancy so that degraded or missing capabilities can be restored by creative use of alternate functionalities. With enough redundancy in the control system, minor battle damage affecting individual control surfaces or actuators, compressor efficiency, etc., can be compensated for such that the closed-loop performance in not noticeably altered. The work is applied to a Black Hawk/T700 system. Author

N90-29026*# Georgia Inst. of Tech., Atlanta. School of Information and Computer Science.

THREE-DIMENSIONAL MOTOR SCHEMA BASED NAVIGATION

Ronald C. Arkin *In* JPL, California Inst. of Tech., Proceedings of the NASA Conference on Space Telerobotics, Volume 1 31 Jan. 1989 p 291-299 (For primary document see N90-29000 23-54)

Avail: NTIS HC A21/MF A03 CSCL 09B

N90-29028*# Hughes Research Labs., Malibu, CA. Artificial Intelligence Center.

EXPLOITING MAP PLANS AS RESOURCES FOR ACTION

David Payton *In* JPL, California Inst. of Tech., Proceedings of the NASA Conference on Space Telerobotics, Volume 1 31 Jan. 1989 p 311-320 (For primary document see N90-29000 23-54)

Avail: NTIS HC A21/MF A03 CSCL 09B

N90-29029*# Old Dominion Univ., Norfolk, VA. Dept. of Computer Science.

LEARNED NAVIGATION IN UNKNOWN TERRAINS: A RETRACTION METHOD

Nageswara S. V. Rao, N. Stoltzfus, and S. Sitharama Iyengar (Louisiana State Univ., Baton Rouge.) *In* JPL, California Inst. of Tech., Proceedings of the NASA Conference on Space Telerobotics, Volume 1 31 Jan. 1989 p 321-330 (For primary document see N90-29000 23-54)

Avail: NTIS HC A21/MF A03 CSCL 09B

N90-29030*# Jet Propulsion Lab., California Inst. of Tech., Pasadena.

COMPUTATIONAL NEURAL LEARNING FORMALISMS FOR MANIPULATOR INVERSE KINEMATICS

Sandeep Gulati, Jacob Barhen, and S. Sitharama Iyengar (Louisiana State Univ., Baton Rouge.) *In its* Proceedings of the NASA Conference on Space Telerobotics, Volume 1 31 Jan. 1989 p 333-342 (For primary document see N90-29000 23-54)

Avail: NTIS HC A21/MF A03 CSCL 09B

N90-29031*# University of Southern Illinois, Carbondale. Dept. of Electrical Engineering.
MULTI-LAYER NEURAL NETWORKS FOR ROBOT CONTROL
Farzad Pourboghrat *In* JPL, California Inst. of Tech., Proceedings of the NASA Conference on Space Telerobotics, Volume 1 31 Jan. 1989 p 343-352 (For primary document see N90-29000 23-54)
Avail: NTIS HC A21/MF A03 CSCL 09B

N90-29032*# Tulane Univ., New Orleans, LA. Dept. of Computer Science.
A HYBRID ARCHITECTURE FOR THE IMPLEMENTATION OF THE ATHENA NEURAL NET MODEL
C. Koutsougeras and C. Papachristou (Case Western Reserve Univ., Cleveland, OH.) *In* JPL, California Inst. of Tech., Proceedings of the NASA Conference on Space Telerobotics, Volume 1 31 Jan. 1989 p 353-361 (For primary document see N90-29000 23-54)
Avail: NTIS HC A21/MF A03 CSCL 09B

N90-29033*# New Mexico Univ., Albuquerque. Dept. of Electrical and Computer Engineering.
A DESIGN PHILOSOPHY FOR MULTI-LAYER NEURAL NETWORKS WITH APPLICATIONS TO ROBOT CONTROL
Nader Vadiee and Mo Jamshidi *In* JPL, California Inst. of Tech., Proceedings of the NASA Conference on Space Telerobotics, Volume 1 31 Jan. 1989 p 363-372 (For primary document see N90-29000 23-54)
Avail: NTIS HC A21/MF A03 CSCL 09B

N90-29034*# Kobe Univ. (Japan). Div. of System Science.
A NEURAL NETWORK FOR CONTROLLING THE CONFIGURATION OF FRAME STRUCTURE WITH ELASTIC MEMBERS
Kazuyoshi Tsutsumi *In* JPL, California Inst. of Tech., Proceedings of the NASA Conference on Space Telerobotics, Volume 1 31 Jan. 1989 p 373-382 (For primary document see N90-29000 23-54)
Avail: NTIS HC A21/MF A03 CSCL 09B

N90-29035*# Edinburgh Univ. (Scotland). Inst. of Artificial Intelligence Applications.
COORDINATING THE ACTIVITIES OF A PLANNER AND AN EXECUTION AGENT
Austin Tate *In* JPL, California Inst. of Tech., Proceedings of the NASA Conference on Space Telerobotics, Volume 1 31 Jan. 1989 p 385-393 (For primary document see N90-29000 23-54)
(Grants GR/D/5898-7; GR/E/98058)
Avail: NTIS HC A21/MF A03 CSCL 09B

N90-29040*# Rensselaer Polytechnic Inst., Troy, NY. Center for Intelligent Robotic Systems for Space Exploration.
A BOLTZMANN MACHINE FOR THE ORGANIZATION OF INTELLIGENT MACHINES
Michael C. Moed and George N. Saridis *In* JPL, California Inst. of Tech., Proceedings of the NASA Conference on Space Telerobotics, Volume 1 31 Jan. 1989 p 437-446 (For primary document see N90-29000 23-54)
(Grant NAGw-1333)
Avail: NTIS HC A21/MF A03 CSCL 09B

N90-29041*# George Mason Univ., Fairfax, VA. School of Information Technology and Engineering.
GRASP PLANNING UNDER UNCERTAINTY
A. M. Erkmen and H. E. Stephanou *In* JPL, California Inst. of Tech., Proceedings of the NASA Conference on Space Telerobotics, Volume 1 31 Jan. 1989 p 447-456 (For primary document see N90-29000 23-54)
Avail: NTIS HC A21/MF A03 CSCL 09B

N90-29042*# Brown Univ., Providence, RI. Dept. of Computer Science.
APPROXIMATION ALGORITHMS FOR PLANNING AND CONTROL
Mark Boddy and Thomas Dean *In* JPL, California Inst. of Tech., Proceedings of the NASA Conference on Space Telerobotics, Volume 1 31 Jan. 1989 p 457-462 (For primary document see N90-29000 23-54)
(Contract F49620-88-C-0132; NSF IRI-86-12644)
Avail: NTIS HC A21/MF A03 CSCL 09B

N90-29043*# Drexel Univ., Philadelphia, PA. Dept. of Electrical and Computer Engineering.
MULTIRESOLUTIONAL MODELS OF UNCERTAINTY GENERATION AND REDUCTION
A. Meystel *In* JPL, California Inst. of Tech., Proceedings of the NASA Conference on Space Telerobotics, Volume 1 31 Jan. 1989 p 463-476 (For primary document see N90-29000 23-54)
Avail: NTIS HC A21/MF A03 CSCL 09B

N90-29062*# Drexel Univ., Philadelphia, PA. Dept. of Electrical and Computer Engineering.
TECHNIQUES AND POTENTIAL CAPABILITIES OF MULTI-RESOLUTIONAL INFORMATION (KNOWLEDGE) PROCESSING
A. Meystel *In* JPL, California Inst. of Tech., Proceedings of the NASA Conference on Space Telerobotics, Volume 2 31 Jan. 1989 p 197-209 (For primary document see N90-29044 23-54)
Avail: NTIS HC A17/MF A03 CSCL 09B

N90-29064*# Michigan Univ., Ann Arbor. Artificial Intelligence Lab.
BUILDING AN ENVIRONMENT MODEL USING DEPTH INFORMATION
Y. Roth-Tabak and Ramesh Jain *In* JPL, California Inst. of Tech., Proceedings of the NASA Conference on Space Telerobotics, Volume 2 31 Jan. 1989 p 221-230 (For primary document see N90-29044 23-54)
(Contract JPL-958086)
Avail: NTIS HC A17/MF A03 CSCL 09B

N90-29078*# Space Telescope Science Inst., Baltimore, MD.
LEARNING IN STOCHASTIC NEURAL NETWORKS FOR CONSTRAINT SATISFACTION PROBLEMS
Mark D. Johnston and Hans-Martin Adorf (European Southern Observatory, Garching, Germany, F.R.) *In* JPL, California Inst. of Tech., Proceedings of the NASA Conference on Space Telerobotics, Volume 2 31 Jan. 1989 p 367-376 (For primary document see N90-29044 23-54)
Avail: NTIS HC A17/MF A03 CSCL 09B

64 NUMERICAL ANALYSIS

Includes iteration, difference equations, and numerical approximation.

N90-29122*# Computational Mechanics Co., Austin, TX.
SECOND ORDER TENSOR FINITE ELEMENT Final Report, Jun. 1990
J. Tinsley Oden, J. Fly, C. Berry, W. Tworzydlo, S. Vadaketh, and J. Bass 22 Jun. 1990 109 p
(Contract NAS8-37283)
(NASA-CR-184008; NAS 1.26:184008; TR-90-03) Avail: NTIS HC A06/MF A01 CSCL 12A

The results of a research and software development effort are presented for the finite element modeling of the static and dynamic behavior of anisotropic materials, with emphasis on single crystal alloys. Various versions of two dimensional and three dimensional hybrid finite elements were implemented and compared with displacement-based elements. Both static and dynamic cases are considered. The hybrid elements developed in the project were

incorporated into the SPAR finite element code. In an extension of the first phase of the project, optimization of experimental tests for anisotropic materials was addressed. In particular, the problem of calculating material properties from tensile tests and of calculating stresses from strain measurements were considered. For both cases, numerical procedures and software for the optimization of strain gauge and material axes orientation were developed. Author

N90-29123# Sandia National Labs., Albuquerque, NM. Applied Mechanics Div.
SUPERCHIEF: A MODIFIED CHIEF (COMBINED HELMHOLZ INTEGRAL EQUATION FORMULATION) METHOD
D. J. Segalman and D. W. Lobitz Jul. 1990 21 p
(Contract DE-AC04-76DP-00789)
(DE90-014744; SAND-90-1266) Avail: NTIS HC A03/MF A01

When the boundary integral equation method is applied to exterior acoustics problems, singularities occur in the resulting algebraic equations at various frequencies associated with the eigenvalues of an interior problem. These frequencies are referred to as forbidden, and various methods have been devised to overcome the computational difficulties presented at these frequencies. The work presented here is an extension to the CHIEF method in that higher derivatives, in addition to the function itself, are constrained to be zero at selected points in the interior domain. Whereas the relative success of either method depends on the quantity and selection of interior points, the SuperCHIEF method requires fewer interior points and is less sensitive to point selection, resulting in improved robustness without significant increase in computational complexity. DOE

N90-29124*# National Aeronautics and Space Administration. Lewis Research Center, Cleveland, OH.
CONSISTENCY AND CONVERGENCE FOR NUMERICAL RADIATION CONDITIONS
Thomas Hagstrom Aug. 1990 12 p Prepared in cooperation with State Univ. of New York, Stony Brook
(Grant NASA Order C-99066-G; NSF DMS-89-05314)
(NASA-TM-103262; ICOMP-90-21; E-5695; NAS 1.15:103262)
Avail: NTIS HC A03/MF A01 CSCL 12A

The problem of imposing radiation conditions at artificial boundaries for the numerical simulation of wave propagation is considered. Emphasis is on the behavior and analysis of the error which results from the restriction of the domain. The theory of error estimation is briefly outlined for boundary conditions. Use is made of the asymptotic analysis of propagating wave groups to derive and analyze boundary operators. For dissipative problems this leads to local, accurate conditions, but falls short in the hyperbolic case. A numerical experiment on the solution of the wave equation with cylindrical symmetry is described. A unified presentation of a number of conditions which have been proposed in the literature is given and the time dependence of the error which results from their use is displayed. The results are in qualitative agreement with theoretical considerations. It was found, however, that for this model problem it is particularly difficult to force the error to decay rapidly in time. Author

N90-29125*# Institute for Computer Applications in Science and Engineering, Hampton, VA.
MULTIGRID FOR HYPERSONIC INVISCID FLOWS Final Report
Naomi H. Decker and Eli Turkel (Tel-Aviv Univ., Israel) Aug. 1990 18 p Submitted for publication
(Contract NAS1-18605)
(NASA-CR-182082; ICASE-90-54; NAS 1.26:182082) Avail: NTIS HC A03/MF A01 CSCL 12A

The use of multigrid methods to solve the Euler equations for hypersonic flow is discussed. The steady state equations are considered with a Runge-Kutta smoother based on the time accurate equations together with local time stepping and residual smoothing. The effect of the Runge-Kutta coefficients on the convergence rate was examined considering both damping characteristics and convection properties. The importance of boundary conditions on the convergence rate for hypersonic flow is discussed. Also of importance are the switch between the second and fourth difference viscosity. Solutions are given for flow around the bump in a channel and flow around a biconic section. Author

N90-29126# Virginia Polytechnic Inst. and State Univ., Blacksburg. Dept. of Mathematics and Physics.
APPLIED MATHEMATICS OF TRANSPORT THEORY Final Report, period ending 1 May 1990
W. Greenberg and P. F. Zweifel 1 May 1990 7 p
(Contract DE-FG05-87ER-25033)
(DE90-014627; DOE/ER-25033/3) Avail: NTIS HC A02/MF A01

Numerous results in many areas of mathematical transport theory and of mathematical physics are reported. Results are presented under the headings: nonlinear kinetic equations, linear kinetic equations, specific transport models, and other areas of mathematical physics. DOE

N90-29127# Argonne National Lab., IL. Mathematics and Computer Science Div.
ELEFUNT TEST RESULTS UNDER AST FORTRAN V1.8.0 ON THE SEQUENT SYMMETRY
W. J. Cody Jul. 1990 19 p
(Contract W-31-109-eng-38)
(DE90-014932; ANL/MCS-TM-138) Avail: NTIS HC A03/MF A01

Testing is discussed of the floating point arithmetic and of the elementary function libraries under AST FORTRAN on a 24-processor Sequent Symmetry computer. The programs MACHAR and PARANOIA were used to check the quality of arithmetic, and the ELEFUNT suite of programs from the book Software Manual for the Elementary Functions by Cody and Waite was used to check function performance. Two complete sets of tests were run, one for each type of floating point processor, Intel 80387 and Weitek 1167, on the machine. DOE

N90-29128*# Institute for Computer Applications in Science and Engineering, Hampton, VA.
NUMERICAL EXPERIMENTS ON THE ACCURACY OF ENO AND MODIFIED ENO SCHEMES Final Report
Chi-Wang Shu (Brown Univ., Providence, RI.) Aug. 1990 26 p Submitted for publication
(Contract NAS1-18605; NSF DMS-88-10150; AF-AFOSR-0093-90)
(NASA-CR-182083; ICASE-90-55; NAS 1.26:182083) Avail: NTIS HC A03/MF A01 CSCL 12A

Further numerical experiments are made assessing an accuracy degeneracy phenomena. A modified essentially non-oscillatory (ENO) scheme is proposed, which recovers the correct order of accuracy for all the test problems with smooth initial conditions and gives comparable results with the original ENO schemes for discontinuous problems. Author

N90-29129*# Institute for Computer Applications in Science and Engineering, Hampton, VA.
NUMERICAL METHODS FOR SYSTEMS OF CONSERVATION LAWS OF MIXED TYPE USING FLUX SPLITTING Final Report
Chi-Wang Shu (Brown Univ., Providence, RI.) Aug. 1990 18 p Submitted for publication
(Contract NAS1-18605; NAG1-1145; NSF DMS-88-10150; AF-AFOSR-0093-90)
(NASA-CR-182084; ICASE-90-56; NAS 1.26:182084) Avail: NTIS HC A03/MF A01 CSCL 12A

The essentially non-oscillatory (ENO) finite difference scheme is applied to systems of conservation laws of mixed hyperbolic-elliptic type. A flux splitting, with the corresponding Jacobi matrices having real and positive/negative eigenvalues, is used. The hyperbolic ENO operator is applied separately. The scheme is numerically tested on the van der Waals equation in fluid dynamics. Convergence was observed with good resolution to weak solutions for various Riemann problems, which are then numerically checked to be admissible as the viscosity-capillarity

limits. The interesting phenomena of the shrinking of elliptic regions if they are present in the initial conditions were also observed.
Author

N90-29130# Oak Ridge National Lab., TN. Fusion Energy Div.
ASYMPTOTIC BEHAVIOR OF SOLUTIONS OF DIFFUSION-LIKE PARTIAL DIFFERENTIAL EQUATIONS INVARIANT TO A FAMILY OF AFFINE GROUPS
Lawrence Dresner Jul. 1990 11 p
(Contract DE-AC05-84OR-21400)
(DE90-014792; ORNL/TM-11559) Avail: NTIS HC A03/MF A01

This report deals with the asymptotic behavior of certain solutions of partial differential equations in one dependent and two independent variables (call them c, z, and t, respectively). The partial differential equations are invariant to one-parameter families of one-parameter affine groups of the form: c' = lambda(sup alpha)c, t' = lambda(sup beta)t, z' = lambda(z), where lambda is the group parameter that labels the individual transformations and alpha and beta are parameters that label groups of the family. The parameters alpha and beta are connected by a linear relation, M(alpha) + N(beta) = L, where M, N, and L are numbers determined by the structure of the partial differential equation. It is shown that when L/M and N/M are less than 0, certain solutions become asymptotic to z(sup L/M)t(sup -N/M) for large z or small t. Some practical applications of this result are discussed.
DOE

N90-29131# Lawrence Livermore National Lab., CA.
DETERMINISTIC TRANSPORT ON AN ARBITRARILY-CONNECTED GRID
Marvin L. Adams Jun. 1990 10 p Presented at the Free Lagrange Conference, Jackson Lake, WY, 3-7 Jun. 1990
(Contract W-7405-eng-48)
(DE90-015148; UCRL-JC-104266; CONF-9006195-6) Avail: NTIS HC A03/MF A01

Spatial discretization is discussed of the transport equation, concentrating on the problems posed by grids with arbitrary connectivity and arbitrarily-shaped computational cells. Both accuracy and efficiency criteria are considered and several candidate discretization schemes with respect to these criteria are examined. It is shown that if arbitrarily-shaped zones are allowed, existing spatial discretization schemes do not provide the desired accuracy in the optically-thick diffusion limit. A new scheme is presented that does appear to perform well in the diffusion limit, regardless of the connectivity of the grid or shape of the zones. It is shown that the new scheme has very nice properties in other limits as well.
DOE

N90-29132# International Centre for Theoretical Physics, Trieste (Italy).
WEIGHTED NORM INEQUALITIES FOR RIEMANN-LIOUVILLE FRACTIONAL INTEGRAL
Christopher Olutunde Imoru (Obafemi Awolowo Univ., Ile-Ife, Nigeria) Dec. 1989 16 p Submitted for publication Sponsored in part by Swedish Agency for Research Cooperation with Developing Countries
(DE90-627153; IC-89/397) Avail: NTIS (US Sales Only) HC A03/MF A01

The main objective of this paper is to prove a result which is more general than the theorem on weighted inequalities for Riemann-Liouville fractional integrals of order n (n is greater than or equal to 1) proved by Martin-Reyes and Sawyer.
DOE

N90-29133# International Centre for Theoretical Physics, Trieste (Italy).
THE CENTER OF THE ENVELOPING ALGEBRA OF THE SEMIDIRECT PRODUCT OF THE HEISENBERG LIE ALGEBRA h(SUB n) AND A REDUCTIVE LIE ALGEBRA S THE RANK OF WHICH IS EQUAL TO 1 OR 2
Van Hop Le (Ho Chi Minh City Univ., Vietnam) Dec. 1989 22 p Submitted for publication
(DE90-627155; IC-89/410) Avail: NTIS (US Sales Only) HC A03/MF A01

Computational methods and some theoretical results about polynomial algebras in several variables (and especially in 2 variables) are used to determine the center of the enveloping algebra of the semidirect product of the Heisenberg Lie algebra and a reductive Lie algebra the rank of which is equal to 1 or 2.
DOE

N90-29134# International Centre for Theoretical Physics, Trieste (Italy).
RECURRENCE RELATIONS AND WEIGHT FUNCTIONS FOR APPROXIMATION BY ORTHONORMAL POLYNOMIALS
A. K. Bisoi (Utkal Univ., Bhubaneswar, India) Dec. 1989 9 p Submitted for publication Sponsored in part by Swedish Agency for Research Cooperation with Developing Countries
(DE90-627156; IC-89/411) Avail: NTIS (US Sales Only) HC A02/MF A01

The popular three-term recurrence relation is found to be a numerically unstable algorithm for generation of higher order orthogonal polynomials. For stability, a k-term recurrence relation for generating the k th order polynomial is suggested. Instead of assigning equal weight to data points with unspecified errors, the use of the Jacobian weight function is suggested for generating the orthogonal polynomials to effect a closer representation.
DOE

N90-29135# International Centre for Theoretical Physics, Trieste (Italy).
BELTRAMI ALGEBRA AND SYMMETRY OF BELTRAMI EQUATION ON RIEMANN SURFACES
Han-Ying Guo, Kai-Wen Xu, Jian-Min Shen, and Shi-Kun Wang (Academia Sinica, Beijing, China) Dec. 1989 16 p Submitted for publication
(DE90-627157; IC-89/412) Avail: NTIS (US Sales Only) HC A03/MF A01

It is shown that the Beltrami equation has an infinite dimensional symmetry, namely the Beltrami algebra, on its solution spaces. The Beltrami algebra with central extension and its supersymmetric version are explicitly found.
DOE

N90-29136# International Centre for Theoretical Physics, Trieste (Italy).
THE COMBINATORICS COMPUTATION FOR CASIMIR OPERATORS OF THE SYMPLECTIC LIE ALGEBRA AND THE APPLICATION FOR DETERMINING THE CENTER OF THE ENVELOPING ALGEBRA OF A SEMIDIRECT PRODUCT
Van Hop Le (Ho Chi Minh City Univ., Vietnam) Dec. 1989 39 p Submitted for publication
(DE90-627161; IC-89/434) Avail: NTIS (US Sales Only) HC A03/MF A01

The combinatorics computation is used to describe the Casimir operators of the symplectic Lie algebra. This result is applied for determining the center of the enveloping algebra of the semidirect product of the Heisenberg Lie algebra and the symplectic Lie algebra.
DOE

N90-29137# International Centre for Theoretical Physics, Trieste (Italy).
ASYMPTOTICS OF LAPLACE-DIRICHLET INTEGRALS
S. M. Kozlov Jan. 1990 7 p
(DE90-627165; IC-90/16) Avail: NTIS (US Sales Only) HC A02/MF A01

The problem of the asymptotic expansion of the Laplace-Dirichlet integral is considered. In homogenization theory such an integral represents the energy, and in general depends on the cohomology class. Here the asymptotic behavior of this integral is found.
DOE

N90-29138# International Centre for Theoretical Physics, Trieste (Italy).
SOLUTION OF THE STOKES SYSTEM BY BOUNDARY INTEGRAL EQUATIONS AND FIXED POINT ITERATIVE SCHEMES
Charles E. Chidume (Nigeria Univ., Nsukka.) and Mbaro-Saman Lubuma Jan. 1990 20 p Submitted for publication
(DE90-627166; IC-90/3) Avail: NTIS (US Sales Only) HC A03/MF A01

The solution to the exterior three dimensional Stokes problem is sought in the form of a single layer potential of unknown density. This reduces the problem to a boundary integral equation of the first kind whose operator is the velocity component of the single layer potential. It is shown that this component is an isomorphism between two appropriate Sobolev spaces containing the unknown densities and the data respectively. The isomorphism corresponds to a variational problem with coercive bilinear form. The latter property allows us to consider various fixed point iterative schemes that converge to the unique solution of the integral equation. Explicit error estimates are also obtained. The successive approximations are also considered in a more computable form by using the product integration method of Atkinson. DOE

N90-29139# International Centre for Theoretical Physics, Trieste (Italy).
THE COUSIN PROBLEMS FOR AN OVERDETERMINED SYSTEM OF COMPLEX PARTIAL DIFFERENTIAL EQUATIONS
Hung Son Le Jan. 1990 8 p
(DE90-627170; IC-90/4) Avail: NTIS (US Sales Only) HC A02/MF A01

The Cousin Problems for an Overdetermined System of complex Partial Differential Equations are considered. It is proven that, under suitable hypotheses on its coefficients, the Cousin Problems can be solved on the domains of C(sup n), which satisfy the same conditions as those in Complex Analysis. DOE

N90-29140# International Centre for Theoretical Physics, Trieste (Italy).
THE FIRST ORDER PHASE TRANSITION FOR SIX-STATE POTTS MODEL ON TWO DIMENSIONAL RANDOM TRIANGLE LATTICE
Tian-Lun Chen, Wu-Qun Huang, and Yun-Wei Xin (Nankai Univ., Tiangjin, China) Dec. 1989 13 p Submitted for publication
(DE90-627210; IC-89/374) Avail: NTIS (US Sales Only) HC A03/MF A01

An optimal Monte Carlo renormalization group method is applied to the 6-state Potts model on a 2-dimensional random triangle lattice. Obviously, the phase transition is of the first order at this phase transition point. The obtained scaling exponent (nu) = 0.54 and the energy gap (delta)E = 0.101 approaches the theoretical and analytical values. DOE

65 STATISTICS AND PROBABILITY

Includes data sampling and smoothing; Monte Carlo method; and stochastic processes.

N90-29141# Southampton Univ. (England). Inst. of Sound and Vibration Research.
ESTIMATION OF INDIVIDUAL COUPLING LOSS FACTORS IN A MULTI-SUBSYSTEM
R. S. Ming, G. J. Stimpson, and N. Lalor Mar. 1990 27 p
(ISVR-TR-184; ETN-90-97516) Avail: NTIS HC A03/MF A01

The estimation of individual loss factors in a complex multisubstructure is experimentally investigated. It is shown that by manipulating the statistical energy analysis power balance equations it is possible to obtain a relationship for the coupling loss factor between two parts of a multi-substructure only in terms of quantities associated with those two components themselves. The whole of the rest of the structure is assumed as a third substructure which completes the energy balance but on which no measurements are made. ESA

66 SYSTEMS ANALYSIS

Includes mathematical modeling; network analysis; and operations research.

N90-29142*# Draper (Charles Stark) Lab., Inc., Cambridge, MA.
MODEL AUTHORING SYSTEM FOR FAIL SAFE ANALYSIS
Scott E. Sikora Washington NASA Aug. 1990 65 p
(Contract NAS2-12451)
(NASA-CR-4317; H-1620; NAS 1.26:4317) Avail: NTIS HC A04/MF A01 CSCL 12B

The Model Authoring System is a prototype software application for generating fault tree analyses and failure mode and effects analyses for circuit designs. Utilizing established artificial intelligence and expert system techniques, the circuits are modeled as a frame-based knowledge base in an expert system shell, which allows the use of object oriented programming and an inference engine. The behavior of the circuit is then captured through IF-THEN rules, which then are searched to generate either a graphical fault tree analysis or failure modes and effects analysis. Sophisticated authoring techniques allow the circuit to be easily modeled, permit its behavior to be quickly defined, and provide abstraction features to deal with complexity. Author

N90-29143*# Draper (Charles Stark) Lab., Inc., Cambridge, MA.
A KNOWLEDGE-BASED SYSTEM DESIGN/INFORMATION TOOL
James G. Allen and Scott E. Sikora Washington NASA Aug. 1990 192 p
(Contract NAS2-12451)
(NASA-CR-4316; H-1621; NAS 1.26:4316) Avail: NTIS HC A09/MF A01 CSCL 12B

The objective of this effort was to develop a Knowledge Capture System (KCS) for the Integrated Test Facility (ITF) at the Dryden Flight Research Facility (DFRF). The DFRF is a NASA Ames Research Center (ARC) facility. This system was used to capture the design and implementation information for NASA's high angle-of-attack research vehicle (HARV), a modified F/A-18A. In particular, the KCS was used to capture specific characteristics of the design of the HARV fly-by-wire (FBW) flight control system (FCS). The KCS utilizes artificial intelligence (AI) knowledge-based system (KBS) technology. The KCS enables the user to capture the following characteristics of automated systems: the system design; the hardware (H/W) design and implementation; the software (S/W) design and implementation; and the utilities (electrical and hydraulic) design and implementation. A generic version of the KCS was developed which can be used to capture the design information for any automated system. The deliverable items for this project consist of the prototype generic KCS and an application, which captures selected design characteristics of the HARV FCS. Author

N90-28636*# National Aeronautics and Space Administration. John F. Kennedy Space Center, Cocoa Beach, FL.
OPERATIONAL COST DRIVERS
Arthur L. Scholz (Boeing Aerospace Co., Kennedy Space Center, FL.) and William J. Dickinson *In* NASA, Marshall Space Flight Center, Advanced Earth-to-Orbit Propulsion Technology 1988, Volume 1 Sep. 1988 p 414-421 (For primary document see N90-28611 23-20)
Avail: NTIS HC A99/MF E06 CSCL 12B

67 THEORETICAL MATHEMATICS

Includes topology and number theory.

N90-29144# Groningen Rijksuniv. (Netherlands).
GEOMETRIC THEORY FOR INFINITE DIMENSIONAL SYSTEMS Ph.D. Thesis
Heiko Johannes Zwart 1988 169 p Previously announced in IAA as A89-51274

(Grant NWO-10-64-06)
(ETN-90-96922) Avail: NTIS HC A08/MF A01

A fundamental treatment of the geometric theory for infinite dimensional systems in Banach spaces is presented. For closed subspaces the concepts of open loop invariance, closed loop invariance and frequency invariance are proved equivalent. The condition that the subspace be closed is essential; there are examples of open loop invariant subspaces which are not closed loop invariant, and the same holds for frequency invariance. ESA

N90-29145# Stanford Univ., CA. Systems Optimization Lab.
LEAST-INDEX RESOLUTION OF DEGENERACY IN LINEAR COMPLEMENTARITY PROBLEMS WITH SUFFICIENT MATRICES
Richard W. Cottle and Yow-Yieh Chang Jun. 1990 14 p
(Contracts DE-FG03-87ER-25028; N00014-89-J-1659; NSF DMS-89-13089)
(DE90-014406; SU-SOL-90-9) Avail: NTIS HC A03/MF A01

The Principal Pivoting Method (PPM) for the Linear Complementarity Problem (LCP) is examined. It is shown that when the matrix M of the LCP (q,M) is (row and column) sufficient, the incorporation of a least index pivot selection rule in the PPM makes it a finite algorithm even when the LCP is degenerate. DOE

N90-29146# International Centre for Theoretical Physics, Trieste (Italy).
ON COMPARABLE L(SUP p)-NORMS OF SUBADDITIVE FUNCTIONS ON TOPOLOGICAL GROUPS
Christopher Olutunde Imoru (Obafemi Awolowo Univ., Ile-Ife, Nigeria) Dec. 1989 7 p Submitted for publication Sponsored in part by Swedish Agency for Research Cooperation with Developing Countries
(DE90-627154; IC-89/398) Avail: NTIS (US Sales Only) HC A02/MF A01

A theorem is proven which contains, as a special case, a result of Beesack on comparable L(sup p)-norms of subadditive functions. DOE

N90-29147# International Centre for Theoretical Physics, Trieste (Italy).
ON AN ISOSPECTRALITY QUESTION OVER COMPACT RIEMANN SURFACES
S. Srinivas Rau (Hyderabad Univ., India) Jan. 1990 5 p Submitted for publication
(DE90-627163; IC-90/13) Avail: NTIS (US Sales Only) HC A01/MF A01

It is proved that for a generic compact Riemann surface X of genus g is greater than 1, (1) there are at most 2(sup 2g) unitary characters of pi(sub 1)(X) whose associated line bundles have laplacians of identical spectrum, and (2) generating cycles for pi(sub 1)(X) can be chosen to be closed geodesics whose length multiplicity is 1. DOE

N90-29148# International Centre for Theoretical Physics, Trieste (Italy).
A COROLLARY TO KODAIRA-SPENCER'S THEOREM ON CONTINUITY OF EIGENVALUES
S. Srinivas Rau (Hyderabad Univ., India) Jan. 1990 10 p
(DE90-627164; IC-90/14) Avail: NTIS (US Sales Only) HC A02/MF A01

An elementary proof is given for continuity of the determinant in the parameter for a smooth family of laplacians (of the same nullity) on a smooth family of holomorphic vector bundles over a compact complex manifold. Families of unitary flat bundles over a compact Riemann surface are discussed, as an example. DOE

N90-29149# Centro Brasileiro de Pesquisas Fisicas, Rio de Janeiro.
GEOMETRICAL PROPERTIES OF AN INTERNAL LOCAL OCTONIONIC SPACE IN A NON-RIEMANNIAN MANIFOLD
Sirley Marques-Bonham 1989 22 p Submitted for publication Sponsored in part by Foundation for Research of Rio de Janeiro, Brazil
(DE90-627175; CBPF-NF-030/89; ISSN-0029-3865) Avail: NTIS (US Sales Only) HC A03/MF A01

A geometrical treatment on a flat tangent space local to a generalized complex, quaternionic, and octonionic space-time is summarized. DOE

N90-29150# Centro Brasileiro de Pesquisas Fisicas, Rio de Janeiro.
ON THE ZETA-FUNCTION REGULARIZATION OF CHIRAL JACOBIANS FOR SINGULAR DIRAC OPERATORS
C. E. I. Carneiro, M. T. Thomas (Universidade Federal Fluminense, Niteroi, Brazil), and S. A. Dias 1989 25 p Submitted for publication Sponsored in part by CNPq, Brazil and Foundation for Research of Rio de Janeiro, Brazil
(DE90-627176; CBPF-NF-037/89; ISSN-0029-3865) Avail: NTIS (US Sales Only) HC A03/MF A01

A definition of the chiral Jacobian which uses the invariance of the generating functional under chiral rotarions is proposed. This definition takes into account the contributions of all terms which after the rotation, get a dependence on the chiral parameter alpha. It is shown that, when the Dirac operator has zero eigenvalues the presence of fermionic sources gives an additional dependence on alpha. The proposed definition, by considering this alpha-dependence, reconciles the zeta-function method of calculating chiral Jacobians with Fujikawa's. DOE

N90-29151# Centro Brasileiro de Pesquisas Fisicas, Rio de Janeiro.
CASIMIR EFFECT IN A D-DIMENSIONAL FLAT SPACETIME AND THE CUT-OFF METHOD
N. F. Svaiter and B. F. Svaiter (Universidade Federal do Rio de Janeiro, Brazil) 1989 23 p Submitted for publication Sponsored in part by CNPq, Brazil
(DE90-627177; CBPF-NF-050/89; ISSN-0029-3965) Avail: NTIS (US Sales Only) HC A03/MF A01

The Casimir effect in a D-dimensional spacetime produced by a Hermitian massless scalar field in the presence of a pair of perfectly reflecting parallel flat plates is discussed. The exponential cut-off regularization method is employed. The regularized vacuum energy and the Casimir energy of this field are evaluated and a detailed analysis of the divergent terms in the regularized vacuum energy is carried out. The two-dimensional version of the Casimir effect is discussed by means of the same cut-off method. A comparison between the above method and the zeta function regularization procedure is presented in a way which gives the unification between these two methods in the present case. DOE

N90-29152# Centro Brasileiro de Pesquisas Fisicas, Rio de Janeiro.
DIRAC'S EQUATION AS A GEODESIC IN RIEMANN SPACE
J. Leite Lopes (Centre de Recherches Nucleaires, Strasbourg, France) 1989 10 p Submitted for publication
(DE90-627194; CBPF-NF-048/89) Avail: NTIS (US Sales Only) HC A02/MF A01

Dirac's equation is derived from a geometrical variational principle which involves a line-element matrix in flat space (for a free fermion and for a fermion in interaction with a gauge field) or in a Riemann space (for a fermion in interaction with the spinor connection, the gauge field of the local Lorentz group). DOE

N90-29153# International Centre for Theoretical Physics, Trieste (Italy).
SUPERCONFORMAL ALGEBRA AND CENTRAL EXTENSION OF MEROMORPHIC VECTOR FIELDS WITH MULTIPOLES ON SUPER-RIEMANN SPHERE
Shi-Kun Wang and Kai-Wen Xu (Zhejiang Univ., China) Dec. 1989 7 p Submitted for publication
(DE90-627211; IC-89/399) Avail: NTIS (US Sales Only) HC A02/MF A01

The superconformal algebras of meromorphic vector fields with

multipoles, the central extension and the relevant abelian differential of the third kind on super Riemann sphere were constructed. The background of the theory is concerned with the interaction of closed superstrings. DOE

N90-29154# International Centre for Theoretical Physics, Trieste (Italy).
TRAJECTORIES OF RENORMALIZATION GROUP FLOWS ON THE PHASE DIAGRAM OF N=2 SUPERCONFORMAL FIELD THEORIES
Kei Ito Dec. 1989 10 p Submitted for publication
(DE90-627212; IC-89/423) Avail: NTIS (US Sales Only) HC A02/MF A01

Trajectories of renormalization group flows of N = 2 super Landau-Ginzburg field theories are mapped out on the phase diagram N = 2 superconformal field theories (SCFTs). It is shown that coupling constants flow on one and the same bifurcation set due to the non-renormalization theorem and the scaling properties of the bifurcation sets. DOE

N90-29155# International Centre for Theoretical Physics, Trieste (Italy).
TOPOLOGY OF SINGULARITIES AND PHASE DIAGRAM OF N=2 SUPERCONFORMAL FIELD THEORIES
Kei Ito Dec. 1989 6 p Presented at the Workshop on Superstrings, Trieste, Italy, 12-14 Jul. 1989 Submitted for publication
(DE90-627213; IC-89/424) Avail: NTIS (US Sales Only) HC A02/MF A01

Relation between chiral primary fields of an N = 2 superconformal model and Milnor monodromy of the corresponding target space singularity is investigated. It is shown that conformal weights of chiral primary fields are identical to one half the difference between spectral numbers and the smallest spectral number. Phase diagram of N = 2 superconformal field theories are mapped out. It is shown that they coincide with bifurcation sets in catastrophe theory. The results are applied to the determination of renormalization group flows triggered by two or more relevant operators. DOE

N90-29156# International Centre for Theoretical Physics, Trieste (Italy).
QUANTUM GRAVITY IN TWO DIMENSIONS AND THE SL(2,R) CURRENT ALGEBRA
Jose A. HelayelNeto, A. William Smith (Centro Brasileiro de Pesquisas Fisicas, Rio de Janeiro.), and Susan Mokhtari Dec. 1989 12 p Submitted for publication Sponsored in part by CNPq, Brazil
(DE90-627215; IC-89/431) Avail: NTIS (US Sales Only) HC A03/MF A01

Gravity coupled to a scalar field in two dimensions is studied and it is shown that in the light-cone gauge there exists a new symmetry associated with the scalar field that leads naturally to SL(2,R)-Kac-Moody current algebra. This algebra is derived from the traceless part of the energy-momentum tensor whose conservation is shown to give the well-known constraint necessary to obtain the chiral SL(2,R) algebra. DOE

N90-29157# International Centre for Theoretical Physics, Trieste (Italy).
ANYONS AND CHERN-SIMONS THEORY ON COMPACT SPACES OF FINITE GENUS
S. Randjbar-Daemi, Abdus Salam (Imperial Coll. of Science and Technology, London, England), and J. A. Strathdee Jan. 1990 8 p Submitted for publication
(DE90-627216; IC-90/11) Avail: NTIS (US Sales Only) HC A02/MF A01

The coupling of an Abelian Chern-Simons field to fermions in space-times of the form R x M(sup 2) is studied, where M(sup 2) is a compact Riemannian manifold. Upon integrating out the non-zero modes of the Chern-Simons field, an effective N-particle Hamiltonian is constructed, which involves a term representing the effects of the zero modes. We also study the transformation to the fractional statistics (anyon) basis. It is shown that unlike the case of the flat Euclidean M(sup 2) the anyon wave equation involves some residual metric dependent interactions, and the wave function is multivalued. DOE

70 PHYSICS (GENERAL)

For precision time and time interval (PTTI) see *35 Instrumentation and Photography;* for geophysics, astrophysics or solar physics see *46 Geophysics, 90 Astrophysics,* or *92 Solar Physics.*

N90-29158# Helsinki Univ. of Technology, Espoo (Finland). Electromagnetics Lab.
CHIRAL MAXWELL-GARNETT MIXING FORMULA
A. H. Sihvola and I. V. Lindell Nov. 1989 11 p
(PB90-189143; ISBN-951-22-0064-3; Rept-55) Avail: NTIS HC A03/MF A01 CSCL 20C

The Maxwell-Garnett mixing formula, previously well-known for dielectric mixtures, is generalized for the first time to cover chiral materials. The mixing formula expresses the permittivity, permeability, and chirality of a two-component mixture with spherical inclusions as functions of the material parameters of the components. The result gives the classical Maxwell-Garnett formula as a special case. GRA

N90-29159# European Space Agency, Paris (France).
SCIENTIFIC COLLOQUIUM IN HONOR OF PROF. DR. RER. NAT. HERMANN L. JORDAN
Peter Hamel, Heinz Winter, Herbert Oertel, Berndt Feuerbacher, Hans Hamacher, Hans Opower, and Ulrich Schumann (Deutsche Forschungsanstalt fuer Luft- und Raumfahrt, Cologne, Germany, F.R.) May 1990 111 p Transl. into ENGLISH of Wissenschaftliches Kolloquim Gewidmet Herrn Professor Dr. Rer. Nat. Hermann L. Jordan zum 65 Geburtstag (Cologne, Fed. Republic of Germany, DFVLR), Jun. 1987 127 p Colloquium held in Cologne, Fed. Republic of Germany, Jun. 1987 Original language document was announced as N88-17432
(ESA-TT-1101; DFVLR-Mitt-87-11; ETN-90-97554) Avail: NTIS HC A06/MF A01

Five scientific contributions presented by institute directors at a scientific colloquium dedicated to Professor Hermann L. Jordan, who retired as chairman of the executive board of the DFVLR (German Aerospace Research Establishment), are presented. The papers were selected to provide an impression of the scientific work performed in the research departments and centers of the DFVLR. Works include energy transmission by means of coherent quasi-monochromatic light beams, microgravity in space, numeric fluids dynamics, and flight test engineering with the ATTAS (Advanced Technologies Testing Aircraft System). For individual titles, see N90-29160 through N90-29163.

N90-29160# European Space Agency, Paris (France).
FLIGHT TEST ENGINEERING WITH THE ATTAS **c01**
Peter Hamel and Heinz Winter (Deutsche Forschungsanstalt fuer Luft- und Raumfahrt, Cologne, Germany, F.R.) *In its* Scientific Colloquium in Honor of Prof. Dr. Rer. Nat. Hermann L. Jordan May 1990 p 10-44 Transl. into ENGLISH from Wissenschaftliches Kolloquim Gewidmet Herrn Professor Dr. Rer. Nat. Hermann L. Jordan zum 65 Geburtstag (Cologne, Fed. Republic of Germany, DFVLR), Jun. 1987 p 9-36 Original language document was announced as N88-17433 (For primary document see N90-29159 23-70)
Avail: NTIS HC A06/MF A01

ATTAS (Advanced Technologies Testing Aircraft System) which is available as technology platform and flying simulator for many research and test projects, predominantly from the field of flight mechanics/flight guidance, into the year 2000, is described. The system engineering of the ATTAS test platform is described and various application programs, which were defined, carried out and evaluated in close collaboration with industrial and official partners

and partly within the framework of international cooperation are discussed. ESA

N90-29161# European Space Agency, Paris (France).
NUMERIC FLUID MECHANICS **c34**
Herbert Oertel (Deutsche Forschungsanstalt fuer Luft- und Raumfahrt, Cologne, Germany, F.R.) *In its* Scientific Colloquium in Honor of Prof. Dr. Rer. Nat. Hermann L. Jordan May 1990 p 45-68 Transl. into ENGLISH from Wissenschaftliches Kolloquim Gewidmet Herrn Professor Dr. Rer. Nat. Hermann L. Jordan zum 65 Geburtstag (Cologne, Fed. Republic of Germany, DFVLR), Jun. 1987 p 37-55 Original language document was announced as N88-17434 (For primary document see N90-29159 23-70)
Avail: NTIS HC A06/MF A01

An introduction into the variety of solutions of the fluid-mechanical model equations is presented. The question of whether the nonlinear interactions of a few modes can describe the transition to turbulent flows and thus open an access to transition and turbulence modeling is discussed. The utilization of numeric methods for practical application in the calculation of transonic wings of commercial aircraft and for the aerodynamic design of re-entry vehicles is presented. ESA

N90-29162# European Space Agency, Paris (France).
MICROGRAVITATION EXPERIMENTS IN SPACE: COMPATIBILITY WITH INTERFERING DYNAMIC INFLUENCES **c29**
Berndt Feuerbacher and Hans Hamacher (Deutsche Forschungsanstalt fuer Luft- und Raumfahrt, Cologne, Germany, F.R.) *In its* Scientific Colloquium in Honor of Prof. Dr. Rer. Nat. Hermann L. Jordan May 1990 p 69-89 Transl. into ENGLISH from Wissenschaftliches Kolloquim Gewidmet Herrn Professor Dr. Rer. Nat. Hermann L. Jordan zum 65 Geburtstag (Cologne, Fed. Republic of Germany, DFVLR), Jun. 1987 p 57-71 Original language document was announced as N88-17435 (For primary document see N90-29159 23-70)
Avail: NTIS HC A06/MF A01

An attempt to establish a relationship between the sensitivity of experiments to disturbances and the accelerations resulting from the dynamic behavior of the spacecraft is presented. For this purpose, simplified physical model concepts are developed, which describe the general behavior so that trends become detectable and the influences of individual part contribution become transparent. These models are set up for both experiment and system side so that the compatibility of the experiments with a particular space vehicle can be qualitatively determined by a direct comparison. ESA

N90-29163# European Space Agency, Paris (France).
ENERGY TRANSMISSION BY MEANS OF COHERENT QUASI-MONO-CHROMATIC LIGHT BEAMS **c74**
Hans Opower (Deutsche Forschungsanstalt fuer Luft- und Raumfahrt, Cologne, Germany, F.R.) *In its* Scientific Colloquium in Honor of Prof. Dr. Rer. Nat. Hermann L. Jordan May 1990 p 90-110 Transl. into ENGLISH from Wissenschaftliches Kolloquim Gewidmet Herrn Professor Dr. Rer. Nat. Hermann L. Jordan zum 65 Geburtstag (Cologne, Fed. Republic of Germany, DFVLR), Jun. 1987 p 73-89 Original language document was announced as N88-17436 (For primary document see N90-29159 23-70)
Avail: NTIS HC A06/MF A01

Light as a medium for energy transmission is considered. General aspects of the propagation of light are discussed. The generation of coherent light with high radiant energy density and the generation of quasi-monochromatic light into electrical energy at the receiver are examined. A summary of current developments is given. ESA

N90-29164# International Centre for Theoretical Physics, Trieste (Italy).
UNEXPECTED PROPERTIES OF THE CENTRIFUGAL FORCE
Marek A. Abramowicz (Scuola Internazionale Superiore di Studi Avanzati, Trieste, Italy) Jan. 1990 24 p Presented at the Summer Workshop on Particle Physics and Cosmology, Trieste, Italy, Jul. 1989; ICTP Colloquia, Trieste, Italy, Nov. 1989; and Relativity Seminar, Garching, Fed. Republic of Germany, Dec. 1989
(DE90-627197; IC-90/17) Avail: NTIS (US Sales Only) HC A03/MF A01

Contrary to what is stated in the Newtonian dynamics, rotation of a reference frame is not sufficient for the occurrence of the centrifugal force. Instead, the necessary and sufficient condition is a motion along a path different from that of a photon trajectory in space. This calls for a rather fundamental change in understanding of the very nature of the centrifugal force. It also has important practical physical consequences: in a strong gravitational field, where light trajectories are substantially curved, centrifugal force is much weaker than the Newtonian theory predicts. In addition, when there are closed (circular) photon trajectories in space, the centrifugal force may reverse its direction - it attracts towards the rotation axis. The weakening of the centrifugal force in strong gravitational fields and the reversal of its direction in the neighborhood of close photon trajectories in space fully and clearly explain puzzling examples of counter intuitive behavior of dynamical effects of rotation found previously by several authors: e.g., reversal of the ellipticity behavior of the relativistic Maclaurin spheroids (Chandrasekhar and Miller, 1974), reversal of the viscous torque action (Anderson and Lemos, 1988), or the fact that rotation increases internal pressure of a sufficiently compact star (Abramowicz and Wagoner, 1974). Weakening of the centrifugal force implies that rotating neutron stars are less oblate (and probably more stable) than the Newtonian theory predicts. This is important for the recently discussed question of how fast can pulsars spin. DOE

N90-29165# Centro Brasileiro de Pesquisas Fisicas, Rio de Janeiro.
SYSTEMATIC APPROACH TO CRITICAL PHENOMENA BY THE EXTENDED VARIATIONAL METHOD AND COHERENT-ANOMALY METHOD
Naoki Kawashima, Makoto Katori, Constantino Tsallis, and Masuookyo Suzuki (Tokyo Univ., Japan) 1989 24 p Submitted for publication
(DE90-627320; CBPF-NF-038/89; ISSN-0029-3865) Avail: NTIS (US Sales Only) HC A03/MF A01

A general procedure to study critical phenomena of magnetic systems is discussed. It consists of systematic series of Landau-like approximations, Extended Variational Method (EVM), and the coherent-anomaly method (CAM). As for susceptibility, the present method is equivalent to the power-series CAM theory. On the other hand, the EVM gives a set of new approximates for other physical quantities. Applications to d-dimensional Ising ferromagnets are also described. The critical points and exponents are estimated with high accuracy. DOE

71 ACOUSTICS

Includes sound generation, transmission and attenuation. For noise pollution see *45 Environmental Pollution.*

N90-29166* National Aeronautics and Space Administration. Langley Research Center, Hampton, VA.
ANNOYANCE CAUSED BY ADVANCED TURBOPROP AIRCRAFT FLYOVER NOISE: COUNTER-ROTATING-PROPELLER CONFIGURATION
David A. McCurdy Washington Sep. 1990 88 p
(NASA-TP-3027; L-16780; NAS 1.60:3027) Avail: NTIS HC A05/MF A01 CSCL 20A

Two experiments were conducted to quantify the annoyance of people to flyover noise of advanced turboprop aircraft with counter rotating propellers. The first experiment examined configurations having an equal number of blades on each rotor and the second experiment examined configurations having an unequal number of blades on each rotor. The objectives were to determine the effects on annoyance of various tonal characteristics,

and to compare annoyance to advanced turboprops with annoyance to conventional turboprops and turbofans. A computer was used to synthesize realistic, time-varying simulations of advanced turboprop aircraft takeoff noise. The simulations represented different combinations fundamental frequency and tone-to-broadband noise ratio. Also included in each experiment were recordings of 10 conventional turboprop and turbofan takeoffs. Each noise was presented at three sound pressure levels in an anechoic chamber. In each experiment, 64 subjects judged the annoyance of each noise stimulus. Analyses indicated that annoyance was significantly affected by the interaction of fundamental frequency with tone-to-broadband noise ratio. No significant differences in annoyance between the advanced turboprop aircraft and the conventional turbofans were found. The use of a duration correction and a modified tone correction improved the annoyance prediction for the stimuli. Author

N90-29167# Composite Industriel, Cadenet (France).
LARGE HYDRODYNAMIC TUNNEL: CALCULATION OF THE ACOUSTIC TRANSPARENCY OF THE JET STREAM [GRAND TUNNEL HYDRODYNAMIQUE: CALCUL DE LA TRANSPARENCE ACOUSTIQUE DE LA VEINE]
Andre Manson 20 Sep. 1989 66 p In FRENCH
(Contract DRET-88-1023)
(Rept-89/115; ETN-90-97487) Avail: NTIS HC A04/MF A01

The purpose of the study is the calculation of the acoustic transparency of the ALTUGLAS jet stream of the large hydrodynamic tunnel. The finite element method and the plane two dimensional hypothesis are used. The results show that the acoustic transparency efficiency occurs for a wall thickness of about 30 mm and frequencies lower than 1300 Hz. Solutions for improving the acoustic transparency are proposed. ESA

N90-29168# Scripps Institution of Oceanography, San Diego, CA. Marine Physical Lab.
LARGE APERTURE ACOUSTIC ARRAYS IN SUPPORT OF REVERBERATION STUDIES Final Report
John A. Hildebrand Apr. 1990 21 p
(Contract N00014-89-J-1935)
(AD-A224002; MPL-U-20/90) Avail: NTIS HC A03/MF A01 CSCL 17/1

In preparation for a major field experiment this report addresses the development of acoustic arrays which are needed in order to make carefully controlled and well-documented measurements of bottom reverberation. The purpose of these measurements is to study the physics of the backscattering process and to quantify backscattering characteristics as a function of physically meaningful parameters (e.g., ensonified area, grazing angle, bottom material properties, bottom roughness, etc.). Specific array systems which are addressed include the following: (1) towed horizontal array, (2) horizontal and vertical array, (3) ship-tethered 64-element vertical array, and (4) self-contained, 16-element vertical array. GRA

N90-29169*# Lockheed Engineering and Sciences Co., Hampton, VA.
VIBRATION RESPONSES OF TWO HOUSE STRUCTURES DURING THE EDWARDS AIR FORCE BASE PHASE OF THE NATIONAL SONIC BOOM PROGRAM
Harvey H. Hubbard Aug. 1990 58 p
(Contract NAS1-19000)
(NASA-CR-182089; NAS 1.26:182089) Avail: NTIS HC A04/MF A01 CSCL 20A

The data are reproduced from NSBEO-1-67, which contains some preliminary results of the test program, and from NASA-Langley working papers 259 and 288 which are now out of print. Included are sample acceleration and strain recordings from F-104, B-58, and XB-70 sonic boom exposures, along with tabulations of the maximum acceleration and strain values measured for each one of about 130 flight tests. These data are compared with similar measurements for engine noise exposures of the building during simulated landing approaches and takeoffs of KC-135 aircraft. Author

72 ATOMIC AND MOLECULAR PHYSICS

Includes atomic structure, electron properties, and molecular spectra.

N90-29170# Oak Ridge National Lab., TN.
FIFTEENTH INTERNATIONAL CONFERENCE ON X RAY AND INNER-SHELL PROCESSES
1990 354 p Conference held in Knoxville, TN, 9-13 Jul. 1990 Prepared in cooperation with Tennessee Univ., Knoxville, TN and Georgia State Univ., Atlanta, GA
(Contract DE-AC05-84OR-21400)
(DE90-013024; ORNL/M-1206-Vol-1; CONF-900757-Vol-1-Absts) Avail: NTIS HC A16/MF A02

Abstracts are presented from invited papers presented at X-90, the fifteenth annual international conference on X ray and Inner-Shell Processes. DOE

N90-29171# University of Western Michigan, Kalamazoo.
CORRELATED CHARGE CHANGING ION-ATOM COLLISIONS
E. M. Bernstein and J. A. Tanis Feb. 1990 17 p
(Contract DE-FG02-87ER-13778)
(DE90-014662; DOE/ER-13778/3) Avail: NTIS HC A03/MF A01

Fundamental atomic interactions of collisions of highly charged projectiles with neutral targets were investigated, with a particular emphasis on two-electron interactions. Inner-shell processes involving excitation, ionization, and charge transfer are investigated using, for the most part, coincidence techniques in which projectile charge-changing events are associated with x ray emission, target recoil ions, or electron emission. Measurements were conducted using accelerators at the Lawrence Berkeley Laboratory (LBL), Argonne National Laboratory (ANL), Hahn-Meitner-Institut, Berlin (HMI), and Western Michigan University (WMU). DOE

73 NUCLEAR AND HIGH-ENERGY PHYSICS

Includes elementary and nuclear particles; and reactor theory.

For space radiation see *93 Space Radiation.*

N90-29172# Rockwell International Corp., Canoga Park, CA. Rocketdyne Div.
HELIUM GENERATION IN FUSION REACTOR MATERIALS Final Report, 15 Sep. 1987 - 31 Mar. 1989
D. W. Kneff and B. M. Oliver May 1990 12 p
(Contract DE-FG03-87ER-52146)
(DE90-013005; DOE/ER-52146/T1) Avail: NTIS HC A03/MF A01

An analysis was made of the multiple-step helium production mechanism discovered in iron following long term mixed-spectrum reactor exposure, the measurement of a large number of samples irradiated in fast-neutron environments for cross section determinations, the initial mapping of the neutron fluence distribution for a high fluence T(d,n) irradiation experiment, the initial measurements of helium production in materials irradiated by 10-MeV neutrons, and the initiation of a joint experiment with ANL to measure the spectrum-integrated Be(n,2n) cross section at lower neutron energies. DOE

N90-29173# Sandia National Labs., Albuquerque, NM. Dept. of Fluid and Thermal Sciences.
THE AFFECT OF GRAVITY ON PARTICLE COLLECTION IN INERTIAL IMPACTORS
V. A. Marple, B. A. Olson (Minnesota Univ., Minneapolis.), and D. J. Rader 1990 4 p Presented at the 3rd International Aerosol Conference, Kyoto, Japan, 24-27 Sep. 1990
(Contract DE-AC04-76DP-00789)
(DE90-013372; SAND-90-1795C; CONF-9009136-2) Avail: NTIS HC A01/MF A01

Gravitational forces were found to be an important factor in

defining the particle collection efficiency curve of inertial impactors for large particles. In general it was found that if the parameter (cftx G) = gW/V(sub 0)(exp 2) (g is the gravitational acceleration, W is the nozzle diameter and V(sub 0) is the average fluid velocity at the nozzle throat) in greater than 10(exp -3), the efficiency curve would shift to lower particle sizes. No effect could be seen for lower values of (cftx G). DOE

N90-29174# Tufts Univ., Medford, MA. Dept. of Physics and Astronomy.
HIGH ENERGY PHYSICS AT TUFTS UNIVERSITY Progress Report, 16 Jul. 1989 - 15 Jul. 1990
R. H. Milburn 15 Jul. 1990 109 p
(Contract DE-AC02-83ER-40085)
(DE90-014664; DOE/ER-40085/21) Avail: NTIS HC A06/MF A01

The high energy physics program is discussed. Some topics are: Soudan II nucleon decay project; neutrino studies; pion and kaon production of charm and charm-strange states; study of heavy flavors at the tagged particle spectrometer; physics at the antiproton-proton collider; planning for physics at the supercollider; and computing and networking. DOE

N90-29175# Los Alamos National Lab., NM.
MOESSBAUER EFFECT APPLICATIONS USING INTENSE RADIOACTIVE ION BEAMS
R. D. Taylor 1990 4 p Presented at the Workshop on the Science of Intense Radioactive Ion Beams, Los Alamos, NM, 10-12 Apr. 1990 Submitted for publication
(Contract W-7405-eng-36)
(DE90-014981; LA-UR-90-2580; CONF-9004209-4) Avail: NTIS HC A01/MF A01

The Moessbauer Effect is reviewed as a promising tool for a number of new solid state studies when used in combination with radioactive beam/implantation facilities. The usual Moessbauer Effect involves long lived radioactive parents (days to years) that populate low-lying nuclear excited states that subsequently decay to the ground state. Resonant emission/absorption of recoil-free gamma rays from these states provide information on a number of properties of the host materials. Radioactive ion beams (RIB) produced on-line allow new Moessbauer nuclei to be studied where there is no suitable parent. The technique allows useful sources to be made having extremely low local concentrations. The ability to separate the beams in both Z and A should provide high specific activity conventional sources, a feature important in some applications such as Moessbauer studies in diamond anvil high pressure cells. Exotic chemistry is proposed using RIB and certain Krypton and Xenon Moessbauer isotopes. DOE

N90-29176# Fermi National Accelerator Lab., Batavia, IL.
BEAM DIAGNOSTICS IN CIRCULAR MACHINES: REVIEW OF NEW DEVELOPMENTS
G. Jackson Jun. 1990 5 p Presented at the 2nd European Particle Accelerator Conference, Nice, France, 11-16 Jun. 1990
(Contract DE-AC02-76CH-03000)
(DE90-014986; FNAL/C-90/122; CONF-900603-28) Avail: NTIS HC A01/MF A01

Recent developments in beam diagnostic equipment and measurement techniques have been driven by commercial technological advances, better data analysis algorithms, and the need to measure complex beam properties. The need for such developments is due to the increased diversity, beam intensity, and luminosity/brightness requirements of charged particle circular accelerators. In addition, the advent of fast analog-to-digital converters and cheap, powerful microprocessors have fundamentally changed the approach to beam diagnosis, allowing designers to create systems where signal processing is performed locally at each detector. New beam monitors from a wide variety of circular accelerators are reviewed. A number of interesting or innovative ideas are presented in detail. DOE

N90-29177# Sandia National Labs., Albuquerque, NM. Pulsed Power Theory Div.
CHARACTERIZATION OF ELECTRON FLOW IN POSITIVE-POLARITY LINEAR-INDUCTION ACCELERATORS
S. E. Rosenthal 1990 9 p Presented at the International Symposium on Discharges and Electrical Insulation in Vacuum, Santa Fe, NM, 17-20 Sep. 1990
(Contract DE-AC04-76DP-00789)
(DE90-014998; SAND-90-1923C; CONF-9009192-5) Avail: NTIS HC A02/MF A01

Experiments at Sandia National Laboratories have studied the operation of the linear-induction accelerators, HELIA and Hermes 3, in positive polarity. These experiments have provided a unique opportunity to explore the consequences of multiple-cathode electron emission in magnetically insulated transmission lines. An examination of the total energy-canonical momentum distribution of the electrons explains the features of the magnetically insulated flow exhibited by these systems. Simple analysis based on the basic concept of pressure balance, in conjunction with particle-in-cell numerical simulations, shows how the line voltage is related to the anode and cathode currents. Two flow designations are introduced that can apply to multiple-cathode magnetically insulated transmission lines: full-gap flow (FGF), and locally emitted flow (LEF). DOE

N90-29178# Stanford Linear Accelerator Center, CA.
RF POWER GENERATION FOR FUTURE LINEAR COLLIDERS
W. R. Fowkes, M. A. Allen, R. S. Callin, G. Caryotakis, K. R. Eppley, K. S. Fant, Z. D. Farkas, J. Feinstein, K. Ko, and R. F. Koontz et al Jun. 1990 8 p Presented at the 8th International Conference on High-power Particle Beams, Novosibirsk, USSR, 2-5 Jul. 1990
(Contract DE-AC03-76SF-00515)
(DE90-014804; SU-SLAC-PUB-5282; CONF-9007111-13) Avail: NTIS HC A02/MF A01

The next linear collider will require 200 MW of RF power per meter of linac structure at relatively high frequency to produce an accelerating gradient of about 100 MV/m. The higher frequencies result in a higher breakdown threshold in the accelerating structure hence permit higher accelerating gradients per meter of linac. The lower frequencies have the advantage that high peak power RF sources can be realized. An 11.42 GHz appears to be a good compromise and the effort at the Stanford Linear Accelerator Center (SLAC) is being concentrated on RF sources operating at this frequency. The filling time of the accelerating structure for each RF feed is expected to be about 80 ns. Under serious consideration at SLAC is a conventional klystron followed by a multistage RF pulse compression system, and the Crossed-Field Amplifier. These are discussed. DOE

N90-29179# Stanford Linear Accelerator Center, CA.
EFFECTS AND TOLERANCES OF INJECTION JITTER IN THE SLC AND FUTURE LINEAR COLLIDERS
T. Limberg, J. T. Seeman, and W. L. Spence May 1990 3 p Presented at the 2nd European Particle Accelerator Conference, Nice, France, 12-16 Jun. 1990
(Contract DE-AC03-76SF-00515)
(DE90-014805; SU-SLAC-PUB-5276; CONF-900603-29) Avail: NTIS HC A01/MF A01

The bunch injected into the main linac of a linear collider may have offsets in transverse angle and position, may have a phase error (longitudinal position offset) and, furthermore, may be optically mismatched. Each of these injection errors reduces the luminosity and must be held within tolerances. The effect of optical mismatches on the emittance at the end of the linac is calculated analytically. The tightest tolerances on magnetic elements stemming from these effects are listed. The phase tolerance is determined by the energy acceptance of the final focus system. It imposes tolerances to the integrated field strength of the damping ring and RTL bending magnets and the bunch compressor RF-phase. In this paper, measurements of injection jitter and the effect of betatron oscillations caused by changes of the angle or position of the incoming beam are described. These measurements

were taken with BNS damping which relaxes certain tolerances by an order of magnitude. The injection jitter tolerances for a linac of the next generation are given. As an example, parameters for the Next Linear Collider (NLC) being designed at SLAC are used. DOE

74 OPTICS

Includes light phenomena; and optical devices.
For lasers see *36 Lasers and Masers.*

N90-29180*# Illinois Univ., Chicago. Dept. of Electrical Engineering and Computer Science.
THEORY OF BIAXIAL GRADED-INDEX OPTICAL FIBER
Stephen F. Kawalko and Piergiorgio L. E. Uslenghi 1990 27 p (Grant NAG2-544)
(NASA-CR-186977; NAS 1.26:186977) Avail: NTIS HC A03/MF A01 CSCL 20F

The problem of wave propagation in a biaxial graded-index fiber with circular symmetry is considered. The problem is formulated in terms of four first-order differential equations for the tangential components of the electric and magnetic fields. A general solution method for solving systems of differential equations is presented. This solution method is then used to solve the system of equations for a particular example of a biaxial graded-index fiber. Numerical results for the propagation constant in the fiber are also given. Author

N90-29181# Mitre Corp., McLean, VA. JASON Program Office.
SOME NOVEL SOURCES OF X RAY BEAMS: CHANNELING, TRANSITION AND CHERENKOV RADIATION
Norval Fortson Mar. 1990 15 p
(Contract DE-AI01-88ER-30142)
(DE90-014442; DOE/ER-30142/T1; JSR-87-301-A) Avail: NTIS (US Sales Only) HC A03/MF A01

Three types of x ray sources are discussed which were investigated as part of a JASON study of novel sources of short wavelength radiation. Other possible sources, such as VUV/XUV Free-Electron Lasers, are discussed in separate reports to DOE. Channeling, transition, and Cherenkov radiation produced by fast electron or positron beams is reviewed. DOE

N90-29182 Institute for Perception RVO-TNO, Soesterberg (Netherlands).
RECOGNITION OF INFRARED IMAGES. PART 3: THE EFFECT OF IMAGE PROCESSING WITH A SIZE-CONTRAST BOX FILTER ON OBSERVATION PERFORMANCE Final Report
B. P. Alblas 9 Oct. 1989 38 p In DUTCH; ENGLISH summary
(Contract R87/KL/094)
(IZF-1989-39; TD-89-4141; ETN-90-97396) Copyright Avail: Inst. for Perception RVO-TNO, P.O. Box 23, 3769 ZG Soesterberg, Netherlands

The size-contrast box filter (which incorporates contrast and expected size of the target) was used in the detection of military targets in infrared images in order to distinguish clutter from targets and to increase the observation performance. The percentage of detected targets by the computer was between 65 and 93 percent, the percentage of false alarms between 14 and 40 percent. All the images were marked with one or two cues (arrows) at the most probable occupied position(s). The effect of cueing is very significant. The type of algorithm and the number of cues has no effect. On average the detection score increased by 20 percent and the percentage of false alarms decreased by 60 percent. These improvements are maintained, when after performing the runs with cueing, the cues were left out. The human observer supported by cueing appeared to always perform much better than the computer with respect to false alarms. ESA

N90-29183 Physics and Electronics Lab. TNO, The Hague (Netherlands).
APPLICATION OF INTEGRATED OPTICAL COMPONENTS IN OPTICAL FIBER COMMUNICATION Final Report
J. L. Joppe Sep. 1989 47 p In DUTCH; ENGLISH summary
(FEL-89-B252; TD-89-3572; ETN-90-97409) Copyright Avail: Physics and Electronics Lab. TNO, P.O. Box 96864, 2509 JG The Hague, Netherlands

Developments in optical fiber communication systems and possible applications of integrated optical components are described. Some concepts of optical communication are explained. The systems characteristics and the properties of the components of the three generations of optical communication are outlined. Coherent optical communication systems and their components are described, and the important role of integrated optics in this detection technique is pointed out. Some present and future commercial applications of optical communication and the contribution of integrated optics are presented. The present and possible future role of integrated optics in optical communication is summarized. ESA

N90-29184# Los Alamos National Lab., NM.
VELOCITY INTERFEROMETER SYSTEM FOR ANY REFLECTOR (VISAR): DISPLACEMENT MODE DATA REDUCTION
W. F. Hemsing 1990 11 p Presented at the SPIE's International Symposium on Optical and Optoelectronic Applied Science and Engineering Exhibit, San Diego, CA, 8-13 Jul. 1990
(Contract W-7405-eng-36)
(DE90-015027; LA-UR-90-2321; CONF-900756-15) Avail: NTIS HC A03/MF A01

A Velocity Interferometer System for Any Reflector (VISAR) is a laboratory tool that measures high velocities by continuously measuring the Doppler shift of laser light reflected from a moving surface. It produces lower output frequencies than a displacement interferometer in which Doppler-shifted laser light from a moving target is mixed with unshifted laser light. To obtain lower frequencies, a VISAR employs a wide-angle Michelson interferometer with a time delay in one leg. Undelayed and delayed light rays are thus mixed to detect the relatively small difference between two Doppler shifts produced by accelerating motion at two slightly different velocities. In most VISAR data reduction programs, the velocity is assumed to be proportional to the interferometer fringe count at any instant. This yields velocity details that are inaccurate over the interferometer delay time. The signal time resolution was shorter than the interferometer delay. A data reduction method that uses the displacement information in suitable VISAR signals to recover velocity features that occur during the interferometer delay. DOE

N90-29185# California Univ., Berkeley. Lawrence Berkeley Lab. Accelerator and Fusion Research Div.
STATUS OF THE ADVANCED LIGHT SOURCE
J. N. Marx Jun. 1990 10 p Presented at the SPIE's International Symposium on Optical and Optoelectronic Applied Science and Engineering Exhibit, San Diego, CA, 8-13 Jul. 1990
(Contract DE-AC03-76SF-00098)
(DE90-015636; LBL-28200; CONF-900756-19) Avail: NTIS HC A02/MF A01

The Advanced Light Source (ALS), now under construction at the Lawrence Berkeley Laboratory, will be a national user facility for the production of high-brightness and partially coherent soft x ray and ultraviolet synchrotron radiation. The ALS is based on a low-emittance electron storage ring optimized for operation at 1.5 GeV with insertion devices in 10 long straight sections and 24 premier bend-magnet ports. High-brightness photon beams, from less than 10 eV to more than 2 keV, will be produced by undulators, thereby providing many research opportunities in materials and surface science, biology, atomic physics and chemistry. Wigglers and bend magnets will provide high-flux, broad-band radiation at energies to 10 keV. DOE

N90-29186# Naval Postgraduate School, Monterey, CA. Dept. of Electrical and Computer Engineering.
NEAR-ANGLE SCATTERING AND BINARY OPTICS M.S. Thesis
Larry Vernon Chizek Dec. 1989 126 p
(AD-A224140) Avail: NTIS HC A07/MF A01 CSCL 20/6

The research objective was to measure near-angle scattering (i.e., scattering less than one degree from the specular beam) from a binary optic and determine if a scalar scattering theory could adequately predict scattering performance. Near-angle scattering was measured from a binary optic beam splitter. A scalar scattering theory was developed and modeled using FORTRAN on a personal computer; results from the computer simulation are compared to the actual measurements. The scalar scattering theory modifies Fraunhofer diffraction by including two types of surface topography which contribute to the scattering, specifically: (1) surface roughness due to micro-irregularities which are considered to be randomly distributed, and (2) large scale surface features (i.e., the binary step pattern) which are deterministic. The random surface roughness, the autocorrelation length of the roughness, and the height of the binary optic's pattern were determined using a talystep surface profilometer. The scalar theory appears to give good results when compared to the measurements. However, higher values were required for the surface roughness and autocorrelation lengths than the talystep indicated, which may be due to the talystep's short scan length. Military and space applications for binary optics are also discussed. GRA

N90-29163# European Space Agency, Paris (France).
ENERGY TRANSMISSION BY MEANS OF COHERENT QUASI-MONO-CHROMATIC LIGHT BEAMS
Hans Opower (Deutsche Forschungsanstalt fuer Luft- und Raumfahrt, Cologne, Germany, F.R.) *In its* Scientific Colloquium in Honor of Prof. Dr. Rer. Nat. Hermann L. Jordan May 1990 p 90-110 Transl. into ENGLISH from Wissenschaftliches Kolloquim Gewidmet Herrn Professor Dr. Rer. Nat. Hermann L. Jordan zum 65 Geburtstag (Cologne, Fed. Republic of Germany, DFVLR), Jun. 1987 p 73-89 Original language document was announced as N88-17436 (For primary document see N90-29159 23-70)
Avail: NTIS HC A06/MF A01

75 PLASMA PHYSICS

Includes magnetohydrodynamics and plasma fusion.
For ionospheric plasmas see *46 Geophysics*. For space plasmas see *90 Astrophysics*.

N90-29187# General Atomic Co., San Diego, CA.
PHYSICS OF THE L TO H TRANSITION IN DIII-D
H. Matsumoto, K. H. Burrell, T. N. Carlstrom, P. Gohil, R. J. Groebner, M. A. Mahdavi, T. H. Osborne, E. J. Doyle, T. Lehecka, and N. C. Luhmann, Jr. (California Univ., Los Angeles.) et al Jun. 1990 6 p Presented at the 17th European Conference on Controlled Fusion and Plasma Heating, Amsterdam, Netherlands, 25-29 Jun. 1990
(Contract DE-AC03-89ER-51114)
(DE90-014120; GA-A-20081; CONF-900602-20) Avail: NTIS HC A02/MF A01

A decrease in the edge magnetic and density fluctuations is always seen at the L-H transitions in DIII-D. Although H-mode is best known for an increase in energy confinement, in fact, the reduction in the edge fluctuations is one of the most reliable indicators of the L-H transition. In DIII-D, a sudden change of the perpendicular rotation, V (perpendicular) in the edge was also observed at the transition. Recently, theories that fluctuations are reduced by sheared poloidal flow were proposed to link these two observations. Also, a theory to explain the mechanism responsible for the observed poloidal flow was proposed. Experimental observations are thus far consistent with these theories. DOE

N90-29188# Texas Univ., Austin. Inst. for Fusion Studies.
TEMPERATURE-GRADIENT INSTABILITY INDUCED BY CONDUCTING END WALLS
H. L. Berk, D. D. Ryutov, and Yu. A. Tsidulko (Academy of Sciences, USSR, Novosibirsk) Apr. 1990 27 p
(Contract DE-FG05-80ET-53088)
(DE90-014334; DOE/ET-53088/431; IFSR-431) Avail: NTIS HC A03/MF A01

A new rapidly growing electron temperature gradient instability is found for a plasma in contact with a conducting wall. The linear instability analysis is presented and speculations are given for its nonlinear consequences. This instability illustrates that conducting walls can produce effects that are detrimental to plasma confinement. This mode should be of importance in open-ended systems including astrophysical plasmas, mirror machines and at the edge of tokamaks where field lines are open and are connected to limiters or divertors. DOE

N90-29189# Massachusetts Inst. of Tech., Cambridge. Plasma Fusion Center.
COMBINED ELECTRON CYCLOTRON RAY TRACING AND TRANSPORT CODE STUDIES IN THE COMPACT IGNITION TOKAMAK
P. T. Bonoli, R. C. Englade, M. Porkolab, and A. H. Kritz (Hunter Coll., New York, NY.) 1990 4 p Presented at the 17th European Conference on Controlled Fusion and Plasma Heating, Amsterdam, Netherlands, 25-29 Jun. 1990
(Contract DE-FG02-84ER-53187)
(DE90-014097; CONF-900602-17) Avail: NTIS HC A01/MF A01

The Compact Ignition Tokamak (CIT) operating scenario is envisaged to consist of a start-up phase in which the toroidal magnetic field (B sub T), plasma current (i sub P) and central electron density (n sub e 0) are simultaneously ramped, followed by a burn cycle and a ramp down cycle. Electron cyclotron radio frequency (ECRF) power at fixed frequency is ideally suited to heating during the ramp up phase of CIT. The angle of injection of the incident microwave beam can be varied as the toroidal field is ramped, so as to maintain central RF-power deposition. Furthermore, since the EC wave is a propagating mode in vacuum, relatively high power densities can be easily coupled into a compact device. Finally, it is noted that recent advances in source technology makes ECR heating at (280 to 310) GHz a viable option. In order to realistically simulate this ramp up scenario, a combined code was developed in which ECRF ray tracing and absorption, and MHD equilibrium calculation, and thermal and particle transport are treated self-consistently. Previous studies of electron cyclotron resonance heating in CIT were carried out using model profiles of RF absorption based on stand-alone ray tracing and absorption calculations. In addition, these studies held the plasma current, toroidal magnetic field, and density constant in time. Herein, a time variation in these plasma quantities is imposed and ECRF power deposition is re-calculated during RF injection so as to more realistically and self-consistently simulate ECH-assisted start-up in CIT. The most recent CIT configuration calls for a toroidal field ramp to 11T. Thus, the present studies consider the use of an ECRF source frequency of 308 GHz, with EC waves launched in the ordinary mode of polarization. DOE

N90-29190# Sandia National Labs., Albuquerque, NM.
PBFA 2 APPLIED B ION DIODE BEAM CHARACTERISTICS AT HIGH VOLTAGES
D. J. Johnson, T. R. Lockner, R. S. Coats, T. A. Mehlhorn, W. E. Nelson, G. A. Chandler, M. P. Desjarlais, M. S. Derzon, R. J. Leeper, and J. E. Maenchen et al 1990 6 p Presented at the International Symposium on Discharges and Electrical Insulation in Vacuum, Santa Fe, NM, 17-20 Sep. 1990
(Contract DE-AC04-76DP-00789)
(DE90-014419; SAND-90-1805C; CONF-9009192-4) Avail: NTIS HC A02/MF A01

An applied B-field ion diode was operated at 21 TW on PBFA 2 to study beam generation and transport physics. The radial focusing 15 cm radius diode utilized a pair of magnet coils in disc

cathode structures to produce an axial B-field to minimize electron loss in the 16 mm anode-cathode gaps. The diode was different than used in the past with the cathodes 20 percent closer together and the B-field increased to 3.3 T at the midplane. The 2.5 MA beam originated from a 5 cm tall ion emitting region and was transported toward the axis in a 12.5 cm radius gas cell with 2 micron thick mylar window and a 5 Torr argon gas fill. A surface flashover plasma created by electron loss on wax filled grooves in the anode produced a beam with comparable currents of proton and carbon ions. The experimental results include the spatial uniformity and time dependence of proton and carbon beam emission from the anode and the divergence and focusability of both beams. DOE

N90-29191# Oak Ridge National Lab., TN. Fusion Energy Div.
FORMATION OF MAGNETIC ISLANDS DUE TO FIELD PERTURBATIONS IN TOROIDAL STELLARATOR CONFIGURATIONS
D. K. Lee, J. H. Harris, and G. S. Lee Jun. 1990 27 p
(Contract DE-AC05-84OR-21400)
(DE90-014789; ORNL/TM-11523) Avail: NTIS HC A03/MF A01

An explicit formulation is developed to determine the width of a magnetic island separatrix generated by magnetic field perturbations in a general toroidal stellarator geometry. A conventional method is employed to recast the analysis in a magnetic flux coordinate system without using any simplifying approximations. The island width is seen to be proportional to the square root of the Fourier harmonic of B sup rho/B sup zeta that is in resonance with the rational value of the rotational transform, where B sup rho and B sup zeta are contravariant normal and toroidal components of the perturbed magnetic field, respectively. The procedure, which is based on a representation of 3-D flux surfaces by double Fourier series, allows rapid and fairly accurate calculation of the island widths in real vacuum field configurations, without the need to follow field lines through numerical integration of the field line equations. Numerical results of the island width obtained in the flux coordinate representation for the Advanced Toroidal Facility agree closely with those determined from Poincare puncture points obtained by following field lines. DOE

N90-29192# Oak Ridge National Lab., TN. Fusion Energy Div.
STELLARATOR STATUS, 1989
J. F. Lyon, G. Grieger, F. Rau, A. Iiyoshi, A. P. Navarro, L. M. Kovrizhnykh, O. S. Pavlichenko, and S. M. Hamberger (Australian National Univ., Canberra.) Jul. 1990 40 p
(Contract DE-AC05-84OR-21400)
(DE90-014791; ORNL/TM-11558) Avail: NTIS HC A03/MF A01

The present status of stellarator experiments and recent progress in stellarator research (both experimental and theoretical) are reported by groups in the United States, the USSR, Japan, Australia, and the European Community (the Federal Republic of Germany and Spain). Experiments under construction and studies of large, next-generation stellarators are also described. DOE

N90-29193# Texas Univ., Austin. Inst. for Fusion Studies.
NONLINEAR TEARING MODE: RUTHERFORD REGIME AND GLOBAL CHARACTERISTICS
Y. Z. Zhang, R. Denton, S. M. Mahajan, Chen Jiayu (Academia Sinica, Hefei, China), and A. Wootton Jun. 1990 13 p
(Contract DE-FG05-80ET-53088)
(DE90-015003; DOE/ER-53088/438; DOE/ER-53267/77; IFSR-438; FRCR-373) Avail: NTIS HC A03/MF A01

Experiments on the TEXT tokamak show that the temporal evolution of a single helicity tearing mode is dominated by the Rutherford regime. Further analysis of the Mirnov signal and sawtooth activity combined with numerical simulation emphasizes the global characteristics of the tearing mode. DOE

N90-29194# Instituto de Pesquisas Espaciais, Sao Jose dos Campos (Brazil).
COMPUTERIZED SIMULATION OF PHENOMENA IN PLASMA VIA PARTICLES [SIMULACAO COMPUTACIONAL DE FENOMENOS EM PLASMAS VIA PARTICULAS]
M. V. Alves and J. A. Bittencourt Jun. 1988 68 p In PORTUGUESE; ENGLISH summary
(INPE-4595-RPE/569) Avail: NTIS HC A04/MF A01

The computerized simulation of plasma by particles has become an efficient tool to investigate the time and spatial evolution of various physical phenomena in plasmas. This method is based on the study of the individual plasma particle motions interacting with one another and with the externally applied fields. Although fairly simple, it allows a nonlinear analysis of complex plasma physical phenomena and diagnostics for regions of the system where experimental measurements would be difficult to make. A general view of the electrostatic one-dimensional computer code ES1, is presented. The main mathematical artifice in this code is the use of a spatial grid in which various plasma particles are represented by superparticles, using a given shape function. The principal characteristics of the model, the approximations made, and the mathematical methods used to solve the equations involved, are described. The specification of the input parameters which characterize the system, the initial conditions, and the graphic diagnostics which can be utilized, are also described. Results are presented illustrating graphically the behavior of the plasma oscillations, the two-stream instability, and the beam-plasma instability. Author

N90-29195# Brookhaven National Lab., Upton, NY.
STUDIES OF CENTRAL INTERACTIONS OF Si IONS AT 14.5 X A GeV/c IN Au AND Cu
S. E. Eiseman, A. Etkin, K. J. Foley, R. W. Hackenburg, R. S. Longacre, W. A. Love, T. W. Morris, E. D. Platner, A. C. Saulys, and S. J. Lindenbaum 1990 21 p Presented at the 25th IUPAP International Conference on High Energy Physics, Singapore, 2-8 Aug. 1990 Prepared in cooperation with City Coll., New York, NY; Johns Hopkins Univ., Baltimore, MD; Rice Univ., Houston, TX Sponsored in part by City Univ. of NY Research Award Program
(Contracts DE-AC02-76CH-00016; DE-AC02-83ER-40107; DE-AS05-81ER-40032; DE-AC02-76ER-03274)
(DE90-015095; BNL-44774; CONF-900822-6) Avail: NTIS HC A03/MF A01

Understanding the growth and saturation of parametric instabilities in laser-produced plasmas requires knowledge of the nonlinear properties of the instabilities and their interaction with each other. Nonlinear behavior of parametric instabilities, which are usually associated with unique optical features, were evidenced in numerous experiments on a variety of laser facilities. Four examples of nonlinear behavior in laser-produced plasmas are discussed: nonlinear stimulated Brillouin scattering spectra, suppression of stimulated Raman scattering by stimulated Brillouin scattering, the parametric decay instability and the onset of turbulence, and the transition to bursting behavior of the two-plasmon decay instability. Experiments are discussed that demonstrate the nonlinear effects which occur as a consequence. DOE

N90-29196# Texas Univ., Austin. Inst. for Fusion Studies.
RESONANT MHD MODES WITH TOROIDAL COUPLING
J. W. Connor, R. J. Hastie (United Kingdom Atomic Energy Authority, Abingdon, England), and J. B. Taylor Jul. 1990 14 p
(Contract DE-FG05-80ET-53088)
(DE90-015185; DOE/ET-53088/439; IFSR-439) Avail: NTIS HC A03/MF A01

This is part 2 of a study of resonant perturbations, such as resistive tearing and ballooning modes, in a torus. These are described by marginal ideal MHD equations in the regions between resonant surfaces; matching across these surfaces provides the dispersion relation. Resistive ballooning, or twisting-modes are discussed which have odd-parity in perturbed magnetic field. It is

shown that, unlike the tearing modes, these odd-parity modes are intrinsically toroidal and are not directly related to the odd-parity modes in a cylinder. This is evident from the analysis of the high-n limit in ballooning-space, where a transition from a stable Delta-prime to an unstable Delta-prime occurs for the twisting mode when the ballooning effect exceeds the interchange effect, which can occur even at large aspect ratio (as in a tokamak). Analysis of the high-n limit in coordinate space, rather than ballooning space, clarifies this singular behavior and indicates how one may define twisting-mode Delta-prime. It also yields a prescription for treating low-n twisting modes and a method for calculating an E-matrix for resistive ballooning modes in a large aspect ratio tokamak. The elements of this matrix are given in terms of cylindrical tearing mode solutions. DOE

N90-29197# Massachusetts Inst. of Tech., Cambridge. Plasma Fusion Center.
IGNITION AND BURN CONTROL CHARACTERISTICS OF THERMONUCLEAR PLASMAS Ph.D. Thesis
Emmanouil Antony Chaniotakis 20 Jun. 1990 238 p
(Contract DE-AC02-78ET-51013)
(DE90-015385; DOE/ET-51013/286; PFC/RR-90-11) Avail: NTIS HC A11/MF A02

Achieving the long sought goal of fusion energy requires the attainment of an ignited and controlled thermonuclear plasma. Obtaining an ignited plasma in a tokamak device requires consideration of both the physics of the plasma and the engineering of the machine. With the aid of a completely analytical procedure, optimized and ignited tokamaks are obtained under various physics assumptions. These designs show the possible advantage of tokamaks characterized by high (approximately 4.5) aspect ratio, and high (approximately 15 T) toroidal magnetic field. The control of an ignited plasma is investigated by using auxiliary power modulation. With auxiliary power stable operating points can be created with Q approx. 50. Recognizing the need for a fast 1(1/2)-D transport model for studying profile effects, the plasma transport equations are solved using variational methods. A computer model based on the variational method has been developed. This model solves the 1(1/2)-D transport equation very fast with little loss of accuracy. DOE

N90-29198# Massachusetts Inst. of Tech., Cambridge. Plasma Fusion Center.
TSC (TOKAMAK SIMULATION CODE) SIMULATIONS OF ALCATOR C-MOD DISCHARGES 3: STUDY OF AXISYMMETRIC STABILITY
J. J. Ramos Jun. 1990 34 p
(Contract DE-AC02-78ET-51013)
(DE90-015386; DOE/ET-51013/284; PFC/RR-90-9) Avail: NTIS HC A03/MF A01

The axisymmetric stability of the single X-point, nominal Alcator C-MOD configuration is investigated with the Tokamak Simulation Code. The resistive wall passive growth rate, in the absence of feedback stabilization, is obtained. The instability is suppressed with an appropriate active feedback system. DOE

N90-29199# International Centre for Theoretical Physics, Trieste (Italy).
ELECTRON ACOUSTIC AND MAGNETOACOUSTIC MODES IN A MAGNETIZED BEAM PLASMA SYSTEM
V. K. Jain and N. L. Tsintsadze (Academy of Sciences of the Georgian SSR, Tbilisi.) Jun. 1989 5 p
(DE90-627473; IC-89/150) Avail: NTIS HC A01/MF A01

The dispersion relation characterizing electrostatic nodes in a cold magnetized plasma penetrated by a hot electron beam is solved analytically. In the limit k(sup 2) lambda(sub b)(sup 2) is much greater than 1, where k is the wavenumber of the mode and lambda(sub b) is the Debye length of electron beams, two new modes viz,. electron acoustic and electron magneto-acoustic, are found to exist. Expressions for the growth rate and threshold beam energy are obtained for the kinetic instabilities of these modes. DOE

76 SOLID-STATE PHYSICS

Includes superconductivity.

For related information, see also *33 Electronics and Electrical Engineering* and *36 Lasers and Masers.*

N90-29200# National Inst. of Standards and Technology, Gaithersburg, MD. Applied and Computational Mathematics Div.
NUMERICAL AND ANALYTICAL STUDY OF NONLINEAR BIFURCATIONS ASSOCIATED WITH THE MORPHOLOGICAL STABILITY OF TWO-DIMENSIONAL SINGLE CRYSTALS
L. N. Brush, R. F. Sekerka, and G. B. McFadden Oct. 1989 43 p Prepared in cooperation with Carnegie-Mellon Univ., Pittsburgh, PA
(PB90-209594; NISTIR-89/4193) Avail: NTIS HC A03/MF A01 CSCL 20L

The nonlinear stability of a two-dimensional single crystal of pure material in an under-cooled melt is studied both analytically and numerically. The quasi-steady state approximation is used for the thermal fields and the effects of different solid and liquid thermal conductivities, isotropic interfacial growth kinetics and isotropic surface tension are included. The bifurcation analysis is performed by calculating the instantaneous value of the fundamental component of the local normal growth speed for an interface perturbed by a single Fourier shape component. Numerically, the fundamental component of the interfacial growth speed is found by Fourier shape component. Numerically, the fundamental component of the interfacial growth speed is found by Fourier analysis of the solution to an integro-differential equation obeyed at the interface. Analytically, an expansion technique is used to derive a solvability condition defining each of these bifurcation points. The analytical and numerical results are in very close agreement. Almost all of the bifurcations are subcritical and the authors present their results by giving values of the Landau coefficient as a function of the different dimensionless parameters used in the model. GRA

N90-29201# National Inst. of Standards and Technology, Gaithersburg, MD. Semiconductor Electronics Div.
SEMICONDUCTOR MEASUREMENT TECHNOLOGY: A SOFTWARE PROGRAM FOR AIDING THE ANALYSIS OF ELLIPSOMETRIC MEASUREMENTS, SIMPLE SPECTROSCOPIC MODELS Final Report
J. F. Marchiando Apr. 1990 364 p
(PB90-216847; NIST/SP-400/84) Avail: NTIS HC A16/MF A02; SOD HC $18.00 as 003-003-03002-3 CSCL 20L

MAIN2 is a software program for analyzing spectroscopic ellipsometric measurements. MAIN2 consists mainly of subroutines written in FORTRAN that are used to invert the standard reflection ellipsometry equations for simple systems. Here, a system is said to be simple if the solid material is characterized by models which assume at least the following: (1) materials are nonmagnetic; (2) samples exhibit depth-dependent optical properties, such as one with layered or laminar structure atop a substrate that behaves like a semi-infinite half-space; (3) layers are flat and of uniform thickness; and (4) the optical medium within each ambient/layer/substrate is isotropic, homogeneous, local, and linear. The ambient region refers to that region of space which lies external to the layer/substrate of the sample. Each layer is characterized by a thickness and a dielectric function. The dielectric function of a region, i.e., ambient, layer, or substrate, is represented by the Bruggeman effective medium approximation (EMA). Within the EMA, the effective medium of a region is characterized by an aggregate mixture of constituent media, and the dielectric function of each constituent medium is known a priori. The ellipsometric equations are formulated as a standard damped nonlinear least-squares problem and then solved by an iterative method when possible. The program is sufficiently modular to allow one to modify some of the models used in the calculations. Author

N90-29202# California Univ., Berkeley. Lawrence Berkeley Lab. Materials and Chemical Sciences Div.
ELECTRON MICROSCOPY OF TRANSITION-METAL DOPED BiCaSrCuO M.S. Thesis

Kim Lester Fortunati Apr. 1990 38 p
(Contracts DE-AC03-76SF-00098; MDA972-88-J-1002)
(DE90-014184; LBL-29039) Avail: NTIS HC A03/MF A01

Superconductivity was discovered in 1911 when H. K. Onnes found no electrical resistance in Hg cooled to 4.1 K. Over one thousand additional low temperature superconductors were discovered prior to Bednorz and Muller's discovery of high temperature (40 K) superconductivity in BaLaCuO compounds in March of 1986. This discovery generated much scientific interest in oxide superconductors. Less than one year later the now well known YBaCuO class of superconductors raised the highest known superconducting transition temperature to 90 K, well above the boiling temperature of liquid nitrogen. In the following year, the highest recorded transition temperature was raised to 105 K by the BiCaSrCuO system. This system extended obtainable values of not only transition temperature, but also critical magnetic field, and critical current. The technology of superconductivity is reviewed. DOE

N90-29203# National Inst. of Standards and Technology, Gaithersburg, MD. Semiconductor Electronics Div.
SEMICONDUCTOR MEASUREMENT TECHNOLOGY. EPROP: AN INTERACTIVE FORTRAN PROGRAM FOR COMPUTING SELECTED ELECTRONIC PROPERTIES OF GALLIUM ARSENIDE AND SILICON Final Report
A. C. Seabaugh, J. J. Mathias, and M. I. Bell May 1990 125 p
Prepared in cooperation with Texas Instruments, Inc., Dallas
(PB90-222738; NIST/SP-400/85) Avail: NTIS HC A06/MF A01 CSCL 20L

A new computer program, Electronic PROPerties (EPROP) is presented for use in interpreting measurements and experiments on gallium arsenide and silicon. EPROP computes a solution of the charge balance equation in thermodynamic equilibrium for up to six different impurities. The user supplies the density, energy level, and degeneracy for each impurity, and in response the program returns as many as 28 output parameters, such as the Fermi level, carrier density, and ionized impurity densities. These can be computed as functions of the temperature (or reciprocal temperature) or the density, energy, or degeneracy of any of the six possible impurities. Listings can also be obtained of various temperature-dependent parameters, such as the bandgap, densities of states, and effective masses. The interactive features of the program allow the user to send the output data to any combination of destinations: a terminal, a listing file, and/or up to four graphic output files, all at the user's direction. The user is also given freedom and ability to customize the data output to these destinations through menu-driven controls. GRA

N90-29204# Solarex Corp., Newtown, PA. Thin Film Div.
RESEARCH ON STABLE, LARGE-AREA, AMORPHOUS SILICON BASED SUBMODULES, PHASE 3 Semiannual Subcontract Report, 1 Feb. - 31 Jul. 1989
A. Catalano, R. R. Arya, M. Bennett, B. Fieselmann, B. Goldstein, J. Morris, J. Newton, J. ODowd, R. S. Oswald, and R. Podlesny et al Jul. 1990 98 p Prepared for Solarex Corp., Newtown, PA
(Contracts DE-AC02-83CH-10093; ZB-7-06003-02)
(DE90-000339; SERI/TP-211-3805) Avail: NTIS HC A05/MF A01

This research program encompasses materials research, non-semiconductor materials research, and submodule research. Researchers studied the materials' considerations that limit transport in the a-SiGe:H alloys, and developed alloys with improved properties. These studies indicated that the homogeneity of the alloy plays an important role in determining electronic properties. P-type a-SiC:H films were also prepared using trimethylboron as a dopant. The conductivity of the films was about an order of magnitude better than the comparable bandgap diborane-doped film. This allowed devices with improved voltage (0.943 V) to be demonstrated. Scientists also investigated the optimum device structures for the bottom, a-SiGe:H cell. This study concluded that grading the i-regions is an important element in obtaining the best performance, but the results differ significantly from those reported elsewhere. The results of this study have been incorporated in a number of tandem and triple-junction devices that have resulted in efficiencies in the range of 10 to 11 percent. A laser-scribing process for the highly reflecting ITO/Ag rear contact has enabled the cell results to be transferred to prototype modules with conversion efficiencies between 9 and 10 percent. DOE

N90-29205# Sandia National Labs., Albuquerque, NM.
TWISTED CRYSTALS: PROPAGATION, GENESIS, AND RELATIONSHIPS WITH OPTICAL ACTIVITY AND MOLECULAR SYMMETRY (EXCERPTS)
F. Bernauer 21 Nov. 1989 47 p Transl. into ENGLISH from Forschungen zur Kristallkunde (Berlin, Fed. Republic of Germany), v. 2, 1929 p 1-7 and 57-77
(Contract DE-AC04-76DP-00789)
(DE90-014259; ALS/TR-89-035) Avail: NTIS HC A03/MF A01

With respect to the screw-like twisting of many crystals, Wallerant has already supposed that twisting is related to a structure dissymetrique of the crystals. In accordance with Pasteur's law, such bodies will in general crystallize in enantiomorphic forms and possess at least the possibility of optical activity. In a few cases, Wallerant has observed a direct relationship between the sense of optical rotation of the substance and the twisting direction of the crystals. The research has dealt only with substances that the literature identifies as possessing holohedric symmetry, lacking optical rotatory power, but nonetheless exhibiting twisted forms. At the same time, it was found that the presence of foreign impurities did not just influence the twisting but was its sole cause in many cases. An obvious further step was to relate the screw-shaped deformation of crystals with the far more frequently observed simple curvature; finally, an attempt was made to elucidate the mechanism of curvature or twisting. DOE

N90-29206# Los Alamos National Lab., NM.
ANTIFERROMAGNETISM AND ENHANCED HEAT IN CeM2Sn (M = Ni, Ir, Cu, Rh, Pd, AND Pt
W. P. Beyermann, M. F. Hundley, P. C. Canfield, Z. Fisk, J. L. Smith, J. D. Thompson, C. Godart, and M. Selsane (Centre National de la Recherche Scientifique, Meudon-Bellevue, France) 1990 13 p Presented at the 6th International Conference on Valence Fluctuations, Rio de Janeiro, Brazil, 9-13 Jul. 1990 Submitted for publication
(Contract W-7405-eng-36)
(DE90-014924; LA-UR-90-2363; CONF-900751-2) Avail: NTIS HC A03/MF A01

Recently a new series of compounds was discovered by M. Selsane et al. which has a structure close to CeCu2Si2. Specific heat, dc susceptibility, and resistivity measurements on annealed, polycrystalline samples of CeM2 Sn2 where M = Ni, Ir, Cu, Rh, Pd, or Pt indicate that each of these compounds orders antiferromagnetically with transition temperatures ranging from T(sub N) = 4.1 K to approximately 0.5 K. All these materials have significant enhancements of the specific heat just before the transition which can be as large as approximately 3.7 J/mole-K sq in some cases. Provided the enhanced heat capacities above T(sub N) are associated with large effective masses, the anomalously low ordering temperature and the very large C/T suggest that T(sub N) and the Kondo temperature T(sub K) are comparable, making these materials particularly attractive for studying the interplay between these competing interactions. In all cases except M = Ir, the susceptibility follows a Curie-Weiss behavior with a high temperature effective moment mu(sub eff) approximately 2.54 mu(sub B)/Ce, while the Ir compound has a very strong mixed-valent nature. DOE

N90-29207# Los Alamos National Lab., NM.
EVIDENCE FOR A COHERENCE GAP IN Ce3Bi4Pt3
M. F. Hundley, P. C. Canfield, J. D. Thompson, J. M. Lawrence (California Univ., Irvine.), and Z. Fisk 1990 12 p Presented at the 6th International Conference on Valence Fluctuations, Rio de Janeiro, Brazil, 9-13 Jul. 1990 Submitted for publication

(Contract W-7405-eng-36)
(DE90-014925; LA-UR-90-2362; CONF-900751-1) Avail: NTIS HC A03/MF A01

The physical properties of the f-electron system Ce3Bi4Pt3 is examined. In the majority of cases f-moment compounds are metallic, and, depending upon the relative strength of competing magnetic interactions, have a superconducting, paramagnetic, or antiferromagnetic ground state. In rare instances f-electron compounds have a narrow-gapped insulating ground state instead. This gap is thought to result from hybridization between conduction and f electrons. We have measured the magnetic susceptibility, low temperature specific heat, resistivity, Hall effect, and thermoelectric power was measured of Ce3Bi4Pt3 and this material was found to be non-metallic at all temperatures. Isostructural lanthanum substitution for cerium suppresses the gap and produces transport and thermodynamic behavior that is characteristic of a relatively heavy Kondo impurity system. Further, the energy scale at which coherence develops is roughly equal to the energy gap in this compound. This suggests that the gap in Ce3Bi4Pt3 appears to stem from the same requirements of lattice periodicity necessary for coherence to manifest itself in metallic systems. Hence, there is strong evidence that the insulating behavior displayed by Ce3Bi4Pt3 results from the presence of a Kondo coherence-induced gap. DOE

N90-29208# Sandia National Labs., Albuquerque, NM.
RADIATION EFFECTS IN InAsSb STRAINED-LAYER SUPERLATTICE PHOTODIODES INDUCED BY DOSE-RATE AND TRANSIENT X RAY ENVIRONMENTS
S. R. Kurtz, L. R. Dawson, and J. G. Snyder (Air Force Weapons Lab., Kirtland AFB, NM.) 1990 12 p Presented at the IRIS Specialty Group Meeting on Passive Sensors and Atmospheric Physics, Laurel, MD, 13 Mar. 1990
(Contract DE-AC04-76DP-00789)
(DE90-015000; SAND-90-0955C; CONF-900396-4) Avail: NTIS HC A03/MF A01

A side-by-side measurement was made of the gamma-flux noise in an InAsSb strained-layer superlattice (SLS) photodiode and a comparable HgCdTe photodiode. Correcting for minor differences in detector quantum efficiency and area, it was found that the SLS can operate in a gamma-flux greater than or = 10x that limits HgCdTe detector performance. Transient photoresponse measurements on an InAsSb SLS detector were performed using a pulsed x ray source. A detector recovery time of 150 nsec was observed, and modeling of the transient response predicted a minority carrier lifetime of 350 nsec and a diffusion length of 2 microns. DOE

N90-29209# Florida Univ., Gainesville. Dept. of Physics.
X RAY SCATTERING STUDIES OF NON-EQUILIBRIUM ORDERING PROCESSES Progress Report, 1 Nov. 1989 - 31 Oct. 1990
S. E. Nagler 1990 16 p
(Contract DE-FG05-86ER-45280)
(DE90-015066; DOE/ER-45280/4) Avail: NTIS HC A03/MF A01

The first synchrotron measurements of ordering in Cu3Au have revealed the presence of an intermediate, non-equilibrium ordered state. Preliminary work involving x ray magnetic scattering was carried out. DOE

N90-29210# Technische Hochschule, Darmstadt (Germany, F.R.). Fachbereich Mathematik.
NOVEL NUMERICAL ANALYSIS METHOD FOR THE STUDY OF CONVOLUTION EQUATIONS IN APPEARANCE POTENTIAL SPECTROSCOPY Ph.D. Thesis [ANALYSIS UND NUMERIK EINES NEUEN VERFAHRENS ZUR UNTERSUCHUNG VON FALTUNGSGLEICHUNGEN BEI DER AUFTRITTSPOTENTIALSPEKTROSKOPIE]
Klaus-Thomas Schleicher 1988 80 p In GERMAN
(ETN-90-97288) Avail: NTIS HC A05/MF A01

Nonlinear convolution equations occurring in the experimental determination of state densities in solid state by Appearance Potential Spectroscopy (APS) were mathematically analyzed. Existence, uniqueness, and regularity are discussed. A numerical method was deduced, providing an approximate solution of the convolution equations which converges to the exact solution. The error between exact solution and numerical approximation was estimated. The method demonstrated the calculation of high resolved AP (Appearance Potential) spectra. The investigation of the solution theory led to modifications of the measuring method. The application of the fast Fourier transformation and its simple use make this method suitable for on-line operation. The programming system for the deconvolution of AP spectra, as well as a few numerical examples are presented. ESA

N90-29211# Brookhaven National Lab., Upton, NY.
ELECTRONIC CONDUCTION IN MOLTEN CRYOLITE SATURATED WITH ALUMINA
Geir M. Haarberg, Karen S. Osen, Jomar Thonstad (Trondheim Univ., Norway), Raymond J. Heus, and J. J. Egan 1990 8 p Presented at the 7th International Symposium on Molten Salts, Montreal, Quebec, 6-11 May 1990 Sponsored by Royal Norwegian Council for Scientific and Industrial Research
(Contract DE-AC02-76CH-00016)
(DE90-015090; BNL-43723; CONF-9005235-3) Avail: NTIS HC A02/MF A01

The Wagner polarization technique was used to study the electronic conduction in the melt Na3AlF6 + Al2O3 at 1000 C. Currents were measured at applied potentials lower than the those which would decompose the melt. In this way ionic currents are suppressed and only electronic currents flow. The electronic conductivity is determined from the current versus potential relation. Transient measurements taken on cell (I) yield the diffusion coefficient of electrons in the melt. DOE

N90-29212# Centro Brasileiro de Pesquisas Fisicas, Rio de Janeiro.
CRITICALITY OF THE THREE-STATE CHIRAL CLOCK MODEL: A RENORMALISATION GROUP STUDY
Marcelo L. Martins and Constantino Tsallis 1989 18 p Submitted for publication Sponsored in part by CNPq, Brazil
(DE90-627321; CBPF-NF-039/89; ISSN-0029-3865) Avail: NTIS (US Sales Only) HC A03/MF A01

Within a real space renormalization group approach, the phase diagram and the universality classes of the three-state chiral clock model in a self-dual planar hierarchical lattice are studied. It is found that, the chiral field Delta is relevant at the pure Potts critical point with a crossover exponent phi is approximate or equal to 0.32. The critical line which separates the ferromagnetic phase from the non-ferromagnetic ones is characterized by a multicritical (Lifshitz) point located at (K, delta) is approximate or equal to (1.452, 0.382). The ferromagnetic phase appears to be divided into two regions by a wetting line which is also located numerically. The various critical lines and point of the phase diagram are believed to be excellent approximations for the square lattice. DOE

N90-29213# Centro Brasileiro de Pesquisas Fisicas, Rio de Janeiro.
A GENERALISED HUBBARD HAMILTONIAN: INFLUENCE OF TEMPERATURE AND FRACTALITY
Sergio A. Cannas, Francisco A. Tamarit, and Constantino Tsallis 1989 18 p
(DE90-627322; CBPF-NF-040/89) Avail: NTIS (US Sales Only) HC A03/MF A01

A generalized Hubbard Hamiltonian which is invariant under a Real Space Renormalization Group is considered. Within the present approximation, the Bravais lattice is replaced by a diamond-like hierarchical lattice. The phase diagram associated with the half-filled band Hubbard Hamiltonian in d = 1, 2 and 3, in the full range of the dimensionless intra-atomic interaction U and hopping t parameters is calculated. The influene of the hierarchical lattice fractality is analyzed as well. DOE

N90-29214# Centro Brasileiro de Pesquisas Fisicas, Rio de Janeiro.
Z(6) MODEL: CRITICALITY AND BREAK-COLLAPE METHOD
A. M. Mariz, L. R. daSilva (Universidade Federal do Rio Grande do Norte, Natal, Brazil), A. C. N. deMagalhaes, and Constantino Tsallis 1989 39 p
(DE90-627323; CBPF-NF-041/89) Avail: NTIS (US Sales Only) HC A03/MF A01

The phase diagram and thermal and crossover exponents of the z (6) ferromagnet on the square lattice are calculated within a real-space renormalization group (RG) scheme. The obtained phase diagram (exhibiting 4 phases corresponding to Z (6), Z (3), Z (2) and completely broken symmetries) contains all exactly known critical points, and possibly is an excellent approximation everywhere except in the high-temperature region where a soft phase is expected to appear. However, all the obtained results are exact in the Wheatstone-bridge hierarchical lattice. In addition to these results, an operational procedure (the break-collapse method) which considerably simplifies the exact calculation of two-spin correlation functions for arbitrary Z (6) two-rooted clusters (frequent in RG approaches) is presented. DOE

N90-29215# Centro Brasileiro de Pesquisas Fisicas, Rio de Janeiro.
SUSCEPTIBILITY OF THE POTTS MODEL IN AN HIERARCHICAL LATTICE: RENORMALISATION GROUP APPROACH
Edson dePinhodaSilva and Constantino Tsallis (Universidade Federal do Rio de Janeiro, Brazil) 1989 29 p
(DE90-627324; CBPF-NF-051/89) Avail: NTIS (US Sales Only) HC A03/MF A01

Using a real space renormalization group method, the thermal dependence of the susceptibility of the q-state Potts model (ferro- and antiferromagnet) on self-dual Wheatstone-bridge-like hierarchical lattices is calculated. The influence of external fields on the antiferromagnetic phase diagram is discussed as well. DOE

N90-29216# International Centre for Theoretical Physics, Trieste (Italy).
SUPERCONDUCTIVITY IN MIXED BOSON-FERMION SYSTEMS
L. Ioffe, A. I. Larkin, Yu. N. Ovchinnikov, and L. Yu (Academia Sinica, Beijing, China) Dec. 1989 9 p Submitted for publication
(DE90-627491; IC-89/390) Avail: NTIS (US Sales Only) HC A02/MF A01

The superconductivity of mixed boson-fermion systems is studied using a simple boson-fermion transformation model. The critical temperature of the superconducting transition is calculated over a wide range of the narrow boson band position relative to the Fermi level. The BCS scenario and boson condensation picture are recovered in two limiting cases of high and low positions of boson band, respectively, with modifications due to boson-fermion interaction. DOE

N90-29217# International Centre for Theoretical Physics, Trieste (Italy).
PARITY VIOLATION AND SUPERCONDUCTIVITY IN DOPED MOTT INSULATORS
D. V. Khveshchenko and Ya. I. Kogan (Academy of Sciences, USSR, Moscow) Dec. 1989 45 p Submitted for publication
(DE90-627493; IC-89/427) Avail: NTIS (US Sales Only) HC A03/MF A01

We study parity violating states of strongly correlated two-dimensional electronic systems. On the basis of mean field theory for the SU(2N)-symmetric generalization of the system involved we give the arguments supporting the existence of these states at a filling number different from one-half. We derive an effective Lagrangian describing the long wavelength dynamics of magnetic excitations and their interaction with charged spinless holes. We establish that the ground state of a doped system is superconducting and discuss the phenomenological manifestations of the parity violation. DOE

N90-29218# Centro Brasileiro de Pesquisas Fisicas, Rio de Janeiro.
DYNAMICAL INFORMATION FOR Fe DOPED YBa2Cu3O7 SUPERCONDUCTING OXIDES OBTAINED FROM HIGH TEMPERATURE MOESSBAUER STUDIES
E. Baggio Saitovitch, R. B. Scorzelli, I. Souza Azevedo, and H. Micklitz (Bochum Univ., Germany, F.R.) 1989 26 p Submitted for publication
(DE90-627871; CBPF-NF-028/89) Avail: NTIS (US Sales Only) HC A03/MF A01

In situ high temperature Fe-57 Moessbauer measurements were performed on samples of YBa2Cu(1-x)Fe(x)3O(7-delta), in pure oxygen or in air, both at a pressure of about 1 atm. Three samples were studied with x = 0.005 and 0.010, respectively in the temperature range from 295 to 640 K. As in previously published papers, the fitted quadrupole doublets were associated to different oxygen configurations around the Fe ions on the Cu(1) chain site, whose temperature dependent behavior can be summarized: (1) the f-factor for the different configurations are very similar; (2) the effective Debye temperature (approx. equal 350 K) is rather insensitive to the Fe content and oxygen coordination; (3) the electronic configuration of Fe is very stable up 320 C; and (4) the quadrupole splitting q(T) can be well described within the picture used for non-cubic metals. Finally a partial change from doublet A to B induced by temperatures is observed. This change is completely or partially reversible, depending on the sample. DOE

N90-29219*# National Aeronautics and Space Administration. Lewis Research Center, Cleveland, OH.
XANES AND EXAFS STUDY OF Au-SUBSTITUTED YBa2Cu3O(7-DELTA)
Mark W. Ruckman (Brookhaven National Lab., Upton, NY.) and Aloysius F. Hepp Sep. 1990 11 p Presented at the 4th Annual Conference on Superconductivity and Applications, Buffalo, NY, 18-20 Sep. 1990; sponsored by The New York State Institute on Superconducitivity
(NASA-TM-103291; E-5751; NAS 1.15:103291) Avail: NTIS HC A03/MF A01 CSCL 20L

The near-edge structure (XANES) of the Au L3 and Cu K edges of YBa2Au(0.3)Cu(2.7)O(7-delta) was studied. X ray diffraction suggests that Au goes on the Cu(1) site and XANES shows that this has little effect on the oxidation state of the remaining copper. The gold L3 edge develops a white line feature whose position lies between that of trivalent gold oxide (Au2O3) and monovalent potassium gold cyanide (KAu(CN)2) and whose intensity relative to the edge step is smaller than in the two reference compounds. The L3 EXAFS for Au in the superconductor resembles that of Au2O3. However, differences in the envelope of the Fourier filtered component for the first shell suggest that the local structure of the Au in the superconductor is not equivalent to Au2O3. Author

N90-29220# Defence Research Establishment, Ottawa (Ontario). Nuclear Effects Section.
TRANSIENT ANNEALING CHARACTERIZATION OF IRRADIATED MOSFETS
T. Cousins and K. M. Qureshi Jan. 1990 44 p
(AD-A223877; DREO-1030) Avail: NTIS HC A03/MF A01 CSCL 20/12

The electrical response of metal-oxide-silicon (MOS) technologies to incident nuclear (especially photon) radiation is a very complex, time-dependent function. This report reviews the physical processes governing this response and then experimentally examines them with the aid of the TATS-400 (Transient Annealing Test System). MOSFET responses to steady-state and pulsed photon and electron beams are characterized in terms of such parameters as threshold voltage shift and interface and oxide trap densities. The results show good agreement between experiment and theory in terms of the expected trends. However in order to conduct more meaningful tests, devices with much better-known geometries must be procured. GRA

N90-29221# Harvard Univ., Cambridge, MA. Div. of Applied Sciences.
DYNAMICAL PROPERTIES OF TWO-DIMENSIONAL JOSEPHSON JUNCTION ARRAYS
Samuel Paul Benz May 1990 147 p
(Contracts N00014-89-J-1023; N00014-89-J-1565; NSF DMR-84-04489; NSF DMR-86-14003; NSF DMR-89-12927)
(AD-A223965; TR-29) Avail: NTIS HC A07/MF A01 CSCL 20/12

We have investigated the dynamical properties of two dimensional (2D) Josephson junction arrays at temperatures below the Kosterlitz-Thouless phase transition. We have completed a comprehensive study, based on experiments and simulations, of the effects of large direct dc and radio-frequency RF bias currents on 2D arrays in the presence of perpendicular magnetic fields. Experiments were performed on large 1000 by 1000 arrays of Nb-Cu-Nb proximity-effects junctions that were fabricated using various photolithographic and thin-film deposition techniques. We present a complete explanation of the dynamic resistance in arrays as a function of both dc bias current and magnetic field. For certain fields, when the number of flux quanta per array unit cell is the ratio of two integers, the field-induced vortices are commensurate with the array and are arranged in ordered superlattices with qxq unit cells. Prominent peaks in the dynamic resistance are observed for these commensurate magnetic fields, and we relate the currents at these peaks with the depinning currents of the vortex superlattices. New exact calculations of the critical current are presented for the cases where f=1/2 and 1/3, which agree well with previous theoretical results and our experimental measurements. GRA

N90-29222# Raytheon Co., Lexington, MA.
MECHANICAL PROPERTY MEASUREMENT OF POLYCRYSTALLINE DIAMOND FILMS
G. F. Cardinale and R. W. Tustison 8 Jul. 1990 11 p Submitted for publication
(Contract N00014-87-C-0251)
(AD-A224037; TR-3) Avail: NTIS HC A03/MF A01 CSCL 20/2

The biaxial modulus and residual (post deposition) stress of polycrystalline diamond (PCD) films deposited by microwave plasma CVD is determined using the bulge test technique. This method involves measuring the deflection of a circular membrane under an applied differential pressure. A calibration parameter for the bulge test is determined by evaluating the biaxial modulus of a silicon specimen standard. The film is characterized using X Ray diffraction. Preliminary results yield a biaxial modulus value of 960 GPa for the PCD film. GRA

N90-29223# Massachusetts Inst. of Tech., Cambridge. Research Lab. of Electronics.
INTERFACE FORMATION AND PERCUSORY DYNAMICS Final Report, 15 Nov. 1986 - 14 Feb. 1990
John D. Joannopoulos 9 May 1990 6 p
(Grant AF-AFOSR-0098-87; AF Proj. 2306)
(AD-A224128; AFOSR-90-0751TR) Avail: NTIS HC A02/MF A01 CSCL 20/11

A completely ab-initio investigation of grain boundaries in solids has been performed for the first time. The electronic and structural properties of two short-period twist boundaries in Ge have been explored and found to be extremely complex. Boundary bonds are found to be distorted and weak, three-fold and five-fold coordinated defects appear to exist, and topological disorder in the form of odd and even numbers of rings of bonds is found to prevail. Complete total energy surfaces as a function of displacement of one grain over the other have also been mapped out. The results predict that there is a large degeneracy in the number of local energy minima, that tunneling-like modes should exist in these boundaries, that the formation energies of the boundaries lie in the range between 4 and 7 eV per unit cell, that the boundary volumes involve expansions in the range of 0.1 to 0.3 A/unit area, that trends toward dimerization exist parallel to the boundary planes, that electronic states will exist deep in the fundamental gaps of these systems. GRA

77 THERMODYNAMICS AND STATISTICAL PHYSICS

Includes quantum mechanics; theoretical physics; and Bose and Fermi statistics.

For related information see also *25 Inorganic and Physical Chemistry* and *34 Fluid Mechanics and Heat Transfer.*

N90-29224# Oak Ridge National Lab., TN. Engineering Physics and Mathematics Div.
PREDICTION, CONTROL, AND DECISION-MAKING ASPECTS FOR CHAOTIC SYSTEMS
V. Protopopescu 1990 8 p Presented at the 8th International Congress on Cybernetics and Systems, New York, NY, 11-15 Jun. 1990
(Contract DE-AC05-84OR-21400)
(DE90-014452; CONF-9006248-1) Avail: NTIS HC A02/MF A01

Several examples of chaotic systems are discussed for which occurrence of chaos, information recovery, control, and decision making processes appear in a new, sometimes counterintuitive light. From case to case, explanations, conjectures, and/or possible applications are indicated. DOE

N90-29225# Rochester Univ., NY. Dept. of Physics and Astronomy.
INTRODUCTION TO GAUGE THEORIES AND UNIFICATION
Aahok Das 1990 57 p Presented at the NATO Advanced Study Inst. on Techniques and Concepts of High Energy Physics, Saint Croix, Virgin Islands, 14-25 Jun. 1990
(Contract DE-AC02-76ER-13065)
(DE90-014473; DOE/ER-13065/630; UR-1172; CONF-900658-1) Avail: NTIS HC A04/MF A01

This paper contains the following lectures on gauge theories: basic notations; dimensional regularization; complex scalar field theory; scalar field theory; self-interacting scalar field theory; Noether's theorem; spontaneous symmetry breaking; dirac field theories; local symmetry; quantum electrodynamics; Higgs mechanism; non-Abelian symmetries; and Weinberg-Salam-Glashow theory. DOE

N90-29226# International Centre for Theoretical Physics, Trieste (Italy).
ON EINSTEINIAN 4-SUBMANIFOLDS IN E(SUP 6)
Georges Zafindratafa (Lyon-1 Univ., Villeurbanne, France) Nov. 1989 11 p Submitted for publication
(DE90-627149; IC-89/329) Avail: NTIS (US Sales Only) HC A03/MF A01

This work contributes to the classification of some Einsteinian 4-submanifolds by determining the second fundamental form. This leads to a characterization of some flat submanifolds of the Euclidean space. In particular, we show that an N-codimensional flat submanifold with flat normal connection in E(sup n+N) is cylindrical. Such a result is important since, in 1919, Elie Cartan asserted without proof the existence of flat, non cylindrical submanifolds of dimension n (ge) 4 in E(sup n+N); at the same time he proved than an n-dimensional submanifold of E(sup n+N), n (le) 3, is flat if and only if it is cylindrical. DOE

N90-29227# International Centre for Theoretical Physics, Trieste (Italy).
DISSIPATIVE QUANTUM MAPS
Hilda A. Cerdeira and Ramakrishna Ramaswamy (Jawaharlal Nehru Univ., New Delhi, India) Dec. 1989 22 p Sponsored in part by Third World Academy of Sciences, Italy; CNPq, Brazil; and Fundacao de Amparo a Pesquisa do Estado de San Paulo, Brazil
(DE90-627179; IC-89/388) Avail: NTIS (US Sales Only) HC A03/MF A01

A quantum kicked oscillator system in contact with a heat

bath is studied. The periodic forcing allows the definition of a quantum map. Using the Caldeira-Leggett approach, the kernel of the Wigner function is solved. The Lyapunov exponent if defined for this quantum system by computing the expectation value for the coordinate variable. This is achieved by taking the average along a semiclassical trajectory weighted by the Wigner function. DOE

N90-29228# International Centre for Theoretical Physics, Trieste (Italy).
QUANTUM CHAOS AND DISSIPATION: LYAPUNOV EXPONENTS
Hilda A. Cerdeira, Ramakrishna Ramaswamy, and Amir O. Caldeira (Universidade Estadual de Campinas, Brazil) Dec. 1989 19 p Submitted for publication Sponsored in part by Third World Academy of Sciences, Italy; Fundacao de Amparo a Pesquisa do Estado de San Paulo, Brazil; and CNPq, Brazil
(DE90-627180; IC-89/394) Avail: NTIS (US Sales Only) HC A03/MF A01

A periodically kicked quantum oscillator system in contact with a heat bath was examined. Using the Caldeira-Leggett approach, the kernel of the Wigner function was solved for all temperatures. Previous results for dissipative quantum maps are recovered as special limits of low damping and slow kicks when the system effectively becomes one-dimensional. The Lyapunov exponent was defined for this quantum system by computing the expectation value for the coordinate variable, by taking the average along a semiclassical trajectory weighted by the Wigner function. In the semiclassical limit, the Lyapunov exponent scales as a positive exponent of Planck's constant. DOE

N90-29229# International Centre for Theoretical Physics, Trieste (Italy).
OLD AND NEW IDEAS IN THE THEORY OF QUANTUM MEASUREMENT
GianCarlo Ghirardi and Alberto Rimini (Pavia Univ., Italy) Dec. 1989 27 p Submitted for publication
(DE90-627181; IC-89/425) Avail: NTIS (US Sales Only) HC A03/MF A01

This work deals with an attempt at incorporating the definite and local character of macroscopic objects in the principles of quantum mechanics and describing reduction as a real physical process, thereby recovering the textbook interpretation of the wave function. DOE

N90-29230# International Centre for Theoretical Physics, Trieste (Italy).
A COMMENT ON ANISOTROPIC SPHERES ADMITTING ONE PARAMETER GROUP OF CONFORMAL MOTIONS
Ashfaque H. Bokhari (Quaid-i-Azam Univ., Islamabad, Pakistan) Dec. 1989 7 p Submitted for publication
(DE90-627195; IC-89/379) Avail: NTIS (US Sales Only) HC A02/MF A01

An earlier solution of the Einstein field equations for spherically symmetric distributions of anisotropic matter (principle stresses unequal) is modified, assuming the existence of a one parameter group of conformal motions. It is shown that the modified solution yields a more general expression of the spacetime metric which includes the earlier metric as a special case. The solution is matched across a separating hypersurface with the Schwarzschild solution. It turns out that the expression for the line element corresponding to the induced metric on the boundary, from the inside, makes geometry look significantly different from the one obtained earlier. DOE

N90-29231# International Centre for Theoretical Physics, Trieste (Italy).
HIGHER LOOP CONTRIBUTIONS TO EFFECTIVE POTENTIAL OF GAUGE THEORY AT HIGH TEMPERATURE
V. M. Belyaev (Academy of Sciences, USSR, Moscow) Oct. 1989 11 p Submitted for publication
(DE90-627208; IC-89/321) Avail: NTIS (US Sales Only) HC A03/MF A01

Higher perturbative contributions to an effective potential for temporal component of gauge field (A(sub 0)(sup alpha) = const) for non-abelian gauge theory at high temperature are discussed. It is shown that one of the most important contributions is due to Debye gluons. The condensate of the field A(sub 0) varies as to gT(g yields 0) does not appear, if we take into account this Debye, one- and two-loop contributions only. The behavior of infrared leading perturbative contributions is investigated. It is argued that asymptotic behavior of these terms still indicates to a possible formation of A(sub 0) varies as to gT condensate. Higher perturbative contributions for Debye mass are also discussed. DOE

N90-29232# International Centre for Theoretical Physics, Trieste (Italy).
ON THE RELATION BETWEEN THE ABSOLUTE PARALLELISM SPACES AND SPACES HAVING A GL(4) CONNECTION
M. Melek Jan. 1990 7 p Submitted for publication
(DE90-627222; IC-90/5) Avail: NTIS (US Sales Only) HC A02/MF A01

It is shown that the difference between an absolute parallelism connection and a GL(4) connection can be expressed as a tensor field omega(sup nu)(sub rho nu) under general coordinate transformations which has the property that the quantity e(sup a)(sub nu) e(sub b)(sup rho) omega(sup nu)(sub rho mu) behaves as a connection under Lorentz transformations. The relations between the equations of geodesics, torsion tensors, and curvature tensors are considered. DOE

N90-29233# International Centre for Theoretical Physics, Trieste (Italy).
MEASUREMENT OF GRAVITATIONAL ACCELERATION OF ANTIMATTER
S. Rouhani (Tehran Univ., Iran) Dec. 1989 10 p Submitted for publication
(DE90-627464; IC-89/405) Avail: NTIS (US Sales Only) HC A02/MF A01

The minute yet effective impact of gravitational potential in the central region of a long tube magnetic container of non-neutral plasmas can be utilized for the measurement of the gravitational acceleration of antimatter particles. The slight change in distribution of plasma particles along the gravitational field affects the internal electric field of the plasma, which in turn affects the frequency of the magnetron motion of its particles. Thus, a rather straightforward relation is established between the gravitational acceleration of the particles and their magnetron frequencies, which is measurable directly, determining the value of the gravitational acceleration. DOE

N90-29234# California Univ., Santa Barbara. Dept. of Physics.
WIGNER SYMBOLS, QUANTUM DYNAMICS, AND THE KICKED ROTATOR
J. H. Jensen and Q. Niu 2 Jul. 1990 26 p
(Contract N00014-89-J-1530)
(AD-A224024; AD-E501248; TR-28) Avail: NTIS HC A03/MF A01 CSCL 20/10

The kicked rotator is used to show how to apply the formalism of Wigner symbols to the study of quantum dynamics. This approach provides a simple and direct method of comparing quantum and classical dynamics. The leading quantum effects are examined in detail for small values of h-bar. The time scales at which quantum effects appear are discussed. GRA

80 SOCIAL SCIENCES (GENERAL)

Includes educational matters.

No abstracts in this category.

81 ADMINISTRATION AND MANAGEMENT

Includes management planning and research.

N90-29235# National Science Foundation, Washington, DC. Div. of Science Resources Studies.
SCIENTISTS, ENGINEERS, AND TECHNICIANS IN NONMANUFACTURING INDUSTRIES: 1987. (DETAILED STATISTICAL TABLES)
1987 43 p
(PB90-226903; NSF-89-321) Avail: NTIS HC A03/MF A01 CSCL 05A

Detailed statistics on scientists, engineers, and technicians (SET) in nonmanufacturing in 1987 are given. The data comes from the Occupational Employment Statistics Survey, a Federal/State program producing national, State, and local data on occupational employment by industry for nonfarm wage and salary workers. Author

N90-29236# National Science Foundation, Washington, DC. Div. of Science Resources Studies.
FEDERAL SUPPORT TO UNIVERSITIES, COLLEGES, AND SELECTED NONPROFIT INSTITUTIONS: FISCAL YEAR 1988 (DETAILED STATISTICAL TABLES)
1990 93 p
(PB90-226887; NSF-89-325) Avail: NTIS HC A05/MF A01 CSCL 05A

The survey is designed to collect information from Federal agencies on total program support in thousands of dollars (encompassing both Science and Engineering (S/E) and non-S/E activities) to academic institutions; total science/engineering support to federally funded research and development centers (FFRDCs) administered by academic institutions; and R and D support to selected non-profit institutions and associated FFRDCs. GRA

N90-29237# National Science Foundation, Washington, DC. Div. of Science Resources Studies.
FEDERAL R AND D FUNDING BY BUDGET FUNCTION: FISCAL YEARS 1989-1991
Apr. 1990 137 p
(PB90-226879; NSF-90-311) Avail: NTIS HC A07/MF A01 CSCL 05A

Information on Federal funding of research and development (R and D) by Federal budget function categories is provided. The focus is exclusively on the R and D components of agency programs as proposed by the administration for fiscal year (FY) 1991. Descriptions of over 500 individual R and D programs are included. Research and development data are classified into the same budget function categories used in the Budget of the United States Government, Fiscal Year 1991. Proposed FY 1991 funding levels are given in budget authority which is the basis for initial congressional action. Detailed data are also included on actual Federal funds directed toward R and D in FY 1989 and estimated funding in FY 1990. GRA

N90-29238# Royal Signals and Radar Establishment, Malvern (England).
GUIDE TO CHARGING FOR THE CCF
R. F. Bateman Dec. 1989 26 p
(RSRE-89022; BR113096; ETN-90-97061) Copyright Avail: NTIS HC A03/MF A01

The method by which the Royal Signals and Radar Establishment (RSRE) Central Computing Facility (CCF) costs are fully recovered using the CCF charging mechanism is reported. The costs to be recovered are capital assets, support, maintenance, consumables and non-distributed, and these are recovered by charging for services i.e., CPU (Central Processing Unit), storage allocated and direct support to tasks, divisions and RSRE. More services will be added which will reduce the existing service charges proportionally. ESA

N90-29239# National Inst. of Standards and Technology, Gaithersburg, MD. Office of Standards Services.
GOVERMENT'S ROLE IN STANDARDS-RELATED ACTIVITIES: ANALYSIS OF COMMENTS
Walter G. Leight Jul. 1990 37 p
(PB90-215534; NISTIR-4367) Avail: NTIS HC A03/MF A01 CSCL 05A

The National Institute of Standards and Technology, supported by a panel of standards experts from other agencies, conducted a hearing on April 3 to 5, 1990, to gather information, insights, and comments relating to improving U.S. participation in international standards related activities and to possible Government actions. Oral presentations were made by 65 organizations and individuals; written submissions were received from 257 others. Thorough review of the hearing transcripts and the complete supplementary written record reveals a number of areas where the private sector and the Federal Government should take constructive actions, especially with respect to coordinating mechanisms for confirmity assessment processes. Author

N90-29240# Army War Coll., Carlisle Barracks, PA.
HOW CAN RESEARCH AND DEVELOPMENT LEADTIME BE REDUCED
Andrew C. Follmer 11 Apr. 1990 58 p
(AD-A224063) Avail: NTIS HC A04/MF A01 CSCL 15/5

Recognizing that the country that can rapidly convert advanced technology into superior weapon systems has a marked advantage, we have continuously increased funding of Research, Development, and Acquisition programs over the last three decades. During this period the leadtime for the development of new equipment has tripled. During the 1960's the stated leadtime objective of the Army was four years or less from initiation of development effort to type classification of the system as standard. This goal was never reached within the Army; instead the acquisition cycle leadtime has grown to ten to fifteen years. As a result of these long leadtimes many of our weapon systems cost too much and have obsolete technology by the time they are fielded. In addition to the premise that any reduction in leadtime means cost savings and a more qualitative combat force for the Army, why is it essential now that we minimize leadtime. The prominent reason is that the military budget will no doubt be significantly reduced due to the changing political environment of the world. Preparing and executing a modernization plan that supports our national security strategy for the present and the future will become complicated by the need for fiscal restraint. GRA

N90-29241# Colorado Univ., Boulder. School of Business.
THE EFFECTS OF MANAGEMENT SUPPORT ON THE SUCCESSFUL IMPLEMENTATION OF GROUP DECISION SUPPORT SYSTEMS M.S. Thesis
George Reno Crouse 23 May 1990 144 p Sponsored by AFIT, Wright-Patterson AFB, OH
(AD-A224473; AFIT/CI/CIA-90-040) Avail: NTIS HC A07/MF A01 CSCL 05/1

During the Information Age, an increased need for group collaboration and group decision making has developed. Companies have concentrated on the processing and distribution of data, and the increased productivity of the individual user. Now more work is done in groups and companies are looking to meet the decision making needs of groups. Group Decision Support Systems (GDSS) are emerging as a solution for those needs. Most companies have no idea what GDSS is, and if they do, they do not have experienced implementing GDSS type technology into their organizations. One problem is that GDSS has many different definitions and different products within each definition. This has led to confusion over this new technology. To implement a GDSS, an organization must match its need with an appropriate technology and an effective implementation strategy. There are many different types of GDSS. This study looks at a GDSS with Face-to-Face-Conferencing capabilities (or decision room). GRA

N90-29076*# National Aeronautics and Space Administration. Ames Research Center, Moffett Field, CA.
A SURVEY OF PLANNING AND SCHEDULING RESEARCH AT THE NASA AMES RESEARCH CENTER
Monte Zweben *In* JPL, California Inst. of Tech., Proceedings of the NASA Conference on Space Telerobotics, Volume 2 31 Jan. 1989 p 353-358 Previously announced as N89-19820 (For primary document see N90-29044 23-54)
Avail: NTIS HC A17/MF A03 CSCL 05A

N90-29077*# Teleos Research, Palo Alto, CA.
INTEGRATING PLANNING AND REACTIVE CONTROL
Stanley J. Rosenschein and Leslie Pack Kaelbling *In* JPL, California Inst. of Tech., Proceedings of the NASA Conference on Space Telerobotics, Volume 2 31 Jan. 1989 p 359-366 Sponsored in part by System Development Foundation (For primary document see N90-29044 23-54)
(Contract NCC2-494; SU Proj. 6359)
Avail: NTIS HC A17/MF A03 CSCL 05A

N90-29079*# Carnegie-Mellon Univ., Pittsburgh, PA. Dept. of Computer Science.
INTEGRATING PLANNING, EXECUTION, AND LEARNING
Daniel R. Kuokka *In* JPL, California Inst. of Tech., Proceedings of the NASA Conference on Space Telerobotics, Volume 2 31 Jan. 1989 p 377-386 Sponsored in part by Hughes Aircraft Co. (For primary document see N90-29044 23-54)
(Contracts NCC2-463; N00014-79-C-0661; N00014-82-C-50767; F33615-84-K-1520)
Avail: NTIS HC A17/MF A03 CSCL 05A

82 DOCUMENTATION AND INFORMATION SCIENCE

Includes information management; information storage and retrieval technology; technical writing; graphic arts; and micrography.

For computer documentation see *61 Computer Programming and Software.*

N90-29242# National Archives and Records Service, Washington, DC. Office of the National Archives.
NATIONAL ARCHIVES PRESERVATION RESEARCH PRIORITIES: PAST AND PRESENT
K. E. Harris, S. Lee-Bechtold, W. K. Wilson, C. W. Mayn, and W. M. Holmes Apr. 1990 21 p
(PB90-206210; NARA/TIP-90/03) Avail: NTIS HC A03/MF A01 CSCL 05B

Preservation research conducted and funded by the National Archives from its creation in 1934 until the present is described. Previous research has concentrated on the stability of record materials, environmental conditions, and the development of standards. The current program incorporates the same components but places greater emphasis on quality control and on systems for the handling of preservation problems. Current research priorities discussed include shrink wrapping, image analysis, film and tape stability, photographic activity testing, and stability of optical media. GRA

N90-29243# National Inst. of Standards and Technology, Gaithersburg, MD. National Computer Systems Lab.
OBJECT DATABASE MANAGEMENT SYSTEMS: CONCEPTS AND FEATURES Final Report
Christopher E. Dabrowski, Elizabeth N. Fong, and Deyuan Yang Apr. 1990 64 p
(PB90-216813; NIST/SP-500/179) Avail: NTIS HC A04/MF A01; SOD HC $3.75 as 003-003-03007-4 CSCL 05B

The last decade has seen the emergence of object concepts and their infusion into information systems technology. This phenomenon began with the advent of programming languages that included object concepts. More recently, object concepts have been merged with database management system technology, resulting in the production of some object database management systems. As a result, the term object database management system (ODBMS) is now becoming a recognized and important topic in the database community. The purpose here is to provide managers and software analysts a state-of-the-art review of object concepts and to describe features associated with object database management systems. Author

N90-29244# Assistant Secretary of Defense (Comptroller), Washington, DC.
AUTOMATED INFORMATION SYSTEM LIFE-CYCLE MANAGEMENT MANUAL
T. Bozek Mar. 1990 37 p
(PB90-219288; DOD-7920.2-M) Avail: NTIS HC A03/MF A01 CSCL 05B

Uniform procedures for the conduct of Automated Information System (AIS) Life-Cycle Management (LCM) activities are given as well as guidelines for the preparation and submission of documentation for LCM reviews. AISs that are integral to or embedded in a weapon system, or that are used exclusively for cryptologic activities, are exempted from the provisions of the Manual. The Manual is mandatory for use by all Department of Defense Components, and is designed for direct use at operating levels without supplementary instructions. GRA

N90-29245# National Inst. of Standards and Technology, Gaithersburg, MD. Information Systems Engineering Div.
INFORMATION MANAGEMENT DIRECTIONS: THE INTEGRATION CHALLENGE Final Report
Elizabeth N. Fong and A. H. Goldfine 1989 178 p
(PB90-219866; NIST/SP-500/167; LC-89-600755) Avail: NTIS HC A09/MF A01; also avail. SOD as SN003-003-02973-4 CSCL 05B

The results of a 3-day workshop on the integration challenge of information management are given. The workshop was the fifth in the Information Management Directions series. The purpose of these workshops is to examine, in depth, key trends and strategies that affect the future of the information management profession. The focus of the fifth workshop was on issues related to integration and productivity. The 72 workshop participants were organized into five working panels, which met to discuss the integration of knowledge and data management; the integration of technical and business data management; the integration of systems planning, development, and maintenance tools and methods; the integration of distributed, heterogeneous computing environments; and architectures and standards for information management. GRA

N90-29246# Patent and Trademark Office, Washington, DC.
INDUSTRIAL PATENT ACTIVITY IN THE US. PART 2: ALPHABETICAL LISTING BY COMPANY, 1969-1989
Jul. 1990 334 p Prepared in ccoperation with National Technical Information Service, Springfield, VA
(PB90-214412) Avail: NTIS HC A15/MF A02; also avail. in set of 2 reports as PB90-214396, HC E99/MF E99 CSCL 05B

An alphabetical listing of U.S. and foreign organizations which received 5 or more U.S. patents during the period 1969 to 1989 is given. Included are some 18,000 corporations, government agencies and universities. For each organization, the total patent count for the 21-year range is shown. Author

N90-29247# Wichita State Univ., KS. National Inst. for Aviation Research.
INTERNATIONAL AIRCRAFT OPERATOR DATA BASE MASTER REQUIREMENTS AND IMPLEMENTATION PLAN Final Report, Sep. 1989 - Jul. 1990
Gary Ott, John Ellis, Raj Sunderraman, John J. Hutchinson, and Frank H. Macheers Aug. 1990 45 p
(Contract DTFA03-89-C-00057)
(DOT/FAA/CT-90/17) Avail: NTIS HC A03/MF A01

This International Aircraft Operator Data Base Master Requirements and Implementation Plan describes the Federal Aviation Administration's (FAA) requirements for aircraft operator information as well as a plan for addressing these requirements.

In order to carry out this responsibility the FAA requirements include a unique description of each aircraft along with the name, address, telephone number, and a fax number of the aircraft operator. It was determined that the FAA has other ad hoc requirements for aircraft operator related information. It was also determined that information needed by the FAA to carry out this responsibility is available through the private sector. The software and computer networking capability is developed to make effective use of this information. The main task of this program is to create an information system which will facilitate and enhance communication between the FAA and the aircraft operator data base suppliers. The plan is presented to make use of these commercial data suppliers to create an aircraft operator information system.

Author

N90-29248 Loughborough Univ. of Technology (England).
EFFICIENCY AND EFFECTIVENESS OF DEEP STRUCTURE-BASED SUBJECT INDEXING LANGUAGES: PRECIS VS. DSIS Ph.D. Thesis
Subal Chandra Biswas 1988 376 p
Avail: Univ. Microfilms Order No. BRDX88181

A Subject Indexing Language (SIL) is an artificial language used for formulating names of subjects. Although classificationists have sought for universals in many fields of study such as, philosophy, biology, general systems theory, etc., the search for a deep structure of SILs formally began with Ranganathan's idea of absolute synthax and was brought to the present by G. Bhattacharyya and D. Austin. Whereas Bhattacharyya's deep structure of SIL is primarily based on classificatory principles (parallel to absolute syntax), the deep structure proposed by Austin has a linguistic connotation. The present study describes and compares two such deep structure-based SILs, viz., PRECIS (PREserved Context Index System) and DSIS (Deep Structure Indexing System), a recent computerized version of POPSI (POstulate-based Permuted Subject Indexing), developed by F. J. Devadason. Both also belong to the category of SILs typified as string indexing languages. The study involves: (1) writing of a suitable DSIS index entry generation program, (2) using both PRECIS (in-house) and DSIS programs to index a collection of representative sample documents from the soft sciences, (3) analyzing and comparing their respective syntactic and semantic aspects in terms of both linguistic and classificatory principles, and (4) applying some measures of efficiency and effectiveness. It was realized that certain modifications in the existing DSIS string manipulation algorithms are necessary to make the program fully operational. Although, no attempts have been made to quantify the measures of effectiveness and efficiency as such, suggestions have been provided as to what these probably would be. Some indications of their searching difficulties for a prospective searcher have been put forward as well. Dissert. Abstr.

N90-29249# Federal Aviation Administration, Atlantic City, NJ.
A GLOSSARY OF TERMS, DEFINITIONS, ACRONYMS, AND ABBREVIATIONS RELATED TO THE NATIONAL AIRSPACE SYSTEM
John M. Fabry Jun. 1990 848 p
(DOT/FAA/CT-TN89/53) Avail: NTIS HC A99/MF E06

The following terms, definitions, acronyms, and abbreviations are defined for the purpose of clarifying their meaning. This unofficial glossary was compiled to provide a common understanding of terms related to the National Airspace System (NAS). The terms contained in this glossary are primarily defined in an operational sense, and are applicable to users, operators, and maintainers of the NAS. This document is not intended to be a arbiter of the official definition. Rather, it is intended to be a general listing of terms, definitions, acronyms, and abbreviations related to NAS projects, system programming, to contractors' documents, and to miscellaneous topics. Author

N90-29250# Oak Ridge National Lab., TN.
BIOMEDICAL AND ENVIRONMENTAL SCIENCES PROGRAM PUBLICATIONS, 1989
C. A. Johnson, J. R. Ellis, K. N. Gibson, V. S. Norman, K. J. Rader, and D. D. Rhew Jul. 1990 113 p
(Contract DE-AC05-84OR-21400)
(DE90-014785; ORNL-6619) Avail: NTIS HC A06/MF A01

This bibliography contains approximately 600 references to journal articles, books, book chapters, proceedings, reports, and abstracts published during 1989 under Oak Ridge National Laboratory Biomedical and Environmental Sciences programs. Some references from 1988 that were not entered into the Laboratory Records data base in time for the previous publication are also included in this document. The bibliography is organized by technical category, then by division, and, within each division, alphabetically by the senior author. An index of authors is also provided. Publications listed in this bibliography include 284 journal articles and abstracts, 224 of which appeared in refereed sources; 196 reports; 54 proceedings; and numerous books, book chapters, and miscellaneous publications. DOE

N90-29251# National Academy of Sciences - National Research Council, Washington, DC. Board on Telecommunications and Computer Applications.
CROSSROADS OF INFORMATION TECHNOLOGY STANDARDS
Jun. 1990 81 p Sponsored by Defense Communications Agency; NAS-NRC; and General Services Administration
(Contract NIST-43NANB007123)
(PB90-239732) Avail: NTIS HC A05/MF A01 CSCL 05B

A group of sixty information technology professionals, including executives from equipment providers, service providers, and user organizations, met for a two-day workshop on information technology standardization. The two key issues discussed were: the timeliness of the standardization process within the U.S. for effective support for a domestic industrial base that is globally competitive, and the degree to which U.S. interests in standardization are effectively developed and represented in worldwide standards-making activities. The workshop drew a number of conclusions as to the importance of information technology to international competitiveness, the need of a state of the art information infrastructure, and the need for accelerating the standards process. They recommended that a blue ribbon panel be convened to set a vision for an information infrastructure and that the American National Standards Institute be reconstituted to better represent the information technology industry and to engage in life cycle planning and in prototyping for information technology standardization. Author

N90-29252# AQUA TERRA Consultants, Decatur, GA.
DATA BASE ANALYZER AND PARAMETER ESTIMATOR (DBAPE) INTERACTIVE COMPUTER PROGRAM USER'S MANUAL
John C. Imhoff, Robert F. Carsel (Environmental Research Lab., Athens, GA.), John L. Kittle, Jr., and Paul R. Hummel Jan. 1990 260 p
(Contract EPA-68-03-3513)
(PB90-193053; EPA/600/3-89/083) Avail: NTIS HC A12/MF A02 CSCL 05B

The Data Base Analyzer and Parameter Estimator (DBAPE) is an interactive computer program that provides a link between two of EPA's development products -- an environmental model and a data base. DBAPE was created to encourage and support the use of the RUSTIC model, a newly developed model that simulates the transport of field-applied pesticides in the crop root zone, the unsaturated zone, and the saturated zone. DBAPE provides an efficient means to obtain soils and meteorologic data needed to run RUSTIC from a data base that contains information on over 8000 agricultural soils and 200 meteorological stations located throughout the contiguous United States. Soils-related RUSTIC input that can be obtained by using DBAPE includes percent organic matter, wilting point, field capacity, residual water content, saturated hydraulic conductivity and values for the van Genuchten parameters for the soil-water characteristic function. Meteorologic data that can be obtained include precipitation, air temperature, pan evaporation, solar radiation, and windspeed. These meteorologic data are not distributed with DBAPE because of their volume.

DBAPE, however, allows the user to identify weather stations near his/her study sites. Meteorologic data for these stations then can be obtained from the EPA's Environmental Research Laboratory, Athens, GA. GRA

N90-29253# Instituto de Pesquisas Espaciais, Sao Jose dos Campos (Brazil).
INPE GEOGRAPHIC DATA BASE [O BANCO DE DADOS GEOGRAFICOS DO INPE]
Guaraci Jose Erthal, Missae Odo BdeOliveira, Carlos Alberto Felgueiras, Gilberto CamaraNeto, and Joao ArgemirodeCarvalho-Paiva Aug. 1988 9 p In PORTUGUESE; ENGLISH summary Presented at the 1st Brazilian Symposium on Data Bases, Rio de Janeiro, 11-12 Apr. 1986
(INPE-4636-PRE/1348) Avail: NTIS HC A02/MF A01

A geographic information system developed at MCT/INPE is presented. This system allows the integration of satellite images, thematic and topographic maps, and tabular data. Its applications include the analysis of complex geoambiental problems. These analyses involve the combination of the various data types to get desired results over a specified region of interest. The input, output, and information extraction procedures available are described. Future developments are also indicated. Author

N90-29254# Army Engineer Waterways Experiment Station, Vicksburg, MS. Information Technology Lab.
OPTICAL STORAGE TECHNOLOGY Final Report
E. D. Keenan and N. Radhakrishnan Apr. 1990 130 p
(AD-A224028; WES/TR/ITL-90-2) Avail: NTIS HC A07/MF A01 CSCL 05/2

User acceptance of optical storage technology has been slow because of problems pertaining to access time, transfer rates, and lack of industry standards. This technology, however, offers three distinct advantages over the present high-density magnetic media: greater storage density; less sensitivity to data corruption, contamination, or malicious alteration; and elimination of mechanical damage. The most prevalent optical storage media are Compact Disc-Read Only Memory (CD-ROM), Write Once Read Many (WORM), and Erasable Optical Discs (EOD). These media are described and evaluated according to their capabilities and limitations within each of the Information Management (IR) areas. The individual IR areas (namely, Library, Printing, Records Management, Visual, Scientific and Engineering, and Automation) are considered in relation to the current level of optical technology, and options for the U.S. Army Corps of Engineers are presented. GRA

N90-29255# Colorado Univ., Boulder. School of Business.
TIME-BASED COMPETITION FOR COMPETITIVE ADVANTAGE: AN INFORMATION TECHNOLOGY PERSPECTIVE M.S. Thesis
Jerry William Hanlin 25 May 1990 178 p Sponsored by AFIT, Wright-Patterson AFB, OH
(AD-A224474; AFIT/CI/CIA-90-041) Avail: NTIS HC A09/MF A01 CSCL 05/3

The environment which business faces today is much more competitive than in the past. Time-based competition is a new competitive strategy through which businesses may gain competitive advantage. Since this strategy is new, there is little information available to managers who are contemplating use of this strategy. Six case studies of time-based competitors are presented and discussed. This thesis had three thrusts. The first was to place time-based competition in current works and models of competitive strategy. Time-based strategy was determined to be a strategic thrust. The second thrust was to identify and validate which elements of time-based strategy are important and/or relevant to time-based competitors. The third thrust was to determine the importance of information technologies (IT) to time-based competition. This thrust also sought information of how time-based competitors support their time thrust by IT. GRA

83 ECONOMICS AND COST ANALYSIS

Includes cost effectiveness studies.

N90-29256# Naval Postgraduate School, Monterey, CA. Dept. of Administrative Science.
EXTENSIONS TO THE LEARNING CURVE: AN ANALYSIS OF FACTORS INFLUENCE UNIT COST OF WEAPON SYSTEMS
O. Douglas Moses May 1990 67 p Prepared for Naval Sea Systems Command, Washington, DC
(AD-A224119; NPS54-90-016) Avail: NTIS HC A04/MF A01 CSCL 05/3

The use of learning curves to analyze unit costs experienced during the manufacture of items produced from a repetitive process is widespread. The assumption implicit in the use of learning curves is that cumulative quantity produced is the primary factor influencing the pattern of unit costs. This paper adds to the learning curve model variables reflecting production rate, company-wide activity and fixed costs, and industry activity. Empirical tests conducted using data from missile weapon systems show that each variable enhances the explanation of unit cost but the importance of the variables depends on the nature of the cost series being analyzed. Additional tests examine the influence of broader economic and political factors on weapon system unit cost. GRA

84 LAW, POLITICAL SCIENCE AND SPACE POLICY

Includes NASA appropriation hearings; aviation law; space law and policy; international law; international cooperation; and patent policy.

No abstracts in this category.

85 URBAN TECHNOLOGY AND TRANSPORTATION

Includes applications of space technology to urban problems; technology transfer; technology assessment; and surface and mass transportation.

For related information see also *03 Air Transportation and Safety, 16 Space Transportation,* and *44 Energy Production and Conversion.*

N90-29257# Congressional Budget Office, Washington, DC.
PRELIMINARY ANALYSIS OF NASA COMMERCIALIZATION INITIATIVES
D. H. Moore and M. Sieverts 17 Feb. 1989 18 p
(PB90-202706) Avail: NTIS HC A03/MF A01 CSCL 05A

The NASA budget request includes support for industry and university collaboration in exploring the potential uses of space for future economic gain and for procurement of launch services from the private sector for NASA missions, and announces NASA's intention to seek private-sector financing for portions of its space transportation and space station programs. The intention to seek private financing for NASA facilities and hardware programs represents a new direction for the NASA program. It would defer some budgetary outlays to the future by means of service contracts and leases to private investors. A complete analysis of these space commercialization initiatives must await more specific information concerning the proposed agreements between the government and private investors, since a variety of options would be open to both parties. Nevertheless, the initiatives included in the 1990 budget raise a number of general issues. Some of these issues are addressed in examining the larger policy behind the proposals, estimating their cost to the government, and briefly examining some budgetary and scoring concerns. GRA

N90-29258# Midwest Research Inst., Golden, CO.
TRANSFERRING BUILDING ENERGY TECHNOLOGIES BY LINKING GOVERNMENT AND PRIVATE-SECTOR PROGRAMS
Barbara C. Farhar Jul. 1990 63 p
(Contract DE-AC02-83CH-10093)
(DE90-000346; SERI/TP-260-3716) Avail: NTIS HC A04/MF A01

The U.S. Department of Energy's Office of Building Technologies (OBT) may wish to use existing networks and infrastructures wherever possible to transfer energy-efficiency technologies for buildings. The advantages of relying on already existing networks are numerous. These networks have in place mechanisms for reaching audiences interested in energy-efficiency technologies in buildings. Because staffs in trade and professional organizations and in state and local programs have responsibilities for brokering information for their members or client organizations, they are open to opportunities to improve their performance in information transfer. OBT, as an entity with primarily R and D functions, is, by cooperating with other programs, spared the necessity of developing an extensive technology transfer program of its own, thus reinventing the wheel. Instead, OBT can minimize its investment in technology transfer by relying extensively on programs and networks already in place. OBT can work carefully with staff in other organizations to support and facilitate their efforts at information transfer and getting energy-efficiency tools and technologies into actual use. Consequently, representatives of some 22 programs and organizations were contacted, and face-to-face conversations held, to explore what the potential might be for transferring technology by linking with OBT. The briefs included in this document were derived from the discussions, the newly published Directory of Energy Efficiency Information Services for the Residential and Commercial Sectors, and other sources provided by respondents. Each brief has been sent to persons contacted for their review and comment one or more times, and each has been revised to reflect the review comments. DOE

N90-29259# Syracuse Research Corp., NY. Science and Technology Policy Center.
STATE SCIENCE AND TECHNOLOGY INDICATORS: AN EXPLORATORY PROFILE AND ANALYSIS Final Report
W. Henry Lambright, Eva M. Price, and Albert H. Teich (American Association for the Advancement of Science, Washington, DC.) 31 Aug. 1989 148 p
(Grant NSF SRS-87-13477)
(PB90-246711) Avail: NTIS HC A07/MF A01 CSCL 05A

One of the more significant changes of the 1980s in the relation of government to science and technology (S/T) has been the rise of the states. To better understand the state role, the project has investigated S/T policies in 13 states. The 13 states were selected to include most of the largest states (presumably having much of the country's S/T activity), as well as a few small states, so as to have a more representative sample. The project developed the following indicators of state S/T activity: state-funded research and development, scientific equipment and facilities, technology transfer activities, special science-education initiatives, state competition for national facilities, and S and T-oriented government institutions. Particular attention was given the role of the new S/T agencies and offices. Also examined was the role of more traditional state agencies and organizations in this emerging function of S/T-based economic development. Finally, the project discussed in depth the indicator of state competition for large national facilities, like the Superconducting Super Collider. GRA

N90-29260*# Medical Technology, Inc., Syracuse, NY. Engine Systems Div.
AUTOMOTIVE STIRLING ENGINE DEVELOPMENT PROGRAM Semiannual Technical Progress Report No. 12, 1 Jan. - 30 Jun. 1987
Roger A. Farrell, A. Richey, and J. Mundy Feb. 1988 73 p
(Contracts DEN3-32; DE-AI01-85CE-50112)
(NASA-CR-180840; NAS 1.26:180840; MTI-87ASE575SA12; DOE/NASA/0032-31) Avail: NTIS HC A04/MF A01 CSCL 10A

A study of high-power kinematic Stirling engines for transportation use, testing of Mod I and Mod II Stirling engines, and component development activities is reviewed. Mod II development testing included performance, emissions, and noise as well as the impact of varying regenerator porosity, working gas, and heater head geometry. Mod I engines were used for Mod II component development and to obtain independent party (U.S. Air Force) evaluation of Stirling engine vehicle performance. Author

88 SPACE SCIENCES (GENERAL)

No abstracts in this category.

89 ASTRONOMY

Includes radio, gamma-ray, and infrared astronomy, and astrometry.

N90-29261*# Dominion Astrophysical Observatory, Victoria (British Columbia).
METALLIC LINE PROFILES OF THE AOV STAR VEGA
J. Murray Fletcher, Austin F. Gulliver, Saul J. Adelman, and Charles R. Crowley (Michigan Univ., Ann Arbor.) Aug. 1990 19 p Submitted for publication Sponsored in part by National Sciences and Engineering Research Council of Canada
(Grant NAG5-921)
(NASA-CR-186906; NAS 1.26:186906) Avail: NTIS HC A03/MF A01 CSCL 03A

High dispersion ultrahigh signal to noise Reticon spectra of Vega were obtained with the coude spectrograph of the 1.2 m telescope. A mean signal to noise ratio of 2500 over the spectral region lambdas from 3825 to 5435 was achieved. Examination of the line profiles confirmed the presence of two different types of profiles which were previously seen in IIIaJ and lower signal to noise Reticon spectra. The profiles of the strong lines are essentially classical rotational profiles with enhanced wings which are slightly stronger than expected while those of weak lines are clearly flat-bottomed resulting in a trapezoidal appearance. A few possible theoretical explanations are presented. Author

N90-29262*# California Inst. of Tech., Pasadena.
STAR FORMATION AND THE DISTRIBUTION OF HI AND INFRARED EMISSION IN M51
Richard J. Rand, Shrinivas R. Kulkarni, and W. Rice (Jet Propulsion Lab., California Inst. of Tech., Pasadena.) 1990 52 p Submitted for publication
(Grants NAG5-1164; NSF AST-97-14405)
(NASA-CR-186928; NAS 1.26:186928) Avail: NTIS HC A04/MF A01 CSCL 03A

H I, infrared, CO, H alpha and beta band observations of M51, the prototypical grand-design spiral galaxy, are used to study the consequences of star formation for the distribution of H I and dust. Using the H I and CO data sets new tests of the idea that the H I is largely a dissociation product in star-forming regions were performed. It was confirmed that the H I spiral arms are generally coincident with the H II region arms, and offset downstream from the CO arms. The radial distributions of total gas, H alpha and H I surface density have a simple explanation in the dissociation picture. The distributions also demonstrate how the surface density of H I might be related to the star formation efficiency in molecule-rich galaxies. The large width of the H I regions along the arms compared to that of the H II regions can be understood in terms of a simple Stroemgren sphere calculation. The longer lifetime of the stars producing dissociating radiation vs. those producing ionizing radiation will also contribute to the greater width of the H I arms if stars are continuously forming on

the arms. The lack of detailed coincidence of the H I and H II regions along the inner arms has a variety of possible explanations within the dissociation scenario. Two simple tests to probe the origin of the IRAS emission in M51 were performed. Author

N90-29263 Delaware Univ., Newark.
AN ANALYSIS OF THE PALOMAR-GREEN SUBDWARFS AND WHITE DWARFS Ph.D. Thesis
Peter Andreas Thejll 1989 166 p
Avail: Univ. Microfilms Order No. DA9010388

It is shown that the scale height of the subdwarfs in the Palomar-Green (PG) survey that show helium and hydrogen lines is larger than suggested by recent work. In two independent determinations of the subdwarf scale height, z(sub 0), in the exponential density distribution above the plane rho(z) = rho(sub o) e(sup -z/z(sub 0) and the subdwarf density in the plane, rho(sub 0), a scale height was found close to 600 pc (-200 pc, +300 pc) with densities ranging from 3 x 10(exp -7) pc(sup -3). The high value for the scale height is supported by two other arguments: First, by using Kitt Peak Downes subdwarf density in the plane and the number of subdwarfs in the PG survey, a scale height of 410 pc was calculated. Second, modeling of the distribution of PG stars per magnitude interval supports high scale heights. No assumption-free values for the life time of the subdwarfs exists and the speculation is that if they are post-HB objects undergoing He-shell flashes they have a lifetime of about 2 x 10(exp 6) years and thus a birthrate that links them to 100 percent of the non-DA white dwarfs and from 15 to 55 percent of the DA white dwarfs. The absolute magnitude of the PG subdwarfs O stars is also found to be in agreement with earlier determinations. Work is also presented that was published in a paper on Sirius B. By using the effective temperature determined by Holberg, et al. (1984) and theoretical work by Ostriker and Hartwick (1968), it was found that the radius of Sirius B lies between 0.76 and 0.81 hundredths of a solar radius and that the rotational velocity lies betwen 0 and 600 km/s at the equator. Furthermore, the impact future observations will have, is discussed. It was found that T(sub eff) and the magnitude are the limiting factors on the accuracy of Sirius B's radius and rotational velocity once the HIPPARCOS satellite determines the parallex to within 1 milliarcsecond.
Dissert. Abstr.

N90-29264 California Univ., Los Angeles.
NEAR-INFRARED SPECKLE OBSERVATIONS OF T TAURI STARS AND A MULTI-WAVELENGTH STUDY OF THE PROTOTYPE STAR T TAURI Ph.D. Thesis
David Andrew Weintraub 1989 407 p
Avail: Univ. Microfilms Order No. DA9013004

If T Tauri stars are low mass pre-main-sequence (PMS) stars similar to the sun, then preplanetary material should surround many T Tauri stars if planetary systems are common. Near-infrared speckle interferometric observations of three dozen T Tauri stars are presented. Most of the observations were made at Lick Observatory using the UCLA Three Color Speckle Photometer at 1.29 (J), 2.28 (K), and 3.84 (L) microns. Of the 36 observed sources, 15 appear resolved, 8 more are possibly resolved, and 10 are apparently unresolved. At least 7 of these are binaries with projected separations of less than 500 AU; one (HL Tau) and maybe as many as three (XZ Tau and Haro 1-4) are resolved as extended structures. A multi-wavelength study of T Tauri, the prototype star of this type, is presented. Using high spatial and spectral resolution observations of the J = 1 yields 0 rotational transition of CO and 13-CO, a 12 second diameter, centrally symmetric structure was found around T Tauri. From the submillimeter spectrum, a gas plus dust mass is estimated at approximately 0.01 solar mass, that is consistent with the mass estimated from the CO observations. At J and K, an infrared array camera and coronagraph were used to observe polarized light scattered off of circumstellar dust grains. At these short wavelengths, a circular structure was again found extending radially out to 13 minutes from T Tauri. Submillimeter observations of other selected T Tauri stars that reveal evidence for approximately 0.01 solar mass of preplanetary material within a 1000 AU radius of a dozen T Tauri stars, and 6 centimeter observations of 12 T Tauri binaries are included. Finally, in the appendix, a catalog of PMS emission-line stars is presented with their IRAS identifications, which were developed and used as a tool for selecting target stars.
Dissert. Abstr.

N90-29265*# Jamieson Science and Engineering, Inc., Scotts Valley, CA.
AN INFRARED SKY MODEL BASED ON THE IRAS POINT SOURCE DATA
Martin Cohen, Russell Walker, Richard Wainscoat, Kevin Volk, Helen Walker, and Deborah Schwartz (National Aeronautics and Space Administration. Ames Research Center, Moffett Field, CA.) Feb. 1990 592 p
(Contract NAS2-12515)
(NASA-CR-177526; NAS 1.26:177526) Avail: NTIS HC A25/MF A04 CSCL 03A

A detailed model for the infrared point source sky is presented that comprises geometrically and physically realistic representations of the galactic disk, bulge, spheroid, spiral arms, molecular ring, and absolute magnitudes. The model was guided by a parallel Monte Carlo simulation of the Galaxy. The content of the galactic source table constitutes an excellent match to the 12 micrometer luminosity function in the simulation, as well as the luminosity functions at V and K. Models are given for predicting the density of asteroids to be observed, and the diffuse background radiance of the Zodiacal cloud. The model can be used to predict the character of the point source sky expected for observations from future infrared space experiments. Author

N90-29266# Los Alamos National Lab., NM. Theoretical Div.
CEPHEID MASSES FOR MODELS WITH ENHANCED OPACITIES
Siobahn M. Morgan (Washington Univ., Seattle.) and Arthur N. Cox 1990 6 p Presented at the Confrontation Between Stellar Pulsation and Evolution, Bologna, Italy, 28-31 May 1990 Submitted for publication
(Contract W-7405-eng-36)
(DE90-014919; LA-UR-90-2369; CONF-9005249-3) Avail: NTIS HC A02/MF A01

Cepheid models with enhanced opacity are constructed and used to determine pulsation constants, Q(sub 0). These are compared to models without an enhanced opacity. Methods of determining Cepheid masses are investigated using the different models and are compared to results obtained by Gieren. The methods to determine the pulsation and Wesselink masses differ significantly, due to the use of a Q(sub 0) that varies with mass, radius and luminosity. DOE

N90-29267# Los Alamos National Lab., NM.
PULSATIONS OF THE WHITE DWARF COMPONENT IN V471 TAURI-LIKE BINARIES
Letizia Stanghellini, Arthur N. Cox, and Sumner G. Starrfield (Arizona State Univ., Tempe.) 1990 5 p Presented at the Confrontation Between Stellar Pulsation and Evolution, Bologna (Italy), 28-31 May 1990
(Contract W-7405-eng-36)
(DE90-014921; LA-UR-90-2367; CONF-9005249-1) Avail: NTIS HC A01

The eclipsing spectroscopic binary V471 Tau has a compact DA component that has been observed to pulsate with multimode, low amplitude oscillations. Three models are tested with different masses (M/Solar mass = 0.6, 0.8, 1.0) against nonradial instability. The models are derived from an evolutionary track calculated by Iben. The results confirm that the pulsations are driven by the kappa and gamma mechanisms operating in the ionization zones of carbon and oxygen. DOE

N90-29268*# National Aeronautics and Space Administration. Marshall Space Flight Center, Huntsville, AL.
NASA MARSHALL SPACE FLIGHT CENTER SOLAR OBSERVATORY REPORT, JANUARY - JUNE 1990

James E. Smith Aug. 1990 85 p
(NASA-TM-103512; NAS 1.15:103512) Avail: NTIS HC A05/MF A01 CSCL 03A

A description of the NASA Marshall Space Flight Center's Solar Vector Magnetograph Facility is presented and a summary of its observations and data reduction is given. The systems that make up the facility are a magnetograph telescope, an H alpha telescope, a Questar telescope, and a computer code. The data are represented by longitudinal contours with azimuth plots. Author

90 ASTROPHYSICS

Includes cosmology; celestial mechanics; space plasmas; and interstellar and interplanetary gases and dust.
For related information see also *75 Plasma Physics*.

N90-29269# California Univ., Berkeley. Lawrence Berkeley Lab. Nuclear Science Div.
ROTATING NEUTRON STARS AND THE EQUATION OF STATE OF DENSE MATTER
F. Weber, N. K. Glendenning, and M. K. Weigel (Technische Univ., Munich, Germany, F.R.) May 1990 16 p Presented at the International Conference on Medium- and High-Energy Physics, Taipei, Taiwan, 14-18 May 1990 Submitted for publication
Sponsored by Max-Kade Foundation, NY
(Contract DE-AC03-76SF-00098)
(DE90-014185; LBL-29081; CONF-9005233-2) Avail: NTIS HC A03/MF A01

The properties of non-rotating as well as rotating neutron stars are investigated in the framework of Einstein's theory of general relativity. The nuclear equation of state of neutron star matter (electrically charge neutral many-baryon/lepton system) is calculated for the relativistic Hartree- and Hartree-Fock approximations. The influence of two-particle correlations on the equation of state is taken into account, too. An important result is that the limiting rotational frequency of a neutron star is set by instability modes caused by gravitational radiation reaction, which set in well below the Kerplerian frequency. DOE

N90-29270# Brookhaven National Lab., Upton, NY. Center for Accelerator Physics.
CONTROL OF NONLINEAR SPACE-CHARGE EMITTANCE GROWTH
Juan C. Gallardo 1990 8 p
(Contract DE-AC02-76CH-00016)
(DE90-014752; BNL-52246) Avail: NTIS HC A02/MF A01

A simple analytical model of the space-charge (self-fields) of a few picosecond electron pulse in a RF photocathode electron gun is presented. The model permits a search for the optimal laser distribution (transverse and longitudinal) that will result in an electron beam with minimum transverse emittance. It is concluded that electron distributions with sharp edges in the transverse dimension and parabolic (inverted) in the longitudinal direction are best to minimize the emittance. These effects were confirmed with extensive simulations using the numerical code PARMELA. DOE

N90-29271 Rice Univ., Houston, TX.
A PLASMA DIAGNOSTIC STUDY OF TWO WIND-BLOWN SHELL NEBULAE: NGC 7635 AND NGC 2359 Ph.D. Thesis
Tamara Elizabeth Jernigan 1989 159 p
Avail: Univ. Microfilms Order No. DA9012813

The first quantitative analysis of the morphology and gaseous-phase properties of two wind-blown shells and their interaction with the interstellar medium by using high spatial resolution emission-line imagery and optical spectrophotometry are presented. The spatially resolved ionization structure are described and the physical mechanisms responsible for the observed emission are analyzed by a detailed comparison of emission characteristics with those predicted by both shock-wave and photoionization models. In NGC77635, imagery reveals variations in density, temperature, and ionization structure on scales ranging from the size of the nebula down to the seeing limit of approximately 2.5 seconds. The overall emission in the nebula is dominated by the overwhelming contribution of the H II region and is characteristic of photoionization processes. The embedded, photoevaporating cloud in NGC 7635 contributes enough mass over a dynamical lifetime to account for the shell mass of 5.0 solar mass. The 'Bubble Nebula' is interpreted as a blister H II region containing a young stellar-wind bubble formed around a post-main-sequence O star. In NGC 2359, imagery reveals variations in density, temperature, and ionization structure on scales ranging from the size of the nebula down to the seeing limit of approximately 2.1 seconds. The structure of the H II region can be understood in terms of a photoionized conical cavity protruding into the surrounding molecular cloud. The emission in the bubble region is characteristic of that produced in the incomplete cooling region behind a stellar-wind shock wave. The results of the spectrophotometry reveal an (OIII) temperature of approximately 27,000 K for the western rim of the bubble, indicative of shock-excited emission. NGC 2359 is interpreted as a blister H II region containing a stellar-wind bubble formed at the edge of a dense, molecular cloud. Dissert. Abstr.

N90-29272 California Univ., Santa Cruz.
THE FORMATION OF GLOBULAR CLUSTERS Ph.D. Thesis
Stephen David Murray 1989 103 p
Avail: Univ. Microfilms Order No. DA9011838

The formation of globular clusters is studied, beginning with star formation. It is proposed that the fragmentation of a protocluster proceeded in two steps. First, perturbations grew rapidly due to thermal instability. The perturbations then had short timescales for the growth of gravitational instabilities, so that fragmentation could be completed on a timescale much less than the dynamical timescale of the parent cloud. The process is modeled using one-dimensional hydrodynamic simulations of clouds both with and without external heat sources. The models include the effects of a nonequilibrium H2 abundance. Cloud-cloud collisions are also simulated. Gravitational instability is investigated by numerically integrating the evolution of Lagrangian perturbations of the fluid variables. Protoclusters form in a protogalactic cloud cooling from its virial temperature. Dynamical effects on the growth of perturbations in these clouds are examined. Finally, collisional mechanisms are examined by which metals can diffuse throughout a protocluster before star formation can occur. It is found that collisional diffusion is too slow for metals to diffuse throughout an entire protocluster on acceptable time scales. Metals may, however, be able to diffuse throughout the star forming regions in cloud-cloud collisions. If the iron and CNO elements are preferentially contained in grains of different sizes, then this latter process might explain the existence of uniformities in (Fe/H) coincidentally in clusters which show CNO variations. Dissert. Abstr.

N90-29273 Tufts Univ., Medford, MA.
ON THE INFRARED BEHAVIOUR OF SOME NON-MINKOWSKIAN QUANTUM FIELDS Ph.D. Thesis
Chandra Pathinayake 1989 74 p
Avail: Univ. Microfilms Order No. DA9011945

The infrared structure of some quantum fields in several spacetimes was studied. Here infrared refers to effects associated with modes whose wave length is large compared to the characteristic scale of the space. Several situations dealing with aspects of this question are analyzed. It is shown that the infrared behavior of a massless scalar field and an antisymmetric tensor field in de Sitter space are different even though these two fields appear to be formally equivalent. The scalar field does not have a de Sitter-invariant quantum state, while the antisymmetric tensor is shown to have a well-behaved de Sitter-invariant vacuum. The second topic considered is the behavior of the expectation value of phi squared for a massless scalar field phi whose quantum state is free from infrared divergences in spatially flat Robertson-Walker universes. If the universe expands as a power of comoving time and the power is greater than 3/2, then phi squared grows for a finite interval of time. The next topic discussed is zero-frequency modes of massless scalar fields and vector fields

in compact spaces. In some spaces they are growing functions of time. It is shown that growth rates can be related to initial conditions of the theory if the mass of the field is a function of time which varies from a constant in the past to 0 in the future. Growth in zero modes of a scalar field phi would lead to growth in phi squared. The relevance of these growing expectation values of squared field operators in global symmetry breaking is studied.
Dissert. Abstr.

N90-29274*# Wheaton Coll., Norton, MA. Dept. of Physics and Astronomy.
THE IONIZATION STRUCTURE OF PLANETARY NEBULAE 10: NGC 2392 Semiannual Report
Timothy Barker (Kitt Peak National Observatory, Tucson, AZ.) 3 Oct. 1989 40 p
(Grants NAG5-1292; NsG-5376)
(NASA-CR-186960; NAS 1.26:186960) Avail: NTIS HC A03/MF A01 CSCL 03B

Spectrophotometric observations of emission-line intensities over the spectral range 1400 to 7200 A were made in six positions in the planetary nebula NGC 2392. Standard equations used to correct for the existence of elements in other than the optically observable ionization stages give consistent results for the different positions that are in excellent agreement with abundances calculated using ultraviolet lines, and there is no evidence for any abundance gradient in the nebula. The logarithmic abundances agree well with determinations by Aller and Keyes. Author

N90-29275*# National Aeronautics and Space Administration. Goddard Space Flight Center, Greenbelt, MD.
PW VUL: A CLASSICAL NOVA WITH NEARLY SOLAR ABUNDANCES
P. Saizar, G. J. Ferland, R. M. Wagner, S. Austin, Sumner G. Starrfield, J. W. Truran, George Sonneborn, S. J. Kenyon, W. M. Sparks, and R. E. Williams (Cerro Tololo Inter-American Observatory, La Serena, Chile) et al 1990 17 p Presented at the Evolution in Astrophysics: IUE Astronomy in the Era of New Space Missions, Toulouse, France, 29 May - 1 Jun. 1990 Submitted for publication
(Contract NAG5-481; W-7405-eng-36; NSF AST-88-18215; NSF AST-87-19607)
(NASA-CR-185080; NAS 1.26:185080; DE90-014912; LA-UR-90-2388; CONF-9005248-3) Avail: NTIS HC A03/MF A01 CSCL 03B

Ultraviolet and optical spectrophotometric data were combined in order to determine the physical parameters in the expanding shell of Nova PW Vul 1984 No. 1. Ultraviolet data were obtained with the IUE satellite from August 2, 1984 (a few days after discovery) until it became too faint to study with the satellite. The last IUE exposure was obtained in June 1988 but is still being followed with ground-based optical telescopes. A plot is presented that shows the variation of electron density and temperature as a function of time. Analysis of the emission line intensities show that the abundances of this very slow nova are solar for helium, carbon, and oxygen while nitrogen is 50 times solar. The CLOUDY code of Ferland is used to model the emission line intensities and find very good agreement with the observations. Plots of representative IUE and optical spectra are displayed. DOE

N90-29276*# National Aeronautics and Space Administration. Goddard Space Flight Center, Greenbelt, MD.
NOVA LMC (LARGE MAGELLANIC CLOUD) 1990 NO. 1: THE FIRST EXTRAGALACTIC NEON NOVA
George Sonneborn, Steven N. Shore, and Sumner G. Starrfield (Los Alamos National Lab., NM.) 1990 5 p Presented at the Evolution in Astrophysics: IUE Astronomy in the Era of New Space Missions, Toulouse, France, 29 May - 1 Jun. 1990 Submitted for publication
(Contract NAG5-181; NAG5-1393; W-7405-eng-36; NSF AST-88-18215)
(NASA-CR-180409; NAS 1.26:180409; DE90-014917; LA-UR-90-2372; CONF-9005248-1) Avail: NTIS HC A01/MF A01 CSCL 03B

IUE observations of Nova LMC 1990 No. 1, the first neon (or ONeMg) nova observed outside the Galaxy, were obtained from 17 January 1990 through March 1990, with especially dense coverage during the first 25 days of the outburst. (The neon nova categorization is based on the detection of forbidden Ne III-V lines in optical spectra; the ultraviolet neon lines were not detected.) During the first 30 days of the outburst, the radiative losses were dominated by the N V wavelength 1240 and C IV wavelength 1550 lines. The maximum ejection velocity was approximately 8000 km/s, based on the blue absorption edge of the C IV P-Cygni profile. Early in the outburst of Nova LMC 1990 No. 1 the UV luminosity alone was approximately 3 x 10(exp 38) erg/sec, implying that the bolometric luminosity was well in excess of the Eddington luminosity for a one solar mass object. DOE

N90-29277# Los Alamos National Lab., NM.
KAPPA EFFECT PULSATIONAL INSTABILITY FOR HOT EXTREME HELIUM STARS
Arthur N. Cox 1990 4 p Presented at the Confrontation Between Stellar Pulsation and Evolution, Bologna, Italy, 28-31 May 1990 Submitted for publication
(Contract W-7405-eng-36)
(DE90-014920; LA-UR-90-2368; CONF-9005249-4) Avail: NTIS HC A01/MF A01

A long standing problem for the hydrogen deficient stars has been the mechanism for the pulsation instability for the hottest members of this class. The usual (kappa) mechanism works well for stars that are in the hydrogen and helium ionization instability strip, and this strip extends to perhaps 20,000K at high luminosity. However, several stars are definitely hotter. Investigations for another ionization instability strip, such as for carbon, have always shown that there is not enough carbon to produce a rapid enough increase of opacity with temperature to give the well-known (kappa) effect. This is so even though these hydrogen deficient stars do show enhanced carbon in their spectra. A strong stellar wind can produce the observed hydrogen deficiency. Another popular mechanism is mass loss in a binary system through the Roche lobe. It now is possible that the missing pulsational instability mechanism is the rapid increase of iron lines absorption as the temperature increases above about 150,000K in the low density envelopes of these luminous stars. Recent calculations shows that the $n = 3$ to $n = 3$ transitions in iron that were assumed unimportant in the earlier Los Alamos calculations can double or triple the opacity suddenly as the iron lines appear in a very sensitive part of the spectrum of the diffusing photons. It has been proposed that these iron lines also cause the many varieties of normal B star pulsations, and the hydrogen deficient stars are merely another example of this new (kappa) effect for pulsating stars. The extreme helium star V2076 Oph at 31,900K, and 38,900 solar luminosity for a solar mass of 1.4, pulsates in the radial fundamental model at about 1 day period with a very large linear growth rate when the iron lines more than double the opacity.
DOE

N90-29278# Los Alamos National Lab., NM. Theoretical Div.
NONRADIAL INSTABILITY STRIPS FOR POST-AGB STARS
Letizia Stanghellini, Arthur N. Cox, and Sumner G. Starrfield (Arizona State Univ., Tempe.) 1990 5 p Presented at the Confrontation Between Stellar Pulsation and Evolution Conference, Bologna, Italy, 28-31 May 1990
(Contract W-7405-eng-36; NSF ASF-88-18215)
(DE90-014922; LA-UR-90-2366; CONF-9005249-2) Avail: NTIS HC A01/MF A01

Several pre-degenerate (PNN and DO) and degenerate (DB) models were tested for stability against nonradial oscillations. These models lie on the 0.6 solar mass evolutionary track calculated by Iben. The post-AGB stars have a residual CO core with only a little surface hydrogen and helium. In order to match all the observed pulsators, three different surface compositions were used for the DO stars, and a pure helium surface for the DB white dwarfs. Three DO and 1 DB instability strips were found that were compared to the available observations. DOE

N90-29279# Los Alamos National Lab., NM.
PULSATIONS OF B STAR MODELS BY AN OPACITY MECHANISM
Arthur N. Cox and Siobahn M. Morgan (Washington Univ., Seattle.) 1990 4 p Presented at the Confrontation Between Stellar Pulsation and Evolution, Bologna, Italy, 28-31 May 1990 Submitted for publication
(Contract W-7405-eng-36)
(DE90-014923; LA-UR-90-2365; CONF-9005249-5) Avail: NTIS HC A01/MF A01

The pulsation mechanism for B stars has been sought for 30 years. No proposed radial or nonradial mechanism, either deeply seated or in the surface layers, has been successful in explaining all the observational details. Perhaps the missing piece in the puzzle is the opacity of the stellar material. Many times the first author has tried to make unconventional surface compositions give instability, but none were ever found. We now propose that the sudden appearance of a tremendous number of iron lines, as the temperature rises above about 150,000 K, gives a high sensitivity of the opacity to temperature at the very low densities found in these blue giants. Opacities need to increase quickly to a factor of three or more above the Cox-Tabor (1976) values in the range around 200,000 K. These increases are the same needed to decrease theoretical period ratios of double-mode Cepheids and (delta) Scuti variables to agree better with observations for conventional yellow giant masses. The reason why not all B stars pulsate is that a slight primordial deficit in the iron abundance in the surface layer (1 times 10 to the minus 6 power of the mass) can reduce the opacity and its sensitivity to temperature. A slight amount of iron concentration by radiative levitation could make a star pulsate even if it did not originally have enough primordial iron to cause this opacity mechanism to operate. Then any slow slight mixing caused by the unstable nonradial pulsations could restabilize the pulsations as actually observed in (alpha) Vir and (beta) CMa. Rapid levitation and mixing for the very luminous B stars with their very low density envelopes could even explain the puzzling luminous blue variables with this standard (kappa) mechanism. Large amplitude pulsations like those seen in BW Vul would indicate a somewhat larger iron abundance compared to all other B stars. DOE

N90-29280*# Columbia Univ., New York, NY. Dept. of Astronomy and Physics.
X RAY SPECTRA OF CATACLYSMIC VARIABLES Final Report, 1 Jun. 1988 - 31 May 1990
Joseph Patterson and Jules Halpern 20 Sep. 1990 33 p
(Grant NAG8-729)
(NASA-CR-187002; NAS 1.26:187002; CAL-1830) Avail: NTIS HC A03/MF A01 CSCL 03B

X ray spectral parameters of cataclysmic variables observed with the 'Einstein' imaging proportional counter were determined by fitting an optically thin, thermal bremsstrahlung spectrum to the raw data. Most of the sources show temperatures of order a few keV, while a few sources exhibit harder spectra with temperatures in excess of 10 keV. Estimated 0.1 to 3.5 keV luminosities are generally in the range from 10(exp 30) to 10(exp 32) erg/sec. The results are consistent with the x rays originating in a disk/white dwarf boundary layer of non-magnetic systems, or in a hot, post-shock region in the accretion column of DQ Her stars, with a negligible contribution from the corona of the companion. In a few objects column densities were found that are unusually high for interstellar material. It was suggested that the absorption occurs in the system itself. Author

N90-29281# International Centre for Theoretical Physics, Trieste (Italy).
QUANTIFYING THE FIR INTERACTION ENHANCEMENT IN PAIRED GALAXIES
Cong Xu and Jack W. Sulentic (Alabama Univ., Tuscaloosa.) Jan. 1990 6 p
(DE90-627485; IC-90/15) Avail: NTIS (US Sales Only) HC A02/MF A01

The Catalog of Isolated Pairs of Galaxies in the Northern Hemisphere, by Karachentsev (1972) was studied and a well matched comparison sample taken from the Catalog of Isolated Galaxies, by Karachentseva (1973) in order to quantify the enhanced FIR emission properties of interacting galaxies. DOE

N90-29282# Centro Brasileiro de Pesquisas Fisicas, Rio de Janeiro.
VISCOUS CAUSAL COSMOLOGIES
M. Novello, J. M. Salim, J. Torres, and H. P. deOliveira (Universidade do Estado do Rio de Janeiro, Brazil) 1989 23 p Submitted for publication
(DE90-627487; CBPF-NF-025/89) Avail: NTIS (US Sales Only) HC A03/MF A01

A set of spatially homogeneous and isotropic cosmological geometries generated by a class of non-perfect fluids is investigated. The irreversibility of this system is studied in the context of causal thermodynamics which provide a useful mechanism to conform to the non-violation of the causal principle. DOE

91 LUNAR AND PLANETARY EXPLORATION

Includes planetology; and manned and unmanned flights.
For spacecraft design or space stations see *18 Spacecraft Design, Testing and Performance.*

N90-29283 State Univ. of New York, Stony Brook.
INFRARED SPECTROSCOPIC MEASUREMENTS ON PLANETARY ATMOSPHERIC GASES Ph.D. Thesis
Suryanarayanan Chudamani 1989 167 p
Avail: Univ. Microfilms Order No. DA9012636

Infrared spectroscopic measurements were performed on trace gas molecules known to be infrared-active in the atmospheres of Earth and the Outer Planets. The measurements were performed at low temperatures relevant to the planetary atmospheres employing the high spectral resolution attainable with a tunable diode laser spectrometer. Accurate data on the intensities, N(2-), O(2-), and air-broadened half-widths of lines in the nu(sub 1)-fundamental band (7.78 microns) of 14-N2O-16 were obtained at several temperatures between 185 and 296 K. These data are needed in remote sensing, ozone depletion, and climate modeling studies of the terrestrial atmosphere. The pressure-induced shifts of some 14-N2O-16 lines were also measured. Intensity data in the 10(sup 0)0-01(sup 1)0 band (13.87 microns) of 12-C16-O2 at 295 K which are useful in studies of the thermal structure of the Earth's atmosphere were measured. They differ significantly from previously published and cataloged data. Measurements of the absolute intensities and the H2-broadened half-widths of several spectral lines in the nu(sub 3) band of GeH4, which was detected in the atmospheres of the Outer Planets, were performed at low temperatures between 94 and 300 K. The combined intensity of the nu(sub 3) bands of all of the five isotopic species of GeH4 as well as that of the Q-branches alone were measured independently at 294 using the Wilson-Wells-Penner-Weber Technique. Absolute intensities, collision-broadened half-widths, and pressure-induced shifts of several lines in the nu(sub 4)-fundamental bands of 12-CH4 and 13-CH4 around 7.70 microns, the nu(sub 2)-fundamantal band of 12-CH3D at 4.55 microns, the nu(sub 3)-fundamental band of 12-CH3D at 7.76 microns, the nu(sub 6)-fundamental band of 12-CH3D at 8.61 microns, and the CO fundamental at 4.67 microns, all of which appear in the spectra of the Outer Planets, were measured at low temperatures. He, Ne, Ar, H2, N2, O2, and air were used as the broadening gases. Dissert. Abstr.

N90-29284*# Iowa Univ., Iowa City. Dept. of Physics and Astronomy.
NEW VOYAGER RADIO SPECTROGRAMS OF URANUS
W. Calvert and D. Tsintikidis Jun. 1990 48 p
(Grant NAGw-1206)
(NASA-CR-180381; NAS 1.26:180381; U-of-Iowa-90-13) Avail: NTIS HC A03/MF A01 CSCL 03B

New, high-resolution spectrograms of the Voyager-2 radio observations at Uranus were produced from the original, six-second Planetary Radio Astronomy (PRA) data and these show a number of new features which were not obvious in previous versions. Among these new features are the detailed structure of the so-called broadband-bursty (b-bursty) emissions, unexpected sloping striations in the smooth high-frequency (SHF) component, and the overlap of these two components during the first rotation after closest approach. In addition, a slightly different planetary rotation rate from the b-bursty emissions, was found, and at the initial onset of the SHF component, what appears to be the shadow of a Uranian plasmasphere. These new spectrograms were prepared using a special dithering algorithm to show signal strengths as gray shadings, and the data were also manually cleaned to suppress noise and interference. This produced spectrograms of exceptional quality and certain details of their production on a stand-alone personal computer are also discussed. Author

92 SOLAR PHYSICS

Includes solar activity, solar flares, solar radiation and sunspots.

For related information see *93 Space Radiation.*

N90-29285# Oak Ridge National Lab., TN.
ENRICHMENT SERVICES FOR CHROMIUM ISOTOPES FOR THE GALLEX (GALLIUM EXPERIMENT) INTERNATIONAL COLLABORATION EXPERIMENT ON SOLAR NEUTRINO FLUX Foreign Trip Report
Andrew J. Szady 16 Jul. 1990 6 p
(Contract DE-AC05-84OR-21400)
(DE90-014300; ORNL/FTR-3672) Avail: NTIS HC A02/MF A01

Detailed discussions were held with members of the Gallium Experiment (GALLEX) international solar neutrino research collaboration concerning negotiations to provide $1.4 million in services to enrich (50)Cr for a (51)Cr neutrino source. The source will be used to calibrate the 20-ton gallium solar neutrino detector currently in place in the Gran Sasso Laboratory in Italy. Funding approval for the enrichment services is expected from the European Common Market by October 19, 1990. The discussions focused on the technical aspects of the enrichment, the health and safety requirements for handling the process gas, cost projections, schedule, the Work-for-Others contract, and the method of payment. Discussions were also held with members of the Nuclear Physics Dept. at the University of Milan concerning the availability of isotopes enriched by the Calutron at the Oak Ridge National Laboratory. Very high purity material is needed to grow crystals for use in double beta decay detectors. Finally, working sessions were held to draft a coauthored paper on the results of using the gas centrifuge to remove trace quantities of (85)Kr from natural xenon. DOE

N90-29286 California Univ., San Diego.
THEORETICAL STUDIES OF PROTON BEAMS IN SOLAR FLARE LOOPS Ph.D. Thesis
David H. Tamres 1989 135 p
Avail: Univ. Microfilms Order No. DA9013714

Physical processes associated with energized streams of protons in the solar flare atmosphere are examined. The importance of proton beam momentum deposition in a flare loop is investigated. Consideration of Coulomb collisions between beam protons and the background plasma leads to general expressions for energy and momentum deposition by polyenergetic protons beams in cold and warm hydrogen targets. It is found that momentum deposition forces are unimportant in comparison with the thermal pressure gradients that arise from nonuniform deposition of beam energy in the case of deka-MeV proton beams, but are potentially important in the case of deka-keV proton beams when the beam energy flux is sufficiently large. The stability of proton beams against resonant scattering by Alfven and magnetoacoustic waves in solar flare loops is addressed by considering the conditions for the effective beam-driven growth of these waves. It is found that proton beams of moderate streaming anisotropy, characterized by an excess of forward momentum in relation to perpendicular momentum, are likely to suffer effective resonant scattering in the loop when the root-mean-square speed V(sub O) exceeds a small multiple of the Alfven speed V(sub A), i.e., when the mean beam energy lies toward the high end of the range 10 to 1000 keV under typical flare conditions of temperature, density, and magnetic field strength. Toward the low end of this range, where V(sub O) is less than or approximately V(sub A), moderately anisotropic proton beams are (unconditionally) stable against resonant scattering by magnetoacoustic waves, and, with assistance from thermal damping, also stable against resonant scattering by Alfven waves. Dissert. Abstr.

N90-29287 Max-Planck-Inst. fuer Physik und Astrophysik, Garching (Germany, F.R.). Inst. fuer Extraterrestrische Physik.
ALFVEN WAVE SOLITONS AND SOLAR INTERMEDIATE DRIFT BURSTS
R. A. Treumann, M. Guedel, and A. O. Benz (Eidgenoessische Technische Hochschule, Zurich, Switzerland) Jan. 1990 30 p Submitted for publication
(MPE-Preprint-173; ETN-90-97425) Copyright Avail: Fachinformationszentrum Karlsruhe, 7514 Eggenstein-Leopoldshafen 2, Fed. Republic of Germany

Stationary solutions for the Alfven solitons propagating obliquely in a homogeneous magnetic field are investigated. Due to their dispersive nature kinetic Alfven waves can evolve into soliton like structures which propagate at velocities of the order of the Alfven velocity in a direction inclined to the magnetic field. In a first model, a cold plasma with beta less than (m sub e/m sub i) is considered. In the second model the plasma contains two electron components, a hot one and a cold one. Differential equations for the plasma density are derived and examples of numerical solutions for the plasma density profiles are presented. Kinetic Alfven solitons can propagate in both cases at Mach numbers M greater or less than 1, as rarefactions or as compressions of the plasma density. In both models rarefaction and compressional solitons are uniquely determined by beta and the propagation velocity vector. Interaction between the hot and cold electron components turn out to be significant for rarefactions of the cold component. Conditions for the existence of soliton solutions are given. The super-Alfvenic kind of solitary waves are applied to solar intermediate drift radio bursts. With a model of the emission process they can be used to determine the magnetic field and the electron density of the source. ESA

N90-29288# Los Alamos National Lab., NM.
SOLAR OSCILLATION FREQUENCY AND SOLAR NEUTRINO PREDICTIONS
Arthur N. Cox Jul. 1990 15 p Presented at the Confrontation Between Stellar Pulsation and Evolution, Bologna, Italy, 28-31 May 1990 Submitted for publication
(Contract W-7405-eng-36)
(DE90-014918; LA-UR-90-2370; CONF-9005249-1) Avail: NTIS HC A03/MF A01

The light and velocity variations of the Sun and solar-like stars are unique among intrinsic variable stars. Unlike all other standard classes, such as Cepheids, B stars, and white dwarfs, the pulsation driving is caused by coupling with the acoustic noise in the upper convection zone. Each global pulsation mode is just another degree of freedom for the turbulent convection, and energy is shared equally between these g(sup (minus))-modes and the solar oscillation modes. This driving and damping, together with the normal stellar pulsation mechanisms produce extremely low amplitude solar oscillations. Actually, the surface layer radiative damping is strong, and the varying oscillation mode amplitudes manifest the stochastic convection driving and the steady damping. Thus stability calculations for solar-like pulsations are difficult and mostly inconclusive, but calculations of pulsation periods are as straightforward as for all the other classes of intrinsic variable stars. The issue that is important for the Sun is its internal structure,

because the mass, radius, and luminosity are extremely well known. Conventionally, we need the pulsation constants for each of millions of modes. Unknown parameters for constructing solar models are the composition and its material pressure, energy, and opacity, as well as the convection mixing length. We treat the nuclear energy and neutrino production formulas as sufficiently well known. The presence of weakly interacting massive particles (WIMPs) orbiting the solar center affects the predicted oscillation frequencies so that they do not agree with observations as well as those for models without WIMPs. DOE

N90-29289# Texas Univ., Austin. Inst. for Fusion Studies.
VLASOV-MAXWELL EQUILIBRIA OF SOLAR CORONAL LOOPS
V. Krishan, T. D. Sreedharan (Indian Inst. of Astrophysics, Bangalore.), and Swadesh M. Mahajan Jul. 1990 26 p
(Contract DE-FG05-80ET-53088)
(DE90-015025; DOE/ET-53088/440; IFSR-440) Avail: NTIS HC A03/MF A01

A Vlasov-Maxwell description of the ubiquitous solar Coronal structures is presented. It is found that an equilibrium plasma configuration can live with spatial gradients in density, temperature, current, and drift speeds of the charged particles. Any stability study must be carried over this inhomogeneous equilibrium state. In addition, the Vlasov description admits the investigation of kinetic processes like heating and radiation. DOE

93 SPACE RADIATION

Includes cosmic radiation; and inner and outer earth's radiation belts.

For biological effects of radiation see *52 Aerospace Medicine*. For theory see *73 Nuclear and High-Energy Physics*.

N90-29290*# National Aeronautics and Space Administration. Langley Research Center, Hampton, VA.
COMPARISON OF DOSE ESTIMATES USING THE BUILDUP-FACTOR METHOD AND A BARYON TRANSPORT CODE (BRYNTRN) WITH MONTE CARLO RESULTS
Judy L. Shinn, John W. Wilson, John E. Nealy, and Francis A. Cucinotta (Rockwell International Corp., Houston, TX.) Washington Oct. 1990 29 p
(NASA-TP-3021; L-16806; NAS 1.60:3021) Avail: NTIS HC A03/MF A01 CSCL 03B

Continuing efforts toward validating the buildup factor method and the BRYNTRN code, which use the deterministic approach in solving radiation transport problems and are the candidate engineering tools in space radiation shielding analyses, are presented. A simplified theory of proton buildup factors assuming no neutron coupling is derived to verify a previously chosen form for parameterizing the dose conversion factor that includes the secondary particle buildup effect. Estimates of dose in tissue made by the two deterministic approaches and the Monte Carlo method are intercompared for cases with various thicknesses of shields and various types of proton spectra. The results are found to be in reasonable agreement but with some overestimation by the buildup factor method when the effect of neutron production in the shield is significant. Future improvement to include neutron coupling in the buildup factor theory is suggested to alleviate this shortcoming. Impressive agreement for individual components of doses, such as those from the secondaries and heavy particle recoils, are obtained between BRYNTRN and Monte Carlo results. Author

N90-29291 Massachusetts Univ., Amherst.
RADIO OUTBURSTS IN EXTRAGALACTIC SOURCES Ph.D. Thesis
Wayne Morris Kinzel 1989 254 p
Avail: Univ. Microfilms Order No. DA9011754

Three aspects of the flux density variability of extragalactic radio sources were examined: millimeter wavelength short timescale variability, the spectral evolution of outbursts, and whether the outbursts are periodically spaced. Observations of extragalactic radio sources were conducted using the Five College Radio Astronomy Observatory between January and June 1985 at 88.2 GHz and during June and July 1985 at 40.0 GHz. Many of the sources exhibited significant flux density variations during the observing span. In addition, the most rapid variations observed were comparable with those reported in previous works. Two sources, 0355+50 and OJ287, both exhibited outbursts whose rise and fall timescales were less than a month. An anomalous flux density dropout was observed in 3C446 and was interpreted as an occultation event. Data at five frequencies between 2.7 and 89.6 GHz from the Dent-Balonek monitoring program were used to investigate the spectral evolution of eight outbursts. Outburst profile fitting was used to deconvolve the individual outbursts from one another at each frequency. The fit profiles were used to generate multiple epoch spectra to investigate the evolution of the outbursts. A phase residual minimization method was used to examine four sources for periodic behavior. Dissert. Abstr.

N90-29292 Durham Univ. (England).
GAMMA RAY EVIDENCE FOR COSMIC RAY SOURCES Ph.D. Thesis
Martin John Rogers 1988 179 p
Avail: Univ. Microfilms Order No. BRD-88170

Strong evidence has been found in recent years that certain classes of object contain and are able to accelerate particles to high energies. The problem of the origin of cosmic rays is addressed in two different ways. Firstly, two different regions of the Galaxy are studied using gamma ray observations from the COS-B satellite combined with atomic and molecular gas measurememts. The Vela region contains a pulsar and a supernova remnant and is a particularly valuable location for cosmic ray studies because of its proximity, the association of the two objects, and the intensity of the gamma ray flux it produces. At greater longitudes, the region around the peculiar object eta Carinae is also studied. It is rich in potential sources of cosmic rays including active stars and a spiral arm seen at a tangent at l approx. 282 deg. Analysis of the Vela region reveals strong evidence for cosmic ray production at all energies observed by COS-B. The supernova remnant seems the most likely candidate. The excess gamma ray emission from around eta Carinae seems to be coming predominantly from the spiral arm, which is the evidence of cosmic ray acceleration by the spiral shock in a particular, known spiral arm which is observed as a feature in the gas. The gamma rays are produced in the gas clouds associated with this arm. The second approach involves a model for cosmic ray production in supernova remnants and is used in association with a Monte Carlo simulation of their occurrence in the Galaxy. The motion of the Sun is also taken into account and the supernova explosions occur mainly in spiral arms. The results are in the form of a time sequence of energy density values and are compared in detail with Be-10 results. It is found that the model accounts for the long term rise in the concentration of this radioisotope and does not predict large excursion from the mean energy density that beset older models. Thus the cosmic ray production by supernova remnants seems to be consistent with the radioisotope data. Dissert. Abstr.

N90-29293 Royal Aerospace Establishment, Farnborough (England).
PREDICTIONS OF RADIATION BACKGROUNDS FOR GRO/OSSE
C. S. Dyer, P. R. Truscott, A. J. Sims, C. Comber, and N. D. A. Hammond (SD-Europe, Farnborough, England) 23 Nov. 1989 21 p
(RAE-TM-Space-372; BR112728; ETN-90-97422) Copyright Avail: NTIS HC A03/MF A01

In view of the important influence of background radiation induced by the charged particle environment on the sensivity of spaceborne gamma ray instrumentation, an extensive series of simulations was performed on representations of the Oriented Scintillation Spectrometer Experiment (OSSE) and Gamma Ray Observatory (GRO) spacecraft. Previously reported results on

shielding are summarized and new results are presented on the influence of detector and spacecraft orientation within anisotropic trapped proton distributions. For the cosmic ray calculation, confidence is obtained by comparison with background observations obtained during a balloon flight of a single detector unit over Alice Springs, Australia. ESA

N90-29294# Instituto de Pesquisas Espaciais, Sao Jose dos Campos (Brazil).
FLUCTUATIONS IN COSMIC BACKGROUND RADIATION [FLUTUACOES NA RADIACAO COSMICA DE FUNDO]
Thyrso VillelaNeto Jun. 1988 13 p In PORTUGUESE; ENGLISH summary Presented at the 1st Seminar on Atmospheric and Space Science of the Brazilian Antarctic Program
(INPE-4579-PRE/1313) Avail: NTIS HC A03/MF A01

The angular distribution of the cosmic background radiation and the need for an experiment in an intermediate angular scale is discussed. This is a region that is not well investigated where the theoretical predictions can be tested. Author

99 GENERAL

N90-29295# Massachusetts Inst. of Tech., Cambridge. Research Lab. of Electronics.
[STATEMENT OF RESEARCH OBJECTIVES AND SUMMARY OF RESEARCH EFFORTS] Progress Report, 1 Jan. - 31 Dec. 1989
Jonathan Allen, Daniel Kleppner, and Barbara Passero, ed. Dec. 1989 374 p
(RLE-PR-132) Avail: NTIS HC A16/MF A02

Each chapter contains both a statement of research objectives and a summary of research efforts for research projects listed. Faculty, research staff, students and others who participated in these projects are identified at the beginning of each project, along with sources of funding. A partial list of some research areas are: Submicron Structures Technology and Research; Microstructural Evolution in Thin Films of Electronic Materials; Focused Ion Beam Fabrication; Chemical Reaction Dynamics at Surfaces; Measurement of Electron-phonon Interactions Through Large-amplitude Phonon Excitation; Optics and Quantum Electronics; Novel Processes and Materials for Infrared Nonlinear Optics; Statistical Mechanics of Surface Systems and Quantum-Correlated Systems; X Ray Diffuse Scattering; Ultralow Temperature Studies of Nanometer Size Semiconductor Devices; Small Angle X Ray and Neutron Scattering - Its Application to Supramolecular Solutions; Plasma Dynamics; Electromagnetic Wave Theory and Applications; Radio Astronomy; Speech Processing Research Program; Computer-Aided Fabrication System Structure; Custom Integrated Circuits; Neurophysiology and Neural Computation; Auditory Psychophysics and Aids for the Deaf; Signal Transmission in the Auditory System; and Linguistics. Author

N90-29296# National Inst. of Standards and Technology, Gaithersburg, MD. Center for Atomic, Molecular, and Optical Physics.
TECHNICAL ACTIVITIES 1989, ELECTRON AND OPTICAL PHYSICS DIVISION
C. W. Clark Feb. 1990 56 p
(PB90-207267; NISTIR-90/4287) Avail: NTIS HC A04/MF A01 CSCL 05D

The report summarizes technical activities of the National Institute of Standard and Technology (NIST) Electron and Optical Physics Division during FY-89. These fall into five general areas: soft x ray radiometry, operation of the SURF-II synchrotron storage ring; electron microscopy and basic surface physics; soft x ray emission studies; and multiphoton processes. A listing is given of calibration services, publications, talks, and other relevant activities of the Division's staff. GRA

N90-29297# National Academy of Engineering, Washington, DC.
ENGINEERING AND THE ADVANCEMENT OF HUMAN WELFARE. TEN OUTSTANDING ACHIEVEMENTS 1964-1989
5 Dec. 1989 51 p LIMITED REPRODUCIBILITY: More than 20% of this document may be affected by color photographs Document contains color illustrations
(ISBN-0-309-04185-6; LC-89-63947; NAS-069) Avail: NTIS HC A04/MF A01

The years 1964 to 1989, the first 25 years of the National Academy of Engineering, have witnessed more advancement in technology and, consequently, greater change in the lives of people than any previous 25-year period in recorded history. As part of its anniversary celebration, the Academy has selected what it considers to be the 10 outstanding engineering achievements that have reached the public since the Academy's founding on December 5, 1964. Each represents a major advance or breakthrough in engineering and a significant contribution to human welfare. This brochure presents each of the 10 achievements in a separate story, where some of the engineering challenge, insight, and excitement that attended the achievements are shared. In doing so, it is hoped also to convey a better understanding of what engineering does and how it has contributed to human welfare over the past quarter century by improving lives, extending possibilities, and expanding horizons. Author

N90-29298# Instituto de Pesquisas Espaciais, Sao Jose dos Campos (Brazil).
ACTIVITIES REPORT FOR THE IBDF-INPE PROJECT SEQE, YEAR 1987
Alberto WaingortSetzer, Marcos daCostaPereira, Alfredo daCostaPereira, Jr., and Sergio Alberto deOliveiraAlmeida (Brazilian Inst. for Forestry Development, Sao Jose dos Campos.) May 1988 96 p In PORTUGUESE; ENGLISH summary
(INPE-4534-RPE/565) Avail: NTIS HC A05/MF A01

The purpose was the detection and assessment in near-real time of large biomass fires in the Brazilian Legal Amazon in 1987 using images of the NOAA-9 meteorological satellite, in compliance with a joint IBDF-INPE project. The periods of April 11 to May 13, in the wet season, without fires, and June 15 to October 2, in the dry season, when the fires were monitored. A conservative estimate based in the images resulted in 20 millions ha (200,000 sq km) of burning areas in 1987, of which at least 40 percent corresponded to recently cut forest. Four hundred thousand hectares (4,000 sq km) of burning areas were detected in specific days (with individual cases of 6,000 ha), and producing dense smoke clouds over areas of 1.5 million sq km, which closed airports and irritated the population. The location of the main fires was regularly sent to IBDF. At state level, the percentages of areas burned in relation to those of the states varied from 18.7 percent in Rondonia to 0.1 percent in Amazon. A reconaissance flight was made in the North of Mato Grosso and confirmed the location and extent of the burned areas detected by the satellite. Field work in the region provided information about the burnings. Tables, graphs, and photographs illustrate data and results obtained. Emission of gases from the fires were estimated at 580 million tons. In general, fires have no ecological considerations and their practice bring severe damage to the environment. Author

Typical Subject Index Listing

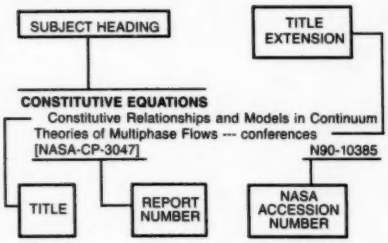

The subject heading is a key to the subject content of the document. Titles, report numbers, and accession numbers of pertinent documents are provided under each subject heading. When the title is insufficiently descriptive of the document content, a title extension has been added, separated from the title by three hyphens. The report number helps to indicate the type of document cited (e.g., NASA report, NASA translation, NASA contractor report). The NASA accession number is the number by which the document abstracts are arranged in this journal and by which the document is sold or requested. The titles, with title extensions if present, are arranged under each subject heading in ascending accession number order. The subject headings have been selected from the latest revision of the *NASA Thesaurus* (NASA SP-7064).

A

A-320 AIRCRAFT
Determination of the ground effect on the characteristics of the A320 aircraft N90-28534
ABEL FUNCTION
Anyons and Chern-Simons theory on compact spaces of finite genus
[DE90-627216] N90-29157
ABILITIES
Predicting F/A-18 fleet replacement squadron performance using an automated battery of performance-based tests
[AD-A223899] N90-28543
Neurophysiological correlates of information processing abilities during divided attention situations in air traffic controllers N90-28989
ABRASION
Mechanical properties testing of diamond and diamond-like films by ultra-low load indentation
[DE90-014456] N90-28861
ABSORPTION SPECTRA
Spectroscopic study of combustion diagnostics on hydroxyl radicals
[NASA-CR-186998] N90-28694
ABSORPTIVITY
XANES and EXAFS study of Au-substituted YBa2Cu3O(7-delta)
[NASA-TM-103291] N90-29219
ABUNDANCE
The ionization structure of planetary nebulae 10: NGC 2392
[NASA-CR-186960] N90-29274
PW Vul: A classical nova with nearly solar abundances
[NASA-CR-185080] N90-29275
ACCELERATION (PHYSICS)
Measurement of gravitational acceleration of antimatter
[DE90-627464] N90-29233
ACCELEROMETERS
Special test and evaluation methods used for a nine-axis accelerometer
[PB90-209578] N90-28622
ACCIDENTS
Helicopter aircrew helmets and head injury: A protective effect
[AD-A223024] N90-29080
ACEE PROGRAM
Energy Efficient Engine high pressure turbine component test performance report
[NASA-CR-168289] N90-28553
Energy Efficient Engine combustor test hardware detailed design report
[NASA-CR-168301] N90-28554
Energy Efficient Engine acoustic supporting technology report
[NASA-CR-174834] N90-28557
Energy Efficient Engine: Flight propulsion system final design and analysis
[NASA-CR-168219] N90-28558
Energy Efficient Engine core design and performance report
[NASA-CR-168069] N90-28559
Energy Efficient Engine integrated core/low spool design and performance report
[NASA-CR-168211] N90-28561
Energy Efficient Engine: Control system component performance report
[NASA-CR-174851] N90-28562
NASA/GE Energy Efficient Engine low pressure turbine scaled test vehicle performance report
[NASA-CR-168290] N90-28563
Energy efficient engine program technology benefit/cost study. Volume 1: Executive summary
[NASA-CR-174766-VOL-1] N90-28564
Energy efficient engine program technology benefit/cost study, volume 2
[NASA-CR-174766-VOL-2] N90-28565
Energy efficient engine pin fin and ceramic composite segmented liner combustor sector rig test report
[NASA-CR-179534] N90-28567
Energy Efficient Engine: Combustor component performance program
[NASA-CR-179533] N90-28568
Energy Efficient Engine: High-pressure compressor test hardware detailed design report
[NASA-CR-180850] N90-28570
ACID RAIN
Preliminary exposure study to determine the effects of acid deposition on coated steel substrates
[PB90-201799] N90-28715
Acid deposition: No such thing as a free launch
[DE90-015085] N90-28920
ACIDITY
Estimating the spatial variability of trace gas deposition velocities
[PB90-208570] N90-28928
ACOUSTIC COUPLING
Combustion instability coupling with feed system acoustics N90-28629
ACOUSTIC FREQUENCIES
The effects of acoustic orientation cues on instrument flight performance in a flight simulator N90-28985
ACOUSTIC MEASUREMENT
Wind tunnel investigation of periodic vortex separation from rough surface circular cylinders by means of acoustic measurements
[ESA-TT-1092] N90-28499
Measuring the vertical directional spectra caused by sea surface sound
[AD-A223883] N90-28957
Large hydrodynamic tunnel: Calculation of the acoustic transparency of the jet stream
[REPT-89/115] N90-29167
Large aperture acoustic arrays in support of reverberation studies
[AD-A224002] N90-29168
ACOUSTIC PROPERTIES
Measuring the vertical directional spectra caused by sea surface sound
[AD-A223883] N90-28957
Electron acoustic and magnetoacoustic modes in a magnetized beam plasma system
[DE90-627473] N90-29199
ACOUSTIC SIMULATION
The simulation of localized sounds for improved situational awareness N90-28984
ACOUSTIC VELOCITY
Thermophysical properties of Helium-4 from 0.8 to 1500 K with pressures to 2000 MPa
[NASA-CR-186992] N90-28681
Measuring the vertical directional spectra caused by sea surface sound
[AD-A223883] N90-28957
ACOUSTICS
Energy Efficient Engine acoustic supporting technology report
[NASA-CR-174834] N90-28557
Liquid Rocket Booster (LRB) for the Space Transportation System (STS) systems study. Appendix B: Liquid rocket booster acoustic and thermal environments
[NASA-CR-183788-APP-B] N90-28602
Methods for detecting low-frequency signals in the presence of strong winds
[AD-A223980] N90-28769
SuperCHIEF: A modified CHIEF (Combined Helmholtz Integral Equation Formulation) method
[DE90-014744] N90-29123
Large aperture acoustic arrays in support of reverberation studies
[AD-A224002] N90-29168
ACTIVE CONTROL
Active control of flexible structures N90-28575
The KALI multi-arm robot programming and control environment N90-29060
ACTUATORS
Active control of flexible structures N90-28575
Liquid Rocket Booster (LRB) for the Space Transportation System (STS) systems study. Appendix C: Battery report for the liquid rocket booster TVC actuators
[NASA-CR-183789-APP-C] N90-28603
Preliminary study of a serial-parallel redundant manipulator N90-29048
Preliminary results on noncollocated torque control of space robot actuators N90-29057
Portable Dextrous Force Feedback Master for robot telemanipulation (PDMFF) N90-29058
ADAPTIVE CONTROL
An expert system to perform on-line controller restructuring for abrupt model changes
[NASA-TM-103609] N90-29121
ADHESION
Factors influencing the mode I interlaminar fracture resistance of toughened matrix composites N90-29668
Scale adherence effects in oxidation and sulfidation N90-28703
ADJUSTING
Adjustable speed drive applications guidebook
[DE90-014151] N90-28780
ADVANCED LAUNCH SYSTEM (STS)
Liquid Rocket Booster (LRB) for the Space Transportation System (STS) systems study. Volume 1: Executive summary
[NASA-CR-183822] N90-28599
Liquid Rocket Booster (LRB) for the Space Transportation System (STS) systems study, volume 2
[NASA-CR-183786] N90-28600
Liquid Rocket Booster (LRB) for the Space Transportation System (STS) systems study. Appendix F: Performance and trajectory for ALS/LRB launch vehicles
[NASA-CR-183792-APP-F] N90-28606
ADVECTION
A nonhydrostatic numerical model in sigma-coordinates and simulations of mesoscale phenomena N90-28932
AEOLIAN TONES
Wind tunnel investigation of periodic vortex separation from rough surface circular cylinders by means of acoustic measurements
[ESA-TT-1092] N90-28499

AEROCAPTURE
Nonequilibrium radiation and chemistry models for aerocapture vehicle flowfields
[NASA-CR-186379] N90-28490
AERODYNAMIC CHARACTERISTICS
Prediction of subsonic vortex shedding from forebodies with chines
[NASA-CR-4323] N90-28494
Projectile supersonic drag characteristics
[AD-A224217] N90-28506
Aerodynamics of Combat Aircraft Controls and of Ground Effects
[AGARD-CP-465] N90-28513
Effects of canard position on the aerodynamic characteristics of a close-coupled canard configuration at low speed N90-28519
The steady and time-dependent aerodynamic characteristics of a combat aircraft with a delta or swept canard N90-28526
Study of ground effects on flying scaled models N90-28532
An in-flight investigation of ground effect on a forward-swept wing airplane N90-28533
Determination of the ground effect on the characteristics of the A320 aircraft N90-28534
Aerodynamic parameters of High-Angle-of attack Research Vehicle (HARV) estimated from flight data
[NASA-TM-102692] N90-28578
AERODYNAMIC COEFFICIENTS
Projectile supersonic drag characteristics
[AD-A224217] N90-28506
A flight dynamic model of aircraft spinning
[AR-005-600] N90-28576
Aerodynamic parameters of High-Angle-of attack Research Vehicle (HARV) estimated from flight data
[NASA-TM-102692] N90-28578
AERODYNAMIC CONFIGURATIONS
Combat aircraft control requirements for agility N90-28517
Energy Efficient Engine high pressure turbine component test performance report
[NASA-CR-168289] N90-28553
Energy Efficient Engine program advanced turbofan nacelle definition study
[NASA-CR-174942] N90-28560
The space transportation main engine phase A' study
[NASA-CR-179399] N90-28610
AERODYNAMIC DRAG
Sting-support interference on afterbody drag at transonic speeds
[NAL-TM-EA-8902] N90-28492
AERODYNAMIC FORCES
Aerodynamic interferences of in-flight thrust reversers in ground effect N90-28529
Turbomachinary rotor forces
[NASA-CR-183779] N90-28852
AERODYNAMIC HEATING
Real-time aerodynamic heating and surface temperature calculations for hypersonic flight simulation
[NASA-TM-4222] N90-28815
AERODYNAMIC INTERFERENCE
Sting-support interference on afterbody drag at transonic speeds
[NAL-TM-EA-8902] N90-28492
Unsteady aerodynamics of controls N90-28525
Aerodynamic interferences of in-flight thrust reversers in ground effect N90-28529
Three-dimensional model testing in the transonic self-streamlining wind tunnel N90-28583
Microgravitation experiments in space: Compatibility with interfering dynamic influences N90-29162
AERODYNAMIC LOADS
NASA/GE Energy Efficient Engine low pressure turbine scaled test vehicle performance report
[NASA-CR-186290] N90-28563
AERODYNAMIC STABILITY
Inflight thrust vectoring: A further degree of freedom in the aerodynamic/flight mechanical design of modern fighter aircraft N90-28528
AERODYNAMIC STALLING
Control research in the NASA high-alpha technology program N90-28516
AERODYNAMICS
Hypersonic Arbitrary-Body Aerodynamics (HABA) for conceptual design
[DE90-014750] N90-28495
Aerodynamics of bodies in shear flow N90-28496
Aerodynamic and propulsive control development of the STOL and maneuver technology demonstrator N90-28514
Aerodynamic control design: Experience and results at Aermacchi N90-28518
Control of vortex aerodynamics at high angles of attack N90-28523
Study of the ground effects in the CEAT aerohydrodynamic tunnel: Using the results N90-28530
Parallelization of a software relating to aerodynamics on MIMD type computers
[ONERA-RT-31/3479-CY] N90-29114
Scientific Colloquium in Honor of Prof. Dr. Rer. Nat. Hermann L. Jordan
[ESA-TT-1101] N90-29159
Numeric fluid mechanics N90-29161
AERONAUTICAL SATELLITES
An aeronautical mobile satellite experiment
[NASA-CR-186971] N90-28593
AEROSOLS
The affect of gravity on particle collection in inertial impactors
[DE90-013372] N90-29173
AEROSPACE ENGINEERING
Fabrication of spherical pressure vessels from composite materials
[INPE-4598-RPE/570] N90-28675
Proceedings of the NASA Conference on Space Telerobotics, volume 2
[NASA-CR-186857] N90-29044
AEROSPACE MEDICINE
Aerospace medicine and biology: A continuing bibliography with indexes (supplement 340)
[NASA-SP-7011(340)] N90-28963
AEROSPACE SYSTEMS
Situational Awareness in Aerospace Operations
[AGARD-CP-478] N90-28972
Automation and robotics technology for intelligent mining systems N90-29018
Causal simulation and sensor planning in predictive monitoring N90-29037
Proceedings of the NASA Conference on Space Telerobotics, volume 2
[NASA-CR-186857] N90-29044
AEROSPACE VEHICLES
Nonequilibrium radiation and chemistry models for aerocapture vehicle flowfields
[NASA-CR-186379] N90-28490
AFTERBODIES
Sting-support interference on afterbody drag at transonic speeds
[NAL-TM-EA-8902] N90-28492
AGGREGATES
Development and testing of rapid repair methods for war damaged runways
[AD-A223970] N90-28586
AGING (MATERIALS)
Development of testing and analysis methodology to assess the long term durability of polymeric composites at high temperatures
[NASA-TM-102714] N90-28871
AGRICULTURE
Data Base Analyzer and Parameter Estimator (DBAPE) interactive computer program user's manual
[PB90-193053] N90-29252
AH-64 HELICOPTER
Plan, execute, and discuss vibration measurements and correlations to evaluate a NASTRAN finite element model of the AH-64 helicopter airframe
[NASA-CR-181973] N90-28866
AIR DATA SYSTEMS
A real time evaluation of the use of a perspective format to promote situational awareness in users of air to air tactical displays N90-28981
AIR DEFENSE
A real time evaluation of the use of a perspective format to promote situational awareness in users of air to air tactical displays N90-28981
Counterair situation awareness display for Army aviation N90-28982
AIR FLOW
A nonhydrostatic numerical model in sigma-coordinates and simulations of mesoscale phenomena N90-28932
AIR JETS
The entrainment rate for a row of turbulent jets
[NASA-CR-185278] N90-28504
AIR MASSES
An investigation of forcing mechanisms during a surprise tornadic thunderstorm
[PB90-216805] N90-28940
AIR POLLUTION
Source emission test of gas turbine engine test facility, Kelly AFB, TX
[AD-A223869] N90-28571
The distribution of middle tropospheric carbon monoxide during early October 1984
[NASA-TM-103485] N90-28906
National air pollutant emission estimates, 1940-1988
[PB90-199266] N90-28908
National air quality and emissions trends report, 1988
[PB90-200114] N90-28909
The global cycle of reactive nitrogen
[DE90-015041] N90-28919
Acid deposition: No such thing as a free launch
[DE90-015085] N90-28920
Tropospheric nitrogen: The influence of anthropogenic sources on distributions and deposition, executive summary
[DE90-015401] N90-28922
Diffusion in the surface layer of the convective boundary layer
[AD-A224125] N90-28924
AIR QUALITY
Source emission test of gas turbine engine test facility, Kelly AFB, TX
[AD-A223869] N90-28571
National air quality and emissions trends report, 1988
[PB90-200114] N90-28909
Diffusion in the surface layer of the convective boundary layer
[AD-A224125] N90-28924
AIR SAMPLING
The affect of gravity on particle collection in inertial impactors
[DE90-013372] N90-29173
AIR TO AIR MISSILES
A real time evaluation of the use of a perspective format to promote situational awareness in users of air to air tactical displays N90-28981
AIR TRAFFIC
Airport capacity enhancement plan 1989
[PB90-197997] N90-28507
AIR TRAFFIC CONTROL
Dallas/Forth Worth simulation. Phase 2: Triple simultaneous parallel Instrument Landing System (ILS) approaches (turbojets)
[DOT/FAA/CT-90/2] N90-28509
Communications Interface Driver (CID) test plan
[DOT/FAA/CT-TN89/35] N90-28762
AIR TRAFFIC CONTROLLERS (PERSONNEL)
Neurophysiological correlates of information processing abilities during divided attention situations in air traffic controllers N90-28989
AIR WATER INTERACTIONS
The role of clouds in CO2-induced climate change
[DE90-014380] N90-28911
Proceedings of the 14th Annual Climate Diagnostics Workshop
[PB90-196573] N90-28938
Measuring the vertical directional spectra caused by sea surface sound
[AD-A223883] N90-28957
AIRBORNE EQUIPMENT
Description of the MARC measuring system
[FEL-89-B170] N90-28887
AIRCRAFT APPROACH SPACING
Dallas/Forth Worth simulation. Phase 2: Triple simultaneous parallel Instrument Landing System (ILS) approaches (turbojets)
[DOT/FAA/CT-90/2] N90-28509
AIRCRAFT COMMUNICATION
An aeronautical mobile satellite experiment
[NASA-CR-186971] N90-28593
AIRCRAFT CONSTRUCTION MATERIALS
Static and dynamic characterization of the ATR 72 rods made of Ti 10.2.3 titanium alloy
[REPT-49-238] N90-28722
AIRCRAFT CONTROL
Aerodynamics of Combat Aircraft Controls and of Ground Effects
[AGARD-CP-465] N90-28513
Combat aircraft control requirements N90-28515
Control research in the NASA high-alpha technology program N90-28516
Combat aircraft control requirements for agility N90-28517
Effective optimal control of a fighter aircraft engine N90-28548
A sensor stabilization/tracking system for unmanned air vehicles
[AD-A224008] N90-28579
Proprioception in aircraft control
[IZF-1989-43] N90-29082
An expert system to perform on-line controller restructuring for abrupt model changes
[NASA-TM-103609] N90-29121
AIRCRAFT DESIGN
Hypersonic Arbitrary-Body Aerodynamics (HABA) for conceptual design
[DE90-014750] N90-28495
Combat aircraft control requirements for agility N90-28517
Effects of canard position on the aerodynamic characteristics of a close-coupled canard configuration at low speed N90-28519
Innovative control concepts and component integration for a generic supercruise fighter N90-28521
Control of vortex aerodynamics at high angles of attack N90-28523

Inflight thrust vectoring: A further degree of freedom in the aerodynamic/flight mechanical design of modern fighter aircraft N90-28528
Dynamic ground effects N90-28531
Determination of the ground effect on the characteristics of the A320 aircraft N90-28534
Life cycle cost in the conceptual design of subsonic commercial aircraft, volumes 1 and 2 N90-28535
System reliability optimization of aircraft wings N90-28536
The aerodynamic design of the oblique flying wing supersonic transport
[NASA-CR-177552] N90-28540
Energy efficient engine program technology benefit/cost study, volume 2
[NASA-CR-174766-VOL-2] N90-28565
Situational Awareness in Aerospace Operations
[AGARD-CP-478] N90-28972
A knowledge-based system design/information tool
[NASA-CR-4316] N90-29143

AIRCRAFT ENGINES
Effective optimal control of a fighter aircraft engine N90-28548
Energy efficient engine program technology benefit/cost study. Volume 1: Executive summary
[NASA-CR-174766-VOL-1] N90-28564
Energy efficient engine program technology benefit/cost study, volume 2
[NASA-CR-174766-VOL-2] N90-28565
Energy Efficient Engine: Control system preliminary definition report
[NASA-CR-179578] N90-28569
High Temperature Surface Interactions
[AGARD-CP-461] N90-28698
Fretting fatigue strength of Ti-6Al-4V at room and elevated temperatures and ways of improving it N90-28709

AIRCRAFT EQUIPMENT
A reliable, maintenance-free oxygen sensor for aircraft using an oxygen-sensitive coating on potentiometric electrodes
[AD-A222696] N90-28545
Military aircrew seating: A human factors engineering approach
[AD-A218049] N90-28999

AIRCRAFT GUIDANCE
Description of the primary flight display and flight guidance system logic in the NASA B-737 transport systems research vehicle
[NASA-TM-102710] N90-28546

AIRCRAFT INDUSTRY
Radiation-curable prepreg composites
[DE90-629740] N90-28674

AIRCRAFT MANEUVERS
Aerodynamics of Combat Aircraft Controls and of Ground Effects
[AGARD-CP-465] N90-28513
Combat aircraft control requirements N90-28515

AIRCRAFT MODELS
The effects of foreplanes on the static and dynamic characteristics of a combat aircraft model N90-28520
Study of ground effects on flying scaled models N90-28532

AIRCRAFT NOISE
Comparison of speech intelligibility in cockpit noise using SPH-4 flight helmet with and without active noise reduction
[NASA-CR-177564] N90-28510

AIRCRAFT RELIABILITY
System reliability optimization of aircraft wings N90-28536

AIRCRAFT SAFETY
Modeling and analysis of airport and aircraft operations
[PB90-222167] N90-28511

AIRCRAFT SPIN
A flight dynamic model of aircraft spinning
[AR-005-600] N90-28576

AIRFOILS
Two-dimensional wind tunnel test and comparison with calculations for a 15.2 percent thick airfoil section for wind turbines
[FFA-TN-1990-16] N90-28501
The effect of rapid spoiler deployment on the transient forces on an aerofoil N90-28527

AIRFRAMES
NASA Langley Research Center National Aero-Space Plane Mission simulation profile sets
[NASA-TM-102670] N90-28541
Correlation of AH-1G airframe flight vibration data with a coupled rotor-fuselage analysis
[NASA-CR-181974] N90-28865
Plan, execute, and discuss vibration measurements and correlations to evaluate a NASTRAN finite element model of the AH-64 helicopter airframe
[NASA-CR-181973] N90-28866

AIRLINE OPERATIONS
Modeling and analysis of airport and aircraft operations
[PB90-222167] N90-28511

AIRPORTS
Airport capacity enhancement plan 1989
[PB90-197997] N90-28507
Modeling and analysis of airport and aircraft operations
[PB90-222167] N90-28511
Proceedings of a workshop on Future Airport Passenger Terminals
[PB90-213620] N90-28580
Development of acceptance plans for airport pavement materials. Volume 1: Development
[DOT/FAA/RD-90/15] N90-28581
Development of a thickness design procedure for stabilized layers under rigid airfield pavements
[DOT/FAA/RD-90/22] N90-28582

AIRSPACE
Airport capacity enhancement plan 1989
[PB90-197997] N90-28507

ALCOHOLS
Analysis of the T63-A-700 engine used in alcohol turbine fuel extender test
[DOT/FAA/CT-TN90/18] N90-28549

ALERTNESS
Loss of alertness and consciousness from pilot position during long range flight N90-28990

ALGEBRA
Beltrami algebra and symmetry of Beltrami equation on Riemann surfaces
[DE90-627157] N90-29135
The combinatorics computation for Casimir operators of the symplectic Lie algebra and the application for determining the center of the enveloping algebra of a semidirect product
[DE90-627161] N90-29136
Superconformal algebra and central extension of meromorphic vector fields with multipoles on super-Riemann sphere
[DE90-627211] N90-29153

ALGORITHMS
Studies in automatic speech recognition and its application in aerospace N90-28759
Real-time aerodynamic heating and surface temperature calculations for hypersonic flight simulation
[NASA-TM-4222] N90-28815
ROSES, a Robot Operating System Expert Scheduler: Methodological framework
[DE90-014782] N90-28851
Tele-Autonomous control involving contact — object localization
[NASA-CR-187004] N90-28854
Selective learning algorithm for certain types of learning failure in multilayer perceptrons
[AD-A223982] N90-28998
Methods and strategies of object localization N90-29020
Robot Acting on Moving Bodies (RAMBO): Interaction with tumbling objects N90-29022
Approximation algorithms for planning and control N90-29042
Multiresolutional models of uncertainty generation and reduction N90-29043
Efficient mapping algorithms for scheduling robot inverse dynamics computation on a multiprocessor system N90-29071
Parallel algorithms for computation of the manipulator inertia matrix N90-29072
Organising geometric computations for space telerobotics N90-29074
Learning in stochastic neural networks for constraint satisfaction problems N90-29078
LINTERP: A numerical algorithm for interpolating quadrilateral and hexahedral meshes
[DE90-014417] N90-29090
The effect of multiprocessor radius on scaling
[DE90-014772] N90-29095
Recursive least-squares learning algorithms for neural networks
[DE90-014926] N90-29096
Block Lanczos algorithm
[AD-A224011] N90-29111
Least-index resolution of degeneracy in linear complementarity problems with sufficient matrices
[DE90-014406] N90-29145
Prediction, control, and decision-making aspects for chaotic systems
[DE90-014452] N90-29224

ALIGNMENT
Using the x ray region of the electromagnetic spectrum for alignment: Overview, geometric optics, and design considerations
[DE90-014798] N90-28752

ALKALI METALS
Thermodynamics and structure of liquid alkali metals from the charged-hard-sphere reference fluid
[DE90-627792] N90-28725

ALKALIES
Structure of metal overlayers by low energy alkali ion scattering: Cu/Ru(0001) and Sn/Pt(111)
[DE90-014453] N90-28718

ALTITUDE
Space station contamination modeling
[NASA-CR-183871] N90-28590

ALTITUDE SIMULATION
Evaluation of the performance capability of the aviator under hypoxic conditions operational experience N90-28991

ALUMINIDES
High temperature protective coatings: Recent trends N90-28710

ALUMINUM
ARALL (ARamid ALuminum Laminate), a literature survey
[FOA-C-20782-2.5] N90-28671
The stability of the martensitic phases in Cu-Zn-Al at an electron concentration of 1.534
[DE90-628628] N90-28727

ALUMINUM ALLOYS
High temperature oxidation of Al-Li alloys N90-28705
Behavior of Al-Mg alloys in hot working and superplasticity
[DE90-015193] N90-28723

ALUMINUM OXIDES
Electronic conduction in molten cryolite saturated with alumina
[DE90-015090] N90-29211

AMAZON REGION (SOUTH AMERICA)
Activities report for the IBDF-INPE project SEQE, year 1987
[INPE-4534-RPE/565] N90-29298

AMBIENCE
Methods for detecting low-frequency signals in the presence of strong winds
[AD-A223980] N90-28769

AMINO RADICAL
Electrochemical surface finishing using amino-substrates on carbon fibers in organic media. Effects of the finishing on the mechanical properties of carbon-epoxy composites
[ONERA-RT-9/3549-M] N90-28672

AMORPHOUS MATERIALS
Research on high-efficiency, multiple-gap, multi-junction amorphous silicon-based alloy thin-film solar cells
[DE90-000338] N90-28896

AMORPHOUS SILICON
Research on the structural and electronic properties of defects in amorphous silicon
[DE90-000342] N90-28730
Research on stable, large-area, amorphous silicon based submodules, phase 3
[DE90-000339] N90-29204

ANALYTIC FUNCTIONS
The Cousin problems for an overdetermined system of complex partial differential equations
[DE90-627170] N90-29139

ANGLE OF ATTACK
Control research in the NASA high-alpha technology program N90-28516
Development of non-conventional control methods for high angle of attack flight using vortex manipulation N90-28522
Control of vortex aerodynamics at high angles of attack N90-28523
Aerodynamic parameters of High-Angle-of attack Research Vehicle (HARV) estimated from flight data
[NASA-TM-102692] N90-28578

ANGULAR ACCELERATION
Special test and evaluation methods used for a nine-axis accelerometer
[PB90-209578] N90-28822

ANGULAR DISTRIBUTION
Fluctuations in cosmic background radiation
[INPE-4579-PRE/1313] N90-29294

ANIONS
Peak analysis in gas chromatography and the development of new stationary phases for anion chromatography
[DE90-014428] N90-28687

ANISOTROPIC PLATES
Structural analysis and optimum design of geodesically stiffened composite panels
[NASA-CR-186944] N90-28862

ANISOTROPY
A comment on anisotropic spheres admitting one parameter group of conformal motions
[DE90-627195] N90-29230

ANNEALING
Transient annealing characterization of irradiated MOSFETS
[AD-A223877] N90-29220
ANNIHILATION REACTIONS
High temperature surface interactions: Overview N90-28699
ANNUAL VARIATIONS
Annual course of precipitation over much of the US: Observed versus GCM simulation
[PB90-221656] N90-28942
ANOMALIES
Study of anomalies in transition vegetation in Alto Xingo-NT, through remote sensing techniques
[INPE-4601-TDL/334] N90-28891
Causal simulation and sensor planning in predictive monitoring N90-29037
Systematic approach to critical phenomena by the extended variational method and coherent-anomaly method
[DE90-627320] N90-29165
ANTARCTIC REGIONS
Ross Sea oceanographic data, 1983-1987: USCGC GLACIER, January-February 1983; USCGC POLAR SEA, January-February 1984; USCGC POLAR STAR, February 1984; USCGC POLAR SEA, February 1987
[PB90-243932] N90-28955
ANTENNA DESIGN
ATDRS payload technology research and development
[NASA-TM-103256] N90-28596
ANTENNA FEEDS
ATDRS payload technology research and development
[NASA-TM-103256] N90-28596
ANTHROPOMETRY
Human factors model concerning the man-machine interface of mining crewstations N90-29011
ANTICYCLONES
Genesis of bow echoes: A rear-inflow induced meso-convective structure
[PB90-209776] N90-28926
ANTIFERROMAGNETISM
Surface and defect excitations in covalently bonded solids
[AD-A221995] N90-28682
Effects of Al substitution by Fe in CeAl2
[DE90-627843] N90-28726
Antiferromagnetism and enhanced heat in CeM2Sn (M = Ni, Ir, Cu, Rh, Pd, and Pt
[DE90-014924] N90-29206
Susceptibility of the Potts model in an hierarchical lattice: Renormalisation group approach
[DE90-627324] N90-29215
ANTIMATTER
Measurement of gravitational acceleration of antimatter
[DE90-627464] N90-29233
ANTIPARTICLES
Measurement of gravitational acceleration of antimatter
[DE90-627464] N90-29233
ANTISEPTICS
Ozone for trace organic contaminant removal
[PB90-221680] N90-28916
APPLICATIONS PROGRAMS (COMPUTERS)
Software development tools
[PB90-250051] N90-29103
Semiconductor measurement technology. EPROP: An interactive FORTRAN program for computing selected electronic properties of Gallium Arsenide and Silicon
[PB90-222738] N90-29203
APPROACH
Vibration responses of two house structures during the Edwards Air Force Base phase of the national sonic boom program
[NASA-CR-182069] N90-29169
APPROPRIATIONS
Our changing planet: The FY 1991 US global change research program. A report by the committee on Earth Sciences to accompany the FY 1991 budget
[PB90-202623] N90-28907
Federal support to universities, colleges, and selected nonprofit institutions: Fiscal year 1988 (detailed statistical tables)
[PB90-226887] N90-29236
APPROXIMATION
Unsteady aerodynamics of controls N90-28525
Finite element analysis of coupled thermoelasticity
[PB90-201211] N90-28860
Planning 3-D collision-free paths using spheres N90-29024
Approximation algorithms for planning and control N90-29042
Recurrence relations and weight functions for approximation by orthonormal polynomials
[DE90-627156] N90-29134
APTITUDE
Air Force Officer Qualifying Test (AFOQT): Development of quick score composites for forms P1 and P2
[AD-A223868] N90-28997
ARC JET ENGINES
Low power arcjet performance
[NASA-TM-103260] N90-28657
High power arcjet
[NASA-CR-183066] N90-28658
ARCHITECTURE (COMPUTERS)
Using embedded microcontrollers in radar test equipment
[DE90-014997] N90-28763
Target detection in Gaussian noise using artificial neural systems
[AD-A223983] N90-28770
DOE/NIST Workshop on Common Architectures for Robotic Systems
[PB90-216839] N90-28840
A system architecture for a planetary rover N90-29015
The NASA/OAST telerobot testbed architecture N90-29016
Three-dimensional motor schema based navigation N90-29026
A hybrid architecture for the implementation of the Athena neural net model N90-29032
A design philosophy for multi-layer neural networks with applications to robot control N90-29033
State-based scheduling: An architecture for telescope observation scheduling N90-29038
The JPL telerobot operator control station. Part 1: Hardware N90-29049
Implementation and design of a teleoperation system based on a VMEBUS/68020 pipelined architecture N90-29053
Integrating planning, execution, and learning N90-29079
A personal computer-based, multitasking data acquisition system
[NASA-TM-4232] N90-29107
A hardware/software environment to support R/D in intelligent machines and mobile robotic systems
[DE90-014458] N90-29119
Information management directions: The integration challenge
[PB90-219866] N90-29245
ARMED FORCES (UNITED STATES)
Air Force Officer Qualifying Test (AFOQT): Development of quick score composites for forms P1 and P2
[AD-A223868] N90-28997
ARRAYS
Phoenix data analysis and numerical simulation
[AD-A224226] N90-28772
Large aperture acoustic arrays in support of reverberation studies
[AD-A224002] N90-29168
Dynamical properties of two-dimensional Josephson junction arrays
[AD-A223965] N90-29221
ARTIFICIAL INTELLIGENCE
Control of intelligent robots in space N90-29013
Automation and robotics technology for intelligent mining systems N90-29018
A design philosophy for multi-layer neural networks with applications to robot control N90-29033
Coordinating the activities of a planner and an execution agent N90-29035
Plan recognition for space telerobotics N90-29036
Approximation algorithms for planning and control N90-29042
Proceedings of the NASA Conference on Space Telerobotics, volume 2
[NASA-CR-186857] N90-29044
HERMIES-3: A step toward autonomous mobility, manipulation, and perception N90-29065
Rice-obot 1: An intelligent autonomous mobile robot N90-29068
Organising geometric computations for space telerobotics N90-29074
Integrating planning and reactive control N90-29077
Learning in stochastic neural networks for constraint satisfaction problems N90-29078
Integrating planning, execution, and learning N90-29079
Who's who in scientific visualization at LLNL
[DE90-014720] N90-29091
Designing intelligent computer aided instruction systems with integrated knowledge representation schemes
[AD-A224178] N90-29113
Overcoming rule-based rigidity and connectionist limitations through massively-parallel case-based reasoning
[NASA-CR-186963] N90-29117
A hardware/software environment to support R/D in intelligent machines and mobile robotic systems
[DE90-014458] N90-29119
Model authoring system for fail safe analysis
[NASA-CR-4317] N90-29142
A knowledge-based system design/information tool
[NASA-CR-4316] N90-29143
ARTIFICIAL SATELLITES
Engineering and the advancement of human welfare. Ten outstanding achievements 1964-1989
[ISBN-0-309-04185-6] N90-29297
ASIA
Responding to the threat of global warming: Options for the Pacific and Asia
[DE90-014756] N90-28918
ASSEMBLING
How do robots take two parts apart N90-29061
ASSESSMENTS
Emerging technologies in electronics and their measurement needs, second edition
[PB90-186087] N90-28773
ASTRONOMICAL CATALOGS
Quantifying the FIR interaction enhancement in paired galaxies
[DE90-627485] N90-29281
ASTRONOMICAL MODELS
Gamma ray evidence for cosmic ray sources N90-29292
ASYMMETRY
Development of non-conventional control methods for high angle of attack flight using vortex manipulation N90-28522
Effects of flowfield turbulence on asymmetric vortices over a slender body
[AD-A224139] N90-28819
ASYMPTOTIC GIANT BRANCH STARS
Nonradial instability strips for post-AGB stars
[DE90-014922] N90-29278
ASYMPTOTIC METHODS
Asymptotic behavior of solutions of diffusion-like partial differential equations invariant to a family of affine groups
[DE90-014792] N90-29130
Asymptotics of Laplace-Dirichlet integrals
[DE90-627165] N90-29137
ASYMPTOTIC SERIES
Consistency and convergence for numerical radiation conditions
[NASA-TM-103262] N90-29124
ATMOSPHERIC CHEMISTRY
Quenching of N(2D) by O(3P)
[AD-A221690] N90-28683
Acid deposition: No such thing as a free launch
[DE90-015085] N90-28920
ATMOSPHERIC CIRCULATION
The global cycle of reactive nitrogen
[DE90-015041] N90-28919
ATMOSPHERIC COMPOSITION
The distribution of middle tropospheric carbon monoxide during early October 1984
[NASA-TM-103485] N90-28906
The role of clouds in CO2-induced climate change
[DE90-014380] N90-28911
The global cycle of reactive nitrogen
[DE90-015041] N90-28919
Tropospheric nitrogen: The influence of anthropogenic sources on distributions and deposition, executive summary
[DE90-015401] N90-28922
Estimating the spatial variability of trace gas deposition velocities
[PB90-208570] N90-28926
Present state of knowledge of the upper atmosphere 1990: An assessment report
[NASA-RP-1242] N90-28929
Infrared spectroscopic measurements on planetary atmospheric gases N90-29283
ATMOSPHERIC GENERAL CIRCULATION MODELS
The role of clouds in CO2-induced climate change
[DE90-014380] N90-28911
Annual course of precipitation over much of the US: Observed versus GCM simulation
[PB90-221656] N90-28942
ATMOSPHERIC MODELS
Tropospheric nitrogen: The influence of anthropogenic sources on distributions and deposition, executive summary
[DE90-015401] N90-28922
Genesis of bow echoes: A rear-inflow induced meso-convective structure
[PB90-209776] N90-28926

Present state of knowledge of the upper atmosphere 1990: An assessment report
[NASA-RP-1242] N90-28929
A nonhydrostatic numerical model in sigma-coordinates and simulations of mesoscale phenomena N90-28932

ATMOSPHERIC MOISTURE
Rain-fade simulation and power augmentation for satellite communication systems
[NASA-TM-103134] N90-28768

ATMOSPHERIC RADIATION
A preliminary ARM (Atmospheric Radiation Measurements) guide for climatic evaluations
[DE90-015135] N90-28937

ATMOSPHERIC TEMPERATURE
Daily temperature, solar radiation, wind speed, cloud cover, and precipitation data recorded at the meteorological station for calendar years 1957--1988
[DE90-014399] N90-28941

ATMOSPHERIC TURBULENCE
Sound propagation through atmospheric turbulence: A literature summary
[RPI-MATH-184] N90-28930

ATMOSPHERICS
Wind lidar for BEST
[CNES-NT-125] N90-28947

ATOMIC COLLISIONS
Correlated charge changing ion-atom collisions
[DE90-014662] N90-29171

ATOMIC EXCITATIONS
Fifteenth International Conference on X Ray and Inner-Shell Processes
[DE90-013024] N90-29170

ATOMIC STRUCTURE
Accurate quantum chemical calculations
[NASA-TM-101932] N90-28680
Research on the structural and electronic properties of defects in amorphous silicon
[DE90-000342] N90-28730

ATTACK AIRCRAFT
Combat aircraft control requirements N90-28515
Combat aircraft control requirements for agility N90-28517
The effects of foreplanes on the static and dynamic characteristics of a combat aircraft model N90-28520
The steady and time-dependent aerodynamic characteristics of a combat aircraft with a delta or swept canard N90-28526

ATTENTION
Evaluation of the Situational Awareness Rating Technique (SART) as a tool for aircrew systems design N90-28977
Attention gradients in situation awareness N90-28978
The three-dimensional structure of visual attention and its implications for display design N90-28980
Neurophysiological correlates of information processing abilities during divided attention situations in air traffic controllers N90-28989

ATTITUDE (INCLINATION)
Maintaining spatial orientation awareness N90-28993
Cognition versus sensation: A paradigm for reorientation
[IZF-1989-20] N90-28995

AUDITORY PERCEPTION
Complex auditory signals
[AD-A224127] N90-28969
Auditory processing of complex sounds across frequency channels
[AD-A224147] N90-28970
The simulation of localized sounds for improved situational awareness N90-28984
Techniques and applications for binaural sound manipulation in human-machine interfaces
[NASA-TM-102279] N90-28996

AUDITORY SIGNALS
Complex auditory signals
[AD-A224127] N90-28969
Auditory processing of complex sounds across frequency channels
[AD-A224147] N90-28970
The effects of acoustic orientation cues on instrument flight performance in a flight simulator N90-28985

AUDITORY STIMULI
Complex auditory signals
[AD-A224127] N90-28969

AUGER SPECTROSCOPY
Use of electron spectroscopies in the tribological evaluation of diamond films
[DE90-014421] N90-28848

AUGMENTATION
Variable mixture ratio performance through nitrogen augmentation N90-28639

AUSTENITIC STAINLESS STEELS
Evaluation of advanced austenitic alloys relative to alloy design criteria for steam service. Part 1: Lean stainless steel
[DE90-014765] N90-28720

AUTOCORRELATION
Near-angle scattering and binary optics
[AD-A224140] N90-29186

AUTOMATIC CONTROL
A sensor stabilization/tracking system for unmanned air vehicles
[AD-A224008] N90-28579
Robotic and automatic welding development at the Marshall Space Flight Center N90-28656
Experiences with the JPL telerobot testbed: Issues and insights N90-29059
Automated information system life-cycle management manual
[PB90-219288] N90-29244

AUTOMOBILES
Special test and evaluation methods used for a nine-axis accelerometer
[PB90-209578] N90-28822
Automotive Stirling engine development program
[NASA-CR-180840] N90-29260

AUTONOMOUS NAVIGATION
Building an environment model using depth information N90-29064
HERMIES-3: A step toward autonomous mobility, manipulation, and perception N90-29065

AUTONOMY
Dynamic interaction of multiple autonomous mobile robots N90-28844
Control of intelligent robots in space N90-29013
Automation and robotics technology for intelligent mining systems N90-29018
Real-time edge tracking using a tactile sensor N90-29023
Three-dimensional motor schema based navigation N90-29026
Periodic gaits for the CMU ambler N90-29027
Exploiting map plans as resources for action N90-29028
Building an environment model using depth information N90-29064
Rice-obot 1: An intelligent autonomous mobile robot N90-29068
Integrating planning, execution, and learning N90-29079

AUTOREGRESSIVE PROCESSES
Autoregressive-moving average models for texture classification
[INPE-4987-PRE/1549] N90-29092

AUXILIARY PROPULSION
Low power arcjet performance
[NASA-TM-103280] N90-28657

AVIONICS
Validation of the F-18 high alpha research vehicle flight control and avionics systems modifications
[NASA-TM-101723] N90-28542
Liquid Rocket Booster (LRB) for the Space Transportion System (STS) systems study. Appendix D: Trade study summary for the liquid rocket booster
[NASA-CR-183790-APP-D] N90-28604
Studies in automatic speech recognition and its application in aerospace N90-28759

AXIAL FLOW
Flow coupling between a rotor and a stator in turbomachinery
[AD-A223882] N90-28572

AXIAL LOADS
Behavior of aramid/epoxy wounded tubes under uniaxial and biaxial loading
[ETCA-89-R-150] N90-28873

AXIAL STRAIN
Microstructure: Property correlation — multiaxial fatigue damage evolution in waspaloy
[NASA-CR-180406] N90-28880

AXISYMMETRIC BODIES
Sting-support interference on afterbody drag at transonic speeds
[NAL-TM-EA-8902] N90-28492
Prediction of subsonic vortex shedding from forebodies with chines
[NASA-CR-4323] N90-28494

AXISYMMETRIC FLOW
Design of an axisymmetric, contoured nozzle for the HEG
[DLR-FB-90-04] N90-28812

B

B STARS
Kappa effect pulsational instability for hot extreme helium stars
[DE90-014920] N90-29277
Pulsations of B star models by an opacity mechanism
[DE90-014923] N90-29279

BACKGROUND NOISE
Methods for detecting low-frequency signals in the presence of strong winds
[AD-A223980] N90-28769

BACKGROUND RADIATION
Fluctuations in cosmic background radiation
[INPE-4579-PRE/1313] N90-29294

BALANCING
Aerodynamic control design: Experience and results at Aermacchi N90-28518

BALL BEARINGS
Evolution and use of combined mechanical and thermal codes for cryogenic turbopump bearings N90-28618
Determination of the SSME high pressure oxidizer turbopump bearing temperature N90-28619
Cryogenic, high speed, turbopump bearing cooling requirements N90-28620
Pool boiling from rotating and stationary spheres in liquid nitrogen N90-28621
Bearing optimization for SSME HPOTP application N90-28622
Development of improved self lubricating cages for SSME HPOTP bearings N90-28623
Cage stability analysis for SSME HPOTP bearings N90-28625
Rocketdyne LOX bearing tester program N90-28626

BALLOONING MODES
Resonant MHD modes with toroidal coupling
[DE90-015185] N90-29196

BANACH SPACE
Geometric theory for infinite dimensional systems
[ETN-90-96922] N90-29144

BARIUM
Dynamical information for Fe doped YBa2Cu3O7 superconducting oxides obtained from high temperature Moessbauer studies
[DE90-627871] N90-29218

BARIUM OXIDES
Synthesis and structural chemistry of Au(III)-substituted Ba2YCu3O(7-delta)
[NASA-TM-103292] N90-28696

BAROCLINIC WAVES
Planetary-scale flow on a two-layer beta-plane channel model with topography N90-28931

BAROCLINITY
Planetary-scale flow on a two-layer beta-plane channel model with topography N90-28931
Vorticity balance study for a tropical region, during the Southern Hemisphere summer
[INPE-4634-TDL/336] N90-28949

BAROTROPIC FLOW
Planetary-scale flow on a two-layer beta-plane channel model with topography N90-28931

BARRIER LAYERS
Thermal analysis of thermal barrier coatings in a high heat flux environment N90-28652
Vacuum application of thermal barrier plasma coatings N90-28653

BATHYTHERMOGRAPHS
Oceanographic data exchange, 1988
[PB90-232596] N90-28952

BCS THEORY
Superconductivity in mixed boson-fermion systems
[DE90-627491] N90-29216

BEAM INJECTION
Some novel sources of x ray beams: Channeling, transition and Cherenkov radiation
[DE90-014442] N90-29181

BEAM SPLITTERS
Near-angle scattering and binary optics
[AD-A224140] N90-29186

BEAMS (RADIATION)
Analysis of vibrational power transmission through a beam system including a flexible section
[ISVR-TR-176] N90-28875
Status of the advanced light source
[DE90-015636] N90-29185

BEARINGS
Solutions to the frictional dynamics problem and the reciprocal variable feedback methodology for design and control of robot mechanisms N90-28846

BED REST
Joint US/USSR study: Comparison of effects of horizontal and head-down bed rest
[NASA-TP-3037] N90-28965

BENDING
Inelastic analysis of laminated composites N90-28689
Ascertaining the fracture toughness of ceramic materials by means of bending testpieces of various notch types at ambient and high temperatures
[ESA-TT-992] N90-28733
A nonlinear finite element formulation for the large displacement analysis of plates N90-28867
Green's functions for dislocations in bonded strips and related crack problems
[NASA-CR-185291] N90-28878
BENDING THEORY
Inelastic analysis of laminated composites N90-28689
BERYLLIUM HYDRIDES
A new low density, high porosity lithium hydride-beryllium hydride foam
[DE90-015150] N90-28739
BETATRONS
Effects and tolerances of injection jitter in the SLC and future linear colliders
[DE90-014805] N90-29179
BIAS
Dynamical properties of two-dimensional Josephson junction arrays
[AD-A223965] N90-29221
BIBLIOGRAPHIES
Technical bibliography of high performance polyethylene fibers
[SNPE-NT-106/89/GTR/RP/NP] N90-28736
Aerospace medicine and biology: A continuing bibliography with indexes (supplement 340)
[NASA-SP-7011(340)] N90-28963
Biomedical and environmental sciences program publications, 1989
[DE90-014785] N90-29250
BINARY STARS
Pulsations of the white dwarf component in V471 tauri-like binaries
[DE90-014921] N90-29267
BINAURAL HEARING
Techniques and applications for binaural sound manipulation in human-machine interfaces
[NASA-TM-102279] N90-28996
BIOASTRONAUTICS
Aerospace medicine and biology: A continuing bibliography with indexes (supplement 340)
[NASA-SP-7011(340)] N90-28963
BIOCHEMICAL FUEL CELLS
Lightweight solid polymer electrolyte fuel cell with stack power density of 3 kW/lb (7 kW/kg)
[AD-A223964] N90-28905
BIOCHEMISTRY
A design tool utilizing stoichiometric structure for the analysis of biochemical reaction networks
[AD-A223873] N90-28961
Joint US/USSR study: Comparison of effects of horizontal and head-down bed rest
[NASA-TP-3037] N90-28965
BIOLOGICAL EFFECTS
Research for electric energy systems
[DE90-014221] N90-28775
Aerospace medicine and biology: A continuing bibliography with indexes (supplement 340)
[NASA-SP-7011(340)] N90-28963
BIOMASS
Activities report for the IBDF-INPE project SEQE, year 1987
[INPE-4534-RPE/565] N90-29298
BIOMEDICAL DATA
The SPECIALIST: Natural language processing system
[PB90-240029] N90-29098
BIOPOLYMERS
Polymer research
[PB90-246636] N90-28737
BIOSYNTHESIS
A design tool utilizing stoichiometric structure for the analysis of biochemical reaction networks
[AD-A223873] N90-28961
BIRD-AIRCRAFT COLLISIONS
User's manual ROBIN: A research and notification system for bird migration
[FEL-1989-103] N90-28508
BISMUTH COMPOUNDS
Evidence for a coherence gap in Ce3Bi4Pt3
[DE90-014925] N90-29207
BLADE TIPS
Blade tip rubbing stress prediction N90-28615
BLOOD PRESSURE
Cardiovascular deconditioning of cosmonauts: Role, importance and applications of the lower body negative pressure
[ETN-90-97507] N90-28964
BLOWING
Control of vortex aerodynamics at high angles of attack N90-28523
BLUFF BODIES
An investigation of the steady and unsteady near wake and its effect on a laminar boundary layer N90-28794
BODY-WING CONFIGURATIONS
Three-dimensional model testing in the transonic self-streamlining wind tunnel N90-28583
Effects of flowfield turbulence on asymmetric vortices over a slender body
[AD-A224139] N90-28819
BONDING
Accurate quantum chemical calculations
[NASA-TM-101932] N90-28680
BOOSTER ROCKET ENGINES
Liquid Rocket Booster (LRB) for the Space Transportation System (STS) systems study. Volume 1: Executive summary
[NASA-CR-183822] N90-28599
Liquid Rocket Booster (LRB) for the Space Transportation System (STS) systems study, volume 2
[NASA-CR-183786] N90-28600
Liquid Rocket Booster (LRB) for the Space Transportation System (STS) systems study. Appendix A: Stress analysis report for the pump-fed and pressure-fed liquid rocket booster
[NASA-CR-183787-APP-A] N90-28601
Liquid Rocket Booster (LRB) for the Space Transportation System (STS) systems study. Appendix B: Liquid rocket booster acoustic and thermal environments
[NASA-CR-183788-APP-B] N90-28602
Liquid Rocket Booster (LRB) for the Space Transportion System (STS) systems study. Appendix D: Trade study summary for the liquid rocket booster
[NASA-CR-183790-APP-D] N90-28604
Liquid Rocket Booster (LRB) for the Space Transportation System (STS) systems study. Appendix E: Pressure-fed booster test bed for the liquid rocket booster study
[NASA-CR-183791-APP-E] N90-28605
Liquid Rocket Booster (LRB) for the Space Transportation System (STS) systems study. Appendix F: Performance and trajectory for ALS/LRB launch vehicles
[NASA-CR-183792-APP-F] N90-28606
Liquid Rocket Booster (LRB) for the Space Transportation System (STS) systems study. Appendix G: LRB for the STS system study level 2 requirements, revision 1
[NASA-CR-183793-APP-G] N90-28607
Summary of booster propulsion/vehicle impact study results N90-28635
High/variable mixture ratio oxygen/hydrogen engines N90-28637
Use of Ni63 overvoltage gap switches in the flight termination systems on boosters launched from US Army Kwajalein Atoll (USAKA)
[AD-A223866] N90-28661
BORON ALLOYS
Tensile behavior of borated stainless steels, phase 1
[DE90-014368] N90-28717
BOROSILICATE GLASS
Strengthening and toughening mechanisms in ceramic fiber-reinforced glass matrix composites N90-28666
BOSONS
Superconductivity in mixed boson-fermion systems
[DE90-627491] N90-29216
BOUNDARY CONDITIONS
Secondary instabilities in compressible boundary layers
[NASA-CR-182091] N90-28502
Calculation of temperature distribution in various turbine blades using a boundary-fitted coordinate transformation method N90-28550
Electromagnetic scattering from two-dimensional thick material junctions
[NASA-CR-186468] N90-28767
On the use of Lagrangian variables in descriptions of unsteady boundary-layer separation
[NASA-CR-182071] N90-28789
An asymptotically induced domain decomposition method for parabolic boundary layer problems
[DE90-014620] N90-28804
Consistency and convergence for numerical radiation conditions
[NASA-TM-103262] N90-29124
BOUNDARY ELEMENT METHOD
Development of an integrated BEM for hot fluid-structure interaction N90-28617
BOUNDARY INTEGRAL METHOD
SuperCHIEF: A modified CHIEF (Combined Helmholz Integral Equation Formulation) method
[DE90-014744] N90-29123
Solution of the Stokes system by boundary integral equations and fixed point iterative schemes
[DE90-627166] N90-29138
BOUNDARY LAYER CONTROL
Control of submersible vortex flows
[NASA-TM-102693] N90-28493
BOUNDARY LAYER EQUATIONS
An investigation of the steady and unsteady near wake and its effect on a laminar boundary layer N90-28794
BOUNDARY LAYER FLOW
Effects of flowfield turbulence on asymmetric vortices over a slender body
[AD-A224139] N90-28819
Numeric fluid mechanics N90-29161
BOUNDARY LAYER SEPARATION
Wind tunnel investigation of periodic vortex separation from rough surface circular cylinders by means of acoustic measurements
[ESA-TT-1092] N90-28499
In-flight flow visualization with pressure measurements at low speeds on the NASA F-18 high alpha research vehicle
[NASA-TM-101726] N90-28505
On the use of Lagrangian variables in descriptions of unsteady boundary-layer separation
[NASA-CR-182071] N90-28789
BOUNDARY LAYER STABILITY
Experimental investigations on the stability and transition of three-dimensional boundary layers
[ESA-TT-1026] N90-28803
BOUNDARY LAYER TRANSITION
Two-dimensional wind tunnel test and comparison with calculations for a 15.2 percent thick airfoil section for wind turbines
[FFA-TN-1990-16] N90-28501
Use of liquid crystals for qualitative and quantitative 2-D studies of transition and skin friction
[RAE-TM-AERO-2159] N90-28800
Experimental investigations on the stability and transition of three-dimensional boundary layers
[ESA-TT-1026] N90-28803
Numeric fluid mechanics N90-29161
BOUNDARY LAYERS
Unsteady aerodynamics of controls N90-28525
An asymptotically induced domain decomposition method for parabolic boundary layer problems
[DE90-014620] N90-28804
Extrapolation procedures at outflow boundaries for the Navier-Stokes equations
[FFA-TN-1990-23] N90-28811
BOUNDARY VALUE PROBLEMS
Solution of the Stokes system by boundary integral equations and fixed point iterative schemes
[DE90-627166] N90-29138
BOW WAVES
Genesis of bow echoes: A rear-inflow induced meso-convective structure
[PB90-209776] N90-28926
BRAIN
Time, space and form in vision
[AD-A213889] N90-28971
BRAZIL
Digital geometric correction for MSS-LANDSAT imagery
[INPE-4627-PRE/1345] N90-28886
Study of anomalies in transition vegetation in Alto Xingo-NT, through remote sensing techniques
[INPE-4601-TDL/334] N90-28891
Computer vision and its potential applications in Brazil
[INPE-4566-NTE/283] N90-29100
Activities report for the IBDF-INPE project SEQE, year 1987
[INPE-4534-RPE/565] N90-29298
BRIGHTNESS DISTRIBUTION
New Voyager radio spectrograms of Uranus
[NASA-CR-180381] N90-29284
BRITTLE MATERIALS
Green's functions for dislocations in bonded strips and related crack problems
[NASA-CR-185291] N90-28878
BRITTLENESS
Is there anything of practical value hidden amongst the composite toughening theories. A Jim Mueller prospective
[DE90-014905] N90-28673
BROADBAND
New approach to HF channel modeling and simulation. Part 2: Stochastic model
[PB90-200338] N90-28755
BROADCASTING
A radio frequency user's guide to the space environment services center geophysical alert broadcasts
[PB90-240631] N90-28935

BROKEN SYMMETRY
Surface and defect excitations in covalently bonded solids
[AD-A221995] N90-28682
Z(6) model: Criticality and break-collape method
[DE90-627323] N90-29214
Introduction to gauge theories and unification
[DE90-014473] N90-29225
On the infrared behaviour of some non-Minkowskian quantum fields N90-29273
BUBBLES
Thermogravimetry-mass spectrometry analysis of gas bubbles in molten glass
[DE90-014116] N90-28684
A plasma diagnostic study of two wind-blown shell nebulae: NGC 7635 and NGC 2359 N90-29271
BUCKLING
Liquid Rocket Booster (LRB) for the Space Transportation System (STS) systems study. Appendix A: Stress analysis report for the pump-fed and pressure-fed liquid rocket booster
[NASA-CR-183787-APP-A] N90-28601
Buckling and postbuckling behavior of compression-loaded isotropic plates with cutouts
[NASA-TP-3024] N90-28859
Structural analysis and optimum design of geodesically stiffened composite panels
[NASA-CR-186944] N90-28862
Parametric solution of nonlinear structure problems
[ONERA-RT-21/3542-RY-082-R] N90-28874
BUILDINGS
Torsional effects in structures subjected to strong ground motion
[PB90-226960] N90-28869
Transferring building energy technologies by linking government and private-sector programs
[DE90-000346] N90-29258
BURNERS
Extended range tankless water heater
[DE90-014474] N90-28750
Radiative heat transfer
[PB90-247602] N90-28813
BURNING RATE
Composite propellants with high burning rates
[FOA-C-20781-2.1] N90-28744

C

C (PROGRAMMING LANGUAGE)
A personal computer-based, multitasking data acquisition system
[NASA-TM-4232] N90-29107
C BAND
Design and realization of a two stage C-band low noise amplifier
[FEL-89-B265] N90-28783
CALCULUS OF VARIATIONS
Dirac's equation as a geodesic in Riemann space
[DE90-627194] N90-29152
Systematic approach to critical phenomena by the extended variational method and coherent-anomaly method
[DE90-627320] N90-29165
Ignition and burn control characteristics of thermonuclear plasmas
[DE90-015385] N90-29197
CALIBRATING
Three-dimensional model testing in the transonic self-streamlining wind tunnel N90-28583
Accurate quantum chemical calculations
[NASA-TM-101932] N90-28680
A microprocessor controlled strain gauge calibration module
[AR-005-579] N90-28821
Rheometer strain and strain-rate errors
[DE90-013845] N90-28824
A laser spectrometer and wavemeter for pulsed lasers
[NASA-CR-181731] N90-28832
Operation and calibration of MRL permeameter for measurement of DC magnetic properties of materials under stress
[MRL-TN-574] N90-28863
CALORIMETERS
Study of the induction time in isothermal decomposition of explosives
[DE90-014906] N90-28745
CANARD CONFIGURATIONS
Aerodynamic and propulsive control development of the STOL and maneuver technology demonstrator N90-28514
Effects of canard position on the aerodynamic characteristics of a close-coupled canard configuration at low speed N90-28519
The effects of foreplanes on the static and dynamic characteristics of a combat aircraft model N90-28520
The steady and time-dependent aerodynamic characteristics of a combat aircraft with a delta or swept canard N90-28526
An in-flight investigation of ground effect on a forward-swept wing airplane N90-28533
CANOPIES (VEGETATION)
A manual for analysis of hemispherical canopy photography
[DE90-014718] N90-28885
CANTILEVER BEAMS
Minimum weight design of a leaf spring tapered in thickness and width for the Hubble Space Telescope-space support equipment
[NASA-TM-4233] N90-28879
CARBON
Mechanical properties testing of diamond and diamond-like films by ultra-low load indentation
[DE90-014456] N90-28861
CARBON DIOXIDE
Study of power generation systems for CO2 collection: LNG combined cycle
[DE90-507881] N90-28901
Natural and anthropogenic climate change
[DE90-015528] N90-28923
CARBON DIOXIDE CONCENTRATION
The role of clouds in CO2-induced climate change
[DE90-014380] N90-28911
CARBON DIOXIDE LASERS
Design of a CO2 laser power control system for a Spacelab microgravity experiment
[NASA-TM-103112] N90-28833
CARBON FIBER REINFORCED PLASTICS
Ultrasonic verification of five wave fronts in unidirectional graphite epoxy composite
[NASA-CR-185288] N90-28858
CARBON FIBERS
Electrochemical surface finishing using amino-substrates on carbon fibers in organic media. Effects of the finishing on the mechanical properties of carbon-epoxy composites
[ONERA-RT-9/3549-M] N90-28872
CARBON MONOXIDE
The distribution of middle tropospheric carbon monoxide during early October 1984
[NASA-TM-103485] N90-28906
Long-range plan for a research project on carbon monoxide production and prediction
[PB90-209602] N90-28910
CARBON-CARBON COMPOSITES
NASA Langley Research Center National Aero-Space Plane Mission simulation profile sets
[NASA-TM-102670] N90-28541
The effects of atomic oxygen on the thermal emittance of high temperature radiator surfaces
[NASA-TM-103224] N90-28870
CARCINOGENS
DNA damage and repair in human skin: Pathways and questions
[DE90-015126] N90-28966
CARDIOVASCULAR SYSTEM
Cardiovascular deconditioning of cosmonauts: Role, importance and applications of the lower body negative pressure
[ETN-90-97507] N90-28964
Prevalence of hypertension among active duty personnel
[AD-A223892] N90-28968
Fluid and electrolyte homeostasis during spaceflight: Elucidation of mechanisms in a primate
[NASA-CR-177548] N90-29085
CARIBBEAN SEA
Puerto Rico Workshop on Land-Based Sources of Marine Pollution in the Wider Caribbean Region
[PB90-184094] N90-28921
Measuring the vertical directional spectra caused by sea surface sound
[AD-A223883] N90-28957
CARRIER LIFETIME
Radiation effects in InAsSb strained-layer superlattice photodiodes induced by dose-rate and transient x ray environments
[DE90-015000] N90-29208
CARTESIAN COORDINATES
Computer program for converting rectangular coordinates to latitude-longitude coordinates
[PB90-231796] N90-28883
Cartesian control of redundant robots N90-29004
Measurement of hand dynamics in a microsurgery environment: Preliminary data in the design of a bimanual telemicro-operation test bed N90-29010
CAST ALLOYS
Micromechanisms of fatigue crack growth and fracture toughness in metal matrix composites
[AD-A223863] N90-28676
CASTING
High temperature oxidation of Al-Li alloys N90-28705
CATACLYSMIC VARIABLES
X ray spectra of cataclysmic variables
[NASA-CR-187002] N90-29280
CATALYSIS
A study of catalysts and mechanisms in synthesis reactions
[DE90-015064] N90-28691
CATALYSTS
Catalytic ignition of hydrogen/oxygen N90-28627
A study of catalysts and mechanisms in synthesis reactions
[DE90-015064] N90-28691
Composite propellants with high burning rates
[FOA-C-20781-2.1] N90-28744
CATHODE RAY TUBES
The interaction of chromostereopsis and stereopsis in stereoscopic CRT (Cathode Ray Tubes) displays
[AD-A217906] N90-28544
Computer simulation of micro-triode performance
[DE90-014191] N90-28774
CATHODES
Unipolar arcing on the cathode surface of a high voltage diode
[AD-A224122] N90-28787
CAVITATION FLOW
Current research in cavitating fluid films
[NASA-TM-103184] N90-28791
CAVITY RESONATORS
Approximation, synthesis, and development of bi-mode cavities microwave filters presenting unsymmetrical quasi-elliptic responses
[CNES-NT-124] N90-28761
CELL DIVISION
Insulin and insulin-like growth factor-1 induce pronounced hypertrophy of skeletal myofibers in tissue culture
[NASA-CR-187026] N90-28960
CEMENTS
Development and testing of rapid repair methods for war damaged runways
[AD-A223970] N90-28586
CENTRIFUGAL FORCE
Target acquisition under load factors: Advantages and disadvantages of a helmet mounted sight N90-28983
Unexpected properties of the centrifugal force
[DE90-627197] N90-29184
CEPHEID VARIABLES
Cepheid masses for models with enhanced opacities
[DE90-014919] N90-29266
CERAMIC COATINGS
High temperature protective coatings: Recent trends N90-28710
Thermal shock and oxidation resistance of ceramic coatings N90-28711
CERAMIC MATRIX COMPOSITES
Ceramic matrix composites in simulated SSME environments N90-28655
Strengthening and toughening mechanisms in ceramic fiber-reinforced glass matrix composites N90-28656
CERAMICS
Energy efficient engine pin fin and ceramic composite segmented liner combustor sector rig test report
[NASA-CR-179534] N90-28567
Friction microprobe studies of composite surfaces
[DE90-014224] N90-28682
Microdamage to ceramic surfaces under sliding conditions N90-28708
Mechanical testing activities related to high-performance structural ceramics
[DE90-014299] N90-28734
Improved silicon carbide for advanced heat engines
[NASA-CR-182186] N90-28735
Proceedings of US Army Research Office Workshop on US Army Applications for Diamond and Diamondlike Materials
[AD-A224193] N90-28741
In-flight investigation of shuttle tile pressure orifice installations
[NASA-TM-4219] N90-28820
CERENKOV RADIATION
Some novel sources of x ray beams: Channeling, transition and Cherenkov radiation
[DE90-014442] N90-29181
CERIUM
Effects of Al substitution by Fe in CeAl2
[DE90-627843] N90-28726
CERIUM COMPOUNDS
Antiferromagnetism and enhanced heat in CeM2Sn (M = Ni, Ir, Cu, Rh, Pd, and Pt
[DE90-014924] N90-29206
Evidence for a coherence gap in Ce3Bi4Pt3
[DE90-014925] N90-29207
CHANNEL FLOW
Free shear layer and swirl flow heat transfer enhancement
[PB90-226123] N90-28798

CHANNELS (DATA TRANSMISSION)
Studies in automatic speech recognition and its application in aerospace N90-28759
CHAOS
An investigation of chaotic Kolmogorov flows [NASA-CR-182079] N90-28816
Prediction, control, and decision-making aspects for chaotic systems [DE90-014452] N90-29224
Quantum chaos and dissipation: Lyapunov exponents [DE90-627180] N90-29228
CHARACTERIZATION
Radiation-curable prepreg composites [DE90-629740] N90-28674
High temperature superconducting thin film microwave circuits: Fabrication, characterization, and applications [NASA-TM-103235] N90-28786
Quality function deployment as a mechanism for process characterization and control [DE90-014755] N90-28857
CHARGE COUPLED DEVICES
Noise performance of microchannel plate imaging systems [DE90-015037] N90-28785
CHARGE TRANSFER
Correlated charge changing ion-atom collisions [DE90-014662] N90-29171
CHARGED PARTICLES
Concept for a neutron spectrometer based on optical detection of (3)He(n, p)-3H reactions in a gas [DE90-014776] N90-28826
Old and new ideas in the theory of quantum measurement [DE90-627181] N90-29229
CHARPY IMPACT TEST
Determination of the NDT temperature and Charpy V-notch impact properties of AAR TC128 grades B steel and A 8XX grade B steel [PB90-207804] N90-28716
CHEMICAL ANALYSIS
Mass spectrometric analysis of hydrogen isotopes in metals and metal hydrides [DE90-014118] N90-28685
Fuels research, volume 1 [DE90-015393] N90-28695
A design tool utilizing stoichiometric structure for the analysis of biochemical reaction networks [AD-A223873] N90-28961
CHEMICAL COMPOSITION
Tripropellant combustion process N90-28631
Reflection Mass Spectrometry (REMS) during 3/5 MBE [DE90-014568] N90-28690
Tensile behavior of borated stainless steels, phase 1 [DE90-014368] N90-28717
Evaluation of advanced austenitic alloys relative to alloy design criteria for steam service. Part 1: Lean stainless steel [DE90-014765] N90-28720
Geothermal fluid genesis in the Great Basin [DE90-014438] N90-28884
CHEMICAL EFFECTS
Strengthening and toughening mechanisms in ceramic fiber-reinforced glass matrix composites N90-28666
CHEMICAL REACTIONS
Assessment of battery technologies for electric vehicles. Volume 2, part 2: Appendices [DE90-014610] N90-28778
CHESAPEAKE BAY (US)
Perspectives on the Chesapeake Bay, 1990: Advances in estuarine sciences [PB90-248600] N90-28954
CHIRAL DYNAMICS
On the zeta-function regularization of chiral Jacobians for singular Dirac operators [DE90-627178] N90-29150
Criticality of the three-state chiral clock model: A renormalisation group study [DE90-627321] N90-29212
CHROMIUM ISOTOPES
Enrichment services for chromium isotopes for the GALLEX (gallium experiment) international collaboration experiment on solar neutrino flux [DE90-014300] N90-29205
CIRCUIT RELIABILITY
Smart microsensors for high temperature applications, phase 1 [AD-A224151] N90-28828
CIRCUITS
Robust controller design by contraction of a pole region [ESA-TT-1042] N90-29118
CIRCULAR TUBES
A study of heat and fluid flow phenomena on the gas side of circular-tube plate-fin heat exchangers N90-28795
CIVIL AVIATION
High-speed civil transport study: Special factors [NASA-CR-181881] N90-28537
CLASSICAL MECHANICS
Unexpected properties of the centrifugal force [DE90-627197] N90-29164
CLASSIFICATIONS
A conceptual weather-type classification procedure for the Philadelphia, Pennsylvania area [PB90-231705] N90-28944
A hybrid architecture for the implementation of the Athena neural net model N90-29032
Autoregressive-moving average models for texture classification [INPE-4987-PRE/1549] N90-29092
Efficiency and effectiveness of deep structure-based subject indexing languages: PRECIS vs. DSIS N90-29248
CLASSIFIERS
A failure diagnosis system based on a neural network classifier for the space shuttle main engine [NASA-TM-103607] N90-28859
CLEANING
Study and analysis of leaking underground storage tank remediation techniques incorporated in states in EPA Region 6 [PB90-214834] N90-28847
CLEARANCES
NASA/GE Energy Efficient Engine low pressure turbine scaled test vehicle performance report [NASA-CR-168290] N90-28563
CLIMATE
A preliminary ARM (Atmospheric Radiation Measurements) guide for climatic evaluations [DE90-015135] N90-28937
Proceedings of the 14th Annual Climate Diagnostics Workshop [PB90-198573] N90-28938
Annual course of precipitation over much of the US: Observed versus GCM simulation [PB90-221656] N90-28942
Program on development of basic understanding of severe weather phenomena [PB90-226564] N90-28943
CLIMATE CHANGE
Our changing planet: The FY 1991 US global change research program. A report by the committee on Earth Sciences to accompany the FY 1991 budget [PB90-202623] N90-28907
The role of clouds in CO2-induced climate change [DE90-014380] N90-28911
Chasing a specter: Risk management for global environmental change [DE90-014455] N90-28917
Responding to the threat of global warming: Options for the Pacific and Asia [DE90-014756] N90-28918
Natural and anthropogenic climate change [DE90-015528] N90-28923
Annual course of precipitation over much of the US: Observed versus GCM simulation [PB90-221656] N90-28942
CLIMATOLOGY
Our changing planet: The FY 1991 US global change research program. A report by the committee on Earth Sciences to accompany the FY 1991 budget [PB90-202623] N90-28907
A preliminary ARM (Atmospheric Radiation Measurements) guide for climatic evaluations [DE90-015135] N90-28937
Proceedings of the 14th Annual Climate Diagnostics Workshop [PB90-198573] N90-28938
Wind lidar for BEST [CNES-NT-125] N90-28947
CLOCKS
Criticality of the three-state chiral clock model: A renormalisation group study [DE90-627321] N90-29212
CLOSED ECOLOGICAL SYSTEMS
Space Station Freedom pressurized element interior design process [NASA-CR-181297] N90-28597
Electrochemical incineration of wastes [NASA-CR-187033] N90-28753
Atmosphere and water quality monitoring on Space Station Freedom [NASA-CR-186707] N90-29084
CLOUD COVER
A preliminary ARM (Atmospheric Radiation Measurements) guide for climatic evaluations [DE90-015135] N90-28937
Daily temperature, solar radiation, wind speed, cloud cover, and precipitation data recorded at the meteorological station for calendar years 1957–1988 [DE90-014399] N90-28941
A conceptual weather-type classification procedure for the Philadelphia, Pennsylvania area [PB90-231705] N90-28944
Study of the relationships between radar structure and the electrical activity of clouds [ETN-90-97488] N90-28946
CLOUD DISPERSAL
Diffusion in the surface layer of the convective boundary layer [AD-A224125] N90-28924
CLOUDS (METEOROLOGY)
The role of clouds in CO2-induced climate change [DE90-014380] N90-28911
The global cycle of reactive nitrogen [DE90-015041] N90-28919
Genesis of bow echoes: A rear-inflow induced meso-convective structure [PB90-209776] N90-28926
A preliminary ARM (Atmospheric Radiation Measurements) guide for climatic evaluations [DE90-015135] N90-28937
CLUTTER
Recognition of infrared images. Part 3: The effect of image processing with a size-contrast box filter on observation performance [IZF-1989-39] N90-29182
COATINGS
Research on high-efficiency, multiple-gap, multi-junction amorphous silicon-based alloy thin-film solar cells [DE90-000338] N90-28896
COAXIAL NOZZLES
Design of an axisymmetric, contoured nozzle for the HEG [DLR-FB-90-04] N90-28812
COCKPITS
Situational Awareness in Aerospace Operations [AGARD-CP-478] N90-28972
Towards a future cockpit: The prototyping and pilot integration of the Mission Management Aid (MMA) N90-28979
COEFFICIENT OF FRICTION
On the application of similarity laws to a scaled railway bogie model [DLR-FB-90-06] N90-28853
COGENERATION
Fuel cells: Their applications, technological status, market and opportunity [DE90-796158] N90-28895
COGNITION
Cognition versus sensation: A paradigm for reorientation [IZF-1989-20] N90-28995
COGNITIVE PSYCHOLOGY
Workload induced spatio-temporal distortions and safety of flight: An investigation of cognitive intrusions in perceptual processes N90-28986
Neurophysiological correlates of information processing abilities during divided attention situations in air traffic controllers N90-28989
COHERENT LIGHT
Energy transmission by means of coherent quasi-mono-chromatic light beams N90-29163
COLLAPSE
Reliability analysis of maintained structural system vulnerable to fatigue and fracture N90-28868
COLLECTION
Robotic sampling system for an unmanned Mars mission N90-29070
COLLISION AVOIDANCE
Dynamic interaction of multiple autonomous mobile robots N90-28844
A 17 degree of freedom anthropomorphic manipulator N90-29001
Planning 3-D collision-free paths using spheres N90-29024
COLLISIONS
Planning 3-D collision-free paths using spheres N90-29024
COLOR
Comparison of methods of space color transformations for enhancement of colored images [INPE-4977-PRE/1542] N90-28881
COLOR CODING
Comparison of methods of space color transformations for enhancement of colored images [INPE-4977-PRE/1542] N90-28881
COMBAT
Combat aircraft control requirements for agility N90-28517
Multiband imaging systems [AD-A223969] N90-28893
Performance-based measures of merit for tactical situation awareness N90-28976
Counterair situation awareness display for Army aviation N90-28982

COMBINATORIAL ANALYSIS
The combinatorics computation for Casimir operators of the symplectic Lie algebra and the application for determining the center of the enveloping algebra of a semidirect product
[DE90-627161] N90-29136
COMBINED CYCLE POWER GENERATION
Study of power generation systems for CO2 collection: LNG combined cycle
[DE90-507881] N90-28901
COMBUSTION
The reduction of smoke emissions from Allison T56 engines
[ARL-PROP-R-182] N90-28547
Energy Efficient Engine combustor test hardware detailed design report
[NASA-CR-168301] N90-28554
Shock dynamics in the sub-nanometer femtosecond domain
[DE90-014390] N90-28689
Study of the radical OH in a high pressure flame by resonant DRASC
[ONERA-RF-57/7131-PY] N90-28692
Ignition and combustion of liquid propellants
[AD-A224150] N90-28746
Radiative heat transfer
[PB90-247602] N90-28813
Development of advanced combustion technology for medium and high speed natural gas engines
[PB90-198565] N90-28836
Activities report for the IBDF-INPE project SEQE, year 1987
[INPE-4534-RPE/565] N90-29298
COMBUSTION CHAMBERS
Energy Efficient Engine combustor test hardware detailed design report
[NASA-CR-168301] N90-28554
Energy Efficient Engine (E3) combustion system component technology performance report
[NASA-CR-168274] N90-28555
Energy efficient engine pin fin and ceramic composite segmented liner combustor sector rig test report
[NASA-CR-179534] N90-28567
Development of comprehensive numerical schemes for predicting evaporating gas-droplets flow processes of a liquid-fueled combustor
[NASA-CR-187018] N90-28693
COMBUSTION EFFICIENCY
Energy Efficient Engine combustor test hardware detailed design report
[NASA-CR-168301] N90-28554
Energy Efficient Engine (E3) combustion system component technology performance report
[NASA-CR-168274] N90-28555
Energy efficient engine program technology benefit/cost study. Volume 1: Executive summary
[NASA-CR-174766-VOL-1] N90-28564
Energy efficient engine program technology benefit/cost study, volume 2
[NASA-CR-174766-VOL-2] N90-28565
Energy Efficient Engine: Combustor component performance program
[NASA-CR-179533] N90-28568
Performance measurements and energy balance of an SPS V160 Stirling motor at the German Aerospace Research Establishment
[DLR-MITT-90-03] N90-28903
COMBUSTION PRODUCTS
The reduction of smoke emissions from Allison T56 engines
[ARL-PROP-R-182] N90-28547
Spectroscopic study of combustion diagnostics on hydroxyl radicals
[NASA-CR-186998] N90-28694
The distribution of middle tropospheric carbon monoxide during early October 1984
[NASA-TM-103485] N90-28906
COMBUSTION STABILITY
Numerical simulations of flowfields in a central-dump ramjet combustor. 3: Effects of chemistry
[AD-A224145] N90-28573
Oxygen/methane combustion stability investigation N90-28628
Combustion instability coupling with feed system acoustics N90-28629
Tripropellant combustion process N90-28631
COMBUSTION TEMPERATURE
Swirl coaxial injector element characterization for booster engines N90-28632
COMFORT
Teleoperator comfort and psychometric stability: Criteria for limiting master-controller forces of operation and feedback during telemanipulation N90-29009
COMMAND AND CONTROL
Research in command and control for the Dutch Army Corps (1NL)
[IZF-1989-28] N90-28760
Experiments in the dynamic and strategic control of cooperating manipulators N90-28845
COMMAND LANGUAGES
Adjustable impedance, force feedback and command language aids for telerobotics (parts 1-4 of an 8-part MIT progress report) N90-29007
COMMERCE
Time-based competition for competitive advantage: An information technology perspective
[AD-A224474] N90-29255
COMMERCIAL AIRCRAFT
World jet airplane inventory at year-end 1989
[PB90-207218] N90-28489
Life cycle cost in the conceptual design of subsonic commercial aircraft, volumes 1 and 2 N90-28535
COMMUNICATION
Communications Interface Driver (CID) test plan
[DOT/FAA/CT-TN89/35] N90-28762
COMMUNICATION NETWORKS
Secure Data Network System (SDNS) network, transport, and message security protocols
[PB90-198946] N90-28757
The NASA/OAST telerobot testbed architecture N90-29016
Coordinating the activities of a planner and an execution agent N90-29035
Design of a monitor and simulation terminal (master) for space station telerobotics and telescience N90-29051
COMMUNICATION SATELLITES
Approximation, synthesis, and development of bi-mode cavities microwave filters presenting unsymmetrical quasi-elliptic responses
[CNES-NT-124] N90-28761
COMPATIBILITY
Ground-based weather radar compatibility with digital radio-relay microwave systems
[PB90-206236] N90-28756
COMPETITION
Mode competition in the quasioptical gyrotron
[AD-A222181] N90-28823
Time-based competition for competitive advantage: An information technology perspective
[AD-A224474] N90-29255
COMPONENT RELIABILITY
Data base for crack growth properties of materials N90-28647
Ceramic matrix composites in simulated SSME environments N90-28655
COMPOSITE MATERIALS
Radiation-curable prepreg composites
[DE90-629740] N90-28674
Fabrication of spherical pressure vessels from composite materials
[INPE-4598-RPE/570] N90-28675
Dissipation of mechanical work and temperature rise in AS4/PEEK thermoplastic composite
[NASA-CR-186893] N90-28678
A constitutive model for AS4/PEEK thermoplastic composites under cyclic loading
[NASA-CR-180393] N90-28679
Technical bibliography of high performance polyethylene fibers
[SNPE-NT-106/89/GTR/RP/NP] N90-28736
Proceedings of US Army Research Office Workshop on US Army Applications for Diamond and Diamondlike Materials
[AD-A224193] N90-28741
Green's functions for dislocations in bonded strips and related crack problems
[NASA-CR-185291] N90-28878
Large hydrodynamic tunnel: Calculation of the acoustic transparency of the jet stream
[REPT-89/115] N90-29167
Engineering and the advancement of human welfare. Ten outstanding achievements 1964-1989
[ISBN-0-309-04185-6] N90-29297
COMPOSITE PROPELLANTS
Composite propellants with high burning rates
[FOA-C-20781-2.1] N90-28744
COMPOSITE STRUCTURES
Energy efficient engine pin fin and ceramic composite segmented liner combustor sector rig test report
[NASA-CR-179534] N90-28567
Mechanical behavior of thick, curved, laminated composites N90-28664
Structural analysis and optimum design of geodesically stiffened composite panels
[NASA-CR-186944] N90-28882
COMPRESSIBILITY
Thermophysical properties of Helium-4 from 0.8 to 1500 K with pressures to 2000 MPa
[NASA-CR-186992] N90-28681
COMPRESSIBLE BOUNDARY LAYER
Secondary instabilities in compressible boundary layers
[NASA-CR-182091] N90-28502
COMPRESSIBLE FLOW
Development of turbulence models for the analysis of compressible or incompressible unsteady flow
[ETN-90-97486] N90-28810
COMPRESSION RATIO
Development of advanced combustion technology for medium and high speed natural gas engines
[PB90-198565] N90-28836
COMPRESSOR EFFICIENCY
Energy Efficient Engine acoustic supporting technology report
[NASA-CR-174834] N90-28557
COMPRESSORS
The effects of a compressor rebuild on gas turbine engine performance: Final results N90-28701
COMPUTATION
Techniques and potential capabilities of multi-resolutional information (knowledge) processing N90-29062
Parallel algorithms for computation of the manipulator inertia matrix N90-29072
Block Lanczos algorithm
[AD-A224011] N90-29111
COMPUTATIONAL FLUID DYNAMICS
The effect of rapid spoiler deployment on the transient forces on an aerofoil N90-28527
Study of the ground effects in the CEAT aerohydrodynamic tunnel: Using the results N90-28530
The aerodynamic design of the oblique flying wing supersonic transport
[NASA-CR-177552] N90-28540
Measurement of the steady surface pressure distribution on a single rotation large scale advanced prop-fan blade at Mach numbers from 0.03 to 0.78
[NASA-CR-182124] N90-28552
Development of comprehensive numerical schemes for predicting evaporating gas-droplets flow processes of a liquid-fueled combustor
[NASA-CR-187018] N90-28693
Spectroscopic study of combustion diagnostics on hydroxyl radicals
[NASA-CR-186998] N90-28694
Numerical simulation of reactive turbulent flows
[ETN-90-97476] N90-28807
Numerical resolution of Navier-Stokes equations using several turbulence models and applications on turbomachines
[ETN-90-97478] N90-28808
Development of turbulence models for the analysis of compressible or incompressible unsteady flow
[ETN-90-97486] N90-28810
Scientific Colloquium in Honor of Prof. Dr. Rer. Nat. Hermann L. Jordan
[ESA-TT-1101] N90-29159
Numeric fluid mechanics N90-29161
COMPUTATIONAL GRIDS
Calculation of temperature distribution in various turbine blades using a boundary-fitted coordinate transformation method N90-28550
Multigrid for hypersonic inviscid flows
[NASA-CR-182082] N90-29125
Deterministic transport on an arbitrarily-connected grid
[DE90-015148] N90-29131
COMPUTER AIDED DESIGN
Hypersonic Arbitrary-Body Aerodynamics (HABA) for conceptual design
[DE90-014750] N90-28495
Flow coupling between a rotor and a stator in turbomachinery
[AD-A223882] N90-28572
Summary of booster propulsion/vehicle impact study results N90-28635
Design and realization of a two stage C-band low noise amplifier
[FEL-89-B265] N90-28783
Automated simulation as part of a design workstation
[NASA-TM-102852] N90-29083
Engineering and the advancement of human welfare. Ten outstanding achievements 1964-1989
[ISBN-0-309-04185-6] N90-29297
COMPUTER AIDED MANUFACTURING
Computerization of Welding Data: Proceedings of the conference and workshop
[PB90-219551] N90-28841
An improved method for choosing sampling points for the inspection of complex surfaces in a computer-aided manufacturing environment N90-29093

Engineering and the advancement of human welfare. Ten outstanding achievements 1964-1989
[ISBN-0-309-04185-6] N90-29297

COMPUTER AIDED TOMOGRAPHY

Geophysical diffraction tomography: A complementary remote sensing technique for hazardous waste site characterization
[DE90-013025] N90-28882

Engineering and the advancement of human welfare. Ten outstanding achievements 1964-1989
[ISBN-0-309-04185-6] N90-29297

COMPUTER ANIMATION

Animated computer-generated video-tape instruction using DIGLIB (Device Independent Graphics Library)
[DE90-015360] N90-29105

COMPUTER ASSISTED INSTRUCTION

Selective learning algorithm for certain types of learning failure in multilayer perceptrons
[AD-A223962] N90-28998

Strategies of computer-based instructional design: A review of guidelines and empirical research
[AD-A224038] N90-29112

Designing intelligent computer aided instruction systems with integrated knowledge representation schemes
[AD-A224178] N90-29113

COMPUTER COMPATIBLE TAPES

Digital geometric correction for MSS-LANDSAT imagery
[INPE-4627-PRE/1345] N90-28886

COMPUTER GRAPHICS

Time, space and form in vision
[AD-A213889] N90-28971

Design of a monitor and simulation terminal (master) for space station telerobotics and telescience N90-29051

Who's who in scientific visualization at LLNL
[DE90-014720] N90-29091

A computer graphics package
[ARE-TM(UDT)-89111] N90-29094

Graph structure model
[DE90-014930] N90-29097

Fast interactive image generation of line and surface oriented objects in raster systems
[ETN-90-97290] N90-29102

Animated computer-generated video-tape instruction using DIGLIB (Device Independent Graphics Library)
[DE90-015360] N90-29105

COMPUTER INFORMATION SECURITY

Secure Data Network System (SDNS) network, transport, and message security protocols
[PB90-198946] N90-28757

A comparison of password techniques for multilevel authentication mechanisms
[AD-A224245] N90-29089

COMPUTER NETWORKS

Secure Data Network System (SDNS) network, transport, and message security protocols
[PB90-198946] N90-28757

The effect of multiprocessor radius on scaling
[DE90-014772] N90-29095

Graph structure model
[DE90-014930] N90-29097

High energy physics at Tufts University
[DE90-014664] N90-29174

International aircraft operator data base master requirements and implementation plan
[DOT/FAA/CT-90/17] N90-29247

COMPUTER PROGRAMMING

LANZ: Software solving the large sparse symmetric generalized eigenproblem
[NASA-CR-182086] N90-28876

A design tool utilizing stoichiometric structure for the analysis of biochemical reaction networks
[AD-A223873] N90-28961

Control of intelligent robots in space N90-29013

The KALI multi-arm robot programming and control environment N90-29060

Integrating planning and reactive control N90-29077

Preparing software conversion studies
[PB90-235623] N90-29099

Software development tools
[PB90-250051] N90-29103

Technical writing for software engineers
[AD-A223872] N90-29109

Strategies of computer-based instructional design: A review of guidelines and empirical research
[AD-A224038] N90-29112

Second order tensor finite element
[NASA-CR-184008] N90-29122

COMPUTER PROGRAMS

Nonequilibrium radiation and chemistry models for aerocapture vehicle flowfields
[NASA-CR-186379] N90-28490

Prediction of subsonic vortex shedding from forebodies with chines
[NASA-CR-4323] N90-28494

Evolution and use of combined mechanical and thermal codes for cryogenic turbopump bearings N90-28618

Bearing optimization for SSME HPOTP application N90-28622

Computer code for the prediction of nozzle admittance N90-28630

High variable mixture ratio oxygen/hydrogen engine N90-28640

NASCRAC (trademark): A fracture mechanics analysis code N90-28645

Comparison of two computer codes for crack growth analysis: NASCRAC versus NASA/FLAGRO N90-28648

Bandwidth and signal-to-noise ratio enhancement of the NPS transient electromagnetic scattering laboratory
[AD-A224144] N90-28771

Simulation of INPE's printed circuit laboratory production line
[INPE-4556-TDL/331] N90-28784

DOE/NIST Workshop on Common Architectures for Robotic Systems
[PB90-216839] N90-28840

LANZ: Software solving the large sparse symmetric generalized eigenproblem
[NASA-CR-182086] N90-28876

Computer program for converting rectangular coordinates to latitude-longitude coordinates
[PB90-231796] N90-28883

A design tool utilizing stoichiometric structure for the analysis of biochemical reaction networks
[AD-A223873] N90-28961

Control of intelligent robots in space N90-29013

Modularity in robotic systems N90-29014

Planning 3-D collision-free paths using spheres N90-29024

State-based scheduling: An architecture for telescope observation scheduling N90-29038

Focus of attention in an activity-based scheduler N90-29039

Planning robot actions under position and shape uncertainty N90-29073

A computer graphics package
[ARE-TM(UDT)-89111] N90-29094

Preparing software conversion studies
[PB90-235623] N90-29099

A stucture dependent software development on a relational basis: An integral approach
[ETN-90-97289] N90-29101

Inference engine for expert systems
[INPE-4565-PRE/1306] N90-29104

Product integration rules at Clenshaw-Curtis and related points: A robust implementation
[DE90-627158] N90-29106

A hardware/software environment to support R/D in intelligent machines and mobile robotic systems
[DE90-014458] N90-29119

ELEFUNT test results under AST FORTRAN V1.8.0 on the sequent symmetry
[DE90-014932] N90-29127

Model authoring system for fail safe analysis
[NASA-CR-4317] N90-29142

Computerized simulation of phenomena in plasma via particles
[INPE-4595-RPE/569] N90-29194

Data Base Analyzer and Parameter Estimator (DBAPE) interactive computer program user's manual
[PB90-193053] N90-29252

NASA Marshall Space Flight Center Solar Observatory report, January - June 1990
[NASA-TM-103512] N90-29268

Comparison of dose estimates using the buildup-factor method and a Baryon transport code (BRYNTRN) with Monte Carlo results
[NASA-TP-3021] N90-29290

COMPUTER SYSTEMS DESIGN

Documenting the decision structure in software development
[NASA-CR-186865] N90-29108

COMPUTER SYSTEMS PERFORMANCE

The effect of multiprocessor radius on scaling
[DE90-014772] N90-29095

Concepts of concurrent programming
[AD-A223897] N90-29110

ELEFUNT test results under AST FORTRAN V1.8.0 on the sequent symmetry
[DE90-014932] N90-29127

COMPUTER SYSTEMS PROGRAMS

Development of acceptance plans for airport pavement materials. Volume 1: Development
[DOT/FAA/RD-90/15] N90-28581

A stucture dependent software development on a relational basis: An integral approach
[ETN-90-97289] N90-29101

COMPUTER TECHNIQUES

Computerization of Welding Data: Proceedings of the conference and workshop
[PB90-219551] N90-28841

Computer aided mechanogenesis of skeletal muscle organs from single cells in vitro
[NASA-CR-187025] N90-28959

Portable Dextrous Force Feedback Master for robot telemanipulation (PDMFF) N90-29058

A personal computer-based, multitasking data acquisition system
[NASA-TM-4232] N90-29107

A knowledge-based system design/information tool
[NASA-CR-4316] N90-29143

COMPUTER VISION

How do robots take two parts apart N90-29061

Techniques and potential capabilities of multi-resolutional information (knowledge) processing N90-29062

Who's who in scientific visualization at LLNL
[DE90-014720] N90-29091

Computer vision and its potential applications in Brazil
[INPE-4666-NTE/283] N90-29100

COMPUTERIZED SIMULATION

Dallas/Forth Worth simulation. Phase 2: Triple simultaneous parallel Instrument Landing System (ILS) approaches (turbojets)
[DOT/FAA/CT-90/2] N90-28509

Shock dynamics in the sub-nanometer femtosecond domain
[DE90-014390] N90-28689

Computer simulation of micro-triode performance
[DE90-014191] N90-28774

Simulation of INPE's printed circuit laboratory production line
[INPE-4556-TDL/331] N90-28784

Numerical simulation of reactive turbulent flows
[ETN-90-97476] N90-28807

Three-dimensional simulations of the generation of one Angstrom radiation by a self-amplified spontaneous emission free-electron laser
[DE90-015032] N90-28830

Dynamic interaction of multiple autonomous mobile robots N90-28844

Tele-Autonomous control involving contact — object localization
[NASA-CR-187004] N90-28854

Reliability analysis of maintained structural system vulnerable to fatigue and fracture N90-28868

Complex auditory signals
[AD-A224127] N90-28969

Three-dimensional motor schema based navigation N90-29026

Causal simulation and sensor planning in predictive monitoring N90-29037

Efficient mapping algorithms for scheduling robot inverse dynamics computation on a multiprocessor system N90-29071

Automated simulation as part of a design workstation
[NASA-TM-102852] N90-29083

LINTERP: A numerical algorithm for interpolating quadrilateral and hexahedral meshes
[DE90-014417] N90-29090

Who's who in scientific visualization at LLNL
[DE90-014720] N90-29091

Block Lanczos algorithm
[AD-A224011] N90-29111

Computerized simulation of phenomena in plasma via particles
[INPE-4595-RPE/569] N90-29194

TSC (Tokamak Simulation Code) simulations of Alcator C-MOD discharges 3: Study of axisymmetric stability
[DE90-015386] N90-29198

Control of nonlinear space-charge emittance growth
[DE90-014752] N90-29270

The formation of globular clusters N90-29272

COMPUTERS

A Boltzmann machine for the organization of intelligent machines N90-29040

Guide to charging for the CCF
[RSRE-89022] N90-29238

CONCENTRATION (COMPOSITION)

Study of the radical OH in a high pressure flame by resonant DRASC
[ONERA-RF-57/7131-PY] N90-28892

CONCENTRIC CYLINDERS

Stabilization of Taylor-Couette flow due to time-periodic outer cylinder oscillation
[PB90-219130] N90-28790

CONCRETES

Development and testing of rapid repair methods for war damaged runways
[AD-A223970] N90-28586

CONCURRENT PROCESSING

Concepts of concurrent programming
[AD-A223897] N90-29110

CONDUCTING POLYMERS
Polymer research
[PB90-246638] N90-28737
CONDUCTIVE HEAT TRANSFER
Radiative heat transfer
[PB90-247602] N90-28813
Frequency response of a thermocouple wire: Effects of axial conduction
[NASA-CR-180454] N90-28827
CONDUCTIVITY
Numerical and analytical study of nonlinear bifurcations associated with the morphological stability of two-dimensional single crystals
[PB90-209594] N90-29200
CONFERENCES
Aerodynamics of Combat Aircraft Controls and of Ground Effects
[AGARD-CP-465] N90-28513
Proceedings of a workshop on Future Airport Passenger Terminals
[PB90-213620] N90-28580
Advanced Earth-to-Orbit Propulsion Technology 1988, volume 1
[NASA-CP-3012-VOL-1] N90-28611
High Temperature Surface Interactions
[AGARD-CP-481] N90-28698
Proceedings of US Army Research Office Workshop on US Army Applications for Diamond and Diamondlike Materials
[AD-A224193] N90-28741
Computerization of Welding Data: Proceedings of the conference and workshop
[PB90-219551] N90-28841
Puerto Rico Workshop on Land-Based Sources of Marine Pollution in the Wider Caribbean Region
[PB90-184094] N90-28921
Drilling the oceanic lower crust and mantle: A global strategy for exploring the deep oceanic crust and mantle in the 1990's
[PB90-240953] N90-28936
Proceedings of the 14th Annual Climate Diagnostics Workshop
[PB90-198573] N90-28938
Situational Awareness in Aerospace Operations
[AGARD-CP-478] N90-28972
Proceedings of the NASA Conference on Space Telerobotics, volume 1
[NASA-CR-186856] N90-29000
Proceedings of the NASA Conference on Space Telerobotics, volume 2
[NASA-CR-186857] N90-29044
Workshop on Neural Networks
[DE90-014794] N90-29120
Fifteenth International Conference on X Ray and Inner-Shell Processes
[DE90-013024] N90-29170
Information management directions: The integration challenge
[PB90-219866] N90-29245
Crossroads of Information Technology Standards
[PB90-239732] N90-29251
CONFIGURATION INTERACTION
Accurate quantum chemical calculations
[NASA-TM-101932] N90-28680
CONFIGURATION MANAGEMENT
A new approach to global control of redundant manipulators N90-29002
CONFINEMENT
An experimental investigation of a single and multiphase confined coaxial jet N90-28796
CONFORMAL MAPPING
Prediction of subsonic vortex shedding from forebodies with chines
[NASA-CR-4323] N90-28494
Beltrami algebra and symmetry of Beltrami equation on Riemann surfaces
[DE90-627157] N90-29135
Trajectories of renormalization group flows on the phase diagram of N=2 superconformal field theories
[DE90-627212] N90-29154
Topology of singularities and phase diagram of N=2 superconformal field theories
[DE90-627213] N90-29155
CONGRESSIONAL REPORTS
Present state of knowledge of the upper atmosphere 1990: An assessment report
[NASA-RP-1242] N90-28929
Federal support to universities, colleges, and selected nonprofit institutions: Fiscal year 1988 (detailed statistical tables)
[PB90-226887] N90-29236
CONSCIOUSNESS
Target acquisition under load factors: Advantages and disadvantages of a helmet mounted sight N90-28983
Loss of alertness and consciousness from pilot position during long range flight N90-28990
CONSERVATION EQUATIONS
Analyses of spray and droplet ignition for pure and multicomponent fuels N90-28688
CONSERVATION LAWS
Numerical experiments on the accuracy of ENO and modified ENO schemes
[NASA-CR-182083] N90-29128
Numerical methods for systems of conservation laws of mixed type using flux splitting
[NASA-CR-182084] N90-29129
CONSISTENCY
Consistency and convergence for numerical radiation conditions
[NASA-TM-103262] N90-29124
CONSTRICTORS
Low power arcjet performance
[NASA-TM-103280] N90-28657
CONTAINERLESS MELTS
Containerless low gravity processing of glass forming and immiscible alloys
[NASA-CR-186999] N90-28747
CONTAMINANTS
Space station contamination modeling
[NASA-CR-183871] N90-28590
National air pollutant emission estimates, 1940-1988
[PB90-199266] N90-28908
National air quality and emissions trends report, 1988
[PB90-200114] N90-28909
CONTINUOUS WAVE LASERS
Tunable CW single-frequency source for injection seeding 2-micrometer lasers
[AD-A223979] N90-28834
CONTRACTION
Robust controller design by contraction of a pole region
[ESA-TT-1042] N90-29118
CONTRACTORS
Procedures for DOE-Navy exchange and approval of engineering information and material management required for production of W88-0/Mk5 RBA (reentry body assembly)
[DE90-014763] N90-28595
CONTROL BOARDS
Description of the primary flight display and flight guidance system logic in the NASA B-737 transport systems research vehicle
[NASA-TM-102710] N90-28546
CONTROL STABILITY
Robust controller design by contraction of a pole region
[ESA-TT-1042] N90-29118
CONTROL SURFACES
Control of submersible vortex flows
[NASA-TM-102693] N90-28493
Aerodynamic control design: Experience and results at Aermacchi N90-28518
Development of non-conventional control methods for high angle of attack flight using vortex manipulation N90-28522
Control of vortex aerodynamics at high angles of attack N90-28523
Unsteady aerodynamics of controls N90-28525
CONTROL SYSTEMS DESIGN
Aerodynamics of Combat Aircraft Controls and of Ground Effects
[AGARD-CP-465] N90-28513
Aerodynamic and propulsive control development of the STOL and maneuver technology demonstrator N90-28514
Combat aircraft control requirements N90-28515
Aerodynamic control design: Experience and results at Aermacchi N90-28518
Innovative control concepts and component integration for a generic supercruise fighter N90-28521
Development of non-conventional control methods for high angle of attack flight using vortex manipulation N90-28522
Unsteady aerodynamics of controls N90-28525
Validation of the F-18 high alpha research vehicle flight control and avionics systems modifications
[NASA-TM-101723] N90-28542
Propulsion system-flight control integration and optimization: Flight evaluation and technology transition
[NASA-TM-4207] N90-28551
Energy Efficient Engine: Control system preliminary definition report
[NASA-CR-179578] N90-28569
A conceptual framework for fighter flight control systems
[PD-CF-9009] N90-28577
A microprocessor controlled strain gauge calibration module
[AR-005-579] N90-28821
Design of a CO2 laser power control system for a Spacelab microgravity experiment
[NASA-TM-103112] N90-28833
Cartesian control of redundant robots N90-29004
The NASA/OAST telerobot testbed architecture N90-29016
Exploiting map plans as resources for action N90-29028
Computational neural learning formaliams for manipulator inverse kinematics N90-29030
Multi-layer neural networks for robot control N90-29031
Plan recognition for space telerobotics N90-29036
Trajectory generation of space telerobots N90-29055
Planning robot actions under position and shape uncertainty N90-29073
Integrating planning and reactive control N90-29077
An expert system to perform on-line controller restructuring for abrupt model changes
[NASA-TM-103609] N90-29121
CONTROL THEORY
Aerodynamic and propulsive control development of the STOL and maneuver technology demonstrator N90-28514
Control research in the NASA high-alpha technology program N90-28516
Innovative control concepts and component integration for a generic supercruise fighter N90-28521
Real time guidance and propulsion control for single-stage-to-orbit airbreathing vehicles N90-28587
An LQR controller design approach for a Large Gap Magnetic Suspension System (LGMSS)
[NASA-TM-101606] N90-28751
Preliminary results on noncollocated torque control of space robot actuators N90-29057
CONTROLLABILITY
Combat aircraft control requirements N90-28515
Combat aircraft control requirements for agility N90-28517
Aerodynamic control design: Experience and results at Aermacchi N90-28518
Innovative control concepts and component integration for a generic supercruise fighter N90-28521
CONTROLLERS
Real time guidance and propulsion control for single-stage-to-orbit airbreathing vehicles N90-28587
Using embedded microcontrollers in radar test equipment
[DE90-014997] N90-28763
Dynamic modeling and payload-adaptation control of a flexible one-link manipulator N90-28843
Experiments in the dynamic and strategic control of cooperating manipulators N90-28845
Cartesian control of redundant robots N90-29004
Teleoperator comfort and psychometric stability: Criteria for limiting master-controller forces of operation and feedback during telemanipulation N90-29009
A neural network for controlling the configuration of frame structure with elastic members N90-29034
Multiple cooperating manipulators: The case of kinematically redundant arms N90-29048
The JPL telerobot operator control station. Part 2: Software N90-29050
Design of a monitor and simulation terminal (master) for space station telerobotics and telescience N90-29051
Performance evaluation of a 6 axis high fidelity generalized force reflecting teleoperator N90-29052
Implementation and design of a teleoperation system based on a VMEBUS/68020 pipelined architecture N90-29053
Human machine interaction via the transfer of power and information signals N90-29054
Trajectory generation of space telerobots N90-29055
On the simulation of space based manipulators with contact N90-29056
Planning robot actions under position and shape uncertainty N90-29073
Robust controller design by contraction of a pole region
[ESA-TT-1042] N90-29118
CONVECTION
Oscillatory convection
[ESA-TT-890] N90-28801
Diffusion in the surface layer of the convective boundary layer
[AD-A224125] N90-28924
Genesis of bow echoes: A rear-inflow induced meso-convective structure
[PB90-209776] N90-28926
CONVECTION CLOUDS
Gravity wave initiated convection
[NASA-CR-186868] N90-28933
CONVECTIVE HEAT TRANSFER
Calculation of temperature distribution in various turbine blades using a boundary-fitted coordinate transformation method N90-28550

Free shear layer and swirl flow heat transfer enhancement
[PB90-226123] N90-28798

CONVERGENCE
An asymptotically induced domain decomposition method for parabolic boundary layer problems
[DE90-014620] N90-28804
An investigation of forcing mechanisms during a surprise tornadic thunderstorm
[PB90-216805] N90-28940
Consistency and convergence for numerical radiation conditions
[NASA-TM-103262] N90-29124
Numerical methods for systems of conservation laws of mixed type using flux splitting
[NASA-CR-182084] N90-29129

CONVOLUTION INTEGRALS
Novel numerical analysis method for the study of convolution equations in appearance potential spectroscopy
[ETN-90-97286] N90-29210

COOLING
Cryogenic, high speed, turbopump bearing cooling requirements N90-28620
Transient cooling of a hot surface by droplets evaporation
[PB90-227968] N90-28799

COOLING SYSTEMS
High/variable mixture ratio oxygen/hydrogen engines N90-28637

COORDINATE TRANSFORMATIONS
Calculation of temperature distribution in various turbine blades using a boundary-fitted coordinate transformation method N90-28550

COORDINATES
A nonhydrostatic numerical model in sigma-coordinates and simulations of mesoscale phenomena N90-28932
Multiple cooperating manipulators: The case of kinematically redundant arms N90-29046

COORDINATION
Motion coordination for mobile robots in unstructured environments
[PB90-199498] N90-28837
Motion coordination for a mobile manipulator system
[PB90-203076] N90-28839
Multiple cooperating manipulators: The case of kinematically redundant arms N90-29046
Parallel algorithms for computation of the manipulator inertia matrix N90-29072

COPPER
Structure of metal overlayers by low energy alkali ion scattering: Cu/Ru(0001) and Sn/Pt(111)
[DE90-014453] N90-28718
The stability of the martensitic phases in Cu-Zn-Al at an electron concentration of 1.534
[DE90-628628] N90-28727
Studies of central interactions of Si ions at 14.5 x A GeV/c in Au and Cu
[DE90-015095] N90-29195

COPPER ALLOYS
Density changes of generation 1.5 and 2.0 copper alloys irradiated at 411 to 414 C and 529 C in FFTF-MOTA
[DE90-015291] N90-28724

COPPER COMPOUNDS
Antiferromagnetism and enhanced heat in CeM2Sn (M = Ni, Ir, Cu, Rh, Pd, and Pt
[DE90-014924] N90-29206

COPPER OXIDES
Synthesis and structural chemistry of Au(III)-substituted Ba2YCu3O(7-delta)
[NASA-TM-103292] N90-28696
Electron microscopy of transition-metal doped BiCaSrCuO
[DE90-014184] N90-29202

CORE FLOW
Energy Efficient Engine core design and performance report
[NASA-CR-168069] N90-28559

CORE SAMPLING
Robotic sampling system for an unmanned Mars mission N90-29070

CORONAL LOOPS
Vlasov-Maxwell equilibria of solar coronal loops
[DE90-015025] N90-29289

CORROSION
Effect of protective coatings on mechanical properties of superalloys N90-28707

CORROSION RESISTANCE
High Temperature Surface Interactions
[AGARD-CP-461] N90-28696
Developments in test procedures for hot-salt corrosion of superalloys N90-28700
Molten salt induced high temperature degradation of thermal barrier coatings N90-28704
Overview on hot gas tests and molten salt corrosion experiments at the DLR N90-28714
Evaluation of advanced austenitic alloys relative to alloy design criteria for steam service. Part 1: Lean stainless steel
[DE90-014765] N90-28720
Proceedings of US Army Research Office Workshop on US Army Applications for Diamond and Diamondlike Materials
[AD-A224193] N90-28741

COSMIC RAYS
Measurements of the single event upset environment in the upper atmosphere
[RAE-TM-SPACE-373] N90-28934
Gamma ray evidence for cosmic ray sources N90-29292
Fluctuations in cosmic background radiation
[INPE-4579-PRE/1313] N90-29294

COSMOLOGY
Viscous causal cosmologies
[DE90-627487] N90-29282

COSMONAUTS
Cardiovascular deconditioning of cosmonauts: Role, importance and applications of the lower body negative pressure
[ETN-90-97507] N90-28964

COST ANALYSIS
Guide to charging for the CCF
[RSRE-89022] N90-29238

COST EFFECTIVENESS
Life cycle cost in the conceptual design of subsonic commercial aircraft, volumes 1 and 2 N90-28535
Energy efficient engine program technology benefit/cost study. Volume 1: Executive summary
[NASA-CR-174766-VOL-1] N90-28564
Energy Efficient Engine: High-pressure compressor test hardware detailed design report
[NASA-CR-180850] N90-28570

COST ESTIMATES
Extensions to the learning curve: An analysis of factors influence unit cost of weapon systems
[AD-A224119] N90-29256

COST REDUCTION
Energy efficient engine program technology benefit/cost study, volume 2
[NASA-CR-174766-VOL-2] N90-28565
How can research and development leadtime be reduced
[AD-A224063] N90-29240

COSTS
Extensions to the learning curve: An analysis of factors influence unit cost of weapon systems
[AD-A224119] N90-29256

COUETTE FLOW
Stabilization of Taylor-Couette flow due to time-periodic outer cylinder oscillation
[PB90-219130] N90-28790

COUNTERMEASURES
Counterair situation awareness display for Army aviation N90-28982

COUNTING
Transformational part-count in layered octahedral-tetrahedral truss configurations
[NASA-TM-102635] N90-28598

COUPLED MODES
Approximation, synthesis, and development of bi-mode cavities microwave filters presenting unsymmetrical quasi-elliptic responses
[CNES-NT-124] N90-28761

COUPLING
The effects of structural flap-lag and pitch-lag coupling on soft inplane hingeless rotor stability in hover
[NASA-TP-3002] N90-28503
Flow coupling between a rotor and a stator in turbomachinery
[AD-A223882] N90-28572

CRACK PROPAGATION
Damage tolerance of the fighter aircraft 37 Viggen. Part 1: Analytical assessment
[FFA-TN-1990-12-PT-1] N90-28538
Damage tolerance of the fighter aircraft 37 Viggen. Part 2: Experimental verification
[FFA-TN-1990-13-PT-2] N90-28539
NASCRAC (trademark): A fracture mechanics analysis code N90-28645
A comparison of single-cycle versus multi-cycle proof testing strategies N90-28646
Data base for crack growth properties of materials N90-28647
Comparison of two computer codes for crack growth analysis: NASCRAC versus NASA/FLAGRO N90-28648
Micromechanisms of fatigue crack growth and fracture toughness in metal matrix composites
[AD-A223863] N90-28676
Crack layer analysis of fatigue fracture of a beta titanium alloy N90-28864
Green's functions for dislocations in bonded strips and related crack problems
[NASA-CR-185291] N90-28878

CRACKS
Crack layer analysis of fatigue fracture of a beta titanium alloy N90-28864

CRASHES
Special test and evaluation methods used for a nine-axis accelerometer
[PB90-209578] N90-28822

CREEP PROPERTIES
NASCRAC (trademark): A fracture mechanics analysis code N90-28645
Inelastic analysis of laminated composites N90-28689

CREEP STRENGTH
Evaluation of advanced austenitic alloys relative to alloy design criteria for steam service. Part 1: Lean stainless steel
[DE90-014765] N90-28720

CREW WORKSTATIONS
Space Station Freedom pressurized element interior design process
[NASA-CR-181297] N90-28597
Human factors model concerning the man-machine interface of mining crewstations N90-29011

CRITERIA
A constitutive model for AS4/PEEK thermoplastic composites under cyclic loading
[NASA-CR-180393] N90-28679
Periodic gaits for the CMU ambler N90-29027

CROSS FLOW
Wind tunnel investigation of periodic vortex separation from rough surface circular cylinders by means of acoustic measurements
[ESA-TT-1092] N90-28499
Experimental investigations on the stability and transition of three-dimensional boundary layers
[ESA-TT-1026] N90-28803

CRYOGENIC FLUIDS
Pratt and Whitney cryogenic turbopump bearing experience N90-28624

CRYOGENICS
Cryogenic, high speed, turbopump bearing cooling requirements N90-28620

CRYOLITE
Electronic conduction in molten cryolite saturated with alumina
[DE90-015090] N90-29211

CRYPTOGRAPHY
Secure Data Network System (SDNS) network, transport, and message security protocols
[PB90-198946] N90-28757

CRYSTAL LATTICES
Shock dynamics in the sub-nanometer femtosecond domain
[DE90-014390] N90-28689
The stability of the martensitic phases in Cu-Zn-Al at an electron concentration of 1.534
[DE90-628628] N90-28727
The first order phase transition for six-state Potts model on two dimensional random triangle lattice
[DE90-627210] N90-29140
Criticality of the three-state chiral clock model: A renormalisation group study
[DE90-627321] N90-29212
A generalised Hubbard Hamiltonian: Influence of temperature and fractality
[DE90-627322] N90-29213
Z(6) model: Criticality and break-collape method
[DE90-627323] N90-29214
Susceptibility of the Potts model in an hierarchical lattice: Renormalisation group approach
[DE90-627324] N90-29215

CRYSTAL STRUCTURE
Twisted crystals: Propagation, genesis, and relationships with optical activity and molecular symmetry (excerpts)
[DE90-014259] N90-29205
Antiferromagnetism and enhanced heat in CeM2Sn (M = Ni, Ir, Cu, Rh, Pd, and Pt
[DE90-014924] N90-29206
X ray scattering studies of non-equilibrium ordering processes
[DE90-015066] N90-29209

CRYSTALLIZATION
Twisted crystals: Propagation, genesis, and relationships with optical activity and molecular symmetry (excerpts)
[DE90-014259] N90-29205

CRYSTALS
Twisted crystals: Propagation, genesis, and relationships with optical activity and molecular symmetry (excerpts)
[DE90-014259] N90-29205

CULTURE TECHNIQUES
Insulin and insulin-like growth factor-1 induce pronounced hypertrophy of skeletal myofibers in tissue culture
[NASA-CR-187026] N90-28960
CURING
Radiation-curable prepreg composites
[DE90-629740] N90-28674
CURRENT ALGEBRA
Quantum gravity in two dimensions and the SL(2,R) current algebra
[DE90-627215] N90-29156
CURRENT DENSITY
Effects of friction and end losses on MHD thruster efficiency
[DE90-013673] N90-28608
Measurement of localized corrosion using current density mapping
[DE90-015086] N90-28721
Unipolar arcing on the cathode surface of a high voltage diode
[AD-A224122] N90-28787
CURRENT DISTRIBUTION
Further studies of 60 Hz exposure effects on human function
[DE90-014377] N90-28962
CURVATURE
The effects of grid-generated turbulence on flat and concave turbulent boundary layers N90-28797
Free shear layer and swirl flow heat transfer enhancement
[PB90-228123] N90-28798
Twisted crystals: Propagation, genesis, and relationships with optical activity and molecular symmetry (excerpts)
[DE90-014259] N90-29205
CYCLIC ACCELERATORS
Beam diagnostics in circular machines: Review of new developments
[DE90-014986] N90-29176
CYCLIC LOADS
A constitutive model for AS4/PEEK thermoplastic composites under cyclic loading
[NASA-CR-180393] N90-28679
CYCLOTRON RADIATION
Combined electron cyclotron ray tracing and transport code studies in the compact ignition tokamak
[DE90-014097] N90-29189
CYCLOTRON RESONANCE DEVICES
Mode competition in the quasioptical gyrotron
[AD-A222181] N90-28823
CYLINDRICAL BODIES
On Einsteinian 4-submanifolds in E(sup 6)
[DE90-627149] N90-29226
CYTOGENESIS
Computer aided mechanogenesis of skeletal muscle organs from single cells in vitro
[NASA-CR-187025] N90-28959

D

DAMAGE
Damage tolerance of the fighter aircraft 37 Viggen. Part 1: Analytical assessment
[FFA-TN-1990-12-PT-1] N90-28538
Damage tolerance of the fighter aircraft 37 Viggen. Part 2: Experimental verification
[FFA-TN-1990-13-PT-2] N90-28539
Development and testing of rapid repair methods for war damaged runways
[AD-A223970] N90-28586
Oxidation, sulfidation, and hot corrosion: Mechanisms and interrelationships N90-28702
Evaluation of high temperature protective coatings for gas turbine engines under simulated service conditions N90-28712
Damage resistant optical coatings prepared using high temperature, plasma chemical-vapor-deposition
[DE90-015042] N90-28738
Minimum weight design of a leaf spring tapered in thickness and width for the Hubble Space Telescope-space support equipment
[NASA-TM-4233] N90-28879
DNA damage and repair in human skin: Pathways and questions
[DE90-015126] N90-28966
DAMAGE ASSESSMENT
The fatigue damage behavior of a single crystal superalloy N90-28644
Microdamage to ceramic surfaces under sliding conditions N90-28708
Activities report for the IBDF-INPE project SEQE, year 1987
[INPE-4534-RPE/565] N90-29298
DAMPING
Effects and tolerances of injection jitter in the SLC and future linear colliders
[DE90-014805] N90-29179
DATA ACQUISITION
Analysis of heliport environmental data, Intracoastal City
[DOT/FAA/CT-TN89/43] N90-28584
On-line object feature extraction for multispectral scene representation
[NASA-CR-187006] N90-28888
A method of classification for multisource data in remote sensing based on interval-valued probabilities
[NASA-CR-187007] N90-28889
How do robots take two parts apart N90-29061
A personal computer-based, multitasking data acquisition system
[NASA-TM-4232] N90-29107
DATA BASE MANAGEMENT SYSTEMS
Object database management systems: Concepts and features
[PB90-216813] N90-29243
DATA BASES
A flight dynamic model of aircraft spinning
[AR-005-600] N90-28576
Data base for crack growth properties of materials N90-28647
High energy-density liquid rocket fuel performance
[NASA-CR-185279] N90-28742
Measuring the vertical directional spectra caused by sea surface sound
[AD-A223883] N90-28957
A design tool utilizing stoichiometric structure for the analysis of biochemical reaction networks
[AD-A223873] N90-28961
Object database management systems: Concepts and features
[PB90-216813] N90-29243
International aircraft operator data base master requirements and implementation plan
[DOT/FAA/CT-90/17] N90-29247
Data Base Analyzer and Parameter Estimator (DBAPE) interactive computer program user's manual
[PB90-193053] N90-29252
DATA LINKS
An aeronautical mobile satellite experiment
[NASA-CR-186971] N90-28593
A FAA Technical Center project transition plan: Mode S
[DOT/FAA/CT-TN90/17] N90-28785
DATA MANAGEMENT
Information management directions: The integration challenge
[PB90-219866] N90-29245
DATA PROCESSING
Phoenix data analysis and numerical simulation
[AD-A224226] N90-28772
Techniques and potential capabilities of multi-resolutional information (knowledge) processing N90-29062
The SPECIALIST: Natural language processing system
[PB90-240029] N90-29098
Preparing software conversion studies
[PB90-235623] N90-29099
INPE geographic data base
[INPE-4636-PRE/1348] N90-29253
DATA STRUCTURES
Treatment of systematic errors 2: Fusion of ultrasound and visual sensor data
[DE90-014780] N90-28850
DATA TRANSMISSION
Secure Data Network System (SDNS) network, transport, and message security protocols
[PB90-198946] N90-28757
DECISION MAKING
Research in command and control for the Dutch Army Corps (1NL)
[IZF-1989-28] N90-28760
Chasing a specter: Risk management for global environmental change
[DE90-014455] N90-28917
A methodology for the objective measurement of pilot situation awareness N90-28974
Situational Awareness Rating Technique (SART): The development of a tool for aircrew systems design N90-28975
Towards a future cockpit: The prototyping and pilot integration of the Mission Management Aid (MMA) N90-28979
Cognition versus sensation: A paradigm for reorientation
[IZF-1989-20] N90-28995
Exploiting map plans as resources for action N90-29028
Perceptual telerobotics N90-29063
Inference engine for expert systems
[INPE-4565-PRE/1306] N90-29104
Documenting the decision structure in software development
[NASA-CR-186865] N90-29108
Overcoming rule-based rigidity and connectionist limitations through massively-parallel case-based reasoning
[NASA-CR-186963] N90-29117
Prediction, control, and decision-making aspects for chaotic systems
[DE90-014452] N90-29224
The effects of management support on the successful implementation of group decision support systems
[AD-A224473] N90-29241
DECISION THEORY
A design philosophy for multi-layer neural networks with applications to robot control N90-29033
DECODING
Automated system for meteorological analysis
[INPE-4586-TDL/332] N90-28945
DECOMPOSITION
Study of the induction time in isothermal decomposition of explosives
[DE90-014906] N90-28745
A complete analytical solution for the inverse instantaneous kinematics of a spherical-revolute-spherical (7R) redundant manipulator N90-29006
DECOMPRESSION SICKNESS
Decompression sickness presenting as a viral syndrome
[AD-A223880] N90-28967
DECONDITIONING
Cardiovascular deconditioning of cosmonauts: Role, importance and applications of the lower body negative pressure
[ETN-90-97507] N90-28984
DECOUPLING
Geometric theory for infinite dimensional systems
[ETN-90-96922] N90-29144
DEFECTS
Research on the structural and electronic properties of defects in amorphous silicon
[DE90-000342] N90-28730
An improved method for choosing sampling points for the inspection of complex surfaces in a computer-aided manufacturing environment N90-29093
DEFENSE PROGRAM
The personal computer: An untapped source for the United States Army War College
[AD-A223976] N90-28087
DEFINITION
Liquid Rocket Booster (LRB) for the Space Transportation System (STS) systems study. Appendix G: LRB for the STS system study level 2 requirements, revision 1
[NASA-CR-183793-APP-G] N90-28607
A glossary of terms, definitions, acronyms, and abbreviations related to the National Airspace System
[DOT/FAA/CT-TN89/53] N90-29249
DEFORMATION
Behavior of Al-Mg alloys in hot working and superplasticity
[DE90-015193] N90-28723
High-temperature deformation and microstructural analysis for Si3N4-Sc2O3
[NASA-TM-103239] N90-28740
A nonlinear finite element formulation for the large displacement analysis of plates N90-28867
Twisted crystals: Propagation, genesis, and relationships with optical activity and molecular symmetry (excerpts)
[DE90-014259] N90-29205
DEGRADATION
Molten salt induced high temperature degradation of thermal barrier coatings N90-28704
Effect of protective coatings on mechanical properties of superalloys N90-28707
Study of meteorological processes important in the degradation of materials through surface temperature
[PB90-222720] N90-28856
DEGREES OF FREEDOM
Inflight thrust vectoring: A further degree of freedom in the aerodynamic/flight mechanical design of modern fighter aircraft N90-28528
A 17 degree of freedom anthropomorphic manipulator N90-29001
Kinematic functions for the 7 DOF robotics research arm N90-29003
A complete analytical solution for the inverse instantaneous kinematics of a spherical-revolute-spherical (7R) redundant manipulator N90-29006
Characterization and control of self-motions in redundant manipulators N90-29045
Reflexive obstacle avoidance for kinematically-redundant manipulators N90-29047

DELAMINATING
Green's functions for dislocations in bonded strips and related crack problems
[NASA-CR-185291] N90-28878
DELTA WINGS
Experimental investigations on the stability and vorticity of the vortex breakdown phenomenon above delta wings, measured by the ultrasonic laser method
[ESA-TT-1079] N90-28498
Control of vortex aerodynamics at high angles of attack N90-28523
The steady and time-dependent aerodynamic characteristics of a combat aircraft with a delta or swept canard N90-28526
The aerodynamic design of the oblique flying wing supersonic transport
[NASA-CR-177552] N90-28540
DENSITY (MASS/VOLUME)
Density changes of generation 1.5 and 2.0 copper alloys irradiated at 411 to 414 C and 529 C in FFTF-MOTA
[DE90-015291] N90-28724
DENSITY DISTRIBUTION
An analysis of the Palomar-Green subdwarfs and white dwarfs N90-29263
DEOXYRIBONUCLEIC ACID
DNA damage and repair in human skin: Pathways and questions
[DE90-015126] N90-28966
DEPLOYMENT
The effect of rapid spoiler deployment on the transient forces on an aerofoil N90-28527
DEPOSITION
Acid deposition: No such thing as a free launch
[DE90-015085] N90-28920
Tropospheric nitrogen: The influence of anthropogenic sources on distributions and deposition, executive summary
[DE90-015401] N90-28922
Estimating the spatial variability of trace gas deposition velocities
[PB90-208570] N90-28928
DEPTH
Building an environment model using depth information N90-29064
DESCENT
Dynamic ground effects N90-28531
DESIGN ANALYSIS
Energy Efficient Engine integrated core/low spool test hardware design report
[NASA-CR-168137] N90-28566
Energy Efficient Engine: High-pressure compressor test hardware detailed design report
[NASA-CR-180850] N90-28570
Development of a thickness design procedure for stabilized layers under rigid airfield pavements
[DOT/FAA/RD-90/22] N90-28582
Liquid Rocket Booster (LRB) for the Space Transportation System (STS) systems study. Appendix G: LRB for the STS system study level 2 requirements, revision 1
[NASA-CR-183793-APP-G] N90-28607
Design optimization of gas generator hybrid propulsion boosters
[NASA-CR-181096] N90-28660
Extended range tankless water heater
[DE90-014474] N90-28750
Using embedded microcontrollers in radar test equipment
[DE90-014997] N90-28763
Minimum weight design of a leaf spring tapered in thickness and width for the Hubble Space Telescope-space support equipment
[NASA-TM-4233] N90-28879
Military aircrew seating: A human factors engineering approach
[AD-A218049] N90-28999
Strategies of computer-based instructional design: A review of guidelines and empirical research
[AD-A224038] N90-29112
A knowledge-based system design/information tool
[NASA-CR-4316] N90-29143
DETECTION
Target detection in Gaussian noise using artificial neural systems
[AD-A223983] N90-28770
Building an environment model using depth information N90-29064
DETERIORATION
Guidelines for pressure vessel safety assessment
[PB90-210619] N90-28749
DETONATION
Shock dynamics in the sub-nanometer femtosecond domain
[DE90-014390] N90-28689
DEUTERIUM
Mass spectrometric analysis of hydrogen isotopes in metals and metal hydrides
[DE90-014118] N90-28685
DEW POINT
Daily temperature, solar radiation, wind speed, cloud cover, and precipitation data recorded at the meteorological station for calendar years 1957--1988
[DE90-014399] N90-28941
DIAGNOSIS
Beam diagnostics in circular machines: Review of new developments
[DE90-014986] N90-29176
DIAMONDS
Proceedings of US Army Research Office Workshop on US Army Applications for Diamond and Diamondlike Materials
[AD-A224193] N90-28741
Use of electron spectroscopies in the tribological evaluation of diamond films
[DE90-014421] N90-28848
Mechanical properties testing of diamond and diamond-like films by ultra-low load indentation
[DE90-014456] N90-28861
Mechanical property measurement of polycrystalline diamond films
[AD-A224037] N90-29222
DICTIONARIES
A glossary of terms, definitions, acronyms, and abbreviations related to the National Airspace System
[DOT/FAA/CT-TN89/53] N90-29249
DIELECTRIC PROPERTIES
Semiconductor measurement technology: A software program for aiding the analysis of ellipsometric measurements, simple spectroscopic models
[PB90-216847] N90-29201
DIELECTRICS
Damage resistant optical coatings prepared using high temperature, plasma chemical-vapor-deposition
[DE90-015042] N90-28738
Research for electric energy systems
[DE90-014221] N90-28775
Investigations into the use of dielectric coatings in magnetic switches
[DE90-014331] N90-28776
Chiral Maxwell-Garnett mixing formula
[PB90-189143] N90-29158
DIESEL ENGINES
Influence of diesel engine exposure on the rupture strength of silicon nitride and partially stabilized zirconia
[DE90-014759] N90-28849
DIFFERENCE EQUATIONS
Numerical methods for systems of conservation laws of mixed type using flux splitting
[NASA-CR-182084] N90-29129
DIFFERENTIAL EQUATIONS
A nonlinear finite element formulation for the large displacement analysis of plates N90-28667
Beltrami algebra and symmetry of Beltrami equation on Riemann surfaces
[DE90-627157] N90-29135
Theory of biaxial graded-index optical fiber
[NASA-CR-186977] N90-29180
DIFFERENTIATION (BIOLOGY)
Computer aided mechanogenesis of skeletal muscle organs from single cells in vitro
[NASA-CR-187025] N90-28959
Insulin and insulin-like growth factor-1 induce pronounced hypertrophy of skeletal myofibers in tissue culture
[NASA-CR-187026] N90-28960
DIFFRACTION
Geophysical diffraction tomography: A complementary remote sensing technique for hazardous waste site characterization
[DE90-013025] N90-28882
Near-angle scattering and binary optics
[AD-A224140] N90-29186
DIFFUSION
Asymptotic behavior of solutions of diffusion-like partial differential equations invariant to a family of affine groups
[DE90-014792] N90-29130
DIFFUSION THEORY
Electrochemistry using nanometer-sized electrodes
[AD-A223890] N90-28697
DIGITAL COMPUTERS
Optical storage technology
[AD-A224028] N90-29254
DIGITAL DATA
A FAA Technical Center project transition plan: Mode S
[DOT/FAA/CT-TN90/17] N90-28765
DIGITAL ELECTRONICS
Energy Efficient Engine: Control system preliminary definition report
[NASA-CR-179578] N90-28589
DIGITAL SYSTEMS
A conceptual framework for fighter flight control systems
[PD-CF-9009] N90-28577
ATDRS payload technology research and development
[NASA-TM-103256] N90-28596
DIODES
Ion divergence and the stability of magnetically insulated diodes
[DE90-014565] N90-28777
PBFA 2 applied B ion diode beam characteristics at high voltages
[DE90-014419] N90-29190
DIRAC EQUATION
On the zeta-function regularization of chiral Jacobians for singular Dirac operators
[DE90-627176] N90-29150
Dirac's equation as a geodesic in Riemann space
[DE90-627194] N90-29152
DIRECT CURRENT
Liquid Rocket Booster (LRB) for the Space Transportation System (STS) systems study. Appendix C: Battery report for the liquid rocket booster TVC actuators
[NASA-CR-183788-APP-C] N90-28603
DIRECTIONAL STABILITY
The effects of foreplanes on the static and dynamic characteristics of a combat aircraft model N90-28520
DIRECTORIES
Who's who in scientific visualization at LLNL
[DE90-014720] N90-29091
DIRICHLET PROBLEM
Asymptotics of Laplace-Dirichlet integrals
[DE90-627165] N90-29137
DISKS
Application of advanced coating techniques to rocket engine components N90-28654
DISORIENTATION
Spatial disorientation incidents in the RNLAF F16 and F5 aircraft and suggestions for prevention N90-28973
DISPERSIONS
Containerless low gravity processing of glass forming and immiscible alloys
[NASA-CR-186999] N90-28747
DISPLACEMENT
Mechanical behavior of thick, curved, laminated composites N90-28664
A nonlinear finite element formulation for the large displacement analysis of plates N90-28667
Parametric solution of nonlinear structure problems
[ONERA-RT-21/3542-RY-082-R] N90-28874
DISPLAY DEVICES
The interaction of chromostereopsis and stereopsis in stereoscopic CRT (Cathode Ray Tubes) displays
[AD-A217906] N90-28544
Description of the primary flight display and flight guidance system logic in the NASA B-737 transport systems research vehicle
[NASA-TM-102710] N90-28545
Situational Awareness in Aerospace Operations
[AGARD-CP-478] N90-28972
The three-dimensional structure of visual attention and its implications for display design N90-28980
A real time evaluation of the use of a perspective format to promote situational awareness in users of air to air tactical displays N90-28981
Counterair situation awareness display for Army aviation N90-28982
Experimental tests on the minimal visual acuity required for safe air crew and air control personnel performance N90-28987
Design of a monitor and simulation terminal (master) for space station telerobotics and telescience N90-29051
Strategies of computer-based instructional design: A review of guidelines and empirical research
[AD-A224038] N90-29112
DISSIPATION
Dissipation of mechanical work and temperature rise in AS4/PEEK thermoplastic composite
[NASA-CR-186893] N90-28678
Dissipative quantum maps
[DE90-627179] N90-29227
Quantum chaos and dissipation: Lyapunov exponents
[DE90-627180] N90-29228
DISTRIBUTED PARAMETER SYSTEMS
Active control of flexible structures N90-28575
DISTRIBUTED PROCESSING
Three-dimensional motor schema based navigation N90-29026

Parallelization of a software relating to aerodynamics on MIMD type computers
[ONERA-RT-31/3479-CY] N90-29114
Piecewise linear models of processor utilization
[DE90-014774] N90-29115
Information management directions: The integration challenge
[PB90-219866] N90-29245

DIVERGENCE
Ion divergence and the stability of magnetically insulated diodes
[DE90-014565] N90-28777
On the infrared behaviour of some non-Minkowskian quantum fields N90-29273

DOCUMENTS
National Archives preservation research priorities: Past and present
[PB90-208210] N90-29242

DOPED CRYSTALS
High-temperature deformation and microstructural analysis for Si3N4-Sc2O3
[NASA-TM-103239] N90-28740
Electron microscopy of transition-metal doped BiCaSrCuO
[DE90-014184] N90-29202
Parity violation and superconductivity in doped Mott insulators
[DE90-627493] N90-29217
Dynamical information for Fe doped YBa2Cu3O7 superconducting oxides obtained from high temperature Moessbauer studies
[DE90-627871] N90-29218
XANES and EXAFS study of Au-substituted YBa2Cu3O(7-delta)
[NASA-TM-103291] N90-29219

DOPPLER EFFECT
Velocity Interferometer System for Any Reflector (VISAR): Displacement mode data reduction
[DE90-015027] N90-29184

DOPPLER RADAR
Phoenix data analysis and numerical simulation
[AD-A224226] N90-28772

DOWNWASH
Analysis of heliport environmental data, Intracoastal City
[DOT/FAA/CT-TN89/43] N90-28584

DRAG
Study of the ground effects in the CEAT aerohydrodynamic tunnel: Using the results N90-28530

DRILLING
Drilling the oceanic lower crust and mantle: A global strategy for exploring the deep oceanic crust and mantle in the 1990's
[PB90-240953] N90-28936

DROP TOWERS
Noncontact measurement of high temperature using optical fiber sensors
[NASA-CR-186975] N90-28825

DROPS (LIQUIDS)
Analyses of spray and droplet ignition for pure and multicomponent fuels N90-28688
Ignition and combustion of liquid propellants
[AD-A224150] N90-28748
Transient cooling of a hot surface by droplets evaporation
[PB90-227968] N90-28799

DUCTILITY
Is there anything of practical value hidden amongst the composite toughening theories. A Jim Mueller prospective
[DE90-014905] N90-28673
Tensile behavior of borated stainless steels, phase 1
[DE90-014368] N90-28717

DURABILITY
The effects of atomic oxygen on the thermal emittance of high temperature radiator surfaces
[NASA-TM-103224] N90-28670

DUST
Near-infrared speckle observations of T Tauri stars and a multi-wavelength study of the prototype star T Tauri N90-29264

DYNAMIC CHARACTERISTICS
The effects of foreplanes on the static and dynamic characteristics of a combat aircraft model N90-28520
Crash-impact behavior of graphite/epoxy composite sine wave webs N90-28667
Static and dynamic characterization of the ATR 72 rods made of Ti 10.2.3 titanium alloy
[REPT-49-238] N90-28722
Mode competition in the quasioptical gyrotron
[AD-A222181] N90-28823
Dynamic interaction of multiple autonomous mobile robots N90-28844
Dynamical properties of two-dimensional Josephson junction arrays
[AD-A223965] N90-29221

DYNAMIC CONTROL
Dynamic modeling and payload-adaptation control of a flexible one-link manipulator N90-28843
Experiments in the dynamic and strategic control of cooperating manipulators N90-28845

DYNAMIC MODELS
A flight dynamic model of aircraft spinning
[AR-005-600] N90-28576
On the application of similarity laws to a scaled railway bogie model
[DLR-FB-90-06] N90-28853
Time, space and form in vision
[AD-A213889] N90-28971
A new approach to global control of redundant manipulators N90-29002

DYNAMIC PROGRAMMING
Robot Acting on Moving Bodies (RAMBO): Interaction with tumbling objects N90-29022

DYNAMIC RESPONSE
Effective optimal control of a fighter aircraft engine N90-28548
Blade tip rubbing stress prediction N90-28615
Cartesian control of redundant robots N90-29004
Kinematics, controls, and path planning results for a redundant manipulator N90-29005

DYNAMIC STRUCTURAL ANALYSIS
A nonlinear finite element formulation for the large displacement analysis of plates N90-28667
Reliability analysis of maintained structural system vulnerable to fatigue and fracture N90-28668
Interface formation and percusory dynamics
[AD-A224128] N90-29223

DYNAMIC TESTS
Military aircrew seating: A human factors engineering approach
[AD-A218049] N90-28999

E

EARPHONES
Techniques and applications for binaural sound manipulation in human-machine interfaces
[NASA-TM-102279] N90-28996

EARTH OBSERVATIONS (FROM SPACE)
Mesoscale Lightning Experiment (MLE): A view of lightning as seen from space during the STS-26 mission
[NASA-TM-103513] N90-28951

EARTHQUAKES
Torsional effects in structures subjected to strong ground motion
[PB90-226960] N90-28869

ECHOES
Genesis of bow echoes: A rear-inflow induced meso-convective structure
[PB90-209776] N90-28926

ECONOMIC DEVELOPMENT
State science and technology indicators: An exploratory profile and analysis
[PB90-246711] N90-29259

ECONOMICS
Proceedings of a workshop on Future Airport Passenger Terminals
[PB90-213620] N90-28580

ECOSYSTEMS
Perspectives on the Chesapeake Bay, 1990: Advances in estuarine sciences
[PB90-248600] N90-28954
Biomedical and environmental sciences program publications, 1989
[DE90-014785] N90-29250

EDDY CURRENTS
Analysis of three-dimensional eddy current field. Application to calculation of magnetic screening effect of the damper system in a model superconducting generator
[DE90-507869] N90-28779

EDGE DETECTION
Robot Acting on Moving Bodies (RAMBO): Interaction with tumbling objects N90-29022
Real-time edge tracking using a tactile sensor N90-29023
Learned navigation in unknown terrains: A retraction method N90-29029

EDUCATION
Selective learning algorithm for certain types of learning failure in multilayer perceptrons
[AD-A223962] N90-28998
The personal computer: An untapped source for the United States Army War College
[AD-A223976] N90-29087
Animated computer-generated video-tape instruction using DIGLIB (Device Independent Graphics Library)
[DE90-015360] N90-29105

EIGENVALUES
LANZ: Software solving the large sparse symmetric generalized eigenproblem
[NASA-CR-182086] N90-28876
Factorization of the characteristic equation for three layer ducts
[AD-A223867] N90-28956
Block Lanczos algorithm
[AD-A224011] N90-29111
SuperCHIEF: A modified CHIEF (Combined Helmholz Integral Equation Formulation) method
[DE90-014744] N90-29123
A corollary to Kodaira-Spencer's theorem on continuity of eigenvalues
[DE90-627164] N90-29148
On the zeta-function regularization of chiral Jacobians for singular Dirac operators
[DE90-627176] N90-29150

EIGENVECTORS
Factorization of the characteristic equation for three layer ducts
[AD-A223867] N90-28956
Block Lanczos algorithm
[AD-A224011] N90-29111

EINSTEIN EQUATIONS
A comment on anisotropic spheres admitting one parameter group of conformal motions
[DE90-627195] N90-29230

EL NINO
Proceedings of the 14th Annual Climate Diagnostics Workshop
[PB90-198573] N90-28938

ELASTIC ANISOTROPY
A hybrid-stress finite element for linear anisotropic elasticity N90-28814

ELASTIC PROPERTIES
A theoretical investigation into the inelastic behavior of metal-matrix composites
[AD-A223973] N90-28677
Factorization of the characteristic equation for three layer ducts
[AD-A223867] N90-28956

ELASTIC SCATTERING
Concept for a neutron spectrometer based on optical detection of (3)He(n, p)-3H reactions in a gas
[DE90-014776] N90-28826

ELASTIC WAVES
Factorization of the characteristic equation for three layer ducts
[AD-A223867] N90-28956

ELASTOSTATICS
Green's functions for dislocations in bonded strips and related crack problems
[NASA-CR-185291] N90-28878

ELECTRIC ARCS
Unipolar arcing on the cathode surface of a high voltage diode
[AD-A224122] N90-28787

ELECTRIC BATTERIES
Assessment of battery technologies for electric vehicles. Volume 2, part 2: Appendices
[DE90-014610] N90-28778

ELECTRIC CORONA
Research for electric energy systems
[DE90-014221] N90-28775

ELECTRIC CURRENT
Measurement of localized corrosion using current density mapping
[DE90-015086] N90-28721

ELECTRIC DISCHARGES
Spacecraft charging effects
[RAE-TM-SPACE-375] N90-28594

ELECTRIC FIELDS
Further studies of 60 Hz exposure effects on human function
[DE90-014377] N90-28962

ELECTRIC GENERATORS
Analysis of three-dimensional eddy current field. Application to calculation of magnetic screening effect of the damper system in a model superconducting generator
[DE90-507869] N90-28779
A 10kW class molten carbonate fuel cell test: The stack with electrolyte plate prepared with paper-making method
[DE90-507841] N90-28900
Performance measurements and energy balance of an SPS V160 Stirling motor at the German Aerospace Research Establishment
[DLR-MITT-90-03] N90-28903
Energy transmission by means of coherent quasi-mono-chromatic light beams N90-29163

ELECTRIC MOTOR VEHICLES
Assessment of battery technologies for electric vehicles. Volume 2, part 2: Appendices
[DE90-014610] N90-28778

ELECTRIC POTENTIAL
Unipolar arcing on the cathode surface of a high voltage diode
[AD-A224122] N90-28787
ELECTRIC PROPULSION
Low power arcjet performance
[NASA-TM-103280] N90-28657
Development of the electric vehicle analyzer
[AD-A224201] N90-28788
ELECTRIC WIRE
Evaluations of new polyimide films for flexible circuit applications at EG and G Mound Applied Technologies
[DE90-014117] N90-28731
ELECTRICAL ENGINEERING
Emerging technologies in electronics and their measurement needs, second edition
[PB90-188087] N90-28773
ELECTRICAL FAULTS
Evaluations of new polyimide films for flexible circuit applications at EG and G Mound Applied Technologies
[DE90-014117] N90-28731
ELECTRICAL INSULATION
Evaluations of new polyimide films for flexible circuit applications at EG and G Mound Applied Technologies
[DE90-014117] N90-28731
Investigations into the use of dielectric coatings in magnetic switches
[DE90-014331] N90-28776
Characterization of electron flow in positive-polarity linear-induction accelerators
[DE90-014998] N90-29177
ELECTRICAL MEASUREMENT
Measurement of localized corrosion using current density mapping
[DE90-015066] N90-28721
Effects of Al substitution by Fe in CeAl2
[DE90-627843] N90-28726
Emerging technologies in electronics and their measurement needs, second edition
[PB90-188087] N90-28773
ELECTRICAL RESISTIVITY
Electronic conduction in molten cryolite saturated with alumina
[DE90-015090] N90-29211
ELECTRICITY
Study of the relationships between radar structure and the electrical activity of clouds
[ETN-90-97488] N90-28946
ELECTRO-OPTICS
Laboratory for Laser Energetics review
[DE90-014666] N90-28829
The III-V semiconductor quantum well lasers and related optoelectronic devices on silicon
[AD-A224120] N90-28835
ELECTROCHEMICAL CORROSION
High temperature surface interactions: Overview N90-28699
ELECTROCHEMICAL OXIDATION
Electrochemical incineration of wastes
[NASA-CR-187033] N90-28753
ELECTROCHEMISTRY
Electrochemical surface finishing using amino-substrates on carbon fibers in organic media. Effects of the finishing on the mechanical properties of carbon-epoxy composites
[ONERA-RT-9/3549-M] N90-28672
Electrochemistry using nanometer-sized electrodes
[AD-A223890] N90-28697
Zinc-bromine battery development
[DE90-014751] N90-28781
ELECTRODE MATERIALS
Electrochemical incineration of wastes
[NASA-CR-187033] N90-28753
ELECTRODEPOSITION
Electrodeposition of wear resistant coatings
[PB90-221839] N90-28732
ELECTRODES
Electrochemistry using nanometer-sized electrodes
[AD-A223890] N90-28697
ELECTROLYTE METABOLISM
Fluid and electrolyte homeostasis during spaceflight: Elucidation of mechanisms in a primate
[NASA-CR-177548] N90-29065
ELECTROLYTES
Assessment of battery technologies for electric vehicles. Volume 2, part 2: Appendices
[DE90-014610] N90-28778
A 10kW class molten carbonate fuel cell test: The stack with electrolyte plate prepared with paper-making method
[DE90-507841] N90-28900
Electronic conduction in molten cryolite saturated with alumina
[DE90-015090] N90-29211
ELECTROLYTIC CELLS
Lightweight solid polymer electrolyte fuel cell with stack power density of 3 kW/lb (7 kW/kg)
[AD-A223964] N90-28905
ELECTROMAGNETIC COMPATIBILITY
Ground-based weather radar compatibility with digital radio-relay microwave systems
[PB90-206236] N90-28756
ELECTROMAGNETIC FIELDS
Research for electric energy systems
[DE90-014221] N90-28775
ELECTROMAGNETIC RADIATION
Propagation of electromagnetic radiation in a random field of gravitational waves and space radio interferometry
[DE90-627196] N90-28764
ELECTROMAGNETIC SCATTERING
Electromagnetic scattering from two-dimensional thick material junctions
[NASA-CR-186468] N90-28767
Bandwidth and signal-to-noise ratio enhancement of the NPS transient electromagnetic scattering laboratory
[AD-A224144] N90-28771
ELECTROMAGNETIC SPECTRA
Using the x ray region of the electromagnetic spectrum for alignment: Overview, geometric optics, and design considerations
[DE90-014798] N90-28752
Methods for multisource data analysis in remote sensing
[NASA-CR-187005] N90-28890
ELECTROMAGNETIC WAVE TRANSMISSION
Propagation of electromagnetic radiation in a random field of gravitational waves and space radio interferometry
[DE90-627196] N90-28764
ELECTRON BEAMS
Radiation-curable prepreg composites
[DE90-629740] N90-28674
Computer simulation of micro-triode performance
[DE90-014191] N90-28774
UV-induced degradation of the Si-SiO2 interface: Applications to the point contact solar cell
[DE90-013843] N90-28898
Characterization of electron flow in positive-polarity linear-induction accelerators
[DE90-014998] N90-29177
Some novel sources of x ray beams: Channeling, transition and Cherenkov radiation
[DE90-014442] N90-29181
Electron acoustic and magnetoacoustic modes in a magnetized beam plasma system
[DE90-627473] N90-29199
ELECTRON DENSITY (CONCENTRATION)
The stability of the martensitic phases in Cu-Zn-Al at an electron concentration of 1.534
[DE90-629628] N90-28727
Combined electron cyclotron ray tracing and transport code studies in the compact ignition tokamak
[DE90-014097] N90-29189
PW Vul: A classical nova with nearly solar abundances
[NASA-CR-185080] N90-29275
Alfven wave solitons and solar intermediate drift bursts
[MPE-PREPRINT-173] N90-29287
ELECTRON EMISSION
Computer simulation of micro-triode performance
[DE90-014191] N90-28774
Unipolar arcing on the cathode surface of a high voltage diode
[AD-A224122] N90-28787
ELECTRON ENERGY
Temperature-gradient instability induced by conducting end walls
[DE90-014334] N90-29188
PW Vul: A classical nova with nearly solar abundances
[NASA-CR-185080] N90-29275
ELECTRON GUNS
Control of nonlinear space-charge emittance growth
[DE90-014752] N90-29270
ELECTRON MICROSCOPY
Technical activities 1989, Electron and Optical Physics Division
[PB90-207267] N90-29296
ELECTRON SPECTROSCOPY
Use of electron spectroscopies in the tribological evaluation of diamond films
[DE90-014421] N90-28848
ELECTRON STATES
Research on the structural and electronic properties of defects in amorphous silicon
[DE90-000342] N90-28730
Interface formation and percusory dynamics
[AD-A224128] N90-29223
ELECTRON TRANSFER
Correlated charge changing ion-atom collisions
[DE90-014662] N90-29171
ELECTRONIC CONTROL
Propulsion system-flight control integration and optimization: Flight evaluation and technology transition
[NASA-TM-4207] N90-28551
ELECTRONIC MODULES
A microprocessor controlled strain gauge calibration module
[AR-005-579] N90-28821
ELECTROSTATIC CHARGE
Spacecraft charging effects
[RAE-TM-SPACE-375] N90-28594
ELECTROSTATICS
Computerized simulation of phenomena in plasma via particles
[INPE-4595-RPE/569] N90-29194
Electron acoustic and magnetoacoustic modes in a magnetized beam plasma system
[DE90-627473] N90-29199
ELLIPSOMETRY
Semiconductor measurement technology: A software program for aiding the analysis of ellipsometric measurements, simple spectroscopic models
[PB90-216847] N90-29201
EMBEDDED COMPUTER SYSTEMS
Concepts of concurrent programming
[AD-A223897] N90-29110
EMBEDDING
Using embedded microcontrollers in radar test equipment
[DE90-014997] N90-28763
EMBRYOS
Computer aided mechanogenesis of skeletal muscle organs from single cells in vitro
[NASA-CR-187025] N90-28959
EMISSION
Acid deposition: No such thing as a free launch
[DE90-015085] N90-28920
EMISSION SPECTRA
The ionization structure of planetary nebulae 10: NGC 2392
[NASA-CR-186960] N90-29274
EMITTANCE
The effects of atomic oxygen on the thermal emittance of high temperature radiator surfaces
[NASA-TM-103224] N90-28670
Effects and tolerances of injection jitter in the SLC and future linear colliders
[DE90-014805] N90-29179
Control of nonlinear space-charge emittance growth
[DE90-014752] N90-29270
EMITTERS
Computer simulation of micro-triode performance
[DE90-014191] N90-28774
END EFFECTORS
Kinematic functions for the 7 DOF robotics research arm N90-29003
A fast lightstripe rangefinding system with smart VLSI sensor N90-29019
Computational neural learning formalisms for manipulator inverse kinematics N90-29030
Grasp planning under uncertainty N90-29041
Characterization and control of self-motions in redundant manipulators N90-29045
ENERGY ABSORPTION
Crash-impact behavior of graphite/epoxy composite sine wave webs N90-28667
ENERGY CONSERVATION
Energy Efficient Engine: Flight propulsion system final design and analysis
[NASA-CR-168219] N90-28558
Energy Efficient Engine core design and performance report
[NASA-CR-168069] N90-28559
Energy Efficient Engine integrated core/low spool design and performance report
[NASA-CR-168211] N90-28561
Energy efficient engine program technology benefit/cost study. Volume 1: Executive summary
[NASA-CR-174766-VOL-1] N90-28564
Energy Efficient Engine: Control system preliminary definition report
[NASA-CR-179578] N90-28569
Open cycle heat pump development for local resource use. Phase 2: District heating case study analysis
[DE90-011123] N90-28904
Transferring building energy technologies by linking government and private-sector programs
[DE90-000346] N90-29258
ENERGY CONVERSION
Ignition and combustion of liquid propellants
[AD-A224150] N90-28746

ENERGY CONVERSION EFFICIENCY
Energy Efficient Engine high pressure turbine component test performance report
[NASA-CR-168289] N90-28553
Energy Efficient Engine acoustic supporting technology report
[NASA-CR-174834] N90-28557
Energy Efficient Engine: Flight propulsion system final design and analysis
[NASA-CR-168219] N90-28558
Energy Efficient Engine program advanced turbofan nacelle definition study
[NASA-CR-174942] N90-28560
Assessment of battery technologies for electric vehicles. Volume 2, part 2: Appendices
[DE90-014610] N90-28778
Fuel cells: Their applications, technological status, market and opportunity
[DE90-796158] N90-28895
Evaluation of the STM4-120 kinematic Stirling engine
[DE90-013836] N90-28897
A 10kW class molten carbonate fuel cell test: The stack with electrolyte plate prepared with paper-making method
[DE90-507841] N90-28900
Study of power generation systems for CO2 collection: LNG combined cycle
[DE90-507881] N90-28901
Performance measurements and energy balance of an SPS V160 Stirling motor at the German Aerospace Research Establishment
[DLR-MITT-90-03] N90-28903
Research on stable, large-area, amorphous silicon based submodules, phase 3
[DE90-000339] N90-29204

ENERGY DISSIPATION
Rain-fade simulation and power augmentation for satellite communication systems
[NASA-TM-103134] N90-28768
Estimation of individual coupling loss factors in a multi-subsystem
[ISVR-TR-184] N90-29141

ENERGY LEVELS
Research on stable, large-area, amorphous silicon based submodules, phase 3
[DE90-000339] N90-29204

ENERGY METHODS
Estimation of individual coupling loss factors in a multi-subsystem
[ISVR-TR-184] N90-29141

ENERGY POLICY
Responding to the threat of global warming: Options for the Pacific and Asia
[DE90-014756] N90-28918

ENERGY STORAGE
Development of the sodium/sulfur technology for energy storage
[DE90-014329] N90-28899

ENERGY TECHNOLOGY
Fuel cells: Their applications, technological status, market and opportunity
[DE90-796158] N90-28895
Solar energy for high temperature technology and applications
[ETN-90-97429] N90-28902
Transferring building energy technologies by linking government and private-sector programs
[DE90-000346] N90-29258

ENERGY TRANSFER
Energy transmission by means of coherent quasi-mono-chromatic light beams N90-29163
Theoretical studies of proton beams in solar flare loops N90-29286

ENGINE CONTROL
Propulsion system-flight control integration and optimization: Flight evaluation and technology transition
[NASA-TM-4207] N90-28551
Smart microsensors for high temperature applications, phase 1
[AD-A224151] N90-28828

ENGINE DESIGN
Energy Efficient Engine combustor test hardware detailed design report
[NASA-CR-168301] N90-28554
Energy Efficient Engine (E3) combustion system component technology performance report
[NASA-CR-168274] N90-28555
Energy Efficient Engine exhaust mixer model technology report addendum; phase 3 test program
[NASA-CR-174799] N90-28556
Energy Efficient Engine: Flight propulsion system final design and analysis
[NASA-CR-168219] N90-28558
Energy Efficient Engine core design and performance report
[NASA-CR-168069] N90-28559
Energy Efficient Engine program advanced turbofan nacelle definition study
[NASA-CR-174942] N90-28560
Energy Efficient Engine: Control system component performance report
[NASA-CR-174851] N90-28562
NASA/GE Energy Efficient Engine low pressure turbine scaled test vehicle performance report
[NASA-CR-168290] N90-28563
Energy Efficient Engine integrated core/low spool test hardware design report
[NASA-CR-168137] N90-28566
Liquid Rocket Booster (LRB) for the Space Transportation System (STS) systems study. Volume 1: Executive summary
[NASA-CR-183822] N90-28599
Liquid Rocket Booster (LRB) for the Space Transportation System (STS) systems study, volume 2
[NASA-CR-183786] N90-28600
Liquid Rocket Booster (LRB) for the Space Transportation System (STS) systems study. Appendix F: Performance and trajectory for ALS/LRB launch vehicles
[NASA-CR-183792-APP-F] N90-28606
The space transportation main engine phase A' study
[NASA-CR-179399] N90-28610
Advanced Earth-to-orbit propulsion technology program overview: Impact of civil space technology initiative N90-28612
Oxygen/hydrogen technology test bed status update N90-28613
Injector element characterization methodology N90-28634
Variable mixture ratio performance through nitrogen augmentation N90-28639
High variable mixture ratio oxygen/hydrogen engine N90-28640
A failure diagnosis system based on a neural network classifier for the space shuttle main engine
[NASA-TM-103607] N90-28659
Automotive Stirling engine development program
[NASA-CR-180840] N90-29260

ENGINE INLETS
Development of advanced combustion technology for medium and high speed natural gas engines
[PB90-198565] N90-28836

ENGINE NOISE
Vibration responses of two house structures during the Edwards Air Force Base phase of the national sonic boom program
[NASA-CR-182089] N90-29169

ENGINE PARTS
Energy Efficient Engine: Control system component performance report
[NASA-CR-174851] N90-28562
A comparison of single-cycle versus multi-cycle proof testing strategies N90-28646
Evaluation of high temperature protective coatings for gas turbine engines under simulated service conditions N90-28712
Surface property improvement in titanium alloy gas turbine components through ion implantation N90-28713
Improved silicon carbide for advanced heat engines
[NASA-CR-182186] N90-28735

ENGINE TESTS
The reduction of smoke emissions from Allison T56 engines
[ARL-PROP-R-182] N90-28547
Energy Efficient Engine: Control system component performance report
[NASA-CR-174851] N90-28562
Energy Efficient Engine integrated core/low spool test hardware design report
[NASA-CR-168137] N90-28566
Energy Efficient Engine: Combustor component performance program
[NASA-CR-179533] N90-28568
Source emission test of gas turbine engine test facility, Kelly AFB, TX
[AD-A223869] N90-28571
Liquid Rocket Booster (LRB) for the Space Transportation System (STS) systems study. Appendix E: Pressure-fed booster test bed for the liquid rocket booster study
[NASA-CR-183791-APP-E] N90-28605
Oxygen/hydrogen technology test bed status update N90-28613
The effects of a compressor rebuild on gas turbine engine performance: Final results N90-28701
Development of advanced combustion technology for medium and high speed natural gas engines
[PB90-198565] N90-28836
Evaluation of the STM4-120 kinematic Stirling engine
[DE90-013836] N90-28897

ENGINEERING
Procedures for DOE-Navy exchange and approval of engineering information and material management required for production of W88-0/Mk5 RBA (reentry body assembly)
[DE90-014763] N90-28595

ENGINEERING MANAGEMENT
Quality function deployment as a mechanism for process characterization and control
[DE90-014755] N90-28857

ENTHALPY
Thermophysical properties of Helium-4 from 0.8 to 1500 K with pressures to 2000 MPa
[NASA-CR-186992] N90-28681
Design of an axisymmetric, contoured nozzle for the HEG
[DLR-FB-90-04] N90-28812

ENTRAINMENT
The entrainment rate for a row of turbulent jets
[NASA-CR-185278] N90-28504

ENTROPY
Thermophysical properties of Helium-4 from 0.8 to 1500 K with pressures to 2000 MPa
[NASA-CR-186992] N90-28681
Viscous causal cosmologies
[DE90-627487] N90-29282

ENVIRONMENT EFFECTS
Chasing a specter: Risk management for global environmental change
[DE90-014455] N90-28917
Puerto Rico Workshop on Land-Based Sources of Marine Pollution in the Wider Caribbean Region
[PB90-184094] N90-28921
Natural and anthropogenic climate change
[DE90-015528] N90-28923

ENVIRONMENT MODELS
Space station contamination modeling
[NASA-CR-183871] N90-28590
Perspectives on the Chesapeake Bay, 1990: Advances in estuarine sciences
[PB90-248600] N90-28954
Building an environment model using depth information N90-29064
Data Base Analyzer and Parameter Estimator (DBAPE) interactive computer program user's manual
[PB90-193053] N90-29252

ENVIRONMENT SIMULATION
Ceramic matrix composites in simulated SSME environments N90-28655

ENVIRONMENTAL MONITORING
National air quality and emissions trends report, 1988
[PB90-200114] N90-28909
Atmosphere and water quality monitoring on Space Station Freedom
[NASA-CR-186707] N90-29084

ENVIRONMENTAL SURVEYS
Use of Ni63 overvoltage gap switches in the flight termination systems on boosters launched from US Army Kwajalein Atoll (USAKA)
[AD-A223866] N90-29661

ENVIRONMENTAL TESTS
Development of testing and analysis methodology to assess the long term durability of polymeric composites at high temperatures
[NASA-TM-102714] N90-28871

EPOXY MATRIX COMPOSITES
Factors influencing the mode I interlaminar fracture resistance of toughened matrix composites N90-28668
Inelastic analysis of laminated composites N90-28669
Behavior of aramid/epoxy wounded tubes under uniaxial and biaxial loading
[ETCA-89-R-150] N90-28873

EPOXY RESINS
Crash-impact behavior of graphite/epoxy composite sine wave webs N90-28667

EQUATIONS OF MOTION
On the application of similarity laws to a scaled railway bogie model
[DLR-FB-90-06] N90-28853
A nonlinear finite element formulation for the large displacement analysis of plates N90-28867

EQUATIONS OF STATE
Estimation of individual coupling loss factors in a multi-subsystem
[ISVR-TR-184] N90-29141
Rotating neutron stars and the equation of state of dense matter
[DE90-014185] N90-29269

EQUIPMENT SPECIFICATIONS
Formulation of design guidelines for automated robotic assembly in outerspace N90-29017

EROSION
Proceedings of US Army Research Office Workshop on US Army Applications for Diamond and Diamondlike Materials
[AD-A224193] N90-28741
ERROR ANALYSIS
Error detection and control for nonlinear shell analysis
[NASA-TM-102723] N90-28677
Consistency and convergence for numerical radiation conditions
[NASA-TM-103282] N90-29124
ERRORS
Studies in automatic speech recognition and its application in aerospace N90-28759
Treatment of systematic errors 2: Fusion of ultrasound and visual sensor data
[DE90-014780] N90-28850
Selective learning algorithm for certain types of learning failure in multilayer perceptrons
[AD-A223982] N90-28908
Plan recognition for space telerobotics N90-29036
ERYTHROCYTES
Regulation of erythropoiesis in rats during space flight
[NASA-CR-177537] N90-29066
ESSENTIALLY NON-OSCILLATORY SCHEMES
Numerical experiments on the accuracy of ENO and modified ENO schemes
[NASA-CR-182063] N90-29126
Numerical methods for systems of conservation laws of mixed type using flux splitting
[NASA-CR-182084] N90-29129
ESTIMATES
National air pollutant emission estimates, 1940-1988
[PB90-199266] N90-28908
ESTIMATING
Estimating the spatial variability of trace gas deposition velocities
[PB90-206570] N90-28928
Data Base Analyzer and Parameter Estimator (DBAPE) interactive computer program user's manual
[PB90-193053] N90-29252
ESTUARIES
Perspectives on the Chesapeake Bay, 1990: Advances in estuarine sciences
[PB90-248800] N90-28954
ETHNIC FACTORS
Air Force Officer Qualifying Test (AFOQT): Development of quick score composites for forms P1 and P2
[AD-A223968] N90-28997
EUCLIDEAN GEOMETRY
On Einsteinian 4-submanifolds in E(sup 6)
[DE90-627149] N90-29226
EULER EQUATIONS OF MOTION
Solution of Euler equations applied to a rotor of a helicopter in steady flight
[ONERA-RSF-1/3731-AY-002A] N90-28500
Multigrid for hypersonic inviscid flows
[NASA-CR-182082] N90-29125
EUTECTICS
Effect of protective coatings on mechanical properties of superalloys N90-28707
EVAPORATION
Transient cooling of a hot surface by droplets evaporation
[PB90-227968] N90-28799
EXCITATION
Surface and defect excitations in covalently bonded solids
[AD-A221995] N90-28682
EXHAUST EMISSION
The reduction of smoke emissions from Allison T56 engines
[ARL-PROP-R-182] N90-28547
Energy Efficient Engine exhaust mixer model technology report addendum; phase 3 test program
[NASA-CR-174799] N90-28556
Source emission test of gas turbine engine test facility, Kelly AFB, TX
[AD-A223869] N90-28571
National air pollutant emission estimates, 1940-1988
[PB90-199266] N90-28908
National air quality and emissions trends report, 1988
[PB90-200114] N90-28909
EXOBIOLOGY
Aerospace medicine and biology: A continuing bibliography with indexes (supplement 340)
[NASA-SP-7011(340)] N90-28963
EXPERT SYSTEMS
ROSES, a Robot Operating System Expert Scheduler: Methodological framework
[DE90-014782] N90-28851
A survey of planning and scheduling research at the NASA Ames Research Center N90-29078
Graph structure model
[DE90-014930] N90-29097
Inference engine for expert systems
[INPE-4565-PRE/1306] N90-29104
A hardware/software environment to support R/D in intelligent machines and mobile robotic systems
[DE90-014458] N90-29119
An expert system to perform on-line controller restructuring for abrupt model changes
[NASA-TM-103609] N90-29121
Model authoring system for fail safe analysis
[NASA-CR-4317] N90-29142
A knowledge-based system design/information tool
[NASA-CR-4316] N90-29143
EXPLOSIONS
Methods for detecting low-frequency signals in the presence of strong winds
[AD-A223980] N90-28769
Unipolar arcing on the cathode surface of a high voltage diode
[AD-A224122] N90-28787
EXPLOSIVES
Shock dynamics in the sub-nanometer femtosecond domain
[DE90-014390] N90-28689
Unipolar arcing on the cathode surface of a high voltage diode
[AD-A224122] N90-28787
EXPOSURE
Oxidation, sulfidation, and hot corrosion: Mechanisms and interrelationships N90-28702
Preliminary exposure study to determine the effects of acid deposition on coated steel substrates
[PB90-201799] N90-28715
Study of meteorological processes important in the degradation of materials through surface temperature
[PB90-222720] N90-28856
EXTRAGALACTIC RADIO SOURCES
Radio outbursts in extragalactic sources N90-29291
EXTRAPOLATION
Extrapolation procedures at outflow boundaries for the Navier-Stokes equations
[FFA-TN-1990-23] N90-28811
EXTRATERRESTRIAL RADIATION
Comparison of dose estimates using the buildup-factor method and a Baryon transport code (BRYNTRN) with Monte Carlo results
[NASA-TP-3021] N90-29290
Predictions of radiation backgrounds for GRO/OSSE
[RAE-TM-SPACE-372] N90-29293
EYE (ANATOMY)
The interaction of chromostereopsis and stereopsis in stereoscopic CRT (Cathode Ray Tubes) displays
[AD-A217906] N90-28544

F

F-18 AIRCRAFT
Predicting F/A-18 fleet replacement squadron performance using an automated battery of performance-based tests
[AD-A223899] N90-28543
A knowledge-based system design/information tool
[NASA-CR-4316] N90-29143
FABRICATION
Strengthening and toughening mechanisms in ceramic fiber-reinforced glass matrix composites N90-28666
Fabrication of spherical pressure vessels from composite materials
[INPE-4598-RPE/570] N90-28675
Zinc-bromine battery development
[DE90-014751] N90-28781
High temperature superconducting thin film microwave circuits: Fabrication, characterization, and applications
[NASA-TM-103235] N90-28786
FABRY-PEROT INTERFEROMETERS
High power arcjet
[NASA-CR-183086] N90-28658
FACTORIZATION
Factorization of the characteristic equation for three layer ducts
[AD-A223867] N90-28956
FAIL-SAFE SYSTEMS
Model authoring system for fail safe analysis
[NASA-CR-4317] N90-29142
FAILURE
Liquid Rocket Booster (LRB) for the Space Transportation System (STS) systems study. Appendix E: Pressure-fed booster test bed for the liquid rocket booster study
[NASA-CR-183791-APP-E] N90-28605
FAILURE ANALYSIS
NASCRAC (trademark): A fracture mechanics analysis code N90-28645
Probabilistic model for fracture mechanics service life analysis N90-28650
Probability models for the failure of fibres and fibrous composite materials N90-28665
Molten salt induced high temperature degradation of thermal barrier coatings N90-28704
Periodic gaits for the CMU ambler N90-29027
FAILURE MODES
System reliability optimization of aircraft wings N90-28536
Probabilistic model for fracture mechanics service life analysis N90-28650
Model authoring system for fail safe analysis
[NASA-CR-4317] N90-29142
FAR INFRARED RADIATION
Quantifying the FIR interaction enhancement in paired galaxies
[DE90-627485] N90-29281
FARADAY EFFECT
Faraday rotation mapping of mercury cadmium telluride
[AD-A224278] N90-28729
FARM CROPS
Data Base Analyzer and Parameter Estimator (DBAPE) interactive computer program user's manual
[PB90-193053] N90-29252
FATIGUE (MATERIALS)
Energy efficient engine pin fin and ceramic composite segmented liner combustor sector rig test report
[NASA-CR-179534] N90-28567
NASCRAC (trademark): A fracture mechanics analysis code N90-28645
Fretting wear and fretting fatigue at temperatures up to 600 C N90-28706
Fretting fatigue strength of Ti-6Al-4V at room and elevated temperatures and ways of improving it N90-28709
Reliability analysis of maintained structural system vulnerable to fatigue and fracture N90-28868
FATIGUE LIFE
Constitutive and life modeling of single crystal blade alloys for root attachment analysis N90-28643
The fatigue damage behavior of a single crystal superalloy N90-28644
FATIGUE TESTS
Application of advanced coating techniques to rocket engine components N90-28654
Static and dynamic characterization of the ATR 72 rods made of Ti 10.2.3 titanium alloy
[REPT-49-238] N90-28722
Microstructure: Property correlation --- multiaxial fatigue damage evolution in waspaloy
[NASA-CR-180406] N90-28880
FEASIBILITY ANALYSIS
Liquid Rocket Booster (LRB) for the Space Transportation System (STS) systems study. Volume 1: Executive summary
[NASA-CR-183822] N90-28599
FEDERAL BUDGETS
Federal R and D funding by budget function: Fiscal years 1989-1991
[PB90-226879] N90-29237
FEED SYSTEMS
Combustion instability coupling with feed system acoustics N90-28629
FEEDBACK
Variable force and visual feedback effects on teleoperator man/machine performance N90-29008
TSC (Tokamak Simulation Code) simulations of Alcator C-MOD discharges 3: Study of axisymmetric stability
[DE90-015386] N90-29196
FEEDBACK CONTROL
Active control of flexible structures N90-28575
Real time guidance and propulsion control for single-stage-to-orbit airbreathing vehicles N90-28587
Solutions to the frictional dynamics problem and the reciprocal variable feedback methodology for design and control of robot mechanisms N90-28846
Kinematics, controls, and path planning results for a redundant manipulator N90-29005
Adjustable impedance, force feedback and command language aids for telerobotics (parts 1-4 of an 8-part MIT progress report) N90-29007
The JPL telerobot operator control station. Part 1: Hardware N90-29049
The JPL telerobot operator control station. Part 2: Software N90-29050
Implementation and design of a teleoperation system based on a VMEBUS/68020 pipelined architecture N90-29053
Human machine interaction via the transfer of power and information signals N90-29054
On the simulation of space based manipulators with contact N90-29056
Preliminary results on noncollocated torque control of space robot actuators N90-29057
Portable Dextrous Force Feedback Master for robot telemanipulation (PDMFF) N90-29058

Robust controller design by contraction of a pole region
[ESA-TT-1042] N90-29118
An expert system to perform on-line controller restructuring for abrupt model changes
[NASA-TM-103609] N90-29121
Geometric theory for infinite dimensional systems
[ETN-90-96922] N90-29144

FEEDFORWARD CONTROL
Active control of flexible structures N90-28575

FERMIONS
Dirac's equation as a geodesic in Riemann space
[DE90-627194] N90-29152
Anyons and Chern-Simons theory on compact spaces of finite genus
[DE90-627216] N90-29157
Superconductivity in mixed boson-fermion systems
[DE90-627491] N90-29216

FERROMAGNETIC MATERIALS
Systematic approach to critical phenomena by the extended variational method and coherent-anomaly method
[DE90-627320] N90-29165
Z(6) model: Criticality and break-collape method
[DE90-627323] N90-29214

FIBER COMPOSITES
Probability models for the failure of fibres and fibrous composite materials N90-28665
Strengthening and toughening mechanisms in ceramic fiber-reinforced glass matrix composites N90-28666
Factors influencing the mode I interlaminar fracture resistance of toughened matrix composites N90-28668
Is there anything of practical value hidden amongst the composite toughening theories. A Jim Mueller prospective
[DE90-014905] N90-28673
Polymer research
[PB90-246638] N90-28737

FIBER OPTICS
Application of integrated optical components in optical fiber communication
[FEL-89-B252] N90-29183
Engineering and the advancement of human welfare. Ten outstanding achievements 1964-1989
[ISBN-0-309-04185-6] N90-29297

FIBERS
Probability models for the failure of fibres and fibrous composite materials N90-28665

FIELD EFFECT TRANSISTORS
Transient annealing characterization of irradiated MOSFETS
[AD-A223877] N90-29220

FIELD OF VIEW
Tracking performance and influence of field of view N90-28988

FIELD THEORY (PHYSICS)
Topology of singularities and phase diagram of N=2 superconformal field theories
[DE90-627213] N90-29155

FIGHTER AIRCRAFT
Innovative control concepts and component integration for a generic supercruise fighter N90-28521
A look at tomorrow today N90-28524
Inflight thrust vectoring: A further degree of freedom in the aerodynamic/flight mechanical design of modern fighter aircraft N90-28528
Aerodynamic interferences of in-flight thrust reversers in ground effect N90-28529
Damage tolerance of the fighter aircraft 37 Viggen. Part 1: Analytical assessment
[FFA-TN-1990-12-PT-1] N90-28538
Damage tolerance of the fighter aircraft 37 Viggen. Part 2: Experimental verification
[FFA-TN-1990-13-PT-2] N90-28539
Effective optimal control of a fighter aircraft engine N90-28548
A conceptual framework for fighter flight control systems
[PD-CF-9009] N90-28577

FILM BOILING
Pool boiling from rotating and stationary spheres in liquid nitrogen N90-28621
Gas-film flow in tubes
[DE90-011528] N90-28793

FILM COOLING
Gas-jet and tangent-slot film cooling tests of a 12.5 deg cone at Mach number of 6.7
[NASA-TP-2786] N90-28806
Effect of vortex circulation on injectant from a single film-cooling hole and a row of film-cooling holes in a turbulent boundary layer. Part 2: Injection beneath the vortex upwash
[AD-A223894] N90-28818

FILTRATION
Ozone for trace organic contaminant removal
[PB90-221680] N90-28916

FINANCIAL MANAGEMENT
Development of acceptance plans for airport pavement materials. Volume 1: Development
[DOT/FAA/RD-90/15] N90-28581
Guide to charging for the CCF
[RSRE-89022] N90-29238

FINE STRUCTURE
Fifteenth International Conference on X Ray and Inner-Shell Processes
[DE90-013024] N90-29170
XANES and EXAFS study of Au-substituted YBa2Cu3O(7-delta)
[NASA-TM-103291] N90-29219

FINITE DIFFERENCE THEORY
Calculation of temperature distribution in various turbine blades using a boundary-fitted coordinate transformation method N90-28550
Numerical methods for systems of conservation laws of mixed type using flux splitting
[NASA-CR-182084] N90-29129

FINITE ELEMENT METHOD
Liquid Rocket Booster (LRB) for the Space Transportation System (STS) systems study. Appendix A: Stress analysis report for the pump-fed and pressure-fed liquid rocket booster
[NASA-CR-183787-APP-A] N90-28601
A hybrid-stress finite element for linear anisotropic elasticity N90-28614
Probabilistic structural analysis methods development for SSME N90-28616
Mechanical behavior of thick, curved, laminated composites N90-28664
Lecture notes on incompressible flow and the finite element method
[DE90-014665] N90-28805
Vortice-propeller interaction
[LIMSI-89-9] N90-28809
Finite element analysis of coupled thermoelasticity
[PB90-201211] N90-28850
Correlation of AH-1G airframe flight vibration data with a coupled rotor-fuselage analysis
[NASA-CR-181974] N90-28865
Plan, execute, and discuss vibration measurements and correlations to evaluate a NASTRAN finite element model of the AH-64 helicopter airframe
[NASA-CR-181973] N90-28866
A nonlinear finite element formulation for the large displacement analysis of plates N90-28867
Application of discrete Fourier series to the finite element stress analysis of axi-symmetric solids
[PB90-231010] N90-28870
Parametric solution of nonlinear structure problems
[ONERA-RT-21/3542-RY-082-R] N90-28874
Error detection and control for nonlinear shell analysis
[NASA-TM-102723] N90-28877
Second order tensor finite element
[NASA-CR-184008] N90-29122
Large hydrodynamic tunnel: Calculation of the acoustic transparency of the jet stream
[REPT-89/115] N90-29167

FINITE VOLUME METHOD
Numerical resolution of Navier-Stokes equations using several turbulence models and applications on turbomachines
[ETN-90-97478] N90-28808

FINS
Damage tolerance of the fighter aircraft 37 Viggen. Part 1: Analytical assessment
[FFA-TN-1990-12-PT-1] N90-28538
Damage tolerance of the fighter aircraft 37 Viggen. Part 2: Experimental verification
[FFA-TN-1990-13-PT-2] N90-28539
A study of heat and fluid flow phenomena on the gas side of circular-tube plate-fin heat exchangers N90-28795

FIRE CONTROL
Performance-based measures of merit for tactical situation awareness N90-28976

FIRES
Activities report for the IBDF-INPE project SEQE, year 1987
[INPE-4534-RPE/565] N90-29298

FIXED POINT ARITHMETIC
Solution of the Stokes system by boundary integral equations and fixed point iterative schemes
[DE90-627166] N90-29138

FLAME IONIZATION
Peak analysis in gas chromatography and the development of new stationary phases for anion chromatography
[DE90-014428] N90-28687

FLAME SPECTROSCOPY
Spectroscopic study of combustion diagnostics on hydroxyl radicals
[NASA-CR-186998] N90-28694

FLAT PLATES
The effects of grid-generated turbulence on flat and concave turbulent boundary layers N90-28797

FLEXIBILITY
Control of intelligent robots in space N90-29013

FLEXIBLE BODIES
Active control of flexible structures N90-28575
The dynamics and control of large flexible space structures - 13
[NASA-CR-186930] N90-28591

FLIGHT CHARACTERISTICS
Solution of Euler equations applied to a rotor of a helicopter in steady flight
[ONERA-RSF-1/3731-AY-002A] N90-28500
Aerodynamic parameters of High-Angle-of attack Research Vehicle (HARV) estimated from flight data
[NASA-TM-102692] N90-28578

FLIGHT CONDITIONS
Effects of canard position on the aerodynamic characteristics of a close-coupled canard configuration at low speed N90-28519

FLIGHT CONTROL
Aerodynamic and propulsive control development of the STOL and maneuver technology demonstrator N90-28514
A look at tomorrow today N90-28524
Validation of the F-18 high alpha research vehicle flight control and avionics systems modifications
[NASA-TM-101723] N90-28542
Description of the primary flight display and flight guidance system logic in the NASA B-737 transport systems research vehicle
[NASA-TM-102710] N90-28546
Propulsion system-flight control integration and optimization: Flight evaluation and technology transition
[NASA-TM-4207] N90-28551
A conceptual framework for fighter flight control systems
[PD-CF-9009] N90-28577
Model authoring system for fail safe analysis
[NASA-CR-4317] N90-29142
Flight test engineering with the ATTAS N90-29160

FLIGHT CREWS
Military aircrew seating: A human factors engineering approach
[AD-A218049] N90-28999
Helicopter aircrew helmets and head injury: A protective effect
[AD-A223024] N90-29080

FLIGHT ENVELOPES
Combat aircraft control requirements N90-28515

FLIGHT INSTRUMENTS
The interaction of chromostereopsis and stereopsis in stereoscopic CRT (Cathode Ray Tubes) displays
[AD-A217906] N90-28544

FLIGHT MECHANICS
Inflight thrust vectoring: A further degree of freedom in the aerodynamic/flight mechanical design of modern fighter aircraft N90-28528
Scientific Colloquium in Honor of Prof. Dr. Rer. Nat. Hermann L. Jordan
[ESA-TT-1101] N90-29159
Flight test engineering with the ATTAS N90-29160

FLIGHT OPERATIONS
Modeling and analysis of airport and aircraft operations
[PB90-222167] N90-28511
A FAA Technical Center project transition plan: Mode S
[DOT/FAA/CT-TN90/17] N90-28765

FLIGHT OPTIMIZATION
Life cycle cost in the conceptual design of subsonic commercial aircraft, volumes 1 and 2 N90-28535

FLIGHT PATHS
Real time guidance and propulsion control for single-stage-to-orbit airbreathing vehicles N90-28587

FLIGHT SAFETY
Modeling and analysis of airport and aircraft operations
[PB90-222167] N90-28511
Spatial disorientation incidents in the RNLAF F16 and F5 aircraft and suggestions for prevention N90-28973
Workload induced spatio-temporal distortions and safety of flight: An investigation of cognitive intrusions in perceptual processes N90-28986
Experimental tests on the minimal visual acuity required for safe air crew and air control personnel performance N90-28987

FLIGHT SIMULATION
Dallas/Forth Worth simulation. Phase 2: Triple simultaneous parallel Instrument Landing System (ILS) approaches (turbojets)
[DOT/FAA/CT-90/2] N90-28509
Aerodynamic control design: Experience and results at Aermacchi N90-28518

An in-flight investigation of ground effect on a forward-swept wing airplane N90-28533
Real-time aerodynamic heating and surface temperature calculations for hypersonic flight simulation [NASA-TM-4222] N90-28815
The effects of acoustic orientation cues on instrument flight performance in a flight simulator N90-28985
Flight test engineering with the ATTAS N90-29160

FLIGHT SIMULATORS
Real-time aerodynamic heating and surface temperature calculations for hypersonic flight simulation [NASA-TM-4222] N90-28815

FLIGHT TESTS
In-flight flow visualization with pressure measurements at low speeds on the NASA F-18 high alpha research vehicle [NASA-TM-101726] N90-28505
Aerodynamic and propulsive control development of the STOL and maneuver technology demonstrator N90-28514
Control research in the NASA high-alpha technology program N90-28516
Study of ground effects on flying scaled models N90-28532
Description of the primary flight display and flight guidance system logic in the NASA B-737 transport systems research vehicle [NASA-TM-102710] N90-28546
Development of the electric vehicle analyzer [AD-A224201] N90-28788
Flight test engineering with the ATTAS N90-29160
Vibration responses of two house structures during the Edwards Air Force Base phase of the national sonic boom program [NASA-CR-182089] N90-29169

FLOATING POINT ARITHMETIC
ELEFUNT test results under AST FORTRAN V1.8.0 on the sequent symmetry [DE90-014932] N90-29127

FLOQUET THEOREM
Stabilization of Taylor-Couette flow due to time-periodic outer cylinder oscillation [PB90-219130] N90-28790

FLOW CHARACTERISTICS
Analysis of vibrational power transmission through a beam system including a flexible section [ISVR-TR-176] N90-28675

FLOW DISTRIBUTION
Nonequilibrium radiation and chemistry models for aerocapture vehicle flowfields [NASA-CR-186379] N90-28490
Control of submersible vortex flows [NASA-TM-102693] N90-28493
Regular and chaotic motion of uniform elliptical vortices in external linear time dependent velocity fields N90-28497
In-flight flow visualization with pressure measurements at low speeds on the NASA F-18 high alpha research vehicle [NASA-TM-101726] N90-28505
Effects of canard position on the aerodynamic characteristics of a close-coupled canard configuration at low speed N90-28519
Numerical simulations of flowfields in a central-dump ramjet combustor. 3: Effects of chemistry [AD-A224145] N90-28573
On the use of Lagrangian variables in descriptions of unsteady boundary-layer separation [NASA-CR-182071] N90-28789
A study of heat and fluid flow phenomena on the gas side of circular-tube plate-fin heat exchangers N90-28795
An experimental investigation of a single and multiphase confined coaxial jet N90-28796
Effects of flowfield turbulence on asymmetric vortices over a slender body [AD-A224139] N90-28819

FLOW MEASUREMENT
Gas-film flow in tubes [DE90-011526] N90-28793

FLOW STABILITY
Experimental investigations on the stability and vorticity of the vortex breakdown phenomenon above delta wings, measured by the ultrasonic laser method [ESA-TT-1079] N90-28496
Secondary instabilities in compressible boundary layers [NASA-CR-182091] N90-28502
Stabilization of Taylor-Couette flow due to time-periodic outer cylinder oscillation [PB90-219130] N90-28790

FLOW VISUALIZATION
In-flight flow visualization with pressure measurements at low speeds on the NASA F-18 high alpha research vehicle [NASA-TM-101726] N90-28505
Free shear layer and swirl flow heat transfer enhancement [PB90-228123] N90-28798
Experimental investigations on the stability and transition of three-dimensional boundary layers [ESA-TT-1026] N90-28803
Studies of vortex interactions [AD-A223864] N90-28817

FLOWMETERS
Specifications, tolerances, and other technical requirements for weighing and measuring devices as adopted by the 74th National Conference on Weights and Measures, 1989 (1990 edition) [PB90-184961] N90-28748

FLUID DYNAMICS
The reduction of smoke emissions from Allison T56 engines [ARL-PROP-R-182] N90-28547

FLUID FILMS
Current research in cavitating fluid films [NASA-TM-103184] N90-28791
Gas-film flow in tubes [DE90-011526] N90-28793

FLUID FLOW
A study of heat and fluid flow phenomena on the gas side of circular-tube plate-fin heat exchangers N90-28795
An experimental investigation of a single and multiphase confined coaxial jet N90-28796

FLUID MECHANICS
Study of ground effects on flying scaled models N90-28532
A hybrid perturbation-Galerkin technique for partial differential equations [NASA-CR-182085] N90-28814

FLUX DENSITY
Ultrasonic verification of five wave fronts in unidirectional graphite epoxy composite [NASA-CR-185288] N90-28858
Theoretical studies of proton beams in solar flare loops N90-29286
Radio outbursts in extragalactic sources N90-29291

FLUX VECTOR SPLITTING
Numerical methods for systems of conservation laws of mixed type using flux splitting [NASA-CR-182084] N90-29129

FLYING PLATFORMS
Multiband imaging systems [AD-A223969] N90-28893

FOAMS
A new low density, high porosity lithium hydride-beryllium hydride foam [DE90-015150] N90-28739

FOCUSING
Target signature modeling and bistatic scattering measurement studies [NASA-CR-186611] N90-28766

FOG
Space-base multispectral imagery: Current and future applications and implications to the United States Army [AD-A224046] N90-28894

FORCE DISTRIBUTION
A flight dynamic model of aircraft spinning [AR-005-600] N90-28578

FOREBODIES
Prediction of subsonic vortex shedding from forebodies with chines [NASA-CR-4323] N90-28494
The effects of foreplanes on the static and dynamic characteristics of a combat aircraft model N90-28520
Development of non-conventional control methods for high angle of attack flight using vortex manipulation N90-28522

FORECASTING
Study of meteorological processes important in the degradation of materials through surface temperature [PB90-222720] N90-28856

FORESTS
A manual for analysis of hemispherical canopy photography [DE90-014718] N90-28885
Activities report for the IBDF-INPE project SEQE, year 1987 [INPE-4534-RPE/565] N90-29298

FORMALISM
Computational neural learning formalisms for manipulator inverse kinematics N90-29030

FORMULATIONS
Chiral Maxwell-Garnett mixing formula [PB90-189143] N90-29158

FORTRAN
LINTERP: A numerical algorithm for interpolating quadrilateral and hexahedral meshes [DE90-014417] N90-29090
Software development tools [PB90-250051] N90-29103
ELEFUNT test results under AST FORTRAN V1.8.0 on the sequent symmetry [DE90-014932] N90-29127
Semiconductor measurement technology. EPROP: An interactive FORTRAN program for computing selected electronic properties of Gallium Arsenide and Silicon [PB90-222738] N90-29203

FOURIER ANALYSIS
Formation of magnetic islands due to field perturbations in toroidal stellarator configurations [DE90-014789] N90-29191
Numerical and analytical study of nonlinear bifurcations associated with the morphological stability of two-dimensional single crystals [PB90-209594] N90-29200

FOURIER SERIES
Stabilization of Taylor-Couette flow due to time-periodic outer cylinder oscillation [PB90-219130] N90-28790
Application of discrete Fourier series to the finite element stress analysis of axi-symmetric solids [PB90-231010] N90-28870

FRACTALS
A generalised Hubbard Hamiltonian: Influence of temperature and fractality [DE90-627322] N90-29213

FRACTURE MECHANICS
NASCRAC (trademark): A fracture mechanics analysis code N90-28645
A comparison of single-cycle versus multi-cycle proof testing strategies N90-28646
Data base for crack growth properties of materials N90-28647
Comparison of two computer codes for crack growth analysis: NASCRAC versus NASA/FLAGRO N90-28648
Probabilistic model for fracture mechanics service life analysis N90-28650
Crack layer analysis of fatigue fracture of a beta titanium alloy N90-28864

FRACTURE STRENGTH
Factors influencing the mode I interlaminar fracture resistance of toughened matrix composites N90-28668
Micromechanisms of fatigue crack growth and fracture toughness in metal matrix composites [AD-A223863] N90-28676
Fretting fatigue strength of Ti-6Al-4V at room and elevated temperatures and ways of improving it N90-28709
Ascertaining the fracture toughness of ceramic materials by means of bending testpieces of various notch types at ambient and high temperatures [ESA-TT-992] N90-28733
Influence of diesel engine exposure on the rupture strength of silicon nitride and partially stabilized zirconia [DE90-014759] N90-28849

FRACTURING
Strengthening and toughening mechanisms in ceramic fiber-reinforced glass matrix composites N90-28666

FRAGMENTATION
The formation of globular clusters N90-29272

FRAMES
A neural network for controlling the configuration of frame structure with elastic members N90-29034

FREE ELECTRON LASERS
Three-dimensional simulations of the generation of one Angstrom radiation by a self-amplified spontaneous emission free-electron laser [DE90-015032] N90-28830
Control of nonlinear space-charge emittance growth [DE90-014752] N90-29270

FREE ENERGY
Thermodynamics and structure of liquid alkali metals from the charged-hard-sphere reference fluid [DE90-627792] N90-28725

FREE FALL
Noncontact measurement of high temperature using optical fiber sensors [NASA-CR-186975] N90-28825

FREE JETS
The entrainment rate for a row of turbulent jets [NASA-CR-185278] N90-28504

FREON
Composite propellants with high burning rates [FOA-C-20781-2.1] N90-28744

FREQUENCIES
Auditory processing of complex sounds across frequency channels [AD-A224147] N90-28970
Solar oscillation frequency and solar neutrino predictions [DE90-014918] N90-29288

FREQUENCY SYNTHESIZERS
Tunable CW single-frequency source for injection seeding 2-micrometer lasers [AD-A223979] N90-28834

FRETTING
Fretting wear and fretting fatigue at temperatures up to 600 C N90-28706
Microdamage to ceramic surfaces under sliding conditions N90-28708
Fretting fatigue strength of Ti-6Al-4V at room and elevated temperatures and ways of improving it N90-28709
Surface property improvement in titanium alloy gas turbine components through ion implantation N90-28713
FRICTION
Effects of friction and end losses on MHD thruster efficiency [DE90-013673] N90-28808
Investigation of maximum achievable body torque for a walking machine with friction cone constraints [PB90-203175] N90-28838
Solutions to the frictional dynamics problem and the reciprocal variable feedback methodology for design and control of robot mechanisms N90-28846
Use of electron spectroscopies in the tribological evaluation of diamond films [DE90-014421] N90-28848
FUEL CELLS
Fuel cells: Their applications, technological status, market and opportunity [DE90-796158] N90-28895
A 10kW class molten carbonate fuel cell test: The stack with electrolyte plate prepared with paper-making method [DE90-507841] N90-28900
FUEL COMBUSTION
Injector element characterization methodology N90-28634
Overview on hot gas tests and molten salt corrosion experiments at the DLR N90-28714
Evaluation of a hybrid kinetics/mixing-controlled combustion model for turbulent premixed and diffusion combustion using KIVA-2 [NASA-TM-103196] N90-28792
FUEL CONSUMPTION
Energy Efficient Engine acoustic supporting technology report [NASA-CR-174834] N90-28557
Energy Efficient Engine core design and performance report [NASA-CR-168069] N90-28559
Energy Efficient Engine program advanced turbofan nacelle definition study [NASA-CR-174942] N90-28560
Energy Efficient Engine integrated core/low spool design and performance report [NASA-CR-168211] N90-28561
Energy efficient engine program technology benefit/cost study, volume 2 [NASA-CR-174766-VOL-2] N90-28565
Energy Efficient Engine: Combustor component performance program [NASA-CR-179533] N90-28568
Energy Efficient Engine: Control system preliminary definition report [NASA-CR-179578] N90-28569
Energy Efficient Engine: High-pressure compressor test hardware detailed design report [NASA-CR-180850] N90-28570
Results from the fourth year of operation of the Federal Methanol Fleet at Lawrence Berkeley Laboratory [DE90-014741] N90-28743
FUEL INJECTION
Computer code for the prediction of nozzle admittance N90-28630
Swirl coaxial injector element characterization for booster engines N90-28632
Heavy hydrocarbon main injector technology N90-28633
Evaluation of a hybrid kinetics/mixing-controlled combustion model for turbulent premixed and diffusion combustion using KIVA-2 [NASA-TM-103196] N90-28792
FUEL-AIR RATIO
Development of advanced combustion technology for medium and high speed natural gas engines [PB90-198565] N90-28836
FUELS
Analyses of spray and droplet ignition for pure and multicomponent fuels N90-28688
Fuels research, volume 1 [DE90-015393] N90-28695
FUNCTIONAL DESIGN SPECIFICATIONS
Communications Interface Driver (CID) test plan [DOT/FAA/CT-TN89/35] N90-28762
A system architecture for a planetary rover N90-29015
FURNACES
Radiative heat transfer [PB90-247602] N90-28813
FUSELAGES
Correlation of AH-1G airframe flight vibration data with a coupled rotor-fuselage analysis [NASA-CR-181974] N90-28885
FUSION REACTORS
Helium generation in fusion reactor materials [DE90-013005] N90-29172

G

GALAXIES
Quantifying the FIR interaction enhancement in paired galaxies [DE90-627485] N90-29281
Gamma ray evidence for cosmic ray sources N90-29292
GALERKIN METHOD
Oscillatory convection [ESA-TT-890] N90-28801
A hybrid perturbation-Galerkin technique for partial differential equations [NASA-CR-182085] N90-28814
GALLIUM
Enrichment services for chromium isotopes for the GALLEX (gallium experiment) international collaboration experiment on solar neutrino flux [DE90-014300] N90-29285
GALLIUM ARSENIDES
Semiconductor measurement technology. EPROP: An interactive FORTRAN program for computing selected electronic properties of Gallium Arsenide and Silicon [PB90-222738] N90-29203
GAMMA RAY OBSERVATORY
Predictions of radiation backgrounds for GRO/OSSE [RAE-TM-SPACE-372] N90-29293
GAMMA RAY SPECTRA
Gamma ray evidence for cosmic ray sources N90-29292
GAMMA RAY SPECTROMETERS
Predictions of radiation backgrounds for GRO/OSSE [RAE-TM-SPACE-372] N90-29293
GAMMA RAYS
Some novel sources of x ray beams: Channeling, transition and Cherenkov radiation [DE90-014442] N90-29181
GAS CHROMATOGRAPHY
Thermogravimetry-mass spectrometry analysis of gas bubbles in molten glass [DE90-014116] N90-28684
Peak analysis in gas chromatography and the development of new stationary phases for anion chromatography [DE90-014426] N90-28687
GAS FLOW
Development of an integrated BEM for hot fluid-structure interaction N90-28617
Current research in cavitating fluid films [NASA-TM-103184] N90-28791
Gas-film flow in tubes [DE90-011528] N90-28793
GAS GENERATORS
Design optimization of gas generator hybrid propulsion boosters [NASA-CR-181096] N90-28660
GAS JETS
Gas-jet and tangent-slot film cooling tests of a 12.5 deg cone at Mach number of 6.7 [NASA-TP-2786] N90-28806
GAS RECOVERY
Study of power generation systems for CO2 collection: LNG combined cycle [DE90-507881] N90-28901
GAS TEMPERATURE
Overview on hot gas tests and molten salt corrosion experiments at the DLR N90-28714
GAS TURBINE ENGINES
Analysis of the T63-A-700 engine used in alcohol turbine fuel extender test [DOT/FAA/CT-TN90/18] N90-28549
Calculation of temperature distribution in various turbine blades using a boundary-fitted coordinate transformation method N90-28550
Energy Efficient Engine exhaust mixer model technology report addendum; phase 3 test program [NASA-CR-174799] N90-28556
Energy Efficient Engine integrated core/low spool design and performance report [NASA-CR-168211] N90-28561
Energy Efficient Engine integrated core/low spool test hardware design report [NASA-CR-168137] N90-28566
Energy Efficient Engine: High-pressure compressor test hardware detailed design report [NASA-CR-180850] N90-28570
Source emission test of gas turbine engine test facility, Kelly AFB, TX [AD-A223869] N90-28571
The effects of a compressor rebuild on gas turbine engine performance: Final results N90-28701
Effect of protective coatings on mechanical properties of superalloys N90-28707
Evaluation of high temperature protective coatings for gas turbine engines under simulated service conditions N90-28712
Surface property improvement in titanium alloy gas turbine components through ion implantation N90-28713
Overview on hot gas tests and molten salt corrosion experiments at the DLR N90-28714
GAS TURBINES
Structural response of SSME turbine blade airfoils N90-28649
Scale adherence effects in oxidation and sulfidation N90-28703
Study of power generation systems for CO2 collection: LNG combined cycle [DE90-507881] N90-28901
GASEOUS ROCKET PROPELLANTS
Catalytic ignition of hydrogen/oxygen N90-28627
GAUGE THEORY
Introduction to gauge theories and unification [DE90-014473] N90-29225
Higher loop contributions to effective potential of gauge theory at high temperature [DE90-627208] N90-29231
GENETIC ENGINEERING
Engineering and the advancement of human welfare. Ten outstanding achievements 1964-1989 [ISBN-0-309-04185-6] N90-29297
GENETICS
Japanese molecular biology 1990: An update [PB90-188707] N90-28958
GEODESIC LINES
On an isospectrality question over compact Riemann surfaces [DE90-627163] N90-29147
Dirac's equation as a geodesic in Riemann space [DE90-627194] N90-29152
On the relation between the absolute parallelism spaces and spaces having a GL(4) connection [DE90-627222] N90-29232
GEODESY
On an isospectrality question over compact Riemann surfaces [DE90-627163] N90-29147
GEOGRAPHIC INFORMATION SYSTEMS
Multiband imaging systems [AD-A223969] N90-28893
INPE geographic data base [INPE-4636-PRE/1348] N90-29253
GEOMETRICAL OPTICS
Using the x ray region of the electromagnetic spectrum for alignment: Overview, geometric optics, and design considerations [DE90-014798] N90-28752
GEOMETRY
Geometrical properties of an internal local octonionic space in a non-Riemannian manifold [DE90-627175] N90-29149
GEOPHYSICS
Geophysical diffraction tomography: A complementary remote sensing technique for hazardous waste site characterization [DE90-013025] N90-28882
A radio frequency user's guide to the space environment services center geophysical alert broadcasts [PB90-240631] N90-28935
GEOTECHNICAL ENGINEERING
Finite element analysis of coupled thermoelasticity [PB90-201211] N90-28860
GEOTHERMAL ENERGY CONVERSION
Geothermal fluid genesis in the Great Basin [DE90-014438] N90-28884
GEOTHERMAL RESOURCES
Geothermal fluid genesis in the Great Basin [DE90-014438] N90-28884
GEOTHERMAL TECHNOLOGY
Geothermal fluid genesis in the Great Basin [DE90-014438] N90-28884
GLACIERS
Ross Sea oceanographic data, 1983-1987: USCGC GLACIER, January-February 1983; USCGC POLAR SEA, January-February 1984; USCGC POLAR STAR, February 1984; USCGC POLAR SEA, February 1987 [PB90-243932] N90-28955

GLASS
Thermogravimetry-mass spectrometry analysis of gas bubbles in molten glass
[DE90-014116] N90-28684
GLOBAL WARMING
Responding to the threat of global warming: Options for the Pacific and Asia
[DE90-014756] N90-28918
GLOBULAR CLUSTERS
The formation of globular clusters N90-29272
GOLD
Synthesis and structural chemistry of Au(III)-substituted Ba2YCu3O(7-delta)
[NASA-TM-103292] N90-28696
XANES and EXAFS study of Au-substituted YBa2Cu3O(7-delta)
[NASA-TM-103291] N90-29219
GOLD ISOTOPES
Studies of central interactions of Si ions at 14.5 x A GeV/c in Au and Cu
[DE90-015095] N90-29195
GOVERNMENT/INDUSTRY RELATIONS
Goverment's role in standards-related activities: Analysis of comments
[PB90-215534] N90-29239
State science and technology indicators: An exploratory profile and analysis
[PB90-246711] N90-29259
GOVERNMENTS
Goverment's role in standards-related activities: Analysis of comments
[PB90-215534] N90-29239
GRAIN BOUNDARIES
High-temperature deformation and microstructural analysis for Si3N4-Sc2O3
[NASA-TM-103239] N90-28740
Interface formation and percusory dynamics
[AD-A224126] N90-29223
GRAIN SIZE
The affect of gravity on particle collection in inertial impactors
[DE90-013372] N90-29173
GRAPH THEORY
Graph structure model
[DE90-014930] N90-29097
GRAPHITE
Crash-impact behavior of graphite/epoxy composite sine wave webs N90-28667
GRAPHITE-EPOXY COMPOSITES
Crash-impact behavior of graphite/epoxy composite sine wave webs N90-28667
Ultrasonic verification of five wave fronts in unidirectional graphite epoxy composite
[NASA-CR-185268] N90-28858
GRASSLANDS
Study of anomalies in transition vegetation in Alto Xingo-NT, through remote sensing techniques
[INPE-4601-TDL/334] N90-28891
GRAVITATION
Quantum gravity in two dimensions and the SL(2,R) current algebra
[DE90-627215] N90-29156
Viscous causal cosmologies
[DE90-627487] N90-29282
GRAVITATIONAL EFFECTS
Development and approach to low-frequency microgravity isolation systems
[NASA-TP-2984] N90-28754
The affect of gravity on particle collection in inertial impactors
[DE90-013372] N90-29173
GRAVITATIONAL FIELDS
Unexpected properties of the centrifugal force
[DE90-627197] N90-29164
Measurement of gravitational acceleration of antimatter
[DE90-627464] N90-29233
GRAVITATIONAL WAVES
Propagation of electromagnetic radiation in a random field of gravitational waves and space radio interferometry
[DE90-627196] N90-28764
GRAVITY WAVES
Gravity wave initiated convection
[NASA-CR-186868] N90-28933
GREAT BASIN (US)
Geothermal fluid genesis in the Great Basin
[DE90-014438] N90-28884
GREEN'S FUNCTIONS
Green's functions for dislocations in bonded strips and related crack problems
[NASA-CR-185291] N90-28878
GREENHOUSE EFFECT
Chasing a specter: Risk management for global environmental change
[DE90-014455] N90-28917
Responding to the threat of global warming: Options for the Pacific and Asia
[DE90-014756] N90-28918
Acid deposition: No such thing as a free launch
[DE90-015085] N90-28920
Tropospheric nitrogen: The influence of anthropogenic sources on distributions and deposition, executive summary
[DE90-015401] N90-28922
Natural and anthropogenic climate change
[DE90-015526] N90-28923
GROOVES
Free shear layer and swirl flow heat transfer enhancement
[PB90-228123] N90-28798
GROUND EFFECT (AERODYNAMICS)
Aerodynamics of Combat Aircraft Controls and of Ground Effects
[AGARD-CP-465] N90-28513
Aerodynamic interferences of in-flight thrust reversers in ground effect N90-28529
Study of the ground effects in the CEAT aerohydrodynamic tunnel: Using the results N90-28530
Dynamic ground effects N90-28531
Study of ground effects on flying scaled models N90-28532
An in-flight investigation of ground effect on a forward-swept wing airplane N90-28533
Determination of the ground effect on the characteristics of the A320 aircraft N90-28534
GROUND STATE
Moessbauer Effect applications using intense radioactive ion beams
[DE90-014981] N90-29175
Evidence for a coherence gap in Ce3Bi4Pt3
[DE90-014925] N90-29207
GROUND STATIONS
An aeronautical mobile satellite experiment
[NASA-CR-186971] N90-28593
GROUND TESTS
Control research in the NASA high-alpha technology program N90-28516
GROUND WATER
Study and analysis of leaking underground storage tank remediation techniques incorporated in states in EPA Region 6
[PB90-214834] N90-28847
Computer program for converting rectangular coordinates to latitude-longitude coordinates
[PB90-231796] N90-28883
GROUP DYNAMICS
The effects of management support on the successful implementation of group decision support systems
[AD-A224473] N90-29241
GUN PROPELLANTS
Ignition and combustion of liquid propellants
[AD-A224150] N90-28746

H

H ALPHA LINE
NASA Marshall Space Flight Center Solar Observatory report, January - June 1990
[NASA-TM-103512] N90-29268
H I REGIONS
Star formation and the distribution of HI and infrared emission in M51
[NASA-CR-186928] N90-29262
H II REGIONS
Star formation and the distribution of HI and infrared emission in M51
[NASA-CR-186928] N90-29262
A plasma diagnostic study of two wind-blown shell nebulae: NGC 7635 and NGC 2359 N90-29271
HABITATS
Flora and threatened and endangered plants of John F. Kennedy Space Center, Florida
[NASA-TM-102791] N90-28925
HAILSTORMS
Program on development of basic understanding of severe weather phenomena
[PB90-226564] N90-28943
HAMILTONIAN FUNCTIONS
Anyons and Chern-Simons theory on compact spaces of finite genus
[DE90-627216] N90-29157
A generalised Hubbard Hamiltonian: Influence of temperature and fractality
[DE90-627322] N90-29213
Dissipative quantum maps
[DE90-627179] N90-29227
Quantum chaos and dissipation: Lyapunov exponents
[DE90-627180] N90-29228
HANDBOOKS
Liquid Rocket Booster (LRB) for the Space Transportation System (STS) systems study, volume 2
[NASA-CR-183786] N90-28600
Specifications, tolerances, and other technical requirements for weighing and measuring devices as adopted by the 74th National Conference on Weights and Measures, 1989 (1990 edition)
[PB90-184961] N90-28748
HARDENING (MATERIALS)
A theoretical investigation into the inelastic behavior of metal-matrix composites
[AD-A223973] N90-28677
HARDNESS
Mechanical properties testing of diamond and diamond-like films by ultra-low load indentation
[DE90-014456] N90-28861
HARMONIC GENERATORS
Tunable CW single-frequency source for injection seeding 2-micrometer lasers
[AD-A223979] N90-28834
HARTREE APPROXIMATION
Rotating neutron stars and the equation of state of dense matter
[DE90-014185] N90-29269
HAZARDS
Geophysical diffraction tomography: A complementary remote sensing technique for hazardous waste site characterization
[DE90-013025] N90-28882
HEAD (ANATOMY)
Helicopter aircrew helmets and head injury: A protective effect
[AD-A223024] N90-29080
HEAD DOWN TILT
Joint US/USSR study: Comparison of effects of horizontal and head-down bed rest
[NASA-TP-3037] N90-28965
HEARING
Auditory processing of complex sounds across frequency channels
[AD-A224147] N90-28970
HEART DISEASES
Prevalence of hypertension among active duty personnel
[AD-A223892] N90-28968
HEAT EXCHANGERS
A study of heat and fluid flow phenomena on the gas side of circular-tube plate-fin heat exchangers N90-28795
Free shear layer and swirl flow heat transfer enhancement
[PB90-228123] N90-28798
Open cycle heat pump development for local resource use. Phase 2: District heating case study analysis
[DE90-011123] N90-28904
HEAT GENERATION
Evolution and use of combined mechanical and thermal codes for cryogenic turbopump bearings N90-28618
HEAT MEASUREMENT
Determination of the SSME high pressure oxidizer turbopump bearing temperature N90-28619
HEAT PUMPS
Open cycle heat pump development for local resource use. Phase 2: District heating case study analysis
[DE90-011123] N90-28904
HEAT RADIATORS
The effects of atomic oxygen on the thermal emittance of high temperature radiator surfaces
[NASA-TM-103224] N90-28670
HEAT RESISTANT ALLOYS
Micromechanics of cyclic deformation in SSME turbopump blade materials N90-28641
High temperature fatigue behavior of Haynes 188 N90-28642
Constitutive and life modeling of single crystal blade alloys for root attachment analysis N90-28643
The fatigue damage behavior of a single crystal superalloy N90-28644
Developments in test procedures for hot-salt corrosion of superalloys N90-28700
Effect of protective coatings on mechanical properties of superalloys N90-28707
HEAT TRANSFER
Development of an integrated BEM for hot fluid-structure interaction N90-28617
A study of heat and fluid flow phenomena on the gas side of circular-tube plate-fin heat exchangers N90-28795
Gas-jet and tangent-slot film cooling tests of a 12.5 deg cone at Mach number of 6.7
[NASA-TP-2786] N90-28806
A hybrid perturbation-Galerkin technique for partial differential equations
[NASA-CR-182085] N90-28814

Effect of vortex circulation on injectant from a single film-cooling hole and a row of film-cooling holes in a turbulent boundary layer. Part 2: Injection beneath the vortex upwash
[AD-A223894] N90-28818
Laboratory for Laser Energetics review
[DE90-014666] N90-28829
Evaluation of the STM4-120 kinematic Stirling engine
[DE90-013836] N90-28897

HEAT TRANSFER COEFFICIENTS
Pool boiling from rotating and stationary spheres in liquid nitrogen N90-28821
A study of heat and fluid flow phenomena on the gas side of circular-tube plate-fin heat exchangers N90-28795

HEATERS
Flight motor set 360L008 (STS-32R). Volume 1: System overview
[NASA-CR-184010] N90-28609

HEAVY IONS
Ion divergence and the stability of magnetically insulated diodes
[DE90-014565] N90-28777

HEISENBERG THEORY
Parity violation and superconductivity in doped Mott insulators
[DE90-627493] N90-29217

HELICOPTERS
Solution of Euler equations applied to a rotor of a helicopter in steady flight
[ONERA-RSF-1/3731-AY-002A] N90-28500
Velocity filtering applied to optical flow calculations
[NASA-TM-102802] N90-28512
Analysis of heliport environmental data, Intracoastal City
[DOT/FAA/CT-TN89/43] N90-28584
Helicopter aircrew helmets and head injury: A protective effect
[AD-A223024] N90-29080

HELIPORTS
Analysis of heliport environmental data, Intracoastal City
[DOT/FAA/CT-TN89/43] N90-28584

HELIUM
Helium generation in fusion reactor materials
[DE90-013005] N90-29172

HELMET MOUNTED DISPLAYS
Target acquisition under load factors: Advantages and disadvantages of a helmet mounted sight N90-28983
Tracking performance and influence of field of view N90-28988

HELMETS
Helicopter aircrew helmets and head injury: A protective effect
[AD-A223024] N90-29080

HEMODYNAMIC RESPONSES
Fluid and electrolyte homeostasis during spaceflight: Elucidation of mechanisms in a primate
[NASA-CR-177548] N90-29085

HERMITIAN POLYNOMIAL
Casimir effect in a D-dimensional flat spacetime and the cut-off method
[DE90-627177] N90-29151

HEURISTIC METHODS
Robot Acting on Moving Bodies (RAMBO): Interaction with tumbling objects N90-29022
Focus of attention in an activity-based scheduler N90-29039
A Boltzmann machine for the organization of intelligent machines N90-29040
Efficient mapping algorithms for scheduling robot inverse dynamics computation on a multiprocessor system N90-29071

HIERARCHIES
A 17 degree of freedom anthropomorphic manipulator N90-29001
Methods and strategies of object localization N90-29020
Techniques and potential capabilities of multi-resolutional information (knowledge) processing N90-29062

HIGH ENERGY INTERACTIONS
High energy physics at Tufts University
[DE90-014664] N90-29174

HIGH ENERGY PROPELLANTS
High energy-density liquid rocket fuel performance
[NASA-CR-185279] N90-28742

HIGH FREQUENCIES
New approach to HF channel modeling and simulation. Part 2: Stochastic model
[PB90-200338] N90-28755

HIGH LEVEL LANGUAGES
Integrating planning and reactive control N90-29077

HIGH SPEED
Development of advanced combustion technology for medium and high speed natural gas engines
[PB90-196565] N90-28836

HIGH TEMPERATURE
Analysis of the T63-A-700 engine used in alcohol turbine fuel extender test
[DOT/FAA/CT-TN90/18] N90-28549
The effects of atomic oxygen on the thermal emittance of high temperature radiator surfaces
[NASA-TM-103224] N90-28670
High Temperature Surface Interactions
[AGARD-CP-461] N90-28698
High temperature surface interactions: Overview N90-28699
Molten salt induced high temperature degradation of thermal barrier coatings N90-28704
High temperature oxidation of Al-Li alloys N90-28705
High temperature protective coatings: Recent trends N90-28710
Evaluation of high temperature protective coatings for gas turbine engines under simulated service conditions N90-28712
Surface property improvement in titanium alloy gas turbine components through ion implantation N90-28713
Mechanical testing activities related to high-performance structural ceramics
[DE90-014299] N90-28734
Improved silicon carbide for advanced heat engines
[NASA-CR-182186] N90-28735
High-temperature deformation and microstructural analysis for Si3N4-Sc2O3
[NASA-TM-103239] N90-28740
High temperature superconducting thin film microwave circuits: Fabrication, characterization, and applications
[NASA-TM-103235] N90-28786
Noncontact measurement of high temperature using optical fiber sensors
[NASA-CR-186975] N90-28825
Dynamical information for Fe doped YBa2Cu3O7 superconducting oxides obtained from high temperature Moessbauer studies
[DE90-627871] N90-29218
Higher loop contributions to effective potential of gauge theory at high temperature
[DE90-627208] N90-29231

HIGH TEMPERATURE ENVIRONMENTS
Evolution and use of combined mechanical and thermal codes for cryogenic turbopump bearings N90-28618

HIGH TEMPERATURE GASES
Development of an integrated BEM for hot fluid-structure interaction N90-28617
Overview on hot gas tests and molten salt corrosion experiments at the DLR N90-28714

HIGH TEMPERATURE PLASMAS
Damage resistant optical coatings prepared using high temperature, plasma chemical-vapor-deposition
[DE90-015042] N90-28738

HIGH TEMPERATURE SUPERCONDUCTORS
Synthesis and structural chemistry of Au(III)-substituted Ba2YCu3O(7-delta)
[NASA-TM-103292] N90-28696
Electron microscopy of transition-metal doped BiCaSrCuO
[DE90-014184] N90-29202
XANES and EXAFS study of Au-substituted YBa2Cu3O(7-delta)
[NASA-TM-103291] N90-29219

HIGH TEMPERATURE TESTS
Ascertaining the fracture toughness of ceramic materials by means of bending testpieces of various notch types at ambient and high temperatures
[ESA-TT-992] N90-28733

HIGH VOLTAGES
PBFA 2 applied B ion diode beam characteristics at high voltages
[DE90-014419] N90-29190

HILBERT SPACE
Accurate quantum chemical calculations
[NASA-TM-101932] N90-28680
Old and new ideas in the theory of quantum measurement
[DE90-627181] N90-29229

HISTORIES
A look at tomorrow today N90-28524

HMX
Study of the induction time in isothermal decomposition of explosives
[DE90-014906] N90-28745

HOLES (ELECTRON DEFICIENCIES)
Parity violation and superconductivity in doped Mott insulators
[DE90-627493] N90-29217

HOMEOSTASIS
Fluid and electrolyte homeostasis during spaceflight: Elucidation of mechanisms in a primate
[NASA-CR-177548] N90-29085

HOT CORROSION
High temperature surface interactions: Overview N90-28699
Developments in test procedures for hot-salt corrosion of superalloys N90-28700
Oxidation, sulfidation, and hot corrosion: Mechanisms and interrelationships N90-28702
Molten salt induced high temperature degradation of thermal barrier coatings N90-28704
Evaluation of high temperature protective coatings for gas turbine engines under simulated service conditions N90-28712
Overview on hot gas tests and molten salt corrosion experiments at the DLR N90-28714

HOT PRESSING
Micromechanics analysis of power consolidation in manufacturing particulate-reinforced MMCs (metal matrix composites)
[DE90-014448] N90-28663
Strengthening and toughening mechanisms in ceramic fiber-reinforced glass matrix composites N90-28665

HOT STARS
Kappa effect pulsational instability for hot extreme helium stars
[DE90-014920] N90-29277

HOT SURFACES
Transient cooling of a hot surface by droplets evaporation
[PB90-227968] N90-28799

HOT WORKING
Behavior of Al-Mg alloys in hot working and superplasticity
[DE90-015193] N90-28723

HOVERING
The effects of structural flap-lag and pitch-lag coupling on soft inplane hingeless rotor stability in hover
[NASA-TP-3002] N90-28503

HOVERING STABILITY
The effects of structural flap-lag and pitch-lag coupling on soft inplane hingeless rotor stability in hover
[NASA-TP-3002] N90-28503

HUBBLE SPACE TELESCOPE
Minimum weight design of a leaf spring tapered in thickness and width for the Hubble Space Telescope-space support equipment
[NASA-TM-4233] N90-28879
State-based scheduling: An architecture for telescope observation scheduling N90-29038
A survey of planning and scheduling research at the NASA Ames Research Center N90-29076

HUMAN FACTORS ENGINEERING
A conceptual framework for fighter flight control systems
[PD-CF-9009] N90-28577
Quality function deployment as a mechanism for process characterization and control
[DE90-014755] N90-28857
Techniques and applications for binaural sound manipulation in human-machine interfaces
[NASA-TM-102279] N90-28996
Military aircrew seating: A human factors engineering approach
[AD-A218049] N90-28999
Human factors model concerning the man-machine interface of mining crewstations N90-29011
Development of a flexible test-bed for robotics, telemanipulation and servicing research N90-29012
Human factors evaluation and validation criteria for quality training programs: Development, presentation, and assessment
[DE90-014724] N90-29081

HUMAN PERFORMANCE
Variable force and visual feedback effects on teleoperator man/machine performance N90-29008

HUMAN TOLERANCES
Annoyance caused by advanced turboprop aircraft flyover noise: Counter-rotating-propeller configuration
[NASA-TP-3027] N90-29166

HUMAN WASTES
Electrochemical incineration of wastes
[NASA-CR-187033] N90-28753

HYBRID PROPELLANTS
Tripropellant combustion process N90-28631

HYBRID PROPULSION
Design optimization of gas generator hybrid propulsion boosters
[NASA-CR-181096] N90-28660

HYDRAULIC JETS
Large hydrodynamic tunnel: Calculation of the acoustic transparency of the jet stream
[REPT-89/115] N90-29167

HYDRAULIC TEST TUNNELS
Large hydrodynamic tunnel: Calculation of the acoustic transparency of the jet stream
[REPT-89/115] N90-29167
HYDROCARBON FUELS
Heavy hydrocarbon main injector technology N90-28833
High energy-density liquid rocket fuel performance
[NASA-CR-185279] N90-28742
HYDRODYNAMICS
Effects of friction and end losses on MHD thruster efficiency
[DE90-013673] N90-28608
Three functions that model empirically measured unfrozen water content data and predict relative hydraulic conductivity
[AD-A223875] N90-28892
The formation of globular clusters N90-29272
HYDROGEN
Catalytic ignition of hydrogen/oxygen N90-28627
Tripropellant combustion process N90-28631
HYDROGEN OXYGEN ENGINES
Oxygen/hydrogen technology test bed status update N90-28813
High/variable mixture ratio oxygen/hydrogen engines N90-28637
High/variable mixture ratio O2/H2 engine N90-28638
Variable mixture ratio performance through nitrogen augmentation N90-28639
High variable mixture ratio oxygen/hydrogen engine N90-28640
HYDROGEOLOGY
Study and analysis of leaking underground storage tank remediation techniques incorporated in states in EPA Region 6
[PB90-214834] N90-28847
HYDROLOGY MODELS
Computer program for converting rectangular coordinates to latitude-longitude coordinates
[PB90-231796] N90-28883
HYDROXYL RADICALS
Study of the radical OH in a high pressure flame by resonant DRASC
[ONERA-RF-57/7131-PY] N90-28692
Spectroscopic study of combustion diagnostics on hydroxyl radicals
[NASA-CR-186998] N90-28694
HYPERCUBE MULTIPROCESSORS
Efficient mapping algorithms for scheduling robot inverse dynamics computation on a multiprocessor system N90-29071
Workshop on Neural Networks
[DE90-014794] N90-29120
HYPERGEOMETRIC FUNCTIONS
Product integration rules at Clenshaw-Curtis and related points: A robust implementation
[DE90-627158] N90-29106
HYPERSONIC FLIGHT
Real-time aerodynamic heating and surface temperature calculations for hypersonic flight simulation
[NASA-TM-4222] N90-28815
HYPERSONIC FLOW
Hypersonic Arbitrary-Body Aerodynamics (HABA) for conceptual design
[DE90-014750] N90-28495
Multigrid for hypersonic inviscid flows
[NASA-CR-182082] N90-29125
HYPERSONIC VEHICLES
Real-time aerodynamic heating and surface temperature calculations for hypersonic flight simulation
[NASA-TM-4222] N90-28815
HYPERSONICS
Hypersonic Arbitrary-Body Aerodynamics (HABA) for conceptual design
[DE90-014750] N90-28495
HYPERTENSION
Prevalence of hypertension among active duty personnel
[AD-A223892] N90-28968
HYPERVELOCITY WIND TUNNELS
Design of an axisymmetric, contoured nozzle for the HEG
[DLR-FB-90-04] N90-28812
HYPOKINESIA
Joint US/USSR study: Comparison of effects of horizontal and head-down bed rest
[NASA-TP-3037] N90-28965
HYPOXIA
Decompression sickness presenting as a viral syndrome
[AD-A223880] N90-28967
Evaluation of the performance capability of the aviator under hypoxic conditions operational experience N90-28991

I

ICE
Three functions that model empirically measured unfrozen water content data and predict relative hydraulic conductivity
[AD-A223875] N90-28892
IGNITION
Analyses of spray and droplet ignition for pure and multicomponent fuels N90-28688
Ignition and combustion of liquid propellants
[AD-A224150] N90-28746
Ignition and burn control characteristics of thermonuclear plasmas
[DE90-015385] N90-29197
IGNITION SYSTEMS
Catalytic ignition of hydrogen/oxygen N90-28627
ILLUSIONS
Spatial disorientation incidents in the RNLAF F16 and F5 aircraft and suggestions for prevention N90-28973
IMAGE ANALYSIS
On-line object feature extraction for multispectral scene representation
[NASA-CR-187006] N90-28888
Detection of ocean inner waves by synthetic aperture radar: Observations at Gibraltar pass
[ETN-90-97477] N90-28953
Techniques and potential capabilities of multi-resolutional information (knowledge) processing N90-29062
National Archives preservation research priorities: Past and present
[PB90-206210] N90-29242
IMAGE ENHANCEMENT
Robot Acting on Moving Bodies (RAMBO): Interaction with tumbling objects N90-29022
IMAGE INTENSIFIERS
Noise performance of microchannel plate imaging systems
[DE90-015037] N90-28785
IMAGE PROCESSING
Target signature modeling and bistatic scattering measurement studies
[NASA-CR-186611] N90-28766
Treatment of systematic errors 2: Fusion of ultrasound and visual sensor data
[DE90-014780] N90-28850
A manual for analysis of hemispherical canopy photography
[DE90-014718] N90-28885
Digital geometric correction for MSS-LANDSAT imagery
[INPE-4627-PRE/1345] N90-28886
A tesselated probabilistic representation for spatial robot perception and navigation N90-29075
Who's who in scientific visualization at LLNL
[DE90-014720] N90-29091
Computer vision and its potential applications in Brazil
[INPE-4666-NTE/283] N90-29100
Fast interactive image generation of line and surface oriented objects in raster systems
[ETN-90-97290] N90-29102
Recognition of infrared images. Part 3: The effect of image processing with a size-contrast box filter on observation performance
[IZF-1989-39] N90-29182
New Voyager radio spectrograms of Uranus
[NASA-CR-180381] N90-29284
IMAGERY
Space-base multispectral imagery: Current and future applications and implications to the United States Army
[AD-A224046] N90-28894
IMAGES
A sensor stabilization/tracking system for unmanned air vehicles
[AD-A224008] N90-28579
Comparison of methods of space color transformations for enhancement of colored images
[INPE-4977-PRE/1542] N90-28881
IMAGING TECHNIQUES
Noncontact measurement of high temperature using optical fiber sensors
[NASA-CR-186975] N90-28825
Comparison of methods of space color transformations for enhancement of colored images
[INPE-4977-PRE/1542] N90-28881
Multiband imaging systems
[AD-A223969] N90-28893
Tropospheric wind profiling using radar interferometry: A feasibility study of a compact mobile system
[PB90-217068] N90-28939
IMPACT RESISTANCE
Determination of the NDT temperature and Charpy V-notch impact properties of AAR TC128 grades B steel and A 8XX grade B steel
[PB90-207804] N90-28716
IMPACT STRENGTH
Determination of the NDT temperature and Charpy V-notch impact properties of AAR TC128 grades B steel and A 8XX grade B steel
[PB90-207804] N90-28716
IMPACT TESTS
Crash-impact behavior of graphite/epoxy composite sine wave webs N90-28667
IMPACTORS
The affect of gravity on particle collection in inertial impactors
[DE90-013372] N90-29173
IMPEDANCE
Electromagnetic scattering from two-dimensional thick material junctions
[NASA-CR-186468] N90-28767
Adjustable impedance, force feedback and command language aids for telerobotics (parts 1-4 of an 8-part MIT progress report) N90-29007
IMPELLERS
Turbomachinery rotor forces
[NASA-CR-183779] N90-28852
IMPROVEMENT
Improved silicon carbide for advanced heat engines
[NASA-CR-182186] N90-28735
IMPURITIES
Microstructure and impurity effects on tungsten heavy alloys
[AD-A224220] N90-28728
Semiconductor measurement technology. EPROP: An interactive FORTRAN program for computing selected electronic properties of Gallium Arsenide and Silicon
[PB90-222738] N90-29203
IN-FLIGHT MONITORING
An in-flight investigation of ground effect on a forward-swept wing airplane N90-28533
In-flight investigation of shuttle tile pressure orifice installations
[NASA-TM-4219] N90-28820
INCOMPRESSIBLE FLOW
Regular and chaotic motion of uniform elliptical vortices in external linear time dependent velocity fields N90-28497
Development of comprehensive numerical schemes for predicting evaporating gas-droplets flow processes of a liquid-fueled combustor
[NASA-CR-187018] N90-28693
Lecture notes on incompressible flow and the finite element method
[DE90-014665] N90-28805
Development of turbulence models for the analysis of compressible or incompressible unsteady flow
[ETN-90-97486] N90-28810
An investigation of chaotic Kolmogorov flows
[NASA-CR-182079] N90-28816
INDEXES (DOCUMENTATION)
Aerospace medicine and biology: A continuing bibliography with indexes (supplement 340)
[NASA-SP-7011(340)] N90-28963
Efficiency and effectiveness of deep structure-based subject indexing languages: PRECIS vs. DSIS N90-29248
INDIUM ANTIMONIDES
Radiation effects in InAsSb strained-layer superlattice photodiodes induced by dose-rate and transient x ray environments
[DE90-015000] N90-29208
INDIUM ARSENIDES
Radiation effects in InAsSb strained-layer superlattice photodiodes induced by dose-rate and transient x ray environments
[DE90-015000] N90-29208
INDOOR AIR POLLUTION
Atmosphere and water quality monitoring on Space Station Freedom
[NASA-CR-186707] N90-29084
INDUSTRIES
Scientists, engineers, and technicians in nonmanufacturing industries: 1987. (Detailed statistical tables)
[PB90-226903] N90-29235
Industrial patent activity in the US. Part 2: Alphabetical listing by company, 1969-1989
[PB90-214412] N90-29246
INEQUALITIES
Weighted norm inequalities for Riemann-Liouville fractional integral
[DE90-627153] N90-29132
INERTIA
Parallel algorithms for computation of the manipulator inertia matrix N90-29072

INERTIAL CONFINEMENT FUSION
Ion divergence and the stability of magnetically insulated diodes
[DE90-014565] N90-28777
Laboratory for Laser Energetics review
[DE90-014666] N90-28829
Characterization of electron flow in positive-polarity linear-induction accelerators
[DE90-014998] N90-29177
INERTIAL FUSION (REACTOR)
Laboratory for Laser Energetics review
[DE90-014666] N90-28829
INFERENCE
Inference engine for expert systems
[INPE-4565-PRE/1306] N90-29104
INFORMATION DISSEMINATION
Procedures for DOE-Navy exchange and approval of engineering information and material management required for production of W88-0/Mk5 RBA (reentry body assembly)
[DE90-014763] N90-28595
Transferring building energy technologies by linking government and private-sector programs
[DE90-000346] N90-29258
INFORMATION MANAGEMENT
Information management directions: The integration challenge
[PB90-219866] N90-29245
INFORMATION PROCESSING (BIOLOGY)
Research in command and control for the Dutch Army Corps (1NL)
[IZF-1989-28] N90-28760
A methodology for the objective measurement of pilot situation awareness N90-28974
Situational Awareness Rating Technique (SART): The development of a tool for aircrew systems design N90-28975
Evaluation of the Situational Awareness Rating Technique (SART) as a tool for aircrew systems design N90-28977
Attention gradients in situation awareness N90-28978
Towards a future cockpit: The prototyping and pilot integration of the Mission Management Aid (MMA) N90-28979
The simulation of localized sounds for improved situational awareness N90-28984
Neurophysiological correlates of information processing abilities during divided attention situations in air traffic controllers N90-28989
INFORMATION RETRIEVAL
The SPECIALIST: Natural language processing system
[PB90-240029] N90-29098
Efficiency and effectiveness of deep structure-based subject indexing languages: PRECIS vs. DSIS N90-29248
INFORMATION SYSTEMS
The personal computer: An untapped source for the United States Army War College
[AD-A223976] N90-29087
A comparison of password techniques for multilevel authentication mechanisms
[AD-A224245] N90-29089
Object database management systems: Concepts and features
[PB90-216813] N90-29243
Automated information system life-cycle management manual
[PB90-219288] N90-29244
International aircraft operator data base master requirements and implementation plan
[DOT/FAA/CT-90/17] N90-29247
Crossroads of Information Technology Standards
[PB90-239732] N90-29251
Optical storage technology
[AD-A224028] N90-29254
Time-based competition for competitive advantage: An information technology perspective
[AD-A224474] N90-29255
INFORMATION THEORY
A Boltzmann machine for the organization of intelligent machines N90-29040
INFRARED ASTRONOMY
Quantifying the FIR interaction enhancement in paired galaxies
[DE90-627485] N90-29281
INFRARED ASTRONOMY SATELLITE
An infrared sky model based on the IRAS point source data
[NASA-CR-177526] N90-29265
INFRARED IMAGERY
Recognition of infrared images. Part 3: The effect of image processing with a size-contrast box filter on observation performance
[IZF-1989-39] N90-29182
INFRARED RADIATION
Transient cooling of a hot surface by droplets evaporation
[PB90-227968] N90-28799
Star formation and the distribution of HI and infrared emission in M51
[NASA-CR-186928] N90-29262
On the infrared behaviour of some non-Minkowskian quantum fields N90-29273
INFRARED SPECTRA
An infrared sky model based on the IRAS point source data
[NASA-CR-177526] N90-29265
INFRARED SPECTROSCOPY
Infrared spectroscopic measurements on planetary atmospheric gases N90-29283
INJECTION
Effect of vortex circulation on injectant from a single film-cooling hole and a row of film-cooling holes in a turbulent boundary layer. Part 2: Injection beneath the vortex upwash
[AD-A223894] N90-28818
Tunable CW single-frequency source for injection seeding 2-micrometer lasers
[AD-A223979] N90-28834
Effects and tolerances of injection jitter in the SLC and future linear colliders
[DE90-014805] N90-29179
INJECTION LASERS
Tunable CW single-frequency source for injection seeding 2-micrometer lasers
[AD-A223979] N90-28834
INJECTION MOLDING
Improved silicon carbide for advanced heat engines
[NASA-CR-182186] N90-28735
INJECTORS
Injector element characterization methodology N90-28634
INJURIES
Helicopter aircrew helmets and head injury: A protective effect
[AD-A223024] N90-29080
INLET NOZZLES
Computer code for the prediction of nozzle admittance N90-28630
INLET TEMPERATURE
High/variable mixture ratio oxygen/hydrogen engines N90-28637
INSPECTION
Guidelines for pressure vessel safety assessment
[PB90-219619] N90-28749
An improved method for choosing sampling points for the inspection of complex surfaces in a computer-aided manufacturing environment N90-29093
INSTALLING
In-flight investigation of shuttle tile pressure orifice installations
[NASA-TM-4219] N90-28820
INSTRUMENT APPROACH
Dallas/Forth Worth simulation. Phase 2: Triple simultaneous parallel Instrument Landing System (ILS) approaches (turbojets)
[DOT/FAA/CT-90/2] N90-28509
INSTRUMENT ERRORS
Rheometer strain and strain-rate errors
[DE90-013845] N90-28824
INSTRUMENT LANDING SYSTEMS
Dallas/Forth Worth simulation. Phase 2: Triple simultaneous parallel Instrument Landing System (ILS) approaches (turbojets)
[DOT/FAA/CT-90/2] N90-28509
INSULATORS
Parity violation and superconductivity in doped Mott insulators
[DE90-627493] N90-29217
INSULIN
Insulin and insulin-like growth factor-1 induce pronounced hypertrophy of skeletal myofibers in tissue culture
[NASA-CR-187026] N90-28960
INTAKE SYSTEMS
Flow coupling between a rotor and a stator in turbomachinery
[AD-A223882] N90-28572
Numerical simulations of flowfields in a central-dump ramjet combustor. 3: Effects of chemistry
[AD-A224145] N90-28573
The equipment for mass flow measurements in the low-speed wind tunnel at DFVLR in Brunswick (Federal Republic of Germany)
[ESA-TT-1125] N90-28585
Development of advanced combustion technology for medium and high speed natural gas engines
[PB90-198565] N90-28836
INTEGERS
The center of the enveloping algebra of the semidirect product of the Heisenberg lie algebra h(sub n) and a reductive Lie algebra S the rank of which is equal to 1 or 2
[DE90-627155] N90-29133
INTEGRALS
Product integration rules at Clenshaw-Curtis and related points: A robust implementation
[DE90-627158] N90-29106
Weighted norm inequalities for Riemann-Liouville fractional integral
[DE90-627153] N90-29132
Asymptotics of Laplace-Dirichlet integrals
[DE90-627165] N90-29137
INTEGRATED OPTICS
Application of integrated optical components in optical fiber communication
[FEL-89-B252] N90-29183
INTELLIGIBILITY
Comparison of speech intelligibility in cockpit noise using SPH-4 flight helmet with and without active noise reduction
[NASA-CR-177564] N90-28510
INTERFACES
UV-induced degradation of the Si-SiO2 interface: Applications to the point contact solar cell
[DE90-013843] N90-28898
INTERFACIAL ENERGY
Interface formation and percusory dynamics
[AD-A224126] N90-29223
INTERFACIAL TENSION
Design of a CO2 laser power control system for a Spacelab microgravity experiment
[NASA-TM-103112] N90-28833
INTERFERENCE DRAG
Sting-support interference on afterbody drag at transonic speeds
[NAL-TM-EA-8902] N90-28492
INTERFEROMETERS
Tropospheric wind profiling using radar interferometry: A feasibility study of a compact mobile system
[PB90-217068] N90-28939
INTERFEROMETRY
Tropospheric wind profiling using radar interferometry: A feasibility study of a compact mobile system
[PB90-217068] N90-28939
INTERMETALLICS
Antiferromagnetism and enhanced heat in CeM2Sn (M = Ni, Ir, Cu, Rh, Pd, and Pt
[DE90-014924] N90-29206
INTERNAL COMBUSTION ENGINES
Results from the fourth year of operation of the Federal Methanol Fleet at Lawrence Berkeley Laboratory
[DE90-014741] N90-28743
Smart microsensors for high temperature applications, phase 1
[AD-A224151] N90-28828
Development of advanced combustion technology for medium and high speed natural gas engines
[PB90-198565] N90-28836
INTERNAL ENERGY
Thermophysical properties of Helium-4 from 0.8 to 1500 K with pressures to 2000 MPa
[NASA-CR-186992] N90-28681
INTERNATIONAL COOPERATION
Goverment's role in standards-related activities: Analysis of comments
[PB90-215534] N90-29239
INTERPOLATION
LINTERP: A numerical algorithm for interpolating quadrilateral and hexahedral meshes
[DE90-014417] N90-29090
INTERSTELLAR CHEMISTRY
The ionization structure of planetary nebulae 10: NGC 2392
[NASA-CR-186960] N90-29274
INTERSTELLAR MATTER
Star formation and the distribution of HI and infrared emission in M51
[NASA-CR-186928] N90-29262
Near-infrared speckle observations of T Tauri stars and a multi-wavelength study of the prototype star T Tauri N90-29264
A plasma diagnostic study of two wind-blown shell nebulae: NGC 7635 and NGC 2359 N90-29271
INVARIANCE
Asymptotic behavior of solutions of diffusion-like partial differential equations invariant to a family of affine groups
[DE90-014792] N90-29130
INVARIANT IMBEDDINGS
Geometric theory for infinite dimensional systems
[ETN-90-96922] N90-29144

INVENTORIES
World jet airplane inventory at year-end 1989
[PB90-207218] N90-28489
INVISCID FLOW
Do inviscid vortex sheets roll-up
[PD-CF-9010] N90-28491
Regular and chaotic motion of uniform elliptical vortices in external linear time dependent velocity fields N90-28497
An investigation of the steady and unsteady near wake and its effect on a laminar boundary layer N90-28794
Multigrid for hypersonic inviscid flows
[NASA-CR-182082] N90-29125
ION ACCELERATORS
Ion divergence and the stability of magnetically insulated diodes
[DE90-014585] N90-28777
ION BEAMS
Ion divergence and the stability of magnetically insulated diodes
[DE90-014585] N90-28777
Mossbauer Effect applications using intense radioactive ion beams
[DE90-014981] N90-29175
PBFA 2 applied B ion diode beam characteristics at high voltages
[DE90-014419] N90-29190
ION CURRENTS
Electronic conduction in molten cryolite saturated with alumina
[DE90-015090] N90-29211
ION IMPLANTATION
Fretting wear and fretting fatigue at temperatures up to 600 C N90-28706
Surface property improvement in titanium alloy gas turbine components through ion implantation N90-28713
Mossbauer Effect applications using intense radioactive ion beams
[DE90-014981] N90-29175
ION SCATTERING
Structure of metal overlayers by low energy alkali ion scattering: Cu/Ru(0001) and Sn/Pt(111)
[DE90-014453] N90-28716
ION SOURCES
Ion divergence and the stability of magnetically insulated diodes
[DE90-014585] N90-28777
PBFA 2 applied B ion diode beam characteristics at high voltages
[DE90-014419] N90-29190
IONIC COLLISIONS
Correlated charge changing ion-atom collisions
[DE90-014662] N90-29171
IONIZATION
Pulsations of the white dwarf component in V471 tauri-like binaries
[DE90-014921] N90-29267
The ionization structure of planetary nebulae 10: NGC 2392
[NASA-CR-186960] N90-29274
IONS
New resonantly photo-pumped x ray laser scheme
[DE90-015044] N90-28831
IRIDIUM
Antiferromagnetism and enhanced heat in CeM2Sn (M = Ni, Ir, Cu, Rh, Pd, and Pt
[DE90-014924] N90-29206
IRON
Effects of Al substitution by Fe in CeAl2
[DE90-627843] N90-28726
Helium generation in fusion reactor materials
[DE90-013005] N90-29172
IRON ISOTOPES
Dynamical information for Fe doped YBa2Cu3O7 superconducting oxides obtained from high temperature Moessbauer studies
[DE90-627871] N90-29218
IRRADIATION
Radiation-curable prepreg composites
[DE90-629740] N90-28674
Density changes of generation 1.5 and 2.0 copper alloys irradiated at 411 to 414 C and 529 C in FFTF-MOTA
[DE90-015291] N90-28724
Transient annealing characterization of irradiated MOSFETS
[AD-A223877] N90-29220
ISING MODEL
Systematic approach to critical phenomena by the extended variational method and coherent-anomaly method
[DE90-627320] N90-29165
ISOTOPE SEPARATION
Enrichment services for chromium isotopes for the GALLEX (gallium experiment) international collaboration experiment on solar neutrino flux
[DE90-014300] N90-29285
ISOTOPIC LABELING
Geothermal fluid genesis in the Great Basin
[DE90-014436] N90-28884
ISOTROPY
Dissipation of mechanical work and temperature rise in AS4/PEEK thermoplastic composite
[NASA-CR-186893] N90-28678
ITERATION
Peak analysis in gas chromatography and the development of new stationary phases for anion chromatography
[DE90-014428] N90-28687
Piecewise linear models of processor utilization
[DE90-014774] N90-29115
ITERATIVE SOLUTION
An asymptotically induced domain decomposition method for parabolic boundary layer problems
[DE90-014620] N90-28804
Error detection and control for nonlinear shell analysis
[NASA-TM-102723] N90-28877
Solution of the Stokes system by boundary integral equations and fixed point iterative schemes
[DE90-627166] N90-29138

J

JAPAN
Japanese molecular biology 1990: An update
[PB90-188707] N90-28958
JET AIRCRAFT
World jet airplane inventory at year-end 1989
[PB90-207218] N90-28489
Predicting F/A-18 fleet replacement squadron performance using an automated battery of performance-based tests
[AD-A223899] N90-28543
Engineering and the advancement of human welfare. Ten outstanding achievements 1964-1989
[ISBN-0-309-04185-6] N90-29297
JET EXHAUST
Numerical resolution of Navier-Stokes equations using several turbulence models and applications on turbomachines
[ETN-90-97478] N90-28806
JET PUMPS
An experimental investigation of a single and multiphase confined coaxial jet N90-28796
JET THRUST
High power arcjet
[NASA-CR-183066] N90-28658
JOINTS (JUNCTIONS)
Flight motor set 360L008 (STS-32R). Volume 1: System overview
[NASA-CR-184010] N90-28609
Solutions to the frictional dynamics problem and the reciprocal variable feedback methodology for design and control of robot mechanisms N90-28846
JOSEPHSON JUNCTIONS
Dynamical properties of two-dimensional Josephson junction arrays
[AD-A223965] N90-29221
JOURNAL BEARINGS
Current research in cavitating fluid films
[NASA-TM-103184] N90-28791

K

K-EPSILON TURBULENCE MODEL
Development of comprehensive numerical schemes for predicting evaporating gas-droplets flow processes of a liquid-fueled combustor
[NASA-CR-187018] N90-28693
Vortice-propeller interaction
[LIMSI-89-9] N90-28809
KAPTON (TRADEMARK)
Evaluations of new polyimide films for flexible circuit applications at EG and G Mound Applied Technologies
[DE90-014117] N90-28731
KEVLAR (TRADEMARK)
ARALL (ARamid ALuminum Laminate), a literature survey
[FOA-C-20782-2.5] N90-28671
Behavior of aramid/epoxy wounded tubes under uniaxial and biaxial loading
[ETCA-89-R-150] N90-28873
KINEMATICS
A theoretical investigation into the inelastic behavior of metal-matrix composites
[AD-A223973] N90-28677
Motion coordination for mobile robots in unstructured environments
[PB90-199498] N90-28837
Evaluation of the STM4-120 kinematic Stirling engine
[DE90-013836] N90-28897
A new approach to global control of redundant manipulators N90-29002
Kinematic functions for the 7 DOF robotics research arm N90-29003
Cartesian control of redundant robots N90-29004
Kinematics, controls, and path planning results for a redundant manipulator N90-29005
Computational neural learning formalisms for manipulator inverse kinematics N90-29030
Grasp planning under uncertainty N90-29041
Characterization and control of self-motions in redundant manipulators N90-29045
Multiple cooperating manipulators: The case of kinematically redundant arms N90-29046
Reflexive obstacle avoidance for kinematically-redundant manipulators N90-29047
On the simulation of space based manipulators with contact N90-29056
Parallel algorithms for computation of the manipulator inertia matrix N90-29072
KINETIC ENERGY
On the dynamics of severe thunderstorms
[DE90-627922] N90-28950
KINETIC EQUATIONS
Applied mathematics of transport theory
[DE90-014627] N90-29128
KINETIC FRICTION
Blade tip rubbing stress prediction N90-28615
KINETICS
Numerical and analytical study of nonlinear bifurcations associated with the morphological stability of two-dimensional single crystals
[PB90-209594] N90-29200
KLYSTRONS
RF power generation for future linear colliders
[DE90-014804] N90-29178
KNOWLEDGE BASES (ARTIFICIAL INTELLIGENCE)
Techniques and potential capabilities of multi-resolutional information (knowledge) processing N90-29062
Perceptual telerobotics N90-29063
Graph structure model
[DE90-014930] N90-29097
Model authoring system for fail safe analysis
[NASA-CR-4317] N90-29142
A knowledge-based system design/information tool
[NASA-CR-4316] N90-29143
KNOWLEDGE REPRESENTATION
Multiresolutional models of uncertainty generation and reduction N90-29043
A survey of planning and scheduling research at the NASA Ames Research Center N90-29076
Integrating planning, execution, and learning N90-29079
Designing intelligent computer aided instruction systems with integrated knowledge representation schemes
[AD-A224178] N90-29113
KONDO EFFECT
Effects of Al substitution by Fe in CeAl2
[DE90-627843] N90-28726
Evidence for a coherence gap in Ce3Bi4Pt3
[DE90-014925] N90-29207

L

LAGRANGE COORDINATES
On the use of Lagrangian variables in descriptions of unsteady boundary-layer separation
[NASA-CR-182071] N90-28789
Deterministic transport on an arbitrarily-connected grid
[DE90-015148] N90-29131
LAMINAR BOUNDARY LAYER
An investigation of the steady and unsteady near wake and its effect on a laminar boundary layer N90-28794
LAMINAR HEAT TRANSFER
Gas-film flow in tubes
[DE90-011528] N90-28793
LAMINATES
Mechanical behavior of thick, curved, laminated composites N90-28664
Inelastic analysis of laminated composites N90-28869
ARALL (ARamid ALuminum Laminate), a literature survey
[FOA-C-20782-2.5] N90-28671
LANDING SIMULATION
Vibration responses of two house structures during the Edwards Air Force Base phase of the national sonic boom program
[NASA-CR-182089] N90-29169

LANGUAGES
Efficiency and effectiveness of deep structure-based subject indexing languages: PRECIS vs. DSIS N90-29248
LARGE SPACE STRUCTURES
The dynamics and control of large flexible space structures - 13
[NASA-CR-186930] N90-28591
Transformational part-count in layered octahedral-tetrahedral truss configurations
[NASA-TM-102635] N90-28598
LASER APPLICATIONS
Engineering and the advancement of human welfare. Ten outstanding achievements 1964-1989
[ISBN-0-309-04185-6] N90-29297
LASER BEAMS
Velocity Interferometer System for Any Reflector (VISAR): Displacement mode data reduction
[DE90-015027] N90-29184
LASER DOPPLER VELOCIMETERS
The effects of grid-generated turbulence on flat and concave turbulent boundary layers N90-28797
LASER HEATING
Unipolar arcing on the cathode surface of a high voltage diode
[AD-A224122] N90-28787
LASER INDUCED FLUORESCENCE
A study of catalysts and mechanisms in synthesis reactions
[DE90-015064] N90-28691
Study of the radical OH in a high pressure flame by resonant DRASC
[ONERA-RF-57/7131-PY] N90-28692
Studies of vortex interactions
[AD-A223864] N90-28817
LASER INTERFEROMETRY
Velocity Interferometer System for Any Reflector (VISAR): Displacement mode data reduction
[DE90-015027] N90-29184
LASER OUTPUTS
Design of a CO2 laser power control system for a Spacelab microgravity experiment
[NASA-TM-103112] N90-28833
LASER PLASMA INTERACTIONS
Unipolar arcing on the cathode surface of a high voltage diode
[AD-A224122] N90-28787
Studies of central interactions of Si ions at 14.5 x A GeV/c in Au and Cu
[DE90-015095] N90-29195
LASER PLASMAS
Unipolar arcing on the cathode surface of a high voltage diode
[AD-A224122] N90-28787
Studies of central interactions of Si ions at 14.5 x A GeV/c in Au and Cu
[DE90-015095] N90-29195
LASER RANGE FINDERS
HERMIES-3: A step toward autonomous mobility, manipulation, and perception N90-29065
LASER SPECTROMETERS
A laser spectrometer and wavemeter for pulsed lasers
[NASA-CR-181731] N90-28832
Infrared spectroscopic measurements on planetary atmospheric gases N90-29283
LASERS
Experimental investigations on the stability and vorticity of the vortex breakdown phenomenon above delta wings, measured by the ultrasonic laser method
[ESA-TT-1079] N90-28498
Wind lidar for BEST
[CNES-NT-125] N90-28947
A laser tracking dynamic robot metrology instrument N90-29021
LATERAL STABILITY
The effects of foreplanes on the static and dynamic characteristics of a combat aircraft model N90-28520
LATITUDE
Computer program for converting rectangular coordinates to latitude-longitude coordinates
[PB90-231796] N90-28883
LATTICE PARAMETERS
Synthesis and structural chemistry of Au(III)-substituted Ba2YCu3O(7-delta)
[NASA-TM-103292] N90-28696
LAUNCH VEHICLES
Liquid Rocket Booster (LRB) for the Space Transportation System (STS) systems study. Appendix F: Performance and trajectory for ALS/LRB launch vehicles
[NASA-CR-183792-APP-F] N90-28606
Summary of booster propulsion/vehicle impact study results N90-28635
Operational cost drivers N90-28636
LEADING EDGES
Genesis of bow echoes: A rear-inflow induced meso-convective structure
[PB90-209776] N90-28926
LEAKAGE
Study and analysis of leaking underground storage tank remediation techniques incorporated in states in EPA Region 6
[PB90-214834] N90-28847
LEARNING
Selective learning algorithm for certain types of learning failure in multilayer perceptrons
[AD-A223982] N90-28998
Designing intelligent computer aided instruction systems with integrated knowledge representation schemes
[AD-A224178] N90-29113
LEARNING CURVES
Extensions to the learning curve: An analysis of factors influence unit cost of weapon systems
[AD-A224119] N90-29256
LEARNING THEORY
A user modelling approach for computer-based critiquing
[AD-A224042] N90-29088
LEAST SQUARES METHOD
Recursive least-squares learning algorithms for neural networks
[DE90-014926] N90-29096
LESIONS
DNA damage and repair in human skin: Pathways and questions
[DE90-015126] N90-28966
LIAPUNOV FUNCTIONS
Dissipative quantum maps
[DE90-627179] N90-29227
Quantum chaos and dissipation: Lyapunov exponents
[DE90-627180] N90-29228
LIBRARIES
Digital geometric correction for MSS-LANDSAT imagery
[INPE-4627-PRE/1345] N90-28886
LIE GROUPS
The center of the enveloping algebra of the semidirect product of the Heisenberg lie algebra h(sub n) and a reductive Lie algebra S the rank of which is equal to 1 or 2
[DE90-627155] N90-29133
The combinatorics computation for Casimir operators of the symplectic Lie algebra and the application for determining the center of the enveloping algebra of a semidirect product
[DE90-627161] N90-29136
LIFE (DURABILITY)
Damage tolerance of the fighter aircraft 37 Viggen. Part 1: Analytical assessment
[FFA-TN-1990-12-PT-1] N90-28538
Damage tolerance of the fighter aircraft 37 Viggen. Part 2: Experimental verification
[FFA-TN-1990-13-PT-2] N90-28539
Development of an integrated BEM for hot fluid-structure interaction N90-28617
Structural response of SSME turbine blade airfoils N90-28649
Thermal analysis of thermal barrier coatings in a high heat flux environment N90-28652
Application of advanced coating techniques to rocket engine components N90-28654
Ceramic matrix composites in simulated SSME environments N90-28655
Automated information system life-cycle management manual
[PB90-219288] N90-29244
LIFE CYCLE COSTS
Life cycle cost in the conceptual design of subsonic commercial aircraft, volumes 1 and 2 N90-28535
Operational cost drivers N90-28636
LIFE SUPPORT SYSTEMS
Automated simulation as part of a design workstation
[NASA-TM-102852] N90-29083
LIFT
Study of the ground effects in the CEAT aerohydrodynamic tunnel: Using the results N90-28530
LIFTING BODIES
Aerodynamics of bodies in shear flow N90-28496
LIGHT BEAMS
Energy transmission by means of coherent quasi-mono-chromatic light beams N90-29163
LIGHT SCATTERING
The spatial scalar structure of premixed turbulent stagnation point flames
[DE90-014189] N90-28686
Near-angle scattering and binary optics
[AD-A224140] N90-29186
LIGHT SOURCES
Status of the advanced light source
[DE90-015636] N90-29185
LIGHTNING
Study of the relationships between radar structure and the electrical activity of clouds
[ETN-90-97488] N90-28946
Mesoscale Lightning Experiment (MLE): A view of lightning as seen from space during the STS-26 mission
[NASA-TM-103513] N90-28951
LIMITERS (FUSION REACTORS)
Temperature-gradient instability induced by conducting end walls
[DE90-014334] N90-29188
LINEAR ACCELERATORS
Characterization of electron flow in positive-polarity linear-induction accelerators
[DE90-014998] N90-29177
RF power generation for future linear colliders
[DE90-014804] N90-29178
Effects and tolerances of injection jitter in the SLC and future linear colliders
[DE90-014805] N90-29179
LINEAR ARRAYS
A laser spectrometer and wavemeter for pulsed lasers
[NASA-CR-181731] N90-28832
Block Lanczos algorithm
[AD-A224011] N90-29111
LINEAR EQUATIONS
Parallel algorithms for computation of the manipulator inertia matrix N90-29072
LINEAR POLARIZATION
Robust controller design by contraction of a pole region
[ESA-TT-1042] N90-29118
LINEAR PROGRAMMING
Investigation of maximum achievable body torque for a walking machine with friction cone constraints
[PB90-203175] N90-28838
Workshop on Neural Networks
[DE90-014794] N90-29120
LINEAR QUADRATIC REGULATOR
An LQR controller design approach for a Large Gap Magnetic Suspension System (LGMSS)
[NASA-TM-101606] N90-28751
LINGUISTICS
Efficiency and effectiveness of deep structure-based subject indexing languages: PRECIS vs. DSIS N90-29248
Statement of research objectives and summary of research efforts
[RLE-PR-132] N90-29295
LININGS
Energy efficient engine pin fin and ceramic composite segmented liner combustor sector rig test report
[NASA-CR-179534] N90-28567
Development of improved self lubricating cages for SSME HPOTP bearings N90-28623
Cage stability analysis for SSME HPOTP bearings N90-28625
LIOUVILLE EQUATIONS
Weighted norm inequalities for Riemann-Liouville fractional integral
[DE90-627153] N90-29132
LIQUID CRYSTALS
Use of liquid crystals for qualitative and quantitative 2-D studies of transition and skin friction
[RAE-TM-AERO-2159] N90-28800
LIQUID FUELS
Ignition and combustion of liquid propellants
[AD-A224150] N90-28746
LIQUID HELIUM 2
Thermophysical properties of Helium-4 from 0.8 to 1500 K with pressures to 2000 MPa
[NASA-CR-186992] N90-28681
LIQUID METALS
Thermodynamics and structure of liquid alkali metals from the charged-hard-sphere reference fluid
[DE90-627792] N90-28725
LIQUID NITROGEN
Pool boiling from rotating and stationary spheres in liquid nitrogen N90-28621
Variable mixture ratio performance through nitrogen augmentation N90-28639
LIQUID OXYGEN
Rocketdyne LOX bearing tester program N90-28626
Oxygen/methane combustion stability investigation N90-28628
LIQUID PHASES
Ignition and combustion of liquid propellants
[AD-A224150] N90-28746
An experimental investigation of a single and multiphase confined coaxial jet N90-28796
LIQUID PROPELLANT ROCKET ENGINES
Liquid Rocket Booster (LRB) for the Space Transportation System (STS) systems study. Volume 1: Executive summary
[NASA-CR-183822] N90-28599

Advanced Earth-to-Orbit Propulsion Technology 1988, volume 1
[NASA-CP-3012-VOL-1] N90-28611
Spectroscopic study of combustion diagnostics on hydroxyl radicals
[NASA-CR-186998] N90-28694

LIQUID ROCKET PROPELLANTS
Liquid Rocket Booster (LRB) for the Space Transportation System (STS) systems study, volume 2
[NASA-CR-183786] N90-28600
Liquid Rocket Booster (LRB) for the Space Transportation System (STS) systems study. Appendix B: Liquid rocket booster acoustic and thermal environments
[NASA-CR-183788-APP-B] N90-28602
Liquid Rocket Booster (LRB) for the Space Transportation System (STS) systems study. Appendix F: Performance and trajectory for ALS/LRB launch vehicles
[NASA-CR-183792-APP-F] N90-28606
Advanced Earth-to-Orbit Propulsion Technology 1988, volume 1
[NASA-CP-3012-VOL-1] N90-28611
High energy-density liquid rocket fuel performance
[NASA-CR-185279] N90-28742

LITHIUM ALLOYS
High temperature oxidation of Al-Li alloys N90-28705

LITHIUM HYDRIDES
A new low density, high porosity lithium hydride-beryllium hydride foam
[DE90-015150] N90-28739

LOAD TESTS
Behavior of aramid/epoxy wounded tubes under uniaxial and biaxial loading
[ETCA-89-R-150] N90-28673

LOADS (FORCES)
The effect of rapid spoiler deployment on the transient forces on an aerofoil N90-28527
Energy Efficient Engine high pressure turbine component test performance report
[NASA-CR-168289] N90-28553
Liquid Rocket Booster (LRB) for the Space Transportation System (STS) systems study. Appendix E: Pressure-fed booster test bed for the liquid rocket booster study
[NASA-CR-183791-APP-E] N90-28605
Probabilistic structural analysis methods development for SSME N90-28616
Mechanical behavior of thick, curved, laminated composites N90-28664
Target acquisition under load factors: Advantages and disadvantages of a helmet mounted sight N90-28983
Variable force and visual feedback effects on teleoperator man/machine performance N90-29008
Measurement of hand dynamics in a microsurgery environment: Preliminary data in the design of a bimanual telemicro-operation test bed N90-29010
Multiple cooperating manipulators: The case of kinematically redundant arms N90-29046

LOCOMOTION
Periodic gaits for the CMU ambler N90-29027
First results in terrain mapping for a roving planetary explorer N90-29066

LONG TERM EFFECTS
Development of testing and analysis methodology to assess the long term durability of polymeric composites at high temperatures
[NASA-TM-102714] N90-28871

LONGITUDE
Computer program for converting rectangular coordinates to latitude-longitude coordinates
[PB90-231796] N90-28883

LOSSES
Regulation of erythropoiesis in rats during space flight
[NASA-CR-177537] N90-29086

LOW CARBON STEELS
Preliminary exposure study to determine the effects of acid deposition on coated steel substrates
[PB90-201799] N90-28715

LOW DENSITY MATERIALS
A new low density, high porosity lithium hydride-beryllium hydride foam
[DE90-015150] N90-28739

LOW GRAVITY MANUFACTURING
Microgravity science and applications: Apparatus and facilities
[NASA-TM-101892] N90-28588

LOW NOISE
Design and realization of a two stage C-band low noise amplifier
[FEL-89-B265] N90-28783

LOW PRESSURE
NASA/GE Energy Efficient Engine low pressure turbine scaled test vehicle performance report
[NASA-CR-168290] N90-28563

LOW SPEED
Effects of canard position on the aerodynamic characteristics of a close-coupled canard configuration at low speed N90-28519

LOW SPEED WIND TUNNELS
Innovative control concepts and component integration for a generic supercruise fighter N90-28521
The equipment for mass flow measurements in the low-speed wind tunnel at DFVLR in Brunswick (Federal Republic of Germany)
[ESA-TT-1125] N90-28585
A microprocessor controlled strain gauge calibration module
[AR-005-579] N90-28821

LOW TEMPERATURE
Mode competition in the quasioptical gyrotron
[AD-A222181] N90-28823

LOWER BODY NEGATIVE PRESSURE
Cardiovascular deconditioning of cosmonauts: Role, importance and applications of the lower body negative pressure
[ETN-90-97507] N90-28964
Joint US/USSR study: Comparison of effects of horizontal and head-down bed rest
[NASA-TP-3037] N90-28965

LUBRICANTS
Use of electron spectroscopies in the tribological evaluation of diamond films
[DE90-014421] N90-28848

LUBRICATION
Pratt and Whitney cryogenic turbopump bearing experience N90-28624
Current research in cavitating fluid films
[NASA-TM-103184] N90-28791

LUMINOSITY
Pulsations of B star models by an opacity mechanism
[DE90-014923] N90-29279

LUNAR LANDING
Engineering and the advancement of human welfare. Ten outstanding achievements 1964-1989
[ISBN-0-309-04185-6] N90-29297

M

MACHINE LEARNING
Multi-layer neural networks for robot control N90-29031
A Boltzmann machine for the organization of intelligent machines N90-29040
Multiresolutional models of uncertainty generation and reduction N90-29043
How do robots take two parts apart N90-29061
A survey of planning and scheduling research at the NASA Ames Research Center N90-29076
Learning in stochastic neural networks for constraint satisfaction problems N90-29078
Integrating planning, execution, and learning N90-29079
Recursive least-squares learning algorithms for neural networks
[DE90-014926] N90-29096

MACHINING
Quality function deployment as a mechanism for process characterization and control
[DE90-014755] N90-28857

MAGELLAN PROJECT (NASA)
The Magellan Venus explorer's guide
[NASA-CR-186968] N90-28592

MAGELLAN SPACECRAFT (NASA)
The Magellan Venus explorer's guide
[NASA-CR-186968] N90-28592

MAGELLANIC CLOUDS
Nova LMC (Large Magellanic Cloud) 1990 no. 1: The first extragalactic neon nova
[NASA-CR-180409] N90-29276

MAGNESIUM ALLOYS
Behavior of Al-Mg alloys in hot working and superplasticity
[DE90-015193] N90-28723

MAGNETIC COMPRESSION
Stellarator status, 1989
[DE90-014791] N90-29192

MAGNETIC CONTROL
Ignition and burn control characteristics of thermonuclear plasmas
[DE90-015385] N90-29197

MAGNETIC CORES
Modeling tape-wound magnetic switches
[DE90-015121] N90-28782

MAGNETIC FIELD CONFIGURATIONS
Formation of magnetic islands due to field perturbations in toroidal stellarator configurations
[DE90-014789] N90-29191

MAGNETIC FIELDS
Further studies of 60 Hz exposure effects on human function
[DE90-014377] N90-28962
Physics of the L to H transition in DIII-D
[DE90-014120] N90-29187
Electron microscopy of transition-metal doped BiCaSrCuO
[DE90-014184] N90-29202
Vlasov-Maxwell equilibria of solar coronal loops
[DE90-015025] N90-29289

MAGNETIC MATERIALS
Optical storage technology
[AD-A224028] N90-29254

MAGNETIC MEASUREMENT
Operation and calibration of MRL permeameter for measurement of DC magnetic properties of materials under stress
[MRL-TN-574] N90-28863

MAGNETIC PERMEABILITY
Systematic approach to critical phenomena by the extended variational method and coherent-anomaly method
[DE90-627320] N90-29165

MAGNETIC PROPERTIES
Surface and defect excitations in covalently bonded solids
[AD-A221995] N90-28682
Operation and calibration of MRL permeameter for measurement of DC magnetic properties of materials under stress
[MRL-TN-574] N90-28863
Antiferromagnetism and enhanced heat in CeM2Sn (M = Ni, Ir, Cu, Rh, Pd, and Pt
[DE90-014924] N90-29206

MAGNETIC SHIELDING
Analysis of three-dimensional eddy current field. Application to calculation of magnetic screening effect of the damper system in a model superconducting generator
[DE90-507869] N90-28779

MAGNETIC SIGNATURES
NASA Marshall Space Flight Center Solar Observatory report, January - June 1990
[NASA-TM-103512] N90-29268

MAGNETIC SUSPENSION
An LQR controller design approach for a Large Gap Magnetic Suspension System (LGMSS)
[NASA-TM-101606] N90-28751

MAGNETIC SWITCHING
Investigations into the use of dielectric coatings in magnetic switches
[DE90-014331] N90-28776
Modeling tape-wound magnetic switches
[DE90-015121] N90-28782

MAGNETIZATION
Effects of Al substitution by Fe in CeAl2
[DE90-627843] N90-28726
Modeling tape-wound magnetic switches
[DE90-015121] N90-28782

MAGNETOACOUSTIC WAVES
Theoretical studies of proton beams in solar flare loops N90-29286

MAGNETOACOUSTICS
Electron acoustic and magnetoacoustic modes in a magnetized beam plasma system
[DE90-627473] N90-29199

MAGNETOHYDRODYNAMIC GENERATORS
Effects of friction and end losses on MHD thruster efficiency
[DE90-013673] N90-28608

MAGNETOHYDRODYNAMIC STABILITY
Temperature-gradient instability induced by conducting end walls
[DE90-014334] N90-29188
Nonlinear tearing mode: Rutherford regime and global characteristics
[DE90-015003] N90-29193
Resonant MHD modes with toroidal coupling
[DE90-015185] N90-29196
TSC (Tokamak Simulation Code) simulations of Alcator C-MOD discharges 3: Study of axisymmetric stability
[DE90-015386] N90-29198

MAGNETOHYDRODYNAMIC WAVES
Theoretical studies of proton beams in solar flare loops N90-29286
Alfven wave solitons and solar intermediate drift bursts
[MPE-PREPRINT-173] N90-29287

MAGNETOHYDRODYNAMICS
Resonant MHD modes with toroidal coupling
[DE90-015185] N90-29196
Solar oscillation frequency and solar neutrino predictions
[DE90-014918] N90-29288

Vlasov-Maxwell equilibria of solar coronal loops
[DE90-015025] N90-29289

MAGNETOSTRICTION
Magnetostrictive direct drive motors
[NASA-CR-186895] N90-28855

MAGNETRONS
Measurement of gravitational acceleration of antimatter
[DE90-627464] N90-29233

MAINTAINABILITY
STOVL fighter propulsion reliability, maintainability, and supportability characterization
[AD-A224221] N90-28574
Reliability analysis of maintained structural system vulnerable to fatigue and fracture N90-28868

MAINTENANCE
Development and testing of rapid repair methods for war damaged runways
[AD-A223970] N90-28586
Results from the fourth year of operation of the Federal Methanol Fleet at Lawrence Berkeley Laboratory
[DE90-014741] N90-28743
Reliability analysis of maintained structural system vulnerable to fatigue and fracture N90-28868
The NASA/OAST telerobot testbed architecture N90-29016

MAN ENVIRONMENT INTERACTIONS
Natural and anthropogenic climate change
[DE90-015528] N90-28923

MAN MACHINE SYSTEMS
A conceptual framework for fighter flight control systems
[PD-CF-9009] N90-28577
Experiments in the dynamic and strategic control of cooperating manipulators N90-28845
Techniques and applications for binaural sound manipulation in human-machine interfaces
[NASA-TM-102279] N90-28996
Proceedings of the NASA Conference on Space Telerobotics, volume 1
[NASA-CR-186856] N90-29000
Adjustable impedance, force feedback and command language aids for telerobotics (parts 1-4 of an 8-part MIT progress report) N90-29007
Variable force and visual feedback effects on teleoperator man/machine performance N90-29008
Teleoperator comfort and psychometric stability: Criteria for limiting master-controller forces of operation and feedback during telemanipulation N90-29009
Human factors model concerning the man-machine interface of mining crewstations N90-29011
The NASA/OAST telerobot testbed architecture N90-29016
Proceedings of the NASA Conference on Space Telerobotics, volume 2
[NASA-CR-186857] N90-29044
The JPL telerobot operator control station. Part 1: Hardware N90-29049
The JPL telerobot operator control station. Part 2: Software N90-29050
Implementation and design of a teleoperation system based on a VMEBUS/68020 pipelined architecture N90-29053
Human machine interaction via the transfer of power and information signals N90-29054

MAN-COMPUTER INTERFACE
A user modelling approach for computer-based critiquing
[AD-A224042] N90-29088

MANAGEMENT
Airport capacity enhancement plan 1989
[PB90-197997] N90-28507

MANAGEMENT INFORMATION SYSTEMS
Optical storage technology
[AD-A224028] N90-29254

MANAGEMENT METHODS
Towards a future cockpit: The prototyping and pilot integration of the Mission Management Aid (MMA) N90-28979
Information management directions: The integration challenge
[PB90-219866] N90-29245
Transferring building energy technologies by linking government and private-sector programs
[DE90-000346] N90-29258

MANAGEMENT PLANNING
Grasp planning under uncertainty N90-29041
The effects of management support on the successful implementation of group decision support systems
[AD-A224473] N90-29241
International aircraft operator data base master requirements and implementation plan
[DOT/FAA/CT-90/17] N90-29247

MANAGEMENT SYSTEMS
The effects of management support on the successful implementation of group decision support systems
[AD-A224473] N90-29241
Automated information system life-cycle management manual
[PB90-219288] N90-29244

MANEUVERABILITY
Combat aircraft control requirements for agility N90-28517

MANIFOLDS
Development of advanced combustion technology for medium and high speed natural gas engines
[PB90-198565] N90-28836

MANIFOLDS (MATHEMATICS)
On Einsteinian 4-submanifolds in E(sup 6)
[DE90-627149] N90-29226

MANIPULATORS
Motion coordination for mobile robots in unstructured environments
[PB90-199498] N90-28837
Motion coordination for a mobile manipulator system
[PB90-203076] N90-28839
Dynamic modeling and payload-adaptation control of a flexible one-link manipulator N90-28843
Experiments in the dynamic and strategic control of cooperating manipulators N90-28845
Proceedings of the NASA Conference on Space Telerobotics, volume 1
[NASA-CR-186856] N90-29000
A 17 degree of freedom anthropomorphic manipulator N90-29001
A new approach to global control of redundant manipulators N90-29002
Kinematic functions for the 7 DOF robotics research arm N90-29003
Kinematics, controls, and path planning results for a redundant manipulator N90-29005
A complete analytical solution for the inverse instantaneous kinematics of a spherical-revolute-spherical (7R) redundant manipulator N90-29006
Development of a flexible test-bed for robotics, telemanipulation and servicing research N90-29012
Modularity in robotic systems N90-29014
Computational neural learning formalisms for manipulator inverse kinematics N90-29030
Multi-layer neural networks for robot control N90-29031
A neural network for controlling the configuration of frame structure with elastic members N90-29034
Proceedings of the NASA Conference on Space Telerobotics, volume 2
[NASA-CR-186857] N90-29044
Characterization and control of self-motions in redundant manipulators N90-29045
Multiple cooperating manipulators: The case of kinematically redundant arms N90-29046
Reflexive obstacle avoidance for kinematically-redundant manipulators N90-29047
Preliminary study of a serial-parallel redundant manipulator N90-29048
Design of a monitor and simulation terminal (master) for space station telerobotics and telescience N90-29051
Performance evaluation of a 6 axis high fidelity generalized force reflecting teleoperator N90-29052
Human machine interaction via the transfer of power and information signals N90-29054
On the simulation of space based manipulators with contact N90-29056
Preliminary results on noncollocated torque control of space robot actuators N90-29057
Portable Dextrous Force Feedback Master for robot telemanipulation (PDMFF) N90-29058
Experiences with the JPL telerobot testbed: Issues and insights N90-29059
The KALI multi-arm robot programming and control environment N90-29060
How do robots take two parts apart N90-29061
HERMIES-3: A step toward autonomous mobility, manipulation, and perception N90-29065
Robotic sampling system for an unmanned Mars mission N90-29070
Efficient mapping algorithms for scheduling robot inverse dynamics computation on a multiprocessor system N90-29071
Parallel algorithms for computation of the manipulator inertia matrix N90-29072
Planning robot actions under position and shape uncertainty N90-29073
A hardware/software environment to support R/D in intelligent machines and mobile robotic systems
[DE90-014458] N90-29119

MANUAL CONTROL
Tele-Autonomous control involving contact — object localization
[NASA-CR-187004] N90-28854

MANUALS
Animated computer-generated video-tape instruction using DIGLIB (Device Independent Graphics Library)
[DE90-015360] N90-29105

MANUFACTURING
Life cycle cost in the conceptual design of subsonic commercial aircraft, volumes 1 and 2 N90-28535
Radiation-curable prepreg composites
[DE90-629740] N90-28874

MAPPING
Map learning with indistinguishable locations N90-29025
Exploiting map plans as resources for action N90-29028
First results in terrain mapping for a roving planetary explorer N90-29066

MARINE PROPULSION
Vortice-propeller interaction
[LIMSI-89-9] N90-28809

MARS SAMPLE RETURN MISSIONS
Robotic sampling system for an unmanned Mars mission N90-29070

MARS SURFACE
Satellite-map position estimation for the Mars rover N90-29069
Robotic sampling system for an unmanned Mars mission N90-29070

MARTENSITE
The stability of the martensitic phases in Cu-Zn-Al at an electron concentration of 1.534
[DE90-628628] N90-28727

MARTENSITIC TRANSFORMATION
The stability of the martensitic phases in Cu-Zn-Al at an electron concentration of 1.534
[DE90-628628] N90-28727

MASS
Cepheid masses for models with enhanced opacities
[DE90-014919] N90-29266

MASS DISTRIBUTION
Near-infrared speckle observations of T Tauri stars and a multi-wavelength study of the prototype star T Tauri N90-29264

MASS FLOW
The equipment for mass flow measurements in the low-speed wind tunnel at DFVLR in Brunswick (Federal Republic of Germany)
[ESA-TT-1125] N90-28585
Specifications, tolerances, and other technical requirements for weighing and measuring devices as adopted by the 74th National Conference on Weights and Measures, 1989 (1990 edition)
[PB90-184961] N90-28748

MASS FLOW RATE
The entrainment rate for a row of turbulent jets
[NASA-CR-185278] N90-28504
The equipment for mass flow measurements in the low-speed wind tunnel at DFVLR in Brunswick (Federal Republic of Germany)
[ESA-TT-1125] N90-28585

MASS SPECTRA
Studies of central interactions of Si ions at 14.5 x A GeV/c in Au and Cu
[DE90-015095] N90-29195

MASS SPECTROMETERS
Thermogravimetry-mass spectrometry analysis of gas bubbles in molten glass
[DE90-014116] N90-28684
Reflection Mass Spectrometry (REMS) during 3/5 MBE
[DE90-014568] N90-28690

MASS SPECTROSCOPY
Mass spectrometric analysis of hydrogen isotopes in metals and metal hydrides
[DE90-014118] N90-28685
Reflection Mass Spectrometry (REMS) during 3/5 MBE
[DE90-014568] N90-28690
Study of the induction time in isothermal decomposition of explosives
[DE90-014906] N90-28745

MASS TRANSFER
Gas-film flow in tubes
[DE90-011528] N90-28793

MASSIVELY PARALLEL PROCESSORS
An even-parity/odd-parity formulation for deterministic transport calculations on massively parallel computers
[DE90-015036] N90-29116
Overcoming rule-based rigidity and connectionist limitations through massively-parallel case-based reasoning
[NASA-CR-186963] N90-29117

MATERIALS RECOVERY
Study of power generation systems for CO2 collection: LNG combined cycle
[DE90-507861] N90-28901
MATHEMATICAL MODELS
Nonequilibrium radiation and chemistry models for aerocapture vehicle flowfields
[NASA-CR-186379] N90-28490
Secondary instabilities in compressible boundary layers
[NASA-CR-182091] N90-28502
The effects of structural flap-lag and pitch-lag coupling on soft inplane hingeless rotor stability in hover
[NASA-TP-3002] N90-28503
Study of ground effects on flying scaled models N90-28532
Cage stability analysis for SSME HPOTP bearings N90-28625
Micromechanics of cyclic deformation in SSME turbopump blade materials N90-28641
High temperature fatigue behavior of Haynes 188 N90-28642
Structural response of SSME turbine blade airfoils N90-28649
Probabilistic model for fracture mechanics service life analysis N90-28650
Thermal analysis of thermal barrier coatings in a high heat flux environment N90-28652
Probability models for the failure of fibres and fibrous composite materials N90-28665
A constitutive model for AS4/PEEK thermoplastic composites under cyclic loading
[NASA-CR-180393] N90-28679
Development of comprehensive numerical schemes for predicting evaporating gas-droplets flow processes of a liquid-fueled combustor
[NASA-CR-187018] N90-28693
An LQR controller design approach for a Large Gap Magnetic Suspension System (LGMSS)
[NASA-TM-101606] N90-28751
New approach to HF channel modeling and simulation. Part 2: Stochastic model
[PB90-200338] N90-28755
Modeling tape-wound magnetic switches
[DE90-015121] N90-28782
Simulation of INPE's printed circuit laboratory production line
[INPE-4556-TDL/331] N90-28784
On the use of Lagrangian variables in descriptions of unsteady boundary-layer separation
[NASA-CR-182071] N90-28789
Evaluation of a hybrid kinetics/mixing-controlled combustion model for turbulent premixed and diffusion combustion using KIVA-2
[NASA-TM-103196] N90-28792
An experimental investigation of a single and multiphase confined coaxial jet N90-28796
Gas-jet and tangent-slot film cooling tests of a 12.5 deg cone at Mach number of 6.7
[NASA-TP-2786] N90-28806
A hybrid perturbation-Galerkin technique for partial differential equations
[NASA-CR-182085] N90-28814
Study of meteorological processes important in the degradation of materials through surface temperature
[PB90-222720] N90-28856
Structural analysis and optimum design of geodesically stiffened composite panels
[NASA-CR-186944] N90-28862
Correlation of AH-1G airframe flight vibration data with a coupled rotor-fuselage analysis
[NASA-CR-181974] N90-28865
Plan, execute, and discuss vibration measurements and correlations to evaluate a NASTRAN finite element model of the AH-64 helicopter airframe
[NASA-CR-181973] N90-28866
Green's functions for dislocations in bonded strips and related crack problems
[NASA-CR-185291] N90-28878
A method of classification for multisource data in remote sensing based on interval-valued probabilities
[NASA-CR-187007] N90-28889
Methods for multisource data analysis in remote sensing
[NASA-CR-187005] N90-28890
Three functions that model empirically measured unfrozen water content data and predict relative hydraulic conductivity
[AD-A223675] N90-28892
Sound propagation through atmospheric turbulence: A literature summary
[RPI-MATH-184] N90-28930
Planetary-scale flow on a two-layer beta-plane channel model with topography N90-28931
Gravity wave initiated convection
[NASA-CR-186868] N90-28933
Automated system for meteorological analysis
[INPE-4586-TDL/332] N90-28945
Vorticity balance study for a tropical region, during the Southern Hemisphere summer
[INPE-4634-TDL/336] N90-28949
Methods and strategies of object localization N90-29020
Planning 3-D collision-free paths using spheres N90-29024
A design philosophy for multi-layer neural networks with applications to robot control N90-29033
A Boltzmann machine for the organization of intelligent machines N90-29040
Autoregressive-moving average models for texture classification
[INPE-4987-PRE/1549] N90-29092
Second order tensor finite element
[NASA-CR-184008] N90-29122
Multigrid for hypersonic inviscid flows
[NASA-CR-182062] N90-29125
Criticality of the three-state chiral clock model: A renormalisation group study
[DE90-627321] N90-29212
Z(6) model: Criticality and break-collapse method
[DE90-627323] N90-29214
An infrared sky model based on the IRAS point source data
[NASA-CR-177526] N90-29265
Cepheid masses for models with enhanced opacities
[DE90-014919] N90-29266
Pulsations of the white dwarf component in V471 tauri-like binaries
[DE90-014921] N90-29267
Radio outbursts in extragalactic sources N90-29291
MATRICES (MATHEMATICS)
Least-index resolution of degeneracy in linear complementarity problems with sufficient matrices
[DE90-014406] N90-29145
MATRIX MATERIALS
Factors influencing the mode I interlaminar fracture resistance of toughened matrix composites N90-28668
MATRIX THEORY
Least-index resolution of degeneracy in linear complementarity problems with sufficient matrices
[DE90-014406] N90-29145
MAXIMUM LIKELIHOOD ESTIMATES
Probability models for the failure of fibres and fibrous composite materials N90-28665
MAXWELL EQUATION
Vlasov-Maxwell equilibria of solar coronal loops
[DE90-015025] N90-29289
MEASURE AND INTEGRATION
Weighted norm inequalities for Riemann-Liouville fractional integral
[DE90-627153] N90-29132
MEASURING INSTRUMENTS
Using embedded microcontrollers in radar test equipment
[DE90-014997] N90-28763
Operation and calibration of MRL permeameter for measurement of DC magnetic properties of materials under stress
[MRL-TN-574] N90-28863
MECHANICAL DRIVES
Adjustable speed drive applications guidebook
[DE90-014151] N90-28780
Solutions to the frictional dynamics problem and the reciprocal variable feedback methodology for design and control of robot mechanisms N90-28846
Preliminary results on noncollocated torque control of space robot actuators N90-29057
MECHANICAL ENGINEERING
Preliminary study of a serial-parallel redundant manipulator N90-29048
MECHANICAL PROPERTIES
Data base for crack growth properties of materials N90-28647
Mechanical behavior of thick, curved, laminated composites N90-28664
Strengthening and toughening mechanisms in ceramic fiber-reinforced glass matrix composites N90-28666
ARALL (ARamid ALuminum Laminate), a literature survey
[FOA-C-20782-2.5] N90-28671
Electrochemical surface finishing using amino-substrates on carbon fibers in organic media. Effects of the finishing on the mechanical properties of carbon-epoxy composites
[ONERA-RT-9/3549-M] N90-28672
Radiation-curable prepreg composites
[DE90-629740] N90-28674
Effect of protective coatings on mechanical properties of superalloys N90-28707
High temperature protective coatings: Recent trends N90-28710
Mechanical testing activities related to high-performance structural ceramics
[DE90-014299] N90-28734
Technical bibliography of high performance polyethylene fibers
[SNPE-NT-106/89/GTR/RP/NP] N90-28736
Some studies of the vibration welding of thermoplastics N90-28842
MELTS (CRYSTAL GROWTH)
Electronic conduction in molten cryolite saturated with alumina
[DE90-015090] N90-29211
MERCURY CADMIUM TELLURIDES
Faraday rotation mapping of mercury cadmium telluride
[AD-A224278] N90-28729
MESH
Crash-impact behavior of graphite/epoxy composite sine wave webs N90-28667
MESOSCALE PHENOMENA
A nonhydrostatic numerical model in sigma-coordinates and simulations of mesoscale phenomena N90-28932
Mesoscale Lightning Experiment (MLE): A view of lightning as seen from space during the STS-26 mission
[NASA-TM-103513] N90-28951
MESSAGE PROCESSING
Communications Interface Driver (CID) test plan
[DOT/FAA/CT-TN89/35] N90-28762
MESSAGES
Secure Data Network System (SDNS) network, transport, and message security protocols
[PB90-198945] N90-28757
METAL COATINGS
Oxidation, sulfidation, and hot corrosion: Mechanisms and interrelationships N90-28702
METAL FATIGUE
High temperature fatigue behavior of Haynes 188 N90-28642
Constitutive and life modeling of single crystal blade alloys for root attachment analysis N90-28643
The fatigue damage behavior of a single crystal superalloy N90-28644
Micromechanisms of fatigue crack growth and fracture toughness in metal matrix composites
[AD-A223863] N90-28676
Fretting fatigue strength of Ti-6Al-4V at room and elevated temperatures and ways of improving it N90-28700
Crack layer analysis of fatigue fracture of a beta titanium alloy N90-28864
Microstructure: Property correlation --- multiaxial fatigue damage evolution in waspaloy
[NASA-CR-180406] N90-28880
METAL HYDRIDES
Mass spectrometric analysis of hydrogen isotopes in metals and metal hydrides
[DE90-014118] N90-28685
METAL IONS
Structure of metal overlayers by low energy alkali ion scattering: Cu/Ru(0001) and Sn/Pt(111)
[DE90-014453] N90-28718
METAL MATRIX COMPOSITES
Micromechanics analysis of power consolidation in manufacturing particulate-reinforced MMCs (metal matrix composites)
[DE90-014448] N90-28663
Inelastic analysis of laminated composites N90-28669
Micromechanisms of fatigue crack growth and fracture toughness in metal matrix composites
[AD-A223863] N90-28676
A theoretical investigation into the inelastic behavior of metal-matrix composites
[AD-A223973] N90-28677
Evaluation of several micromechanics models for discontinuously reinforced metal matrix composites
[NASA-TM-102719] N90-28872
METAL PLATES
Electrodeposition of wear resistant coatings
[PB90-221839] N90-28732
Buckling and postbuckling behavior of compression-loaded isotropic plates with cutouts
[NASA-TP-3024] N90-28859
METAL POWDER
Micromechanics analysis of power consolidation in manufacturing particulate-reinforced MMCs (metal matrix composites)
[DE90-014448] N90-28663
METALLIC GLASSES
Containerless low gravity processing of glass forming and immiscible alloys
[NASA-CR-186999] N90-28747

METALLOGRAPHY
Determination of the NDT temperature and Charpy V-notch impact properties of AAR TC128 grades B steel and A 8XX grade B steel
[PB90-207804] N90-28716
METALS
Mass spectrometric analysis of hydrogen isotopes in metals and metal hydrides
[DE90-014118] N90-28685
High temperature surface interactions: Overview
N90-28699
METASTABLE STATE
Research on the structural and electronic properties of defects in amorphous silicon
[DE90-000342] N90-28730
METEOROLOGICAL CHARTS
Automated system for meteorological analysis
[INPE-4586-TDL/332] N90-28945
METEOROLOGICAL PARAMETERS
Atmospheric environment for Space Shuttle (STS-32) launch
[NASA-TM-100400] N90-28912
Atmospheric environment for Space Shuttle (STS-31) launch
[NASA-TM-103508] N90-28913
Atmospheric environment for space shuttle (STS-36) launch
[NASA-TM-100403] N90-28914
Atmospheric environment for space shuttle (STS-34) launch
[NASA-TM-100396] N90-28915
Estimating the spatial variability of trace gas deposition velocities
[PB90-208570] N90-28928
Automated system for meteorological analysis
[INPE-4586-TDL/332] N90-28945
METEOROLOGICAL RADAR
Ground-based weather radar compatibility with digital radio-relay microwave systems
[PB90-206236] N90-28756
A personal computer-based, multitasking data acquisition system
[NASA-TM-4232] N90-29107
METEOROLOGICAL SERVICES
Program on development of basic understanding of severe weather phenomena
[PB90-226564] N90-28943
METEOROLOGY
Study of meteorological processes important in the degradation of materials through surface temperature
[PB90-222720] N90-28856
Estimating the spatial variability of trace gas deposition velocities
[PB90-208570] N90-28928
An investigation of forcing mechanisms during a surprise tornadic thunderstorm
[PB90-216805] N90-28940
Automated system for meteorological analysis
[INPE-4586-TDL/332] N90-28945
Vorticity balance study for a tropical region, during the Southern Hemisphere summer
[INPE-4634-TDL/336] N90-28949
On the dynamics of severe thunderstorms
[DE90-627922] N90-28950
METHANE
Oxygen/methane combustion stability investigation
N90-28828
METHYL ALCOHOL
Results from the fourth year of operation of the Federal Methanol Fleet at Lawrence Berkeley Laboratory
[DE90-014741] N90-28743
METROLOGY
A laser tracking dynamic robot metrology instrument
N90-29021
MICHELSON INTERFEROMETERS
Velocity Interferometer System for Any Reflector (VISAR): Displacement mode data reduction
[DE90-015027] N90-29184
MICROANALYSIS
Friction microprobe studies of composite surfaces
[DE90-014224] N90-28862
MICROCHANNEL PLATES
Noise performance of microchannel plate imaging systems
[DE90-015037] N90-28785
MICROCRACKS
Crack layer analysis of fatigue fracture of a beta titanium alloy N90-28864
MICROELECTRONICS
Polymer research
[PB90-246638] N90-28737
Adjustable speed drive applications guidebook
[DE90-014151] N90-28780
Measurements of the single event upset environment in the upper atmosphere
[RAE-TM-SPACE-373] N90-28934
MICROMECHANICS
Micromechaniams of fatigue crack growth and fracture toughness in metal matrix composites
[AD-A223863] N90-28676
Evaluation of several micromechanics models for discontinuously reinforced metal matrix composites
[NASA-TM-102719] N90-28872
MICROMINIATURIZATION
Smart microsensors for high temperature applications, phase 1
[AD-A224151] N90-28828
MICROPROCESSORS
Using embedded microcontrollers in radar test equipment
[DE90-014997] N90-28763
Adjustable speed drive applications guidebook
[DE90-014151] N90-28780
A microprocessor controlled strain gauge calibration module
[AR-005-579] N90-28821
Engineering and the advancement of human welfare. Ten outstanding achievements 1964-1989
[ISBN-0-309-04185-6] N90-29297
MICROSTRUCTURE
Friction microprobe studies of composite surfaces
[DE90-014224] N90-28862
High temperature oxidation of Al-Li alloys N90-28705
Microstructure and impurity effects on tungsten heavy alloys
[AD-A224220] N90-28728
High-temperature deformation and microstructural analysis for Si3N4-Sc2O3
[NASA-TM-103239] N90-28740
Containerless low gravity processing of glass forming and immiscible alloys
[NASA-CR-186999] N90-28747
Some studies of the vibration welding of thermoplastics N90-28842
Evaluation of several micromechanics models for discontinuously reinforced metal matrix composites
[NASA-TM-102719] N90-28872
Electron microscopy of transition-metal doped BiCaSrCuO
[DE90-014184] N90-29202
XANES and EXAFS study of Au-substituted YBa2Cu3O(7-delta)
[NASA-TM-103291] N90-29219
MICROWAVE AMPLIFIERS
Design and realization of a two stage C-band low noise amplifier
[FEL-89-B265] N90-28783
MICROWAVE ANTENNAS
Design and performance of a long, over-water microwave radio link
[PB90-207994] N90-28758
MICROWAVE CIRCUITS
High temperature superconducting thin film microwave circuits: Fabrication, characterization, and applications
[NASA-TM-103235] N90-28786
MICROWAVE EQUIPMENT
Ground-based weather radar compatibility with digital radio-relay microwave systems
[PB90-206236] N90-28756
MICROWAVE FILTERS
Approximation, synthesis, and development of bi-mode cavities microwave filters presenting unsymmetrical quasi-elliptic responses
[CNES-NT-124] N90-28781
MICROWAVE OSCILLATORS
High temperature superconducting thin film microwave circuits: Fabrication, characterization, and applications
[NASA-TM-103235] N90-28786
MICROWAVES
Design and performance of a long, over-water microwave radio link
[PB90-207994] N90-28758
MIGRATION
User's manual ROBIN: A research and notification system for bird migration
[FEL-1989-103] N90-28508
MILITARY AIR FACILITIES
Source emission test of gas turbine engine test facility, Kelly AFB, TX
[AD-A223869] N90-28571
MILITARY OPERATIONS
Space-base multispectral imagery: Current and future applications and implications to the United States Army
[AD-A224046] N90-28894
MILLIMETER WAVES
Radio outbursts in extragalactic sources N90-29291
MIMD (COMPUTERS)
Parallelization of a software relating to aerodynamics on MIMD type computers
[ONERA-RT-31/3479-CY] N90-29114
MINIATURIZATION
Special test and evaluation methods used for a nine-axis accelerometer
[PB90-209578] N90-28822
Measurement of hand dynamics in a microsurgery environment: Preliminary data in the design of a bimanual telemicro-operation test bed N90-29010
MINING
Human factors model concerning the man-machine interface of mining crewstations N90-29011
Automation and robotics technology for intelligent mining systems N90-29018
MINKOWSKI SPACE
Introduction to gauge theories and unification
[DE90-014473] N90-29225
MISS DISTANCE
Dallas/Forth Worth simulation. Phase 2: Triple simultaneous parallel Instrument Landing System (ILS) approaches (turbojets)
[DOT/FAA/CT-90/2] N90-28509
MISSILE BODIES
Effects of flowfield turbulence on asymmetric vortices over a slender body
[AD-A224139] N90-28819
MISSILE COMPONENTS
Proceedings of US Army Research Office Workshop on US Army Applications for Diamond and Diamondlike Materials
[AD-A224193] N90-28741
MISSION PLANNING
Life cycle cost in the conceptual design of subsonic commercial aircraft, volumes 1 and 2 N90-28535
Development of the electric vehicle analyzer
[AD-A224201] N90-28788
Coordinating the activities of a planner and an execution agent N90-29035
MIXERS
Energy Efficient Engine exhaust mixer model technology report addendum; phase 3 test program
[NASA-CR-174799] N90-28556
MIXING
Regular and chaotic motion of uniform elliptical vortices in external linear time dependent velocity fields
N90-28497
An experimental investigation of a single and multiphase confined coaxial jet N90-28796
Chiral Maxwell-Garnett mixing formula
[PB90-189143] N90-29158
MIXING LAYERS (FLUIDS)
Numerical simulation of the formation of two-dimensional and three-dimensional structures in shear layers and wakes
[ESA-TT-1008] N90-28802
MOBILITY
Motion coordination for mobile robots in unstructured environments
[PB90-199498] N90-28837
Motion coordination for a mobile manipulator system
[PB90-203076] N90-28839
Remote atmospheric profiling systems for tropospheric monitoring
[PB90-216789] N90-28927
HERMIES-3: A step toward autonomous mobility, manipulation, and perception N90-29065
Planetary rover technology development requirements
N90-29067
A hardware/software environment to support R/D in intelligent machines and mobile robotic systems
[DE90-014458] N90-29119
MODELS
Multiresolutional models of uncertainty generation and reduction N90-29043
MODULARITY
Modularity in robotic systems N90-29014
MODULES
Modularity in robotic systems N90-29014
MOISTURE CONTENT
Three functions that model empirically measured unfrozen water content data and predict relative hydraulic conductivity
[AD-A223875] N90-28892
MOLECULAR ABSORPTION
Fifteenth International Conference on X Ray and Inner-Shell Processes
[DE90-013024] N90-29170
MOLECULAR BEAM EPITAXY
Reflection Mass Spectrometry (REMS) during 3/5 MBE
[DE90-014568] N90-28890
MOLECULAR BIOLOGY
Japanese molecular biology 1990: An update
[PB90-188707] N90-28958
Biomedical and environmental sciences program publications, 1989
[DE90-014785] N90-29250

MOLECULAR CLOUDS
A plasma diagnostic study of two wind-blown shell nebulae: NGC 7635 and NGC 2359 N90-29271
MOLECULAR STRUCTURE
Accurate quantum chemical calculations [NASA-TM-101932] N90-28680
Surface and defect excitations in covalently bonded solids [AD-A221995] N90-28682
Fuels research, volume 1 [DE90-015393] N90-28695
MOLECULES
Infrared spectroscopic measurements on planetary atmospheric gases N90-29283
MOLTEN SALTS
Molten salt induced high temperature degradation of thermal barrier coatings N90-28704
Overview on hot gas tests and molten salt corrosion experiments at the DLR N90-28714
MOMENT DISTRIBUTION
A flight dynamic model of aircraft spinning [AR-005-600] N90-28576
MOMENTUM
Quantum gravity in two dimensions and the SL(2,R) current algebra [DE90-627215] N90-29156
MONITORS
Preliminary exposure study to determine the effects of acid deposition on coated steel substrates [PB90-201799] N90-28715
Simulation of INPE's printed circuit laboratory production line [INPE-4556-TDL/331] N90-28784
Remote atmospheric profiling systems for tropospheric monitoring [PB90-216789] N90-28927
Causal simulation and sensor planning in predictive monitoring N90-29037
Design of a monitor and simulation terminal (master) for space station telerobotics and telescience N90-29051
MONOCHROMATIC RADIATION
Scientific Colloquium in Honor of Prof. Dr. Rer. Nat. Hermann L. Jordan [ESA-TT-1101] N90-29159
Energy transmission by means of coherent quasi-mono-chromatic light beams N90-29163
MONOTECTIC ALLOYS
Containerless low gravity processing of glass forming and immiscible alloys [NASA-CR-186999] N90-28747
MONTE CARLO METHOD
Surface and defect excitations in covalently bonded solids [AD-A221995] N90-28682
A study of heat and fluid flow phenomena on the gas side of circular-tube plate-fin heat exchangers N90-28795
An improved method for choosing sampling points for the inspection of complex surfaces in a computer-aided manufacturing environment N90-29093
The first order phase transition for six-state Potts model on two dimensional random triangle lattice [DE90-627210] N90-29140
An infrared sky model based on the IRAS point source data [NASA-CR-177526] N90-29265
Comparison of dose estimates using the buildup-factor method and a Baryon transport code (BRYNTRN) with Monte Carlo results [NASA-TP-3021] N90-29290
MORPHOLOGY
Structure of metal overlayers by low energy alkali ion scattering: Cu/Ru(0001) and Sn/Pt(111) [DE90-014453] N90-28718
Numerical and analytical study of nonlinear bifurcations associated with the morphological stability of two-dimensional single crystals [PB90-209594] N90-29200
A plasma diagnostic study of two wind-blown shell nebulae: NGC 7635 and NGC 2359 N90-29271
MOSAICS
Digital geometric correction for MSS-LANDSAT imagery [INPE-4627-PRE/1345] N90-28886
MOSSBAUER EFFECT
Moessbauer Effect applications using intense radioactive ion beams [DE90-014981] N90-29175
MOTION PERCEPTION
Effects of short-term weightlessness on roll circularvection N90-28992
MOTION PICTURES
Animated computer-generated video-tape instruction using DIGLIB (Device Independent Graphics Library) [DE90-015360] N90-29105
MOTION SIMULATION
On the application of similarity laws to a scaled railway bogie model [DLR-FB-90-06] N90-28853
On the simulation of space based manipulators with contact N90-29056
MOTORS
Performance measurements and energy balance of an SPS V160 Stirling motor at the German Aerospace Research Establishment [DLR-MITT-90-03] N90-28903
MOUNTING
Constitutive and life modeling of single crystal blade alloys for root attachment analysis N90-28643
MULTIGRID METHODS
Numerical resolution of Navier-Stokes equations using several turbulence models and applications on turbomachines [ETN-90-97478] N90-28808
MULTIPLE ACCESS
ATDRS payload technology research and development [NASA-TM-103256] N90-28596
MULTIPOLES
Superconformal algebra and central extension of meromorphic vector fields with multipoles on super-Riemann sphere [DE90-627211] N90-29153
MULTIPROCESSING (COMPUTERS)
Efficient mapping algorithms for scheduling robot inverse dynamics computation on a multiprocessor system N90-29071
The effect of multiprocessor radius on scaling [DE90-014772] N90-29095
Piecewise linear models of processor utilization [DE90-014774] N90-29115
MULTISENSOR APPLICATIONS
A method of classification for multisource data in remote sensing based on interval-valued probabilities [NASA-CR-187007] N90-28889
Workshop on Neural Networks [DE90-014794] N90-29120
MULTISPECTRAL BAND SCANNERS
Description of the MARC measuring system [FEL-89-B170] N90-28887
On-line object feature extraction for multispectral scene representation [NASA-CR-187006] N90-28888
Methods for multisource data analysis in remote sensing [NASA-CR-187005] N90-28890
Space-base multispectral imagery: Current and future applications and implications to the United States Army [AD-A224046] N90-28894
MULTISPECTRAL RADAR
Multiband imaging systems [AD-A223969] N90-28893
MULTISTATIC RADAR
Target signature modeling and bistatic scattering measurement studies [NASA-CR-186611] N90-28766
MUSCLES
Computer aided mechanogenesis of skeletal muscle organs from single cells in vitro [NASA-CR-187025] N90-28959
MUSCULOSKELETAL SYSTEM
Insulin and insulin-like growth factor-1 induce pronounced hypertrophy of skeletal myofibers in tissue culture [NASA-CR-187026] N90-28960

N

NACELLES
Energy Efficient Engine program advanced turbofan nacelle definition study [NASA-CR-174942] N90-28560
NARROWBAND
New approach to HF channel modeling and simulation. Part 2: Stochastic model [PB90-200338] N90-28755
NASA PROGRAMS
A survey of planning and scheduling research at the NASA Ames Research Center N90-29076
Preliminary analysis of NASA commercialization initiatives [PB90-202706] N90-29257
NASTRAN
Liquid Rocket Booster (LRB) for the Space Transportation System (STS) systems study. Appendix E: Pressure-fed booster test bed for the liquid rocket booster study [NASA-CR-183791-APP-E] N90-28805
Plan, execute, and discuss vibration measurements and correlations to evaluate a NASTRAN finite element model of the AH-64 helicopter airframe [NASA-CR-181973] N90-28868
NATIONAL AEROSPACE PLANE PROGRAM
NASA Langley Research Center National Aero-Space Plane Mission simulation profile sets [NASA-TM-102670] N90-28541
NATIONAL AIRSPACE SYSTEM
A glossary of terms, definitions, acronyms, and abbreviations related to the National Airspace System [DOT/FAA/CT-TN89/53] N90-29249
NATURAL GAS
Development of advanced combustion technology for medium and high speed natural gas engines [PB90-198565] N90-28836
NATURAL LANGUAGE (COMPUTERS)
The SPECIALIST: Natural language processing system [PB90-240029] N90-29098
NAVIER-STOKES EQUATION
Secondary instabilities in compressible boundary layers [NASA-CR-182091] N90-28502
Numerical resolution of Navier-Stokes equations using several turbulence models and applications on turbomachines [ETN-90-97478] N90-28808
Extrapolation procedures at outflow boundaries for the Navier-Stokes equations [FFA-TN-1990-23] N90-28811
An investigation of chaotic Kolmogorov flows [NASA-CR-182079] N90-28816
NAVIGATION
An aeronautical mobile satellite experiment [NASA-CR-186971] N90-28593
Dynamic interaction of multiple autonomous mobile robots N90-28844
Treatment of systematic errors 2: Fusion of ultrasound and visual sensor data [DE90-014780] N90-28850
Proceedings of the NASA Conference on Space Telerobotics, volume 1 [NASA-CR-186856] N90-29000
Automation and robotics technology for intelligent mining systems N90-29018
Map learning with indistinguishable locations N90-29025
Three-dimensional motor schema based navigation N90-29026
Learned navigation in unknown terrains: A retraction method N90-29029
A hardware/software environment to support R/D in intelligent machines and mobile robotic systems [DE90-014458] N90-29119
NEAR WAKES
An investigation of the steady and unsteady near wake and its effect on a laminar boundary layer N90-28794
NEBULAE
A plasma diagnostic study of two wind-blown shell nebulae: NGC 7635 and NGC 2359 N90-29271
NEON
Nova LMC (Large Magellanic Cloud) 1990 no. 1: The first extragalactic neon nova [NASA-CR-180409] N90-29276
NEURAL NETS
A failure diagnosis system based on a neural network classifier for the space shuttle main engine [NASA-TM-103607] N90-28659
Target detection in Gaussian noise using artificial neural systems [AD-A223983] N90-28770
Proceedings of the NASA Conference on Space Telerobotics, volume 1 [NASA-CR-186856] N90-29000
Computational neural learning formalisms for manipulator inverse kinematics N90-29030
Multi-layer neural networks for robot control N90-29031
A hybrid architecture for the implementation of the Athena neural net model N90-29032
A design philosophy for multi-layer neural networks with applications to robot control N90-29033
A neural network for controlling the configuration of frame structure with elastic members N90-29034
Design of a monitor and simulation terminal (master) for space station telerobotics and telescience N90-29051
Learning in stochastic neural networks for constraint satisfaction problems N90-29078
Recursive least-squares learning algorithms for neural networks [DE90-014926] N90-29096
Overcoming rule-based rigidity and connectionist limitations through massively-parallel case-based reasoning [NASA-CR-186963] N90-29117

Workshop on Neural Networks
[DE90-014794] N90-29120

NEUROPHYSIOLOGY
Time, space and form in vision
[AD-A213889] N90-28971
Neurophysiological correlates of information processing abilities during divided attention situations in air traffic controllers N90-28989
Statement of research objectives and summary of research efforts
[RLE-PR-132] N90-29295

NEUTRINOS
Solar oscillation frequency and solar neutrino predictions
[DE90-014918] N90-29288

NEUTRON CROSS SECTIONS
Helium generation in fusion reactor materials
[DE90-013005] N90-29172

NEUTRON SPECTROMETERS
Concept for a neutron spectrometer based on optical detection of (3)He(n, p)-3H reactions in a gas
[DE90-014776] N90-28826

NEUTRON STARS
Rotating neutron stars and the equation of state of dense matter
[DE90-014185] N90-29269

NEUTRONS
Measurements of the single event upset environment in the upper atmosphere
[RAE-TM-SPACE-373] N90-28934

NICKEL ALLOYS
Density changes of generation 1.5 and 2.0 copper alloys irradiated at 411 to 414 C and 529 C in FFTF-MOTA
[DE90-015291] N90-28724

NICKEL COMPOUNDS
Antiferromagnetism and enhanced heat in CeM2Sn (M = Ni, Ir, Cu, Rh, Pd, and Pt
[DE90-014924] N90-29206

NITRIC ACID
The global cycle of reactive nitrogen
[DE90-015041] N90-28919

NITROGEN
The global cycle of reactive nitrogen
[DE90-015041] N90-28919

NITROGEN ATOMS
Quenching of N(2D) by O(3P)
[AD-A221690] N90-28683

NITROGEN OXIDES
Quenching of N(2D) by O(3P)
[AD-A221690] N90-28683
The global cycle of reactive nitrogen
[DE90-015041] N90-28919
Acid deposition: No such thing as a free launch
[DE90-015085] N90-28920
Tropospheric nitrogen: The influence of anthropogenic sources on distributions and deposition, executive summary
[DE90-015401] N90-28922

NITROUS OXIDES
Natural and anthropogenic climate change
[DE90-015528] N90-28923

NOISE (SOUND)
Methods for detecting low-frequency signals in the presence of strong winds
[AD-A223980] N90-28769
Measuring the vertical directional spectra caused by sea surface sound
[AD-A223983] N90-28957

NOISE INTENSITY
Studies in automatic speech recognition and its application in aerospace N90-28759
Annoyance caused by advanced turboprop aircraft flyover noise: Counter-rotating-propeller configuration
[NASA-TP-3027] N90-29166

NOISE POLLUTION
High-speed civil transport study: Special factors
[NASA-CR-181881] N90-28537

NOISE REDUCTION
Comparison of speech intelligibility in cockpit noise using SPH-4 flight helmet with and without active noise reduction
[NASA-CR-177564] N90-28510
Methods for detecting low-frequency signals in the presence of strong winds
[AD-A223980] N90-28769

NOISE TOLERANCE
Annoyance caused by advanced turboprop aircraft flyover noise: Counter-rotating-propeller configuration
[NASA-TP-3027] N90-29166

NONDESTRUCTIVE TESTS
A comparison of single-cycle versus multi-cycle proof testing strategies N90-28646
Ultrasonic verification of five wave fronts in unidirectional graphite epoxy composite
[NASA-CR-185288] N90-28858

NONEQUILIBRIUM RADIATION
Nonequilibrium radiation and chemistry models for aerocapture vehicle flowfields
[NASA-CR-186379] N90-28490

NONLINEAR OPTICS
Statement of research objectives and summary of research efforts
[RLE-PR-132] N90-29295

NONLINEAR SYSTEMS
Mode competition in the quasioptical gyrotron
[AD-A222181] N90-28823
Parametric solution of nonlinear structure problems
[ONERA-RT-21/3542-RY-082-R] N90-28874
Error detection and control for nonlinear shell analysis
[NASA-TM-102723] N90-28877
Numeric fluid mechanics N90-29161

NONLINEARITY
A nonlinear finite element formulation for the large displacement analysis of plates N90-28867
Computerized simulation of phenomena in plasma via particles
[INPE-4595-RPE/569] N90-29194
Numerical and analytical study of nonlinear bifurcations associated with the morphological stability of two-dimensional single crystals
[PB90-209594] N90-29200
Control of nonlinear space-charge emittance growth
[DE90-014752] N90-29270

NORTH AMERICA
Acid deposition: No such thing as a free launch
[DE90-015085] N90-28920

NOTCH TESTS
Ascertaining the fracture toughness of ceramic materials by means of bending testpieces of various notch types at ambient and high temperatures
[ESA-TT-992] N90-28733

NOTCHES
Ascertaining the fracture toughness of ceramic materials by means of bending testpieces of various notch types at ambient and high temperatures
[ESA-TT-992] N90-28733

NOVAE
PW Vul: A classical nova with nearly solar abundances
[NASA-CR-185080] N90-29275

NOZZLE DESIGN
High/variable mixture ratio O2/H2 engine N90-28838
Design of an axisymmetric, contoured nozzle for the HEG
[DLR-FB-90-04] N90-28812

NOZZLE EFFICIENCY
The affect of gravity on particle collection in inertial impactors
[DE90-013372] N90-29173

NOZZLE GEOMETRY
Low power arcjet performance
[NASA-TM-103280] N90-28657
Design of an axisymmetric, contoured nozzle for the HEG
[DLR-FB-90-04] N90-28812

NUCLEAR MEDICINE
Biomedical and environmental sciences program publications, 1989
[DE90-014785] N90-29250

NUCLEAR PHYSICS
Biomedical and environmental sciences program publications, 1989
[DE90-014785] N90-29250

NUMERICAL ANALYSIS
Novel numerical analysis method for the study of convolution equations in appearance potential spectroscopy
[ETN-90-97288] N90-29210

NUMERICAL CONTROL
A system architecture for a planetary rover N90-29015
Reflexive obstacle avoidance for kinematically-redundant manipulators N90-29047

NUMERICAL FLOW VISUALIZATION
An investigation of chaotic Kolmogorov flows
[NASA-CR-182079] N90-28816

O

O STARS
An analysis of the Palomar-Green subdwarfs and white dwarfs N90-29263

OBLIQUE WINGS
The aerodynamic design of the oblique flying wing supersonic transport
[NASA-CR-177552] N90-28540

OBSTACLE AVOIDANCE
Velocity filtering applied to optical flow calculations
[NASA-TM-102802] N90-28512
Motion coordination for mobile robots in unstructured environments
[PB90-199498] N90-28837
Cartesian control of redundant robots N90-29004
Reflexive obstacle avoidance for kinematically-redundant manipulators N90-29047

OCEAN BOTTOM
Drilling the oceanic lower crust and mantle: A global strategy for exploring the deep oceanic crust and mantle in the 1990's
[PB90-240953] N90-28936
Large aperture acoustic arrays in support of reverberation studies
[AD-A224002] N90-29168

OCEAN CURRENTS
Ross Sea oceanographic data, 1983-1987: USCGC GLACIER, January-February 1983; USCGC POLAR SEA, January-February 1984; USCGC POLAR STAR, February 1984; USCGC POLAR SEA, February 1987
[PB90-243932] N90-28955

OCEAN MODELS
Factorization of the characteristic equation for three layer ducts
[AD-A223867] N90-28956

OCEAN SURFACE
Detection of ocean inner waves by synthetic aperture radar: Observations at Gibraltar pass
[ETN-90-97477] N90-28953
Measuring the vertical directional spectra caused by sea surface sound
[AD-A223883] N90-28957

OCEANOGRAPHIC PARAMETERS
Detection of ocean inner waves by synthetic aperture radar: Observations at Gibraltar pass
[ETN-90-97477] N90-28953

OCEANOGRAPHY
Drilling the oceanic lower crust and mantle: A global strategy for exploring the deep oceanic crust and mantle in the 1990's
[PB90-240953] N90-28936
Proceedings of the 14th Annual Climate Diagnostics Workshop
[PB90-198573] N90-28938
Oceanographic data exchange, 1988
[PB90-232596] N90-28952
Ross Sea oceanographic data, 1983-1987: USCGC GLACIER, January-February 1983; USCGC POLAR SEA, January-February 1984; USCGC POLAR STAR, February 1984; USCGC POLAR SEA, February 1987
[PB90-243932] N90-28955

OCEANS
Design and performance of a long, over-water microwave radio link
[PB90-207994] N90-28758
Ross Sea oceanographic data, 1983-1987: USCGC GLACIER, January-February 1983; USCGC POLAR SEA, January-February 1984; USCGC POLAR STAR, February 1984; USCGC POLAR SEA, February 1987
[PB90-243932] N90-28955

OFFGASSING
Space station contamination modeling
[NASA-CR-183871] N90-28590

ON-LINE SYSTEMS
On-line object feature extraction for multispectral scene representation
[NASA-CR-187006] N90-28888
Coordinating the activities of a planner and an execution agent N90-29035
Grasp planning under uncertainty N90-29041
An expert system to perform on-line controller restructuring for abrupt model changes
[NASA-TM-103609] N90-29121

OPENINGS
Buckling and postbuckling behavior of compression-loaded isotropic plates with cutouts
[NASA-TP-3024] N90-28859

OPERATING COSTS
Energy Efficient Engine program advanced turbofan nacelle definition study
[NASA-CR-174942] N90-28560
Energy Efficient Engine: High-pressure compressor test hardware detailed design report
[NASA-CR-180850] N90-28570
Operational cost drivers N90-28636

OPERATING SYSTEMS (COMPUTERS)
ROSES, a Robot Operating System Expert Scheduler: Methodological framework
[DE90-014782] N90-28851
Concepts of concurrent programming
[AD-A223897] N90-29110

OPERATIONAL PROBLEMS
Spacecraft charging effects
[RAE-TM-SPACE-375] N90-28594

OPERATOR PERFORMANCE
Situational Awareness Rating Technique (SART): The development of a tool for aircrew systems design N90-28975
Tracking performance and influence of field of view N90-28968
Teleoperator comfort and psychometric stability: Criteria for limiting master-controller forces of operation and feedback during telemanipulation N90-29009
OPERATORS (MATHEMATICS)
On the zeta-function regularization of chiral Jacobians for singular Dirac operators
[DE90-627176] N90-29150
Casimir effect in a D-dimensional flat spacetime and the cut-off method
[DE90-627177] N90-29151
OPTICAL COMMUNICATION
Application of integrated optical components in optical fiber communication
[FEL-89-B252] N90-29183
OPTICAL COMPUTERS
A hybrid architecture for the implementation of the Athena neural net model N90-29032
OPTICAL DATA PROCESSING
A hybrid architecture for the implementation of the Athena neural net model N90-29032
OPTICAL DATA STORAGE MATERIALS
Optical storage technology
[AD-A224026] N90-29254
OPTICAL FIBERS
Noncontact measurement of high temperature using optical fiber sensors
[NASA-CR-186975] N90-28825
Theory of biaxial graded-index optical fiber
[NASA-CR-186977] N90-29180
OPTICAL FILTERS
Velocity filtering applied to optical flow calculations
[NASA-TM-102602] N90-28512
OPTICAL ILLUSION
Effects of short-term weightlessness on roll circularvection N90-28992
OPTICAL MEASUREMENT
Concept for a neutron spectrometer based on optical detection of (3)He(n, p)-3H reactions in a gas
[DE90-014776] N90-28826
OPTICAL PATHS
Mode competition in the quasioptical gyrotron
[AD-A222181] N90-28823
OPTICAL PROPERTIES
Experimental study of the optical constants of metals at high temperatures
[DE90-014732] N90-28719
Semiconductor measurement technology: A software program for aiding the analysis of ellipsometric measurements, simple spectroscopic models
[PB90-216847] N90-29201
OPTICAL PUMPING
New resonantly photo-pumped x ray laser scheme
[DE90-015044] N90-28831
OPTICAL RADAR
Wind lidar for BEST
[CNES-NT-125] N90-28947
OPTICAL SCANNERS
Near-angle scattering and binary optics
[AD-A224140] N90-29186
OPTIMAL CONTROL
Effective optimal control of a fighter aircraft engine N90-28548
The dynamics and control of large flexible space structures - 13
[NASA-CR-186930] N90-28591
OPTIMIZATION
Aerodynamic interferences of in-flight thrust reversers in ground effect N90-28529
System reliability optimization of aircraft wings N90-28536
Bearing optimization for SSME HPOTP application N90-28622
Summary of booster propulsion/vehicle impact study results N90-28635
Design optimization of gas generator hybrid propulsion boosters
[NASA-CR-181096] N90-28660
High temperature oxidation of Al-Li alloys N90-28705
Minimum weight design of a leaf spring tapered in thickness and width for the Hubble Space Telescope-space support equipment
[NASA-TM-4233] N90-28879
A neural network for controlling the configuration of frame structure with elastic members N90-29034
Efficient mapping algorithms for scheduling robot inverse dynamics computation on a multiprocessor system N90-29071
Least-index resolution of degeneracy in linear complementarity problems with sufficient matrices
[DE90-014406] N90-29145
OPTOELECTRONIC DEVICES
The III-V semiconductor quantum well lasers and related optoelectronic devices on silicon
[AD-A224120] N90-28835
ORDER-DISORDER TRANSFORMATIONS
X ray scattering studies of non-equilibrium ordering processes
[DE90-015066] N90-29209
Interface formation and percusory dynamics
[AD-A224128] N90-29223
ORIFICES
In-flight investigation of shuttle tile pressure orifice installations
[NASA-TM-4219] N90-28820
OROGRAPHY
A nonhydrostatic numerical model in sigma-coordinates and simulations of mesoscale phenomena N90-28932
ORTHOGONAL FUNCTIONS
Recurrence relations and weight functions for approximation by orthonormal polynomials
[DE90-627156] N90-29134
ORTHOSTATIC TOLERANCE
Cardiovascular deconditioning of cosmonauts: Role, importance and applications of the lower body negative pressure
[ETN-90-97507] N90-28964
OSCILLATING FLOW
Numerical simulations of flowfields in a central-dump ramjet combustor. 3: Effects of chemistry
[AD-A224145] N90-28573
Oscillatory convection
[ESA-TT-890] N90-28801
OSCILLATIONS
Regular and chaotic motion of uniform elliptical vortices in external linear time dependent velocity fields N90-28497
Stabilization of Taylor-Couette flow due to time-periodic outer cylinder oscillation
[PB90-219130] N90-28790
Oscillatory convection
[ESA-TT-890] N90-28801
Effects and tolerances of injection jitter in the SLC and future linear colliders
[DE90-014805] N90-29179
Nonradial instability strips for post-AGB stars
[DE90-014922] N90-29278
OSCILLATORS
Computer simulation of micro-triode performance
[DE90-014191] N90-28774
Dissipative quantum maps
[DE90-627179] N90-29227
Quantum chaos and dissipation: Lyapunov exponents
[DE90-627180] N90-29228
OUTGASSING
Space station contamination modeling
[NASA-CR-183871] N90-28590
OVERVOLTAGE
Use of Ni63 overvoltage gap switches in the flight termination systems on boosters launched from US Army Kwajalein Atoll (USAKA)
[AD-A223666] N90-28661
OXIDATION
A study of catalysts and mechanisms in synthesis reactions
[DE90-015064] N90-28691
Oxidation, sulfidation, and hot corrosion: Mechanisms and interrelationships N90-28702
Scale adherence effects in oxidation and sulfidation N90-28703
Molten salt induced high temperature degradation of thermal barrier coatings N90-28704
High temperature oxidation of Al-Li alloys N90-28705
Fretting wear and fretting fatigue at temperatures up to 600 C N90-28706
Evaluation of high temperature protective coatings for gas turbine engines under simulated service conditions N90-28712
OXIDATION RESISTANCE
NASA Langley Research Center National Aero-Space Plane Mission simulation profile sets
[NASA-TM-102670] N90-28541
Thermal shock and oxidation resistance of ceramic coatings N90-28711
OXIDES
High temperature surface interactions: Overview N90-28699
Dynamical information for Fe doped YBa2Cu3O7 superconducting oxides obtained from high temperature Moessbauer studies
[DE90-627871] N90-29218
OXYGEN
Catalytic ignition of hydrogen/oxygen N90-28627
OXYGEN ANALYZERS
A reliable, maintenance-free oxygen sensor for aircraft using an oxygen-sensitive coating on potentiometric electrodes
[AD-A222696] N90-28545
OXYGEN ATOMS
The effects of atomic oxygen on the thermal emittance of high temperature radiator surfaces
[NASA-TM-103224] N90-28670
Quenching of N(2D) by O(3P)
[AD-A221690] N90-28683
OXYGEN-HYDROCARBON ROCKET ENGINES
Advanced Earth-to-Orbit Propulsion Technology 1988, volume 1
[NASA-CP-3012-VOL-1] N90-28611
Computer code for the prediction of nozzle admittance N90-28630
OZONE
Ozone for trace organic contaminant removal
[PB90-221680] N90-28918
The global cycle of reactive nitrogen
[DE90-015041] N90-28919
Acid deposition: No such thing as a free launch
[DE90-015085] N90-28920
Tropospheric nitrogen: The influence of anthropogenic sources on distributions and deposition, executive summary
[DE90-015401] N90-28922
Present state of knowledge of the upper atmosphere 1990: An assessment report
[NASA-RP-1242] N90-28929
OZONE DEPLETION
Present state of knowledge of the upper atmosphere 1990: An assessment report
[NASA-RP-1242] N90-28929

P

P-3 AIRCRAFT
The reduction of smoke emissions from Allison T56 engines
[ARL-PROP-R-182] N90-28547
PACIFIC OCEAN
Responding to the threat of global warming: Options for the Pacific and Asia
[DE90-014756] N90-28918
PALLADIUM COMPOUNDS
Antiferromagnetism and enhanced heat in CeM2Sn (M = Ni, Ir, Cu, Rh, Pd, and Pt
[DE90-014924] N90-29206
PANEL METHOD (FLUID DYNAMICS)
Study of the ground effects in the CEAT aerohydrodynamic tunnel: Using the results N90-28530
PANELS
Transformational part-count in layered octahedral-tetrahedral truss configurations
[NASA-TM-102635] N90-28598
Study of meteorological processes important in the degradation of materials through surface temperature
[PB90-222720] N90-28856
PARALLEL COMPUTERS
An even-parity/odd-parity formulation for deterministic transport calculations on massively parallel computers
[DE90-015036] N90-29116
PARALLEL PROCESSING (COMPUTERS)
ROSES, a Robot Operating System Expert Scheduler: Methodological framework
[DE90-014782] N90-28851
The effect of multiprocessor radius on scaling
[DE90-014772] N90-29095
Parallelization of a software relating to aerodynamics on MIMD type computers
[ONERA-RT-31/3479-CY] N90-29114
An even-parity/odd-parity formulation for deterministic transport calculations on massively parallel computers
[DE90-015036] N90-29116
Overcoming rule-based rigidity and connectionist limitations through massively-parallel case-based reasoning
[NASA-CR-186963] N90-29117
PARALLEL PROGRAMMING
Concepts of concurrent programming
[AD-A223697] N90-29110
Piecewise linear models of processor utilization
[DE90-014774] N90-29115
PARAMETER IDENTIFICATION
A failure diagnosis system based on a neural network classifier for the space shuttle main engine
[NASA-TM-103607] N90-28659
PARAMETERIZATION
Robust controller design by contraction of a pole region
[ESA-TT-1042] N90-29118

PARITY
An even-parity/odd-parity formulation for deterministic transport calculations on massively parallel computers [DE90-015036] N90-29116
Parity violation and superconductivity in doped Mott insulators [DE90-627493] N90-29217

PARTIAL DIFFERENTIAL EQUATIONS
A hybrid perturbation-Galerkin technique for partial differential equations [NASA-CR-182085] N90-28814
The effect of multiprocessor radius on scaling [DE90-014772] N90-29095
Asymptotic behavior of solutions of diffusion-like partial differential equations invariant to a family of affine groups [DE90-014792] N90-29130
The Cousin problems for an overdetermined system of complex partial differential equations [DE90-627170] N90-29139

PARTICLE ACCELERATORS
PBFA 2 applied B ion diode beam characteristics at high voltages [DE90-014419] N90-29190

PARTICLE BEAMS
Beam diagnostics in circular machines: Review of new developments [DE90-014986] N90-29176

PARTICLE DENSITY (CONCENTRATION)
The affect of gravity on particle collection in inertial impactors [DE90-013372] N90-29173

PARTICLE INTERACTIONS
Ion divergence and the stability of magnetically insulated diodes [DE90-014565] N90-28777

PARTICLE MOTION
Computerized simulation of phenomena in plasma via particles [INPE-4595-RPE/569] N90-29194

PARTICLE PRODUCTION
High energy physics at Tufts University [DE90-014664] N90-29174

PARTICLE SIZE DISTRIBUTION
Micromechanics analysis of power consolidation in manufacturing particulate-reinforced MMCs (metal matrix composites) [DE90-014448] N90-28663

PARTICLE TRAJECTORIES
Unexpected properties of the centrifugal force [DE90-627197] N90-29164

PARTICLES
An experimental investigation of a single and multiphase confined coaxial jet N90-28796

PARTICULATES
Evaluation of several micromechanics models for discontinuously reinforced metal matrix composites [NASA-TM-102719] N90-28872
Estimating the spatial variability of trace gas deposition velocities [PB90-208570] N90-28928

PATENTS
Industrial patent activity in the US. Part 2: Alphabetical listing by company, 1969-1989 [PB90-214412] N90-29246

PATHOGENESIS
Regulation of erythropoiesis in rats during space flight [NASA-CR-177537] N90-29086

PATTERN RECOGNITION
Studies in automatic speech recognition and its application in aerospace N90-28759
Tele-Autonomous control involving contact — object localization [NASA-CR-187004] N90-28854
On-line object feature extraction for multispectral scene representation [NASA-CR-187006] N90-28888
A method of classification for multisource data in remote sensing based on interval-valued probabilities [NASA-CR-187007] N90-28889
Real-time edge tracking using a tactile sensor N90-29023
Perceptual telerobotics N90-29063
Recognition of infrared images. Part 3: The effect of image processing with a size-contrast box filter on observation performance [IZF-1989-39] N90-29182

PAVEMENTS
Development of acceptance plans for airport pavement materials. Volume 1: Development [DOT/FAA/RD-90/15] N90-28581
Development of a thickness design procedure for stabilized layers under rigid airfield pavements [DOT/FAA/RD-90/22] N90-28582

PAYLOADS
ATDRS payload technology research and development [NASA-TM-103256] N90-28596
Development and approach to low-frequency microgravity isolation systems [NASA-TP-2984] N90-28754
Dynamic modeling and payload-adaptation control of a flexible one-link manipulator N90-28843

PEEK
Dissipation of mechanical work and temperature rise in AS4/PEEK thermoplastic composite [NASA-CR-186893] N90-28678
A constitutive model for AS4/PEEK thermoplastic composites under cyclic loading [NASA-CR-180393] N90-28679

PELLETS
Noncontact measurement of high temperature using optical fiber sensors [NASA-CR-186975] N90-28825

PERCEPTION
How do robots take two parts apart N90-29061
Perceptual telerobotics N90-29063
A tesselated probabilistic representation for spatial robot perception and navigation N90-29075

PERCHLORATES
Composite propellants with high burning rates [FOA-C-20781-2.1] N90-28744

PERFORMANCE PREDICTION
Blade tip rubbing stress prediction N90-28615
Developments in test procedures for hot-salt corrosion of superalloys N90-28700

PERFORMANCE TESTS
A look at tomorrow today N90-28524
Validation of the F-18 high alpha research vehicle flight control and avionics systems modifications [NASA-TM-101723] N90-28542
Energy Efficient Engine exhaust mixer model technology report addendum; phase 3 test program [NASA-CR-174799] N90-28556
Energy efficient engine pin fin and ceramic composite segmented liner combustor sector rig test report [NASA-CR-179534] N90-28567
Source emission test of gas turbine engine test facility, Kelly AFB, TX [AD-A223869] N90-28571
Liquid Rocket Booster (LRB) for the Space Transportation System (STS) systems study. Appendix F: Performance and trajectory for ALS/LRB launch vehicles [NASA-CR-183792-APP-F] N90-28606
A comparison of single-cycle versus multi-cycle proof testing strategies N90-28646
Mechanical testing activities related to high-performance structural ceramics [DE90-014299] N90-28734
Communications Interface Driver (CID) test plan [DOT/FAA/CT-TN89/35] N90-28762
Special test and evaluation methods used for a nine-axis accelerometer [PB90-209578] N90-28822
Performance measurements and energy balance of an SPS V160 Stirling motor at the German Aerospace Research Establishment [DLR-MITT-90-03] N90-28903
Air Force Officer Qualifying Test (AFOQT): Development of quick score composites for forms P1 and P2 [AD-A223868] N90-28997
Performance evaluation of a 6 axis high fidelity generalized force reflecting teleoperator N90-29052

PERIPHERAL VISION
Maintaining spatial orientation awareness N90-28993

PERMAFROST
Three functions that model empirically measured unfrozen water content data and predict relative hydraulic conductivity [AD-A223875] N90-28892

PERMEABILITY
Chiral Maxwell-Garnett mixing formula [PB90-189143] N90-29158

PERMITTIVITY
Chiral Maxwell-Garnett mixing formula [PB90-189143] N90-29158

PERSONAL COMPUTERS
The personal computer: An untapped source for the United States Army War College [AD-A223976] N90-29087
A personal computer-based, multitasking data acquisition system [NASA-TM-4232] N90-29107

PERSONNEL
Scientists, engineers, and technicians in nonmanufacturing industries: 1987. (Detailed statistical tables) [PB90-226903] N90-29235

PERSONNEL SELECTION
Air Force Officer Qualifying Test (AFOQT): Development of quick score composites for forms P1 and P2 [AD-A223868] N90-28997

PERTURBATION
Aerodynamics of bodies in shear flow N90-28496
Regular and chaotic motion of uniform elliptical vortices in external linear time dependent velocity fields N90-28497
An investigation of the steady and unsteady near wake and its effect on a laminar boundary layer N90-28794
A hybrid perturbation-Galerkin technique for partial differential equations [NASA-CR-182085] N90-28814
Geometric theory for infinite dimensional systems [ETN-90-96922] N90-29144
The formation of globular clusters N90-29272

PERTURBATION THEORY
Real time guidance and propulsion control for single-stage-to-orbit airbreathing vehicles N90-28587
Formation of magnetic islands due to field perturbations in toroidal stellarator configurations [DE90-014789] N90-29191
Higher loop contributions to effective potential of gauge theory at high temperature [DE90-627208] N90-29231

PESTICIDES
Data Base Analyzer and Parameter Estimator (DBAPE) interactive computer program user's manual [PB90-193053] N90-29252

PHASE DIAGRAMS
Trajectories of renormalization group flows on the phase diagram of N=2 superconformal field theories [DE90-627212] N90-29154
Topology of singularities and phase diagram of N=2 superconformal field theories [DE90-627213] N90-29155

PHASE TRANSFORMATIONS
Evaluation of advanced austenitic alloys relative to alloy design criteria for steam service. Part 1: Lean stainless steel [DE90-014765] N90-28720
The first order phase transition for six-state Potts model on two dimensional random triangle lattice [DE90-627210] N90-29140

PHASED ARRAYS
ATDRS payload technology research and development [NASA-TM-103256] N90-28596

PHOTOCHEMICAL REACTIONS
Tropospheric nitrogen: The influence of anthropogenic sources on distributions and deposition, executive summary [DE90-015401] N90-28922

PHOTOCONDUCTIVITY
Research on stable, large-area, amorphous silicon based submodules, phase 3 [DE90-000339] N90-29204

PHOTODIODES
Radiation effects in InAsSb strained-layer superlattice photodiodes induced by dose-rate and transient x ray environments [DE90-015000] N90-29208

PHOTOELECTRICITY
A fast lightstripe rangefinding system with smart VLSI sensor N90-29019

PHOTOELECTRON SPECTROSCOPY
Preliminary exposure study to determine the effects of acid deposition on coated steel substrates [PB90-201799] N90-28715

PHOTOGRAPHS
Multiband imaging systems [AD-A223969] N90-28893
National Archives preservation research priorities: Past and present [PB90-206210] N90-29242

PHOTOGRAPHY
A manual for analysis of hemispherical canopy photography [DE90-014718] N90-28885

PHOTOINTERPRETATION
Comparison of methods of space color transformations for enhancement of colored images [INPE-4977-PRE/1542] N90-28881

PHOTOIONIZATION
Fifteenth International Conference on X Ray and Inner-Shell Processes [DE90-013024] N90-29170
A plasma diagnostic study of two wind-blown shell nebulae: NGC 7635 and NGC 2359 N90-29271

PHOTOLITHOGRAPHY
Dynamical properties of two-dimensional Josephson junction arrays [AD-A223965] N90-29221

PHOTON BEAMS
Transient annealing characterization of irradiated MOSFETS
[AD-A223877] N90-29220
PHOTONS
Unexpected properties of the centrifugal force
[DE90-627197] N90-29164
PHYSICAL EXERCISE
Joint US/USSR study: Comparison of effects of horizontal and head-down bed rest
[NASA-TP-3037] N90-28965
PHYSICAL WORK
Teleoperator comfort and psychometric stability: Criteria for limiting master-controller forces of operation and feedback during telemanipulation N90-29009
PHYSIOLOGICAL EFFECTS
Further studies of 60 Hz exposure effects on human function
[DE90-014377] N90-28962
PHYSIOLOGICAL RESPONSES
Fluid and electrolyte homeostasis during spaceflight: Elucidation of mechanisms in a primate
[NASA-CR-177548] N90-29085
PHYSIOLOGICAL TESTS
Predicting F/A-18 fleet replacement squadron performance using an automated battery of performance-based tests
[AD-A223899] N90-28543
PHYSIOLOGY
Joint US/USSR study: Comparison of effects of horizontal and head-down bed rest
[NASA-TP-3037] N90-28965
PILOT ERROR
Spatial disorientation incidents in the RNLAF F16 and F5 aircraft and suggestions for prevention N90-28973
Loss of alertness and consciousness from pilot position during long range flight N90-28990
PILOT PERFORMANCE
Situational Awareness in Aerospace Operations
[AGARD-CP-478] N90-28972
Spatial disorientation incidents in the RNLAF F16 and F5 aircraft and suggestions for prevention N90-28973
A methodology for the objective measurement of pilot situation awareness N90-28974
Performance-based measures of merit for tactical situation awareness N90-28976
Evaluation of the Situational Awareness Rating Technique (SART) as a tool for aircrew systems design N90-28977
Attention gradients in situation awareness N90-28978
Towards a future cockpit: The prototyping and pilot integration of the Mission Management Aid (MMA) N90-28979
The three-dimensional structure of visual attention and its implications for display design N90-28980
Counterair situation awareness display for Army aviation N90-28982
The simulation of localized sounds for improved situational awareness N90-28984
The effects of acoustic orientation cues on instrument flight performance in a flight simulator N90-28985
Experimental tests on the minimal visual acuity required for safe air crew and air control personnel performance N90-28987
Loss of alertness and consciousness from pilot position during long range flight N90-28990
Evaluation of the performance capability of the aviator under hypoxic conditions operational experience N90-28991
Effects of short-term weightlessness on roll circularvection N90-28992
Maintaining spatial orientation awareness N90-28993
Proprioception in aircraft control
[IZF-1989-43] N90-29082
PILOT SELECTION
Predicting F/A-18 fleet replacement squadron performance using an automated battery of performance-based tests
[AD-A223899] N90-28543
PILOT TRAINING
Predicting F/A-18 fleet replacement squadron performance using an automated battery of performance-based tests
[AD-A223899] N90-28543
Maintaining spatial orientation awareness N90-28993
PIONEER VENUS SPACECRAFT
A survey of planning and scheduling research at the NASA Ames Research Center N90-29076
PIPELINING (COMPUTERS)
Implementation and design of a teleoperation system based on a VMEBUS/68020 pipelined architecture N90-29053
PIPES (TUBES)
Behavior of aramid/epoxy wounded tubes under uniaxial and biaxial loading
[ETCA-89-R-150] N90-28873
PITCHING MOMENTS
Study of the ground effects in the CEAT aerohydrodynamic tunnel: Using the results N90-28530
PLANE WAVES
Electromagnetic scattering from two-dimensional thick material junctions
[NASA-CR-186468] N90-28767
PLANETARY ATMOSPHERES
Infrared spectroscopic measurements on planetary atmospheric gases N90-29283
PLANETARY BOUNDARY LAYER
Diffusion in the surface layer of the convective boundary layer
[AD-A224125] N90-28924
PLANETARY EVOLUTION
Near-infrared speckle observations of T Tauri stars and a multi-wavelength study of the prototype star T Tauri N90-29264
PLANETARY MAPPING
The Magellan Venus explorer's guide
[NASA-CR-186966] N90-28592
First results in terrain mapping for a roving planetary explorer N90-29066
PLANETARY NEBULAE
The ionization structure of planetary nebulae 10: NGC 2392
[NASA-CR-186960] N90-29274
PLANETARY SURFACES
A system architecture for a planetary rover N90-29015
Planetary rover technology development requirements N90-29067
PLANNING
Integrating planning and reactive control N90-29077
Integrating planning, execution, and learning N90-29079
PLANTS (BOTANY)
Flora and threatened and endangered plants of John F. Kennedy Space Center, Florida
[NASA-TM-102791] N90-28925
PLASMA ARC WELDING
Robotic and automatic welding development at the Marshall Space Flight Center N90-28656
PLASMA CONTROL
Physics of the L to H transition in DIII-D
[DE90-014120] N90-29187
Temperature-gradient instability induced by conducting end walls
[DE90-014334] N90-29188
Stellarator status, 1989
[DE90-014791] N90-29192
PLASMA CURRENTS
Combined electron cyclotron ray tracing and transport code studies in the compact ignition tokamak
[DE90-014097] N90-29189
PLASMA DIAGNOSTICS
High power arcjet
[NASA-CR-183066] N90-28658
PBFA 2 applied B ion diode beam characteristics at high voltages
[DE90-014419] N90-29190
Computerized simulation of phenomena in plasma via particles
[INPE-4595-RPE/569] N90-29194
PLASMA DIODES
Unipolar arcing on the cathode surface of a high voltage diode
[AD-A224122] N90-28787
PLASMA DYNAMICS
Statement of research objectives and summary of research efforts
[RLE-PR-132] N90-29295
PLASMA OSCILLATIONS
Computerized simulation of phenomena in plasma via particles
[INPE-4595-RPE/569] N90-29194
PLASMA PHYSICS
Physics of the L to H transition in DIII-D
[DE90-014120] N90-29187
PLASMA SPRAYING
Vacuum application of thermal barrier plasma coatings N90-28653
PLASMA WAVES
Electron acoustic and magnetoacoustic modes in a magnetized beam plasma system
[DE90-627473] N90-29199
PLASMAS (PHYSICS)
Computerized simulation of phenomena in plasma via particles
[INPE-4595-RPE/569] N90-29194
Ignition and burn control characteristics of thermonuclear plasmas
[DE90-015385] N90-29197
Measurement of gravitational acceleration of antimatter
[DE90-627464] N90-29233
A plasma diagnostic study of two wind-blown shell nebulae: NGC 7635 and NGC 2359 N90-29271
Theoretical studies of proton beams in solar flare loops N90-29286
PLASMASPHERE
New Voyager radio spectrograms of Uranus
[NASA-CR-180381] N90-29284
PLASTIC DEFORMATION
Micromechanics of cyclic deformation in SSME turbopump blade materials N90-28841
Microstructure: Property correlation --- multiaxial fatigue damage evolution in waspaloy
[NASA-CR-180406] N90-28880
PLATES (STRUCTURAL MEMBERS)
A nonlinear finite element formulation for the large displacement analysis of plates N90-28867
PLATING
Electrodeposition of wear resistant coatings
[PB90-221839] N90-28732
PLATINUM
Structure of metal overlayers by low energy alkali ion scattering: Cu/Ru(0001) and Sn/Pt(111)
[DE90-014453] N90-28718
PLATINUM COMPOUNDS
Antiferromagnetism and enhanced heat in CeM2Sn (M = Ni, Ir, Cu, Rh, Pd, and Pt
[DE90-014924] N90-29206
Evidence for a coherence gap in Ce3Bi4Pt3
[DE90-014925] N90-29207
PLOTTERS
A computer graphics package
[ARE-TM(UDT)-89111] N90-29094
PLOTTING
A computer graphics package
[ARE-TM(UDT)-89111] N90-29094
POINT SOURCES
An infrared sky model based on the IRAS point source data
[NASA-CR-177526] N90-29265
POLARIZED LIGHT
Near-infrared speckle observations of T Tauri stars and a multi-wavelength study of the prototype star T Tauri N90-29264
POLICIES
State science and technology indicators: An exploratory profile and analysis
[PB90-246711] N90-29259
POLLUTION CONTROL
National air quality and emissions trends report, 1988
[PB90-200114] N90-28909
POLLUTION MONITORING
The distribution of middle tropospheric carbon monoxide during early October 1984
[NASA-TM-103485] N90-28906
POLYCARBONATES
Some studies of the vibration welding of thermoplastics N90-28842
POLYCRYSTALS
Mechanical property measurement of polycrystalline diamond films
[AD-A224037] N90-29222
POLYETHYLENES
Technical bibliography of high performance polyethylene fibers
[SNPE-NT-106/89/GTR/RP/NP] N90-28736
POLYHEDRONS
Investigation of maximum achievable body torque for a walking machine with friction cone constraints
[PB90-203175] N90-28838
POLYIMIDES
Evaluations of new polyimide films for flexible circuit applications at EG and G Mound Applied Technologies
[DE90-014117] N90-28731
POLYMER MATRIX COMPOSITES
Development of testing and analysis methodology to assess the long term durability of polymeric composites at high temperatures
[NASA-TM-102714] N90-28871
POLYMERIC FILMS
A reliable, maintenance-free oxygen sensor for aircraft using an oxygen-sensitive coating on potentiometric electrodes
[AD-A222696] N90-28545
POLYMERIZATION
Polymer research
[PB90-246638] N90-28737
POLYNOMIALS
Product integration rules at Clenshaw-Curtis and related points: A robust implementation
[DE90-627158] N90-29106

The center of the enveloping algebra of the semidirect product of the Heisenberg lie algebra h(sub n) and a reductive Lie algebra S the rank of which is equal to 1 or 2
[DE90-627155] N90-29133
Recurrence relations and weight functions for approximation by orthonormal polynomials
[DE90-627156] N90-29134

POLYPROPYLENE
Some studies of the vibration welding of thermoplastics N90-28842

POROSITY
The fatigue damage behavior of a single crystal superalloy N90-28644
A new low density, high porosity lithium hydride-beryllium hydride foam
[DE90-015150] N90-28739

POROUS MATERIALS
Asymptotic behavior of solutions of diffusion-like partial differential equations invariant to a family of affine groups
[DE90-014792] N90-29130

POSITION (LOCATION)
Using the x ray region of the electromagnetic spectrum for alignment: Overview, geometric optics, and design considerations
[DE90-014798] N90-28752
Study of the relationships between radar structure and the electrical activity of clouds
[ETN-90-97488] N90-28946
Kinematics, controls, and path planning results for a redundant manipulator N90-29005
Methods and strategies of object localization N90-29020
Robot Acting on Moving Bodies (RAMBO): Interaction with tumbling objects N90-29022
Real-time edge tracking using a tactile sensor N90-29023
Map learning with indistinguishable locations N90-29025
Satellite-map position estimation for the Mars rover N90-29089
An improved method for choosing sampling points for the inspection of complex surfaces in a computer-aided manufacturing environment N90-29093

POSITION SENSING
Tele-Autonomous control involving contact --- object localization
[NASA-CR-187004] N90-28854

POSITIONING
Measurement of hand dynamics in a microsurgery environment: Preliminary data in the design of a bimanual telemicro-operation test bed N90-29010

POSTURE
Motion coordination for mobile robots in unstructured environments
[PB90-199498] N90-28837

POTABLE WATER
Ozone for trace organic contaminant removal
[PB90-221680] N90-28916

POTENTIAL FLOW
Flow coupling between a rotor and a stator in turbomachinery
[AD-A223882] N90-28572

POTENTIAL THEORY
Higher loop contributions to effective potential of gauge theory at high temperature
[DE90-627208] N90-29231

POTENTIOMETRIC ANALYSIS
A reliable, maintenance-free oxygen sensor for aircraft using an oxygen-sensitive coating on potentiometric electrodes
[AD-A222696] N90-28545

POWDER METALLURGY
Micromechanics analysis of power consolidation in manufacturing particulate-reinforced MMCs (metal matrix composites)
[DE90-014448] N90-28563
Micromechanisms of fatigue crack growth and fracture toughness in metal matrix composites
[AD-A223863] N90-28676

POWDERED ALUMINUM
High energy-density liquid rocket fuel performance
[NASA-CR-185279] N90-28742

POWER BEAMING
Analysis of vibrational power transmission through a beam system including a flexible section
[ISVR-TR-176] N90-28875

POWER EFFICIENCY
Energy Efficient Engine exhaust mixer model technology report addendum; phase 3 test program
[NASA-CR-174799] N90-28556

POWER LINES
Characterization of electron flow in positive-polarity linear-induction accelerators
[DE90-014998] N90-29177

PRE-MAIN SEQUENCE STARS
Near-infrared speckle observations of T Tauri stars and a multi-wavelength study of the prototype star T Tauri N90-29264

PRECIPITATION (METEOROLOGY)
Daily temperature, solar radiation, wind speed, cloud cover, and precipitation data recorded at the meteorological station for calendar years 1957--1988
[DE90-014399] N90-28941

PRECIPITATION HARDENING
Density changes of generation 1.5 and 2.0 copper alloys irradiated at 411 to 414 C and 529 C in FFTF-MOTA
[DE90-015291] N90-28724

PREDICTION ANALYSIS TECHNIQUES
Prediction of subsonic vortex shedding from forebodies with chines
[NASA-CR-4323] N90-28494
Control research in the NASA high-alpha technology program N90-28516
Unsteady aerodynamics of controls N90-28525
Flow coupling between a rotor and a stator in turbomachinery
[AD-A223882] N90-28572
High temperature fatigue behavior of Haynes 188 N90-28642
Constitutive and life modeling of single crystal blade alloys for root attachment analysis N90-28643
The fatigue damage behavior of a single crystal superalloy N90-28644
Probabilistic model for fracture mechanics service life analysis N90-28650
Thermal analysis of thermal barrier coatings in a high heat flux environment N90-28652

PREMIXED FLAMES
The spatial scalar structure of premixed turbulent stagnation point flames
[DE90-014189] N90-28686

PREPREGS
Radiation-curable prepreg composites
[DE90-629740] N90-28674

PRESERVING
National Archives preservation research priorities: Past and present
[PB90-206210] N90-29242

PRESIDENTIAL REPORTS
Federal support to universities, colleges, and selected nonprofit institutions: Fiscal year 1988 (detailed statistical tables)
[PB90-226887] N90-29236

PRESSURE DISTRIBUTION
Study of the ground effects in the CEAT aerohydrodynamic tunnel: Using the results N90-28530
Measurement of the steady surface pressure distribution on a single rotation large scale advanced prop-fan blade at Mach numbers from 0.03 to 0.78
[NASA-CR-182124] N90-28552
Military aircrew seating: A human factors engineering approach
[AD-A218049] N90-28999

PRESSURE DRAG
Sting-support interference on afterbody drag at transonic speeds
[NAL-TM-EA-8902] N90-28492

PRESSURE EFFECTS
Liquid Rocket Booster (LRB) for the Space Transportation System (STS) systems study. Appendix A: Stress analysis report for the pump-fed and pressure-fed liquid rocket booster
[NASA-CR-183787-APP-A] N90-28601

PRESSURE MEASUREMENT
In-flight flow visualization with pressure measurements at low speeds on the NASA F-18 high alpha research vehicle
[NASA-TM-101726] N90-28505
Determination of the ground effect on the characteristics of the A320 aircraft N90-28534
Gas-jet and tangent-slot film cooling tests of a 12.5 deg cone at Mach number of 6.7
[NASA-TP-2786] N90-28806

PRESSURE SENSORS
A reliable, maintenance-free oxygen sensor for aircraft using an oxygen-sensitive coating on potentiometric electrodes
[AD-A222696] N90-28545

PRESSURE VESSELS
Fabrication of spherical pressure vessels from composite materials
[INPE-4598-RPE/570] N90-28675
Guidelines for pressure vessel safety assessment
[PB90-219619] N90-28749

PRIMATES
Time, space and form in vision
[AD-A213889] N90-28971

PRINTED CIRCUITS
Simulation of INPE's printed circuit laboratory production line
[INPE-4556-TDL/331] N90-28784

PRINTING
A computer graphics package
[ARE-TM(UDT)-89111] N90-29094

PRIORITIES
National Archives preservation research priorities: Past and present
[PB90-206210] N90-29242

PROBABILITY THEORY
Probabilistic structural analysis methods development for SSME N90-28616
Probability models for the failure of fibres and fibrous composite materials N90-28665
A method of classification for multisource data in remote sensing based on interval-valued probabilities
[NASA-CR-187007] N90-28889
Multiresolutional models of uncertainty generation and reduction N90-29043

PROBLEM SOLVING
Parametric solution of nonlinear structure problems
[ONERA-RT-21/3542-RY-082-R] N90-28874
Learned navigation in unknown terrains: A retraction method N90-29029
State-based scheduling: An architecture for telescope observation scheduling N90-29038
Approximation algorithms for planning and control N90-29042
A tesselated probabilistic representation for spatial robot perception and navigation N90-29075
A user modelling approach for computer-based critiquing
[AD-A224042] N90-29088
Documenting the decision structure in software development
[NASA-CR-186865] N90-29108
Technical writing for software engineers
[AD-A223872] N90-29109
Asymptotics of Laplace-Dirichlet integrals
[DE90-627165] N90-29137
The Cousin problems for an overdetermined system of complex partial differential equations
[DE90-627170] N90-29139

PROCESS CONTROL (INDUSTRY)
Adjustable speed drive applications guidebook
[DE90-014151] N90-28780

PROCUREMENT
Preparing software conversion studies
[PB90-235623] N90-29099

PRODUCT DEVELOPMENT
Application of integrated optical components in optical fiber communication
[FEL-89-B252] N90-29183

PRODUCTION
Long-range plan for a research project on carbon monoxide production and prediction
[PB90-209602] N90-28910

PRODUCTION MANAGEMENT
Quality function deployment as a mechanism for process characterization and control
[DE90-014755] N90-28857

PROJECT MANAGEMENT
Procedures for DOE-Navy exchange and approval of engineering information and material management required for production of W88-0/Mk5 RBA (reentry body assembly)
[DE90-014763] N90-28595
A FAA Technical Center project transition plan: Mode S
[DOT/FAA/CT-TN90/17] N90-28765
Long-range plan for a research project on carbon monoxide production and prediction
[PB90-209602] N90-28910
Planetary rover technology development requirements N90-29067

PROJECT PLANNING
A FAA Technical Center project transition plan: Mode S
[DOT/FAA/CT-TN90/17] N90-28765
Long-range plan for a research project on carbon monoxide production and prediction
[PB90-209602] N90-28910
A survey of planning and scheduling research at the NASA Ames Research Center N90-29076

PROJECTILES
Projectile supersonic drag characteristics
[AD-A224217] N90-28506

PROP-FAN TECHNOLOGY
Measurement of the steady surface pressure distribution on a single rotation large scale advanced prop-fan blade at Mach numbers from 0.03 to 0.78
[NASA-CR-182124] N90-28552

PROPELLANT ADDITIVES
High energy-density liquid rocket fuel performance
[NASA-CR-185279] N90-28742
PROPELLANT COMBUSTION
Energy Efficient Engine (E3) combustion system component technology performance report
[NASA-CR-168274] N90-28555
Oxygen/methane combustion stability investigation N90-28628
Combustion instability coupling with feed system acoustics N90-28629
Tripropellant combustion process N90-28631
High/variable mixture ratio oxygen/hydrogen engines N90-28637
High energy-density liquid rocket fuel performance
[NASA-CR-185279] N90-28742
Evaluation of the STM4-120 kinematic Stirling engine
[DE90-013836] N90-28897
PROPELLER BLADES
Vortice-propeller interaction
[LIMSI-89-9] N90-28809
PROPELLER NOISE
Annoyance caused by advanced turboprop aircraft flyover noise: Counter-rotating-propeller configuration
[NASA-TP-3027] N90-29166
PROPORTIONAL COUNTERS
X ray spectra of cataclysmic variables
[NASA-CR-187002] N90-29280
PROPRIOCEPTION
Proprioception in aircraft control
[IZF-1989-43] N90-29082
PROPULSION
STOVL fighter propulsion reliability, maintainability, and supportability characterization
[AD-A224221] N90-28574
Real time guidance and propulsion control for single-stage-to-orbit airbreathing vehicles N90-28587
Operational cost drivers N90-28636
PROPULSION SYSTEM CONFIGURATIONS
Liquid Rocket Booster (LRB) for the Space Transportation System (STS) systems study. Appendix B: Liquid rocket booster acoustic and thermal environments
[NASA-CR-183788-APP-B] N90-28602
High/variable mixture ratio O2/H2 engine N90-28638
PROPULSION SYSTEM PERFORMANCE
Propulsion system-flight control integration and optimization: Flight evaluation and technology transition
[NASA-TM-4207] N90-28551
Liquid Rocket Booster (LRB) for the Space Transportation System (STS) systems study. Appendix B: Liquid rocket booster acoustic and thermal environments
[NASA-CR-183788-APP-B] N90-28602
Effects of friction and end losses on MHD thruster efficiency
[DE90-013673] N90-28608
Advanced Earth-to-Orbit Propulsion Technology 1988, volume 1
[NASA-CP-3012-VOL-1] N90-28611
Low power arcjet performance
[NASA-TM-103260] N90-28657
PROPULSIVE EFFICIENCY
Energy Efficient Engine (E3) combustion system component technology performance report
[NASA-CR-168274] N90-28555
Energy Efficient Engine core design and performance report
[NASA-CR-168069] N90-28559
Energy Efficient Engine integrated core/low spool test hardware design report
[NASA-CR-168137] N90-28566
Energy Efficient Engine: High-pressure compressor test hardware detailed design report
[NASA-CR-180850] N90-28570
Effects of friction and end losses on MHD thruster efficiency
[DE90-013673] N90-28608
PROTECTIVE COATINGS
Molten salt induced high temperature degradation of thermal barrier coatings N90-28704
Effect of protective coatings on mechanical properties of superalloys N90-28707
High temperature protective coatings: Recent trends N90-28710
Evaluation of high temperature protective coatings for gas turbine engines under simulated service conditions N90-28712
Overview on hot gas tests and molten salt corrosion experiments at the DLR N90-28714
Preliminary exposure study to determine the effects of acid deposition on coated steel substrates
[PB90-201799] N90-28715
Electrodeposition of wear resistant coatings
[PB90-221839] N90-28732
Use of electron spectroscopies in the tribological evaluation of diamond films
[DE90-014421] N90-28848
PROTEIN SYNTHESIS
Insulin and insulin-like growth factor-1 induce pronounced hypertrophy of skeletal myofibers in tissue culture
[NASA-CR-187026] N90-28960
PROTOCOL (COMPUTERS)
Secure Data Network System (SDNS) network, transport, and message security protocols
[PB90-196946] N90-28757
Coordinating the activities of a planner and an execution agent N90-29035
PROTONS
Theoretical studies of proton beams in solar flare loops N90-29286
PROTOTYPES
Extended range tankless water heater
[DE90-014474] N90-28750
A laser spectrometer and wavemeter for pulsed lasers
[NASA-CR-181731] N90-28832
PSYCHOACOUSTICS
Complex auditory signals
[AD-A224127] N90-28969
Annoyance caused by advanced turboprop aircraft flyover noise: Counter-rotating-propeller configuration
[NASA-TP-3027] N90-29166
PSYCHOLOGY
Human factors evaluation and validation criteria for quality training programs: Development, presentation, and assessment
[DE90-014724] N90-29081
PSYCHOMOTOR PERFORMANCE
Predicting F/A-18 fleet replacement squadron performance using an automated battery of performance-based tests
[AD-A223899] N90-28543
Evaluation of the performance capability of the aviator under hypoxic conditions operational experience N90-28991
PSYCHOPHYSICS
Complex auditory signals
[AD-A224127] N90-28969
Auditory processing of complex sounds across frequency channels
[AD-A224147] N90-28970
Time, space and form in vision
[AD-A213889] N90-28971
Statement of research objectives and summary of research efforts
[RLE-PR-132] N90-29295
PUBLIC HEALTH
Further studies of 60 Hz exposure effects on human function
[DE90-014377] N90-28962
PULSARS
Kappa effect pulsational instability for hot extreme helium stars
[DE90-014920] N90-29277
Pulsations of B star models by an opacity mechanism
[DE90-014923] N90-29279
Gamma ray evidence for cosmic ray sources N90-29292
PULSED LASERS
A laser spectrometer and wavemeter for pulsed lasers
[NASA-CR-181731] N90-28832
Tunable CW single-frequency source for injection seeding 2-micrometer lasers
[AD-A223979] N90-28834
PYROMETERS
Noncontact measurement of high temperature using optical fiber sensors
[NASA-CR-186975] N90-28825

Q

QUALITY CONTROL
Development of acceptance plans for airport pavement materials. Volume 1: Development
[DOT/FAA/RD-90/15] N90-28581
Adjustable speed drive applications guidebook
[DE90-014151] N90-28780
Automated system for meteorological analysis
[INPE-4586-TDL/332] N90-28945
Human factors evaluation and validation criteria for quality training programs: Development, presentation, and assessment
[DE90-014724] N90-29081
QUANTUM CHEMISTRY
Accurate quantum chemical calculations
[NASA-TM-101932] N90-28680
QUANTUM EFFICIENCY
Research on high-efficiency, multiple-gap, multi-junction amorphous silicon-based alloy thin-film solar cells
[DE90-000338] N90-28896
QUANTUM ELECTRODYNAMICS
Introduction to gauge theories and unification
[DE90-014473] N90-29225
QUANTUM ELECTRONICS
The III-V semiconductor quantum well lasers and related optoelectronic devices on silicon
[AD-A224120] N90-28835
Statement of research objectives and summary of research efforts
[RLE-PR-132] N90-29295
QUANTUM MECHANICS
Dissipative quantum maps
[DE90-627179] N90-29227
Quantum chaos and dissipation: Lyapunov exponents
[DE90-627180] N90-29228
Old and new ideas in the theory of quantum measurement
[DE90-627181] N90-29229
QUANTUM THEORY
Wigner symbols, quantum dynamics, and the kicked rotator
[AD-A224024] N90-29234
QUANTUM WELLS
The III-V semiconductor quantum well lasers and related optoelectronic devices on silicon
[AD-A224120] N90-28835
QUASI-STEADY STATES
Numerical and analytical study of nonlinear bifurcations associated with the morphological stability of two-dimensional single crystals
[PB90-209594] N90-29200
QUATERNIONS
Geometrical properties of an internal local octonionic space in a non-Riemannian manifold
[DE90-627175] N90-29149
QUENCHING (ATOMIC PHYSICS)
Quenching of N(2D) by O(3P)
[AD-A221690] N90-28683

R

RADAR
Using embedded microcontrollers in radar test equipment
[DE90-014997] N90-28763
Target detection in Gaussian noise using artificial neural systems
[AD-A223983] N90-28770
RADAR ANTENNAS
Target signature modeling and bistatic scattering measurement studies
[NASA-CR-186611] N90-28766
RADAR DATA
Study of the relationships between radar structure and the electrical activity of clouds
[ETN-90-97488] N90-28946
A personal computer-based, multitasking data acquisition system
[NASA-TM-4232] N90-29107
RADAR MAPS
The Magellan Venus explorer's guide
[NASA-CR-186968] N90-28592
RADAR SCATTERING
Target signature modeling and bistatic scattering measurement studies
[NASA-CR-186611] N90-28766
RADAR SIGNATURES
Target signature modeling and bistatic scattering measurement studies
[NASA-CR-186611] N90-28766
RADAR TARGETS
Target detection in Gaussian noise using artificial neural systems
[AD-A223983] N90-28770
RADAR TRACKING
User's manual ROBIN: A research and notification system for bird migration
[FEL-1989-103] N90-28508
RADAR TRANSMITTERS
Ground-based weather radar compatibility with digital radio-relay microwave systems
[PB90-206236] N90-28756
RADIANT FLUX DENSITY
Energy transmission by means of coherent quasi-mono-chromatic light beams N90-29163
RADIATION DAMAGE
Use of Ni63 overvoltage gap switches in the flight termination systems on boosters launched from US Army Kwajalein Atoll (USAKA)
[AD-A223866] N90-28661
RADIATION DETECTORS
Enrichment services for chromium isotopes for the GALLEX (gallium experiment) international collaboration experiment on solar neutrino flux
[DE90-014300] N90-29285

RADIATION DISTRIBUTION
Propagation of electromagnetic radiation in a random field of gravitational waves and space radio interferometry
[DE90-627196] N90-28764
Fluctuations in cosmic background radiation
[INPE-4579-PRE/1313] N90-29294

RADIATION DOSAGE
Further studies of 60 Hz exposure effects on human function
[DE90-014377] N90-28962
Comparison of dose estimates using the buildup-factor method and a Baryon transport code (BRYNTRN) with Monte Carlo results
[NASA-TP-3021] N90-29290

RADIATION EFFECTS
Density changes of generation 1.5 and 2.0 copper alloys irradiated at 411 to 414 C and 529 C in FFTF-MOTA
[DE90-015291] N90-28724
Bandwidth and signal-to-noise ratio enhancement of the NPS transient electromagnetic scattering laboratory
[AD-A224144] N90-28771
Natural and anthropogenic climate change
[DE90-015528] N90-28923
Radiation effects in InAsSb strained-layer superlattice photodiodes induced by dose-rate and transient x ray environments
[DE90-015000] N90-29208
Transient annealing characterization of irradiated MOSFETS
[AD-A223877] N90-29220

RADIATION SHIELDING
Comparison of dose estimates using the buildup-factor method and a Baryon transport code (BRYNTRN) with Monte Carlo results
[NASA-TP-3021] N90-29290

RADIATION SOURCES
Gamma ray evidence for cosmic ray sources
N90-29292

RADIATION TRANSPORT
An even-parity/odd-parity formulation for deterministic transport calculations on massively parallel computers
[DE90-015036] N90-29116
Comparison of dose estimates using the buildup-factor method and a Baryon transport code (BRYNTRN) with Monte Carlo results
[NASA-TP-3021] N90-29290
Predictions of radiation backgrounds for GRO/OSSE
[RAE-TM-SPACE-372] N90-29293

RADIATIVE HEAT TRANSFER
Radiative heat transfer
[PB90-247602] N90-28813

RADIATIVE LIFETIME
UV-induced degradation of the Si-SiO2 interface: Applications to the point contact solar cell
[DE90-013843] N90-28898

RADIO ASTRONOMY
New Voyager radio spectrograms of Uranus
[NASA-CR-180381] N90-29284
Radio outbursts in extragalactic sources N90-29291
Statement of research objectives and summary of research efforts
[RLE-PR-132] N90-29295

RADIO ATTENUATION
Rain-fade simulation and power augmentation for satellite communication systems
[NASA-TM-103134] N90-28768

RADIO BURSTS
Radio outbursts in extragalactic sources N90-29291

RADIO COMMUNICATION
Design and performance of a long, over-water microwave radio link
[PB90-207994] N90-28758
Rain-fade simulation and power augmentation for satellite communication systems
[NASA-TM-103134] N90-28768

RADIO FREQUENCIES
A radio frequency user's guide to the space environment services center geophysical alert broadcasts
[PB90-240631] N90-28935
RF power generation for future linear colliders
[DE90-014804] N90-29178

RADIO OBSERVATION
New Voyager radio spectrograms of Uranus
[NASA-CR-180381] N90-29284

RADIO RELAY SYSTEMS
Ground-based weather radar compatibility with digital radio-relay microwave systems
[PB90-206236] N90-28756

RADIO WAVES
RF power generation for future linear colliders
[DE90-014804] N90-29178

RADIOACTIVE ISOTOPES
Use of Ni63 overvoltage gap switches in the flight termination systems on boosters launched from US Army Kwajalein Atoll (USAKA)
[AD-A223866] N90-28661
Moessbauer Effect applications using intense radioactive ion beams
[DE90-014981] N90-29175

RADIOACTIVITY
Predictions of radiation backgrounds for GRO/OSSE
[RAE-TM-SPACE-372] N90-29293

RADIOBIOLOGY
Biomedical and environmental sciences program publications, 1989
[DE90-014785] N90-29250

RADIOMETERS
Technical activities 1989, Electron and Optical Physics Division
[PB90-207267] N90-29296

RAIL TRANSPORTATION
On the application of similarity laws to a scaled railway bogie model
[DLR-FB-90-06] N90-28853

RAIN
A nonhydrostatic numerical model in sigma-coordinates and simulations of mesoscale phenomena N90-28932
Annual course of precipitation over much of the US: Observed versus GCM simulation
[PB90-221656] N90-28942

RAIN FORESTS
Study of anomalies in transition vegetation in Alto Xingo-NT, through remote sensing techniques
[INPE-4601-TDL/334] N90-28891

RAMAN SPECTROSCOPY
Study of the radical OH in a high pressure flame by resonant DRASC
[ONERA-RF-57/7131-PY] N90-28692

RAMJET ENGINES
Numerical simulations of flowfields in a central-dump ramjet combustor. 3: Effects of chemistry
[AD-A224145] N90-28573

RANGEFINDING
Velocity filtering applied to optical flow calculations
[NASA-TM-102802] N90-28512
A fast lightstripe rangefinding system with smart VLSI sensor N90-29019
A laser tracking dynamic robot metrology instrument N90-29021

RASTER SCANNING
Fast interactive image generation of line and surface oriented objects in raster systems
[ETN-90-97290] N90-29102

RATINGS
Proceedings of a workshop on Future Airport Passenger Terminals
[PB90-213620] N90-28580

RAY TRACING
Combined electron cyclotron ray tracing and transport code studies in the compact ignition tokamak
[DE90-014097] N90-29189

RDX
Study of the induction time in isothermal decomposition of explosives
[DE90-014906] N90-28745

REACTION KINETICS
Numerical simulations of flowfields in a central-dump ramjet combustor. 3: Effects of chemistry
[AD-A224145] N90-28573
Quenching of N(2D) by O(3P)
[AD-A221690] N90-28683
The spatial scalar structure of premixed turbulent stagnation point flames
[DE90-014189] N90-28686
Analyses of spray and droplet ignition for pure and multicomponent fuels N90-28688
Evaluation of a hybrid kinetics/mixing-controlled combustion model for turbulent premixed and diffusion combustion using KIVA-2
[NASA-TM-103196] N90-28792
Numerical simulation of reactive turbulent flows
[ETN-90-97476] N90-28807

REACTIVITY
Reflection Mass Spectrometry (REMS) during 3/5 MBE
[DE90-014568] N90-28690
The global cycle of reactive nitrogen
[DE90-015041] N90-28919

REACTOR MATERIALS
Density changes of generation 1.5 and 2.0 copper alloys irradiated at 411 to 414 C and 529 C in FFTF-MOTA
[DE90-015291] N90-28724
Helium generation in fusion reactor materials
[DE90-013005] N90-29172

READ-ONLY MEMORY DEVICES
Optical storage technology
[AD-A224028] N90-29254

REAL TIME OPERATION
Real time guidance and propulsion control for single-stage-to-orbit airbreathing vehicles N90-28587
Using the x ray region of the electromagnetic spectrum for alignment: Overview, geometric optics, and design considerations
[DE90-014798] N90-28752
Real-time aerodynamic heating and surface temperature calculations for hypersonic flight simulation
[NASA-TM-4222] N90-28815
A laser spectrometer and wavemeter for pulsed lasers
[NASA-CR-181731] N90-28832
Experiments in the dynamic and strategic control of cooperating manipulators N90-28845
Solutions to the frictional dynamics problem and the reciprocal variable feedback methodology for design and control of robot mechanisms N90-28846
A real time evaluation of the use of a perspective format to promote situational awareness in users of air to air tactical displays N90-28981
A 17 degree of freedom anthropomorphic manipulator N90-29001
Real-time edge tracking using a tactile sensor N90-29023
Coordinating the activities of a planner and an execution agent N90-29035
Perceptual telerobotics N90-29063
Parallel algorithms for computation of the manipulator inertia matrix N90-29072
An expert system to perform on-line controller restructuring for abrupt model changes
[NASA-TM-103609] N90-29121

RECONNAISSANCE
Space-base multispectral imagery: Current and future applications and implications to the United States Army
[AD-A224046] N90-28894

RECRYSTALLIZATION
Behavior of Al-Mg alloys in hot working and superplasticity
[DE90-015193] N90-28723

RECTANGULAR PLATES
Buckling and postbuckling behavior of compression-loaded isotropic plates with cutouts
[NASA-TP-3024] N90-28859
A nonlinear finite element formulation for the large displacement analysis of plates N90-28867

RECURSIVE FUNCTIONS
Recursive least-squares learning algorithms for neural networks
[DE90-014926] N90-29096

REDUCED GRAVITY
Microgravity science and applications: Apparatus and facilities
[NASA-TM-101892] N90-28588
Containerless low gravity processing of glass forming and immiscible alloys
[NASA-CR-186999] N90-28747
Development and approach to low-frequency microgravity isolation systems
[NASA-TP-2984] N90-28754
Design of a CO2 laser power control system for a Spacelab microgravity experiment
[NASA-TM-103112] N90-28833
Cardiovascular deconditioning of cosmonauts: Role, importance and applications of the lower body negative pressure
[ETN-90-97507] N90-28964
Fluid and electrolyte homeostasis during spaceflight: Elucidation of mechanisms in a primate
[NASA-CR-177548] N90-29085
Microgravitation experiments in space: Compatibility with interfering dynamic influences N90-29162

REDUNDANCY
Combat aircraft control requirements N90-28515
Motion coordination for mobile robots in unstructured environments
[PB90-199498] N90-28837
A new approach to global control of redundant manipulators N90-29002
Cartesian control of redundant robots N90-29004
Kinematics, controls, and path planning results for a redundant manipulator N90-29005
Control of intelligent robots in space N90-29013
Multiple cooperating manipulators: The case of kinematically redundant arms N90-29046
Preliminary study of a serial-parallel redundant manipulator N90-29048

REDUNDANT COMPONENTS
Reliability analysis of maintained structural system vulnerable to fatigue and fracture N90-28868

REFINING
Building an environment model using depth information N90-29064

REFLECTION
Casimir effect in a D-dimensional flat spacetime and the cut-off method
[DE90-627177] N90-29151
REFRACTIVITY
Design and performance of a long, over-water microwave radio link
[PB90-207994] N90-28758
REFRACTORIES
Radiative heat transfer
[PB90-247602] N90-28813
REGULATIONS
System reliability optimization of aircraft wings N90-28536
REGULATORY MECHANISMS (BIOLOGY)
Regulation of erythropoiesis in rats during space flight
[NASA-CR-177537] N90-29086
REINFORCING FIBERS
Ceramic matrix composites in simulated SSME environments N90-28655
Is there anything of practical value hidden amongst the composite toughening theories. A Jim Mueller prospective
[DE90-014905] N90-28673
REINFORCING MATERIALS
Evaluation of several micromechanics models for discontinuously reinforced metal matrix composites
[NASA-TM-102719] N90-28672
RELATIVITY
Unexpected properties of the centrifugal force
[DE90-627197] N90-29164
Rotating neutron stars and the equation of state of dense matter
[DE90-014185] N90-29269
RELIABILITY
STOVL fighter propulsion reliability, maintainability, and supportability characterization
[AD-A224221] N90-29574
Methods for multisource data analysis in remote sensing
[NASA-CR-187005] N90-28690
RELIABILITY ANALYSIS
Reliability analysis of maintained structural system vulnerable to fatigue and fracture N90-28668
RELIABILITY ENGINEERING
Adjustable speed drive applications guidebook
[DE90-014151] N90-28780
Smart microsensors for high temperature applications, phase 1
[AD-A224151] N90-28828
RELIEF MAPS
Satellite-map position estimation for the Mars rover N90-29069
REMOTE CONTROL
Remote atmospheric profiling systems for tropospheric monitoring
[PB90-216789] N90-28927
A neural network for controlling the configuration of frame structure with elastic members N90-29034
Plan recognition for space telerobotics N90-29036
REMOTE SENSING
Comparison of methods of space color transformations for enhancement of colored images
[INPE-4977-PRE/1542] N90-28681
On-line object feature extraction for multispectral scene representation
[NASA-CR-187006] N90-28688
A method of classification for multisource data in remote sensing based on interval-valued probabilities
[NASA-CR-187007] N90-28689
Methods for multisource data analysis in remote sensing
[NASA-CR-187005] N90-28690
Study of anomalies in transition vegetation in Alto Xingo-NT, through remote sensing techniques
[INPE-4801-TDL/334] N90-28691
Remote atmospheric profiling systems for tropospheric monitoring
[PB90-216789] N90-28927
Gravity wave initiated convection
[NASA-CR-186868] N90-28933
Detection of ocean inner waves by synthetic aperture radar: Observations at Gibraltar pass
[ETN-90-97477] N90-28953
Proceedings of the NASA Conference on Space Telerobotics, volume 1
[NASA-CR-186856] N90-29000
RENORMALIZATION GROUP METHODS
Trajectories of renormalization group flows on the phase diagram of N=2 superconformal field theories
[DE90-627212] N90-29154
Criticality of the three-state chiral clock model: A renormalisation group study
[DE90-627321] N90-29212
A generalised Hubbard Hamiltonian: Influence of temperature and fractality
[DE90-627322] N90-29213
Z(6) model: Criticality and break-collapse method
[DE90-627323] N90-29214
Susceptibility of the Potts model in an hierarchical lattice: Renormalisation group approach
[DE90-627324] N90-29215
REPLACING
Preparing software conversion studies
[PB90-235623] N90-29099
REQUIREMENTS
Emerging technologies in electronics and their measurement needs, second edition
[PB90-188087] N90-28773
RESEARCH
Japanese molecular biology 1990: An update
[PB90-188707] N90-28958
RESEARCH AIRCRAFT
Aerodynamic parameters of High-Angle-of attack Research Vehicle (HARV) estimated from flight data
[NASA-TM-102692] N90-28578
A knowledge-based system design/information tool
[NASA-CR-4316] N90-29143
RESEARCH AND DEVELOPMENT
Scientific Colloquium in Honor of Prof. Dr. Rer. Nat. Hermann L. Jordan
[ESA-TT-1101] N90-29159
Federal support to universities, colleges, and selected nonprofit institutions: Fiscal year 1988 (detailed statistical tables)
[PB90-226887] N90-29236
Federal R and D funding by budget function: Fiscal years 1989-1991
[PB90-226879] N90-29237
State science and technology indicators: An exploratory profile and analysis
[PB90-246711] N90-29259
RESEARCH FACILITIES
Dynamic ground effects N90-28531
Study of ground effects on flying scaled models N90-28532
Microgravity science and applications: Apparatus and facilities
[NASA-TM-101892] N90-28588
RESEARCH MANAGEMENT
Strategies of computer-based instructional design: A review of guidelines and empirical research
[AD-A224038] N90-29112
Federal R and D funding by budget function: Fiscal years 1989-1991
[PB90-226879] N90-29237
How can research and development leadtime be reduced
[AD-A224063] N90-29240
RESEARCH VEHICLES
Validation of the F-18 high alpha research vehicle flight control and avionics systems modifications
[NASA-TM-101723] N90-28542
Aerodynamic parameters of High-Angle-of attack Research Vehicle (HARV) estimated from flight data
[NASA-TM-102692] N90-28578
RESIN MATRIX COMPOSITES
Factors influencing the mode I interlaminar fracture resistance of toughened matrix composites N90-28668
RESINS
Factors influencing the mode I interlaminar fracture resistance of toughened matrix composites N90-28668
RESONANCE
Preliminary results on noncollocated torque control of space robot actuators N90-29057
RESONANT FREQUENCIES
Numerical simulations of flowfields in a central-dump ramjet combustor. 3: Effects of chemistry
[AD-A224145] N90-28573
RESOURCES MANAGEMENT
Chasing a specter: Risk management for global environmental change
[DE90-014455] N90-28917
REUSABLE ROCKET ENGINES
Advanced Earth-to-orbit propulsion technology program overview: Impact of civil space technology initiative N90-28812
REVENUE
Proceedings of a workshop on Future Airport Passenger Terminals
[PB90-213620] N90-28580
REVERBERATION
Large aperture acoustic arrays in support of reverberation studies
[AD-A224002] N90-29168
REVERSING
Aerodynamic and propulsive control development of the STOL and maneuver technology demonstrator N90-28514
Inflight thrust vectoring: A further degree of freedom in the aerodynamic/flight mechanical design of modern fighter aircraft N90-28528
REVISIONS
Preparing software conversion studies
[PB90-235623] N90-29099
REYNOLDS NUMBER
Hypersonic Arbitrary-Body Aerodynamics (HABA) for conceptual design
[DE90-014750] N90-28495
Wind tunnel investigation of periodic vortex separation from rough surface circular cylinders by means of acoustic measurements
[ESA-TT-1092] N90-28499
Two-dimensional wind tunnel test and comparison with calculations for a 15.2 percent thick airfoil section for wind turbines
[FFA-TN-1990-16] N90-28501
An experimental investigation of a single and multiphase confined coaxial jet N90-28796
RHEOLOGY
Rheometer strain and strain-rate errors
[DE90-013845] N90-28824
RHEOMETERS
Rheometer strain and strain-rate errors
[DE90-013845] N90-28824
RHODIUM COMPOUNDS
Antiferromagnetism and enhanced heat in CeM2Sn (M = Ni, Ir, Cu, Rh, Pd, and Pt
[DE90-014924] N90-29206
RIEMANN MANIFOLD
Beltrami algebra and symmetry of Beltrami equation on Riemann surfaces
[DE90-627157] N90-29135
On an isospectrality question over compact Riemann surfaces
[DE90-627163] N90-29147
A corollary to Kodaira-Spencer's theorem on continuity of eigenvalues
[DE90-627164] N90-29148
Geometrical properties of an internal local octonionic space in a non-Riemannian manifold
[DE90-627175] N90-29149
Dirac's equation as a geodesic in Riemann space
[DE90-627194] N90-29152
Superconformal algebra and central extension of meromorphic vector fields with multipoles on super-Riemann sphere
[DE90-627211] N90-29153
Anyons and Chern-Simons theory on compact spaces of finite genus
[DE90-627216] N90-29157
RIGID ROTORS
The effects of structural flap-lag and pitch-lag coupling on soft inplane hingeless rotor stability in hover
[NASA-TP-3002] N90-28503
RIGID STRUCTURES
A nonlinear finite element formulation for the large displacement analysis of plates N90-28867
RISK
Chasing a specter: Risk management for global environmental change
[DE90-014455] N90-28917
ROBOT ARMS
Motion coordination for a mobile manipulator system
[PB90-203076] N90-28839
Modularity in robotic systems N90-29014
A fast lightstripe rangefinding system with smart VLSI sensor N90-29019
Grasp planning under uncertainty N90-29041
Preliminary study of a serial-parallel redundant manipulator N90-29045
The JPL telerobot operator control station. Part 1: Hardware N90-29049
The JPL telerobot operator control station. Part 2: Software N90-29050
Performance evaluation of a 6 axis high fidelity generalized force reflecting teleoperator N90-29052
Human machine interaction via the transfer of power and information signals N90-29054
Experiences with the JPL telerobot testbed: Issues and insights N90-29059
The KALI multi-arm robot programming and control environment N90-29060
ROBOT DYNAMICS
Motion coordination for mobile robots in unstructured environments
[PB90-199498] N90-28837
Motion coordination for a mobile manipulator system
[PB90-203076] N90-28839
Dynamic interaction of multiple autonomous mobile robots N90-28844
Experiments in the dynamic and strategic control of cooperating manipulators N90-28845

Solutions to the frictional dynamics problem and the reciprocal variable feedback methodology for design and control of robot mechanisms N90-28846
Tele-Autonomous control involving contact — object localization
[NASA-CR-187004] N90-28854
Magnetostrictive direct drive motors
[NASA-CR-186895] N90-28855
Proceedings of the NASA Conference on Space Telerobotics, volume 1
[NASA-CR-186856] N90-29000
A new approach to global control of redundant manipulators N90-29002
Kinematic functions for the 7 DOF robotics research arm N90-29003
A complete analytical solution for the inverse instantaneous kinematics of a spherical-revolute-spherical (7R) redundant manipulator N90-29006
Adjustable impedance, force feedback and command language aids for telerobotics (parts 1-4 of an 8-part MIT progress report) N90-29007
A laser tracking dynamic robot metrology instrument N90-29021
Map learning with indistinguishable locations N90-29025
Three-dimensional motor schema based navigation N90-29026
Exploiting map plans as resources for action N90-29028
Grasp planning under uncertainty N90-29041
Efficient mapping algorithms for scheduling robot inverse dynamics computation on a multiprocessor system N90-29071
Planning robot actions under position and shape uncertainty N90-29073

ROBOT SENSORS
Dynamic interaction of multiple autonomous mobile robots N90-28844
Real-time edge tracking using a tactile sensor N90-29023
Reflexive obstacle avoidance for kinematically-redundant manipulators N90-29047

ROBOTICS
Robotic and automatic welding development at the Marshall Space Flight Center N90-28656
Motion coordination for mobile robots in unstructured environments
[PB90-199498] N90-28837
Motion coordination for a mobile manipulator system
[PB90-203076] N90-28839
DOE/NIST Workshop on Common Architectures for Robotic Systems
[PB90-216839] N90-28840
Experiments in the dynamic and strategic control of cooperating manipulators N90-28845
Solutions to the frictional dynamics problem and the reciprocal variable feedback methodology for design and control of robot mechanisms N90-28846
Proceedings of the NASA Conference on Space Telerobotics, volume 1
[NASA-CR-186856] N90-29000
A 17 degree of freedom anthropomorphic manipulator N90-29001
Kinematic functions for the 7 DOF robotics research arm N90-29003
A complete analytical solution for the inverse instantaneous kinematics of a spherical-revolute-spherical (7R) redundant manipulator N90-29006
Adjustable impedance, force feedback and command language aids for telerobotics (parts 1-4 of an 8-part MIT progress report) N90-29007
Measurement of hand dynamics in a microsurgery environment: Preliminary data in the design of a bimanual telemicro-operation test bed N90-29010
Development of a flexible test-bed for robotics, telemanipulation and servicing research N90-29012
Control of intelligent robots in space N90-29013
Modularity in robotic systems N90-29014
A system architecture for a planetary rover N90-29015
The NASA/OAST telerobot testbed architecture N90-29016
Formulation of design guidelines for automated robotic assembly in outerspace N90-29017
Automation and robotics technology for intelligent mining systems N90-29018
A fast lightstripe rangefinding system with smart VLSI sensor N90-29019
Computational neural learning formalisms for manipulator inverse kinematics N90-29030
A neural network for controlling the configuration of frame structure with elastic members N90-29034
Plan recognition for space telerobotics N90-29036
Proceedings of the NASA Conference on Space Telerobotics, volume 2
[NASA-CR-186857] N90-29044
Reflexive obstacle avoidance for kinematically-redundant manipulators N90-29047
Preliminary study of a serial-parallel redundant manipulator N90-29048
The JPL telerobot operator control station. Part 1: Hardware N90-29049
The JPL telerobot operator control station. Part 2: Software N90-29050
Design of a monitor and simulation terminal (master) for space station telerobotics and telescience N90-29051
Performance evaluation of a 6 axis high fidelity generalized force reflecting teleoperator N90-29052
Implementation and design of a teleoperation system based on a VMEBUS/68020 pipelined architecture N90-29053
Human machine interaction via the transfer of power and information signals N90-29054
Trajectory generation of space telerobots N90-29055
On the simulation of space based manipulators with contact N90-29056
Experiences with the JPL telerobot testbed: Issues and insights N90-29059
The KALI multi-arm robot programming and control environment N90-29060
Perceptual telerobotics N90-29063
Planetary rover technology development requirements N90-29067
Robotic sampling system for an unmanned Mars mission N90-29070
Organising geometric computations for space telerobotics N90-29074
A tesselated probabilistic representation for spatial robot perception and navigation N90-29075
Integrating planning and reactive control N90-29077
Integrating planning, execution, and learning N90-29079
A hardware/software environment to support R/D in intelligent machines and mobile robotic systems
[DE90-014458] N90-29119

ROBOTS
Motion coordination for mobile robots in unstructured environments
[PB90-199498] N90-28837
Motion coordination for a mobile manipulator system
[PB90-203076] N90-28839
DOE/NIST Workshop on Common Architectures for Robotic Systems
[PB90-216839] N90-28840
Dynamic interaction of multiple autonomous mobile robots N90-28844
Experiments in the dynamic and strategic control of cooperating manipulators N90-28845
Solutions to the frictional dynamics problem and the reciprocal variable feedback methodology for design and control of robot mechanisms N90-28846
Treatment of systematic errors 2: Fusion of ultrasound and visual sensor data
[DE90-014780] N90-28850
ROSES, a Robot Operating System Expert Scheduler: Methodological framework
[DE90-014782] N90-28851
Proceedings of the NASA Conference on Space Telerobotics, volume 1
[NASA-CR-186856] N90-29000
A 17 degree of freedom anthropomorphic manipulator N90-29001
Cartesian control of redundant robots N90-29004
Adjustable impedance, force feedback and command language aids for telerobotics (parts 1-4 of an 8-part MIT progress report) N90-29007
Development of a flexible test-bed for robotics, telemanipulation and servicing research N90-29012
Control of intelligent robots in space N90-29013
Modularity in robotic systems N90-29014
The NASA/OAST telerobot testbed architecture N90-29016
Formulation of design guidelines for automated robotic assembly in outerspace N90-29017
Methods and strategies of object localization N90-29020
A laser tracking dynamic robot metrology instrument N90-29021
Robot Acting on Moving Bodies (RAMBO): Interaction with tumbling objects N90-29022
Three-dimensional motor schema based navigation N90-29026
Periodic gaits for the CMU ambler N90-29027
Exploiting map plans as resources for action N90-29028
Learned navigation in unknown terrains: A retraction method N90-29029
Multi-layer neural networks for robot control N90-29031
A design philosophy for multi-layer neural networks with applications to robot control N90-29033
Plan recognition for space telerobotics N90-29036
Causal simulation and sensor planning in predictive monitoring N90-29037
A Boltzmann machine for the organization of intelligent machines N90-29040
Grasp planning under uncertainty N90-29041
Reflexive obstacle avoidance for kinematically-redundant manipulators N90-29047
The JPL telerobot operator control station. Part 1: Hardware N90-29049
The JPL telerobot operator control station. Part 2: Software N90-29050
Design of a monitor and simulation terminal (master) for space station telerobotics and telescience N90-29051
Performance evaluation of a 6 axis high fidelity generalized force reflecting teleoperator N90-29052
Implementation and design of a teleoperation system based on a VMEBUS/68020 pipelined architecture N90-29053
Human machine interaction via the transfer of power and information signals N90-29054
Trajectory generation of space telerobots N90-29055
On the simulation of space based manipulators with contact N90-29056
Preliminary results on noncollocated torque control of space robot actuators N90-29057
Portable Dextrous Force Feedback Master for robot telemanipulation (PDMFF) N90-29058
Experiences with the JPL telerobot testbed: Issues and insights N90-29059
The KALI multi-arm robot programming and control environment N90-29060
How do robots take two parts apart N90-29061
Techniques and potential capabilities of multi-resolutional information (knowledge) processing N90-29062
Perceptual telerobotics N90-29063
Building an environment model using depth information N90-29064
HERMIES-3: A step toward autonomous mobility, manipulation, and perception N90-29065
Rice-obot 1: An intelligent autonomous mobile robot N90-29068
Satellite-map position estimation for the Mars rover N90-29069
Planning robot actions under position and shape uncertainty N90-29073
A tesselated probabilistic representation for spatial robot perception and navigation N90-29075
Integrating planning, execution, and learning N90-29079
A hardware/software environment to support R/D in intelligent machines and mobile robotic systems
[DE90-014458] N90-29119

ROBUSTNESS (MATHEMATICS)
Robust controller design by contraction of a pole region
[ESA-TT-1042] N90-29118
SuperCHIEF: A modified CHIEF (Combined Helmholz Integral Equation Formulation) method
[DE90-014744] N90-29123

ROCKET ENGINE CONTROL
Liquid Rocket Booster (LRB) for the Space Transportion System (STS) systems study. Appendix D: Trade study summary for the liquid rocket booster
[NASA-CR-183790-APP-D] N90-28604

ROCKET ENGINE DESIGN
Low power arcjet performance
[NASA-TM-103280] N90-28657
High power arcjet
[NASA-CR-183086] N90-28658

ROCKET ENGINES
Effects of friction and end losses on MHD thruster efficiency
[DE90-013673] N90-28608
Data base for crack growth properties of materials N90-28647

ROCKET EXHAUST
Spectroscopic study of combustion diagnostics on hydroxyl radicals
[NASA-CR-186998] N90-28694

ROCKET NOZZLES
Computer code for the prediction of nozzle admittance N90-28630

ROCKET PROPELLANTS
Tripropellant combustion process N90-28631
Summary of booster propulsion/vehicle impact study results N90-28635

ROCKS
Robotic sampling system for an unmanned Mars mission N90-29070

RODS
Static and dynamic characterization of the ATR 72 rods made of Ti 10.2.3 titanium alloy
[REPT-49-238] N90-28722

ROLLER BEARINGS
Pratt and Whitney cryogenic turbopump bearing experience N90-28624
ROLLING CONTACT LOADS
On the application of similarity laws to a scaled railway bogie model
[DLR-FB-90-06] N90-28853
ROTARY WINGS
Solution of Euler equations applied to a rotor of a helicopter in steady flight
[ONERA-RSF-1/3731-AY-002A] N90-28500
The effects of structural flap-lag and pitch-lag coupling on soft inplane hingeless rotor stability in hover
[NASA-TP-3002] N90-28503
ROTATION
Faraday rotation mapping of mercury cadmium telluride
[AD-A224278] N90-28729
A nonlinear finite element formulation for the large displacement analysis of plates N90-28867
Situational awareness and vestibular stimulation: The influence of whole-body rotation upon task performance
[IZF-1989-14] N90-28994
Robot Acting on Moving Bodies (RAMBO): Interaction with tumbling objects N90-29022
ROTONS
Wigner symbols, quantum dynamics, and the kicked rotator
[AD-A224024] N90-29234
ROTOR AERODYNAMICS
Analysis of heliport environmental data, Intracoastal City
[DOT/FAA/CT-TN89/43] N90-28584
ROTOR BLADES (TURBOMACHINERY)
Measurement of the steady surface pressure distribution on a single rotation large scale advanced prop-fan blade at Mach numbers from 0.03 to 0.78
[NASA-CR-182124] N90-28552
Flow coupling between a rotor and a stator in turbomachinery
[AD-A223882] N90-28572
Analysis of heliport environmental data, Intracoastal City
[DOT/FAA/CT-TN89/43] N90-28584
Turbomachinery rotor forces
[NASA-CR-183779] N90-28852
ROTOR DYNAMICS
Turbomachinery rotor forces
[NASA-CR-183779] N90-28852
Correlation of AH-1G airframe flight vibration data with a coupled rotor-fuselage analysis
[NASA-CR-181974] N90-28665
ROTORS
Flow coupling between a rotor and a stator in turbomachinery
[AD-A223882] N90-28572
ROVING VEHICLES
A system architecture for a planetary rover N90-29015
Planetary rover technology development requirements N90-29067
Satellite-map position estimation for the Mars rover N90-29069
A survey of planning and scheduling research at the NASA Ames Research Center N90-29076
RP-1 ROCKET PROPELLANTS
Heavy hydrocarbon main injector technology N90-28633
RUN TIME (COMPUTERS)
ROSES, a Robot Operating System Expert Scheduler: Methodological framework
[DE90-014782] N90-28851
RUNGE-KUTTA METHOD
Numerical experiments on the accuracy of ENO and modified ENO schemes
[NASA-CR-182083] N90-29128
RUNWAYS
Development and testing of rapid repair methods for war damaged runways
[AD-A223970] N90-28586
RUPTURING
Influence of diesel engine exposure on the rupture strength of silicon nitride and partially stabilized zirconia
[DE90-014759] N90-28849
RUTHENIUM
Structure of metal overlayers by low energy alkali ion scattering: Cu/Ru(0001) and Sn/Pt(111)
[DE90-014453] N90-28718

S

SAFETY
Procedures for DOE-Navy exchange and approval of engineering information and material management required for production of W88-0/Mk5 RBA (reentry body assembly)
[DE90-014763] N90-28595
Guidelines for pressure vessel safety assessment
[PB90-219619] N90-28749
SALINITY
Ross Sea oceanographic data, 1983-1987: USCGC GLACIER, January-February 1983; USCGC POLAR SEA, January-February 1984; USCGC POLAR STAR, February 1984; USCGC POLAR SEA, February 1987
[PB90-243932] N90-28955
SAMPLES
Robotic sampling system for an unmanned Mars mission N90-29070
SAMPLING
A system architecture for a planetary rover N90-29015
A fast lightstripe rangefinding system with smart VLSI sensor N90-29019
Robotic sampling system for an unmanned Mars mission N90-29070
An improved method for choosing sampling points for the inspection of complex surfaces in a computer-aided manufacturing environment N90-29093
SATELLITE COMMUNICATION
Rain-fade simulation and power augmentation for satellite communication systems
[NASA-TM-103134] N90-28768
SATELLITE IMAGERY
Digital geometric correction for MSS-LANDSAT imagery
[INPE-4627-PRE/1345] N90-28886
Study of anomalies in transition vegetation in Alto Xingo-NT, through remote sensing techniques
[INPE-4601-TDL/334] N90-28891
INPE geographic data base
[INPE-4638-PRE/1348] N90-29253
SATELLITE TRANSMISSION
Rain-fade simulation and power augmentation for satellite communication systems
[NASA-TM-103134] N90-28768
SATURABLE REACTORS
Investigations into the use of dielectric coatings in magnetic switches
[DE90-014331] N90-28776
SCALARS
The spatial scalar structure of premixed turbulent stagnation point flames
[DE90-014189] N90-28686
Casimir effect in a D-dimensional flat spacetime and the cut-off method
[DE90-627177] N90-29151
Quantum gravity in two dimensions and the SL(2,R) current algebra
[DE90-627215] N90-29156
On the infrared behaviour of some non-Minkowskian quantum fields N90-29273
SCALE (CORROSION)
High temperature surface interactions: Overview N90-28699
Scale adherence effects in oxidation and sulfidation N90-28703
SCALE HEIGHT
An analysis of the Palomar-Green subdwarfs and white dwarfs N90-29263
SCALING LAWS
On the application of similarity laws to a scaled railway bogie model
[DLR-FB-90-06] N90-28853
SCATTERING
New approach to HF channel modeling and simulation. Part 2: Stochastic model
[PB90-200338] N90-28755
SCATTERING FUNCTIONS
New approach to HF channel modeling and simulation. Part 2: Stochastic model
[PB90-200338] N90-28755
SCENE ANALYSIS
On-line object feature extraction for multispectral scene representation
[NASA-CR-187006] N90-28888
SCHEDULES
Focus of attention in an activity-based scheduler N90-29039
SCHEDULING
ROSES, a Robot Operating System Expert Scheduler: Methodological framework
[DE90-014782] N90-28851
State-based scheduling: An architecture for telescope observation scheduling N90-29036
Focus of attention in an activity-based scheduler N90-29039
Approximation algorithms for planning and control N90-29042
Efficient mapping algorithms for scheduling robot inverse dynamics computation on a multiprocessor system N90-29071
SCHWARZSCHILD METRIC
A comment on anisotropic spheres admitting one parameter group of conformal motions
[DE90-627195] N90-29230
SCINTILLATION
Predictions of radiation backgrounds for GRO/OSSE
[RAE-TM-SPACE-372] N90-29293
SEA ICE
Ross Sea oceanographic data, 1983-1987: USCGC GLACIER, January-February 1983; USCGC POLAR SEA, January-February 1984; USCGC POLAR STAR, February 1984; USCGC POLAR SEA, February 1987
[PB90-243932] N90-28955
SEA STATES
Measuring the vertical directional spectra caused by sea surface sound
[AD-A223883] N90-28957
SEATS
Military aircrew seating: A human factors engineering approach
[AD-A218049] N90-28999
SECONDARY FLOW
Free shear layer and swirl flow heat transfer enhancement
[PB90-228123] N90-28798
SELF LUBRICATION
Development of improved self lubricating cages for SSME HPOTP bearings N90-28623
SELF ORGANIZING SYSTEMS
Selective learning algorithm for certain types of learning failure in multilayer perceptrons
[AD-A223982] N90-28998
SEMANTICS
A user modelling approach for computer-based critiquing
[AD-A224042] N90-29088
The SPECIALIST: Natural language processing system
[PB90-240029] N90-29098
Inference engine for expert systems
[INPE-4565-PRE/1306] N90-29104
Efficiency and effectiveness of deep structure-based subject indexing languages: PRECIS vs. DSIS N90-29248
SEMICONDUCTOR LASERS
The III-V semiconductor quantum well lasers and related optoelectronic devices on silicon
[AD-A224120] N90-28835
SEMICONDUCTORS (MATERIALS)
Fifteenth International Conference on X Ray and Inner-Shell Processes
[DE90-013024] N90-29170
Semiconductor measurement technology: A software program for aiding the analysis of ellipsometric measurements, simple spectroscopic models
[PB90-216847] N90-29201
Semiconductor measurement technology. EPROP: An interactive FORTRAN program for computing selected electronic properties of Gallium Arsenide and Silicon
[PB90-222738] N90-29203
SENSORY PERCEPTION
Situational Awareness in Aerospace Operations
[AGARD-CP-478] N90-28972
A methodology for the objective measurement of pilot situation awareness N90-28974
Situational Awareness Rating Technique (SART): The development of a tool for aircrew systems design N90-28975
Performance-based measures of merit for tactical situation awareness N90-28976
Evaluation of the Situational Awareness Rating Technique (SART) as a tool for aircrew systems design N90-28977
Attention gradients in situation awareness N90-28978
Workload induced spatio-temporal distortions and safety of flight: An investigation of cognitive intrusions in perceptual processes N90-28986
Loss of alertness and consciousness from pilot position during long range flight N90-28990
Situational awareness and vestibular stimulation: The influence of whole-body rotation upon task performance
[IZF-1989-14] N90-28994
Cognition versus sensation: A paradigm for reorientation
[IZF-1989-20] N90-28995

SEPARATED FLOW
Wind tunnel investigation of periodic vortex separation from rough surface circular cylinders by means of acoustic measurements
[ESA-TT-1092] N90-28499
The effect of rapid spoiler deployment on the transient forces on an aerofoil N90-28527
SERIES EXPANSION
Application of discrete Fourier series to the finite element stress analysis of axi-symmetric solids
[PB90-231010] N90-28870
SERVICE LIFE
NASA Langley Research Center National Aero-Space Plane Mission simulation profile sets
[NASA-TM-102670] N90-28541
Energy Efficient Engine (E3) combustion system component technology performance report
[NASA-CR-168274] N90-28555
Probabilistic structural analysis methods development for SSME N90-28616
Cryogenic, high speed, turbopump bearing cooling requirements N90-28620
Bearing optimization for SSME HPOTP application N90-28622
Development of improved self lubricating cages for SSME HPOTP bearings N90-28623
Cage stability analysis for SSME HPOTP bearings N90-28625
Comparison of two computer codes for crack growth analysis: NASCRAC versus NASA/FLAGRO N90-28648
Probabilistic model for fracture mechanics service life analysis N90-28650
Durability of thermal barrier coatings in a high heat flux environment N90-28651
Study of meteorological processes important in the degradation of materials through surface temperature
[PB90-222720] N90-28856
Development of testing and analysis methodology to assess the long term durability of polymeric composites at high temperatures
[NASA-TM-102714] N90-28871
Development of the sodium/sulfur technology for energy storage
[DE90-014329] N90-28899
SHAFTS (MACHINE ELEMENTS)
Preliminary results on noncollocated torque control of space robot actuators N90-29057
SHAPES
Organising geometric computations for space telerobotics N90-29074
SHEAR FLOW
Aerodynamics of bodies in shear flow N90-28496
SHEAR LAYERS
Free shear layer and swirl flow heat transfer enhancement
[PB90-228123] N90-28798
Numerical simulation of the formation of two-dimensional and three-dimensional structures in shear layers and wakes
[ESA-TT-1008] N90-28802
SHEAR PROPERTIES
Is there anything of practical value hidden amongst the composite toughening theories. A Jim Mueller prospective
[DE90-014905] N90-28673
SHELL THEORY
Error detection and control for nonlinear shell analysis
[NASA-TM-102723] N90-28877
SHIPS
Automated system for meteorological analysis
[INPE-4586-TDL/332] N90-28945
SHOCK LAYERS
Gas-jet and tangent-slot film cooling tests of a 12.5 deg cone at Mach number of 6.7
[NASA-TP-2786] N90-28806
SHOCK RESISTANCE
Thermal shock and oxidation resistance of ceramic coatings N90-28711
SHOCK WAVES
Shock dynamics in the sub-nanometer femtosecond domain
[DE90-014390] N90-28689
A plasma diagnostic study of two wind-blown shell nebulae: NGC 7635 and NGC 2359 N90-29271
SHORT TAKEOFF AIRCRAFT
Aerodynamic and propulsive control development of the STOL and maneuver technology demonstrator N90-28514
SHOT PEENING
Fretting fatigue strength of Ti-6Al-4V at room and elevated temperatures and ways of improving it N90-28709
SIGNAL DETECTION
A reliable, maintenance-free oxygen sensor for aircraft using an oxygen-sensitive coating on potentiometric electrodes
[AD-A222696] N90-28545
SIGNAL PROCESSING
Methods for detecting low-frequency signals in the presence of strong winds
[AD-A223980] N90-28769
Target detection in Gaussian noise using artificial neural systems
[AD-A223983] N90-28770
SIGNAL TO NOISE RATIOS
Comparison of speech intelligibility in cockpit noise using SPH-4 flight helmet with and without active noise reduction
[NASA-CR-177564] N90-28510
Methods for detecting low-frequency signals in the presence of strong winds
[AD-A223980] N90-28769
Bandwidth and signal-to-noise ratio enhancement of the NPS transient electromagnetic scattering laboratory
[AD-A224144] N90-28771
Noise performance of microchannel plate imaging systems
[DE90-015037] N90-28785
Metallic line profiles of the AOV star Vega
[NASA-CR-186906] N90-29261
SIGNATURE ANALYSIS
Bandwidth and signal-to-noise ratio enhancement of the NPS transient electromagnetic scattering laboratory
[AD-A224144] N90-28771
SIGNS AND SYMPTOMS
Decompression sickness presenting as a viral syndrome
[AD-A223880] N90-28967
SILICON
The III-V semiconductor quantum well lasers and related optoelectronic devices on silicon
[AD-A224120] N90-28835
Use of electron spectroscopies in the tribological evaluation of diamond films
[DE90-014421] N90-28848
Research on high-efficiency, multiple-gap, multi-junction amorphous silicon-based alloy thin-film solar cells
[DE90-000338] N90-28896
Semiconductor measurement technology. EPROP: An interactive FORTRAN program for computing selected electronic properties of Gallium Arsenide and Silicon
[PB90-222738] N90-29203
SILICON CARBIDES
Ascertaining the fracture toughness of ceramic materials by means of bending testpieces of various notch types at ambient and high temperatures
[ESA-TT-992] N90-28733
Improved silicon carbide for advanced heat engines
[NASA-CR-182186] N90-28735
SILICON DIOXIDE
Damage resistant optical coatings prepared using high temperature, plasma chemical-vapor-deposition
[DE90-015042] N90-28738
SILICON ISOTOPES
Studies of central interactions of Si ions at 14.5 x A GeV/c in Au and Cu
[DE90-015095] N90-29195
SILICON NITRIDES
Microdamage to ceramic surfaces under sliding conditions N90-28708
Ascertaining the fracture toughness of ceramic materials by means of bending testpieces of various notch types at ambient and high temperatures
[ESA-TT-992] N90-28733
Influence of diesel engine exposure on the rupture strength of silicon nitride and partially stabilized zirconia
[DE90-014759] N90-28849
SILVER ZINC BATTERIES
Liquid Rocket Booster (LRB) for the Space Transportation System (STS) systems study. Appendix C: Battery report for the liquid rocket booster TVC actuators
[NASA-CR-183789-APP-C] N90-28603
SIMILARITY NUMBERS
On the application of similarity laws to a scaled railway bogie model
[DLR-FB-90-06] N90-28853
SIMULATION
A flight dynamic model of aircraft spinning
[AR-005-600] N90-28576
Overview on hot gas tests and molten salt corrosion experiments at the DLR N90-28714
Genesis of bow echoes: A rear-inflow induced meso-convective structure
[PB90-209776] N90-28926
A nonhydrostatic numerical model in sigma-coordinates and simulations of mesoscale phenomena N90-28932
Design of a monitor and simulation terminal (master) for space station telerobotics and telescience N90-29051
SINE WAVES
Crash-impact behavior of graphite/epoxy composite sine wave webs N90-28667
SINGLE CRYSTALS
The fatigue damage behavior of a single crystal superalloy N90-28644
Second order tensor finite element
[NASA-CR-184008] N90-29122
Numerical and analytical study of nonlinear bifurcations associated with the morphological stability of two-dimensional single crystals
[PB90-209594] N90-29200
SINGLE EVENT UPSETS
Measurements of the single event upset environment in the upper atmosphere
[RAE-TM-SPACE-373] N90-28934
SINGLE STAGE TO ORBIT VEHICLES
Real time guidance and propulsion control for single-stage-to-orbit airbreathing vehicles N90-28587
High/variable mixture ratio O2/H2 engine N90-28638
High variable mixture ratio oxygen/hydrogen engine N90-28640
SINGULARITY (MATHEMATICS)
Topology of singularities and phase diagram of N=2 superconformal field theories
[DE90-627213] N90-29155
SINTERING
Microstructure and impurity effects on tungsten heavy alloys
[AD-A224220] N90-28728
SKIN (ANATOMY)
DNA damage and repair in human skin: Pathways and questions
[DE90-015126] N90-28966
SKIN FRICTION
The effects of grid-generated turbulence on flat and concave turbulent boundary layers N90-28797
Use of liquid crystals for qualitative and quantitative 2-D studies of transition and skin friction
[RAE-TM-AERO-2159] N90-28800
SKY SURVEYS (ASTRONOMY)
An infrared sky model based on the IRAS point source data
[NASA-CR-177526] N90-29265
SLABS
Electromagnetic scattering from two-dimensional thick material junctions
[NASA-CR-186468] N90-28767
SLENDER BODIES
Effects of flowfield turbulence on asymmetric vortices over a slender body
[AD-A224139] N90-28819
SLENDER WINGS
Effects of flowfield turbulence on asymmetric vortices over a slender body
[AD-A224139] N90-28819
SLEWING
The dynamics and control of large flexible space structures - 13
[NASA-CR-186930] N90-28591
SLIDING
Microdamage to ceramic surfaces under sliding conditions N90-28708
SLIDING FRICTION
Friction microprobe studies of composite surfaces
[DE90-014224] N90-28662
SLOTS
Gas-jet and tangent-slot film cooling tests of a 12.5 deg cone at Mach number of 6.7
[NASA-TP-2786] N90-28806
SLURRIES
An experimental investigation of a single and multiphase confined coaxial jet N90-28796
SMART STRUCTURES
Smart microsensors for high temperature applications, phase 1
[AD-A224151] N90-28828
SMOKE
The reduction of smoke emissions from Allison T56 engines
[ARL-PROP-R-182] N90-28547
Diffusion in the surface layer of the convective boundary layer
[AD-A224125] N90-28924
Activities report for the IBDF-INPE project SEQE, year 1987
[INPE-4534-RPE/565] N90-29298
SODIUM SULFUR BATTERIES
Development of the sodium/sulfur technology for energy storage
[DE90-014329] N90-28899

SOFTWARE ENGINEERING
A conceptual framework for fighter flight control systems
[PD-CF-9009] N90-28577
Data base for crack growth properties of materials N90-28647
DOE/NIST Workshop on Common Architectures for Robotic Systems
[PB90-216839] N90-28840
Experiments in the dynamic and strategic control of cooperating manipulators N90-28845
The JPL telerobot operator control station. Part 2: Software N90-29050
The KALI multi-arm robot programming and control environment N90-29060
Preparing software conversion studies
[PB90-235823] N90-29099
A stucture dependent software development on a relational basis: An integral approach
[ETN-90-97289] N90-29101
Documenting the decision structure in software development
[NASA-CR-186865] N90-29108
A knowledge-based system design/information tool
[NASA-CR-4316] N90-29143
SOFTWARE TOOLS
Graph structure model
[DE90-014930] N90-29097
A stucture dependent software development on a relational basis: An integral approach
[ETN-90-97289] N90-29101
Software development tools
[PB90-250051] N90-29103
Parallelization of a software relating to aerodynamics on MIMD type computers
[ONERA-RT-31/3479-CY] N90-29114
Piecewise linear models of processor utilization
[DE90-014774] N90-29115
SOILS
Development and testing of rapid repair methods for war damaged runways
[AD-A223970] N90-28586
Robotic sampling system for an unmanned Mars mission N90-29070
Data Base Analyzer and Parameter Estimator (DBAPE) interactive computer program user's manual
[PB90-193053] N90-29252
SOLAR ACTIVITY EFFECTS
A radio frequency user's guide to the space environment services center geophysical alert broadcasts
[PB90-240631] N90-28935
SOLAR CELLS
Research on high-efficiency, multiple-gap, multi-junction amorphous silicon-based alloy thin-film solar cells
[DE90-000338] N90-28896
Research on stable, large-area, amorphous silicon based submodules, phase 3
[DE90-000339] N90-29204
SOLAR CORONA
Vlasov-Maxwell equilibria of solar coronal loops
[DE90-015025] N90-29289
SOLAR DYNAMIC POWER SYSTEMS
Solar energy for high temperature technology and applications
[ETN-90-97429] N90-28902
SOLAR ENERGY
Development of the sodium/sulfur technology for energy storage
[DE90-014329] N90-28899
Solar energy for high temperature technology and applications
[ETN-90-97429] N90-28902
SOLAR ENERGY CONVERSION
Solar energy for high temperature technology and applications
[ETN-90-97429] N90-28902
SOLAR FLARES
Theoretical studies of proton beams in solar flare loops N90-29286
SOLAR NEUTRINOS
Enrichment services for chromium isotopes for the GALLEX (gallium experiment) international collaboration experiment on solar neutrino flux
[DE90-014300] N90-29285
SOLAR OBSERVATORIES
NASA Marshall Space Flight Center Solar Observatory report, January - June 1990
[NASA-TM-103512] N90-29268
SOLAR OSCILLATIONS
Solar oscillation frequency and solar neutrino predictions
[DE90-014918] N90-29288
SOLAR RADIATION
A manual for analysis of hemispherical canopy photography
[DE90-014718] N90-28885
Natural and anthropogenic climate change
[DE90-015528] N90-28923
Daily temperature, solar radiation, wind speed, cloud cover, and precipitation data recorded at the meteorological station for calendar years 1957--1988
[DE90-014399] N90-28941
SOLAR RADIO BURSTS
Alfven wave solitons and solar intermediate drift bursts
[MPE-PREPRINT-173] N90-29287
SOLAR RADIO EMISSION
Alfven wave solitons and solar intermediate drift bursts
[MPE-PREPRINT-173] N90-29287
SOLAR THERMAL ELECTRIC POWER PLANTS
Solar energy for high temperature technology and applications
[ETN-90-97429] N90-28902
SOLID ELECTRODES
Lightweight solid polymer electrolyte fuel cell with stack powar density of 3 kW/lb (7 kW/kg)
[AD-A223964] N90-28905
SOLID ELECTROLYTES
Lightweight solid polymer electrolyte fuel cell with stack power density of 3 kW/lb (7 kW/kg)
[AD-A223964] N90-28905
SOLID PROPELLANT IGNITION
Flight motor set 360L008 (STS-32R). Volume 1: System overview
[NASA-CR-184010] N90-28609
SOLID PROPELLANT ROCKET ENGINES
Liquid Rocket Booster (LRB) for the Space Transportation System (STS) systems study. Appendix C: Battery report for the liquid rocket booster TVC actuators
[NASA-CR-183789-APP-C] N90-28603
SOLID STATE LASERS
New resonantly photo-pumped x ray laser scheme
[DE90-015044] N90-28831
SOLID-SOLID INTERFACES
Lightweight solid polymer electrolyte fuel cell with stack power density of 3 kW/lb (7 kW/kg)
[AD-A223964] N90-28905
Interface formation and percusory dynamics
[AD-A224128] N90-29223
SOLIDIFICATION
High temperature oxidation of Al-Li alloys N90-28705
SOLIDS
Surface and defect excitations in covalently bonded solids
[AD-A221995] N90-28682
Application of discrete Fourier series to the finite element stress analysis of axi-symmetric solids
[PB90-231010] N90-28870
SOLIDS FLOW
Lightweight solid polymer electrolyte fuel cell with stack power density of 3 kW/lb (7 kW/kg)
[AD-A223964] N90-28905
SOLITARY WAVES
Alfven wave solitons and solar intermediate drift bursts
[MPE-PREPRINT-173] N90-29287
SONIC BOOMS
Vibration responses of two house structures during the Edwards Air Force Base phase of the national sonic boom program
[NASA-CR-182089] N90-29169
SOUND LOCALIZATION
The simulation of localized sounds for improved situational awareness N90-28984
The effects of acoustic orientation cues on instrument flight performance in a flight simulator N90-28985
SOUND PRESSURE
Annoyance caused by advanced turboprop aircraft flyover noise: Counter-rotating-propeller configuration
[NASA-TP-3027] N90-29166
SOUND PROPAGATION
Sound propagation through atmospheric turbulence: A literature summary
[RPI-MATH-184] N90-28930
SOUND WAVES
Wind tunnel investigation of periodic vortex separation from rough surface circular cylinders by means of acoustic measurements
[ESA-TT-1092] N90-28499
Combustion instability coupling with feed system acoustics N90-28629
SOUTHERN HEMISPHERE
Vorticity balance study for a tropical region, during the Southern Hemisphere summer
[INPE-4634-TDL/336] N90-28949
SPACE ADAPTATION SYNDROME
Regulation of erythropoiesis in rats during space flight
[NASA-CR-177537] N90-29086
SPACE CHARGE
Control of nonlinear space-charge emittance growth
[DE90-014752] N90-29270
SPACE COMMERCIALIZATION
Preliminary analysis of NASA commercialization initiatives
[PB90-202706] N90-29257
SPACE ENVIRONMENT SIMULATION
Microgravity science and applications: Apparatus and facilities
[NASA-TM-101892] N90-28588
SPACE FLIGHT
Joint US/USSR study: Comparison of effects of horizontal and head-down bed rest
[NASA-TP-3037] N90-28965
Regulation of erythropoiesis in rats during space flight
[NASA-CR-177537] N90-29086
SPACE FLIGHT STRESS
Fluid and electrolyte homeostasis during spaceflight: Elucidation of mechanisms in a primate
[NASA-CR-177548] N90-29085
SPACE HABITATS
Space Station Freedom pressurized element interior design process
[NASA-CR-181297] N90-28597
SPACE MISSIONS
Formulation of design guidelines for automated robotic assembly in outerspace N90-29017
SPACE POWER REACTORS
The effects of atomic oxygen on the thermal emittance of high temperature radiator surfaces
[NASA-TM-103224] N90-28670
SPACE PROCESSING
Noncontact measurement of high temperature using optical fiber sensors
[NASA-CR-186975] N90-28825
Scientific Colloquium in Honor of Prof. Dr. Rer. Nat. Hermann L. Jordan
[ESA-TT-1101] N90-29159
Microgravitation experiments in space: Compatibility with interfering dynamic influences N90-29162
SPACE SHUTTLE ASCENT STAGE
Atmospheric environment for Space Shuttle (STS-32) launch
[NASA-TM-100400] N90-28912
Atmospheric environment for Space Shuttle (STS-31) launch
[NASA-TM-103508] N90-28913
Atmospheric environment for space shuttle (STS-36) launch
[NASA-TM-100403] N90-28914
Atmospheric environment for space shuttle (STS-34) launch
[NASA-TM-100396] N90-28915
SPACE SHUTTLE BOOSTERS
Liquid Rocket Booster (LRB) for the Space Transportation System (STS) systems study. Appendix C: Battery report for the liquid rocket booster TVC actuators
[NASA-CR-183789-APP-C] N90-28603
Flight motor set 360L008 (STS-32R). Volume 1: System overview
[NASA-CR-184010] N90-28609
Operational cost drivers N90-28636
SPACE SHUTTLE MAIN ENGINE
The space transportation main engine phase A' study
[NASA-CR-179399] N90-28610
Probabilistic structural analysis methods development for SSME N90-28616
Determination of the SSME high pressure oxidizer turbopump bearing temperature N90-28619
Cryogenic, high speed, turbopump bearing cooling requirements N90-28620
Bearing optimization for SSME HPOTP application N90-28622
Development of improved self lubricating cages for SSME HPOTP bearings N90-28623
Cage stability analysis for SSME HPOTP bearings N90-28625
Rocketdyne LOX bearing tester program N90-28626
Structural response of SSME turbine blade airfoils N90-28649
A failure diagnosis system based on a neural network classifier for the space shuttle main engine
[NASA-TM-103607] N90-28659
SPACE SHUTTLE MISSION 61-B
Atmospheric environment for Space Shuttle (STS-31) launch
[NASA-TM-103508] N90-28913
SPACE SHUTTLE MISSION 61-C
Flight motor set 360L008 (STS-32R). Volume 1: System overview
[NASA-CR-184010] N90-28609
Atmospheric environment for Space Shuttle (STS-32) launch
[NASA-TM-100400] N90-28912

SPACE SHUTTLE MISSION 61-E
Atmospheric environment for space shuttle (STS-34) launch
[NASA-TM-100396] N90-28915
SPACE SHUTTLE MISSIONS
Atmospheric environment for space shuttle (STS-36) launch
[NASA-TM-100403] N90-28914
SPACE SHUTTLE ORBITERS
Microgravity science and applications: Apparatus and facilities
[NASA-TM-101892] N90-28588
Liquid Rocket Booster (LRB) for the Space Transportation System (STS) systems study. Appendix B: Liquid rocket booster acoustic and thermal environments
[NASA-CR-183788-APP-B] N90-28602
In-flight investigation of shuttle tile pressure orifice installations
[NASA-TM-4219] N90-28820
SPACE SHUTTLE PAYLOADS
Regulation of erythropoiesis in rats during space flight
[NASA-CR-177537] N90-29086
SPACE SHUTTLES
Shuttle to Shuttle 2: Subsystem weight reduction potential (estimated 1992 technology readiness date)
[NASA-TM-89114] N90-28589
Development and approach to low-frequency microgravity isolation systems
[NASA-TP-2984] N90-28754
SPACE STATION STRUCTURES
Space Station Freedom pressurized element interior design process
[NASA-CR-181297] N90-28597
SPACE STATIONS
Space station contamination modeling
[NASA-CR-183871] N90-28590
Development and approach to low-frequency microgravity isolation systems
[NASA-TP-2984] N90-28754
Design of a monitor and simulation terminal (master) for space station telerobotics and telescience N90-29051
Atmosphere and water quality monitoring on Space Station Freedom
[NASA-CR-186707] N90-29084
Preliminary analysis of NASA commercialization initiatives
[PB90-202706] N90-29257
SPACE TRANSPORTATION
Development of the electric vehicle analyzer
[AD-A224201] N90-28788
Preliminary analysis of NASA commercialization initiatives
[PB90-202706] N90-29257
SPACE TRANSPORTATION SYSTEM
Liquid Rocket Booster (LRB) for the Space Transportation System (STS) systems study. Volume 1: Executive summary
[NASA-CR-183822] N90-28599
Liquid Rocket Booster (LRB) for the Space Transportation System (STS) systems study, volume 2
[NASA-CR-183786] N90-28600
Liquid Rocket Booster (LRB) for the Space Transportation System (STS) systems study. Appendix A: Stress analysis report for the pump-fed and pressure-fed liquid rocket booster
[NASA-CR-183787-APP-A] N90-28601
Liquid Rocket Booster (LRB) for the Space Transportation System (STS) systems study. Appendix B: Liquid rocket booster acoustic and thermal environments
[NASA-CR-183788-APP-B] N90-28602
Liquid Rocket Booster (LRB) for the Space Transportation System (STS) systems study. Appendix C: Battery report for the liquid rocket booster TVC actuators
[NASA-CR-183789-APP-C] N90-28603
Liquid Rocket Booster (LRB) for the Space Transportion System (STS) systems study. Appendix D: Trade study summary for the liquid rocket booster
[NASA-CR-183790-APP-D] N90-28604
Liquid Rocket Booster (LRB) for the Space Transportation System (STS) systems study. Appendix E: Pressure-fed booster test bed for the liquid rocket booster study
[NASA-CR-183791-APP-E] N90-28605
Liquid Rocket Booster (LRB) for the Space Transportation System (STS) systems study. Appendix F: Performance and trajectory for ALS/LRB launch vehicles
[NASA-CR-183792-APP-F] N90-28606
Liquid Rocket Booster (LRB) for the Space Transportation System (STS) systems study. Appendix G: LRB for the STS system study level 2 requirements, revision 1
[NASA-CR-183793-APP-G] N90-28607
The space transportation main engine phase A' study
[NASA-CR-179399] N90-28610
Advanced Earth-to-orbit propulsion technology program overview: Impact of civil space technology initiative N90-28612
SPACE-TIME FUNCTIONS
Geometrical properties of an internal local octonionic space in a non-Riemannian manifold
[DE90-627175] N90-29149
Casimir effect in a D-dimensional flat spacetime and the cut-off method
[DE90-627177] N90-29151
A comment on anisotropic spheres admitting one parameter group of conformal motions
[DE90-627195] N90-29230
SPACEBORNE ASTRONOMY
Predictions of radiation backgrounds for GRO/OSSE
[RAE-TM-SPACE-372] N90-29293
SPACEBORNE EXPERIMENTS
Microgravity science and applications: Apparatus and facilities
[NASA-TM-101892] N90-28588
Development and approach to low-frequency microgravity isolation systems
[NASA-TP-2984] N90-28754
Design of a CO2 laser power control system for a Spacelab microgravity experiment
[NASA-TM-103112] N90-28833
Microgravitation experiments in space: Compatibility with interfering dynamic influences N90-29162
SPACEBORNE PHOTOGRAPHY
Mesoscale Lightning Experiment (MLE): A view of lightning as seen from space during the STS-26 mission
[NASA-TM-103513] N90-28951
SPACECRAFT CHARGING
Spacecraft charging effects
[RAE-TM-SPACE-375] N90-28594
SPACECRAFT COMMUNICATION
Design of a monitor and simulation terminal (master) for space station telerobotics and telescience N90-29051
SPACECRAFT COMPONENTS
Transformational part-count in layered octahedral-tetrahedral truss configurations
[NASA-TM-102635] N90-28598
A comparison of single-cycle versus multi-cycle proof testing strategies N90-28646
SPACECRAFT CONFIGURATIONS
Shuttle to Shuttle 2: Subsystem weight reduction potential (estimated 1992 technology readiness date)
[NASA-TM-89114] N90-28589
The space transportation main engine phase A' study
[NASA-CR-179399] N90-28610
SPACECRAFT CONSTRUCTION MATERIALS
Shuttle to Shuttle 2: Subsystem weight reduction potential (estimated 1992 technology readiness date)
[NASA-TM-89114] N90-28589
SPACECRAFT CONTAMINATION
Space station contamination modeling
[NASA-CR-183871] N90-28590
SPACECRAFT DESIGN
Shuttle to Shuttle 2: Subsystem weight reduction potential (estimated 1992 technology readiness date)
[NASA-TM-89114] N90-28589
SPACECRAFT ENVIRONMENTS
Space station contamination modeling
[NASA-CR-183871] N90-28590
Space Station Freedom pressurized element interior design process
[NASA-CR-181297] N90-28597
Electrochemical incineration of wastes
[NASA-CR-187033] N90-28753
Atmosphere and water quality monitoring on Space Station Freedom
[NASA-CR-186707] N90-29084
SPACECRAFT LAUNCHING
Flight motor set 360L008 (STS-32R). Volume 1: System overview
[NASA-CR-184010] N90-28609
Atmospheric environment for Space Shuttle (STS-32) launch
[NASA-TM-100400] N90-28912
Atmospheric environment for Space Shuttle (STS-31) launch
[NASA-TM-103508] N90-28913
Atmospheric environment for space shuttle (STS-36) launch
[NASA-TM-100403] N90-28914
Atmospheric environment for space shuttle (STS-34) launch
[NASA-TM-100396] N90-28915
SPACECRAFT MANEUVERS
The dynamics and control of large flexible space structures - 13
[NASA-CR-186930] N90-28591
SPACECRAFT ORBITS
Space station contamination modeling
[NASA-CR-183871] N90-28590
SPACECRAFT POWER SUPPLIES
Liquid Rocket Booster (LRB) for the Space Transportation System (STS) systems study. Appendix C: Battery report for the liquid rocket booster TVC actuators
[NASA-CR-183789-APP-C] N90-28603
SPACECRAFT PROPULSION
Low power arcjet performance
[NASA-TM-103280] N90-28857
SPACECRAFT STRUCTURES
Transformational part-count in layered octahedral-tetrahedral truss configurations
[NASA-TM-102635] N90-28598
SPACELAB
Microgravity science and applications: Apparatus and facilities
[NASA-TM-101892] N90-28588
SPACETENNAS
Tropospheric wind profiling using radar interferometry: A feasibility study of a compact mobile system
[PB90-217068] N90-28939
SPALLATION
Scale adherence effects in oxidation and sulfidation N90-28703
SPARK IGNITION
Evaluation of a hybrid kinetics/mixing-controlled combustion model for turbulent premixed and diffusion combustion using KIVA-2
[NASA-TM-103196] N90-28792
SPATIAL DISTRIBUTION
Mode competition in the quasioptical gyrotron
[AD-A222181] N90-28823
SPATIAL RESOLUTION
Spatial disorientation incidents in the RNLAF F16 and F5 aircraft and suggestions for prevention N90-28973
Attention gradients in situation awareness N90-28978
The three-dimensional structure of visual attention and its implications for display design N90-28980
Workload induced spatio-temporal distortions and safety of flight: An investigation of cognitive intrusions in perceptual processes N90-28986
SPECIFICATIONS
Procedures for DOE-Navy exchange and approval of engineering information and material management required for production of W88-0/Mk5 RBA (reentry body assembly)
[DE90-014763] N90-28595
Specifications, tolerances, and other technical requirements for weighing and measuring devices as adopted by the 74th National Conference on Weights and Measures, 1989 (1990 edition)
[PB90-184961] N90-28748
Adjustable speed drive applications guidebook
[DE90-014151] N90-28780
Quality function deployment as a mechanism for process characterization and control
[DE90-014755] N90-28857
SPECTRA
Measuring the vertical directional spectra caused by sea surface sound
[AD-A223883] N90-28957
SPECTRAL BANDS
Peak analysis in gas chromatography and the development of new stationary phases for anion chromatography
[DE90-014428] N90-28687
Study of anomalies in transition vegetation in Alto Xingo-NT, through remote sensing techniques
[INPE-4601-TDL/334] N90-28891
Metallic line profiles of the AOV star Vega
[NASA-CR-186906] N90-29261
SPECTRAL RESOLUTION
A laser spectrometer and wavemeter for pulsed lasers
[NASA-CR-181731] N90-28832
Infrared spectroscopic measurements on planetary atmospheric gases N90-29283
SPECTRAL THEORY
Planetary-scale flow on a two-layer beta-plane channel model with topography N90-28931
SPECTROGRAMS
New Voyager radio spectrograms of Uranus
[NASA-CR-180381] N90-29284
SPECTROSCOPIC ANALYSIS
Novel numerical analysis method for the study of convolution equations in appearance potential spectroscopy
[ETN-90-97288] N90-29210
SPECTROSCOPY
Semiconductor measurement technology: A software program for aiding the analysis of ellipsometric measurements, simple spectroscopic models
[PB90-216847] N90-29201

SPECTRUM ANALYSIS
X ray spectra of cataclysmic variables
[NASA-CR-187002] N90-29280
SPECULAR REFLECTION
Near-angle scattering and binary optics
[AD-A224140] N90-29186
SPEECH RECOGNITION
Studies in automatic speech recognition and its application in aerospace N90-28759
SPHERES
Planning 3-D collision-free paths using spheres N90-29024
Superconformal algebra and central extension of meromorphic vector fields with multipoles on super-Riemann sphere
[DE90-627211] N90-29153
A comment on anisotropic spheres admitting one parameter group of conformal motions
[DE90-627195] N90-29230
SPIRAL GALAXIES
Star formation and the distribution of HI and infrared emission in M51
[NASA-CR-186926] N90-29262
SPOILERS
The effect of rapid spoiler deployment on the transient forces on an aerofoil N90-28527
SPONTANEOUS EMISSION
Three-dimensional simulations of the generation of one Angstrom radiation by a self-amplified spontaneous emission free-electron laser
[DE90-015032] N90-28830
SPRAYERS
Analyses of spray and droplet ignition for pure and multicomponent fuels N90-28688
SPRINGS (ELASTIC)
Minimum weight design of a leaf spring tapered in thickness and width for the Hubble Space Telescope-space support equipment
[NASA-TM-4233] N90-28879
SQUEEZE FILMS
Current research in cavitating fluid films
[NASA-TM-103184] N90-28791
STABILITY
Fretting wear and fretting fatigue at temperatures up to 600 C N90-28706
Ion divergence and the stability of magnetically insulated diodes
[DE90-014565] N90-28777
Teleoperator comfort and psychometric stability: Criteria for limiting master-controller forces of operation and feedback during telemanipulation N90-29009
Computational neural learning formalisms for manipulator inverse kinematics N90-29030
Electron acoustic and magnetoacoustic modes in a magnetized beam plasma system
[DE90-627473] N90-29199
Numerical and analytical study of nonlinear bifurcations associated with the morphological stability of two-dimensional single crystals
[PB90-209584] N90-29200
Theoretical studies of proton beams in solar flare loops N90-29286
STABILITY DERIVATIVES
Aerodynamic interferences of in-flight thrust reversers in ground effect N90-28529
STABILITY TESTS
Aerodynamic control design: Experience and results at Aermacchi N90-28518
STABILIZATION
Development and testing of rapid repair methods for war damaged runways
[AD-A223970] N90-28586
Stabilization of Taylor-Couette flow due to time-periodic outer cylinder oscillation
[PB90-219130] N90-28790
STABILIZERS (FLUID DYNAMICS)
A sensor stabilization/tracking system for unmanned air vehicles
[AD-A224008] N90-28579
STAGNATION POINT
The spatial scalar structure of premixed turbulent stagnation point flames
[DE90-014189] N90-28686
Real-time aerodynamic heating and surface temperature calculations for hypersonic flight simulation
[NASA-TM-4222] N90-28815
STAINLESS STEELS
Thermogravimetry-mass spectrometry analysis of gas bubbles in molten glass
[DE90-014116] N90-28684
Tensile behavior of borated stainless steels, phase 1
[DE90-014368] N90-28717
STANDARDIZATION
Crossroads of Information Technology Standards
[PB90-239732] N90-29251
STANDARDS
Liquid Rocket Booster (LRB) for the Space Transportation System (STS) systems study. Appendix G: LRB for the STS system study level 2 requirements, revision 1
[NASA-CR-183793-APP-G] N90-28607
Specifications, tolerances, and other technical requirements for weighing and measuring devices as adopted by the 74th National Conference on Weights and Measures, 1989 (1990 edition)
[PB90-164961] N90-28748
Goverment's role in standards-related activities: Analysis of comments
[PB90-215534] N90-29239
STAR FORMATION
Star formation and the distribution of HI and infrared emission in M51
[NASA-CR-186928] N90-29262
The formation of globular clusters N90-29272
STATIC CHARACTERISTICS
The effects of foreplanes on the static and dynamic characteristics of a combat aircraft model N90-28520
Static and dynamic characterization of the ATR 72 rods made of Ti 10.2.3 titanium alloy
[REPT-49-238] N90-28722
STATISTICAL ANALYSIS
Development of acceptance plans for airport pavement materials. Volume 1: Development
[DOT/FAA/RD-90/15] N90-28581
Phoenix data analysis and numerical simulation
[AD-A224226] N90-28772
Methods for multisource data analysis in remote sensing
[NASA-CR-187005] N90-28890
A conceptual weather-type classification procedure for the Philadelphia, Pennsylvania area
[PB90-231705] N90-28944
Autoregressive-moving average models for texture classification
[INPE-4987-PRE/1549] N90-29092
Estimation of individual coupling loss factors in a multi-subsystem
[ISVR-TR-184] N90-29141
Prediction, control, and decision-making aspects for chaotic systems
[DE90-014452] N90-29224
Data Base Analyzer and Parameter Estimator (DBAPE) interactive computer program user's manual
[PB90-193053] N90-29252
STATISTICAL CORRELATION
System reliability optimization of aircraft wings N90-28536
STATISTICAL DISTRIBUTIONS
Autoregressive-moving average models for texture classification
[INPE-4987-PRE/1549] N90-29092
STATISTICAL MECHANICS
Statement of research objectives and summary of research efforts
[RLE-PR-132] N90-29295
STATORS
Flow coupling between a rotor and a stator in turbomachinery
[AD-A223882] N90-28572
STEADY FLOW
Prediction of subsonic vortex shedding from forebodies with chines
[NASA-CR-4323] N90-28494
Regular and chaotic motion of uniform elliptical vortices in external linear time dependent velocity fields N90-28497
Solution of Euler equations applied to a rotor of a helicopter in steady flight
[ONERA-RSF-1/3731-AY-002A] N90-28500
STEADY STATE
Unsteady aerodynamics of controls N90-28525
Radiative heat transfer
[PB90-247602] N90-28813
Planetary-scale flow on a two-layer beta-plane channel model with topography N90-28931
Multigrid for hypersonic inviscid flows
[NASA-CR-182082] N90-29125
STEELS
Determination of the NDT temperature and Charpy V-notch impact properties of AAR TC128 grades B steel and A 8XX grade B steel
[PB90-207804] N90-28716
Study of meteorological processes important in the degradation of materials through surface temperature
[PB90-222720] N90-28856
Operation and calibration of MRL permeameter for measurement of DC magnetic properties of materials under stress
[MRL-TN-574] N90-28863
STEERING
A sensor stabilization/tracking system for unmanned air vehicles
[AD-A224008] N90-28579
STELLAR ATMOSPHERES
Metallic line profiles of the AOV star Vega
[NASA-CR-186906] N90-29261
STELLAR COLOR
Near-infrared speckle observations of T Tauri stars and a multi-wavelength study of the prototype star T Tauri N90-29264
Nova LMC (Large Magellanic Cloud) 1990 no. 1: The first extragalactic neon nova
[NASA-CR-180409] N90-29276
STELLAR ENVELOPES
Near-infrared speckle observations of T Tauri stars and a multi-wavelength study of the prototype star T Tauri N90-29264
STELLAR EVOLUTION
Cepheid masses for models with enhanced opacities
[DE90-014919] N90-29266
Nonradial instability strips for post-AGB stars
[DE90-014922] N90-29278
STELLAR LUMINOSITY
Nova LMC (Large Magellanic Cloud) 1990 no. 1: The first extragalactic neon nova
[NASA-CR-180409] N90-29276
Quantifying the FIR interaction enhancement in paired galaxies
[DE90-627485] N90-29281
STELLAR MAGNITUDE
An analysis of the Palomar-Green subdwarfs and white dwarfs N90-29263
STELLAR MASS
Pulsations of the white dwarf component in V471 tauri-like binaries
[DE90-014921] N90-29267
A plasma diagnostic study of two wind-blown shell nebulae: NGC 7635 and NGC 2359 N90-29271
Nova LMC (Large Magellanic Cloud) 1990 no. 1: The first extragalactic neon nova
[NASA-CR-180409] N90-29276
Nonradial instability strips for post-AGB stars
[DE90-014922] N90-29278
STELLAR MODELS
Cepheid masses for models with enhanced opacities
[DE90-014919] N90-29266
STELLAR OSCILLATIONS
Pulsations of the white dwarf component in V471 tauri-like binaries
[DE90-014921] N90-29267
STELLAR PHYSICS
Kappa effect pulsational instability for hot extreme helium stars
[DE90-014920] N90-29277
Pulsations of B star models by an opacity mechanism
[DE90-014923] N90-29279
STELLAR ROTATION
Rotating neutron stars and the equation of state of dense matter
[DE90-014185] N90-29269
STELLAR SPECTRA
Metallic line profiles of the AOV star Vega
[NASA-CR-186906] N90-29261
X ray spectra of cataclysmic variables
[NASA-CR-187002] N90-29280
***STELLAR SPECTROPHOTOMETRY**
Metallic line profiles of the AOV star Vega
[NASA-CR-186906] N90-29261
STELLAR WINDS
A plasma diagnostic study of two wind-blown shell nebulae: NGC 7635 and NGC 2359 N90-29271
STELLARATORS
Formation of magnetic islands due to field perturbations in toroidal stellarator configurations
[DE90-014789] N90-29191
Stellarator status, 1989
[DE90-014791] N90-29192
STEREOSCOPIC VISION
The interaction of chromostereopsis and stereopsis in stereoscopic CRT (Cathode Ray Tubes) displays
[AD-A217906] N90-28544
STIFFENING
Structural analysis and optimum design of geodesically stiffened composite panels
[NASA-CR-186944] N90-28862
STIFFNESS
Buckling and postbuckling behavior of compression-loaded isotropic plates with cutouts
[NASA-TP-3024] N90-28859
STIMULATION
Situational awareness and vestibular stimulation: The influence of whole-body rotation upon task performance
[IZF-1989-14] N90-28994

STIRLING ENGINES
Evaluation of the STM4-120 kinematic Stirling engine [DE90-013836] N90-28897
Performance measurements and energy balance of an SPS V160 Stirling motor at the German Aerospace Research Establishment [DLR-MITT-90-03] N90-28903
Automotive Stirling engine development program [NASA-CR-180840] N90-29260
STOCHASTIC PROCESSES
New approach to HF channel modeling and simulation. Part 2: Stochastic model [PB90-200338] N90-28755
Simulation of INPE's printed circuit laboratory production line [INPE-4556-TDL/331] N90-28784
Study of meteorological processes important in the degradation of materials through surface temperature [PB90-222720] N90-28856
Learning in stochastic neural networks for constraint satisfaction problems N90-29078
STOICHIOMETRY
Reflection Mass Spectrometry (REMS) during 3/5 MBE [DE90-014568] N90-28690
Synthesis and structural chemistry of Au(III)-substituted Ba2YCu3O(7-delta) [NASA-TM-103292] N90-28696
A design tool utilizing stoichiometric structure for the analysis of biochemical reaction networks [AD-A223873] N90-28961
STOPPING
Use of Ni63 overvoltage gap switches in the flight termination systems on boosters launched from US Army Kwajalein Atoll (USAKA) [AD-A223866] N90-28661
STORAGE RINGS (PARTICLE ACCELERATORS)
Status of the advanced light source [DE90-015636] N90-29185
Technical activities 1989, Electron and Optical Physics Division [PB90-207267] N90-29296
STORAGE TANKS
Guidelines for pressure vessel safety assessment [PB90-219619] N90-28749
Study and analysis of leaking underground storage tank remediation techniques incorporated in states in EPA Region 6 [PB90-214834] N90-28847
STORMS (METEOROLOGY)
Gravity wave initiated convection [NASA-CR-186868] N90-28933
STRAIN GAGE BALANCES
A microprocessor controlled strain gauge calibration module [AR-005-579] N90-28821
STRAIN RATE
Inelastic analysis of laminated composites N90-28669
Rheometer strain and strain-rate errors [DE90-013845] N90-28824
STRAKES
Development of non-conventional control methods for high angle of attack flight using vortex manipulation N90-28522
STRATEGY
Studies in automatic speech recognition and its application in aerospace N90-28759
Methods and strategies of object localization N90-29020
Map learning with indistinguishable locations N90-29025
How do robots take two parts apart N90-29061
STREAMLINING
Three-dimensional model testing in the transonic self-streamlining wind tunnel N90-28583
STRESS ANALYSIS
Calculation of temperature distribution in various turbine blades using a boundary-fitted coordinate transformation method N90-28550
Development of a thickness design procedure for stabilized layers under rigid airfield pavements [DOT/FAA/RD-90/22] N90-28582
Liquid Rocket Booster (LRB) for the Space Transportation System (STS) systems study. Appendix A: Stress analysis report for the pump-fed and pressure-fed liquid rocket booster [NASA-CR-183787-APP-A] N90-28601
Liquid Rocket Booster (LRB) for the Space Transportation System (STS) systems study. Appendix E: Pressure-fed booster test bed for the liquid rocket booster study [NASA-CR-183791-APP-E] N90-28605
Blade tip rubbing stress prediction N90-28615
Constitutive and life modeling of single crystal blade alloys for root attachment analysis N90-28643
Mechanical behavior of thick, curved, laminated composites N90-28664
Application of discrete Fourier series to the finite element stress analysis of axi-symmetric solids [PB90-231010] N90-28870
Mechanical property measurement of polycrystalline diamond films [AD-A224037] N90-29222
STRESS CORROSION CRACKING
Measurement of localized corrosion using current density mapping [DE90-015086] N90-28721
STRESS DISTRIBUTION
A hybrid-stress finite element for linear anisotropic elasticity N90-28614
STRESS INTENSITY FACTORS
Damage tolerance of the fighter aircraft 37 Viggen. Part 1: Analytical assessment [FFA-TN-1990-12-PT-1] N90-28538
STRESS MEASUREMENT
Mechanical property measurement of polycrystalline diamond films [AD-A224037] N90-29222
STRESS-STRAIN DIAGRAMS
Inelastic analysis of laminated composites N90-28669
STRESS-STRAIN RELATIONSHIPS
Inelastic analysis of laminated composites N90-28669
STRESSES
A theoretical investigation into the inelastic behavior of metal-matrix composites [AD-A223973] N90-28677
STRUCTURAL ANALYSIS
Liquid Rocket Booster (LRB) for the Space Transportation System (STS) systems study. Appendix E: Pressure-fed booster test bed for the liquid rocket booster study [NASA-CR-183791-APP-E] N90-28605
Probabilistic structural analysis methods development for SSME N90-28616
Development of an integrated BEM for hot fluid-structure interaction N90-28617
Structural response of SSME turbine blade airfoils N90-28649
Probabilistic model for fracture mechanics service life analysis N90-28650
Inelastic analysis of laminated composites N90-28669
Structure of metal overlayers by low energy alkali ion scattering: Cu/Ru(0001) and Sn/Pt(111) [DE90-014453] N90-28718
Simulation of INPE's printed circuit laboratory production line [INPE-4556-TDL/331] N90-28784
Structural analysis and optimum design of geodesically stiffened composite panels [NASA-CR-186944] N90-28862
Torsional effects in structures subjected to strong ground motion [PB90-226960] N90-28869
Analysis of vibrational power transmission through a beam system including a flexible section [ISVR-TR-176] N90-28875
Error detection and control for nonlinear shell analysis [NASA-TM-102723] N90-28877
Human factors model concerning the man-machine interface of mining crewstations N90-29011
Second order tensor finite element [NASA-CR-184008] N90-29122
STRUCTURAL DESIGN
Study of ground effects on flying scaled models N90-28532
Measurement of the steady surface pressure distribution on a single rotation large scale advanced prop-fan blade at Mach numbers from 0.03 to 0.78 [NASA-CR-182124] N90-28552
Operational cost drivers N90-28636
Design optimization of gas generator hybrid propulsion boosters [NASA-CR-181096] N90-28660
Formulation of design guidelines for automated robotic assembly in outerspace N90-29017
STRUCTURAL ENGINEERING
Statement of research objectives and summary of research efforts [RLE-PR-132] N90-29295
STRUCTURAL RELIABILITY
Reliability analysis of maintained structural system vulnerable to fatigue and fracture N90-28868
STRUCTURAL VIBRATION
Active control of flexible structures N90-28575
Analysis of vibrational power transmission through a beam system including a flexible section [ISVR-TR-176] N90-28875
STRUTS
Transformational part-count in layered octahedral-tetrahedral truss configurations [NASA-TM-102635] N90-28598
SUBDWARF STARS
An analysis of the Palomar-Green subdwarfs and white dwarfs N90-29263
SUBMARINES
Control of submersible vortex flows [NASA-TM-102693] N90-28493
SUBROUTINES
Automated system for meteorological analysis [INPE-4586-TDL/332] N90-28945
Software development tools [PB90-250051] N90-29103
Semiconductor measurement technology: A software program for aiding the analysis of ellipsometric measurements, simple spectroscopic models [PB90-216847] N90-29201
SUBSONIC AIRCRAFT
Life cycle cost in the conceptual design of subsonic commercial aircraft, volumes 1 and 2 N90-28535
High-speed civil transport study: Special factors [NASA-CR-181881] N90-28537
SUBSONIC FLOW
Extrapolation procedures at outflow boundaries for the Navier-Stokes equations [FFA-TN-1990-23] N90-28811
SUBSONIC WIND TUNNELS
Dynamic ground effects N90-28531
SULFIDATION
Oxidation, sulfidation, and hot corrosion: Mechanisms and interrelationships N90-28702
Scale adherence effects in oxidation and sulfidation N90-28703
SULFUR DIOXIDES
Preliminary exposure study to determine the effects of acid deposition on coated steel substrates [PB90-201799] N90-28715
SULFUR FLUORIDES
Research for electric energy systems [DE90-014221] N90-28775
SULFUR OXIDES
Acid deposition: No such thing as a free launch [DE90-015085] N90-28920
SUMMER
Vorticity balance study for a tropical region, during the Southern Hemisphere summer [INPE-4634-TDL/336] N90-28949
SUN
Solar oscillation frequency and solar neutrino predictions [DE90-014918] N90-29288
SUPERCONDUCTING SUPER COLLIDER
High energy physics at Tufts University [DE90-014664] N90-29174
SUPERCONDUCTIVITY
Thermogravimetry-mass spectrometry analysis of gas bubbles in molten glass [DE90-014116] N90-28684
High temperature superconducting thin film microwave circuits: Fabrication, characterization, and applications [NASA-TM-103235] N90-28786
Superconductivity in mixed boson-fermion systems [DE90-627491] N90-29216
Parity violation and superconductivity in doped Mott insulators [DE90-627493] N90-29217
SUPERCONDUCTORS
Analysis of three-dimensional eddy current field. Application to calculation of magnetic screening effect of the damper system in a model superconducting generator [DE90-507869] N90-28779
High temperature superconducting thin film microwave circuits: Fabrication, characterization, and applications [NASA-TM-103235] N90-28786
Dynamical information for Fe doped YBa2Cu3O7 superconducting oxides obtained from high temperature Moessbauer studies [DE90-627871] N90-29218
SUPERFLUIDITY
Thermophysical properties of Helium-4 from 0.8 to 1500 K with pressures to 2000 MPa [NASA-CR-186992] N90-28681
SUPERLATTICES
The III-V semiconductor quantum well lasers and related optoelectronic devices on silicon [AD-A224120] N90-28835
Radiation effects in InAsSb strained-layer superlattice photodiodes induced by dose-rate and transient x ray environments [DE90-015000] N90-29208
Dynamical properties of two-dimensional Josephson junction arrays [AD-A223965] N90-29221

SUPERNOVA REMNANTS
Gamma ray evidence for cosmic ray sources N90-29292
SUPERPLASTICITY
Behavior of Al-Mg alloys in hot working and superplasticity
[DE90-015193] N90-28723
SUPERSONIC AIRCRAFT
High-speed civil transport study: Special factors
[NASA-CR-181881] N90-28537
SUPERSONIC COMBUSTION RAMJET ENGINES
Real time guidance and propulsion control for single-stage-to-orbit airbreathing vehicles N90-28587
SUPERSONIC DRAG
Projectile supersonic drag characteristics
[AD-A224217] N90-28506
SUPERSONIC SPEED
Projectile supersonic drag characteristics
[AD-A224217] N90-28506
SUPERSONIC TRANSPORTS
The aerodynamic design of the oblique flying wing supersonic transport
[NASA-CR-177552] N90-28540
Measurements of the single event upset environment in the upper atmosphere
[RAE-TM-SPACE-373] N90-28934
SUPPORTS
Sting-support interference on afterbody drag at transonic speeds
[NAL-TM-EA-8902] N90-28492
SURFACE DEFECTS
Surface and defect excitations in covalently bonded solids
[AD-A221995] N90-28682
SURFACE DIFFUSION
Diffusion in the surface layer of the convective boundary layer
[AD-A224125] N90-28924
SURFACE FINISHING
Electrochemical surface finishing using amino-substrates on carbon fibers in organic media. Effects of the finishing on the mechanical properties of carbon-epoxy composites
[ONERA-RT-9/3549-M] N90-28672
Fretting fatigue strength of Ti-6Al-4V at room and elevated temperatures and ways of improving it N90-28709
SURFACE LAYERS
High temperature oxidation of Al-Li alloys N90-28705
SURFACE NAVIGATION
Rice-obot 1: An intelligent autonomous mobile robot N90-29068
A tesselated probabilistic representation for spatial robot perception and navigation N90-29075
SURFACE PROPERTIES
Surface property improvement in titanium alloy gas turbine components through ion implantation N90-28713
Structure of metal overlayers by low energy alkali ion scattering: Cu/Ru(0001) and Sn/Pt(111)
[DE90-014453] N90-28718
Technical bibliography of high performance polyethylene fibers
[SNPE-NT-106/89/GTR/RP/NP] N90-28736
SURFACE REACTIONS
High Temperature Surface Interactions
[AGARD-CP-461] N90-28698
High temperature surface interactions: Overview N90-28699
Oxidation, sulfidation, and hot corrosion: Mechanisms and interrelationships N90-28702
SURFACE ROUGHNESS
Wind tunnel investigation of periodic vortex separation from rough surface circular cylinders by means of acoustic measurements
[ESA-TT-1092] N90-28499
Friction microprobe studies of composite surfaces
[DE90-014224] N90-28662
Large aperture acoustic arrays in support of reverberation studies
[AD-A224002] N90-29168
Near-angle scattering and binary optics
[AD-A224140] N90-29186
SURFACE TEMPERATURE
Determination of the SSME high pressure oxidizer turbopump bearing temperature N90-28619
Transient cooling of a hot surface by droplets evaporation
[PB90-227968] N90-28799
Real-time aerodynamic heating and surface temperature calculations for hypersonic flight simulation
[NASA-TM-4222] N90-28815
Study of meteorological processes important in the degradation of materials through surface temperature
[PB90-222720] N90-28856
SURFACES
An improved method for choosing sampling points for the inspection of complex surfaces in a computer-aided manufacturing environment N90-29093
SURGERY
Measurement of hand dynamics in a microsurgery environment: Preliminary data in the design of a bimanual telemicro-operation test bed N90-29010
SURVEYS
Severe thunderstorm forecasting: An operational review
[PB90-215484] N90-28948
Scientists, engineers, and technicians in nonmanufacturing industries: 1987. (Detailed statistical tables)
[PB90-226903] N90-29235
An analysis of the Palomar-Green subdwarfs and white dwarfs N90-29263
SWEPT FORWARD WINGS
A look at tomorrow today N90-28524
An in-flight investigation of ground effect on a forward-swept wing airplane N90-28533
SWEPT WINGS
The steady and time-dependent aerodynamic characteristics of a combat aircraft with a delta or swept canard N90-28526
SWIRLING
Swirl coaxial injector element characterization for booster engines N90-28632
SWITCHES
Use of Ni63 overvoltage gap switches in the flight termination systems on boosters launched from US Army Kwajalein Atoll (USAKA)
[AD-A223866] N90-28661
Investigations into the use of dielectric coatings in magnetic switches
[DE90-014331] N90-28776
Modeling tape-wound magnetic switches
[DE90-015121] N90-28782
SYMBOLS
Wigner symbols, quantum dynamics, and the kicked rotator
[AD-A224024] N90-29234
SYMMETRY
Numerical simulations of flowfields in a central-dump ramjet combustor. 3: Effects of chemistry
[AD-A224145] N90-28573
Beltrami algebra and symmetry of Beltrami equation on Riemann surfaces
[DE90-627157] N90-29135
On the zeta-function regularization of chiral Jacobians for singular Dirac operators
[DE90-627176] N90-29150
Twisted crystals: Propagation, genesis, and relationships with optical activity and molecular symmetry (excerpts)
[DE90-014259] N90-29205
SYNCHRONIZED OSCILLATORS
Tunable CW single-frequency source for injection seeding 2-micrometer lasers
[AD-A223979] N90-28834
SYNCHROTRON RADIATION
Status of the advanced light source
[DE90-015636] N90-29185
SYNCHROTRONS
Technical activities 1989, Electron and Optical Physics Division
[PB90-207267] N90-29296
SYNOPTIC METEOROLOGY
Atmospheric environment for Space Shuttle (STS-32) launch
[NASA-TM-100400] N90-28912
Atmospheric environment for Space Shuttle (STS-31) launch
[NASA-TM-103508] N90-28913
Atmospheric environment for space shuttle (STS-36) launch
[NASA-TM-100403] N90-28914
Atmospheric environment for space shuttle (STS-34) launch
[NASA-TM-100396] N90-28915
SYNTAX
The SPECIALIST: Natural language processing system
[PB90-240029] N90-29096
SYNTHESIS (CHEMISTRY)
A study of catalysts and mechanisms in synthesis reactions
[DE90-015064] N90-28691
Synthesis and structural chemistry of Au(III)-substituted Ba2YCu3O(7-delta)
[NASA-TM-103292] N90-28696
A new low density, high porosity lithium hydride-beryllium hydride foam
[DE90-015150] N90-28739
SYNTHETIC APERTURE RADAR
Detection of ocean inner waves by synthetic aperture radar: Observations at Gibraltar pass
[ETN-90-97477] N90-28953
SYNTHETIC FUELS
Analysis of the T63-A-700 engine used in alcohol turbine fuel extender test
[DOT/FAA/CT-TN90/18] N90-28549
SYSTEM FAILURES
System reliability optimization of aircraft wings N90-28536
SYSTEMS ANALYSIS
Liquid Rocket Booster (LRB) for the Space Transportation System (STS) systems study. Appendix G: LRB for the STS system study level 2 requirements, revision 1
[NASA-CR-183793-APP-G] N90-28607
SYSTEMS ENGINEERING
System reliability optimization of aircraft wings N90-28536
Design and realization of a two stage C-band low noise amplifier
[FEL-89-B265] N90-28783
Evaluation of the Situational Awareness Rating Technique (SART) as a tool for aircrew systems design N90-28977
The JPL telerobot operator control station. Part 1: Hardware N90-29049
Designing intelligent computer aided instruction systems with integrated knowledge representation schemes
[AD-A224178] N90-29113
A knowledge-based system design/information tool
[NASA-CR-4316] N90-29143
Flight test engineering with the ATTAS N90-29160
SYSTEMS INTEGRATION
A look at tomorrow today N90-28524
Description of the primary flight display and flight guidance system logic in the NASA B-737 transport systems research vehicle
[NASA-TM-102710] N90-28546
Propulsion system-flight control integration and optimization: Flight evaluation and technology transition
[NASA-TM-4207] N90-28551
Experiences with the JPL telerobot testbed: Issues and insights N90-29059
Information management directions: The integration challenge
[PB90-219866] N90-29245

T

T TAURI STARS
Near-infrared speckle observations of T Tauri stars and a multi-wavelength study of the prototype star T Tauri N90-29264
TABLES (DATA)
World jet airplane inventory at year-end 1989
[PB90-207218] N90-28489
Industrial patent activity in the US. Part 2: Alphabetical listing by company, 1969-1989
[PB90-214412] N90-29246
TAKEOFF
Vibration responses of two house structures during the Edwards Air Force Base phase of the national sonic boom program
[NASA-CR-182089] N90-29169
TARGET ACQUISITION
Target detection in Gaussian noise using artificial neural systems
[AD-A223983] N90-28770
Target acquisition under load factors: Advantages and disadvantages of a helmet mounted sight N90-28983
Tracking performance and influence of field of view N90-28988
TARGET RECOGNITION
Target signature modeling and bistatic scattering measurement studies
[NASA-CR-186611] N90-28766
Target detection in Gaussian noise using artificial neural systems
[AD-A223983] N90-28770
TASK COMPLEXITY
Maintaining spatial orientation awareness N90-28993
TASKS
Focus of attention in an activity-based scheduler N90-29039
TATB
Study of the induction time in isothermal decomposition of explosives
[DE90-014906] N90-28745
TAXONOMY
Flora and threatened and endangered plants of John F. Kennedy Space Center, Florida
[NASA-TM-102791] N90-28925

TDR SATELLITES
ATDRS payload technology research and development
[NASA-TM-103256] N90-28596
TEARING MODES (PLASMAS)
Nonlinear tearing mode: Rutherford regime and global characteristics
[DE90-015003] N90-29193
TECHNICAL WRITING
Technical writing for software engineers
[AD-A223872] N90-29109
TECHNOLOGIES
Federal support to universities, colleges, and selected nonprofit institutions: Fiscal year 1988 (detailed statistical tables)
[PB90-226887] N90-29236
Goverment's role in standards-related activities: Analysis of comments
[PB90-215534] N90-29239
State science and technology indicators: An exploratory profile and analysis
[PB90-246711] N90-29259
TECHNOLOGY ASSESSMENT
Energy efficient engine program technology benefit/cost study. Volume 1: Executive summary
[NASA-CR-174766-VOL-1] N90-28564
TECHNOLOGY TRANSFER
Transferring building energy technologies by linking government and private-sector programs
[DE90-000346] N90-29258
State science and technology indicators: An exploratory profile and analysis
[PB90-246711] N90-29259
TELEMETRY
Special test and evaluation methods used for a nine-axis accelerometer
[PB90-209578] N90-28822
A system architecture for a planetary rover N90-29015
A personal computer-based, multitasking data acquisition system
[NASA-TM-4232] N90-29107
TELEOPERATORS
Tele-Autonomous control involving contact --- object localization
[NASA-CR-187004] N90-28854
Adjustable impedance, force feedback and command language aids for telerobotics (parts 1-4 of an 8-part MIT progress report) N90-29007
Variable force and visual feedback effects on teleoperator man/machine performance N90-29008
Teleoperator comfort and psychometric stability: Criteria for limiting master-controller forces of operation and feedback during telemanipulation N90-29009
Development of a flexible test-bed for robotics, telemanipulation and servicing research N90-29012
The NASA/OAST telerobot testbed architecture N90-29016
Exploiting map plans as resources for action N90-29028
A neural network for controlling the configuration of frame structure with elastic members N90-29034
Plan recognition for space telerobotics N90-29036
The JPL telerobot operator control station. Part 1: Hardware N90-29049
The JPL telerobot operator control station. Part 2: Software N90-29050
Design of a monitor and simulation terminal (master) for space station telerobotics and telescience N90-29051
Performance evaluation of a 6 axis high fidelity generalized force reflecting teleoperator N90-29052
Implementation and design of a teleoperation system based on a VMEBUS/68020 pipelined architecture N90-29053
Trajectory generation of space telerobots N90-29055
Portable Dextrous Force Feedback Master for robot telemanipulation (PDMFF) N90-29056
Experiences with the JPL telerobot testbed: Issues and insights N90-29059
The KALI multi-arm robot programming and control environment N90-29060
Perceptual telerobotics N90-29063
Organising geometric computations for space telerobotics N90-29074
TELESCOPES
Wind lidar for BEST
[CNES-NT-125] N90-28947
NASA Marshall Space Flight Center Solar Observatory report, January - June 1990
[NASA-TM-103512] N90-29268
TEMPERATURE DEPENDENCE
The stability of the martensitic phases in Cu-Zn-Al at an electron concentration of 1.534
[DE90-628628] N90-28727
TEMPERATURE DISTRIBUTION
Calculation of temperature distribution in various turbine blades using a boundary-fitted coordinate transformation method N90-28550
Transient cooling of a hot surface by droplets evaporation
[PB90-227968] N90-28799
Frequency response of a thermocouple wire: Effects of axial conduction
[NASA-CR-180454] N90-28827
Theoretical studies of proton beams in solar flare loops N90-29286
TEMPERATURE EFFECTS
Liquid Rocket Booster (LRB) for the Space Transportation System (STS) systems study. Appendix B: Liquid rocket booster acoustic and thermal environments
[NASA-CR-183788-APP-B] N90-28602
High temperature fatigue behavior of Haynes 188 N90-28642
Durability of thermal barrier coatings in a high heat flux environment N90-28651
Vacuum application of thermal barrier plasma coatings N90-28653
Dissipation of mechanical work and temperature rise in AS4/PEEK thermoplastic composite
[NASA-CR-186893] N90-28678
High Temperature Surface Interactions
[AGARD-CP-461] N90-28698
Fretting wear and fretting fatigue at temperatures up to 600 C N90-28706
Fretting fatigue strength of Ti-6Al-4V at room and elevated temperatures and ways of improving it N90-28709
High-temperature deformation and microstructural analysis for Si3N4-Sc2O3
[NASA-TM-103239] N90-28740
Radiative heat transfer
[PB90-247602] N90-28813
Frequency response of a thermocouple wire: Effects of axial conduction
[NASA-CR-180454] N90-28827
Influence of diesel engine exposure on the rupture strength of silicon nitride and partially stabilized zirconia
[DE90-014759] N90-28849
UV-induced degradation of the Si-SiO2 interface: Applications to the point contact solar cell
[DE90-013843] N90-28898
Numerical and analytical study of nonlinear bifurcations associated with the morphological stability of two-dimensional single crystals
[PB90-209594] N90-29200
A generalised Hubbard Hamiltonian: Influence of temperature and fractality
[DE90-627322] N90-29213
TEMPERATURE GRADIENTS
Temperature-gradient instability induced by conducting end walls
[DE90-014334] N90-29188
TEMPERATURE MEASUREMENT
Gas-jet and tangent-slot film cooling tests of a 12.5 deg cone at Mach number of 6.7
[NASA-TP-2786] N90-28806
Noncontact measurement of high temperature using optical fiber sensors
[NASA-CR-186975] N90-28825
Wind lidar for BEST
[CNES-NT-125] N90-28947
TEMPERATURE PROBES
A reliable, maintenance-free oxygen sensor for aircraft using an oxygen-sensitive coating on potentiometric electrodes
[AD-A222696] N90-28545
TEMPERATURE SENSORS
Smart microsensors for high temperature applications, phase 1
[AD-A224151] N90-28828
TEMPORAL RESOLUTION
Workload induced spatio-temporal distortions and safety of flight: An investigation of cognitive intrusions in perceptual processes N90-28986
TENSILE CREEP
Evaluation of advanced austenitic alloys relative to alloy design criteria for steam service. Part 1: Lean stainless steel
[DE90-014765] N90-28720
TENSILE PROPERTIES
Evaluations of new polyimide films for flexible circuit applications at EG and G Mound Applied Technologies
[DE90-014117] N90-28731
TENSILE STRENGTH
Behavior of aramid/epoxy wounded tubes under uniaxial and biaxial loading
[ETCA-89-R-150] N90-28873
TENSILE STRESS
Microstructure: Property correlation --- multiaxial fatigue damage evolution in waspaloy
[NASA-CR-180406] N90-28880
TENSILE TESTS
Tensile behavior of borated stainless steels, phase 1
[DE90-014368] N90-28717
Static and dynamic characterization of the ATR 72 rods made of Ti 10.2.3 titanium alloy
[REPT-49-238] N90-28722
TENSORS
Second order tensor finite element
[NASA-CR-184008] N90-29122
On the relation between the absolute parallelism spaces and spaces having a GL(4) connection
[DE90-627222] N90-29232
On the infrared behaviour of some non-Minkowskian quantum fields N90-29273
TERMS
A glossary of terms, definitions, acronyms, and abbreviations related to the National Airspace System
[DOT/FAA/CT-TN89/53] N90-29249
TERRAIN
Multiband imaging systems
[AD-A223969] N90-28893
Learned navigation in unknown terrains: A retraction method N90-29029
First results in terrain mapping for a roving planetary explorer N90-29066
TERRAIN ANALYSIS
Description of the MARC measuring system
[FEL-89-B170] N90-28887
TEST EQUIPMENT
Using embedded microcontrollers in radar test equipment
[DE90-014997] N90-28763
TEST FACILITIES
Source emission test of gas turbine engine test facility, Kelly AFB, TX
[AD-A223869] N90-28571
Oxygen/hydrogen technology test bed status update N90-28613
Flight test engineering with the ATTAS N90-29160
TEST FIRING
Ceramic matrix composites in simulated SSME environments N90-28655
TEST STANDS
Energy Efficient Engine acoustic supporting technology report
[NASA-CR-174834] N90-28557
Liquid Rocket Booster (LRB) for the Space Transportation System (STS) systems study. Appendix E: Pressure-fed booster test bed for the liquid rocket booster study
[NASA-CR-183791-APP-E] N90-28605
Development of a flexible test-bed for robotics, telemanipulation and servicing research N90-29012
The NASA/OAST telerobot testbed architecture N90-29016
TEXTS
The SPECIALIST: Natural language processing system
[PB90-240029] N90-29098
TEXTURES
Autoregressive-moving average models for texture classification
[INPE-4987-PRE/1549] N90-29092
THEMATIC MAPPING
INPE geographic data base
[INPE-4636-PRE/1348] N90-29253
THEOREM PROVING
Weighted norm inequalities for Riemann-Liouville fractional integral
[DE90-627153] N90-29132
On comparable L(sup p)-norms of subadditive functions on topological groups
[DE90-627154] N90-29146
A corollary to Kodaira-Spencer's theorem on continuity of eigenvalues
[DE90-627164] N90-29148
THEOREMS
On comparable L(sup p)-norms of subadditive functions on topological groups
[DE90-627154] N90-29146
A corollary to Kodaira-Spencer's theorem on continuity of eigenvalues
[DE90-627164] N90-29148
On Einsteinian 4-submanifolds in E(sup 6)
[DE90-627149] N90-29226
THERAPY
Decompression sickness presenting as a viral syndrome
[AD-A223880] N90-28967
THERMAL ANALYSIS
Thermal analysis of thermal barrier coatings in a high heat flux environment N90-28652

Finite element analysis of coupled thermoelasticity
[PB90-201211] N90-28860
THERMAL CONDUCTIVITY
Thermophysical properties of Helium-4 from 0.8 to 1500 K with pressures to 2000 MPa
[NASA-CR-186992] N90-28681
Investigations into the use of dielectric coatings in magnetic switches
[DE90-014331] N90-28776
Transient cooling of a hot surface by droplets evaporation
[PB90-227968] N90-28799
Frequency response of a thermocouple wire: Effects of axial conduction
[NASA-CR-180454] N90-28827
THERMAL CONTROL COATINGS
Durability of thermal barrier coatings in a high heat flux environment N90-28651
Thermal analysis of thermal barrier coatings in a high heat flux environment N90-28652
Vacuum application of thermal barrier plasma coatings N90-28653
Application of advanced coating techniques to rocket engine components N90-28654
Molten salt induced high temperature degradation of thermal barrier coatings N90-28704
Effect of protective coatings on mechanical properties of superalloys N90-28707
High temperature protective coatings: Recent trends N90-28710
Thermal shock and oxidation resistance of ceramic coatings N90-28711
THERMAL DEGRADATION
UV-induced degradation of the Si-SiO2 interface: Applications to the point contact solar cell
[DE90-013843] N90-28898
THERMAL ENERGY
Solar energy for high temperature technology and applications
[ETN-90-97429] N90-28902
THERMAL ENVIRONMENTS
Liquid Rocket Booster (LRB) for the Space Transportation System (STS) systems study. Appendix B: Liquid rocket booster acoustic and thermal environments
[NASA-CR-183788-APP-B] N90-28602
THERMAL FATIGUE
High temperature fatigue behavior of Haynes 188 N90-28642
Structural response of SSME turbine blade airfoils N90-28649
Evaluation of high temperature protective coatings for gas turbine engines under simulated service conditions N90-28712
THERMAL INSTABILITY
The formation of globular clusters N90-29272
THERMAL RADIATION
Experimental study of the optical constants of metals at high temperatures
[DE90-014732] N90-28719
THERMAL RESISTANCE
NASA Langley Research Center National Aero-Space Plane Mission simulation profile sets
[NASA-TM-102670] N90-28541
THERMAL SHOCK
Durability of thermal barrier coatings in a high heat flux environment N90-28651
Vacuum application of thermal barrier plasma coatings N90-28653
Ceramic matrix composites in simulated SSME environments N90-28655
Thermal shock and oxidation resistance of ceramic coatings N90-28711
THERMAL STABILITY
Cryogenic, high speed, turbopump bearing cooling requirements N90-28620
THERMAL STRESSES
Calculation of temperature distribution in various turbine blades using a boundary-fitted coordinate transformation method N90-28550
THERMOCOUPLES
Frequency response of a thermocouple wire: Effects of axial conduction
[NASA-CR-180454] N90-28827
THERMODYNAMIC CYCLES
Open cycle heat pump development for local resource use. Phase 2: District heating case study analysis
[DE90-011123] N90-28904
THERMODYNAMIC EFFICIENCY
Overview on hot gas tests and molten salt corrosion experiments at the DLR N90-28714
THERMODYNAMIC EQUILIBRIUM
Research on the structural and electronic properties of defects in amorphous silicon
[DE90-000342] N90-28730
Semiconductor measurement technology. EPROP: An interactive FORTRAN program for computing selected electronic properties of Gallium Arsenide and Silicon
[PB90-222738] N90-29203
THERMODYNAMIC PROPERTIES
Fuels research, volume 1
[DE90-015393] N90-28695
THERMODYNAMICS
Molten salt induced high temperature degradation of thermal barrier coatings N90-28704
Thermodynamics and structure of liquid alkali metals from the charged-hard-sphere reference fluid
[DE90-627792] N90-28725
Genesis of bow echoes: A rear-inflow induced meso-convective structure
[PB90-209776] N90-28926
Viscous causal cosmologies
[DE90-627487] N90-29282
THERMOELASTICITY
Finite element analysis of coupled thermoelasticity
[PB90-201211] N90-28860
THERMOGRAPHY
Transient cooling of a hot surface by droplets evaporation
[PB90-227968] N90-28799
THERMOGRAVIMETRY
Thermogravimetry-mass spectrometry analysis of gas bubbles in molten glass
[DE90-014116] N90-28684
THERMONUCLEAR REACTIONS
Ignition and burn control characteristics of thermonuclear plasmas
[DE90-015385] N90-29197
THERMOPLASTIC RESINS
Some studies of the vibration welding of thermoplastics N90-28842
THERMOPLASTICITY
Dissipation of mechanical work and temperature rise in AS4/PEEK thermoplastic composite
[NASA-CR-186893] N90-28678
A constitutive model for AS4/PEEK thermoplastic composites under cyclic loading
[NASA-CR-180393] N90-28679
THICKNESS
Minimum weight design of a leaf spring tapered in thickness and width for the Hubble Space Telescope-space support equipment
[NASA-TM-4233] N90-28879
THIN FILMS
A reliable, maintenance-free oxygen sensor for aircraft using an oxygen-sensitive coating on potentiometric electrodes
[AD-A222696] N90-28545
High temperature superconducting thin film microwave circuits: Fabrication, characterization, and applications
[NASA-TM-103235] N90-28786
Use of electron spectroscopies in the tribological evaluation of diamond films
[DE90-014421] N90-28848
Mechanical properties testing of diamond and diamond-like films by ultra-low load indentation
[DE90-014456] N90-28861
Research on high-efficiency, multiple-gap, multi-junction amorphous silicon-based alloy thin-film solar cells
[DE90-000338] N90-28896
Research on stable, large-area, amorphous silicon based submodules, phase 3
[DE90-000339] N90-29204
Dynamical properties of two-dimensional Josephson junction arrays
[AD-A223965] N90-29221
Mechanical property measurement of polycrystalline diamond films
[AD-A224037] N90-29222
THREE DIMENSIONAL FLOW
Oscillatory convection
[ESA-TT-890] N90-28801
Numerical simulation of the formation of two-dimensional and three-dimensional structures in shear layers and wakes
[ESA-TT-1008] N90-28802
Experimental investigations on the stability and transition of three-dimensional boundary layers
[ESA-TT-1026] N90-28803
THREE DIMENSIONAL MODELS
Three-dimensional model testing in the transonic self-streamlining wind tunnel N90-28583
Three-dimensional simulations of the generation of one Angstrom radiation by a self-amplified spontaneous emission free-electron laser
[DE90-015032] N90-28830
Building an environment model using depth information N90-29064
THREE DIMENSIONAL MOTION
The dynamics and control of large flexible space structures - 13
[NASA-CR-186930] N90-28591
THRUST CHAMBER PRESSURE
Swirl coaxial injector element characterization for booster engines N90-28832
Heavy hydrocarbon main injector technology N90-28833
THRUST CONTROL
High power arcjet
[NASA-CR-183086] N90-28658
THRUST REVERSAL
Aerodynamic interferences of in-flight thrust reversers in ground effect N90-28529
Dynamic ground effects N90-28531
THRUST VECTOR CONTROL
Aerodynamics of Combat Aircraft Controls and of Ground Effects
[AGARD-CP-465] N90-28513
Aerodynamic and propulsive control development of the STOL and maneuver technology demonstrator N90-28514
Inflight thrust vectoring: A further degree of freedom in the aerodynamic/flight mechanical design of modern fighter aircraft N90-28528
THUNDERSTORMS
An investigation of forcing mechanisms during a surprise tornadic thunderstorm
[PB90-216805] N90-28940
Severe thunderstorm forecasting: An operational review
[PB90-215484] N90-28948
On the dynamics of severe thunderstorms
[DE90-627922] N90-28950
Mesoscale Lightning Experiment (MLE): A view of lightning as seen from space during the STS-26 mission
[NASA-TM-103513] N90-28951
TILES
In-flight investigation of shuttle tile pressure orifice installations
[NASA-TM-4219] N90-28820
TIME
How can research and development leadtime be reduced
[AD-A224063] N90-29240
TIME DEPENDENCE
Regular and chaotic motion of uniform elliptical vortices in external linear time dependent velocity fields N90-28497
The steady and time-dependent aerodynamic characteristics of a combat aircraft with a delta or swept canard N90-28526
Time-based competition for competitive advantage: An information technology perspective
[AD-A224474] N90-29255
TIN
Structure of metal overlayers by low energy alkali ion scattering: Cu/Ru(0001) and Sn/Pt(111)
[DE90-014453] N90-28718
TIN COMPOUNDS
Antiferromagnetism and enhanced heat in CeM2Sn (M = Ni, Ir, Cu, Rh, Pd, and Pt
[DE90-014924] N90-29206
TITANIUM ALLOYS
Fretting fatigue strength of Ti-6Al-4V at room and elevated temperatures and ways of improving it N90-28709
Surface property improvement in titanium alloy gas turbine components through ion implantation N90-28713
Static and dynamic characterization of the ATR 72 rods made of Ti 10.2.3 titanium alloy
[REPT-49-238] N90-28722
Crack layer analysis of fatigue fracture of a beta titanium alloy N90-28864
TOKAMAK DEVICES
Combined electron cyclotron ray tracing and transport code studies in the compact ignition tokamak
[DE90-014097] N90-29189
Nonlinear tearing mode: Rutherford regime and global characteristics
[DE90-015003] N90-29193
Ignition and burn control characteristics of thermonuclear plasmas
[DE90-015385] N90-29197
TSC (Tokamak Simulation Code) simulations of Alcator C-MOD discharges 3: Study of axisymmetric stability
[DE90-015386] N90-29198
TOMOGRAPHY
Geophysical diffraction tomography: A complementary remote sensing technique for hazardous waste site characterization
[DE90-013025] N90-28882

TOPOGRAPHY
Planetary-scale flow on a two-layer beta-plane channel model with topography N90-28931
Near-angle scattering and binary optics [AD-A224140] N90-29186
INPE geographic data base [INPE-4636-PRE/1348] N90-29253

TOPOLOGY
Beltrami algebra and symmetry of Beltrami equation on Riemann surfaces [DE90-627157] N90-29135
On comparable L(sup p)-norms of subadditive functions on topological groups [DE90-627154] N90-29146
On an isospectrality question over compact Riemann surfaces [DE90-627163] N90-29147
Topology of singularities and phase diagram of N=2 superconformal field theories [DE90-627213] N90-29155

TORNADOES
An investigation of forcing mechanisms during a surprise tornadic thunderstorm [PB90-216805] N90-28940
Program on development of basic understanding of severe weather phenomena [PB90-226564] N90-28943

TOROIDAL PLASMAS
Combined electron cyclotron ray tracing and transport code studies in the compact ignition tokamak [DE90-014097] N90-29189
Resonant MHD modes with toroidal coupling [DE90-015185] N90-29196

TORQUE
Investigation of maximum achievable body torque for a walking machine with friction cone constraints [PB90-203175] N90-28838
Performance evaluation of a 6 axis high fidelity generalized force reflecting teleoperator N90-29052
Preliminary results on noncollocated torque control of space robot actuators N90-29057

TORQUE MOTORS
Magnetostrictive direct drive motors [NASA-CR-186895] N90-28855

TORSION
Torsional effects in structures subjected to strong ground motion [PB90-226960] N90-28869

TORSIONAL STRESS
Microstructure: Property correlation --- multiaxial fatigue damage evolution in waspaloy [NASA-CR-180406] N90-28880

TOUCH
Human machine interaction via the transfer of power and information signals N90-29054

TOUGHNESS
Factors influencing the mode I interlaminar fracture resistance of toughened matrix composites N90-28668
Electrochemical surface finishing using amino-substrates on carbon fibers in organic media. Effects of the finishing on the mechanical properties of carbon-epoxy composites [ONERA-RT-9/3549-M] N90-28672
Is there anything of practical value hidden amongst the composite toughening theories. A Jim Mueller prospective [DE90-014905] N90-28673
Static and dynamic characterization of the ATR 72 rods made of Ti 10.2.3 titanium alloy [REPT-49-238] N90-28722

TOWERS
Design and performance of a long, over-water microwave radio link [PB90-207994] N90-28758

TOXICITY
Acid deposition: No such thing as a free launch [DE90-015085] N90-28920

TRACE CONTAMINANTS
Ozone for trace organic contaminant removal [PB90-221680] N90-28916

TRACE ELEMENTS
Estimating the spatial variability of trace gas deposition velocities [PB90-208570] N90-28928
Infrared spectroscopic measurements on planetary atmospheric gases N90-29283

TRACKING (POSITION)
A sensor stabilization/tracking system for unmanned air vehicles [AD-A224008] N90-28579
Tracking performance and influence of field of view N90-28988

TRACKING PROBLEM
Cartesian control of redundant robots N90-29004

TRADEOFFS
Liquid Rocket Booster (LRB) for the Space Transportion System (STS) systems study. Appendix D: Trade study summary for the liquid rocket booster [NASA-CR-183790-APP-D] N90-28604

TRAINING ANALYSIS
Human factors evaluation and validation criteria for quality training programs: Development, presentation, and assessment [DE90-014724] N90-29081

TRAJECTORIES
Robot Acting on Moving Bodies (RAMBO): Interaction with tumbling objects N90-29022
Multiple cooperating manipulators: The case of kinematically redundant arms N90-29046
Trajectory generation of space telerobots N90-29055
Trajectories of renormalization group flows on the phase diagram of N=2 superconformal field theories [DE90-627212] N90-29154

TRAJECTORY CONTROL
Kinematics, controls, and path planning results for a redundant manipulator N90-29005
Robot Acting on Moving Bodies (RAMBO): Interaction with tumbling objects N90-29022
Planning 3-D collision-free paths using spheres N90-29024
Grasp planning under uncertainty N90-29041
Characterization and control of self-motions in redundant manipulators N90-29045
Trajectory generation of space telerobots N90-29055

TRAJECTORY MEASUREMENT
A laser tracking dynamic robot metrology instrument N90-29021

TRAJECTORY OPTIMIZATION
Real time guidance and propulsion control for single-stage-to-orbit airbreathing vehicles N90-28587

TRANSDUCERS
Special test and evaluation methods used for a nine-axis accelerometer [PB90-209578] N90-28822
Preliminary results on noncollocated torque control of space robot actuators N90-29057

TRANSFER ORBITS
Advanced Earth-to-Orbit Propulsion Technology 1988, volume 1 [NASA-CP-3012-VOL-1] N90-28611
Advanced Earth-to-orbit propulsion technology program overview: Impact of civil space technology initiative N90-28612
Development of the electric vehicle analyzer [AD-A224201] N90-28788

TRANSFORMATIONS (MATHEMATICS)
Comparison of methods of space color transformations for enhancement of colored images [INPE-4977-PRE/1542] N90-28881
Parallel algorithms for computation of the manipulator inertia matrix N90-29072
On the relation between the absolute parallelism spaces and spaces having a GL(4) connection [DE90-627222] N90-29232

TRANSIENT LOADS
Reliability analysis of maintained structural system vulnerable to fatigue and fracture N90-28868

TRANSIENT RESPONSE
Bandwidth and signal-to-noise ratio enhancement of the NPS transient electromagnetic scattering laboratory [AD-A224144] N90-28771

TRANSITION TEMPERATURE
Electron microscopy of transition-metal doped BiCaSrCuO [DE90-014184] N90-29202
Superconductivity in mixed boson-fermion systems [DE90-627491] N90-29216

TRANSMITTER RECEIVERS
Ground-based weather radar compatibility with digital radio-relay microwave systems [PB90-206236] N90-28756

TRANSMITTERS
Special test and evaluation methods used for a nine-axis accelerometer [PB90-209578] N90-28822

TRANSONIC FLOW
Solution of Euler equations applied to a rotor of a helicopter in steady flight [ONERA-RSF-1/3731-AY-002A] N90-28500
Unsteady aerodynamics of controls N90-28525

TRANSONIC SPEED
Sting-support interference on afterbody drag at transonic speeds [NAL-TM-EA-8902] N90-28492

TRANSONIC WIND TUNNELS
Three-dimensional model testing in the transonic self-streamlining wind tunnel N90-28583

TRANSPARENCE
Large hydrodynamic tunnel: Calculation of the acoustic transparency of the jet stream [REPT-89/115] N90-29167

TRANSPORT AIRCRAFT
High-speed civil transport study: Special factors [NASA-CR-181881] N90-28537
Energy Efficient Engine: Flight propulsion system final design and analysis [NASA-CR-168219] N90-28558

TRANSPORT THEORY
Lecture notes on incompressible flow and the finite element method [DE90-014665] N90-28805
Applied mathematics of transport theory [DE90-014827] N90-29126
Deterministic transport on an arbitrarily-connected grid [DE90-015148] N90-29131

TRAVELING WAVE TUBES
Rain-fade simulation and power augmentation for satellite communication systems [NASA-TM-103134] N90-28768

TRENDS
Developments in test procedures for hot-salt corrosion of superalloys N90-28700
High temperature protective coatings: Recent trends N90-28710
National air quality and emissions trends report, 1988 [PB90-200114] N90-28909

TRIANGLES
The first order phase transition for six-state Potts model on two dimensional random triangle lattice [DE90-627210] N90-29140

TRIBOLOGY
Friction microprobe studies of composite surfaces [DE90-014224] N90-28662
Fretting wear and fretting fatigue at temperatures up to 600 C N90-28706
Microdamage to ceramic surfaces under sliding conditions N90-28708
Use of electron spectroscopies in the tribological evaluation of diamond films [DE90-014421] N90-28848

TRITIUM
Mass spectrometric analysis of hydrogen isotopes in metals and metal hydrides [DE90-014118] N90-28685

TROPICAL METEOROLOGY
Wind lidar for BEST [CNES-NT-125] N90-28947

TROPICAL REGIONS
Study of anomalies in transition vegetation in Alto Xingo-NT, through remote sensing techniques [INPE-4601-TDL/334] N90-28891
Vorticity balance study for a tropical region, during the Southern Hemisphere summer [INPE-4634-TDL/336] N90-28949

TROPOSPHERE
The distribution of middle tropospheric carbon monoxide during early October 1984 [NASA-TM-103485] N90-28906
Tropospheric nitrogen: The influence of anthropogenic sources on distributions and deposition, executive summary [DE90-015401] N90-28922
Remote atmospheric profiling systems for tropospheric monitoring [PB90-216789] N90-28927
Tropospheric wind profiling using radar interferometry: A feasibility study of a compact mobile system [PB90-217068] N90-28939

TRUSSES
Transformational part-count in layered octahedral-tetrahedral truss configurations [NASA-TM-102635] N90-28598

TUMBLING MOTION
Robot Acting on Moving Bodies (RAMBO): Interaction with tumbling objects N90-29022

TUNABLE LASERS
Tunable CW single-frequency source for injection seeding 2-micrometer lasers [AD-A223979] N90-28834

TUNGSTEN
Experimental study of the optical constants of metals at high temperatures [DE90-014732] N90-28719

TUNGSTEN ALLOYS
Microstructure and impurity effects on tungsten heavy alloys [AD-A224220] N90-28728

TURBINE BLADES
Calculation of temperature distribution in various turbine blades using a boundary-fitted coordinate transformation method N90-28550

Flow coupling between a rotor and a stator in turbomachinery
[AD-A223882] N90-28572
Micromechanics of cyclic deformation in SSME turbopump blade materials N90-28641
Constitutive and life modeling of single crystal blade alloys for root attachment analysis N90-28643
Structural response of SSME turbine blade airfoils N90-28649
Durability of thermal barrier coatings in a high heat flux environment N90-28651
Thermal analysis of thermal barrier coatings in a high heat flux environment N90-28652
Vacuum application of thermal barrier plasma coatings N90-28653
Application of advanced coating techniques to rocket engine components N90-28654
The effects of a compressor rebuild on gas turbine engine performance: Final results N90-28701

TURBINE ENGINES
Energy Efficient Engine: Flight propulsion system final design and analysis
[NASA-CR-168219] N90-28558
Energy Efficient Engine core design and performance report
[NASA-CR-168069] N90-28559
NASA/GE Energy Efficient Engine low pressure turbine scaled test vehicle performance report
[NASA-CR-168290] N90-28563

TURBINE PUMPS
Evolution and use of combined mechanical and thermal codes for cryogenic turbopump bearings N90-28618
Determination of the SSME high pressure oxidizer turbopump bearing temperature N90-28619
Cryogenic, high speed, turbopump bearing cooling requirements N90-28620
Pool boiling from rotating and stationary spheres in liquid nitrogen N90-28621
Bearing optimization for SSME HPOTP application N90-28622
Pratt and Whitney cryogenic turbopump bearing experience N90-28624
Injector element characterization methodology N90-28634
Micromechanics of cyclic deformation in SSME turbopump blade materials N90-28641
Turbomachinery rotor forces
[NASA-CR-183779] N90-28852

TURBINES
Flow coupling between a rotor and a stator in turbomachinery
[AD-A223882] N90-28572

TURBOFAN AIRCRAFT
Energy efficient engine program technology benefit/cost study. Volume 1: Executive summary
[NASA-CR-174766-VOL-1] N90-28564
Energy efficient engine program technology benefit/cost study, volume 2
[NASA-CR-174766-VOL-2] N90-28565

TURBOFAN ENGINES
Effective optimal control of a fighter aircraft engine N90-28548
Energy Efficient Engine combustor test hardware detailed design report
[NASA-CR-168301] N90-28554
Energy Efficient Engine (E3) combustion system component technology performance report
[NASA-CR-168274] N90-28555
Energy Efficient Engine acoustic supporting technology report
[NASA-CR-174834] N90-28557
Energy Efficient Engine program advanced turbofan nacelle definition study
[NASA-CR-174942] N90-28560
Energy Efficient Engine: Control system component performance report
[NASA-CR-174651] N90-28562
Energy efficient engine program technology benefit/cost study. Volume 1: Executive summary
[NASA-CR-174766-VOL-1] N90-28564
Energy efficient engine program technology benefit/cost study, volume 2
[NASA-CR-174766-VOL-2] N90-28565

TURBULENCE
The spatial scalar structure of premixed turbulent stagnation point flames
[DE90-014189] N90-28686
An investigation of chaotic Kolmogorov flows
[NASA-CR-182079] N90-28816
Diffusion in the surface layer of the convective boundary layer
[AD-A224125] N90-28924
A nonhydrostatic numerical model in sigma-coordinates and simulations of mesoscale phenomena N90-28932

TURBULENCE EFFECTS
The effects of grid-generated turbulence on flat and concave turbulent boundary layers N90-28797
Effects of flowfield turbulence on asymmetric vortices over a slender body
[AD-A224139] N90-28819

TURBULENCE MODELS
Numerical resolution of Navier-Stokes equations using several turbulence models and applications on turbomachines
[ETN-90-97478] N90-28808
Development of turbulence models for the analysis of compressible or incompressible unsteady flow
[ETN-90-97486] N90-28810

TURBULENT BOUNDARY LAYER
Phoenix data analysis and numerical simulation
[AD-A224226] N90-28772
The effects of grid-generated turbulence on flat and concave turbulent boundary layers N90-28797
Vortice-propeller interaction
[LIMSI-89-9] N90-28809
Effect of vortex circulation on injectant from a single film-cooling hole and a row of film-cooling holes in a turbulent boundary layer. Part 2: Injection beneath the vortex upwash
[AD-A223894] N90-28818

TURBULENT FLOW
Development of comprehensive numerical schemes for predicting evaporating gas-droplets flow processes of a liquid-fueled combustor
[NASA-CR-187018] N90-28693
Numerical simulation of reactive turbulent flows
[ETN-90-97476] N90-28807
Numeric fluid mechanics N90-29161

TURBULENT JETS
The entrainment rate for a row of turbulent jets
[NASA-CR-185278] N90-28504

TURBULENT WAKES
Effects of flowfield turbulence on asymmetric vortices over a slender body
[AD-A224139] N90-28819

TWO DIMENSIONAL BODIES
Aerodynamics of bodies in shear flow N90-28496

TWO DIMENSIONAL FLOW
Regular and chaotic motion of uniform elliptical vortices in external linear time dependent velocity fields N90-28497
Two-dimensional wind tunnel test and comparison with calculations for a 15.2 percent thick airfoil section for wind turbines
[FFA-TN-1990-16] N90-28501
The effect of rapid spoiler deployment on the transient forces on an aerofoil N90-28527
Use of liquid crystals for qualitative and quantitative 2-D studies of transition and skin friction
[RAE-TM-AERO-2159] N90-28800
An investigation of chaotic Kolmogorov flows
[NASA-CR-182079] N90-28816

TWO DIMENSIONAL MODELS
Electromagnetic scattering from two-dimensional thick material junctions
[NASA-CR-186468] N90-28767
Radiative heat transfer
[PB90-247602] N90-28813
Studies of vortex interactions
[AD-A223864] N90-28817

TWO STAGE TURBINES
Energy Efficient Engine high pressure turbine component test performance report
[NASA-CR-168289] N90-28553

U

U.S.S.R. SPACE PROGRAM
The Magellan Venus explorer's guide
[NASA-CR-186968] N90-28592

ULTRASONIC RADIATION
Ultrasonic verification of five wave fronts in unidirectional graphite epoxy composite
[NASA-CR-185288] N90-28858

ULTRASONICS
Experimental investigations on the stability and vorticity of the vortex breakdown phenomenon above delta wings, measured by the ultrasonic laser method
[ESA-TT-1079] N90-28498
Treatment of systematic errors 2: Fusion of ultrasound and visual sensor data
[DE90-014780] N90-28850

ULTRAVIOLET RADIATION
UV-induced degradation of the Si-SiO2 interface: Applications to the point contact solar cell
[DE90-013843] N90-28898
DNA damage and repair in human skin: Pathways and questions
[DE90-015126] N90-28966

ULTRAVIOLET SPECTRA
The ionization structure of planetary nebulae 10: NGC 2392
[NASA-CR-186960] N90-29274
PW Vul: A classical nova with nearly solar abundances
[NASA-CR-185080] N90-29275

UNDERGROUND STORAGE
Study and analysis of leaking underground storage tank remediation techniques incorporated in states in EPA Region 6
[PB90-214834] N90-28847

UNDERWATER ACOUSTICS
Measuring the vertical directional spectra caused by sea surface sound
[AD-A223883] N90-28957

UNITED STATES
A preliminary ARM (Atmospheric Radiation Measurements) guide for climatic evaluations
[DE90-015135] N90-28937
Federal R and D funding by budget function: Fiscal years 1989-1991
[PB90-226879] N90-29237

UNIVERSE
On the infrared behaviour of some non-Minkowskian quantum fields N90-29273

UNIVERSITIES
The personal computer: An untapped source for the United States Army War College
[AD-A223976] N90-29087
Federal support to universities, colleges, and selected nonprofit institutions: Fiscal year 1988 (detailed statistical tables)
[PB90-226887] N90-29236

UNSTEADY AERODYNAMICS
Unsteady aerodynamics of controls N90-28525
Turbomachinery rotor forces
[NASA-CR-183779] N90-28852

UNSTEADY FLOW
Regular and chaotic motion of uniform elliptical vortices in external linear time dependent velocity fields N90-28497
Development of turbulence models for the analysis of compressible or incompressible unsteady flow
[ETN-90-97486] N90-28810

UPPER ATMOSPHERE
Present state of knowledge of the upper atmosphere 1990: An assessment report
[NASA-RP-1242] N90-28929
Measurements of the single event upset environment in the upper atmosphere
[RAE-TM-SPACE-373] N90-28934

UPWASH
Effect of vortex circulation on injectant from a single film-cooling hole and a row of film-cooling holes in a turbulent boundary layer. Part 2: Injection beneath the vortex upwash
[AD-A223894] N90-28818

URANIUM
Experimental study of the optical constants of metals at high temperatures
[DE90-014732] N90-28719

URANUS (PLANET)
New Voyager radio spectrograms of Uranus
[NASA-CR-180381] N90-29284

USER MANUALS (COMPUTER PROGRAMS)
User's manual ROBIN: A research and notification system for bird migration
[FEL-1989-103] N90-28508
Data Base Analyzer and Parameter Estimator (DBAPE) interactive computer program user's manual
[PB90-193053] N90-29252

USER REQUIREMENTS
Liquid Rocket Booster (LRB) for the Space Transportation System (STS) systems study, volume 2
[NASA-CR-183786] N90-28600
Optical storage technology
[AD-A224028] N90-29254

UTILITIES
Ozone for trace organic contaminant removal
[PB90-221680] N90-28916

V

V/STOL AIRCRAFT
STOVL fighter propulsion reliability, maintainability, and supportability characterization
[AD-A224221] N90-28574

VANES
Validation of the F-18 high alpha research vehicle flight control and avionics systems modifications
[NASA-TM-101723] N90-28542
Analysis of the T63-A-700 engine used in alcohol turbine fuel extender test
[DOT/FAA/CT-TN90/18] N90-28549

The effects of a compressor rebuild on gas turbine engine performance: Final results N90-28701
VAPOR DEPOSITION
Strengthening and toughening mechanisms in ceramic fiber-reinforced glass matrix composites N90-28666
Mechanical property measurement of polycrystalline diamond films
[AD-A224037] N90-29222
VAPOR PHASES
A study of catalysts and mechanisms in synthesis reactions
[DE90-015064] N90-28691
VAPORIZING
Transient cooling of a hot surface by droplets evaporation
[PB90-227968] N90-28799
VARIABILITY
Estimating the spatial variability of trace gas deposition velocities
[PB90-208570] N90-28928
Radio outbursts in extragalactic sources N90-29291
VARIABLE STARS
Nonradial instability strips for post-AGB stars
[DE90-014922] N90-29278
VARIATIONS
Fluctuations in cosmic background radiation
[INPE-4579-PRE/1313] N90-29294
VECTOR SPACES
On the infrared behaviour of some non-Minkowskian quantum fields N90-29273
VECTORS (MATHEMATICS)
Superconformal algebra and central extension of meromorphic vector fields with multipoles on super-Riemann sphere
[DE90-627211] N90-29153
VEGETATION
Study of anomalies in transition vegetation in Alto Xingo-NT, through remote sensing techniques
[INPE-4601-TDL/334] N90-28891
VELOCITY
Velocity filtering applied to optical flow calculations
[NASA-TM-102802] N90-28512
A complete analytical solution for the inverse instantaneous kinematics of a spherical-revolute-spherical (7R) redundant manipulator N90-29006
Alfven wave solitons and solar intermediate drift bursts
[MPE-PREPRINT-173] N90-29287
VELOCITY DISTRIBUTION
Regular and chaotic motion of uniform elliptical vortices in external linear time dependent velocity fields N90-28497
An experimental investigation of a single and multiphase confined coaxial jet N90-28796
Numerical simulation of the formation of two-dimensional and three-dimensional structures in shear layers and wakes
[ESA-TT-1008] N90-28802
Extrapolation procedures at outflow boundaries for the Navier-Stokes equations
[FFA-TN-1990-23] N90-28811
Tropospheric wind profiling using radar interferometry: A feasibility study of a compact mobile system
[PB90-217068] N90-28939
Velocity Interferometer System for Any Reflector (VISAR): Displacement mode data reduction
[DE90-015027] N90-29184
VELOCITY MEASUREMENT
Determination of the ground effect on the characteristics of the A320 aircraft N90-28534
An investigation of the steady and unsteady near wake and its effect on a laminar boundary layer N90-28794
VENUS (PLANET)
The Magellan Venus explorer's guide
[NASA-CR-186968] N90-28592
VENUS SURFACE
The Magellan Venus explorer's guide
[NASA-CR-186968] N90-28592
VERTICAL AIR CURRENTS
Genesis of bow echoes: A rear-inflow induced meso-convective structure
[PB90-209776] N90-28926
An investigation of forcing mechanisms during a surprise tornadic thunderstorm
[PB90-216805] N90-28940
VERTICAL ORIENTATION
Measuring the vertical directional spectra caused by sea surface sound
[AD-A223883] N90-28957
VERY LARGE SCALE INTEGRATION
A fast lightstripe rangefinding system with smart VLSI sensor N90-29019
VESTIBULAR TESTS
Situational awareness and vestibular stimulation: The influence of whole-body rotation upon task performance
[IZF-1989-14] N90-28994
VIBRATION
Studies in automatic speech recognition and its application in aerospace N90-28759
Some studies of the vibration welding of thermoplastics N90-28842
Correlation of AH-1G airframe flight vibration data with a coupled rotor-fuselage analysis
[NASA-CR-181974] N90-28865
Vibration responses of two house structures during the Edwards Air Force Base phase of the national sonic boom program
[NASA-CR-182089] N90-29169
Effects and tolerances of injection jitter in the SLC and future linear colliders
[DE90-014805] N90-29179
VIBRATION DAMPING
The dynamics and control of large flexible space structures - 13
[NASA-CR-186930] N90-28591
Minimum weight design of a leaf spring tapered in thickness and width for the Hubble Space Telescope-space support equipment
[NASA-TM-4233] N90-28879
VIBRATION ISOLATORS
Development and approach to low-frequency microgravity isolation systems
[NASA-TP-2984] N90-28754
VIBRATION MEASUREMENT
Plan, execute, and discuss vibration measurements and correlations to evaluate a NASTRAN finite element model of the AH-64 helicopter airframe
[NASA-CR-181973] N90-28866
VIBRATION TESTS
Studies of vortex interactions
[AD-A223864] N90-28817
Plan, execute, and discuss vibration measurements and correlations to evaluate a NASTRAN finite element model of the AH-64 helicopter airframe
[NASA-CR-181973] N90-28866
Military aircrew seating: A human factors engineering approach
[AD-A218049] N90-28999
VIDEO DATA
Animated computer-generated video-tape instruction using DIGLIB (Device Independent Graphics Library)
[DE90-015360] N90-29105
VISCOSITY
Thermophysical properties of Helium-4 from 0.8 to 1500 K with pressures to 2000 MPa
[NASA-CR-186992] N90-28681
VISCOUS DAMPING
A 17 degree of freedom anthropomorphic manipulator N90-29001
VISCOUS FLOW
Do inviscid vortex sheets roll-up
[PD-CF-9010] N90-28491
VISCOUS FLUIDS
Viscous causal cosmologies
[DE90-627487] N90-29282
VISIBILITY
Diffusion in the surface layer of the convective boundary layer
[AD-A224125] N90-28924
VISION
Treatment of systematic errors 2: Fusion of ultrasound and visual sensor data
[DE90-014780] N90-28850
VISUAL ACUITY
Experimental tests on the minimal visual acuity required for safe air crew and air control personnel performance N90-28987
VISUAL AIDS
Experimental tests on the minimal visual acuity required for safe air crew and air control personnel performance N90-28987
VISUAL FIELDS
Tracking performance and influence of field of view N90-28988
Effects of short-term weightlessness on roll circularvection N90-28992
VISUAL PERCEPTION
Time, space and form in vision
[AD-A213889] N90-28971
The three-dimensional structure of visual attention and its implications for display design N90-28980
A real time evaluation of the use of a perspective format to promote situational awareness in users of air to air tactical displays N90-28981
Target acquisition under load factors: Advantages and disadvantages of a helmet mounted sight N90-28983
The effects of acoustic orientation cues on instrument flight performance in a flight simulator N90-28985
Maintaining spatial orientation awareness N90-28993
VLASOV EQUATIONS
Vlasov-Maxwell equilibria of solar coronal loops
[DE90-015025] N90-29289
VOICE COMMUNICATION
Comparison of speech intelligibility in cockpit noise using SPH-4 flight helmet with and without active noise reduction
[NASA-CR-177564] N90-28510
VOIDS
Shock dynamics in the sub-nanometer femtosecond domain
[DE90-014390] N90-28689
VORTEX BREAKDOWN
Control of submersible vortex flows
[NASA-TM-102693] N90-28493
Experimental investigations on the stability and vorticity of the vortex breakdown phenomenon above delta wings, measured by the ultrasonic laser method
[ESA-TT-1079] N90-28498
In-flight flow visualization with pressure measurements at low speeds on the NASA F-18 high alpha research vehicle
[NASA-TM-101726] N90-28505
VORTEX INJECTORS
Swirl coaxial injector element characterization for booster engines N90-28632
VORTEX SHEDDING
Prediction of subsonic vortex shedding from forebodies with chines
[NASA-CR-4323] N90-28494
Numerical simulations of flowfields in a central-dump ramjet combustor. 3: Effects of chemistry
[AD-A224145] N90-28573
Studies of vortex interactions
[AD-A223864] N90-28817
VORTEX SHEETS
Do inviscid vortex sheets roll-up
[PD-CF-9010] N90-28491
Numerical simulation of the formation of two-dimensional and three-dimensional structures in shear layers and wakes
[ESA-TT-1008] N90-28802
VORTICES
Control of submersible vortex flows
[NASA-TM-102693] N90-28493
Prediction of subsonic vortex shedding from forebodies with chines
[NASA-CR-4323] N90-28494
Aerodynamics of bodies in shear flow N90-28496
Regular and chaotic motion of uniform elliptical vortices in external linear time dependent velocity fields N90-28497
Wind tunnel investigation of periodic vortex separation from rough surface circular cylinders by means of acoustic measurements
[ESA-TT-1092] N90-28499
In-flight flow visualization with pressure measurements at low speeds on the NASA F-18 high alpha research vehicle
[NASA-TM-101726] N90-28505
Development of non-conventional control methods for high angle of attack flight using vortex manipulation N90-28522
Control of vortex aerodynamics at high angles of attack N90-28523
Dynamic ground effects N90-28531
A flight dynamic model of aircraft spinning
[AR-005-600] N90-28576
Vortice-propeller interaction
[LIMSI-89-9] N90-28809
Studies of vortex interactions
[AD-A223864] N90-28817
Effect of vortex circulation on injectant from a single film-cooling hole and a row of film-cooling holes in a turbulent boundary layer. Part 2: Injection beneath the vortex upwash
[AD-A223894] N90-28818
Genesis of bow echoes: A rear-inflow induced meso-convective structure
[PB90-209776] N90-28926
VORTICITY
Regular and chaotic motion of uniform elliptical vortices in external linear time dependent velocity fields N90-28497
On the use of Lagrangian variables in descriptions of unsteady boundary-layer separation
[NASA-CR-182071] N90-28789
An investigation of forcing mechanisms during a surprise tornadic thunderstorm
[PB90-216805] N90-28940
Vorticity balance study for a tropical region, during the Southern Hemisphere summer
[INPE-4634-TDL/336] N90-28949

W

WAFERS
Reflection Mass Spectrometry (REMS) during 3/5 MBE
[DE90-014566] N90-28690

WAKES
Do inviscid vortex sheets roll-up
[PD-CF-9010] N90-28491
Numerical simulation of the formation of two-dimensional and three-dimensional structures in shear layers and wakes
[ESA-TT-1008] N90-28802

WALKING
Periodic gaits for the CMU ambler N90-29027

WALKING MACHINES
Investigation of maximum achievable body torque for a walking machine with friction cone constraints
[PB90-203175] N90-28838
First results in terrain mapping for a roving planetary explorer N90-29066

WALL FLOW
Three-dimensional model testing in the transonic self-streamlining wind tunnel N90-28583

WALLS
Free shear layer and swirl flow heat transfer enhancement
[PB90-228123] N90-28798

WASPALOY
Microstructure: Property correlation — multiaxial fatigue damage evolution in waspaloy
[NASA-CR-180406] N90-28880

WASTE TREATMENT
Electrochemical incineration of wastes
[NASA-CR-187033] N90-28753

WASTES
Geophysical diffraction tomography: A complementary remote sensing technique for hazardous waste site characterization
[DE90-013025] N90-28882

WATER
Three functions that model empirically measured unfrozen water content data and predict relative hydraulic conductivity
[AD-A223875] N90-28892

WATER DEPTH
Ross Sea oceanographic data, 1983-1987: USCGC GLACIER, January-February 1983; USCGC POLAR SEA, January-February 1984; USCGC POLAR STAR, February 1984; USCGC POLAR SEA, February 1987
[PB90-243932] N90-28955

WATER HEATING
Extended range tankless water heater
[DE90-014474] N90-28750

WATER POLLUTION
Puerto Rico Workshop on Land-Based Sources of Marine Pollution in the Wider Caribbean Region
[PB90-184094] N90-28921

WATER QUALITY
Puerto Rico Workshop on Land-Based Sources of Marine Pollution in the Wider Caribbean Region
[PB90-184094] N90-28921
Atmosphere and water quality monitoring on Space Station Freedom
[NASA-CR-186707] N90-29084

WATER VAPOR
A nonhydrostatic numerical model in sigma-coordinates and simulations of mesoscale phenomena N90-28932

WAVE ATTENUATION
Analysis of vibrational power transmission through a beam system including a flexible section
[ISVR-TR-176] N90-28875

WAVE DIFFRACTION
Electromagnetic scattering from two-dimensional thick material junctions
[NASA-CR-186468] N90-28767

WAVE DISPERSION
Electron acoustic and magnetoacoustic modes in a magnetized beam plasma system
[DE90-627473] N90-29199

WAVE EQUATIONS
Consistency and convergence for numerical radiation conditions
[NASA-TM-103262] N90-29124

WAVE FRONTS
Ultrasonic verification of five wave fronts in unidirectional graphite epoxy composite
[NASA-CR-185288] N90-28858

WAVE FUNCTIONS
Anyons and Chern-Simons theory on compact spaces of finite genus
[DE90-627216] N90-29157
Old and new ideas in the theory of quantum measurement
[DE90-627181] N90-29229

WAVE PROPAGATION
Propagation of electromagnetic radiation in a random field of gravitational waves and space radio interferometry
[DE90-627196] N90-28764
Ultrasonic verification of five wave fronts in unidirectional graphite epoxy composite
[NASA-CR-185288] N90-28858
Study of the relationships between radar structure and the electrical activity of clouds
[ETN-90-97488] N90-28948
Detection of ocean inner waves by synthetic aperture radar: Observations at Gibraltar pass
[ETN-90-97477] N90-28953
Factorization of the characteristic equation for three layer ducts
[AD-A223867] N90-28956
Consistency and convergence for numerical radiation conditions
[NASA-TM-103262] N90-29124
Theory of biaxial graded-index optical fiber
[NASA-CR-186977] N90-29180

WAVE REFLECTION
Velocity Interferometer System for Any Reflector (VISAR): Displacement mode data reduction
[DE90-015027] N90-29184

WAVEFORMS
Studies in automatic speech recognition and its application in aerospace N90-28759

WEAPON SYSTEMS
How can research and development leadtime be reduced
[AD-A224063] N90-29240
Extensions to the learning curve: An analysis of factors influence unit cost of weapon systems
[AD-A224119] N90-29256

WEAR
Determination of the SSME high pressure oxidizer turbopump bearing temperature N90-28619
Fretting wear and fretting fatigue at temperatures up to 600 C N90-28706
Microdamage to ceramic surfaces under sliding conditions N90-28708
Surface property improvement in titanium alloy gas turbine components through ion implantation N90-28713
Electrodeposition of wear resistant coatings
[PB90-221839] N90-28732
Results from the fourth year of operation of the Federal Methanol Fleet at Lawrence Berkeley Laboratory
[DE90-014741] N90-28743
Use of electron spectroscopies in the tribological evaluation of diamond films
[DE90-014421] N90-28848
Mechanical properties testing of diamond and diamond-like films by ultra-low load indentation
[DE90-014456] N90-28861

WEAR RESISTANCE
Pratt and Whitney cryogenic turbopump bearing experience N90-28624
Rocketdyne LOX bearing tester program N90-28626
Electrodeposition of wear resistant coatings
[PB90-221839] N90-28732

WEATHER
An investigation of forcing mechanisms during a surprise tornadic thunderstorm
[PB90-216805] N90-28940
Annual course of precipitation over much of the US: Observed versus GCM simulation
[PB90-221656] N90-28942
Program on development of basic understanding of severe weather phenomena
[PB90-226564] N90-28943
A conceptual weather-type classification procedure for the Philadelphia, Pennsylvania area
[PB90-231705] N90-28944

WEATHER FORECASTING
Proceedings of the 14th Annual Climate Diagnostics Workshop
[PB90-198573] N90-28938
Program on development of basic understanding of severe weather phenomena
[PB90-226564] N90-28943
Automated system for meteorological analysis
[INPE-4586-TDL/332] N90-28945
Severe thunderstorm forecasting: An operational review
[PB90-215484] N90-28948

WEATHER STATIONS
Data Base Analyzer and Parameter Estimator (DBAPE) interactive computer program user's manual
[PB90-193053] N90-29252

WEIBULL DENSITY FUNCTIONS
Probability models for the failure of fibres and fibrous composite materials N90-28665

WEIGHT REDUCTION
Shuttle to Shuttle 2: Subsystem weight reduction potential (estimated 1992 technology readiness date)
[NASA-TM-89114] N90-28589

WEIGHTING FUNCTIONS
Weighted norm inequalities for Riemann-Liouville fractional integral
[DE90-627153] N90-29132
Recurrence relations and weight functions for approximation by orthonormal polynomials
[DE90-627156] N90-29134

WEIGHTLESSNESS
Effects of short-term weightlessness on roll circularvection N90-28992
Formulation of design guidelines for automated robotic assembly in outerspace N90-29017

WEIGHTLESSNESS SIMULATION
Cardiovascular deconditioning of cosmonauts: Role, importance and applications of the lower body negative pressure
[ETN-90-97507] N90-28964

WELD STRENGTH
Robotic and automatic welding development at the Marshall Space Flight Center N90-28656
Some studies of the vibration welding of thermoplastics N90-28842

WELDING
Computerization of Welding Data: Proceedings of the conference and workshop
[PB90-219551] N90-28841
Some studies of the vibration welding of thermoplastics N90-28842

WHISKER COMPOSITES
Mechanical testing activities related to high-performance structural ceramics
[DE90-014299] N90-28734
Evaluation of several micromechanics models for discontinuously reinforced metal matrix composites
[NASA-TM-102719] N90-28872

WHITE DWARF STARS
An analysis of the Palomar-Green subdwarfs and white dwarfs N90-29263
Nonradial instability strips for post-AGB stars
[DE90-014922] N90-29278

WIGGLER MAGNETS
Status of the advanced light source
[DE90-015836] N90-29185

WIND (METEOROLOGY)
The global cycle of reactive nitrogen
[DE90-015041] N90-28919
On the dynamics of severe thunderstorms
[DE90-627922] N90-28950

WIND DIRECTION
A conceptual weather-type classification procedure for the Philadelphia, Pennsylvania area
[PB90-231705] N90-28944

WIND EFFECTS
A plasma diagnostic study of two wind-blown shell nebulae: NGC 7635 and NGC 2359 N90-29271

WIND MEASUREMENT
Tropospheric wind profiling using radar interferometry: A feasibility study of a compact mobile system
[PB90-217068] N90-28939

WIND PRESSURE
Methods for detecting low-frequency signals in the presence of strong winds
[AD-A223980] N90-28769

WIND PROFILES
Atmospheric environment for Space Shuttle (STS-32) launch
[NASA-TM-100400] N90-28912
Atmospheric environment for Space Shuttle (STS-31) launch
[NASA-TM-103508] N90-28913
Atmospheric environment for space shuttle (STS-36) launch
[NASA-TM-100403] N90-28914
Atmospheric environment for space shuttle (STS-34) launch
[NASA-TM-100396] N90-28915
Tropospheric wind profiling using radar interferometry: A feasibility study of a compact mobile system
[PB90-217068] N90-28939
An investigation of forcing mechanisms during a surprise tornadic thunderstorm
[PB90-216805] N90-28940

WIND SHEAR
Genesis of bow echoes: A rear-inflow induced meso-convective structure
[PB90-209776] N90-28926

WIND TUNNEL TESTS
Two-dimensional wind tunnel test and comparison with calculations for a 15.2 percent thick airfoil section for wind turbines
[FFA-TN-1990-16] N90-28501

Aerodynamic and propulsive control development of the STOL and maneuver technology demonstrator N90-28514
Control research in the NASA high-alpha technology program N90-28516
Aerodynamic control design: Experience and results at Aermacchi N90-28518
Effects of canard position on the aerodynamic characteristics of a close-coupled canard configuration at low speed N90-28519
Innovative control concepts and component integration for a generic supercruise fighter N90-28521
The steady and time-dependent aerodynamic characteristics of a combat aircraft with a delta or swept canard N90-28526
Determination of the ground effect on the characteristics of the A320 aircraft N90-28534
Aerodynamic parameters of High-Angle-of attack Research Vehicle (HARV) estimated from flight data [NASA-TM-102692] N90-28578
The equipment for mass flow measurements in the low-speed wind tunnel at DFVLR in Brunswick (Federal Republic of Germany) [ESA-TT-1125] N90-28585

WIND TURBINES
Two-dimensional wind tunnel test and comparison with calculations for a 15.2 percent thick airfoil section for wind turbines [FFA-TN-1990-16] N90-28501

WIND VELOCITY
Tropospheric wind profiling using radar interferometry: A feasibility study of a compact mobile system [PB90-217068] N90-28939
Daily temperature, solar radiation, wind speed, cloud cover, and precipitation data recorded at the meteorological station for calendar years 1957--1988 [DE90-014399] N90-28941

WINDSHIELDS
Methods for detecting low-frequency signals in the presence of strong winds [AD-A223980] N90-28769

WING LOADING
In-flight investigation of shuttle tile pressure orifice installations [NASA-TM-4219] N90-28820

WING OSCILLATIONS
The steady and time-dependent aerodynamic characteristics of a combat aircraft with a delta or swept canard N90-28526

WING PROFILES
Study of the ground effects in the CEAT aerohydrodynamic tunnel: Using the results N90-28530
The aerodynamic design of the oblique flying wing supersonic transport [NASA-CR-177552] N90-28540

WING TIP VORTICES
Experimental investigations on the stability and vorticity of the vortex breakdown phenomenon above delta wings, measured by the ultrasonic laser method [ESA-TT-1079] N90-28498

WINGS
Do inviscid vortex sheets roll-up [PD-CF-9010] N90-28491
Study of the ground effects in the CEAT aerohydrodynamic tunnel: Using the results N90-28530
System reliability optimization of aircraft wings N90-28536
Damage tolerance of the fighter aircraft 37 Viggen. Part 1: Analytical assessment [FFA-TN-1990-12-PT-1] N90-28538
Damage tolerance of the fighter aircraft 37 Viggen. Part 2: Experimental verification [FFA-TN-1990-13-PT-2] N90-28539
In-flight investigation of shuttle tile pressure orifice installations [NASA-TM-4219] N90-28820

WIRE
Frequency response of a thermocouple wire: Effects of axial conduction [NASA-CR-180454] N90-28827

WORDS (LANGUAGE)
A comparison of password techniques for multilevel authentication mechanisms [AD-A224245] N90-29089

WORKLOADS (PSYCHOPHYSIOLOGY)
A methodology for the objective measurement of pilot situation awareness N90-28974
Situational Awareness Rating Technique (SART): The development of a tool for aircrew systems design N90-28975
Performance-based measures of merit for tactical situation awareness N90-28976
Evaluation of the Situational Awareness Rating Technique (SART) as a tool for aircrew systems design N90-28977
Attention gradients in situation awareness N90-28978
Workload induced spatio-temporal distortions and safety of flight: An investigation of cognitive intrusions in perceptual processes N90-28986

WORKSTATIONS
Automated simulation as part of a design workstation [NASA-TM-102852] N90-29083

WORLD DATA CENTERS
Oceanographic data exchange, 1988 [PB90-232596] N90-28952

X

X RAY DIFFRACTION
Mechanical property measurement of polycrystalline diamond films [AD-A224037] N90-29222

X RAY LASERS
New resonantly photo-pumped x ray laser scheme [DE90-015044] N90-28831

X RAY SCATTERING
X ray scattering studies of non-equilibrium ordering processes [DE90-015066] N90-29209

X RAY SOURCES
Using the x ray region of the electromagnetic spectrum for alignment: Overview, geometric optics, and design considerations [DE90-014798] N90-28752
Some novel sources of x ray beams: Channeling, transition and Cherenkov radiation [DE90-014442] N90-29181

X RAY SPECTRA
X ray spectra of cataclysmic variables [NASA-CR-187002] N90-29280

X RAY SPECTROSCOPY
Preliminary exposure study to determine the effects of acid deposition on coated steel substrates [PB90-201799] N90-28715

X RAYS
Using the x ray region of the electromagnetic spectrum for alignment: Overview, geometric optics, and design considerations [DE90-014798] N90-28752
Fifteenth International Conference on X Ray and Inner-Shell Processes [DE90-013024] N90-29170
Technical activities 1989, Electron and Optical Physics Division [PB90-207267] N90-29296

X-29 AIRCRAFT
A look at tomorrow today N90-28524
An in-flight investigation of ground effect on a forward-swept wing airplane N90-28533

Y

YAG LASERS
Tunable CW single-frequency source for injection seeding 2-micrometer lasers [AD-A223979] N90-28834

YAWING MOMENTS
Development of non-conventional control methods for high angle of attack flight using vortex manipulation N90-28522

YIELD POINT
Damage tolerance of the fighter aircraft 37 Viggen. Part 1: Analytical assessment [FFA-TN-1990-12-PT-1] N90-28538
Damage tolerance of the fighter aircraft 37 Viggen. Part 2: Experimental verification [FFA-TN-1990-13-PT-2] N90-28539

YIELD STRENGTH
Comparison of two computer codes for crack growth analysis: NASCRAC versus NASA/FLAGRO N90-28648
Tensile behavior of borated stainless steels, phase 1 [DE90-014368] N90-28717

YTTRIUM
Dynamical information for Fe doped YBa2Cu3O7 superconducting oxides obtained from high temperature Moessbauer studies [DE90-627871] N90-29218

Z

ZINC
The stability of the martensitic phases in Cu-Zn-Al at an electron concentration of 1.534 [DE90-628628] N90-28727

ZINC-BROMIDE BATTERIES
Zinc-bromine battery development [DE90-014751] N90-28781

ZIRCONIUM OXIDES
Influence of diesel engine exposure on the rupture strength of silicon nitride and partially stabilized zirconia [DE90-014759] N90-28849

Typical Personal Author Index Listing

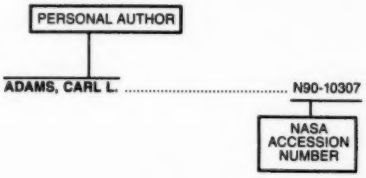

Listings in this index are arranged alphabetically by personal author. The NASA accession number denotes the number by which the citation is identified.

A

AARON, JOHN N90-28597
ABDUL-AZIZ, A. N90-28649
ABE, T. N90-28900
ABRAMOWICZ, MAREK A. N90-29164
ADAM, GH. N90-29106
ADAMS, A. N90-28638
ADAMS, MARVIN L. N90-29131
ADDIS, ROBERT B. N90-28752
ADELMAN, SAUL J. N90-29261
ADORF, HANS-MARTIN N90-29078
AHLERS, MANFRED N90-28727
AKINLADE, O. N90-28725
AKITA, S. N90-28779
ALBERT, GEORGE N90-28781
ALBLAS, B. P. N90-29182
ALLEN, JAMES G. N90-29143
ALLEN, JONATHAN N90-29295
ALLEN, M. A. N90-29178
ALPERINE, SERGE N90-28704
ALVES, M. V. N90-29194
ALVIS, ROBERT L. N90-28595
AMIN-JAVAHERI, MASOUD N90-29072
ANDERSON, B. J. N90-29054
ANDERSON, CARL M. N90-28814
ANDERSON, K. R. N90-28724
ANDREWS, J. BARRY N90-28747
ANDRO, M. N90-28596
ANNIS, CHARLES N90-28650
ANTOLOVICH, STEPHEN D. N90-28641
ANTON, D. L. N90-28643
ANZIC, G. N90-28596
ARBIT, H. A. N90-28633
ARDAI, J. L. N90-28955
ARGEMIRODECARVALHOPAIVA, JOAO N90-29253
ARKIN, RONALD C. N90-29026
ARMSTRONG, ELIZABETH S. N90-28622
ARNDT, NORBERT N90-28852
ARONSON, ALAN R. N90-29098
ARP, VINCENT D. N90-28681
ARYA, R. R. N90-29204
ARYA, V. K. N90-28649
ASHFORD, N. N90-28511
ATHERTON, C. S. N90-28919
N90-28922
AUGUSTOMII, FERNANDO N90-28886
AUSTIN, S. N90-29275
AUWETER-KURTZ, M. N90-28658
AZEVEDO, I. SOUZA N90-29218

B

BACKES, PAUL N90-29060
BAILEY, STEVEN A. N90-29107
BAINUM, PETER M. N90-28591
BAIR, E. K. N90-28639
BAJCSY, RUZENA K. N90-29061
BAK, JOE N90-28643
BAKER, LEONARD H. N90-28765
BALARAM, BOB N90-29059
BALDWIN, STEPHEN N90-28795
BALL, J. H. N90-28791
BALLARINI, R. N90-28878
BALLTRIP, D. L. N90-28720
BANERJEA, A. N90-28696
BANERJEE, P. K. N90-28617
BANERJEE, S. N90-29017
BANKS, WILLIAM W. N90-29081
BARBAGALLO, PHILIP S. N90-28765
BARBER, S. A. N90-28623
BARBIER, B. N90-28672
BARHEN, J. N90-28851
BARHEN, JACOB N90-29030
BARKER, TIMOTHY N90-29274
BARKOCY, EDWARD J. N90-28595
BARNDEN, JOHN N90-29117
BARNIV, YAIR N90-28512
BAROL, D. N90-28511
BARRETT, CHRISTOPHER L. N90-28986
BARRY, P. E. N90-28739
BASS, J. N90-29122
BASYE, KENNETH N90-29025
BATEMAN, R. F. N90-29238
BATTS, G. W. N90-28912
N90-28913
N90-28914
N90-28915
BAUSCHLICHER, CHARLES W., JR. N90-28680
BAYTOS, JOHN F. N90-28745
BDEOLIVEIRA, MISSAE ODO N90-29253
BEAHAN, JOHN N90-29059
BEARMAN, P. W. N90-28527
BEATTY, R. F. N90-28626
BECKER, F. E. N90-28904
BECKER, M. N90-28902
BECKERMAN, M. N90-28850
BECLE, J. P. N90-28534
BEDARD, ROGER J., JR. N90-29067
BEGAULT, DURAND R. N90-28996
BEGG, ZIA N90-29105
BEGUN, G. M. N90-28849
BEICHEL, R. N90-28639
BEIN, THOMAS W. N90-28572
BEITLER, R. S. N90-28562
BELL, M. I. N90-29203
BELLINGER, N. C. N90-28713
BELYAEV, V. M. N90-29231
BENEDIKTSSON, JON ATLI N90-28890
BENNETT, G. W. N90-28562
BENNETT, M. N90-29204
BENSMAN, D. N90-28766
BENZ, A. O. N90-29287
BENZ, SAMUEL PAUL N90-29221
BERA, RAJENDRA K. N90-28491
N90-28577
BERBERIAN, D. N90-29068
BERG, BRUCE G. N90-28969
BERGER, ALAN D. N90-29023
BERGMANN, JUERGEN R. N90-29101
BERK, H. L. N90-29188
BERNAUER, F. N90-29205
BERNSTEIN, E. M. N90-29171
BERRY, C. N90-29122
BESTUL, THOR N90-29022
BEVERIDGE, JOHN H. N90-28637
BEYERMANN, W. P. N90-29206
BHARDWAJ, R. C. N90-28753
BHASIN, K. B. N90-28786
BINNEY, RICHARD S. N90-28763
BIRD, F. J. N90-28821
BIRT, M. J. N90-28872
BISOI, A. K. N90-29134
BISSET, JOHN W. N90-28568
BISWAS, SUBAL CHANDRA N90-29248
BITTENCOURT, J. A. N90-29194
BJOERCK, ANDERS N90-28501
BLACK, PATRICK B. N90-28892
BLASS, ECKHART N90-28793
BLATT, J. R. N90-28556
BLAU, PETER J. N90-28662
BLES, W. N90-28994
BLOM, ANDERS F. N90-28538
N90-28539
BOCKRIS, J. OM. N90-28753
BODDY, MARK N90-29042
BOER, L. C. N90-28995
BOERS, JACK E. N90-28774
BOGEGARD, SVEN N90-28671
BOISSON, H. C. N90-28810
BOKHARI, ASHFAQUE H. N90-29230
BOLLING, E. N90-28720
BOMAN, PER-OLOF N90-28538
N90-28539
BONNER, SUSAN N90-29024
BONOLI, P. T. N90-29189
BOOGERS, J. A. M. N90-28711
BOOKER, J. R. N90-28860
N90-28870
BORGHI, R. N90-28807
BORIS, JAY P. N90-28573
BORNSTEIN, N. S. N90-28703
BOSCHET, C. N90-28761
BOURUET-AUBERTOT, PASCALE N90-28953
BOUSMAN, WILLIAM G. N90-28503
BOWERS, J. S. N90-28739
BOYCE, J. B. N90-28730
BOZEK, T. N90-29244
BRADLEY, D. K. N90-28829
BRAGER, H. R. N90-28724
BRAGINSKY, V. B. N90-28764
BRANDER, J. R. G. N90-28511
BRANDON, JEANNE N90-28731
BRATTON, THOMAS N90-28762
BRAZA, M. N90-28810
BREISACHER, KEVIN J. N90-28629
BRENNAN, T. M. N90-28690
BRESINA, JOHN J. N90-28541
BREWE, D. E. N90-28791
BRIDGEMAN, M. J. N90-28563
BRIGGS, CRAIG N90-28747
BRINDLEY, WILLIAM J. N90-28651
N90-28652
BRINKMAN, C. R. N90-28849
BROSIUS, E. B. N90-28956
BROWN, ROBERT M. N90-28937
BROWNE, ALLEN C. N90-29098
BRUSASCO, R. M. N90-28738
BRUSH, L. N. N90-29200
BRUSHER, GERALD A. N90-28615
BUCHANAN, P. K. N90-28884
BUCK, M. E. N90-28898
BUEHLER, CH. N90-29013
BUFACCHI, B. N90-28518
BURCHAM, FRANK W., JR. N90-28551
BURDEA, GRIGORE C. N90-29058
BURDICK, J. N90-29045
BURKS, B. L. N90-29065
BURNSIDE, W. D. N90-28766
BURRELL, K. H. N90-29187
BURRUS, D. L. N90-28554
N90-28555
BURSEY, R. W., JR. N90-28624
BUSHNELL, D. M. N90-28493
BUSHNELL, PETER N90-28552
BUSTARD, DAVID W. N90-29110
BUTLER, MICHAEL S. N90-29014
BUZAN, FORREST T. N90-29007
BYER, ROBERT L. N90-28834

C

CABON, PH. N90-28990
CAILLAS, C. N90-29066
CALDEIRA, AMIR O. N90-29228
CALLIN, R. S. N90-29178
CALVERT, W. N90-29284
CAMARANETO, GILBERTO N90-28886
N90-29253
CAMERON, STEPHEN N90-29074
CAMPAGNAC, M. H. N90-28722
CAMPBELL, J. H. N90-28738
CANFIELD, P. C. N90-29206
N90-29207
CANNAS, SERGIO A. N90-29213
CANNON, JAMES L. N90-28620
CANTWELL, ELIZABETH N90-29083

CARDINALE, G. F. N90-29222
CARLEY, L. RICHARD N90-29019
CARLSON, LELAND A. N90-28490
CARLSTROM, T. N. N90-29187
CARMICHAEL, ALISTAIR A. N90-28674
CARNEIRO, C. E. I. N90-29150
CARROLL, R. G. N90-28631
CARSEL, ROBERT F. N90-29252
CARTAXOMODESTODESOUZA, RICARDO N90-28886
CARTER, J. P. N90-28860
CARYOTAKIS, G. N90-29178
CASAS, JOSEPH C. N90-28906
CATALANO, A. N90-29204
CELMINS, ILMARS N90-28506
CERDEIRA, HILDA A. N90-29227
N90-29228
CHACON, VINCE N90-28542
CHAHROUR, C. A. N90-28554
N90-28555
CHALON, G. N90-28947
CHAMIS, C. C. N90-28616
CHAN, JEFFREY W. N90-28510
CHAN, S. T. N90-28605
CHANDLER, G. A. N90-29190
CHANG, BILIN N90-28867
CHANG, C. N90-28684
CHANG, YOW-YIEH N90-29145
CHANIOTAKIS, EMMAHOUIL ANTONY N90-29197
CHAPMAN, K. S. N90-28813
CHARLES, STEVE N90-29010
CHASSAING, P. N90-28810
CHEN, C. L. N90-29071
CHEN, C. P. N90-28693
CHEN, JIAN-SHIANG N90-28843
CHEN, P. C. N90-28851
CHEN, TIAN-LUN N90-29140
CHENG, R. K. N90-28686
CHEONG, DEOCK-SOO N90-28740
CHERRY, D. G. N90-28563
CHIDUME, CHARLES E. N90-29138
CHIZEK, LARRY VERNON N90-29186
CHODY, JOSEPH R. N90-28517
CHOLLET, J. P. N90-28807
CHOREY, C. M. N90-28786
CHOURA, SLIM N90-28575
CHRISTENSEN, C. R. N90-28729
CHUDAMANI, SURYANARAYANAN N90-29283
CHUN, WENDELL N90-29070
CHURCHILL, SUSANNE N90-29085
CISCON, L. N90-29068
CLABORN, G. W. N90-29116
CLARK, C. W. N90-29296
CLAUS, R. O. N90-28825
CLIFFORD, STEVEN F. N90-28939
CLOUGH, S. A. N90-28923
COATS, R. S. N90-29190
COBLEIGH, BRENT R. N90-28578
COBLENTZ, A. N90-28990
COCQUEREZ, J. L. N90-28532
CODY, JOE C. N90-28618
N90-28620
CODY, W. J. N90-29127
COE, HAROLD H. N90-28622
COHEN, HARVEY D. N90-28962
COHEN, MARTIN N90-29265
COLBAUGH, R. N90-29004
COLEMAN, K. C. N90-28684
COMBER, C. N90-29293
CONDAMINAS, A. N90-28534
CONNOLLY, D. J. N90-28596
CONNOR, J. W. N90-29196
CONNORS, VICKIE S. N90-28906
CONTE, A. N90-28708
CONWAY, LYNN N90-28854
CORBAN, JOHN ERIC N90-28587
CORIELL, S. R. N90-28790
COTNOIR, L. J. N90-28832
COTON, P. N90-28532
COTTLE, RICHARD W. N90-29145
COUSINS, T. N90-29220
COWLEY, STEPHEN J. N90-28789
COX, ARTHUR N. N90-29266
N90-29267
N90-29277
N90-29278
N90-29279
N90-29288
COX, GEORGE B., JR. N90-28634
CROUSE, GEORGE RENO N90-29241
CROWLEY, CHARLES R. N90-29261
CROWLEY, JOHN STEPHEN N90-29080
CUAN, WINSTON M. N90-28621
CUCINOTTA, FRANCIS A. N90-29290
CUPERTINODURAO, OTAVIO S. N90-29100
CURRAN, FRANCIS M. N90-28657
CURRAN, T. C. N90-28909
CURRY, ROBERT E. N90-28533

D

DABROWSKI, CHRISTOPHER E. N90-29243
DACOSTAPEREIRA, ALFREDO, JR. N90-29296
DACOSTAPEREIRA, MARCOS N90-29298
DACUNHA, S. F. N90-28726
DARGUSH, G. F. N90-28617
DAS, AAHOK N90-29225
DASILVA, L. R. N90-29214
DAVENPORT, A. J. N90-28721
DAVID, G. D. N90-28715
DAVIDSON, DAVID L. N90-28676
DAVIES, BARRY F. N90-29012
DAVILAMASCARENHAS, NELSON DELFINO N90-29092
DAVIS, DONALD Y. N90-28558
DAVIS, GARY A. N90-28615
DAVIS, JAMES N90-28762
DAVIS, LARRY S. N90-29022
DAWSON, L. R. N90-28690
N90-29208
DEAN, THOMAS N90-29025
N90-29042
N90-29069
DEBELLIS, WILLIAM B. N90-28982
DEBONI, T. M. N90-28689
DECASTRO, EMORY S. N90-28545
DECKER, NAOMI H. N90-29125
DECRESCENTE, M. A. N90-28703
DECRUYENAERE, JEAN-PAUL N90-28579
DEDHIA, D. D. N90-28645
DEFIGUEIREDO, R. N90-29068
DEHOFF, P. H. N90-28855
DEJONG, A. N. N90-28887
DELAPLATA, LUIS MARQUEZ N90-28991
DELFRATE, JOHN H. N90-28505
DELLERBA, G. N90-28989
DELOURDESBUENOTRINDADE, MARIA N90-28891
DEMAGALHAES, A. C. N. N90-29214
DEMENTHON, DANIEL N90-29022
DENN, M. M. N90-28824
DENTON, R. N90-29193
DEOLIVEIRA, H. P. N90-29282
DEOLIVEIRAALMEIDA, SERGIO ALBERTO N90-29298
DEPINHODASILVA, EDSON N90-29215
DERZON, M. S. N90-29190
DESARMOT, G. N90-28672
DESCHAMPS, JACQUES N90-28530
DESJARLAIS, M. P. N90-29190
DESSOUKY, K. I. N90-28593
DEVELICE, R. L. N90-28942
DIAS, S. A. N90-29150
DIBELLA, F. A. N90-28904
DICKEY, MICHAEL R. N90-28788
DICKINSON, WILLIAM J. N90-28636
DICKSON, LAWRENCE W. N90-28674
DIMARZO, M. N90-28799
DINKEL, C. N90-28757
DIONISE, JOSEPH N90-29056
DODSON, H. N90-28628
DOLAN, FRED J. N90-28620
DOLINSKY, S. N90-29016
DONALDSON, C. D. N90-28493
DOOGOOD, P. N. N90-28547
DOSS, E. D. N90-28608
DOYLE, E. J. N90-29187
DOYLE, RICHARD J. N90-29037
DRAEGER, J. N90-28987
DREICER, JARED S. N90-29097
DRESNER, LAWRENCE N90-29130
DUBIEL, D. J. N90-28567
N90-28568
DUBOIS, FREDERICK W. N90-28745
DUDAS, CHARLES N90-28762
DUFRANE, K. F. N90-28623
DUNKLE, SUSAN B. N90-29109
DUTRA, LUCIANO VIEIRA N90-29092
DUYAR, AHMET N90-28659
DVORCHAK, STEPHEN R. N90-28976
DWIVEDI, SUREN N. N90-29017
N90-29027
DYE, RAYMOND H. N90-28970
DYER, C. S. N90-28934
N90-29293

E

EBLEN, LARRY H. N90-28948
ECKEL, ANDREW J. N90-28655
EGAN, J. J. N90-29211
EICHENBERG, DENNIS J. N90-28833
EINSTEIN, J. R. N90-29065
EISEMAN, S. E. N90-29195
EISMANN, PAUL H. N90-29001
ELDER, J. E. N90-28713
ELFES, ALBERTO N90-29075
ELLEFSON, R. E. N90-28685
ELLIOTT, C. J. N90-28830
ELLIS, J. R. N90-29250
ELLIS, JOHN N90-29247
EMERICK, KEN N90-29057
EMMETT, J. L. N90-28738
EMRICH, M. L. N90-29120
ENDSLEY, MICA R. N90-28974
ENGLADE, R. C. N90-29189
ENGLER, ROLF H. N90-28498
ENNIX, KIMBERLY A. N90-28788
EPPLEY, K. R. N90-29178
ERCOLINE, WILLIAM R. N90-28985
ERICKSON, C. M. N90-28640
ERKMEN, A. M. N90-29041
ERLEBACHER, GORDON N90-28502
ERTHAL, GUARACI JOSE N90-29253
ESSENS, P. J. M. D. N90-28760
ETKIN, A. N90-29195
ETZKORN, H. W. N90-28738

F

FABRY, JOHN M. N90-29249
FANT, K. S. N90-29178
FAORO, R. N90-28909
FARHAR, BARBARA C. N90-29258
FARKAS, L. A. N90-28850
FARKAS, Z. D. N90-29178
FARRELL, JAMES D. N90-29001
N90-29047
FARRELL, ROGER A. N90-29260
FARREN, J. N90-28934
FARROW, JOSEPH E. N90-28758
FAVROW, L. H. N90-28643
FEEZELL, R. R. N90-29065
FEINSTEIN, J. N90-29178
FELDMAN, JEROME A. N90-28971
FELGUEIRAS, CARLOS ALBERTO N90-29253
FELL, C. N90-28683
FENTON, R. G. N90-29006
FERBER, M. K. N90-28734
FERG, D. N90-28866
FERLAND, G. J. N90-29275
FERREIRAMESILVA, ANTONIO JOSE N90-28886
FEUERBACHER, BERNDT N90-29159
N90-29162
FIESELMANN, B. N90-29204
FINK, LAWRENCE E. N90-28635
N90-28660
FINNSTROM, B. N90-28902
FISHER, DAVID F. N90-28505
FISHER, MARK N90-28731
FISHER, S. C. N90-28633
FISK, Z. N90-29206
N90-29207
FITZ-SIMONS, T. N90-28909
FITZMAURICE, N. N90-28816
FLANIGAN, L. A. N90-28656
FLETCHER, J. MURRAY N90-29261
FLIFLET, A. W. N90-28823
FLY, GERALD W. N90-28614
FLY, J. N90-29122
FLYNN, T. N90-28884
FOLEY, K. J. N90-29195
FOLLMER, ANDREW C. N90-29240
FOLTZ, H. L. N90-28554
N90-28555
FONG, ELIZABETH N. N90-29243
N90-29245
FOOTE, L. N90-28866
FORGET, PHILIPPE N90-28953
FORGY, C. L. N90-28952
FORMAN, ROYCE G. N90-28647
FORNEY, G. P. N90-29103
FORNEY, L. J. N90-28827
FORTSON, NORVAL N90-29181
FORTUNATI, KIM LESTER N90-29202
FOSLIEN, W. K. N90-29054
FOSTER, JOHN E. N90-28581
FOUILLOT, J.-P. N90-28990
FOWKES, W. R. N90-29178
FOX, MARK S. N90-29039
FRACKER, MARTIN L. N90-28978
FRALICK, G. C. N90-28827
FRANCIS, COLIN M. N90-29057
FRANK, N. N90-28909
FREAS, W. N90-28909
FREEMAN, ROBERT A. N90-29046
FREUND, E. N90-29013
FRIEDRICHS, REINHARD N90-28585
FUJIKAWA, G. N90-28596

G

GAC, FRANK D. N90-28673
GAIER, J. R. N90-28696
GALLARDO, JUAN C. N90-29270
GALLIEN, RANDY N90-28661
GANGE, R. W. N90-28966
GARDNER, JOHN H. N90-28573
GARDNER, WILLIAM B. N90-28564
N90-28565
GARECHT, D. M. N90-28609
GARNER, F. A. N90-28724
GARRETT, A. J. N90-28979
GAUDET, L. N90-28800
GAWTHROP, P. E. N90-28756
GEER, JAMES F. N90-28814
GELL, T. G. N90-28800
GEMAYEL, CHAOUKI A. N90-28582
GEORGIOU, I. N90-28678
GERA, JOSEPH N90-28516
GERMAN, RANDALL M. N90-28728
GEYER, H. K. N90-28608
GHASSEMIAN, HASSAN N90-28888
GHIRARDI, GIANCARLO N90-29229
GIBBONS, T. B. N90-28700
GIBSON, C. P. N90-28979
GIBSON, HOWARD G. N90-28620
GIBSON, K. N. N90-29250
GIBSON, W. A. N90-28826
GILBERT, WILLIAM P. N90-28516
N90-28531
GILES, D. W. N90-28824
GILLESPIE, L. N90-28857
GILLESPIE, L. K. N90-28857
GILLINGHAM, KENT K. N90-28985
GILYARD, GLENN B. N90-28551
GIRARD, R. N90-28874
GLAESER, JOHN S. N90-28549
GLASS, K. N90-29004
GLEESON, J. N90-28623
GLENDENNING, N. K. N90-29269
GLICK, J. F. N90-28904
GLOCKER, B. N90-28658
GODART, C. N90-29206
GOELZ, T. M. N90-28658
GOGOUSSIS, ARISTIDES N90-28846
GOHIL, P. N90-29187
GOIX, P. J. N90-28686
GOLDENBERG, A. A. N90-29006
GOLDFINE, A. H. N90-29245
GOLDSTEIN, B. N90-29204
GOLDSTEIN, J. C. N90-28830
GOMESMARINHO, CELSO VALIM N90-28949
GONG, LESLIE N90-28815
GOODMAN, BRADLEY A. N90-29036
GORDON, ELIOTT B. N90-28504
GORDON, T. D. N90-28590
GORE, ROBERT ALLEN N90-28796
GORMSEN, BARBARA B. N90-28906
GOSSANT, MICHEL N90-28736
GRAFF, EHOUD N90-28664
GRAHAM, CHARLES N90-28962
GRAHAM, J. M. R. N90-28527
GRANT, RICHARD L. N90-28597
GRASSE, W. N90-28902
GRAVES, R. L. N90-28849
GRAY, D. E. N90-28564
N90-28565
GREBER, ISAAC N90-28504
GREEN, DAVID M. N90-28969
GREEN, JAMES M. N90-28627
GREEN, JOHN N90-28695
GREENBERG, W. N90-29126
GREINER, M. N90-28798
GRESHO, P. M. N90-28805
GRETZ, BRUCE N90-29005
GRIEGER, G. N90-29192
GRIFFIN, G. R. N90-28543
GRIGORIEV, ANATOLI I. N90-28965
GRISHAM, J. A. N90-28729
GRODSINSKY, CARLOS M. N90-28754
GROEBNER, R. J. N90-29187
GROOM, NELSON J. N90-28751
GROSCHE, FRIEDRICH R. N90-28499
GRUSS, ANDREW N90-29019
GUEDEL, M. N90-29287
GUEDRY, F. E., JR. N90-28993
GUERDAL, ZAFER N90-28862
GUHA, S. N90-28896
GUICHAOUA, C. N90-28761
GUIRAUD, D. N90-29114
GULATI, SANDEEP N90-29030
GULLIVER, AUSTIN F. N90-29261
GUO, HAN-YING N90-29135
GUPTA, A. K. N90-28712
GUSTAFSSON, BERTIL N90-28811
GUTOWSKI, W. J. N90-28923
GUVENEN, HALDUN N90-28496

H

HAARBERG, GEIR M. N90-29211
HABIGER, H. N90-28658
HACHAM, H. N90-28966
HACKENBURG, R. W. N90-29195
HAGA, WILLIAM J. N90-29089
HAGANS, K. N90-28785
HAGSTROM, THOMAS N90-29124
HAHNE, DAVID E. N90-28521
HAINES, W. E. N90-28955
HAIRE, MICHAEL N90-28954
HALBERT, E. C. N90-28851
HALFORD, GARY R. N90-28642
HALL, WILLIAM J. N90-28869
HALPERN, JULES N90-29280
HAMACHER, HANS N90-29159
N90-29162
HAMAMATSU, T. N90-28900
N90-28901
HAMBERGER, S. M. N90-29192
HAMBOURGER, P. D. N90-28696
HAMEED, S. N90-28919
HAMEL, PETER N90-29159
N90-29160
HAMILTON, WILLIAM L. N90-28976
HAMINH, H. N90-28810
HAMM, R. N. N90-28826
HAMMOND, N. D. A. N90-29293
HAMMONS, B. E. N90-28690
HAMPEL, H. N90-28715
HANCOCK, G. J. N90-28525
HANKLA, A. N90-28785
HANLIN, JERRY WILLIAM N90-29255
HANNAFORD, BLAKE N90-29052
HANNEMANN, KLAUS N90-28812
HARDY, J. R. N90-28689
HARJES, H. C. N90-28776
HARMON, P. N90-29051
HARRIS, D. O. N90-28645
HARRIS, J. H. N90-29191
HARRIS, JAMES A. N90-28750
HARRIS, K. E. N90-29242
HARVEY, J. F. N90-28821
HARWOOD, DAVID N90-29022
HASTIE, R. J. N90-29196
HAVSTAD, MARK A. N90-28719
HAYASAKA, T. N90-28900
HAYASHI, AKIRA N90-29069
HAYATI, SAMAD N90-29060
HAYWARD, VINCENT N90-29048
N90-29060
HEBEN, MICHAEL J. N90-28697
HEBERT, M. N90-29066
HEINEN, V. O. N90-28786
HELAYELNETO, JOSE A. N90-29156
HEMON, ALAIN N90-28809
HEMSING, W. F. N90-29184
HENRIKSEN, G. L. N90-28778
HEPP, A. F. N90-28696
HEPP, ALOYSIUS F. N90-29219
HERBELL, THOMAS P. N90-28655
HERSBACH, H. J. C. N90-28711
HERSHKOWITZ, ELAINE N90-29009
HESSBURG, T. M. N90-29054
HEUS, RAYMOND J. N90-29211
HIBRAY, R. E. N90-28690
HICHO, G. E. N90-28716
HICKS, THOMAS M. N90-28948
HILDEBRAND, JOHN A. N90-29168
HILL, S. D. N90-28576
HILLIS, S. L. N90-28743
HIMSOLT, GUENTHER N90-28733
HINKLE, C. ROSS N90-28925
HIRMAN, JOSEPH W. N90-28935
HIRSCHBEIN, MURRAY S. N90-29067
HO, P. Y. N90-28557
HODGKINSON, JOHN N90-26517
HOEFER, HANS N90-28499
HOFFMEYER, J. A. N90-28755
HOLLAND, J. ALVIN N90-28906
HOLLARS, MICHAEL G. N90-29057
HOLMES, R. R. N90-28653
HOLMES, W. M. N90-29242
HOLONYAK, N., JR. N90-28835
HONG, BOR ZEN N90-28669
HOPKINS, D. A. N90-28616
HOPSON, GEORGE D. N90-28597
HORNER, JANE LOUISE N90-28875
HOSHIHNING, CARLOS N90-28945
HOTES, DEBORAH L. N90-28670
HOWE, DAVID C. N90-28560
N90-28566
N90-28569
N90-28570
HSIEH, K. C. N90-28835
HUANG, WU-QUN N90-29140
HUBBARD, HARVEY H. N90-29169
HUBERSON, SERGE N90-28809
HUDAK, STEPHEN J., JR. N90-28648
HUDIONO, H. N90-28838
HUELSKAMP, MARGARET N90-28731
HUMMEL, D. N90-28519
HUMMEL, PAUL R. N90-29252
HUNDLEY, M. F. N90-29206
N90-29207
HUNG, R. J. N90-28694
N90-28933
HUNKA, GEORGE W. N90-29049
HUNT, D. R. N90-28547
HURST, G. S. N90-28826
HUSTON, T. E. N90-28826
HUTCHINSON, JOHN J. N90-29247
HWANG, JENQ-NENG N90-29096

I

IACONO, M. N90-28923
IDE, KAYO N90-28497
IIYOSHI, A. N90-29192
IMHOFF, JOHN C. N90-29252
IMMARIGEON, J.-P. N90-28712
IMORU, CHRISTOPHER OLUTUNDE N90-29132
N90-29146
IOFFE, L. N90-29216
ISAACS, H. S. N90-28721
ISHIKAWA, H. N90-28900
N90-28901
ITO, KEI N90-29154
N90-29155
IYENGAR, S. SITHARAMA N90-29029
N90-29030
IZAKI, Y. N90-28900

J

JACKSON, G. N90-29176
JACKSON, M. E. N90-28656
JACKSON, W. B. N90-28730
JACOBS, S. S. N90-28955
JACOBSON, M. J. N90-28930
JAIN, RAMESH N90-29084
JAIN, V. K. N90-29199
JAMSHIDI, MO N90-29033
JARRY, P. N90-28761
JASCHINSKI, ALFRED N90-28853
JASPER, G. L. N90-28912
N90-28913
N90-28914
N90-28915
JAYARAMAN, N. N90-28880
JEDREY, T. C. N90-28593
JENSEN, J. H. N90-29234
JENSEN, M. A. N90-28856
JENSEN, R. J. N90-28628
JERNIGAN, TAMARA ELIZABETH N90-29271
JIANG, IVAN CHEN WEN N90-28572
JIAYU, CHEN N90-29193
JOANNOPOULOS, JOHN D. N90-28682
N90-29223
JOGUET, P. N90-28873
JOHNSON, C. A. N90-29250
JOHNSON, C. E. N90-28732
JOHNSON, D. J. N90-29190
JOHNSON, N. N90-28730
JOHNSON, PAUL LESLIE N90-28797
JOHNSON, VICKI S. N90-28535
JOHNSON, W. STEVEN N90-28871
N90-28872
JOHNSTON, MARK D. N90-29078
JOHNSTON, S. E. N90-28850
JONES, C. S. N90-28656
JONES, GARY N90-29017
JONES, J. E. N90-28841
JONES, MARK T. N90-28876
JONES, W. W. N90-29103
JOPPE, J. L. N90-29183
JOSEF, J. A. N90-29116

K

KAELBLING, LESLIE PACK N90-29077
KAESBAUER, DIETER N90-29118
KAHL, W. K. N90-28849
KAILASANATH, KAZHIKATHRA N90-28573

KAIMAL, J. C. N90-28927
KAISUWAN, PISUT N90-28818
KALKANIS, P. N90-28527
KALLURI, SREERAMESH N90-28642
KAN, EDWIN P. N90-29049
N90-29050
KANADE, TAKEO N90-29019
N90-29066
KANNEL, J. W. N90-28623
N90-28625
KAPPERS, A. N90-28973
KARDASHEV, N. S. N90-28764
KARLEN, JAMES P. N90-29001
N90-29047
KARLISCH, PATRICIA N90-28959
N90-28960
KARO, A. M. N90-28689
KASSNER, M. E. N90-28723
KATORI, MAKOTO N90-29165
KAWALKO, STEPHEN F. N90-29180
KAWAMOTO, T. N90-28779
KAWASHIMA, NAOKI N90-29165
KAZEROONI, H. N90-29054
KEBA, J. E. N90-28626
KEENAN, E. D. N90-29254
KELLER, PETER N90-29091
KELLEY, D. R. N90-28732
KELLEY, ROBERT B. N90-29024
KELLY, STEPHEN EDWARD N90-28961
KEMMERLY, GUY T. N90-28531
KEMP, R. A. W. N90-28887
KENNEDY, E. N90-28847
KENNEDY, P. J. N90-28708
KENNEDY, R. M. N90-28957
KENYON, S. J. N90-29275
KERSTEN, R. TH. N90-28738
KESSLER, ROLAND N90-28801
KHONSARI, M. M. N90-28791
KHOSLA, PRADEEP K. N90-29023
KHVESHCHENKO, D. V. N90-29217
KIM, HAKIL N90-28889
KING, G. A. N90-28942
KING, J. F. N90-28720
KING, S. N90-29051
KING, W. CHRIS N90-28882
KINZEL, WAYNE MORRIS N90-29291
KIRCHER, T. A. N90-28702
KITTLE, JOHN L., JR. N90-29252
KLASSEN, M. N90-28799
KLEIN, C. A. N90-28837
KLEIN, VLADISLAV N90-28578
KLEPPNER, DANIEL N90-29295
KLUCZ, RAYMOND S. N90-28788
KMIEC, T. D. N90-28631
KNEFF, D. W. N90-29172
KNIGHT, NORMAN F., JR. N90-28877
KNOX, CHARLES E. N90-28546
KNUTH, WILLIAM H. N90-28637
KO, K. N90-29176
KOEL, B. N90-28718
KOFFSKEY, W. E. N90-28916
KOGAN, YA. I. N90-29217
KOHN, STARR D. N90-28582
KONKEL, C. N90-29051
KOONTZ, R. F. N90-29178
KORKOSZ, G. N90-28866
KOURTA, A. N90-28810
KOUTSOUGERAS, C. N90-29032
KOVRIZHNYKH, L. M. N90-29192
KOZLOV, S. M. N90-29137
KRESSE, JOHN N90-28533
KREUTZ, K. N90-29003
KRISHAN, V. N90-29289
KRITZ, A. H. N90-29189
KROME, ELIZABETH C. N90-28954
KROO, ILAN N90-28540
KROTKOV, E. N90-29066
KUIPERS, A. N90-28973
KULKARNI, SHRINIVAS R. N90-29262
KUNATH, R. R. N90-28596
KUOKKA, DANIEL R. N90-29079
KURTZ, H. L. N90-28658
KURTZ, RONALD N90-29048
KURTZ, S. R. N90-29208
KURYLO, M. J. N90-28929
KUSUNOSE, N. N90-28900
KWEON, I. S. N90-29066

L

LABREZE, LAURENT N90-28964
LADD, JUDSON W. N90-28948
LAFLAMME, J. C. G. N90-28701
LAI, J. Y. N90-28870
LAI, S. K. N90-28725
LALOR, N. N90-29141
LALVANI, HARESH N90-28598
LAM, SHUI T. N90-28789
LAMBRIGHT, W. HENRY N90-29259
LANDELL, B. PATRICK N90-29050
LANDGREBE, ALBERT N90-28899
LANDGREBE, DAVID N90-28888
LANDOLT, J. P. N90-28992
LANGE, ROBERT D. N90-29086
LANGHOFF, STEPHEN R. N90-28680
LAPOTIN, NANCY T. N90-28893
LARKIN, A. I. N90-29216
LARKIN, M. J. N90-28556
LASHMORE, D. S. N90-28732
LATAITIS, RICHARD J. N90-28939
LAUFER, P. M. N90-28832
LAUGHREY, JAMES A. N90-28514
LAUGIER, CHRISTIAN N90-29073
LAVIN, S. P. N90-28557
LAW, CHUNG K. N90-28746
LAWRENCE, J. M. N90-29207
LAWRENCE, VICTOR B. N90-28647
LAY, N. E. N90-28593
LE, HUNG SON N90-29139
LE, VAN HOP N90-29133
N90-29136
LEE-BECHTOLD, S. N90-29242
LEE, C. S. G. N90-29071
LEE, D. K. N90-29191
LEE, G. S. N90-29191
LEE, SUCK GYU N90-28844
LEE, T. H. N90-28766
LEE, THOMAS S. N90-29053
LEE, YU-TAI N90-28572
LEEPER, R. J. N90-29190
LEGER, A. N90-28983
LEGER, ALAIN N90-28988
LEHECKA, T. N90-29187
LEIGHT, WALTER G. N90-29239
LEMER, A. C. N90-28580
LENIHAN, J. N90-28942
LEO, ANTHONY N90-28781
LESIEUTRE, DANIEL J. N90-28494
LEVINE, LINDA N90-29109
LEWIS, LIANE C. N90-28522
LEWIS, NATHAN S. N90-28697
LEWIS, PAUL S. N90-29096
LI, FEIYUE N90-28591
LIGOMENIDES, PANOS A. N90-29063
LILJEGEN, TORSTEN N90-28744
LILLY, DOUGLAS K. N90-28772
LIMBERG, T. N90-29179
LINDELL, I. V. N90-29158
LINDENBAUM, S. J. N90-29195
LINKER, KEVIN L. N90-28897
LITMAN, DIANE J. N90-29036
LITT, JONATHAN S. N90-29121
LIU, K. C. N90-28849
LIVINGS, JEFFREY G. N90-28762
N90-28765
LOBITZ, D. W. N90-29123
LOCKNER, T. R. N90-29190
LOHMANN, R. P. N90-28567
LONG, M. N90-29003
LONGACRE, R. S. N90-29195
LONGIN, TERESA L. N90-28897
LOPATA, VINCE J. N90-28674
LOPES, J. LEITE N90-29152
LOPEZ, L. N90-29051
LOTT, STEPHEN N90-28781
LOVE, W. A. N90-29195
LU, SHI N90-28869
LUBUMA, MBARO-SAMAN N90-29138
LUCCHESINI, M. N90-28518
LUHMANN, N. C., JR. N90-29187
LUMIA, R. N90-29055
LUMSDEN, J. B. N90-28619
LUO, H. A. N90-28878
LYKINS, B. W. N90-28916
LYON, J. F. N90-29192
LYONS, TERENCE J. N90-28985

M

MABEY, D. G. N90-28525
N90-28526
MACCONOCHIE, IAN O. N90-28589
MACHEERS, FRANK H. N90-29247
MACLEOD, J. D. N90-28701
MAENCHEN, J. E. N90-29190
MAGNANI, NICHOLAS J. N90-28899
MAHAJAN, S. M. N90-29193
MAHAJAN, SWADESH M. N90-29289
MAHALINGAM, SWAMINATHAN N90-29027
MAHDAVI, M. A. N90-29187
MAHMOUD, SAAD MUSTAFA N90-28548
MAIENSCHEIN, J. L. N90-28739
MAJIDZADEH, KAMRAN N90-28581
MALCOLM, GERALD N. N90-28522
MALKIN, FRANK J. N90-28982
MALLOCH, CHARLES BERNARD N90-29093
MALY, KURT N90-29108
MANE, L. N90-29114
MANFRIANI, L. N90-28518
MANGES, W. W. N90-29065
MANGOLD, P. N90-28528
N90-28529
MANN, G. A. N90-28776
MANN, REINHOLD C. N90-29119
MANSON, ANDRE N90-29167
MARCHANT, R. D. N90-28570
MARCHIANDO, J. F. N90-29201
MARCUS, STEVEN I. N90-29046
MARHEFKA, R. J. N90-28766
MARIZ, A. M. N90-29214
MARKS, BRET A. N90-28521
MARPLE, V. A. N90-29173
MARQUES-BONHAM, SIRLEY N90-29149
MARSHALL, DANIEL N90-28769
MARTIN, C. A. N90-28576
MARTIN, C. R. N90-28905
MARTIN, J. W. N90-28856
MARTINS, MARCELO L. N90-29212
MARTINSSERRA, PAULO ROBERTO N90-28886
MARTY, DAVID E. N90-28618
MARX, J. N. N90-29185
MASSIMINO, MICHAEL J. N90-29008
MASSINES, J. N90-28808
MASTAGLIO, THOMAS WALTER N90-29088
MATECZUN, A. N90-28993
MATHIAS, J. J. N90-29203
MATIJEVIC, J. R. N90-29015
N90-29016
MATSUMOTO, H. N90-29187
MATUSZAK, LEO M. N90-28788
MAURER, M. N90-28857
MAWID, MOHAMMD AHMED N90-28688
MAY, PETER T. N90-28939
MAYER, J. R. R. N90-29021
MAYN, C. W. N90-29242
MAYTUM, D. N90-28966
MAZIASZ, P. J. N90-28720
MCBRAYER, J. D. N90-28898
MCCABE, GREGORY J., JR. N90-28944
MCCAMMON, D. F. N90-28956
MCCAMMON, K. N90-28785
MCCARTHY, G. J. N90-28643
MCCARTY, ROBERT D. N90-28681
MCCLAIN, JAMES ENNIS N90-28544
MCCLEARY, SUSAN L. N90-28877
MCCRAY, ALEXA T. N90-29098
MCCURDY, DAVID A. N90-29166
MCFADDEN, G. B. N90-28790
N90-29200
MCGAW, MICHAEL A. N90-28644
MCGILL, R. N. N90-28743
MCHARGUE, CARL J. N90-28881
MCKAY, J. A. N90-28832
MCKECHNIE, T. N. N90-28653
MCKIM, HARLAN L. N90-28893
MCMILLEN, R. T. N90-28928
MCMURPHY, F. E. N90-28739
MCQUEEN, H. J. N90-28723
MEAGHER, GREGORY M. N90-28632
MEHLHORN, T. A. N90-29190
MEIBURG, ECKART N90-28602
MELE, P. A. N90-28955
MELEK, M. N90-29232
MENDENHALL, MICHAEL R. N90-28494
MERRILL, WALTER N90-28659
MERRIMAN, T. L. N90-28625
MERRY, CAROLYN J. N90-28893
MEYREL, REMY N90-28707
N90-28710
MEYER, J. N90-28810
MEYER, ROBERT R., JR. N90-28820
MEYER, T. G. N90-28643
MEYERHOFF, MARK E. N90-28545
MEYERS, CHARLES A. N90-28648
MEYSTEL, A. N90-29043
N90-29082
MICKLITZ, H. N90-29218
MILBURN, R. H. N90-29174
MILLER, S. N90-28683
MILLIGAN, WALTER W. N90-28641
MING, R. S. N90-29141
MINNICK, STEPHEN A. N90-28787
MOBLEY, RICHARD M. N90-28774
MOED, MICHAEL C. N90-29040
MOES, TIMOTHY R. N90-28820
MOFFATT, R. E. N90-28952

MOKHTARI, SUSAN N90-29156
MOLLARD, R. N90-28990
MOLNAR, G. N90-28923
MONTEMERLO, MELVIN D. N90-29067
MOODY, STEPHEN MARK N90-28842
MOORE, D. H. N90-29257
MOORE, JAMES D. N90-28618
MOORHOUSE, DAVID J. N90-28514
MORAN, P. J. N90-28715
MOREL, J. E. N90-29116
MORGAN, F. A. N90-28776
MORGAN, SIOBAHN M. N90-29266
N90-29279
MORIMOTO, CARL N90-29050
MORITSUKA, H. N90-28901
MORRIS, J. N90-29204
MORRIS, P. M. N90-28567
MORRIS, T. W. N90-29195
MOSES, O. DOUGLAS N90-29256
MOSTAFA, IBRAHIM MOHAMMED N90-28864
MOULTON, BRYAN J. N90-28533
MUGIKURA, Y. N90-28900
MUIRHEAD, BRIAN K. N90-29067
MULLEN, J. L. N90-28732
MULLINS, D. R. N90-28718
MUNDY, J. N90-29260
MURRAY, B. T. N90-28790
MURRAY, STEPHEN DAVID N90-29272
MURRI, DANIEL G. N90-28522
MUSCETTOLA, NICOLA N90-29038
MUSS, JEFFREY A. N90-28632
MYERS, LAWRENCE P. N90-28551

N

NAERHEIM, Y. N90-28619
NAGLER, S. E. N90-29209
NAGY, LAWRENCE A. N90-28768
NAIK, DIPAK N90-28855
NAISH, PETER L. N. N90-28984
NAVARRO, A. P. N90-29192
NEAL, GRAEME N90-28583
NEALY, JOHN E. N90-29290
NEILSON, R. P. N90-28942
NELSON, E. E. N90-28845
NELSON, W. E. N90-29190
NEMETH, MICHAEL P. N90-28859
NESBITT, JAMES A. N90-28851
N90-28852
NEWTON, J. N90-29204
NG, LIAN N90-28502
NG, T. TERRY N90-28522
NGUY, HENRY L. N90-28647
NGUYEN, H. LEE N90-28792
NGUYEN, LUAT T. N90-28516
NGUYEN, THONG V. N90-28630
NICE, D. STEPHEN N90-28968
NILSEN, JOSEPH N90-28831
NITSCHKE-KOWSKY, PETRA N90-28803
NIU, Q. N90-29234
NIU, WILLIAM N90-29084
NOBILE, A. N90-29106
NORDSTROEM, JAN N90-28811
NORMAN, V. S. N90-29250
NOVELLO, M. N90-29282
NOVIKOV, I. D. N90-28764
NOWAK, ROBERT J. N90-28806
NOYES, GEROLD N90-28903

O

OAKLEY, CAROLYN N90-28985
OBRIEN, C. J. N90-28639
ODEN, J. TINSLEY N90-28614
N90-29122
ODOWD, J. N90-29204
OELKER, HANS-CHRISTOPH N90-28519
OERTEL, HERBERT N90-29159
N90-29161
OH, BYEONG SOO N90-28550
OHERN, MICHAEL E. N90-28861
OHLHORST, CRAIG W. N90-28541
OLEARY, C. O. N90-28520
OLIVER, B. M. N90-29172
OLSON, B. A. N90-29173
OLSSON, MATS-OLOF N90-28538
N90-28539
OLVEY, LAURA A. N90-29116
OOSTERVELD, W. J. N90-28973
OPOWER, HANS N90-29159
N90-29163
OPPERMANN, H. V. N90-28748
ORAN, ELAINE S. N90-28573
ORIN, DAVID E. N90-29072
ORIO, C. G. N90-28930
ORIORDAN, TIMOTHY N90-28917
ORMOND, F. M. N90-28929
OSBORNE, T. H. N90-29187
OSEN, KAREN S. N90-29211
OSWALD, R. S. N90-29204
OTT, GARY N90-29247
OVCHINNIKOV, YU. N. N90-29216
OVERBURY, S. H. N90-28718
OXENBERG, SHELDON N90-29050
OXOKA, A. I. N90-28511
OYTANA, C. N90-28873

P

PAFFETT, M. T. N90-28718
PAHLE, JOSEPH W. N90-28542
PALMBERG, BJORN N90-28538
N90-28539
PAPACHRISTOU, C. N90-29032
PAQUET, V. N90-28738
PARK, JONG N90-29007
PARKER, DOUGLAS SCOTT N90-28868
PARKER, G. A. N90-29021
PARSLEY, R. C. N90-28636
PARTHASARATHY, A. N90-28905
PARTRIDGE, P. G. N90-28705
PASSERO, BARBARA N90-29295
PATCH, K. D. N90-28904
PATHINAYAKE, CHANDRA N90-29273
PATNAIK, P. C. N90-28712
N90-28713
PATRICK, G. M. N90-28756
PATRICK, MERRELL L. N90-28876
PATTERSON, JOSEPH N90-29280
PAULSEN, PHILLIP E. N90-28670
PAULSON, JOHN W., JR. N90-28531
PAVLICHENKO, O. S. N90-29192
PAXSON, DANIEL EDWIN N90-28794
PAYTON, DAVID N90-29028
PEARSON, MARK L. N90-28614
PEDERSEN, J. N90-28563
PEEBLES, D. E. N90-28848
PELEGRINA, J. L. N90-28727
PENNER, J. E. N90-28919
N90-28922
PENNER, REGINALD M. N90-28697
PERONTI, M. N90-28989
PERSYN, CHARLES E. N90-29087
PESANTE, LINDA H. N90-29109
PHILLIPS, DWIGHT U. N90-28635
N90-28660
PHILLIPS, JOHN L. N90-28862
PICART, A. N90-28807
PINAIRE, JAMES A., JR. N90-28819
PISHVA, M. R. N90-28713
PITTS, WILLIAM M. N90-28910
PLATNER, E. D. N90-29195
PLATT, N. N90-28816
PODHORODESKI, R. P. N90-29006
PODLESNY, R. N90-29204
POLNAREV, A. G. N90-28764
POOLE, W. E. N90-28624
POPE, L. E. N90-28848
PORCU, S. N90-28989
PORKOLAB, M. N90-29189
POUCH, J. J. N90-28696
POURBOGHRAT, FARZAD N90-29031
PRATER, JOHN T. N90-28741
PRATHER, M. J. N90-28929
PREVIC, FRED H. N90-28980
PRICE, EVA M. N90-29259
PRIEM, RICHARD J. N90-28629
PROTOPOPESCU, V. N90-29224
PUFAHL, INGRID N90-29098
PYNE, C. R. N90-28526

Q

QUINN, ROBERT D. N90-28815
QUINTERO, RICHARD N90-28840
QURESHI, K. M. N90-29220

R

RADER, D. J. N90-29173
RADER, K. J. N90-29250
RADHAKRISHNAN, N. N90-29254
RAETZER-SCHEIBE, H.-J. N90-28714
RAGONIDEMORAESCORREIA, VIRGINIA N90-28881
RAGSDALE, DANIEL JOSEPH N90-29113
RAINER, F. N90-28738
RAJENDRA, G. N90-28492
RAJU, G. JAGGANATH N90-29007
RAMADHYANI, S. N90-28813
RAMAMURTHY, H. N90-28813
RAMASWAMY, RAMAKRISHNA N90-29227
N90-29228
RAMBOZ, JOHN D. N90-28822
RAMOS, D. N90-28857
RAMOS, J. J. N90-29198
RAND, RICHARD J. N90-29262
RANDALL, DAVID A. N90-28911
RANDJBAR-DAEMI, S. N90-29157
RAO, NAGESWARA S. V. N90-29029
RAPP, DOUGLAS C. N90-28742
RAPP, ROBERT A. N90-28699
RASPET, RICHARD N90-28769
RATNER, E. Z. N90-28778
RATVASKY, THOMAS R. N90-28578
RAU, F. N90-29192
RAU, S. SRINIVAS N90-29147
N90-29148
RAWLINSON, K. SCOTT N90-28897
RAYNER, STEVE N90-28917
READY, S. E. N90-28730
REE, MALCOLM JAMES N90-28997
REEBER, ROBERT R. N90-28741
REGENIE, VICTORIA A. N90-28542
REICHLE, HENRY G., JR. N90-28906
REITER, EDNA N90-28804
RHEW, D. D. N90-29250
RIBLETT, LOREN E. N90-28763
RICCIO, L. N90-28989
RICE, W. N90-29262
RICH, PAUL M. N90-28885
RICHARDS, J. S. N90-28613
RICHARDS, LEW N90-28781
RICHARDSON, C. N90-29094
RICHEY, A. N90-29260
RICHMOND, ROBERT J. N90-28611
RICOY, M. A. N90-28767
RIDER, JAMES P. N90-29011
RIDLEY, D. N90-28981
RIMINI, ALBERTO N90-29229
RIX, JOACHIM N90-29102
RIYOPOULOS, S. N90-28823
ROBERTS, L. N90-28523
ROBERTSON, I. M. N90-28863
ROBINSON, M. B. N90-28747
ROBINSON, P. N90-29083
RODRIGUE, GARRY N90-28804
RODRIGUEZ, CESAR ALONSO N90-28991
RODRIGUEZ, GUILLERMO N90-29000
N90-29044
RODRIGUEZ, P. I. N90-28879
ROGASH, JOSEPH A. N90-28940
ROGERS, GEORGE N90-28770
N90-28998
ROGERS, MARTIN JOHN N90-29292
ROJAS, R. N90-28766
ROMANOFSKY, R. R. N90-28788
ROMERO, JUAN J. CANTON N90-28991
ROSENSCHEIN, STANLEY J. N90-29077
ROSENTHAL, DAVID A. N90-28935
ROSENTHAL, S. E. N90-29177
ROSHKO, ANATOL N90-28817
ROTH-TABAK, Y. N90-29064
ROUHANI, S. N90-29233
RUCKMAN, MARK W. N90-29219
RUDGE, FREDERICK W. N90-28967
RUI, YUTING N90-28679
RUPERT, A. N90-28993
RUSSELL, DALE A. N90-28646
RUTLEDGE, A. T. N90-28883
RUTLEDGE, SHARON K. N90-28670
RYUTOV, D. D. N90-29188

S

SABLA, P. E. N90-28554
N90-28555
SADEH, NORMAN N90-29039
SAGE, J.-P. N90-28947
SAITOVITCH, E. BAGGIO N90-29218
SAIZAR, P. N90-29275
SALAM, ABDUS N90-29157
SALGUERO, DAVID E. N90-28495
SALIM, J. M. N90-29282
SALTSMAN, JAMES F. N90-28642
SANDERS, WILLIAM A. N90-28740
SANDLER, HAROLD N90-28965
SANDOR, PATRICK N90-28983
N90-28988
SANGHA, K. N90-28865
SARIDIS, GEORGE N. N90-29040
SARMIENTO, CHARLES J. N90-28657
SAULYS, A. C. N90-29195
SAUNDERS, CHRIS B. N90-28674

SAUNDERS, S. C. N90-28856
SAUNDERS, S. R. J. N90-28700
SAUNDERS, T. B. N90-28515
SAUVAGEOT, HENRI N90-28946
SAZAMA, C. L. N90-28952
SCHAEFER, RAINER N90-28709
SCHAFFNER, PHILIP R. N90-28751
SCHLEICHER, KLAUS-THOMAS N90-29210
SCHMALZER, PAUL A. N90-28925
SCHMITT, M. J. N90-28830
SCHNEIDER, STANLEY AARON N90-28845
SCHOENTHAL, MARK N90-28762
SCHOLZ, ARTHUR L. N90-28636
SCHOMER, PAUL D. N90-28769
SCHRADE, H. O. N90-28658
SCHUBERT, W. K. N90-28898
SCHUETZ, WALTER N90-28709
SCHUMANN, ULRICH N90-29159
SCHURMAN, I. W. N90-28930
SCHWARTZ, DEBORAH N90-29265
SCHWARTZ, R. N90-28987
SCHWARTZ, SIDNEY H. N90-28621
SCHWARTZ, STEPHEN E. N90-28920
SCORZELLI, R. B. N90-29218
SCOTT, PAUL T. N90-28571
SEABAUGH, A. C. N90-29203
SEEMAN, J. T. N90-29179
SEGALMAN, D. J. N90-29123
SEKERKA, R. F. N90-29200
SELCON, S. J. N90-28977
SELSANE, M. N90-29206
SEMPLE, WOLSEY A. N90-29105
SENG, HAN-SONG N90-28858
SENGER, R. N90-28722
SENNE, EDSON L. F. N90-29104
SERAJI, HOMAYOUN N90-29000
N90-29002
N90-29003
N90-29044
N90-29045
SETO, S. P. N90-28554
N90-28555
SEVRAIN, A. N90-28810
SHALKHAUSER, KURT A. N90-28768
SHAMIE, J. N90-28865
SHANSKY, JANET N90-28960
SHAO, LEJUN N90-28854
N90-29020
SHARMA, D. K. N90-28753
SHARP, D. J. N90-28776
SHARP, G. R. N90-28596
SHAW, B. A. N90-28715
SHAW, THOMAS LEOMIL N90-28675
SHEA, DANIEL M. N90-28615
SHEFT, STANLEY N90-28970
SHEN, JIAN-MIN N90-29135
SHEN, STEWART N. N90-29108
SHENK, T. N90-29083
SHEPHERD, I. G. N90-28686
SHERIDAN, THOMAS B. N90-29007
N90-29008
SHERRILL, ROBERT T. N90-28906
SHIMAZU, K. N90-28900
SHIN, WON-TAE KWON N90-28931
SHINN, JUDY L. N90-29290
SHOFNER, WILLIAM P. N90-28970
SHORE, STEVEN N. N90-29276
SHU, CHI-WANG N90-29128
N90-29129
SHULL, R. H. N90-28543
SHUNDO, Y. N90-28900
SIDDALINGAIAH, MADHU N90-29022
SIDDIQI, TOUFIC A. N90-28918
SIDES, J. N90-28500
SIEGMANN, W. L. N90-28930
SIEVERTS, M. N90-29257
SIEWERT, T. A. N90-28841
SIHVOLA, A. H. N90-29158
SIKORA, SCOTT E. N90-29142
N90-29143
SIMPSON, CAROL A. N90-28510
SIMPSON, T. C. N90-28715
SIMS, A. J. N90-28934
N90-29293
SIMS, J. N90-28857
SINGH, AJIT N90-28674
SIRE, R. A. N90-28645
SIROVICH, L. N90-28816
SKELLY, W. A. N90-28941
SKIDMORE, F. W. N90-28547
SKOW, ANDREW M. N90-28517
SLUTZ, S. A. N90-28777
SMITH, A. WILLIAM N90-29156
SMITH, ANDRA N90-28731
SMITH, D. B. N90-29015
SMITH, GREG N90-28697
SMITH, J. H. N90-28716
SMITH, J. L. N90-29206
SMITH, JAMES E. N90-29268
SMITH, STEPHEN F. N90-29038
SMYTH, CHRISTOPHER C. N90-28982
SNYDER, B. N90-28798
SNYDER, J. G. N90-29206
SNYDER, W. E. N90-28836
SOARES, PAUL A. N90-28586
SOLKA, JEFFREY L. N90-28770
N90-28998
SONNEBORN, GEORGE N90-29275
N90-29276
SORENSON, K. B. N90-28717
SPARKS, W. M. N90-29275
SPEETER, THOMAS H. N90-29058
SPENCE, W. L. N90-29179
SPERL, TODD C. N90-28997
SPRATT, RANDOLPH W. N90-28574
SREEDHARAN, T. D. N90-29289
SRINIVAS, KANKANAHALLI N90-29117
SRINIVASAN, H. V. N90-29022
SRINIVASAN, S. N90-28905
SRINIVASAN, SURESH N90-29098
SRIVASTAVA, S. N90-29017
STALLWORTH, RODERICK N90-28648
STANGHELLINI, LETIZIA N90-29267
N90-29278
STARRFIELD, SUMNER G. N90-29267
N90-29275
N90-29276
N90-29278
STEARNS, E. MARSHALL N90-28558
N90-28559
N90-28561
STEINFELD, J. I. N90-28683
STENSBY, J. A. N90-28729
STEPHANOU, H. E. N90-29041
STEPHEN, J. N90-28934
STEPHENS, J. J. N90-28717
STEPHENSON, FRANK W., JR. N90-28612
STIEWITT, HORST N90-28499
STILLMAN, G. E. N90-28835
STIMPSON, G. J. N90-29141
STINECIPHER, MARY MARGARET N90-28745
STINSON, HELEN C. N90-28648
STOCKER, P. J. N90-28619
STOLTZFUS, N. N90-29029
STONE, HENRY W. N90-29059
STRACK, JOHN R. N90-29091
STRASBURG, ROY FRANCIS N90-28687
STRATHDEE, J. A. N90-29157
STRAUB, F. N90-28866
STREET, R. A. N90-28730
STREETS, DAVID G. N90-28918
SULENTIC, JACK W. N90-29281
SUN, C. T. N90-28678
N90-28679
SUNDERRAMAN, RAJ N90-29247
SUTHERLAND, B. M. N90-28966
SUTHERLAND, J. C. N90-28966
SUTTON, C. W. N90-28821
SUZUKI, MASUOOKYO N90-29165
SVAITER, B. F. N90-29151
SVAITER, N. F. N90-29151
SVOBODA, JAMES S. N90-28768
SWAIN, PHILIP H. N90-28889
N90-28890
SWAN, D. H. N90-28905
SWASDISON, SOMPORN N90-28959
SWINDEMAN, R. W. N90-28720
SZABLYA, H. M. N90-28780
SZADY, ANDREW J. N90-29285

T

TACKETT, J. R. N90-28684
TAKEUCHI, A. Y. N90-28726
TAKUMA, T. N90-28779
TAMARIT, FRANCISCO A. N90-29213
TAMRES, DAVID H. N90-29286
TANIS, J. A. N90-29171
TANRIKUT, S. N90-28567
TANTON, G. A. N90-28729
TARJANYI, MIKE N90-28781
TATE, AUSTIN N90-29035
TAYLOR, J. B. N90-29196
TAYLOR, J. R. N90-28554
N90-28555
TAYLOR, MICHAEL ROBINSON N90-28759
TAYLOR, PETER R. N90-28680
TAYLOR, R. D. N90-29175
TAYLOR, R. M. N90-28975
N90-28977
TEAS, DON C. N90-28985
TEICH, ALBERT H. N90-29259
TEJADA, FRANCISCO RIOS N90-28991
TENWOLDE, J. G. N90-28508
TERADA, T. N90-28712
TERRELL, DUDLEY J. N90-29112
TESAR, DELBERT N90-29014
THAMBURAJ, R. N90-28713
THEJLL, PETER ANDREAS N90-29263
THOMAS, ANTHONY N90-29105
THOMAS, M. T. N90-29150
THOMAS, RICHARD W. N90-28514
THOMPSON, D. H. N90-29065
THOMPSON, J. D. N90-29206
N90-29207
THOMPSON, JACK M., JR. N90-29001
N90-29047
THOMPSON, R. N90-28730
THOMPSON, R. L. N90-28649
THONSTAD, JOMAR N90-29211
TIDD, JOHN PATRICK N90-29113
TIEMAN, T. C. B. N90-28783
TILLEY, SCOTT W. N90-29005
N90-29057
TIMKO, L. P. N90-28553
TINGLEY, J. W. N90-28898
TOOSSI, M. N90-28866
TORGOGOMES, ARTHUR N90-28784
TORNG, TONY YI N90-28868
TORRES, J. N90-29282
TOSI, M. P. N90-28725
TOWER, JOHN T. N90-29049
TRAMMELL, E. G. N90-28952
TRENT, LINDA KELLY N90-28968
TRETOUT, B. N90-28692
TREUMANN, R. A. N90-29287
TRUEBLOOD, B. N90-28628
TRURAN, J. W. N90-29275
TRUSCOTT, P. R. N90-29293
TSAI, C. C. N90-28730
TSALLIS, CONSTANTINO N90-29165
N90-29212
N90-29213
N90-29214
N90-29215
TSAO, J. Y. N90-28690
TSIDULKO, YU. A. N90-29188
TSIKOS, CONSTANTINE J. N90-29061
TSINTIKIDIS, D. N90-29284
TSINTSADZE, N. L. N90-29199
TSO, KAM N90-29060
TSUTSUMI, KAZUYOSHI N90-29034
TSZENG, T. C. N90-28663
TU, W. H. N90-28640
TUCKER, J. H. N90-28515
TURKEL, ELI N90-29125
TURNER, J. E. N90-28826
TUSTISON, R. W. N90-29222
TWORZYDLO, W. N90-29122

U

UHRIG, ROBERT E. N90-29120
UNGER, RICHARD L. N90-29011
UPADHYE, R. N90-29083
USLENGHI, PIERGIORGIO L. E. N90-29180

V

VADAKETH, S. N90-29122
VADIEE, NADER N90-29033
VALTORTA, E. N90-28518
VANBERGEN, J. H. W. N90-28973
VANBRUNT, RICHARD J. N90-28775
VANDENBURGH, HERMAN H. N90-28959
N90-28960
VANDERVELDEN, ALEXANDER J. M. N90-28540
VANDOMMELEN, LEON L. N90-28789
VANDYKE, PALMER T. N90-29091
VANGENT, R. N. H. W. N90-29082
VANHOLTEN, C. R. N90-28973
VANSANT, GLENN J. N90-29049
VANSCHALWIJK, WALTER N90-28781
VAUGHAN, O. H., JR. N90-28951
VAUGHN, RONALD W. N90-28571
VAUGHN, WALLACE L. N90-28541
VELEV, O. N90-28905
VENTURI, P. N90-28989
VENTURINO, MICHAEL N90-28976
VERBRUGGE, R. N90-28532
VERMA, S. K. N90-28654
VEYS, JEAN-MARIE N90-28707
VIDAL, GEORGES N90-28530
VIEIRADUTRA, LUCIANO N90-28881
VILLELANETO, THYRSO N90-29294

VINCENT, P. S. N90-28883
VISKANTA, R. N90-28813
VISWANATH, P. R. N90-28492
VOGLER, L. E. N90-28755
VOLAKIS, JOHN L. N90-28767
VOLD, HAVARD I. N90-29001
N90-29047
VOLK, KEVIN N90-29265
VOLPE, RICHARD N90-29023
VOLZ, RICHARD A. N90-28854
N90-29020
VONKARMAN, THEODORE N90-28817
VOSE, MICHAEL D. N90-29115

W

WAGNER, MARK N90-28769
WAGNER, R. M. N90-29275
WAHAB, M. ABDEL N90-28950
WAINGORTSETZER, ALBERTO N90-29298
WAINSCOAT, RICHARD N90-29265
WALCHLI, LAWRENCE A. N90-28524
WALDSPURGER, THERESA A. N90-29098
WALKER, DOUGLAS N90-28769
WALKER, HELEN N90-29265
WALKER, IAN D. N90-29046
WALKER, J. N90-28730
WALKER, MICHAEL W. N90-28854
N90-29056
WALKER, RUSSELL N90-29265
WALLIO, H. ANDREW N90-28906
WALSH, NORMAN J. N90-28771
WALTON, J. J. N90-28919
N90-28922
WANG, SHI-KUN N90-29135
N90-29153
WANG, W.-C. N90-28923
WANHILL, R. J. H. N90-28711
WARD, WILLIAM F. N90-28677
WARNER, J. D. N90-28786
WATANABE, T. N90-28900
WATERHOUSE, R. B. N90-28706
WATKINS, TOMMIE N90-28650
WATSON, R. T. N90-28929
WATT, D. G. D. N90-28992
WAVERING, A. J. N90-29055
WEBER, F. N90-29269
WEDEKIND, G. N90-28528
N90-28529
WEGMANN, T. N90-28658
WEIGEL, M. K. N90-29269
WEIL, J. C. N90-28924
WEILBRENNER, JAMES M. N90-28894
WEINTRAUB, DAVID ANDREW N90-29264
WEIR, B. N90-28520
WEISBIN, C. R. N90-29065
WEISENBURGER, R. N90-28866
WEISGERBER, SCOTT A. N90-28986
WEISMAN, M. L. N90-28926
WEISS, A. H. N90-28640
WEISS, G. A. N90-28689
WEISS, ROSANNE M. N90-28584
WELDON, VINCENT N90-28660
WELDON, VINCENT A. N90-28635
WELSH, B. L. N90-28526
WELSH, JEFFREY H. N90-29018
WENZEL, ELIZABETH M. N90-28996
WENZLER, CARL J. N90-28833
WEST, B. H. N90-28743
N90-28849
WEY, MING-JYH N90-28792
WHALEN, THOMAS J. N90-28735
WHEELER, C. F. N90-28511
WHITELEY, JAMES DAVID N90-28999
WICKNER, R. B. N90-28958
WIENTJES, C. J. E. N90-28994
WIKER, STEVEN F. N90-29009
WILD, J. CHRISTIAN N90-29108
WILLIAMS, JAMES H., JR. N90-28858
WILLIAMS, MELVIN K. N90-28731
WILLIAMS, R. E. N90-29275
WILLIAMS, ROY N90-29010
WILSON, JOHN W. N90-29290
WILSON, T. L. N90-29090
WILSON, W. K. N90-29242
WINER, K. N90-28730
WINKEL, J. N90-28887
WINTER, HEINZ N90-29159
N90-29160
WIRTZ, R. A. N90-28798
WITTBERG, THOMAS N90-28731
WITTEN, ALAN J. N90-28882
WOLSTENHOLME, LINDA C. N90-28665
WOOD, LAURIE N90-29052
WOOD, N. J. N90-28523
WOOTTON, A. N90-29193
WORLEY, PATRICK H. N90-29095
WOYTOWITZ, P. J. N90-28645
WRENN, G. L. N90-28594
WRIGHT, H. A. N90-28826
WU, S. T. N90-28611
WYNOSKY, T. A. N90-28560

X

XIN, YUN-WEI N90-29140
XU, CONG N90-29261
XU, JIANKE N90-28591
XU, KAI-WEN N90-29135
N90-29153
XUE, MING N90-28932

Y

YANG, DEYUAN N90-29243
YANG, JU-SUNG N90-28536
YAO, M. N90-28895
YARED, WAEL N90-29007
YELTON, W. G. N90-28778
YONG, JOO KIM N90-29111
YOST, WILLIAM A. N90-28970
YOUNG, CAROLYNN N90-28592
YU, L. N90-29216
YUKAWA, S. N90-28749

Z

ZAFINDRATAFA, GEORGES N90-29226
ZAVRACKY, PAUL M. N90-28828
ZEIK, A. C. N90-28839
ZENTLER, JAN-MARK N90-28782
ZERN, CHERYL ANN N90-28866
ZHANG, Y. Z. N90-29193
ZHOU, WEIYU N90-28867
ZIAVRAS, SOTIRIOS N90-29022
ZIEGENFUSS, H. G. N90-28841
ZIK, JOHN N90-29009
ZIMMERMAN, W. F. N90-29018
ZUNIGA, FANNY A. N90-28505
ZURAWSKI, ROBERT L. N90-28827
ZVIRAN, MOSHE N90-29089
ZWART, HEIKO JOHANNES N90-29144
ZWEBEN, MONTE N90-29076
ZWEIFEL, P. F. N90-29126

Typical Corporate Source Index Listing

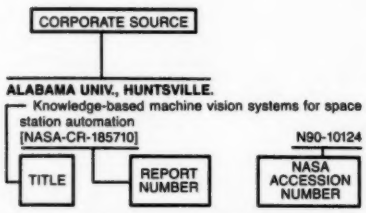

Listings in this index are arranged alphabetically by corporate source. The title of the document provides the user with a brief description of the subject matter. The report number helps to indicate the type of document cited (e.g., NASA report, translation, NASA contractor report). The NASA accession number denotes the number by which the citation is identified. The titles are arranged under each corporate source in ascending accession number order.

A

ACUREX CORP., HUNTSVILLE, AL.
High/variable mixture ratio oxygen/hydrogen engines N90-28637

ADMIRALTY RESEARCH ESTABLISHMENT, PORTLAND (ENGLAND).
A computer graphics package [ARE-TM(UDT)-89111] N90-29094

ADVISORY GROUP FOR AEROSPACE RESEARCH AND DEVELOPMENT, NEUILLY-SUR-SEINE (FRANCE).
Aerodynamics of Combat Aircraft Controls and of Ground Effects [AGARD-CP-465] N90-28513
High Temperature Surface Interactions [AGARD-CP-461] N90-28698
Situational Awareness in Aerospace Operations [AGARD-CP-478] N90-28972

AEROJET TECHSYSTEMS CO., SACRAMENTO, CA.
Computer code for the prediction of nozzle admittance N90-28630
Swirl coaxial injector element characterization for booster engines N90-28632
Variable mixture ratio performance through nitrogen augmentation N90-28639

AERONAUTICA MACCHI S.P.A., VARESE (ITALY).
Aerodynamic control design: Experience and results at Aermacchi N90-28518

AERONAUTICAL RESEARCH INST. OF SWEDEN, STOCKHOLM.
Two-dimensional wind tunnel test and comparison with calculations for a 15.2 percent thick airfoil section for wind turbines [FFA-TN-1990-16] N90-28501
Damage tolerance of the fighter aircraft 37 Viggen. Part 1: Analytical assessment [FFA-TN-1990-12-PT-1] N90-28538
Damage tolerance of the fighter aircraft 37 Viggen. Part 2: Experimental verification [FFA-TN-1990-13-PT-2] N90-28539
Extrapolation procedures at outflow boundaries for the Navier-Stokes equations [FFA-TN-1990-23] N90-28811

AERONAUTICAL RESEARCH LABS., MELBOURNE (AUSTRALIA).
The reduction of smoke emissions from Allison T56 engines [ARL-PROP-R-182] N90-28547
A flight dynamic model of aircraft spinning [AR-005-600] N90-28576
A microprocessor controlled strain gauge calibration module [AR-005-579] N90-28821

AEROSPACE MEDICAL RESEARCH LABS., WRIGHT-PATTERSON AFB, OH.
Performance-based measures of merit for tactical situation awareness N90-28976
Attention gradients in situation awareness N90-28978
Military aircrew seating: A human factors engineering approach [AD-A218049] N90-28999

AEROSPATIALE, SURESNES (FRANCE).
Static and dynamic characterization of the ATR 72 rods made of Ti 10.2.3 titanium alloy [REPT-49-238] N90-28722

AEROSPATIALE, TOULOUSE (FRANCE).
Determination of the ground effect on the characteristics of the A320 aircraft N90-28534

AIR FORCE ASTRONAUTICS LAB., EDWARDS AFB, CA.
Development of the electric vehicle analyzer [AD-A224201] N90-28788

AIR FORCE HUMAN RESOURCES LAB., BROOKS AFB, TX.
Source emission test of gas turbine engine test facility, Kelly AFB, TX [AD-A223869] N90-28571
Air Force Officer Qualifying Test (AFOQT): Development of quick score composites for forms P1 and P2 [AD-A223868] N90-28997

AIR FORCE WRIGHT AERONAUTICAL LABS., WRIGHT-PATTERSON AFB, OH.
The interaction of chromostereopsis and stereopsis in stereoscopic CRT (Cathode Ray Tubes) displays [AD-A217906] N90-28544

ALABAMA UNIV., BIRMINGHAM.
Containerless low gravity processing of glass forming and immiscible alloys [NASA-CR-186999] N90-28747

ALABAMA UNIV., HUNTSVILLE.
Development of comprehensive numerical schemes for predicting evaporating gas-droplets flow processes of a liquid-fueled combustor [NASA-CR-187018] N90-28693
Spectroscopic study of combustion diagnostics on hydroxyl radicals [NASA-CR-186998] N90-28694
Gravity wave initiated convection [NASA-CR-186868] N90-28933

ALLIED-SIGNAL AEROSPACE CO., KANSAS CITY, MO.
Using embedded microcontrollers in radar test equipment [DE90-014997] N90-28763
Quality function deployment as a mechanism for process characterization and control [DE90-014755] N90-28857

AMERICAN WELDING INST., LOUISVILLE, TN.
Computerization of Welding Data: Proceedings of the conference and workshop [PB90-219551] N90-28841

AMERICAN WELDING SOCIETY, MIAMI, FL.
Computerization of Welding Data: Proceedings of the conference and workshop [PB90-219551] N90-28841

AMES LAB., IA.
Peak analysis in gas chromatography and the development of new stationary phases for anion chromatography [DE90-014428] N90-28687

ANACAPA SCIENCES, INC., FORT RUCKER, AL.
Strategies of computer-based instructional design: A review of guidelines and empirical research [AD-A224038] N90-29112

APPLIED RESEARCH LAB., STATE COLLEGE, PA.
Factorization of the characteristic equation for three layer ducts [AD-A223867] N90-28956

AQUA TERRA CONSULTANTS, DECATUR, GA.
Data Base Analyzer and Parameter Estimator (DBAPE) interactive computer program user's manual [PB90-193053] N90-29252

AQUANAUTICS CORP., ALAMEDA, CA.
A reliable, maintenance-free oxygen sensor for aircraft using an oxygen-sensitive coating on potentiometric electrodes [AD-A222696] N90-28545

ARGONNE NATIONAL LAB., IL.
Effects of friction and end losses on MHD thruster efficiency [DE90-013673] N90-28608
Responding to the threat of global warming: Options for the Pacific and Asia [DE90-014756] N90-28918
ELEFUNT test results under AST FORTRAN V1.8.0 on the sequent symmetry [DE90-014932] N90-29127

ARIZONA UNIV., TUCSON.
Aerodynamics of bodies in shear flow N90-28496
Reliability analysis of maintained structural system vulnerable to fatigue and fracture N90-28868

ARMY AVIATION SYSTEMS COMMAND, CLEVELAND, OH.
An expert system to perform on-line controller restructuring for abrupt model changes [NASA-TM-103609] N90-29121

ARMY AVIATION SYSTEMS COMMAND, CORPUS CHRISTI, TX.
Analysis of the T63-A-700 engine used in alcohol turbine fuel extender test [DOT/FAA/CT-TN90/18] N90-28549

ARMY AVIATION SYSTEMS COMMAND, MOFFETT FIELD, CA.
The effects of structural flap-lag and pitch-lag coupling on soft inplane hingeless rotor stability in hover [NASA-TP-3002] N90-28503
Comparison of speech intelligibility in cockpit noise using SPH-4 flight helmet with and without active noise reduction [NASA-CR-177564] N90-28510

ARMY COLD REGIONS RESEARCH AND ENGINEERING LAB., HANOVER, NH.
Three functions that model empirically measured unfrozen water content data and predict relative hydraulic conductivity [AD-A223875] N90-28892
Multiband imaging systems [AD-A223969] N90-28893

ARMY CONSTRUCTION ENGINEERING RESEARCH LAB., CHAMPAIGN, IL.
Methods for detecting low-frequency signals in the presence of strong winds [AD-A223980] N90-28769

ARMY ENGINEER WATERWAYS EXPERIMENT STATION, VICKSBURG, MS.
Optical storage technology [AD-A224028] N90-29254

ARMY MISSILE COMMAND, REDSTONE ARSENAL, AL.
Faraday rotation mapping of mercury cadmium telluride [AD-A224278] N90-28729

ARMY PROPULSION LAB., CLEVELAND, OH.
Current research in cavitating fluid films [NASA-TM-103184] N90-28791

ARMY RESEARCH OFFICE, RESEARCH TRIANGLE PARK, NC.
Proceedings of US Army Research Office Workshop on US Army Applications for Diamond and Diamondlike Materials [AD-A224193] N90-28741

ARMY SAFETY CENTER, FORT RUCKER, AL.
Helicopter aircrew helmets and head injury: A protective effect [AD-A223024] N90-29080

ARMY STRATEGIC DEFENSE COMMAND, HUNTSVILLE, AL.
Use of Ni63 overvoltage gap switches in the flight termination systems on boosters launched from US Army Kwajalein Atoll (USAKA) [AD-A223866] N90-28861

ARMY WAR COLL., CARLISLE BARRACKS, PA.
Space-base multispectral imagery: Current and future applications and implications to the United States Army [AD-A224046] N90-28894

The personal computer: An untapped source for the United States Army War College
[AD-A223976] N90-29087
How can research and development leadtime be reduced
[AD-A224063] N90-29240
ASSISTANT SECRETARY OF DEFENSE (COMPTROLLER), WASHINGTON, DC.
Automated information system life-cycle management manual
[PB90-219288] N90-29244
ATMOSPHERIC AND ENVIRONMENTAL RESEARCH, INC., CAMBRIDGE, MA.
Natural and anthropogenic climate change
[DE90-015528] N90-28923
ATOMIC ENERGY OF CANADA LTD., PINAWA (MANITOBA).
Radiation-curable prepreg composites
[DE90-629740] N90-28674

B

BALLISTIC RESEARCH LABS., ABERDEEN PROVING GROUND, MD.
Projectile supersonic drag characteristics
[AD-A224217] N90-28506
BATTELLE COLUMBUS LABS., OH.
Development of improved self lubricating cages for SSME HPOTP bearings N90-28823
Cage stability analysis for SSME HPOTP bearings N90-28825
BIONETICS CORP., COCOA BEACH, FL.
Flora and threatened and endangered plants of John F. Kennedy Space Center, Florida
[NASA-TM-102791] N90-28925
BOEING AEROSPACE CO., SEATTLE, WA.
Summary of booster propulsion/vehicle impact study results N90-28635
Design optimization of gas generator hybrid propulsion boosters
[NASA-CR-181096] N90-28660
BOEING COMMERCIAL AIRPLANE CO., SEATTLE, WA.
World jet airplane inventory at year-end 1989
[PB90-207218] N90-28489
High-speed civil transport study: Special factors
[NASA-CR-181881] N90-28537
BOLT, BERANEK, AND NEWMAN, INC., CAMBRIDGE, MA.
Plan recognition for space telerobotics N90-29036
BONNEVILLE POWER ADMINISTRATION, PORTLAND, OR.
Adjustable speed drive applications guidebook
[DE90-014151] N90-28760
BORDEAUX 2 UNIV. (FRANCE).
Cardiovascular deconditioning of cosmonauts: Role, importance and applications of the lower body negative pressure
[ETN-90-97507] N90-28964
BRITISH AEROSPACE PUBLIC LTD. CO., BRISTOL (ENGLAND).
Development of a flexible test-bed for robotics, telemanipulation and servicing research N90-29012
BRITISH AEROSPACE PUBLIC LTD. CO., LANCASHIRE (ENGLAND).
Combat aircraft control requirements N90-28515
BROOKHAVEN NATIONAL LAB., UPTON, NY.
Measurement of localized corrosion using current density mapping
[DE90-015066] N90-28721
Acid deposition: No such thing as a free launch
[DE90-015065] N90-28920
A preliminary ARM (Atmospheric Radiation Measurements) guide for climatic evaluations
[DE90-015135] N90-28937
DNA damage and repair in human skin: Pathways and questions
[DE90-015126] N90-28968
Studies of central interactions of Si ions at 14.5 x A GeV/c in Au and Cu
[DE90-015095] N90-29195
Electronic conduction in molten cryolite saturated with alumina
[DE90-015090] N90-29211
Control of nonlinear space-charge emittance growth
[DE90-014752] N90-29270
BROWN UNIV., PROVIDENCE, RI.
Map learning with indistinguishable locations N90-29025
Approximation algorithms for planning and control N90-29042
BUREAU OF MINES, PITTSBURGH, PA.
Human factors model concerning the man-machine interface of mining crewstations N90-29011
Automation and robotics technology for intelligent mining systems N90-29018

C

CAELUM RESEARCH CORP., SILVER SPRING, MD.
Perceptual telerobotics N90-29063
CALIFORNIA INST. OF TECH., PASADENA.
Regular and chaotic motion of uniform elliptical vortices in external linear time dependent velocity fields N90-28497
Electrochemistry using nanometer-sized electrodes
[AD-A223690] N90-28697
Studies of vortex interactions
[AD-A223864] N90-28817
Turbomachinery rotor forces
[NASA-CR-183779] N90-28852
Star formation and the distribution of HI and infrared emission in M51
[NASA-CR-186928] N90-29262
CALIFORNIA UNIV., BERKELEY.
Rheometer strain and strain-rate errors
[DE90-013845] N90-28824
CALIFORNIA UNIV., BERKELEY. LAWRENCE BERKELEY LAB.
The spatial scalar structure of premixed turbulent stagnation point flames
[DE90-014189] N90-28686
Rheometer strain and strain-rate errors
[DE90-013845] N90-28824
Status of the advanced light source
[DE90-015836] N90-29185
Electron microscopy of transition-metal doped BiCaSrCuO
[DE90-014184] N90-29202
Rotating neutron stars and the equation of state of dense matter
[DE90-014185] N90-29269
CALIFORNIA UNIV., DAVIS.
Ignition and combustion of liquid propellants
[AD-A224150] N90-28746
CALIFORNIA UNIV., LOS ANGELES.
Dynamic interaction of multiple autonomous mobile robots N90-28844
Near-infrared speckle observations of T Tauri stars and a multi-wavelength study of the prototype star T Tauri N90-29264
CALIFORNIA UNIV., SAN DIEGO.
Theoretical studies of proton beams in solar flare loops N90-29286
CALIFORNIA UNIV., SANTA BARBARA.
Wigner symbols, quantum dynamics, and the kicked rotator
[AD-A224024] N90-29234
CALIFORNIA UNIV., SANTA CRUZ.
The formation of globular clusters N90-29272
CARNEGIE-MELLON UNIV., PITTSBURGH, PA.
A fast lightstripe rangefinding system with smart VLSI sensor N90-29019
Real-time edge tracking using a tactile sensor N90-29023
Periodic gaits for the CMU ambler N90-29027
State-based scheduling: An architecture for telescope observation scheduling N90-29038
Focus of attention in an activity-based scheduler N90-29039
First results in terrain mapping for a roving planetary explorer N90-29066
A tesselated probabilistic representation for spatial robot perception and navigation N90-29075
Integrating planning, execution, and learning N90-29079
Technical writing for software engineers
[AD-A223872] N90-29109
Concepts of concurrent programming
[AD-A223897] N90-29110
Numerical and analytical study of nonlinear bifurcations associated with the morphological stability of two-dimensional single crystals
[PB90-209594] N90-29200
CASE WESTERN RESERVE UNIV., CLEVELAND, OH.
The entrainment rate for a row of turbulent jets
[NASA-CR-185278] N90-28504
Crack layer analysis of fatigue fracture of a beta titanium alloy N90-28864
Green's functions for dislocations in bonded strips and related crack problems
[NASA-CR-185291] N90-28878
CENTER FOR ENGINEERING APPLICATIONS, MEMPHIS, TN.
Measurement of hand dynamics in a microsurgery environment: Preliminary data in the design of a bimanual telemicro-operation test bed N90-29010
CENTRAL ELECTRICITY GENERATING BOARD, GLOUCESTER (ENGLAND).
A real time evaluation of the use of a perspective format to promote situational awareness in users of air to air tactical displays N90-28981
CENTRAL RESEARCH INST. OF ELECTRIC POWER INDUSTRY, TOKYO (JAPAN).
Analysis of three-dimensional eddy current field. Application to calculation of magnetic screening effect of the damper system in a model superconducting generator
[DE90-507869] N90-28779
A 10kW class molten carbonate fuel cell test: The stack with electrolyte plate prepared with paper-making method
[DE90-507841] N90-28900
Study of power generation systems for CO2 collection: LNG combined cycle
[DE90-507881] N90-28901
CENTRE D'ESSAIS AERONAUTIQUE TOULOUSE (FRANCE).
Study of the ground effects in the CEAT aerohydrodynamic tunnel: Using the results N90-28530
CENTRE NATIONAL D'ETUDES SPATIALES, TOULOUSE (FRANCE).
Approximation, synthesis, and development of bi-mode cavities microwave filters presenting unsymmetrical quasi-elliptic responses
[CNES-NT-124] N90-28761
Wind lidar for BEST
[CNES-NT-125] N90-28947
CENTRO BRASILEIRO DE PESQUISAS FISICAS, RIO DE JANEIRO.
Effects of Al substitution by Fe in CeAl2
[DE90-627843] N90-28726
Geometrical properties of an internal local octonionic space in a non-Riemannian manifold
[DE90-627175] N90-29149
On the zeta-function regularization of chiral Jacobians for singular Dirac operators
[DE90-627176] N90-29150
Casimir effect in a D-dimensional flat spacetime and the cut-off method
[DE90-627177] N90-29151
Dirac's equation as a geodesic in Riemann space
[DE90-627194] N90-29152
Systematic approach to critical phenomena by the extended variational method and coherent-anomaly method
[DE90-627320] N90-29165
Criticality of the three-state chiral clock model: A renormalisation group study
[DE90-627321] N90-29212
A generalised Hubbard Hamiltonian: Influence of temperature and fractality
[DE90-627322] N90-29213
Z(6) model: Criticality and break-collape method
[DE90-627323] N90-29214
Susceptibility of the Potts model in an hierarchical lattice: Renormalisation group approach
[DE90-627324] N90-29215
Dynamical information for Fe doped YBa2Cu3O7 superconducting oxides obtained from high temperature Moessbauer studies
[DE90-627871] N90-29218
Viscous causal cosmologies
[DE90-627487] N90-29282
CHESAPEAKE RESEARCH CONSORTIUM, INC., GLOUCESTER POINT, VA.
Perspectives on the Chesapeake Bay, 1990: Advances in estuarine sciences
[PB90-248600] N90-28954
CINCINNATI UNIV., OH.
Microstructure: Property correlation
[NASA-CR-180406] N90-28880
CITY COLL. OF THE CITY UNIV. OF NEW YORK, NY.
Studies of central interactions of Si ions at 14.5 x A GeV/c in Au and Cu
[DE90-015095] N90-29195
COLORADO STATE UNIV., FORT COLLINS.
The role of clouds in CO2-induced climate change
[DE90-014380] N90-28911
COLORADO UNIV., BOULDER.
Diffusion in the surface layer of the convective boundary layer
[AD-A224125] N90-28924
A user modelling approach for computer-based critiquing
[AD-A224042] N90-29088
The effects of management support on the successful implementation of group decision support systems
[AD-A224473] N90-29241
Time-based competition for competitive advantage: An information technology perspective
[AD-A224474] N90-29255
COLUMBIA UNIV., NEW YORK, NY.
X ray spectra of cataclysmic variables
[NASA-CR-187002] N90-29280

COMISION NACIONAL DE ENERGIA ATOMICA, SAN CARLOS DE BARILOCHE (ARGENTINA).
The stability of the martensitic phases in Cu-Zn-Al at an electron concentration of 1.534
[DE90-628628] N90-28727
COMMERCE DEPT., WASHINGTON, DC.
Japanese molecular biology 1990: An update
[PB90-188707] N90-28958
COMPOSITE INDUSTRIEL, CADENET (FRANCE).
Large hydrodynamic tunnel: Calculation of the acoustic transparency of the jet stream
[REPT-89/115] N90-29167
COMPUTATIONAL MECHANICS CO., AUSTIN, TX.
A hybrid-stress finite element for linear anisotropic elasticity N90-28614
Second order tensor finite element
[NASA-CR-184008] N90-29122
COMPUTER TECHNOLOGY ASSOCIATES, INC., MCKEE CITY, NJ.
Dallas/Forth Worth simulation. Phase 2: Triple simultaneous parallel Instrument Landing System (ILS) approaches (turbojets)
[DOT/FAA/CT-90/2] N90-28509
CONGRESSIONAL BUDGET OFFICE, WASHINGTON, DC.
Preliminary analysis of NASA commercialization initiatives
[PB90-202706] N90-29257
COUNCIL FOR NATIONAL ACADEMIC AWARDS (ENGLAND).
Studies in automatic speech recognition and its application in aerospace N90-28759
A study of heat and fluid flow phenomena on the gas side of circular-tube plate-fin heat exchangers N90-28795

D

DEFENCE AND CIVIL INST. OF ENVIRONMENTAL MEDICINE, TORONTO (ONTARIO).
Effects of short-term weightlessness on roll circularvection N90-28992
DEFENCE RESEARCH ESTABLISHMENT, OTTAWA (ONTARIO).
Transient annealing characterization of irradiated MOSFETS
[AD-A223877] N90-29220
DEFENCE RESEARCH ESTABLISHMENT SUFFIELD, RALSTON (ALBERTA).
A sensor stabilization/tracking system for unmanned air vehicles
[AD-A224008] N90-28579
DELAWARE UNIV., NEWARK.
An analysis of the Palomar-Green subdwarfs and white dwarfs N90-29263
DEUTSCHE FORSCHUNGS- UND VERSUCHSANSTALT FUER LUFT- UND RAUMFAHRT, COLOGNE (GERMANY, F.R.).
Solar energy for high temperature technology and applications
[ETN-90-97429] N90-28902
DEUTSCHE FORSCHUNGSANSTALT FUER LUFT- UND RAUMFAHRT, COLOGNE (GERMANY, F.R.).
Overview on hot gas tests and molten salt corrosion experiments at the DLR N90-28714
DEUTSCHE FORSCHUNGSANSTALT FUER LUFT- UND RAUMFAHRT, GOETTINGEN (GERMANY, F.R.).
Design of an axisymmetric, contoured nozzle for the HEG
[DLR-FB-90-04] N90-28812
DEUTSCHE FORSCHUNGSANSTALT FUER LUFT- UND RAUMFAHRT, OBERPFAFFENHOFEN (GERMANY, F.R.).
On the application of similarity laws to a scaled railway bogie model
[DLR-FB-90-06] N90-28853
DEUTSCHE FORSCHUNGSANSTALT FUER LUFT- UND RAUMFAHRT, STUTTGART (GERMANY, F.R.).
Performance measurements and energy balance of an SPS V160 Stirling motor at the German Aerospace Research Establishment
[DLR-MITT-90-03] N90-28903
DOMINION ASTROPHYSICAL OBSERVATORY, VICTORIA (BRITISH COLUMBIA).
Metallic line profiles of the AOV star Vega
[NASA-CR-186906] N90-29261
DORNIER-WERKE G.M.B.H., FRIEDRICHSHAFEN (GERMANY, F.R.).
Inflight thrust vectoring: A further degree of freedom in the aerodynamic/flight mechanical design of modern fighter aircraft N90-28528
Aerodynamic interferences of in-flight thrust reversers in ground effect N90-28529
DORTMUND UNIV. (GERMANY, F.R.).
Control of intelligent robots in space N90-29013
DRAPER (CHARLES STARK) LAB., INC., CAMBRIDGE, MA.
Model authoring system for fail safe analysis
[NASA-CR-4317] N90-29142
A knowledge-based system design/information tool
[NASA-CR-4316] N90-29143
DRESSER INDUSTRIES, INC., WAUKESHA, WI.
Development of advanced combustion technology for medium and high speed natural gas engines
[PB90-198565] N90-28836
DREXEL UNIV., PHILADELPHIA, PA.
Multiresolutional models of uncertainty generation and reduction N90-29043
Techniques and potential capabilities of multi-resolutional information (knowledge) processing N90-29062
DURHAM UNIV. (ENGLAND).
Gamma ray evidence for cosmic ray sources N90-29292

E

EA-MUELLER, INC., BALTIMORE, MD.
Adjustable speed drive applications guidebook
[DE90-014151] N90-28780
EAST ANGLIA UNIV., NORWICH (ENGLAND).
Chasing a specter: Risk management for global environmental change
[DE90-014455] N90-28917
EBASCO SERVICES, INC., BELLEVUE, WA.
Adjustable speed drive applications guidebook
[DE90-014151] N90-28780
EDGERTON, GERMESHAUSEN AND GRIER, INC., IDAHO FALLS, ID.
Assessment of battery technologies for electric vehicles. Volume 2, part 2: Appendices
[DE90-014610] N90-28778
EDINBURGH UNIV. (SCOTLAND).
Coordinating the activities of a planner and an execution agent N90-29035
EG AND G ENERGY MEASUREMENTS, INC., WOBURN, MA.
Computer simulation of micro-triode performance
[DE90-014191] N90-28774
EG AND G MOUND APPLIED TECHNOLOGIES, MIAMISBURG, OH.
Thermogravimetry-mass spectrometry analysis of gas bubbles in molten glass
[DE90-014116] N90-28684
Mass spectrometric analysis of hydrogen isotopes in metals and metal hydrides
[DE90-014118] N90-28685
Evaluations of new polyimide films for flexible circuit applications at EG and G Mound Applied Technologies
[DE90-014117] N90-28731
EIDETICS INTERNATIONAL, INC., TORRANCE, CA.
Combat aircraft control requirements for agility N90-28517
ENERGY CONVERSION DEVICES, INC., TROY, MI.
Research on high-efficiency, multiple-gap, multi-junction amorphous silicon-based alloy thin-film solar cells
[DE90-000338] N90-28896
ENERGY RESEARCH CORP., DANBURY, CT.
Zinc-bromine battery development
[DE90-014751] N90-28781
ENVIRONMENTAL PROTECTION AGENCY, CINCINNATI, OH.
Ozone for trace organic contaminant removal
[PB90-221680] N90-28916
ENVIRONMENTAL PROTECTION AGENCY, RESEARCH TRIANGLE PARK, NC.
National air pollutant emission estimates, 1940-1988
[PB90-199266] N90-28908
National air quality and emissions trends report, 1988
[PB90-200114] N90-28909
ENVIRONMENTAL PROTECTION AGENCY, WASHINGTON, DC.
Study and analysis of leaking underground storage tank remediation techniques incorporated in states in EPA Region 6
[PB90-214834] N90-28847
ETABLISSEMENT TECHNIQUE CENTRAL DE L'ARMEMENT, ARCUEIL (FRANCE).
Behavior of aramid/epoxy wounded tubes under uniaxial and biaxial loading
[ETCA-89-R-150] N90-28873
EUROPEAN SPACE AGENCY, PARIS (FRANCE).
Experimental investigations on the stability and vorticity of the vortex breakdown phenomenon above delta wings, measured by the ultrasonic laser method
[ESA-TT-1079] N90-28498
Wind tunnel investigation of periodic vortex separation from rough surface circular cylinders by means of acoustic measurements
[ESA-TT-1092] N90-28499
The equipment for mass flow measurements in the low-speed wind tunnel at DFVLR in Brunswick (Federal Republic of Germany)
[ESA-TT-1125] N90-28585
Ascertaining the fracture toughness of ceramic materials by means of bending testpieces of various notch types at ambient and high temperatures
[ESA-TT-992] N90-28733
Oscillatory convection
[ESA-TT-890] N90-28801
Numerical simulation of the formation of two-dimensional and three-dimensional structures in shear layers and wakes
[ESA-TT-1008] N90-28802
Experimental investigations on the stability and transition of three-dimensional boundary layers
[ESA-TT-1026] N90-28803
Robust controller design by contraction of a pole region
[ESA-TT-1042] N90-29118
Scientific Colloquium in Honor of Prof. Dr. Rer. Nat. Hermann L. Jordan
[ESA-TT-1101] N90-29159
Flight test engineering with the ATTAS N90-29160
Numeric fluid mechanics N90-29161
Microgravitation experiments in space: Compatibility with interfering dynamic influences N90-29162
Energy transmission by means of coherent quasi-mono-chromatic light beams N90-29163

F

FAILURE ANALYSIS ASSOCIATES, INC., PALO ALTO, CA.
NASCRAC (trademark): A fracture mechanics analysis code N90-28645
FEDERAL AVIATION ADMINISTRATION, ATLANTIC CITY, NJ.
Dallas/Forth Worth simulation. Phase 2: Triple simultaneous parallel Instrument Landing System (ILS) approaches (turbojets)
[DOT/FAA/CT-90/2] N90-28509
Analysis of heliport environmental data, Intracoastal City
[DOT/FAA/CT-TN89/43] N90-28584
Communications Interface Driver (CID) test plan
[DOT/FAA/CT-TN89/35] N90-28762
A FAA Technical Center project transition plan: Mode S
[DOT/FAA/CT-TN90/17] N90-28765
A glossary of terms, definitions, acronyms, and abbreviations related to the National Airspace System
[DOT/FAA/CT-TN89/53] N90-29249
FEDERAL AVIATION ADMINISTRATION, WASHINGTON, DC.
Development of acceptance plans for airport pavement materials. Volume 1: Development
[DOT/FAA/RD-90/15] N90-28581
FERMI NATIONAL ACCELERATOR LAB., BATAVIA, IL.
Beam diagnostics in circular machines: Review of new developments
[DE90-014986] N90-29176
FLORIDA UNIV., GAINESVILLE.
Complex auditory signals
[AD-A224127] N90-28969
X ray scattering studies of non-equilibrium ordering processes
[DE90-015066] N90-29209
FORD AEROSPACE AND COMMUNICATIONS CORP., PALO ALTO, CA.
Kinematics, controls, and path planning results for a redundant manipulator N90-29005
FORD AEROSPACE CORP., PALO ALTO, CA.
Preliminary results on noncollocated torque control of space robot actuators N90-29057
FORD MOTOR CO., DEARBORN, MI.
Improved silicon carbide for advanced heat engines
[NASA-CR-182186] N90-28735

G

GENERAL ATOMIC CO., SAN DIEGO, CA.
Physics of the L to H transition in DIII-D
[DE90-014120] N90-29187
GENERAL ELECTRIC CO., CINCINNATI, OH.
Energy Efficient Engine high pressure turbine component test performance report
[NASA-CR-168289] N90-28553
Energy Efficient Engine combustor test hardware detailed design report
[NASA-CR-168301] N90-28554
Energy Efficient Engine (E3) combustion system component technology performance report
[NASA-CR-168274] N90-28555

Energy Efficient Engine acoustic supporting technology report
[NASA-CR-174834] N90-28557
Energy Efficient Engine core design and performance report
[NASA-CR-168069] N90-28559
NASA/GE Energy Efficient Engine low pressure turbine scaled test vehicle performance report
[NASA-CR-168290] N90-28563

GENERAL ELECTRIC CO., EVENDALE, OH.
Energy Efficient Engine: Flight propulsion system final design and analysis
[NASA-CR-168219] N90-28558
Energy Efficient Engine integrated core/low spool design and performance report
[NASA-CR-168211] N90-28561
Energy Efficient Engine: Control system component performance report
[NASA-CR-174851] N90-28562

GEOLOGICAL SURVEY, TALLAHASSEE, FL.
Computer program for converting rectangular coordinates to latitude-longitude coordinates
[PB90-231796] N90-28883

GEOLOGICAL SURVEY, TRENTON, NJ.
A conceptual weather-type classification procedure for the Philadelphia, Pennsylvania area
[PB90-231705] N90-28944

GEORGE MASON UNIV., FAIRFAX, VA.
Grasp planning under uncertainty N90-29041

GEORGIA INST. OF TECH., ATLANTA.
Real time guidance and propulsion control for single-stage-to-orbit airbreathing vehicles N90-28587
Micromechanics of cyclic deformation in SSME turbopump blade materials N90-28641
Crash-impact behavior of graphite/epoxy composite sine wave webs N90-28667
A theoretical investigation into the inelastic behavior of metal-matrix composites
[AD-A223973] N90-28677
Three-dimensional motor schema based navigation N90-29026

GEORGIA STATE UNIV., ATLANTA.
Fifteenth International Conference on X Ray and Inner-Shell Processes
[DE90-013024] N90-29170

GRENOBLE-1 UNIV. (FRANCE).
Planning robot actions under position and shape uncertainty N90-29073

GRONINGEN RIJKSUNIV. (NETHERLANDS).
Geometric theory for infinite dimensional systems
[ETN-90-98922] N90-29144

H

HAMBURG UNIV. (GERMANY, F.R.).
Experimental tests on the minimal visual acuity required for safe air crew and air control personnel performance N90-28987

HAMILTON STANDARD, WINDSOR LOCKS, CT.
Measurement of the steady surface pressure distribution on a single rotation large scale advanced prop-fan blade at Mach numbers from 0.03 to 0.78
[NASA-CR-182124] N90-28552

HARMONY THERMAL CO., WICHITA, KS.
Extended range tankless water heater
[DE90-014474] N90-28750

HARVARD UNIV., CAMBRIDGE, MA.
Dynamical properties of two-dimensional Josephson junction arrays
[AD-A223965] N90-29221

HAUTE-NORMANDIE UNIV., MONT SAINT AIGNAN (FRANCE).
Numerical simulation of reactive turbulent flows
[ETN-90-97476] N90-28807

HAWKER SIDDELEY CANADA LTD., TORONTO (ONTARIO).
Surface property improvement in titanium alloy gas turbine components through ion implantation N90-28713

HELSINKI UNIV. OF TECHNOLOGY, ESPOO (FINLAND).
Fuel cells: Their applications, technological status, market and opportunity
[DE90-796158] N90-28695
Chiral Maxwell-Garnett mixing formula
[PB90-189143] N90-29158

HOWARD UNIV., WASHINGTON, DC.
The dynamics and control of large flexible space structures - 13
[NASA-CR-186930] N90-28591

HUGHES RESEARCH LABS., MALIBU, CA.
Exploiting map plans as resources for action N90-29028

HUMAN ENGINEERING LABS., ABERDEEN PROVING GROUND, MD.
Counterair situation awareness display for Army aviation N90-28982

I

IIT RESEARCH INST., BARTLESVILLE, OK.
Fuels research, volume 1
[DE90-015393] N90-28695

IIT RESEARCH INST., CHICAGO, IL.
Application of advanced coating techniques to rocket engine components N90-28654

ILLINOIS UNIV., CHICAGO.
Analyses of spray and droplet ignition for pure and multicomponent fuels N90-28688
A nonlinear finite element formulation for the large displacement analysis of plates N90-28867
Theory of biaxial graded-index optical fiber
[NASA-CR-186977] N90-29180

ILLINOIS UNIV., URBANA.
The III-V semiconductor quantum well lasers and related optoelectronic devices on silicon
[AD-A224120] N90-28835

ILLINOIS UNIV., URBANA-CHAMPAIGN.
Torsional effects in structures subjected to strong ground motion
[PB90-226960] N90-28869

IMPERIAL COLL. OF SCIENCE AND TECHNOLOGY, LONDON (ENGLAND).
The effect of rapid spoiler deployment on the transient forces on an aerofoil N90-28527

INDUSTRIEANLAGEN-BETRIEBSGESELLSCHAFT M.B.H., OTTOBRUNN (GERMANY, F.R.).
Fretting fatigue strength of Ti-6Al-4V at room and elevated temperatures and ways of improving it N90-28709

INSTITUT DE MECANIQUE DES FLUIDES DE LILLE (FRANCE).
Study of ground effects on flying scaled models N90-28532

INSTITUT DE MECANIQUE DES FLUIDES DE TOULOUSE (FRANCE).
Development of turbulence models for the analysis of compressible or incompressible unsteady flow
[ETN-90-97486] N90-28810

INSTITUT NATIONAL DES SCIENCES DE L'UNIVERS, PARIS (FRANCE).
Study of the relationships between radar structure and the electrical activity of clouds
[ETN-90-97488] N90-28946

INSTITUTE FOR CIRCADIAN PHYSIOLOGY, BOSTON, MA.
Fluid and electrolyte homeostasis during spaceflight: Elucidation of mechanisms in a primate
[NASA-CR-177548] N90-29085

INSTITUTE FOR COMPUTER APPLICATIONS IN SCIENCE AND ENGINEERING, HAMPTON, VA.
On the use of Lagrangian variables in descriptions of unsteady boundary-layer separation
[NASA-CR-182071] N90-28789
A hybrid perturbation-Galerkin technique for partial differential equations
[NASA-CR-182085] N90-28814
An investigation of chaotic Kolmogorov flows
[NASA-CR-182079] N90-28816
LANZ: Software solving the large sparse symmetric generalized eigenproblem
[NASA-CR-182086] N90-28876
Multigrid for hypersonic inviscid flows
[NASA-CR-182082] N90-29125
Numerical experiments on the accuracy of ENO and modified ENO schemes
[NASA-CR-182083] N90-29128
Numerical methods for systems of conservation laws of mixed type using flux splitting
[NASA-CR-182084] N90-29129

INSTITUTE FOR PERCEPTION RVO-TNO, SOESTERBERG (NETHERLANDS).
Research in command and control for the Dutch Army Corps (1NL)
[IZF-1989-28] N90-28760
Situational awareness and vestibular stimulation: The influence of whole-body rotation upon task performance
[IZF-1989-14] N90-28994
Cognition versus sensation: A paradigm for reorientation
[IZF-1989-20] N90-28995
Proprioception in aircraft control
[IZF-1989-43] N90-29082
Recognition of infrared images. Part 3: The effect of image processing with a size-contrast box filter on observation performance
[IZF-1989-39] N90-29182

INSTITUTE FOR TELECOMMUNICATION SCIENCES, BOULDER, CO.
Design and performance of a long, over-water microwave radio link
[PB90-207994] N90-28758

INSTITUTE OF AVIATION MEDICINE, MADRID (SPAIN).
Evaluation of the performance capability of the aviator under hypoxic conditions operational experience N90-28991

INSTITUTO DE PESQUISAS ESPACIAIS, SAO JOSE DOS CAMPOS (BRAZIL).
Fabrication of spherical pressure vessels from composite materials
[INPE-4598-RPE/570] N90-28675
Simulation of INPE's printed circuit laboratory production line
[INPE-4556-TDL/331] N90-28784
Comparison of methods of space color transformations for enhancement of colored images
[INPE-4977-PRE/1542] N90-28881
Digital geometric correction for MSS-LANDSAT imagery
[INPE-4627-PRE/1345] N90-28888
Study of anomalies in transition vegetation in Alto Xingo-NT, through remote sensing techniques
[INPE-4601-TDL/334] N90-28891
Automated system for meteorological analysis
[INPE-4586-TDL/332] N90-28945
Vorticity balance study for a tropical region, during the Southern Hemisphere summer
[INPE-4634-TDL/336] N90-28949
Autoregressive-moving average models for texture classification
[INPE-4987-PRE/1549] N90-29092
Computer vision and its potential applications in Brazil
[INPE-4666-NTE/283] N90-29100
Inference engine for expert systems
[INPE-4565-PRE/1306] N90-29104
Computerized simulation of phenomena in plasma via particles
[INPE-4595-RPE/569] N90-29194
INPE geographic data base
[INPE-4636-PRE/1348] N90-29253
Fluctuations in cosmic background radiation
[INPE-4579-PRE/1313] N90-29294
Activities report for the IBDF-INPE project SEQE, year 1987
[INPE-4534-RPE/565] N90-29298

INTERNATIONAL CENTRE FOR THEORETICAL PHYSICS, TRIESTE (ITALY).
Thermodynamics and structure of liquid alkali metals from the charged-hard-sphere reference fluid
[DE90-627792] N90-28725
Propagation of electromagnetic radiation in a random field of gravitational waves and space radio interferometry
[DE90-627196] N90-28764
On the dynamics of severe thunderstorms
[DE90-627922] N90-28950
Product integration rules at Clenshaw-Curtis and related points: A robust implementation
[DE90-627158] N90-29106
Weighted norm inequalities for Riemann-Liouville fractional integral
[DE90-627153] N90-29132
The center of the enveloping algebra of the semidirect product of the Heisenberg lie algebra h(sub n) and a reductive Lie algebra S the rank of which is equal to 1 or 2
[DE90-627155] N90-29133
Recurrence relations and weight functions for approximation by orthonormal polynomials
[DE90-627156] N90-29134
Beltrami algebra and symmetry of Beltrami equation on Riemann surfaces
[DE90-627157] N90-29135
The combinatorics computation for Casimir operators of the symplectic Lie algebra and the application for determining the center of the enveloping algebra of a semidirect product
[DE90-627161] N90-29136
Asymptotics of Laplace-Dirichlet integrals
[DE90-627165] N90-29137
Solution of the Stokes system by boundary integral equations and fixed point iterative schemes
[DE90-627166] N90-29138
The Cousin problems for an overdetermined system of complex partial differential equations
[DE90-627170] N90-29139
The first order phase transition for six-state Potts model on two dimensional random triangle lattice
[DE90-627210] N90-29140
On comparable L(sup p)-norms of subadditive functions on topological groups
[DE90-627154] N90-29146

On an isospectrality question over compact Riemann surfaces
[DE90-627163] N90-29147
A corollary to Kodaira-Spencer's theorem on continuity of eigenvalues
[DE90-627164] N90-29148
Superconformal algebra and central extension of meromorphic vector fields with multipoles on super-Riemann sphere
[DE90-627211] N90-29153
Trajectories of renormalization group flows on the phase diagram of N=2 superconformal field theories
[DE90-627212] N90-29154
Topology of singularities and phase diagram of N=2 superconformal field theories
[DE90-627213] N90-29155
Quantum gravity in two dimensions and the SL(2,R) current algebra
[DE90-627215] N90-29156
Anyons and Chern-Simons theory on compact spaces of finite genus
[DE90-627216] N90-29157
Unexpected properties of the centrifugal force
[DE90-627197] N90-29164
Electron acoustic and magnetoacoustic modes in a magnetized beam plasma system
[DE90-627473] N90-29199
Superconductivity in mixed boson-fermion systems
[DE90-627491] N90-29216
Parity violation and superconductivity in doped Mott insulators
[DE90-627493] N90-29217
On Einsteinian 4-submanifolds in E(sup 6)
[DE90-627149] N90-29226
Dissipative quantum maps
[DE90-627179] N90-29227
Quantum chaos and dissipation: Lyapunov exponents
[DE90-627180] N90-29228
Old and new ideas in the theory of quantum measurement
[DE90-627181] N90-29229
A comment on anisotropic spheres admitting one parameter group of conformal motions
[DE90-627195] N90-29230
Higher loop contributions to effective potential of gauge theory at high temperature
[DE90-627208] N90-29231
On the relation between the absolute parallelism spaces and spaces having a GL(4) connection
[DE90-627222] N90-29232
Measurement of gravitational acceleration of antimatter
[DE90-627464] N90-29233
Quantifying the FIR interaction enhancement in paired galaxies
[DE90-627485] N90-29281

IOWA UNIV., IOWA CITY.
New Voyager radio spectrograms of Uranus
[NASA-CR-180381] N90-29284

ITALIAN AIR FORCE AEROSPACE MEDICAL CENTER, ROME.
Neurophysiological correlates of information processing abilities during divided attention situations in air traffic controllers N90-28989

J

JAMIESON SCIENCE AND ENGINEERING, INC., SCOTTS VALLEY, CA.
An infrared sky model based on the IRAS point source data
[NASA-CR-177526] N90-29265

JET PROPULSION LAB., CALIFORNIA INST. OF TECH., PASADENA.
The Magellan Venus explorer's guide
[NASA-CR-186968] N90-28592
An aeronautical mobile satellite experiment
[NASA-CR-186971] N90-28593
Proceedings of the NASA Conference on Space Telerobotics, volume 1
[NASA-CR-186856] N90-29000
A new approach to global control of redundant manipulators N90-29002
Kinematic functions for the 7 DOF robotics research arm N90-29003
A system architecture for a planetary rover N90-29015
The NASA/OAST telerobot testbed architecture N90-29016
Computational neural learning formalisms for manipulator inverse kinematics N90-29030
Causal simulation and sensor planning in predictive monitoring N90-29037
Proceedings of the NASA Conference on Space Telerobotics, volume 2
[NASA-CR-186857] N90-29044
Characterization and control of self-motions in redundant manipulators N90-29045
The JPL telerobot operator control station. Part 1: Hardware N90-29049
The JPL telerobot operator control station. Part 2: Software N90-29050
Performance evaluation of a 6 axis high fidelity generalized force reflecting teleoperator N90-29052
Implementation and design of a teleoperation system based on a VMEBUS/68020 pipelined architecture N90-29053
Experiences with the JPL telerobot testbed: Issues and insights N90-29059
The KALI multi-arm robot programming and control environment N90-29060

JOHNS HOPKINS UNIV., BALTIMORE, MD.
Preliminary exposure study to determine the effects of acid deposition on coated steel substrates
[PB90-201799] N90-28715
Studies of central interactions of Si ions at 14.5 x A GeV/c in Au and Cu
[DE90-015095] N90-29195

K

KANSAS UNIV., LAWRENCE.
Life cycle cost in the conceptual design of subsonic commercial aircraft, volumes 1 and 2 N90-28535

KOBE UNIV. (JAPAN).
A neural network for controlling the configuration of frame structure with elastic members N90-29034

KOPIN CORP., TAUNTON, MA.
Smart microsensors for high temperature applications, phase 1
[AD-A224151] N90-28828

KRUG INTERNATIONAL, HOUSTON, TX.
The effects of acoustic orientation cues on instrument flight performance in a flight simulator N90-28985

L

LABORATOIRE D'INFORMATIQUE POUR LA MECANIQUE ET LES SCIENCES DE L'INGENIEUR, PARIS (FRANCE).
Vortice-propeller interaction
[LIMSI-89-9] N90-28809

LABORATOIRE DE MEDECINE AEROSPATIALE, BRETIGNY-SUR-ORGE (FRANCE).
Target acquisition under load factors: Advantages and disadvantages of a helmet mounted sight N90-28983
Tracking performance and influence of field of view N90-28988

LAMONT-DOHERTY GEOLOGICAL INST., PALISADES, NY.
Ross Sea oceanographic data, 1983-1987: USCGC GLACIER, January-February 1983; USCGC POLAR SEA, January-February 1984; USCGC POLAR STAR, February 1984; USCGC POLAR SEA, February 1987
[PB90-243932] N90-28955

LAWRENCE LIVERMORE NATIONAL LAB., CA.
Shock dynamics in the sub-nanometer femtosecond domain
[DE90-014390] N90-28689
Experimental study of the optical constants of metals at high temperatures
[DE90-014732] N90-28719
Behavior of Al-Mg alloys in hot working and superplasticity
[DE90-015193] N90-28723
Damage resistant optical coatings prepared using high temperature, plasma chemical-vapor-deposition
[DE90-015042] N90-28738
A new low density, high porosity lithium hydride-beryllium hydride foam
[DE90-015150] N90-28739
Using the x ray region of the electromagnetic spectrum for alignment: Overview, geometric optics, and design considerations
[DE90-014798] N90-28752
Modeling tape-wound magnetic switches
[DE90-015121] N90-28782
Noise performance of microchannel plate imaging systems
[DE90-015037] N90-28785
An asymptotically induced domain decomposition method for parabolic boundary layer problems
[DE90-014620] N90-28804
Lecture notes on incompressible flow and the finite element method
[DE90-014665] N90-28805
New resonantly photo-pumped x ray laser scheme
[DE90-015044] N90-28831
The global cycle of reactive nitrogen
[DE90-015041] N90-28919
Tropospheric nitrogen: The influence of anthropogenic sources on distributions and deposition, executive summary
[DE90-015401] N90-28922
Human factors evaluation and validation criteria for quality training programs: Development, presentation, and assessment
[DE90-014724] N90-29081
Who's who in scientific visualization at LLNL
[DE90-014720] N90-29091
Animated computer-generated video-tape instruction using DIGLIB (Device Independent Graphics Library)
[DE90-015360] N90-29105
Deterministic transport on an arbitrarily-connected grid
[DE90-015148] N90-29131

LEEDS UNIV. (ENGLAND).
Some studies of the vibration welding of thermoplastics N90-28842

LISTER HILL NATIONAL CENTER FOR BIOMEDICAL COMMUNICATIONS, BETHESDA, MD.
The SPECIALIST: Natural language processing system
[PB90-240029] N90-29098

LOCKHEED ENGINEERING AND SCIENCES CO., HAMPTON, VA.
Vibration responses of two house structures during the Edwards Air Force Base phase of the national sonic boom program
[NASA-CR-182089] N90-29169

LONDON UNIV. (ENGLAND).
Unsteady aerodynamics of controls N90-28525

LOS ALAMOS NATIONAL LAB., NM.
Is there anything of practical value hidden amongst the composite toughening theories. A Jim Mueller prospective
[DE90-014905] N90-28673
Study of the induction time in isothermal decomposition of explosives
[DE90-014906] N90-28745
Three-dimensional simulations of the generation of one Angstrom radiation by a self-amplified spontaneous emission free-electron laser
[DE90-015032] N90-28830
A manual for analysis of hemispherical canopy photography
[DE90-014718] N90-28885
Workload induced spatio-temporal distortions and safety of flight: An investigation of cognitive intrusions in perceptual processes N90-28986
LINTERP: A numerical algorithm for interpolating quadrilateral and hexahedral meshes
[DE90-014417] N90-29090
Recursive least-squares learning algorithms for neural networks
[DE90-014926] N90-29096
Graph structure model
[DE90-014930] N90-29097
An even-parity/odd-parity formulation for deterministic transport calculations on massively parallel computers
[DE90-015036] N90-29116
Moessbauer Effect applications using intense radioactive ion beams
[DE90-014981] N90-29175
Velocity Interferometer System for Any Reflector (VISAR): Displacement mode data reduction
[DE90-015027] N90-29184
Antiferromagnetism and enhanced heat in CeM2Sn (M = Ni, Ir, Cu, Rh, Pd, and Pt
[DE90-014924] N90-29206
Evidence for a coherence gap in Ce3Bi4Pt3
[DE90-014925] N90-29207
Cepheid masses for models with enhanced opacities
[DE90-014919] N90-29266
Pulsations of the white dwarf component in V471 tauri-like binaries
[DE90-014921] N90-29267
Kappa effect pulsational instability for hot extreme helium stars
[DE90-014920] N90-29277
Nonradial instability strips for post-AGB stars
[DE90-014922] N90-29278
Pulsations of B star models by an opacity mechanism
[DE90-014923] N90-29279
Solar oscillation frequency and solar neutrino predictions
[DE90-014918] N90-29288

LOUGHBOROUGH UNIV. OF TECHNOLOGY (ENGLAND).
Efficiency and effectiveness of deep structure-based subject indexing languages: PRECIS vs. DSIS N90-29248

LOYOLA UNIV., CHICAGO, IL.
Auditory processing of complex sounds across frequency channels
[AD-A224147] N90-28970

M

MARTIN MARIETTA CORP., DENVER, CO.
Robotic sampling system for an unmanned Mars mission N90-29070
MARTIN MARIETTA CORP., NEW ORLEANS, LA.
Liquid Rocket Booster (LRB) for the Space Transportation System (STS) systems study. Volume 1: Executive summary
[NASA-CR-183822] N90-28599
Liquid Rocket Booster (LRB) for the Space Transportation System (STS) systems study, volume 2
[NASA-CR-183786] N90-28600
Liquid Rocket Booster (LRB) for the Space Transportation System (STS) systems study. Appendix A: Stress analysis report for the pump-fed and pressure-fed liquid rocket booster
[NASA-CR-183787-APP-A] N90-28601
Liquid Rocket Booster (LRB) for the Space Transportation System (STS) systems study. Appendix B: Liquid rocket booster acoustic and thermal environments
[NASA-CR-183788-APP-B] N90-28602
Liquid Rocket Booster (LRB) for the Space Transportation System (STS) systems study. Appendix C: Battery report for the liquid rocket booster TVC actuators
[NASA-CR-183789-APP-C] N90-28603
Liquid Rocket Booster (LRB) for the Space Transportion System (STS) systems study. Appendix D: Trade study summary for the liquid rocket booster
[NASA-CR-183790-APP-D] N90-28604
Liquid Rocket Booster (LRB) for the Space Transportation System (STS) systems study. Appendix E: Pressure-fed booster test bed for the liquid rocket booster study
[NASA-CR-183791-APP-E] N90-28605
Liquid Rocket Booster (LRB) for the Space Transportation System (STS) systems study. Appendix F: Performance and trajectory for ALS/LRB launch vehicles
[NASA-CR-183792-APP-F] N90-28606
Liquid Rocket Booster (LRB) for the Space Transportation System (STS) systems study. Appendix G: LRB for the STS system study level 2 requirements, revision 1
[NASA-CR-183793-APP-G] N90-28607
MARTIN MARIETTA LABS., BALTIMORE, MD.
Preliminary exposure study to determine the effects of acid deposition on coated steel substrates
[PB90-201799] N90-28715
MARYLAND UNIV., COLLEGE PARK.
Transient cooling of a hot surface by droplets evaporation
[PB90-227966] N90-28799
Robot Acting on Moving Bodies (RAMBO): Interaction with tumbling objects N90-29022
Perceptual telerobotics N90-29063
MASSACHUSETTS INST. OF TECH., CAMBRIDGE.
Surface and defect excitations in covalently bonded solids
[AD-A221995] N90-28682
Quenching of N(2D) by O(3P)
[AD-A221690] N90-28683
Polymer research
[PB90-246636] N90-28737
Ultrasonic verification of five wave fronts in unidirectional graphite epoxy composite
[NASA-CR-185286] N90-28858
Adjustable impedance, force feedback and command language aids for telerobotics (parts 1-4 of an 8-part MIT progress report) N90-29007
Variable force and visual feedback effects on teleoperator man/machine performance N90-29008
Combined electron cyclotron ray tracing and transport code studies in the compact ignition tokamak
[DE90-014097] N90-29189
Ignition and burn control characteristics of thermonuclear plasmas
[DE90-015385] N90-29197
TSC (Tokamak Simulation Code) simulations of Alcator C-MOD discharges 3: Study of axisymmetric stability
[DE90-015386] N90-29198
Interface formation and percusory dynamics
[AD-A224128] N90-29223
Statement of research objectives and summary of research efforts
[RLE-PR-132] N90-29295
MASSACHUSETTS UNIV., AMHERST.
Radio outbursts in extragalactic sources N90-29291
MATERIALS RESEARCH LABS., ASCOT VALE (AUSTRALIA).
Operation and calibration of MRL permeameter for measurement of DC magnetic properties of materials under stress
[MRL-TN-574] N90-28863
MAX-PLANCK-INST. FUER PHYSIK UND ASTROPHYSIK, GARCHING (GERMANY, F.R.).
Alfven wave solitons and solar intermediate drift bursts
[MPE-PREPRINT-173] N90-29287
MCDONNELL-DOUGLAS HELICOPTER CO., MESA, AZ.
Correlation of AH-1G airframe flight vibration data with a coupled rotor-fuselage analysis
[NASA-CR-181974] N90-28865
Plan, execute, and discuss vibration measurements and correlations to evaluate a NASTRAN finite element model of the AH-64 helicopter airframe
[NASA-CR-181973] N90-28866
MCGILL UNIV., MONTREAL (QUEBEC).
Effects of short-term weightlessness on roll circularvection N90-28992
Preliminary study of a serial-parallel redundant manipulator N90-29048
MEDICAL TECHNOLOGY, INC., SYRACUSE, NY.
Automotive Stirling engine development program
[NASA-CR-180840] N90-29260
MICHIGAN UNIV., ANN ARBOR.
Factors influencing the mode I interlaminar fracture resistance of toughened matrix composites N90-28668
Electromagnetic scattering from two-dimensional thick material junctions
[NASA-CR-186468] N90-28767
Tele-Autonomous control involving contact
[NASA-CR-187004] N90-28854
Methods and strategies of object localization N90-29020
On the simulation of space based manipulators with contact N90-29056
Building an environment model using depth information N90-29064
MIDWEST RESEARCH INST., GOLDEN, CO.
Research on the structural and electronic properties of defects in amorphous silicon
[DE90-000342] N90-28730
Research on high-efficiency, multiple-gap, multi-junction amorphous silicon-based alloy thin-film solar cells
[DE90-000338] N90-28896
Research on stable, large-area, amorphous silicon based submodules, phase 3
[DE90-000339] N90-29204
Transferring building energy technologies by linking government and private-sector programs
[DE90-000346] N90-29258
MIDWEST RESEARCH INST., KANSAS CITY, MO.
Further studies of 60 Hz exposure effects on human function
[DE90-014377] N90-28962
MINNESOTA UNIV., MINNEAPOLIS.
Solutions to the frictional dynamics problem and the reciprocal variable feedback methodology for design and control of robot mechanisms N90-28846
Human machine interaction via the transfer of power and information signals N90-29054
MIRIAM HOSPITAL, PROVIDENCE, RI.
Computer aided mechanogenesis of skeletal muscle organs from single cells in vitro
[NASA-CR-187025] N90-28959
Insulin and insulin-like growth factor-1 induce pronounced hypertrophy of skeletal myofibers in tissue culture
[NASA-CR-187026] N90-28960
MITRE CORP., MCLEAN, VA.
Some novel sources of x ray beams: Channeling, transition and Cherenkov radiation
[DE90-014442] N90-29181

N

NATIONAL ACADEMY OF ENGINEERING, WASHINGTON, DC.
Engineering and the advancement of human welfare. Ten outstanding achievements 1964-1989
[ISBN-0-309-04185-6] N90-29297
NATIONAL ACADEMY OF SCIENCES - NATIONAL RESEARCH COUNCIL, WASHINGTON, DC.
Proceedings of a workshop on Future Airport Passenger Terminals
[PB90-213620] N90-28580
Crossroads of Information Technology Standards
[PB90-239732] N90-29251
NATIONAL ACID PRECIPITATION ASSESSMENT PROGRAM, WASHINGTON, DC.
Estimating the spatial variability of trace gas deposition velocities
[PB90-208570] N90-28928
NATIONAL AERONAUTICAL ESTABLISHMENT, OTTAWA (ONTARIO).
Evaluation of high temperature protective coatings for gas turbine engines under simulated service conditions N90-28712
NATIONAL AERONAUTICAL LAB., BANGALORE (INDIA).
Do inviacid vortex sheets roll-up
[PD-CF-9010] N90-28491
Sting-support interference on afterbody drag at transonic speeds
[NAL-TM-EA-8902] N90-28492
A conceptual framework for fighter flight control systems
[PD-CF-9009] N90-28577
NATIONAL AERONAUTICS AND SPACE ADMINISTRATION, WASHINGTON, DC.
Advanced Earth-to-orbit propulsion technology program overview: Impact of civil space technology initiative N90-28612
Present state of knowledge of the upper atmosphere 1990: An assessment report
[NASA-RP-1242] N90-28929
Aerospace medicine and biology: A continuing bibliography with indexes (supplement 340)
[NASA-SP-7011(340)] N90-28963
Planetary rover technology development requirements N90-29067
NATIONAL AERONAUTICS AND SPACE ADMINISTRATION. AMES RESEARCH CENTER, MOFFETT FIELD, CA.
The effects of structural flap-lag and pitch-lag coupling on soft inplane hingeless rotor stability in hover
[NASA-TP-3002] N90-28503
Velocity filtering applied to optical flow calculations
[NASA-TM-102802] N90-28512
Accurate quantum chemical calculations
[NASA-TM-101932] N90-28680
Joint US/USSR study: Comparison of effects of horizontal and head-down bed rest
[NASA-TP-3037] N90-28965
Techniques and applications for binaural sound manipulation in human-machine interfaces
[NASA-TM-102279] N90-28996
A survey of planning and scheduling research at the NASA Ames Research Center N90-29076
Automated simulation as part of a design workstation
[NASA-TM-102852] N90-29083
NATIONAL AERONAUTICS AND SPACE ADMINISTRATION. GODDARD SPACE FLIGHT CENTER, GREENBELT, MD.
Formulation of design guidelines for automated robotic assembly in outerspace N90-29017
PW Vul: A classical nova with nearly solar abundances
[NASA-CR-185080] N90-29275
Nova LMC (Large Magellanic Cloud) 1990 no. 1: The first extragalactic neon nova
[NASA-CR-180409] N90-29276
NATIONAL AERONAUTICS AND SPACE ADMINISTRATION. HUGH L. DRYDEN FLIGHT RESEARCH FACILITY, EDWARDS, CA.
In-flight flow visualization with pressure measurements at low speeds on the NASA F-18 high alpha research vehicle
[NASA-TM-101726] N90-28505
An in-flight investigation of ground effect on a forward-swept wing airplane N90-28533
Validation of the F-18 high alpha research vehicle flight control and avionics systems modifications
[NASA-TM-101723] N90-28542
Propulsion system-flight control integration and optimization: Flight evaluation and technology transition
[NASA-TM-4207] N90-28551
Real-time aerodynamic heating and surface temperature calculations for hypersonic flight simulation
[NASA-TM-4222] N90-28815
In-flight investigation of shuttle tile pressure orifice installations
[NASA-TM-4219] N90-28820
NATIONAL AERONAUTICS AND SPACE ADMINISTRATION. JOHN F. KENNEDY SPACE CENTER, COCOA BEACH, FL.
Operational cost drivers N90-28636
NATIONAL AERONAUTICS AND SPACE ADMINISTRATION. LYNDON B. JOHNSON SPACE CENTER, HOUSTON, TX.
Data base for crack growth properties of materials N90-28647

NATIONAL AERONAUTICS AND SPACE ADMINISTRATION. LANGLEY RESEARCH CENTER, HAMPTON, VA.
Control of submersible vortex flows [NASA-TM-102693] N90-28493
Secondary instabilities in compressible boundary layers [NASA-CR-182091] N90-28502
Control research in the NASA high-alpha technology program N90-28516
Innovative control concepts and component integration for a generic supercruise fighter N90-28521
Development of non-conventional control methods for high angle of attack flight using vortex manipulation N90-28522
Dynamic ground effects N90-28531
NASA Langley Research Center National Aero-Space Plane Mission simulation profile sets [NASA-TM-102670] N90-28541
Description of the primary flight display and flight guidance system logic in the NASA B-737 transport systems research vehicle [NASA-TM-102710] N90-28546
Aerodynamic parameters of High-Angle-of attack Research Vehicle (HARV) estimated from flight data [NASA-TM-102692] N90-28578
Shuttle to Shuttle 2: Subsystem weight reduction potential (estimated 1992 technology readiness date) [NASA-TM-89114] N90-28589
Transformational part-count in layered octahedral-tetrahedral truss configurations [NASA-TM-102635] N90-28598
An LQR controller design approach for a Large Gap Magnetic Suspension System (LGMSS) [NASA-TM-101606] N90-28751
Gas-jet and tangent-slot film cooling tests of a 12.5 deg cone at Mach number of 6.7 [NASA-TP-2766] N90-28806
Buckling and postbuckling behavior of compression-loaded isotropic plates with cutouts [NASA-TP-3024] N90-28859
Development of testing and analysis methodology to assess the long term durability of polymeric composites at high temperatures [NASA-TM-102714] N90-28871
Evaluation of several micromechanics models for discontinuously reinforced metal matrix composites [NASA-TM-102719] N90-28872
Error detection and control for nonlinear shell analysis [NASA-TM-102723] N90-28877
The distribution of middle tropospheric carbon monoxide during early October 1984 [NASA-TM-103485] N90-28906
Annoyance caused by advanced turboprop aircraft flyover noise: Counter-rotating-propeller configuration [NASA-TP-3027] N90-29166
Comparison of dose estimates using the buildup-factor method and a Baryon transport code (BRYNTRN) with Monte Carlo results [NASA-TP-3021] N90-29290

NATIONAL AERONAUTICS AND SPACE ADMINISTRATION. LEWIS RESEARCH CENTER, CLEVELAND, OH.
ATDRS payload technology research and development [NASA-TM-103256] N90-28596
Probabilistic structural analysis methods development for SSME N90-28616
Bearing optimization for SSME HPOTP application N90-28622
Catalytic ignition of hydrogen/oxygen N90-28627
Combustion instability coupling with feed system acoustics N90-28629
High temperature fatigue behavior of Haynes 188 N90-28642
The fatigue damage behavior of a single crystal superalloy N90-28644
Structural response of SSME turbine blade airfoils N90-28649
Durability of thermal barrier coatings in a high heat flux environment N90-28651
Thermal analysis of thermal barrier coatings in a high heat flux environment N90-28652
Ceramic matrix composites in simulated SSME environments N90-28655
Low power arcjet performance [NASA-TM-103280] N90-28657
A failure diagnosis system based on a neural network classifier for the space shuttle main engine [NASA-TM-103607] N90-28659
The effects of atomic oxygen on the thermal emittance of high temperature radiator surfaces [NASA-TM-103224] N90-28670
Synthesis and structural chemistry of Au(III)-substituted Ba2YCu3O(7-delta) [NASA-TM-103292] N90-28696
High-temperature deformation and microstructural analysis for Si3N4-Sc2O3 [NASA-TM-103239] N90-28740
Development and approach to low-frequency microgravity isolation systems [NASA-TP-2984] N90-28754
Rain-fade simulation and power augmentation for satellite communication systems [NASA-TM-103134] N90-28768
High temperature superconducting thin film microwave circuits: Fabrication, characterization, and applications [NASA-TM-103235] N90-28786
Evaluation of a hybrid kinetics/mixing-controlled combustion model for turbulent premixed and diffusion combustion using KIVA-2 [NASA-TM-103196] N90-28792
Frequency response of a thermocouple wire: Effects of axial conduction [NASA-CR-180454] N90-28827
Design of a CO2 laser power control system for a Spacelab microgravity experiment [NASA-TM-103112] N90-28833
An expert system to perform on-line controller restructuring for abrupt model changes [NASA-TM-103609] N90-29121
Consistency and convergence for numerical radiation conditions [NASA-TM-103282] N90-29124
XANES and EXAFS study of Au-substituted YBa2Cu3O(7-delta) [NASA-TM-103291] N90-29219

NATIONAL AERONAUTICS AND SPACE ADMINISTRATION. MARSHALL SPACE FLIGHT CENTER, HUNTSVILLE, AL.
Microgravity science and applications: Apparatus and facilities [NASA-TM-101892] N90-28588
Space Station Freedom pressurized element interior design process [NASA-CR-181297] N90-28597
Advanced Earth-to-Orbit Propulsion Technology 1988, volume 1 [NASA-CP-3012-VOL-1] N90-28611
Oxygen/hydrogen technology test bed status update N90-28613
Cryogenic, high speed, turbopump bearing cooling requirements N90-28620
Comparison of two computer codes for crack growth analysis: NASCRAC versus NASA/FLAGRO N90-28648
Vacuum application of thermal barrier plasma coatings N90-28653
Robotic and automatic welding development at the Marshall Space Flight Center N90-28656
Minimum weight design of a leaf spring tapered in thickness and width for the Hubble Space Telescope-space support equipment [NASA-TM-4233] N90-28679
Atmospheric environment for Space Shuttle (STS-32) launch [NASA-TM-100400] N90-28912
Atmospheric environment for Space Shuttle (STS-31) launch [NASA-TM-103508] N90-28913
Atmospheric environment for space shuttle (STS-36) launch [NASA-TM-100403] N90-28914
Atmospheric environment for space shuttle (STS-34) launch [NASA-TM-100396] N90-28915
Mesoscale Lightning Experiment (MLE): A view of lightning as seen from space during the STS-26 mission [NASA-TM-103513] N90-28951
NASA Marshall Space Flight Center Solar Observatory report, January - June 1990 [NASA-TM-103512] N90-29268

NATIONAL AERONAUTICS AND SPACE ADMINISTRATION. WALLOPS FLIGHT FACILITY, WALLOPS ISLAND, VA.
A personal computer-based, multitasking data acquisition system [NASA-TM-4232] N90-29107

NATIONAL AEROSPACE LAB., EMMELOORD (NETHERLANDS).
Thermal shock and oxidation resistance of ceramic coatings N90-28711

NATIONAL ARCHIVES AND RECORDS SERVICE, WASHINGTON, DC.
National Archives preservation research priorities: Past and present [PB90-206210] N90-29242

NATIONAL DEFENCE RESEARCH ESTABLISHMENT, STOCKHOLM (SWEDEN).
ARALL (ARamid ALuminum Laminate), a literature survey [FOA-C-20782-2.5] N90-28671
Composite propellants with high burning rates [FOA-C-20781-2.1] N90-28744

NATIONAL INST. OF STANDARDS AND TECHNOLOGY, BOULDER, CO.
Thermophysical properties of Helium-4 from 0.8 to 1500 K with pressures to 2000 MPa [NASA-CR-186992] N90-28681
Guidelines for pressure vessel safety assessment [PB90-219619] N90-28749

NATIONAL INST. OF STANDARDS AND TECHNOLOGY, GAITHERSBURG, MD.
Determination of the NDT temperature and Charpy V-notch impact properties of AAR TC128 grades B steel and A 8XX grade B steel [PB90-207804] N90-28716
Electrodeposition of wear resistant coatings [PB90-221839] N90-28732
Specifications, tolerances, and other technical requirements for weighing and measuring devices as adopted by the 74th National Conference on Weights and Measures, 1989 (1990 edition) [PB90-184961] N90-28748
Secure Data Network System (SDNS) network, transport, and message security protocols [PB90-198946] N90-28757
Emerging technologies in electronics and their measurement needs, second edition [PB90-186087] N90-28773
Research for electric energy systems [DE90-014221] N90-28775
Stabilization of Taylor-Couette flow due to time-periodic outer cylinder oscillation [PB90-219130] N90-28790
Special test and evaluation methods used for a nine-axis accelerometer [PB90-209578] N90-28822
DOE/NIST Workshop on Common Architectures for Robotic Systems [PB90-216839] N90-28840
Computerization of Welding Data: Proceedings of the conference and workshop [PB90-219551] N90-28841
Study of meteorological processes important in the degradation of materials through surface temperature [PB90-222720] N90-28856
Long-range plan for a research project on carbon monoxide production and prediction [PB90-209602] N90-28910
Genesis of bow echoes: A rear-inflow induced meso-convective structure [PB90-209776] N90-28926
Trajectory generation of space telerobots N90-29055
Software development tools [PB90-250051] N90-29103
Numerical and analytical study of nonlinear bifurcations associated with the morphological stability of two-dimensional single crystals [PB90-209594] N90-29200
Semiconductor measurement technology: A software program for aiding the analysis of ellipsometric measurements, simple spectroscopic models [PB90-216847] N90-29201
Semiconductor measurement technology. EPROP: An interactive FORTRAN program for computing selected electronic properties of Gallium Arsenide and Silicon [PB90-222738] N90-29203
Goverment's role in standards-related activities: Analysis of comments [PB90-215534] N90-29239
Object database management systems: Concepts and features [PB90-216813] N90-29243
Information management directions: The integration challenge [PB90-219866] N90-29245
Technical activities 1989, Electron and Optical Physics Division [PB90-207267] N90-29296

NATIONAL OCEANIC AND ATMOSPHERIC ADMINISTRATION, BOULDER, CO.
Remote atmospheric profiling systems for tropospheric monitoring [PB90-216789] N90-28927
A radio frequency user's guide to the space environment services center geophysical alert broadcasts [PB90-240831] N90-28935
Tropospheric wind profiling using radar interferometry: A feasibility study of a compact mobile system [PB90-217068] N90-28939

NATIONAL OCEANIC AND ATMOSPHERIC ADMINISTRATION, OAK RIDGE, TN.
Estimating the spatial variability of trace gas deposition velocities [PB90-208570] N90-28928

NATIONAL OCEANIC AND ATMOSPHERIC ADMINISTRATION, WASHINGTON, DC.
Oceanographic data exchange, 1988
[PB90-232596] N90-28952
NATIONAL PHYSICAL LAB., TEDDINGTON (ENGLAND).
Developments in test procedures for hot-salt corrosion of superalloys N90-28700
NATIONAL RESEARCH COUNCIL OF CANADA, OTTAWA (ONTARIO).
The effects of a compressor rebuild on gas turbine engine performance: Final results N90-28701
NATIONAL SCIENCE FOUNDATION, WASHINGTON, DC.
Scientists, engineers, and technicians in nonmanufacturing industries: 1987. (Detailed statistical tables)
[PB90-226903] N90-29235
Federal support to universities, colleges, and selected nonprofit institutions: Fiscal year 1988 (detailed statistical tables)
[PB90-226887] N90-29236
Federal R and D funding by budget function: Fiscal years 1989-1991
[PB90-226879] N90-29237
NATIONAL SEVERE STORMS LAB., NORMAN, OK.
Program on development of basic understanding of severe weather phenomena
[PB90-226564] N90-28943
NATIONAL TECHNICAL INFORMATION SERVICE, SPRINGFIELD, VA.
Industrial patent activity in the US. Part 2: Alphabetical listing by company, 1969-1989
[PB90-214412] N90-29246
NATIONAL TELECOMMUNICATIONS AND INFORMATION ADMINISTRATION, ANNAPOLIS, MD.
Ground-based weather radar compatibility with digital radio-relay microwave systems
[PB90-206236] N90-28756
NATIONAL TELECOMMUNICATIONS AND INFORMATION ADMINISTRATION, BOULDER, CO.
New approach to HF channel modeling and simulation. Part 2: Stochastic model
[PB90-200336] N90-28755
NATIONAL WEATHER SERVICE, FORT WORTH, TX.
An investigation of forcing mechanisms during a surprise tornadic thunderstorm
[PB90-216805] N90-28940
Severe thunderstorm forecasting: An operational review
[PB90-215484] N90-28948
NATIONAL WEATHER SERVICE, WASHINGTON, DC.
Proceedings of the 14th Annual Climate Diagnostics Workshop
[PB90-198573] N90-28938
NAVAL AEROSPACE MEDICAL RESEARCH LAB., PENSACOLA, FL.
Predicting F/A-18 fleet replacement squadron performance using an automated battery of performance-based tests
[AD-A223899] N90-28543
Maintaining spatial orientation awareness N90-28993
NAVAL AIR DEVELOPMENT CENTER, WARMINSTER, PA.
Oxidation, sulfidation, and hot corrosion: Mechanisms and interrelationships N90-28702
Microdamage to ceramic surfaces under sliding conditions N90-28708
NAVAL HEALTH RESEARCH CENTER, SAN DIEGO, CA.
Prevalence of hypertension among active duty personnel
[AD-A223892] N90-28968
NAVAL POSTGRADUATE SCHOOL, MONTEREY, CA.
Development and testing of rapid repair methods for war damaged runways
[AD-A223970] N90-28586
Bandwidth and signal-to-noise ratio enhancement of the NPS transient electromagnetic scattering laboratory
[AD-A224144] N90-28771
Unipolar arcing on the cathode surface of a high voltage diode
[AD-A224122] N90-28787
Effect of vortex circulation on injectant from a single film-cooling hole and a row of film-cooling holes in a turbulent boundary layer. Part 2: Injection beneath the vortex upwash
[AD-A223894] N90-28818
Effects of flowfield turbulence on asymmetric vortices over a slender body
[AD-A224139] N90-28819
A comparison of password techniques for multilevel authentication mechanisms
[AD-A224245] N90-29089
Block Lanczos algorithm
[AD-A224011] N90-29111
Designing intelligent computer aided instruction systems with integrated knowledge representation schemes
[AD-A224178] N90-29113
Near-angle scattering and binary optics
[AD-A224140] N90-29186
Extensions to the learning curve: An analysis of factors influence unit cost of weapon systems
[AD-A224119] N90-29256
NAVAL RESEARCH LAB., WASHINGTON, DC.
Numerical simulations of flowfields in a central-dump ramjet combustor. 3: Effects of chemistry
[AD-A224145] N90-28573
Mode competition in the quasioptical gyrotron
[AD-A222181] N90-28823
NAVAL SEA SYSTEMS COMMAND, WASHINGTON, DC.
Extensions to the learning curve: An analysis of factors influence unit cost of weapon systems
[AD-A224119] N90-29256
NAVAL SHIP RESEARCH AND DEVELOPMENT CENTER, BETHESDA, MD.
Flow coupling between a rotor and a stator in turbomachinery
[AD-A223882] N90-28572
NAVAL SURFACE WARFARE CENTER, DAHLGREN, VA.
Target detection in Gaussian noise using artificial neural systems
[AD-A223983] N90-28770
Selective learning algorithm for certain types of learning failure in multilayer perceptrons
[AD-A223982] N90-28998
NAVAL UNDERWATER SYSTEMS CENTER, WEST PALM BEACH, FL.
Measuring the vertical directional spectra caused by sea surface sound
[AD-A223883] N90-28957
NETHERLANDS AEROSPACE MEDICAL CENTRE, SOESTERBERG.
Spatial disorientation incidents in the RNLAF F16 and F5 aircraft and suggestions for prevention N90-28973
NEVADA UNIV., RENO.
Free shear layer and swirl flow heat transfer enhancement
[PB90-228123] N90-28798
Geothermal fluid genesis in the Great Basin
[DE90-014438] N90-28884
NEW MEXICO STATE UNIV., LAS CRUCES.
Cartesian control of redundant robots N90-29004
Overcoming rule-based rigidity and connectionist limitations through massively-parallel case-based reasoning
[NASA-CR-186963] N90-29117
NEW MEXICO UNIV., ALBUQUERQUE.
A design philosophy for multi-layer neural networks with applications to robot control N90-29033
NIELSEN ENGINEERING AND RESEARCH, INC., MOUNTAIN VIEW, CA.
Prediction of subsonic vortex shedding from forebodies with chines
[NASA-CR-4323] N90-28494
NORTH CAROLINA UNIV., CHARLOTTE.
Magnetostrictive direct drive motors
[NASA-CR-186895] N90-28855
NORTHROP CORP., HAWTHORNE, CA.
A methodology for the objective measurement of pilot situation awareness N90-28974
NORTHWEST FLORIDA WATER MANAGEMENT DISTRICT, TALLAHASSEE.
Computer program for converting rectangular coordinates to latitude-longitude coordinates
[PB90-231796] N90-28883
NOTTINGHAM UNIV. (ENGLAND).
Fretting wear and fretting fatigue at temperatures up to 600 C N90-28706
NSI TECHNOLOGY SERVICES CORP., CORVALLIS, OR.
Annual course of precipitation over much of the US: Observed versus GCM simulation
[PB90-221656] N90-28942

O

OAK RIDGE NATIONAL LAB., TN.
Friction microprobe studies of composite surfaces
[DE90-014224] N90-28662
Micromechanics analysis of power consolidation in manufacturing particulate-reinforced MMCs (metal matrix composites)
[DE90-014448] N90-28663
Structure of metal overlayers by low energy alkali ion scattering: Cu/Ru(0001) and Sn/Pt(111)
[DE90-014453] N90-28718
Evaluation of advanced austenitic alloys relative to alloy design criteria for steam service. Part 1: Lean stainless steel
[DE90-014765] N90-28720
Mechanical testing activities related to high-performance structural ceramics
[DE90-014299] N90-28734
Results from the fourth year of operation of the Federal Methanol Fleet at Lawrence Berkeley Laboratory
[DE90-014741] N90-28743
Gas-film flow in tubes
[DE90-011528] N90-28793
Concept for a neutron spectrometer based on optical detection of (3)He(n, p)-3H reactions in a gas
[DE90-014776] N90-28826
Influence of diesel engine exposure on the rupture strength of silicon nitride and partially stabilized zirconia
[DE90-014759] N90-28849
Treatment of systematic errors 2: Fusion of ultrasound and visual sensor data
[DE90-014780] N90-28850
ROSES, a Robot Operating System Expert Scheduler: Methodological framework
[DE90-014782] N90-28851
Mechanical properties testing of diamond and diamond-like films by ultra-low load indentation
[DE90-014456] N90-28861
Geophysical diffraction tomography: A complementary remote sensing technique for hazardous waste site characterization
[DE90-013025] N90-28882
HERMIES-3: A step toward autonomous mobility, manipulation, and perception N90-29065
The effect of multiprocessor radius on scaling
[DE90-014772] N90-29095
Piecewise linear models of processor utilization
[DE90-014774] N90-29115
A hardware/software environment to support R/D in intelligent machines and mobile robotic systems
[DE90-014458] N90-29119
Workshop on Neural Networks
[DE90-014794] N90-29120
Asymptotic behavior of solutions of diffusion-like partial differential equations invariant to a family of affine groups
[DE90-014792] N90-29130
Fifteenth International Conference on X Ray and Inner-Shell Processes
[DE90-013024] N90-29170
Formation of magnetic islands due to field perturbations in toroidal stellarator configurations
[DE90-014789] N90-29191
Stellarator status, 1989
[DE90-014791] N90-29192
Prediction, control, and decision-making aspects for chaotic systems
[DE90-014452] N90-29224
Biomedical and environmental sciences program publications, 1989
[DE90-014785] N90-29250
Enrichment services for chromium isotopes for the GALLEX (gallium experiment) international collaboration experiment on solar neutrino flux
[DE90-014300] N90-29285
OFFICE NATIONAL D'ETUDES ET DE RECHERCHES AEROSPATIALES, PARIS (FRANCE).
Solution of Euler equations applied to a rotor of a helicopter in steady flight
[ONERA-RSF-1/3731-AY-002A] N90-28500
Electrochemical surface finishing using amino-substrates on carbon fibers in organic media. Effects of the finishing on the mechanical properties of carbon-epoxy composites
[ONERA-RT-9/3549-M] N90-28672
Study of the radical OH in a high pressure flame by resonant DRASC
[ONERA-RF-57/7131-PY] N90-28692
Molten salt induced high temperature degradation of thermal barrier coatings N90-28704
Effect of protective coatings on mechanical properties of superalloys N90-28707
High temperature protective coatings: Recent trends N90-28710
Parametric solution of nonlinear structure problems
[ONERA-RT-21/3542-RY-082-R] N90-28874
Parallelization of a software relating to aerodynamics on MIMD type computers
[ONERA-RT-31/3479-CY] N90-29114
OFFICE OF SCIENCE AND TECHNOLOGY, WASHINGTON, DC.
Our changing planet: The FY 1991 US global change research program. A report by the committee on Earth Sciences to accompany the FY 1991 budget
[PB90-202623] N90-28907
OFFICE OF SOFTWARE DEVELOPMENT, FALLS CHURCH, VA.
Preparing software conversion studies
[PB90-235623] N90-29099

OHIO STATE UNIV., COLUMBUS.
High temperature surface interactions: Overview N90-28699
Target signature modeling and bistatic scattering measurement studies
[NASA-CR-186611] N90-28766
Motion coordination for mobile robots in unstructured environments
[PB90-199498] N90-28837
Investigation of maximum achievable body torque for a walking machine with friction cone constraints
[PB90-203175] N90-28838
Motion coordination for a mobile manipulator system
[PB90-203076] N90-28839
Dynamic modeling and payload-adaptation control of a flexible one-link manipulator N90-28843
Parallel algorithms for computation of the manipulator inertia matrix N90-29072
OKLAHOMA UNIV., NORMAN.
Phoenix data analysis and numerical simulation
[AD-A224226] N90-28772
OLD DOMINION UNIV., NORFOLK, VA.
Learned navigation in unknown terrains: A retraction method N90-29029
Documenting the decision structure in software development
[NASA-CR-186865] N90-29108
OREGON STATE UNIV., CORVALLIS.
Annual course of precipitation over much of the US: Observed versus GCM simulation
[PB90-221656] N90-28942
OXFORD UNIV. (ENGLAND).
Organising geometric computations for space telerobotics N90-29074

P

PACIFIC NORTHWEST LAB., RICHLAND, WA.
Density changes of generation 1.5 and 2.0 copper alloys irradiated at 411 to 414 C and 529 C in FFTF-MOTA
[DE90-015291] N90-28724
PARIS V UNIV. (FRANCE).
Loss of alertness and consciousness from pilot position during long range flight N90-28990
PATENT AND TRADEMARK OFFICE, WASHINGTON, DC.
Industrial patent activity in the US. Part 2: Alphabetical listing by company, 1969-1989
[PB90-214412] N90-29246
PENNSYLVANIA STATE UNIV., UNIVERSITY PARK.
Genesis of bow echoes: A rear-inflow induced meso-convective structure
[PB90-209776] N90-28926
PENNSYLVANIA UNIV., PHILADELPHIA.
How do robots take two parts apart N90-29061
PERKIN-ELMER CORP., POMONA, CA.
Atmosphere and water quality monitoring on Space Station Freedom
[NASA-CR-186707] N90-29084
PHYSICAL SCIENCES, INC., ALEXANDRIA, VA.
A laser spectrometer and wavemeter for pulsed lasers
[NASA-CR-181731] N90-28832
PHYSICS AND ELECTRONICS LAB. TNO, THE HAGUE (NETHERLANDS).
User's manual ROBIN: A research and notification system for bird migration
[FEL-1989-103] N90-28508
Design and realization of a two stage C-band low noise amplifier
[FEL-89-B265] N90-28783
Description of the MARC measuring system
[FEL-89-B170] N90-28887
Application of integrated optical components in optical fiber communication
[FEL-89-B252] N90-29183
PRATT AND WHITNEY AIRCRAFT, EAST HARTFORD, CT.
Energy Efficient Engine exhaust mixer model technology report addendum; phase 3 test program
[NASA-CR-174799] N90-28556
Energy Efficient Engine program advanced turbofan nacelle definition study
[NASA-CR-174942] N90-28560
Energy efficient engine program technology benefit/cost study. Volume 1: Executive summary
[NASA-CR-174766-VOL-1] N90-28564
Energy efficient engine program technology benefit/cost study, volume 2
[NASA-CR-174766-VOL-2] N90-28565
Energy Efficient Engine integrated core/low spool test hardware design report
[NASA-CR-168137] N90-28566
Energy efficient engine pin fin and ceramic composite segmented liner combustor sector rig test report
[NASA-CR-179534] N90-28567
Energy Efficient Engine: Combustor component performance program
[NASA-CR-179533] N90-28568
Energy Efficient Engine: Control system preliminary definition report
[NASA-CR-179578] N90-28569
Energy Efficient Engine: High-pressure compressor test hardware detailed design report
[NASA-CR-180850] N90-28570
Constitutive and life modeling of single crystal blade alloys for root attachment analysis N90-28843
PRATT AND WHITNEY AIRCRAFT, WEST PALM BEACH, FL.
Pratt and Whitney cryogenic turbopump bearing experience N90-28624
Tripropellant combustion process N90-28631
Injector element characterization methodology N90-28634
High/variable mixture ratio O2/H2 engine N90-28638
Probabilistic model for fracture mechanics service life analysis N90-28650
PRINCETON UNIV., NJ.
Ignition and combustion of liquid propellants
[AD-A224150] N90-28746
PURDUE UNIV., WEST LAFAYETTE, IN.
Dissipation of mechanical work and temperature rise in AS4/PEEK thermoplastic composite
[NASA-CR-186893] N90-28678
A constitutive model for AS4/PEEK thermoplastic composites under cyclic loading
[NASA-CR-180393] N90-28679
Radiative heat transfer
[PB90-247602] N90-28813
On-line object feature extraction for multispectral scene representation
[NASA-CR-187006] N90-28888
A method of classification for multisource data in remote sensing based on interval-valued probabilities
[NASA-CR-187007] N90-28889
Methods for multisource data analysis in remote sensing
[NASA-CR-187005] N90-28890
Efficient mapping algorithms for scheduling robot inverse dynamics computation on a multiprocessor system N90-29071

R

RAYTHEON CO., LEXINGTON, MA.
Mechanical property measurement of polycrystalline diamond films
[AD-A224037] N90-29222
READING UNIV. (ENGLAND).
A nonhydrostatic numerical model in sigma-coordinates and simulations of mesoscale phenomena N90-28932
RENSSELAER POLYTECHNIC INST., TROY, NY.
Inelastic analysis of laminated composites N90-28669
Microstructure and impurity effects on tungsten heavy alloys
[AD-A224220] N90-28728
An investigation of the steady and unsteady near wake and its effect on a laminar boundary layer N90-28794
Sound propagation through atmospheric turbulence: A literature summary
[RPI-MATH-184] N90-28930
Planning 3-D collision-free paths using spheres N90-29024
A Boltzmann machine for the organization of intelligent machines N90-29040
An improved method for choosing sampling points for the inspection of complex surfaces in a computer-aided manufacturing environment N90-29093
RICARDO CONSULTING ENGINEERS PLC, SHOREHAM-BY-SEA (ENGLAND).
Development of advanced combustion technology for medium and high speed natural gas engines
[PB90-198565] N90-28836
RICE UNIV., HOUSTON, TX.
Rice-obot 1: An intelligent autonomous mobile robot N90-29068
Studies of central interactions of Si ions at 14.5 x A GeV/c in Au and Cu
[DE90-015095] N90-29195
A plasma diagnostic study of two wind-blown shell nebulae: NGC 7635 and NGC 2359 N90-29271
ROBOTICS RESEARCH CORP., MILFORD, OH.
A 17 degree of freedom anthropomorphic manipulator N90-29001
Reflexive obstacle avoidance for kinematically-redundant manipulators N90-29047
ROCHESTER UNIV., NY.
Laboratory for Laser Energetics review
[DE90-014666] N90-28829
Time, space and form in vision
[AD-A213889] N90-28971
Introduction to gauge theories and unification
[DE90-014473] N90-29225
ROCKWELL INTERNATIONAL CORP., CANOGA PARK, CA.
The space transportation main engine phase A' study
[NASA-CR-179399] N90-28610
Blade tip rubbing stress prediction N90-28615
Pool boiling from rotating and stationary spheres in liquid nitrogen N90-28621
Rocketdyne LOX bearing tester program N90-28626
Oxygen/methane combustion stability investigation N90-28628
Heavy hydrocarbon main injector technology N90-28633
High variable mixture ratio oxygen/hydrogen engine N90-28640
Helium generation in fusion reactor materials
[DE90-013005] N90-29172
ROCKWELL INTERNATIONAL SCIENCE CENTER, THOUSAND OAKS, CA.
Determination of the SSME high pressure oxidizer turbopump bearing temperature N90-28619
ROYAL AEROSPACE ESTABLISHMENT, BEDFORD (ENGLAND).
The effects of foreplanes on the static and dynamic characteristics of a combat aircraft model N90-28520
The steady and time-dependent aerodynamic characteristics of a combat aircraft with a delta or swept canard N90-28526
ROYAL AEROSPACE ESTABLISHMENT, FARNBOROUGH (ENGLAND).
Spacecraft charging effects
[RAE-TM-SPACE-375] N90-28594
High temperature oxidation of Al-Li alloys N90-28705
Use of liquid crystals for qualitative and quantitative 2-D studies of transition and skin friction
[RAE-TM-AERO-2159] N90-28800
Measurements of the single event upset environment in the upper atmosphere
[RAE-TM-SPACE-373] N90-28934
Towards a future cockpit: The prototyping and pilot integration of the Mission Management Aid (MMA) N90-28979
The simulation of localized sounds for improved situational awareness N90-28984
Predictions of radiation backgrounds for GRO/OSSE
[RAE-TM-SPACE-372] N90-29293
ROYAL AIR FORCE INST. OF AVIATION MEDICINE, FARNBOROUGH (ENGLAND).
Situational Awareness Rating Technique (SART): The development of a tool for aircrew systems design N90-28975
Evaluation of the Situational Awareness Rating Technique (SART) as a tool for aircrew systems design N90-28977
ROYAL SIGNALS AND RADAR ESTABLISHMENT, MALVERN (ENGLAND).
Guide to charging for the CCF
[RSRE-89022] N90-29238
RUTGERS - THE STATE UNIV., NEW BRUNSWICK, NJ.
Strengthening and toughening mechanisms in ceramic fiber-reinforced glass matrix composites N90-28666
RUTGERS - THE STATE UNIV., PISCATAWAY, NJ.
Portable Dextrous Force Feedback Master for robot telemanipulation (PDMFF) N90-29058

S

SAINT JOHN'S RIVER WATER MANAGEMENT DISTRICT, PLATKA, FL.
Computer program for converting rectangular coordinates to latitude-longitude coordinates
[PB90-231796] N90-28883
SANDIA NATIONAL LABS., ALBUQUERQUE, NM.
Hypersonic Arbitrary-Body Aerodynamics (HABA) for conceptual design
[DE90-014750] N90-28495
Procedures for DOE-Navy exchange and approval of engineering information and material management required for production of W88-0/Mk5 RBA (reentry body assembly)
[DE90-014763] N90-28595
Reflection Mass Spectrometry (REMS) during 3/5 MBE
[DE90-014568] N90-28690
Tensile behavior of borated stainless steels, phase 1
[DE90-014368] N90-28717
Investigations into the use of dielectric coatings in magnetic switches
[DE90-014331] N90-28776
Ion divergence and the stability of magnetically insulated diodes
[DE90-014565] N90-28777

Zinc-bromine battery development
[DE90-014751] N90-28781
Use of electron spectroscopies in the tribological evaluation of diamond films
[DE90-014421] N90-28848
Evaluation of the STM4-120 kinematic Stirling engine
[DE90-013836] N90-28897
UV-induced degradation of the Si-SiO2 interface: Applications to the point contact solar cell
[DE90-013843] N90-28898
Development of the sodium/sulfur technology for energy storage
[DE90-014329] N90-28899
SuperCHIEF: A modified CHIEF (Combined Helmholz Integral Equation Formulation) method
[DE90-014744] N90-29123
The affect of gravity on particle collection in inertial impactors
[DE90-013372] N90-29173
Characterization of electron flow in positive-polarity linear-induction accelerators
[DE90-014998] N90-29177
PBFA 2 applied B ion diode beam characteristics at high voltages
[DE90-014419] N90-29190
Twisted crystals: Propagation, genesis, and relationships with optical activity and molecular symmetry (excerpts)
[DE90-014259] N90-29205
Radiation effects in InAsSb strained-layer superlattice photodiodes induced by dose-rate and transient x ray environments
[DE90-015000] N90-29208

SCHOOL OF AEROSPACE MEDICINE, BROOKS AFB, TX.
Decompression sickness presenting as a viral syndrome
[AD-A223880] N90-28967
The three-dimensional structure of visual attention and its implications for display design N90-28980
The effects of acoustic orientation cues on instrument flight performance in a flight simulator N90-28985

SCIENCE AND ENGINEERING ASSOCIATES, INC., ENGLEWOOD, CO.
Space station contamination modeling
[NASA-CR-183871] N90-28590

SCIENTIFIC CONSULTING SERVICES, PULLMAN, WA.
Study of meteorological processes important in the degradation of materials through surface temperature
[PB90-222720] N90-28856

SCRIPPS INSTITUTION OF OCEANOGRAPHY, SAN DIEGO, CA.
Large aperture acoustic arrays in support of reverberation studies
[AD-A224002] N90-29168

SHELADIA ASSOCIATES, INC., ROCKVILLE, MD.
Assessment of battery technologies for electric vehicles. Volume 2, part 2: Appendices
[DE90-014810] N90-28778

SOCIETE NATIONALE D'ETUDE ET DE CONSTRUCTION DE MOTEURS D'AVIATION, MOISSY-CRAMAYEL (FRANCE).
Numerical resolution of Navier-Stokes equations using several turbulence models and applications on turbomachines
[ETN-90-97478] N90-28808

SOCIETE NATIONALE DES POUDRES ET EXPLOSIFS, VERT-LE-PETIT (FRANCE).
Technical bibliography of high performance polyethylene fibers
[SNPE-NT-106/89/GTR/RP/NP] N90-28736

SOIL AND MATERIALS ENGINEERS, INC., ANN ARBOR, MI.
Development of a thickness design procedure for stabilized layers under rigid airfield pavements
[DOT/FAA/RD-90/22] N90-28582

SOLAREX CORP., NEWTOWN, PA.
Research on stable, large-area, amorphous silicon based submodules, phase 3
[DE90-000339] N90-29204

SOUTH FLORIDA WATER MANAGEMENT DISTRICT, WEST PALM BEACH.
Computer program for converting rectangular coordinates to latitude-longitude coordinates
[PB90-231796] N90-28883

SOUTHAMPTON UNIV. (ENGLAND).
Three-dimensional model testing in the transonic self-streamlining wind tunnel N90-28583
Analysis of vibrational power transmission through a beam system including a flexible section
[ISVR-TR-176] N90-28875
Estimation of individual coupling loss factors in a multi-subsystem
[ISVR-TR-184] N90-29141

SOUTHWEST FLORIDA WATER MANAGEMENT DISTRICT, TALLAHASSEE.
Computer program for converting rectangular coordinates to latitude-longitude coordinates
[PB90-231796] N90-28883

SOUTHWEST RESEARCH INST., SAN ANTONIO, TX.
A comparison of single-cycle versus multi-cycle proof testing strategies N90-28646
Micromechanisms of fatigue crack growth and fracture toughness in metal matrix composites
[AD-A223863] N90-28676

SPACE TELESCOPE SCIENCE INST., BALTIMORE, MD.
Learning in stochastic neural networks for constraint satisfaction problems N90-29078

SPECTRA RESEARCH SYSTEMS, INC., HUNTSVILLE, AL.
Evolution and use of combined mechanical and thermal codes for cryogenic turbopump bearings N90-28618

STANFORD LINEAR ACCELERATOR CENTER, CA.
RF power generation for future linear colliders
[DE90-014804] N90-29178
Effects and tolerances of injection jitter in the SLC and future linear colliders
[DE90-014805] N90-29179

STANFORD UNIV., CA.
Control of vortex aerodynamics at high angles of attack N90-28523
The aerodynamic design of the oblique flying wing supersonic transport
[NASA-CR-177552] N90-28540
Mechanical behavior of thick, curved, laminated composites N90-28664
The effects of grid-generated turbulence on flat and concave turbulent boundary layers N90-28797
Tunable CW single-frequency source for injection seeding 2-micrometer lasers
[AD-A223979] N90-28834
Experiments in the dynamic and strategic control of cooperating manipulators N90-28845
Least-index resolution of degeneracy in linear complementarity problems with sufficient matrices
[DE90-014406] N90-29145

STATE DEPT., WASHINGTON, DC.
Puerto Rico Workshop on Land-Based Sources of Marine Pollution in the Wider Caribbean Region
[PB90-184094] N90-28921

STATE UNIV. OF NEW YORK, BUFFALO.
Development of an integrated BEM for hot fluid-structure interaction N90-28617

STATE UNIV. OF NEW YORK, STONY BROOK.
Calculation of temperature distribution in various turbine blades using a boundary-fitted coordinate transformation method N90-28550
Consistency and convergence for numerical radiation conditions
[NASA-TM-103262] N90-29124
Infrared spectroscopic measurements on planetary atmospheric gases N90-29283

STUTTGART UNIV. (GERMANY, F.R.).
High power arcjet
[NASA-CR-183066] N90-28658

SURREY UNIV., GUILDFORD (ENGLAND).
A laser tracking dynamic robot metrology instrument N90-29021

SURREY UNIV., LONDON (ENGLAND).
Probability models for the failure of fibres and fibrous composite materials N90-28665

SVERDRUP TECHNOLOGY, INC., BROOK PARK, OH.
High energy-density liquid rocket fuel performance
[NASA-CR-185279] N90-28742

SYDNEY OBSERVATORY (AUSTRALIA).
Application of discrete Fourier series to the finite element stress analysis of axi-symmetric solids
[PB90-231010] N90-28870

SYDNEY UNIV. (AUSTRALIA).
Finite element analysis of coupled thermoelasticity
[PB90-201211] N90-28860

SYRACUSE RESEARCH CORP., NY.
State science and technology indicators: An exploratory profile and analysis
[PB90-246711] N90-29259

T

TECHNISCHE HOCHSCHULE, DARMSTADT (GERMANY, F.R.).
A stucture dependent software development on a relational basis: An integral approach
[ETN-90-97289] N90-29101
Fast interactive image generation of line and surface oriented objects in raster systems
[ETN-90-97290] N90-29102
Novel numerical analysis method for the study of convolution equations in appearance potential spectroscopy
[ETN-90-97288] N90-29210

TECHNISCHE UNIV., BRUNSWICK (GERMANY, F.R.).
Effects of canard position on the aerodynamic characteristics of a close-coupled canard configuration at low speed N90-28519

TECOGEN, INC., WALTHAM, MA.
Open cycle heat pump development for local resource use. Phase 2: District heating case study analysis
[DE90-011123] N90-28904

TELEDYNE BROWN ENGINEERING, HUNTSVILLE, AL.
Design of a monitor and simulation terminal (master) for space station telerobotics and telescience N90-29051

TELEOS RESEARCH, PALO ALTO, CA.
Integrating planning and reactive control N90-29077

TENNESSEE UNIV., KNOXVILLE.
Regulation of erythropoiesis in rats during space flight
[NASA-CR-177537] N90-29086
Fifteenth International Conference on X Ray and Inner-Shell Processes
[DE90-013024] N90-29170

TEXAS A&M UNIV., COLLEGE STATION.
Nonequilibrium radiation and chemistry models for aerocapture vehicle flowfields
[NASA-CR-186379] N90-28490
Active control of flexible structures N90-28575
A study of catalysts and mechanisms in synthesis reactions
[DE90-015084] N90-28691
Electrochemical incineration of wastes
[NASA-CR-187033] N90-28753
Tele-Autonomous control involving contact
[NASA-CR-187004] N90-28854
Lightweight solid polymer electrolyte fuel cell with stack power density of 3 kW/lb (7 kW/kg)
[AD-A223964] N90-28905
Planetary-scale flow on a two-layer beta-plane channel model with topography N90-28931

TEXAS INSTRUMENTS, INC., DALLAS.
Semiconductor measurement technology. EPROP: An interactive FORTRAN program for computing selected electronic properties of Gallium Arsenide and Silicon
[PB90-222738] N90-29203

TEXAS UNIV., AUSTIN.
Modularity in robotic systems N90-29014
Multiple cooperating manipulators: The case of kinematically redundant arms N90-29046
Satellite-map position estimation for the Mars rover N90-29069
Temperature-grzdient instability induced by conducting end walls
[DE90-014334] N90-29188
Nonlinear tearing mode: Rutherford regime and global characteristics
[DE90-015003] N90-29193
Resonant MHD modes with toroidal coupling
[DE90-015185] N90-29196
Vlasov-Maxwell equilibria of solar coronal loops
[DE90-015025] N90-29289

THIOKOL CORP., BRIGHAM CITY, UT.
Flight motor set 360L008 (STS-32R). Volume 1: System overview
[NASA-CR-184010] N90-28609

TORONTO UNIV. (ONTARIO).
A complete analytical solution for the inverse instantaneous kinematics of a spherical-revolute-spherical (7R) redundant manipulator N90-29006

TOTAL ARMY PERSONNEL AGENCY (PROVISIONAL), ALEXANDRIA, VA.
A design tool utilizing stoichiometric structure for the analysis of biochemical reaction networks
[AD-A223873] N90-28961

TRANSPORTATION RESEARCH BOARD, WASHINGTON, DC.
Modeling and analysis of airport and aircraft operations
[PB90-222167] N90-28511

TRANSPORTATION SYSTEMS CENTER, CAMBRIDGE, MA.
Airport capacity enhancement plan 1989
[PB90-197997] N90-28507

TUFTS UNIV., MEDFORD, MA.
High energy physics at Tufts University
[DE90-014664] N90-29174
On the infrared behaviour of some non-Minkowskian quantum fields N90-29273

TULANE UNIV., NEW ORLEANS, LA.
A hybrid architecture for the implementation of the Athena neural net model N90-29032

U

UNITED TECHNOLOGIES RESEARCH CENTER, EAST HARTFORD, CT.
Scale adherence effects in oxidation and sulfidation N90-28703
UNIVERSAL TECHNOLOGY CORP., DAYTON, OH.
STOVL fighter propulsion reliability, maintainability, and supportability characterization
[AD-A224221] N90-28574
UNIVERSIDAD NACIONAL DE CUYO, MENDOZA (ARGENTINA).
The stability of the martensitic phases in Cu-Zn-Al at an electron concentration of 1.534
[DE90-628628] N90-28727
UNIVERSITE DE TOULON ET DU VAR (FRANCE).
Detection of ocean inner waves by synthetic aperture radar: Observations at Gibraltar pass
[ETN-90-97477] N90-28953
UNIVERSITY OF SOUTHERN ILLINOIS, CARBONDALE.
Multi-layer neural networks for robot control N90-29031
UNIVERSITY OF TECHNOLOGY, LOUGHBOROUGH (ENGLAND).
Effective optimal control of a fighter aircraft engine N90-28548
UNIVERSITY OF WESTERN MICHIGAN, KALAMAZOO.
Correlated charge changing ion-atom collisions
[DE90-014662] N90-29171

V

VERSAR, INC., COLUMBIA, MD.
Preliminary exposure study to determine the effects of acid deposition on coated steel substrates
[PB90-201799] N90-28715
VIRGINIA POLYTECHNIC INST. AND STATE UNIV., BLACKSBURG.
System reliability optimization of aircraft wings N90-28536
Noncontact measurement of high temperature using optical fiber sensors
[NASA-CR-186975] N90-28825
Structural analysis and optimum design of geodesically stiffened composite panels
[NASA-CR-186944] N90-28862
Applied mathematics of transport theory
[DE90-014627] N90-29126

W

WASHINGTON STATE UNIV., PULLMAN.
An experimental investigation of a single and multiphase confined coaxial jet N90-28796
WESTINGHOUSE HANFORD CO., RICHLAND, WA.
Daily temperature, solar radiation, wind speed, cloud cover, and precipitation data recorded at the meteorological station for calendar years 1957--1988
[DE90-014399] N90-28941
WHEATON COLL., NORTON, MA.
The ionization structure of planetary nebulae 10: NGC 2392
[NASA-CR-186960] N90-29274
WICHITA STATE UNIV., KS.
International aircraft operator data base master requirements and implementation plan
[DOT/FAA/CT-90/17] N90-29247
WISCONSIN UNIV., MADISON.
Teleoperator comfort and psychometric stability: Criteria for limiting master-controller forces of operation and feedback during telemanipulation N90-29009
WOODS HOLE OCEANOGRAPHIC INST., MA.
Drilling the oceanic lower crust and mantle: A global strategy for exploring the deep oceanic crust and mantle in the 1990's
[PB90-240953] N90-28936
WRIGHT RESEARCH DEVELOPMENT CENTER, WRIGHT-PATTERSON AFB, OH.
Aerodynamic and propulsive control development of the STOL and maneuver technology demonstrator N90-28514
A look at tomorrow today N90-28524

X

XEROX PALO ALTO RESEARCH CENTER, CA.
Research on the structural and electronic properties of defects in amorphous silicon
[DE90-000342] N90-28730

Typical Contract Number Index Listing

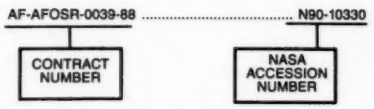

Listings in this index are arranged alphanumerically by contract number. Under each contract number the NASA accession numbers denoting documents that have been produced as a result of research done under that contract are arranged in ascending order. The NASA accession number denotes the number by which the citation is identified.

AF PROJ. 2306 ..... N90-29223
AF PROJ. 2313 ..... N90-28969
N90-28970
AF PROJ. 2864 ..... N90-28788
AF PROJ. 3066 ..... N90-28574
AF PROJ. 7231 ..... N90-28999
AF PROJ. 7930 ..... N90-28545
AF-AFOSR-0029-88 ..... N90-29048
AF-AFOSR-0093-90 ..... N90-29128
N90-29129
AF-AFOSR-0098-87 ..... N90-29223
AF-AFOSR-0117-88 ..... N90-28876
AF-AFOSR-0215-88 ..... N90-29117
AF-AFOSR-0333-88 ..... N90-28969
AF-AFOSR-0335-89 ..... N90-28970
ANE-2/87-STEP2 ..... N90-28811
ASL-89-8025 ..... N90-28927
N90-28939
A85/K/077 ..... N90-28995
A85/KLU/103 ..... N90-28508
A86/KLU/048 ..... N90-28994
A87/KL/154 ..... N90-28760
CNPQ-200.986-80 ..... N90-29075
C87-101249 ..... N90-28778
DA PROJ. 1L1-61102-AH-45 ..... N90-29121
DA PROJ. 1L1-62618-AH-80 ..... N90-28506
DA PROJ. 2Q2-63007-A-795 ..... N90-29112
DAAG29-84-K-0061 ..... N90-29061
DAAG29-85-K-0198 ..... N90-28772
DAAG60-90-M-1463 ..... N90-28930
DAAL03-86-K-0098 ..... N90-28746
DAAL03-87-K-0072 ..... N90-28728
DAAL03-88-K-0036 ..... N90-28924
DAAL03-89-C-0024 ..... N90-28828
DAAL03-89-K-0008 ..... N90-28835
DAAL03-89-K-0012 ..... N90-28746
DACA-76-88-C-0008 ..... N90-29022
DE-AC02-76CH-00016 ..... N90-28721
N90-28920
N90-28937
N90-28966
N90-29195
N90-29211
N90-29270
DE-AC02-76CH-03000 ..... N90-29176
DE-AC02-76ER-03274 ..... N90-29195
DE-AC02-76ER-13065 ..... N90-29225
DE-AC02-78ET-51013 ..... N90-29197
N90-29198
DE-AC02-83CH-10093 ..... N90-28730
N90-28896
N90-29204
N90-29258
DE-AC02-83ER-40085 ..... N90-29174
DE-AC02-83ER-40107 ..... N90-29195
DE-AC03-76SF-00098 ..... N90-28686
N90-28824
N90-29185
N90-29202
N90-29269
DE-AC03-76SF-00515 ..... N90-29178
N90-29179
DE-AC03-89ER-51114 ..... N90-29187
DE-AC04-76DP-00611 ..... N90-28763
DE-AC04-76DP-00613 ..... N90-28857
DE-AC04-76DP-00789 ..... N90-28495
N90-28595
N90-28690
N90-28717
N90-28776
N90-28777
N90-28781
N90-28848
N90-28897
N90-28898
N90-28899
N90-29123
N90-29173
N90-29177
N90-29190
N90-29205
N90-29206
DE-AC04-88DP-43495 ..... N90-28684
N90-28685
N90-28731
DE-AC05-84OR-21400 ..... N90-28662
N90-28663
N90-28718
N90-28720
N90-28734
N90-28743
N90-28793
N90-28826
N90-28849
N90-28850
N90-28851
N90-28861
N90-28882
N90-28917
N90-29095
N90-29115
N90-29119
N90-29120
N90-29130
N90-29170
N90-29191
N90-29192
N90-29224
N90-29250
N90-29285
DE-AC06-76RL-01830 ..... N90-28724
DE-AC06-87RL-10930 ..... N90-28941
DE-AC07-76ID-01570 ..... N90-28778
DE-AC08-88NV-10617 ..... N90-28774
DE-AC79-87BP-34906 ..... N90-28780
DE-AI01-85CE-50112 ..... N90-29260
DE-AI01-87CE-34011 ..... N90-28775
DE-AI01-88ER-30142 ..... N90-29181
DE-AL05-83ER-52092 ..... N90-28823
DE-AS05-81ER-40032 ..... N90-29195
DE-FC03-85DP-40200 ..... N90-28829
DE-FC22-83FE-60149 ..... N90-28695
DE-FG01-88CE-26561 ..... N90-28904
DE-FG01-89CE-15407 ..... N90-28750
DE-FG01-89CE-34025 ..... N90-28962
DE-FG02-84ER-53187 ..... N90-29189
DE-FG02-86ER-60485 ..... N90-28923
DE-FG02-87ER-13778 ..... N90-29171
DE-FG02-89ER-69027 ..... N90-28911
DE-FG03-87ER-25028 ..... N90-29145
DE-FG03-87ER-52146 ..... N90-29172
DE-FG05-80ET-53088 ..... N90-29186
N90-29193
N90-29196
N90-29289
DE-FG05-86ER-45280 ..... N90-29209
DE-FG05-87ER-25033 ..... N90-29126
DE-FG05-88ER-13829 ..... N90-28691
DE-FG07-88ID-12784 ..... N90-28684
DEN3-32 ..... N90-29260
DFG-HU-254/8 ..... N90-28519
DOT-HS-9-02193IA N90-28822
DRET-86-176 ..... N90-28809
DRET-86-199 ..... N90-28807
DRET-87-131 ..... N90-28810
DRET-87-1170 ..... N90-28946
DRET-87-1171 ..... N90-28953
DRET-88-34-001 ..... N90-28672
N90-28874
N90-29114
DRET-88-302-15 ..... N90-28736
DRET-88-1023 ..... N90-29167
DRET-88-1457 ..... N90-28808
DRET-89-34-001 ..... N90-28500
DRET-89-001-40 ..... N90-28692
DTFA01-81-Y-10555 ..... N90-28582
DTFA01-86-Y-01046 ..... N90-28581
DTFA03-89-C-00023 ..... N90-28509
DTFA03-89-C-00057 ..... N90-29247
EPA-DW-89932676-01-0 ..... N90-28922
EPA-R-814347-01 ..... N90-28715
EPA-68-C8-0006 ..... N90-28942
EPA-68-03-3513 ..... N90-29252
FAA-T0701U N90-28584
FAA-T1006B N90-28765
FMV-88260-88-203-73-001 ..... N90-28811
F04611-85-C-0100 ..... N90-28830
F19628-85-C-0139 ..... N90-28683
F19628-90-C-0003 ..... N90-29109
N90-29110
F30602-88-C-0001 ..... N90-29039
F33615-84-K-1520 ..... N90-29079
F33615-86-C-3623 ..... N90-28522
F33615-88-C-0638 ..... N90-28545
F33615-88-C-2823 ..... N90-28574
F44620-78-C-0083 ..... N90-28686
F49620-85-K-0018 ..... N90-29061
F49620-86-C-0045 ..... N90-29048
F49620-86-10-0020 ..... N90-28523
F49620-88-C-0132 ..... N90-29025
N90-29042
N90-29069
GR/D/5898-7 ..... N90-29035
GR/E/98058 ..... N90-29035
GRI-5084-243-0094 ..... N90-28836
GRI-5086-260-1293 ..... N90-28813
GRI-5087-260-1562 ..... N90-28798
HB-7-08056-1 ..... N90-28730
IR/D PROJ. D-46S N90-29070
JPL-958086 ..... N90-29064
MDA903-87-C-0523 ..... N90-29112
MDA972-88-J-1002 ..... N90-29202
MDA972-88-K-0003 ..... N90-28838
MIPR-FY1457-89-5004 ..... N90-28848
MRI PROJ. RA-111-C N90-28962
NAGW-925 ..... N90-28888
N90-28889
N90-28890
NAGW-1165 ..... N90-29033
NAGW-1175 ..... N90-29066
NAGW-1206 ..... N90-29284
NAGW-1333 ..... N90-29040
NAGW-1592 ..... N90-29117
NAGW-1736 ..... N90-28658
NAGW-1779 ..... N90-28753
NAG1-466 ..... N90-28876
NAG1-643 ..... N90-28862
NAG1-825 ..... N90-28878
N90-28879
NAG1-831 ..... N90-28825
NAG1-1003 ..... N90-28490
NAG1-1026 ..... N90-29108
NAG1-1145 ..... N90-29129
NAG2-414 ..... N90-28959
N90-28960
NAG2-541 ..... N90-28767
NAG2-542 ..... N90-28766
NAG2-544 ..... N90-29180
NAG3-251 ..... N90-28504
NAG3-503 ..... N90-28641
NAG3-506 ..... N90-28880
NAG3-856 ..... N90-28878
NAG3-1105 ..... N90-28858
NAG5-181 ..... N90-29276
NAG5-481 ..... N90-29275
NAG5-921 ..... N90-29261
NAG5-1024 ..... N90-28854

NAG5-1045	N90-29061
NAG5-1164	N90-29262
NAG5-1169	N90-28855
NAG5-1292	N90-29274
NAG5-1393	N90-29276
NAG8-072	N90-28747
NAG8-092	N90-28693
NAG8-102	N90-28694
NAG8-729	N90-29280
NAG9-208	N90-29068
NANB8H0690	N90-28799
NASA ORDER C-99066-G	N90-29124
NASA ORDER H-80598-B	N90-28590
NAS1-17077	N90-28494
NAS1-17498	N90-28865
	N90-28866
NAS1-18243	N90-28832
NAS1-18377	N90-28537
NAS1-18584	N90-29108
NAS1-18599	N90-28502
NAS1-18605	N90-28502
	N90-28789
	N90-28814
	N90-28816
	N90-28876
	N90-29125
	N90-29128
	N90-29129
NAS1-19000	N90-29189
NAS2-10547	N90-29085
NAS2-11586	N90-29086
NAS2-12425	N90-28510
NAS2-12451	N90-29142
	N90-29143
NAS2-12515	N90-29265
NAS2-13188	N90-28510
NAS3-20643	N90-28553
	N90-28554
	N90-28555
	N90-28557
	N90-28558
	N90-28559
	N90-28561
	N90-28562
	N90-28563
NAS3-20646	N90-28556
	N90-28560
	N90-28564
	N90-28565
	N90-28566
	N90-28567
	N90-28568
	N90-28569
	N90-28570
NAS3-23051	N90-28552
NAS3-23939	N90-28643
NAS3-24384	N90-28735
NAS3-24612	N90-28628
NAS3-25266	N90-28742
	N90-28768
NAS7-918	N90-28592
	N90-28593
	N90-29000
	N90-29044
NAS8-4000	N90-28619
	N90-28626
NAS8-30490	N90-28609
NAS8-33108	N90-28652
NAS8-36361	N90-28615
NAS8-36667	N90-28639
NAS8-36869	N90-28610
	N90-28640
NAS8-36901	N90-28650
NAS8-36944	N90-28635
NAS8-37136	N90-28599
	N90-28600
	N90-28601
	N90-28602
	N90-28603
	N90-28604
	N90-28605
	N90-28606
	N90-28607
NAS8-37283	N90-28614
	N90-29122
NAS8-37451	N90-28648
NAS8-37776	N90-28660
NAS8-40000	N90-28621
NAS8-50000	N90-28597
	N90-29084
NAS10-10285	N90-28925
NAS10-11624	N90-28925
NCA2-343	N90-28540
NCC2-371	N90-28680
NCC2-463	N90-29079
NCC2-494	N90-29077
NCC2-531	N90-29038
NCC3-135	N90-28827
NCGS-1-RO-1-23636-01	N90-29061
NIST-43NANB007123	N90-29251
NR PROJ. 039283	N90-28676
NS-10939-11	N90-29061
NSC79-0208-M008-23	N90-28725
NSF ASF-88-18215	N90-29278
NSF AST-87-19607	N90-29275
NSF AST-88-18215	N90-29275
	N90-29276
NSF AST-97-14405	N90-29262
NSF ATM-87-09659	N90-28926
NSF BCS-88-03920	N90-28869
NSF CDR-88-03017	N90-29071
NSF CES-88-03920	N90-28869
NSF DCR-82-19196	N90-29061
NSF DCR-83-20136	N90-28971
NSF DDM-84-21321	N90-28839
NSF DFR-84-19191	N90-28869
NSF DMC-84-21321	N90-28837
	N90-28838
NSF DMC-85-17315	N90-29061
NSF DMR-84-04489	N90-29221
NSF DMR-86-14003	N90-29221
NSF DMR-86-20311	N90-28699
NSF DMR-89-12927	N90-29221
NSF DMS-88-10150	N90-29128
	N90-29129
NSF DMS-89-05314	N90-29124
NSF DMS-89-13089	N90-29145
NSF ECS-80-0324	N90-28890
NSF ECS-86-17860	N90-29048
NSF EET-87-18434	N90-29072
NSF INT-85-14199	N90-29061
NSF IRI-86-12844	N90-29025
	N90-29042
	N90-29069
NSF IRI-87-01874	N90-29036
NSF ROA-86-15072	N90-29027
NSF SRS-87-13477	N90-29259
NSG-1414	N90-28591
NSG-5376	N90-29274
NWO-10-84-06	N90-29144
N00014-79-C-0681	N90-29079
N00014-81-K-0503	N90-29075
N00014-82-C-50767	N90-29079
N00014-84-C-0618	N90-28817
N00014-84-K-0655	N90-28971
N00014-85-C-0206	N90-28676
N00014-86-K-0158	N90-28682
N00014-87-C-0251	N90-29222
N00014-87-K-0030	N90-28699
N00014-88-K-0389	N90-28905
N00014-88-K-0482	N90-28697
N00014-88-K-0576	N90-28834
N00014-88-K-0632	N90-29061
N00014-89-F-0064	N90-28808
N00014-89-F-0082	N90-28689
N00014-89-J-1023	N90-29221
N00014-89-J-1530	N90-29234
N00014-89-J-1565	N90-29221
N00014-89-J-1659	N90-29145
N00014-89-J-1935	N90-29168
N00039-88-C-0051	N90-28956
ONR-SB-35923-0	N90-29061
ORNL ORDER 19X-SB154C	N90-28699
R87/KL/094	N90-29182
STEV-506266-489-06-22	N90-28501
STPA-86-91-021-00-471-75-86	N90-28722
STU-89/90	N90-28811
SU PROJ. 6359	N90-29077
W-31-109-ENG-38	N90-28808
	N90-28918
	N90-29127
W-7405-ENG-36	N90-28673
	N90-28745
	N90-28830
	N90-28885
	N90-29090
	N90-29096
	N90-29097
	N90-29116
	N90-29175
	N90-29184
	N90-29206
	N90-29207
	N90-29266
	N90-29267
	N90-29275
	N90-29276
	N90-29277
	N90-29278
	N90-29279
	N90-29288
W-7405-ENG-48	N90-28689
	N90-28719
	N90-28723
	N90-28738
	N90-28739
	N90-28752
	N90-28782
	N90-28785
	N90-28804
	N90-28805
	N90-28831
	N90-28919
	N90-28922
	N90-29081
	N90-29091
	N90-29105
	N90-29131
W-7405-ENG-82	N90-28687
ZB-7-06003-4	N90-28896
ZB-7-06003-02	N90-29204
106-30-01-40	N90-29086
106-30-02-40	N90-29085
188-41-53	N90-29265
199-04-16-11	N90-29290
199-21-12	N90-28965
316-60-13	N90-28596
324-02-00	N90-28832
505-60-00	N90-28540
505-60-01-02	N90-28493
505-61-41	N90-28820
505-61-51	N90-28510
505-62-0K	N90-29121
505-62-21	N90-28504
	N90-29124
505-63-1A	N90-28735
	N90-28740
505-63-01-05	N90-28871
	N90-28872
505-63-01-08	N90-28859
505-63-01-10	N90-28877
505-63-31	N90-28815
505-63-51-01	N90-28865
	N90-28866
505-63-51-09	N90-29166
505-66-41	N90-28546
505-66-51	N90-28512
505-66-91-02	N90-28751
505-68-27	N90-29142
505-68-71	N90-28505
	N90-28542
	N90-28578
505-68-71-03	N90-28494
505-69-01	N90-28996
505-90-01	N90-28858
505-90-21-01	N90-28502
	N90-28789
	N90-28814
	N90-28816
	N90-28876
	N90-29125
	N90-29128
	N90-29129
506-40-21-01	N90-28806
506-41-11	N90-28696
506-41-61	N90-29083
506-42-31	N90-28657
506-42-51	N90-28742
506-43-41-02	N90-28598
506-44-2C	N90-28786
506-44-26	N90-29219
506-63-31	N90-28878
533-02-01	N90-28551
535-03-01	N90-28552
535-03-11-03	N90-29189
537-01-37-01	N90-28537
537-02-11	N90-28792
582-01-11	N90-28659
586-01-11	N90-28670
650-60-23	N90-28768
694-03-03	N90-28754
783-01-41-17	N90-28541
889-62-20-10-02	N90-28592
906-65-05-01	N90-28589
992-21-01	N90-28503

Typical Report Number Index Listing

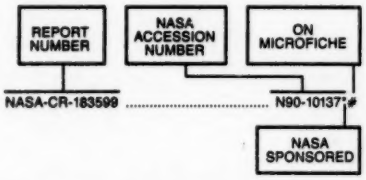

Listings in this index are arranged alphanumerically by report number. The NASA accession number denotes the number by which the citation is identified. An asterisk (*) indicates that the item is a NASA report. A pound sign (#) indicates that the item is available on microfiche.

A-85177 ..... N90-28965* #
A-89093 ..... N90-28503* #
A-90068 ..... N90-28996* #
A-90095 ..... N90-29085* #
A-90108 ..... N90-28512* #
A-90168 ..... N90-28540* #
A-90245 ..... N90-29083* #
A-90264 ..... N90-28510* #

AAMRL-TR-89-046 ..... N90-28999 #

ACCN-79353 ..... N90-29094 #

AD-A213889 ..... N90-28971 #
AD-A217906 ..... N90-28544 #
AD-A218049 ..... N90-28999 #
AD-A221690 ..... N90-28683 #
AD-A221995 ..... N90-28682 #
AD-A222181 ..... N90-28823 #
AD-A222696 ..... N90-28545 #
AD-A223024 ..... N90-29080 #
AD-A223863 ..... N90-28676 #
AD-A223864 ..... N90-28817 #
AD-A223866 ..... N90-28661 #
AD-A223867 ..... N90-28956 #
AD-A223868 ..... N90-28997 #
AD-A223869 ..... N90-28571 #
AD-A223872 ..... N90-29109 #
AD-A223873 ..... N90-28961 #
AD-A223875 ..... N90-28892 #
AD-A223877 ..... N90-29220 #
AD-A223880 ..... N90-28967 #
AD-A223882 ..... N90-28572 #
AD-A223883 ..... N90-28957 #
AD-A223890 ..... N90-28697 #
AD-A223892 ..... N90-28968 #
AD-A223894 ..... N90-28818 #
AD-A223897 ..... N90-29110 #
AD-A223899 ..... N90-28543 #
AD-A223964 ..... N90-28905 #
AD-A223965 ..... N90-29221 #
AD-A223969 ..... N90-28893 #
AD-A223970 ..... N90-28586 #
AD-A223973 ..... N90-28677 #
AD-A223976 ..... N90-29087 #
AD-A223979 ..... N90-28834 #
AD-A223980 ..... N90-28769 #
AD-A223982 ..... N90-28998 #
AD-A223983 ..... N90-28770 #
AD-A224002 ..... N90-29168 #
AD-A224008 ..... N90-28579 #
AD-A224011 ..... N90-29111 #
AD-A224024 ..... N90-29234 #
AD-A224028 ..... N90-29254 #
AD-A224037 ..... N90-29222 #
AD-A224038 ..... N90-29112 #
AD-A224042 ..... N90-29088 #
AD-A224046 ..... N90-28894 #
AD-A224063 ..... N90-29240 #
AD-A224119 ..... N90-29256 #
AD-A224120 ..... N90-28835 #
AD-A224122 ..... N90-28787 #
AD-A224125 ..... N90-28924 #
AD-A224127 ..... N90-28969 #
AD-A224128 ..... N90-29223 #
AD-A224139 ..... N90-28819 #
AD-A224140 ..... N90-29186 #
AD-A224144 ..... N90-28771 #
AD-A224145 ..... N90-28573 #
AD-A224147 ..... N90-28970 #
AD-A224150 ..... N90-28746 #
AD-A224151 ..... N90-28828 #
AD-A224178 ..... N90-29113 #
AD-A224193 ..... N90-28741 #
AD-A224201 ..... N90-28788 #
AD-A224217 ..... N90-28506 #
AD-A224220 ..... N90-28726 #
AD-A224221 ..... N90-28574 #
AD-A224226 ..... N90-28772 #
AD-A224245 ..... N90-29089 #
AD-A224278 ..... N90-28729 #
AD-A224473 ..... N90-29241 #
AD-A224474 ..... N90-29255 #

AD-E501218 ..... N90-28882 #
AD-E501248 ..... N90-29234 #
AD-E951507 ..... N90-28729 #

AD-F000153 ..... N90-28894 #
AD-F000153 ..... N90-29088 #

AECL-9560 ..... N90-28674 #

AFHRL-TR-90-3 ..... N90-28997 #

AFIT/CI/CIA-89-027 ..... N90-28544 #
AFIT/CI/CIA-90-040 ..... N90-29241 #
AFIT/CI/CIA-90-041 ..... N90-29255 #

AFOEHL-90-064EQ00094DEF ..... N90-28571 #

AFOSR-90-0749TR ..... N90-28969 #
AFOSR-90-0751TR ..... N90-29223 #
AFOSR-90-0754TR ..... N90-28970 #

AGARD-CP-461 ..... N90-28698 #
AGARD-CP-465 ..... N90-28513 #
AGARD-CP-478 ..... N90-28972 #

AIAA-90-1968 ..... N90-28742* #
AIAA-90-2450 ..... N90-28792* #
AIAA-90-2578 ..... N90-28657* #

AL-TR-90-006 ..... N90-28788 #

ALS/TR-89-035 ..... N90-29205 #

AMSMI/CR-RD-RE-90-1 ..... N90-28729 #

ANL/EAIS/TM-17 ..... N90-28918 #

ANL/MCS-TM-138 ..... N90-29127 #

APL/PSU-TR-90-008 ..... N90-28956 #

AR-005-579 ..... N90-28821 #
AR-005-600 ..... N90-28576 #
AR-006-055 ..... N90-28547 #

ARE-TM(UDT)-89111 ..... N90-29094 #

ARI-TR-888 ..... N90-29112 #

ARL-FLIGHT-MECH-R-180 ..... N90-28576 #

ARL-FLIGHT-MECH-TM-2 ..... N90-28821 #

ARL-PROP-R-182 ..... N90-28547 #

ARO-WRKSP-RP8901 ..... N90-28741 #

ARO-22880.1-GS ..... N90-28772 #
ARO-23610.5-EG ..... N90-28746 #
ARO-24667.16-MS ..... N90-28726 #
ARO-25882.3-GS ..... N90-28924 #
ARO-26308.1-EG ..... N90-28746 #
ARO-26434.3-EL ..... N90-28835 #
ARO-27323.1-SBI ..... N90-28828 #

ASI890-324-89 ..... N90-29112 #

AVSCOM-TR-89-A-002 ..... N90-28503* #
AVSCOM-TR-90-C-018 ..... N90-29121* #

BIO-2 ..... N90-28925* #
BIO-4595 ..... N90-28966 #

BNL-43723 ..... N90-29211 #
BNL-44770 ..... N90-28937 #
BNL-44774 ..... N90-29195 #
BNL-44821 ..... N90-28920 #
BNL-44830 ..... N90-28721 #
BNL-44839 ..... N90-28966 #
BNL-52246 ..... N90-29270 #

BRL-MR-3843 ..... N90-28506 #

BR112416 ..... N90-28800 #
BR112728 ..... N90-29293
BR112976 ..... N90-29094 #
BR113096 ..... N90-29238 #
BR113427 ..... N90-28934 #
BR113453 ..... N90-28594 #

CAL-1830 ..... N90-29260* #

CBP/TRS-41/90 ..... N90-28954 #

CBPF-NF-025/89 ..... N90-29282 #
CBPF-NF-028/89 ..... N90-29218 #
CBPF-NF-030/89 ..... N90-29149 #
CBPF-NF-037/89 ..... N90-29150 #
CBPF-NF-038/89 ..... N90-29165 #
CBPF-NF-039/89 ..... N90-29212 #
CBPF-NF-040/89 ..... N90-29213 #
CBPF-NF-041/89 ..... N90-29214 #
CBPF-NF-046/89 ..... N90-28726 #
CBPF-NF-048/89 ..... N90-29152 #
CBPF-NF-050/89 ..... N90-29151 #
CBPF-NF-051/89 ..... N90-29215 #

CCMS-90-05 ..... N90-28862* #

CERL-TR-N-90/09 ..... N90-28769 #

CESAR-89/38 ..... N90-28850 #
CESAR-90/30 ..... N90-29119 #

CML-90-2 ..... N90-28678* #
CML-90-3 ..... N90-28679* #

CNEA-CAB-89/22 ..... N90-28727 #

CNES-NT-124 ..... N90-28761 #
CNES-NT-125 ..... N90-28947 #

CONF-891113-12 ..... N90-28721 #
CONF-900160-4 ..... N90-28673 #
CONF-900396-4 ..... N90-29208 #
CONF-900513-2 ..... N90-28862 #
CONF-900602-17 ..... N90-29189 #
CONF-900602-20 ..... N90-29187 #
CONF-900603-28 ..... N90-29176 #
CONF-900603-29 ..... N90-29179 #
CONF-900617-17 ..... N90-28717 #
CONF-900658-1 ..... N90-29225 #
CONF-900704-11 ..... N90-28688 #
CONF-900731-1 ..... N90-28861 #
CONF-900751-1 ..... N90-29207 #
CONF-900751-2 ..... N90-29206 #
CONF-900756-15 ..... N90-29184 #
CONF-900756-17 ..... N90-28785 #
CONF-900756-18 ..... N90-28739 #
CONF-900756-19 ..... N90-29185 #
CONF-900757-VOL-1-ABSTS ..... N90-29170 #
CONF-900801-23 ..... N90-28897 #
CONF-900822-6 ..... N90-29195 #

CONF-8906244 ..... N90-28915 #
CONF-8910354-2 ..... N90-28966 #
CONF-8910434-1 ..... N90-28917 #
CONF-8911136-VUGRAPHS ..... N90-29120 #
CONF-8911192-5 ..... N90-28736 #
CONF-9002131-1 ..... N90-28804 #
CONF-9002135-1 ..... N90-28723 #
CONF-9004209-4 ..... N90-29175 #
CONF-9004232-2 ..... N90-28830 #
CONF-9004234-1 ..... N90-28689 #
CONF-9005149-6 ..... N90-28882 #
CONF-9005175-2 ..... N90-28763 #
CONF-9005233-2 ..... N90-29269 #
CONF-9005235-3 ..... N90-29211 #
CONF-9005248-1 ..... N90-29276* #
CONF-9005248-3 ..... N90-29275* #
CONF-9005249-1 ..... N90-29267 #
CONF-9005249-1 ..... N90-29288 #
CONF-9005249-2 ..... N90-29278 #
CONF-9005249-3 ..... N90-29266 #
CONF-9005249-4 ..... N90-29277 #
CONF-9005249-5 ..... N90-29279 #
CONF-9005252-1 ..... N90-28919 #
CONF-9005253-1 ..... N90-28831 #
CONF-9006105-9 ..... N90-28608 #
CONF-9006121-7 ..... N90-28731 #
CONF-9006176-10 ..... N90-28776 #
CONF-9006176-11 ..... N90-28782 #
CONF-9006195-4 ..... N90-29116 #
CONF-9006195-6 ..... N90-29131 #
CONF-9006241-1 ..... N90-28685 #
CONF-9006241-3 ..... N90-28684 #
CONF-9006243-1 ..... N90-28899 #
CONF-9006246-1 ..... N90-28690 #
CONF-9006248-1 ..... N90-29224 #
CONF-9006249-1 ..... N90-28920 #
CONF-9007106-43 ..... N90-29097 #
CONF-9007111-10 ..... N90-28777 #
CONF-9007111-13 ..... N90-29178 #
CONF-9007117-3 ..... N90-29096 #
CONF-9007125-1 ..... N90-28774 #
CONF-9007131-1 ..... N90-28718 #
CONF-9007134-1 ..... N90-29119 #
CONF-9008124-1 ..... N90-28896 #
CONF-9008127-1 ..... N90-28848 #
CONF-9009136-2 ..... N90-29173 #
CONF-9009147-1 ..... N90-28663 #
CONF-9009192-4 ..... N90-29190 #
CONF-9009192-5 ..... N90-29177 #
CONF-9009209-1 ..... N90-28824 #
CONF-9009223-1 ..... N90-28745 #

CRIE-T-89015 ..... N90-28779 #

CRIE-W-89012 ..... N90-28900 #
CRIE-W-89016 ..... N90-28901 #

CRREL-SR-90-15 ..... N90-28893 #

CRREL-90-5 ..... N90-28892 #

DE90-000338 ..... N90-28896 #
DE90-000339 ..... N90-29204 #
DE90-000342 ..... N90-28730 #
DE90-000346 ..... N90-29258 #
DE90-011123 ..... N90-28904 #
DE90-011528 ..... N90-28793 #
DE90-013005 ..... N90-29172 #
DE90-013024 ..... N90-29170 #
DE90-013025 ..... N90-28882 #
DE90-013372 ..... N90-29173 #
DE90-013673 ..... N90-28608 #
DE90-013836 ..... N90-28897 #
DE90-013843 ..... N90-28898 #
DE90-013845 ..... N90-28824 #
DE90-014097 ..... N90-29189 #
DE90-014116 ..... N90-28684 #
DE90-014117 ..... N90-28731 #
DE90-014118 ..... N90-28685 #
DE90-014120 ..... N90-29187 #
DE90-014151 ..... N90-28780 #
DE90-014184 ..... N90-29202 #
DE90-014185 ..... N90-29269 #
DE90-014189 ..... N90-28686 #
DE90-014191 ..... N90-28774 #
DE90-014221 ..... N90-28775 #
DE90-014224 ..... N90-28662 #
DE90-014259 ..... N90-29205 #
DE90-014299 ..... N90-28734 #
DE90-014300 ..... N90-29265 #
DE90-014329 ..... N90-28899 #
DE90-014331 ..... N90-28776 #
DE90-014334 ..... N90-29188 #
DE90-014368 ..... N90-28717 #
DE90-014377 ..... N90-28962 #
DE90-014380 ..... N90-28911 #
DE90-014390 ..... N90-28689 #
DE90-014399 ..... N90-28941 #
DE90-014406 ..... N90-29145 #
DE90-014417 ..... N90-29090 #
DE90-014419 ..... N90-29190 #
DE90-014421 ..... N90-28848 #
DE90-014428 ..... N90-28687 #
DE90-014438 ..... N90-28884 #
DE90-014442 ..... N90-29181 #
DE90-014448 ..... N90-28663 #
DE90-014452 ..... N90-29224 #
DE90-014453 ..... N90-28718 #
DE90-014455 ..... N90-28917 #
DE90-014456 ..... N90-28861 #
DE90-014458 ..... N90-29119 #
DE90-014473 ..... N90-29225 #
DE90-014474 ..... N90-28750 #
DE90-014565 ..... N90-28777 #
DE90-014568 ..... N90-28690 #
DE90-014610 ..... N90-28778 #
DE90-014620 ..... N90-28804 #
DE90-014627 ..... N90-29126 #
DE90-014662 ..... N90-29171 #
DE90-014664 ..... N90-29174 #
DE90-014665 ..... N90-28805 #
DE90-014686 ..... N90-28829 #
DE90-014718 ..... N90-28685 #
DE90-014720 ..... N90-29091 #
DE90-014724 ..... N90-29081 #
DE90-014732 ..... N90-28719 #
DE90-014741 ..... N90-28743 #
DE90-014744 ..... N90-29123 #
DE90-014750 ..... N90-28495 #
DE90-014751 ..... N90-28781 #
DE90-014752 ..... N90-29270 #
DE90-014755 ..... N90-28857 #
DE90-014756 ..... N90-28918 #
DE90-014759 ..... N90-28849 #
DE90-014763 ..... N90-28595 #
DE90-014765 ..... N90-28720 #
DE90-014772 ..... N90-29095 #
DE90-014774 ..... N90-29115 #
DE90-014776 ..... N90-28826 #
DE90-014780 ..... N90-28850 #
DE90-014782 ..... N90-28851 #
DE90-014785 ..... N90-29250 #
DE90-014789 ..... N90-29191 #
DE90-014791 ..... N90-29192 #
DE90-014792 ..... N90-29130 #
DE90-014794 ..... N90-29120 #
DE90-014798 ..... N90-28752 #
DE90-014804 ..... N90-29178 #
DE90-014805 ..... N90-29179 #
DE90-014905 ..... N90-28673 #
DE90-014906 ..... N90-28745 #
DE90-014912 ..... N90-29275* #
DE90-014917 ..... N90-29276* #
DE90-014918 ..... N90-29288 #
DE90-014919 ..... N90-29266 #
DE90-014920 ..... N90-29277 #
DE90-014921 ..... N90-29267 #
DE90-014922 ..... N90-29278 #
DE90-014923 ..... N90-29279 #
DE90-014924 ..... N90-29206 #
DE90-014925 ..... N90-29207 #
DE90-014926 ..... N90-29096 #
DE90-014930 ..... N90-29097 #
DE90-014932 ..... N90-29127 #
DE90-014981 ..... N90-29175 #
DE90-014986 ..... N90-29176 #
DE90-014997 ..... N90-28763 #
DE90-014998 ..... N90-29177 #
DE90-015000 ..... N90-29208 #
DE90-015003 ..... N90-29193 #
DE90-015025 ..... N90-29289 #
DE90-015027 ..... N90-29184 #
DE90-015032 ..... N90-28830 #
DE90-015036 ..... N90-29116 #
DE90-015037 ..... N90-28785 #
DE90-015041 ..... N90-28919 #
DE90-015042 ..... N90-28738 #
DE90-015044 ..... N90-28831 #
DE90-015064 ..... N90-28691 #
DE90-015066 ..... N90-29209 #
DE90-015085 ..... N90-28920 #
DE90-015086 ..... N90-28721 #
DE90-015090 ..... N90-29211 #
DE90-015095 ..... N90-29195 #
DE90-015121 ..... N90-28782 #
DE90-015126 ..... N90-28966 #
DE90-015135 ..... N90-28937 #
DE90-015148 ..... N90-29131 #
DE90-015150 ..... N90-28739 #
DE90-015185 ..... N90-29196 #
DE90-015193 ..... N90-28723 #
DE90-015291 ..... N90-28724 #
DE90-015360 ..... N90-29105 #
DE90-015385 ..... N90-29197 #
DE90-015386 ..... N90-29198 #
DE90-015393 ..... N90-28695 #
DE90-015401 ..... N90-28922 #
DE90-015528 ..... N90-28923 #
DE90-015636 ..... N90-29185 #
DE90-507841 ..... N90-28900 #
DE90-507869 ..... N90-28779 #
DE90-507881 ..... N90-28901 #
DE90-627149 ..... N90-29226 #
DE90-627153 ..... N90-29132 #
DE90-627154 ..... N90-29146 #
DE90-627155 ..... N90-29133 #
DE90-627156 ..... N90-29134 #
DE90-627157 ..... N90-29135 #
DE90-627158 ..... N90-29106 #
DE90-627161 ..... N90-29136 #
DE90-627163 ..... N90-29147 #
DE90-627164 ..... N90-29148 #
DE90-627165 ..... N90-29137 #
DE90-627166 ..... N90-29138 #
DE90-627170 ..... N90-29139 #
DE90-627175 ..... N90-29149 #
DE90-627176 ..... N90-29150 #
DE90-627177 ..... N90-29151 #
DE90-627179 ..... N90-29227 #
DE90-627180 ..... N90-29228 #
DE90-627181 ..... N90-29229 #
DE90-627194 ..... N90-29152 #
DE90-627195 ..... N90-29230 #
DE90-627196 ..... N90-28764 #
DE90-627197 ..... N90-29164 #
DE90-627208 ..... N90-29231 #
DE90-627210 ..... N90-29140 #
DE90-627211 ..... N90-29153 #
DE90-627212 ..... N90-29154 #
DE90-627213 ..... N90-29155 #
DE90-627215 ..... N90-29156 #
DE90-627216 ..... N90-29157 #
DE90-627222 ..... N90-29232 #
DE90-627320 ..... N90-29165 #
DE90-627321 ..... N90-29212 #
DE90-627322 ..... N90-29213 #
DE90-627323 ..... N90-29214 #
DE90-627324 ..... N90-29215 #
DE90-627464 ..... N90-29233 #
DE90-627473 ..... N90-29199 #
DE90-627485 ..... N90-29281 #
DE90-627487 ..... N90-29282 #
DE90-627491 ..... N90-29216 #
DE90-627493 ..... N90-29217 #
DE90-627792 ..... N90-28725 #
DE90-627843 ..... N90-28726 #
DE90-627871 ..... N90-29218 #
DE90-627922 ..... N90-28950 #
DE90-628626 ..... N90-28727 #
DE90-629740 ..... N90-28674 #
DE90-796158 ..... N90-28895 #

DFVLR-FB-84-14 ..... N90-28801 #
DFVLR-FB-85-67 ..... N90-28733 #
DFVLR-FB-86-10 ..... N90-28802 #
DFVLR-FB-86-24 ..... N90-28803 #
DFVLR-FB-86-34 ..... N90-29118 #
DFVLR-FB-87-06 ..... N90-28498 #
DFVLR-FB-87-24 ..... N90-28499 #

DFVLR-MITT-87-11 ..... N90-29159 #
DFVLR-MITT-88-02 ..... N90-28585 #

DLR-FB-90-04 ..... N90-28812 #
DLR-FB-90-06 ..... N90-28853 #

DLR-MITT-90-03 ..... N90-28903 #

DOD-7920.2-M ..... N90-29244 #

DOE/BP-34906/1 ..... N90-28780 #

DOE/CE-15407/T5 ..... N90-28750 #
DOE/CE-26561/1 ..... N90-28904 #
DOE/CE-34025/T4 ..... N90-28962 #

DOE/DP-40200/124 ..... N90-28829 #

DOE/ER-13065/630 ..... N90-29225 #
DOE/ER-13778/3 ..... N90-29171 #
DOE/ER-13829/3 ..... N90-28691 #
DOE/ER-25033/3 ..... N90-29126 #
DOE/ER-30142/T1 ..... N90-29181 #
DOE/ER-40085/21 ..... N90-29174 #
DOE/ER-45280/4 ..... N90-29209 #
DOE/ER-52146/T1 ..... N90-29172 #
DOE/ER-53088/438 ..... N90-29193 #
DOE/ER-53267/77 ..... N90-29193 #

DOE/ER-60485/3 ..... N90-28923 #
DOE/ER-69027/T1 ..... N90-28911 #

DOE/ET-51013/284 ..... N90-29196 #
DOE/ET-51013/286 ..... N90-29197 #
DOE/ET-53068/431 ..... N90-29188 #
DOE/ET-53068/439 ..... N90-29196 #
DOE/ET-53068/440 ..... N90-29289 #

DOE/ID-10243/2-VOL-2-APP-PT-2 ..... N90-28778 #
DOE/ID-12784/1 ..... N90-28884 #

DOE/NASA/0032-31 ..... N90-29260* #

DOT-TSC-FAA-89-1 ..... N90-28507 #

DOT/FAA/CP-89-4 ..... N90-28507 #

DOT/FAA/CT-TN89/35 ..... N90-28782 #
DOT/FAA/CT-TN89/43 ..... N90-28584 #
DOT/FAA/CT-TN89/53 ..... N90-29249 #
DOT/FAA/CT-TN90/17 ..... N90-28765 #
DOT/FAA/CT-TN90/18 ..... N90-28549 #

DOT/FAA/CT-90/2 ..... N90-28509 #
DOT/FAA/CT-90/17 ..... N90-29247 #

DOT/FAA/RD-90/15 ..... N90-28581 #
DOT/FAA/RD-90/22 ..... N90-28582 #

DREO-1030 ..... N90-29220 #

DRES-SM-1321 ..... N90-28579 #

DTRC/PAS-90/15 ..... N90-28572 #

E-4137 ..... N90-28552* #
E-4924 ..... N90-28791* #
E-5287 ..... N90-28754* #
E-5436 ..... N90-28633* #
E-5478 ..... N90-28768* #
E-5515 ..... N90-28786* #
E-5590 ..... N90-28792* #
E-5593 ..... N90-28740* #
E-5640 ..... N90-28670* #
E-5667 ..... N90-28742* #
E-5687 ..... N90-28596* #
E-5695 ..... N90-29124* #
E-5734 ..... N90-28657* #
E-5751 ..... N90-29219* #
E-5752 ..... N90-28696* #
E-5756 ..... N90-28659* #
E-5761 ..... N90-29121* #

EGG-10617-1088 ..... N90-28774 #

EPA/DF/DK-90/038A ..... N90-28847 #

EPA/450/4-90/001 ..... N90-28908 #
EPA/450/4-90/002 ..... N90-28909 #
EPA/600/D-90/016 ..... N90-28916 #
EPA/600/D-90/019 ..... N90-28942 #
EPA/600/3-89/083 ..... N90-29252 #
EPA/600/3-90/032 ..... N90-28715 #

ESA-TT-890 ..... N90-28801 #
ESA-TT-992 ..... N90-28733 #
ESA-TT-1008 ..... N90-28802 #
ESA-TT-1026 ..... N90-28803 #
ESA-TT-1042 ..... N90-29118 #
ESA-TT-1079 ..... N90-28498 #
ESA-TT-1092 ..... N90-28499 #
ESA-TT-1101 ..... N90-29159 #
ESA-TT-1125 ..... N90-28585 #

ETCA-89-R-150 ..... N90-28873 #

ETN-90-96922 ..... N90-29144 #
ETN-90-97061 ..... N90-29238 #
ETN-90-97063 ..... N90-28800 #
ETN-90-97070 ..... N90-29094 #
ETN-90-97100 ..... N90-28744 #
ETN-90-97101 ..... N90-28671 #
ETN-90-97288 ..... N90-29210 #
ETN-90-97289 ..... N90-29101 #
ETN-90-97290 ..... N90-29102 #
ETN-90-97386 ..... N90-28994
ETN-90-97388 ..... N90-28995
ETN-90-97393 ..... N90-28760
ETN-90-97396 ..... N90-29182
ETN-90-97397 ..... N90-29082
ETN-90-97403 ..... N90-28508
ETN-90-97406 ..... N90-28887
ETN-90-97409 ..... N90-29183
ETN-90-97410 ..... N90-28783
ETN-90-97422 ..... N90-29293

ETN-90-97425 ..... N90-29287
ETN-90-97429 ..... N90-28902
ETN-90-97456 ..... N90-28736 #
ETN-90-97470 ..... N90-28873 #
ETN-90-97476 ..... N90-28807 #
ETN-90-97477 ..... N90-28953 #
ETN-90-97478 ..... N90-28808 #
ETN-90-97484 ..... N90-28722 #
ETN-90-97485 ..... N90-28809 #
ETN-90-97486 ..... N90-28810 #
ETN-90-97487 ..... N90-29167 #
ETN-90-97488 ..... N90-28946 #
ETN-90-97489 ..... N90-28672 #
ETN-90-97498 ..... N90-29114 #
ETN-90-97500 ..... N90-28692 #
ETN-90-97501 ..... N90-28874 #
ETN-90-97502 ..... N90-28500 #
ETN-90-97505 ..... N90-28761 #
ETN-90-97506 ..... N90-28947 #
ETN-90-97507 ..... N90-28964 #
ETN-90-97510 ..... N90-28538 #
ETN-90-97511 ..... N90-28539 #
ETN-90-97512 ..... N90-28501 #
ETN-90-97514 ..... N90-28811 #
ETN-90-97515 ..... N90-28875 #
ETN-90-97516 ..... N90-29141 #
ETN-90-97526 ..... N90-28934 #
ETN-90-97529 ..... N90-28594 #
ETN-90-97538 ..... N90-28903 #
ETN-90-97543 ..... N90-28812 #
ETN-90-97544 ..... N90-28853 #
ETN-90-97547 ..... N90-28801 #
ETN-90-97548 ..... N90-28733 #
ETN-90-97549 ..... N90-28802 #
ETN-90-97550 ..... N90-28803 #
ETN-90-97551 ..... N90-29118 #
ETN-90-97552 ..... N90-28498 #
ETN-90-97553 ..... N90-28499 #
ETN-90-97554 ..... N90-29159 #
ETN-90-97555 ..... N90-28585 #

E19-666-1 ..... N90-28827* #

FEL-89-B170 ..... N90-28887
FEL-89-B252 ..... N90-29183
FEL-89-B265 ..... N90-28783
FEL-1989-103 ..... N90-28508

FFA-TN-1990-12-PT-1 ..... N90-28538 #
FFA-TN-1990-13-PT-2 ..... N90-28539 #
FFA-TN-1990-16 ..... N90-28501 #
FFA-TN-1990-23 ..... N90-28811 #

FNAL/C-90/122 ..... N90-29176 #

FOA-C-20781-2.1 ..... N90-28744 #
FOA-C-20782-2.5 ..... N90-28671 #

FRCR-373 ..... N90-29193 #

GA-A-20081 ..... N90-29187 #

GL-TR-90-0122 ..... N90-28683 #

GL-4697 ..... N90-28834 #

GRI-89/0196 ..... N90-28836 #
GRI-90/0088 ..... N90-28798 #
GRI-90/0133 ..... N90-28813 #

H-1575 ..... N90-28820* #
H-1602 ..... N90-28815* #
H-1603 ..... N90-28551* #
H-1620 ..... N90-29142* #
H-1621 ..... N90-29143* #
H-1632 ..... N90-28542* #
H-1651 ..... N90-28505* #

IC-89/150 ..... N90-29199 #
IC-89/244 ..... N90-28950 #
IC-89/321 ..... N90-29231 #
IC-89/329 ..... N90-29226 #
IC-89/374 ..... N90-29140 #
IC-89/379 ..... N90-29230 #
IC-89/388 ..... N90-29227 #
IC-89/390 ..... N90-29216 #
IC-89/392 ..... N90-28764 #
IC-89/394 ..... N90-29228 #
IC-89/397 ..... N90-29132 #
IC-89/398 ..... N90-29146 #
IC-89/399 ..... N90-29153 #
IC-89/405 ..... N90-29233 #
IC-89/410 ..... N90-29133 #
IC-89/411 ..... N90-29134 #
IC-89/412 ..... N90-29135 #
IC-89/418 ..... N90-28725 #

IC-89/422 ..... N90-29106 #
IC-89/423 ..... N90-29154 #
IC-89/424 ..... N90-29155 #
IC-89/425 ..... N90-29229 #
IC-89/427 ..... N90-29217 #
IC-89/431 ..... N90-29156 #
IC-89/434 ..... N90-29136 #
IC-90/3 ..... N90-29138 #
IC-90/4 ..... N90-29139 #
IC-90/5 ..... N90-29232 #
IC-90/11 ..... N90-29157 #
IC-90/13 ..... N90-29147 #
IC-90/14 ..... N90-29148 #
IC-90/15 ..... N90-29281 #
IC-90/16 ..... N90-29137 #
IC-90/17 ..... N90-29164 #

ICASE-IR-12 ..... N90-28876* #

ICASE-90-47 ..... N90-28789* #
ICASE-90-50 ..... N90-28818* #
ICASE-90-54 ..... N90-29125* #
ICASE-90-55 ..... N90-29128* #
ICASE-90-56 ..... N90-29129* #
ICASE-90-57 ..... N90-28814* #
ICASE-90-58 ..... N90-28502* #

ICOMP-90-21 ..... N90-29124* #

IFSR-431 ..... N90-29188 #
IFSR-438 ..... N90-29193 #
IFSR-439 ..... N90-29196 #
IFSR-440 ..... N90-29289 #

INPE-4534-RPE/565 ..... N90-29298 #
INPE-4556-TDL/331 ..... N90-28784 #
INPE-4565-PRE/1306 ..... N90-29104 #
INPE-4579-PRE/1313 ..... N90-29294 #
INPE-4586-TDL/332 ..... N90-28945 #
INPE-4595-RPE/569 ..... N90-29194 #
INPE-4598-RPE/570 ..... N90-28675 #
INPE-4601-TDL/334 ..... N90-28891 #
INPE-4627-PRE/1345 ..... N90-28886 #
INPE-4634-TDL/336 ..... N90-28949 #
INPE-4636-PRE/1348 ..... N90-29253 #
INPE-4666-NTE/283 ..... N90-29100 #
INPE-4977-PRE/1542 ..... N90-28881 #
INPE-4987-PRE/1549 ..... N90-29092 #

IRS-90-P7 ..... N90-28858* #

IS-T-1467 ..... N90-28687 #

ISBN-0-309-04185-6 ..... N90-29297 #
ISBN-0-309-04817-6 ..... N90-28511 #
ISBN-92-835-0533-6 ..... N90-28698 #
ISBN-92-835-0554-9 ..... N90-28972 #
ISBN-92-835-0555-7 ..... N90-28513 #
ISBN-951-22-0064-3 ..... N90-29158 #

ISSN-0029-3865 ..... N90-29149 #
ISSN-0029-3865 ..... N90-29150 #
ISSN-0029-3865 ..... N90-29165 #
ISSN-0029-3865 ..... N90-29212 #
ISSN-0029-3965 ..... N90-29151 #
ISSN-0067-0367 ..... N90-28674 #
ISSN-0069-4274 ..... N90-28869 #
ISSN-0171-1342 ..... N90-28812 #
ISSN-0171-1342 ..... N90-28853 #
ISSN-0176-7739 ..... N90-28903 #
ISSN-0347-3694 ..... N90-28671 #
ISSN-0347-3694 ..... N90-28744 #

ISVR-TR-176 ..... N90-28875 #
ISVR-TR-184 ..... N90-29141 #

IZF-1989-14 ..... N90-28994
IZF-1989-20 ..... N90-28995
IZF-1989-28 ..... N90-28760
IZF-1989-39 ..... N90-29182
IZF-1989-43 ..... N90-29082

JPL-PUBL-89-7-VOL-1 ..... N90-29000* #
JPL-PUBL-89-7-VOL-2 ..... N90-29044* #
JPL-PUBL-90-14 ..... N90-28593* #
JPL-PUBL-90-24 ..... N90-28592* #

JSR-87-301-A ..... N90-29181 #

KCP-613-4276 ..... N90-28857 #
KCP-613-4292 ..... N90-28763 #

L-16148 ..... N90-28806* #
L-16780 ..... N90-29166*
L-16789 ..... N90-28859* #
L-16806 ..... N90-29290* #

LA-UR-90-2268 ..... N90-29118 #
LA-UR-90-2294 ..... N90-28830 #
LA-UR-90-2321 ..... N90-29184 #
LA-UR-90-2342 ..... N90-29097 #
LA-UR-90-2358 ..... N90-29096 #
LA-UR-90-2362 ..... N90-29207 #
LA-UR-90-2363 ..... N90-29206 #
LA-UR-90-2365 ..... N90-29279 #
LA-UR-90-2366 ..... N90-29278 #
LA-UR-90-2367 ..... N90-29267 #
LA-UR-90-2368 ..... N90-29277 #
LA-UR-90-2369 ..... N90-29266 #
LA-UR-90-2370 ..... N90-29268 #
LA-UR-90-2372 ..... N90-29276* #
LA-UR-90-2388 ..... N90-29275* #
LA-UR-90-2427 ..... N90-28745 #
LA-UR-90-2431 ..... N90-28673 #
LA-UR-90-2580 ..... N90-29175 #

LA-11733-MS ..... N90-28885 #
LA-11902-MS ..... N90-29090 #

LBL-28200 ..... N90-29185 #
LBL-28684 ..... N90-28686 #
LBL-29039 ..... N90-29202 #
LBL-29040 ..... N90-28524 #
LBL-29061 ..... N90-29269 #

LC-86-23 ..... N90-28587* #
LC-89-63947 ..... N90-29297 #
LC-89-600755 ..... N90-29245 #
LC-90-31527 ..... N90-28511 #

LDGO-89-5 ..... N90-28955 #

LIMSI-89-9 ..... N90-28809 #

M-593-VOL-1 ..... N90-28611* #

MCCS-90-187 ..... N90-29117* #

MISC-90024-VOL-2-APP-PT-2 ..... N90-28778 #

MLM-3641(OP) ..... N90-28684 #
MLM-3642(OP) ..... N90-28685 #
MLM-3644(OP) ..... N90-28731 #

MPE-PREPRINT-173 ..... N90-29287

MPL-U-20/90 ..... N90-29168 #

MRL-TN-574 ..... N90-28883 #

MSAT-X-183 ..... N90-28593* #

MTI-87ASE575SA12 ..... N90-29260* #

MU-025921-14-T ..... N90-28767* #

NAL-TM-EA-8902 ..... N90-28492 #

NAMRL-1354 ..... N90-28543 #

NARA/TIP-90/03 ..... N90-29242 #

NAS 1.15:4207 ..... N90-28551* #
NAS 1.15:4219 ..... N90-28520* #
NAS 1.15:4222 ..... N90-28615* #
NAS 1.15:4232 ..... N90-29107* #
NAS 1.15:4233 ..... N90-28679* #
NAS 1.15:89114 ..... N90-28589* #
NAS 1.15:100396 ..... N90-28915* #
NAS 1.15:100400 ..... N90-28912* #
NAS 1.15:100403 ..... N90-28914* #
NAS 1.15:101606 ..... N90-28751* #
NAS 1.15:101723 ..... N90-28542* #
NAS 1.15:101726 ..... N90-28505* #
NAS 1.15:101802 ..... N90-28588* #
NAS 1.15:101932 ..... N90-28680* #
NAS 1.15:102279 ..... N90-28096* #
NAS 1.15:102635 ..... N90-28598* #
NAS 1.15:102670 ..... N90-28541* #
NAS 1.15:102692 ..... N90-28578* #
NAS 1.15:102693 ..... N90-28493* #
NAS 1.15:102710 ..... N90-29546* #
NAS 1.15:102714 ..... N90-28671* #
NAS 1.15:102719 ..... N90-28672* #
NAS 1.15:102723 ..... N90-28877* #
NAS 1.15:102791 ..... N90-28925* #
NAS 1.15:102802 ..... N90-28512* #
NAS 1.15:102852 ..... N90-29083* #
NAS 1.15:103112 ..... N90-28833* #
NAS 1.15:103134 ..... N90-28766* #
NAS 1.15:103184 ..... N90-28791* #
NAS 1.15:103196 ..... N90-28792* #
NAS 1.15:103224 ..... N90-28670* #
NAS 1.15:103235 ..... N90-28786* #
NAS 1.15:103239 ..... N90-28740* #
NAS 1.15:103256 ..... N90-28596* #
NAS 1.15:103262 ..... N90-29124* #
NAS 1.15:103280 ..... N90-28657* #
NAS 1.15:103291 ..... N90-29219* #
NAS 1.15:103292 ..... N90-28696* #
NAS 1.15:103485 ..... N90-28906* #
NAS 1.15:103506 ..... N90-28913* #
NAS 1.15:103512 ..... N90-29268* #
NAS 1.15:103513 ..... N90-28951* #
NAS 1.15:103607 ..... N90-28659* #
NAS 1.15:103609 ..... N90-29121* #
NAS 1.21:7011(340) N90-28963*
NAS 1.26:4316 ..... N90-29143* #
NAS 1.26:4317 ..... N90-29142* #
NAS 1.26:4323 ..... N90-28494* #
NAS 1.26:168069 ..... N90-28559* #
NAS 1.26:168137 ..... N90-28566* #
NAS 1.26:168211 ..... N90-28561* #
NAS 1.26:168219 ..... N90-28558* #
NAS 1.26:168274 ..... N90-28555* #
NAS 1.26:168289 ..... N90-28553* #
NAS 1.26:168290 ..... N90-28563* #
NAS 1.26:168301 ..... N90-28554* #
NAS 1.26:174651 ..... N90-28562* #
NAS 1.26:174766-VOL-1 ..... N90-28564* #
NAS 1.26:174766-VOL-2 ..... N90-28565* #
NAS 1.26:174799 ..... N90-28556* #
NAS 1.26:174834 ..... N90-28557* #
NAS 1.26:174942 ..... N90-28560* #
NAS 1.26:177526 ..... N90-29265* #
NAS 1.26:177537 ..... N90-29086* #
NAS 1.26:177548 ..... N90-29085* #
NAS 1.26:177552 ..... N90-28540* #
NAS 1.26:177564 ..... N90-28510* #
NAS 1.26:179399 ..... N90-28610* #
NAS 1.26:179533 ..... N90-28568* #
NAS 1.26:179534 ..... N90-28567* #
NAS 1.26:179578 ..... N90-28569* #
NAS 1.26:180381 ..... N90-29284* #
NAS 1.26:180393 ..... N90-28679* #
NAS 1.26:180406 ..... N90-28880* #
NAS 1.26:180409 ..... N90-29276* #
NAS 1.26:180454 ..... N90-28827* #
NAS 1.26:180840 ..... N90-29260* #
NAS 1.26:180850 ..... N90-28570* #
NAS 1.26:181096 ..... N90-28660* #
NAS 1.26:181297 ..... N90-28597* #
NAS 1.26:181731 ..... N90-28832* #
NAS 1.26:181881 ..... N90-28537* #
NAS 1.26:181973 ..... N90-28866* #
NAS 1.26:181974 ..... N90-28665* #
NAS 1.26:182071 ..... N90-28789* #
NAS 1.26:182079 ..... N90-28816* #
NAS 1.26:182082 ..... N90-29125* #
NAS 1.26:182083 ..... N90-29126* #
NAS 1.26:182084 ..... N90-29129* #
NAS 1.26:182085 ..... N90-28614* #
NAS 1.26:182086 ..... N90-28876* #
NAS 1.26:182089 ..... N90-29169* #
NAS 1.26:182091 ..... N90-28502* #
NAS 1.26:182124 ..... N90-28552* #
NAS 1.26:182186 ..... N90-28735* #
NAS 1.26:183066 ..... N90-28658* #
NAS 1.26:183779 ..... N90-28652* #
NAS 1.26:183786 ..... N90-28600* #
NAS 1.26:183787-APP-A ..... N90-28601* #
NAS 1.26:183788-APP-B ..... N90-28602* #
NAS 1.26:183789-APP-C ..... N90-28603* #
NAS 1.26:183790-APP-D ..... N90-28604* #
NAS 1.26:183791-APP-E ..... N90-28605* #
NAS 1.26:183792-APP-F ..... N90-28606* #
NAS 1.26:183793-APP-G ..... N90-28607* #
NAS 1.26:183822 ..... N90-28599* #
NAS 1.26:183871 ..... N90-28590* #
NAS 1.26:184008 ..... N90-29122* #
NAS 1.26:184010 ..... N90-28609* #
NAS 1.26:185080 ..... N90-29275* #
NAS 1.26:185278 ..... N90-28504* #
NAS 1.26:185279 ..... N90-28742* #
NAS 1.26:185288 ..... N90-28658* #
NAS 1.26:185291 ..... N90-28878* #
NAS 1.26:186379 ..... N90-28490* #
NAS 1.26:186488 ..... N90-28767* #
NAS 1.26:186611 ..... N90-28766* #
NAS 1.26:186707 ..... N90-29084* #
NAS 1.26:186856 ..... N90-29000* #
NAS 1.26:186857 ..... N90-29044* #
NAS 1.26:186865 ..... N90-29108* #
NAS 1.26:186868 ..... N90-28933* #
NAS 1.26:186893 ..... N90-28678* #
NAS 1.26:186895 ..... N90-28855* #
NAS 1.26:186906 ..... N90-29281* #
NAS 1.26:186928 ..... N90-29262* #
NAS 1.26:186930 ..... N90-28591* #
NAS 1.26:186944 ..... N90-28862* #
NAS 1.26:186960 ..... N90-29274* #
NAS 1.26:186963 ..... N90-29117* #
NAS 1.26:186968 ..... N90-28592* #
NAS 1.26:186971 ..... N90-28593* #
NAS 1.26:186975 ..... N90-28825* #
NAS 1.26:186977 ..... N90-29180* #
NAS 1.26:186992 ..... N90-28681* #
NAS 1.26:186998 ..... N90-28694* #
NAS 1.26:186999 ..... N90-28747* #
NAS 1.26:187002 ..... N90-29280* #
NAS 1.26:187004 ..... N90-28854* #
NAS 1.26:187005 ..... N90-28890* #
NAS 1.26:187006 ..... N90-28888* #
NAS 1.26:187007 ..... N90-28889* #
NAS 1.26:187018 ..... N90-28693* #
NAS 1.26:187025 ..... N90-28959* #
NAS 1.26:187026 ..... N90-28960* #
NAS 1.26:187033 ..... N90-28753* #
NAS 1.55:3012-VOL-1 ..... N90-28611* #
NAS 1.60:2786 ..... N90-28806* #
NAS 1.60:2984 ..... N90-28754* #
NAS 1.60:3002 ..... N90-28503* #
NAS 1.60:3021 ..... N90-29290* #
NAS 1.60:3024 ..... N90-28859* #
NAS 1.60:3027 ..... N90-29166*
NAS 1.60:3037 ..... N90-28965* #
NAS 1.61:1242 ..... N90-28929* #

NAS-069 ..... N90-29297 #

NASA-CP-3012-VOL-1 ..... N90-28611* #

NASA-CR-4316 ..... N90-29143* #
NASA-CR-4317 ..... N90-29142* #
NASA-CR-4323 ..... N90-28494* #
NASA-CR-168069 ..... N90-28559* #
NASA-CR-168137 ..... N90-28566* #
NASA-CR-168211 ..... N90-28561* #
NASA-CR-168219 ..... N90-28558* #
NASA-CR-168274 ..... N90-28555* #
NASA-CR-168289 ..... N90-28553* #
NASA-CR-168290 ..... N90-28563* #
NASA-CR-168301 ..... N90-28554* #
NASA-CR-174651 ..... N90-28562* #
NASA-CR-174766-VOL-1 ..... N90-28564* #
NASA-CR-174766-VOL-2 ..... N90-28565* #
NASA-CR-174799 ..... N90-28556* #
NASA-CR-174834 ..... N90-28557* #
NASA-CR-174942 ..... N90-28560* #
NASA-CR-177526 ..... N90-29265* #
NASA-CR-177537 ..... N90-29086* #
NASA-CR-177548 ..... N90-29085* #
NASA-CR-177552 ..... N90-28540* #
NASA-CR-177564 ..... N90-28510* #
NASA-CR-179399 ..... N90-28610* #
NASA-CR-179533 ..... N90-28568* #
NASA-CR-179534 ..... N90-28567* #
NASA-CR-179578 ..... N90-28569* #
NASA-CR-180381 ..... N90-29284* #
NASA-CR-180393 ..... N90-28679* #
NASA-CR-180406 ..... N90-28880* #
NASA-CR-180409 ..... N90-29276* #
NASA-CR-180454 ..... N90-28827* #
NASA-CR-180840 ..... N90-29260* #
NASA-CR-180850 ..... N90-28570* #
NASA-CR-181096 ..... N90-28660* #
NASA-CR-181297 ..... N90-28597* #
NASA-CR-181731 ..... N90-28832* #
NASA-CR-181881 ..... N90-28537* #
NASA-CR-181973 ..... N90-28866* #
NASA-CR-181974 ..... N90-28665* #
NASA-CR-182071 ..... N90-28789* #
NASA-CR-182079 ..... N90-28816* #
NASA-CR-182082 ..... N90-29125* #
NASA-CR-182083 ..... N90-29126* #
NASA-CR-182084 ..... N90-29129* #
NASA-CR-182085 ..... N90-28814* #
NASA-CR-182086 ..... N90-28876* #
NASA-CR-182089 ..... N90-29169* #
NASA-CR-182091 ..... N90-28502* #
NASA-CR-182124 ..... N90-28552* #
NASA-CR-182186 ..... N90-28735* #
NASA-CR-183066 ..... N90-28658* #
NASA-CR-183779 ..... N90-28852* #
NASA-CR-183786 ..... N90-28600* #
NASA-CR-183787-APP-A ..... N90-28601* #
NASA-CR-183788-APP-B ..... N90-28602* #
NASA-CR-183789-APP-C ..... N90-28603* #
NASA-CR-183790-APP-D ..... N90-28604* #
NASA-CR-183791-APP-E ..... N90-28605* #
NASA-CR-183792-APP-F ..... N90-28606* #
NASA-CR-183793-APP-G ..... N90-28607* #
NASA-CR-183822 ..... N90-28599* #
NASA-CR-183871 ..... N90-28590* #
NASA-CR-184008 ..... N90-29122* #

NASA-CR-184010 N90-28609* #
NASA-CR-185080 N90-29275* #
NASA-CR-185278 N90-28504* #
NASA-CR-185279 N90-28742* #
NASA-CR-185288 N90-28858* #
NASA-CR-185291 N90-28878* #
NASA-CR-186379 N90-28490* #
NASA-CR-186468 N90-28767* #
NASA-CR-186611 N90-28766* #
NASA-CR-186707 N90-29084* #
NASA-CR-186856 N90-29000* #
NASA-CR-186857 N90-29044* #
NASA-CR-186865 N90-29108* #
NASA-CR-186868 N90-28933* #
NASA-CR-186893 N90-28678* #
NASA-CR-186895 N90-28855* #
NASA-CR-186906 N90-29261* #
NASA-CR-186928 N90-29262* #
NASA-CR-186930 N90-28591* #
NASA-CR-186944 N90-28862* #
NASA-CR-186960 N90-29274* #
NASA-CR-186963 N90-29117* #
NASA-CR-186966 N90-28592* #
NASA-CR-186971 N90-28593* #
NASA-CR-186975 N90-28825* #
NASA-CR-186977 N90-29180* #
NASA-CR-186992 N90-28681* #
NASA-CR-186998 N90-28694* #
NASA-CR-186999 N90-28747* #
NASA-CR-187002 N90-29280* #
NASA-CR-187004 N90-28854* #
NASA-CR-187005 N90-28890* #
NASA-CR-187006 N90-28888* #
NASA-CR-187007 N90-28889* #
NASA-CR-187018 N90-28693* #
NASA-CR-187025 N90-28959* #
NASA-CR-187026 N90-28960* #
NASA-CR-187033 N90-28753* #

NASA-RP-1242 N90-28929* #

NASA-SP-7011(340) N90-28963*

NASA-TM-4207 N90-28551* #
NASA-TM-4219 N90-28820* #
NASA-TM-4222 N90-28815* #
NASA-TM-4232 N90-29107* #
NASA-TM-4233 N90-28879* #
NASA-TM-89114 N90-28589* #
NASA-TM-100396 N90-28915* #
NASA-TM-100400 N90-28912* #
NASA-TM-100403 N90-28914* #
NASA-TM-101606 N90-28751* #
NASA-TM-101723 N90-28542* #
NASA-TM-101726 N90-28505* #
NASA-TM-101892 N90-28588* #
NASA-TM-101932 N90-28680* #
NASA-TM-102279 N90-28996* #
NASA-TM-102635 N90-28598* #
NASA-TM-102670 N90-28541* #
NASA-TM-102692 N90-28578* #
NASA-TM-102693 N90-28493* #
NASA-TM-102710 N90-28546* #
NASA-TM-102714 N90-28871* #
NASA-TM-102719 N90-28872* #
NASA-TM-102723 N90-28877* #
NASA-TM-102791 N90-28925* #
NASA-TM-102802 N90-28512* #
NASA-TM-102852 N90-29083* #
NASA-TM-103112 N90-28833* #
NASA-TM-103134 N90-28768* #
NASA-TM-103184 N90-28791* #
NASA-TM-103196 N90-28792* #
NASA-TM-103224 N90-28670* #
NASA-TM-103235 N90-28786* #
NASA-TM-103239 N90-28740* #
NASA-TM-103256 N90-28596* #
NASA-TM-103262 N90-29124* #
NASA-TM-103280 N90-28657* #
NASA-TM-103291 N90-29219* #
NASA-TM-103292 N90-28696* #
NASA-TM-103485 N90-28906* #
NASA-TM-103508 N90-28913* #
NASA-TM-103512 N90-29268* #
NASA-TM-103513 N90-28951* #
NASA-TM-103607 N90-28659* #
NASA-TM-103609 N90-29121* #

NASA-TP-2786 N90-28806* #
NASA-TP-2984 N90-28754* #
NASA-TP-3002 N90-28503* #
NASA-TP-3021 N90-29290* #
NASA-TP-3024 N90-28659* #
NASA-TP-3027 N90-29166* #
NASA-TP-3037 N90-28965* #

NCAR/CT-125 N90-28926 #

NEMO-4 N90-28895 #

NHRC-90-5 N90-28968 #

NIPER-479-VOL-1 N90-28695 #

NIST-TN/1334 N90-28681* #

NIST/GCR-90/575 N90-28799 #

NIST/HB-44 N90-28748 #

NIST/SP-400/84 N90-29201 #
NIST/SP-400/85 N90-29203 #
NIST/SP-500/167 N90-29245 #
NIST/SP-500/179 N90-29243 #
NIST/SP-780 N90-28749 #
NIST/SP-784 N90-28840 #

NIST/TN-1275 N90-28856 #

NISTIR-89/4185 N90-28910 #
NISTIR-89/4193 N90-29200 #
NISTIR-89/4195 N90-28822 #
NISTIR-90/4250 N90-28757 #
NISTIR-90/4260 N90-28773 #
NISTIR-90/4283 N90-28790 #
NISTIR-90/4287 N90-29296 #
NISTIR-4300 N90-28716 #
NISTIR-4301 N90-28732 #
NISTIR-4339 N90-28775 #
NISTIR-4363 N90-29103 #
NISTIR-4367 N90-29239 #

NLM/LHC-90-02 N90-29098 #

NOAA-TM-ERL-SEL-80 N90-28935 #

NOAA-TM-ERL-WPL-175 N90-28927 #
NOAA-TM-ERL-WPL-177 N90-28939 #

NOAA-TM-ERL-181 N90-28928 #

NOAA-TM-NWS-SR-128 N90-28940 #
NOAA-TM-NWS-SR-130 N90-28948 #

NPS54-90-014 N90-29089 #
NPS54-90-016 N90-29256 #

NRL-MR-6532 N90-28823 #
NRL-MR-6682 N90-28573 #

NSF-89-321 N90-29235 #
NSF-89-325 N90-29236 #
NSF-90-311 N90-29237 #

NSF/ENG-89056 N90-28839 #
NSF/ENG-89058 N90-28838 #
NSF/ENG-90001 N90-28837 #

NST/SP-781 N90-28841 #

NSWC/TR-90-167 N90-28998 #
NSWC/TR-90-171 N90-28770 #

NTIA-90-255 N90-28755 #
NTIA-90-256 N90-28758 #
NTIA-90-260 N90-28756 #

NUSC-TD-8733 N90-28957 #

ONERA-RF-57/7131-PY N90-28692 #

ONERA-RSF-1/3731-AY-002A N90-28500 #

ONERA-RT-9/3549-M N90-28672 #
ONERA-RT-21/3542-RY-082-R N90-28874 #
ONERA-RT-31/3479-CY N90-29114 #

ORNL-6612 N90-28849 #
ORNL-6619 N90-29250 #
ORNL-6629/P1 N90-28720 #

ORNL/DSRD-25 N90-29120 #

ORNL/FTR-3672 N90-29285 #
ORNL/FTR-3675 N90-28734 #

ORNL/M-1206-VOL-1 N90-29170 #

ORNL/TM-9987 N90-28851 #
ORNL/TM-11349 N90-28850 #
ORNL/TM-11523 N90-29191 #
ORNL/TM-11531 N90-28826 #

ORNL/TM-11558 N90-29192 #
ORNL/TM-11559 N90-29130 #
ORNL/TM-11566 N90-29115 #
ORNL/TM-11579 N90-29095 #
ORNL/TM-11590 N90-28743 #

ORNL/TR-90/9 N90-28793 #

OSU-721432-2 N90-28766* #
OSU-721446-2 N90-28766* #
OSU-721447-2 N90-28766* #
OSU-721711-3 N90-28766* #

PB90-183351 N90-28681* #
PB90-184094 N90-28921 #
PB90-184961 N90-28748 #
PB90-188087 N90-28773 #
PB90-188707 N90-28958 #
PB90-189143 N90-29158 #
PB90-193053 N90-29252 #
PB90-197997 N90-28507 #
PB90-198585 N90-28836 #
PB90-198573 N90-28938 #
PB90-198946 N90-28757 #
PB90-199266 N90-28908 #
PB90-199498 N90-28837 #
PB90-200114 N90-28909 #
PB90-200338 N90-28755 #
PB90-201211 N90-28860 #
PB90-201799 N90-28715 #
PB90-202623 N90-28907 #
PB90-202706 N90-29257 #
PB90-203076 N90-28839 #
PB90-203175 N90-28838 #
PB90-206210 N90-29242 #
PB90-206236 N90-28756 #
PB90-207218 N90-28489 #
PB90-207267 N90-29296 #
PB90-207804 N90-28716 #
PB90-207994 N90-28758 #
PB90-208570 N90-28928 #
PB90-209578 N90-28822 #
PB90-209594 N90-29200 #
PB90-209602 N90-28910 #
PB90-209776 N90-28926 #
PB90-213620 N90-28580 #
PB90-214412 N90-29246 #
PB90-214834 N90-28847 #
PB90-215484 N90-28948 #
PB90-215534 N90-29239 #
PB90-216789 N90-28927 #
PB90-216805 N90-28940 #
PB90-216813 N90-29243 #
PB90-216839 N90-28840 #
PB90-216847 N90-29201 #
PB90-217068 N90-28939 #
PB90-219130 N90-28790 #
PB90-219288 N90-29244 #
PB90-219551 N90-28841 #
PB90-219619 N90-28749 #
PB90-219866 N90-29245 #
PB90-221656 N90-28942 #
PB90-221680 N90-28916 #
PB90-221839 N90-28732 #
PB90-222167 N90-28511 #
PB90-222720 N90-28856 #
PB90-222738 N90-29203 #
PB90-226564 N90-28943 #
PB90-226879 N90-29237 #
PB90-226887 N90-29236 #
PB90-226903 N90-29235 #
PB90-226980 N90-28869 #
PB90-227968 N90-28799 #
PB90-228123 N90-28798 #
PB90-231010 N90-28870 #
PB90-231705 N90-28944 #
PB90-231796 N90-28883 #
PB90-232596 N90-28952 #
PB90-235623 N90-29099 #
PB90-239732 N90-29251 #
PB90-240029 N90-29098 #
PB90-240631 N90-28935 #
PB90-240953 N90-28936 #
PB90-243932 N90-28955 #
PB90-246638 N90-28737 #
PB90-246711 N90-29259 #
PB90-247602 N90-28813 #
PB90-248600 N90-28954 #
PB90-250051 N90-29103 #

PD-CF-9009 N90-28577 #
PD-CF-9010 N90-28491 #

PFC/RR-90-9 N90-29198 #
PFC/RR-90-11 N90-29197 #

PNL-SA-17636 ..... N90-28724 #

PSI-1011/TR-800 ..... N90-28832* #

PWA-5394-315 ..... N90-28560* #
PWA-5594-231 ..... N90-28566* #
PWA-5594-251-VOL-2 ..... N90-28565* #
PWA-5594-258-VOL-1 ..... N90-28564* #
PWA-5594-271-ADD ..... N90-28556* #
PWA-5594-287 ..... N90-28570* #
PWA-5594-329 ..... N90-28568* #
PWA-5594-331 ..... N90-28569* #
PWA-5594-333 ..... N90-28567* #

R-599 ..... N90-28660 #
R-603 ..... N90-28670 #

RAE-TM-AERO-2159 ..... N90-28800 #

RAE-TM-SPACE-372 ..... N90-29293
RAE-TM-SPACE-373 ..... N90-28934 #
RAE-TM-SPACE-375 ..... N90-28594 #

REMTECH-RTN-186-02 ..... N90-28602* #

REPT-20 ..... N90-28716 #
REPT-49-236 ..... N90-28722 #
REPT-55 ..... N90-29158 #
REPT-89/115 ..... N90-29167 #
REPT-90B00133 ..... N90-29107* #
REPT-249.9 ..... N90-28652* #

RF-8035 ..... N90-28905 #

RI/RD87-207-2 ..... N90-28610* #

RLE-PR-132 ..... N90-29295 #

RPI-MATH-184 ..... N90-28930 #

RSRE-89022 ..... N90-29238 #

R82AEB401 ..... N90-28555* #
R82AEB406 ..... N90-28553* #
R82AEB470 ..... N90-28559* #
R82AEB472 ..... N90-28554* #
R83AEB143 ..... N90-28563* #
R83AEB488 ..... N90-28558* #
R83AEB503 ..... N90-28561* #
R83AEB623 ..... N90-28562* #
R84AEB246 ..... N90-28557* #

SAND-85-2523-REV-2 ..... N90-28595 #
SAND-89-2907C ..... N90-28777 #
SAND-90-0009C ..... N90-28897 #
SAND-90-0078 ..... N90-28495 #
SAND-90-0186C ..... N90-28848 #
SAND-90-0415C ..... N90-28776 #
SAND-90-0955C ..... N90-29208 #
SAND-90-1247C ..... N90-28717 #
SAND-90-1266 ..... N90-29123 #
SAND-90-1582C ..... N90-28690 #
SAND-90-1767C ..... N90-28898 #
SAND-90-1795C ..... N90-29173 #
SAND-90-1805C ..... N90-29190 #
SAND-90-1829C ..... N90-28899 #
SAND-90-1923C ..... N90-29177 #
SAND-90-7016 ..... N90-28781 #

SEA-D470-2 ..... N90-28590* #

SEI-CM-23 ..... N90-29109 #
SEI-CM-24 ..... N90-29110 #

SERI/TP-211-3804 ..... N90-28896 #
SERI/TP-211-3805 ..... N90-29204 #
SERI/TP-211-3830 ..... N90-28730 #
SERI/TP-260-3716 ..... N90-29258 #

SNPE-NT-106/89/GTR/RP/NP ..... N90-28736 #

SRS-552 ..... N90-28869 #

SU-SLAC-PUB-5276 ..... N90-29179 #
SU-SLAC-PUB-5282 ..... N90-29178 #

SU-SOL-90-9 ..... N90-29145 #

TAMRF-6382-90-01 ..... N90-28490* #

TD-89-1050 ..... N90-28995
TD-89-1051 ..... N90-28994
TD-89-1053 ..... N90-28760
TD-89-3097 ..... N90-28506
TD-89-3572 ..... N90-29183
TD-89-3576 ..... N90-28783
TD-89-3873 ..... N90-28887
TD-89-4141 ..... N90-29182
TD-89-4143 ..... N90-29062

TR-EE-87-26 ..... N90-28890* #
TR-EE-88-34 ..... N90-28888* #

TR-EE90-48 ..... N90-28889* #

TR-3 ..... N90-29222 #
TR-28 ..... N90-29234 #
TR-29 ..... N90-29221 #
TR-90-03 ..... N90-29122* #
TR-244 ..... N90-28971 #
TR-391 ..... N90-28494* #
TR-4455-038-90 ..... N90-28904 #

TRB/TRR-1214 ..... N90-28511 #

TWR-17547-1-VOL-1 ..... N90-28809* #

U-OF-IOWA-90-13 ..... N90-29284* #

UCRL-CR-104308 ..... N90-29105 #
UCRL-CR-104490-EXEC-SUMM ..... N90-28922 #

UCRL-ID-103169 ..... N90-28805 #
UCRL-ID-103792 ..... N90-29081 #
UCRL-ID-103911 ..... N90-28719 #
UCRL-ID-104341 ..... N90-28752 #

UCRL-JC-103246 ..... N90-28689 #
UCRL-JC-103631 ..... N90-28723 #
UCRL-JC-103743 ..... N90-28739 #
UCRL-JC-104001 ..... N90-28804 #
UCRL-JC-104052 ..... N90-28919 #
UCRL-JC-104125 ..... N90-28831 #
UCRL-JC-104266 ..... N90-29131 #
UCRL-JC-104336 ..... N90-28785 #

UCRL-53941 ..... N90-29091 #
UCRL-101769 ..... N90-28736 #
UCRL-102850 ..... N90-28782 #

UILU-ENG-89-2006 ..... N90-28869 #

UR-1172 ..... N90-29225 #

USAAVSCOM-TR-90-G-1 ..... N90-28510* #

USAFSAM-JA-90-22 ..... N90-28967 #

USAFSAM-TP-89-20 ..... N90-28545 #

USASC-TR-90-1 ..... N90-29060 #

USGS/WRI-89-4070 ..... N90-28883 #
USGS/WRI-89-4183 ..... N90-28944 #

VPI-E-90-08 ..... N90-28862* #

WDCA-OC-89-2 ..... N90-28952 #

WES/TR/ITL-90-2 ..... N90-29254 #

WHC-MR-0165 ..... N90-28941 #

WHOI-89-39 ..... N90-28936 #

WRDC-TR-89-2150 ..... N90-28574 #

Appendix—About STAR

Scientific and Technical Aerospace Reports (STAR) is a major component of a comprehensive National Aeronautics and Space Administration information system covering aeronautics, space, and supporting disciplines. *STAR* is issued on the 8th and 23rd of each month and announces current publications of the following types:

- NASA, NASA contractor, and NASA grantee reports
- Reports issued by other U.S. Government agencies, domestic and foreign institutions, universities, and private firms
- Translations in report form
- NASA-owned patents and patent applications
- Other U.S. Government agency and foreign patents and patent applications
- Domestic and foreign dissertations and theses

Journal, book, and conference literature, cover-to-cover journal translations, and certain foreign dissertations are announced in a companion journal, *International Aerospace Abstracts (IAA),* available on subscription from the American Institute of Aeronautics and Astronautics, Technical Information Service, 555 West 57th Street, 12th Floor, New York, NY 10019.

SUBJECT SCOPE

The subject scope of *STAR* and *IAA* includes all aspects of aeronautics and space research and development, supporting basic and applied research, and applications. Aerospace aspects of earth resources, energy development, conservation, oceanography, environmental protection, urban transportation, and other topics of high national priority are also covered.

OTHER NASA PUBLICATIONS

Other NASA publications and information services are described in the publication, *The NASA Scientific and Technical Information System ... and How to Use It,* available without charge from the NASA Scientific and Technical Information Facility, P.O. Box 8757, BWI Airport, MD 21240.

HOW TO USE *STAR* SUBJECT CATEGORIES

STAR is categorized by 10 major subject divisions broken down further into 76 specific subject categories and one general division/category. The major subject divisions are listed on page ii in the Table of Contents, together with a note for each that defines its scope and provides any cross-references. For example:

AERONAUTICS

Includes aeronautics (general); aerodynamics; air transportation and safety; aircraft communications and navigation; aircraft design, testing and performance; aircraft instrumentation; aircraft propulsion and power; aircraft stability and control; and research and support facilities (air).

For related information see also *Astronautics.*

Each major division is further divided into as many as nine specific categories, which are identified by category numbers.

Abstracts in *STAR* are grouped by subject category, the categories appearing in sequential order. Category breaks in the abstract section are identified by the category number and title, and a scope note. Cross-references to other categories are provided as appropriate. For example:

02 AERODYNAMICS

Includes aerodynamics of bodies, combinations, wings, rotors, and control surfaces; and internal flow in ducts and turbomachinery.

For related information see also *34 Fluid Mechanics and Heat Transfer.*

CROSS-REFERENCES

Individual *STAR* abstracts are not ordinarily cross-referenced, except for certain conference reports or book translations that have had separate abstracts written for their component papers or chapters. Citations and abstracts of the components follow immediately after those of the parent document. When the subject content of a component differs sufficiently from the general content of the parent, a cross-reference citation also is printed at the end of the category to which it normally would have been assigned if it were independent.

DOCUMENTS ON MICROFICHE

Documents on microfiche[1] are designated by a pound sign (#) following the accession number. The pound sign is used without regard to the source or quality of the microfiche.

LIMITED REPRODUCIBILITY

A Note of Limited Reproducibility appears in the citation, if one or a combination of the following factors affect the reproducibility of more than 20% of the document. These factors include: faint or broken type, color photographs, black and white photographs, foldouts, dot matrix print, charts/graphs with script notation, non-Roman alphabet, or some other factor that limits the reproducibility of that document. This notation also appears on the microfiche header, with the specific causing factor checked off on a list visible in the second frame.

COLOR COPIES

An increasing number of NASA scientific and technical reports are being produced with color graphs, charts, illustrations, and photographs. A message indicating that a document has color pages follows the Sales and Pricing (SAP) information in the *STAR* citation.

Registered users of the NASA Scientific and Technical Information System will receive ordered documents with color at no *additional* cost, as long as stock copies of that document are available. Otherwise, an additional fee of $2.00 per color page, over and above the standard document price will be charged. The NASA STI Facility staff will work with registered users over the telephone to inform and meet each individual's ordering needs.

AVAILABILITIES

One or more sources from which a document announced in *STAR* is available to the public is given in each citation. The most commonly indicated sources and their acronyms or abbreviations are listed below. If the publication is available from a source other than those listed, the publisher and his address will be displayed on the availability line or in combination with the corporate source line.

Avail: NTIS. Sold by the National Technical Information Service. Prices for hard copy (HC) and microfiche (MF) are indicated by a price code following the letters HC or MF in the *STAR* citation. Current values for the price codes are given in the tables on page A-7.

(1) A microfiche is a transparent sheet of film, 105 by 148 mm in size, containing as many as 60 to 98 pages of information reduced to micro images (not to exceed 26:1 reduction).

Initially distributed microfiche under the NTIS SRIM (Selected Research in Microfiche) is available at greatly reduced unit prices. For this service and for information concerning subscription to NASA printed reports, consult the NTIS Subscription Section, Springfield, VA 22161.

NOTE ON ORDERING DOCUMENTS: When ordering NASA publications (those followed by the * symbol), use the N accession number. NASA patent applications (only the specifications are offered) should be ordered by the US-Patent-Appl-SN number. Non-NASA publications (no asterisk) should be ordered by the AD, PB, or other *report number* shown on the last line of the citation, not by the N accession number. It is also advisable to cite the title and other bibliographic identification.

Avail: SOD (or GPO). Sold by the Superintendent of Documents, U.S. Government Printing Office, in hard copy. The current price and order number are given following the availability line. (NTIS will fill microfiche requests, as indicated above, for those documents identified by a # symbol.)

Avail: BLL (formerly NLL): British Library Lending Division, Boston Spa, Wetherby, Yorkshire, England. Photocopies available from this organization at the price shown. (If none is given, address inquiry to the BLL.)

Avail: DOE Depository Libraries. Organizations in U.S. cities and abroad that maintain collections of Department of Energy reports, usually in microfiche form, are listed in *Energy Research Abstracts*. Services available from the DOE and its depositories are described in a booklet, *DOE Technical Information Center - Its Functions and Services* (TID-4660), which may be obtained without charge from the DOE Technical Information Center.

Avail: ESDU. Pricing information on specific data, computer programs, and details on Engineering Sciences Data Unit (ESDU) topic categories can be obtained from ESDU International Ltd. Requesters in North America should use the Virginia address while all other requesters should use the London address, both of which are on page A-6.

Avail: Fachinformationszentrum, Karlsruhe. Sold by the Fachinformationszentrum Energie, Physik, Mathematik GMBH, Eggenstein Leopoldshafen, Federal Republic of Germany, at the price shown in deutschmarks (DM).

Avail: HMSO. Publications of Her Majesty's Stationery Office are sold in the U.S. by Pendragon House, Inc. (PHI), Redwood City, CA. The U.S. price (including a service and mailing charge) is given, or a conversion table may be obtained from PHI.

Avail: NASA Public Document Rooms. Documents so indicated may be examined at or purchased from the National Aeronautics and Space Administration, Public Documents Room (Room 126), 600 Independence Ave., S.W., Washington, DC 20546, or public document rooms located at NASA installations, and the NASA Pasadena Office at the Jet Propulsion Laboratory.

Avail: Univ. Microfilms. Documents so indicated are dissertations selected from *Dissertation Abstracts* and are sold by University Microfilms as xerographic copy (HC) and microfilm. All requests should cite the author and the Order Number as they appear in the citation.

Avail: US Patent and Trademark Office. Sold by Commissioner of Patents and Trademarks, U.S. Patent and Trademark Office, at the standard price of

$1.50 each, postage free. (See discussion of NASA patents and patent applications below.)

Avail: (US Sales Only). These foreign documents are available to users within the United States from the National Technical Information Service (NTIS). They are available to users outside the United States through the International Nuclear Information Service (INIS) representative in their country, or by applying directly to the issuing organization.

Avail: USGS. Originals of many reports from the U.S. Geological Survey, which may contain color illustrations, or otherwise may not have the quality of illustrations preserved in the microfiche or facsimile reproduction, may be examined by the public at the libraries of the USGS field offices whose addresses are listed in this Introduction. The libraries may be queried concerning the availability of specific documents and the possible utilization of local copying services, such as color reproduction.

Avail: Issuing Activity, or Corporate Author, or no indication of availability. Inquiries as to the availability of these documents should be addressed to the organization shown in the citation as the corporate author of the document.

NASA PATENTS AND PATENT APPLICATIONS

Patents and patent applications owned by NASA are announced in *STAR* under appropriate subject categories and are referenced in the *STAR* indexes. In the Report/Accession Number Index, patents are indexed by the NASA Case Number (which appears in lieu of the report number in other indexes), the U.S. Patent Number, the U.S. Patent Application Serial Number, and the U.S. Patent Class. Patent applications for which patents have not yet been issued are indexed by the NASA Case Number and the U.S. Patent Application Serial Number.

NASA *patent application specifications* are sold in paper copy and microfiche by the National Technical Information Service (NTIS). The US-Patent-Appl-SN- number should be used in ordering either paper copy or microfiche from NTIS. Printed copies of *patents* (which are not microfiched) are available for purchase from:

Commissioner of Patents and Trademarks
U.S. Patent and Trademark Office
Washington, DC 20231

When ordering patents, the U.S. Patent Number should be used, and payment must be remitted in advance, by money order or check payable to the Commissioner of Patents and Trademarks. Prepaid purchase coupons for ordering are also available from the Patent and Trademark Office. The patents and patent applications announced in *STAR* are owned by NASA and are available for royalty-free licensing. Requests for licensing terms and further information should be addressed to:

Associate General Counsel for Intellectual Property/Code GP
National Aeronautics and Space Administration
Washington, DC 20546

ELIGIBILITY AND REGISTRATION FOR NASA INFORMATION PRODUCTS AND SERVICES

A variety of services is available to organizations of the following types that have registered with NASA to receive specific services or products:

1. NASA offices and installations, contractors, subcontractors, grantees, and consultants;
2. Other U.S. Government agencies and their contractors;
3. Libraries in the United States that have arrangements with NASA to maintain collections of NASA documents for public reference;
4. Other organizations in the United States having a need for NASA documents in work related to aeronautics and space research;
5. Organizations abroad that have established reciprocal document exchange arrangements with NASA.

Only the central service points or central points of document acquisition and control within qualified organizations are eligible to register for NASA products and services. Domestic organizations that may be eligible to receive various classes of NASA publications and services should address their requests for registration or for further information to:

NASA Scientific and Technical Information Facility
ATTN: Registration Services
P.O. Box 8757
BWI Airport, MD 21240
301-621-0153

Organizations abroad should direct requests to Manager, International STI Activities, NTT, NASA Headquarters, Washington, DC 20546.

AVAILABILITY OF *STAR* ABSTRACTS ON MICROFICHE

Microfiche of the abstract sections of this issue and other issues of *STAR* are available on annual subscription from NTIS as PB90-911300, Attn: Subscriptions, 5285 Port Royal Road, Springfield, VA 22161. Annual subscription rates are $75.50 North America; $151.00 foreign. Abstract sections for previous years retroactive to 1964 are available at the current rates. Microfiche for individual *STAR* issue abstract sections are not available.

PUBLIC COLLECTIONS OF NASA DOCUMENTS

DOMESTIC: NASA and NASA-sponsored documents and a large number of aerospace publications are available to the public for reference purposes at the library maintained by the American Institute of Aeronautics and Astronautics, Technical Information Service, 555 West 57th Street, 12th Floor, New York, NY 10019.

EUROPEAN: An extensive collection of NASA and NASA-sponsored publications is maintained by the British Library Lending Division, Boston Spa, Wetherby, Yorkshire, England, for public access. The British Library Lending Division also has available many of the non-NASA publications cited in *STAR*. European requesters may purchase facsimile copy or microfiche of NASA and NASA-sponsored documents, those identified by both the symbols # and * from ESA - Information Retrieval Service, European Space Agency, 8-10 rue Mario-Nikis, 75738 Paris CEDEX 15, France.

FEDERAL DEPOSITORY LIBRARY PROGRAM

In order to provide the general public with greater access to U.S. Government publications, Congress established the Federal Depository Library Program under the Government Printing Office (GPO), with 51 regional depositories responsible for permanent retention of material, inter-library loan, and reference services. At least one copy of nearly every NASA and NASA-sponsored publication, either in printed or microfiche format, is received and retained by the 51 regional depositories. A list of the regional GPO libraries, arranged alphabetically by state, appears on the inside back cover. These libraries are *not* sales outlets. A local library can contact a Regional Depository to help locate specific reports, or direct contact may be made by an individual.

ADDRESSES OF ORGANIZATIONS

American Institute of Aeronautics and Astronautics
Technical Information Service
555 West 57th Street, 12th Floor
New York, New York 10019

British Library Lending Division,
Boston Spa, Wetherby, Yorkshire,
England

Commissioner of Patents and Trademarks
U.S. Patent and Trademark Office
Washington, DC 20231

Department of Energy
Technical Information Center
P.O. Box 62
Oak Ridge, Tennessee 37830

European Space Agency-Information Retrieval Service
ESRIN
Via Galileo Galilei
00044 Frascati (Rome) Italy

Engineering Sciences Data Unit International
P.O. Box 1633
Manassas, Virginia 22110

Engineering Sciences Data Unit International, Ltd.
251-259 Regent Street
London, W1R 7AD, England

Fachinformationszentrum Energie, Physik, Mathematik
GMBH
7514 Eggenstein Leopoldshafen
Federal Republic of Germany

Her Majesty's Stationery Office
P.O. Box 569, S.E. 1
London, England

NASA Scientific and Technical Information Facility
P.O. Box 8757
BWI Airport, Maryland 21240

National Aeronautics and Space Administration
Scientific and Technical Information Division (NTT)
Washington, DC 20546

National Technical Information Service
5285 Port Royal Road
Springfield, Virginia 22161

Pendragon House, Inc.
899 Broadway Avenue
Redwood City, California 94063

Superintendent of Documents
U.S. Government Printing Office
Washington, DC 20402

University Microfilms
A Xerox Company
300 North Zeeb Road
Ann Arbor, Michigan 48106

University Microfilms, Ltd.
Tylers Green
London, England

U.S. Geological Survey Library National Center
MS 950
12201 Sunrise Valley Drive
Reston, Virginia 22092

U.S. Geological Survey Library
2255 North Gemini Drive
Flagstaff, Arizona 86001

U.S. Geological Survey
345 Middlefield Road
Menlo Park, California 94025

U.S. Geological Survey Library
Box 25046
Denver Federal Center, MS914
Denver, Colorado 80225

NTIS PRICE SCHEDULES

(Effective January 1, 1990)

Schedule A
STANDARD PRICE DOCUMENTS AND MICROFICHE

PRICE CODE	NORTH AMERICAN PRICE	FOREIGN PRICE
A01	$ 8.00	$ 16.00
A02	11.00	22.00
A03	15.00	30.00
A04-A05	17.00	34.00
A06-A09	23.00	46.00
A10-A13	31.00	62.00
A14-A17	39.00	78.00
A18-A21	45.00	90.00
A22-A25	53.00	106.00
A99	*	*
N01	60.00	120.00
N02	59.00	118.00
N03	20.00	40.00

Schedule E
EXCEPTION PRICE DOCUMENTS AND MICROFICHE

PRICE CODE	NORTH AMERICAN PRICE	FOREIGN PRICE
E01	$10.00	$ 20.00
E02	12.00	24.00
E03	14.00	28.00
E04	16.50	33.00
E05	18.50	37.00
E06	21.50	43.00
E07	24.00	48.00
E08	27.00	54.00
E09	29.50	59.00
E10	32.50	65.00
E11	35.00	70.00
E12	38.50	77.00
E13	41.00	82.00
E14	45.00	90.00
E15	48.50	97.00
E16	53.00	106.00
E17	57.50	115.00
E18	62.00	124.00
E19	69.00	138.00
E20	80.00	160.00
E99	*	*

* Contact NTIS for price quote.

IMPORTANT NOTICE

NTIS Shipping and Handling Charges

U.S., Canada, Mexico — ADD $3.00 per TOTAL ORDER

All Other Countries — ADD $4.00 per TOTAL ORDER

Exceptions — Does NOT apply to:

ORDERS REQUESTING NTIS RUSH HANDLING
ORDERS FOR SUBSCRIPTION OR STANDING ORDER PRODUCTS *ONLY*

NOTE: Each additional delivery address on an order requires a separate shipping and handling charge.

FEDERAL REGIONAL DEPOSITORY LIBRARIES

ALABAMA

AUBURN UNIV. AT MONTGOMERY LIBRARY
Documents Department
Montgomery, AL 36193
(205) 279-9110 ext.253

UNIV. OF ALABAMA LIBRARY
Reference Department/Documents
Box S
Tuscaloosa, AL 35486
(205) 348-6046

ARIZONA

DEPT. OF LIBRARY, ARCHIVES, AND PUBLIC RECORDS
Third Floor State Capitol
1700 West Washington
Phoenix, AZ 85007
(602) 255-4121

ARKANSAS

ARKANSAS STATE LIBRARY
Documents Service Section
One Capitol Mall
Little Rock, AR 72201
(501) 371-2090

CALIFORNIA

CALIFORNIA STATE LIBRARY
Govt. Publications Section
914 Capitol Mall
Sacramento, CA 95814
(916) 322-4572

COLORADO

UNIV. OF COLORADO
Norlin Library
Government Publications Division
Campus Box 184
Boulder, CO 80309
(303) 492-8834

DENVER PUBLIC LIBRARY
Govt. Pub. Department
1357 Broadway
Denver, CO 80203
(303) 571-2346

CONNECTICUT

CONNECTICUT STATE LIBRARY
231 Capitol Avenue
Hartford, CT 06106
(203) 566-4971

FLORIDA

UNIV. OF FLORIDA LIBRARIES
Documents Department
Library West
Gainesville, FL 32611
(904) 392-0367

GEORGIA

UNIV. OF GEORGIA LIBRARIES
Government Documents Dept.
Athens, GA 30602
(404) 542-8949

HAWAII

UNIV. OF HAWAII
Hamilton Library
Government Documents Collection
2550 The Mall
Honolulu, HI 96822
(808) 948-8230

IDAHO

UNIV. OF IDAHO LIBRARY
Documents Section
Moscow, ID 83843
(208) 885-6344

ILLINOIS

ILLINOIS STATE LIBRARY
Federal Documents
Centennial Building
Springfield, IL 62756
(217) 782-5012

INDIANA

INDIANA STATE LIBRARY
Serials Section
140 North Senate Avenue
Indianapolis, IN 46204
(317) 232-3686

IOWA

UNIV. OF IOWA LIBRARIES
Government Publications Dept.
Iowa City, IA 52242
(319) 335-5926

KANSAS

UNIVERSITY OF KANSAS
Spencer Research Library
Government Documents
Lawrence, KS 66045
(913) 864-4662

KENTUCKY

UNIV. OF KENTUCKY LIBRARIES
Government Publications/Maps Dept.
Lexington, KY 40506
(606) 257-8400

LOUISIANA

LOUISIANA STATE UNIVERSITY
Middleton Library
Government Documents Dept.
Baton Rouge, LA 70803
(504) 388-2570

LOUISIANA TECHNICAL UNIV.
Prescott Memorial Library
Government Documents Dept.
Ruston, LA 71272
(318) 257-4962

MAINE

UNIVERSITY OF MAINE
Raymond H. Fogler Library
Govt. Documents & Microforms Dept.
Orono, ME 04469
(207) 581-1680

MARYLAND

UNIVERSITY OF MARYLAND
McKeldin Library
Documents/Maps Room
College Park, MD 20742
(301) 454-3034

MASSACHUSETTS

BOSTON PUBLIC LIBRARY
Government Documents Dept.
666 Boylston Street
Boston, MA 02117
(617) 536-5400 ext.226

MICHIGAN

DETROIT PUBLIC LIBRARY
5201 Woodward Avenue
Detroit, MI 48202
(313) 833-1409

LIBRARY OF MICHIGAN
Government Documents
P.O. Box 30007
735 E. Michigan Avenue
Lansing, MI 48909
(517) 373-1593

MINNESOTA

UNIVERSITY OF MINNESOTA
Wilson Library
Government Publications
309 Nineteenth Avenue South
Minneapolis, MN 55455
(612) 373-7813

MISSISSIPPI

UNIV. OF MISSISSIPPI LIB.
Government Documents Dept.
106 Old Gym Bldg.
University, MS 38677
(601) 232-5857

MISSOURI

University of Missouri at Columbia Library
Government Documents
Columbia, MO 65201
(314) 882-6733

MONTANA

UNIV. OF MONTANA
Mansfield Library
Documents Division
Missoula, MT 59812
(406) 243-6700

NEBRASKA

UNIVERSITY OF NEBRASKA - LINCOLN
Love Memorial Library
Documents Department
Lincoln, NE 68588
(402) 472-2562

NEVADA

UNIV. OF NEVADA-RENO LIB.
Govt. Pub. Department
Reno, NV 89557
(702) 784-6579

NEW JERSEY

NEWARK PUBLIC LIBRARY
U.S. Documents Division
5 Washington Street
P.O. Box 630
Newark, NJ 07101
(201) 733-7812

NEW MEXICO

UNIVERSITY OF NEW MEXICO
General Library
Government Publications/Maps Dept.
Albuquerque, NM 87131
(505) 277-5441

NEW MEXICO STATE LIBRARY
325 Don Gaspar Avenue
Santa Fe, NM 87501
(505) 827-3826

NEW YORK

NEW YORK STATE LIBRARY
Documents Sect. Cultural Educ. Ctr.
Empire State Plaza
Albany, NY 12230
(518) 474-5563

NORTH CAROLINA

UNIVERSITY OF NORTH CAROLINA AT CHAPEL HILL
Davis Library 080A
BA/SS Department Documents
Chapel Hill, NC 27514
(919) 962-1151

NORTH DAKOTA

NORTH DAKOTA STATE UNIVERSITY LIBRARY
Government Documents Dept.
Fargo, ND 58105
(701) 237-8352
In cooperation with Univ. of North Dakota, Chester Fritz Library
Grand Forks

OHIO

STATE LIBRARY OF OHIO
Documents Section
65 South Front Street
Columbus, OH 43266
(614) 644-7051

OKLAHOMA

OKLAHOMA DEPT. OF LIBRARIES
Government Documents
200 NE 18th Street
Oklahoma City, OK 73105
(405) 521-2502, ext. 252

OKLAHOMA STATE UNIV. LIB.
Documents Department
Stillwater, OK 74078
(405) 624-0489

OREGON

PORTLAND STATE UNIV.
Millar Library
934 SW Harrison - P.O. Box 1151
Portland, OR 97207
(503) 229-3673

PENNSYLVANIA

STATE LIBRARY OF PENN.
Government Publications Section
Box 1601
Walnut St. & Commonwealth Ave.
Harrisburg, PA 17105
(717) 787-3752

SOUTH CAROLINA

CLEMSON UNIV. COOPER LIB.
Documents Department
Clemson, SC 29634
(803) 656-5174
In cooperation with Univ. of South Carolina, Thomas Cooper Library, Columbia

TEXAS

TEXAS STATE LIBRARY
Public Services Department
P.O. Box 12927 - 1201 Brazos
Austin, TX 78711
(512) 463-5455

TEXAS TECH. UNIV. LIBRARY
Documents Department
Lubbock, TX 79409
(806) 742-2268

UTAH

UTAH STATE UNIVERSITY
Merrill Library & Learning Resources Center, UMC-30
Documents Department
Logan, UT 84322
(801) 750-2682

VIRGINIA

UNIVERSITY OF VIRGINIA
Alderman Library
Government Documents
Charlottesville, VA 22903
(804) 924-3133

WASHINGTON

WASHINGTON STATE LIBRARY
Document Section
Olympia, WA 98504
(206) 753-4027

WEST VIRGINIA

WEST VIRGINIA UNIV. LIB.
Government Documents Section
P.O. Box 6069
Morgantown, WV 26506
(304) 293-3640

WISCONSIN

ST. HIST SOC. OF WISCONSIN LIB.
Government Pub. Section
816 State Street
Madison, WI 53706
(608) 262-2781
In cooperation with Univ. of Wisconsin-Madison, Memorial Library

MILWAUKEE PUBLIC LIBRARY
Documents Division
814 West Wisconsin Avenue
Milwaukee, WI 53233
(414) 278-3065

WYOMING

WYOMING STATE LIBRARY
Supreme Court & Library Bldg.
Cheyenne, WY 82002
(307) 777-5919

National Aeronautics and
Space Administration
Code NTT
Washington, D.C.
20546
Official Business
Penalty for Private Use, $300

SPECIAL FOURTH-CLASS RATE
POSTAGE & FEES PAID
NASA
PERMIT No. G27

NASA

POSTMASTER: If Undeliverable (Section 158
Postal Manual) Do Not Return